FUSE

Volume 12, December 2023

Fungal Systematics and Evolution

WESTERDIJK FUNGAL BIO DIVERSITY INSTITUTE

EDITORIAL BOARD

Cover: *Niveomyces multisynnematus* growing on *Ophiocordyceps aff. flavida*

SCOPE AND AIMS

SCOPE
All aspects of systematics and evolution of fungi.

AIMS
Fungal Systematics and Evolution is an international, peer-reviewed, open-access, full colour, fast-track journal. Papers will include reviews, research articles, methodology papers, taxonomic monographs, and the description of fungi. The journal strongly supports good practice policies, and requires voucher specimens to be deposited in a fungarium, cultures in long-term genetic resource collection, sequences in GenBank, alignments in TreeBASE, and taxonomic novelties in MycoBank.

ABOUT FUNGAL SYSTEMATICS AND EVOLUTION
Fungal Systematics and Evolution has an OPEN ACCESS publishing policy. All manuscripts will undergo peer review before acceptance, and will be published as quickly as possible following acceptance. There are no page charges or length restrictions, or fees for colour plates. The official journal language is English. All content submitted to Fungal Systematics and Evolution is checked for plagiarism.

PUBLISHED BY
Westerdijk Fungal Biodiversity Institute, P.O. Box 85167, 3508 AD Utrecht, The Netherlands.

FREQUENCY
Twice per year (June and December).

ISSN: 2589-3823
E-ISSN: 2589-3831

CONTENTS

Research papers

FUSE

Fungal Systematics and Evolution

Volume 12
DECEMBER 2023
PAGES 1–30

doi.org/10.3114/fuse.2023.12.01

Eight novel cave fungi in Thailand's Satun Geopark

S. Preedanon[1], S. Suetrong[1*], C. Srihom[1], S. Somrithipol[2], N. Kobmoo[2], S. Saengkaewsuk[1], P. Srikitikulchai[1], A. Klaysuban[1], S. Nuankaew[2], C. Chuaseeharonnachai[2], B. Chainuwong[1], C. Muangsong[3], Z.F. Zhang[4], L. Cai[5], N. Boonyuen[2*]

[1]National Biobank of Thailand (NBT), National Science and Technology Development Agency (NSTDA), Khlong Nueng, Khlong Luang, Pathum Thani 12120, Thailand
[2]National Center for Genetic Engineering and Biotechnology (BIOTEC), National Science and Technology Development Agency (NSTDA), Khlong Nueng, Khlong Luang, Pathum Thani 12120, Thailand
[3]Innovation for Social and Environmental Management, Mahidol University (MU), Amnatcharoen Campus, Amnatcharoen 37000, Thailand
[4]Southern Marine Science and Engineering Guangdong Laboratory (Guangzhou), Guangzhou 51145, China
[5]State Key Laboratory of Mycology, Institute of Microbiology, Chinese Academy of Sciences (CAS), Beijing 100101, China

*Corresponding author: S. Suetrong, satinee.sue@nstda.or.th; N. Boonyuen, nattawut@biotec.or.th

Key words:
karst cave
morpho-phylo systematics
multi-locus phylogenies
new taxa
palaeozoic satun era
taxonomy

Abstract: Karst caves are unique oligotrophic ecosystems characterised by the scarcity of organic litter, darkness, low to moderate temperatures, and high humidity, supporting diverse fungal communities. Despite their importance, little is known about the fungi in karst caves in Thailand. In 2019, we explored the culturable mycobiota associated with three selected types of substrates (air, soil/sediment and organic litter samples) from two karst caves, the Le Stegodon and Phu Pha Phet Caves, in the Satun UNESCO Global Geopark in southern Thailand. Based on morphological characters and multilocus phylogenetic analyses, eight new species (*Actinomortierella caverna, Hypoxylon phuphaphetense, Leptobacillium latisporum, Malbranchea phuphaphetensis, Scedosporium satunense, Sesquicillium cavernum, Thelonectria satunensis* and *Umbelopsis satunensis*) were described, illustrated, and compared to closely related species. These new fungal taxa form independent lineages distinct from other previously described species and classified into eight different families across six orders and two phyla (*Ascomycota* and *Mucoromycota*). This paper provides additional evidence that the karst caves located within the Satun UNESCO Global Geopark, situated in the southern region of Thailand, harbour a diverse range of newly discovered species.

Citation: Preedanon S, Suetrong S, Srihom C, Somrithipol S, Kobmoo N, Saengkaewsuk S, Srikitikulchai P, Klaysuban A, Nuankaew S, Chuaseeharonnachai C, Chainuwong B, Muangsong C, Zhang ZF, Cai L, Boonyuen N (2023). Eight novel cave fungi in Thailand's Satun Geopark. *Fungal Systematics and Evolution* **12**: 1–30. doi: 10.3114/fuse.2023.12.01
Received: 4 April 2023; **Accepted:** 12 June 2023; **Effectively published online:** 24 July 2023
Corresponding editor: P.W. Crous

INTRODUCTION

Fungi constitute a remarkably diverse group of organisms that exhibit a wide range of morphological, ecological, metabolic, and phylogenetic characteristics. They can be found in various forms, including single-celled and multicellular filamentous structures. Fungi play crucial roles in ecosystems as saprophytes, decomposers, mutualists, and pathogens (Schoch *et al.* 2009, Bastian *et al.* 2010, Naranjo-Ortiz & Gabaldón 2019). The current estimate of fungal diversity is highly uncertain, ranging from 2.2 to 3.8 M, but only approximately 146 000–150 000 species, or 3–4 %, are currently accepted taxa; thus, 96 % of fungal species remain unknown (Hawksworth & Lucking 2017, Banki *et al*. 2021). Fungal communities exist in every ecosystem on Earth, and the species compositions of the communities can be adjusted to adapt to various environmental conditions, including caves (Vanderwolf *et al.* 2013). Karst caves are dark, relatively cool, humid, nutrient-limited, and subterranean (Lee *et al.* 2012, Zhang *et al*. 2017, 2018). The unique environmental ecosystems in cave environments provide an opportunity to identify and study unusual fungi that are adapted to extreme conditions associated with oligotrophy (Gabriel & Northup 2013). According to research on karst cave fungi, they play important roles in the formation and characteristics of speleothems in caves by controlling major biogeochemical cycling and cave evolution (Vanderwolf *et al.* 2013, Zhu *et al.* 2022). Furthermore, it has been reported that the microbial communities in caves can obtain energy by breaking down aromatic compounds, fixing nitrogen from the atmosphere and interacting with minerals in terms of fungal metabolism and cave biogeochemistry (Boblitt *et al.* 2018, Jones & Northup 2021, Zada *et al.* 2021, Zhu *et al.* 2022). This evidence suggests that fungi living in extreme and harsh conditions might potentially produce novel compounds, bioactive secondary metabolites and/or enzymes that enable them to survive in these environments (Belyagoubi *et al.* 2018, Fernández-Remacha *et al.* 2022, Gubiani *et al.* 2022). Most of the fungal genera found in caves have also been isolated from natural substrates, such as sediment, cave walls, speleothems,

guano, water, air, and various fauna (including bats) from different regions of the world; many of the fungi are not native to caves but have likely been introduced and dispersed by humans, fauna, water, and air currents (Jurado *et al.* 2008, Shapiro & Pringle 2010, Vanderwolf *et al.* 2013, 2016, Martin-Sanchez *et al.* 2014, Nováková *et al.* 2018, Carvalho *et al.* 2022, Leplat *et al.* 2022).

The cave-dwelling fungi found in the tropics, particularly in Thailand, are not well documented. In a recent study, Nuankaew *et al.* (2022) discovered two new species of *Talaromyces* in soil samples collected from the Satun UNESCO Global Geopark in southern Thailand. As part of a project that addresses the mycological diversity of the Satun UNESCO Global Geopark (Satun province, Thailand), two karst caves (Phu Pha Phet Cave and Le Stegodon Cave) were surveyed in this study. The fungal species in these two caves were identified using culturable morphotypes and BLAST queries against the fungal sequence database. Morphological characteristics, in combination with molecular data from seven loci (the ribosomal small subunit (SSU), the ribosomal large subunit (LSU), translation elongation factor 1-alpha (*TEF-1α*), beta-tubulin (*TUB*), α-actin (*ACT*), RNA polymerase II largest subunit (*RPB1*) and second largest subunit of ribosomal polymerase II (*RPB2*) regions) summarised in a multi-locus phylogeny, permitted the characterisation, description and illustration of eight new fungal species found in these caves.

MATERIALS AND METHODS

Cave information and sampling sites

Satun Province in southern Thailand, known as the "Land of Palaeozoic fossils", was designated as the first UNESCO Global Geopark in the country on 17 April 2018 (Cheablam *et al.* 2021, Nantakat & Vorachart 2021). The Satun UNESCO Global Geopark covers four districts of Satun Province: Thungwa, Manang, La-Ngu, and Muang Satun. The region is renowned for its high diversity of fossil species from the Palaeozoic Era as well as for its diverse karst topography, which includes limestone, sandstone, mudstone, shale, and chert.

Phu Pha Phet Cave, also known as the "Diamond Mountain Cave", is located within the Satun UNESCO Global Geopark at an elevation of 21 m (7°7'25"N 99°47'54"E) in Thungwa, Manang District (Fig. 1). It is the fourth largest cave in the world and the largest cave in Thailand, covering an area of more than 0.16 ha, and is approximately 536.65 m in length. The cave, which has a high ceiling and a unique atmosphere, contains sparkling stalactites and stalagmites resembling diamond flakes. More than 20 chambers are present within the cave, which can be accessed via a wooden bridge and is illuminated by installed lights. This cave is open to tourists and has therefore experienced some level of anthropogenic disturbance. However, certain areas of the cave are closed to the public to assure the protection of natural resources and promote sustainable tourism. As a result, the number of visitors to the cave is limited. Overall, the level of

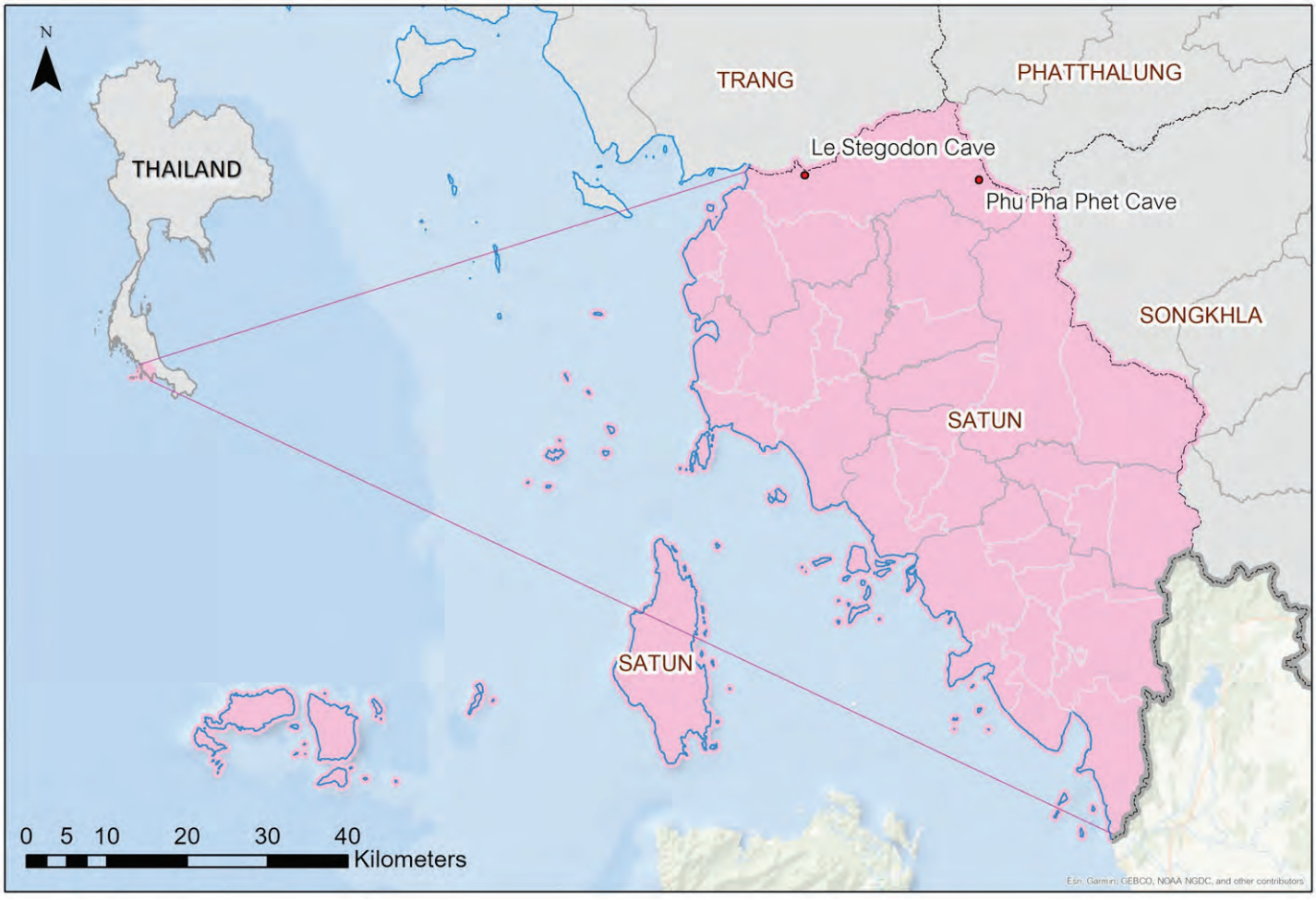

Fig. 1. Map of Thailand and location of the two sampling sites Satun UNESCO Global Geopark in Satun Province in the southern part of Thailand.

human disturbance in the Phu Pha Phet Cave can be considered moderate (Nantakat & Vorachart 2021; https://www.dmr.go.th/department-of-mineral-resources-thailand; accessed 26 May 2023). The depicted areas in Le Stegodon Cave indicate the sampling sites/zones: A (A1–A5), B (B1–B5), and C (C1–C5) (Fig. 2).

Le Stegodon Cave (Tham Le Stegodon; 107 m elevation; 7°7'35"N 99°59'49"E), located in the Thung Wa Subdistrict, Thung Wa District, is a sea cave with seawater intrusions on its western outlet (Fig. 1). It consists of three winding tunnels that converge within the mountain and have a total length of approximately three to four km. The tunnels are 10–20 m wide and 10–20 m high. The western outlet of Le Stegodon Cave is connected to a brackish stream that flows through a mangrove forest. The water level in the cave is influenced both by the stream and by the daily tides from the western outlet. While the cave is open to tourists, certain areas are closed to the public for the same reasons as in the case of Phu Pha Phet Cave. The level of human disturbance in some areas of the cave is considered low to moderate. Each of the two caves in this study was divided into three main zones for fungal sampling purposes (Duangkrayom *et al.* 2018, Nantakat & Vorachart 2021). Additionally, the positions of sampling sites/zones A (A1–A5), B (B1–B5), and C (C1–C5) within Phu Pha Phet Cave are also illustrated (Fig. 2).

Sample collection and fungal isolation

Sampling (Fig. 3) was performed in November 2019. The collection and isolation methods used were specific to the type of sample collected as follows: 1) Air samples (A) were collected using the Koch sedimentation method (Zhang *et al.* 2017). For each air sample, 3–5 Petri dishes containing 2 % potato dextrose agar (PDA, Difco) containing two antibiotics (50 µg/mL ampicillin and 50 µg/mL streptomycin) were exposed to the atmosphere in the cave for 15–20 min. The dishes were then sealed with Parafilm and placed in zip-lock plastic bags (Jiang *et al.* 2017). 2) Soil samples (S) of approximately 10–20 g was collected from the top 1–5 cm surface, placed in zip-lock bags, and stored at 4 °C in an ice box until it could be transferred to the laboratory for analysis. 3) Organic litter (O) consisting of guano, other animal dung, carcasses, and plant debris were collected in plastic zip-lock bags and kept at 4 °C in an ice box. All samples were transferred to the laboratory and kept at 4 °C in a refrigerator until used for further fungal isolation.

Isolation of cave fungi

Samples were processed according to the methods described by Zhang *et al.* (2017, 2021). One gram of S or O was added to 9 mL of sterile water in a sterile 15 mL centrifuge tube, and shaken by hand or mechanically for 10 min. The suspensions of S were diluted to 10^{-1}–10^{-5} and 10^{-2}–10^{-5} for O. Two hundred mL of suspension at each concentration were spread on PDA containing streptomycin (50 µg/mL) and ampicillin (50 µg/mL); three replicate plates were prepared for each dilution. All fungal plates were incubated at room temperature (23–25 °C) and examined at 24 h intervals for 2–3 wk. Single colonies were picked from the plates and transferred to PDA plates without antibiotics.

Morphological characterisation

The size, colour, shape, and arrangement of sporangiophores and conidiophores, sporangia and conidiogenous cells (*i.e.*, phialides), spores, and conidia (n = 10–30) were observed after placing the material in a drop of lactophenol blue and examining it using a light microscope (OLYMPUS CX31; Olympus Corporation, Japan) at high magnification, following published procedures and techniques (Seifert *et al.* 2011, Zhang *et al.* 2017, Nuankaew *et al.* 2022, Watanabe 2002). Measurements were made of fresh cultures suspended in water, and the fungi were photographed using a Nomarski differential interference contrast microscope (OLYMPUS DP70). Species were determined using a morphological species concept, but DNA sequences were used to support the morphological data (Crous *et al.* 2021, 2022).

Candidate strains of potential new species were identified based on comparison of their Internal Transcribed Spacers (ITS) sequences with those of known genera and species using BLASTn tool; if the highest match was less than 97 %, the strain was considered a potential new species, according to the method outlined by Zhang *et al.* (2017). Candidate strains of potential new species were transferred to new plates containing PDA, malt extract agar (MEA), oatmeal agar (OA) or cornmeal agar (CMA) based on the given genera. The cultures were incubated at room temperature (23–25 °C) until morphological characterisation and molecular studies were performed. Colony characteristics and pigment production were examined after 14 d. Colony size was measured after 7 d for fast-growing strains, after 14 d for the slower strains, and after 8 wk for the most fastidious strains. The colour codes used in the fungal description follow the "Methuen Handbook of Colour" (Kornerup & Wanscher 1978). Fungal karst cave cultures were examined periodically for the development of reproductive structures according to the modified method of Réblová *et al.* (2016).

To maintain axenic cultures of fungi from karst caves, slant agar plates containing PDA were inoculated with small pieces of mycelium or with spore suspensions. Fungal strains were selected based on their morphotypes and stored at 4 °C for further study; the stored cultures were transferred to fresh medium every 6 mo. Fungal cultures of new species are maintained in the Thailand Bioresource Research Center (TBRC; https://www.tbrcnetwork.org, accessed 26 May 2023) and the National Biobank of Thailand (NBT; https://www.nationalbiobank.in.th; accessed 26 May 2023), and dry cultures were deposited at the BIOTEC Bangkok Fungarium (BBH; https://www.nationalbiobank.in.th/microbe-services; accessed 26 May 2023). The new taxa were registered at MycoBank Database (Crous *et al.* 2004; https://www.mycobank.org/, accessed 26 May 2023).

DNA extraction, PCR amplification, and Sequencing

Total genomic DNA was extracted from 7-d-old axenic cultures grown on PDA, according to the modified method of Boonyuen *et al.* (2021). The Internal transcribed spacers 1 and 2, including the intervening 5.8S nrDNA gene (ITS), were sequenced for every fungal isolate, and SSU, LSU, *TEF-1α*, *TUB*, *ACT*, *RPB1* and *RPB2* regions (White *et al.* 1990, Vilgalys & Hester 1990, Glass & Donaldson 1995, O'Donnell & Cigelnik 1997, Carbone & Kohn 1999, Liu *et al.* 1999, Voigt & Wöstemeyer 2000, Matheny *et al.* 2002, Castlebury *et al.* 2004, Rehner & Buckley 2005) were sequenced for each fungal strain that represented a new species candidate.

PCR was performed in a 50 µL reaction mixture containing 35.8 µL of nanopurified water, 5 µL of 10X Taq buffer with

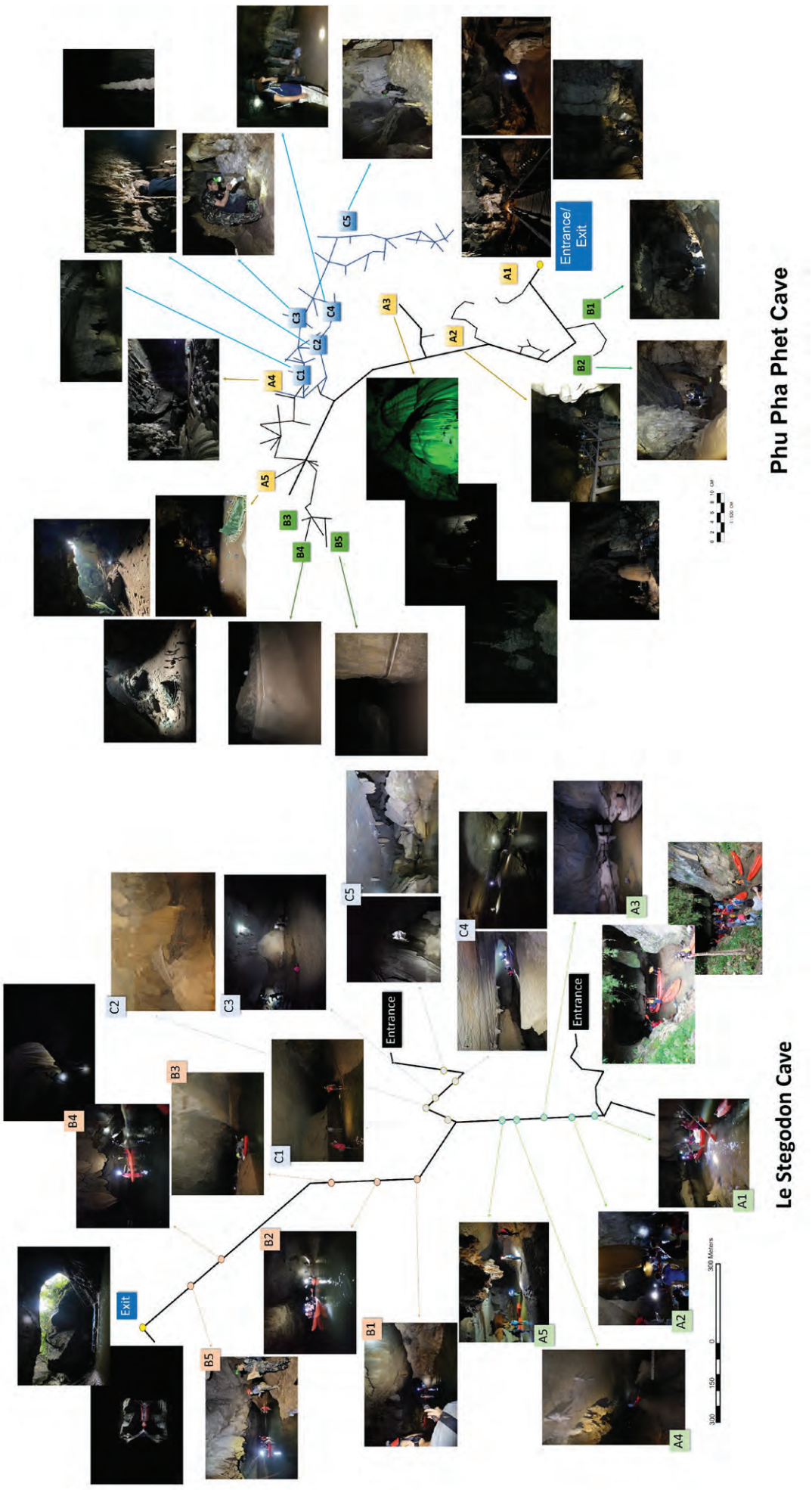

Fig. 2. Map of visited caves. Sampling sites/zones in Le Stegodon Cave and Phu Pha Phet Cave are shown, as are the locations of sampling sites/zones A (A1–A5), B (B1–B5) and C (C1–C5) in Phu Pha Phet Cave.

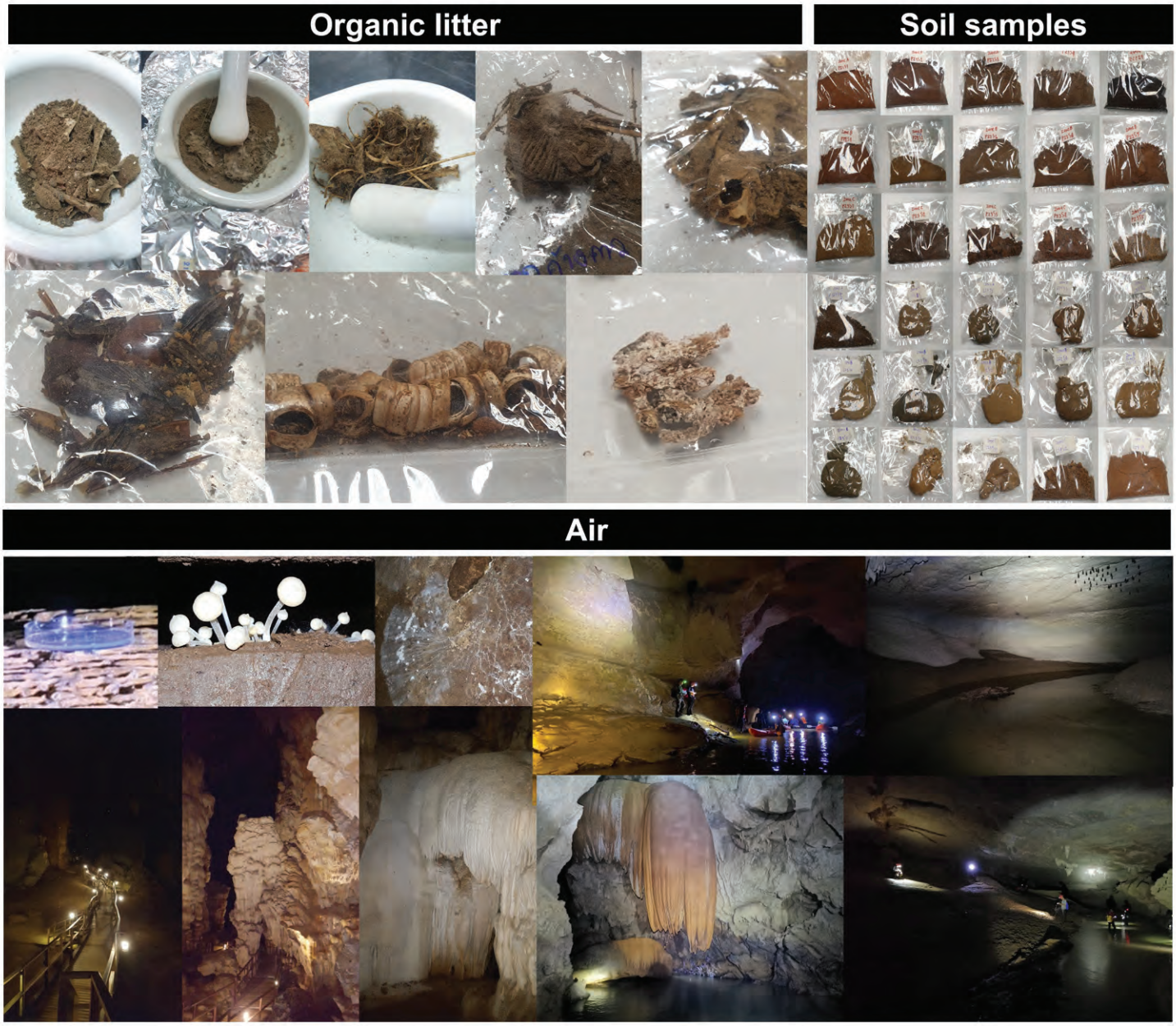

Fig. 3. Samples (soil sediment, organic litter).

$(NH_4)_2SO_4$, 5 µL of 25 mM $MgCl_2$, 1 µL of 10 mM dNTP, 1 µL of each primer, 0.2 µL of recombinant Taq DNA polymerase (Thermo Scientific™) and 1 µL of fungal DNA. The primers ITS5/ITS4, ITS1F/4, NS1/NS4 (White *et al.* 1990), LROR/LR5 (Vilgalys & Hester 1990), Bt2a/Bt2b (Glass & Donaldson 1995), T1/T22 (O'Donnell & Cigelnik 1997), 983F/2218R (Rehner & Buckley 2005), tef1-728/tef1-1576 (Carbone & Kohn 1999), act1/act4 (Voigt & Wöstemeyer 2000), crpb1a/rpb1c (Castlebury *et al.* 2004) and RPB2-5F2/fRPB2-7cR (Liu *et al.* 1999) were employed. PCR profiles were obtained using the 100TM Thermal Cycler (BIO–RAD Laboratories, Inc., California) as described by Zhang *et al.* (2017, 2021). PCR products were checked by electrophoresis on 1 % agarose gels together with a DNA ladder containing DNA molecules of known sizes. To confirm the presence of amplicons at the expected molecular weight. PCR products were purified using a DNA purification kit (MACHEREY-NAGEL, Germany). The PCR products were used directly for DNA sequencing. DNA sequencing was performed at Macrogen Inc. in South Korea using the primers listed above. Forward and reverse reads were paired and consensus sequences, and they were checked for ambiguous bases and trimmed at both ends using BioEdit v. 7.2.3 (Hall 1999). The new sequences identified in this study were deposited in GenBank (National Center for Biotechnology Information; NCBI; accessed 26 May 2023). A BLASTn search of the GenBank database for the newly generated sequences was performed to exclude contamination and to search for related taxa (www.ncbi.nlm.nih.gov/blast; accessed 26 May 2023).

Sequence homologies were analysed using the BLAST search engine at NCBI and compared with the sequences reported in GenBank. If the ITS sequence of the highest BLAST hit for a given isolate had a closest similarity to potential genera and species of less than 97 %, the isolate was recognized as a potential novel species and was further identified using morphological data and multilocus phylogenetic analysis according to Zhang *et al.* (2017). The morphological data for potential novel species were compared with morphological data for known species identified to at least the genus or species level. Alignments were checked and manually optimised along with other sequences obtained from the GenBank nucleotide database.

Phylogenetic analysis

Multilocus phylogenetic analysis was conducted using the method of Boonyuen *et al.* (2011). Multiple alignments of the sequences generated from the novel species with other sequences obtained from GenBank were performed, and the results were refined manually in BioEdit v. 7.2.3 (Hall 1999), and automatically aligned using MUSCLE v. 3.8.1 (Edgar 2004). Manual gap adjustments were made to improve the alignment. Nine datasets were compiled in BioEdit v. 7.2.3, and the formats of multiple sequence alignments were changed using AliView (Larsson 2014). Bayesian posterior probabilities of the branches were obtained using MrBayes v. 3.2.6 (Ronquist *et al.* 2012) with the best-fit model (GTR+I+G) selected by AIC in MrModeltest v. 2.2 (Nylander 2004), which was tested with hierarchical likelihood ratios (hLRTs) and evaluated for the number of distinct data patterns under this model. Three million generations were run in four Markov chains and sampled every 100 generations with a burn-in value set at 3 000 sampled trees. Finally, maximum likelihood (ML) and bootstrap analyses were conducted using the CIPRES Science Gateway platform (Miller *et al.* 2010) with RAxML–HPC2 on XSEDE v. 8.2.8 (Stamatakis 2014) under the GTR + GAMMA model with the BFGS method to optimize GTR rate parameters. The resulting consensus tree was displayed using Interactive Tree Of Life (iTOL) (Letunic & Bork 2021; https://itol.embl.de/, accessed 26 May 2023) and adjusted in Adobe Photoshop 2020. All sequences generated in this study were deposited in GenBank and their respective accession numbers are given in Table 1. The resulting alignments were submitted to TreeBASE under submission IDs (30019, 29986, 29985, 29988, 29990, 29983, 29989, 29987 and 29984; https://www.treebase.org/treebase-web/home.html, accessed 26 May 2023).

RESULTS

Phylogenetic analyses

The ITS phylogenetic analysis consists of 92 fungal taxa. *Taphrina americana* (CBS 331.55) and *T. antarctica* (CCFEE 5198) were used to root the tree (Fig. 4). Phylogenetic analyses showed that the eight novel species found in the karst cave (shown in red bold font in the figure) were distributed among eight families belonging to six different orders, *i.e.*, *Onygenales, Hypocreales, Microascales, Xylariales, Mortierellales* and *Umbelopsidales*. The Bayesian inference (BI) tree is not shown because its topology is similar to that of the ML tree shown in the figure. Credible ML bootstrap values (≥ 50 %) and Bayesian posterior probabilities (≥ 0.95) are shown in the phylogenetic tree.

Taxonomy

Based on the morphological and molecular results provided above, several new species are proposed, namely *Actinomortierella caverna*, *Hypoxylon phuphaphetense*, *Leptobacillium latisporum*, *Malbranchea phuphaphetensis*, *Scedosporium satunense*, *Sesquicillium cavernum*, *Thelonectria satunensis*, and *Umbelopsis satunensis*.

Table 1. Strain numbers and sequence accession numbers of eight novel species.

Species name	Family	Strain number	GenBank accession numbers[2]						
			ITS	LSU	SSU	*TEF-1α*	*TUB*	*RPB1*	*RPB2*	*ACT*
Actinomortierella caverna	*Mortierellaceae*	TBRC 16274[1]	OP856536	OP856526	OP850837	NA	NA	NA	NA	NA
Hypoxylon phuphaphetense	*Hypoxylaceae*	TBRC 16277[1]	OP856538	OP856528	NA	NA	OQ144973	NA	OQ108849	NA
Leptobacillium latisporum	*Cordycipitaceae*	TBRC 16288[1]	OP856540	OP856529	OP850838	NA	NA	NA	NA	NA
Malbranchea phuphaphetensis	*Malbrancheaceae*	TBRC 16252[1]	OP856532	OP856522	NA	OQ116929	OQ144969	NA	NA	NA
Scedosporium satunense	*Microascaceae*	TBRC 16285[1]	OP856539	NA	NA	NA	OQ144974	NA	NA	NA
Sesquicillium cavernum	*Bionectriceae*	TBRC 16268[1]	OP856535	OP856525	NA	OQ116931	OQ144971	NA	NA	NA
Thelonectria satunensis	*Nectriaceae*	TBRC 16275[1]	OP856537	OP856527	NA	OQ116932	OQ144972	OQ076387	NA	OQ116938
Umbelopsis satunensis	*Umbelopsidaceae*	TBRC 16254[1]	OP856533	OP856524	OP850836	NA	NA	NA	NA	OQ116937

[1]Ex-holotype strains.

[2]NA = not available.

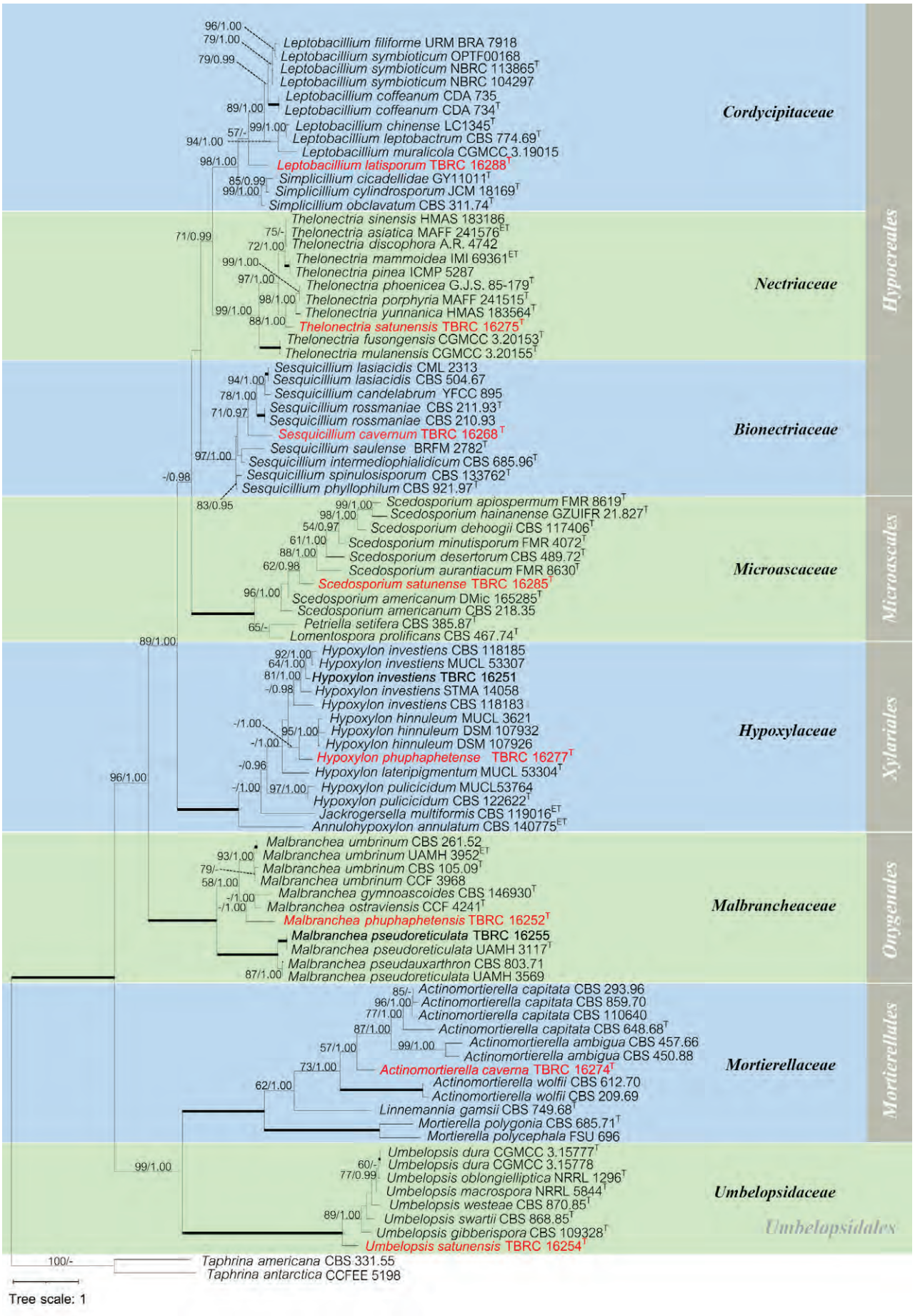

Fig. 4. RAxML Phylogenetic tree of selected fungal groups showing the eight new species based on ITS region (90 ingroup taxa). Maximum likelihood bootstrap values (BSML, left) ≥ 50 % are shown at the nodes. Bayesian posterior probabilities (BYPP, right) ≥ 0.95 are given at the nodes. Highly supported nodes with 100 % bootstrap supports and with 1.00 posterior probabilities are shown as thick lines. Abbreviations: T = ex-holotype; ET = ex-epitype. Novel species are indicated by red bold font.

Actinomortierella caverna C. Srihom, Preedanon, S. Saengkaewsuk & Somrith*.*, ***sp. nov.*** MycoBank MB 846891. Fig. 5.

Etymology: "*caverna*" in Latin means "cave" and refers to the habitat in which this fungus was initially discovered.

Typus: **Thailand**, Satun Province, Thung Wa District, Satun UNESCO Global Geopark, Le Stegodon Cave, 7°7'35"N 99°59'49"E, 107 m elevation, isolated from soil, Dec. 2019, coll. *N. Boonyuen, P. Srikitikulchai & S. Preedanon*, isol., *S. Preedanon*, *cultura dessicata* (**holotype** BBH 49442; ex-type culture BCC 91669 = TBRC 16274 = NBTF

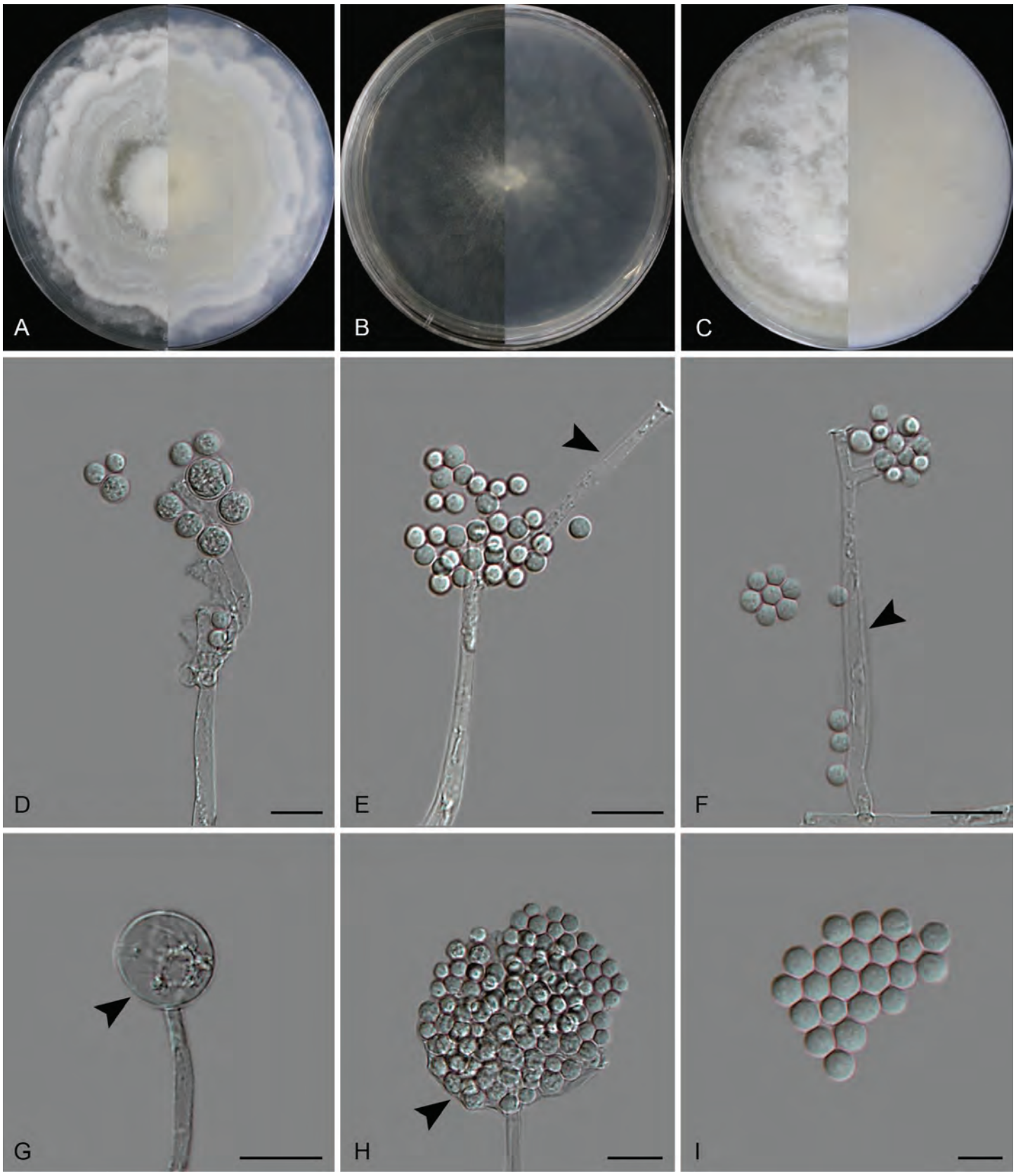

Fig. 5. *Actinomortierella caverna* (TBRC 16274). **A–C.** Obverse and reverse views of cultures on PDA, MEA 2 % and OA after 14 d. **D, F.** Sporangiophore (arrow) with sporangiospores. **E.** uppermost branching of sporangiophore (arrow). **G.** Vesicle (arrow). **H.** sporangium wall (arrow) with sporangiospores. **I.** Sporangiospores. Scale bars: D–H = 20 µm; I =10 µm.

002290 = isolate CV00251). The GenBank accession numbers of ITS, LSU and SSU are OP856536, OP856526 and OP850837, respectively.

Classification: *Mortierellaceae, Mortierellales, Incertae sedis, Mortierellomycetes, Mortierellomycotina, Mucoromycota*

Description: *Vegetative hyphae* aseptate, 1.1–4.6 µm (n = 15) wide, smooth and hyaline. *Sporangiophores* arising from the mycelia, hyaline, 79.9–353 × 6.4–18.2 µm wide; branched sporangiophores forming sporangia, 7.6–60 × 2.2–4.8 µm wide. *Sporangia* globose to subglobose, 13–37.6 µm wide. *Vesicle* 56–60.1 µm diam. *Sporangiospores* hyaline, globose to subglobose, one-celled, 5.9–12.6 × 5.8–11.8 µm (n = 30),.

Culture characteristics: Colonies after 14 d on: PDA attaining 85 mm diam, umbonate, undulate, floccose, fluffy, margins curled, mycelia white (1A1); reverse yellowish white (1A2) to white (1A1) at margin. On MEA attaining 85 mm diam, filamentous, flat, margin rhizoids, striate, aerial mycelia extremely sparse and white (1A1); reverse white (1A1). On OA attaining 85 mm diam, convex, floccose, fluffy, tufts, dense and white (1A1), margin entire; reverse white (1A1). Sporulation within 9 wk on PDA.

Notes: *Actinomortierella* is characterised by sporangiophores with an inflated upper part bearing branches to form the sporangium (Chalabuda 1868, Degawa 1997, Degawa & Gams 2004, Vandepol *et al.* 2020). This genus is typically found in soils, manure, compost, decaying wood, and the rhizosphere (Seviour *et al.* 1987, Lorch *et al.* 2013, Macias *et al.* 2019). According to indexfungorum.org (accessed 26 May 2023), three species, *A. ambigua*, *A. capitata*, and *A. wolfii*, are currently accepted in the genus; these were initially described as *Mortierella* by Marchal (1891), Mehrotra *et al.* (1963), and Mehrotra & Baijal (1963), respectively. Based on phylogenetic analysis the new species belongs to *Actinomortierella*, and is related to *A. capitata*, (BSML = 99 %) (Fig. 6). However, the Bayesian posterior probability is less than 0.95. Additionally, comparison of the ITS barcode regions of *A. capitata* and *A. caverna* showed a sequence similarity of 85.81–89 %. Morphologically, *A. caverna* branches at the uppermost portion of the sporangiophore, but the inflation part from which the branches arise is rarely observed. Additionally, the new species has only a few branches, unlike the other two species. *Actinomortierella capitata* has sporangia that are much larger than those of the new species (Supplementary Table S1). *Actinomortierella caverna* differs from *A. ambigua* and *A. wolfii* in the shape of its spores. Spores of *A. caverna* are globose to subglobose, while spores of *A. ambigua* are oblong, and those of *A. wolfii* are ellipsoid-reniform. Distinctions between the novel taxa and their close relatives are presented in Supplementary Table S1. The new species was discovered in the cave habitat for the first time. Morphological characteristics and phylogenetic analyses of combined ITS, LSU and SSU sequences support the new species and the placement of *A. caverna* in the *Mortierellaceae.*

Hypoxylon phuphaphetense C. Srihom, Preedanon, S. Saengkaewsuk & Somrith., ***sp. nov.*** MycoBank MB 846894. Fig. 7.

Etymology: "*phuphaphetense*", pertaining to Phu Pha Phet cave in which the fungus was first discovered.

Typus: **Thailand**, Satun Province, Manang District, Satun UNESCO Global Geopark, Phu Pha Phet Cave, 7°7'25"N 99°47'54"E, 21 m elevation, isolated from soil, Dec. 2019, coll. *N. Boonyuen, P. Srikitikulchai & S. Preedanon*, isol., S. Preedanon, *cultura dessicata* (**holotype** BBH 49444; ex-type culture BCC 91956 = TBRC 16277 = NBTF 002284, isolate CV00283). The GenBank accession numbers of ITS, LSU, *RPB2* and *TUB* are OP856538, OP856528, OQ108849, and OQ144973, respectively.

Classification: *Hypoxylaceae, Xylariales, Xylariomycetidae, Sordariomycetes, Pezizomycotina, Ascomycota.*

Description: *Conidiophores* micro- to semi-macronematous, hyaline, simple or branched, smooth to slightly roughened, 1.7–17 × 0.8–2.2 µm. *Conidiogenous cells* holoblastic, mono- or polyblastic, aggregated, hyaline to brown, straight to curved with scars. *Conidia* ellipsoid, pale brown to dark brown, smooth- to rough-walled, 5–10.2 × 4–5 µm (n = 30) with protruding hilum, more abundant on PDA than on 2 % MEA or on OA. *Sexual morph* not observed.

Culture characteristics: Colonies after 14 d on: PDA attaining 60 mm diam, circular, flat, felt, annular, margin radially striate with lobate edge and greyish brown (5F3) to orange grey (5B2) at margin; reverse dark brown (6F8) to reddish yellow (4A6) at margin. On 2 % MEA attaining 40 mm diam, circular, flat, entire, more intense near the medium surface, sparse and greyish brown (5F3); reverse yellowish brown (5D8). On OA attaining 60 mm diam, irregular, flat, undulate, and more intense near the medium surface, dull and brownish grey (5F2); reverse greyish yellow (4B3). Sporulation within 6 wk on PDA.

Notes: The genus *Hypoxylon* within the family *Hypoxylaceae* (*Xylariales, Ascomycota*) was proposed by Bulliard (1791). More than 200 species have been recorded (Becker *et al.* 2020, Pourmoghaddam *et al.* 2020, Cedeño-Sanchez *et al.* 2023). It is a common fungus in natural forests, and some species of the genus reside in dead plants or as endophytes, while others are beneficial and play important roles in the ecosystem (Dayarathne *et al.* 2020, Hyde *et al.* 2020, Ma *et al.* 2022, Song *et al*. 2022).

Phylogenetically, *H. phuphaphetense* forms a sister clade with *H. hinnuleum* in *Hypoxylon* clade H1 with BSML = 100 % and BYPP = 1.00, as shown in Fig. 8. However, these two clades appear highly different based on their morphological data. *Hypoxylon hinnuleum* was proposed as the sexual morph of *Nodulisporium hinnuleum* (Sir *et al.* 2019). The asexual morph of *H. hinnuleum* is *Virgariella* or *Nodulisporium*, with a long conidiophore with branches and a denticulate conidiogenous cell. Smith (1962) first described *Nodulisporium hinnuleum* from sorghum and oat in Kansas, USA, as a culture contaminant. Later, Sir *et al.* (2019) collected a number of *Hypoxylon* specimens in Texas, USA and considered *N. hinnuleum* as their asexual morph. In contrast, *H. phuphaphetense* is unique in that it only possesses an asexual morph. It produces a simple or clustered conidiogenous cell that is short and lacks denticulation (small tooth-like projections). Its asexual morphology differs significantly from the typical asexual morphs observed in the genus, which usually exhibit characteristics resembling *Nodulisporium*. Furthermore, the conidia of *H. hinnuleum* are hyaline and thin-walled, while those of the new species are pale to dark brown and relatively thick-walled. Additionally, the conidia of the new species are markedly larger (4.9–10.2 × 4.1–5.6 µm in *H. phuphaphetense vs*. 3.6–5.1 × 2.1–3.1 µm in *H. hinnuleum*). The ITS barcode

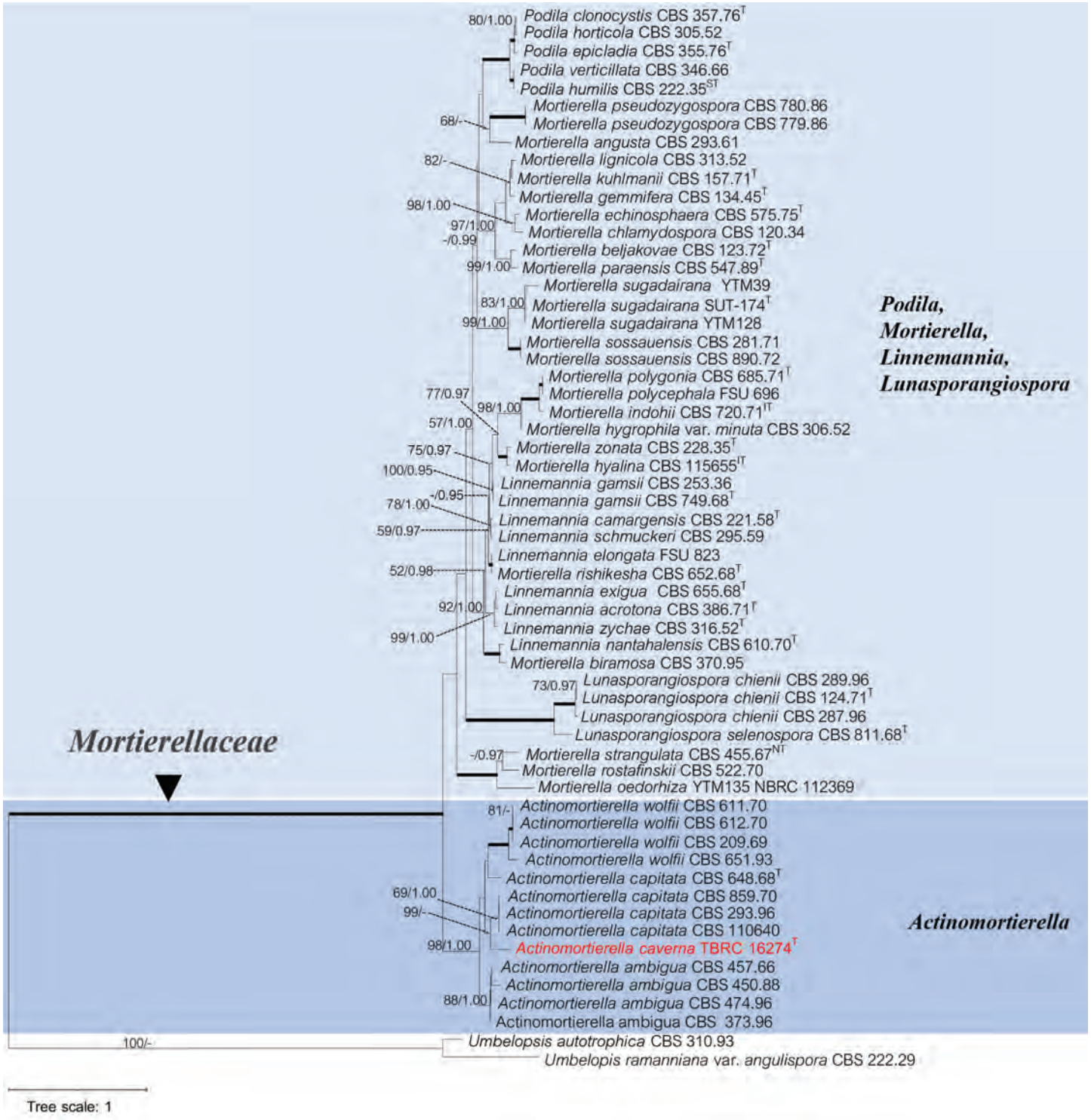

Fig. 6. RAxML phylogenetic tree of *Actinomortierella caverna* (TBRC 16274) and related taxa resulting from the combination of ITS, LSU and SSU sequences (57 ingroup taxa). Maximum likelihood bootstrap values (BSML, left) ≥ 50 % are shown at the nodes. Bayesian posterior probabilities (BYPP, right) ≥ 0.95 are given at the nodes. Highly supported nodes with 100 % bootstrap supports and with 1.00 posterior probabilities are shown as thick lines. Abbreviations: T = ex-holotype; ST = ex-syntype; NT = ex-neotype; IT = ex-isotype. Novel species is shown in red bold font.

region of *H. phuphaphetense* was compared with those of *H. hinnuleum* (MUCL 3621, DSM 107932, DSM 107926) sequences, and the results showed 494/564 = 89.36 % similarity with 10 substitutions, 491/563 = 89.34 % similarity with 10 substitutions and 493/565 = 89.03 % similarity with 10 substitutions, respectively. Based on the observed morphology and phylogeny, we introduce our karst cave collection as a new taxon.

Leptobacillium latisporum C. Srihom, Preedanon, S. Saengkaewsuk & Somrith., ***sp. nov.*** MycoBank MB 846897. Fig. 9.

Etymology: "*latis*" from Latin, lati- means broad, and "*sporum*" means spores or conidia, referring to the broad conidia of this species compared with those of other species.

Typus: **Thailand**, Satun Province, Manang District, Satun UNESCO Global Geopark, Phu Pha Phet Cave, 7°7'25"N 99°47'54"E, 21 m elevation,

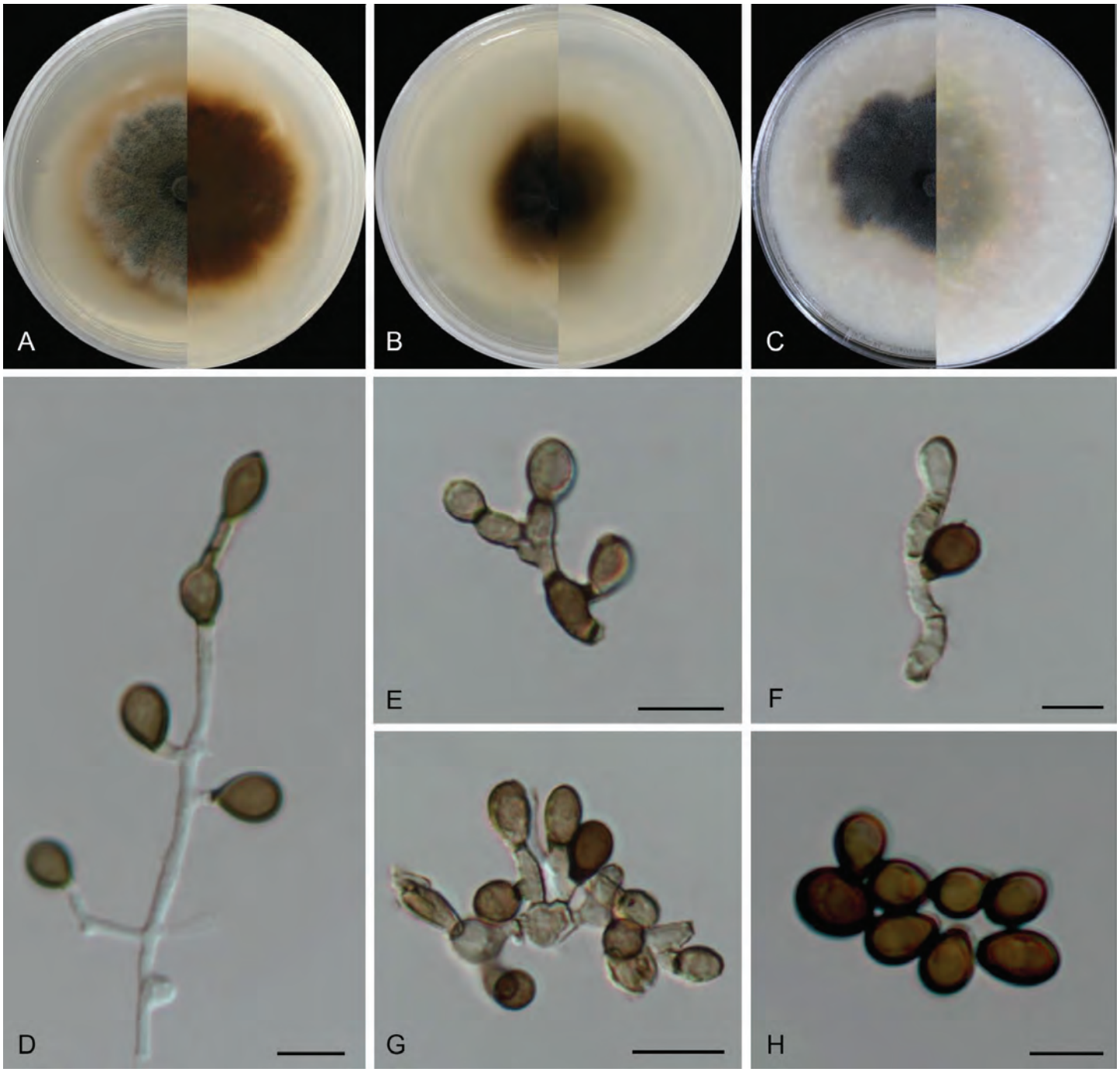

Fig. 7. *Hypoxylon phuphaphetense* (TBRC 16277). **A–C.** Obverse and reverse views of cultures on PDA, MEA 2 %, and OA after 14 d after. **D.** Conidiophores with conidia. **E–G.** Conidiogenous cells with conidia. **H.** Conidia. Scale bars: D–H = 10 µm.

isolated from soil, Dec. 2019, coll. *N. Boonyuen, P. Srikitikulchai & S. Preedanon*, isol., *S. Preedanon*, *cultura dessicata* (**holotype** BBH 49446; ex-type culture BCC 91807 = TBRC 16288 = NBTF 002288 = isolate CV00353). The GenBank accession numbers of ITS, LSU, and SSU are OP856540, OP856529 and OP850838, respectively.

Classification: *Cordycipitaceae, Hypocreales, Hypocreomycetidae, Sordariomycetes, Pezizomycotina, Ascomycota.*

Description: *Vegetative hyphae* hyaline, 1.2–3.6 µm wide (n = 15), *Conidiophores* macronematous, mostly solitary, cylindrical. *Conidiogenous cells* phialide, often branched with two or three phialides which being furcate (= schizophialides), hyaline, 13.2–40.8 × 3–4.8 µm. *Conidia* mostly formed in a long dry chain, slightly fusoid to narrowly cylindrical, 4–6.3 × 1.9–3.8 µm. *Chlamydospores* and *sexual morph* not observed.

Culture characteristics: Colonies after 14 d on: PDA attaining 45 mm diam, circular, raised, entire, velvety, fluffy, dense, delicate and white (5A1); reverse smooth with indistinct radial furrows, greyish orange (5B4) to orange white (5A2) at margin. On MEA attaining 70 mm diam, circular, raised, entire, velvety, fluffy, dense, delicate and white (5A1); reverse smooth with indistinct radial furrows, brownish orange (5C4) to orange white (5A2) at margin. On OA attaining 45 mm diam, circular, raised, entire, velvety, fluffy, dense, delicate and white (5A1); reverse orange white (5A2). Sporulation within 6 wk on PDA.

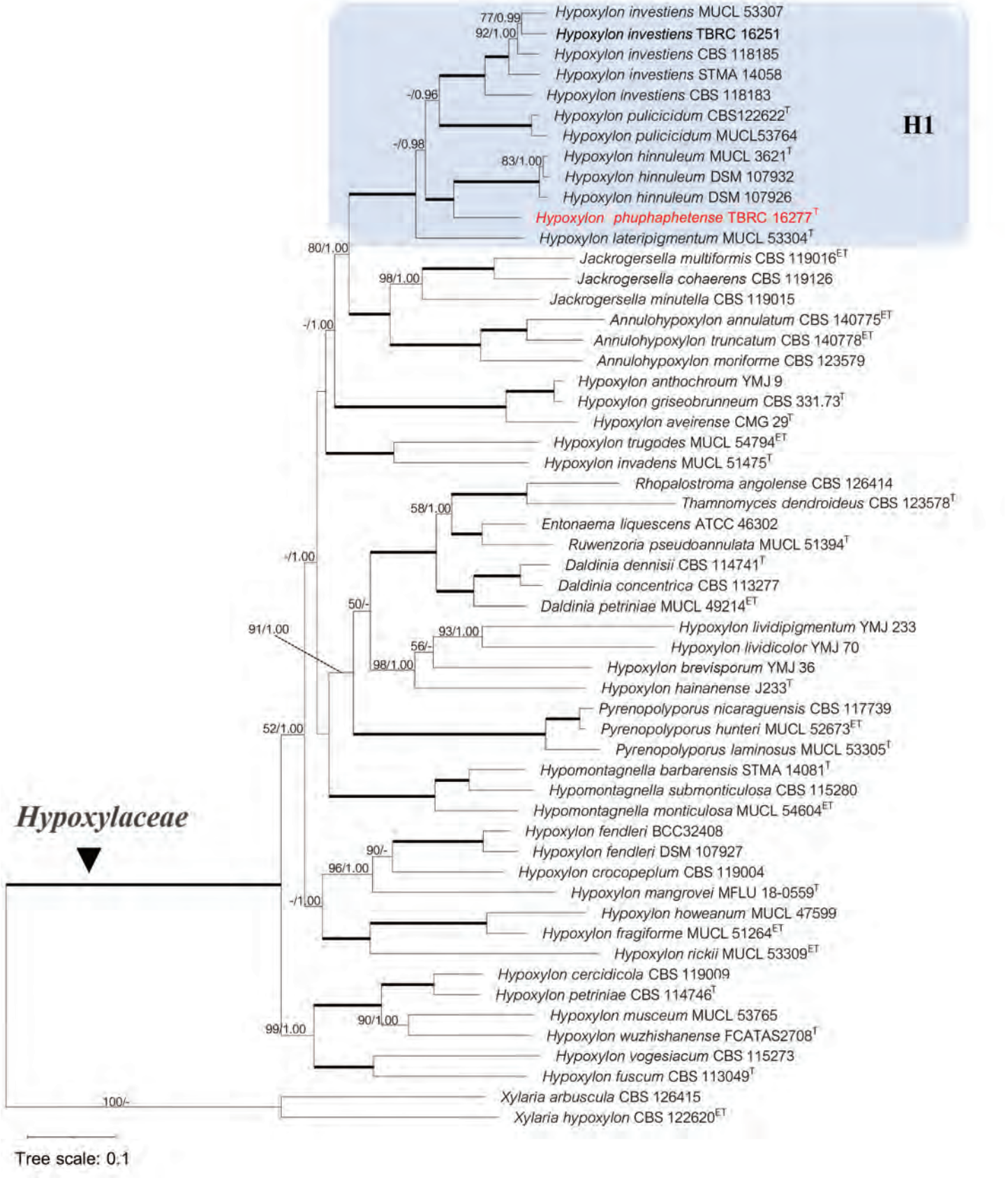

Fig. 8. The RAxML phylogenetic tree of *Hypoxylon phuphaphetense* (TBRC 16277) and related taxa based on sequences at four loci (ITS, LSU, *RPB2* and *TUB*) consists of 53 ingroup taxa. Maximum likelihood bootstrap values (BSML, left) ≥ 50 % are shown at the nodes. Bayesian posterior probabilities (BYPP, right) ≥ 0.95 are given at the nodes. Highly supported nodes with 100 % bootstrap supports and with 1.00 posterior probabilities are shown as thick lines. Abbreviations: T = ex-holotype; ET = ex-epitype. Novel species is shown in red bold font. H1 represents a sister clade of *Hypoxylon* spp., in which our new species is closed.

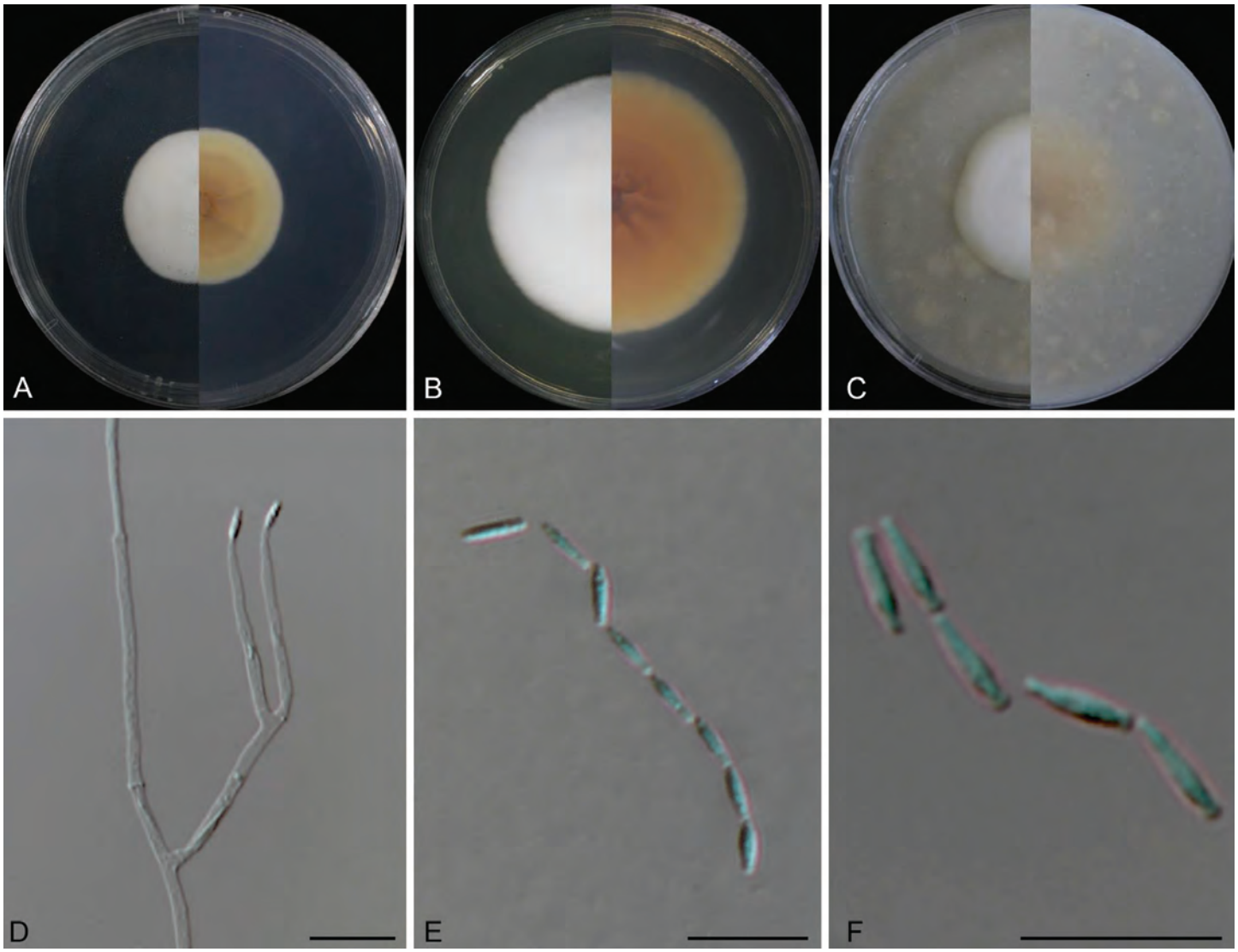

Fig. 9. *Leptobacillium latisporum* (TBRC 16288). **A–C.** Obverse and reverse views of cultures on PDA, MEA 2 %, and OA after 14 d. **D.** Conidiophores with conidia. **E, F.** Chains of conidia. Scale bars: D = 15 µm; E, F = 5 µm.

Notes: The genus *Leptobacillium* was proposed by Zare & Gams (2016) with *L. leptobactrum* as the type species. This genus is a member of the *Cordycipitaceae*. The genus is characterised by fusoid to cylindrical conidia born in chains and accumulated at the tip of a phialide that is usually solitary on hyphae. Molecular phylogeny supports the segregation of *Leptobacillium* from *Simplicillium*, a closely related genus (Chen *et al.* 2021). Based on indexfungorum.org (accessed 26 May 2023), *Leptobacillium* currently includes seven species. Recently, *L. cavernicola* from palaeolithic-decorated caves in France was described (Leplat *et al.* 2022), and *L. symbioticum* and *L. leptobactrum* were found in air samples from show caves in Spain (Dominguez-Moñino *et al.* 2021), India (Phookamsak *et al.* 2019) and Japan (Okane *et al*. 2020). In this study, the new species was identified as *Leptobacillium* based on its morphological and phylogenetic data. However, the new species differs markedly from other species in having the widest conidia. Furthermore, the conidiophores of the new species are often branched with two or three phialides, while the conidiophores of other species are mainly solitary phialides. Phylogenetic analysis also supports the distinction because the new species forms a sister clade of the cluster of the described species, with strong support (MSML= 92 % and BYPP = 1.00) (Fig. 10). Morphological comparisons between the new species and closely related *Leptobacillium* are provided in Supplementary Table S2. Our fungus represents a new karst cave taxon that is morphologically and phylogenetically distinguished from other species, and we propose it *L. latisporum*.

Malbranchea phuphaphetensis C. Srihom, Preedanon, S. Saengkaewsuk & Somrith., ***sp. nov.*** MycoBank MB 846887. Fig. 11.

Etymology: "*phuphaphetensis*" refers to the name of the cave in which the fungus was first discovered.

Typus: **Thailand**, Satun Province, Manang District, Satun UNESCO Global Geopark, Phu Pha Phet Cave, 7°7'25"N 99°47'54"E, 21 m elevation, isolated from soil, Dec. 2019, coll. *N. Boonyuen, P. Srikitikulchai & S. Preedanon*, isol., *S. Preedanon*, *cultura dessicata* (**holotype** BBH 49439; ex-type culture BCC 91900 = TBRC 16252 = NBTF 002285 = isolate CV 00115). The GenBank accession numbers of ITS, LSU, *BenA* and *TEF-1α* are OP856532, OP856522, OQ144969 and OQ116929, respectively.

Classification: Onygenaceae, Onygenales, Eurotiomycetidae, Eurotiomycetes, Pezizomycotina, Ascomycota.

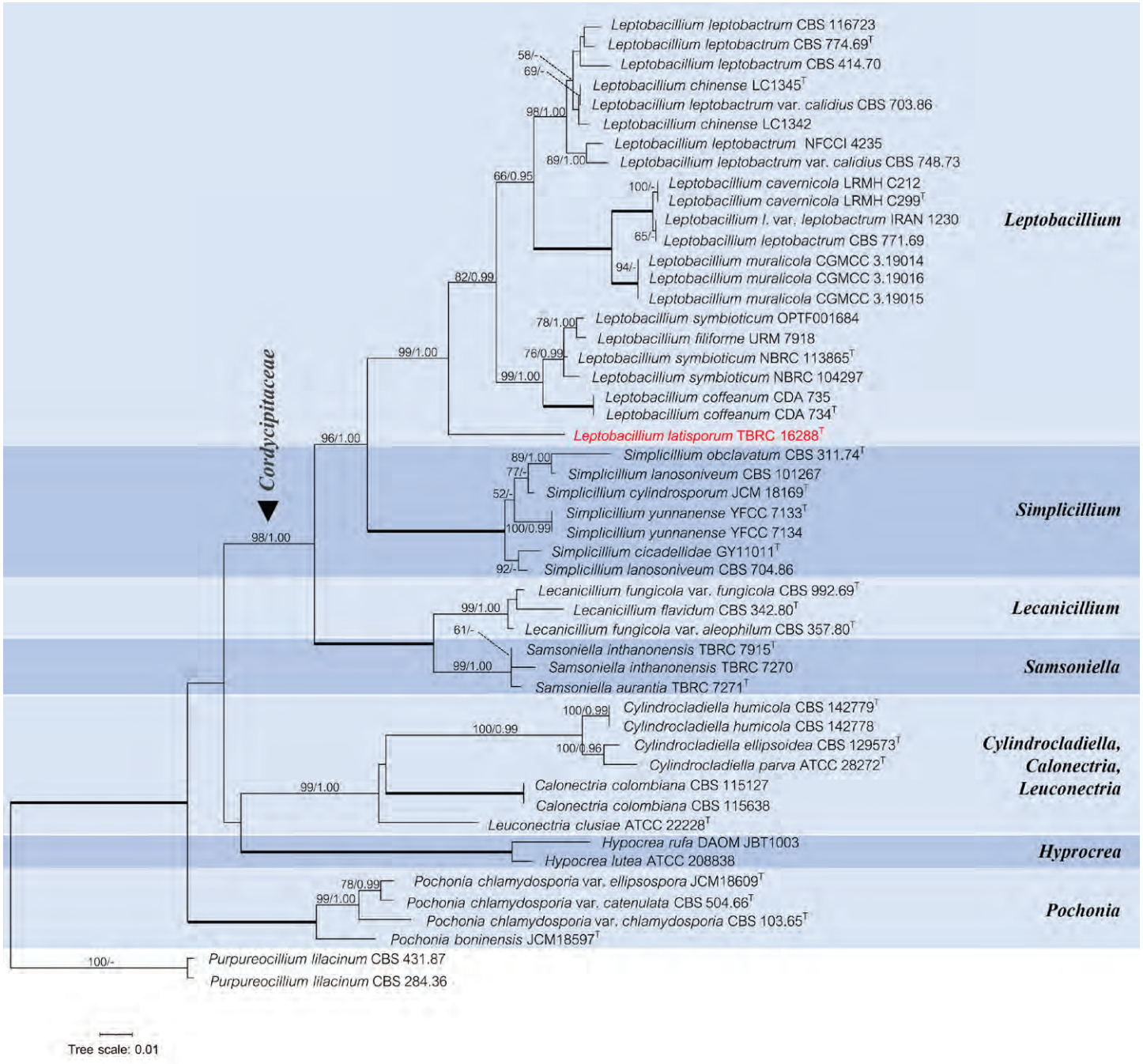

Fig. 10. RAxML phylogenetic tree of *Leptobacillium latisporum* (TBRC 16288) and related taxa resulting from the combined datasets of ITS, LSU and SSU sequences (48 ingroup taxa). Maximum likelihood bootstrap values (BSML, left) ≥ 50 % are shown at the nodes. Bayesian posterior probabilities (BYPP, right) ≥ 0.95 are given at the nodes. Highly supported nodes with 100 % bootstrap supports and with 1.00 posterior probabilities are shown as thick lines. Abbreviation: T = ex-holotype. Novel species is shown in red bold font.

Description: *Vegetative hyphae* hyaline, septate, 1.5–3.6 µm wide (n = 15). *Arthroconidia* formed from narrow hyphae, one-celled, hyaline smooth and thin-walled, cylindrical or short-cylindrical, straight, 4.2–9.4 × 2.4–4.5 µm (n = 30). *Chlamydospores* and *sexual morph* not observed.

Culture characteristics: Colonies after 14 d on: PDA attaining 35 mm diam, circular, flat, entire, more intense near the medium surface, velutinous and deep orange (6A8) to light yellow (4A5) at margin; reverse deep orange (6A8) to light yellow (4A5) at margin. On MEA attaining 25–30 mm diam, circular, flat, entire, velutinous, and dark orange (5A8) to pale yellow (4A3) at margin; reverse dark orange (5A8) to pale yellow (4A3) at margin. On OA attaining 30 mm diam, circular, flat, entire, woolly and brownish orange (5C5) to light yellow (4A4) at margin; reverse greyish orange (5B3). Sporulation within 9 wk on PDA.

Notes: Saccardo (1882) proposed *Malbranchea* with *M. pulchella* as the type species. The genus is characterised by alternate arthroconidia originating from vegetative hyphae in its asexual morph. In its sexual morph, it exhibits distinct features including orange to brown coloration, appendages, and/or spines. It forms gymnothecial ascomata, which are structures that enclose the reproductive organs. These ascomata have a prototunicate structure, meaning they consist of a single layer. Within the ascomata, the genus produces eight-spored inflated asci, which are sac-like structures. These asci contain globose to oblate ascospores that have a reticulate pattern on their

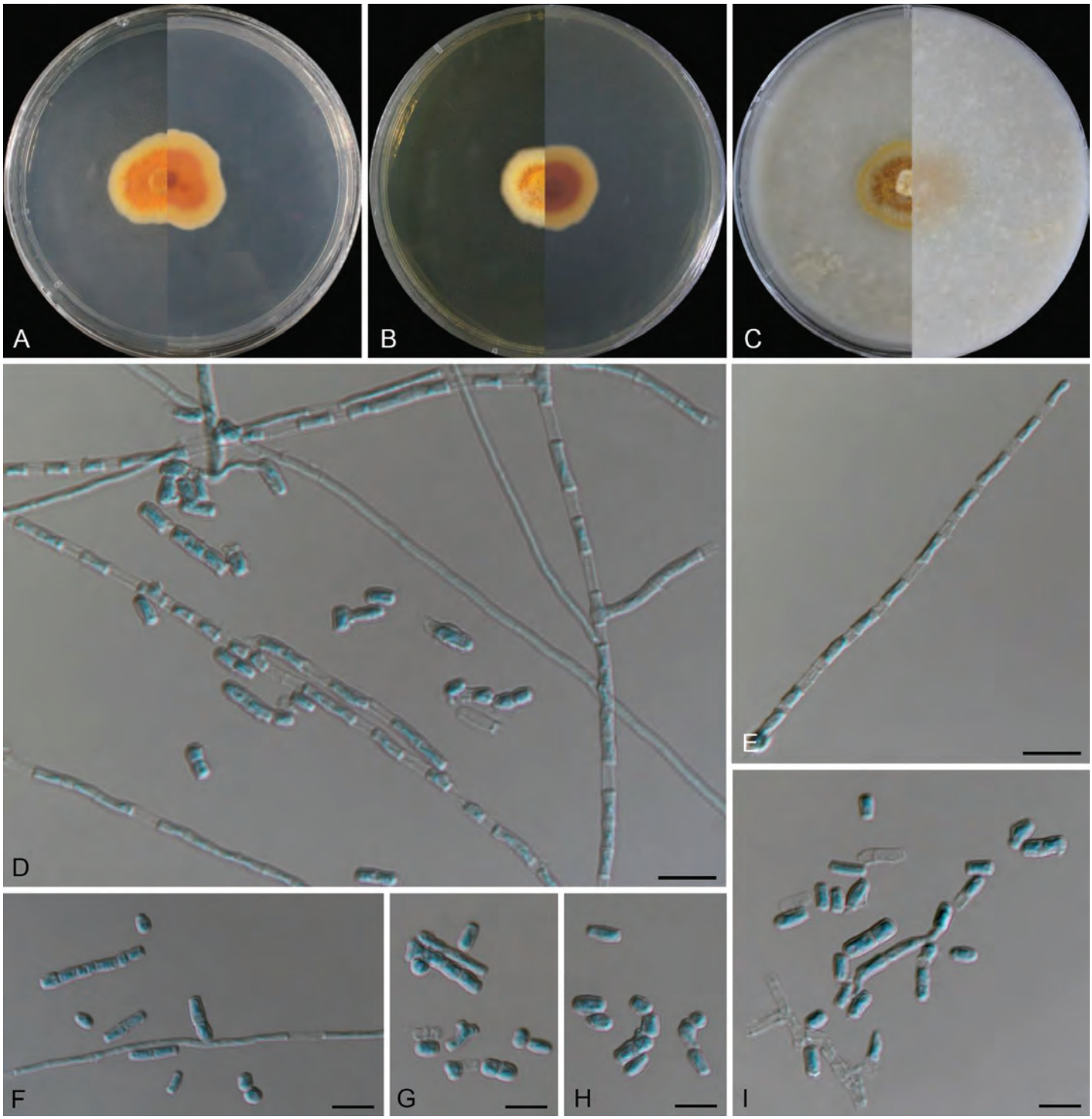

Fig. 11. *Malbranchea phuphaphetensis* (TBRC 16252). **A–C.** Obverse and reverse views of cultures on PDA, MEA 2 %, and OA after 14 d. **D, E.** Intercalary arthroconidia (arrow) along the fertile hyphae. **F–I.** Arthroconidia. Scale bars D, E = 5 µm; F–I = 10 µm.

surface. Based on indexfungorum.org (accessed 26 May 2023), 43 species are presently referred to the genus *Malbranchea*, and 42 species have sequences of at least one locus in GenBank. Phylogenetic analysis based on ITS, LSU, *BenA* and *TEF-1α* sequences showed that our isolate clustered within the genus *Malbranchea* (Fig. 12). The new taxon, *M. phuphaphetensis* is phylogenetically related to *M. ostraviensis*, which was originally described as *Auxarthron ostraviense* by Hubka *et al.* (2013), and *M. gymnoascoides* (Rodríguez-Andrade *et al.* 2021) (Fig. 12). The ITS barcode region of *M. phuphaphetensis* was compared with those of *M. ostraviensis* and *M. gymnoascoides*, and the results showed 416/459 = 92.37 % similarity with 8 substitutions and 414/459 = 92.16 % similarity with 9 substitutions, respectively. These species have similar orange shade of colony colour (Rodríguez-Andrade *et al.* 2021, Kandemir *et al.* 2022). However, *M. phuphaphetensis* has a much longer arthroconidium (4.2–19.4 × 2.4–4.5 µm) than *M. gymnoascoides* (1.5–2 × 6–10 µm) and *M. ostraviensis* (1.5–2.5 × 3.8–12.6 µm). Therefore, we propose *M. phuphaphetensis* as new species.

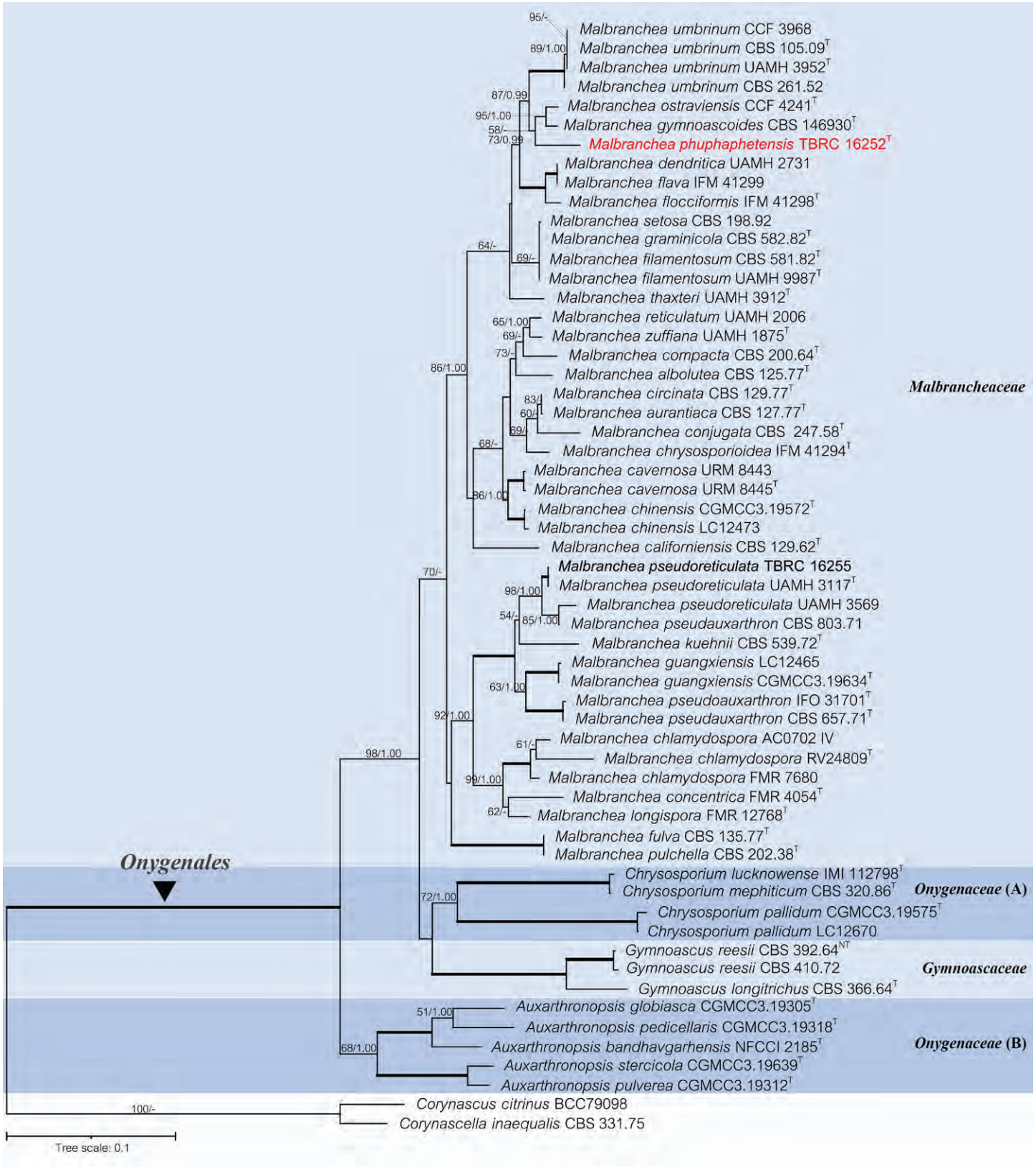

Fig. 12. RAxML phylogenetic tree of *Malbranchea phuphaphetensis* (TBRC 16252) and related taxa based on ITS, LSU, *BenA* and *TEF-1α* sequences (56 ingroup taxa). Maximum likelihood bootstrap values (BSML, left) ≥ 50 % are shown at the nodes. Bayesian posterior probabilities (BYPP, right) ≥ 0.95 are given at the nodes. Highly supported nodes with 100 % bootstrap supports and with 1.00 posterior probabilities are shown as thick lines. Abbreviations: T = ex-holotype; NT = ex-neotype. Novel species is shown in red bold font.

Scedosporium satunense C. Srihom, Preedanon, S. Saengkaewsuk & Somrith., ***sp. nov.*** MycoBank MB 846896. Fig. 13.

Etymology: "*satunense*" was named after the province from which this fungus was initially collected.

Typus: **Thailand**, Satun Province, Thung Wa District, Satun UNESCO Global Geopark, Le Stegodon Cave, 7°7'35"N 99°59'49"E, 107 m elevation, isolated from soil, Dec. 2019, coll. *N. Boonyuen, P. Srikitikulchai & S. Preedanon*, isol., *S. Preedanon*, *cultura dessicata*, (**holotype** BBH 49445; ex-type culture BCC 91803 = TBRC 16285 = NBTF

Fig. 13. *Scedosporium satunense* (TBRC 16285). **A, B.** Obverse and reverse views of cultures on PDA and CMA after 14 d. **C, E.** Conidiophores. **D, F.** Phialides with conidia. **G, H.** Conidia. Scale bars: D = 5 µm; C, E–H = 10 µm.

002291 = isolate CV00322). The GenBank accession numbers of ITS and *BenA* are OP856539 and OQ144974, respectively.

Classification: *Microascaceae, Microascales, Hypocreomycetidae, Sordariomycetes, Pezizomycotina, Ascomycota.*

Description: *Vegetative hyphae* hyaline to pale brown, septate, branched, smooth or slightly rough, hyphae 1.7–3.3 µm wide. *Conidiophores* macronematous, hyaline, solitary, frequently reduced to a single conidiogenous cell arising laterally from hypha, or forming short-stalked, penicilloid, 10.2–33.2 × 1.4–3.1 µm, bearing two or three conidiogenous cells at the top. *Conidiogenous cells* annellidic, hyaline, smooth and thin-walled, cylindrical, 3.8–14.7 × 1.7–3.2 µm. *Conidia* enteroblastic, one-celled, solitary, hyaline, ellipsoidal to cylindrical, 5.7–10.5 × 4.1–5.6 µm, brown, smooth and thick-walled. *Sexual morph* not observed.

Culture characteristics: Colonies after 14 d on: PDA attaining 60 mm diam, circular, umbonate, filiform, dense, felt, smooth with indistinct radial furrows and grey (1D1) to white (1A1) at the margin; reverse medium grey (1E1) to white (1A1) at margin. On CMA attaining 50 mm diam, circular, flat, filiform, aerial mycelia extremely sparse and greyish brown (5D3); reverse dark blond (5D4) to white (5A1) at margin. Sporulation within 6 wk on PDA.

Notes: The genus *Scedosporium*, designed by Sacc. ex Castell. & Chalm. (1919), includes saprobic fungi, with a few species

reported to cause disease in humans (de Hoog *et al.* 2000, Rainer & de Hoog 2006, Lackner *et al.* 2014, Abrantes *et al.* 2021). *Scedosporium* is characterised by cylindrical to flask-shaped and annellidic conidiogenous cells borne in solitary on the hyphae or in penicillate groups on the conidiophore. The genus is also reported to include the morphology of the pseudallescheria-like sexual morph, which is characterised by fusiform one-celled ascospores borne in an oval or spherical ascus inside the cleistothecia (Tapia 2012, Lackner *et al.* 2014). Molecular phylogeny usually assists in species separation (Gilgado *et al.* 2008, Lackner *et al.* 2012, Subedi & Chen 2015). In our findings, *S. satunense* clusters together with *S. americanum* (96 % ML bootstrap proportion and 1.00 Bayesian posterior probability) (Fig. 14). In particular, the ITS rDNA sequence of *S. satunense*

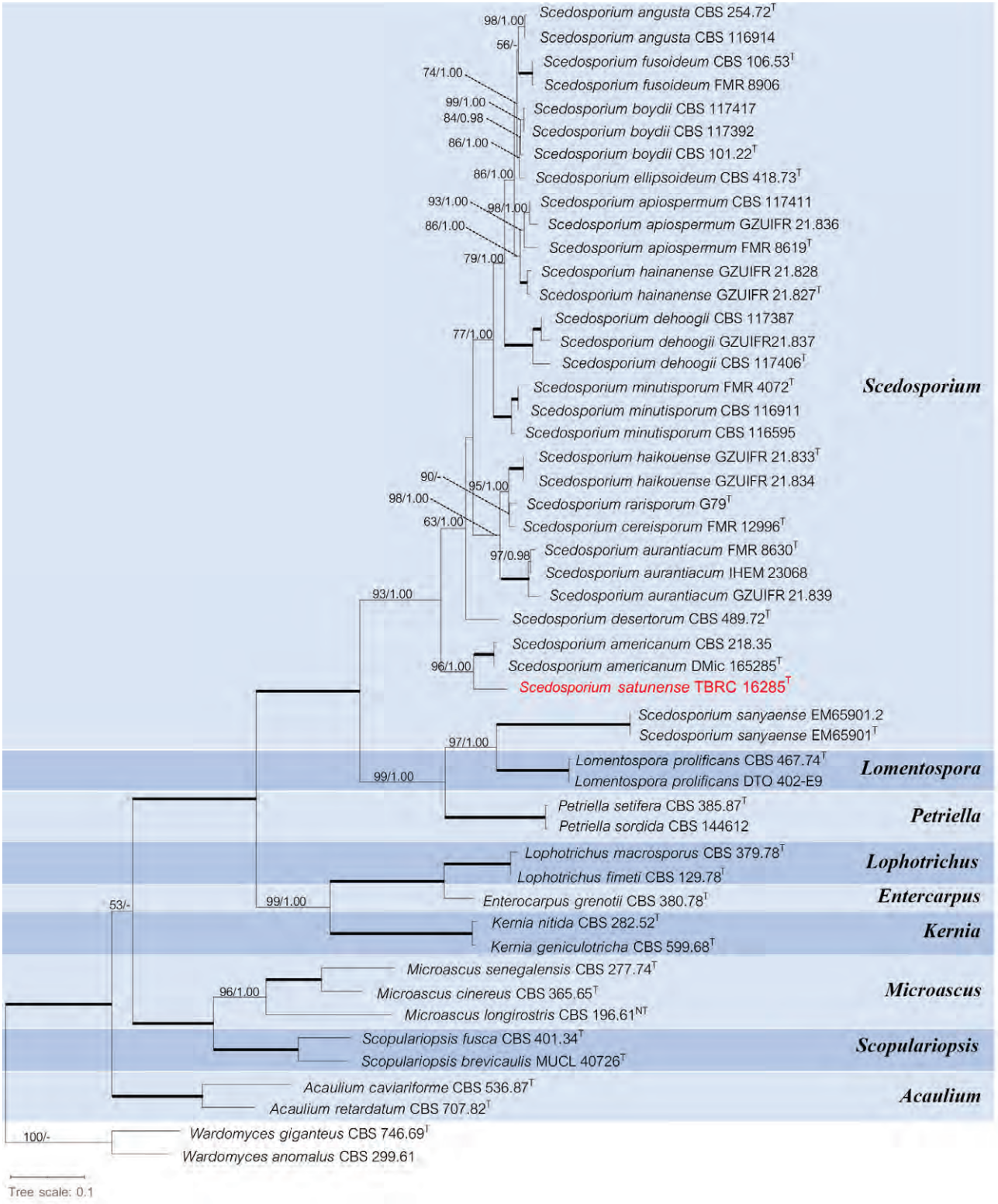

Fig. 14. The RAxML phylogenetic tree of *Scedosporium satunense* (TBRC 16285) and related taxa based on sequences at two loci (ITS and *BenA*) consists of 48 ingroup taxa. Maximum likelihood bootstrap values (BSML, left) ≥ 50 % are shown at the nodes. Bayesian posterior probabilities (BYPP, right) ≥ 0.95 are given at the nodes. Highly supported nodes with 100 % bootstrap supports and with 1.00 posterior probabilities are shown as thick lines. Abbreviations: T = ex-holotype; NT = ex-neotype. Novel species is shown in red bold font.

was compared with ITS rDNA sequences in *S. americanum* (CBS 218.35 and DMic 165285); the results showed 523/555 = 94.23 % similarity with no substitution and 530/556 = 95.32 % similarity with no substitution, respectively. Analysis of the *BenA* gene showed that there were base substitutions at multiple positions, resulting in 94.25 % similarity with nine substitutions. The new species differs from *S. americanum* in several aspects. For example, colonies of the new species are shades of white to grey and grow faster (reaching diameters of approximately 60 mm in 14 d), while those of *S. americanum* are brown to olive-brown and reach diameters of approximately 30 mm in 14 d (Abrantes *et al.* 2021). The conidia of *S. americanum* are ellipsoid to clavate and smaller (5.4–6.8 × 4.2–4.8 µm, Abrantes *et al.* 2021) than those of the new species, which are ellipsoid to oblong and slightly larger (5.8–10.5 × 4.1–5.6 µm). Additionally, synnemata are not present in *S. satunense*, while they are clearly observed in *S. americanum* (Abrantes *et al.* 2021). Both morphological and DNA sequence data support the distinction of *S. satunense* as a novel karst cave taxon in this study.

Sesquicillium cavernum C. Srihom, Preedanon, S. Saengkaewsuk & Somrith., ***sp. nov.*** MycoBank MB 846889. Fig. 15.

Etymology: "*cavernum*" in Latin means "cave" and refers to the habitat in which this species was first discovered.

Typus: **Thailand**, Satun Province, Thung Wa District, Satun UNESCO Global Geopark, Le Stegodon Cave, 7°7'35"N 99°59'49"E, 107 m elevation, isolated from shells of dead snails, Dec. 2019, coll. *N. Boonyuen, P. Srikitikulchai & S. Preedanon*, isol., *S. Preedanon*, *cultura dessicata* (**holotype** BBH 49441; ex-type culture BCC 91623 = TBRC 16268 = NBTF 002289 = isolate CV00218). The GenBank accession numbers of ITS, LSU, *TUB* and *TEF-1α* are OP856535, OP856525, OQ144971 and OQ116931, respectively.

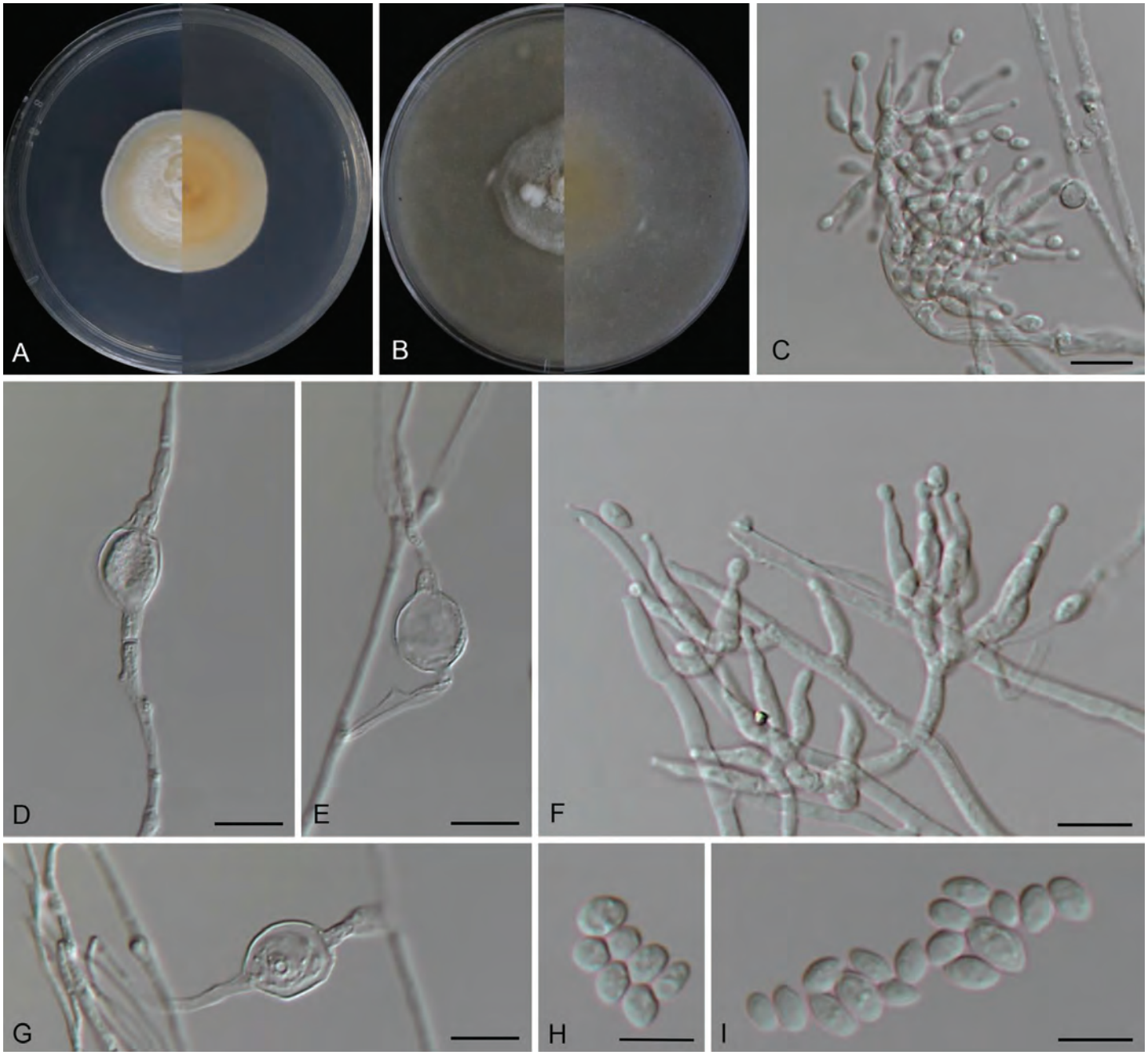

Fig. 15. *Sesquicillium cavernum* (TBRC 16268). **A, B.** Obverse and reverse views of cultures on PDA and OA after 14 d. **C, F.** Penicillate conidiophores with phialides and conidia. **D, E, G.** Chlamydospores. **H, I.** Conidia. Scale bars: C = 20 µm; D, E, G–I = 10 µm; F = 5 µm.

Classification: Bionectriaceae, Hypocreales, Hypocreomycetidae, Sordariomycetes, Pezizomycotina, Ascomycota.

Description: *Vegetative hyphae* hyaline to pale brown, septate, smooth, 1.2–3.2 µm wide. *Conidiophores* hyaline to pale brown, septate, short and solitary or penicillate branched; conidiophores from aerial hyphae were septate with dense phialides, 20.1 × 33–36 µm. *Phialides* subulate, tapering towards the apex, 10.2–12.5 µm long, 1.5–4 µm wide at the base, and 0.2–0.3 µm wide at the tip, intercalary phialides are rarely observed. *Conidia* enteroblastic, one-celled, solitary, hyaline, subglobose to broadly ellipsoidal, 3.9–6 × 2.3–4.6 µm, smooth and thick-walled. *Chlamydospores* solitary, hyaline, intercalary, broadly ellipsoidal, smooth, 6.0–7.5 × 5.0–6.3 µm wide. *Sexual morph* not observed.

Culture characteristics: After 14 d Colonies on PDA attaining 35 mm diam, circular, raised, entire, velvety, dense, delicate and orange, white (5A2) to white (5A1) at margin; reverse light orange (5A4) to orange, white (5A2) at the margin. On OA attaining 45–55 mm diam, circular, umbonate, entire, mycelia extremely tufted at the centre, margin annular and white (3A1); reverse yellowish white (3A2). Sporulation within 6 wk on PDA.

Notes: *Sesquicillium* was erected by Gams (1968). Recently, Zhao *et al.* (2023) revealed that *Clonostachys* and *Sesquicillium* are closely related and constitute sister clades based on multiple gene phylogenetic analyses. Furthermore, some species of *Clonostachys* were allocated to *Sesquicillium* when the genus was revised. Morphologically, there is little differentiation of the asexual morphs (*i.e.*, penicillium-, verticillium-, gliocladium-, or acremonium-like conidiophores) among the species; thus, molecular phylogeny is usually employed for species identification (Corda 1839, Moreira *et al.* 2016, Rossman *et al.* 2013, Torcato *et al.* 2020, Zeng & Zhuang 2022, Zhao *et al.* 2023). In this study, *S. cavernum* was found to be distantly related to *S. candelabrum* (originally *Verticillium candelabrum* according to Bonorden 1851) and *S. rossmaniae* with BSML = 71 % and BYPP = 1.00 (Fig. 16). *Sesquicillium cavernum* differs from those two species in having relatively wider conidia (3.9–6 × 2.3–4.6 µm in *S. cavernum vs*. 3–5.5 × 1.8–3.4 µm in *S. candelabrum* and 4.2–6.6 × 2–2.8 µm in *S. rossmaniae*). The morpho-phylogenetic evidence presented here allow us to describe *S. cavernum* as a new species that occurs on shells of dead snails inside a cave in Thailand.

Thelonectria satunensis Chuaseehar., Nuankaew, Preedanon & Somrith., ***sp. nov.*** MycoBank MB 846893. Fig. 17.

Etymology: "*satunensis*" meaning "derived from Satun", the province in which this fungus was first discovered.

Typus: **Thailand**, Satun Province, Manang District, Satun UNESCO Global Geopark, Phu Pha Phet Cave, 7°7'25"N 99°47'54"E, 21 m elevation, airborne, Dec. 2019, coll. *N. Boonyuen, P. Srikitikulchai & S. Preedanon*, isol., *S. Preedanon, cultura dessicata* (**holotype** BBH 49443; ex-type culture BCC 91755 = TBRC 16275 = NBTF 002337 = isolate CV00255). The GenBank accession numbers of *ACT*, ITS, LSU, *RPB1*, *TEF-1α* and *TUB* are OQ116938, OP856537, OP856527, OQ076387, OQ116932, and OQ144972, respectively.

Classification: *Nectriaceae, Hypocreales, Hypocreomycetidae, Sordariomycetes, Pezizomycotina, Ascomycota.*

Description: *Ascomata* on 1/4-strength PDA after 30 d perithecial, solitary to gregarious, up to five in a group, superficial, sometimes immersed in agar medium or with the base immersed in agar medium on a minute stroma, pyriform to subglobose, papillate, yellowish-brown to brown, no colour change in 3 % KOH or 100 % lactic acid, 350–500 × 350–370 µm (n = 10). *Perithecial surface* smooth or slightly roughened. *Perithecial wall* lacking a definite outline, appearing to be intertwined hyphae with angular cells and flattened fusoid cells, 29–39 µm thick. *Asci* unitunicate, cylindrical to clavate, 8-spored, 57–88 × 10–13 µm (n = 30), with a refractive ring at the apex. *Ascospores* uniseriate, ellipsoid, finely spinulose, 1-septate, symmetrically two-celled, initially hyaline, becoming pale brown at maturity, 10–17.5 × 7.5 µm (n = 30). *Asexual morph*: *Mycelia* smooth, branched, septate, hyaline hyphae, pale brown, and 1.5–4.5 µm in diam. *Conidiophores* arising laterally from hyphae, unbranched to diverticillate branched, septate, 19–33 × 2.5–4.5 µm (n = 10). *Phialides* cylindrical or ampulliform, borne solitary or apically on irregularly branching clusters of cells or directly from hyphae, 7–18 × 2.5–4.5 µm (n = 10), with periclinal thickening and collarette. *Conidia* hyaline, slimy droplets on aerial mycelium or arising from the agar surface. *Macroconidia* cylindrical or falcate, curved, rounded on both ends, smooth, 3–5-septate, hyaline, 27.5–45 × 7.5–10 µm (n = 30). *Chlamydospores* and *microconidia* not observed.

Culture characteristics: Colonies after 21 d on: PDA reaching 64–69 mm diam, irregular, raised, margins curled, mycelia white, floccose; sporulation absent, soluble pigment absent, exudates absent; reverse yellowish white (1A2) with margins white. On 1/4-strength PDA attaining 55–56 mm diam, irregular, flat, margins curled, mycelia white with centre yellowish brown (5D8), mostly glabrous surface with sparsely aerial hyphae; sporulation producing asexual morph moderately and ascomata sparsely after 30 d of incubation, conidia in mas white, soluble pigment absent, exudates absent; reverse white with centre yellowish brown (5D8).

Notes: *Thelonectria,* previously placed in the genus *Neonectria,* is a recently established genus of common and ubiquitous fungi that is found on living and decaying woody substrates, soil, other fungi, and insects (Salgado-Salazar *et al.* 2012, Zeng & Zhuang 2019, Crous *et al.* 2022b, Zeng & Zhuang 2022). In the phylogenetic analysis, *T. satunensis* grouped as a separate clade with *T. asiatica*, *T. brayfordii*, *T. conchyliata*, *T. discophora*, *T. guangdongensis*, *T. japonica*, *T. lucida*, *T. mammoidea*, *T. ostrina*, *T. phoenicea*, *T. pinea*, *T. porphyria*, *T. purpurea*, *T. rubi*, *T. sinensis* and *T. yunnanica*. In the phylogenetic analysis, placement of this new species in a major clade in the *Nectriaceae* (*Hypocreales*) was strongly supported with 100 % ML bootstrap and 1.00 BI posterior probabilities. In this study, *T. satunensis* is well separated from the other species, with a number of nucleotide base substitutions in *ACT* (97.40–97.77 %), ITS (93.80–94.60 %), LSU (97.89–98.26 %), *RPB1* (89.37–90 %), *TEF-1α* (92.67–94.11 %), and *TUB* (91.98–92.75 %), as shown in Fig. 18. Among the known phylogenetically related species, *T. satunensis* is morphologically similar to *T. ostrina* and *T. porphyria*; these three species share papillate perithecia and 3–5-septate macroconidia (Salgado-Salazar *et al.* 2015). However, *T. satunensis* differs from

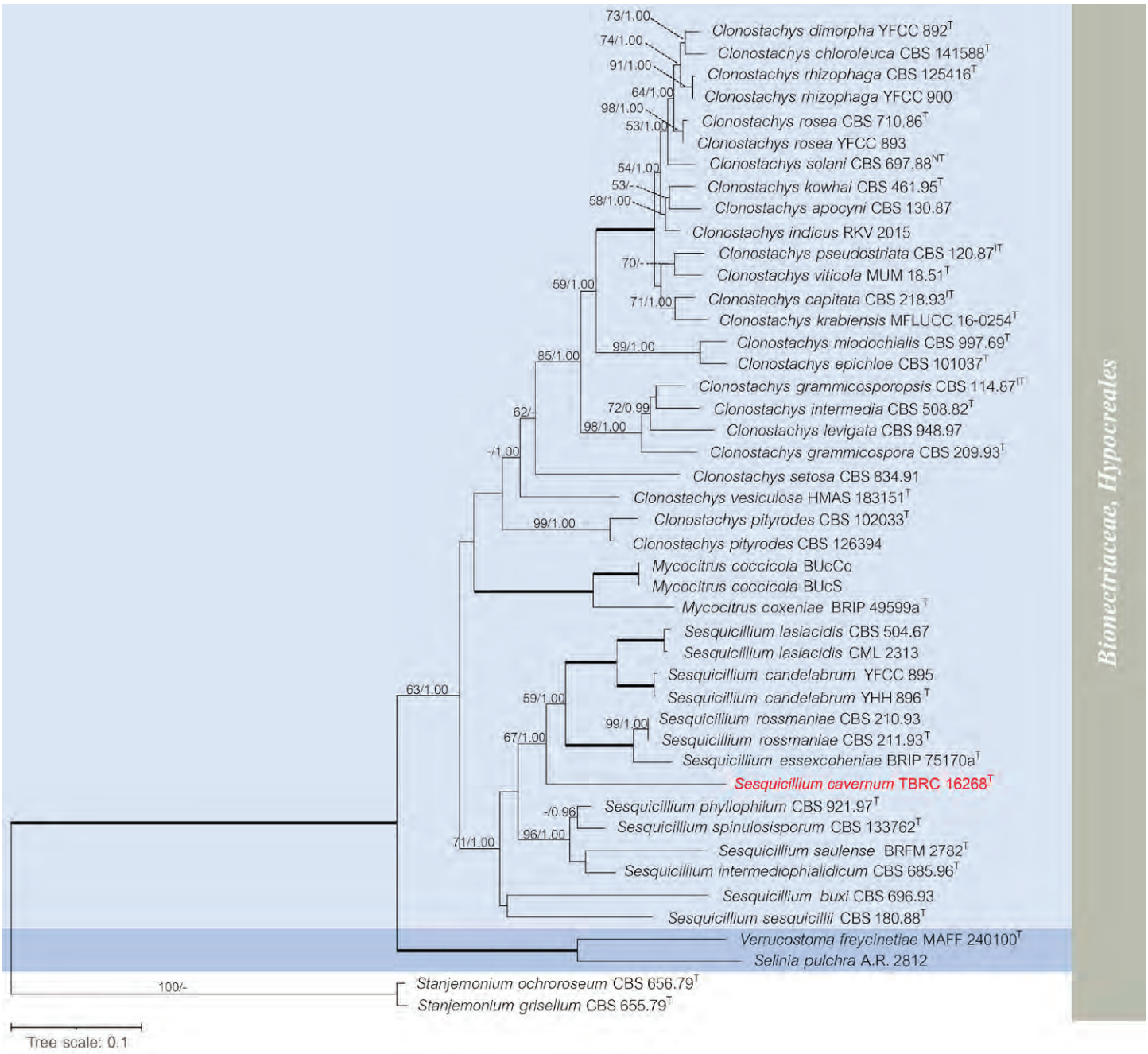

Fig. 16. The RAxML phylogenetic tree of *Sesquicillium cavernum* (TBRC 16268) and related taxa based on sequences at four loci (ITS, LSU, *TUB* and *TEF-1α*) consists of 43 ingroup taxa. Maximum likelihood bootstrap (BSML, left) values ≥ 50 % are shown. Bayesian posterior probabilities (BYPP, right) ≥ 0.95 are given at the nodes. Highly supported nodes with 100 % bootstrap supports and with 1.00 posterior probabilities are shown as thick lines. Abbreviations: T = ex-holotype; IT = ex-isotype; NT = ex-neotype. Novel species is shown in red bold font.

those two species in forming white colonies and having shorter macroconidia (27.5–45 × 7.5–10 µm), while *T. ostrina* and *T. porphyria* form purple colonies and have longer conidia (40–108 × 5–9 µm in *T. ostrina* and 42.5–88.5 × 4.5–7.5 µm in *T. porphyria*; Salgado-Salazar *et al.* 2015). Thus, *T. satunensis* is newly introduced on the basis of its morphological characteristics and on DNA sequence analysis of combined datasets of its *ACT*, ITS, LSU, *RPB1, TEF-1α* and *TUB* sequences.

Umbelopsis satunensis C. Srihom, Preedanon, S. Saengkaewsuk & Somrith., ***sp. nov.*** MycoBank MB 846888. Fig. 19.

Etymology: *"satunensis"* refers to "Satun province", from which the ex-type strain was collected.

Typus: **Thailand**, Satun Province, Thung Wa District, Satun UNESCO Global Geopark, Le Stegodon Cave, 7°7'35"N 99°59'49"E, 107 m elevation, isolated from shells of dead snails, Dec. 2019, coll. *N. Boonyuen, P. Srikitikulchai & S. Preedanon*, isol., *S. Preedanon*, *cultura dessicata*, (**holotype** BBH 49440; ex-type culture BCC 91926 = TBRC 16254 = NBTF 002286 = isolate CV00129). The GenBank accession numbers of SSU, ITS, LSU and *ACT* are OP856533, OP856524, OP850836 and OQ116937, respectively.

Classification: Umbelopsidaceae, Umbelopsidales, Incertae sedis, Umbelopsidomycetes, Mucoromycotina, Mucoromycota.

Description: *Vegetative hyphae*, smooth, hyaline 1.2–3.6 µm (n = 15) wide, *Sporangiophores* developing from abundant aerial

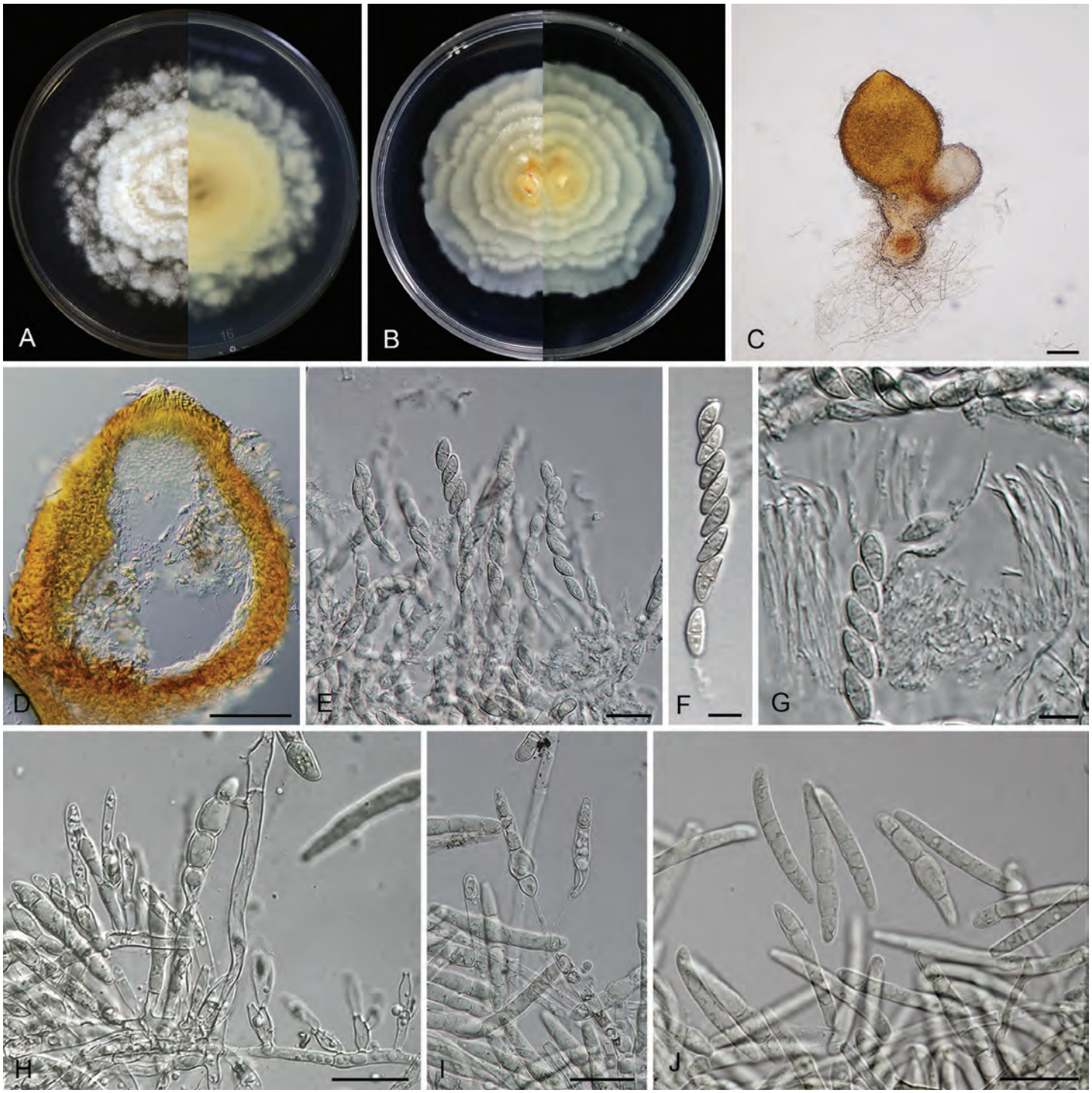

Fig. 17. *Thelonectria satunensis* (TBRC 16275). **A, B.** Obverse and reverse views of cultures on PDA and 1/4–strength PDA after 21 d. **C.** Perithecia produced on 1/4–strength PDA. **D.** Longitudinal section of perithecium. **E, F.** Asci and ascospores. **G.** Periphyses and asci with ascospores. **H.** Conidiophores, phialides and macroconidia. **I, J.** Macroconidia. Scale bars: C, D = 100 µm; E, H–J = 20 µm; F, G = 10 µm.

hyphae, hyaline, smooth, with compactly sympodial branching from slightly swollen stalks, 2.2–4 µm wide, up to 125 µm long. *Sporangia* at tips of sporangiophores globose, thin-walled and double-layered, 22.7–34 µm in diam. *Sporangiospores* smooth, angular, 3.6–4.0 × 3.3–3.9 µm in diam (n = 30). *Chlamydospores* hyaline, smooth, globose to subglobose, 6.3–6.8 × 6.5–6.9 µm in diam. *Zygospores* not observed.

Culture characteristics: Colonies after 14 d on: PDA attaining 75 mm diam, circular, flat, entire, more intense near the medium surface, sparse, butter-like and vivid yellow (3A8) to yellowish white (3A2) at margin; reverse vivid yellow (3A8) to yellowish white (3A2). On MEA attaining 75 mm diam, circular, flat, entire, more intense near the medium surface, membranous and pale yellow (3A3) to yellowish white (3A2); reverse yellowish white (3A2). On CMA attaining 85 mm diam, circular, flat, entire, more intense near the medium surface, membranous, butter-like and pale yellow (3A3); reverse pale yellow (3A3). Sporulation within 6 wk on PDA.

Notes: *Umbelopsis* (*Umbelopsidaceae, Umbelopsidales, Mucoromycota*) was initially described by Amos & Barnett

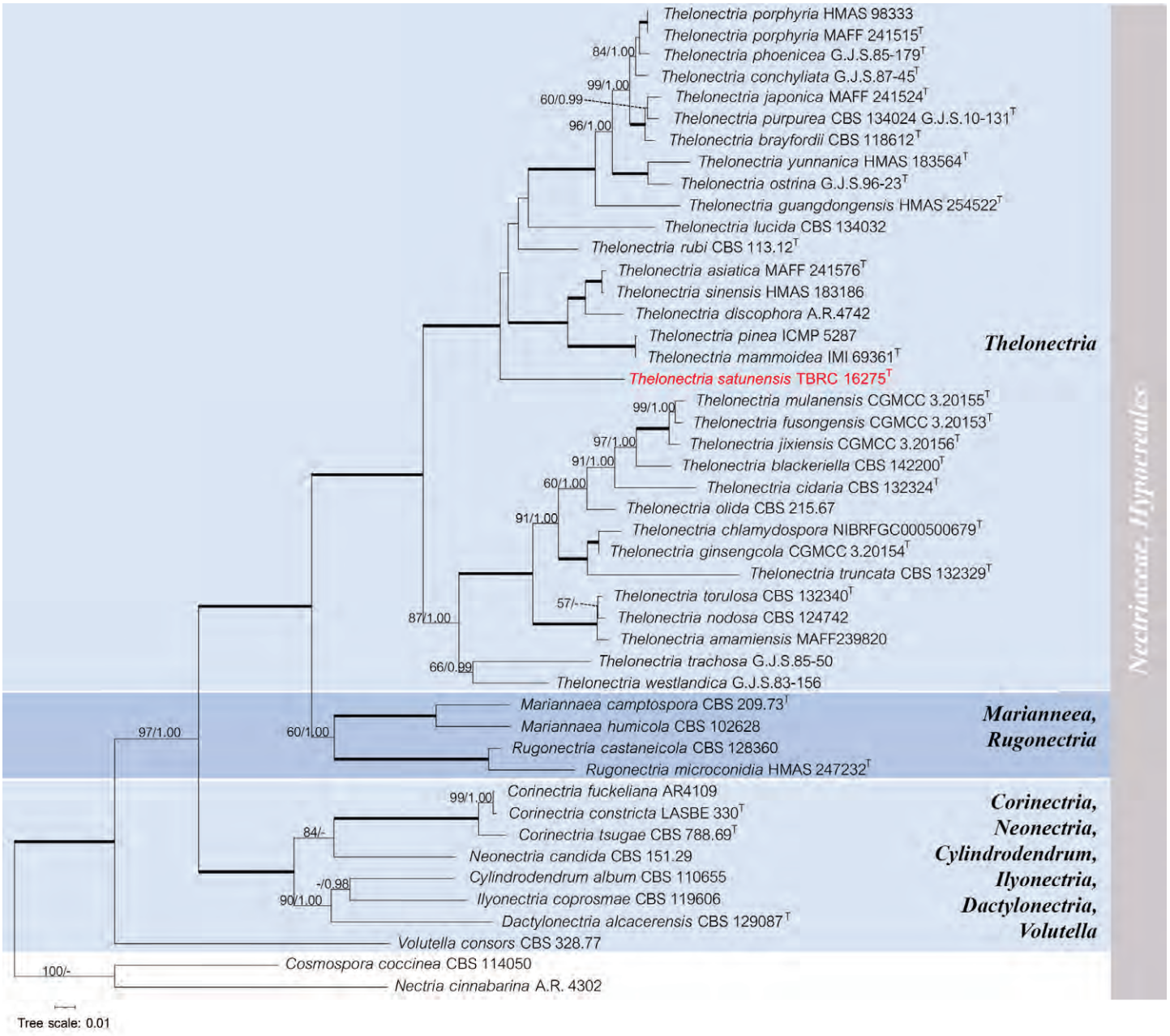

Fig. 18. The RAxML phylogenetic tree of *Thelonectria satunensis* (TBRC 16275) and related taxa based on the sequences from six loci (*ACT*, ITS, LSU, *RPB1*, *TEF-1α* and *TUB*) consisting of 44 ingroup taxa. Maximum likelihood bootstrap values (BSML, left) ≥ 50 % are shown at the nodes. Bayesian posterior probabilities (BYPP, right) ≥ 0.95 are given at the nodes. Highly supported nodes with 100 % bootstrap supports and with 1.00 posterior probabilities are shown as thick lines. Abbreviations: T = ex-holotype. Novel species is shown in red bold font.

(1966) with *U. versiformis* as type species. The MycoBank database currently recognises 25 species in this genus (https://www.mycobank.org, accessed 26 May 2023). Environmentally, *Umbelopsis* species are a common and important constituent of forest soils (Domsch *et al.* 1980, Parshikov *et al.* 1999, Summerbell 2005, Wang *et al.* 2015, Ikeda *et al.* 2016).

Based on phylogenetic analysis (Fig. 20), *Umbelopsis satunensis* is well placed in the genus *Umbelopsis* and forms a sister clade with *U. dura*, *U. macrospora* and *U. oblongielliptica.* These three species share morphological characteristics in that they lack vesicles from which the sporangiophores develop. However, *U. satunensis* differs markedly in that it produces spores that are angular in shape, while the spores of *U. macrospora* and *U. oblongielliptica* are oblong-ellipsoidal, and those of *U. dura* are ovoid. *Umbelopsis satunensis* is further distinguished from other species in this genus by the relatively larger sizes of its sporangium and sporangiospores. The spores of *U. satunensis* are up to 7 µm diam, while the spores of *U. dura*, *U. macrospora* and *U. oblongielliptica* range from 2.8 to 5 µm in length and 1.6 to 2.8 µm in width. In addition, based on DNA sequence *U. satunensis* differs from other related species like *U. dura, U. macrospora* and *U. oblongielliptica* sequences in that it displays a number of nucleotide base substitutions in SSU (99.43–99.52 %), ITS (94.83–95.16 %), LSU (98.62–99.04 %), and *ACT* (95.37–95.87 %).

DISCUSSION

Our research on cave-dwelling fungi in the Satun UNESCO Global Geopark in southern Thailand revealed eight new species which are described in this study (*Ascomycota* and

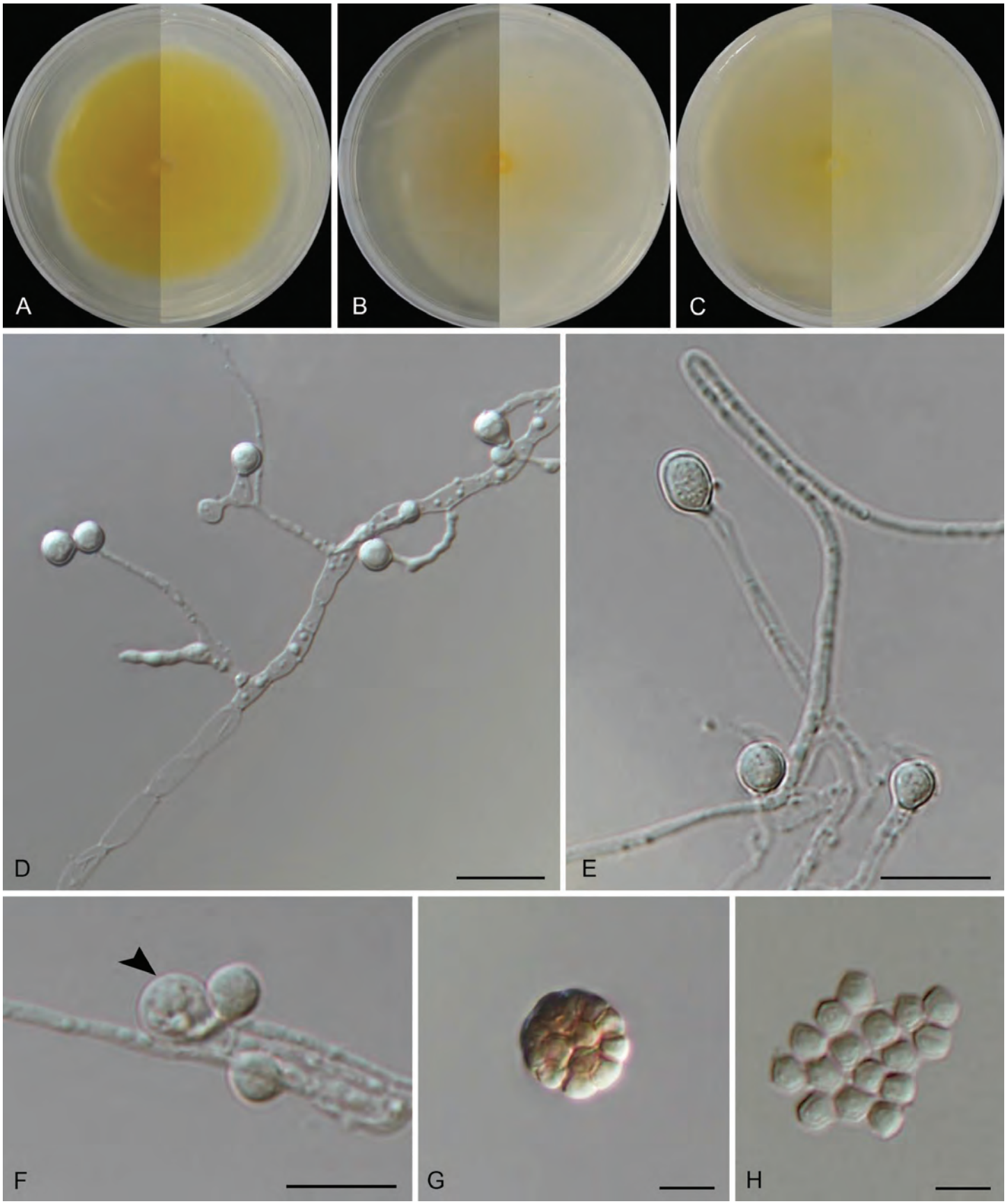

Fig. 19. *Umbelopsis satunensis* (TBRC 16254). **A–C.** Obverse and reverse views of cultures on PDA, MEA 2 %, and CMA after 14 d. **D.** Chlamydospores. **E, F**. Immature sporangia with sporangiospores (arrow). **G.** Mature sporangium with angular sporangiospores. **H.** Sporangiospores in the angular shape. Scale bars: D–F = 20 µm; G, H = 10 µm.

Mucoromycota). Approximately 1 600 species of fungi have been recorded from caves worldwide (Vanderwolf *et al.* 2013, Jiang *et al.* 2017, Zhang *et al.* 2017, 2020, Visagie *et al.* 2021); the most species-rich phylum is *Ascomycota*, followed by *Basidiomycota* and *Mucoromycota*. The common genera belonging to the *Ascomycota* are mostly cosmopolitan, *i.e.*,

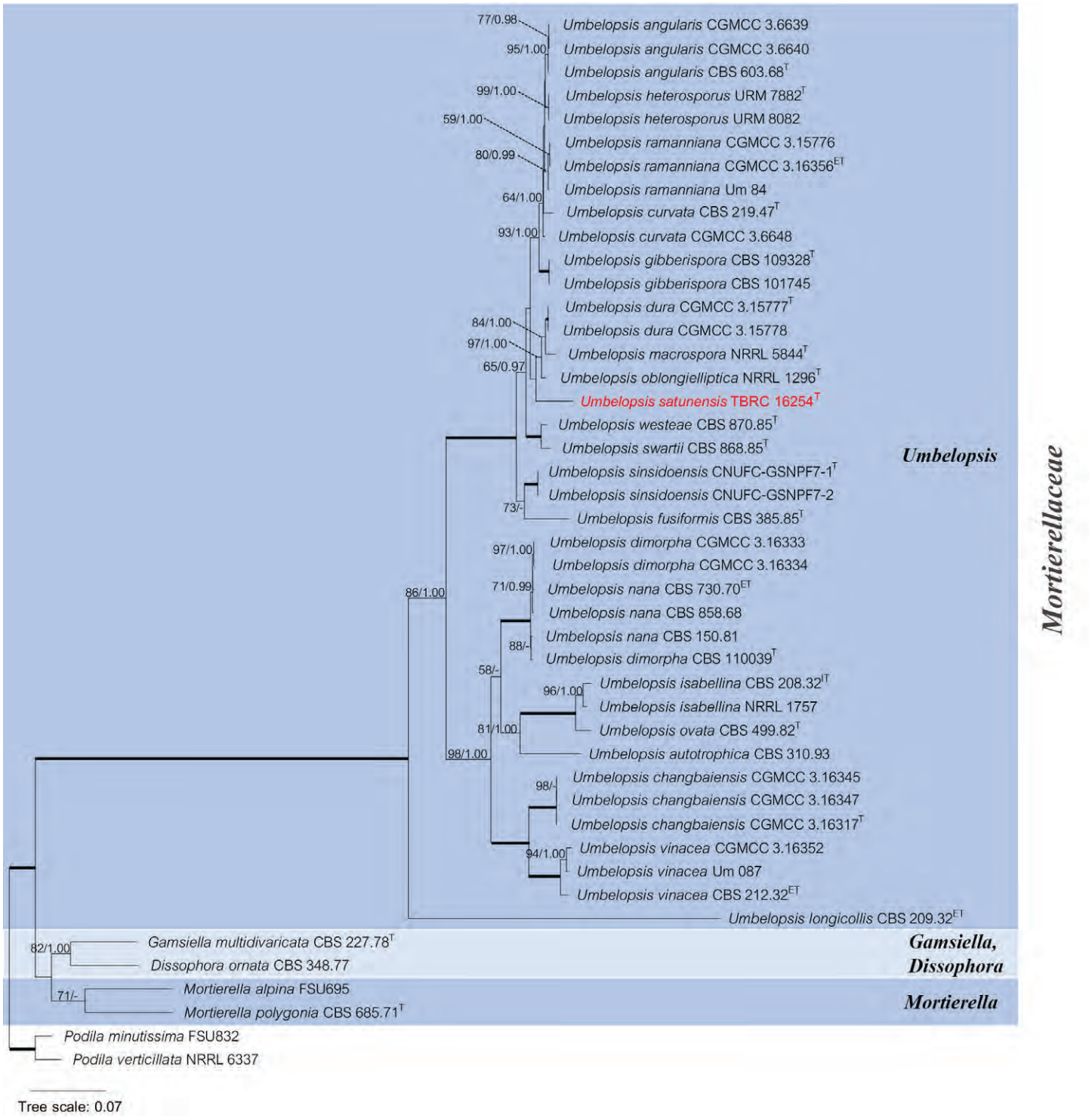

Fig. 20. RAxML phylogenetic tree of *Umbelopsis satunensis* (TBRC 16254) and related taxa based on sequences from four loci (SSU, ITS, LSU and *ACT*) consisting of 43 ingroup taxa. Maximum likelihood bootstrap values (BSML, left) ≥ 50 % are shown at the nodes. Bayesian posterior probabilities (BYPP, right) ≥ 0.95 are given at the nodes. Highly supported nodes with 100 % bootstrap supports and with 1.00 posterior probabilities are shown as thick lines. Abbreviations: T = ex-holotype; ET = ex-epitype; IT = ex-isotype. Novel species is shown in red bold font.

Aspergillus, Penicillium, Fusarium and *Trichoderma* (Vanderwolf *et al.* 2013, Cunha *et al.* 2020, Zhang *et al.* 2021, Wasti *et al.* 2021); these genera were found in various substrates/hosts in caves (Raudabaugh *et al.* 2021, Martin-Pozas *et al.* 2022, Ogórek *et al.* 2022, Zalar *et al.* 2022). Three recent studies investigated cave fungi in China (Jiang *et al.* 2017, Zhang *et al.* 2017, 2021), and reported three, 20, and 33 novel species, respectively. In parallel investigations, such as those undertaken within Brazilian cave systems by Alves *et al.* (2022), *Pseudolecanicillium* was delineated as a new genus within the *Cordycipitaceae.* Concurrently, six new species were discovered from sediments and atmospheric samples: *Aspergillus lebretii, Malbranchea cavernosa, Pseudohumicola cecavii, Pseudolecanicillium caatingaense, Talaromyces cavernicola,* and *Tritirachium brasiliense.* Additionally, through morphological and multi-locus phylogenetic examinations, fungi were identified in association with bat flies in a Caatinga dry forest cave in Brazil. This analysis resulted in the description of two new species: *Allophoma*

brasiliensis and *Pyrenochaetopsis cecavii* as reported by Carvalho *et al.* (2022). A number of studies have explored the diversity of fungi found in caves during 2020–2022; the results of these studies indicated high species diversity and demonstrated the presence of many new fungal taxa obtained from several hosts/substrates in caves in various parts of the world (Karunarathna *et al.* 2020, Takashima *et al.* 2020, Crous *et al.* 2020, Liu *et al.* 2021, Leplat *et al.* 2021, 2022, Pereira *et al.* 2022, Visagie *et al.* 2022). The description of these new species highlights the need for further research and documentation of the mycobiota that live in this environment. This study adds to our knowledge of the fungi that exist in harsh cave environments and highlights the importance of sustainable conservation and exploitation of these resources. Future research, including the integration of omics technologies (metagenomics) and culture-independent techniques, has the potential to deepen our understanding of the ecology of these fungi and their ecological functions within karst caves. This knowledge will be essential in identifying how cave microbiomes respond to increased human presence, establishing effective management practices, and implementing methods for restoring cave microbiomes affected by tourism in the Satun UNESCO Global Geopark.

ACKNOWLEDGEMENTS

This research was jointly supported by the RDI Management for National Strategic and Network Division–NSTDA under research grant number P1951709 as part of the project titled "Diversity of rock-dwelling microbes in Satun UNESCO Global Geopark". Scientific and English editing services related to this work were partially supported by the integrated technology platform, NSTDA (P1952580). Lei Cai wishes to express appreciation to the CAS-NSTDA Joint Research Program (NO. 153211KYSB20200039). We wish to thank Theerayut Toojinda, Sissades Tongsima and Wonnop Visessanguan for their support with fungal research at BIOTEC (NSTDA). We acknowledge Rungsima Tantalakha at RDI Management for National Strategic and Network Division for coordinating for this research on a collaboration between Thailand and China based on BIOTEC, NBT, and IMCAS (Institute of Microbiology, Chinese Academy of Sciences). We thank Lily Eurwilaichitr and Supawadee Ingsriswang for their contributions to the Thailand-China Joint Laboratory on Microbial Biotechnology under the collaboration between TBRC (BIOTEC) and CGMCC. We are grateful to Bumrungrat Ploydam and Narongrit Thungprue (the Khao Banthat Wildlife Sanctuary and the Satun Geopark Network) for permission to collect samples at Phu Pha Phet and Le Stegodon Caves. Chaiyaporn Siripornpibul, Kittapha Malimart and Umapon Chareonkunnatum are thank for their help with fungal collection in two caves. The authors are deeply grateful for pre-submission comments and suggestions provided by Jennifer Luangsa-ard (BIOTEC-NSTDA). Additional special thanks are also given to the editors and anonymous reviewers for their constructive comments on the manuscript. We would like to express our gratitude to the corresponding editor, Pedro W. Crous, and to Lin Zhao for their indispensable assistance in creating a phylogenetic tree using ITS, LSU, and *TEF1* data for the new species, *Sesquicillium cavernum.*

Conflict of interest: The authors declare that there is no conflict of interest.

REFERENCES

Abrantes RA, Refojo N, Hevia AI, *et al.* (2021). *Scedosporium* spp. from clinical setting in Argentina, with the proposal of the new pathogenic species *Scedosporium americanum*. *Journal of Fungi* **7**: 160.

Amos RE, Barnett HL (1966). *Umbelopsis versiformis*, a new genus and species of the Imperfects. *Mycologia* **58**: 805–808.

Alves VCS, Lira RA, Lima JMS, Barbosa RN, Bento DM, Barbier E, Bernard E, Souza-Motta CM, Bezerra JDP (2022). Unravelling the fungal darkness in a tropical cave: richness and the description of one new genus and six new species. *Fungal Systematics and Evolution* **10**: 139–167.

Bánki O, Roskov Y, Vandepitte L, *et al*. (2021). Catalogue of Life Checklist. *Catalogue of Life*. 10.48580/d4t2

Bastian F, Jurado V, Nováková A, *et al.* (2010). The microbiology of Lascaux Cave. *Microbiology* **156**: 644–652.

Becker K, Lambert C, Wieschhaus J, *et al.* (2020). Phylogenetic assignment of the fungicolous *Hypoxylon invadens* (*Ascomycota, Xylariales*) and investigation of its secondary metabolites. *Microorganisms* **8**: 1–14.

Belyagoubi L, Belyagoubi-Benhammou N, Jurado V, *et al.* (2018). Antimicrobial activities of culturable microorganisms (actinomycetes and fungi) isolated from Chaabe Cave, Algeria. *International Journal of Speleology* **47**: 189–199.

Bercea S, Năstase-Bucur R, Mirea IC, *et al*. (2018). Novel approach to microbiological air monitoring in show caves. *Aerobiologia* **34**: 445–468.

Boblitt CM, Plotnick RE, Kenig F, *et al*. (2018). Determining taphonomic controls and rates of decay in cave environments using microcosms. *Palaios* **33**: 141–153.

Bonorden HF (1851). *Handbuch der allgemeinen Mykologie*. Stuttgart, Schweizerbart.

Boonyuen N, Chuaseeharonnachai C, Suetrong S, *et al.* (2011). *Savoryellales* (*Hypocreomycetidae, Sordariomycetes*): A novel lineage of aquatic ascomycetes inferred from multiple-gene phylogenies of the genera *Ascotaiwania*, *Ascothailandia*, and *Savoryella*. *Mycologia* **103**: 1351–1371.

Boonyuen N, Chuaseeharonnachai C, Nuankaew S, *et al*. (2021). Novelties in *Fuscosporellaceae* (*Fuscosporellales*): Two new *Parafuscosporella* from Thailand revealed by morphology and phylogenetic analyses. *Diversity* **13**: 517.

Brad T, Itcus C, Pascu MD, *et al*. (2018). Fungi in perennial ice from Scărişoara Ice Cave (Romania). *Scientific Reports* **8**: 10096.

Bulliard P (1791). *Histoire des champignons de la France, ou traité élémentaire. renfermant dans un ordre méthodique les descriptions et les figures des champignons qui croissent naturellement en France.* Imprimerie de la Société typographique (Paris).

Carbone I, Kohn LM (1999). A method for designing primer sets for speciation studies in filamentous ascomycetes. *Mycologia* **91**: 553–556.

Carvalho JLVR, Lima JMS, Barbier E, *et al.* (2022). Ticket to ride: Fungi from bat ectoparasites in a tropical cave and the description of two new species. *Brazilian Journal of Microbiology* **53**: 2077–2091.

Castellani A, Chalmers AJ (1919). *Manual of Tropical Medicine*. Baillière, Tindall and Cox, UK.

Castlebury LA, Rossman AY, Sung GH, *et al.* (2004). Multigene phylogeny reveals new lineage for *Stachybotrys chartarum*, the indoor air fungus. *Mycological Research* **108**: 864–872.

Cedeño-Sanchez M, Charria-Girón E, Lambert C, *et al*. (2023). Segregation of the genus *Parahypoxylon* (*Hypoxylaceae, Xylariales*) from *Hypoxylon* by a polyphasic taxonomic approach. *MycoKeys* **95**: 131–162.

Chalabuda TV (1968). Systemica familiae *Mortierella*. *Novosti Sistematiki Nizshikh Rastenii* **5**: 120–131.

Chao A, Gotelli NJ, Hsieh TC, *et al.* (2014). Rarefaction and extrapolation with Hill numbers: a framework for sampling and estimation in species diversity studies. *Ecological Monographs* **84**: 45–67.

Cheablam O, Tansakul P, Nantakat B, *et al*. (2021). Assessment of the geotourism resource potential of the Satun UNESCO global geopark, Thailand. *Geoheritage* **13**: 87.

Chen WH, Han YF, Liang JD, *et al*. (2021). Taxonomic and phylogenetic characterizations reveal four new species of *Simplicillium* (*Cordycipitaceae, Hypocreales*) from Guizhou, China. *Scientific Reports* **11**: 15300.

Corda ACJ (1839). *Pracht-Flora Europaeischer Schimmelbildungen*. Gerhard Fleischer, Leipzig, Berlin.

Crous PW, Boers J, Holdom D, *et al.* (2022b). Fungal planet description sheets: 1383–1435. *Persoonia* **48**: 261–371.

Crous PW, Cowan DA, Maggs-Kölling G, *et al*. (2020). Fungal planet description sheets: 1112–1181. *Persoonia* **45**: 251–409.

Crous PW, Gams W, Stalpers JA, *et al.* (2004). MycoBank: An online initiative to launch mycology into the 21st century. *Studies in Mycology* **50**: 19–22.

Crous PW, Luangsa-ard J, Wingfield MJ, *et al.* (2018). Fungal Planet description sheets: 785 – 867. *Persoonia* **41**: 238–417.

Crous PW, Osieck ER, Jurjević Z, *et al.* (2021). Fungal planet description sheets: 1284-1382. *Persoonia* **47**: 178–374.

Crous PW, Sandoval-Denis M, Costa MM, *et al.* (2022a). *Fusarium* and allied fusarioid taxa. *Fungal Systematics and Evolution* **9**: 161–200.

Cunha AOB, Bezerra JDP, Oliveira TGL, *et al*. (2020). Living in the dark: Bat caves as hotspots of fungal diversity. *PLoS ONE* **15**: e0243494.

Dayarathne MC, Jones EBG, Maharachchikumbura SSN, *et al*. (2020). Morpho-molecular characterization of microfungi associated with marine based habitats. *Mycosphere* **11**: 1–188.

de Hoog GS, Guarro J,Gené J, Figueras MJ (2000). *Atlas of Clinical Fungi.* Centraalbureau voor schimmelcultures. Universitat Rovira i Virgili / Utrecht, the Netherlands.

Degawa Y (1997). Zygospore formation in *Mortierella capitata*. *Mycoscience* **38**: 387–389.

Degawa Y, Gams W (2004). A new species of *Mortierella*, and an associated sporangiiferous mycoparasite in a new genus, Nothadelphia. *Studies in Mycology* **50**: 567–572.

Dominguez-Moñino I, Jurado V, Rogerio-Candelera MA, *et al.* (2021). Airborne fungi in show caves from southern Spain. *Applied Sciences* **11**: 5027.

Domsch KH, Gams W, Anderson TH (1980). *Compendium of Soil Fungi.* Volume 1. Academic Press, London, UK.

Duangkrayom J, Nishioka Y, Shaokun C, *et al.* (2018). Proboscidean fossils (Mammalia) from the Quaternary deposits on Stegodon Cave, Thungwa, Satun Province, southern Thailand. *WIAS Discussion Paper* **2018-001**: 1–19.

Edgar R (2004). MUSCLE: Multiple sequence alignment with high accuracy and high throughput. *Nucleic Acids Research* **32**: 1792–1797.

Fernández-Remacha D, González-Riancho C, Lastra Osua M, *et al.* (2022). Analysis of laccase-like enzymes secreted by fungi isolated from a cave in northern Spain. *MicrobiologyOpen* **11**: e1279.

Gabriel CR, Northup DE (2013). Microbial ecology: Caves as an extreme habitat. In: *Cave Microbiomes: A Novel Resource for Drug Discovery* (Cheeptham N, ed), Springer, New York, USA.

Gams W (1968). Die systematische Stellung der Schimmelpilze *Fusidium buxi* und *Verticillium candelabrum. Acta Botanica Neerlandica* **17**: 455–460.

Gilgado F, Cano J, Gené J, *et al.* (2008). Molecular and phenotypic data supporting distinct species statuses for *Scedosporium apiospermum* and *Pseudallescheria boydii* and the proposed new species *Scedosporium dehoogii*. *Journal of Clinical Microbiology* **46**: 766–771.

Glass NL, Donaldson GC (1995). Development of primer sets designed for use with the PCR to amplify conserved genes from filamentous ascomycetes. *Applied and Environmental Microbiology* **61**: 1323–1330.

Guan YM, Ma YY, Jin Q, *et al.* (2020). Multi-locus phylogeny and taxonomy of the fungal complex associated with rusty root rot of Panax ginseng in China. *Frontiers in Microbiology* **11**: 618942.

Gubiani JR, Bernardi DI, De Paula CCP, *et al.* (2022). Absolute configuration of cytotoxic anthraquinones from a Brazilian cave soil-derived fungus, *Aspergillus* sp. SDC28. *Archiv der Pharmazie* **355**: 2100441.

Hall TA (1999). BioEdit: A user-friendly biological sequence alignment editor and analysis program for Windows 95/98/NT. *Nucleic Acids Symposium Series* **41**: 95–98.

Hawksworth DL, Lucking R (2017). Fungal diversity revisited: 2.2 to 3.8 million species. *Microbiology Spectrum* **5**: FUNK-0052-2016.

He D, Wu F, Ma W, *et al.* (2021). Insights into the bacterial and fungal communities and microbiome that causes a microbe outbreak on ancient wall paintings in the Maijishan Grottoes. *International Biodeterioration and Biodegradation* **163**: 105250.

Houbraken J, de Vries RP, Samson, RA (2014). Modern taxonomy of biotechnologically important *Aspergillus* and *Penicillium* species. *Advances in Applied Microbiology* **86**: 199–249.

Hsieh TC, Ma KH, Chao A (2022). iNEXT: Interpolation and Extrapolation for Species Diversity. R package version 3.0.0.

Hubka V, Dobiasova S, Lyskova P, *et al.* (2013). *Auxarthron ostraviense sp. nov*., and *A. umbrinum* associated with non-dermatophytic onychomycosis. *Medical Mycology* **51**: 614–624.

Hyde KD, Norphanphoun C, Maharachchikumbura SSN, *et al.* (2020). Refined families of *Sordariomycetes. Mycosphere* **11**: 305–1059.

Ikeda H, Fukuda T, Yokoyama J (2016). Endophytic fungi associated with a holoparasitic pant, *Balanophora japonica* (*Balanophoraceae*). *American Journal of Plant Science* **7**: 152–158.

Jiang JR, Cai L, Liu F (2017). Oligotrophic fungi from a carbonate cave, with three new species of *Cephalotrichum*. *Mycology* **8**: 164–177.

Jones DS, Northup DE (2021). Cave decorating with microbes: Geomicrobiology of caves. *Elements* **17**: 107–112.

Jurado V, Sanchez-Moral S, Saiz-Jimenez C (2008). Entomogenous fungi and the conservation of the cultural heritage: A review. *International Biodeterioration and Biodegradation* **62**: 325–330.

Kandemir H, Dukik K, de Melo Teixeira M, *et al.* (2022). Phylogenetic and ecological re-evaluation of the order *Onygenales*. *Fungal Diversity* **115**: 1–72.

Karunarathna SC, Dong Y, Karasaki S, *et al*. (2020). Discovery of novel fungal species and pathogens on bat carcasses in a cave in Yunnan province, China. *Emerging Microbes and Infections* **9**: 1554–1566.

Kornerup A, Wanscher JH (1978). *Methuen Handbook of Colour.* Eyre Methuen, London, UK.

Lackner M, Klaassen CH, Meis JF, *et al.* (2012). Molecular identification tools for sibling species of *Scedosporium* and *Pseudallescheria*. *Medical Mycology* **50**: 497–508.

Lackner M, de Hoog GS, Yang L, *et al.* (2014). Proposed nomenclature for *Pseudallescheria, Scedosporium* and related genera. *Fungal Diversity* **67**: 1–10.

Larsson A (2014). AliView: A fast and lightweight alignment viewer and editor for large datasets. *Bioinformatics* **30**: 3276–3278.

Lawrence DP, Nouri MT, Trouillas FP (2019). Taxonomy and multi-locus phylogeny of cylindrocarpon-like species associated with diseased roots of grapevine and other fruit and nut crops in California. *Fungal Systematics and Evolution* **4**: 59–75.

Lee NM, Meisinger DB, Aubrecht R, *et al.* (2012). Caves and karst environments. In: *Life at Extremes: Environments, Organisms and Strategies for Survival.* (Bell EM, ed). CABI London, UK: 320–344.

Leplat J, François A, Bousta F (2021). *Simplicillium pechmerlensis*, a new fungal species isolated of the pechmerle show cave. *Phytotaxa* **521**: 80–94.

Leplat J, Francois A, Bousta F (2022). *Leptobacillium cavernicola*, a newly discovered fungal species isolated from several paleolithic-decorated caves in France. *Phytotaxa* **571**: 186–196.

Letunic I, Bork P (2021). Interactive Tree Of Life (iTOL) v5: An online tool for phylogenetic tree display and annotation. *Nucleic Acids Research* **49**: 293–296.

Liu F, Cai L (2012). Morphological and molecular characterization of a novel species of *Simplicillium* from China. *Cryptogamie, Mycologie* **33**: 137–144.

Liu YL, Whelen S, Hall BD (1999). Phylogenetic relationships among ascomycetes: Evidence from an RNA polymerase II subunit. *Molecular Biology and Evolution* **16**: 1799–1808.

Liu X, Tibpromma S, Zhang F, *et al*. (2021). *Neopestalotiopsis cavernicola sp. nov*. from gem cave in Yunnan province, China. *Phytotaxa* **512**: 1–27.

Lorch JJ, Lindner DD, Gargas A, *et al.* (2013). A culture-based survey of fungi in soil from bat hibernacula in the eastern united states and its implications for detection of *Geomyces destructans*, the causal agent of bat white-nose syndrome. *Mycologia* **105**: 237–252.

Ma H, Song Z, Pan X, *et al.* (2022). Multi-gene phylogeny and taxonomy of *Hypoxylon* (*Hypoxylaceae, Ascomycota*) from China. *Diversity* **14**: 37.

Macias AM, Marek PE, Morrissey EM, *et al.* (2019). Diversity and function of fungi associated with the fungivorous millipede, *Brachycybe lecontii*. *Fungal Ecology* **41**: 187–197.

Mang SM, Scrano L, Camele I (2020). Preliminary studies on fungal contamination of two rupestrian churches from matera (Southern Italy). *Sustainability* **12**: 6988.

Marchal M (1891). Champignons coprophiles de Belgique VI. Mucoririees et Sphaeropsidees nouvelles. *Bulletin de la Société Royale de Botanique de Belgique* **30**: 134–146.

Martin-Pozas T, Nováková A, Jurado V, *et al.* (2022). Diversity of microfungi in a high radon cave ecosystem. *Frontiers in Microbiology* **13**: 869661.

Martin-Sanchez PM, Bastian F, Alabouvette C, *et al.* (2013). Real-time PCR detection of *Ochroconis lascauxensis* involved in the formation of black stains in the Lascaux Cave, France. *Science of the Total Environment* **443**: 478–484.

Martin-Sanchez PM, Jurado V, Porca E, *et al.* (2014). Airborne microorganisms in Lascaux Cave (France). *International Journal of Speleology* **43**: 295–303.

Matheny PB, Liu YJ, Ammirati JF, *et al.* (2002). Using *RPB1* sequences to improve phylogenetic inference among mushrooms (*Inocybe, Agaricales*). *American Journal of Botany* **89**: 688–698.

Mehrotra BS, Baijal U (1963). Species of *Mortierella* from India - III. *Mycopathologia et Mycologia Applicata* **20**: 49–54.

Mehrotra BS, Baijal U, Mehrotra BR (1963). Two new species of *Mortierella* from India. *Mycologia* **55**: 289–296.

Miller MA, Pfeiffer W, Schwartz T (2010). *Creating the CIPRES Science Gateway for inference of large phylogenetic trees.* Proceedings of the Gateway Computing Environments Workshop (GCE), New Orleans, LA.: 1–8.

Moreira GM, Abreu LM, Carvalho VG, *et al.* (2016). Multilocus phylogeny of *Clonostachys* subgenus *Bionectria* from Brazil and description of *Clonostachys chloroleuca sp. nov. Mycological Progress* **15**: 1031–1039.

Muangsong C, Cai B, Pumijumnong N, *et al.* (2019). A preliminary study on teak tree-ring cellulose δ18O from northwestern Thailand: the potential for developing multi-proxy records of Thailand summer monsoon variability. *Theoretical and Applied Climatology* **136**: 575–586.

Nantakat B, Vorachart V (2021). Designing tourism identity communication in Satun UNESCO Global Geopark. *Geojournal Tour Geosites* **35**: 275–281.

Naranjo-Ortiz MA, Gabaldón T (2019). Fungal evolution: Major ecological adaptations and evolutionary transitions. *Biological Review* **94**: 1443–1476.

Nieves-Rivera Á, Santos-Flores C, Dugan F, *et al.* (2009). Guanophilic fungi in three caves of southwestern Puerto Rico. *International Journal of Speleology* **38**: 61–70.

Nováková A (2009). Microscopic fungi isolated from the Domica Cave system (Slovak Karst National Park, Slovakia). A review. *International Journal of Speleology* **38**: 71–82.

Nováková A, Kubátová A, Sklenar F, *et al.* (2018). Microscopic fungi on cadavers and skeletons from cave and mine environments. *Czech Mycology* **70**: 101–121.

Nuankaew S, Chuaseeharonnachai C, Preedanon, S, *et al*. (2022). Two novel species of *Talaromyces* discovered in a Karst Cave in the Satun UNESCO Global Geopark of Southern Thailand. *Journal of Fungi* **8**: 825.

Nylander JAA (2004). *MrModeltest v2. Program distributed by the author.* Evolutionary Biology Centre, Uppsala University.

O'Donnell K, Cigelnik E (1997). Two divergent intragenomic rDNA ITS2 types within a monophyletic. *Molecular Phylogenetics and Evolution* **7**: 103–116.

Ogórek R, Suchodolski J, Piecuch A, *et al.* (2022). Keratinophilic and keratinolytic fungi in cave ecosystems: A culture-based study of Brestovská cave and Demänovská L'adová and slobody caves (Slovakia). *Applied Sciences* **12**: 1455.

Okane I, Nonaka K, Kurihara Y, *et al.* (2020). A new species of *Leptobacillim, L. symbioticum*, isolated from mites and sori of soybean rust. *Mycoscience* **61**: 165–171.

Oksanen J, Simpson G, Blanchet F, *et al.* (2022). Vegan: Community Ecology Package. R package version 2.6-4.

Parshikov IA, Freeman JP, Lay JO, *et al.* (1999). Regioselective transformation of ciprofloxacin to N-acetylciprofloxacin by the fungus *Mucor ramannianus*. *FEMS Microbiology Letters* **177**: 131–135.

Pereira MLS, Carvalho JLVR, Lima JMS, *et al.* (2022). Richness of *Cladosporium* in a tropical bat cave with the description of two new species. *Mycological Progress* **21**: 345–357.

Phookamsak R, Hyde KD, Jeewon R, *et al.* (2019). Fungal diversity notes 929–1035: Taxonomic and phylogenetic contributions on genera and species of fungi. *Fungal Diversity* **95**: 1–273.

Pourmoghaddam MJ, Lambert C, Surup F, *et al.* (2020). Discovery of a new species of the *Hypoxylon rubiginosum* complex from Iran and antagonistic activities of *Hypoxylon* spp. against the ash dieback pathogen, *Hymenoscyphus fraxineus*, in dual culture. *MycoKeys* **66**: 105–133.

Rainer J, de Hoog GS (2006). Molecular taxonomy and ecology of *Pseudallescheria, Petriella* and *Scedosporium prolificans* (*Microascaceae*) containing opportunistic agents on humans. *Mycological Research* **110**: 151–160.

Raudabaugh DB, Rivera NA, Anchor GC, *et al.* (2021). Preliminary study of cave sample storage conditions on fungal community diversity. *Diversity* **13**: 188.

Réblová M, Miller AN, Rossman AY, *et al.* (2016). Recommendations for competing sexual-asexually typified generic names in

Sordariomycetes (except *Diaporthales*, *Hypocreales*, and *Magnaporthales*). *IMA Fungus* **7**: 131–153.

Rehner SA, Buckley E (2005). A *Beauveria* phylogeny inferred from nuclear ITS and EF1-α sequences: Evidence for cryptic diversification and links to *Cordyceps* teleomorphs. *Mycologia* **97**: 84–98.

Rodríguez-Andrade E, Cano-Lira JF, Wiederhold N, *et al.* (2021). A revision of *Malbranchea*-like fungi from clinical specimens in the United States of America reveals unexpected novelty. *IMA Fungus* **12**: 25.

Ronquist F, Teslenko M, van der Mark P, *et al.* (2012). MrBayes 3.2: Efficient Bayesian phylogenetic inference and model choice across a large model space. *Systematic Biology* **61**: 539–542.

Rossman AY, Seifert KA, Samuel GJ, *et al.* (2013). Genera in *Bionectriaceae*, *Hypocreaceae*, and *Nectriaceae* (*Hypocreales*) proposed for acceptance or rejection. *IMA Fungus* **4**: 41–51.

Saccardo PA (1882). Fungi Gallici lecti a Cl. viris P. Brunaud, C.C. Gillet, Abb. Letendre, A. Malbranche, J. Therry & Doma Libert. Series IV. *Michelia* **2**: 583–648.

Salgado-Salazar C, Rossman A, Samuels GJ, *et al.* (2012). Multigene phylogenetic analyses of the *Thelonectria coronata* and *T. veuillotiana* species complexes. *Mycologia* **104**: 1325–1350.

Salgado-Salazar C, Rossman AY, Samuels GJ, *et al*. (2015). Phylogeny and taxonomic revision of *Thelonectriadiscophora* (*Ascomycota, Hypocreales, Nectriaceae*) species complex. *Fungal Diversity* **70**: 1–29.

Samson RA, Hoekstra ES, Frisvad JC (2004). *Introduction to Food-and Airborne Fungi*. CBS-KNAW Fungal Biodiversity Centre, Utrecht, Netherlands.

Schoch CL, Sung G-, López-Giráldez F, *et al.* (2009). The Ascomycota tree of life: A phylum-wide phylogeny clarifies the origin and evolution of fundamental reproductive and ecological traits. *Systemic Biology* **58**: 224–239.

Schroers HJ (2001). A monograph of *Bionectria* (*Ascomycota, Hypocreales, Bionectriaceae*) and its *Clonostachys* anamorphs. *Studies in Mycology* **46**: 1–214.

Seifert K, Morgan-Jones G, Gams W, *et al.* (2011). *The Genera of Hyphomycetes. CBS Biodiversity Series no. 9*: 1–997. CBS-KNAW Fungal Biodiversity Centre, Utrecht, Netherlands.

Seviour RJ, Cooper AL, Skilbeck NW (1987). Identification of *Mortierella wolfii*, a causative agent of mycotic abortion in cattle. *Journal of Medical and Veterinary Mycology* **25**: 115–123.

Shapiro J, Pringle A (2010). Anthropogenic influences on the diversity of fungi isolated from caves in Kentucky and Tennessee. *The American Midland Naturalist* **163**: 76–86.

Singh SK, Thapliyal M, Guleri S, *et al*. (2022). First report on occurrence of *Clonostachys* in cave ecosystem from India. *Journal of Mycopathological Research* **60**: 267–271.

Sir EB, Becker K, Lambert C, *et al.* (2019). Observations on Texas hypoxylons, including two new *Hypoxylon* species and widespread environmental isolates of the *H. croceum* complex identified by polyphasic approach. *Mycologia* **11**: 832–856.

Siripattharapurinont R (2015). Official Report of Cave Survey and Mapping for Phu Pha Phet Cave. Department of Mineral Resources. (Printed in Thai).

Siripattharapurinont R (2016). Official Report of Cave Survey and Mapping for Le Stegodon Cave. Department of Mineral Resources. (Printed in Thai).

Smith G (1962). Some new and interesting species of micro-fungi. III. *Transactions of the British Mycological Society* **45**: 387–394.

Song ZK, Zhu AH, Liu ZD, *et al*. (2022). Three new species of *Hypoxylon* (*Xylariales, Ascomycota*) on a multigene phylogeny from Medog in Southwest China. *Journal of Fungi*: **8**: 500.

Stamatakis A (2014). RAxML version 8: A tool for phylogenetic analysis and post-analysis of large phylogenies. *Bioinformatics* **30**: 1312–1313.

Subedi S, Chen SC (2015). Epidemiology of scedosporiosis. *Current Fungal Infection Reports* **9**: 275–184.

Summerbell RC (2005). Root endophyte and mycorrhizosphere fungi of black spruce, *Picea mariana*, in a boreal forest habitat: Influence of site factors on fungal distributions. *Studies in Mycology* **53**: 121–145.

Sun JZ, Ge QY, Zhu ZB, *et al*. (2019). Three dominating hypocrealean fungi of the 'white mold spots' on acrylic varnish coatings of the murals in a Koguryo tomb in China. *Phytotaxa* **397**: 225–236.

Takashima M, Kurakado S, Cho O, *et al*. (2020). Description of four apiotrichum and two cutaneotrichosporon species isolated from guano samples from bat-inhabited caves in Japan. *International Journal of Systematic and Evolutionary Microbiology* **70**: 4458–4469.

Tapia C (2012). *Scedosporium/Pseudallescheria*. *Revista Chilena de Infectologia* **29**: 335–336.

Torcato C, Gonçalves MFM, Rodríguez-Gálvez E, *et al.* (2020). *Clonostachys viticola sp. nov*., a novel species isolated from *Vitis vinifera*. *International Journal of Systematic and Evolutionary Microbiology* **70**: 4321–4328.

Vandepol N, Liber J, Desirò A, *et al.* (2020). Resolving the *Mortierellaceae* phylogeny through synthesis of multi-gene phylogenetics and phylogenomics. *Fungal Diversity* **104**: 267–289.

Vanderwolf KJ, Malloch D, Mcalpine DF, *et al.* (2013). A world review of fungi, yeasts, and slime molds in caves. *International Journal of Speleology* **42**: 77–96.

Vanderwolf KJ, Malloch D, McAlpine DF (2016). Ectomycota associated with arthropods from bat hibernacula in eastern Canada, with particular reference to *Pseudogymnoascus destructans*. *Insects* **7**: 16.

Vilgalys R, Hester M (1990). Rapid genetic identification and mapping of enzymatically amplified ribosomal DNA from several *Cryptococcus* species. *Journal of Bacteriology* **172**: 4238–4246.

Visagie CM, Boekhout T, Theelen B, *et al*. (2022). Da Vinci's yeast: *Blastobotrys davincii f.a., sp. nov*. *Yeast* **40**: 7–31.

Visagie CM, Goodwell M, Nkwe DO (2021). *Aspergillus* diversity from the Gcwihaba Cave in Botswana and description of one new species. *Fungal Systematics and Evolution* **8**: 81–89.

Voigt K, Wöstemeyer J (2000). Reliable amplification of actin genes facilitates deep-level phylogeny. *Microbiological Research* **155**: 179–195.

Wanasinghe DN, Phukhamsakda C, Hyde KD, *et al.* (2018). Fungal diversity notes 709–839: Taxonomic and phylogenetic contributions to fungal taxa with an emphasis on fungi on Rosaceae. *Fungal Diversity* **89**: 1–236.

Wang Y, Cheng X, Wang H, *et al.* (2022). The characterization of microbiome and interactions on weathered rocks in a subsurface karst cave, Central China. *Frontiers in Microbiology* **13**: 909494.

Wang YN, Liu XY, Zheng RY (2013). Four new species records of *Umbelopsis* (*Mucoromycotina*) from China. *Journal of Mycology* **2013**: ID970216.

Wang YN, Liu XY, Zheng RY (2014). *Umbelopsis changbaiensis sp. nov*. from China and the typification of *Mortierella vinacea*. *Mycological Progress* **13**: 657–669.

Wang YN. Liu XY, Zheng RY (2015). *Umbelopsis longicollis comb. nov*. and the synonymy of *U. roseonana* and *U. versiformis* with *U. nana*. *Mycologia* **107**: 1023–1032.

Wang YN, Liu XY, Zheng RY (2022). The *Umbelopsis ramanniana sensu lato* consists of five cryptic species. *Journal of Fungi* **8**: 895.

Watanabe T (2002). *Pictorial Atlas of Soil and Seed fungi: Morphologies of Cultured Fungi and Key to Species*. Taylor and Francis Group, London, UK.

Wasti IG, Khan FAA, Bernard H, *et al.* (2021). Fungal communities in bat guano, speleothem surfaces, and cavern water in Madai Cave, Northern Borneo (Malaysia). *Mycology* **12**: 188–202.

White TJ, Bruns T, Lee S, *et al.* (1990). Amplification and direct sequencing of fungal ribosomal RNA genes for phylogenetics. In: *PCR Protocols: A Guide to Methods and Applications* (Innis MA, Gelfand DH, Sninsky JJ, *et al.,* eds). Academic Press, New York: 315–322.

Zada S, Xie J, Yang M, *et al.* (2021). Composition and functional profiles of microbial communities in two geochemically and mineralogically different caves. *Applied Microbiology and Biotechnology* **105**: 8921–8936.

Zalar P, Gubenšek A, Gostincar C, *et al.* (2022). Cultivable skin mycobiota of healthy and diseased blind cave salamander (*Proteus anguinus*). *Frontiers in Microbiology* **13**: 926558.

Zhao L, Groenewald JZ, Hernández-Restrepo M, *et al.* (2023). Revising *Clonostachys* and allied genera in *Bionectriaceae*. *Studies in Mycology* **105**: 205–266.

Zare R, Gams W (2016). More white *Verticillium*-like anamorphs with erect conidiophores. *Mycological Progress* **15**: 993–1030.

Zeng ZQ, Zhuang WY (2013). Four new taxa of *Ilyonectria* and *Thelonectria* (*Nectriaceae*) revealed by morphology and combined ITS and β-tubulin sequence data. *Phytotaxa* **85**: 15–25.

Zeng ZQ, Zhuang WY (2019). The genera *Rugonectria* and *Thelonectria* (*Hypocreales, Nectriaceae*) in China. *MycoKeys* **55**: 101–120.

Zeng ZQ, Zhuang WY (2022). New species of *Nectriaceae* (*Hypocreales*) from China. *Journal of Fungi* **8**: 1075.

Zhang ZF, Liu F, Zhou X, *et al.* (2017). Culturable mycobiota from karst caves in China, with descriptions of 20 new species. *Persoonia* **39**: 1–31.

Zhang ZF, Zhao P, Cai L (2018). Origin of cave fungi. *Frontiers in Microbiology* **9**: 1407.

Zhang ZF, Zhou SY, Eurwilaichitr L, *et al.* (2021). Culturable mycobiota from karst caves in China II, with descriptions of 33 new species. *Fungal Diversity* **106**: 29–136.

Zhu H, Jiang C, Liu S (2022). Microbial roles in cave biogeochemical cycling. *Frontiers in Microbiology* **13**: 950005.

Supplementary information

Table S1. Morphological comparisons of the new species (*Actinomortierella caverna*) with its close relatives.

Table S2. Morphological comparison of the new species (*Leptobacillium latisporum*) with its close relatives.

FUSE

Fungal Systematics and Evolution

Volume 12
DECEMBER 2023
PAGES 31–45

doi.org/10.3114/fuse.2023.12.02

Kgaria (*Boletaceae, Boletoideae*) *gen. nov*. in Australia: Neither a *Tylopilus* nor a *Porphyrellus*

R.E. Halling[1*], N.A. Fechner[2], G. Holmes[3], N. Davoodian[3]

[1]Department of Research & Conservation, Denver Botanic Gardens, 909 York St, Denver CO 80206 USA; Institute of Systematic Botany, New York Botanical Garden, 2900 Southern Blvd, Bronx, NY 10458, USA
[2]Queensland Herbarium, Mt Coot-tha Road, Toowong, Brisbane, QLD 4066, Australia
[3]Royal Botanic Gardens Victoria, South Yarra, VIC 3141, Australia

*Corresponding author: R.E. Halling, rhalling@nybg.org

Key words:
boletes
cyanogranules
molecular phylogenetics
new taxa
ribosomal DNA

Abstract: *Kgaria* is described as a new porphyrellus-like genus of *Boletaceae* to accommodate *Tylopilus cyanogranulifer*, a dark brown to dull lilac/violet, or rarely, nearly black bolete with a series of oxidation reactions progressing from blue to red then nearly black and a dark brown spore deposit. Idiosyncratic blue-green pigment encrustations (cyanogranules) and a similarly colored reaction of the hyphae located on pileus and stipe surfaces are also diagnostic. Phylogenetic analyses of nuclear large-subunit rDNA (nrLSU), translation elongation factor 1-alpha (*tef-1*), and the second largest subunit of RNA polymerase II (*rpb2*) infer *Kgaria* as a unique generic lineage with two species, one of which is newly described (*K. similis*). *Tylopilus olivaceoporus*, originally described at the same time and as distinct from *T. cyanogranulifer*, appears to be conspecific with the latter. Some darkly pigmented taxa with similar oxidation reactions that were recently described from Brazil, Guyana, and China are further supported by morphology and molecular data as discrete lineages in separate genera in subfamily *Boletoideae*.

Citation: Halling RE, Fechner NA, Holmes G, Davoodian N (2023). *Kgaria* (*Boletaceae, Boletoideae*) *gen. nov*. in Australia: Neither a *Tylopilus* nor a *Porphyrellus*. *Fungal Systematics and Evolution* **12**: 31–45. doi: 10.3114/fuse.2023.12.02
Received: 9 June 2023; **Accepted:** 23 July 2023; **Effectively published online:** 26 July 2023
Corresponding editor: P.W. Crous

INTRODUCTION

Watling & Gregory (1989a) suggested *Tylopilus* (including *Porphyrellus*) was abundant in Australasia and that there were many species still undocumented. Watling & Gregory (1986, 1988a, b, 1989a, b, 1991), and Li & Watling (1999) produced treatments on boletes specifically from Queensland's Cooloola Sandmass and elsewhere in Australia. Based on those works, a preliminary survey of Australian boletes was published by Watling & Li (1999). Further work by Bougher & Thiers (1991), Castellano *et al*. (1992), Wolfe & Bougher (1993), Halling *et al*. (2006, 2008, 2012a,b, 2014, 2015), Halling & Fechner (2011), Trappe *et al*. (2013), Fechner *et al*. (2017), Gelardi *et al*. (2017), Davoodian *et al*. (2018, 2019), and Crous *et al*. (2020, 2021) added to these efforts to document novel taxa, clarify concepts, and infer phylogenetic relationships of some Australian boletes. Recently, Osmundson *et al.* (2021) went into further detail deciphering earlier concepts used to delimit *Tylopilus* worldwide.

It is of particular importance here to note that a broad circumscription of *Tylopilus* was employed by Watling & Gregory (1989a) that included *Porphyrellus* (type species, *T. porphyrosporus*) in the generic concept. They stated at the time that there were no records of porphyrelloid species from Queensland. Although there is a reference to Hilton's (1982) listing of *P. pseudoscaber nom. inval*. (= *P. porphyrosporus*) from Western Australia, all available fungarium specimens collected in Australia that they examined did not match the extant European concept of that species.

However, Watling & Gregory (1989a, p. 23) described, in some detail under species group 6, *T. olivaceoporus* as a *nom. prov*. with a morphological alliance to *T. porphyrosporus* based on pore color and cyanescent context. Due to the poor condition of the two cited specimens collected at Queensland's Cooloola Sandmass (*Watling 16227*, *16308*; both in E), a formal description was not offered. This Sandmass is on the Australian mainland and part of the Great Sandy National Park in SE Queensland and lies just south of K'gari [also known as Fraser Island], which is also part of the national park. The authors mentioned some distinctive macroscopic features such as: a roughened, purple brown pileus surface, a white context and olivaceous grey hymenophore that stains blue. Portions of the pileipellis assumed a "Prussian blue" color when mounted in alkaline solutions and hyphae were constricted at the septa. Some conjecture on similar macro-chemical reactions was noted for African specimens cited by Heinemann (1966), as he (Heinemann 1951) described "Prussian blue" reactions in ammoniacal mounts of cell walls on the hyphae of the pilei- and stipitipellis of *T. violaceus* and *T. beelii*.

In further commentary following the description of the *nom. prov*., Watling & Gregory (1989a, p. 24) also mentioned two specimens (*JECA 84/117*, BRIP 9254; *JECA 84/119*, BRIP 9255) with ". . . similar bluish coloration . . ." when observed in alkaline solutions. Those specimens (now in BRI: AQ0646036;

AQ0813158 respectively) are clearly different because of faintly ornamented spores, and we confirm they represent *Ionosporus australis* of subfamily *Leccinoideae* described by Khmelnitsky *et al*. (2019).

Following the details circumscribing *T. olivaceoporus nom. prov*., additional categories of distinction such as hymenial cystidium features and spore size were listed for other Queensland specimens (Watling & Gregory 1989a). These groupings were noted in order to aid workers for identification of future specimens. Of relevance here, a specimen labelled as BRIP 9175 (*JECA80/580*, now in BRI: AQ0809781) is listed in a group with colored cystidial contents and large spores, and is briefly described under group 12, as *Tylopilus* sp. 6 (Watling & Gregory 1989a, p. 27). It is noteworthy that this specimen is compared to *T. olivaceoporus* because of bluish green colors in the pileipellis and bluish incrustations on those hyphae in alkaline solutions on microscope slide preparations. Also, irregularly roughened pileus surfaces and punctate dotted stipe surfaces are mentioned in both descriptions.

Eventually, Li & Watling (1999) formally described, via Latin diagnoses, *T. olivaceoporus* and *T. cyanogranulifer* (for *Tylopilus* sp. 6) as distinct, separate species without comparison. In the original publication (Watling & Gregory1989a), those authors noted that the pileipellis of *T. olivaceoporus* was distinctly blue in ammoniacal solutions, the hyphae were constricted at the septa, and the pileus context had some elements that were strongly blue. In the brief description of *T. cyanogranulifer* (as *Tylopilus* sp. 6), the pileipellis hyphae are brown, smooth and interwoven and some hyphae of the pileipellis possessed blueish incrustations in alkali mounts. The single specimen cited (BRIP 9175) became the holotype for *T. cyanogranulifer* and another specimen (C. Sandercoe & J. Milne, *JECA 86/79*, BRIP 19810; now in BRI: AQ0809780) was cited as the holotype for *T. olivaceoporus*. No illustrations were provided and only Latin diagnoses were given with a comment that *T. olivaceoporus* is ". . . characterized by the bluish encrustations in alkaline solution and the dark squamulose or rimose cuticle." (Li & Watling 1999, p. 147).

Here, we revisit the concepts of *T. olivaceoporus* and *T. cyanogranulifer*. In our evaluation of the diagnoses, there is little difference between them other than possible variation in oxidation reaction of the exposed context, and whether or not the septa of the hyphae in the pileipellis are constricted. Both taxa are noted as having bluish green granules in the pileipellis. Later that year, Watling & Li (1999) published some additional details of these species based on other specimens from the Cooloola Sandmass. In a complicated dichotomous key, the two species are separated (p. 17) by subtle distinctions of stipe surface morphology, pileus color and texture, oxidation reactions of exposed context, pore color and oxidation reaction, and a spore width difference of 0.5 µm. Unfortunately, only one of the additional specimens determined as *T. olivaceoporus* is extant (*JECA 83/45*, BRIP 19451; now in BRI: AQ0813159). According to Roger Shivas at BRIP (pers. comm., 26 June 2023), 4 920 specimens of larger fungi at that institution were sent on permanent loan to BRI in January 2002 and subsequently have been accessioned with AQ barcodes at BRI.

We examined the type specimens and documented and sequenced additional fresh material of porphyrelloid boletes, particularly from the Cooloola Sandmass and adjacent K'gari in Queensland, as well as specimens from New South Wales, Victoria, and Tasmania. Based on our morphological and molecular analyses, we believe that *T. olivaceoporus* and *T. cyanogranulifer* are conspecific, and so we offer an updated description of *T. cyanogranulifer* along with description of a new species. We hypothesize that neither *Tylopilus* nor *Porphyrellus* are appropriate genera for these entities and a new genus, *Kgaria*, in the *Boletoideae* is warranted and described here.

MATERIALS & METHODS

Morphology

Macromorphological data were obtained from fresh specimens. General color terms are approximations, and the color codes (*e.g.*, 7D8) are page, column and grid designations from Kornerup & Wanscher (1983). Microscopic structures were observed with an Olympus BHS compound microscope equipped with Nomarski differential interference contrast (DIC) optics, and measured from dried material revived in freshly prepared 3 % KOH or 20 % NH_4OH. The presence or absence and abundance of cyanogranules and pigmentation were noted using freshly prepared radial and paradermal sections of the pileus surface and longitudinal and paradermal sections from the stipe surface. These were often acquired several times from different portions of the same basidiome. The letter abbreviation *Q* refers to the range of length/width ratios measured from *n* basidiospores, and *x* refers to the mean length × mean width. Light micrographs were obtained via Spot 5.6 Imaging software using a Spot Insight Gigabit 4.0 Mp digital camera from Diagnostic Instruments. Fungarium codes (Thiers 2023) are cited for all collections from which morphological features were examined and included in the descriptions.

DNA isolation, PCR amplification, DNA sequencing

DNA was extracted from dried specimens using either the E.Z.N.A. Forensic DNA Kit (Omega Bio-tek) or the DNeasy Plant Pro Kit (Qiagen). Partial nuclear large subunit rDNA (nrLSU) genes were PCR amplified with primers LROR and LR5 under the following cycling conditions: (1) 95 °C for 15 min, (2) then 30 cycles of 94 °C for 30 s, 60 °C for 30 s, and 72 °C for 1 min, (3) then 72 °C for 5 min. Partial translation elongation factor 1 alpha (*tef1*) and second largest subunit of RNA polymerase II (*rpb2*) genes (both nuclear protein-coding genes) were PCR amplified based on primers and protocols outlined in Davoodian *et al*. (2021) and Khmelnitsky *et al*. (2019), respectively. In some cases, it was necessary to dilute the gDNA extractions with 10 parts distilled, deionized water prior to PCR to achieve successful amplification. Sanger sequencing was conducted in forward and reverse directions at the Australian Genome Research Facility in Melbourne, Australia and Macrogen in the USA (formerly https://www.macrogenusa.com).

Sequence alignment and phylogenetic analysis

Each of the three genes used in this study were aligned separately with MAFFT online (Katoh *et al*. 2017). Additional exemplars outside of our proposed genus were acquired from GenBank by downloading top BLAST hits (http://www.ncbi.nlm.nih.gov/BLAST/) by using our newly generated sequences as queries and from our knowledge of existing sequences on GenBank of morphologically similar species. Alignments were

visually inspected and manually adjusted as required. After preliminary phylogenetic analysis of each locus individually to confirm concordance for critical groups, all three loci were concatenated. The concatenated alignment had 44 terminals and a length of 2 388 and has been supplied as Supplementary File S1.

Phylogenetic analysis was conducted via CIPRES (Miller *et al*. 2011). MrBayes v. 3.2.6 (Ronquist *et al*. 2012) was used for Bayesian phylogenetic analysis. The alignments were partitioned by gene, and the protein-coding genes were further partitioned by coding regions and introns. The following was specified in the MrBayes block for analysis: lset applyto = (all); coding = all; nst = 6; nucmodel = 4by4; rates = invgamma; ngammacat = 5; nbetacat = 5; unlink shape = (all); tratio = (all); revmat = (all); statefreq = (all); omega = (all); pinvar = (all); mcmc ngen = 30 000 000; printfreq = 10 000; samplefreq = 1 000; nruns = 2; nchains = 4; temp = 0.200; swapfreq = 1; nswaps = 1; mcmcdiagn = Yes; minpartfreq = 0.1; allchains = No; relburnin = Yes; burninfrac = 0.5; stoprule = No; Savebrlens = Yes; Ordertaxa = No; sump burnin = 7 500; nruns = 2; sumt burnin = 7 500; nruns = 2; ntrees = 1; contype = Halfcompat; conformat = Figtree. A maximum likelihood (ML) phylogenetic analysis was conducted using RAxML (Stamatakis 2014) with RAxML-HPC BlackBox on CIPRES, using the same model (GTR+G+I) as our Bayesian analysis as it is the most parameter-rich.

RESULTS

Molecular analyses

Exemplars are listed in Table 1 with taxon names, voucher numbers, location, GenBank accession numbers and reference citations for prior accessions used. Newly acquired sequences are in bold face.

Bayesian and ML analyses (Fig. 1) inferred a robustly supported clade corresponding to our hypothesized new genus, including two species with 100 % bootstrap support and Bayesian posterior probability (BPP) of 1. This clade is quite separate from *Tylopilus s*. *str*., but both are clearly in the *Boletoideae*. The sister clade to *Kgaria* that includes *Porphyrellus* and *Afrocastellanoa* is weakly supported with low bootstrap support and low BPP. A larger clade (with 72 % bootstrap support and 0.99 BPP) includes *Kgaria*, *Porphyrellus* and *Afrocastellanoa* along with other similarly pigmented boletes such as *Brasilioporus*, *Indoporus*, *Anthracoporus*, and *Nevesoporus* from Brazil, India, and China. These genera have some similar overall macromorphology and oxidation reactions (bluing, reddening, and/or blackening) reminiscent of *Tylopilus s.l*. and *Porphyrellus s.l*. as clarified by Wu *et al*. (2014) and Li & Yang (2021). Also, this larger clade includes other genera such as *Strobilomyces* and *Boletus s*. *str*. Three exemplars from the *Chalciporoideae* are shown as basal to the *Boletoideae* clade along with two exemplars from the *Paxillaceae*, rooted outside of the *Boletaceae*.

Taxonomy

Kgaria Halling, Fechner, & Davoodian, ***gen. nov.*** MycoBank MB 848732.

Etymology: Derived from the Butchulla (Badjala) Traditional Landowners' name "K'gari" (pronounced *gurri*, which translates to 'paradise'), a site where the genus routinely occurs. K'gari, also known as Fraser Island, is the world's largest sand island, a UNESCO designated World Heritage Area.

Typus: *Tylopilus cyanogranulifer* T.-H. Li, Watling & N.M. Greg. *in* Li & Watling, *Edinburgh J. Bot.* **56**: 146. 1999.

Diagnosis: *Basidiomata* epigeous and boletoid. *Pileus* brown to dark brown or nearly black with overtones of lilac to dull violet, even or irregularly bumpy to roughened, sometimes appressed scaly-areolate with age, viscid or dry. *Context* white, typically oxidizing blue to red then black. *Hymenophore* tubulose, white, then mineral green to dull yellow to olive brown, red to blue then black when bruised. *Stipe* dry, finely scurfy to subpruinose to finely granulose above, fibrillose streaked downward, variously colored with mineral green, lilac to pale violet, and dark brown pigmentation. *Spores* brown in deposit, smooth, subfusoid. *Hymenial cystidia* present, typically with homogenous brown content in alkaline mounts. *Pileipellis* and s*tipitipellis* with cyanogranular encrusting pigment. *Clamp connections* absent. *Phylogenetically* robustly distinct from *Porphyrellus* and *Afrocastellanoa*.

Kgaria cyanogranulifera (T.-H. Li, Watling & N.M. Greg.) Halling, Fechner & Davoodian, ***comb. nov.*** MycoBank MB 848733. Figs 2–4, 8.
Basionym: *Tylopilus cyanogranulifer* T.-H. Li, Watling & N.M. Greg. in Li & Watling, *Edinburgh J. Bot.* **56**: 146. 1999. MycoBank MB 450217.

Typus: **Australia**, Queensland, Cooloola, Noosa River Soil Landscape (Wolsi 985167), in rainforest, 29 Aug. 1980, *J.E.C. Aberdeen et al*., *JECA 80/580,* BRIP 9175, now in BRI (**holotype** BRI AQ0809781!).

Synonyms: *Tylopilus olivaceoporus* T.H. Li *et al*., *Edinburgh J. Bot*. **56**: 146. 1999. MycoBank MB 662322.
"*Tylopilus olivaceoporus*" Watling & N.M. Greg., *Proc. Roy. Soc. Queensland* **100**: 23. 1989, as "*nom. prov.*", *nom. inval*. MycoBank MB 129797.

Typus: **Australia**, Queensland, Cooloola NP, Harry's Hut Road, on side of dead tree trunk, 11 Jun. 1986, *C. Sandercoe & J. Milne*, *JECA 86/79*, BRIP 19810, now in BRI (**holotype** BRI AQ0809780!).

Pileus (4–)5–7.5(–14) cm broad, convex to plano-convex to plane, brown (6, 7E6) to dark brown (7,8E–F8), sometimes with lilac to dull violet tints (12F7, 14F4), occasionally paler at margin, dry, matted tomentose, sometimes granular to bumpy, becoming finely areolate and agglutinating into fine squamules. *Tubes* adnexed, with *pores* and *tubes* whitish to a pale mineral green to greenish gray (1B2–3) to dull yellow (3B3) to dull yellowish green to dull olive brown (4D–E5, 4), staining dull red to cyanescent then becoming dark brown to black. *Stipe* 5–13 cm long, 1–3.5(–4) cm broad, straight or curved, equal, subclavate to clavate, sometimes pinched at the base, dry, very finely scurfy to finely matted above and granulose ("punctate dotted" *fide* Li & Watling 1999) to fibrillose streaked below, sometimes with low, obscure ridges, pale mineral green to dull green (25–26–27E5, 4) above, pale lilac to dull violet (15E5) to nearly violet brown (9–10D4) below the apex, with a white to pinkish ochraceous base. *Flesh* white, cyanescent, soon pale reddish to dull red then becoming dark brown to black, sometimes with some deep lilac brown in

Table 1. Taxon names, Collection information, GenBank accession numbers, References.

Taxon	Voucher	Location	28S	*tef1*	*rpb2*	Reference(s)
Abtylopilus scabrosus	HKAS50211	China	KT990552	KT990752	KT990389	Li & Yang (2021)
Afroboletus multijugus	PC0723571	Burundi	—	KX869299	KX869426	Han *et al.* (2018)
Afrocastellanoa ivoryana	OSC150015	Zimbabwe	KX685721	KX685715	—	Orihara & Smith (2017)
Anthracoporus cystidiatus	HKAS55375	China	KT990622	KT990816	—	Wu *et al.* (2016b)
Anthracoporus holophaeus	HKAS50508	China	KF112465	KF112244	—	Wu *et al.* (2014)
Anthracoporus nigropurpureus	HKAS52685	China	KT990627	KT990821	KT990459	Wu *et al.* (2016b)
Boletus albobrunnescens	OR131	Thailand	—	KT824039	KT824006	Raspé *et al.* (2016)
Boletus edulis	Be3	Germany	KF030282	GU187682	GU187774	Nuhn *et al.* (2013), Binder *et al.* (2010)
Boletus reticuloceps	HKAS57671	China	KF112454	KF112201	KF112703	Wu *et al.* (2014)
Brasilioporus olivaceoflavidus	VIES9901322	Brazil	OM068912	OM160555	OM160576	Magnago *et al.* (2022)
Brasilioporus simoniarum	VIES9901327	Brazil	OM068914	OM160557	OM160577	Magnago *et al.* (2022)
Buchwaldoboletus lignicola	HKAS84904	Germany	KT990538	KT990740	KT990377	Wu *et al.* (2016b)
Chalciporus piperatus	HKAS84882	Germany	KT990562	KT990758	KT990397	Wu *et al.* (2016b)
Chalciporus rubinelloides	HKAS57362	China	KT990563	KT990759	KT990398	Wu *et al.* (2016b)
Guyanaporus albipodus	Henkel 8848	Guyana	LC043081	—	LC043083	Henkel *et al.* (2016)
Gyrodon lividus	REG Gl1	Germany	AF098378	GU187701	GU187786	Bresinsky *et al.* (1999), Binder *et al.* (2010)
Gyrodon sp.	HKAS59448	China	KF112349	KF112276	KF112818	Wu *et al.* (2014)
Imleria badia	HKAS53502	Germany	KC215213	KC215247	KC215235	Zhu *et al.* (2014)
Indoporus shoreae	AP6697	India	MK123976	—	MK243368	Parihar *et al.* (2018)
Indoporus squamulosus	HKAS107153	China	—	MT110335	MT110409	Li & Yang (2021)
Kgaria cyanogranulifera	NY1115382 (REH9153)	Australia	—	—	**OR263674**	this study
Kgaria cyanogranulifera	NY1115381 (REH9189)	Australia	**OR063859**	**OR232707**	**OR263675**	this study
Kgaria cyanogranulifera	NY1115380 (REH9196)	Australia	**OR063860**	—	**OR263676**	this study
Kgaria cyanogranulifera	NY1115418 (REH9207)	Australia	**OR063861**	—	**OR263677**	this study
Kgaria cyanogranulifera	NY1194100 (REH9359)	Australia	**OR063862**	**OR232708**	**OR263678**	this study
Kgaria cyanogranulifera	NY1194081 (REH9488)	Australia	**OR063863**	—	**OR263679**	this study
Kgaria cyanogranulifera	NY1194066 (REH9508)	Australia	JX889646	JX889688	**OR263680**	Halling *et al.* (2012), this study
Kgaria cyanogranulifera	NY1194065 (REH9527)	Australia	JX889647	JX889689	**OR263681**	Halling *et al.* (2012), this study
Kgaria cyanogranulifera	NY1194090 (REH9549)	Australia	**OR063864**	**OR232709**	**OR263682**	this study
Kgaria similis	NY1193974 (REH9031) TYPE	Australia	**OR063865**	—	**OR263683**	this study
Kgaria similis	NY1193966 (REH9033)	Australia	**OR063866**	—	**OR263684**	this study
Kgaria similis	NY1193839 (REH9406)	Australia	**OR063867**	**OR113660**	**OR263685**	this study
Kgaria similis	NY1193816 (REH9409)	Australia	**OR063868**	—	—	this study
Kgaria similis	NY1193840 (REH9426)	Australia	**OR063869**	—	**OR263686**	this study
Nevesoporus nigrostipitatus	VIES9901383	Brazil	OM068918	OM160562	—	Magnago *et al.* (2022)
Porphyrellus orientifumosipes	HKAS53372	China	KT990629	KT990823	KT990461	Wu *et al.* (2016b)
Porphyrellus porphyrosporus	MB97-023	Germany	DQ534643	GU187734	GU187800	Binder *et al.* (2010)
Porphyrellus porphyrosporus	HKAS48585	China	KT990543	KT990745	KT990382	Wu *et al.* (2016b)
Strobilomyces strobilaceus	MB001177	Germany	—	KX869313	KX869440	Han *et al.* (2014)
Strobilomyces sp.	HKAS59420	China	KF112463	KF112256	KF112810	Wu *et al.* (2014)
Tylopilus aurantiacus	HKAS59700	China	KF112458	KF112223	KF112740	Li & Yang (2021)
Tylopilus felleus	HKAS90203	China	KT990545	KT990913	KT990384	Wu *et al.* (2016b)
Tylopilus felleus	CFMR: BOS780	USA	MK601814	MK721168	MK766370	Kuo & Ortiz-Santana (2020)
Tylopilus violaceobrunneus	HKAS8944	China	KT990702	KT990886	KT990504	Wu *et al.* (2016b)

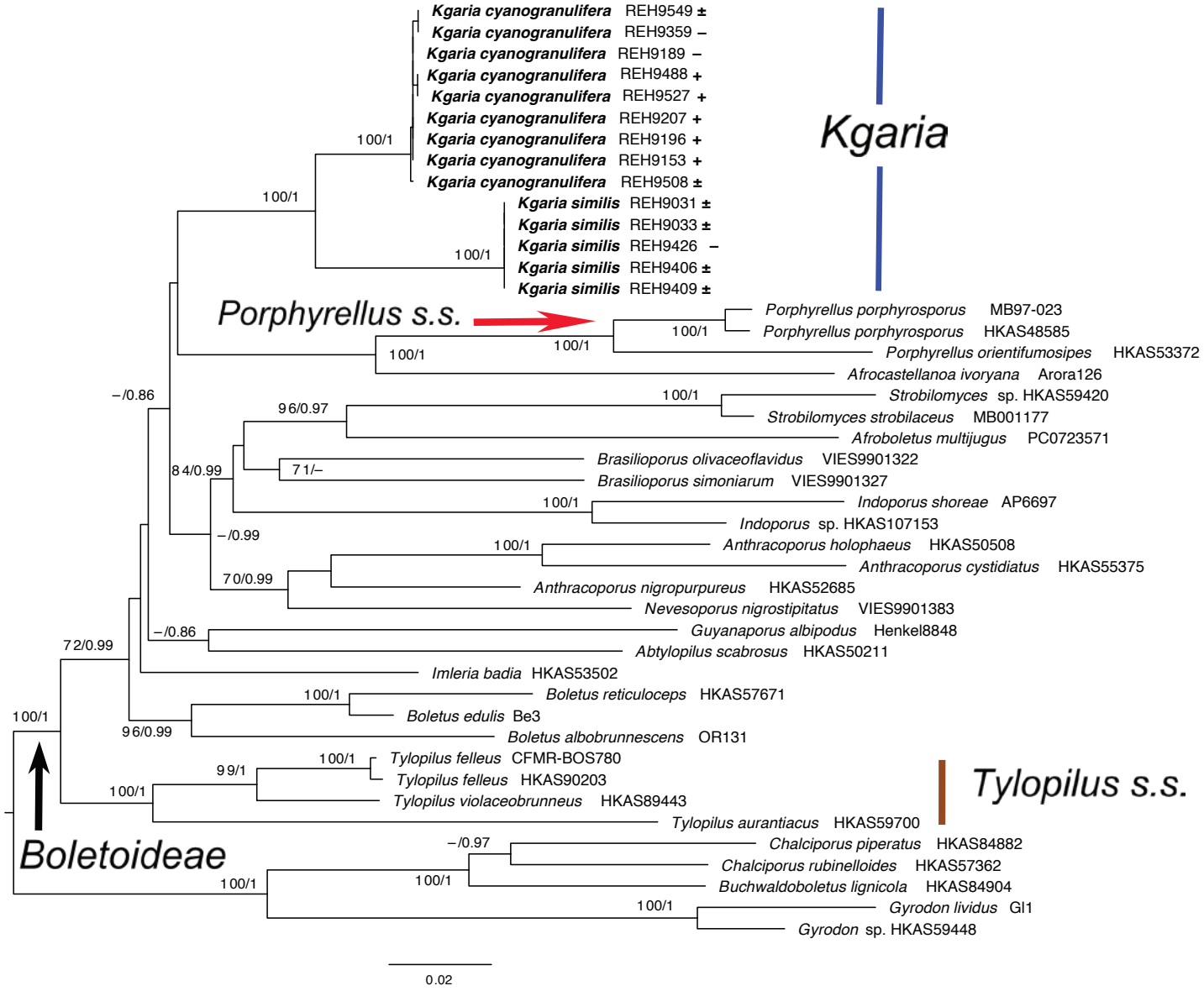

Fig. 1. Phylogenetic relationships and placement of *Kgaria* in the *Boletaceae* inferred from the combined large-subunit rDNA (nrLSU), translation elongation factor 1-alpha (*tef1*) and second largest subunit of RNA polymerase II (*rpb2*) dataset. The tree topology corresponds to the maximum likelihood (ML) tree in increasing order with midpoint rooting. Support values > 70 % bootstrap support (BS) are shown followed by Bayesian posterior probability (PP) values > 0.80. Symbols following the *Kgaria* exemplars denote presence (+), average abundance (±), or absence (–) of cyanogranules. Scale bar shows substitutions/site.

the stipe base. *Odor* mild or rarely mealy-earthy; *taste* mild.

Spores chocolate brown to cocoa brown to umber brown (5F8) in deposit, (11.5–)12.5–14.5(–16) × 3.5–4.5 µm, (*n* = 40; *x* = 13.82 × 4.19 µm; *Q* = 2.6–4.5), subfusiform to subcylindric, smooth, thin-walled, hyaline in KOH, weakly dextrinoid in Melzer's. *Basidia* 27–36 × 9–11 µm, clavate, with brown colloidal content or hyaline, 4-sterigmate. *Hymenial cystidia* 45–63 × 10–16 µm, abundant, ventricose to ventricose-rostrate, thin-walled, with uniformly brown or colloidal brown contents. *Hymenophoral trama* of the *Boletus*-subtype, with a central strand often with oleiferous elements, with divergent, lateral strata made up of hyphae 3–9 µm broad, hyaline. *Pileipellis* a suberect tangled trichodermium, with hyphae 10–20(–45) µm broad, some hyphae constricted at the septa, and palisadic, typically with scattered, fine, blue green encrusting pigment (cyanogranules) on pale olive-green walls in alkali, sometimes lacking cyanogranules; sometimes with pale blue green, thin walls, or with hyaline to pale brown encrusting pigment, otherwise hyaline to pale cinnamon brown or cocoa brown, with contents sometimes brown or deep blue green, and then occasionally almost oleiferous; *subpellis* sometimes blue green to olive green to pale blue in alkali. *Stipitipellis* often with cyanogranules and blue green hyphae, sometimes lacking cyanogranules and then hyphae hyaline to pale brown; *caulocystidia* usually clustered, 33–45 × 16–31 µm, short-clavate or short-ventricose with broad venter and short mucro, rarely sphaeropedunculate, then up to 79 × 34 µm; *subpellis* and *stipe context* sometimes pale blue green in alkali mounts, otherwise hyaline. *Clamp connections* absent.

Habit, habitat, distribution: Solitary to gregarious on sand or soil in rainforest or wet or dry sclerophyll bush presumably ectomycorrhizal with members of the *Myrtaceae* and *Casuarinaceae* (*Angophora costata*, *Allocasuarina*, *Eucalyptus*

Fig. 2. Basidiomata of *Kgaria cyanogranulifera*. **A.** *Halling 9153*. **B.** *Halling 9527*. Scale bars = 1 cm.

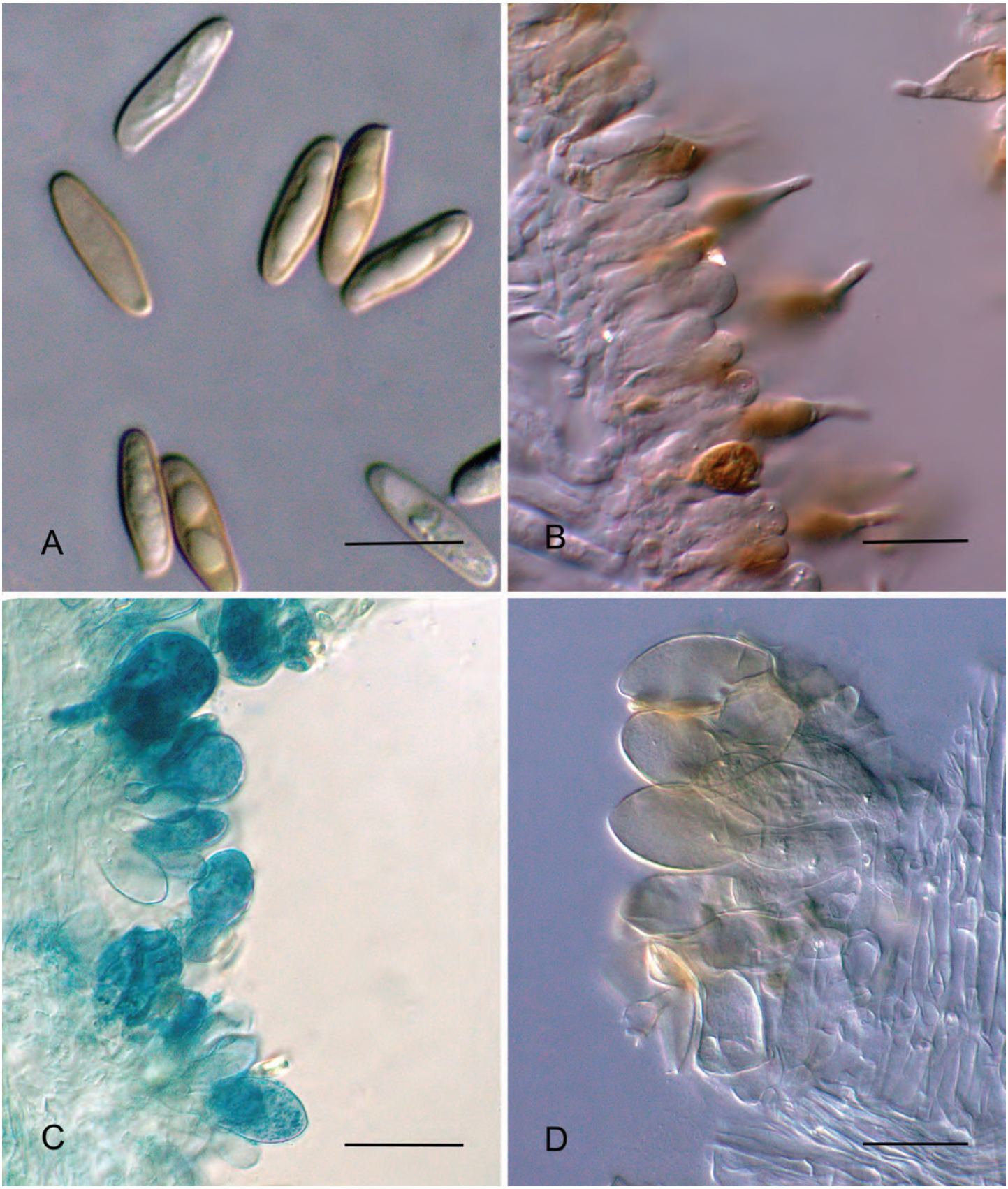

Fig. 3. Microscopic features of *Kgaria cyanogranulifera*. **A.** Basidiospores (*Halling 9153*). **B.** Hymenial cystidia (*Halling 9330*). **C.** Stipitipellis (*Halling 9549*). **D.** Stipitipellis (*Halling 9189*). Scale bars: A = 10 µm; B–D = 25 µm.

acmenoides, *E. botryoides*, *E. pilularis*, *E. racemosa*, *E. saligna*, *E. signata*, *Leptospermum*, *Lophostemon confertus*, *Syncarpia glomulifera*, *S. hillii*). So far, known only from Australia in New South Wales, Queensland, Tasmania, and Victoria.

Materials examined: **Australia**, Queensland, Wide Bay District, Great Sandy National Park, K'gari [Fraser Island], road from Central Station to Lake Birrabeen, 25.4972°S, 153.051°E, 160 m, 13 Feb. 2009, *R.E. Halling 9074* (BRI AQ0797943; NY1193997); K'gari [Fraser Island],

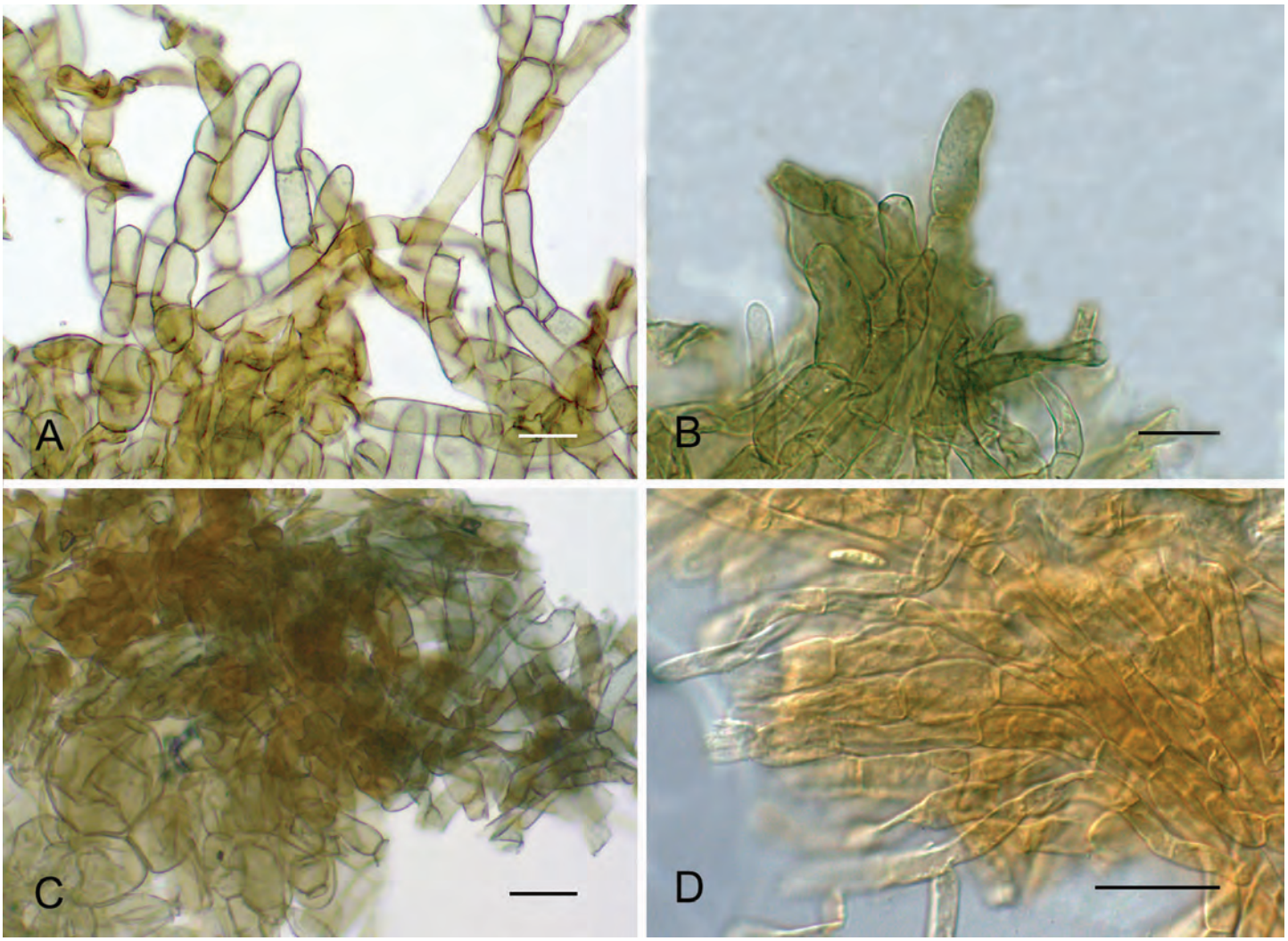

Fig. 4. Pileipellis of *Kgaria cyanogranulifera*. **A.** Palisadal orientation (*Halling 9344*). **B.** Palisadal orientation with cyanogranules (*BRI AQ0809781!*, holotype). **C.** Constricted hyphal septa and cyanogranules (*Halling 9344*). **D.** Constricted hyphal septa (*BRI AQ0809781!*, holotype). Scale bars = 20 µm.

Central Station, 25.4762°S, 153.056°E, 90 m, 2 Jun. 2009, *R.E. Halling 9125* (BRI; NY1115422); K'gari [Fraser Island], walking track S of Central Station, 25.48°S, 153.058°E, 155 m, 3 Jun. 2009, *R.E. Halling 9140* (BRI; NY1115388); K'gari [Fraser Island], Lake Birrabeen, 25.5008°S, 153.05°E, 117 m, 4 Jun. 2009, *R.E. Halling 9153* (BRI AQ0797781; NY1115382); K'gari [Fraser Island], roads from Central Station to Valley of the Giants, 25.4095°S, 153.086°E, 112 m, 6 Jun. 2009, *R.E. Halling 9170* (BRI AQ0797057; NY1115407); K'gari [Fraser Island], road from Wanggoolba Creek Ferry landing to Central Station, 25.4608°S, 153.024°E, 90 m, 7 Jun. 2009, *R.E. Halling 9189* (BRI AQ0794294; NY1115381); K'gari [Fraser Island], NE of Lake McKenzie, Lake McKenzie Road, 25.4409°S, 153.055°E, 115 m, 8 Jun. 2009, *R.E. Halling 9196* (BRI AQ0794301; NY1115380); K'gari [Fraser Island], Ungowa Road, 25.4585°S, 153.011°E, 24 m, 9 Jun. 2009, *R.E. Halling 9207* (BRI AQ0794312; NY1115418); K'gari [Fraser Island], Kingfisher Bay, 25.3932°S, 153.031°E, 8 m, 10 Jun. 2009, *R.E. Halling 9225* (BRI AQ0794328; NY1115411); K'gari [Fraser Island], Lake Wabby Lookout car park, 25.4529°S, 153.124°E, 141 m, 11 Jun. 2009, *R.E. Halling 9234* (BRI AQ0794334; NY1115385); K'gari [Fraser Island], Wanggoolba Creek Road, 25.4609°S, 153.024°E, 25 m, 29 Mar. 2010, *R.E. Halling 9307* (BRI AQ0875872; NY1115394); K'gari [Fraser Island], 6.9 km along Lake Garawongera Drive, 25.3246°S, 153.159°E, 176 m, 20 May 2010, *R.E. Halling 9330* (BRI AQ0794280; NY1193986); K'gari [Fraser Island], road from Eurong to Central Station, 25.4977°S, 153.098°E, 105 m, 22 May 2010, *R.E. Halling 9344* (BRI AQ0794252; NY 1115359); K'gari [Fraser Island], Kingfisher Bay, 25.3932°S, 153.031°E, 8 m, 24 May 2010, *R.E. Halling 9359* (BRI AQ0794251; NY1194100); K'gari [Fraser Island], Northern Road, 6.8 km N of Cornwells Road, 25.3904°S, 153.082°E, 129 m, 26 May 2010, *R.E. Halling 9384* (BRI AQ0794253; NY1115364); K'gari [Fraser Island], Valley of the Giants, 25.3854°S, 153.131°E, 130 m, 26 May 2010, *R.E. Halling 9391* (BRI AQ0794250; NY1115361); K'gari [Fraser Island], 3 km W of Central Station, Wanggoolba Creek Road, 25.4711°S, 153.036°E, 24 m, 18 Feb. 2011, *R.E. Halling 9431* (BRI AQ0796545; NY1193814); K'gari [Fraser Island], road from Eurong to Central Station, 25.5003°S, 153.102°E, 82 m, 17 May 2011, *R.E. Halling 9488* (BRI AQ0875871; NY1194081); K'gari [Fraser Island], Lake Birrabeen, 25.5008°S, 153.05°E, 117 m, 19 May 2011, *R.E. Halling 9508* (BRI AQ0875867; NY1194066); K'gari [Fraser Island], from Wanggoolba Road toward Bennett Road, 25.4712°S, 153.036°E, 24 m, 20 May 2011, *R.E. Halling 9527* (BRI AQ0796263; NY11940650); K'gari [Fraser Island], Lake Garawongera Road, 25.3252°S, 153.168°E, 150 m, 21 May 2011, *R.E. Halling 9536* (BRI AQ0875866; NY1194056); Cooloola, King's Bore track, 12 Dec. 1983, *JECA 83/45* (BRIP 19451; BRI AQ813159); Cooloola, near Frankis Gulch, 26.0478°S, 153.083°E, 68 m, 24 May 2011, *R.E. Halling 9549* (BRI AQ0875870; NY1194090); Cooloola, Freshwater Road, near Freshwater Camping Area, 25.9986°S, 153.144°E, 73 m, 11 Mar. 2012, *R.E. Halling 9692* (BRI AQ0798429; NY1491216); New South Wales, Central Coast, Palm Grove, 7 km W of intersection of Pacific Hwy and Ourimbah Creek Rd, O'Sullivan's Way, 33.3319°S, 151.308°E, 240 m, 13 Mar. 2017, *R.E. Halling 10152* (DAR83375; NY02686011);

Tasmania, Tasmanian Southern Ranges, Huon Valley, Duckhole Lake track, 43.3728°S, 146.892°E, 110 m, 4 Feb. 2014, *R.E. Halling 9874* (HO; NY02449678); Victoria, Gippsland Plain, Lang Lang Conservation Reserve (Adam's Creek), Vic. Grid Ref.: T 10, 60 m, 12 May 2005, *R.E. Halling 8688* (MEL2265012; NY1034455); Mornington Peninsula, Buckley Nature Reserve (Myers and Balnarring Roads [Melway 162 H8]), Vic. Grid Ref.: P 25, 7 May 2010, *N.H. Sinnott 3790* (MEL2341318; NY01293298); East Gippsland, Cape Conran-Sydenham Inlet Coastal Park, near Cape Conran Cabins, 20 m, 1 Jul. 2004, *J.M. Trappe 28325* (NY02072438).

Kgaria similis Halling, Fechner & Davoodian, ***sp. nov.*** MycoBank MB 848734. Figs 5–7.

Etymology: *similis* (Latin): like, resembling, or similar to *K. cyanogranulifera*.

Typus: **Australia**, Queensland, Wide Bay District, Great Sandy National Park, K'gari [Fraser Island], road between Lake Birrabeen and Lake Boomanjin, 25.4972°S, 153.051°E, 140 m, 8 Feb. 2009, *R.E. Halling 9031* (**holotype** BRI AQ0797944; **isotype** NY1193974).

Pileus 2.5–10.5 cm broad, convex to plano-convex, dry, viscid when wet but often dry when collected, even or sometimes finely wrinkled on the disc, appressed fibrillose, matted to matted subtomentose, then finely areolate to matted subsquamulose, dark brown to near violet brown (11F5–4) with pale brown between areoles, matted fibrillose at margin. *Tubes* adnate to adnexed, mineral greenish to pale olive to grayish yellow (4B4), staining blue green, then slowly red becoming black. *Stipe* 5–8.5 cm long, 1–2(–3.5) cm broad, strict, equal to subclavate to clavate-ventricose and then pinched at base, dry, subpruinose to matted to fibrillose streaked, very rarely slightly ridged, white to pale yellowish green to mineral greenish at apex, pale brown to brownish below, staining an obscure reddish color then brown to black when bruised, white to pinkish brown at base. *Flesh* white, cyanescent, becoming reddish orange or slowly dull red, then eventually black, with some blue staining above tubes. *Odor* mild to slightly pungent; *taste* rarely bitter.

Spores cocoa brown in deposit, (11–)12.5–16(–17) × 3.5–4.5(–5.5) µm, (*n* = 40; *x* = 13.93 × 4.16 µm; *Q* = 2.4–4.75), subfusiform to subcylindric, smooth, thin-walled, hyaline in KOH, weakly dextrinoid in Melzer's. *Basidia* 30–35 × 8–11 µm, subclavate to clavate, 4-sterigmate, hyaline and thin-walled. *Hymenial cystidia* 50–83 × 10–18 µm, abundant, ventricose to ventricose-rostrate, thin-walled, with uniformly brown or colloidal brown contents. *Hymenophoral trama* of the *Boletus*-subtype, with a central strand often with oleiferous elements, with lateral strata cells 3–9 µm broad, divergent, hyaline. *Pileipellis* a tangled trichodermium, becoming repent, with hyphae 4.5–9 µm broad, not palisadal, without constricted septa, brown walled, hyaline or with brown contents, occasionally with dull, pale olive walls, with some encrusting bands, and some rare scattered cyanogranules; *subpellis* sometimes with a pale blue to blue green color at junction with context in alkali. *Stipitipellis* with scattered, rare cyanogranules; *caulocystidia* 14–37 × 6–15 µm, narrowly clavate to rarely fusiform, with uniformly pale brown contents or sometimes blue green. *Stipe context hyphae* hyaline, sometimes with a pale blue green tint in alkali. *Clamp connections* absent.

Habit, *habitat*, *distribution*: Solitary to gregarious or sometimes cespitose, on soil or sand in wet or dry sclerophyll bush presumably ectomycorrhizal with members of the *Myrtaceae* and *Casuarinaceae* (*Allocasuarina*, *Eucalyptus*, *Leptospermum*, *Lophostemon*, *Syncarpia glomulifera*). So far, known only from Australia in Queensland and Victoria.

Materials examined: **Australia**, Queensland, Wide Bay District: Great Sandy National Park, K'gari [Fraser Island], road between Lake Birrabeen and Lake Boomanjin, 25.5106°S, 153.052°E, 110 m, 8 Feb. 2009, *R.E. Halling 9033*, (BRI; NY1193966); K'gari [Fraser Island], road from Pile Valley to Lake McKenzie, 25.4739°S, 153.064°E, 83 m, 23 Mar. 2010, *R.E. Halling 9243* (BRI AQ0875876; NY1115386); K'gari [Fraser Island], Wanggoolba Road, 25.4739°S, 153.036°E, 100 m, 24 Mar. 2010, *R.E. Halling 9261* (BRI AQ0875875; NY1115387); K'gari [Fraser Island], track from Central Station to Kingfisher Bay, 25.428°S, 153.061°E, 96 m, 28 Mar. 2010, *R.E. Halling 9289* (BRI AQ0875873; NY1115377); K'gari [Fraser Island], road from Eurong to Central Station, 25.4998°S, 153.103°E, 90 m, 15 Feb. 2011, *R.E. Halling 9406* (BRI AQ0796544; NY1193839); K'gari [Fraser Island], road from Central Station to Ungowa Road, 25.4621°S, 153.026°E, 33 m, 15 Feb. 2011, *R.E. Halling 9409* (BRI AQ0797784; NY1193816); K'gari [Fraser Island], along Cornwell's Road, 25.4146°S, 153.051°E, 95 m, 16 Feb. 2011, *R.E. Halling 9419* (BRI AQ0875898; NY1193815); K'gari [Fraser Island], Lake Birrabeen, 25.5008°S, 153.05°E, 117 m, 17 Feb. 2011, *R.E. Halling 9426* (BRI AQ0796262; NY1193840); Cooloola, Camp Milo, Western Firebreak, 25.9954°S, 153.075°E, 58–68 m, 25 Feb. 2012, *R.E. Halling 9635* (BRI; NY1491108). VICTORIA, Otway Plain, Colac Otway Shire, Carlisle State Park, Old Carlisle Track, 15.1 km W of Gellibrand, Vic. Grid Ref.: K 33, 100 m, 9 May 2005, *R.E. Halling 8683* (MEL2265007; NY1034454).

DISCUSSION

Two exemplars of *Kgaria cyanogranulifera* (*REH 9508*, NY1194066; *REH 9527*, NY1194065) were first included in a phylogenetic inference using nrLSU and *tef-1* by Halling *et al*. (2012b) where specimens were determined to be *Porphyrellus brunneus*. An 84 % bootstrap support in the extended dataset of that study inferred a clade with *Porphyrellus porphyrosporus* and *Strobilomyces floccopus* (= *strobilaceus*) as sister to the *K. cyanogranulifera* exemplars. Those same two exemplars, re-determined as *T. cyanogranulifer*, were used by Magnago *et al*. (2022) in a study of South American boletes with similar macromorphology. The inference offered there shows with less than 70 % ML support and less than 0.95 BPP support that *K. cyanogranulifera* is sister to two clades identified as various *Porphyrellus* spp., and with similarly weak support they were distant from *Porphyrellus s. str.*; those other *Porphyrellus* spp. had been re-evaluated by Li & Yang (2021) to represent another porphyrelloid genus, *Anthracoporus*. Orihara & Smith (2017) used the nrLSU and *tef-1* sequences from *REH 9527* (NY1194065) and inferred *P. brunneus* (*sensu* Halling *et al*. 2012b, = *K. cyanogranulifera*) was likewise a sister clade to *Porphyrellus s. str*. and the newly described *Afrocastellanoa*. Similarly, Wang *et al*. (2023) used the nrLSU and *tef-1* sequences from *REH 9508* (NY1194066) and inferred *P. brunneus* (*sensu* Halling *et al*. 2012b, = *K. cyanogranulifera*) and *Guyanaporus* and *Brasilioporus*, with 63 % bootstrap support, as a sister clade to *Porphyrellus s. str*. and *Afrocastellanoa*. Based on our 3-gene phylogenetic analyses offered here, a clade with additional Australian material (14 exemplars) of *Kgaria cyanogranulifera* and *K. similis* is supported as monophyletic with Bayesian

Fig. 5. Basidiomata of *Kgaria similis*. **A.** *Halling 9031* (holotype). **B.** *Halling 9419*. Scale bars = 2 cm.

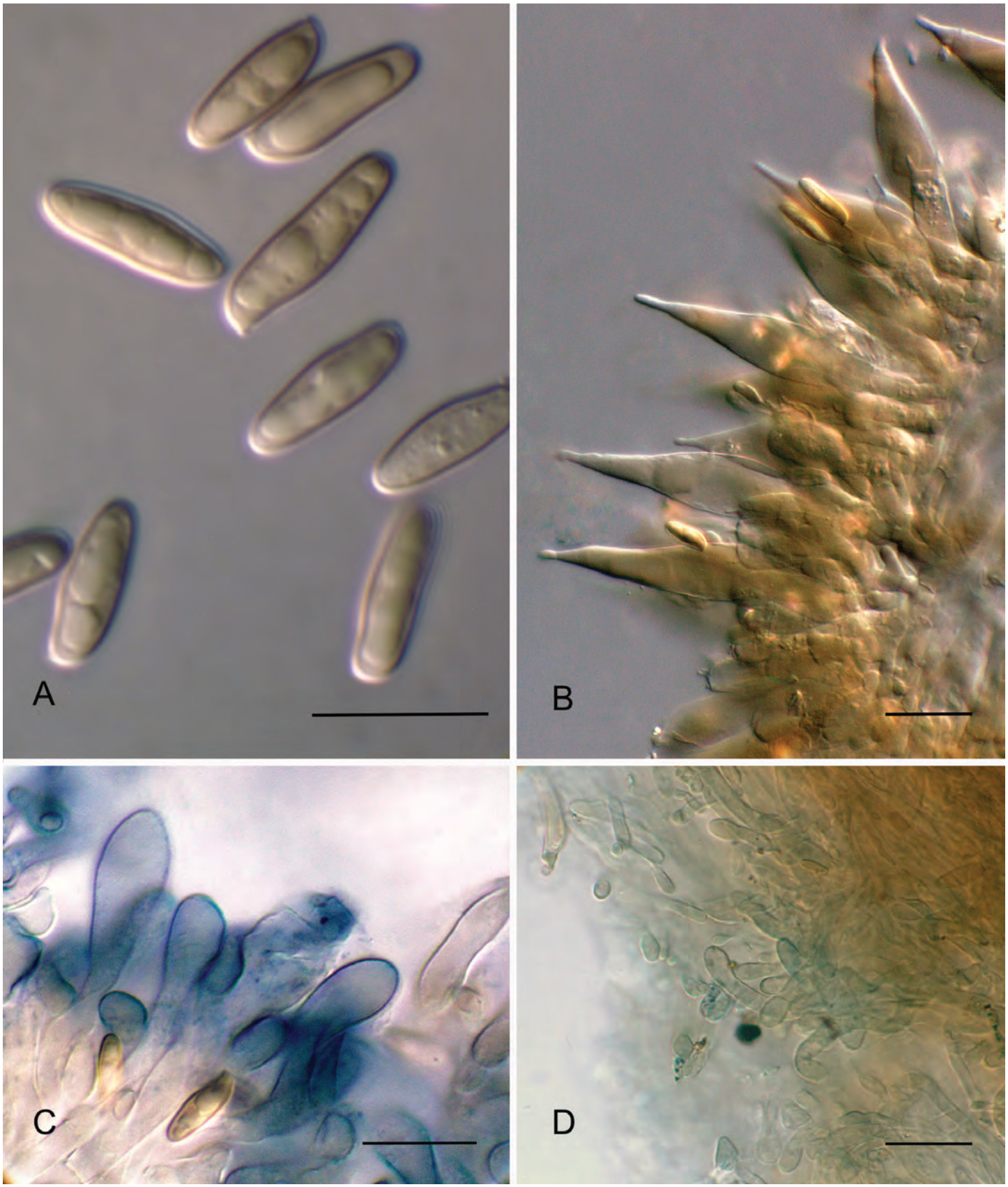

Fig. 6. Microscopic features of *Kgaria similis*. **A.** Basidiospores (*Halling 9261*). **B.** Hymenial cystidia (*Halling 9409*). **C.** Caulocystidia (*Halling 9426*). **D.** Stipitipellis with some cyanogranules (*Halling 9243*). Scale bars: A, C = 10 µm; B, D = 20 µm.

posterior probability of 1 and bootstrap support of 100 % as a separate and distinct clade sister to *Porphyrellus s. str*. from the Northern Hemisphere and *Afrocastellanoa* from Zimbabwe (Fig. 1), although the sister condition is poorly supported based on ML and BPP values. Thus, based on our study and inferences supported in the other four independent phylogenetic studies, we propose *Kgaria* as a separate genus encompassing two species.

An alternative hypothesis would be to consider *Kgaria* as a subgeneric entity in *Porphyrellus*. However, based on the

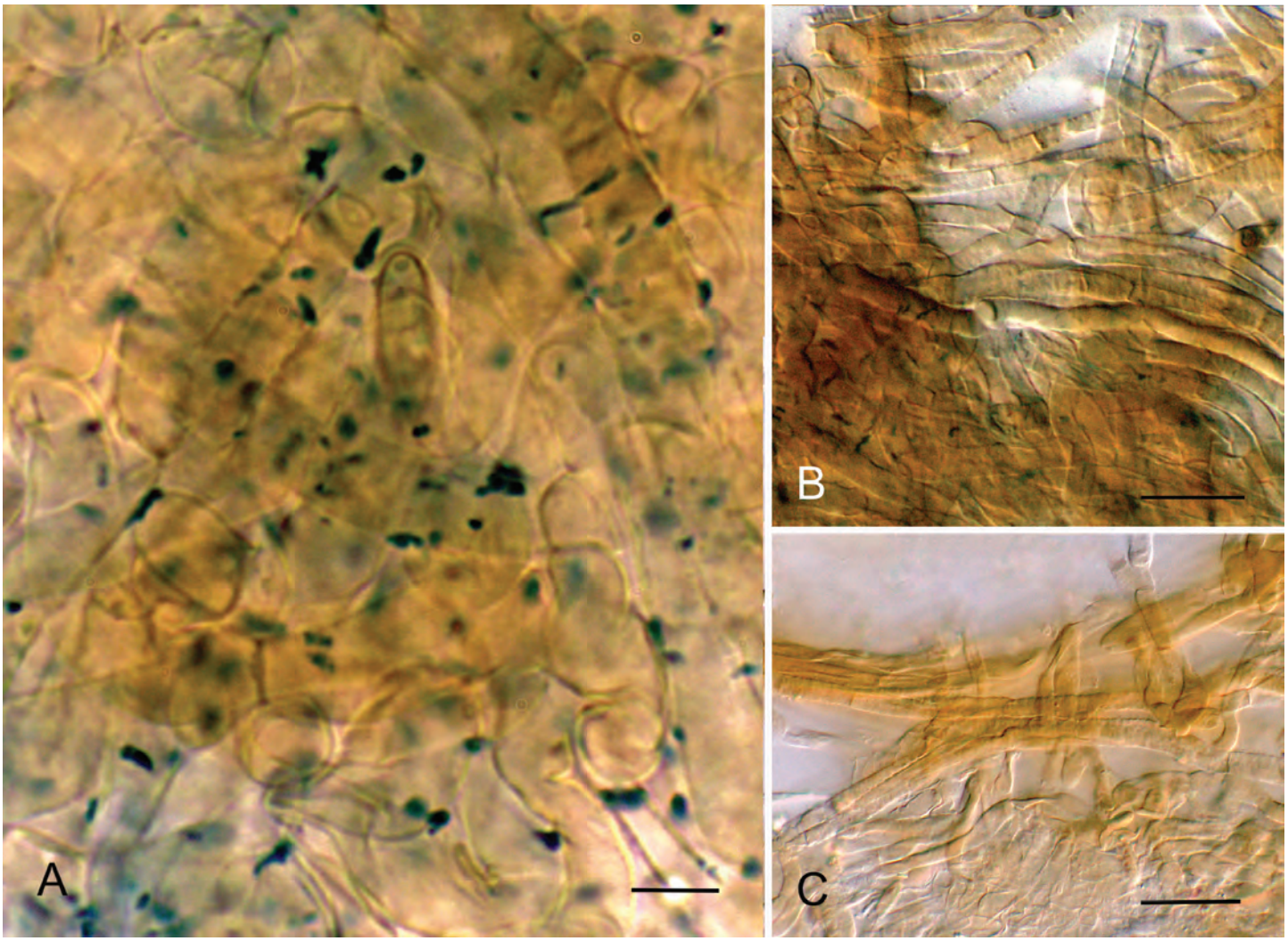

Fig. 7. Pileipellis of *Kgaria similis* **A.** Cyanogranules (*Halling 9406*). **B.** Portion of tangled, collapsed trichodermium with encrusted cells and cyanogranules (*Halling 9406*). **C.** Portion of tangled, collapsed trichodermium lacking cyanogranules (*Halling 9301*, holotype). Scale bars: A = 10 µm; B, C = 20 µm.

most recent morphological and 4-gene molecular phylogenetic analyses of *Porphyrellus* presented by Li & Yang (2021), there are enigmatic relationships among the taxa they infer as belonging in that genus. Further, any other hypothesis lumping *Kgaria* into any other existing genus except for the inclusive clade including *Boletus* is not strongly supported. If lumped into *Boletus*, then everything else, other than *Tylopilus* and the outgroups, would have to be lumped into *Boletus s. str*. as well, but even this clade only receives 72 % bootstrap support and 0.99 BPP. Our analyses on the other hand, show much stronger support for recognizing *Kgaria* as a distinct genus.

The predominance of cyanogranules and blue green pigments in alkaline solutions offer further support to differentiate *Kgaria* from all the other porphyrelloid entities that lack those features. Also, there is a considerable biogeographical disjunction. Based on the most recent treatment of *Tylopilus s. l.* (including *Porphyrellus*) by Li & Yang (2021), no other genera or species have been described as having cyanogranules or similarly colored hyphal walls in alkaline solutions. The two species of *Kgaria* are distinct in the molecular phylogeny and can be distinguished by differences in the pileipellis: *K. cyanogranulifera* has a trichodermium with broad, palisadic hyphae showing constricted septa; *K. similis* has a tangled, collapsing trichodermium that is not palisadic and with narrow hyphae lacking constricted septa. The stipitipellis of *K. cyanogranulifera* has cyanogranules and clusters of short-clavate to short-ventricose, sometimes sphaeropedunculate caulocystidia, whereas *K. similis* rarely possesses cyanogranules and the caulocystidia are narrowly clavate to sometimes fusiform. However, they might not be easy to differentiate in the field, but *K. cyanogranulifera* usually exhibits a lilac to pale violet pigmentation on the upper part of the stipe (Fig. 2); such colors are lacking in *K. similis* (Fig. 5).

The original descriptions of *T. olivaceoporus* and *T. cyanogranulifer* refer to the presence of cyanogranules for both species. Both type specimens consist of one half of a basidioma each. Cyanogranules were usually present in both type specimens and obvious in any given section of the pileus or stipe, but depending on the random location of a section, cyanogranules were either present or absent. Descriptions of the stipitipellis in the protologues are lacking, but based on our examinations, the caulocystidial morphology and arrangement along with the distribution of cyanogranules and blue green hyphal wall pigmentation are additional characteristic features. Both holotypes of *T. cyanogranulifer* and *T. olivaceoporus* possess the same anatomical features in the pileipellis and stipitipellis, and thus are considered taxonomic synonyms.

There is variation in the presence/absence and abundance of cyanogranules among our specimens cited above (Fig. 1). For

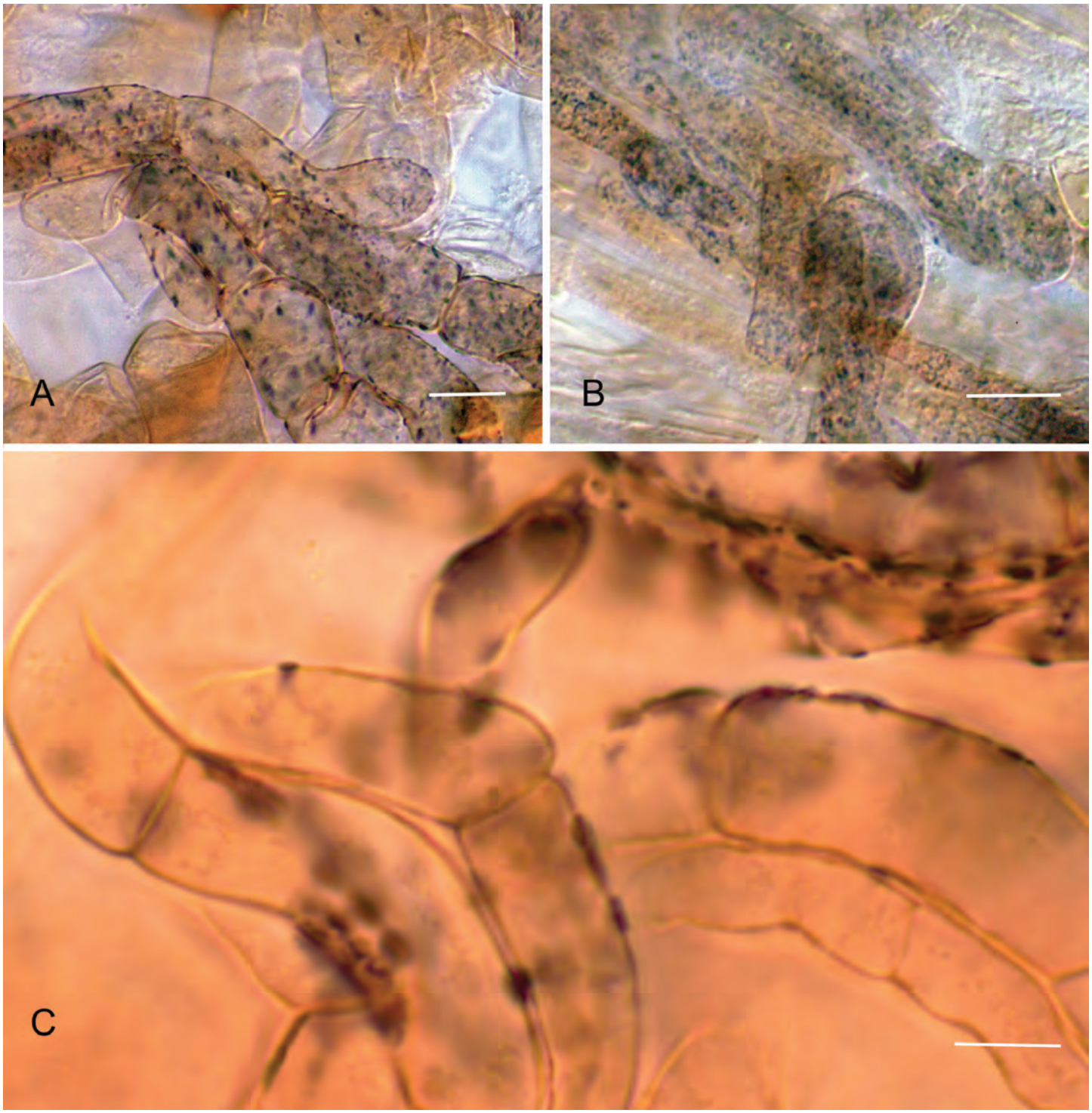

Fig. 8. Pileipellis and stipitipellis of *Kgaria cyanogranulifera* in water and Melzer's mounts. **A.** Pileipellis in water (*Halling 9153*). **B.** Stipitipellis in water (*Halling 9153*). **C.** Pileipellis in Melzer's (*Halling 9508*). Scale bars: A, B = 10 µm; C = 5 µm.

example, one sequenced specimen (Fig. 3D, *Halling 9189*) seems to completely lack the cyanogranules, but the phylogenetic analyses infer it as the same species as another sequenced specimen (Fig. 4C, *Halling 9549*). The latter has an abundance of blue green hyphae, cyanogranules are usually present, and the other micro-morphological features are similar. It is important to note that solutions of alkali for microscopic examinations, either KOH or NH_4OH, need to be fresh, or the blue green reactions will not appear. It is also noteworthy that the cyanogranules, if present, will be visible in mounts of Melzer's or water, but the blue green reaction is absent (Fig. 8).

The expanded distribution of *Kgaria* from subtropical southern Queensland to temperate regions in SE Australia is the result of detailed, broader exploration of understudied areas. Further research for new taxa and additional exemplars for genomic sequencing, should help to resolve more firmly the relationships between *Kgaria* and allied taxa. We would suggest that *T. beelii* and *T. violaceus* described by Heinemann (1951, 1966) from Africa need further investigation as to their generic placement and potential relationship to *Kgaria*. It is also clear that some obvious characters, such as similar or different colors of various parts of the basidiomata (including spore color and ornamentation) and various oxidation reactions are widespread within the *Boletaceae*, but not all relationships have been

sufficiently and rigorously resolved via molecular phylogenetics. In general terms, the study presented here is just another step in an effort to understand and describe the diversity of Australian bolete species. There are still many taxa to be discovered and properly documented, especially from underexplored areas elsewhere in the Southern Hemisphere. For example, some boletes included in the field guide to Tasmanian fungi by Gates & Ratkowsky (2014) most likely represent additional new taxa.

ACKNOWLEDGEMENTS

We acknowledge the Traditional Owners and Custodians of lands throughout Australia, and pay our respects to Elders past, present and emerging. The senior author (REH) is grateful to the National Science Foundation (USA) for funding under grants (DEB #0414665, and DEB #1020421 with M. Binder, D. Hibbett) and to the National Geographic Society Committee for Research and Exploration (USA) for funding under grant #8457–08. Governmental agencies in New South Wales, Queensland, Victoria, and Tasmania are thanked for permission to collect specimens in bushlands under their supervision. The Queensland Herbarium (BRI) provided assistance and logistical support to REH for herbarium and field studies while in Queensland, and facilitated access to critical herbarium specimens. Herbaria in New South Wales (DAR), Victoria (MEL), and Tasmania (HO) also assisted in deposition of newly collected specimens. The Queensland Parks and Wildlife Service offered accommodation and orientation at K'gari. J. Ackerfield, A. Wilson, M. Yousse (DBG) and E. Sessa, L. Briscoe (NY) kindly facilitated loans of specimens for REH. REH is especially grateful to L. Briscoe for her forensic work and patience in locating relevant specimens deposited in NY. O. Khmelnitsky and P. Singh helped with DNA extractions and PCR in the L.B. & D. Cullman Laboratory at the New York Botanical Garden. We are indebted to S. Abell, T. Baroni, N. Bougher, M. Castellano, E. Cox, I. Dodd, G. Gates, F. Guard, T. Lebel, S. McMullan-Fisher, G. Mueller, T. Osmundson, P. & J. O'Sullivan, C. Pearce, K. Querengasser, D. Ratkowsky, R. Robinson, K. Syme, J. Trappe, and J. & T. Van Der Heul for field assistance and logistical guidance at various sites in New South Wales, Queensland, Tasmania, Victoria, and Western Australia. We are grateful to P.B. Matheny, B. Thiers and E. Vellinga for helpful comments and suggestions as well as input from anonymous reviewers.

Conflict of interest: The authors declare that there is no conflict of interest.

REFERENCES

Binder M, Larsson K-H, Matheny PB, *et al.* (2010). *Amylocorticiales ord. nov*. and *Jaapiales ord. nov.*: Early diverging clades of *Agaricomycetidae* dominated by corticioid forms. *Mycologia* **102**: 865–880.

Bougher NL, Thiers HD (1991). An indigenous species of *Leccinum* (*Boletaceae*) from Australia. *Mycotaxon* **42**: 255–262.

Bresinsky A, Jarosch M, Fischer M, *et al*. (1999). Phylogenetic relationships within *Paxillus s.l.* (*Basidiomycetes, Boletales*): Separation of a Southern Hemisphere genus. *Plant Biology* **1**: 327–333.

Castellano MA, Trappe JM, Malajczuk N (1992). Australasian truffle-like Fungi. III. *Royoungia gen. nov*. and *Mycoamaranthus gen. nov*. (*Basidiomycotina*). *Australian Systematic Botany* **5**: 613–616.

Crous PW, Cowan DA, Maggs-Kölling G, *et al*. (2020). Fungal Planet description sheets: 1112–1181. *Persoonia* **45**: 251–409.

Crous PW, Osieck ER, Jurjević Ž, *et al*. (2021). Fungal Planet description sheets: 1284–1382. *Persoonia* **47**: 178–374.

Davoodian N, Bergemann SE, Hosaka K, *et al*. (2018). A global view of *Gyroporus*: molecular phylogenetics, diversity patterns, and new species. *Mycologia* **110**: 985–995.

Davoodian N, Bougher NL, Fechner NA, *et al*. (2019). Three new species of *Gyroporus* (*Boletales, Basidiomycota*) from Australia. *Muelleria* **37**: 101–107.

Davoodian N, Lebel T, Castellano MA, *et al*. (2021). *Hysterangiales* revisited: expanded phylogeny reveals new genera and two new suborders. *Fungal Systematics and Evolution* **8**: 65–80.

Fechner N, Bonito G, Bougher NL, *et al*. (2017). New species of *Austroboletus* (*Boletaceae*) in Australia. *Mycological Progress* **16**: 769–775.

Gates G, Ratkowsky D (2014). *A Field Guide to Tasmanian Fungi*, Tasmanian Field Naturalists Club, Hobart.

Gelardi M, Fechner N, Halling RE, *et al*. (2017). *Gymnogaster boletoides* J.W. Cribb (*Boletaceae, Boletales*), a striking Australian secotioid bolete. *Austrobaileya* **10**: 121–129.

Halling RE, Fechner N (2011). *Heimioporus* (*Boletineae*) in Australia. *Australasian Mycologist* **29**: 47–51.

Halling RE, Osmundson TW, Neves M-A (2006). *Austroboletus mutabilis sp. nov*. from Northern Queensland. *Muelleria* **23**: 31–36.

Halling RE, Osmundson TW, Neves M-A (2008). Pacific boletes: Implications for biogeographic relationships. *Mycological Research* **112**: 437–447.

Halling RE, Nuhn M, Fechner NA, *et al*. (2012a). *Sutorius*: a new genus for *Boletus eximius*. *Mycologia* **104**: 951–961.

Halling RE, Nuhn M, Osmundson T, *et al.* (2012b). Affinities of the *Boletus chromapes* group to *Royoungia* and the description of two new genera, *Harrya* and *Australopilus*. *Australian Systematic Botany* **25**: 418–431.

Halling RE, Desjardin DE, Fechner N, *et al*. (2014). New porcini (*Boletus* sect. *Boletus*) from Australia and Thailand. *Mycologia* **106**: 830–834.

Halling RE, Fechner N, Nuhn M, *et al*. (2015). Evolutionary relationships of *Heimioporus* and *Boletellus* (*Boletales*), with an emphasis on Australian taxa including new species and new combinations in *Aureoboletus*, *Hemileccinum*, and *Xerocomus*. *Australian Systematic Botany* **28**: 1–22.

Han LH, Feng B, Wu G, *et al.* (2018). African origin and global distribution patterns: Evidence inferred from phylogenetic and biogeographical analyses of ectomycorrhizal fungal genus *Strobilomyces*. *Journal of Biogeography* **45**: 201–212.

Heinemann P (1951). Champignons récoltés au Congo belge par Madame M. Goossens-Fontana I. *Boletineae*. *Bulletin du Jardin botanique de l'État à Bruxelles* **21**: 223–346.

Heinemann P (1966). *Hygrophoraceae*, *Laccaria et Boletineae* II (complément). *Flore Iconographique de Champignons du Congo* **15**: 279–308.

Henkel TW, Obase K, Husbands D, *et al.* (2016). New *Boletaceae* taxa from Guyana: *Binderoboletus segoi gen*. and *sp. nov*., *Guyanaporus albipodus gen*. and *sp. nov*., *Singerocomus rubriflavus gen*. and *sp. nov*., and a new combination for *Xerocomus inundabilis*. *Mycologia* **108**: 157–173.

Hilton RN (1982). A census of the larger fungi of Western Australia. *Journal of the Royal Society of Western Australia* **65**: 1–15.

Katoh K, Rozewicki J, Yamada KD (2017). MAFFT online service: multiple sequence alignment, interactive sequence choice and visualization. *Briefings in Bioinformatics* **20**: 1160–1166.

Khmelnitsky O, Davoodian N, Singh P, *et al.* (2019). *Ionosporus*: a new genus for *Boletus longipes* (*Boletaceae*), with a new species, *I*.

australis, from Australia. *Mycological Progress* **18**: 439–451.
Kornerup A, Wanscher JH (1983). *Methuen Handbook of Colour*, 3rd ed. reprint, Eyre Methuen, Ltd, London.
Kuo M, Ortiz-Santana B (2020). Revision of leccinoid fungi, with emphasis on North American taxa, based on molecular and morphological data. *Mycologia* **112**: 197–211
Li T-H, Watling R (1999). New taxa and combinations of Australian boletes. *Edinburgh Journal of Botany* **56**: 143–148.
Li Y-C, Yang ZL (2021). *The Boletes of China*: *Tylopilus s.l.* Science Press, Beijing and Springer Nature, Singapore.
Magnago AC, Alves-Silva G, Henkel TW, *et al.* (2022). New genera, species and combinations of *Boletaceae* from Brazil and Guyana. *Mycologia* **114**: 607–625.
Miller MA, Pfeiffer W, Schwartz T (2011). The CIPRES science gateway: a community resource for phylogenetic analyses. In: *Proceedings of the 2011 TeraGrid Conference: Extreme Digital Discovery*. Article 41: 1–8. doi.org/10.1145/2016741.2016785.
Nuhn ME, Binder M, Taylor AFS, *et al.* (2013). Phylogenetic overview of the *Boletineae*. *Fungal Biology* **117**: 479–511.
Orihara T, Smith ME (2017). Unique phylogenetic position of the African truffle-like fungus, *Octaviania ivoryana* (*Boletaceae, Boletales*), and the proposal of a new genus, *Afrocastellanoa*. *Mycologia* **109**: 323–332.
Osmundson TW, Bougher NL, Robinson RM, *et al.* (2021). *Rubinoboletus phaseolisporus* (*Boletaceae*) from Western Australia is a *Tylopilus* with bean-shaped spores. *Nuytsia* **32**: 87–97.
Parihar A, Hembrom ME, Vizzini A, *et al*. (2018). *Indoporus shoreae gen. et sp. nov.* (*Boletaceae*) from tropical India. *Cryptogamie*, *Mycologie* **39**: 447–466.
Raspé O, Vadthanarat S, De Kesel A, *et al.* (2016). *Pulveroboletus fragrans*, a new *Boletaceae* species from northern Thailand, with a remarkable aromatic odor. *Mycological Progress* **15**: 38.
Ronquist F, Teslenko M, Van Der Mark P, *et al*. (2012). MrBayes 3.2: efficient Bayesian phylogenetic inference and model choice across a large model space. *Systematic Biology* **61**: 539–542.
Stamatakis A (2014). RAxML Version 8: A tool for Phylogenetic Analysis and Post-Analysis of Large Phylogenies. *Bioinformatics* **30**: 1312–1313.
Thiers BM (2023 continuously updated). Index Herbariorum: A global directory of public herbaria and associated staff. New York Botanical Garden's Virtual Herbarium. http://sweetgum.nybg.org/science/ih.
Trappe JM, Castellano MA, Halling RE, *et al*. (2013). Australian sequestrate fungi 18: *Solioccasus polychromus gen. & sp. nov*., a richly colored, tropical to subtropical, hypogeous fungus. *Mycologia* **105**: 888–895.
Wang Y, Wang L-Y, Dai D, *et al*. (2023). *Boletaceae* in China: Taxonomy and phylogeny reveal a new genus, two new species, and a new record. *Frontiers in Microbiology* **13**: 1052948.
Watling R, Gregory NM (1986). Observations on the boletes of the Cooloola Sandmass, Queensland and notes on their distribution in Australia. *Proceedings of the Royal Society of Queensland* **97**: 97–128.
Watling R, Gregory NM (1988a). Observations on the boletes of the Cooloola Sandmass, Queensland and notes on their distribution in Australia. Part 2A. Smooth spored taxa — Introduction, keys, references. *Proceedings of the Royal Society of Queensland* **99**: 45–63.
Watling R, Gregory NM (1988b). Observations on the boletes of the Cooloola Sandmass, Queensland and notes on their distribution in Australia. Part 2B: Smooth spored taxa of the family *Gyrodontaceae* and the genus *Pulveroboletus*. *Proceedings of the Royal Society of Queensland* **99**: 65–76.
Watling R, Gregory NM (1989a). Observations on the boletes of the Cooloola Sandmass, Queensland and notes on their distribution in Australia Part 2C: Smooth spored taxa —*Strobilomycetaceae*. *Proceedings of the Royal Society of Queensland* **100**: 13–30.
Watling R, Gregory NM (1989b). Observations on the boletes of the Cooloola Sandmass, Queensland and notes on their distribution in Australia Part 2D: Smooth spored taxa —*Boletaceae*, *Xerocomaceae*. *Proceedings of the Royal Society of Queensland* **100**: 31–47.
Watling R, Gregory NM (1991). Observations on the boletes of the Cooloola Sandmass, Queensland and notes on their distribution in Australia: Part 3. Lamellate taxa. *Edinburgh Journal of Botany* **48**: 353–391.
Watling R, Li T-H (1999). *Australian Boletes: A Preliminary Survey.* Royal Botanic Garden, Edinburgh.
Wolfe CB, Bougher NL (1993). Systematics, mycogeography, and evolutionary history of *Tylopilus* subg. *Roseoscabra* in Australia elucidated by comparison with Asian and American species. *Australian Systematic Botany* **6**: 187–213.
Wu G, Feng B, Xu J, *et al.* (2014). Molecular phylogenetic analyses redefine seven major clades and reveal 22 new generic clades in the fungal family *Boletaceae*. *Fungal Diversity* **69**: 93–115.
Wu G, Li Y-C, Zhu X-T, *et al.* (2016). One hundred noteworthy boletes from China. *Fungal Diversity* **81**: 25–188.
Zhu X-T, Li Y-C, Wu G, *et al.* (2014). The genus *Imleria* in East Asia. *Phytotaxa* **191**: 81–98.

Supplementary information

File S1. Concatenated 3-gene (nrLSU, *tef1*, *rpb2*) DNA alignment of *Kgaria*.

FUSE

Fungal Systematics and Evolution

Volume 12
DECEMBER 2023
PAGES 47–57

doi.org/10.3114/fuse.2023.12.03

Fulvifomes wrightii (*Hymenochaetales*), a new species related to *F. robiniae* from Argentina and Paraguay

M. Martínez[1,2*], C.A. Salvador-Montoya[2,3], A. de Errasti[1,2], O.F. Popoff[3], M. Rajchenberg[1,2]

[1]Centro Forestal CIEFAP - CONICET, CC14, 9200 Esquel, Chubut, Argentina, Ruta 259 km 16.2, 9200 Esquel, Chubut, Argentina
[2]Consejo Nacional de Investigaciones Científicas y Técnicas (CONICET), Buenos Aires, Argentina
[3]Instituto de Botánica del Nordeste (IBONE - CONICET), Sargento Cabral 2131, W3402BKG Corrientes, Argentina

*Corresponding author: M. Martínez, mariby9@gmail.com

Key words:
distribution
host
Hymenochaetaceae
new taxa
phylogenetic analysis
taxonomy

Abstract: Morphological revision and phylogenetic analysis based on nITS and nLSU of specimens previously considered to be a species related to *Fulvifomes robiniae* from South America revealed a new species of *Fulvifomes*, *i.e*. *Fulvifomes wrightii*. It grows on *Libidibia paraguariensis*, a *Fabaceae* distributed in the Chaco Region. The new species is characterised by a perennial, ungulate basidioma with a rimose pileal surface, 6–7 pores per mm, a homogenous context, indistinct stratified tubes and abundant crystals in tube trama and hymenia. Illustrations, taxonomic analyses and a key to the *Fulvifomes* species recorded from the Americas is provided.

Citation: Martínez M, Salvador-Montoya CA, de Errasti A, Popoff OF, Rajchenberg M (2023). *Fulvifomes wrightii* (*Hymenochaetales*), a new species related to *F. robiniae* from Argentina and Paraguay. *Fungal Systematics and Evolution* **12**: 47–57. doi: 10.3114/fuse.2023.12.03
Received: 26 May 2023; **Accepted:** 18 July 2023; **Effectively published online:** 28 July 2023
Corresponding editor: P.W. Crous

INTRODUCTION

Fulvifomes (Murrill 1914) is characterised by perennial basidiomata with or without a crust on the pileal surface, a monomitic to dimitic hyphal system, with or without dark lines in the context, and subglobose to ellipsoid, yellowish basidiospores, occasionally with a flattened side that turn darker in KOH solution (Zhou 2014, Salvador-Montoya *et al.* 2018, 2022). For many decades the genus was considered a synonym of *Phellinus* (*Phellinus s.l.*) or a subgenus of *Phellinus* (Dai 1999). However, molecular studies confirmed that *Fulvifomes* is a distinct taxon (Wagner & Fisher 2001, 2002). Wagner & Fischer (2002), Larsson *et al*. (2006) and Dai (2010) showed that *Fulvifomes* is closely related to *Aurificaria luteoumbrina* in their phylogenetic inferences. Currently, *Aurificaria* is considered a synonym of *Fulvifomes* (Zhou 2014). Ecologically, *Fulvifomes* includes species that grow on dead trunks and living angiosperm trees in temperate and tropical regions (Salvador-Montoya *et al*. 2018, Olou *et al.* 2019, Wu *et al.* 2022).

Fulvifomes robiniae (type species of the genus) is considered a parasitic polypore of *Robinia* species (recurrent host is *R. pseudoacacia*) in temperate North America (Salvador-Montoya *et al.* 2018). This species was related to *Fulvifomes rimosus* (Kotlaba & Pouzar 1978). However, Kotlaba & Pouzar (1978, 1979) showed *F. robiniae* and *F. rimosus* to exhibit morphological differences in the shape of pileal and pore surfaces, as well as in the size of basidiospores. Furthermore, *F. robiniae* was initially considered to have a variable morphology and wide geographic distribution in North and Central America (USA, Bahamas, Puerto Rico and Jamaica) (Kotlaba & Pouzar 1978, 1979, Gilbertson & Ryvarden 1987). Nevertheless, based on morphological, ecological and molecular data, Salvador-Montoya *et al.* (2018, 2022) have shown that specimens resembling *F. robiniae* from different parts of the Americas correspond to different entities.

During surveys in Paraguay and Argentina, specimens that resemble *F. robiniae* were collected in the Chaco Region of both countries. The aim of the present study was to taxonomically establish and describe a new species within the *F. robiniae* complex in the Chaco region in South America.

MATERIAL AND METHODS

Morphological studies

The specimens studied are deposited in the Fungarium of the Centro de Investigación y Extensión Forestal Andino Patagónico (HCFC) and Fungarium CTES. Morphological and microscopic procedures follow Robledo & Urcelay (2009). Colours were determined following Kornerup & Wanscher (1978). Spores were measured from sections from the tubes of basidiomata. For the spore measurements ImageJ software was used (González 2018). The following abbreviations were used: KOH = 5 % potassium hydroxide, IKI = Melzer's reagent, IKI– = neither amyloid nor dextrinoid, CB = cyanophilous, CB– = acyanophilous, L = mean spore length (arithmetic mean of all spores), W = mean spore width (arithmetic average of all spores), Q = variation in L/W ratios among specimens studied, n = number of spores

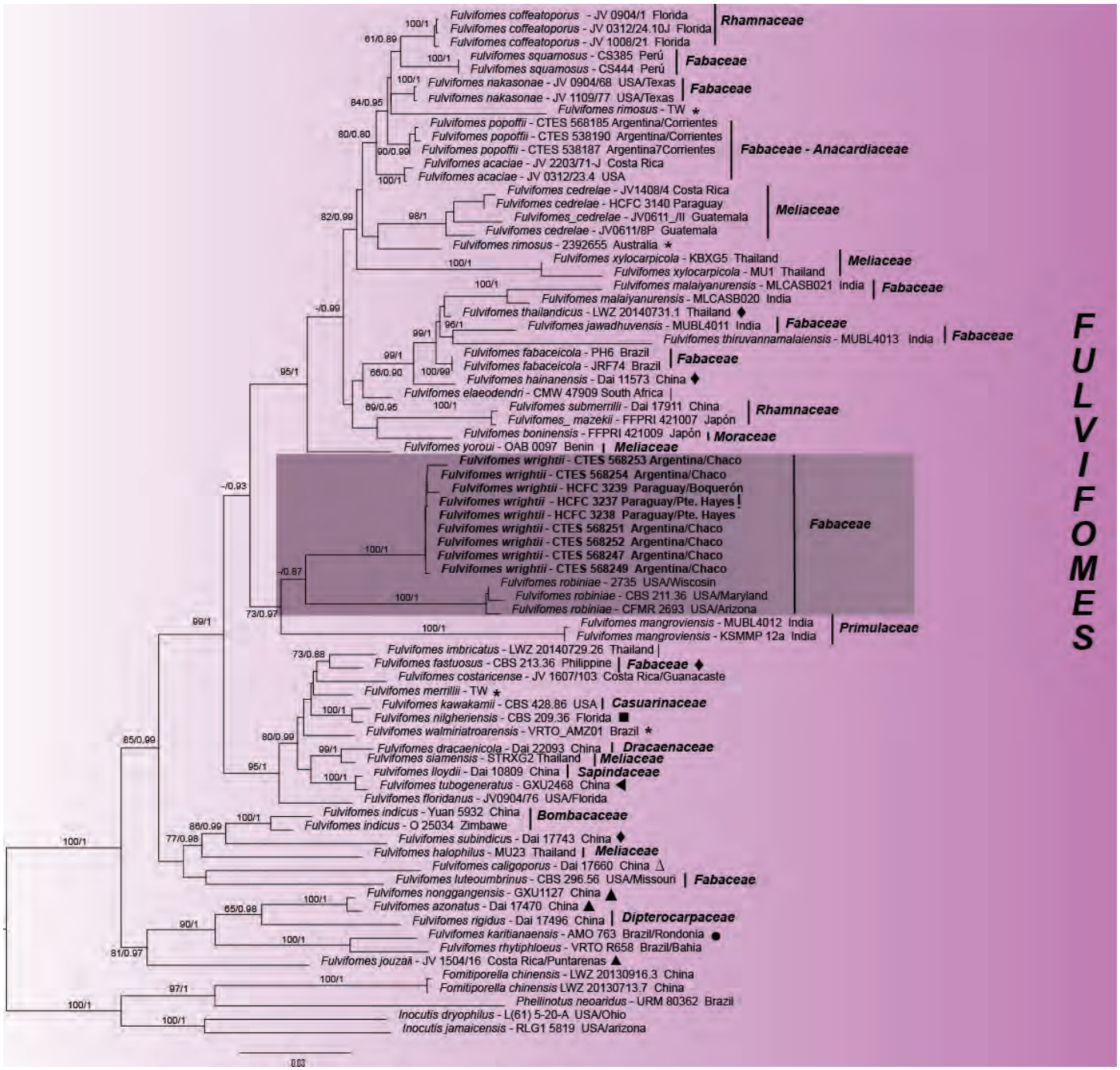

Fig. 1. Maximun likelihood (ML) tree of *Fulvifomes* based on dataset of ITS and nLSU sequences. Bayesian posterior probability above 0.80 and bootstrap values above 60 % are shown. Species studied in this work are in bold and the different substrates on which the species in the genus grow (! = type material; ♦ = angiosperm; ▲ = dead angiosperm; ◀ = living angiosperm; *= decaying wood; ● =dead deciduous wood; ■ dead trunk; Δ = unknown).

measured from a given number of specimens. The maps were prepared with QGIS 3.12 "Bucuresti" free software (https://www.qgis.org/en/site/).

Isolates

A fungal culture was obtained from the basidiomata by transferring small pieces from the context or tubes to Petri dishes containing 2 % malt extract agar (MEA) (Nobles 1965, Rajchenberg & Greslebin 1995) and deposited in the Culture Collection of Centro de Investigación y Extensión Forestal Andino Patagónico (CIEFAPcc).

DNA extraction, PCR amplification and sequencing

Extraction of total genomic DNA from dried basidiomata and culture followed the protocol of Doyle & Doyle (1990) modified by Tamari & Hinkley (2016). Primers pairs LR0R, LR5 and LR7 (Vilgalys & Hester 1990) were used to amplify nLSU sequences, while the ITS region was amplified using primers ITS1 and ITS4 (White *et al.* 1990). The PCR procedure for ITS and LSU followed Ji *et al.* (2017). For ITS the amplification was: initial denaturation at 95 °C for 3 min, followed by 35 cycles at 94 °C for 40 s, 54 °C for 45 s, and 72 °C for 1 min, and a final extension of 72 °C for 10 min. For nLSU the amplification was: denaturation at 94 °C

for 1 min, followed by 35 cycles of 94 °C for 30 s, 50 °C for 1 min and 72 °C for 1.5 min, with a final extension of 72 °C for 10 min. The PCR product was purified and sequenced in Macrogen Inc. (Republic of Korea).

Phylogenetic analyses

The new sequences obtained from each region were assembled and manually edited using the Bioedit program, Geneious v. 6.1.8 and CromasPro DNA Sequencing Software (Hall 1999, Treves 2010, Kearse *et al.* 2012). New nITS and nLSU sequences were added to sequences obtained from GenBank (NCBI) (Table 1). The sequences used in this work represent species endorsed by Ji *et al.* (2017), Salvador-Montoya *et al*. (2018, 2022) and Olou *et al*. (2019).

The dataset was aligned with Guidance (Sela *et al.* 2015), under L-INS-I criteria for nLSU region and Q-INS-I for ITS, then manually inspected and edited using the MEGA v. 6 program (Tamura *et al.* 2013) when needed. Potential ambiguously aligned segments were detected with the software Gblock v. 0.91b (Castresana 2000) for the nITS region. The combined dataset was constructed combining the nLSU and nITS regions and was subdivided into four data partitions: ITS1, 5.8S, ITS2 and LSU. *Phellinotus neoaridus, Fomitiporella chinensis*, *Inocutis dryophilus* and *Inonotus hispidus* were used as outgroups for phylogenetic inferences, based on works performed by Salvador-Montoya *et al.* (2018), Pildain *et al.* (2018) and Olou *et al*. (2019).

The best evolutionary model was selected with AIC (Akaike Information Criterion) with the jModelTest2 v. 1.6 on XEDE program in CIPRESS online (Darriba *et al.* 2012). Maximum likelihood (ML) and Bayesian inference (BI) were employed to perform phylogenetic analysis of the final combined dataset. Maximum likelihood was conducted with RaxMLv. 8.1 program (Stamatakis 2014) to find the best score trees with GTRGAMMA model for the single marker and the data set. The analysis first involved 1 000 independent ML searches each one starting from one randomised stepwise addition parsimony tree. The BI analysis was carried out in the Mr.Bayes v. 3.2.6 program (Ronquist & Huelsenbeck 2003) with two independent runs, each one starting from random trees with four independent simultaneous chains. A total of 8 000 000 million generations were made in total, sampling a tree every 1000 generations. The final alignment were deposited in TreeBASE (http://purl.org/phylo/treebase/phylows/study/TB2:S30336).

RESULTS

Molecular phylogeny

The final combined database (28S + ITS1 + 5.8S + ITS2), had 68 sequences (including the new sequences), resulting in a total of 1 995 characters of which 628 were constant. The Jmodeltest results indicated that the best evolutionary model for each partition was TIM2+I+G, TrN+G, K80+I and TIM3+G for LSU, ITS1, 5.8S, ITS2, respectively.

The phylogenetic inferences based on the combined dataset showed that *Fulvifomes* was recovered as monophyletic (BS = 100/BPP = 1). Within *Fulvifomes*, the sequences of the new species formed a monophyletic group (BS = -/BPP = 0.87) closely related to *F. robiniae* (BS = 100/BPP = 1), but forming a distinct linage here named as *Fulvifomes wrightii* (Fig. 1).

Taxonomy

Fulvifomes wrightii M. Martínez, Salvador-Montoya & Rajchenb., ***sp. nov.*** MycoBank MB 848322. Figs 2, 3.

Typus: **Paraguay**, Pte. Hayes, Chaco Húmedo, residence "Frigorífico Concepción SA". Coord.: 23°26'39'' S57°27'54''W, on living stems of *Libidibia paraguariensis*, 18 May 2019, *M. Martínez, M. Vera & C. Insfrán, N° 415A,* CIEFAPcc 707 (**holotype** HCFC 3237).

Diagnosis: *Basidioma* perennial, ungulate, pileal surface rimose, dark gray, pore surface flat to convex, 6–7 pores/mm. *Context* homogenous. *Hyphal system* monomitic in the context and dimitic in tube trama. *Hymenia* with abundant crystals. *Basidiospores* subglobose to broadly ellipsoidal with a flattened side, (4.5–)5–6 × (4–)4.5–5 µm, thick-walled, yellow to brown in water, turning darker in KOH solution, on living trees of *Libidibia paraguariensis*.

Etymology: In honour of Dr. Jorge Eduardo Wright for his contributions to Paraguayan mycology.

Description: *Basidiomata* perennial, sessile, solitary, woody hard. *Pilei* dimidiate, ungulate to slightly applanate, projecting up to 100–143 mm long, 48–81 mm wide and 30–145 mm thick at the base. *Pileal surface* with brown tomentose zones (5E6 – 5F7), soon glabrous and black, dark grey (1F1) to greyish green (1C2 – 1D2), in juvenile specimens concentrically furrowed with small cracks, in the mature basidioma the pileal surface becoming radially to concentrically rimose, glabrous, margin slightly acute to obtuse, entire, brown reddish (6C7) to dark brown (6FA). *Hymenophore* poroid, flat to convex, brown (5E7 – 5E4), dark brown (6F8) to greyish brown (5E3); *pores* round to regular (5)6–7(8) per mm, (90–)100–190(–200) µm diam, dissepiments entire, (30–)40–170(–190) µm thick. *Tubes* indistinctly stratified, with whitish mycelial cords filling the more developed tubes, up to 105 mm long, brown (6E7). *Context* homogenous, golden brown (5D7), woody hard, up to 5–8 mm in juvenile specimen, almost lacking when mature. In KOH the context becomes reddish brown and, the tubes, dark brown.

Hyphal system monomitic in the context and dimitic in tube trama; generative hyphae thin- to thick-walled, branched, regularly simple-septate, (1.5–)2.5–4.5(–6) µm diam; *trama* with unbranched skeletal hyphae, 90–526 × (3–)3.5–4 um, lumen almost solid, tapering to the apex with 2–4 adventitious septa. *Generative hyphae* thin- to thick-walled, covered with small crystals, 1.5–4 µm diam, branched and simple septate. *Basidiospores* (4.5–)5–6 × (4–)4.5–5 µm, (L = 5.4 µm, W = 4.6 µm) Q = 1.10–1.25 (Q av. = 1.18), broadly ellipsoid to subglobose, with a flattened side, smooth and thick-walled, yellow to brown in water, dark brown in KOH, IKI–, CB–. Rhomboid and quadrangular crystals present in hymenia. *Basidia* and *cystidia* not observed.

Cultural characters: Growth slow, 0.5–3.5 cm in MEA in 25 d, at first mat somewhat compacted, then cottony, especially the central area, to somewhat homogeneously appressed, scant fluffy aerial mycelium to somewhat cottony present, pale yellow at first, then becoming deep yellow, margin irregular. Aerial hyphae composed of dominant generative hyphae, 1–4 µm diam, frequently branched, thickened in some sections and

Table 1. List of species, localities, sources and GenBank accession numbers of taxa used in this study.

Species	Geographic Origin	Collection Reference	Substrate	GenBank accession number	
Fulvifomes azonatus	China/Yunnan	Dai 17470	Angiosperm	MH390395	MH390418
F. acaciae	Costa Rica	JV 2203/71-J	*Acacia* sp.	OP828596	OP828594
	USA	JV 0312/23.4	*Acacia* sp.	OP828597	OP828595
F. boninensis	Japón	FFPRI421009	*Morus boninensis*	LC315777	LC315786
F. caligoporus	China/Hainan	Dai 17660	On living angiosperm tree	MH390391	MH390421
F. cedrelae (as *F. centroamericanus*)	Guatemala	JV 0611/III	On living angiosperm tree	KX960764	KX960763
	Guatemala	JV 0611/8P	On living angiosperm tree	–	KX960757
	Costa Rica	JV 1408/4	On living angiosperm tree	KX960768	–
F. costaricense	Costa Rica/Guanacaste	JV 1607/103-J	Angiosperm	MH390386	MH390414
F. dracaenicola	China/Hainan	Dai 22093	*Dracaena cambodiana*	MW559804	MW559799
F. elaeodendri	South Africa	CMW 47909	*Elaeodendron croceum*	MH599132	MH599096
F. fastuosus	Philippines	CBS 213.36	*Gliricidia sepium*	AY059057	AY558615
	Thailand	LWZ 20140801-1	*Angiosperm*	KR905669	KR905675
F. floridanus	USA/Florida	JV 0904/76	*Lysiloma latisiliqua*	MH390388	MH390424
F. fabaceicola	Brazil/Pernambuco	JRF 74	–	MH048087	MH048097
	Brazil/Pernambuco	PH 6	–	MH048086	MH048096
F. fastuosus	Philippines	CBS 213.36	*Gliricidia sepium*	AY059057	AY558615
F. hainanensis	China	Dai 11573	*Angiosperm*	JX866779	KC879263
F. halophilus	Thailand	MU23	*Xylocarpus granatum*	JX104740	JX104693
F. imbricatus	Thailand	LWZ 20140729-26	*Angiosperm*	KR905671	KR905679
F. indicus	China	Yuan 5932	*Bombax ceiba*	JX866777	KC879261
	Zimbabwe	O 25034	Unknown	KC879259	KC879262
F. jouzaii	Costa Rica/Puntarenas	JV 1504/16-J	Angiosperm	MH390400	MH390425
F. jawadhuvensis	India	MUBL4011	*Albizia amara*	MW048886	MW040079
F. coffeatoporus	USA/Florida	JV0904/1	*Krugiodendron ferreum*	KX960765	KX960762
	USA/Florida	JV0312/24.10J	*K. ferreum*	KX960766	KX960760
	USA/Florida	JV1008/21	*K. ferreum*	KX960767	KX960761
F. karitianaensis	Brazil/Rondonia	AMO 763	–	MH048081	MH048091
F. kawakamii	USA	CBS 428.86	*Casuarina equisetifolia*	AY059028	–
F. merrillii	Taiwan	–	Unknown	JX484002	JX484013
F. mangroviensis	India	MUBL4012	*Aegiceras corniculatum*	MW048909,	MW040083
	India	KSM-MP12a	*A. corniculatum*	OM897221	OM897222
F. malaiyanurensis	India	CAL 1618	*Tamarindus indica*	MW048883	MF155651
F. nakasoneae	JV 0904/68	USA/Florida	Angiosperm	MH390373	MH390408
	JV 1109/77	USA/Texas	*Condalia hookeri*	MH390374	MH390409
F. nilgheriensis	USA	CBS 209.36	On dead deciduous wood	AY059023	AY558633
F. nonggangensis	China/Guangxi	GXU 1127	Angiosperm	MT571502	MT571504
F. popoffii	Argentina/Corrientes	CTES 568185	*Peltophorum dubium*	ON754378	ON754383
	Argentina/Corrientes	CTES 568187	*P. dubium*	ON754377	–
	Argentina/Corrientes	CTES 568190	*Schinopsis balansae*	ON754379	ON754384
	Argentina/Corrientes	CTES 568186	*P. dubium*	ON754376	ON754382
F. rhytiphloeus	Brazil/Bahia	VRTOR658	–	MT906624	MT908357
F. rigidus	China/Yunnan	Dai 17496	*Shorea chinensis*	MH390398	MH390432
F. rimosus	Taiwan	–	Unknown	JX484003	JX484016
	Australia	2392655	Unknown	–	MH628255
F. robiniae	USA/Maryland	CBS 211.36	*Robinia pseudoacacia*	AY059038	AY558646
	USA/Arizona	CFMR 2693	*R. neomexicana*	KX065995	KX065961

Table 1. (Continued).

Species	Geographic Origin	Collection Reference	Substrate	GenBank accession number	
	USA/Wisconsin	CFMR 2735	*R. pseudoacacia*	KX065996	KX065962
F. siamensis	Thailand	STRXG2	*Xylocarpus granatum*	JX104755	JX104708
F. squamosus	Peru/Piura	USM 258349	*Acacia macracantha*	MF479264	MF479269
	Peru/Piura	USM 258361	*A. macracantha*	MF479266	MF479267
F. subindicus	China/Hainan	Dai 17743	Angiosperm	MH390393	MH390435
F. submerrillii	China/Hubei	Dai 17911	On angiosperm stump	MH390371	MH390405
Fulvifomes sp.	Australia	MEL 2382673	Unknown	KP013036	KP013036
F. thailandicus	Thailand	LWZ 20140731-1	Angiosperm	KR905665	KR905672
F. tubogeneratus	China/Guangxi	GXU 2468	On dead trunk	MT580800	MT580805
F.thiruvannamalaiensis	India	MUBL4013	*Albizia amara*	MZ221600	MZ221598
F. xylocarpicola	Thailand	KBXG5	*Xylocarpus granatum*	JX104716	JX104669
	Thailand	MU1	*X. granatum*	JX104718	JX104671
F. yoroui	Benin/Collines	OAB 0097	*Pseudocedrela kotschyi*	MN017120	MN017126
F. wrightii	Paraguay/Pte.Hayes	HCFC 3237	*Libidibia paraguariensis*	OQ924554	OQ807188
	Paraguay/Pte.Hayes	HCFC 3238	*L. paraguariensis*	OQ924556	OQ807189
	Paraguay/Boquerón	HCFC 3239	*L. paraguariensis*	OQ924555	–
	Argentina/Chaco	CTES 568247	*L. paraguariensis*	OQ924562	OQ807190
	Argentina/Chaco	CTES 568252	*L. paraguariensis*	OQ924561	OQ807191
	Argentina/Chaco	CTES 568254	*L. paraguariensis*	OQ924557	OQ807195
	Argentina/Chaco	CTES 568251	*L. paraguariensis*	OQ924560	OQ807192
	Argentina/Chaco	CTES 568249	*L. paraguariensis*	OQ924559	OQ807193
	Argentina/Chaco	CTES 568253	*L. paraguariensis*	OQ924558	OQ807194
F. waimiriatroarensis	Brazil/Amazonas	VTROAMZ01	Unknown	OK086356	OK086370
Fomitiporia chinensis	China	LWZ 20130713-7	Deciduous wood	KJ787808	KJ787817
F. chinensis	China	LWZ 20130916-3	Deciduous wood	KJ787809	KJ787818
Inonotus hispidus	Spain	S45	*Vitis vinifera*	EU282484	EU282482
I. porrectus	USA/Missouri	CBS 296.56	*Gleditschia triacanthos*	AY059051	AY558603
Inocutis dryophilus	USA/Ohio	L(61)5-20-A	*Quercus prinus*	AM269846	AM269783
I. jamaicensis	USA/Arizona	RLG 15819	*Q. arizonica*	KY907703	–
Phellinotus neoaridus	Brazil/Pernambuco	URM 80362	*Caesalpiania sp.*	KM211286	KM211294

with some cytoplasmic contents, regularly septate. Fibre hyphae present, not dominant, little branched, 2.5–3.5 µm diam, lumen almost solid. Chlamydospores abundant, globose, ellipsoid, terminal and intercalated 3.7–11.9 × 4.7– 9.9 µm. The hyphae are pale yellow in water, turning reddish on contact with KOH (Fig. 4).

Habitat and Distribution: Basidiomata are found on living trees of *L. paraguariensis* (*Fabaceae*). This polypore is distributed in the Chaco region of Paraguay and Argentina (Fig. 5).

Specimens examined: **Argentina,** Chaco, Presidencia de la Plaza, Capitán Solari, Parque Nacional Chaco, on living tree of *L. paraguariensis*, 29 Mar. 1990, *O.F. Popoff* 693 (CTES 568261); *ibid*., on living tree of *L. paraguariensis*, 17 Sep. 2016, *C.A. Salvador-Montoya et al*. 715, 717 and 716 (CTES 568247, 568254 and 568252, respectively); *ibid*., on living tree of *L. paraguariensis*, 18 Sep. 2016, *C.A. Salvador-Montoya & O.F. Popoff* 723, 724, 725, 726 and 727 (CTES 568250, 568249, 568253, 568251, 568248, respectively); *ibid*., on living tree of *L. paraguariensis* (*as Caesalpinia melanocarpa*), Jun. 1947, *Wright, C. Iaconis & J.A. Stevenson* (BACF 53440 as *Fomes dependens*); *ibid*., Apr. 1949, *Martinoli* (BACF 53441, as *Fomes dependens*). **Paraguay,** Pte. Hayes, Chaco Húmedo, residence "Frigorífico Concepción SA", 23°26'39''S 57°27'54''W, on living tree of *L. paraguariensis*, 18 May 2019, *M. Martínez, M. Vera & C. Insfran* 415A (HCFC 3237, **holotype**); *ibid*., 18 May 2019, M. *Martínez, M. Vera & C. Insfran* 415B (HCFC 3238); *ibid*., 16 Nov. 2018, M. *Martínez, B. De Madrignac & Cristian* 393 (HCFC 3239).

Additional specimens examined: *Fulvifomes robiniae*: EE. UU. Ohio #223 (*ex* NY, **lectotype** *fide* Lowe) (BACF 27561, **isotype**). *Fulvifomes aff. robiniae*: **Tayikistan**, Tadzhik SSR, Nurek, on living *Pistacia vera*, 25 Apr. 1980, *E. Parmasto* 102813 (BAFC 28043, as *Phellinus robiniae*).

Fig. 2. *Fulvifomes wrightii sp. nov*. **A–I.** Basidiomata: A. CTES 568247; B. CTES 568248; C. CTES 568252; D. CTES 568250; E. CTES 568251; F. CTES 568249; G. CTES 568254; H. CTES 568253; I. HCFC 3238; J. HCFC 3237 (holotype). **K, L.** Pore surface. **M–O.** Basidiospores: M. In water; N. In Melzer's reagent; O. In 5 % KOH. Scale bars: A–D = 2cm; E, F = 1 cm; G = 5 cm; H = 2 cm; I = 5 cm; J = 1cm; K, L = 3 cm; M–O = 5 µm.

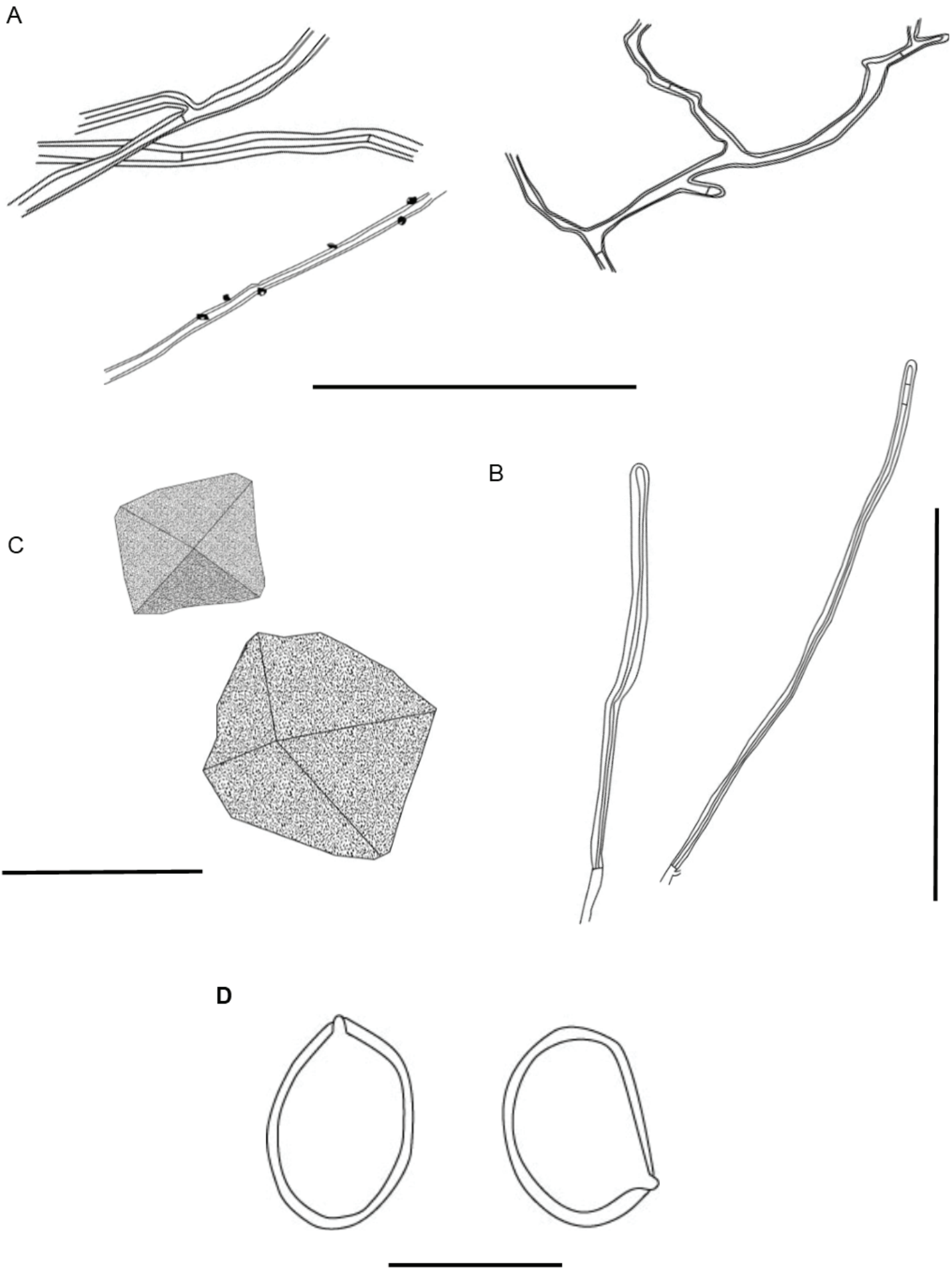

Fig. 3. Microscopical features of *Fulvifomes wrightii*. **A.** Thin- to thick-walled generative hyphae of the context. **B.** Skeletal hyphae from the tubes. **C.** Crystals. **D.** Basidiospores. Scale bars: A = 100 µm; B = 100 µm; C = 15 µm; D = 10 µm.

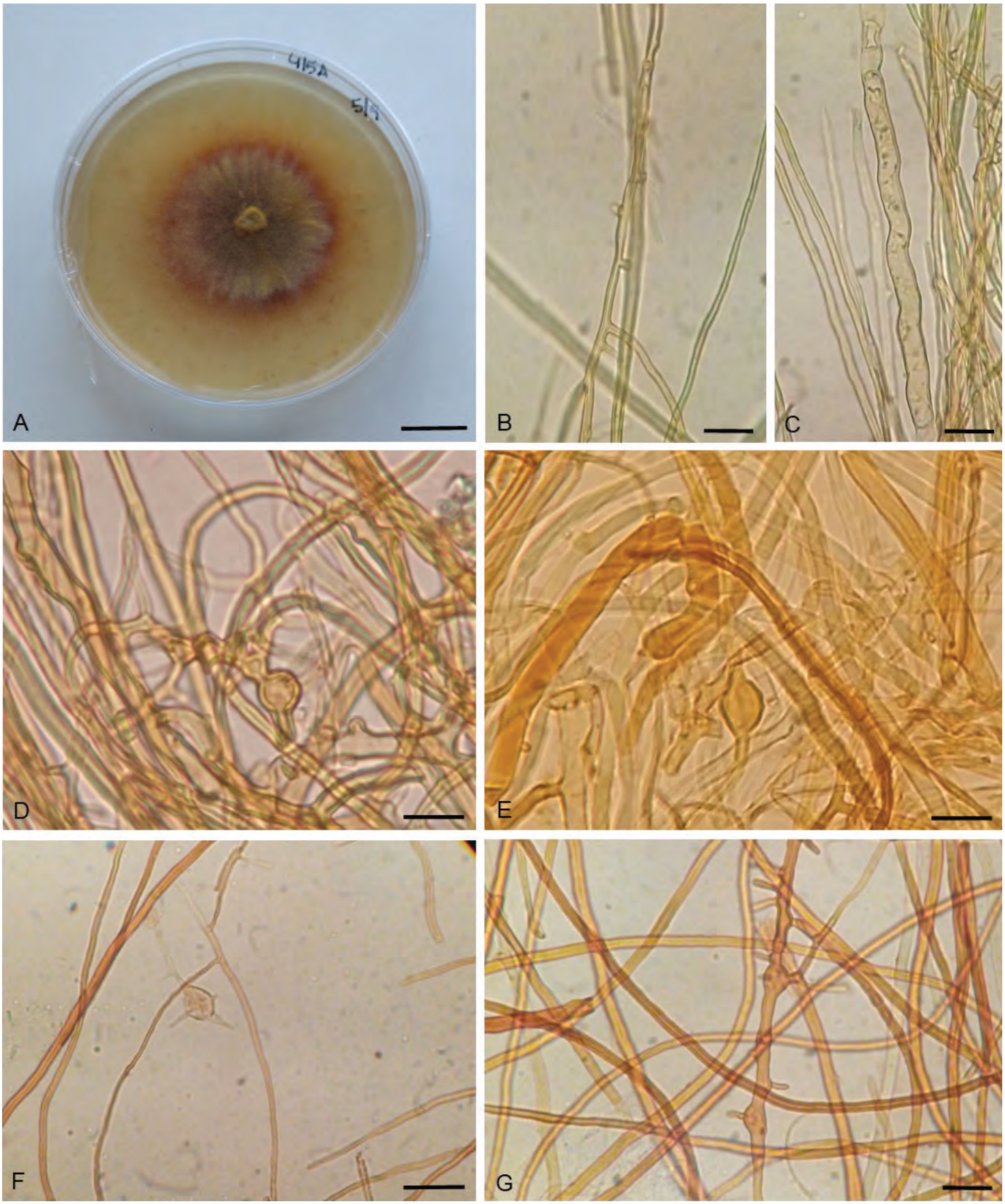

Fig. 4. *Fulvifomes wrightii.* Macro- and microscopic cultural features. **A.** Mycelial mat, **B, C.** Generative hyphae, in water. **D–F.** Ellipsoid and globose chlamydospores, in KOH. **G.** Fiber hyphae, in KOH. Scale bars: A = 2 cm; B, C = 5 µm; D–F = 15 µm; G = 5 µm.

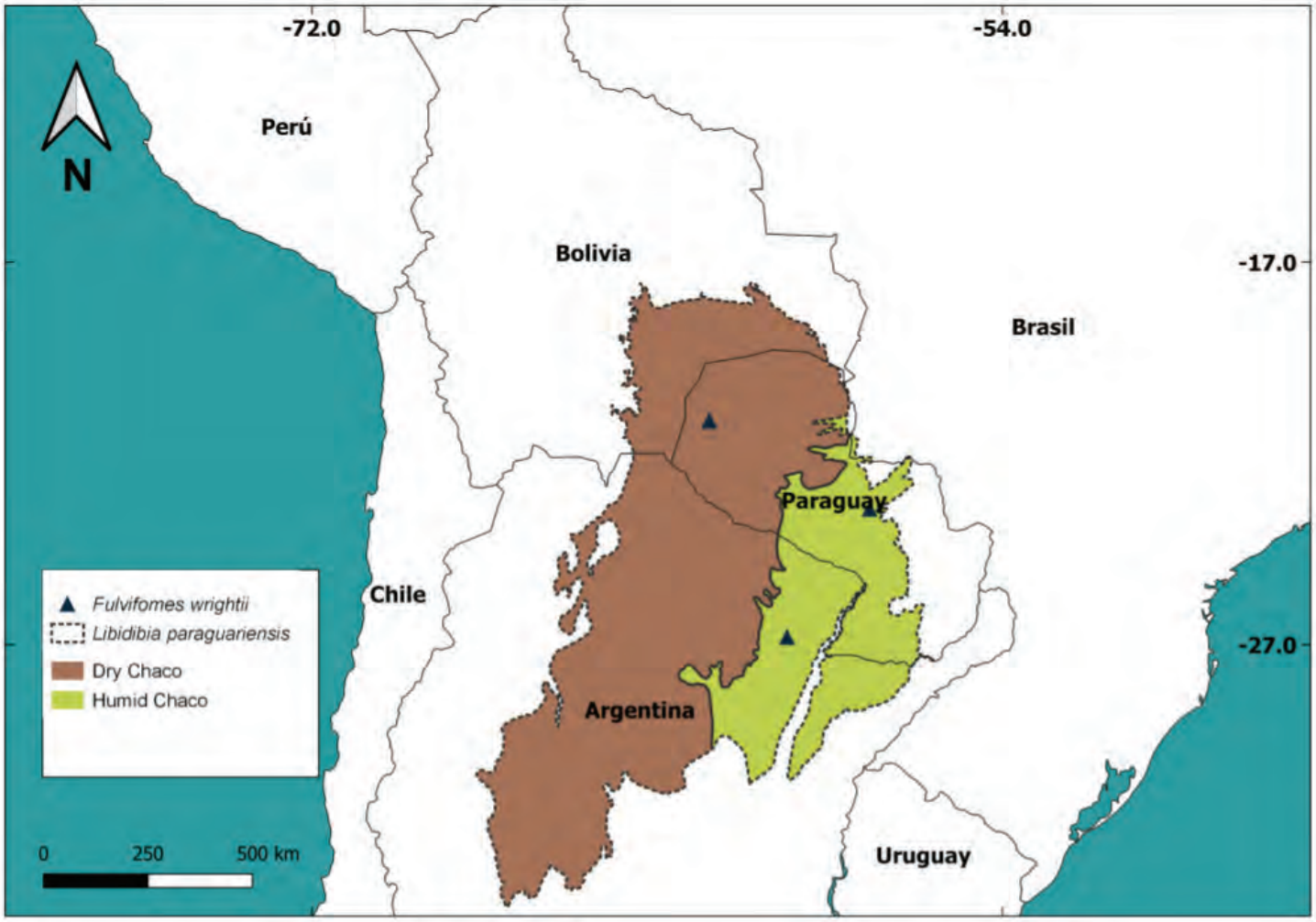

Fig. 5. Map of the geographic distribution of specimens of *Fulvifomes wrightii* and the host *Libidibia paraguariensis* in subtropical region (the black lines represent the estimated distribution of the host).

DISCUSSION

Fulvifomes wrightii is characterised by its perennial ungulate basidiomata with rimose and dark grey pileal surface, a convex pore surface with 6–7 pores per mm, indistinctly stratified tubes, the homogenous context, a dimitic hyphal system that is restricted to the tubes (*viz*., monomitc in the context), and hymenia and tube trama with abundant crystals in well-developed specimens (Fig. 3). *In vitro*, the culture has chlamydospores (Fig. 4).

Fulvifomes wrightii resembles *Fulvifomes robiniae* by the shape of basidiomata and basidiospores. However, *F. robiniae* has a cracked and dark brown pileal surface, a flat pore surface with 5–6 pores per mm, and lacks crystals in the hymenium (Gilbertson & Ryvarden 1987, Salvador-Montoya *et al*. 2018). Additionally, *F. robiniae* has a geographic distribution in temperate zones of the USA, growing mainly on living trees of *Robinia pseudoacacia* (Kotlaba & Pouzar 1978, Salvador-Montoya *et al.* 2018), a *Fabaceae* that is native in North America (IPNI 2022). Outside the Americas, *R. pseudoacacia* is a naturalised and invasive species in the temperate regions of Europe, as well as in Asia and Southern Africa (Capdevila-Argüelles *et al.* 2011). Regarding *F. wrightii*, it is found in the subtropical region of South America, growing on living trees of *L. paraguariensis* [common name is "Guayacán", considered the South American ebony tree according to Aronson & Toledo (1992)]. *Libidibia paraguariensis* is considered endemic to the Chaco region and is distributed in north and central Argentina, southern Bolivia, Brazil (specifically in Matto Grosso do Sul state), Paraguay (Giménez *et al.* 2017). According to Mereles (2005), *L. paraguariensis* appears in xerophytic forests in the Chaco region, and grows in structured, floodable and asphyxiated soils. Nevertheless, Imaña-Encinas *et al*. (2019) mention it as a tree species of the humid Chaco, conditioned by topographic gradients and floods.

Fulvifomes wrightii also resembles *F. cedrelae, F. rimosus*, *F. popoffii* and *Phellinus chaquensis*. Nevertheless, *F. cedrelae* differs by smaller basidiospores (5–5.5 × 4–4.5 µm) and by growing on *Meliaceae* where it induces a heart-rot (*e.g*. *Cedrela fissilis, C. odorata* and *Swietenia mahagoni*) (Salvador-Montoya *et al.* 2018, 2022). Regarding *F. rimosus*, it has larger pores (4–5 pores/mm) (Kotlaba & Pouzar 1978). In the case of *F. popoffii*, this species has a rimose pileal surface, a flat pore surface with 5–6 pores/mm and grows on living trees of *Peltophorum dubium* (Salvador-Montoya *et al*. 2022). Finally, *P. chaquensis* differs from *F. wrigthii* by its smaller pores (6–7 pores/mm), presence of hymenial setae and by growing on standing trees of *Astronium balansae*, *L. paraguariensis* and species of *Schinopsis* (Luna *et al.* 2012, Rajchenberg & Robledo 2013, Salvador-Montoya *et al.* 2018).

Key to species of *Fulvifomes* in America

1 Pileal surface rimose[1] 2
1 Pileal surface fissured, cracked or squamulate[2] 9

2 Hyphal system dimitic throughout the basidioma 3
2 Hyphal system monomitic in the context and dimitic in the tubes 4

3 Tubes distinctly stratified, spores cyanophilous, pores 9–10 per mm ..... *F. jouzaii*
3 Tubes indistinctly stratified, spores acyanophilous, pores 3–5 per mm ..... *F. rimosus*

4 Basidioma triquetrous, on *Polygonaceae* ..... *F. minutiporus*
4 Basidioma ungulate, another host 5

5 Pores (5–)6–7(–8) per mm 6
5 Pores 3–4 per mm 8

6 Crystals lacking, context with indistinct dark lines ..... *F. cedrelae*
6 Crystals present in the hymeniun and tubes, context without black lines 7

7 Growing on *Peltophorum dubium* and *Schinopsis balansae* ..... *F. popoffii*
7 Growing on *Libidibia paraguariensis* ..... *F. wrigthii*

8 Tubes stratified, basidiospores ellipsoid ..... *F. fabaceicola*
8 Tubes indistinctly stratified, basidiospores subglobose to globose ..... *F. coffeatoporus*

9 Tubes distinctly stratified, dimitic hyphal system throughout the basidioma 10
9 Tubes indistinctly stratified, dimitic hyphal system restricted to the tubes 11

10 Pores 7–9 per mm ..... *F. rhytiphloeus*
10 Pores 4–7 per mm ..... *F. grenadensis*

11 Context with black lines 12
11 Context without black lines 13

12 Basidiospores ellipsoid, chlamydospores present ..... *F. kawakamii*
12 Basidiospores subglobose, chlamydospores absent ..... *F. costaricense*

13 Pilear surface squamulate, on *Acacia macracantha* ..... *F. squamosus*
13 Pilear surface cracked with crusted or scrupose zone, host different 14

14 Growing on *Robinia pseudoacacia* ..... *F. robiniae*
14 Growing on *Acacia* 15

15 Basidiospores broadly ellipsoidal, 5–6 × 4–5 µm ..... *F. acaciae*
15 Basidiospores ellipsoid, 4–5 × 3–4 µm 16

16 Pileal surface glabrous ..... *F. karitianaensis*
16 Pileal surface velutinate ..... *F. waimiriatroariensis*

ACKNOWLEDGEMENTS

We thank the curators of the fungaria BAFC and CTES for providing access to collections. The first author thanks Luis Oakley and Christian Vogt for helping with commentaries on Chaco's biogeography and distribution of *L. paraguariensis*, Pablo Masera for helping with the geoprocessing and map confection and to Belén Pildain for her help with the phylogenetic tree. Funding by PICT-MinCyT (Ministerio de Ciencia y Tecnología, Argentina) for projects 2015/1933 and 3234/2018 are also acknowledged.

Conflict of interest: The authors declare that there is no conflict of interest.

[1]Rimose: having a surface covered with a network of cracks radial-concentrically and small crevices.
[2]Fissured: having long irregularly, narrow cracks or openings.

REFERENCES

Aronson J, Toledo SC (1992). *Caesalpinia paraguariensis* (*Fabaceae*): Forage Tree for All Seasons. *Economic Botany* **46**: 121–132.

Capdevila-Argüelles L, Zilleti A, Suarez VA (GEIB) (2011). *Manual de las especies exóticas invasoras de los ríos y riberas de la cuenca hidrográfica del Duero.* Confederación Hidrográfica del Duero Ministerio de Medio Ambiente, y Medio Rural y Marino, España.

Castresana J (2000). Selection of conserved blocks from multiple alignments for their use in phylogenetic analysis. *Molecular Biology and Evolution* **17**: 540–552.

Darriba D, Taboada GL, Doallo R, *et al.* (2012). jModelTest 2: more models, new heuristics and parallel computing. *Nature Methods* **9**: 772.

Dai YC (1999) *Phellinus sensu lato* (*Aphyllophorales, Hymenochaetaceae*) in East Asia. *Acta Botanica Fennica* **166**: 43–103.

Dai YC (2010). *Hymenochaetaceae* (*Basidiomycota*) in China. *Fungal Diversity* **45**: 131–343

Doyle JJ, Doyle JL (1990). Isolation of plant DNA from fresh tissue. *Focus* **12**: 13–15.

Gilbertson RL, Ryvarden L (1987). *North American Polypores* vol 2. Oslo, Fungiflora.

Giménez AM, Bolzon Muniz GBM, Moglia, JGM, *et al.* (2017) Ecoanatomía del ébano sudamericano: "guayacán" (*Libidibia paraguariensis*, *Fabaceae*). *Boletín de la Sociedad Argentina de Botánica.* **52**: 45–54.

González AM (2018). ImageJ: una herramienta indispensable para medir el mundo biológico. *Folium relatos botánicos* **1**: 6–17.

Hall T (1999). BioEdit: a user-friendly biological sequence alignment editor and analysis program for Windows 95/98/NT. *Nucleic Acids Symposium Series* **4**: 95–98.

Imaña-Encinas J, Campos da Nóbrega R, Woo Jong-Choon, *et al.* (2019). Delimitación por SIG de un área de la ecorregión Chaco Húmedo a la margen derecha del río Paraguay. *Investigación Agraria* **21**: 54–64.

IPNI (2022). *International Plant Names Index*. Published on the Internet http://www.ipni.org. The Royal Botanic Gardens, Kew, Harvard University Herbaria & Libraries and Australian National Botanic Gardens [Retrieved 23 August 2022].

Ji XH, Wu F, Dai, YC, *et al.* (2017). Two new species of *Fulvifomes* (*Hymenochaetales*, *Basidiomycota*) from America. *MycoKeys* **22**: 1–13.

Kearse M, Moir R, Wilson A, *et al*. (2012). Geneious Basic: an integrated and extendable desktop software platform for the organization and analysis of sequence data. *Bioinformatics* **28**: 1647–1649.

Kornerup A, Wanscher JH (1978). *Methuen Handbook of Colour* (3rd ed.). Eyre Methuen, London.

Kotlaba F, Pouzar Z (1978). Notes on *Phellinus rimosus* complex (*Hymenochaetaceae*). *Acta Botanica Croatica* **37**: 171–182.

Kotlaba F, Pouzar Z (1979). Two new setae-less *Phellinus* species with large coloured spores (*Fungi*, *Hymenochaetaceae*). *Folia Geobotanica & Phytotaxonomica* **14**: 259–263.

Larsson KH, Parmasto E, Fischer M, *et al.* (2006). *Hymenochaetales*: a molecular phylogeny of the hymenochaetoid clade. *Mycologia* **98**: 926–936.

Luna MJ, Murace MA, Robledo GL, *et al.* (2012). Characterization of *Schinopsis haenkeana* wood decayed by *Phellinus chaquensis* (*Basidiomycota, Hymenochaetales*). *IAWA Journal* **33**: 91–104.

Mereles F (2005). Una aproximación al conocimiento de las formaciones vegetales del Chaco Boreal, Paraguay. *Rojasiana* **6**: 5–48.

Murrill WA (1914). North American Polypores. *The New Era Printing Company*, New York.

Nobles MK (1965). Identification of cultures of wood-inhabiting Hymenomycetes. *Canadian Journal of Botany* **43**: 1097–1139.

Olou BA, Ordynets A, Langer E (2019). First new species of *Fulvifomes* (*Hymenochaetales*, *Basidiomycota*) from tropical Africa. *Mycological Progress* **18**: 1383–1393.

Pildain MB, Reinoso-Cendoya R, Ortiz-Santana B, *et al.* (2018). A discussion on the genus *Fomitiporella* (*Hymenochaetaceae, Hymenochaetales*) and first record of *F. americana* from southern South America. *MycoKeys* **38**: 77–91.

Rajchenberg M, Greslebin A (1995). Cultural characters, compatibility tests and taxonomic remarks of selected polypores of the Patagonian Andes forest of Argentina. *Mycotaxon* **56**: 325–346.

Rajchenberg M, Robledo G (2013). Pathogenic polypores in Argentina. *Forest Pathology* **43**: 171–184.

Robledo G, Urcelay C (2009). *Hongos de la madera en árboles nativos del Centro de la Argentina*. Editorial Universidad Nacional de Córdoba.

Ronquist F, Huelsenbeck JP (2003). MrBayes version 3.0: Bayesian phylogenetic inference under mixed models. *Bioinformatics* **19**: 1572–1574.

Salvador-Montoya CA, Popoff OF, Reck MA, *et al.* (2018). Taxonomic delimitation of *Fulvifomes robiniae* (Hymenochaetales, Basidiomycota) and related species in America: *F. squamosus* sp. nov. *Plant Systematics and Evolution* **304**: 445–459.

Salvador-Montoya CA, Martínez M, Drechsler-Santos ER (2022). Taxonomic update of species closely related to *Fulvifomes robiniae* in America: *F. popoffii sp. nov*. *Mycological Progress* **21**: 95.

Sela I, Ashkenazy H, Katoh K, *et al.* (2015). GUIDANCE2: accurate detection of unreliable alignment regions accounting for the uncertainty of multiple parameters. *Nucleic Acids Research* 2015 Jul. 1; **43** (Web Server issue): W7–W14.

Stamatakis A (2014). RaxML Version 8: a tool phylogenetic analysis and post-analysis of large phylogenies. *Bioinformatics* **30**: 1312–1313.

Tamura K, Stecher G, Peterson D, *et al.* (2013). MEGA6: Molecular Evolutionary Genetics Analysis Version 6.0. *Molecular Biology and Evolution* **30**: 2725–2729.

Tamari F, Hinkley CS (2016). Extraction of DNA from Plant Tissue: Review and Protocols. In: *Sample Preparation Techniques for Soil, Plant, and Animal Samples*, (Micic M, ed.). Humana Press, New York: 245–263.

Treves DS (2010). Review of three DNA analysis applications for use in the microbiology or genetics classroom. *Journal of Microbiology & Biology Education* **11**: 186–187.

Vilgalys R, Hester M (1990). Rapid genetic identification and mapping of enzymatically amplified ribosomal DNA from several *Cryptococcus* species. *Journal of Bacteriology* **172**: 4239–4246.

Wagner T, Fischer M (2001). Natural groups and a revised system for the European poroid *Hymenochaetales* (*Basidiomycota*) supported by nLSU rDNA sequence data. *Mycological Research* **105**: 773–782.

Wagner T, Fischer M (2002). Proceedings towards a natural classification of the worldwide taxa *Phellinus s.l.* and *Inonotus s.l.*, and phylogenetic relationships of allied genera. *Mycologia* **94**: 998–1016.

White T, Bruns T, Lee S, *et al.* (1990). Amplification and direct sequencing of fungal ribosomal RNA genes for phylogenetics. In: *PCR Protocols: a guide to methods and applications* (Innis M, Gelfand D, Sninsky J, White T, eds.) Academic Press, New York: 315–322.

Wu F, Zhou LW, Vlasák J, *et al.* (2022). Global diversity and systematics of *Hymenochaetaceae* with poroid hymenophore. *Fungal Diversity* **113**: 1–192.

Zhou LW (2014). *Fulvifomes hainanensis sp. nov*. and *F. indicus comb. nov*. (*Hymenochaetales*, *Basidiomycota*) evidenced by a combination of morphology and phylogeny. *Mycoscience* **55**: 70–77.

FUSE

Fungal Systematics and Evolution

Volume 12
DECEMBER 2023
PAGES 59–71

doi.org/10.3114/fuse.2023.12.04

Microfungi associated with dying *Euphorbia mauritanica* in South Africa and their relative pathogenicity

S. Marincowitz[1*], N.Q. Pham[2], B.D. Wingfield[1], F. Roets[3], M.J. Wingfield[1]

[1]Department of Biochemistry, Genetics and Microbiology, Forestry and Agricultural Biotechnology Institute (FABI), University of Pretoria, Private Bag X20, Hatfield, 0028, South Africa
[2]Department of Plant and Soil Sciences, Forestry and Agricultural Biotechnology Institute (FABI), University of Pretoria, Private Bag X20, Hatfield, 0028, South Africa
[3]Department of Conservation Ecology and Entomology, Stellenbosch University, Private Bag X1, Matieland, 7602, South Africa

*Corresponding author: seonju.marincowitz@fabi.up.ac.za

Key words:
Euphorbia
fungal pathogens
new taxa
phoma-like
plant disease
taxonomy

Abstract: *Euphorbia mauritanica* is a succulent shrub that is indigenous to South Africa and widely distributed throughout the country. Dying plants have been observed in their natural habitat in the Northern and Western Cape Provinces of South Africa in recent years. Stems displaying lesions were collected and the emerging cultures were identified based on ITS, LSU, *ACT*, *RPB2*, *TEF1* and/or *TUB2* sequence data. Four filamentous fungi were consistently observed and isolated. One was identified as *Alanphillipsia* (*Ala.*) *aloes*, and the other three were new to science and are described here as *Cytospora euphorbiicola sp. nov.*, *Nothomicrosphaeropsis namakwaensis sp. nov*. and *Austrophoma* (*Aus.*) *euphorbiae gen. et sp. nov.* These new species and *Ala. aloes* were the most commonly encountered, and their pathogenicity was tested on *E. mauritanica* plants in a greenhouse trial. All four species gave rise to lesions that were significantly larger than those associated with the controls, but they were not significantly different to each other. Although the lesions associated with the inoculations were well-developed, they did not give rise to plant death, suggesting that they are not responsible for the large-scale die-off of *E. mauritanica* in the field. The primary cause of the death of *E. mauritanica* in the studied area remains unknown and could be due to environmental factors such as has been found with the die-off of *Euphorbia ingens* in South Africa.

Citation: Marincowitz S, Pham NQ, Wingfield BD, Roets F, Wingfield MJ (2023). Microfungi associated with dying *Euphorbia mauritanica* in South Africa and their relative pathogenicity. *Fungal Systematics and Evolution* **12**: 59–71. doi: 10.3114/fuse.2023.12.04
Received: 30 May 2023; **Accepted:** 27 July 2023; **Effectively published online:** 31 July 2023
Corresponding editor: P.W. Crous

INTRODUCTION

During the course of the last few decades, the die-off of *Euphorbia* species, particularly the woody *Euphorbia*, *E. ingens*, has occurred in South Africa. Intensive studies have been conducted on these die-offs considering both possible biotic and abiotic factors that might explain the problem (Roux *et al*. 2008, Van der Linde *et al.* 2011, 2012a, b, 2016, 2017a, b, 2018). These studies led to the identification of a relatively large number of insect pests and pathogens associated with the observed symptoms. Among them were *Lasiodiplodia theobromae* and *L. mahajangana*, and weevil-associated *Gondwanamyces serotectus* and *G. ubusi*, which showed significant disease development in pathogenicity trials (Van der Linde *et al*. 2011, 2012b). However, the overall conclusions were that environmental factors predisposed trees to damage by opportunistic fungal pathogens and aggressive insects, eventually leading to tree mortality.

During routine plant disease surveys, large numbers of *E. mauritanica* plants have been observed dying in the Northern and Western Cape Provinces of South Africa. Typically, the plants had symptomatic branches with discolouration that extended down to the base. The widespread nature of the die-off and the disease symptoms raised concerns that fungal pathogens might be involved. Unlike *E. ingens* which grows as a tree, *E. mauritanica* is a shrub growing up to 1.5 m high with many succulent stems branching at the base and with small leaves. It is native to Africa with a wide distribution in South Africa and grows in dry climates, mainly in coastal and inland areas with colder winters (Bruyns 2022). A fungus, *Endoconidioma euphorbiae* (*Dothioraceae*, *Dothideales*), was reported from the leaves of *E. mauritanica* (Crous *et al.* 2020). However, no extensive studies have been conducted regarding fungi associated with *E. mauritanica* or the die-offs of the plant.

The aim of this study was to identify the fungi commonly associated with the die-offs of *E. mauritanica* plants, primarily utilising DNA sequence analyses. Furthermore, their possible contribution to plant death was assessed using artificial inoculations under greenhouse conditions.

MATERIALS AND METHODS

Field observations and isolations

Dying *E. mauritanica* plants (Figs 1, 2), common in areas in the vicinity of Clanwilliam (Western Cape Province) and Nieuwoudtville (Northern Cape Province), were visited in August 2020. Initial symptoms were distinct lesions on the stems that appeared to extend rapidly downwards. Eleven stem pieces from different plants with incipient lesions were transferred to the laboratory, and isolations were made from fungal structures present on the lesions. Spores taken from sporocarps were plated on malt extract agar (MEA: 20 g Biolab malt extract, 20 g Difco agar, 1 L deionised water) supplemented with 100 mg streptomycin. Pure cultures were established from the primary isolations on MEA and on water agar (WA: 20 g Difco agar, 1 L deionised water), where autoclaved bamboo toothpicks had been placed on the agar surface to induce sporulation.

Fungal structures produced on WA, MEA or toothpicks were studied under a compound microscope (Nikon Eclipse Ni, Japan). The structures were initially mounted in water and later replaced with 85 % lactic acid, in which all micrographs and measurements were done. Vertical sections of sporocarps formed on media or toothpicks were prepared using a Leica Cryomicrotome (Leica Biosystem, Germany). The sporocarps were mounted in a freezing medium, cut in 10–12 µm thickness, and mounted in 85 % lactic acid for observation. Up to 50 measurements were made for key morphological structures, if available, and presented in minimum–maximum (average ± standard deviation).

For growth characteristics, 5 mm diam mycelial plugs taken from the leading edges of 7 d-old cultures were placed at the centres of 90 mm Petri dishes containing 2 % MEA. The cultures were incubated in the dark at temperatures ranging from 10–35 °C at 5 °C intervals. Colonies were observed daily, and when the fastest growing cultures reached the edges of the Petri dishes, two measurements of colony diameter, perpendicular to each other were taken, and the averages, as well as the daily growth rates, were computed. Culture characteristics were described after growth for 28 d in the dark, and colony colours were described using the colour charts of Rayner (1970).

All cultures were stored in the culture collection (CMW) of the Forestry and Agricultural Biotechnology Institute (FABI),

Fig. 1. Locations where dying *Euphorbia mauritanica* were observed and the samples collected: Clanwilliam (Western Cape Province) and Nieuwoudtville (Northern Cape Province), South Africa.

Fig. 2. Dying *Euphorbia mauritanica* in the fields close to Nieuwoudtville, Northern Cape Province, South Africa. **A, B.** Dead and dying shrubs. **C–E.** Lesions observed in the stems of dying plants.

University of Pretoria, Pretoria, South Africa. The type specimens and ex-type cultures were lodged in the H.G.W.L. Schweickerdt herbarium (PRU) and the culture collection of the Innovation-Africa (CMW-IA), University of Pretoria, South Africa.

DNA extraction, PCR amplification and sequencing

Isolates grown on 2 % MEA for 7 d at 25 °C were used for DNA extraction. Mycelium was scraped from the surface of the media using sterile needles and transferred to 1.5 mL Eppendorf tubes. DNA was extracted using Prepman® Ultra Sample Preparation Reagent (Thermo Fisher Scientific, Waltham, MA, USA) following the protocols suggested by the manufacturer. The regions targeted for PCR amplification and subsequent sequencing are listed in Table 1. PCR reactions were conducted using the Applied Biosystems ProFlex PCR System (Thermo Fisher Scientific, Waltham, MA, USA) following the preparation described by Pham *et al.* (2019). Amplified fragments were cleaned using an ExoSAP-IT™ PCR Product Cleanup Reagent (Thermo Fisher Scientific, Waltham, MA, USA). Amplicons were sequenced in both directions using an ABI PRISM™ 3100 DNA sequencer (Applied Biosystems, USA) at the Sequencing Facility of the Faculty of Natural and Agricultural Sciences, University of Pretoria, South Africa. Geneious Prime v. 2022.1.1 (https://www.geneious.com) was used to assemble and edit the raw sequences. All sequences generated in this study were deposited in GenBank (http://www.ncbi.nlm.nih.gov) (Supplementary Tables S1–S3).

Phylogenetic analyses

The ITS and LSU regions were sequenced for all isolates obtained in this study. Preliminary identification was made by performing a nucleotide BLAST search using the ITS and LSU sequences against the NCBI GenBank database (http://www.ncbi.nlm.nih.gov) to identify the isolates to genus and closest species level. This information was then used to generate the datasets for further phylogenetic analyses. Sequences for species closely related to those emerging from this study were sourced from GenBank (Supplementary Tables S1–S3). All sequences were aligned with MAFFT v. 7 (Katoh & Standley 2013) and inspected manually using

Table 1. Primers used in this study, with sequences and sources.

Region	Primer	Direction	Sequence	Annealing temperature	References	*Alanphilipsia*	*Didymelaceae*	*Cytospora*
Internal transcribed spacer regions 1 and 2 and the 5.8S gene of the ribosomal RNA (ITS)	ITS-1F	Forward	CTTGGTCATTTAGAGGAAGTAA	56 °C	Gardes & Bruns (1993)	v	v	v
	ITS-4	Reverse	TCCTCCGCTTATTGATATGC		White *et al*. (1990)			
Nuclear large subunit of the ribosomal RNA (LSU)	LR0R	Forward	ACCCGCTGAACTTAAGC	55 °C	Rehner & Samuels (1994)	v	v	v
	LR5	Reverse	TCCTGAGGGAAACTTCG		Vilgalys and Hester (1990)			
DNA-directed RNA polymerase II second largest subunit (*RPB2*)	fRPB2-5F2	Forward	GGGGWGAYCAGAAGAAGGC	58 °C	Sung *et al*. (2007)	n/a	v	v
	fRPB2-7cR	Reverse	CCCATRGCTTGYTTRCCCAT		Liu *et al*. (1999)			
β-Tubulin 2 (*TUB2*)	BT2a	Forward	GGTAACCAAATCGGTGCTGCTTTC	52 °C	Glass & Donaldson (1995)	n/a	v	v
	BT2b	Reverse	ACCCTCAGTGTAGTGACCCTTGGC		Glass & Donaldson (1995)			
Actin (*ACT*)	ACT-512F	Forward	ATGTGCAAGGCCGGTTTCGC	55 °C	Carbone & Kohn (1999)	n/a	n/a	v
	ACT-783R	Reverse	TACGAGTCCTTCTGGCCCAT		Carbone & Kohn (1999)			
Translation elongation factor 1-α (*TEF1*)	EF1-728F	Forward	CATCGAGAAGTTCGAGAAGG	52 °C	Carbone & Kohn (1999)	n/a	n/a	v
	EF1-986R	Reverse	TACTTGAAGGAACCCTTACC		Carbone & Kohn (1999)			

MEGA v. 7 (Kumar *et al.* 2016). The most appropriate model for analyses was obtained using the software jModeltest v. 1.2.5 (Posada 2008). Bayesian inference (BI) analyses were performed using MrBayes v. 3.2.6 (Ronquist *et al.* 2012) on the CIPRES Science Gateway v. 3.3 (Miller *et al.* 2010). Four Markov chain Monte Carlo (MCMC) chains were run from a random starting tree for five million generations, and trees were sampled every 100th generation. The first 25 % of the trees sampled were eliminated as burn-in, and the remaining trees were used to determine the posterior probabilities. Maximum-likelihood (ML) analysis was conducted using RAxML v. 8.2.4 (Stamatakis 2014) on the CIPRES Science Gateway v. 3.3, with default GTR substitution matrix and 1 000 rapid bootstraps. Final consensus trees were viewed using MEGA v. 7 (Kumar *et al.* 2016).

Pathogenicity tests

Five representative isolates of four species that were obtained in this study were selected for an inoculation trial to determine the pathogenicity of the fungi. Three isolates, CMW 56355, CMW 56351 and CMW 56352, each represented a species, and two isolates, CMW 56344 and CMW 56346, represented a single species. Plants of *E. mauritanica* were grown from branch cuttings taken from a single plant and thus representing a single clone. The rooted cuttings were maintained in individual pots in a greenhouse where the temperature was adjusted to approximately 25 °C.

Plants with main stems ranging in 5–8 mm diam were selected for inoculation. The inoculum was prepared by first soaking toothpicks in malt extract broth that had been cut in half and thus 3 cm in length. The toothpicks were autoclaved twice and placed onto the surface of potato dextrose agar in 90 mm Petri dishes (PDA: Difco potato dextrose agar 24 g, 1 L deionised water) under sterile conditions. A plug of agar taken from the actively growing margins of the test fungi was then placed at the centre of the plates containing two half-length toothpicks, which were placed approximately 10 mm apart from each other and from the inoculum source. These plates were incubated at 25 °C in the dark for 7 wk until the toothpicks were completely overgrown by fungal hyphae. Toothpicks on non-inoculated plates were maintained under the same conditions to be used as controls.

Fifteen plants per isolate and an equal number of controls were inoculated. The inoculated plants were kept in a greenhouse where the temperature was adjusted to approximately 25 °C and exposed to a natural light cycle. The plants were watered twice a week. Toothpicks overgrown by mycelium and sterile toothpicks for the controls were inserted into the main stem to a depth of 2–3 mm. After 8 wk, the toothpicks were removed from the inoculated stems that were then dissected lengthwise. The pathogenicity test was not repeated. A transparent mica sheet (210 × 297 mm) was placed directly on the freshly cut branches, and the area of infection was traced on the sheet using a marker. The sheet with the traced outlines and a ruler were transferred to a flatbed scanner (Epson Perfection V700 photo, China) for image processing. The image files created were loaded into Adobe Photoshop 2021 (Adobe Systems Incorporated), and the lesion area was measured. The experimental data were analysed statistically using R software v. 4.2.1 (R Core Team 2021) by performing the Kruskal-Wallis Rank Sum test (Kruskal & Wallis 1952) and the Dwass-Steele-Critchlow-Fligner all-pairs test for pairwise comparisons (Dwass 1960, Steel 1960, Critchlow & Fligner 1991).

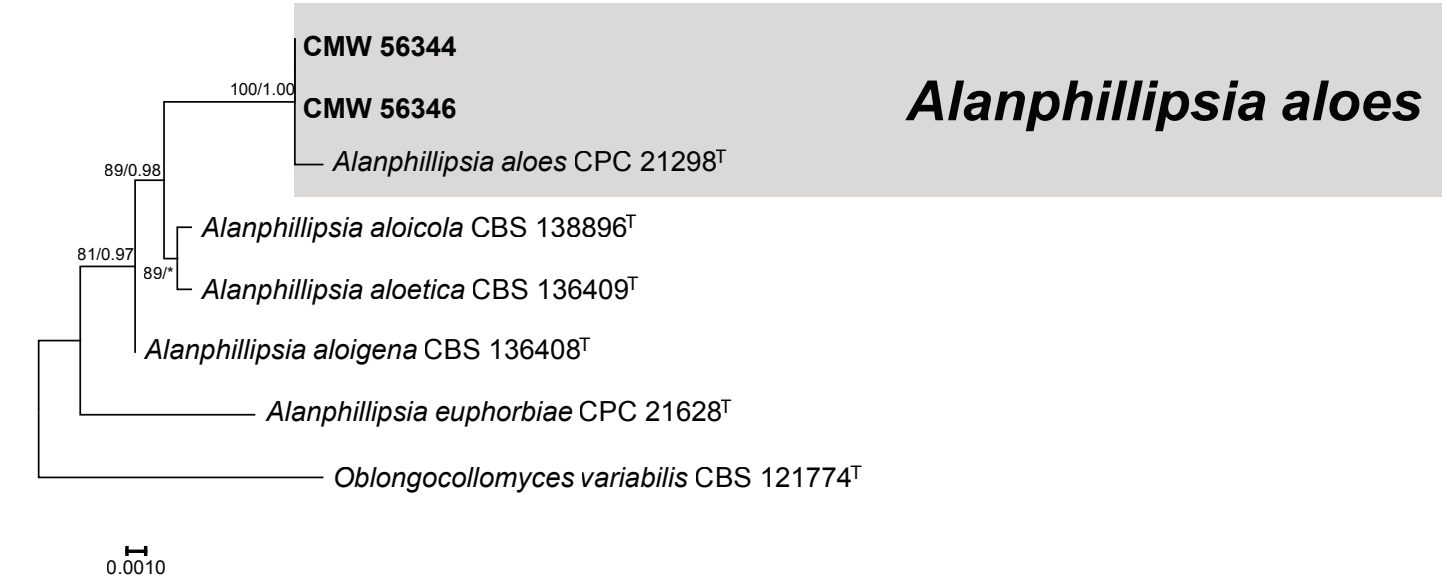

Fig. 3. Phylogenetic tree based on maximum likelihood (ML) analysis of a combined DNA data set of the ITS and LSU sequences for *Alanphillipsia* spp. Isolates sequenced in this study are presented in boldface. Bootstrap values ≥ 60 % for ML analyses and posterior probabilities values ≥ 0.9 obtained from Bayesian inference (BI) are indicated at the nodes as ML/BI. Bootstrap values < 60 % or probabilities values < 0.9 are marked with "*". Isolates representing the ex-type material are marked with "T". *Oblongocollomyces variabilis* (isolate CBS 121774) represent the outgroup.

Re-isolations were made from the tissues close to the point of inoculation onto MEA. The resulting isolates were identified based on their colony morphology, and a representative sample of these was sequenced for the ITS region.

RESULTS

Identification of isolates

Four fungal taxa were consistently found present on the infected tissues, and pure cultures were produced for them. An initial BLAST search using generated ITS and LSU sequences against the NCBI GenBank database identified these isolates as members of *Alanphillipsia* (*Botryospheriaceae*, *Botryosphaeriales*, *Dothideomycetes*), *Cytospora* (*Cytosporaceae*, *Diaporthales*, *Sordariomycetes*), *Nothomicrosphaeropsis* (*Didymellaceae*, *Pleosporales*, *Dothideomycetes*) and a didymellaceous fungus.

Two isolates (CMW 56344, CMW 56346) were identified as species of *Alanphillipsia* based on the BLAST search using the ITS and LSU sequences. Five previously described *Alanphillipsia* spp. and *Oblongocollomyces variabilis* (CBS 121774) as the outgroup were included in the phylogenetic analyses. Maximum likelyhood and BI analyses were performed based on the combined sequences of the ITS and LSU region. The concatenated aligned dataset consisted of seven ingroup taxa and 1 401 characters, including alignment gaps. Based on the result of jModeltest, the TrNef+I model was selected for ITS and the Tim2+G for LSU, and these models were applied to individual loci in the combined dataset for the BI analysis. The ML tree for *Alanphillipsia* with bootstrap support values of the ML and the posterior probabilities obtained from the BI analysis is presented in Fig. 3. The two isolates obtained in this study had identical sequences and clustered in a well-supported clade (ML/BI = 100) that includes the ex-type isolate of *Alanphillipsia aloes* (CPC 21298). The two isolates were thus identified as *Alanphillipsia aloes*.

The phylogenetic placement of the *Cytospora* isolate (CMW 56355) obtained was confirmed based on the analyses of the concatenated dataset of six regions (ITS+LSU+*ACT*+*RPB2*+*TEF1*+*TUB2*). This combined dataset consisted of 36 ingroup taxa and 3 558 characters with alignment gaps. Sequences for *Diaporthe eres* (AR5193) were used as the outgroup. Based on the results of jModeltest, BI analysis was performed applying the TIMef+I+G substitution model for ITS region, the TrN+I+G for LSU, the TPMIuf+G for *ACT*, the TIM3+I+G for *RPB2*, the TIM2+G for *TEF1,* and the TPM2uf+G for *TUB2*. The isolate CMW 56355 collected in this study represented a new lineage, clearly distinct from the most closely related species, *Cytospora tibouchinae* (CPC 26333) and *Cytospora myrtagena* (CBS 116843) (Fig. 4).

For the two taxa in *Didymellaceae* (CMW 56351, CMW 56352), the concatenated aligned dataset including sequences of four gene regions (ITS+LSU+*RPB2*+*TUB2*) consisted of 88 ingroup taxa and 2 291 characters, including alignment gaps. Two isolates of *Pleiochaeta setosa* (CBS 118.25, CBS 496.63) were used as the outgroup taxon. Based on the results of jModeltest, the TIM2+I+G model was selected for *RPB2* and LSU, the TVM+I+G for *TUB2*, and the GTR+I+G for ITS. These models were applied to individual loci in the concatenated dataset for the BI analysis. The ML and BI analyses resulted in phylogenetic trees with concordant topologies and showed similar phylogenetic relationships between taxa. The ML tree with bootstrap support values of the ML and the posterior probabilities obtained from the BI analysis is presented in Fig. 5. The isolate CMW 56351 formed a lineage, which was separated and distinct from all other genera in the *Didymellaceae*, representing a novel genus (Fig. 5). The isolate CMW 56352 clustered within *Nothomicrosphaeropsis*, was closely related but clearly distinct from the ex-type isolate

Cytospora - ITS+LSU+*ACT*+*RPB2*+*TEF1*+*TUB2*

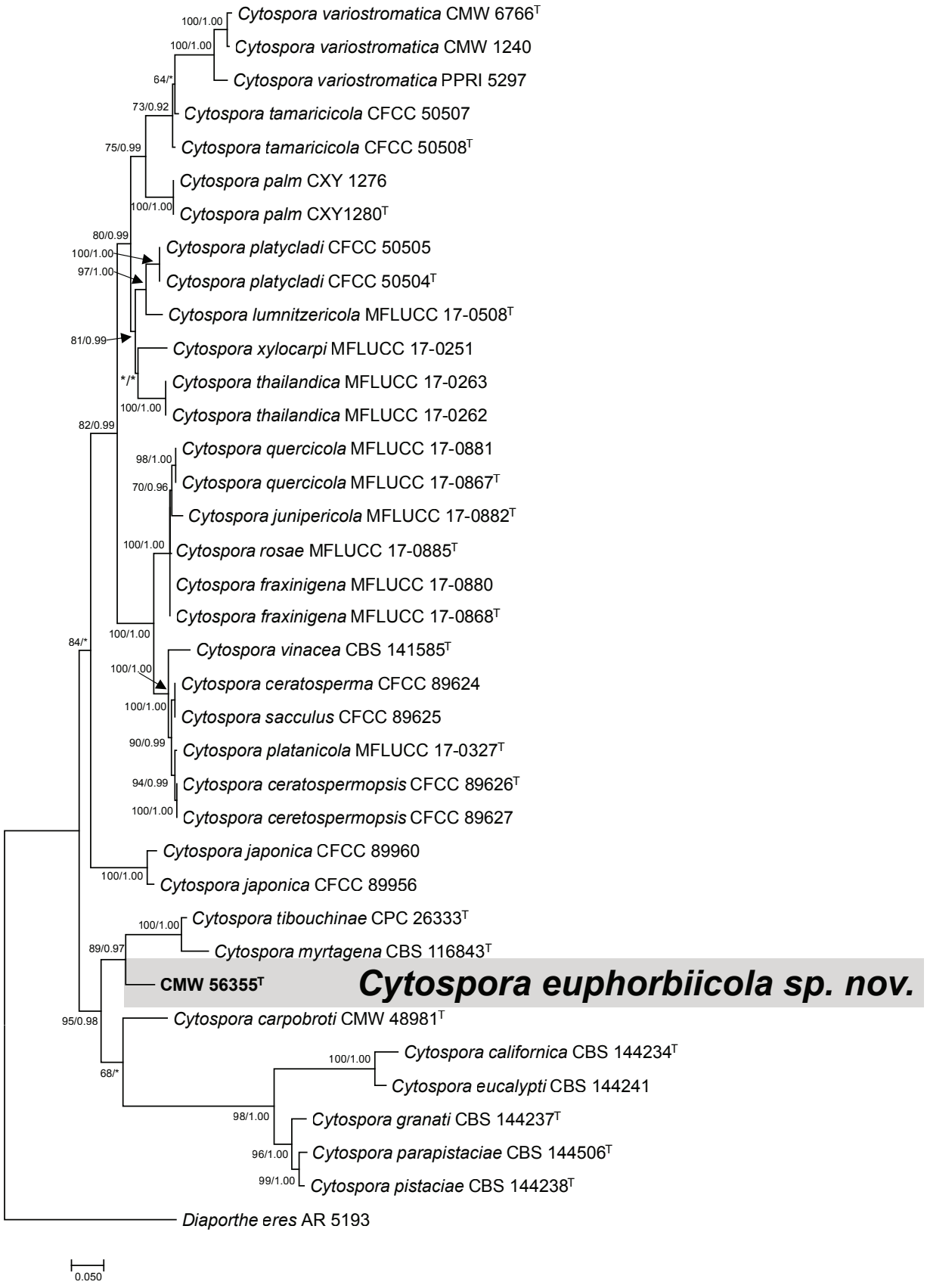

Fig. 4. Phylogenetic tree based on maximum likelihood (ML) analysis of a combined DNA data set of the ITS, LSU, *ACT*, *RPB2*, *TEF1* and *TUB2* sequences for *Cytospora* spp. Isolates sequenced in this study are presented in bold face. Bootstrap values ≥ 60 % for ML analyses and posterior probabilities values ≥ 0.9 obtained from Bayesian inference (BI) are indicated at the nodes as ML/BI. Bootstrap values < 60 % or probabilities values < 0.9 are marked with "*", and nodes lacking the support values are marked with "–". Isolates representing the ex-type material are marked with "T". *Diaporthe eres* (isolate AR5193) represents the outgroup.

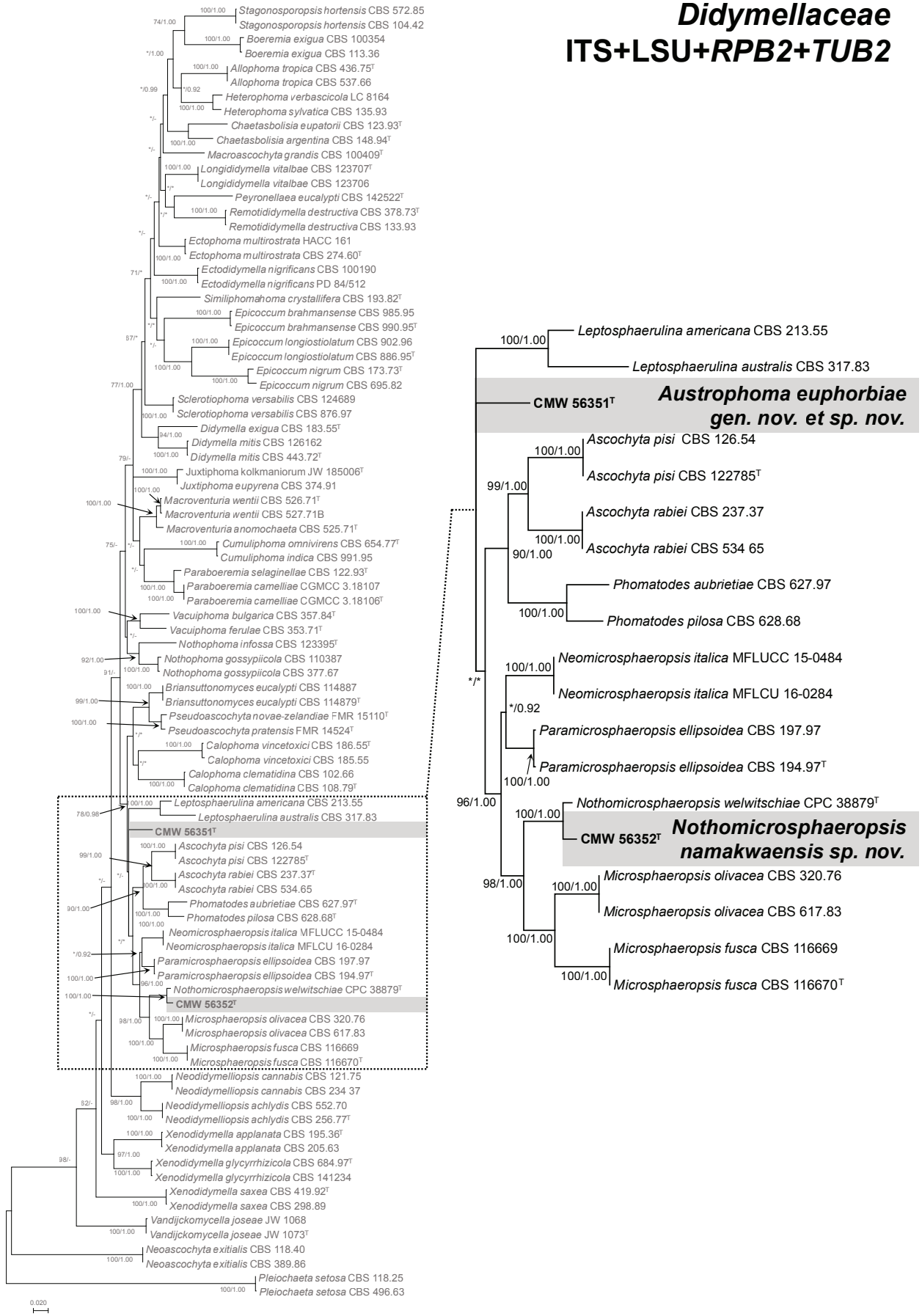

Fig. 5. Phylogenetic tree based on maximum likelihood (ML) analysis of a combined DNA data set of the ITS, LSU, *RPB2*, and *TUB2* sequences representing species of the *Didymellaceae*. Isolates sequenced in this study are presented in bold face. Bootstrap values ≥ 60 % for ML analyses and posterior probabilities values ≥ 0.9 obtained from Bayesian inference (BI) are indicated at the nodes as ML/BI. Bootstrap values < 60 % or probabilities values < 0.9 are marked with "*", and nodes lacking the support values are marked with "–". Isolates representing the ex-type material are marked with "T". Two isolates of *Pleiochaeta setosa* (CBS 118.25 and CBS 496.63) represent the outgroup.

of its sister species, *N. welwitschiae*. This isolate was thus recognised as a novel species of *Nothomicrosphaeropsis*.

Three fungi which are found to be a new species of *Nothomicrosphaeropsis, Cytospora* and a new genus of the *Didymellaceae*, are described and introduced here.

Taxonomy

Austrophoma N.Q. Pham, Marinc. & M.J. Wingf.***, gen. nov.*** MycoBank MB 849172.

Type: *Austrophoma euphorbiae* N.Q. Pham, Marinc. & M.J. Wingf.

Etymology: The name refers to a similarity to *Phoma* and its distribution in the Southern Hemisphere.

Diagnosis: Similar to phoma-like didymellaceous genera, but differs in its hyaline, cylindrical (rectangular in side view) conidia and dark colony colour at 25 °C on 2 % MEA.

Description: *Conidiomata* on MEA pycnidial, papillate or with short neck. *Conidiophores* reduced to conidiogenous cells lining the hymenial layer inside conidioma. *Conidiogenous cells* hyaline, holoblastic, doliiform to lageniform. *Conidia* hyaline, cylindrical, with round apex and flat base, straight or slightly curved, aseptate, rarely 1-septate.

Austrophoma euphorbiae N.Q. Pham, Marinc. & M.J. Wingf. ***sp. nov*.** MycoBank MB 849173. Fig. 6.

Etymology: The name refers to the host genus *Euphorbia*.

Diagnosis: Similar to other phoma-like species but differs in having hyaline and rectangular-shaped (in side view) conidia.

Typus: **South Africa**, Northern Cape Province, Namakwa District Municipality, Nieuwoudtville Falls, from dying *Euphorbia mauritanica*, Aug. 2020, *M.J. Wingfield* (**holotype** PRU(M) 4548, culture ex-type CMW-IA 49, CMW 56351). GenBank: OR198840 (ITS); OR198846 (LSU); OR211854 (*TUB2*); OR211851 (*RPB2*).

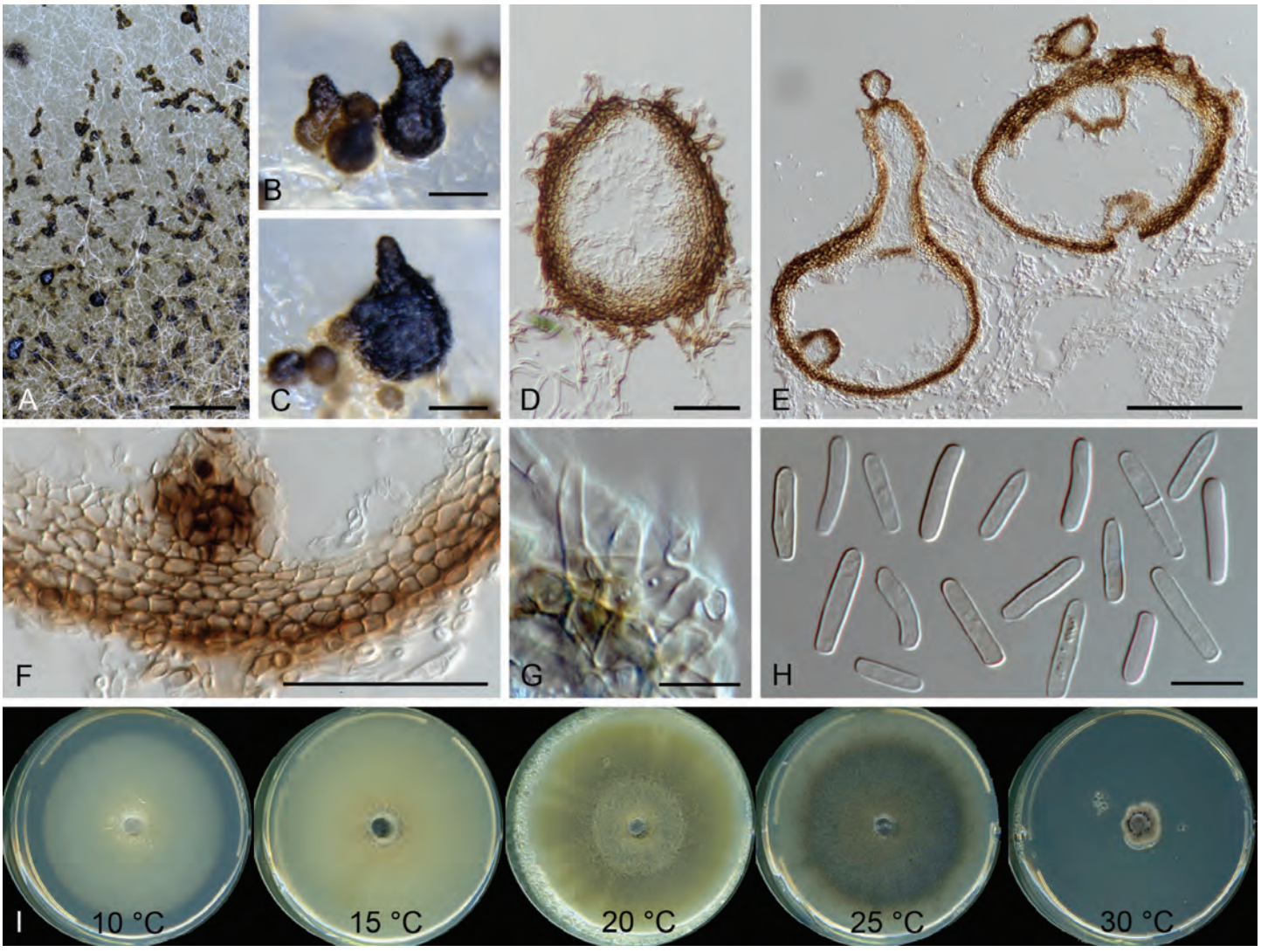

Fig. 6. Micrographs of *Austrophoma euphorbiae sp. nov.* (ex-type: CMW-IA 49, CMW 56351). **A.** Colony with abundant pycnidia on 2 % MEA after 60 d in the dark at room temperature. **B, C.** Young and mature pycnidia with ostiolar protruding, single or multiple necks. **D, E.** Vertical sections through pycnidia. **F.** Pycnidial wall. **G.** Conidiogenous cells. **H.** Conidia. **I.** Colony morphology on 2 % MEA incubated in the dark for 28 d at different temperatures. Scale bars: A = 1 mm; B, C = 100 µm; D–F = 50 µm; G, H = 10 µm.

Description: *Sexual morph* unknown. *Asexual morph* on 2 % MEA. *Conidiomata* pycnidial, immersed to superficial in medium, globose to ellipsoidal, ovoid; base pale brown when young becoming dark brown to black with age, 122–396 × 91–490 (214 ± 64.1 × 197 ± 100.5) µm; protruding ostioles, or necks absent or present, single or multiple when present, 72–533 µm long. *Conidiomatal walls* pseudoparenchymatous, *textura angularis*, in two tiers, 16–34 (25 ± 4.3) µm thick, outer tier composed of 3–5 layers of thick-walled, moderately compressed, brown cells, inner tier composed of thin-walled, compressed, hyaline cells. *Conidiophores* on entire layer of inner cavity, reduced to conidiogenous cells. *Conidiogenous cells* holoblastic, cylindrical. *Conidia* hyaline, cylindrical, with round apex and flat base, mostly straight, occasionally curved, aseptate, rarely 1-septate, 8–14 × 3–4 (10.4 ± 1.37 × 3.2 ± 0.32) µm, oozing out in milky slimy mass.

Culture characteristics: Colonies on MEA showing optimum growth at 25 °C (5.3 mm/d), followed by 20 °C (5.2 mm/d), 15 °C (4 mm/d), 10 °C (2.5 mm/d), 30 °C (0.5 mm/d) and 35 °C (0.4 mm/d). Colonies on MEA at 25 °C in the dark for 28 d fuscous black (3''''k) above and reverse, sparse aerial hyphae, with even edge. Colonies at lower temperatures colour becoming paler.

Host: *Euphorbia mauritanica*.

Distribution: South Africa (Northern Cape Province).

Notes: *Austrophoma* had a close affinity to phoma-like genera in the *Didymellaceae* in multi-gene analyses. The most closely related genera were *Ascochyta*, *Leptosphaerulina*, *Microsphaeropsis*, *Neomicrosphaeropsis*, *Nothomicrosphaeropsis*, *Paramicrosphaeropsis* and *Phomatodes*. In addition to its differences in molecular characteristics, *Austrophoma* can be distinguished from *Ascochyta* by producing pycnidia (on MEA) with papilla or distinguishing necks. *Ascochyta* produces ostiolate or poroid pycnidia, without a distinct form of neck (Chen *et al*. 2015). *Austrophoma* is different from *Microsphaeropsis* and its derivative genera containing the name 'microsphaeropsis' by having hyaline conidia: *Microsphaeropsis*, *Paramicrosphaeropsis*, (Hou *et al*. 2020), *Nothomicrosphaeropsis* (Crous *et al*. 2021) and *Neomicrosphaeropsis* (Thambugala *et al*. 2016) produce pigmented conidia. *Austrophoma* and *Phomatodes* (Chen *et al*. 2015) are morphologically similar to each other in having hyaline conidia in allantoid to cylindrical conidia, but combined sequence data separate them into distinct lineages. No sexual morph was found with *Austrophoma*, whereas *Leptosphaerulina* and *Neomicrosphaeropsis* have sexual morphs producing muriform ascospores.

Nothomicrosphaeropsis namakwaensis N.Q. Pham, Marinc. & M.J. Wingf., ***sp. nov.*** MycoBank MB 849174. Fig. 7.

Etymology: The name refers to the District Municipality Namakwa, where the host plant grows naturally.

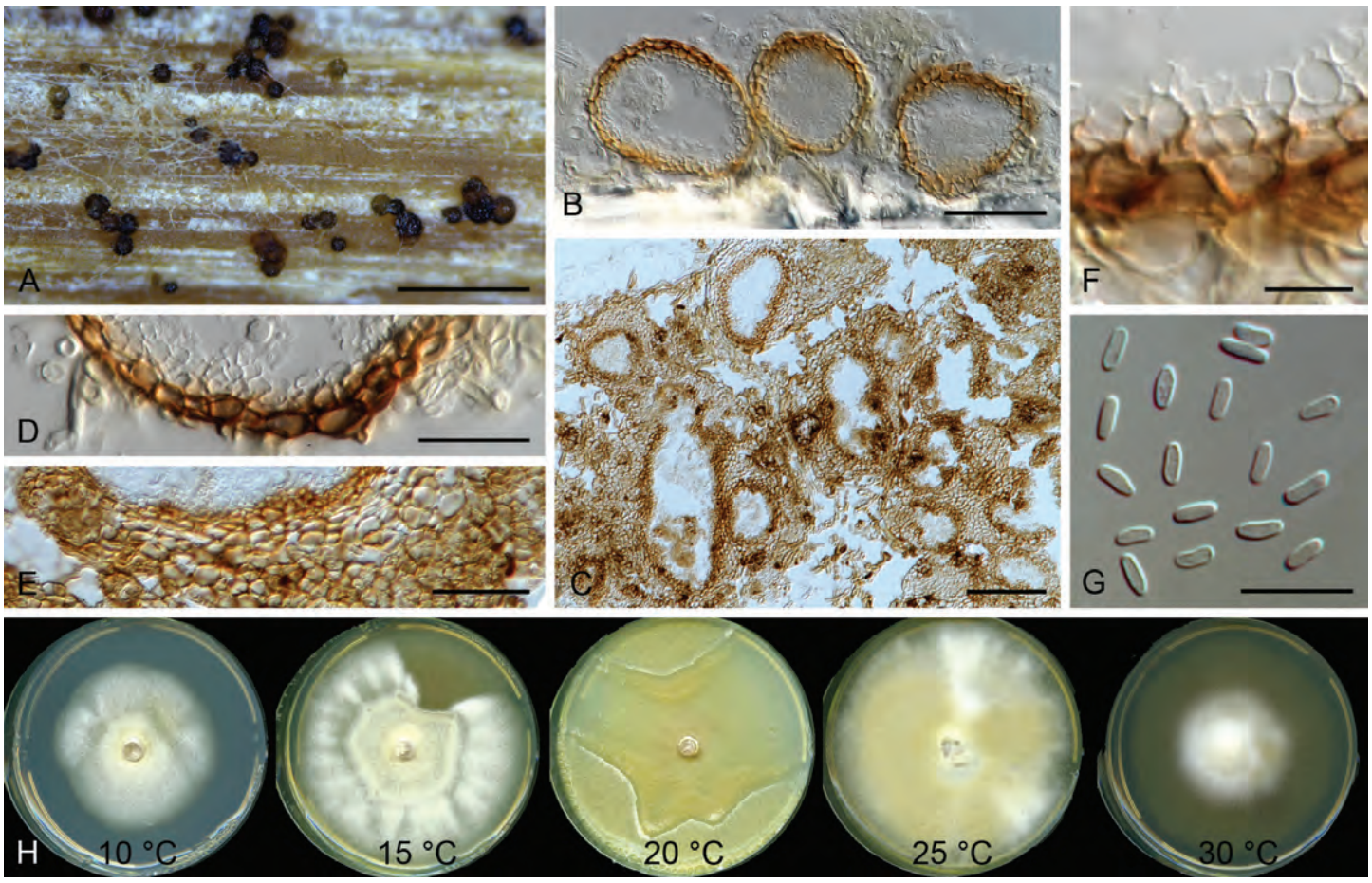

Fig. 7. Micrographs of *Nothomicrosphaeropsis namakwaensis sp. nov.* (ex-type: CMW-IA 50, CMW 56352). **A.** Pycnidia formed on toothpick. **B.** Vertical section through pycnidia. **C.** Vertical section through eustroma formed on MEA with pycinidal locules connected by *textura angularis* tissue. **D, E.** Conidiomatal wall (D) and pycnidial locule (E). **F.** Conidiogenous cells. **G.** Conidia. **H.** Colony morphology on 2 % MEA in the dark for 28 d at different temperatures. Scale bars: A = 500 µm; B, E = 50 µm; C = 100 µm; D = 25 µm; F, G = 10 µm.

Diagnosis: Similar to *N. welwitschiae* but differs in conidial dimensions (3–5 × 1.5–2 µm, oblong to ellipsoidal) from *N. welwitschiae* (4–7 × 2–2.5 µm, sub-cylindrical). It can be differentiated from *N. welwitschiae* by the LSU (1 bp), *RPB2* (9 bp) and *TUB2* (5 bp) sequences.

Typus: **South Africa**, Northern Cape Province, Namakwa District Municipality, Nieuwoudtville Falls, from dying *Euphorbia mauritanica*, Aug. 2020, *M.J. Wingfield* (**holotype** PRU(M) 4549, culture ex-type CMW 56352, CMW-IA 50). GenBank: OR198841 (ITS); OR198847 (LSU); OR211855 (*TUB2*); OR211852 (*RPB2*).

Description: *Sexual morph* unknown. *Asexual morph* on toothpicks in WA. *Conidiomata* pycnidial or eustromatic, 50–238 × 46.5–172 (89.3 ± 33.82 × 83.1 ± 26.49) µm; when pycnidial, separate, immersed to superficial on media or superficial on toothpicks with base attached, globose to ellipsoidal, single or gregarious, base often missing when immersed in media; when eustromatic, stromata consisting of brown, thick-walled *textura angularis* tissues connecting pycnidial locules. *Ostioles* inconspicuous. *Conidiomatal walls* pseudoparenchymatous, composed of two tiers, 7–17 (11.3 ± 2.79) µm thick, inner tiers consisting of a few layers of sub-hyaline, thin-walled cells, outer tiers consisting of 1–3 layers of thick-walled, brown, compressed cells. *Conidiophores* borne along hymenial walls of inner cavity, reduced to conidiogenous cells, 4–6 × 3–5 µm. *Conidiogenous cells* blastic, doliiform. *Conidia* hyaline, oblong to ellipsoidal, aseptate, 3–5 × 1.5–2 (3.8 ± 0.35 × 1.5 ± 0.11) µm.

Culture characteristics: Colonies on MEA showing optimal growth at 25 °C showing 7.5 mm/d, followed by 20 °C (6.4 mm/d), 15 °C (4.2 mm/d), 10 °C (2.8 mm/d), 30 °C (2.4 mm/d) and 35 °C (0.5 mm/d). Cultures on MEA at 25 °C for 28 d in the dark, sterile, showing circular growth with even margin, aerial mycelia medium dense, cottony, colour above saffron (13d) to pale luteous (17d), reverse luteous (19b).

Host: *Euphorbia mauritanica*.

Distribution: South Africa (Northern Cape Province).

Notes: *Nothomicrosphaeropsis namakwaensis* grouped with *N. welwitschiae* in a well-supported clade (Fig. 5). The genus accommodates only one other species, *N. welwitschiae* isolated from dead leaves of *Welwitschia mirabilis* in Namibia (Crous *et al*. 2021). *Nothomicrosphaeropsis namakwaensis* can be distinguished from *N. welwitschiae* by its hyaline conidia, which do not darken with age and larger conidial dimensions.

Cytospora euphorbiicola N.Q. Pham, Marinc. & M.J. Wingf., ***sp. nov*.** MycoBank MB 849175. Fig. 8.

Etymology: The name refers to the host plant, *Euphorbia.*

Diagnosis: Similar to *C. tibouchinae* and *C. myrtagena* but differs in larger conidial dimensions (*C. euphorbiicola* 4–7 × 1–2 µm; *C. tibouchinae* 3–4 × 1–1.5 µm; *C. myrtagena* 3–4 × 1 µm). It can be differentiated from *C. tibouchinae* by the ITS (90 bp) and LSU (10 bp) sequences and *C. myrtagena* by the ITS (99 bp) sequence.

Typus: **South Africa**, Northern Cape Province, Namakwa District Municipality, Nieuwoudtville Falls, from dying *Euphorbia mauritanica*, Aug. 2020, *M.J. Wingfield* (**holotype** PRU(M) 4550, culture ex-type CMW 56355, CMW-IA 51). GenBank: OR198839 (ITS); OR198845 (LSU); OR211853 (*TUB2*); OR211850 (*RPB2*); OR211857 (*TEF1*); OR211856 (*ACT*).

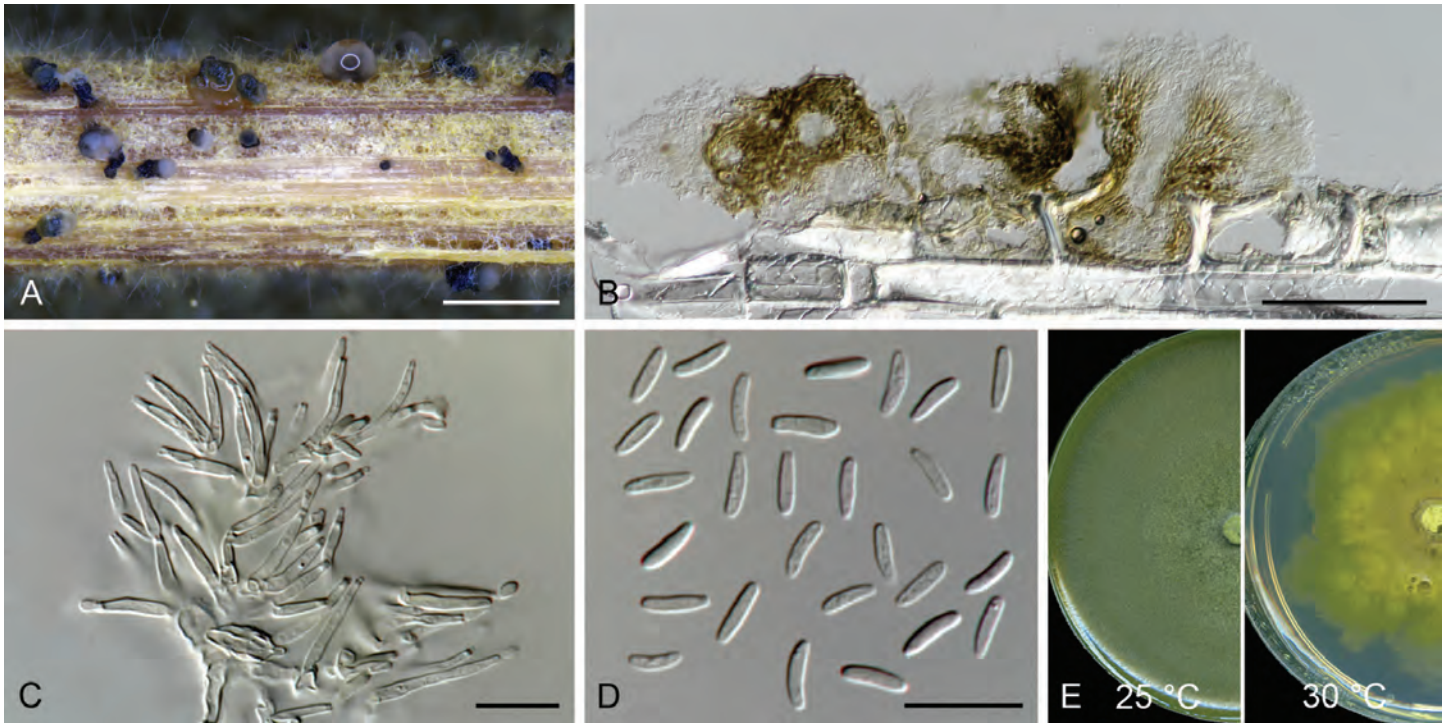

Fig. 8. Micrographs of *Cytospora euphorbiicola sp. nov*. (ex-type: CMW-IA 51, CMW 56355). **A.** Sporodochia formed on toothpick. **B.** Vertical section through sporodochia. **C.** Conidiophores and conidiogenous cells. **D.** Conidia. **E.** Colony morphology on 2 % MEA incubated in the dark for 28 d at 25 °C and 30 °C. Scale bars: A = 1 mm; B = 100 µm; C, D = 10 µm.

Description: *Sexual morph* unknown. *Asexual morph* on toothpicks placed on WA medium. *Conidiomata* sporodochial. *Conidiophores* borne on hymenial layer inner cavity, branched irregularly at the base and above. *Conidiogenous cells* phialidic, cylindrical tapering towards apex, integrated, acropleurogenous, collarette minute, 7.5–16 × 1–2 (10.6 ± 1.59 × 1.5 ± 1.82) µm. *Conidia* hyaline, aseptate, fusiform to allantoid, straight or curved, 4–7 × 1–2 (5.3 ± 0.52 1.3 ± 0.15) µm, in slimy milky mass or droplets.

Culture characteristics: Colonies on MEA showing optimal growth at 25 °C showing 13.7 mm growth per day, followed by 20 °C (13.2 mm/d), 15 °C (9 mm/d), 10 °C (3.9 mm/d), 30 °C (3.3 mm/d) and 35 °C (growth only on the plug). Cultures on MEA for 28 d in the dark at 25 °C sterile, showing circular growth with even edge, aerial mycelia flat, medium dense, colour above and reverse citrine (21k); at 30 °C circular growth with uneven margin, colour above amber (21'b), at 10 °C above pale luteous (19d).

Host: *Euphorbia mauritanica*.

Distribution: South Africa (Northern Cape Province).

Notes: *Cytospora euphorbiicola* shows close phylogenetic affinity to *C. tibouchinae* and *C. myrtagena*, both isolated from members of the *Myrtales*. *Cytospora tibouchinae* was reported from *Tibouchina semidecandra* in La Réunion (Crous *et al*. 2016), and *C. myrtagena* from *Eucalyptus grandis* and *Tibouchina urvilleana* in Sumatra (Indonesia) and Hilo (Hawaii, USA) (Adams *et al*. 2005, Rossman *et al*. 2015). *Cytospora euphorbiicola* (4–7 × 1–2 µm) can be differentiated from both species by its larger conidial dimensions (*C. tibouchinae* 3–4 × 1–1.5 µm; *C. myrtagena* 3–4 × 1 µm). No sexual morph is known for *Cytospora euphorbiicola* and *C. tibouchinae* (Crous *et al*. 2016), but one is known for *C. myrtagena* (Adams *et al.* 2005)

Pathogenicity

Eight weeks after inoculation, all inoculated *Euphorbia* stems remained living, but those inoculated with fungi had distinct lesions around the points of inoculation. In contrast, there were only small areas of wound-associated discolouration for the control inoculations. Mean lesion area associated with five fungal isolates did not differ significantly from each other, but they were all significantly larger than the lesions associated with the controls ($p < 0.05$) (Fig. 9). Re-isolations from the lesion margins resulted in 100 % recovery of the inoculated fungi, while isolations made from the control inoculations yielded either nothing or only secondary contaminant fungi.

DISCUSSION

Dying *E. mauritanica* shrubs such as those examined in this study have been observed in parts of the Western and Northern Cape Provinces of South Africa for at least five years. The results of this study showed that a number of fungi are present on the primary lesions associated with the die-off of these plants. These included some known fungi as well as the various new taxa described here. The greenhouse pathogenicity test confirmed that these fungi were opportunists and most likely contributed to the die-off of the shrubs, possibly predisposed by environmental factors.

Alanphillipsia aloes (*Botryosphaeriaceae*) was originally reported from dark lesions associated with dying *Aloidendron* (*Aloe) dichotoma* in South Africa (Crous *et al*. 2013). Five species are known in the genus, including *Ala. aloes*, *Ala. aloetica*, *Ala. aloicola*, *Ala. aloigena* and *Ala. euphorbiae*. They have been reported exclusively from indigenous *Aloe* and *Euphorbia* trees in arid regions of South Africa (Crous *et al*. 2013, 2014). Members of the *Botryosphaeriaceae* (Slippers & Wingfield 2007) are well-known opportunistic fungi that tend to become active under conditions of host plant stress. It was thus not surprising that *Ala. aloes* did not emerge as a primary pathogen in our inoculation studies.

Two pycnidia-producing isolates represented two new taxa in the *Didymellaceae*, *Austrophoma eugeniae* and *Nothomicrosphaeropsis namakwaensis*. The phylogenetic placement of these fungi with closely-related genera within the family was well supported in multi-gene analyses. The only species in the genus *Nothomicrosphaeropsis*, *N. welwitschiae*, was isolated from dead leaves of *Welwitschia mirabilis*, which is found in the Namib desert (Crous *et al*. 2021). *Nothomicrosphaeropsis namakwaensis* described here is the second species to be described in the genus and can be clearly differentiated from *N. welwitschiae* based on the sequences of *RPB2* and *TUB2* regions. It showed some degree of pathogenicity to the *E. mauritanica* plants, but it did not result in death.

Austrophoma is introduced here as a new genus in the *Didymellaceae*, with *Aus. euphorbiae* as the type species. Although only a single isolate of this fungus was collected, its unique habitat justified our decision to describe it. As in the case of *Nothomicrosphaeropsis,* in which we discovered a second species in this study, it is reasonable to anticipate that additional

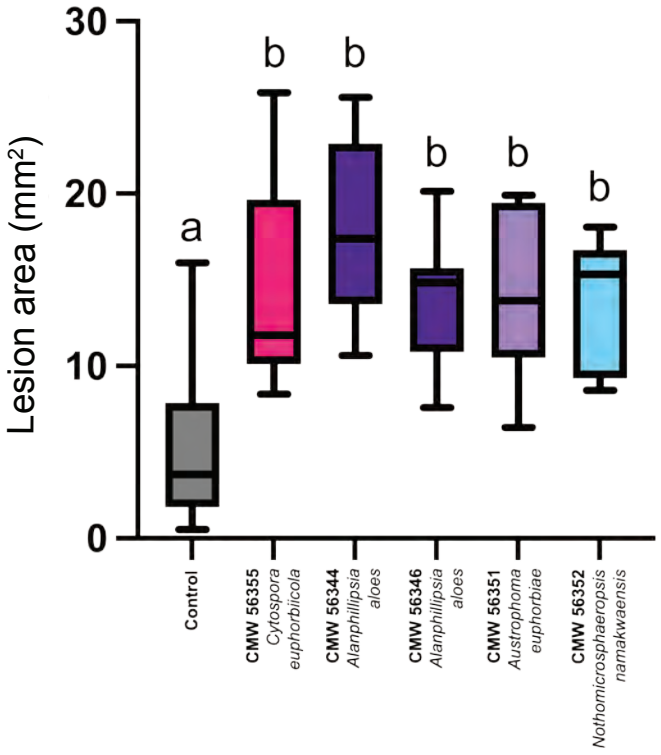

Fig. 9. Boxplots indicating lesion area resulting from inoculations with five fungal isolates and the control on *Euphorbia mauritanica*. Vertical bars represent standard error of the means. Bars with different letters indicate statistically significance at $P \leq 0.05$.

species of *Austrophoma* will emerge as studies in this unusual and arid environment are undertaken. *Austrophoma euphorbiae* showed significant lesion development in the pathogenicity tests but is unlikely to have contributed to disease development.

Cytospora euphorbiicola (*Cytosporaceae*) grouped with *C. tibouchinae* (La Réunion) and *C. myrtagena* (North Sumatra, Indonesia; Hawaii, USA) (Adams *et al*. 2005, Crous *et al*. 2016, Rossman *et al.* 2015). *Cytospora* spp. are well-known opportunistic fungi, having a cosmopolitan distribution and commonly occurring in healthy woody plants as asymptomatic endophytes. However, they can also cause diseases in various woody plants, usually under conditions of stress (Adams *et al*. 2005, Mehrabi *et al*. 2011, Zhang *et al*. 2012, Du *et al*. 2013, Palavouzis *et al*. 2015). An extensive study by Adams *et al*. (2006) identified 14 *Cytospora* spp. from South Africa, and later Jami *et al*. (2018) described *C. carpobroti* causing disease on sour fig, *Carpobrotus edulis*. *Cytospora euphorbiicola* is the 16th species of *Cytospora* to be described from South Africa. It was able to cause lesions on the stems of *Euphorbia* plants but, like all other fungi considered in this study, did not result in plant death.

Greenhouse inoculations with the fungi most commonly encountered in this study showed that they are all able to cause lesions, but none were found to be primary pathogens and able to kill *E. mauritanica*. We thus conclude that the fungi most commonly associated with the die-off of *E. mauritanica* are not the primary cause of the observed disease. This situation could be similar to the case of *E. ingens* plants that are dying in large numbers where they occur naturally in South Africa (Van der Linde *et al*. 2012a). The die-off of *E. ingens* plants is associated with a suite of complex stress factors, including biotic and abiotic agents and anthropogenic activities in their habitats (Van der Linde *et al.* 2011, 2012a, b, 2016, 2017a, b, 2018). A particular interest was in *Lasiodiplodia theobromae*, *Gondwanamyces serotectus* and *G. ubusi*, which in pathogenicity tests, gave rise to extensive internal rot and lesions in the succulent branches (Van der Linde *et al.* 2011, 2012b). Apart from biotic agents, moisture deficiency resulting from increasing temperatures and decreasing precipitation was noted as a major abiotic contribution to the die-off of *E. ingens* (Van der Linde *et al.* 2012a).

It is reasonable to assume that the death of *E. mauritanica* plants considered in this study has been subjected to stress since the sampling took place after a prolonged drought. The fungi encountered are likely endophytes that have proliferated under these stressful conditions resulting in large-scale die-offs.

ACKNOWLEDGEMENTS

We are grateful to the University of Pretoria for funding to make this study possible. Mrs W.J. Wingfield kindly provided the plant material of *E. mauritanica,* and Dr H. Suzuki assisted with data analyses, for which we are most grateful.

Conflict of interest: The authors declare that there is no conflict of interest.

REFERENCES

Adams GC, Wingfield MJ, Common R, *et al*. (2005). Phylogenetic relationships and morphology of *Cytospora* species and related teleomorphs (*Ascomycota*, *Diaporthales*, *Valsaceae*) from *Eucalyptus*. *Studies in Mycology* **52**: 1–142.

Adams GC, Roux J, Wingfield MJ (2006). *Cytospora* species (*Ascomycota*, *Diaporthales*, *Valsaceae*): introduced and native pathogens of trees in South Africa. *Australasian Plant Pathology* **35**: 521–548.

Bruyns PV (2022). *Euphorbia* in Southern Africa: Volume 2. Springer International Publishing AG.

Carbone I, Kohn LM (1999). A method for designing primer sets for speciation studies in filamentous ascomycetes. *Mycologia* **91**: 553–556.

Chen Q, Jiang JR, Zhang GZ, *et al*. (2015). Resolving the *Phoma* enigma. *Studies in Mycology* **82**: 137–217.

Critchlow DE, Fligner MA (1991). On distribution-free multiple comparisons in the one-way analysis of variance. *Communications in Statistics - Theory and Methods* **20**: 127–139.

Crous PW, Cowan DA, Maggs-Kölling G, *et al.* (2020). Fungal Planet description sheets. *Persoonia* **45**: 251–409.

Crous PW, Hernández-Restrepo M, Schumacher RK, *et al*. (2021). New and Interesting Fungi 4. *Fungal Systematics and Evolution* **7**: 255–343.

Crous PW, Wingfield MJ, Guarro J, *et al*. (2013). Fungal Planet description sheets: 154–213. *Persoonia* **31**: 188–296.

Crous PW, Wingfield MJ, Schumacher RK, *et al.* (2014). Fungal Planet Description Sheets: 281–319. *Persoonia* **33**: 212–289.

Crous PW, Wingfield MJ, Richardson DM, *et al*. (2016). Fungal Planet description sheets: 400–468. *Persoonia* **36**: 316–458.

Du Q, Zhao SF, Wu CL, *et al.* (2013). Root rot of Chinese jujube (*Ziziphus jujuba*) caused by *Cytospora sacculus* in China. *Plant Disease* **97**: 1661.

Dwass M (1960). Some k-sample rank-order tests. In: *Contributions to Probability and Statistics* (Olkin S, Ghurye G, Hoeffding W, Madow W G, Mann H B, eds). Stanford University Press, Stanford, California, USA: 198–202.

Fan XL, Bezerra JDP, Tian CM, *et al*. (2020). *Cytospora* (*Diaporthales*) in China. *Persoonia* **45**: 1–45.

Gardes M, Bruns TD (1993). ITS primers with enhanced specificity for basidiomycetes–application to the identification of mycorrhizae and rusts. *Molecular Ecology* **2**: 113–118.

Glass NL, Donaldson GC (1995). Development of primer sets designed for use with the PCR to amplify conserved genes from filamentous ascomycetes. *Applied and Environmental Microbiology* **61**: 1323–1330.

Hou LW, Groenewald JZ, Pfenning LH, *et al*. (2020). The phoma-like dilemma. *Studies in Mycology* **96**: 309–396.

Jami F, Marincowitz S, Crous PW, *et al*. (2018). A new *Cytospora* species pathogenic on *Carpobrotus edulis* in its native habitat. *Fungal Systematics and Evolution* **2**: 34–43.

Jiang N, Yang Q, Fan X-L, *et al*. (2020) Identification of six *Cytospora* species on Chinese chestnut in China. *MycoKeys* **62**: 1–25.

Katoh K, Standley DM (2013). MAFFT multiple sequence alignment software version 7: improvements in performance and usability. *Molecular Biology and Evolution* **30**: 772–780.

Kumar S, Stecher G, Tamura K (2016). MEGA7: Molecular Evolutionary Genetics Analysis version 7.0 for bigger datasets. *Molecular Biology and Evolution* **33**: 1870–1874.

Kruskal WH, Wallis WA (1952). Use of ranks in one-criterion variance analysis. *Journal of American Statistical Association* **47**: 583–621 and *errata, ibid*. **48**: 907–911.

Lawrence DP, Holland LA, Nouri MT, *et al.* (2018). Molecular phylogeny of *Cytospora* species associated with canker diseases of fruit and nut crops in California, with the descriptions of ten new species and one new combination. *IMA Fungus* **9**: 333–369.

Liu YJ, Whelen S, Hall BD (1999). Phylogenetic relationships among ascomycetes: evidence from an RNA polymerse II subunit. *Molecular Biology and Evolution* **16**: 1799–1808.

Mehrabi ME, Mohammadi GE, Fotouhifar KB. (2011). Studies on *Cytospora* canker disease of apple trees in Semirom region of Iran. *Journal of Agricultural Technology* **7**: 967–982

Miller MA, Pfeiffer W, Schwartz T (2010). Creating the CIPRES Science Gateway for inference of large phylogenetic trees. In: *Proceedings of the Gateway Computing Environments Workshop (GCE), 14 Nov. 2010*. New Orleans, Louisiana: 1–8.

Norphanphoun C, Raspé O, Jeewon R, *et al.* (2018). Morphological and phylogenetic characterisation of novel *Cytospora* species associated with mangroves. *MycoKeys* **38**: 93–120.

Palavouzis SC, Tzamos S, Paplomatas E, Thomidis T (2015). First report of *Cytospora punicae* isolated from pomegranate plants with symptom of collar rot in northern Greece. *Journal of Plant Pathology* **97(1)**: 1125–4653.

Pham NQ, Barnes I, Chen SF, *et al*. (2019). Ten new species of *Calonectria* from Indonesia and Vietnam. *Mycologia* **111**: 78–102.

Posada D (2008). jModelTest: phylogenetic model averaging. *Molecular Biology and Evolution* **25**: 1253–1256.

R Core Team (2021). R: A language and environment for statistical computing. R Foundation for Statistical Computing, Vienna, Austria. https://www.R-project.org/.

Rayner RW (1970). A mycological colour chart. Commonwealth Mycological Institute: British Mycological society. Kew, Surrey, UK.

Rehner SA, Samuels GJ (1994). Taxonomy and phylogeny of *Gliocladium* analysed from nuclear large subunit ribosomal DNA sequences. *Mycological Research* **98**: 625–634.

Ronquist F, Teslenko M, Van der Mark P, *et al.* (2012). MrBayes 3.2: efficient Bayesian phylogenetic inference and model choice across a large model space. *Systematic Biology* **61:** 539–542.

Rossman AY, Adams GC, Cannon PF, *et al*. (2015). Recommendations of generic names in *Diaporthales* competing for protection or use. *IMA Fungus* **6**: 145–154.

Roux J, Malan R, Howitt M, *et al.* (2008). Discovery of new fungi associated with the decline and death of *Euphorbia ingens* in the Limpopo province of South Africa. *South African Journal of Botany* **74**: 377–378.

Senanayake IC, Crous PW, Groenewald JZ, *et al*. (2017). Families of *Diaporthales* based on morphological and phylogenetic evidence. *Studies in Mycology* **86**: 217– 296.

Stamatakis A (2014). RAxML version 8: a tool for phylogenetic analysis and post-analysis of large phylogenies. *Bioinformatics* **30**: 1312–1313.

Steel RGD (1960). A rank sum test for comparing all pairs of treatments. *Technometrics* **2**: 197–207.

Thambugala KM, Daranagama DA, Phillips AJL, *et al*. (2016). Microfungi on *Tamarix*. *Fungal Diversity* **82**: 239–306.

Sung GH, Sung JM, Hywel-Jones NL, *et al.* (2007). A multi-gene phylogeny of *Clavicipitaceae* (Ascomycota Fungi): identification of localised incongruence using a combinational bootstrap approach. *Molecular Phylogenetics and Evolution* **44**: 1204–1223.

Udayanga D, Castlebury LA, Rossman AY, *et al.* (2014). Insights into the genus *Diaporthe*: phylogenetic species delimitation in the *D. eres* species complex. *Fungal Diversity* **67**: 203–229.

Van der Linde JA, Roux J, Wingfield MJ, *et al*. (2012a). Die-off of giant *Euphorbia* trees in South Africa: Symptoms and relationships to climate. *South African Journal of Botany* **83**: 172–185.

Van der Linde JA, Six DL, De Beer ZW, *et al*. (2016). Novel ophiostomatalean fungi from galleries of *Cyrtogenius africus* (*Scolytinae*) infesting dying *Euphorbia ingens*. *Antonie van Leeuwenhoek* **109**: 589–601.

Van der Linde JA, Six DL, Wingfield MJ, *et al*. (2011). *Lasiodiplodia* species associated with dying *Euphorbia ingens* in South Africa. *Southern Forests: a Journal of Forest Science* **73**: 165–173.

Van der Linde JA, Six DL, Wingfield MJ, *et al*. (2012b). New species of *Gondwanamyces* from dying *Euphorbia* trees in South Africa. *Mycologia* **104**: 574–584.

Van der Linde JA, Six DL, Wingfield MJ, *et al*. (2017a). Fungi and insects associated with *Euphorbia ingens* die-off in South Africa. *Southern Forests* **80**: 21–28.

Van der Linde JA, Wingfield MJ, Crous CJ, *et al.* (2017b). Landscape degradation may contribute to large-scale die-offs of *Euphorbia ingens* in South Africa. *South African Journal of Botany* **111**: 144–152.

Van der Linde JA, Wingfield MJ, Six DL, *et al*. (2018). Seasonal flight patterns of *Curculionidae* (*Cossoninae* and *Scolytinae*) infesting dying *Euphorbia ingens* in South Africa. *Journal of Entomological Science* **53**: 70–81.

Vilgalys R, Hester M (1990). Rapid genetic identification and mapping of enzymatically amplified ribosomal DNA from several *Cryptococcus* species. *Journal of Bacteriology* **172**: 4238–4246.

White TJ, Bruns T, Lee S, *et al.* (1990). Amplification and direct sequencing of fungal ribosomal RNA genes for phylogenetics. In: *PCR protocols: a guide to methods and applications* (Innis MA, Gelfand DH, Sninsky JJ, White TJ, eds), Academic Press, San Diego, California, USA: 315–322.

Yang T, Groenewald JZ, Cheewangkoon R, *et al.* (2017). Families, genera, and species of *Botryosphaeriales*. *Fungal Biology* **121**: 322–346.

Zhang QT, He M, Zhang XY, *et al*. (2012). Canker on bark of *Populus* spp. caused by *Cytospora tritici*, a new disease in China. *Plant Disease* **96**: 1578.

Zhang Q-T, Lu Q, He M, *et al.* (2014). *Cytospora palm sp. nov*. (*Diaporthales, Ascomycota*), a canker agent on *Cotinus coggygria* (*Anacardiaceae*) in Northern China. *Cryptogamie, Mycologie* **35**: 211–220.

Supplementary information

Table S1. Collection details and GenBank accessions of *Alanphillipsia* isolates included in the phylogenetic analyses.

Table S2. Collection details and GenBank accessions of *Cytospora* isolates included in the phylogenetic analyses.

Table S3. Collection details and GenBank accessions of *Didymellaceae* isolates included in the phylogenetic analyses.

FUSE

Fungal Systematics and Evolution

Volume 12
DECEMBER 2023
PAGES 73–80

doi.org/10.3114/fuse.2023.12.05

A novel species of *Microsphaeropsis* causing cankers on *Rafnia amplexicaulis* in South Africa

T. Paap[1], S. Marincowitz[1], N.Q. Pham[2], F. Roets[3], R.J. Basson[3], B.D. Wingfield[1], K. Oberlander[4], M.J. Wingfield[1]

[1]Department of Biochemistry, Genetics and Microbiology; Forestry and Agricultural Biotechnology Institute, University of Pretoria, Private Bag X20, Hatfield, Pretoria, 0028, South Africa
[2]Department of Plant and Soil Sciences, Forestry and Agricultural Biotechnology Institute (FABI), University of Pretoria, Private Bag X20, Hatfield, Pretoria, 0028, South Africa
[3]Department of Conservation Ecology and Entomology, Stellenbosch University, Private Bag X1, Matieland, 7602, South Africa
[4]H.G.W.J. Schweickerdt Herbarium, Department of Plant and Soil Sciences, University of Pretoria, Private Bag X20, Hatfield, Pretoria, 0028, South Africa

*Corresponding author: trudy.paap@fabi.up.ac.za

Key words:
multigene phylogeny
new taxon
pathogenicity
stem canker

Abstract: Cankers leading to branch, stem and plant death were observed on the South African endemic *Rafnia amplexicaulis* (*Fabaceae*) in the Cederberg Wilderness Area, South Africa, during September 2021. Conidiomatal pycnidia were found developing on the cankers, and isolations consistently yielded a *Microsphaeropsis* species. Phylogenetic analysis based on partial nucleotide sequences of the internal transcribed spacers (ITS), the nuclear large subunit (LSU) and RNA polymerase II second largest subunit (*RPB2*) regions showed that the fungus represented an undescribed species. Based on the multigene phylogeny and morphological characteristics, we describe the species here as *M. rafniae sp. nov*. Pathogenicity tests and the fulfilment of Koch's postulates confirmed that *M. rafniae sp. nov*. is the cause of the cankers of *R. amplexicaulis*. Presently, this disease is known from a single location in South Africa, and further surveys are required to determine its distribution and relative importance.

Citation: Paap T, Marincowitz S, Pham NQ, Roets F, Basson RJ, Wingfield BD, Oberlander K, Wingfield MJ (2023). A novel species of *Microsphaeropsis* causing cankers on *Rafnia amplexicaulis* in South Africa. *Fungal Systematics and Evolution* **12**: 73–80. doi: 10.3114/fuse.2023.12.05
Received: 13 July 2023; **Accepted:** 28 July 2023; **Effectively published online:** 1 August 2023
Corresponding editor: P.W. Crous

INTRODUCTION

Rafnia amplexicaulis (*Fabaceae*) is a perennial, woody shrub endemic to the Northern and Western Cape Provinces of South Africa. As a resprouter, coppice shoots are produced from an underground lignotuber following fire, resulting in plants being multi-stemmed at ground level (Campbell & van Wyk 2001). The leaves and roots of *R. amplexicaulis* have been utilised as traditional remedies by the local Cape indigenous communities (Kinfe *et al.* 2015).

During a field visit to the Cederberg mountains in September 2021, yellowing and dying *R. amplexicaulis* shrubs were observed in a single location within the Cederberg Wilderness Area, Western Cape Province, South Africa. Closer inspection revealed girdling cankers present on the symptomatic stems. Fungal structures (pycnidia) characteristic of a *Microsphaeropsis* species were visible on the surface of the cankers.

Microsphaeropsis (*Didymellaceae*) was introduced by Von Höhnel (1917) to accommodate pycnidial fungi with small dark aseptate conidia produced from phialides. The genus has a cosmopolitan distribution, with species commonly described as plant endophytes or saprophytes. The genus also contains a number of plant pathogens described from necrotic spots and/or lesions on leaves and twigs (Swart *et al*. 1998, Hou *et al*. 2020). The aim of this study was to describe the disease occurring on *R. amplexicaulis* and identify its causal agent.

METHODS AND METHODS

Disease description and isolations

The diseased *R. amplexicaulis* plants were restricted to an area of approximately 1 000 m^2 on a south-east facing slope within the Cederberg Wilderness Area, Western Cape Province, South Africa (-32.412743, 19.174894). Shrubs were visibly yellowing, and on closer examination cankers were commonly found on symptomatic stems and branches. In instances where cankers were girdling, these led to stem and branch death (Fig. 1). Removal of the outer bark showed distinct necrosis of the cambium at the leading edges of the lesions. Sections of symptomatic stems were removed from plants, placed in brown paper bags and transported to the laboratory for further examination.

Conidiomatal pycnidia that oozed conidial masses typical of *Microsphaeropsis* species were observed on the surfaces of the cankers. Conidia were lifted from the pycnidia using a sterile hypodermic needle and transferred to the surface of 2 % malt

Fig. 1. *Rafnia amplexicaulis* in the field. **A.** Population of *Rafnia amplexicaulis* in the Cedarberg Wilderness Area, Western Cape Province, South Africa. **B.** Symptomatic stems.

extract agar (MEA: 20 g Biolab malt extract, 20 g Difco agar, 1 L deionised water) amended with 1 % streptomycin sulphate (Sigma-Aldrich). Cultures were purified by transferring single hyphal tips to fresh MEA plates and maintained at 25 °C.

The resulting cultures were deposited in the culture collection (CMW) of the Forestry and Agricultural Biotechnology Institute (FABI), University of Pretoria, Lunnon Road, Pretoria, South Africa. The holotype and ex-holotype were deposited in the H.G.W.J. Schweickerdt Herbarium (PRU) and the culture collection of Innovation Africa (CMW-IA), respectively, at the University of Pretoria, Lunnon Road, Pretoria, South Africa.

Morphology

The top part of pycnidial structures were cut with a scalpel. The exposed insides of the structures were moistened with a piece of agar, and conidiogenous cells and conidia were extracted and mounted on slides in water. For measurements, the water was replaced with 85 % lactic acid. Images were captured using Nikon microscopes (Eclipse Ni and SMZ18, Japan) mounted with a DS-Ri2 camera. The image program NIS-Elements BR was used for measurements and taking photos. Bark samples containing pycnidia were cut into small pieces. The pieces were boiled for a few seconds to soften the structures and mounted on a disc with freezing medium. Vertical sections were prepared in 10–12 µm thickness using a cryomicrotome (Leica CM1520, Germany). The sections were mounted in 85 % lactic acid for observation. Fifty conidia were measured and presented as min–max (average ± standard deviation), whereas less than ten structures were measured for conidiogenous cells and conidiomata and presented as min–max, due to the shortage of samples.

Isolate CMW 57792 was used for the growth study and colony morphology. Culture characteristics and growth rates were determined on MEA, potato dextrose agar (PDA; BD Difco) and oatmeal agar (OA; liquid extract of 30 g of oats cooked in 800 mL water for an hour used to make 1 L, 20 g Difco agar). Colours were described using the colour chart of Rayner (1970). Cultures were grown at seven temperatures, ranging from 5 to 35 °C in 5 °C intervals. At each temperature, five replicates of the isolate were incubated in the dark. Diameters perpendicular to each other were measured after 10 d, when the colony margins reached the edges of the Petri-dishes at optimum temperature. After measuring the diameters, the plates were returned to the incubators for an additional few weeks to observe possible changes with age. An NaOH spot test was performed on a culture grown on OA (Boerema *et al*. 2004).

DNA isolation, PCR amplification and sequencing

DNA was extracted from 7-d-old isolates grown on 2 % MEA at 25 °C using Prepman® Ultra Sample Preparation Reagent (Thermo Fisher Scientific, Waltham, MA, USA) following the manufacturer's protocols. The nuclear internal transcribed spacer regions 1 and 2 (ITS), including the 5.8S rRNA gene region, were amplified using primers ITS1F and ITS4 (White *et al*. 1990, Gardes & Bruns 1993); part of the nuclear large subunit (LSU) of ribosomal RNA gene with primers LR0R and LR5 (Vilgalys & Hester 1990, Rehner & Samuels 1994) and a fragment of the DNA-directed RNA polymerase II second largest subunit gene (*RPB2*) with primer pair RPB2-5F2 and fRBP2-7cR (Liu *et al.* 1999; Sung *et al*. 2007). PCR amplifications were prepared following the protocols described by Pham *et al*. (2019). For ITS and LSU regions, the thermal cycling included an initial denaturation at 95 °C for 5 min followed by 10 primary amplification cycles of 30 s at 95 °C, 30 s at 56 °C, and 60 s at 72 °C, then 30 additional cycles of the same reaction sequence, with a 5 s increase in the annealing step per cycle, and the reactions were completed with a final extension at 72 °C for 10 min. The amplification for *RPB2* was performed following the method of Liu *et al.* (2020). Amplified fragments of all loci were purified using ExoSAP-IT™ PCR Product Cleanup Reagent (Thermo Fisher Scientific, Waltham, MA, USA). Amplicons were sequenced in both directions using an ABI PRISM™ 3100 DNA sequencer (Applied Biosystems, USA) at the Sequencing Facility

Table 1. Collection details and GenBank accessions of isolates included in the phylogenetic analyses.

Species	Isolates	Substrate	Locality	GenBank accessions			References
				RPB2	LSU	ITS	
Microsphaeropsis fusca	CBS 116669	*Sarothamnus scoparius*	The Netherlands	MT018219	EU754170	MN973572	Hou *et al*. (2020)
	CBS 116670^{T}	*Sarothamnus scoparius*	The Netherlands	MT018220	MN943779	MN973573	Hou *et al*. (2020)
	CBS 139603; MFLUCC 14-0507	*Sarothamnus scoparius*	Germany	MT018218	MN943778	MN973571	Hou *et al*. (2020)
Microsphaeropsis olivacea	CBS 233.77	*Pinus laricio*	France	MT018217	GU237988	GU237803	Hou *et al*. (2020)
	CBS 320.76	*Cronartium ribicola*	France	MT018214	MN943775	MN973568	Hou *et al*. (2020)
	CBS 617.83	*Pinus sylvestris*	Switzerland	MT018213	MN943774	MN973567	Hou *et al*. (2020)
	CBS 608.72	*Tremella foliacea*	The Netherlands	MT018216	MN943777	MN973570	Hou *et al*. (2020)
	CBS 336.78	*Picea abies*	Germany	MT018215	MN943776	MN973569	Hou *et al*. (2020)
Microsphaeropsis proteae	CBS 113685; UPSC 1926	*Dryas octopetala*	Sweden	MT018262	MN943800	MN973593	Hou *et al*. (2020)
	CBS 111303^{T}; CPC 1423	*Protea nitida*	N/A	MT018221	JN712561	JN712495	Hou *et al*. (2020)
	CBS 111319; CPC 1425	*Protea nitida*	N/A	MT018223	JN712563	JN712497	Hou *et al*. (2020)
	CBS 111320; CPC 1424	*Protea nitida*	N/A	MT018222	JN712562	JN712496	Hou *et al*. (2020)
Microsphaeropsis rafniae	**CMW 57792^{T}**	*Rafnia amplexicaulis*	South Africa	**OR211858**	**OR209716**	**OR209698**	This study
	CMW 57793	*Rafnia amplexicaulis*	South Africa	**OR211859**	**OR209717**	**OR209699**	This study
	CMW 57794	*Rafnia amplexicaulis*	South Africa	**OR211861**	**OR209718**	**OR209700**	This study
	CMW 57795	*Rafnia amplexicaulis*	South Africa	**OR211862**	**OR209719**	**OR209701**	This study
Microsphaeropsis taxicola	CBS 469.80	*Rhus typhina*	The Netherlands	MT018210	MN943772	MN973565	Hou *et al*. (2020)
	CBS 442.83	*Taxus baccata*	The Netherlands	MT018211	EU754171	GU237865	Hou *et al*. (2020)
	CBS 427.92	*Opuntia cladodes*	The Netherlands	MT018212	MN943773	MN973566	Hou *et al*. (2020)
Microsphaeropsis viridis	CBS 763.73	*Populus tremula*	France	MT018205	MN943768	MN973561	Hou *et al*. (2020)
	CBS 762.73	*Pseudotsuga menziesii*	France	MT018206	MN943769	MN973562	Hou *et al*. (2020)
	CBS 354.69	*Berberis* sp.	The Netherlands	MT018207	MN943770	MN973563	Hou *et al*. (2020)
	CBS 432.71^{T}	*Sarothamnus* sp.	The Netherlands	MT018209	GU237987	GU237863	Hou *et al*. (2020)
	CBS 639.80	*Abies alba*	Germany	MT018208	MN943771	MN973564	Hou *et al*. (2020)
Neomicrosphaeropsis alhagi-pseudalhagi	MFLUCC 17-0825^{T}	*Alhagi maurorum*	Uzbekistan	MH069682	MH069670	MH069664	Hou *et al*. (2020)
Neomicrosphaeropsis elaeagni	MFLUCC 17-0740^{T}	*Elaeagnus angustifolia*	Russia	MH069684	MH069672	MH069666	Hou *et al*. (2020)
Neomicrosphaeropsis italica	MFLUCC 15-0484	*Tamarix* sp.	Italy	KU695539	KU729853	KU900319	Hou *et al*. (2020)
	MFLUCC 16-0284	*Tamarix* sp.	Italy	KU714604	KU900296	KU900321	Hou *et al*. (2020)
Nothomicrosphaeropsis welwitschiae	CBS 146829^{T}; CPC 38879	*Welwitschia mirabilis*	Namibia	MW890067	MW883826	MW883434	Crous *et al*. (2021)
Paramicrosphaeropsis ellipsoidea	CBS 197.97	*Quercus ilex*	Spain	MT018224	MN943780	MN973574	Hou *et al*. (2020)
	CBS 194.97^{T}	*Quercus ilex*	Spain	MT018225	MN943781	MN973575	Hou *et al*. (2020)
Calophoma parvula	CBS 620.68	*Aegopodium podagraria*	The Netherlands	MT018234	MN943783	MN973577	Hou *et al*. (2020)

CBS = culture collection of Westerdijk Fungal Biodiversity Institute, Utrecht, the Netherlands; CMW = culture collection of the FABI, University of Pretoria, Pretoria, South Africa; CMW-IA = culture collection of Innovation Africa, University of Pretoria, Pretoria, South Africa; CPC = culture collection of Pedro Crous, housed at Westerdijk Fungal Biodiversity Institute; MFLUCC = Mae Fah Luang University Culture Collection, Chiang Rai, Thailand; UPSC: Uppsala University Culture Collection, Sweden.

ITS = internal transcribed spacer regions 1 & 2 including the 5.8S region of the nrRNA; LSU = 28S large subunit of the nrRNA; *RPB2* = DNA-directed RNA polymerase II second largest subunit gene.

^{T}Denotes ex-type strain.

Isolates and sequences obtained in this study are indicated in **bold**.

of the Faculty of Natural and Agricultural Sciences, University of Pretoria, South Africa. Geneious Prime v. 2022.1.1 was used for assembling and editing raw sequences (https://www.geneious.com). All sequences generated in this study were deposited in GenBank (http://www.ncbi.nlm.nih.gov) (Table 1).

Phylogenetic analyses

Reference sequences for species closely related to those emerging from this study were downloaded from the GenBank nucleotide database (Table 1). All sequences were aligned using MAFFT v. 7 (http://mafft.cbrc.jp/alignment/server/) (Katoh & Standley 2013), then confirmed manually in MEGA v. 7 (Kumar *et al*. 2016) where necessary. Maximum likelihood (ML) and Bayesian inference (BI) analyses were performed on the combined dataset of three regions. The most appropriate model was obtained using the software jModeltest v. 1.2.5 (Posada 2008). For ML, analyses were conducted using RAxML v. 8.2.4 on the CIPRES Science Gateway v. 3.3 (Stamatakis 2014) with default GTR substitution matrix and 1 000 rapid bootstraps. For BI, analyses were performed using MrBayes v. 3.2.6 (Ronquist *et al.* 2012) on the CIPRES Science Gateway v. 3.3. Four Markov chain Monte Carlo (MCMC) chains were run from a random starting tree for five million generations and trees were sampled every 100th generation. The first 25 % of trees sampled were eliminated as burn-in and the remaining trees were used to determine the posterior probabilities. *Calophoma parvula* (CBS 620.68) was used as the outgroup taxon. Resulting trees were viewed using MEGA v. 7 (Kumar *et al*. 2016) and FigTree v. 1.4.3 (Rambaut 2010).

Pathogenicity tests

The pathogenicity of the isolated *Microsphaeropsis* species towards *R. amplexicaulis* was determined in a natural population of the host plant in the Cedarberg Wilderness Area, Western Cape Province, South Africa (-32.42956; 19.15981). Inoculations were initiated during spring (October) of 2021 using two isolates (CMW 57792 and CMW 57793).

Thirty plants were randomly chosen for inoculation, distributed in an area of approximately 1 ha. A 7-mm-diam cork borer was used to remove the bark and expose the cambium on a single branch (2–3 cm diam) per plant. Similar sized discs, taken from the actively growing margins of 2-wk-old cultures on PDA, were inserted into these wounds with the mycelial growth facing the xylem (n = 10 branches per isolate). Each branch received only one inoculation. An additional 10 branches were inoculated with an agar-only control. Wounds were covered with Parafilm™ (Amcor, Zürich, Switzerland) to prevent desiccation and contamination by other organisms.

After 7 wk, inoculated branches were harvested by removal at the base of the main stem, and transferred in brown paper bags to the laboratory for assessment. Leaves were removed from the branches, and the length of the lesions (mm) was determined by removing the bark around each inoculation point with a sterile scalpel and measuring the length of the longest distance of the stained portion of the vascular tissues using digital calipers.

Isolations were made from stained portions of vascular tissues of all inoculated branches including control treatments, to determine whether *Microsphaeropsis* was the causal agent for lesion development. Branch sections containing lesions were surface sterilised with 70 % ethanol for 1 min, after which approximately 5 mm^3 sections from the leading edges of lesions were plated onto ½ PDA. These were incubated in the dark at 25 °C for approximately 7–10 d and resulting fungal cultures were morphologically evaluated to confirm identity.

Lesion length data were normally distributed after implementing a Shapiro-Wilks test (W = 0.931, p = 0.053) using R Software v. 3.6.3 (https://www.rstudio.com). The influence of treatment (different isolates and controls) on lesion length data was thereafter tested using a linear model (*lm*) using base R. Significant main effects were separated using a conservative Tukey post-hoc test in the multcomp package in R (Hothorn *et al*. 2008). A probability level of 5 % was considered significant.

Permitting

Permission to collect samples was provided by the Western Cape Nature Conservation Board. Collections were made under permit number CN44-87-16977.

RESULTS

Disease description and pathogen identification

A *Microsphaeropsis* species was consistently found sporulating on cankered *R. amplexicaulis* stems. Four isolates (CMW 57792, CMW 57793, CMW 57794 and CMW 57795), originating from separate shrubs, were purified and used for further morphological study and molecular identification. Two isolates (CMW 57792 and CMW 57793) were used in the pathogenicity trials.

Phylogenetic analyses

Amplicons of approximately 520 bp were generated for the ITS region, 900 bp for the LSU, and 880 bp for the *RPB2.* The concatenated aligned dataset consisted of 31 ingroup taxa and 1 835 characters, including alignment gaps. Based on the results of jModeltest, a TrNef+G model was selected for ITS, the TPM1uf for LSU and the TIM3+I for *RPB2,* and these models were applied to individual loci in the concatenated dataset for the BI analyses. ML and BI analyses resulted in phylogenetic trees with concordant topologies and showed similar phylogenetic relationships between taxa. The ML tree with bootstrap support values, and the posterior probabilities obtained from BI, is presented in Fig. 2. The four isolates considered in this study were identical and clustered in a well-supported clade (ML/BI = 100/1.00), clearly distinct from the most closely related species, *Microsphaeropsis proteae,* and thus represent a novel taxon.

Taxonomy

Microsphaeropsis rafniae M.J. Wingf., N.Q. Pham & Marinc., ***sp. nov*.** MycoBank MB 849562. Fig. 3.

Etymology: Name refers to *Rafnia*, the host genus on which it occurs.

Diagnosis: Similar to *M. proteae* (conidia 5–8 × 3.5–4 µm *in vivo*) but differs in its smaller conidial dimensions (3–5 × 2–3 µm *in vivo*).

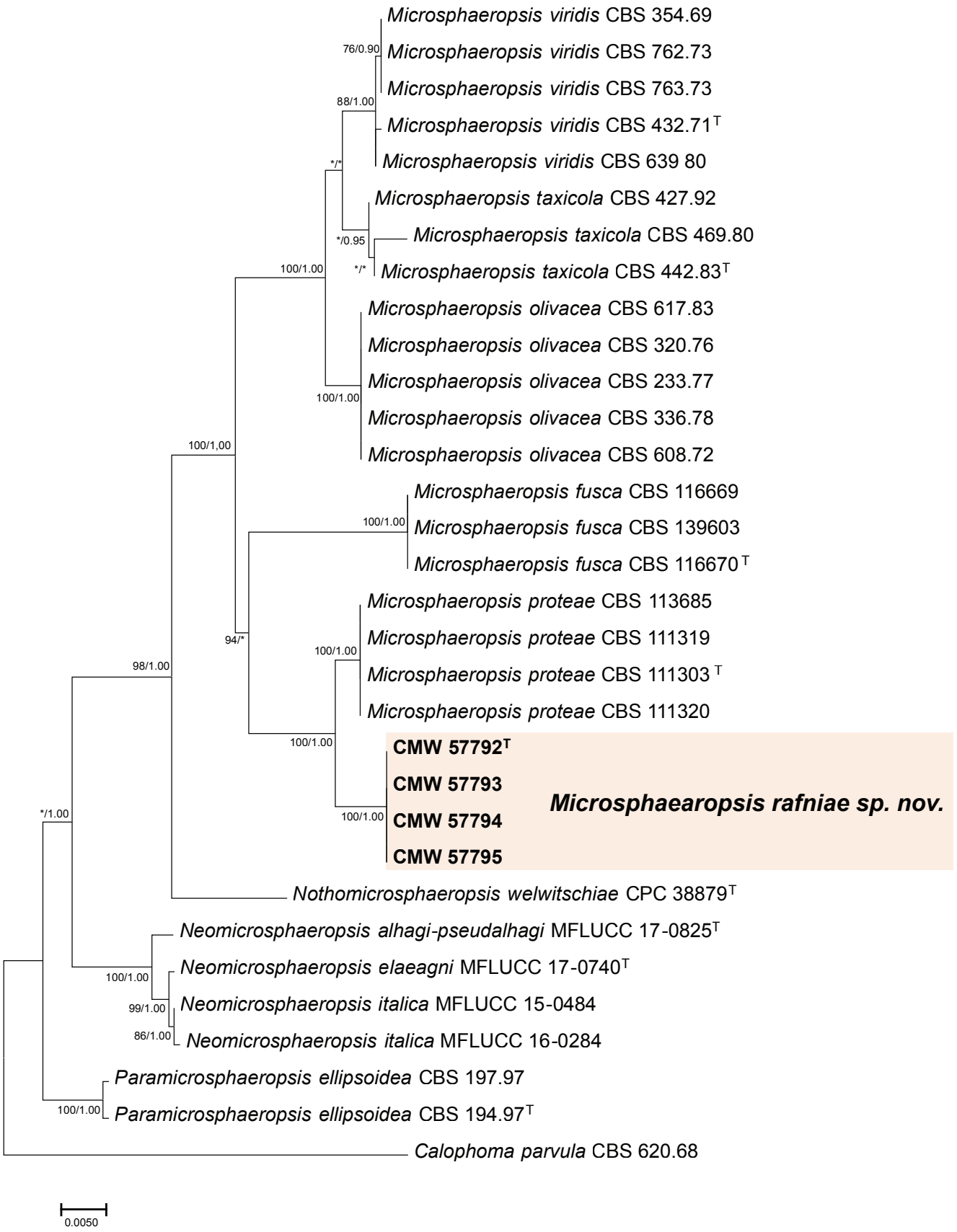

Fig. 2. Phylogenetic tree based on a Maximum Likelihood (ML) analysis of a combined DNA data set of ITS, LSU and *RPB2* sequences representing *Microsphaeropsis* spp. and closely related groups in *Didymellaceae*. Isolates sequenced in this study are presented in bold face. Bootstrap values ≥ 70 % for ML analyses and posterior probabilities values ≥ 0.90 obtained from Bayesian inference (BI) are indicated at the nodes as ML/BI. Isolates representing ex-type cultures are marked with a "T". *Calophoma parvula* (CBS 620.68) represents the outgroup taxon.

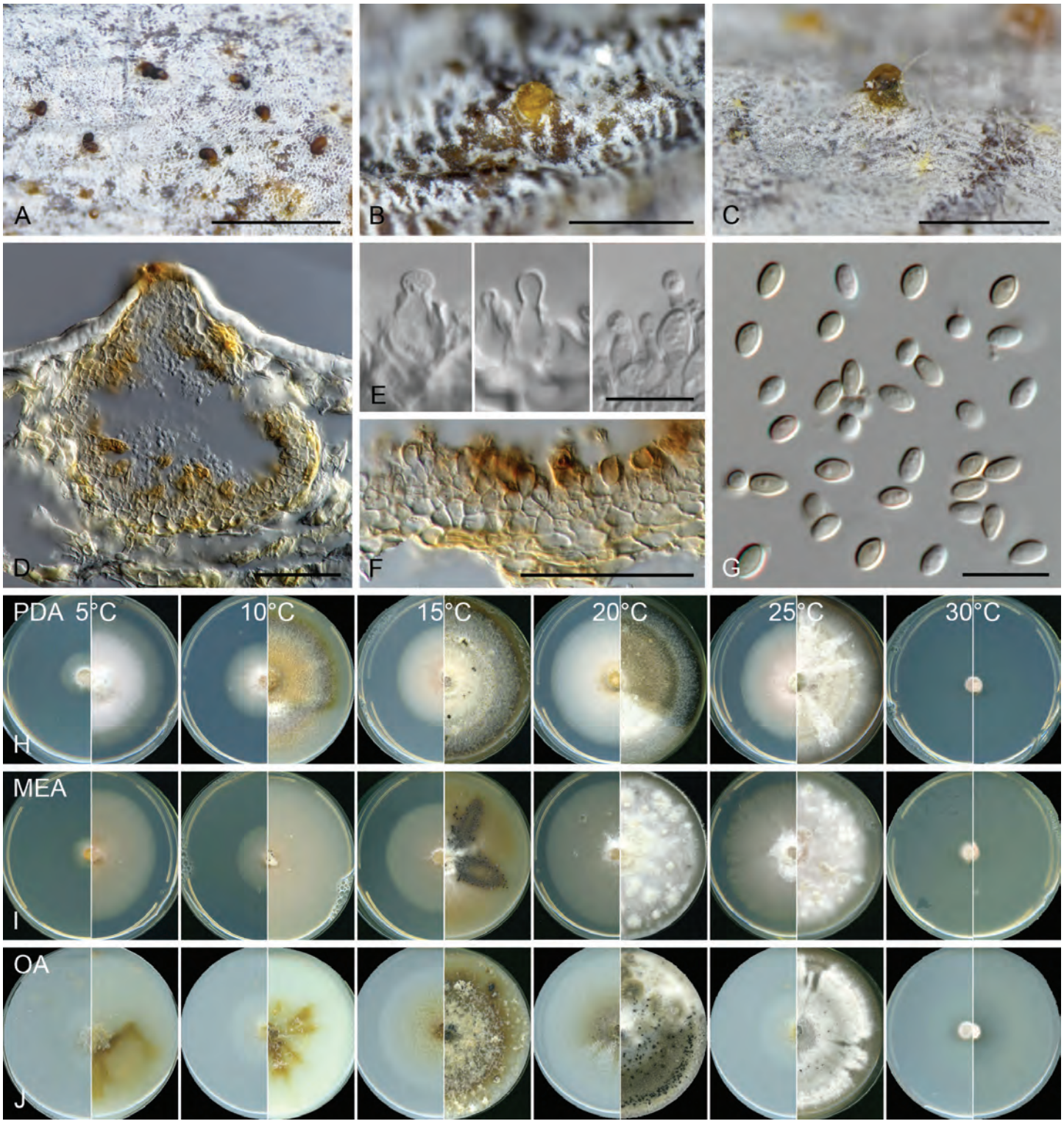

Fig. 3. Micrographs and culture characteristics of *Microsphaeropsis rafniae sp. nov.* (holotype: PRU(M) 4551, ex-holotype CMW-IA 52, CMW 57792). **A.** Conidiomata immersed in the substrate. **B, C.** Conidioma with protruding ostiole and conidial mass on the tip. **D.** Vertical section of conidioma in the substrate. **E.** Conidiogenous cells showing periclinal thickening (left) or percurrent proliferation (middle). **F.** Conidiomatal wall. **G.** Conidia. **H–J.** Colonies of the ex-holotype grown at six temperatures after 10 d (left) /30 d (right) in the dark on PDA (H), MEA (I) and OA (J).

Typus: **South Africa**, Western Cape Province, West Coast District, Cederberg Mountains, *Rafnia amplexicaulis*, 4 Sep. 2021, *M.J. Wingfield* (**holotype** PRU(M) 4552; ex-holotype culture CMW-IA 52, CMW 57792), [GenBank: OR209698 (ITS), OR209716 (LSU), OR211858 (*RPB2*)].

Description: *Sexual morph* not observed. *Conidiomata* in substrate pycnidial, solitary, scattered, immersed becoming erumpent, subglobose, 159 × 149 µm; ostiole inconspicuous; pycnidial wall pseudoparenchymatous, consisting of 3–4 layers of compressed cells, outer layers pale brown. *Conidiophores* reduced to conidiogenous cells, formed along pycinidial cavity. *Conidiogenous cells* phialidic, hyaline, ampulliform to lageniform, 4–8 × 3–4 µm, showing periclinal thickening or percurrent proliferation. *Conidia* oozing out in yellow mass, becoming brown droplets at tip of ostiole, ellipsoidal, ovoid, rarely pyriform, hyaline, thin-walled at beginning, becoming sub-

hyaline to pale brown, thick-walled with age, smooth, aseptate, 3–5 × 2–3 (4.2 ± 0.35 × 2.4 ± 0.14) µm *in vivo*, 3–6 × 2–3 (4.2 ± 0.45 × 2.4 ± 0.27) µm *in vitro*, guttulate.

Culture characters: Colonies on PDA in the dark for 10 d, optimum growth temperature at 20 °C reaching 68.6 mm, followed by 25 °C (61.3 mm), 15 °C (52.1 mm), 5 °C (17.1 mm), 30 °C (10.5 mm) and 35 °C (no growth); on MEA optimum growth temperature at 20 °C reaching 71.5 mm, followed by 25 °C (65.3 mm), 15 °C (52.6 mm), 5 °C (18.6 mm), 30 °C (12 mm) and 35 °C (no growth). Colonies on PDA, MEA and OA showing circular growth with smooth margins, with superficial, flat and medium dense mycelia, fertile in 30 d, morphology homogeneous in 10 d, becoming diverse with age, having streaks or patches of white aerial mycelia. Colony colours on PDA and MEA in 10 d above peach (7d) to sienna (13i), fading towards edges, in 30 d sienna, umber (13m) to olivaceous grey (21''''''i) at higher temperatures, covered with white aerial mycelia partly or in patches. Colony colours on OA in 10 d colourless with tint of citrin (21k) near centre, in 30 d greenish olivaceous (23'''i) streaks to olivaceous gray with white aerial mycelial patches or streaks and black fruiting structure.

Distribution: South Africa, Western Cape Province, West Coast District, Cederberg Wilderness Area.

Additional specimens examined: **South Africa**, Western Cape Province, West Coast District, Cederberg Wilderness Area, -32.412743, 19.174894, on stems and branches of *Rafnia amplexicaulis*, 4 Sep. 2021, *M.J. Wingfield,* PRU(M) 4552, culture CMW-IA 53, CMW 57793 [GenBank: OR209699 (ITS), OR209717 (LSU), OR211859 (*RPB2*)]; PRU(M) 4553, culture CMW-IA 54, CMW 57794 [GenBank: OR209700 (ITS), OR209718 (LSU), OR211861 (*RPB2*)]; PRU(M) 4554, culture CMW 57795 [GenBank: OR209701 (ITS), OR209719 (LSU), OR211862 (*RPB2*)].

Notes: *Microsphaeropsis rafniae* is phylogenetically close to *M. proteae* and *M. fusca*. However, it can be distinguished from those species by its smaller conidia (3–5 × 2–3 µm *in vivo*); *M. fusca* (5–10.5 × 3.5–6.5 µm *in vitro*) (Hou *et al.* 2020) and *M. proteae* (5–8 × 3.5–4 µm *in vivo*) (Swart *et al*. 1998, Crous *et al.* 2011). *Microsphaeropsis fusca* was originally isolated from twig lesions of *Sarothamnus scoparius* (*Fabaceae*) in the Netherlands, and *M. proteae* from leaves of *Protea nitida* (*Proteaceae*) in Hermanus, Western Cape Province, South Africa (Swart *et al*. 1998, Hou *et al*. 2020). The NaOH spot test was positive on OA, turning from pale luteous to sienna colour, whereas *M. fusca* was reported as negative (Hou *et al.* 2020). There is no record of a spot test for *M. proteae*. The species showed strong growth at lower temperatures (5–25 °C). Cultures at 35 °C failed to grow when plates were returned to an optimum temperature (20 °C) and incubated for another 10 d, indicating this temperature results in death.

Pathogenicity tests: After 7 wk of incubation, lesions were evident around the inoculation points under the bark of the hosts. These consisted of dark brown to reddish-brown vascular staining in the form of streaks. Controls showed similar staining, but this did not extend far from the inoculation points. *Microsphaeropsis rafniae* was consistently isolated from the stained areas of the treatments but was never recovered from the controls. Treatment had a significant effect on lesion length ($F = 35.83$, $DF = 2, 27$, $p < 0.001$). Post-hoc analyses revealed that lesions caused by the two isolates were significantly longer than those caused by the controls, but lesion length did not differ between the two test isolates (Fig. 4).

DISCUSSION

A previously unreported canker disease was observed on stems and branches of *R. amplexicaulis* in the Cederberg Wilderness Area, Western Cape, South Africa. *Microsphaeropsis* isolates were recovered from these cankers and identified based on multi-locus (ITS, LSU and *RPB2*) phylogenetic analyses and

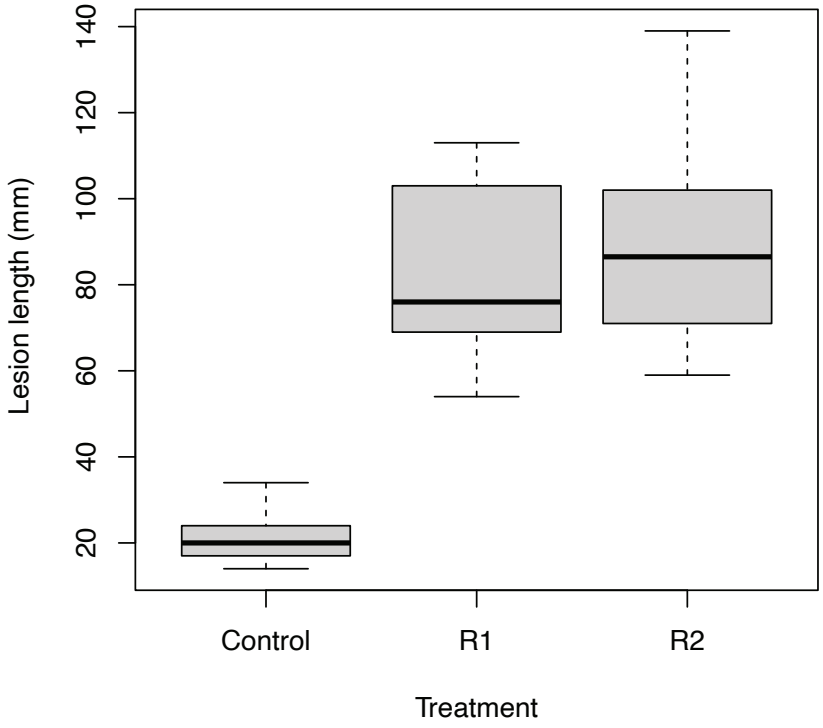

Fig. 4. Lesion length of two isolates of *Microsphaeropsis rafniae sp. nov*. (R1: CMW 57792, R2: CMW 57793) inoculated into *Rafnia amplexicaulis* branches after 7 w of incubation. Boxes indicating a 25–75 % data range, whiskers indicating a 1.5 × interquartile range.

morphological characters. These analyses revealed the isolates represented a novel species, described here as *M. rafniae*. Pathogenicity tests confirmed that *M. rafniae* is a canker pathogen of *R. amplexicaulis*.

The genus *Microsphaeropsis* was originally placed in *Montagnulaceae*, a family established to accommodate species with pigmented, phoma-like conidia. De Gruyter *et al*. (2009) proposed the family *Didymellaceae* to accommodate species in *Phoma* s. *l*. and related genera, including *Microsphaeropsis*. A new family, *Microsphaeropsidaceae*, was introduced to accommodate the genus by Chen *et al*. (2015). However, Hou *et al.* (2020) found that *Microsphaeropsis* spp. clearly reside in the *Didymellaceae* and reduced *Microsphaeropsidaceae* to synonymy, with *Microsphaeropsis* again placed in *Didymellaceae*.

Microsphaeropsis spp. have been reported from a wide variety of plant hosts, including as pathogens causing twig lesions (Hou *et al*. 2020) and leaf spots (Swart *et al*. 1998). This study characterised a novel pathogenic *Microsphaeropsis* species, *M. rafniae,* causing cankers on *R. amplexicaulis*, an endemic South African shrub. *Microsphaeropsis rafniae* is phylogenetically closest to *M. proteae*, also described from an endemic South African plant, *Protea nitida* (Swart *et al.* 1998). The two species are, however, phylogenetically distinct, with all isolates of *M. proteae* clustered in a well-supported clade. While morphologically similar, the two species can be distinguished based on their conidial size. Currently, neither the distribution range nor epidemiology of *M. rafniae* are known, with further studies required to better understand the role of this fungus as a disease-causing agent of *R. amplexicaulis.*

ACKNOWLEDGEMENTS

Members of the Tree Protection Cooperative Programme (TPCP), the DST/NRF Centre of Excellence in Plant Health Biotechnology (CPHB) and the University of Pretoria, South Africa, are acknowledged for financial support.

Conflict of interest: The authors declare that there is no conflict of interest.

REFERENCES

Boerema GH, de Gruyter J, Noordeloos ME, *et al.* (2004). *Phoma identification manual. Differentiation of specific and infra-specific taxa in culture*. CABI, UK.

Campbell GJ, van Wyk B-E (2001). A taxonomic revision of *Rafnia* (*Fabaceae, Crotalarieae*). *South African Journal of Botany* **67**: 90–149.

Chen Q, Jiang JR, Zhang GZ, Cai L, *et al.* (2015). Resolving the *Phoma* enigma. *Studies in Mycology* **82**: 137–217.

Crous PW, Hernández-Restrepo M, Schumacher RK, *et al*. (2021). New and Interesting Fungi. 4. *Fungal Systematics and Evolution* **7**: 255–343.

Crous PW, Summerell BA, Swart L, *et al.* (2011). Fungal pathogens of *Proteaceae*. *Persoonia* **27**: 20–45.

de Gruyter J, Aveskamp MM, Woudenberg JHC, *et al*. (2009). Molecular phylogeny of *Phoma* and allied anamorph genera: Towards a reclassification of the *Phoma* complex. *Mycological Research* **113**: 508–519.

Gardes M, Bruns TD (1993). ITS primers with enhanced specificity for *Basidiomycetes* — Application to the identification of mycorrhizae and rusts. *Molecular Ecology* **2**: 113–118.

Hothorn T, Bretz F, Westfall P (2008). Simultaneous inference in general parametric models. *Biometrical Journal* **50**: 346–363.

Hou LW, Groenewald JZ, Pfenning LH, *et al.* (2020). The phoma-like dilemma. *Studies in Mycology* **96**: 309–396.

Katoh K, Standley DM (2013). MAFFT multiple sequence alignment software version 7: improvements in performance and usability. *Molecular Biology and Evolution* **30**: 772–780.

Kinfe HH, Long HS, Stander MA, *et al.* (2015). The major phenolic compound of the roots and leaves of *Rafnia amplexicaulis* (*Fabaceae*), a liquorice substitute and traditional tea used in Cape Herbal Medicine. *South African Journal of Botany* **100**: 75–79.

Kumar S, Stecher G, Tamura K (2016). MEGA7: molecular evolutionary genetics analysis version 7.0 for bigger datasets. *Molecular Biology and Evolution* **33**: 1870–1874.

Liu QL, Li JQ, Wingfield MJ, Duong TA, *et al.* (2020). Reconsideration of species boundaries and proposed DNA barcodes for *Calonectria*. *Studies in Mycology* **97**: 100106.

Liu YJ, Whelen S, Hall BD (1999). Phylogenetic relationships among ascomycetes: evidence from an RNA polymerase II subunit. *Molecular Biology and Evolution* **16**: 1799–1808.

Pham NQ, Barnes I, Chen SF, *et al.* (2019). Ten new species of *Calonectria* from Indonesia and Vietnam. *Mycologia* **111**: 78–102.

Posada D (2008). jModelTest: phylogenetic model averaging. *Molecular Biology and Evolution* **25**: 1253–1256.

Rambaut A (2010). *FigTree v. 1.3.1*. Institute of Evolutionary Biology, University of Edinburgh, Edinburgh.

Rayner RW (1970). *A mycological colour chart*. Commonwealth Mycological Institute, Kew, Surrey, UK.

Rehner SA, Samuels GJ (1994). Taxonomy and phylogeny of *Gliocladium* analysed from nuclear large subunit ribosomal DNA sequences. *Mycological Research* **98**: 625–634.

Ronquist F, Teslenko M, Van Der Mark P, *et al.* (2012). MrBayes 3.2: efficient Bayesian phylogenetic inference and model choice across a large model space. *Systematic Biology* **61**: 539–542.

Stamatakis A (2014). RAxML version 8: a tool for phylogenetic analysis and post-analysis of large phylogenies. *Bioinformatics* **30**: 1312–1313.

Sung GH, Sung JM, Hywel-Jones NL, *et al.* (2007). A multi-gene phylogeny of *Clavicipitaceae* (*Ascomycota, Fungi*): identification of localised incongruence using a combinational bootstrap approach. *Molecular Phylogenetics and Evolution* **44**: 1204–1223.

Swart L, Crous PW, Denman S, *et al.* (1998). Fungi occurring on *Proteaceae*. I. *South African Journal of Botany* **64**: 137–145.

Vilgalys R, Hester M (1990). Rapid genetic identification and mapping of enzymatically amplified ribosomal DNA from several *Cryptococcus* species. *Journal of Bacteriology* **172**: 4239–4246.

Von Höhnel F (1917). Fungi imperfecti. Beiträge zur Kenntnis derselben. *Hedwigia* **59**: 236–284.

White T, Bruns T, Lee S, *et al.* (1990). Amplification and direct sequencing of fungal ribosomal RNA genes for phylogenetics. In: *PCR – Protocols and applications: a guide to methods and applications* (Innis MA, Gelfand DH, Sninsky JJ, *et al.*, eds). Cambridge, MA: Academic Press: 315–322.

FUSE

Fungal Systematics and Evolution

Volume 12
DECEMBER 2023
PAGES 81–89

doi.org/10.3114/fuse.2023.12.06

Phylloporia mutabilis sp. nov. from Benin, West Africa

B.A. Olou[1*], F.-S. Krah[2], M. Piepenbring[3], N.S. Yorou[1]

[1]Research Unit Tropical Mycology and Plant-Soil Fungi Interactions (MyTIPS), Faculty of Agronomy, University of Parakou, BP 123 Parakou, Benin
[2]Fungal Ecology and Bayreuth Center of Ecology and Environmental Research (BayCEER), University of Bayreuth, Universitätsstr. 30, 95440 Bayreuth, Germany
[3]Mycology Research Group, Faculty of Biological Sciences, Goethe University Frankfurt am Main, Biologicum, Max-von-Laue-Str. 13, 60438 Frankfurt am Main, Germany

*Corresponding author: borisolou@yahoo.fr

Key words:
Hymenochaetaceae
integrative taxonomy
new taxon
Phylloporia
polypore

Abstract: *Phylloporia* is a widespread genus of *Hymenochaetales* (*Basidiomycota*) with polyporoid basidiomata found mainly in the tropics. Species of *Phylloporia* are predominantly parasitic of woody plant hosts, while some species grow as saprotrophs. Data on the genus is still scarce for tropical Africa, where we expect a high diversity given the high plant diversity in this area. Two specimens of this genus were collected in Benin (West Africa) and analysed morphologically and phylogenetically based on a multigene dataset (ITS, LSU, *EF1α*). Strong support for a species new to science was found, described here as *Phylloporia mutabilis*. It differs from other *Phylloporia* species by stipitate, coriaceous basidiomata, earth coloured to dark brown when fresh and changing upon drying from golden to yellowish brown, the margin being large in young specimens, becoming narrower with maturity. Basidiomata of *Phylloporia mutabilis grow* on the soil under angiosperm trees in a dense dry forest, so its lifestyle (saprotrophic, parasitic or mycorrhizal) is not evident, and future ecological studies will be required to elucidate this aspect.

Citation: Olou BA, Krah F-S, Piepenbring M, Yorou NS (2023). *Phylloporia mutabilis sp. nov.* from Benin, West Africa. *Fungal Systematics and Evolution* **12**: 81–89. doi: 10.3114/fuse.2023.12.06
Received: 7 June 2023; **Accepted:** 22 July 2023; **Effectively published online:** 2 August 2023
Corresponding editor: P.W. Crous

INTRODUCTION

Phylloporia typified by *P. parasitica* is a polypore genus mainly distributed in the tropics (Murrill 1904, Ryvarden & Johansen 1980, Gilbertson & Ryvarden 1987, Wagner & Ryvarden 2002), with some species reported from temperate zones (Dai 2010, 2012, Ryvarden & Melo 2014, Bernicchia & Gorjón 2020). *Phylloporia* species mostly grow parasitically on living angiosperm trees or bushes, including roots, trunks, branches, petioles or leaves, with high levels of host specificity, causing white rot (Wagner & Ryvarden 2002, Zhou 2015a, Qin *et al.* 2018, Wu *et al.* 2019, Zhou *et al.* 2022). However, some species were recorded on dead wood (Ryvarden & Johansen 1980, Ferreira-Lopes *et al.* 2016, Wagner & Ryvarden 2002, Zhou & Dai 2012, Zhou *et al.* 2022) or with basidiomata on soil (Ipulet & Ryvarden 2005, Yombiyeni *et al.* 2015, Zhou 2015b, Chamorro-Martínez *et al.* 2022). The genus was described over a century ago (Murrill 1904) but it was rarely cited until the type specimen was re-examined and 12 species were recognised on the basis of morphological and phylogenetic data (Ryvarden 1972, Wagner & Ryvarden 2002). Species of *Phylloporia* differ from other polyporoid genera by annual or perennial, effused-reflexed, pileate or stipitate, soft corky to hard corky basidiomata, tomentose to velutinate pileal surface, a context mostly duplex with a black line between upper tomentum and lower contextual layer, a monomitic hyphal system in most species, generative hyphae with simple septa, absence of setal elements (with the exception of *Phylloporia mori*; Wu *et al.* 2020), and subglobose, ellipsoid or cylindric, hyaline to yellowish, fairly thick-walled basidiospores (Wagner & Ryvarden 2002, Zhou et al. 2022). From then on, *Phylloporia* gained more attention and currently 76 species are known worldwide (https://www.catalogueoflife.org). Fifteen species have been reported from tropical Africa, including two species from Benin (West Africa) (Olou *et al.* 2021). Given the parasitic nature of most species of *Phylloporia* and the high diversity of plants in Benin, *Phylloporia* species are probably more diverse than presently known. To explore this hidden diversity, we conducted surveys in Benin and collected two specimens corresponding morphologically to *Phylloporia*.

MATERIAL AND METHODS

Field collections

During a mycological survey in Benin from July to September 2021, two specimens belonging to the genus *Phylloporia* were collected in the dense dry forest of Pahou. The specimens were photographed in their natural environment using a Sony DSC-HX400V camera prior to recording. The geographical coordinates of each specimen were recorded. Small pieces of fresh basidiomata were placed in plastic bags half-filled with silica

gel for subsequent DNA extraction. The remaining basidiomata were air or oven dried at 45–50 °C for 1–2 d depending on the consistency of the basidiomata. The dried basidiomata were then preserved in plastic bags for morphological study and deposited at the mycological herbarium of the University of Parakou (UNIPAR) in Benin.

DNA extraction, amplification, and sequencing

We extracted the DNA from dried fragments of the *Phylloporia* sp. using the innuSPEED DNA Isolation Kits by Analytik Jena. The D1–D4 domains of the nuclear ribosomal large subunit of ribosomal DNA (LSU; 28S rDNA) is the DNA region mainly analysed in the context of previous studies on species delimitation in *Phylloporia*. Here, in addition to LSU, we amplified the internal transcribed spacer region of rDNA (ITS) and the translation elongation factor 1-alpha (*EF1α*). The primer pairs ITS-1F/ITS4 (White *et al.* 1990, Gardes & Bruns 1993), LR0R/LR5 (Vilgalys & Hester 1990), and EF1-983F/2218R (Rehner & Buckley 2008) were used to amplify the target DNA regions. The polymerase chain reaction (PCR) procedure, the PCR products purification, and Sanger sequencing followed Olou *et al.* (2020). Table 1 presents the accession numbers for all the sequences obtained in the context of the present study and obtained from GenBank for the phylogenetic analysis. The alignment used in the present study was deposited in TreeBASE (S30614).

Phylogenetic analyses

To study phylogenetic relationships, newly generated sequences were aligned with other sequences retrieved from GenBank. Thirty-seven ITS sequences were aligned with two ITS sequences generated in this study. In addition, 125 LSU sequences retrieved from GenBank and used by previous studies on *Phylloporia* (Olou *et al.* 2021, Wu *et al.* 2022, Zhou *et al.* 2022) were aligned together with two newly generated LSU sequences. Eighteen *EF1α* sequences were aligned with two newly generated sequences. Each region was aligned separately using the online mode of MAFFT v. 7 (Katoh *et al.* 2017). *Inonotus andersonii* and *Inonotus hispidus* were chosen as outgroups (Wu *et al.* 2019, Olou *et al.* 2021, Zhou *et al.* 2022). Multiple sequence alignments were inspected and some bases were manually adjusted using AliView v. 1.28 (Larsson 2014). One dataset of combined ITS-LSU-*EF1α* was assembled for the phylogenetic analysis. The best-fit evolutionary model was estimated for each partition using the standard model selection (Kalyaanamoorthy *et al.* 2017) implemented in IQ-TREE v. 1.6.12 (Minh *et al.* 2020, http://www.iqtree.org/) with the command line –m TESTONLY. Following this substitution model, the phylogenetic tree inference of Maximum likelihood (ML) and Bayesian Inference (BI) were performed to verify the phylogenetic position of the newly generated sequences. The ML was run using IQ-TREE v. 1.6.12 and the branch support was evaluated using the Ultrafast Bootstrap (UFBoot) (Hoang *et al.* 2018) with 5 000 replicates. The BI was executed using MrBayes v. 3.2.7 in command line mode (https://github.com/NBISweden/MrBayes) for five million generations until the standard deviation of split frequencies reached 0.01. Chain convergence was determined using Tracer v. 1.7.1 (http://tree.bio.ed.ac.uk/software/tracer/) and the first 25 % (5 000) trees were discarded as burn-in. The remaining trees were used to build the consensus tree using the Phylogenetic Tree Summarization (SumTrees) program within DendroPy v. 4.3.0. (Sukumaran & Holder 2010, https://github.com/jeetsukumaran/DendroPy). The topology of the species trees resulting from ML and BI analyses is congruent which enabled us to combine them. To combine both trees, the Phylogenetic Tree Summarization (SumTrees) program within DendroPy v. 4.3.0. (Sukumaran & Holder 2010, https://github.com/jeetsukumaran/DendroPy) was used to add the posterior probabilities (PP) of the BI on the ML tree. Then, the UFBoot values were added to the best tree obtained by ML that already had values of the posterior probabilities using IQ-TREE (Trifinopoulos *et al.* 2016). The resulting tree with (UFBoot /PP) is presented below and the support values of UFBoot and PP are indicated on each node.

Morphological examination

Macro- and microstructure descriptions were based on dried fungarium specimens of *Phylloporia* sp. Macro-morphological characters were described with the aid of a dissecting microscope. The colours of basidiomata were coded according to the Handbook of Colour of Kornerup & Wanscher (1981) and indicated in parentheses in the description. The microstructures were described using a LEICA DM2700M compound light microscope. For the microstructures, fine sections through the basidiomata were prepared for observation using a razor blade under a dissecting microscope and mounted in 10 % aqueous solution of potassium hydroxide (KOH). Melzer's reagent and Cotton Blue were used to test dextrinoid or amyloid and cyanophilic reactions. The following abbreviations are used: IKI = Melzer's reagent, IKI– = neither amyloid nor dextrinoid, CB = Cotton Blue, CB– = acyanophilous. The basidiospore size is given as length and width of the spores. For measurements we present the mean with standard deviation and minimum and maximum values in parentheses. The length (L), arithmetic average of all spore lengths, and the width (W), arithmetic average of all spore widths, were calculated. In addition, the ratio of length/width (Q) was calculated.

RESULTS

Molecular phylogeny

Two specimens of *Phylloporia* sp. recently collected in Benin (OAB0643 and OAB0666) were placed in a phylogenetic analysis of *Phylloporia* spp. Therefore, six sequences, namely two sequences of ITS rDNA, two of LSU rDNA, and two of the *EF1α* gene, were generated and combined with sequences retrieved from GenBank. The combined ITS, LSU, and *EF1α* alignment includes 128 sequences with 3 064 characters, of which 1 508 are distinct patterns, 959 are parsimony-informative, 326 singleton sites, and 1 779 constant sites. Three well supported major clades corresponding to the genera *Fomitiporella* (100/100), *Fulvifomes* (100/100), and *Phylloporia* (100/100) were recovered from the phylogenetic analyses inferred from the ITS-LSU-*EF1α* analysis (Fig. 1). Our newly generated sequences clustered together and form a distinct and well-supported clade (100/100) within *Phylloporia*, that is a sister clade of the bigger clade including *P. parasitica*, *P. flacourtiae*, and *P. littoralis*. As no further morphologically identical species of *Phylloporia* is known, we introduce them as a new species and provide a detailed description of this species.

Table 1. Species names, sample data, and GenBank accession numbers of sequences of *Phylloporia* spp. and closely related species of *Hymenochaetales* obtained in the context of the present study and those retrieved from GenBank.

Species	Voucher or Strain	Origin	ITS	LSU	*EF1α*	References
Fomitiporella resupinata	DMC76	Cameroon	KJ787822	JF712935	–	Zhou & Dai (2012)
Fomitiporella sinica	LWZ 20130809-5	China	KJ787819	KJ787810	–	Zhou (2014)
Fomitiporella tenuissima	Dai 12245	China	KC456242	KC999902	–	Yu *et al.* (2013)
Fomitiporella umbrinella	JV 0509/114	USA	KX181314	KX181336	–	Ji *et al.* (2017)
Fulvifomes fastuosus	CBS 213.36	Philippines	AY558615	AY059057	–	Wagner & Fischer (2002)
Fulvifomes robiniae	CFMR 2693	USA	KX065961	KX065995	–	Sayers *et al.* (2020)
Fulvifomes yoroui	OAB0097	Benin	MN017126	MN017120	–	Olou *et al.* (2019)
Inonotus andersonii	JV1209_66	USA	MN318443	MN318443	–	Sayers *et al.* (2020)
Inonotus hispidus	92-829	Germany	AY624993	AF311014	–	Wagner & Fischer (2001)
Phylloporia afrospathulata	MUCL 54511	Gabon	–	KJ743248	–	Yombiyeni *et al.* (2015)
	MUCL 53983	Gabon	–	KJ743249	–	Yombiyeni *et al.* (2015)
Phylloporia alyxiae	Chen 1182	Taiwan	–	LC514407	–	Wu *et al.* (2020)
	GC 1604-28	Taiwan	–	LC514408	–	Wu *et al.* (2020)
Phylloporia atlantica	JRF142	Brazil	–	MG738813	–	Wu *et al.* (2019)
	JRF151	Brazil	–	MG738814	–	Wu *et al.* (2019)
Phylloporia beninensis	OAB0107	Benin	–	MW244097	–	Olou *et al.* (2021)
	OAB0142	Benin	MW244094	MW244099	–	Olou *et al.* (2021)
	OAB0511	Benin	–	MW244096	–	Olou *et al.* (2021)
Phylloporia bibulosa	Ahmad27088	Pakistan	–	AF411824	–	Wagner & Ryvarden (2002)
Phylloporia boldo	CIEFAPcc532	Chile	–	MK193759	–	Rajchenberg *et al.* (2019)
	CIEFAPcc584	Chile	–	MK193758	–	Rajchenberg *et al.* (2019)
Phylloporia capucina	Robledo1610	Argentina	–	KJ651919	–	Sayers *et al.* (2020)
Phylloporia chrysites	MUCL 52862	Mexico	–	HM635667	–	Valenzuela *et al.* (2011)
Phylloporia chrysites	MUCL 52764	Mexico	–	HM635666	–	Valenzuela *et al.* (2011)
Phylloporia clariceae	FLOR:51258	Brazil	–	KJ631406	–	Ferreira-Lopes *et al.* (2016)
Phylloporia clausenae	Yuan 3528	China	–	KJ787795	–	Zhou (2015a)
	Cui8463	China	MH151186	MH165868	MH167424	Zhou (2015a)
Phylloporia crataegi	Dai18133	China	MH151191	MH165865	MH167431	Zhou & Dai (2012)
	Dai 11016	China	–	JF712923	–	Zhou & Dai (2012)
Phylloporia crystallina	JV2106/102	Ecuador	–	ON006467	–	Zhou *et al.* (2022)
Phylloporia cylindrispora	Yuan6144	China	–	KJ787798	–	Zhou (2015a)
	Yuan6148	China	–	KJ787797	–	Zhou (2015a)
Phylloporia cystidiolophora	Dai13953	China	–	MG738799	MH167438	Wu *et al.* (2019)
	Dai13945	China	–	MG738798	–	Wu *et al.* (2019)
Phylloporia dependens	Cui 13763	China	MH151190	KX242353	–	Chen *et al.* (2017)
Phylloporia elegans	FLOR:51179	Brazil	–	KJ631409	–	Ferreira-Lopes *et al.* (2016)
	FLOR:51178	Brazil	–	KJ631408	–	Ferreira-Lopes *et al.* (2016)
Phylloporia ephedrae	TAA 72-2	Turkmenistan	MH151184	AF411826	–	Wagner & Ryvarden (2002)
Phylloporia flabelliforma	MUCL 55570	Gabon	NR_154332	KU198350	–	Decock *et al.* (2015)
	MUCL 55569	Gabon	KU198356	KU198349	–	Decock *et al.* (2015)
Phylloporia flacourtiae	Yuan 6362	China	–	KJ787801	–	Zhou (2015a)
	Yuan 6360	China	–	KJ787800	–	Zhou (2015a)
Phylloporia fontanesiae	Cui12356	China	MH151188	MH165871	–	Zhou & Dai (2012)
	Li 199	China	–	JF712925	–	Zhou & Dai (2012)
Phylloporia fruticum	MUCL 52762	Mexico	–	HM635668	–	Valenzuela *et al.* (2011)
	ENCB TR&RV858	Mexico	–	HM635669	–	Valenzuela *et al.* (2011)
Phylloporia fulva	MUCL 54472	Gabon	–	KJ743247	–	Yombiyeni *et al.* (2015)

Table 1. (Continued).

Species	Voucher or Strain	Origin	ITS	LSU	*EF1α*	References
Phylloporia gabonensis	MUCL 55572	Gabon	KU198354	KU198352	–	Decock *et al.* (2015)
	MUCL 55571	Gabon	NR_154331	KU198353	–	Decock *et al.* (2015)
Phylloporia gutta	Dai16070	China	MH151183	MH165863	MH167423	Zhou & Dai (2012)
	Dai 4197	China	–	JF712927	–	Zhou & Dai (2012)
Phylloporia hainaniana	Dai 9460	China	–	JF712928	–	Cui *et al.* (2010)
Phylloporia homocarnica	Yuan 5766	China	–	KJ787804	–	Zhou (2015a)
	Yuan 5750	China	MH151195	KJ787803	–	Zhou (2015a)
Phylloporia inonotoides	MUCL 54468	China	–	KJ743250	–	Yombiyeni *et al.* (2015)
Phylloporia lespedezae	Dai17065	China	MH151179	KY242602	MH167419	Ren & Wu (2017)
	Dai17067	China	MH151180	KY242603	MH167420	Ren & Wu (2017)
Phylloporia littoralis	MUCL: 56145	Gabon	–	KY349141	–	Yombiyeni & Decock (2017)
	MUCL: 56144	Gabon	–	KY349140	–	Yombiyeni & Decock (2017)
	OAB0204	Benin	MW244095	MW244098	–	Olou *et al.* (2021)
Phylloporia lonicerae	Dai17900	China	MH151175	MG738802	MH167418	Qin *et al.* (2018)
Phylloporia lonicerae	Dai17899	China	MH151174	MG738801	MH167417	Qin *et al.* (2018)
	Dai17898	China	MH151173	MG738800	MH167416	Qin *et al.* (2018)
Phylloporia manglietiae	Cui 13709	China	MF410324	KX242358	MH167430	Chen *et al.* (2017)
Phylloporia minuta	FURB 55088	Brazil	–	NG_064479	–	Bittencourt *et al.* (2018)
Phylloporia minutipora	Dai16172	China	–	MH165873	MH167436	Zhou (2016)
	LWZ-2016	China	–	KU904466	–	Sayers *et al.* (2020)
	Dai 9257	China	–	KU904464	–	Sayers *et al.* (2020)
	Ipulet 706	Uganda	–	JF712929	–	Ipulet & Ryvarden (2005)
	MUCL 52865	Congo	–	HM635671	–	Valenzuela *et al.* (2011)
	Dai-21223	China	–	MZ437408	–	Wu *et al.* (2022)
Phylloporia montana	BDNA2409	Brazil	–	MG738811	–	Wu *et al.* (2019)
	BDNA2388	Brazil	–	MG738810	–	Wu *et al.* (2019)
Phylloporia mori	Wu 1105 2	Taiwan	–	LC514412	–	Wu *et al.* (2020)
	Wu 1105 3	Taiwan	–	LC514413	–	Wu *et al.* (2020)
Phylloporia moricola	Wu1807 1	China	–	LC589617	–	Wu *et al.* (2021)
	Wu1807 5	China	–	LC589618	–	Wu *et al.* (2021)
	Wu1807 6	China	–	LC589619	–	Wu *et al.* (2021)
Phylloporia murrayae	Wu 1404-4	Taiwan	–	LC514409	–	Wu *et al.* (2020)
	Wu 1404-5	Taiwan	–	LC514410	–	Wu *et al.* (2020)
Phylloporia mutabilis	OAB0643	Benin	OR096158	OR096136	OR161068	This study
	OAB0666	Benin	OR096159	OR096137	OR359376	This study
Phylloporia nandinae	Dai 10588	China	–	JF712930	–	Zhou & Dai (2012)
	Dai 10625	China	–	JF712931	MH167439	Zhou & Dai (2012)
Phylloporia nodostipitata	FLOR:51173	Brazil	KJ639057	KJ631412	–	Ferreira-Lopes *et al.* (2016)
	FLOR:51175	Brazil	–	KJ631413	–	Ferreira-Lopes *et al*. (2016)
Phylloporia nouraguensis	MUCL/FG-11-404	Guyana	–	KC136223	–	Decock *et al.* (2013)
	MUCL/FG-11-409	Guyana	–	KC136224	–	Decock et al. (2013)
Phylloporia oblongospora	Zhou179	China	MH151197	JF712932	–	Cui *et al.* (2010)
Phylloporia oreophila	CUI2219	China	MH151196	JF712933	–	Zhou & Dai (2012)
	Cui 9503	China	–	JF712934	–	Zhou & Dai (2012)
Phylloporia osmanthi	Yuan 5655	China	–	KF729938	–	Zhou (2015b)
Phylloporia parasitica	LR 19843	Argentina	KU198361		–	Decock *et al.* (2015)
Phylloporia pectinata	R.Coveny 113	Australia	–	AF411823	–	Wagner & Ryvarden (2002)
Phylloporia pendula	Cui 13691	China	–	KX242357	MH167426	Chen *et al.* (2017)

Table 1. (Continued).

Species	Voucher or Strain	Origin	ITS	LSU	*EF1α*	References
	Cui 13876	China	–	KX901670	MH167427	Chen *et al.* (2017)
Phylloporia perangusta	Dai18139	China	MH151169	MG738803	MH167413	Wu *et al.* (2019)
Phylloporia pseudopectinata	Cui 13746	China	–	KX242355	MF977778	Chen *et al.* (2017)
	Cui 13749	China	–	KX242356	MH167429	Chen *et al.* (2017)
Phylloporia pulla	Cui 5251	China	–	KU904468	–	Zhou (2016)
	Dai 9627	China	–	KU904469	–	Zhou (2016)
Phylloporia radiata	LWZ-2016a	China	–	KU904470	–	Zhou (2016)
Phylloporia rattanicola	Dai18233	China	–	MG738807	–	Wu *et al.* (2019)
	Dai18235	China	MH151172	MG738808	MH167415	Wu *et al.* (2019)
Phylloporia ribis	82-828	Germany	–	AF311040	–	Wagner & Ryvarden (2002)
Phylloporia rinoreae	MUCL: 56283	Gabon	–	MN243144	–	Jerusalem *et al.* (2019)
	MUCL: 57328	Gabon	–	MN243146	–	Jerusalem *et al*. (2019)
Phylloporia rubiacearum	Chen 3583	Taiwan	–	LC514416	–	Wu *et al.* (2020)
	Chen 3584	Taiwan	–	LC514417	–	Wu *et al.* (2020)
Phylloporia rzedowskii	MUCL 52859	Mexico	–	HM635673	–	Valenzuela *et al.* (2011)
	MUCL 52860	Mexico	–	HM635674	–	Valenzuela *et al.* (2011)
Phylloporia sumacoensis	JV2109/73	Ecuador	–	ON006468	–	Zhou *et al.* (2022)
Phylloporia solicola	JRF145	Brazil	–	MG738815	–	Wu *et al.* (2019)
Phylloporia sp.	Robledo1220	Argentina	–	KC136225	–	Sayers *et al.* (2020)
	ISA007	Brazil	–	KJ743265	–	Sayers *et al.* (2020)
Phylloporia spathulata	Chay456	Mexico	–	AF411822	–	Ferreira-Lopes *et al.* (2016)
Phylloporia splendida	Dai6282	China	–	MG738805	–	Wu *et al.* (2019)
	Cui8429	China	–	MG738804	–	Wu *et al.* (2019)
Phylloporia tabernaemontanae	*Dai 18852*	Australia	–	MZ437409	–	Wu *et al.* (2022)
	Dai 18853	Australia	–	MZ437410	–	Wu *et al.* (2022)
Phylloporia terrestris	Yuan 5738	China	–	KC778784	–	Zhou (2015b)
	He2359	China	MH151189	MH165869	–	Zhou (2015b)
Phylloporia tiliae	Yuan 5491	China	–	KJ787805	–	Zhou (2013)
Phylloporia ulloai	MUCL 52866	Mexico	–	HM635677	–	Valenzuela *et al.* (2011)
	MUCL 52867	Mexico	–	HM635678	–	Valenzuela *et al.* (2011)
Phylloporia weberiana	Dai 9242	China	–	JF712936	–	Sayers *et al.* (2020)
Phylloporia yuchengii	YG 051	Uzbekistan	–	KM264325	–	Gafforov *et al.* (2014)

Taxonomy

Phylloporia mutabilis Olou, ***sp. nov.*** MycoBank MB 849082. Figs 2, 3.

Etymology: *mutabilis* (Latin), referring to the colour of basidiomata, changing as it dries.

Typus: **Benin**, Atlantic Province, dry dense forest of Pahou near Ouidah city, 6°23'2.97"N, 2°9'15.90"E, alt. 33.1 m, on soil under angiosperm of dry dense forest, 8 Jul. 2021, *leg*. *B.A. Olou*, OAB0643 (**holotype** UNIPAR, OAB0643). Holotype sequences: ITS OR096158, LSU OR096136, and *EF1α* OR161068.

Diagnosis: *Phylloporia mutabilis* differs from known species of *Phylloporia* by the combination of the following characteristics: *Basidiomata* stipitate, caespitose, coriaceous, pileus surface and margin with bands of white and dark brown colours in fresh specimens, margin large in young specimens and becoming narrower with maturity, earth coloured to dark brown when fresh and golden brown to yellowish brown after drying. *Pilei* semi-circular to circular, up to 5 cm wide and 2 mm thick at base. *Setae*, *cystidia* and *cystidioles* absent. *Basidia* 9–12 × 4–6 µm. *Basidiospores* ellipsoid to subglobose, 2.7–3.8 × 2–2.9 µm.

Description: *Basidiomata* eccentrically to laterally stipitate, caespitose, two to several pilei rising from a common base, coriaceous, without odour or taste. Pilei semi-circular to circular, up to 5 cm wide and 2 mm thick at base. *Pileal surface* tomentose, shiny when fresh, earth coloured (5F2) to dark brown (6F8) when fresh and golden brown (5D7) to yellowish brown (5E8) when dry, concentrically zonate; margin entire, yellowish white, with a distinct groove between the margin and the central part of the pileal surface. *Pore surface* golden yellow (4C6); pores angular, 6–8 per mm, slightly decurrent on stipe. Context up to 1.5 mm thick, duplex, the lower context woody,

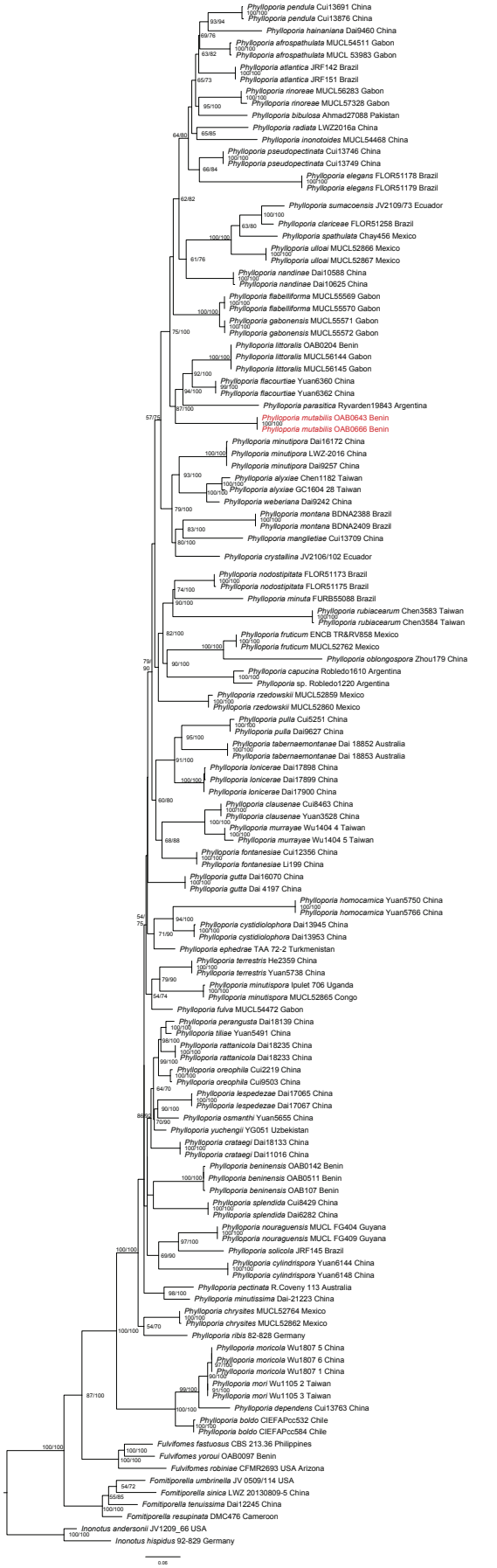

Fig. 1. Summarised tree from the Maximum likelihood (ML) and Bayesian analysis (BI) analyses of the combined ITS-LSU- EF1α dataset of *Phylloporia* and closely related genera. Branch support values given as UFBoot/PP. Newly generated sequences are highlighted in red. The sequence names are followed by voucher or strain number and country of origin.

Fig. 2. Basidiomata of *Phylloporia mutabilis* (OAB0643). **A.** Fresh basidiomata in the field. **B.** Basidiomata after drying. Scale bars = 1 cm.

golden brown, up to 1.4 mm thick, upper context very narrow, up to 0.1 mm thick, the two parts separated by a black line. *Tubes* golden yellow, woody, up to 1 mm long at the base and in the middle of basidiomata, narrow toward the margin. Stipe yellow brown, cylindrical or more frequently flattened, up to 4 cm long and 1 cm in diam., duplex, inner part woody, outer part as tomentum, corky, the two parts separated by a black line. *Hyphal system* monomitic; generative hyphae septate without clamps. Contextual hyphae golden yellow, thick-walled, septate without clamps, unbranched, CB–, 4–7 µm diam. *Tramal hyphae* golden yellow to golden brown, thick-walled, unbranched, septate without clamps, CB–, 2.5–4.5 µm diam. Setae, cystidia, and cystidioles absent. *Basidia* with four sterigmata, 9–12 × 4–6 µm; basidioles similar to basidia. *Basidiospores* broadly ellipsoid to subglobose, yellowish, thick-walled, smooth, IKI–, CB–, (2.6–) 2.7–3.8(–4.1) × 2.0–2.9(–3.1) µm, L = 3.2 µm, W = 2.4 µm, Q = 1.33 (n = 54/1).

Ecology and distribution: Basidiomata grow on the soil under angiosperm trees in a dense dry forest. This species is currently only known from the type locality in southern Benin.

Additional specimen examined: **Benin**, Atlantic Province, dense dry forest of Pahou in Ouidah, 6°23'2.97"N, 2°9'15.90"E, alt. 33.1m, on soil under angiosperms of dense dry forest, 8 Jul. 2021, *leg*. B.A. Olou, OAB0666 (UNIPAR).

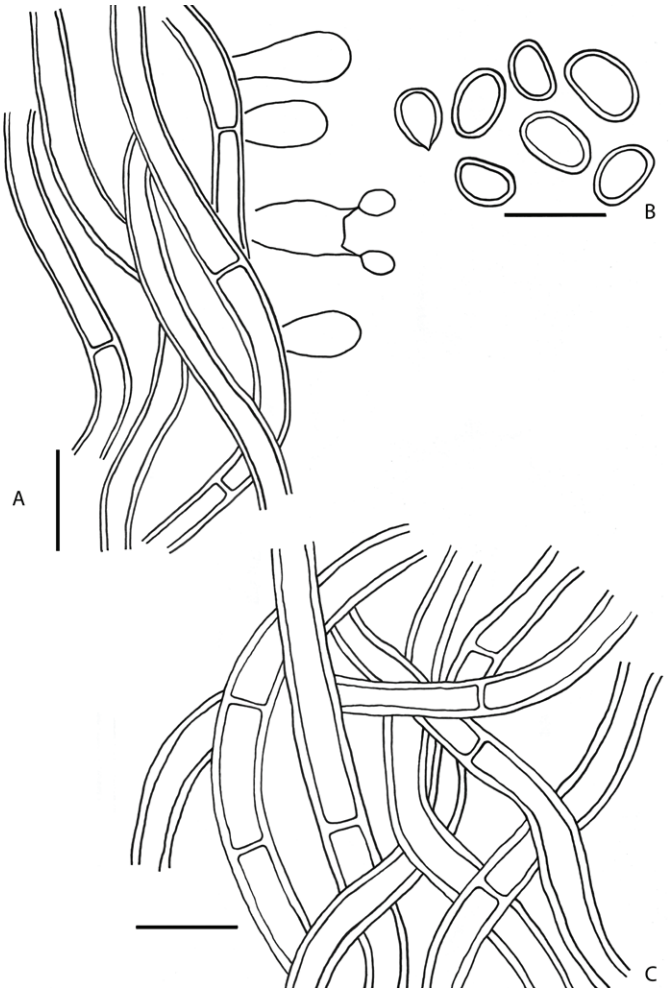

Fig. 3. *Phylloporia mutabilis* (OAB0643). **A.** Hyphae of the trama close to a pore and basidia, one basidium with young basidiospores. **B.** Basidiospores. **C.** Contextual hyphae. Scale bars: A, C = 10 µm; B = 5 µm.

DISCUSSION

Sequences generated from two specimens of *Phylloporia mutabilis* were added to the phylogeny of the genus *Phylloporia*. Our phylogenetic analyses of combined ITS-LSU-*EF1α* dataset reveal that sequences of *Phylloporia mutabilis* form a distinct clade which has a sister clade, including *P. littoralis*, *P. flacourtiae*, and *P. parasitica*. The three latter species differ from *P. mutabilis* by resupinate or pileate-sessile basidiomata (Murrill 1904, Yombiyeni & Decock 2017, Zhou 2015a).

Among the 76 known *Phylloporia* species, 10 species have pileate-stipitate basidiomata like *P. mutabilis*. Of these 10 species, seven, namely *P. afrospathulata*, *P. elegans*, *P. minutispora*, *P. nodostipitata*, *P. spathulata*, *P. solicola* and *P. terrestris* are not phylogenetically closely related to the new species. The remaining three species, *P. rajchenbergii*, *P. ryvardenii* and *P. verae-crucis* were not included in the phylogenetic analyses because their sequences are not available (Chamorro-Martínez *et al.* 2022)

Phylloporia rajchenbergii differs from *P. mutabilis* by its lateral stipitate basidiomata, a reddish brown pileus, polygonal to elongate and smaller pores, 14–16 per mm (Chamorro-Martínez *et al.* 2022).

Phylloporia ryvardenii differs from *P. mutabilis* by its neotropical origin, the lack of black in the context and stipe, and smaller spores, 10–12 per mm (Chamorro-Martínez *et al.* 2022).

Phylloporia veracrucis differs from *P. mutabilis* by its larger ellipsoid basidiospores, 4.5 × 3.5 µm (Wagner & Ryvarden 2002) (smaller in *P. mutabilis*, 3.8 × 2.9 µm). In addition, *P. veracrucis* is only known from Mexico (North America) (Wagner & Ryvarden 2002) while *P. mutabilis* is known from Benin (West Africa). *Phylloporia mutabilis* is newly described here and its distribution will have to be reassessed once more collections become available.

Phylloporia rajchenbergii, *P. ryvardenii* and *P. veracrucis* were reported to be related to *P. spathulata* (Wagner & Ryvarden 2002, Chamorro-Martínez *et al.* 2022). *Phylloporia spathulata* was reported from tropical Africa (Ryvarden & Johansen 1980), but the species was considered to have a neotropical distribution by Ferreira-Lopes *et al.* (2016). In addition, the sequences of *P. spathulata* did not match with those of *P. mutabilis*, so it is obvious that *P. mutabilis* and *P. spathulata* are two different species. Records of *P. spathulata* from tropical Africa need to be examined microscopically and phylogenetically as these specimens might represent another species.

The lifestyle of *P. mutabilis* is not known. Its basidiomata were found on soil and its mycelium could develop on the roots of nearby living trees or on dead wood debris buried in the soil. It might also have a mycorrhizal lifestyle like some species of *Coltricia*. Future studies on the ecology of terrestrial *Phylloporia* species will shed light on our understanding of the lifestyle of terrestrial *Phylloporia* species.

The description of *P. mutabilis* brings the diversity of *Phylloporia* in Benin to three species, namely *P. beninensis*, *P. littoralis* and *P. mutabilis*. *Phylloporia beninensis* and *P. littoralis* are recorded from woodlands with open canopy in central and northern Benin (dry habitats) and these species are characterised by pileate-sessile or effused-reflexed basidiomata attached to wood. *Phylloporia mutabilis* is the only species recorded from a dense dry forest with a closed canopy in southern Benin (wet habitat) and is characterised by pileate-stipitate basidiomata on soil. Although it is still too early to draw this conclusion, our data seem to indicate that species in dry habitats are characterised by pileate-sessile basidiomata and species in wet habitats by pileate-stipitate species. Previous studies have shown that morphological traits of the basidiomata are linked to microclimate (Krah *et al.* 2022). Similarly, the size of the basidiomata, its colour, lightness and toughness are linked to harsh microclimatic conditions (Krah *et al.* 2019, Bässler *et al.* 2021). However, at present we know little about whether the presence or absence of the stipe in a basidioma can be linked to habitat types or microclimatic adaptations. Further mycological surveys on *Phylloporia* in Benin will increase the diversity of species of *Phylloporia* and this will facilitate ecological studies to answer these outstanding questions.

ACKNOWLEDGEMENTS

This research was funded by The German Federal Ministry of Education and Research, BMBF (grant No. 01D20015). Boris Armel Olou also received support from the Mohamed Bin Zayed Species Conservation Fund (grant No. 192520581) for the field work.

Conflict of interest: The authors declare that there is no conflict of interest.

REFERENCES

Bässler C, Brandl R, Müller J, *et al.* (2021). Global analysis reveals an environmentally driven latitudinal pattern in mushroom size across fungal species. *Ecology Letters* **24**: 658–667.

Bernicchia A, Gorjón SP (2020). *Polypores of the Mediterranean Region*. Romar.

Bittencourt F, Stürmer SL, Reck MA, *et al.* (2018). *Phylloporia minuta*. *Phytotaxa* **348**: 199–210.

Chamorro-Martínez HA, Raymundo T, Martínez-González CR, *et al.* (2022). Two new stipitate species of *Phylloporia* (*Basidiomycota, Hymenochaetaceae*) from Chamela Biology Station, U.N.A.M. in Jalisco, Mexico. *Lilloa* **59**: 359–375.

Chen Y, Zhu L, Xing J, *et al.* (2017). Three new species of *Phylloporia* (*Hymenochaetales*) with dimitic hyphal systems from tropical China. *Mycologia* **109**: 951–964.

Cui BK, Yuan HS, Dai YC (2010). Two new species of *Phylloporia* (*Basidiomycota*, *Hymenochaetaceae*) from China. *Mycotaxon* **113**: 171–178.

Dai YC (2010). *Hymenochaetaceae* (*Basidiomycota*) in China. *Fungal Diversity* **45**: 131–343.

Dai YC (2012). Polypore diversity in China with an annotated checklist of Chinese polypores. *Mycoscience* **53**: 49–80.

Decock C, Amalfi M, Robledo G, *et al.* (2013). *Phylloporia nouraguensis*, an undescribed species on *Myrtaceae* from French Guiana. *Cryptogamie, Mycologie* **34**: 15–27.

Decock C, Yombiyeni P, Memiaghe H (2015). *Hymenochaetaceae* from the Guineo-Congolian Rainforest: *Phylloporia flabelliforma sp. nov*. and *Phylloporia gabonensis sp. nov.*, two undescribed species from Gabon. *Cryptogamie, Mycologie* **36**: 449–467.

Ferreira-Lopes V, Robledo GL, Reck MA, *et al.* (2016). *Phylloporia spathulata sensu stricto* and two new South American stipitate species of *Phylloporia* (*Hymenochaetaceae*). *Phytotaxa* **257**: 133–148.

Gafforov Y, Tomšovský M, Langer E, *et al.* (2014). *Phylloporia yuchengii sp. nov*. (*Hymenochaetales, Basidiomycota*) from Western Tien Shan Mountains of Uzbekistan based on phylogeny and morphology. *Cryptogamie, Mycologie* **35**: 313–322.

Gardes M, Bruns TD (1993). ITS primers with enhanced specificity for basidiomycetes - application to the identification of mycorrhizae and rusts. *Molecular Ecology* **2**: 113–118.

Gilbertson RL, Ryvarden L (1987). *North American Polypores.* Vol. 2. *Megasporoporia - Wrightoporia*, 2nd edn. *Fungiflora*, Oslo.

Hoang DT, Chernomor O, Von Haeseler A, *et al.* (2018). UFBoot2: Improving the ultrafast bootstrap approximation. *Molecular Biology and Evolution* **35**: 518–522.

Ipulet P, Ryvarden L (2005). New and interesting polypores from Uganda. *Synopsis Fungorum* **20**: 87–99.

Jerusalem M, Yombiyeni P, Castillo G, *et al.* (2019). *Hymenochaetaceae* (*Basidiomycota, Hymenochaetales*) from the guineo-congolian phytochorion: *Phylloporia rinoreae sp. nov*., an additional undescribed species from the forest global earth observatory plot in Gabon. *Plant Ecology and Evolution* **152**: 531–538.

Ji XH, Vlasák J, Zhou LW, *et al.* (2017). Phylogeny and diversity of *Fomitiporella* (*Hymenochaetales, Basidiomycota*). *Mycologia* **109**: 308–322.

Kalyaanamoorthy S, Minh BQ, Wong TKF, *et al.* (2017). ModelFinder: Fast model selection for accurate phylogenetic estimates. *Nature Methods* **14**: 587–589.

Katoh K, Rozewicki J, Yamada KD (2017). MAFFT online service: multiple sequence alignment, interactive sequence choice and visualization. *Briefings in Bioinformatics* **20**: 1160–1166.

Krah FS, Büntgen U, Schaefer H, *et al.* (2019). European mushroom assemblages are darker in cold climates. *Nature Communications* **10**: 2890.

Krah FS, Hagge J, Schreiber J, *et al.* (2022). Fungal fruit body assemblages are tougher in harsh microclimates. *Scientific Reports* **12**: 1633.

Larsson A (2014). AliView: A fast and lightweight alignment viewer and editor for large datasets. *Bioinformatics* **30**: 3276–3278.

Minh BQ, Schmidt HA, Chernomor O, *et al.* (2020). IQ-TREE 2: New models and efficient methods for phylogenetic inference in the genomic era. *Molecular Biology and Evolution* **37**: 1530–1534.

Murrill WA (1904). A new polyporoid genus from South America. *Torreya* **4**: 141–142.

Olou BA, Krah F, Piepenbring M, *et al.* (2020). Diversity of *Trametes* (*Polyporales, Basidiomycota*) in tropical Benin and description of new species *Trametes parvispora*. *MycoKeys* **65**: 25–47.

Olou BA, Ordynets A, Langer E (2019). First new species of *Fulvifomes* (*Hymenochaetales, Basidiomycota*) from tropical Africa. *Mycological Progress* **18**: 1383–1393.

Olou BA, Yorou NS, Langer E (2021). New species and a new record of *Phylloporia* from Benin. *Scientific Reports* **11**: 8879.

Qin WM, Wang XW, Sawahata T, *et al.* (2018). *Phylloporia lonicerae* (*Hymenochaetales, Basidiomycota*), a new species on *Lonicera japonica* from Japan and an identification key to worldwide species of *Phylloporia*. *MycoKeys* **30**: 17–30.

Rajchenberg M, Pildain MB, Madriaga DC, *et al.* (2019). New poroid *Hymenochaetaceae* (*Basidiomycota, Hymenochaetales*) from Chile. *Mycological Progress* **18**: 865–877.

Rehner SA, Buckley E (2008). A *Beauveria* phylogeny inferred from nuclear ITS and *EF1*- sequences: evidence for cryptic diversification and links to *Cordyceps* teleomorphs. *Mycologia* **97**: 84–98.

Ren GJ, Wu F (2017). *Phylloporia lespedezae sp. nov.* (*Hymenochaetaceae, Basidiomycota*) from China. *Phytotaxa* **299**: 243–251.

Ryvarden L (1972). A critical checklist of the *Polyporaceae* in tropical East Africa. *Norwegian Journal of Botany* **19**: 229–238.

Ryvarden L, Johansen I (1980). *A preliminary Polypore flora of East Africa*. Fungiflora, Oslo.

Ryvarden L, Melo I (2014). *Poroid fungi of Europe*. Fungiflora, Oslo.

Sayers EW, Cavanaugh M, Clark K, *et al.* (2020). GenBank. *Nucleic Acids Research* **48**: D84–D86.

Sukumaran J, Holder MT (2010). DendroPy: A Python library for phylogenetic computing. *Bioinformatics* **26**: 1569–1571.

Trifinopoulos J, Nguyen LT, von Haeseler A, *et al.* (2016). W-IQ-TREE: a fast online phylogenetic tool for maximum likelihood analysis. *Nucleic Acids Research* **44**: W232–W235.

Valenzuela R, Raymundo T, Cifuentes J, *et al.* (2011). Two undescribed species of *Phylloporia* from Mexico based on morphological and phylogenetic evidence. *Mycological Progress* **10**: 341–349.

Vilgalys R, Hester M (1990). Rapid genetic identification and mapping of enzymatically amplified ribosomal DNA from several *Cryptococcus* species. *Journal of Bacteriology* **172**: 4238–4246.

Wagner T, Fischer M (2002). Proceedings towards a natural classification of the worldwide taxa *Phellinus s.l.* and *Inonotus s.l.*, and phylogenetic relationships of allied genera. *Mycologia* **94**: 998–1016.

Wagner T, Fischer M (2001). Natural groups and a revised system for the European poroid *Hymenochaetales* (*Basidiomycota*) supported by nLSU rDNA sequence data. *Mycological Research* **105**: 773–782.

Wagner T, Ryvarden L (2002). Phylogeny and taxonomy of the genus *Phylloporia* (*Hymenochaetales*). *Mycological Progress* **1**: 105–116.

White TJ, Bruns T, Lee S, *et al.* (1990). Amplification and direct sequencing of fungal ribosomal RNA genes for phylogenetics. In: *PCR protocols: a guide to methods and applications* (Innis MA,

Gelfand DH, Sninsky JJ, White TJ, eds), Academic Press, San Diego, California, USA: 315–322.

Wu F, Ren GJ, Wang L, *et al.* (2019). An updated phylogeny and diversity of *Phylloporia* (*Hymenochaetales*): eight new species and keys to species of the genus. *Mycological Progress* **18**: 615–639.

Wu F, Zhou LW, Vlasák J, *et al.* (2022). Global diversity and systematics of *Hymenochaetaceae* with poroid hymenophore. *Fungal Diversity* **113**: 1–192.

Wu SH, Chang CC, Wei CL, *et al.* (2020). Four new species of *Phylloporia* (*Hymenochaetales, Basidiomycota*) from southeastern Taiwan. *Mycological Progress* **19**: 743–752.

Wu SH, Chang CC, Wei CL, *et al.* (2021). *Phylloporia moricola sp. nov*. (*Hymenochaetales*, *Basidiomycota*) from China. *Phytotaxa* **501**: 181–188.

Yombiyeni P, Balezi A, Amalfi M, *et al.* (2015). *Hymenochaetaceae* from the Guineo-Congolian rainforest: Three new species of *Phylloporia* based on morphological, DNA sequences and ecological data. *Mycologia* **107**: 996–1011.

Yombiyeni P, Decock C (2017). *Hymenochaetaceae* (*Hymenochaetales*) from the Guineo-Congolian phytochorion: *Phylloporia littoralis sp. nov*. from coastal vegetation in Gabon, with an identification key to the local species. *Plant Ecology and Evolution* **150**: 160–172.

Yu HY, Zhao CL, Dai YC (2013). *Inonotus niveomarginatus* and *I. tenuissimus spp. nov*. (*Hymenochaetales*), resupinate species from tropical China. *Mycotaxon* **124**: 61–68.

Zhou LW (2014). Notes on the taxonomic positions of some *Hymenochaetaceae* (*Basidiomycota*) species with colored basidiospores. *Phytotaxa* **177**: 183.

Zhou L (2013). *Phylloporia tiliae sp. nov*. from China. *Mycotaxon* **124**: 361–365.

Zhou LW (2015a). Four new species of *Phylloporia* (*Hymenochaetales, Basidiomycota*) from tropical China with a key to *Phylloporia* species worldwide. *Mycologia* **107**: 1184–1192.

Zhou LW (2015b). *Phylloporia osmanthi* and *P. terrestris spp. nov*. (*Hymenochaetales, Basidiomycota*) from Guangxi, South China. *Nova Hedwigia* **100**: 239–249.

Zhou LW (2016). *Phylloporia minutipora* and *P. radiata spp. nov*. (*Hymenochaetales, Basidiomycota*) from China and a key to worldwide species of *Phylloporia*. *Mycological Progress* **15**: 1–11.

Zhou LW, Dai YC (2012). Phylogeny and taxonomy of *Phylloporia* (*Hymenochaetales*): New species and a worldwide key to the genus. *Mycologia* **104**: 211–222.

Zhou M, Wu F, Dai YC, *et al.* (2022). Two new species of *Phylloporia* (*Hymenochaetales*) from the Neotropics. *MycoKeys* **90**: 71–83.

FUSE

Fungal Systematics and Evolution

Volume 12
DECEMBER 2023
PAGES 91–110

doi.org/10.3114/fuse.2023.12.07

New mycoparasitic species in the genera *Niveomyces* and *Pseudoniveomyces gen. nov.* (*Hypocreales*: *Cordycipitaceae*), with sporothrix-like asexual morphs, from Thailand

N. Kobmoo[1*], K. Tasanathai[1], J.P.M. Araújo[2], W. Noisripoom[1], D. Thanakitpipattana[1], S. Mongkolsamrit[1], W. Himaman[3], J. Houbraken[4], J.J. Luangsa-ard[1*]

[1]National Center for Genetic Engineering and Biotechnology (BIOTEC), National Science and Technology Development Agency (NSTDA), 111 Thailand Science Park, Khlong Nueng, Khlong Luang, Pathum Thani 12120, Thailand
[2]Institute of Systematic Botany, The New York Botanical Garden, Bronx - NY, USA, 10458
[3]Forest Entomology and Microbiology Research Group, Forest and Plant Conservation Research Office, 61 Department of National Parks, Wildlife and Plant Conservation, Phahonyothin Road, Chatuchak, Bangkok, 10900, Thailand
[4]Westerdijk Fungal Biodiversity Institute, Uppsalalaan 8, 3584 CT, Utrecht, The Netherlands

*Corresponding author: jajen@biotec.or.th, noppol.kob@biotec.or.th

Key words:
Cordycipitaceae
entomopathogenic fungi
mycoparasitism
new taxa
Sporothrix

Abstract: Four new species of the genus *Niveomyces* are described from Thailand. They were found as mycoparasites on: *Ophiocordyceps* infecting flies (*Diptera*) for *Niveomyces albus*; ants (*Hymenoptera*) for *N. formicidarum*; and leafhoppers (*Hemiptera*) for *N. hirsutellae* and *N. multisynnematus*. A new genus, *Pseudoniveomyces* with two species: *Pseudoniveo. blattae* (type species), parasitic on *Ophiocordyceps* infecting cockroaches, and *Pseudoniveo. arachnovorum*, found on a spider egg sac, are also described. These fungi share a common feature which is a sporothrix-like asexual morph. Based on our molecular data, *Sporothrix insectorum* is shown to be affiliated to the genus *Niveomyces*, and thus a new combination *N. insectorum comb. nov*. is proposed. *Niveomyces coronatus*, *N. formicidarum* and *N. insectorum* formed the *N. coronatus* species complex found on ant-pathogenic *Ophiocordyceps* from different continents. *Pseudoniveomyces* species are distinguished from *Niveomyces* spp. based on the presence of fusoid macroconidia in culture and a red pigment diffused in the medium, resembling to *Gibellula* and *Hevansia*. The molecular phylogenetic analyses also confirmed its generic status. The host/substrates associated with the genera within *Cordycipitaceae* were mapped onto the phylogeny to demonstrate that mycoparasitism also evolved independently multiple times in this family.

Citation: Kobmoo N, Tasanathai K, Araújo JPM, Noisripoom W, Thanakitpipattana D, Mongkolsamrit S, Himaman W, Houbraken J, Luangsa-ard JJ (2023). New mycoparasitic species in the genera *Niveomyces* and *Pseudoniveomyces gen. nov*. (*Hypocreales*: *Cordycipitaceae*), with sporothrix-like asexual morphs, from Thailand. *Fungal Systematics and Evolution* **12**: 91–110. doi: 10.3114/fuse.2023.12.07
Received: 13 July 2023; **Accepted:** 9 August 2023; **Effectively published online:** 28 August 2023
Corresponding editor: P.W. Crous

INTRODUCTION

Fungi constitute the most diverse kingdom of living organisms (Blackwell 2011) with highly diversified lifestyles and ecologies (Smith & Read 2008, Gibson & Hunter 2010, Pineda *et al.* 2013, Lacey *et al.* 2015). Some fungi evolved to exploit other fungi which are themselves pathogenic or parasitic on other organisms, a lifestyle called "hyperparasitism" (Boosalis 1964, Parratt & Laine 2016). Hyperparasitism by fungi on fungal pathogens of other organisms is commonly called "mycoparasitism" (Bushley *et al.* 2013, Wang *et al.* 2015, Crous *et al.* 2017, Araújo *et al.* 2020, 2022) although the initial meaning of the latter term referred to fungi parasitising other fungi whether the hosts be parasites/pathogens or not (Barnett 1963). Mycoparasitism has evolved multiple times in the Kingdom *Fungi* (Gleason *et al.* 2014). Within the *Ascomycota*, the order *Hypocreales* contains almost 3 000 species, composed of plant and animal pathogens, endophytes, insect endosymbionts, saprophytes and mycoparasites (Spatafora *et al.* 2007, Sung *et al.* 2007a, Blackwell 2010, Boomsma *et al.* 2014, Matsuura *et al.* 2018). The mycoparasitic lifestyle has evolved independently multiple times in *Hypocreales* (Spatafora *et al.* 2007, Sung *et al.* 2008). For example, within *Cordycipitaceae, Lecanicillium* and *Simplicillium* are found to infect plant pathogens (*e.g.* coffee rust fungus *Hemileia vastatrix*) and entomopathogens (Vandermeer *et al.* 2009, Baiswar *et al.* 2014, Wei *et al.* 2019). *Pseudogibellula* is found to grow directly on *Ophiocordyceps*, suggesting an apparent mycoparasitism (Araújo *et al.* 2020, Mongkolsamrit *et al.* 2021), and the genus *Niveomyces* has been recently proposed as a mycoparasite of *Ophiocordyceps camponoti-floridani* (Araújo *et al*. 2022). Within *Hypocreaceae*, *Syspastospora parasitica* is found to infect a well-known insect pathogen/endophyte, *Beauveria bassiana* (Posada *et al.* 2004). Within *Ophiocordycipitaceae*, *Polycephalomyces* and *Pleurocordyceps* are found to infect a variety of cordycipitaceous entomopathogens and most recently, *Torrubiellomyces* was proposed to infect ant-pathogenic *Ophiocordyceps camponoti-*

floridani (Kaitsu *et al.* 2013, Wang *et al.* 2015, 2021, Zhong *et al.* 2016, Araújo *et al.* 2022).

The genus *Sporothrix* (*Ophiostomataceae*, *Ophiostomatales*) was established in the early 20th century by Hektoen & Perkins (1900) with *S. schenckii*, a human pathogen, as the type species of the genus. Subsequently, a link was established to the sexually reproductive genus *Ophiostoma* found essentially as pathogens of various organisms including plants and insects (Münch 1907). De Beer *et al.* (2016) established the distinction between *Ophiostoma sensu stricto* and *Sporothrix s.s*. based on molecular phylogenies. Before the monograph of de Hoog (1974), there were inconsistencies regarding what "*Sporothrix*" really was. Due to morphological plasticity, *Sporothrix* species had been linked to various ascomycetous genera such as *Graphium*, *Cephalosporium*, *Cladosporium* (Hedgcock 1906, Münch 1907), and even *Sporotrichum*, which is now recognised as being affiliated to *Basidiomycota* (von Arx 1971, Stalpers 1978). "Sporothrix-like" asexual morphs are characterised by hyaline mycelia occasionally producing holoblastic conidia on variably denticulate conidiogenous cells, forming conidia sympodially (de Hoog 1974, de Beer *et al.* 2016). This type of asexual morph is very similar to what can be found in *Beauveria* which are insect pathogens of the family *Cordycipitaceae*. *Sporothix insectorum*, a species initially found on insects (de Hoog 1974), is a good example of uncertainty regarding "*Sporothrix*". De Hoog (1993) suggested a "clavicipitalean relationship" to *Spor. insectorum* while de Beer *et al.* (2016) also suggested that this species should be compared with fungi in *Cordycipitaceae*. De Hoog (1974) described the type specimen of *Spor. insectorum* as being found on "*Paltothyreus tarsatus*" (*Hymenoptera, Formicidae)* "associated with *Gibellula* [= *Pseudogibellula*] *formicarum*", which was further supported and discussed by Araújo *et al.* (2020) and considered to be a mycoparasite of *Ophiocordyceps paltothyreum*, a commonly found ant parasite in West Africa.

Through our continuous exploration of the diversity of entomopathogenic fungi from Thailand and their associated mycoparasites, we have found new specimens with sporothrix-like asexual morphs resembling the recently proposed new genus *Niveomyces* (Araújo *et al.* 2022). They were found on dead insects infected with hypocrealean entomopathogenic fungi, strongly suggesting a mycoparasitic nutritional mode. In order to confirm whether these specimens belong to *Niveomyces* but are different from *N. coronatus* described by Araújo *et al.* (2022) and to check the taxonomic affiliation of *Spor. insectorum*, we conducted a taxonomic study including the newly found specimens and the ex-type culture of *Spor. insectorum* (CBS 756.73). We propose four new mycoparasitic species of *Niveomyces*, and the new genus, *Pseudoniveomyces*, represented so far by two species, *Pseudoniveo. arachnovorum* and *Pseudoniveo. blattae*. With these new taxa added to the *Cordycipitaceae*, we also reconstructed the ancestral host/substrate association to gain insights into the evolution of mycoparasitism in this family. Our hypothesis is that different lineages of mycoparasites have evolved multiple times independently in *Cordycipitaceae*.

MATERIALS AND METHODS

Fungal isolation, DNA extractions and PCR

The samples were found while inspecting the underside and topside of understory leaves in natural parks and community forests of Thailand (Table 1). The samples were placed in plastic boxes and transported back to the laboratory. To establish cultures, small pieces of sterile potatoes dextrose agar (PDA; potato 200 g/L, dextrose 15 g/L, agar 15 g/L) were cut with a flamed sterile needle and gently brought into contact with synnemata bearing abundant conidia, then placed on sterile PDA Petri dishes. The inoculated PDA plates were examined daily for fungal gemination and contamination. The germinating conidia without contaminations were sub-cultured on fresh PDA plates. The pure cultures were maintained at 25 °C for 2–3 wk before further examination.

The DNA of 15 samples was extracted using a procedure based on Cetyl-trimethyl-ammonium bromide (CTAB); mycelial mass grown on PDA (40–50 mg) was collected and placed into a micro centrifuge tube (1.5 mL), ground manually with a pestle in 600 µL of CTAB buffer (NaCl 1.4 M; Tris-HCl 100 mM pH 8.0; EDTA 20 mM pH 8.0, 2 % CTAB and 1 % PVP-40). The suspension was thoroughly mixed and incubated for 1 h at 65 °C. After the suspension had cooled to approximately room temperature, 600 µL of chloroform/isoamyl alcohol (24:1 v/v) was added and homogenised until an emulsion was obtained; the mixture was then centrifuged at 12 000 rpm for 15 min at 25 °C. The supernatant was transferred to a new tube (1.5 mL) and 300 µL of cold (~ 4 °C) isopropanol was added, the suspension was left in a refrigerator for 15–30 min and centrifuged at 12 000 rpm for 15 min at 4 °C. Subsequently, the supernatant was discarded, and the pellet was washed in 300 mL 70 % (v/v) ethanol then air-dried at room temperature. Finally, the DNA pellet was dissolved in 50 mL TE buffer (10 mM Tris-HCl pH 8.0, 1 mM, EDTA pH 8.0).

PCR and sequencing

Amplification of the whole internal transcribed spacer region (ITS), partial region of the large subunit of the nuclear ribosomal DNA (LSU), the translation elongation factor 1-α (*TEF1*), partial regions of genes encoding the largest (*RPB1*) and second largest (*RPB2*) subunits of RNA polymerase II were amplified. The primers used were ITS5 and ITS4 (White *et al.* 1990; ITS), LR0R and LR7 (Vilgalys & Hester 1990; LSU), EF1-983F and EF1-2218R (Rehner & Buckley 2005; *TEF1*), CRPB1 and RPB1Cr (Castlebury *et al.* 2004; *RPB1*) and RPB2-5F2 (Sung *et al.* 2007b) and fRPB2-7cR (Liu *et al.* 1999; *RPB2*). All amplification reactions were performed in 25 µL volumes consisting of 10× *Taq* Buffer with $(NH_4)_2SO_4$, 2.5 mM $MgCl_2$, 1 U *Taq* DNA polymerase (Thermo Scientific), 200 µM of each of the four dNTPs (Promega, Madison, WI, USA), 0.4 M betaine and 0.2 µM of each primer, using a T100 Thermal Cycler (Bio-Rad). The amplification reactions were checked for positive amplification on 1 % agarose gel. The PCR amplicons were sent to MACROGEN (Korea) for purification and Sanger sequencing.

Molecular phylogenies

Nucleotide sequences were assembled and edited in BioEdit v. 7.1.3 (Hall 1999). Sequences of ITS, LSU, *TEF1*, *RPB1* and *RPB2* from related cordycipitaceous species, selected from previous studies (Sung *et al.* 2001, 2007a, b, Sung & Spatafora 2004, Bischoff *et al.* 2005, Chaverri *et al.* 2005, Luangsa-Ard *et al.* 2005, Spatafora *et al.* 2007, Zare & Gams 2008, Johnson *et al.* 2009, Rehner *et al.* 2011, Kepler *et al.* 2012, 2017, Sanjuan *et al.* 2014, Tsang *et al.* 2016, Mongkolsamrit *et al.* 2018, 2020, 2021, 2022, Vu *et al.* 2019, Thanakitpipattana *et al.* 2020, Wang *et al.*

Table 1. List of taxa included in the phylogenetic analyses and their GenBank accession numbers. The accession numbers marked in **bold** font refer to sequences new in this study or have been generated by our group in Thailand. T= ex-type culture.

Species	Strain	Host/Substratum	GenBank Accession no.				
			ITS	LSU	*TEF1*	*RPB1*	*RPB2*
Akanthomyces aculeatus	HUA 186145^{T}	*Lepidoptera*	–	MF416520[1]	MF416465[1]	–	–
	HUA 772	*Lepidoptera*; *Sphingidae*	KC519371[2]	KC519370[2]	KC519366[2]	–	–
Akanthomyces sulphureus	TBRC 7248^{T}	*Araneae*; spider	MF140758[3]	MF140722[3]	MF140843[3]	MF140787[3]	MF140812[3]
Ascopolyporus polychrous	P.C. 546	*Hemiptera*	–	DQ118737[4]	DQ118745[4]	DQ127236[4]	–
Ascopolyporus villosus	ARSEF 6355	*Hemiptera*	AY886544[5]	AY886544[5]	DQ118750[4]	DQ127241[4]	–
Beauveria bassiana	ARSEF 1564^{T}	*Lepidoptera*	HQ880761[6]	–	HQ880974[6]	HQ880833[6]	HQ880905[6]
	ARSEF 7518	*Hymenoptera*	HQ880762[6]	–	HQ880975[6]	HQ880834[6]	HQ880906[6]
Blackwellomyces cardinalis	OSC 93609	*Lepidopteran*	–	AY184962[7]	DQ522325[8]	DQ522370[8]	DQ522422[8]
	OSC 93610	*Lepidopteran*	JN049843[9]	AY184963[7]	EF469059[10]	EF469088[10]	EF469106[10]
Cordyceps militaris	OSC 93623	*Lepidoptera*	JN049825[9]	AY184966[7]	DQ522332[8]	DQ522377[8]	–
	YFCC 6587	*Lepidoptera*	–	MN576818[11]	MN576988[11]	MN576878[11]	MN576932[11]
Engyodontium parvisporum	IHEM 22910	Human bronchoscopy specimen	LC092896[12]	LC092915[12]	LC425558[13]	–	–
Engyodontium rectidentatum	CBS 206.74	Air	LC092893[12]	LC092912[12]	LC425553[13]	–	–
	CBS 641.74	Buried keratinous substance	LC092895[12]	LC092914[12]	LC425540[13]	–	–
Flavocillium bifurcatum	YFCC 6101^{T}	*Lepidoptera*; *Noctuidae*	–	MN576781[11]	MN576951[11]	MN576841[11]	MN576897[11]
Gamszarea humicola	CGMCC 3.19303^{T}	Soil	MK329092[14]	MK328997[14]	MK336027[14]	–	MK335979[14]
Gamszarea wallacei	CBS 101237 ^{T}	*Lepidoptera*	EF641891[15]	AY184967[7]	EF469073[10]	EF469102[10]	EF469119[10]
Gibellula gamsii	BCC 28797	*Arachnida*; *Araneida*	MH152531[16]	MH152541[16]	MH152562[16]	MH152549[16]	MH152557[16]
	BCC 27968^{T}	*Arachnida*; *Araneida*	MH152529[16]	MH152539[16]	MH152560[16]	MH152547[16]	–
Gibellula pulchra	BCC 47555	*Arachnida*; *Araneida*	MH532885[17]	OK040714[17]	MH521897[17]	MH521804[17]	
Hevansia novoguineensis	CBS 610.80^{T}	*Arachnida*	MH532831[18]	MH394646[19]	MH521885[19]	–	MH521844[19]
	BCC 42675	*Arachnida*	MZ684089[20]	MZ684004[20]	MZ707814[20]	–	MZ707835[20]
Jenniferia thomisidarum	BCC 37881^{T}	*Araneae*, *Diaea cf. dorsata*	MZ684099[20]	MZ684010[20]	MZ707823[20]	MZ707830[20]	MZ707843[20]
	BCC 37882	*Araneae*, *Diaea cf.* dorsata	MZ684100[20]	MZ684011[20]	MZ707824[20]	MZ707831[20]	MZ707844[20]

Table 1. (Continued).

Species	Strain	Host/Substratum	GenBank Accession no.				
			ITS	LSU	*TEF1*	*RPB1*	*RPB2*
Lecanicillium antillanum	CBS 350.85	*Arachnida*	–	AF339536[21]	DQ522350[8]	DQ522396[8]	DQ522450[8]
Lecanicillium aranearum	CBS 726.73a	*Arachnida*; *Araneae*	–	AF339537[21]	EF468781[10]	EF468887[10]	EF468934[10]
Lecanicillium tenuipes	CBS 309.85	*Arachnida*	–	AF339526[21]	DQ522341[1]	DQ522387[1]	DQ522439[1]
Liangia sinensis	YFCC3103^T	*Beauveria yunnanensis*	–	MN576782[11]	MN576952[11]	MN576842[11]	MN576898[11]
	YFCC3104	*Beauveria yunnanensis*	–	MN576783[11]	MN576953[11]	MN576843[11]	MN576899[11]
Neohyperdermium piperis	CBS 116719	*Hemiptera*	–	AY466442[22]	DQ118749[1]	DQ127240[4]	EU369083[23]
Neohyperdermium pulvinatum	P.C. 602	*Hemiptera*	–	DQ118738[4]	DQ118746[4]	DQ127237[4]	–
Neotorrubiella chinghridicola	BCC 39684	*Orthopterida*	–	MK632096[24]	MK632148[24]	MK632071[24]	MK632181[24]
	BCC 80733^T	*Orthopterida*	–	MK632097[24]	MK632149[24]	MK632072[24]	MK632176[24]
Niveomyces albus	**BCC 83025^T**	***Ophiocordyceps* sp. on *Diptera***	**ON103032**	**ON103157**	**ON125015**	**ON286876**	**ON125027**
	BCC 74477	***Ophiocordyceps* sp. on *Arachnida* (*Araneae*)**	**ON103033**	**ON103158**	**ON125016**	**ON286877**	**ON125028**
	BCC 73628	***Ophiocordyceps* sp. on *Arachnida* (*Araneae*)**	**ON103034**	**ON103159**	**ON125017**	–	**ON125029**
Niveomyces coronatus	NY 04434800^T	*Ophiocordyceps camponoti-floridani*	–	ON493606[25]	ON513397[25]	ON513399[25]	ON513400[25]
Niveomyces formicidarum	**BCC 79346**	***Ophiocordyceps* sp. on *Hymenoptera***	**ON103035**	**ON103160**	**ON125018**	**ON286878**	**ON125030**
	BCC 83026^T	***Ophiocordyceps* sp. on *Hymenoptera***	**ON103036**	**ON103161**	**ON125019**	**ON286879**	–
Niveomyces hirsutellae	**BCC 36631^T**	***Ophiocordyceps* sp. on *Hemiptera***	**ON103039**	**ON103164**	**ON125022**	**ON286882**	**ON125033**
	BCC 36632	***Ophiocordyceps* sp. on *Hemiptera***	**ON103040**	**ON103165**	**ON125023**	**ON286883**	**ON125034**
	BCC 78482	***Ophiocordyceps* sp. on *Hemiptera***	**ON103041**	**ON103166**	**ON125024**	**ON286884**	**ON125035**
Niveomyces insectorum	CBS 756.73^T	"*Palthothyreus tarsatus* in *Rubiaceae*, associated with *Gibellula formicarum*" *	MH860798[26]	**ON103169**	**ON125026**	**ON286887**	**ON125038**
Niveomyces multisynnematus	**BCC 90307**	***Ophiocordyceps* sp. on *Hemiptera***	**ON103037**	**ON103162**	**ON125020**	**ON286880**	**ON125031**
	BCC 90308^T	***Ophiocordyceps* sp. on *Hemiptera***	**ON103038**	**ON103163**	**ON125021**	**ON286881**	**ON125032**
Parahevansia koratensis	NHJ 666.01	*Arachnida*	GQ250010[20]	GQ249981[20]	GQ250031[20]		
	NHJ 2662	*Lepidoptera*	GQ250008[20]	GQ249982[20]	GQ250032[20]	ON470206[20]	ON470208[20]
Parengyodontium album	CBS 368.72	A fresco	LC092891[12]	LC092910[12]	LC382183[13]	–	–
	CBS 504.83^T	Human brain abscess	LC092880[12]	LC092899[12]	LC382177[13]	–	–

Table 1. (Continued).

Species	Strain	Host/Substratum	GenBank Accession no.				
			ITS	LSU	*TEF1*	*RPB1*	*RPB2*
Pleurodesmospora lepidopterorum	DY 10501[T]	*Lepidoptera*	MW826576[27]	–	MW834317[27]	MW834315[27]	MW834316[27]
	DY 10502	*Lepidoptera*	MW826577[27]	–	MW834319[27]	–	MW834318[27]
Polystromomyces araneae	BCC 93301[T]	*Arachnida*	MZ684101[20]	MZ684016[20]	MZ707825[20]	MZ707832[20]	MZ707845[20]
Pseudogibellula formicarum	BCC 84257	*Ophiocordyceps flavida*	MT508782[19]	MT512653[19]	MT533480[19]	MT533473[19]	–
	CBS 433.73	*Palthothyreus tarsatus*	MH860731[26]	MH872442[26]	MT533481[19]	MT533475[19]	–
Pseudoniveomyces arachnovorum	**BCC 95818[T]**	***Arachnida*** (of spider eggs)	**OR098526**	–	**OR133172**	**OR133173**	**OR133173**
Pseudoniveomyces blattae	**BCC 53567[T]**	***Blattodea***	**ON103042**	**ON103167**	–	**ON286885**	**ON125036**
	BCC 53568	***Blattodea***	**ON103043**	**ON103168**	**ON125025**	**ON286886**	**ON125037**
Purpureocillium lilacinum	CBS 431.87	*Meloidogyn* sp. (*Nematoda*)	AY624188[28]	EF468844[10]	EF468791[10]	EF468897[10]	EF468940[10]
	CBS 284.36[T]	Soil	AY624189[28]	FR775484[29]	EF468792[10]	EF468898[10]	EF468941[10]
Samsoniella inthanonensis	TBRC 7915[T]	*Lepidoptera*	MF140761[3]	MF140725[3]	MF140849[3]	MF140790[3]	MF140815[3]
	TBRC 7916	*Lepidoptera*	MF140760[3]	MF140724[3]	MF140848[3]	MF140789[3]	MF140814[3]
Simplicillium lanosoniveum	CBS 101267	*Hemileia vastatrix*	–	AF339554[21]	DQ522357[8]	DQ522405[8]	DQ522463[8]
	CBS 704.86	*Hemileia vastatrix*	AJ292396[30]	AF339553[21]	DQ522358[8]	DQ522406[8]	DQ522464[8]

References: [1]Kepler *et al.* (2017), [2]Sanjuan *et al.* (2014), [3]Mongkolsamrit *et al.* (2018), [4]Chaverri *et al.* (2005), [5]Bischoff *et al.* (2005), [6]Rehner *et al.* (2011), [7]Sung & Spatafora (2004), [8]Spatafora *et al.* (2007), [9]Kepler *et al.* (2012), [10]Sung *et al.* (2007), [11]Wang *et al.* (2020), [12]Tsang *et al.* (2016), [13]Lee *et al.* (2018, unpublished), [14]Zhang *et al.* (2021), [15]Zare & Gams (2008), [16]Kuephadungphan *et al.* (2019), [17]Kuephadungphan *et al.* (2022), [18]Helaly *et al.* (2019), [19]Mongkolsamrit *et al.* (2021), [20]Mongkolsamrit *et al.* (2022), [21]Sung *et al.* (2001), [22]Bischoff & White (2004), [23]Johnson *et al.* (2009), [24]Thanakitpipattana *et al.* (2020), [25]Araújo *et al.* (2022), [26]Vu *et al.* (2019), [27]Chen *et al.* (2021), [28]Luangsa-ard *et al.* (2005), [29]Perdomo *et al.* (2013), [30]Zare *et al.* (2000).

* Literal description of *Sporothrix insectorum* from de Hoog (1974).

2020, Chen *et al.* 2021, Zhang *et al.* 2021) were downloaded from GenBank for phylogenetic analyses (Table 1). Sequences from the ex-type culture of *Sporothrix insectorum* (CBS 756.73) were also included, as its affiliation to *Cordycipitaceae* had been previously hypothesised (de Beer *et al.* 2016). The sequences from each marker were aligned using ClustalW (Thompson *et al.* 1994) in BioEdit (Hall 1999). A "Randomized Accelerated Maximum Likelihood" (RAxML) phylogenetic analysis was performed using RAxML-VI-HPC2 v. 8.2.12 (Stamatakis 2006, 2014) on XSEDE (http://www.phylo.org/), with the GTRGAMMA + I model and 1 000 bootstrap iterations (BS) were executed to evaluate the branch support. Bayesian inference (BI) analyses were performed by MrBayes v. 3.2 (Ronquist *et al.* 2012), with the GTR + G + I model as inferred by MrModeltest v. 2.2 (Nylander 2004). Five million generations of Markov chain Monte Carlo (MCMC) simulation were run with sampling every 1 000 generations, and discarding the first 10 % as burn-in after which the Bayesian posterior probabilities (PP) were calculated on the remaining trees. The molecular divergence based on p-distances calculated using MEGA v. 11 (Tamura *et al.* 2021) was used to aid the decision of splitting species within the *Niveomyces coronatus* complex. The sequence alignments for all datasets used in this study were submitted to Figshare https://doi.org/10.6084/m9.figshare.22716451.v4.

Morphological examination

Macro-morphological characters were described based on dry materials and photographs by using a digital Nikon D5100 camera. Micro-morphological characters, examined under a compound microscope (Olympus CX23, Olympus Corporation, Japan), were mounted with lactophenol cotton blue before measuring the sizes of the conidiogenous cells and conidia. Morphological characteristics of colonies, consisting of colour, texture, pigmentation and growth rates, were observed on two kinds of media: oatmeal agar (OA, Difco, oatmeal 60 g, agar 12.5 g, in 1 L distilled water) and PDA and incubated at 25 °C for 20 d. The colours of specimens and cultures incubated on OA and PDA were described and codified following the Sixth Royal Horticultural Society (R.H.S.) Colour Chart (2015).

Reconstruction of ancestral hosts and substrates

The hosts or substrates from which the fungal strains were isolated were classified into five categories: environment, insect, arachnid, nematode and fungus. The strains isolated from soil (*Gamzarea humicola* CGMCC3 19303, *Purpureocillium lilacinum* CBS 284.36) and from a fresco (mural painting) (*Parengyodontium album* CBS 368.72) were categorised as coming from the environment. The strains of *Simplicillium lasonovineum* and *Liangia sinensis* were reported to grow on the rust *Hemileia vastatrix* (Sung *et al.* 2001), and the entomopathogen *Beauveria bassiana* (Wang *et al.* 2020) respectively; the hosts of these two species were thus categorised as fungi. The novel taxa described in this study, *Niveomyces* spp. and *Pseudoniveomyces blattae* are mycoparasites; the hosts were also classified as fungi. Other prominent entomopathogenic fungi of the family are classified as associated with insects or arachnids.

The host/substrate information was mapped on the 5-locus phylogenetic tree and used to reconstruct the ancestral host and substrate association for the species presented in the tree, using a stochastic mapping approach (Huelsenbeck *et al.* 2003, Bollback 2006) with Markov Chain Monte Carlo to sample characters histories from posterior probability of characters distribution. This was done with the R package "phytools" (Revell 2012).

RESULTS

Phylogenetic analyses

The 5-locus phylogeny (ITS-LSU-*TEF1-RPB1-RPB2*: Fig. 1) revealed that the 15 specimens exhibiting sporothrix-like asexual morphs (*i.e. Niveomyces* spp. and *Pseudoniveomyces gen. nov*.) included in this study formed two strongly supported monophyletic clades; one included *N. insectorum* (= *Spor. insectorum*, CBS 756.73) and *N. coronatus* (NY04434800) (*i.e*. the genus *Niveomyces*, BS = 92 % / BPP = 1.00; Fig. 1), branching as a sister clade to *Pseudogibellula formicarum*, and another independent clade with full support (BS = 100 % / BPP = 1.00; *Pseudoniveomyces gen. nov*.), represented by *Pseudoniveo. blattae* and *Pseudoniveo. arachnovorum sp. nov*., which branches as a sister taxon to a clade comprising *Gibellula*, *Hevansia* and *Jenniferia*. Four fully supported subclades could be observed within *Niveomyces,* with one subclade containing both *N. insectorum* (= *Spor. insectorum*) and the recently proposed type species for *Niveomyces*, *N. coronatus* (Araújo *et al.* 2022). This subclade is herein considered as the *N. coronatus* complex, which also includes *N. formicidarum sp. nov*. (BCC79346, BCC83026) (Fig. 1).

The single-locus phylogenetic trees from respective markers (Supplementary Figs S1–S5) consistently showed a strong grouping of BCC79346/BCC83026, separated from *N. insectorum* and *N. coronatus*. The pair BCC79346/BCC83026 is thus proposed as a new species, namely *N. formicidarum sp. nov*. Furthermore, the p-distances between the two strains of *N. formicidarum* from different markers were always lower compared to those between these strains and *Spor. insectorum* or *N. coronatus* (Fig. 2). The divergences between *N. formicidarum* and *Spor. insectorum*, and the one between *N. formicidarum* and *N. coronatus* are lower than the 3 % divergence (p-distance = 0.03) that is the required threshold for separating Operational Taxonomic Units (OTUs), but higher than the 1 % (except LSU), which has been recently used for separating species within *Cordycipitaceae* (Kuephadungphan *et al.* 2022). Based on all the markers combined, the p-distance between the two strains of *N. formicidarum* (0.0015) is also lower than those between this species and *Spor. insectorum* (mean ± sd = 0.0165 ± 0.0018), and *N. coronatus* (mean ± sd = 0.0255 ± 0.0031). The all-loci p-distance between *Spor. insectorum* and *N. coronatus* is 0.0244.

Beside the *N. coronatus* complex, the phylogenetic tree (Fig. 1) also revealed three other highly supported subclades within *Niveomyces*. These subclades are thus proposed respectively as novel species, namely *Niveomyces albus*, *N. multisynnematus* and *N. hirsutellae*. The monophyly of these new species was mostly recovered in the single-locus phylogenetic trees (Supplementary Figs S1–S5) except for *N. albus* for LSU. The *RPB1* phylogeny showed that the *N. coronatus* complex and *Pseudoniveo blattae* clustered together without separation (Supplementary Fig. S4) while all the other markers consistently placed *Pseudoniveo. blattae* with *Pseudoniveo. arachnovorum*, forming the new genus close to the genera *Hevansia*, *Gibellula* and *Jenniferia* with variable levels of support. The difference of *Pseudoniveomyces* to *Niveomyces* is also supported by morphological characteristics (see Taxonomy below).

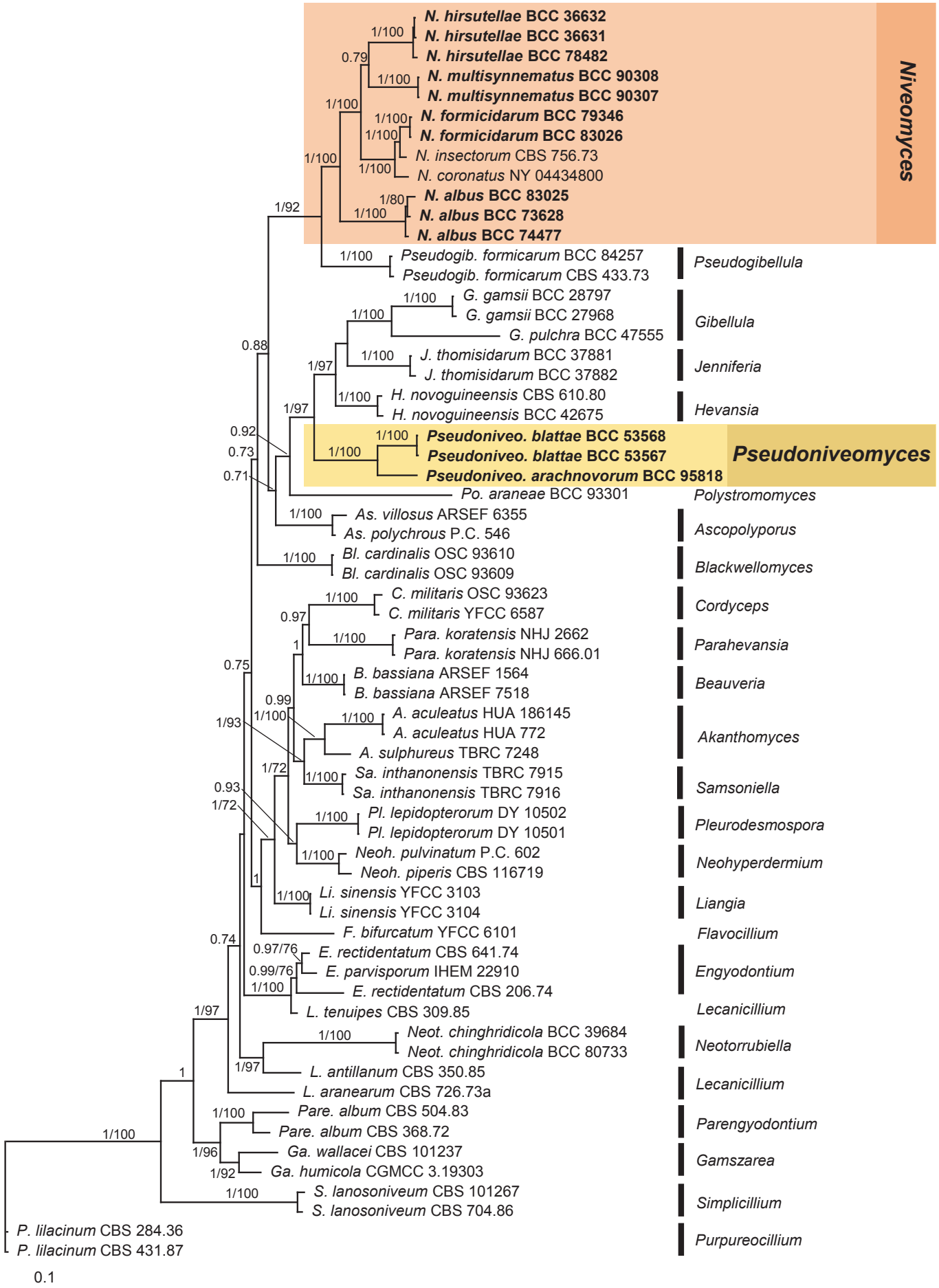

Fig. 1. The best phylogenetic tree from the Bayesian inference based on a multi-locus alignment (ITS-LSU-*TEF1-RPB1-RPB2*). The statistical support values, namely Bayesian posterior probability (PP; > 0.70) and maximum likelihood-based bootstrap (BS; > 70 %), are shown above the nodes (PP/BS).

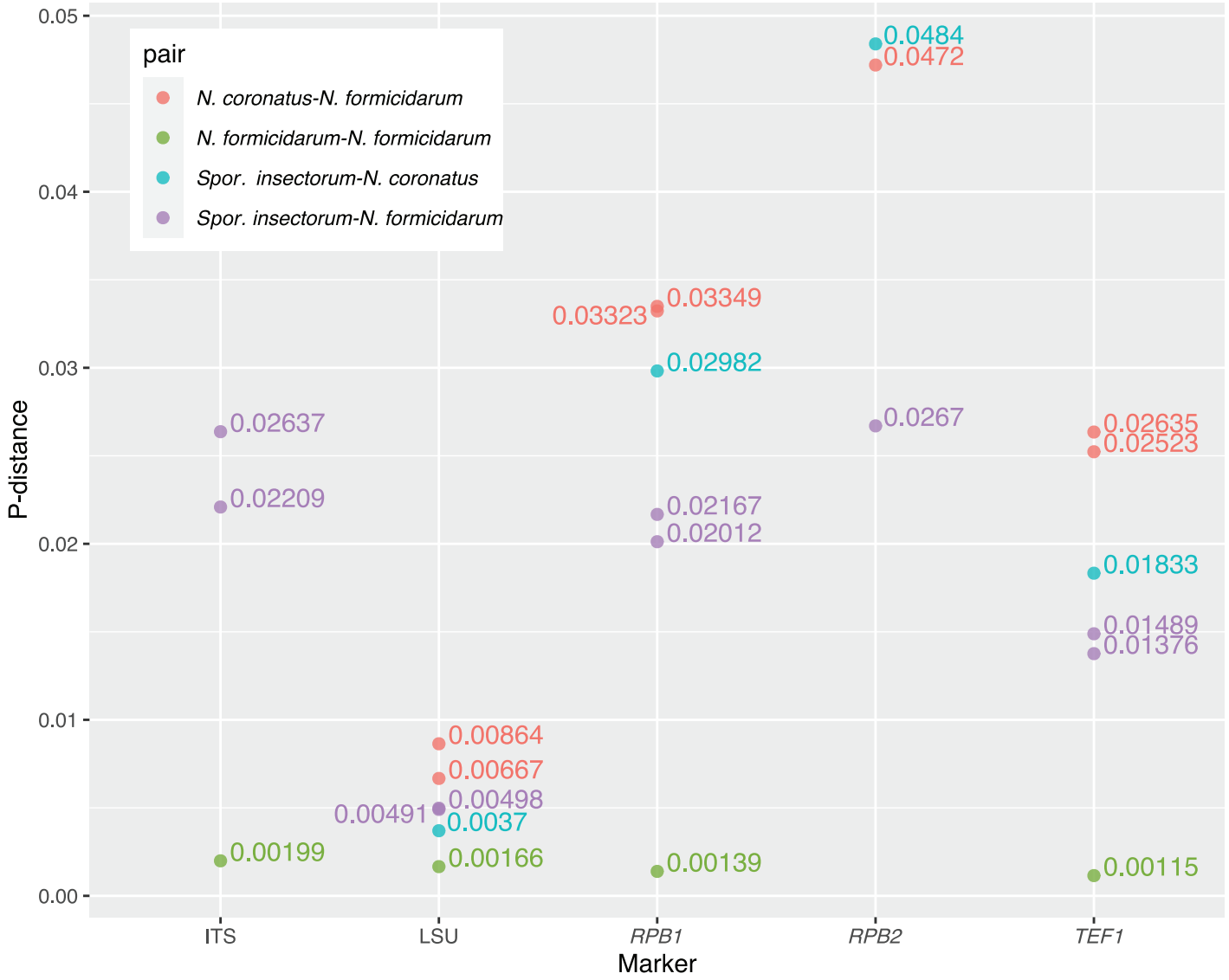

Fig. 2. A dot plot representing the p-distance values calculated between pairs of strains within the *Niveomyces coronatus* species complex for the five markers used in the molecular phylogenetic analyses.

Taxonomy

Niveomyces albus Tasanathai, Noisripoom & Kobmoo, ***sp. nov.*** MycoBank MB 846659. Fig. 3.

Etymology: The name refers to the white colour of fresh specimens in nature.

Typus: **Thailand**, Nakhon Ratchasima Province, Khao Yai National Park, on *Ophiocordyceps dipterigena s.l.* on *Diptera*, on the underside of leaves, 1 Nov. 2016, *D. Thanakitpipattana, N. Kobmoo, R. Somnuk & B. Sakolrak* (**holotype** BBH 42322, culture ex-type BCC 83025).

Sexual morph: Unknown. *Asexual morph*: *Host* covered by dense, white and cottony mycelium forming on the stromata of *Ophiocordyceps dipterigena s.l. Hyphae* septate, hyaline, smooth-walled, irregularly branched, 1–2 µm wide. *Conidiophores* mono- or synnematous, septate, cylindrical, simple, dichotomously or irregularly branched of variable length. *Conidiogenous cells* arising directly from the hyphae, cylindrical, (12–)14.5–36(–60) × 1–2 µm, bearing a rather irregularly, geniculate rachis. *Conidia* forming singly on denticles, cylindrical with rounded ends and on apiculus, hyaline, smooth-walled, aseptate, 5–7(–10) × 1–2 µm.

Culture characteristics: Colonies on OA attaining a diam of 20–22 mm in 20 d at 25 °C, cottony, yellow white (NN155A). Colonies on PDA attaining a diam of 13–15 mm in 20 d at 25 °C, cottony, pale yellow (11D); reverse colonies with light yellow colour (12C).

Additional specimen examined: **Thailand**, Saraburi Province, Khao Yai National Park, Chet Kot Waterfall, parasitic on a fungal pathogen of spider, on the underside of leaves, 1 Jul. 2014, *K. Tasanathai, A. Khonsanit, W. Noisripoom & D. Thanakitpipattana* (BBH 38780, culture BCC 73628).

Notes: *Niveomyces albus* shows similarity to *N. formicidarum*, *N. hirsutellae* and *N. multisynnematus* in the length of the conidiogenous cells. *Niveomyces albus* differs from the three species in the size of the conidia, *N. albus* (5–10 × 1–2 µm) is larger than *N. formicidarum* (3–5 × 1–1.5 µm), *N. hirsutellae* (2–5 × 1–1.5 µm) and *N. multisynnematus* (2–5 × 1–1.5 µm).

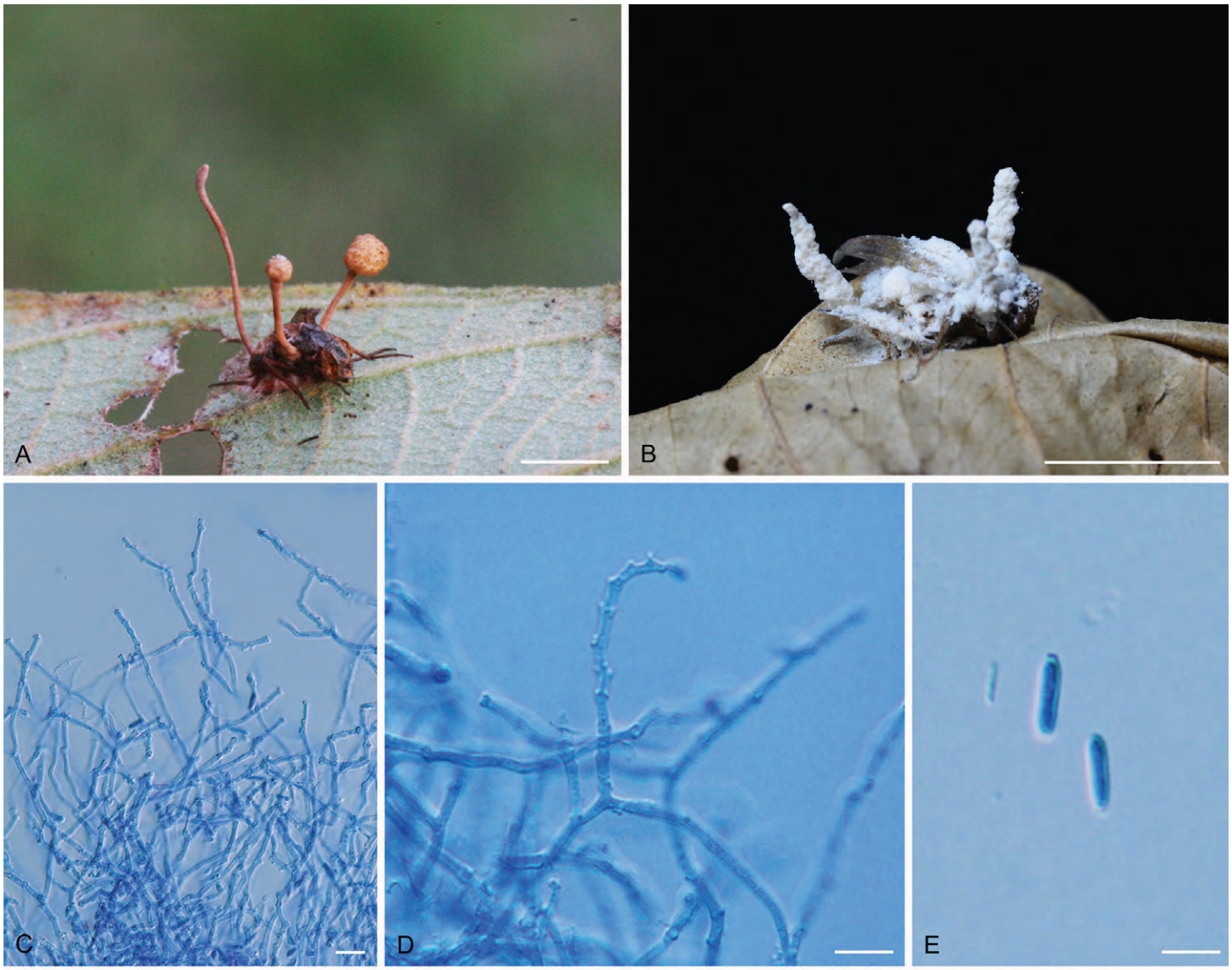

Fig. 3. *Niveomyces albus.* **A.** *Ophiocordyceps dipterigena s.l.* on a fly. **B.** *Niveomyces albus* growing on *Ophiocordyceps dipterigena s.l.* **C.** Conidiogenous cells. **D.** Close-up of conidiogenous cells with characteristic denticles. **E.** Conidia. Scale bars: A, B = 5 mm; C, D = 10 µm; E = 5 µm.

Niveomyces formicidarum Tasanathai, Noisripoom & Kobmoo, ***sp. nov.*** MycoBank MB 846660. Fig. 4.

Etymology: The name refers to the ant family *Formicidae.*

Typus: **Thailand**, Nakhon Ratchasima Province, Khao Yai National Park, on *Ophiocordyceps polyrhachis-furcata* (*Ophiocordycipitaceae*, *Hypocreales*, *Ascomycota*) on *Polyrhachis furcata* (*Hymenoptera, Formicidae*), attached to the underside of leaves, 1 Nov. 2016, *D. Thanakitpipattana, N. Kobmoo, R. Somnuk & B. Sakolrak* (**holotype** BBH 42323, culture ex-type BCC 83026).

Sexual morph: Unknown. *Asexual morph*: White and cottony mycelium forming on the stroma of *Ophiocordyceps polyrhachis-furcata*. *Hyphae* septate, hyaline, smooth-walled, irregularly branched, 1–2 µm wide. *Synnemata* > 2 mm long and 80–100 µm wide, indeterminate, simple, cylindrical, curved, occasionally dichotomously branched, consisting of longitudinal paralleled cells. *Conidiophores* mono- or synnematous, septate, cylindrical to linear, simple, dichotomously or irregularly branched of variable length. *Conidiogenous cells* arising directly from the hyphae, cylindrical, (10–)13–23.5(–33) × 1 µm, bearing a rather irregular, geniculate rachis. *Conidia* forming on denticles, ellipsoidal to cylindrical with rounded ends and an apiculus, hyaline, smooth-walled, aseptate, (3–)4–5 × 1–1.5 µm.

Additional specimen examined: **Thailand**, Phetchabun Province, Nam Nao National Park, on *Hymenoptera* (ant), on the underside of leaves, 6 Oct. 2015, *K. Tasanathai, S. Mongkolsamrit, W. Noisripoom, N. Kobmoo & R. Promharn* (BBH 44067, culture BCC 79346).

Notes: *Niveomyces formicidarum* is similar to *N. hirsutellae* and *N. multisynnematus* in the length of conidiogenous cells and conidia but differs in host association and molecular segregation. *Niveomyces formicidarum* was found on an ant (*Hymenoptera*) while *N. hirsutellae* and *N. multisynnematus* were found on leafhoppers (*Hemiptera*).

Niveomyces hirsutellae Tasanathai, Noisripoom & Kobmoo, ***sp. nov.*** MycoBank MB 846661. Fig. 5.

Etymology: The name refers to the hyperparasite of *Hirsutella* species.

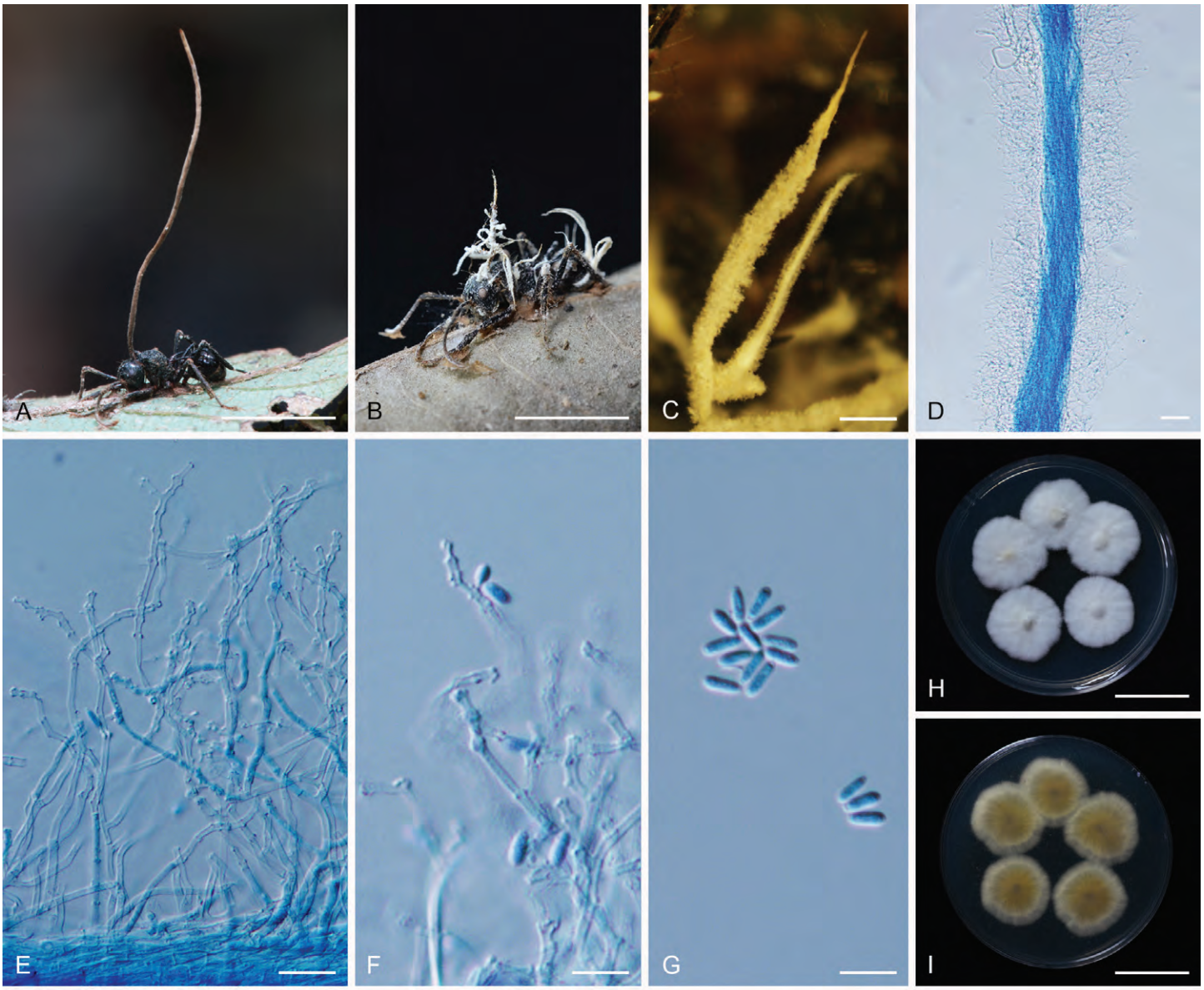

Fig. 4. *Niveomyces formicidarum.* **A.** *Ophiocordyceps polyrhachis-furcata* on *Polyrhachis furcata*. **B.** *Niveomyces formicidarum* growing on *Ophiocordyceps polyrhachis-furcata*. **C.** Close-up of synnemata. **D.** Close-up of synnema. **E.** Conidiogenous cells. **F.** Close-up of conidiogenous cells with characteristic of denticles with conidia. **G.** Conidia. **H, I.** Colonies on PDA: (H) obverse, (I) reverse. Scale bars: A, B = 5 mm; C = 500 µm; D = 80 µm; E–G = 10 µm; H, I = 15 mm.

Typus: **Thailand**, Phetchabun Province, Nam Nao National Park, on *Hirsutella aff. versicolor* on *Hemiptera* (leafhopper, *Cicadellidae*), on the underside of leaves, 29 May 2009, *K. Tasanathai, S. Mongkolsamrit & T. Chohmee* (**holotype** BBH 27064, culture ex-type BCC 36631).

Sexual morph: Unknown. *Asexual morph*: *Host* covered by dense, white to cream and cottony mycelium forming on *Hirsutella aff. versicolor*. *Hyphae* septate, hyaline, smooth-walled, irregularly branched, 1–2 µm wide. *Synnemata* indeterminate, simple, cylindrical, curved, occasionally dichotomously branched, > 4 mm long, 80–100 µm wide, consisting of longitudinal parallel layers of cells. *Conidiophores* mono- or synnematous, septate, cylindrical to linear, simple, dichotomously or irregularly branched of variable length. *Conidiogenous cells* arising directly from the hyphae, cylindrical, (15–)18.5–25.5(–30) × 1–1.5 µm, bearing a rather irregular, geniculate rachis. *Conidia* forming singly on denticles, ellipsoidal with an apiculus, hyaline, smooth-walled, aseptate, (2–)3–5 × 1–1.5 µm.

Additional specimens examined: **Thailand**, Phetchabun Province, Nam Nao National Park, on *Hemiptera* (leafhopper, *Cicadellidae*), on the underside of leaves, 29 May 2009, *K. Tasanathai, S. Mongkolsamrit & T. Chohmee* (BBH 26747, culture BCC36632); Samut Songkhram Province, Bang Khonthi, on *Hemiptera* (leafhopper), on the underside of leaves, 17 Aug. 2015, *K. Tasanathai, A. Khonsanit, D. Thanakitpipattana, W. Noisripoom & R. Promharn* (BBH 42358, culture BCC 78482).

Notes: *Niveomyces hirsutellae* is closely related to *N. multisynnematus*. Both species can be found on leafhoppers (insect species could not be determined) but differ in the production of multiple synnemata for *N. multisynnematus*, in the shape of conidia, and in the molecular segregation.

Niveomyces insectorum (de Hoog & H.C. Evans) Kobmoo, Tasanathai & Luangsa-ard, ***comb. nov.*** MycoBank MB 323936. *Basionym*: *Sporothrix insectorum* de Hoog & H.C. Evans, *Stud. Mycol*. **7**: 25. 1974.

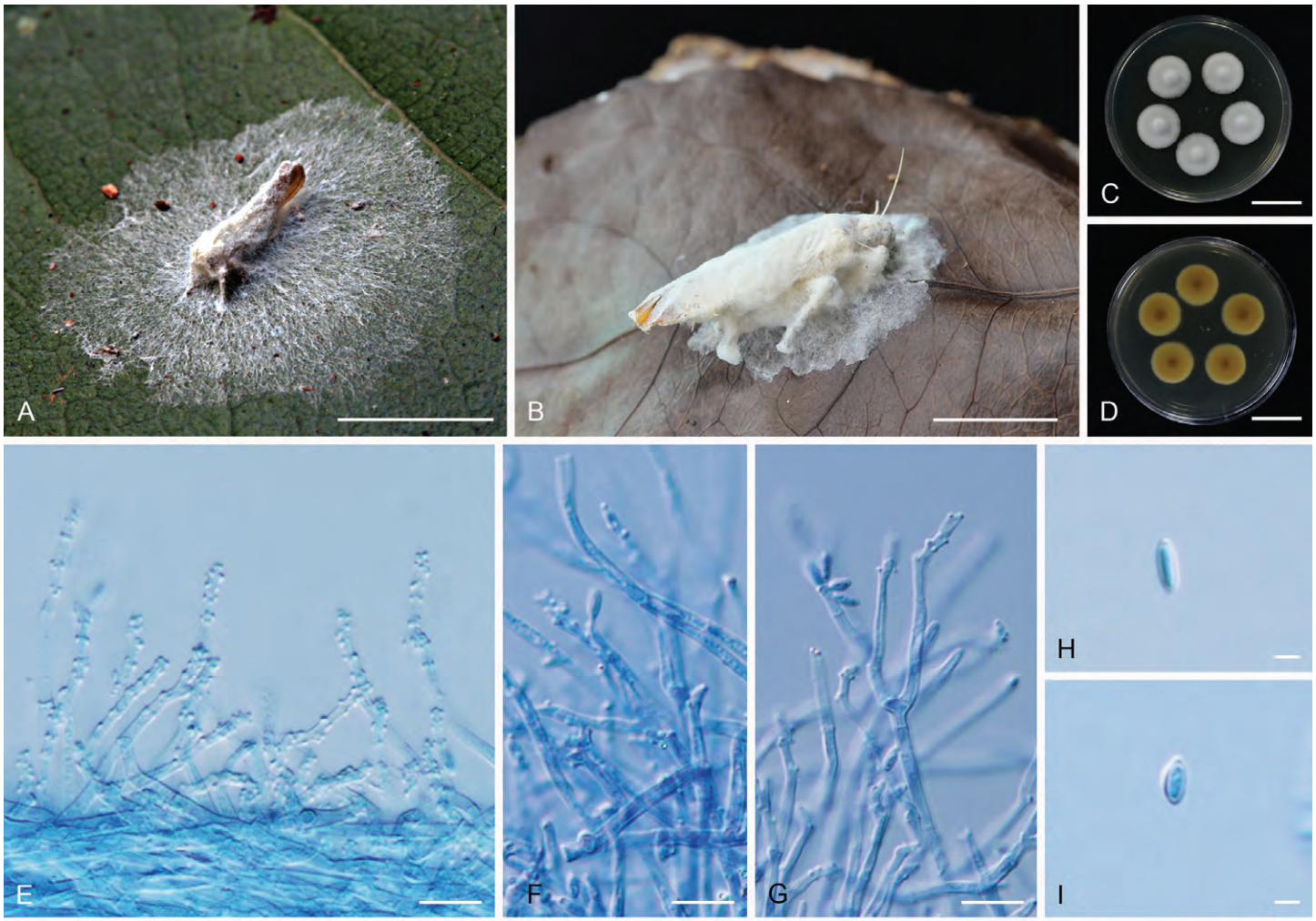

Fig. 5. *Niveomyces hirsutellae*. **A.** *Hirsutella aff. versicolor* on leafhopper. **B.** *Niveomyces hirsutellae* growing on *Hirsutella aff. versicolor.* **C, D.** Colonies on PDA: (C) obverse, (D) reverse. **E.** Conidiogenous cells. **F, G.** Close-up of conidiogenous cells with characteristic denticles with conidia attached. **H, I.** Conidium. Scale bars: A = 10 mm; B = 8 mm; C, D = 15 mm; E–G = 10 µm; H, I = 1.5 µm.

Notes: The ex-type culture of *Sporothrix insectorum* is shown here to cluster inside *Niveomyces* (Fig. 1) and therefore a new combination is proposed for this species.

Niveomyces multisynnematus Tasanathai, Noisripoom & Kobmoo, ***sp. nov.*** MycoBank MB 846662. Fig. 6.

Etymology: The name reflects the production of multiple synnemata.

Typus: **Thailand**, Samut Songkhram Province, Bang Khonthi, on *Ophiocordyceps aff. flavida* on *Hemiptera* (leafhopper, *Cicadellidae*), on the underside of leaves, 25 Mar. 2019, *K. Tasanathai, J. Luangsa-ard, S. Mongkolsamrit & R. Promharn* (**holotype** BBH 47491, culture ex-type BCC 90308).

Sexual morph: Unknown. *Asexual morph*: White and cottony mycelium forming on *Ophiocordyceps aff. flavida*. Hyphae septate, hyaline, smooth-walled, irregularly branched, 1–2 µm wide. *Synnemata* indeterminate, simple, cylindrical, curved, occasionally dichotomously branched, > 1 mm long, 50–60 µm wide, consisting of longitudinal parallel layers of cells. *Conidiophores* mono- or synnematous, septate, cylindrical, simple, dichotomously or irregularly branched of variable length. *Conidiogenous cells* arising directly from the hyphae, cylindrical, (20–)26–40(–50) × 1 µm, bearing a rather irregularly, geniculate rachis. *Conidia* singly forming on denticles, oval to ellipsoidal with an apiculus, occasionally cylindrical with rounded ends, aseptate, hyaline, smooth-walled, (2–)2.5–4(–5) × 1–1.5 µm.

Additional specimen examined: **Thailand**, Samut Songkhram Province, Bang Khonthi, on *Hemiptera* (leafhopper), on the underside of leaves, 25 Mar. 2019, *K. Tasanathai, J. Luangsa-ard, S. Mongkolsamrit & R. Promharn* (BBH 47490, culture BCC 90307).

Notes: *Niveomyces multisynnematus* is closely related to *N. hirsutellae*, found on *Hemiptera* (leafhopper) on the underside of leaves. It differs from *N. hirsutellae* in the production of multiple synnemata, and in the conidial shape.

Pseudoniveomyces Tasanathai, Noisripoom & Kobmoo, ***gen. nov.*** MycoBank MB 846491.

Etymology: Referring to the phenotypic similarity of the asexual morph to *Niveomyces.*

Type species: *Pseudoniveomyces blattae* Tasanathai, Noisripoom & Kobmoo

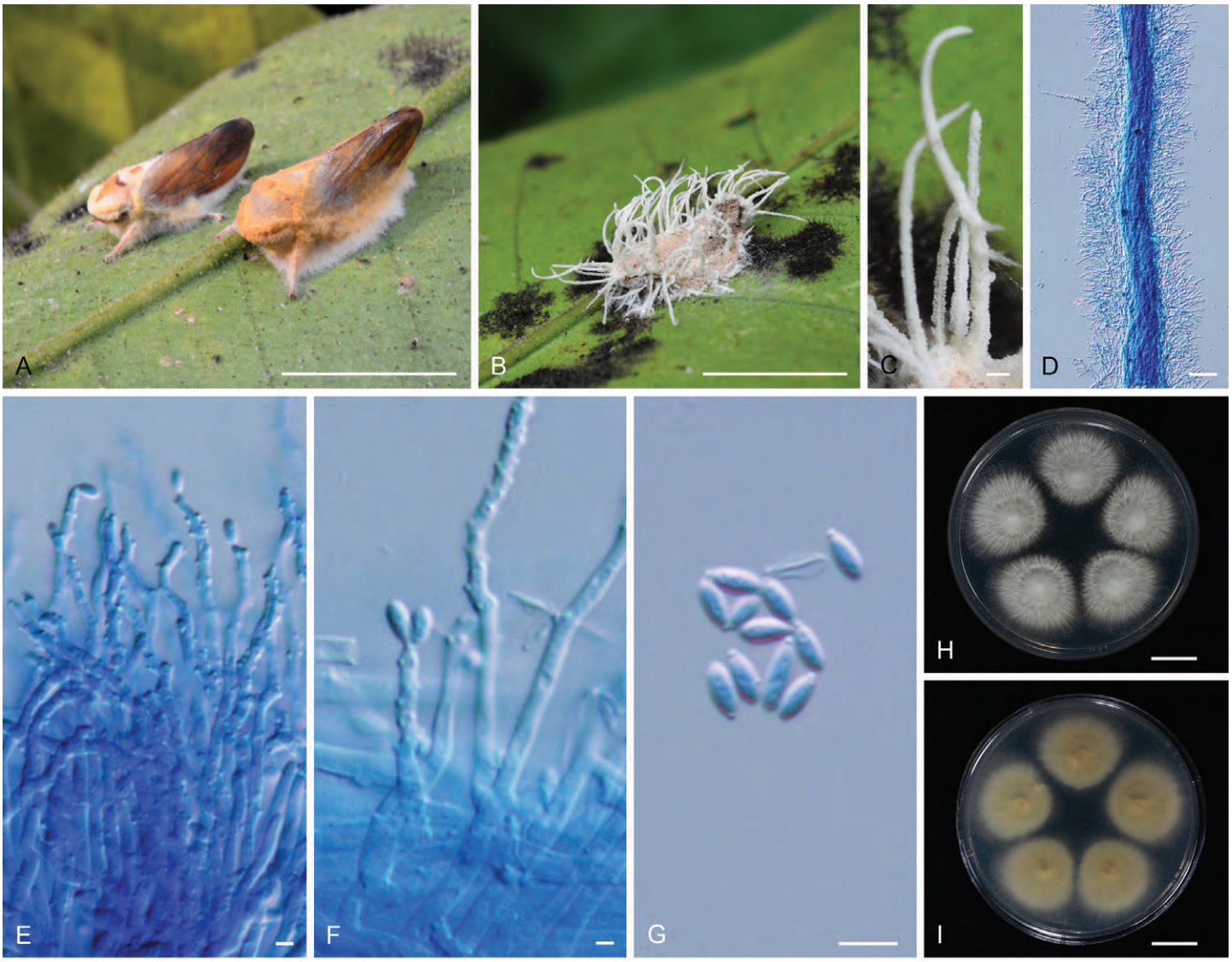

Fig. 6. *Niveomyces multisynnematus.* **A.** *Ophiocordyceps aff. flavida* on hopper. **B.** *Niveomyces multisynnematus* growing on *Ophiocordyceps aff. flavida*. **C.** Close-up of synnemata. **D.** Close-up of synnema. **E.** Conidiogenous cells. **F.** Close-up of conidiogenous cells with characteristic of denticles with conidia. **G.** Conidia. **H, I.** Colonies on PDA: (H) obverse, (I) reverse. Scale bars: A, B = 10 mm; C = 100 µm; D = 50 µm; E, F = 1 µm; G = 4 µm; H, I = 10 mm.

Sexual morph: Unknown. *Asexual morph*: *Mycelium* white to cream, covering the host. *Vegetative hyphae* septate and hyaline. *Conidiogenous cells* arising from undifferentiated hyphae, consisting of elongate or cylindrical cells, with characteristic denticles that are crowded at the apex and less frequent towards the base. *Type I conidia (microconidia)*, hyaline, aseptate, smooth- and thin-walled, ovoid to ellipsoid, formed singly on the denticles, produced on specimen and solid media. *Type II conidia (macroconidia)* hyaline, aseptate, smooth, thin-walled, fusoid, produced on solid media. Colonies on PDA, OA produce a pale red diffusate in solid medium.

Pseudoniveomyces blattae Tasanathai, Noisripoom & Kobmoo, ***sp. nov.*** MycoBank MB 846762. Fig. 7.

Etymology: The name refers to the host – a cockroach.

Typus: **Thailand**, Nakhon Nayok Province, Khao Yai National Park, *Ophiocordyceps* sp. on cockroach, on the underside of leaves, 7 Jun. 2012, *K. Tasanathai, S. Mongkolsamrit, A. Khonsanit, W. Noisripoom & P. Srikitikulchai* (**holotype** BBH 32477, culture ex-type BCC 53567).

Sexual morph: Unknown. *Asexual morph*: White to cream and cottony mycelium forming on the stromata of *Ophiocordyceps* sp. on cockroach, flattened, scattered. *Conidiophores* mono- or synnematous, *conidiogenous cells* arising from undifferentiated cylindrical to linear cells, (12–)15–71(–90) × (1.5–)2–2.5(–3) µm bearing a rather irregular, geniculate rachis, scattered. Two types of *conidia*: *Type I (microconidia)*, produced on specimen and on OA, forming singly on denticles, hyaline, smooth-walled, one-celled, ovoid to ellipsoid, 5–7(–8) × 2–3 µm; *Type II (macroconidia)*, produced on PDA, hyaline, fusoid, occasionally septate, 5–9(–12) × 1–2 µm.

Culture characteristics: Colonies on OA attaining a diam of 15–18 mm in 20 d at 25 °C, cottony with high mycelium density, flattened, white, reverse deep pink (180D) produce pale red pigment diffusing in the medium. Sporulation observed after 14 d. Conidiogenous cells cylindrical arising from aerial hyphae, producing microconidia, hyaline, oval to ellipsoidal, 5–7(–8) × 2–3 µm. Colonies on PDA attaining a diam of 12–15 mm in 20 d at 25 °C, cottony with high mycelium density, white, moderate purplish red to dark purplish pink pigment diffusing in the

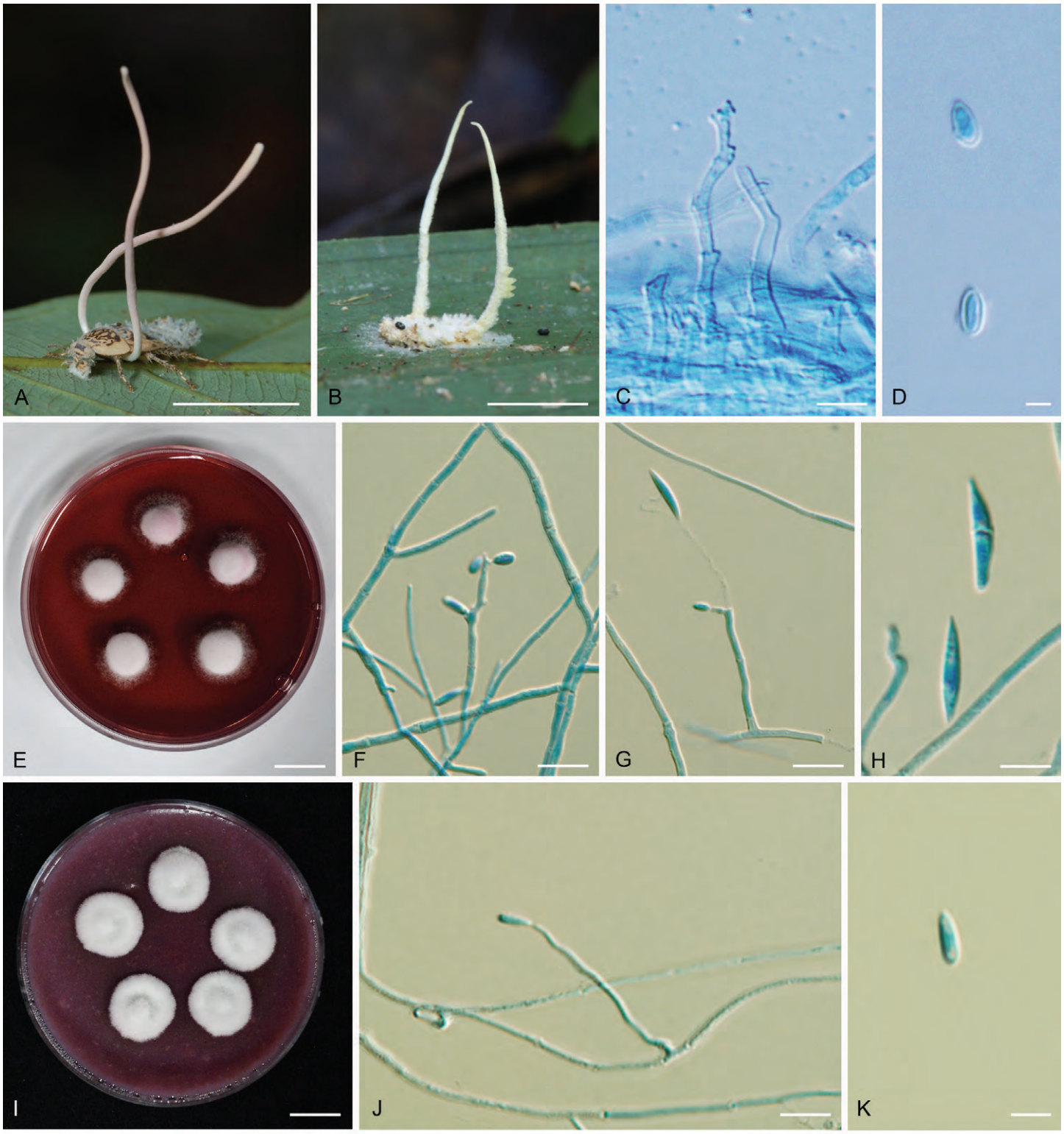

Fig. 7. *Pseudoniveomyces blattae.* **A.** *Ophiocordyceps* sp. on cockroach. **B.** *Pseudoniveomyces blattae* growing on *Ophiocordyceps* sp. **C.** Conidiogenous cells observed directly on the specimen. **D.** Conidia. **E.** Colonies on PDA. **F.** Conidiogenous cells and Type I conidia on PDA**. G.** Conidiogenous cells with a Type I and a Type II conidium on PDA. **H.** Type II conidia on PDA. **I.** Colonies on OA. **J.** Conidiogenous cells and Type I conidia on OA. **K.** Type I conidium on OA. Scale bars: A, B = 5 mm; C, F, G, J = 10 µm; D = 3 µm; E, I = 10 mm; H = 5 µm; K = 4 µm.

medium, reverse moderate red. Sporulation observed after 14 d. Conidiogenous cells arising from aerial hyphae, solitary, producing both microconidia and macroconidia. Macroconidia hyaline, fusiform, 5–9(–12) × 1–2 µm, occasionally septate.

Notes: *Pseudoniveomyces blattae* shows similarity to *Pseudoniveo. arachnovorum* in the production of a pale red pigment diffused in OA and PDA. Morphological comparison between *Pseudoniveo. blattae* and *Pseudoniveo. arachnovorum* shows similarity in the conidial shape but *Pseudoniveo. blattae* has shorter conidia than *Pseudoniveo. arachnovorum*.

Pseudoniveomyces arachnovorum Tasanathai, Noisripoom & Kobmoo, ***sp. nov.*** MycoBank MB 849232. Fig. 8.

Etymology: The name refers to the host - spider egg sac.

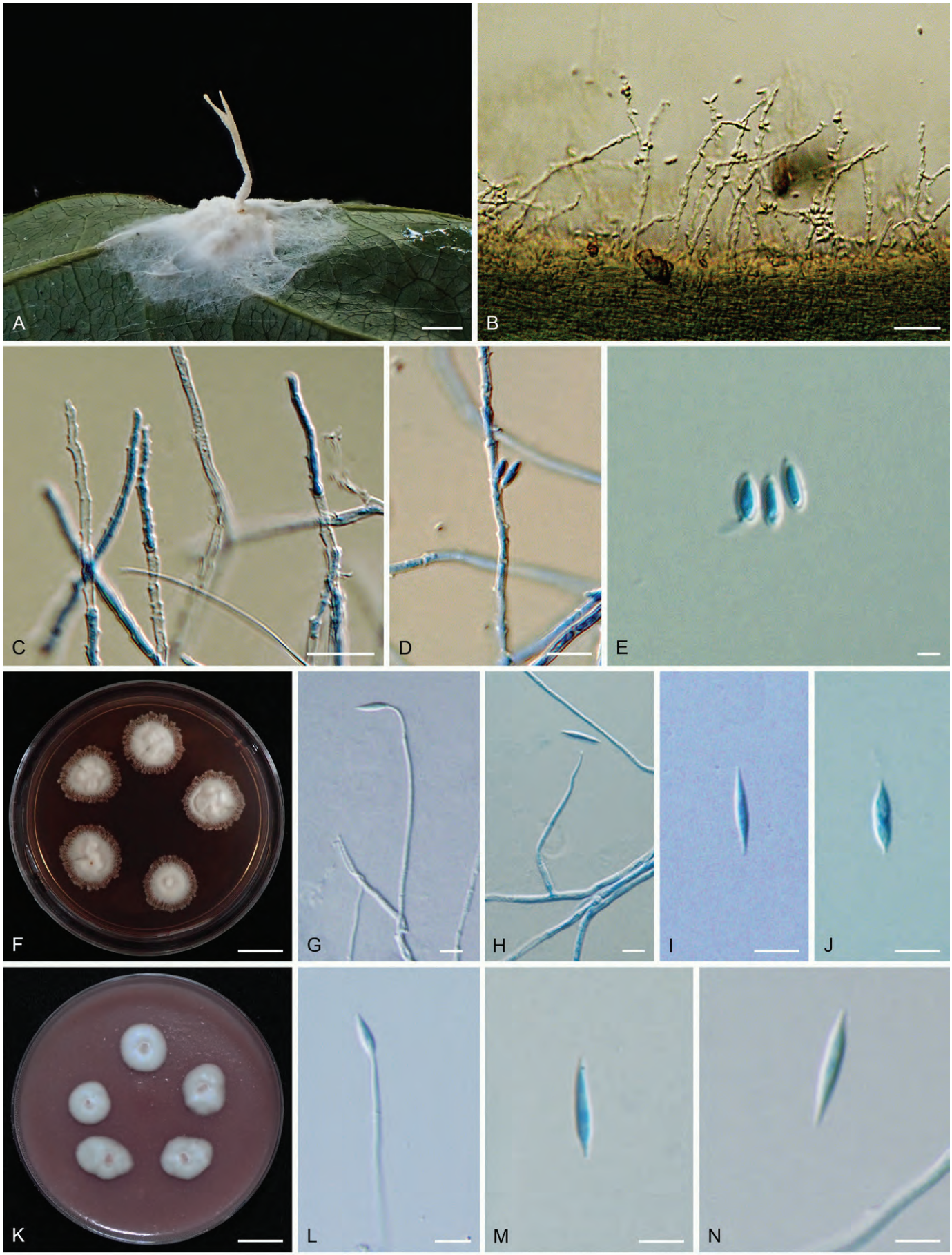

Fig. 8. *Pseudoniveomyces arachnovorum*. **A.** *Pseudoniveomyces arachnovorum* on spider eggs in the sac. **B.** Conidiogenous cells with Type I conidia observed directly on the specimen. **C, D.** Close-up of conidiogenous cells with characteristic denticles and Type I conidia. **E.** Type I conidia extracted from the specimen. **F.** Colonies on PDA. **G, H.** Conidiogenous cells with Type II conidia on PDA. **I, J.** Type II Conidia on PDA. **K.** Colonies on OA. **L.** Conidiogenous cells with a conidium on OA. **M, N.** Type II Conidia on OA. Scale bars: A = 1 mm; B = 150 µm; C, D = 20 µm; E = 3 µm; F, K = 10 mm; G–J, L = 10 µm; M, N = 5 µm.

Typus: **Thailand**, Songkhla Province, Khao Nam Khang National Park, on spider eggs in the sac on the underside of leaves, 15 Dec. 2022, *B. Sakolrak, W. Himaman & P. Jangsantear* (**holotype** BBH49635, culture ex-type BCC 95818).

Sexual morph: Unknown. *Asexual morph*: White to cream and cottony mycelium forming on spider egg sacs. *Conidiophores* mono- or synnematous. *Conidiogenous cells* directly from the hyphae, cylindrical, > 420 µm long, 15–20 µm wide, bearing a rather irregularly, geniculate rachis. Two types of *conidia*: *Type I* (*microconidia*), produced on specimen, forming singly on denticles, ovoid to ellipsoidal with an apiculus, occasionally cylindrical with rounded ends, aseptate, hyaline, smooth-walled, (4–)5–6(–7) × 2–3 µm; *Type II* (*macroconidia*) produced on solid media (OA and PDA), fusiform, smooth-walled, 10–19 × 1.5–2 µm.

Culture characteristics: Colonies on OA attaining 10–15 mm diam in 20 d at 25 °C, cottony with high mycelium density, white, reverse deep pink (180D) produce pale red pigment diffusing in the medium. Conidiogenous cells cylindrical arising from aerial hyphae. Conidia forming on denticles, fusiform, smooth-walled, aseptate, (10–11)–16 × 1.5–2 µm. Colonies on PDA attaining a diam of 10–12 mm in 20 d at 25 °C, cottony with high mycelium density, white, moderate purplish red to dark purplish pink pigment diffusing in the medium, reverse moderate red. Conidiogenous cells arising from aerial hyphae, solitary. Conidia hyaline, fusiform, (10–)12–16(–19) × 1.5–2 µm.

Notes: *Pseudoniveomyces arachnovorum* shows similarity to *Pseudoniveo. blattae* in the production of a pale red pigment diffused in OA and PDA but differ in the conidial length of *Pseudoniveo. arachnovorum* in being longer than that of *Pseudoniveo. blattae*.

Reconstruction of ancestral hosts/substrates

The reconstruction of ancestral hosts/substrates from the 5-locus phylogenetic tree (Fig. 9 and Table 2) showed that the most recent common ancestor (MRCA) of *Cordycipitaceae* (MRCA 1) was versatile with the highest probability of being an environmental fungus (0.430). The genus *Simplicillium* constitutes a deep basal lineage departing from the MRCA 1 along with the other genera which have the MRCA (MRCA 2) also the most probably being from the environment. The genera *Parengyodontium* and *Gamszarea* appeared also as a deep lineage of *Cordycipitaceae* with the MRCA (MRCA 3) being the most probably from the environment. The remaining taxa formed a conspicuous lineage including in majority pathogens of insects and spiders, with the MRCA (MRCA 4) inferred to be

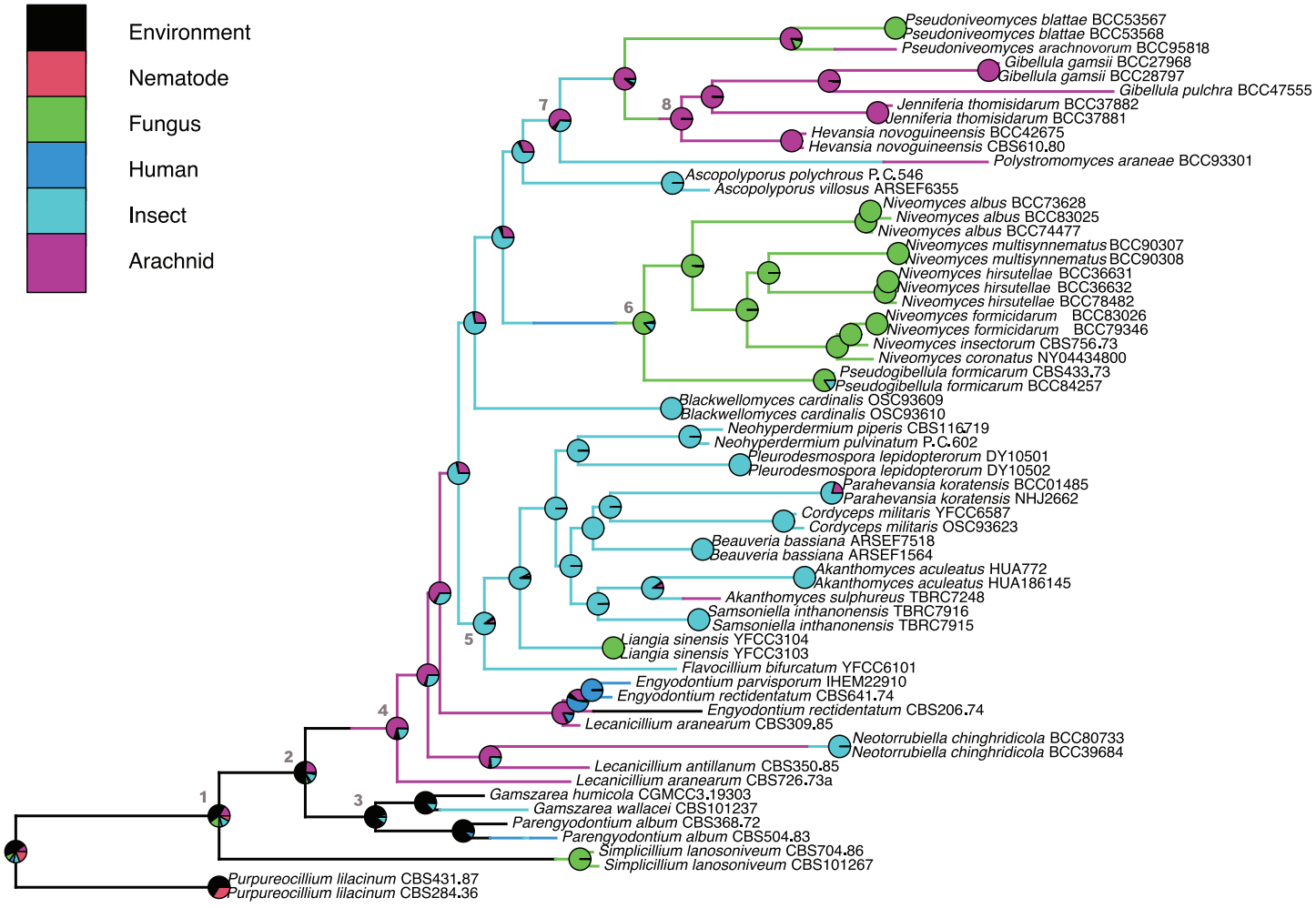

Fig. 9. Evolution of hosts/substrates association as inferred by mapping the hosts/substrates, from which the fungal strains were isolated, onto the 5-locus phylogenetic tree. The pie charts on the internal nodes showed the posterior probabilities of association to different hosts/substrates of the most recent common ancestors (MRCAs) at those nodes. The numbers denote major MRCAs of the evolutionary history of the *Cordycipitaceae*.

Table 2. Posterior probabilities (PP) of ancestral hosts/substrates at major nodes (MRCAs: most recent common ancestors) inferred from the 5-locus Bayesian phylogenetic tree. The MRCA numbers correspond to those appearing in Fig. 9. The PP corresponding to different hosts/substrates are written in the following order: environment/human/nematode/insect/arachnid/fungus. The highest PP value per MRCA is highlighted with a **bold** font.

MRCA	Posterior Probability
1	**0.430** / 0.051 / 0.078 / 0.123 / 0.167 / 0.151
2	**0.522** / 0.031 / 0.026 / 0.134 / 0.235 / 0.052
3	**0.815** / 0.030 / 0.006 / 0.098 / 0.042 / 0.009
4	0.068 / 0.010 / 0.003 / 0.208 / **0.701** / 0.010
5	0.003 / 0.005 / 0.001 / **0.897** / 0.073 / 0.021
6	0.009 / 0.006 / 0.005 / 0.121 / 0.019 / **0.840**
7	0.010 / 0.008 / 0.013 / 0.316 / **0.622** / 0.031
8	0.000 / 0.000 / 0.001 / 0.005 / **0.992** / 0.002

most probably associated to spiders. In this lineage, we can notice a lineage of mostly insect fungi (MRCA 5). There is an almost exclusive lineage of mycoparasites (MRCA 6), including the new *Niveomyces* species discovered in this study with the highest probability as a pathogen of fungi (0. 849). The new genus *Pseudoniveomyces* did not depart from the MRCA 7 but branched as the sister clade to the group of *Gibellula*, *Hevansia* and *Jenniferia* whose most recent common ancestor (MRCA 8) was found to be most probably a spider pathogen. In effect, *Pseudoniveomyces* branched within an almost exclusive clade of spider pathogens whose most recent common ancestor (MRCA 7) was thus inferred to be versatile but with the predominance for arachnids. *Liangia sinensis*, purported mycoparasite of *Beauveria yunnanensis*, appeared among taxa of which the MRCA is most probably an entomopathogen (MRCA 5).

DISCUSSION

New species and a new genus of mycoparasites in *Cordycipitaceae*

In this study, we describe four new species within *Niveomyces* (*N. albus*, *N. formicidarum*, *N. multisynnematus* and *N. hirsutellae*) and a new genus, *Pseudoniveomyces*, with two species (*Pseudoniveo. arachnovorum* and *Pseudoniveo. blattae*). *Niveomyces* and *Pseudoniveomyces* species are characterised by the presence of a sporothrix-like asexual morph and their mostly mycoparasitic nutritional mode.

The species within *Niveomyces* share common morphological features which are scattered, denticulate, conidiogenous cells arising either from undifferentiated hyphae (*N. albus*), or from indeterminate synnemata (*N. formicidarum*, *N. hirsutellae* and *N. multisynnematus*) forming terminally or laterally. The conidia are hyaline, smooth-walled, aseptate and formed singly on denticles, having an ovoid to cylindrical shape with rounded ends. The new genus, *Pseudoniveomyces*, is characterised by the presence of two types of conidia, Type I (microconidia), which is homologous to the conidia in *Niveomyces*, and Type II (macroconidia), fusoid and occasionally septate, was observed only on solid media. The phylogenetic analyses suggest that it is more related to *Hevansia*, *Gibellula* and *Jenniferia*. *Pseudoniveomyces* shares similar morphological features to *Niveomyces* but differs in the production of the two types of conidia (Fig. 7D, H) and the colour of axenic culture on solid media resembling *Hevansia* and *Gibellula*. The phylogenetic evidence with the distinctive macroconidia of *Pseudoniveo. blattae* and *Pseudoniveo. arachnovorum* supports the status of a distinct genus to *Niveomyces* although both genera produce sporothrix-like asexual morphs. The size of conidiophores and conidia are largely overlapping between the species within *Niveomyces* and *Pseudoniveomyces*. Our finding reinforces the idea that the species diversity of hypocrealean entomopathogenic and mycoparasitic fungi is still largely underexploited due to the existence of cryptic species. There are many closely related species with overlapped morphological characters as shown by molecular phylogenies (Tasanathai *et al.* 2019, 2022, Khonsanit *et al.* 2020, Mongkolsamrit *et al.* 2020) and genomics data (Kobmoo *et al.* 2019, 2021). Most of the novel species described here were found on entomopathogenic fungi which are *Ophiocordyceps* (or *Hirsutella*) growing on different insects: *Niveomyces albus* on *Diptera*-associated *Ophiocordyceps*, *N. multisynnematus* and *N. hirsutellae* on *Hemiptera*-associated *Ophiocordyceps* (= *Hirsutella*), *N. formicidarum* (as well as *N. coronatus* complex) on ant-associated *Ophiocordyceps*. *Pseudoniveomyces blattae* was found on an undescribed *Ophiocordyceps* infecting a cockroach. *Pseudoniveomyces arachnovorum* was found on a spider egg sac. *Pseudoniveomyces arachnovorum* is thus not a strict mycoparasite. Due to the limited number of specimens per species, we do not recommend the insect host identity as an absolute criterion for identification. However, our findings suggest the association of *Niveomyces* species with *Ophiocordyceps* parasitising specific host groups. For example, the *N. coronatus* complex is associated with *Ophiocordyceps* infecting ants (*O. camponoti-floridani* infecting *Camponotus floridanus* for *N. coronatus*, *O. polyrhachis-furcata* infecting *Polyrhachis furcata* for *N. formicidarum* and *N. insectorum* for *O. paltothyreum* infecting *Paltothyreus tarsatus*) (de Hoog 1974, Araújo *et al.* 2020, 2022). Other species are formed by an association with *Ophiocordyceps* infecting *Hemiptera* (*N. hirsutellae* and *N. multisynnematus* on *Hirsutella*) and *Diptera* (*N. albus* in *O. dipterigena s.l.*). The fact that *Niveomyces* species appeared to only parasitise *Ophiocorydyceps* (*Hirsutella*) which are specific pathogens to various insects, warrants further investigation as to why this ecological niche produces such a host-specific diversification. Furthermore, no sexual morph is yet known for *Niveomyces* and *Pseudoniveomyces*. The potential lack of sexual reproduction could contribute to a reduced gene flow between host-specific species, exacerbating the specialisation to different *Ophiocordyceps* species. Future studies further exploring the diversity of *Niveomyces* that infect entomopathogens associated with other hosts should contribute to confirm or refute this pattern.

The affiliation of *Sporothrix insectorum* to *Cordycipitaceae*

De Hoog (1993) proposed a "clavicipitalean" relationship for *Sporothrix insectorum*. De Beer *et al.* (2016) even suggested that its sequences should be compared to *Cordycipitaceae*. Our study presents strong molecular evidence that *Sporothrix*

insectorum is affiliated to the *N. coronatus* species complex in the *Cordycipitaceae*. Considering that the *Spor. insectorum* ex-type strain (CBS 756.73) was isolated in Ghana while *N. coronatus* has been described from North America (Araújo *et al.* 2022), and the two specimens of *N. formicidarum* are from Thailand (BCC79346 and BCC83026); they were thus discovered from different biogeographic regions. The divergence between these taxa is also higher than 1 %, further supporting the status of *N. formicidarum* as a new species from Thailand, and that *Spor. insectorum* becomes a synonym of *N. insectorum*.

The evolution of mycoparasitism in *Cordycipitaceae* and *Hypocreales*

It was established that the fungi of the order *Hypocreales* were derived from a plant pathogenic ancestor (Spatafora *et al.* 2007, Zhang *et al.* 2018). This order contains the most conspicuous group of fungal pathogens of plants and animals (Berbee 2001). The evolution of host specificity of fungal pathogens has received much attention during the last decade, particularly through genomic studies to elucidate underlying molecular mechanisms (Baroncelli *et al.* 2016, Zhang *et al.* 2018, St. Leger & Wang 2020). The existence of mycoparasites within *Hypocreales* has been increasingly documented (Wang *et al.* 2014, Zhong *et al.* 2016, Crous *et al.* 2017, Mongkolsamrit *et al.* 2021). Our study has added supplementary taxa to the list. Mycoparasitism appears overall relatively minor within this order and has evolved independently multiple times. *Niveomyces* formed with *Pseudogibellula* a unique lineage of mycoparasites while *Pseudoniveomyces* might have evolved independently from the common ancestor shared with *Gibellula*, *Hevansia* and *Jenniferia*. *Pseudoniveomyces arachnovorum* was found on a spider egg sac and thus cannot be described as a mycoparasite. It is possible that mycoparasites from *Cordycipitaceae* can maintain a potent entomopathogenicity and be occasionally found on insects and spiders. The exoskeleton of insects and arachnids as well as fungal cell wall are composed of chitins. Entomopathogenic fungi are specialised to secrete enzymes such as chitinases allowing the penetration into the insect body (Da Silva *et al.* 2005, Staats *et al.* 2013). They are therefore evolutionarily weaponised to also exploit fungi. Other mycoparasites exist also in other *Hypocrealean* families, *e.g.*, *Polycephalomyces* and *Torrubiellomyces* in *Ophiocordycipitaceae* (Wang *et al.* 2015, Crous *et al.* 2017, Araújo *et al.* 2022) and *Syspastospora* in *Hypocreaceae* (Posada *et al.* 2004). Overall, our finding confirms the fact that mycoparasitism has evolved multiple times in the evolution of *Hypocreales*.

Previous studies of *Cordycipitaceae* show that *Simplicillium* and *Lecanicillium* are basal to other genera in *Cordycipitaceae* (Sung *et al.* 2007a, Mongkolsamrit *et al.* 2018, 2020). However, these did not include *Gamszarea* and *Parengyodontium*. Our study includes a comprehensive list of genera of *Cordycipitaceae*, showing that *Gamszarea* and *Parengyodontium* constitute basal lineages in *Cordycipitaceae*. *Simplicillium* and *Lecanicillium* have a broad spectrum of hosts and substrates including fungal pathogens of plants (Vandermeer *et al.* 2009, Baiswar *et al.* 2014) and insects (Wei *et al.* 2019) and are also known for their entomopathogenic potentials (Zhou *et al.* 2020, Sujithra *et al.* 2021). *Parengyodontium* has been isolated as a human pathogen and from environmental samples (soil, air, material clean surface) (Tsang *et al.* 2016, Zhang *et al.* 2021). *Gamzarea* also appeared to be an ecologically versatile genus with species found from soil and insects (Zhang *et al.* 2021). Both *Parengyodontium* and *Gamszarea* form a deep lineage close to *Simplicillium* and *Lecanicillium*. Otherwise, *Cordycipitaceae* contains prominent entomopathogenic genera such as *Beauveria* (Imoulan *et al.* 2017, Khonsanit *et al.* 2020), *Blackwellomyces* (Mongkolsamrit *et al.* 2020), *Cordyceps* (Mongkolsamrit *et al.* 2018), *Gibellula* and *Hevansia* (Kuephadungphan *et al.* 2020, 2022). These genera are known only as entomopathogens, except *Beauveria* which was reported to cause an infection in an immune-suppressed human individual (Henke *et al.* 2002), and occasionally as endophytes (Brownbridge *et al.* 2012).

Overall, it seems that *Cordycipitaceae* might have originated from an ecologically versatile ancestor with the capacity to exploit various substrates and hosts. It then evolved to become specialised pathogens of insects and spiders while some lineages, as evidenced by *Niveomyces* and *Pseudoniveo. blattae*, have evolved as specialised mycoparasites. *Sporothrix insectorum* was described as growing on an ant "associated to *Gibellula formicarum*" following de Hoog (1974). It has been thus unclear whether it is an entomopathogen co-occurring with *G. formicarum* which is now reclassified as *Pseudogibellula formicarum* (Samson & Evans 1973, Mongkolsamrit *et al.* 2021), or a mycoparasite exploiting *Pseudogib. formicarum*. As *Spor. insectorum* is clearly affiliated to *Niveomyces* which has been shown to be mycoparasites (Araújo *et al.* 2022), it is highly probable that this species is also parasitic on entomopathogens. *Pseudogibellula formicarum* was originally described as an ant pathogen (Samson & Evans 1973, Samson *et al.* 1989) and later documented as pathogenic to the glassy-winged sharpshooter (*Homalodisca coagulata*, *Hemiptera*) (Kanga *et al.* 2004, Boucias *et al.* 2007) whereas Mongkolsamrit *et al.* (2021) has found it growing on *Ophiocordyceps flavida* occurring on leafhoppers in Thailand, which suggests a mycoparasitism. The ecology of *Pseudogib. formicarum* is thus ambiguous. It is possible that *Pseudogib. formicarum* is a mycoparasite which still has a potent entomopathogenicity. The genus *Liangia* with a lecanicillium-like asexual morph has been shown to be a mycoparasite on *Beauveria yunnanensis* (Wang *et al.* 2020). Therefore, it appears that mycoparasitism has also evolved multiple times in the *Cordycipitaceae*. It would be interesting in the future to sequence the genome of these fungal mycoparasites and compare them to other species with different substrate utilisation from the same family as well as to mycoparasites from other families of *Hypocreales*. This will contribute to a better understanding of the genetic and genomic mechanisms behind the evolutionary trajectory towards mycoparasitism.

ACKNOWLEDGEMENTS

This work was supported by the National Center for Genetic Engineering and Biotechnology (BIOTEC) Platform Technology Management (Grant no. P19-50231), National Science and Technology Development Agency (NSTDA). The National Park, Wildlife and Plant Conservation Department in Thailand is gratefully acknowledged for permission to conduct a study in the protected area. The authors would like to thank Mr Artit Khonsanit for pictures of specimens taken from the field, and Dr Andrew Rodrigues from the Global Biodiversity Information Facility (GBIF) for the linguistic correction of the manuscript.

Conflict of interest: The authors declare that there is no conflict of interest.

REFERENCES

Araújo JPM, Evans HC, Fernandes IO, *et al.* (2020). Zombie-ant fungi cross continents: II. Myrmecophilous hymenostilboid species and a novel zombie lineage. *Mycologia* **112**: 1138–1170.

Araújo JPM, Lebert BM, Vermeulen S, *et al.* (2022). Masters of the manipulator: two new hypocrealean genera, *Niveomyces* (*Cordycipitaceae*) and *Torrubiellomyces* (*Ophiocordycipitaceae*), parasitic on the zombie ant fungus *Ophiocordyceps camponoti-floridani*. *Persoonia* 171–194.

Baiswar P, Ngachan SV, Rymbai H, *et al.* (2014). *Simplicillium lanosoniveum*, a hyperparasite on *Aecidium elaeagni-latifoliae* in India. *Australasian Plant Disease Notes* **9**: 144.

Barnett HL (1963). The nature of mycoparasitism by Fungi. *Annual Review of Microbiology* **17**: 1–14.

Baroncelli R, Amby DB, Zapparata A, *et al.* (2016). Gene family expansions and contractions are associated with host range in plant pathogens of the genus *Colletotrichum*. *BMC Genomics* **17**: 1–17.

Berbee ML (2001). The phylogeny of plant and animal pathogens in the *Ascomycota*. *Physiological and Molecular Plant Pathology* **59**: 165–187.

Bischoff JF, White JF (2004). *Torrubiella piperis sp. nov.* (*Clavicipitaceae*, *Hypocreales*), a new teleomorph of the *Lecanicillium* complex. *Studies in Mycology* **50**: 89–94.

Bischoff JF, Chaverri P, White JF (2005). Clarification of the host substrate of *Ascopolyporus* and description of *Ascopolyporus philodendrus sp. nov*. *Mycologia* **97**: 710–717.

Blackwell M (2010). Fungal evolution and taxonomy. *BioControl* **55**: 7–16.

Blackwell M (2011). The Fungi: 1, 2, 3 … 5.1 million species? *American Journal of Botany* **98**: 426–438.

Bollback JP (2006). SIMMAP: Stochastic character mapping of discrete traits on phylogenies. *BMC Bioinformatics* **7**: 1–7.

Boomsma JJ, Jensen AB, Meyling NV, *et al.* (2014). Evolutionary interaction networks of insect pathogenic fungi. *Annual Review of Entomology* **59**: 467–485.

Boosalis G (1964). Hyperparasitism. *Annual Review of Phytopathology* **2**: 363–376.

Boucias DG, Scharf DW, Breaux SE, *et al.* (2007). Studies on the fungi associated with the glassy-winged sharpshooter *Homalodisca coagulata* with emphasis on a new species *Hirsutella homalodiscae nom. prov*. *BioControl* **52**: 231–258.

Brownbridge M, Reay SD, Nelson TL, *et al.* (2012). Persistence of *Beauveria bassiana* (*Ascomycota*: *Hypocreales*) as an endophyte following inoculation of radiata pine seed and seedlings. *Biological Control* **61**: 194–200.

Bushley KE, Raja R, Jaiswal P, *et al.* (2013). The genome of *Tolypocladium inflatum*: evolution, organization, and expression of the cyclosporin biosynthetic gene cluster. *PLoS Genetics* **9**(6): e1003496.

Castlebury LA, Rossman AY, Sung GH, *et al.* (2004). Multigene phylogeny reveals new lineage for *Stachybotrys chartarum*, the indoor air fungus. *Mycological Research* **108**: 864–872.

Chaverri P, Bischoff JF, Evans HC, *et al.* (2005). *Regiocrella*, a new entomopathogenic genus with a pycnidial anamorph and its phylogenetic placement in the *Clavicipitaceae*. *Mycologia* **97**: 1225–1237.

Chen WH, Han YF, Liang JD, *et al.* (2021). Multi-gene phylogenetic evidence indicates that *Pleurodesmospora* belongs in *Cordycipitaceae* (*Hypocreales*, *Hypocreomycetidae*) and *Pleurodesmospora lepidopterorum sp. nov.* on pupa from China. *MycoKeys* **80**: 45–55.

Crous PW, Wingfield MJ, Burgess TI, *et al.* (2017). Fungal Planet description sheets: 625–715. *Persoonia* **39**: 270–467.

Da Silva MV, Santi L, Staats CC, *et al.* (2005). Cuticle-induced endo/exoacting chitinase CHIT30 from *Metarhizium anisopliae* is encoded by an ortholog of the chi3 gene. *Research in Microbiology* **156**: 382–392.

de Beer ZW, Duong TA, Wingfield MJ (2016). The divorce of *Sporothrix* and *Ophiostoma*: solution to a problematic relationship. *Studies in Mycology* **83**: 165–191.

de Hoog GS (1974). The genera *Blastobotrys*, *Sporothrix*, *Calcarisporium* and *Calcarisporiella gen. nov. Studies in Mycology* **7**: 1–84.

de Hoog GS (1993). *Sporothrix*-like anamorphs of *Ophiostoma* species and other fungi. In: *Ceratocystis and Ophiostoma: taxonomy, ecology and pathogenicity* (Wingfield MJ, Seifert KA, Webber J, eds). APS Press, St. Paul, Minnesota: 53–60.

Gibson CM, Hunter MS (2010). Extraordinarily widespread and fantastically complex: Comparative biology of endosymbiotic bacterial and fungal mutualists of insects. *Ecology Letters* **13**: 223–34.

Gleason FH, Lilje O, Marano AV, Sime-Ngando T, *et al.* (2014). Ecological functions of zoosporic hyperparasites. *Frontiers in Microbiology* **5**: 1–10.

Hall TA (1999). BioEdit: A User-Friendly Biological Sequence Alignment Editor and Analysis Program for Windows 95/98/NT. *Nucleic Acids Symposium Series* **41**: 95–98.

Hedgcock GG (1906). Studies upon some chromogenic fungi which discolor wood. *Missouri Botanical Garden Annual Report* **17**: 59–114.

Hektoen L, Perkins CF (1900). Refractory subcutaneous abscesses caused by *Sporothrix schenckii*. a new pathogenic fungus. *Journal of Experimental Medicine* **5**: 77–89.

Henke MO, de Hoog GS, *et al.* (2002). Human deep tissue infection with an entomopathogenic *Beauveria* species. *Journal of Clinical Microbiology* **40**: 2698–2702.

Huelsenbeck JP, Nielsen R, Bollback JP (2003). Stochastic mapping of morphological characters. *Systematic Biology* **52**: 131–158.

Imoulan A, Hussain M, Kirk PM, *et al.* (2017). Entomopathogenic fungus *Beauveria*: Host specificity, ecology and significance of morpho-molecular characterization in accurate taxonomic classification. *Journal of Asia-Pacific Entomology* **20**: 1204–1212.

Johnson D, Sung GH, Hywel-Jones NL, *et al.* (2009). Systematics and evolution of the genus *Torrubiella* (*Hypocreales*, *Ascomycota*). *Mycological Research* **113**: 279–289.

Kaitsu Y, Shimizu K, Tanaka E, *et al.* (2013). *Ophiocordyceps sessilis sp. nov*., a new species of *Ophiocordyceps* on *Camponotus* ants in Japan. *Mycological Progress* **12**: 755–761.

Kanga LHB, Jones WA, Humber RA, *et al.* (2004). Fungal pathogens of the glassy-winged sharpshooter *Homalodisca coagulata* (*Homoptera*: *Cicadellidae*). *Florida Entomologist* **87**: 225–228.

Kepler RM, Luangsa-Ard JJ, Hywel-Jones NL, *et al.* (2017). A phylogenetically-based nomenclature for *Cordycipitaceae* (*Hypocreales*). *IMA Fungus* **8**: 335–353.

Kepler RM, Sung G-H, Ban S, *et al.* (2012). New teleomorph combinations in the entomopathogenic genus *Metacordyceps*. *Mycologia* **104**: 182–197.

Khonsanit A, Luangsa-ard JJ, Thanakitpipattana D, *et al.* (2020). Cryptic diversity of the genus *Beauveria* with a new species from Thailand. *Mycological Progress* **19**: 291–315.

Kobmoo N, Arnamnart N, Pootakham W, *et al.* (2021). The integrative taxonomy of *Beauveria asiatica* and *B. bassiana* species complexes with whole-genome sequencing, morphometric and chemical analyses. *Persoonia* **47**: 136–150.

Kobmoo N, Mongkolsamrit S, Arnamnart N, *et al.* (2019). Population genomics revealed cryptic species within host-specific zombie-ant

fungi (*Ophiocordyceps unilateralis*). *Molecular Phylogenetics and Evolution* **140**: 106580.

Kuephadungphan W, Macabeo APG, Luangsa-ard JJ, *et al.* (2019). Studies on the biologically active secondary metabolites of the new spider parasitic fungus *Gibellula gamsii*. *Mycological Progress* **18**: 135–146.

Kuephadungphan W, Tasanathai K, Petcharad B, *et al.* (2020). Phylogeny- and morphology-based recognition of new species in the spider-parasitic genus *gibellula* (*Hypocreales*, *C ordycipitaceae*) from Thailand. *MycoKeys* **72**: 17–42.

Kuephadungphan W, Petcharad B, Tasanathai K, *et al.* (2022). Multi-locus phylogeny unmasks hidden species within the specialised spider- parasitic fungus, *Gibellula* (*Hypocreales*, *Cordycipitaceae*) in Thailand. *Studies in Mycology* **101**: 245–286.

Lacey LAA, Grzywacz D, Shapiro-Ilan DII, *et al.* (2015). Insect pathogens as biological control agents: Back to the future. *Journal of Invertebrate Pathology* **132**: 1–41.

St. Leger RJ, Wang JB (2020). *Metarhizium*: jack of all trades, master of many. *Open Biology* **10**: 200307.

Liu YJ, Whelen S, Hall BD (1999). Phylogenetic relationships among ascomycetes: evidence from an RNA polymerse II subunit. *Molecular Biology and Evolution* **16**: 1799–1808.

Luangsa-Ard JJ, Hywel-Jones NL, Manoch L, *et al.* (2005). On the relationships of *Paecilomyces* sect. *Isarioidea* species. *Mycological Research* **109**: 581–589.

Matsuura Y, Moriyama M, Łukasik P, *et al.* (2018). Recurrent symbiont recruitment from fungal parasites in cicadas. *Proceedings of the National Academy of Sciences of the USA* **115**: E5970–E5979.

Mongkolsamrit S, Khonsanit A, Thanakitpipattana D, *et al.* (2020). Revisiting *Metarhizium* and the description of new species from Thailand. *Studies in Mycology* **95**: 171–251.

Mongkolsamrit S, Noisripoom W, Tasanathai K, *et al.* (2022). Comprehensive treatise of *Hevansia* and three new genera *Jenniferia*, *Parahevansia* and *Polystromomyces* on spiders in *Cordycipitaceae* from Thailand. *MycoKeys* **91**: 113–149.

Mongkolsamrit S, Noisripoom W, Thanakitpipattana D, *et al.* (2018). Disentangling cryptic species with *Isaria*-like morphs in *Cordycipitaceae*. *Mycologia* **110**: 230–257.

Mongkolsamrit S, Noisripoom W, Tasanathai K, *et al.* (2020). Molecular phylogeny and morphology reveal cryptic species in *Blackwellomyces* and *Cordyceps* (*Cordycipitaceae*) from Thailand. *Mycological Progress* **19**: 957–983.

Mongkolsamrit S, Noisripoom W, Pumiputikul S, *et al.* (2021). *Ophiocordyceps flavida sp. nov.* (*Ophiocordycipitaceae*), a new species from Thailand associated with *Pseudogibellula formicarum* (*Cordycipitaceae*), and their bioactive secondary metabolites. *Mycological Progress* **20**: 477–492.

Münch E (1907). Die Blaufäule des Nadelhozes. I–II. *Naturwissenschaftliche Zeitschrift für Forst- und Landwirtschaft* **5**: 531–573.

Nylander JAA (2004). *MrModeltest*. Available from: https://github.com/nylander/MrModeltest2.

Parratt SR, Laine AL (2016). The role of hyperparasitism in microbial pathogen ecology and evolution. *ISME Journal* **10**: 1815–1822.

Perdomo H, Cano J, García D, *et al.* (2013). Polyphasic analysis of *Purpureocillium lilacinum* isolates from different origins and proposal of the new species *Purpureocillium lavendulum*. *Mycologia* **105**: 151–161.

Pineda A, Dicke M, Pieterse CMJ, *et al.* (2013). Beneficial microbes in a changing environment: Are they always helping plants to deal with insects? *Functional Ecology* **27**: 574–586.

Posada F, Vega FE, Rehner SA, *et al.* (2004). *Syspastospora parasitica*, a mycoparasite of the fungus *Beauveria bassiana* attacking the Colorado potato beetle *Leptinotarsa decemlineata*: A tritrophic association. *Journal of Insect Science* **4**: 3–5.

Rehner SA, Buckley E (2005). A *Beauveria* phylogeny inferred from nuclear ITS and EF1-α sequences: evidence for cryptic diversification and links to *Cordyceps* teleomorphs. *Mycologia* **97**: 84–98.

Rehner SA, Minnis AM, Sung G-H, *et al.* (2011). Phylogeny and systematics of the anamorphic, entomopathogenic genus *Beauveria*. *Mycologia* **103**: 1055–1073.

Revell LJ (2012). Phytools: An R package for phylogenetic comparative biology (and other things). *Methods in Ecology and Evolution* **3**: 217–223.

Ronquist F, Teslenko M, van der Mark P, *et al.* (2012). MrBayes 3.2: Efficient Bayesian phylogenetic inference and model choice a cross a large model space. *Systematic Biology* **61**: 539–542.

Samson RA, Evans HC (1973). Notes on entomogeneous fungi from Ghana I. The genera *Gibellula* and *Pseudogibellula*. *Acta Botanica Neerlandica* **22**: 522–528.

Samson RA, van Reenen-Hoekstra ES, Evans HC (1989). New species of *Torrubiella* (*Ascomycotina*: *Clavicipitales*) on insects from Ghana. *Studies in Mycology* **31**: 123–132.

Sanjuan T, Tabima J, Restrepo S, *et al.* (2014). Entomopathogens of Amazonian stick insects and locusts are members of the *Beauveria* species complex (*Cordyceps sensu stricto*). *Mycologia* **106**: 260–275.

Smith SE, Read D (2008). *Mycorrhizal Symbiosis*. 3rd ed. Academic Press (Ed.). Elsevier, London.

Spatafora JW, Sung GH, Sung JM, *et al.* (2007). Phylogenetic evidence for an animal pathogen origin of ergot and the grass endophytes. *Molecular Ecology* **16**: 1701–1711.

Stalpers JA (1978). Identification of wood-inhabiting *Aphyllophorales* in pure culture. *Studies in Mycology* **16**: 1–248.

Stamatakis A (2006). RAxML-VI-HPC: Maximum likelihood-based phylogenetic analyses with thousands of taxa and mixed models. *Bioinformatics* **22**: 2688–2690.

Stamatakis A (2014). RAxML version 8: A tool for phylogenetic analysis and post-analysis of large phylogenies. *Bioinformatics* **30**: 1312–1313.

Staats CC, Kmetzsch L, Lubeck I, *et al.* (2013). *Metarhizium anisopliae* chitinase CHIT30 is involved in heat-shock stress and contributes to virulence against *Dysdercus peruvianus*. *Fungal Biology* **117**: 37–144.

Sujithra M, Prathibha HV, Rajkumar M, *et al.* (2021). Entomopathogenic potential of *Simplicillium lanosoniveum* native strain in suppressing invasive whitefly, *Aleurodicus rugioperculatus* Martin (*Hemiptera*: *Aleyrodidae*), infesting coconut. *Journal of Fungi* **7**: 1–13.

Sung GH, Spatafora JW (2004). *Cordyceps cardinalis sp. nov.*, a new species of *Cordyceps* with an east asian-eastern north american distribution. *Mycologia* **96**: 658–666.

Sung GH, Hywel-Jones NL, Sung JM, *et al.* (2007a). Phylogenetic classification of *Cordyceps* and the clavicipitaceous fungi. *Studies in Mycology* **57**: 5–59.

Sung GH, Sung JM, Hywel-Jones NL, *et al.* (2007b). A multi-gene phylogeny of *Clavicipitaceae* (*Ascomycota*, *Fungi*): Identification of localized incongruence using a combinational bootstrap approach. *Molecular Phylogenetics and Evolution* **44**: 1204–1223.

Sung GH, Poinar GO, Spatafora JW (2008). The oldest fossil evidence of animal parasitism by fungi supports a Cretaceous diversification of fungal-arthropod symbioses. *Molecular Phylogenetics and Evolution* **49**: 495–502.

Sung GH, Spatafora JW, Zare R, *et al.* (2001). A revision of *Verticillium* sect. *Prostrata*. II. Phylogenetic analyses of SSU and LSU nuclear rDNA sequences from anamorphs and teleomorphs of the *Clavicipitaceae*. *Nova Hedwigia* **72**: 311–328.

Tamura K, Stecher G, Kumar S (2021). MEGA11: Molecular Evolutionary Genetics Analysis Version 11. *Molecular Biology and Evolution* **38**: 3022–3027.

Tasanathai K, Khonsanit A, Noisripoom W, *et al.* (2022). Hidden species behind *Ophiocordyceps* (*Ophiocordycipitaceae*, *Hypocreales*) on termites: four new species from Thailand. *Mycological Progress* **21**: 86.

Tasanathai K, Noisripoom W, Chaitika T, *et al.* (2019). Phylogenetic and morphological classification of *Ophiocordyceps* species on termites from Thailand. *MycoKeys* **56**: 101–129.

Thanakitpipattana D, Tasanathai K, Mongkolsamrit S, *et al.* (2020). Fungal pathogens occurring on *Orthopterida* in Thailand. *Persoonia* **44**: 140–160.

Thompson JD, Higgins DG, Gibson TJ (1994). CLUSTAL W: Improving the sensitivity of progressive multiple sequence alignment through sequence weighting, position-specific gap penalties and weight matrix choice. *Nucleic Acids Research* **22**: 4673–4680.

Tsang CC, Chan JFW, Pong WM, *et al.* (2016). Cutaneous hyalohyphomycosis due to *Parengyodontium album gen. et comb. nov. Medical Mycology* **54**: 699–713.

Vandermeer J, Perfecto I, Liere H (2009). Evidence for hyperparasitism of coffee rust (*Hemileia vastatrix*) by the entomogenous fungus, *Lecanicillium lecanii*, through a complex ecological web. *Plant Pathology* **58**: 636–641.

Vilgalys R, Hester M (1990). Rapid genetic identification and mapping of enzymatically amplified ribosomal DNA from several *Cryptococcus* species. *Journal of Bacteriology* **172**: 4238–4246.

von Arx JA (1971). Über die Typusart, zwei neue und einige weitere arten der Gattung *Sporotrichum*. *Persoonia* **6**: 179–184.

Vu D, Groenewald M, de Vries M, *et al.* (2019). Large-scale generation and analysis of filamentous fungal DNA barcodes boosts coverage for kingdom fungi and reveals thresholds for fungal species and higher taxon delimitation. *Studies in Mycology* **92**: 135–154.

Wang L, Li HH, Chen YQ, *et al.* (2014). *Polycephalomyces lianzhouensis sp. nov*., a new species, co-occurs with *Ophiocordyceps crinalis*. *Mycological Progress* **13**: 1089–1096.

Wang YB, Wang Y, Fan Q, *et al.* (2020). Multigene phylogeny of the family *Cordycipitaceae* (*Hypocreales*): new taxa and the new systematic position of the Chinese cordycipitoid fungus *Paecilomyces hepiali*. *Fungal Diversity* **103**: 1–46.

Wang YB, Yu H, Dai YD, *et al.* (2015). *Polycephalomyces agaricus*, a new hyperparasite of *Ophiocordyceps* sp. infecting melolonthid larvae in southwestern China. *Mycological Progress* **14**: 70.

Wang YH, Ban S, Wang WJ, *et al.* (2021). *Pleurocordyceps gen. nov*. for a clade of fungi previously included in *Polycephalomyces* based on molecular phylogeny and morphology. *Journal of Systematics and Evolution* **59**: 1065–1080.

Wei D PP, Wanasinghe DN, Hyde KD, *et al.* (2019). The genus *Simplicillium*. *MycoKeys* **60**: 69–92.

White T, Bruns T, Lee S, *et al.* (1990). Amplification and direct sequencing of fungal ribosomal RNA genes for phylogenetics. In: *PCR – Protocols and Applications: A Guide to Methods and Applications* (Innis MA, Gelfand DH, Sninsky JJ, *et al.*, eds). Cambridge, MA: Academic Press: 315–322.

Zare R, Gams W (2008). A revision of the *Verticillium fungicola* species complex and its affinity with the genus *Lecanicillium*. *Mycological Research* **112**: 811–824.

Zhang W, Zhang X, Li K, *et al.* (2018). Introgression and gene family contraction drive the evolution of lifestyle and host shifts of hypocrealean fungi. *Mycology* **9**: 176–188.

Zhang ZF, Zhou SY, Eurwilaichitr L, *et al.* (2021). Culturable mycobiota from Karst caves in China II, with descriptions of 33 new species. *Fungal Diversity* **106**: 29–136.

Zhong X, Li S, Peng Q, *et al.* (2016) A *Polycephalomyces* hyperparasite of *Ophiocordyceps sinensis* leads to shortened duration of production and reduced numbers of host ascospores. *Fungal Ecology* **21**: 24–31.

Zhou Y, Zou X, Zhi J, *et al.* (2020). Fast Recognition of *Lecanicillium* spp., and its virulence against *Frankliniella occidentalis*. *Frontiers in Microbiology* **11**: 1–12.

Supplementary information

Fig. S1. The best phylogenetic tree from Bayesian inference based on ITS. The statistical support values, namely Bayesian posterior probability (PP; > 0.70) and maximum likelihood-based bootstrap (BS; > 70 %), are shown above the nodes (PP/BS).

Fig. S2. The best phylogenetic tree from Bayesian inference based on LSU. The statistical support values, namely Bayesian posterior probability (PP; > 0.70) and maximum likelihood-based bootstrap (BS; > 70 %), are shown above the nodes (PP/BS).

Fig. S3. The best phylogenetic tree from Bayesian inference based on *TEF1*. The statistical support values, namely Bayesian posterior probability (PP; > 0.70) and maximum likelihood-based bootstrap (BS; > 70 %), are shown above the nodes (PP/BS).

Fig. S4. The best phylogenetic tree from Bayesian inference based on *RPB1*. The statistical support values, namely Bayesian posterior probability (PP; > 0.70) and maximum likelihood-based bootstrap (BS; > 70 %), are shown above the nodes (PP/BS).

Fig. S5. The best phylogenetic tree from Bayesian inference based on *RPB2*. The statistical support values, namely Bayesian posterior probability (PP; > 0.70) and maximum likelihood-based bootstrap (BS; > 70 %), are shown above the nodes (PP/BS).

FUSE

Fungal Systematics and Evolution

Volume 12
DECEMBER 2023
PAGES 111–152

doi.org/10.3114/fuse.2023.12.08

Phylogeny and species diversity of the genus *Helvella* with emphasis on eighteen new species from China

N. Mao[#], Y.Y. Xu[#], Y.X. Zhang, H. Zhou, X.B. Huang, C.L. Hou, L. Fan[*]

College of Life Science, Capital Normal University, Xisanhuanbeilu 105, Haidian, Beijing 100048, China

[#]These authors contributed equally to this work
[*]Corresponding author: fanli@mail.cnu.edu.cn

Key words:
molecular analysis
new taxa
Pezizales
phylogeny
saddle fungi
taxonomy

Abstract: *Helvella* is a widespread, frequently encountered fungal group appearing in forests, but the species diversity and molecular phylogeny of *Helvella* in China remains incompletely understood. In this work, we performed comprehensive phylogenetic analyses using multilocus sequence data. Six datasets were employed, including a five-locus concatenated dataset (ITS, nrLSU, *tef1-α*, *rpb2*, *hsp*), a two-locus concatenated dataset (ITS, nrLSU), and four single-locus datasets (ITS) that were divided based on the four different phylogenetic clades of *Helvella* recognized in this study. A total of 1 946 sequences were used, of which 713 were newly generated, including 170 sequences of ITS, 174 sequences of nrLSU, 131 sequences of *tef1-α*, 107 sequences of *rpb2* and 131 sequences of *hsp*. The phylogeny based on the five-locus concatenated dataset revealed that *Helvella s. str*. is monophyletic and four phylogenetic clades are clearly recognized, *i.e*., *Acetabulum* clade, *Crispa* clade, *Elastica* clade, and *Lacunosa* clade. A total of 24 lineages or subclades were recognized, 11 of which were new, the remaining 13 corresponding with previous studies. Chinese *Helvella* species are distributed in 22 lineages across four clades. Phylogenetic analyses based on the two-locus concatenated dataset and four single-locus datasets confirmed the presence of at least 93 phylogenetic species in China. Among them, 58 are identified as known species, including a species with a newly designated lectotype and epitype, 18 are newly described in this paper, and the remaining 17 taxa are putatively new to science but remain unnamed due to the paucity or absence of ascomatal materials. In addition, the *Helvella* species previously recorded in China are discussed. A list of 76 confirmed species, including newly proposed species, is provided. The occurrence of *H. crispa* and *H. elastica* are not confirmed although both are commonly recorded in China.

Citation: Mao N, Xu YY, Zhang YX, Zhou H, Huang XB, Hou CL, Fan L (2023). Phylogeny and species diversity of the genus *Helvella* with emphasis on eighteen new species from China. *Fungal Systematics and Evolution* **12**: 111–152. doi: 10.3114/fuse.2023.12.08
Received: 2 March 2023; **Accepted:** 17 August 2023; **Effectively published online:** 29 August 2023
Corresponding editor: P.W. Crous

INTRODUCTION

Helvella (1753) is one of the most conspicuous members of *Helvellaceae*. Almost all *Helvella* species have saddle-shaped ascocarps with cupulate or lobed caps on a distinct stipe, and ellipsoid ascospores with a large central oil drop with the exception of the *H. macropus* complex which has subfusoid ascospores. *Helvella* species are extraordinarily common and widely distributed in terrestrial biomes of the Northern and Southern Hemispheres (Skrede *et al*. 2017, 2020). Some of them have great dietary and health value, such as, *H*. *bachu*, *H*. *lacunosa* and *H*. *taiyuanensis* (Liu *et al.* 1985, Shameem *et al.* 2016, Zhao *et al*. 2016a). Ecologically, some species in this genus form ectomycorrhizal associations with host plants (*Pinaceae* and *Fagaceae*) (Maia *et al*. 1996, Tedersoo *et al.* 2006, Hwang *et al*. 2015).

As a frequently encountered and important fungal group, the systematics and species diversity of *Helvella* have been widely studied by mycologists from different parts of the world, especially from Europe and North America (Dissing 1966a, b, Korf 1972, Weber 1972, 1975, Harmaja 1979, Häffner 1987, Abbott & Currah 1997, Landeros *et al*. 2012, 2015, Nguyen *et al.* 2013, Skrede *et al.* 2017, 2020, 2023, Hansen *et al.* 2019, Løken *et al.* 2019). The ascoma shape and colour, pubescence on the apothecium receptacle surface, ascospore size and shape are highlighted in the identification of *Helvella* species. However, it's difficult to discriminate the difference between *Helvella* species with only morphology. Molecular systematics and DNA barcode sequences as a robust tool to identify fungal species have been applied to taxonomic studies of *Helvella*, which are useful for establishing the species concepts of *Helvella* (Landvik *et al.* 1999, Hansen & Pfister 2006, Tedersoo *et al.* 2006, Laessoe & Hansen 2007, Nguyen *et al.* 2013, Landeros *et al.* 2015, Skrede *et al.* 2017, 2020, 2023, Hansen *et al.* 2019, Wang *et al.* 2019, 2023a, b, Lu *et al.* 2023, Yu *et al.* 2023). For example, Landeros *et al.* (2015) revealed *Helvella* is monophyletic by analysing partial nrLSU data. Skrede *et al.* (2017) assessed species boundaries within *Helvella* in Europe by using morphology and phylogenetic evidence from four loci – heat shock protein 90 (*hsp*), translation elongation factor alpha (*tef1-α*), RNA polymerase II second

largest subunit (*rpb2*) and the nuclear large subunit ribosomal DNA (nrLSU), in which a total of 55 species in Europe were identified, 30 species were designated neo- and epitypes, and seven new species were described.

In China, based on morphology, or both morphology and molecular data, a lot of research has been focused on the taxonomy of *Helvella* (Teng 1963, Liu *et al.* 1985, Cao 1988, Liu & Cao 1988, Cao & Liu 1990, Cao *et al.* 1990, Zhuang 1995, 1996, 1997, 1998a, b, Zhuang & Wang 1998, Wang & Chen 2002, Xu 2002, Zhuang 2004, Zhuang & Yang 2008, Ariyawansa *et al.* 2015, Zhao *et al.* 2015, Hyde *et al.* 2016, Wang *et al.* 2016, 2019, 2023a, b, Zhao *et al.* 2016a, b, Tibpromma *et al.* 2017, Xu *et al.* 2022, Yu *et al.* 2023). Recently, 16 new species and two new Chinese records were determined based on morphology and molecular phylogenies infered from ITS, LSU, *tef1-α*, and *hsp* (Wang *et al.* 2023a). Presently, a total of 90 species are recorded from China, but molecular evidence lack for 37 species. Moreover, many newly introduced collections did not match to previously known species either in morphology or molecular analysis. It is therefore necessary to thoroughly revise records of Chinese *Helvella* spp. In the present study, five highly informative genetic markers (ITS, nrLSU, *tef1-α*, *rpb2*, *hsp*) were used in our molecular analyses. Morphological features and DNA-based molecular analyses were conducted based on the specimens gathered from many parts of China, combined with existing type specimens and sequences available in the GenBank database. Our aims were to: 1) readdress the infrageneric group limits and relationships within *Helvella*; 2) clarify the species diversity and phylogenetic relationships of *Helvella* in China, and 3) describe and illustrate new species found in China based on both molecular and morphological data.

MATERIALS AND METHODS

Sample collections

Samples collected in China were examined. Voucher specimens were accessioned in the Herbarium Biology Department at Capital Normal University (BJTC). Additional specimens on loan from other fungaria were also studied. The principal fungaria were the Herbarium Mycologicum Academiae Sinicaea at the Institute of Microbiology, Chinese Academy of Sciences (HMAS) and the Herbarium of Cryptogams at the Kunming Institute of Botany, Chinese Academy of Sciences (HKAS), Herbarium of Mycology of Jilin Agricultural University (HMJAU), and the Hebarium of Shanxi Institute for Functional Foods, Shanxi Agricultural University (HSA). Macroscopic characters were described from fresh and dried material. Microscopic characteristics were observed in sections obtained from dried specimens mounted in 5 % KOH, Congo Red, cotton blue, Melzer's reagent, or water.

DNA extraction, PCR amplification, sequencing and nucleotide alignment

Dried specimens were crushed by shaking for 3 min at 30 Hz (Mixer Mill MM 301, Retsch, Haan, Germany) in a 1.5 mL tube together with one 3-mm-diam tungsten carbide ball, and total genomic DNA was extracted using the E.Z.N.A. Fungal DNA kit (Omega Bio-Tek Inc. Norcross, Georgia, USA) following the manufacturer's protocol. Polymerase chain reactions (PCR) were performed to amplify partial sequences from the five partial genes (ITS, nrLSU, *tef1-α*, *rpb2*, *hsp*) with previously published primer sets. The details of primer combinations, optimized PCR annealing temperatures and references for published primers are provided (Table 1).

Amplification reactions were performed in 25 µL reaction volumes containing 2 µL DNA template, 1 µL per primer (10 µM), 12.5 µL 2× Master Mix (TiangenBiotech Co., Beijing, China), and 8.5 µL ddH_2O.

Amplification reactions were performed as follows: for the ITS or ITS2 gene: initial denaturation at 94 °C for 3 min, followed by 35 cycles at 94 °C for 30 s, 53 or 55 °C for 45 s, 72 °C for 55 s, and a final extension at 72 °C for 10 min; for the nrLSU gene: initial denaturation at 94 °C for 4 min, followed by 35 cycles at 94 °C for 30 s, 55 °C for 45 s, 72 °C for 1 min, and a final extension at 72 °C for 10 min; for the *tef1-α* gene: initial denaturation at 94 °C for 3 min, followed by 11 cycles including denaturation at 94 °C for 30 s, annealing temperature started at 64 °C (decreased by 1 °C per cycle, until to 54 °C) for 45 s and extension at 72 °C for 1 min, then followed by 30 cycles at 94 °C for 35 s, 56 °C for 45 s, 72 °C for 1 min, and a final extension at 72 °C for 10 min; for the *rpb2* gene: initial denaturation at 94 °C for 3 min, followed by 11 cycles including denaturation at 94 °C for 30 s, annealing temperature started at 62 °C (decreased by 1 °C per cycle, until to 52 °C) for 45 s and extension at 72 °C for 1 min, then followed by 30 cycles at 94 °C for 35 s, 55 °C for 45 s, 72 °C for 1 min, and a final extension at 72 °C for 10 min; for the *hsp* gene: initial denaturation at 94 °C for 4 min, followed by 35 cycles at 94 °C for 30 s, 58 °C for 45 s, 72 °C for 1 min, and a final extension at 72 °C for 10 min. The PCR products were sent to Beijing Zhongkexilin Biotechnology Co. Ltd. (Beijing, China) for purification and sequencing. The newly generated sequences were assembled and edited using SeqMan (DNA STAR package; DNAStar Inc., Madison, WI, USA) with generic-level identities for sequences confirmed via BLAST queries of GenBank.

Table 1. Sequences of primers, citations for previously published primers and annealing temperature used for PCR amplification of sequences generated for this study.

Gene region	Forward primer	Primer sequence (5'–3')	Reverse primer	Primer sequence (5'–3')	PCR annealing temp (°C)	References
ITS	ITS1-F	CTTGGTCATTTAGAGGAAGTAA	ITS4	TCCTCCGCTTATTGATATGC	53 or 55	White *et al*. (1990)
ITS2	ITS3	GCATCGATGAAGAACGCAGC	ITS4	(see above)	55	White *et al*. (1990)
nrLSU	LROR	ACCCGCTGAACTTAAGC	LR5	TCCTGAGGGAAACTTCG	55	Vilgalys & Hester (1990)
tef1-α	EF1-983F	GCYCCYGGHCAYCGTGAYTTYAT	EF1-2218R	ATGACACCRACRGCRACRGTYTG	touchdown	Rehner & Buckley (2005)
rpb2	fRPB2-7cF	ATGGGYAARCAAGCYATGGG	fRPB2-11aR	GCRTGGATCTTRTCRTCSACC	touchdown	Liu *et al*. (1999)
hsp	H_hspf	CRGGCATCCGGGTGACGTAAT	H_hspr	AGGGKGTTGTCGACTCCGAGG	58	Skrede *et al*. (2017)

A total of 713 *Helvella* sequences from our 186 collections were used in the molecular phylogenetic analyses, of which 170 in ITS, 174 in nrLSU, 131 in *tef1-α*, 107 in *rpb2*, and 131 in *hsp*. Sequences of all DNA regions generated in this study were deposited in GenBank. Other sequences of *Helvella* and related species obtained from GenBank are based on published literature (Nguyen *et al*. 2013, Landeros *et al*. 2012, 2015, Zhao *et al*. 2015, Hyde *et al*. 2016, Wang *et al*. 2016, 2019, 2023a, Zhao *et al*. 2016a, b, Skrede *et al*. 2017, 2020, 2023, Hansen *et al*. 2019, Løken *et al.* 2019), or selected by using the BLASTn search function of the NCBI database to find similar matches with taxa in *Helvella*. For ITS sequence data, the genus search tool in GenBank database was used for retrieving *Helvella*-related ITS sequences. The accession numbers of new and downloaded sequences stored in the NCBI GenBank nucleotide database (http://www.ncbi.nlm.nih.gov/) are provided in Supplementary Tables S1–S6.

Six molecular datasets were assembled for this study. Dataset I was comprised of five gene fragments (ITS/nrLSU/*tef1-α*/*rpb2*/*hsp*) and contained all the *Helvella* species with available DNA data worldwide. The phylogenetic trees derived from the single-gene dataset (including ITS, nrLSU, *tef1-α*, *rpb2* and *hsp*) did not exhibit any incongruence because no well-supported (BS > 70 %) conflict was detected among the topologies of the five genes. The concatenated five-gene dataset was used to infer the phylogenetic placement of *Helvella* species and to assess subgeneric limits and relationships within *Helvella*. *Dissingia oblongispora* and *Pindara terrestris* were used as outgroup taxa. Datasets II–V were comprised of single gene fragment (ITS), which respectively corresponded to four subgeneric phylogenetic clades of *Helvella* that were recognized in this study based on the phylogenetic analyses for Dataset I, *i.e*., *Acetabulum* clade (Datasets II), *Crispa* clade (Datasets III), *Elastica* clade (Datasets IV), and *Lacunosa* clade (Datasets V). Each dataset contained all corresponded and qualified ITS sequences that were newly provided in this study and downloaded from GenBank. The four single-gene datasets were used to delimit and detect *Helvella* species and assess the species diversity. Dataset VI was comprised of two gene fragments (ITS/nrLSU) and contained all Chinese *Helvella* species recognized in this study except for the species lacking available molecular data. This concatenated two-gene dataset was used to show the species diversity of *Helvella* in China excluding the species lacking DNA data, and to infer the phylogenetic relationships between Chinese *Helvella* species.

Sequences were aligned and edited in MAFFT (Katoh & Frith 2012) under default parameters, and manually adjusted for maximum sequence similarity in Se-Al v. 2.03a (Rambaut 2000). Ambiguously aligned regions and gaps in the alignment were excluded before the analyses. For the concatenated dataset (Datasets I, VI), alignments were constructed separately for each of the gene fragments using MAFFT (Katoh & Frith 2012), optimized using BioEdit v. 7.0.9 (Hall 1999), then concatenated using SequenceMatrix v. 1.7.8 (Vaidya *et al.* 2011). Unsampled gene regions were coded as missing data and the intron regions of protein-coding genes were retained in the final analyses. Poorly aligned sites were identified by Gblocks v. 0.91b (http://www.phylogeny.fr/one_task.cgi?task_type=gblocks&tab_index=2; Castresana 2000; using default options except ALLOWED GAP POSITIONS 5 half) with default parameters. All identified ambiguous sites were excluded before the analyses. Alignments of all datasets used in this study were submitted to TreeBASE (No. 30611).

Phylogenetic analyses

Maximum likelihood (ML) analyses on all six datasets in this study were conducted with RAxML v. 8.0.14 (Stamatakis *et al.* 2014) and the GTRGAMMAI substitution model with parameters unlinked. The ML bootstrap replicates (1 000) were computed in RAxML with a rapid bootstrap analysis and search for the best-scoring ML tree.

Bayesian inference (BI) was performed with MrBayes v. 3.2.2 (Ronquist & Huelsenbeck 2003) as an additional method for determining branch support. The best substitution model that fit the data at each locus was evaluated using MrModeltest v. 2.3 (Nylander 2004). For the concatenated analyses (Datasets I and VI), each locus was considered a partition and assigned its own best-fitting substitution model, that was GTR+I+G for ITS, nrLSU, *rpb2* and *hsp*, and SYM+I+G for *tef1-α*. We used two independent runs with four Markov chains Monte Carlo (MCMC) for 5 155 000 (Dataset I) and 4 420 000 (Dataset VI) generations under the default settings. For the ITS analysis (Datasets II–V), the best substitution model for each dataset respectively was GTR+I+G (Datasets II, III), GTR+G (Datasets IV, V). The MCMC analysis were run for 825 000 (Dataset II), 1 430 000 (Dataset III), 2 330 000 (Dataset IV) and 3 010 000 (Dataset V) generations under the default settings. Average standard deviations of split frequency (ASDSF) values were far lower than 0.01 at the end of the generations. Trees were sampled every 100 generations after burn-in (25 % of trees were discarded as the burn-in phase of the analyses, set up well after convergence), and 50 % majority-rule consensus trees were constructed.

Clades with bootstrap support (BS) ≥ 70 % and Bayesian posterior probability (PP) ≥ 0.95 were considered as significantly supported (Hillis & Bull 1993, Alfaro *et al.* 2003). All phylogenetic trees were viewed with TreeView (Page 2001).

RESULTS

Phylogenetic analyses

Combined five-gene phylogeny of Helvella

Dataset I (ITS/nrLSU/*tef1-α*/*rpb2*/*hsp*) contained 1 348 sequences from 136 species, including 629 sequences newly generated from Chinese collections. The length of the aligned dataset was 2 726 bp after exclusion of poorly aligned sites (all in ITS), with 565 bp for ITS, 666 bp for nrLSU, 908 bp for *tef1-α*, 346 bp for *rpb2*, and 241 bp for *hsp*. Maximum likelihood and BI analyses yielded similar tree topologies and only the tree inferred from the ML analysis is illustrated with strong statistical bootstrap from ML and posterior probability from BI support values shown (Fig. 1). Our present analysis revealed that the genus *Helvella* is monophyletic, and four distinct clades in *Helvella* can be recognized (Fig. 1), *i.e*., *Acetabulum* clade, *Crispa* clade, *Elastica* clade, and *Lacunosa* clade.

Within the *Acetabulum* clade, two lineages were furthermore recognized, *i.e*., the *acetabulum* lineage and *solitaria* lineage. Within the *Crispa* clade, *H. crispa* and its allies consisted of a well-supported lineage which was designated as *crispa* lineage hereafter, and the other two species, *H. maculata* and *H. maculatoides*, both outside *crispa* lineage, formed their own independent branches. Within the *Elastica* clade, eight individual evolving lineages were recognized, *i.e*., *bicolor-elastica* lineage, *capucina-danica* lineage, *carnosa* lineage, *corbierei-stevensii* lineage, *fallax-*

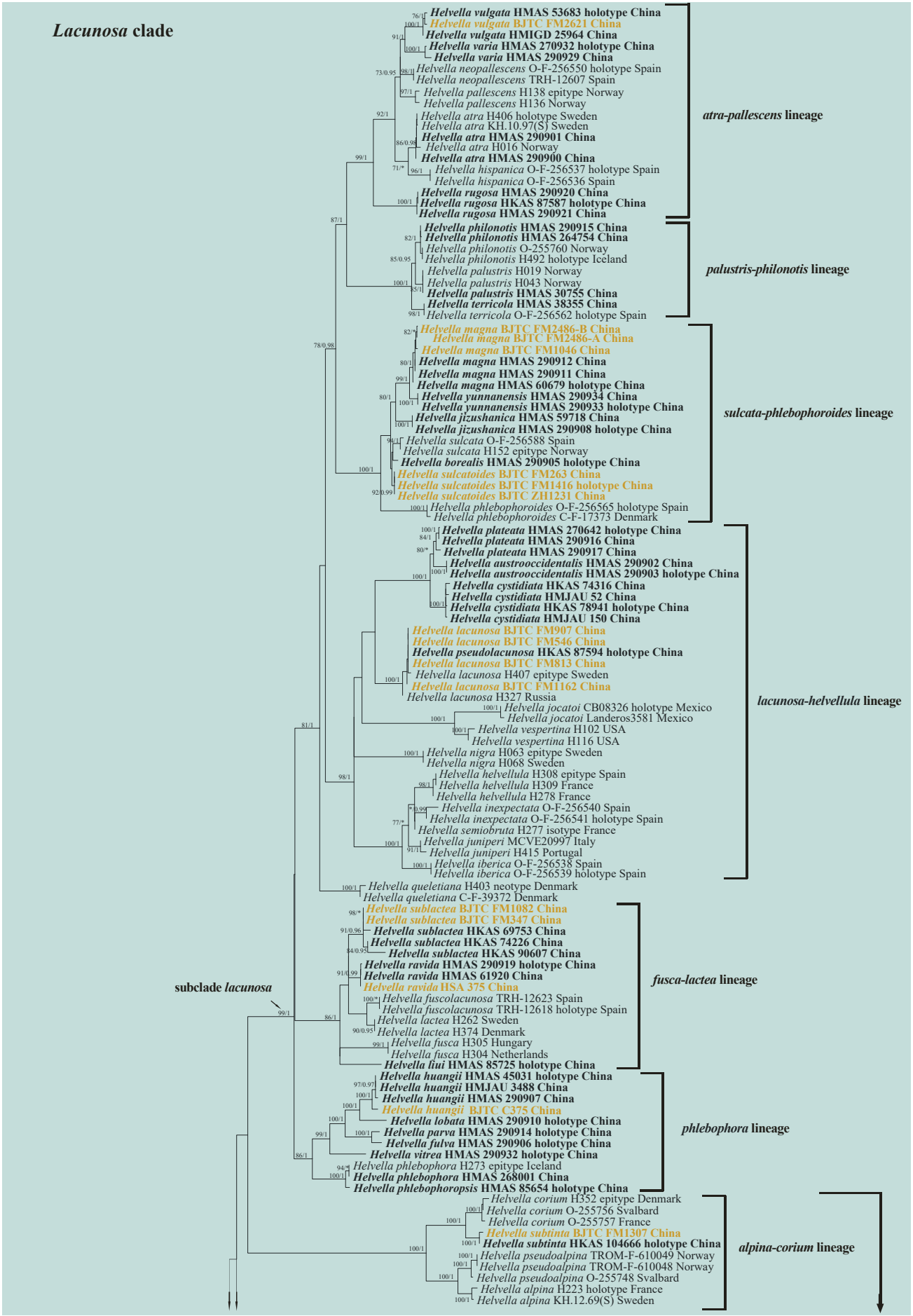

Fig. 1. Phylogeny of Chinese *Helvella* inferred from the Dataset I (ITS/nrLSU/*tef1-α*/*rpb2*/*hsp*) using the maximum likelihood (ML) analysis. Numbers representing likelihood bootstrap support values (MLBS ≥ 70 %, left) and significant Bayesian posterior probability (BPP ≥ 0.95, right) are indicated above the nodes. Chinese *Helvella* species are printed in **bold**. New species and new sequences are printed in golden font.

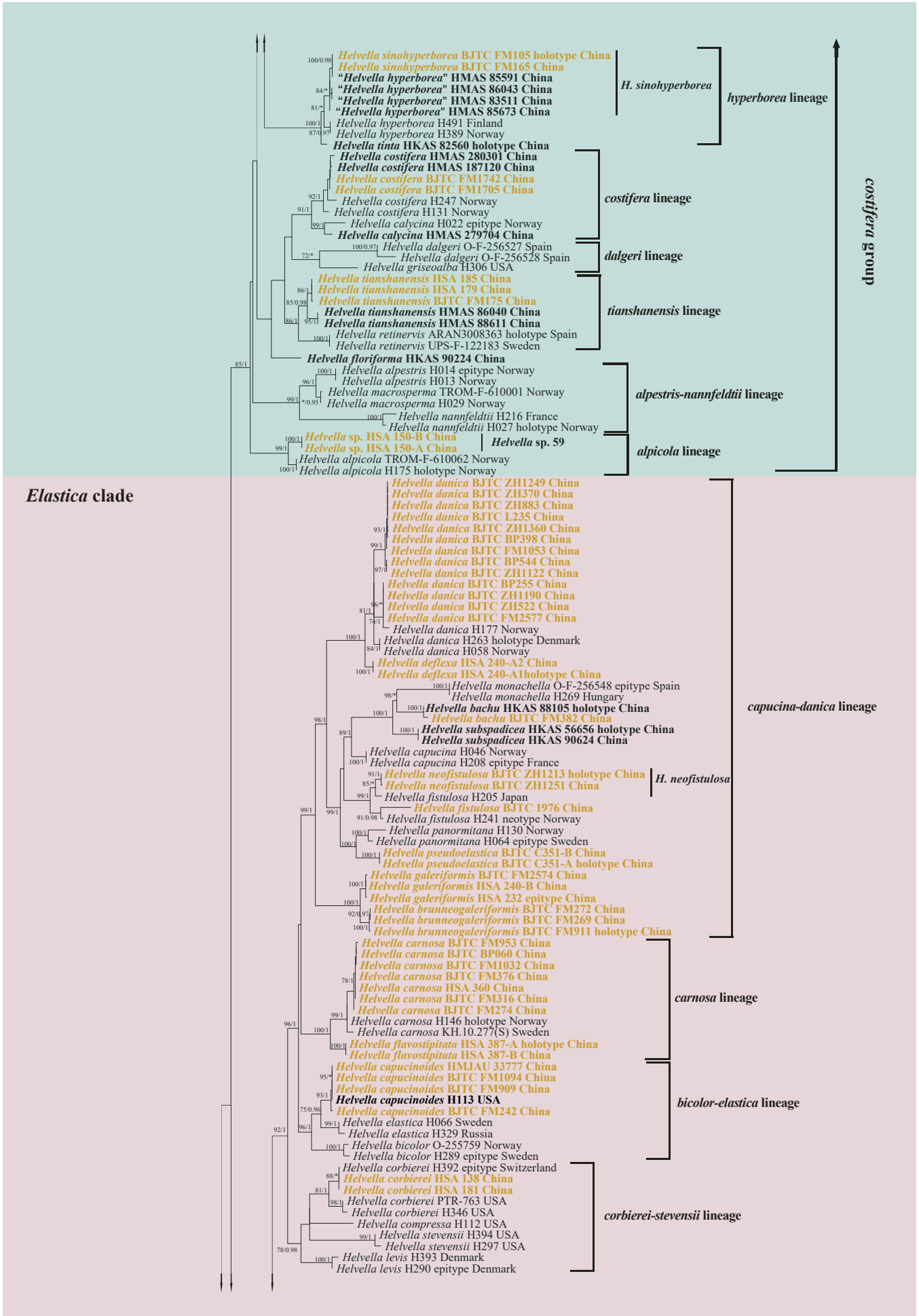

Fig. 1. (Continued).

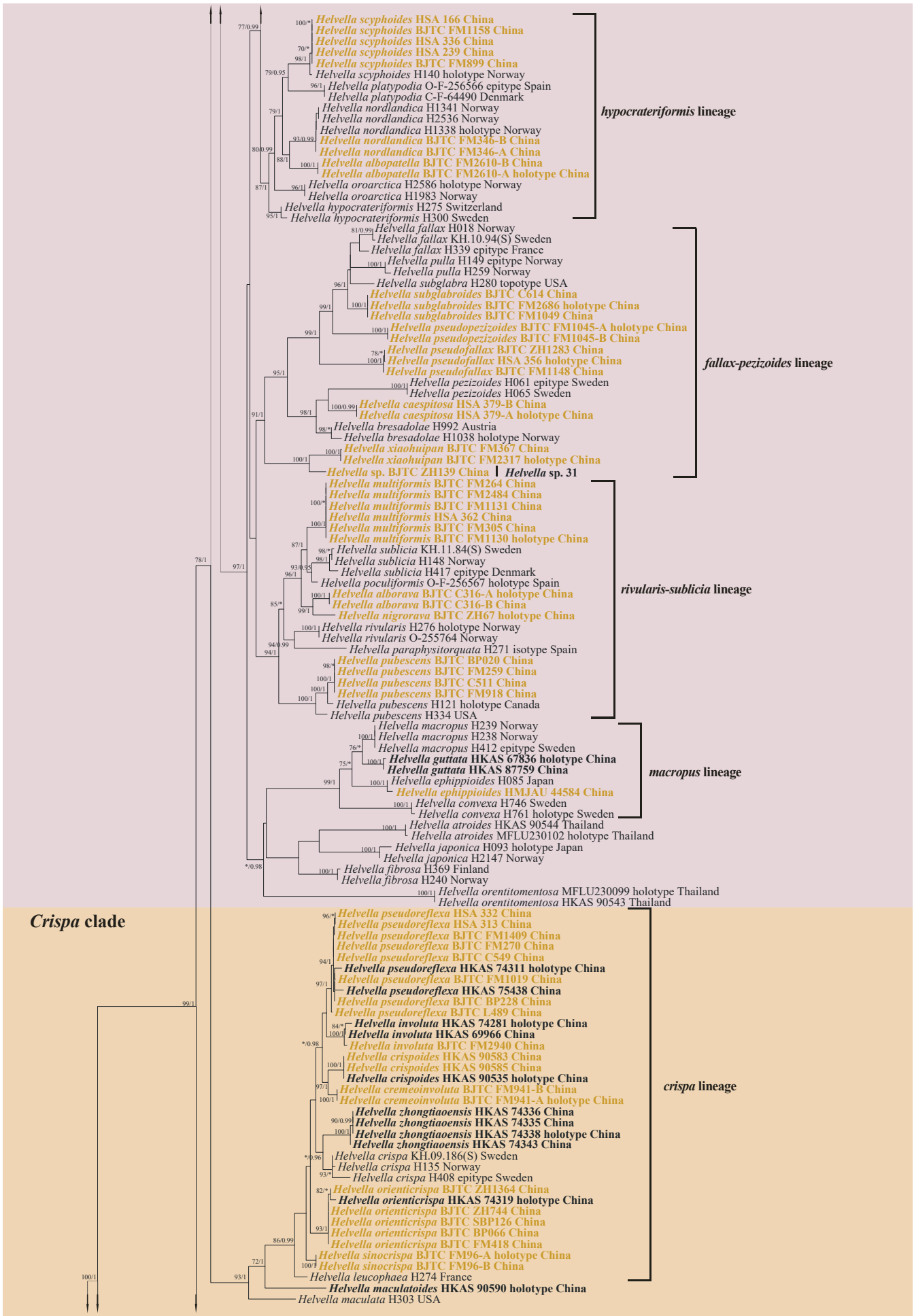

Fig. 1. (Continued).

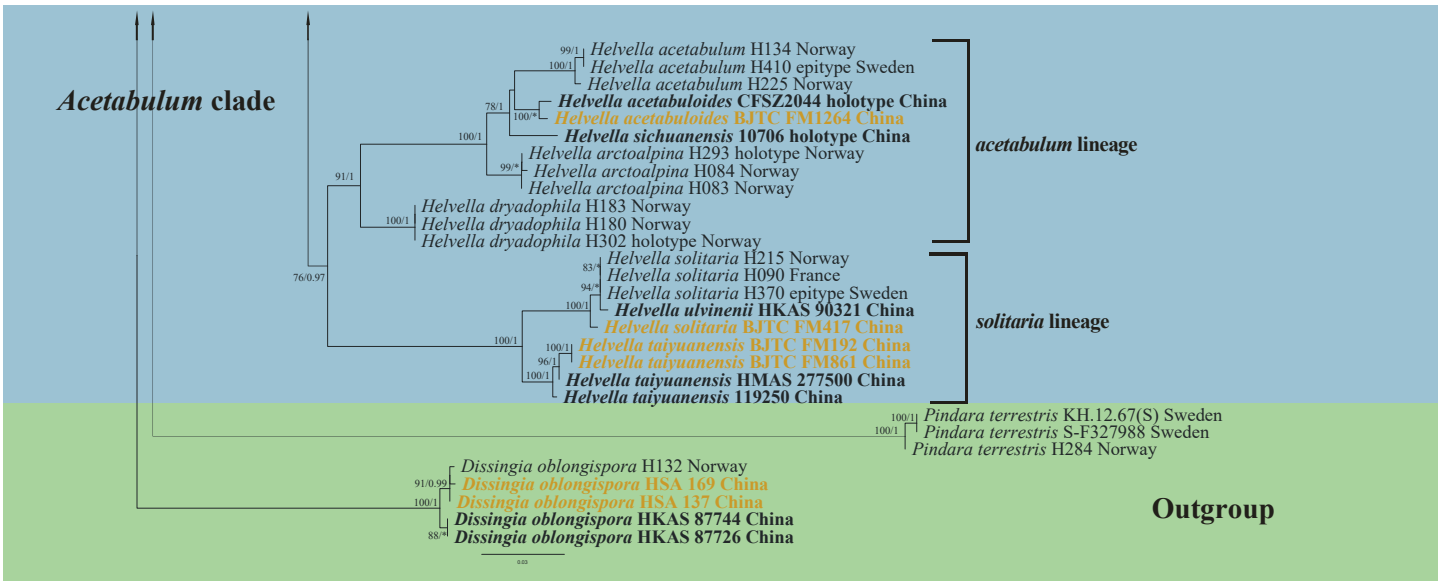

Fig. 1. (Continued).

pezizoides lineage, *hypocrateriformis* lineage, *macropus* lineage, and *rivularis-sublicia* lineage. The species *H. atroides*, *H. fibrosa*, *H. japonica* and *H. orientitomentosa* are outside the *macropus* lineages and formed their own independent branches. Within the *Lacunosa* clade, 13 lineages were recognized, *i.e.*, *alpestris-nannfeldtii* lineage, *alpicola* lineage, *alpina-corium* lineage, *atra-pallescens* lineage, *costifera* lineage, *dalgeri* lineage, *fusca-lactea* lineage, *hyperborea* lineage, *lacunosa-helvellula* lineage, *palustris-philonotis* lineage, *phlebophora* lineage, *sulcata-phlebophoroides* lineage, and *tianshanensis* lineage. Both *H. floriforma* and *H. queletiana* are outside all lineages and formed their own independent branches. Furthermore, six of the 13 lineages (*atra-pallescens* lineage, *fusca-lactea* lineage, *lacunosa-helvellula* lineage, *palustris-philonotis* lineage, *phlebophora* lineage and *sulcata-phlebophoroides* lineage) and the species *H. queletiana* gathered into a distinct and strong supported group, which was recognized as the *lacunosa* subclade. The remaining seven lineages and *H. floriforma* in the *Lacunosa* clade were scattered outside the *lacunosa* subclade. For improving the discussion, they were designated as a group, *i.e.*, *costifera* group (Fig. 1).

ITS-based phylogenetic analysis

The ITS dataset was employed to delimit and detect the Chinese *Helvella* species diversity in this study. ITS sequence is considered a universal barcode for fungi (Schoch *et al.* 2012) and helpful for analyses of *Helvella* groups from ectomycorrhizal root tips. A total of 715 ITS sequences, including 168 novel sequences from Chinese collections, were obtained for this study. Our multigene phylogenetic analysis (Fig. 1) revealed that Chinese *Helvella* collections were classified in four clades, therefore these ITS sequences were accordingly split into four parts (Datasets II–V) that represented four clades (*Acetabulum* clade, *Crispa* clade, *Elastica* clade and *Lacunosa* clade). This parsing of species facilitates the molecular phylogenetic analyses for delimiting many Chinese *Helvella* species and detecting the phylogenetic relationships between these *Helvella* species. The phylogenetic analyses for all four clades are documented below.

Acetabulum clade: Dataset II (ITS) was used to delimit and detect the *Helvella* species of the *Acetabulum* clade. This dataset comprised 30 sequences of the *Acetabulum* clade, in which eight sequences were isolated from our *Helvella* specimens. The length of the dataset was 321 bp after alignment and exclusion of poorly aligned sites. Maximum likelihood and BI analyses yielded identical tree topologies; only the tree inferred from the ML analysis is shown (Supplementary Fig. S1). This ITS-based phylogenetic analysis resolved seven clusters from this clade. Of these, five clusters were identified as known species because each cluster contains the authentic sequence(s) of these species, *i.e.*, *H. acetabulum*, *H. acetabuloides*, *H. solitaria*, *H. sichuanensis*, and *H. taiyuanensis*. They all occur in China. The remaining two clusters represent two putatively unknown species, marked as *Helvella* sp. 1, 2, which are respectively from Iran or an unknown country (See Supplementary Fig. S1, Supplementary Table S3).

Crispa clade: Dataset III (ITS) was used to delimit and detect the *Helvella* species of the *Crispa* clade. This dataset comprised 126 sequences from the *Crispa* clade, in which 35 sequences were isolated from our *Helvella* specimens. The length of the dataset was 794 bp after alignment and exclusion of poorly aligned sites. Maximum likelihood and BI analyses yielded identical tree topologies; only the tree inferred from the ML analysis is shown (Supplementary Fig. S2). A total of 13 clusters with strong support were recognized in this clade. Of these, six clusters were identified as known species, *i.e.*, *H. crispoides*, *H. involuta*, *H. maculatoides*, *H. orienticrispa*, *H. pseudoreflexa*, and *H. zhongtiaoensis*, and they all occur in China. Two clusters composed of Chinese collections were new to science, which are described as new species in this study (see Taxonomy). The remaining five clusters were suggested as putatively unknown species, marked as *Helvella* sp. 3–7. Notably, *Helvella* sp. 5 occurs in China and an unknown country. The other four species are respectively from France, Germany or the United States (See Supplementary Fig. S2, Supplementary Table S4).

Elastica clade: Dataset IV (ITS) was used to delimit and detect the *Helvella* species of the *Elastica* clade. This dataset comprised 318 sequences, including 102 sequences newly isolated from our *Helvella* specimens. The length of the dataset was 578 bp after alignment and exclusion of poorly aligned sites. Maximum likelihood and BI analyses yielded identical tree topologies; only the tree inferred from the ML analysis is shown (Supplementary Fig. S3). A total of 66 strong support clusters corresponding to 66 *Helvella* species were resolved in this clade. Of these, 26 clusters corresponded to known species because each cluster contains the authentic sequence(s) of these species. Sixteen species of them occur in China, *i.e*., *H*. *atroides*, *H*. *bachu*, *H*. *capucinoides*, *H*. *carnosa*, *H*. *corbierei*, *H*. *danica*, *H*. *ephippioides*, *H*. *fistulosa*, *H*. *galeriformis*, *H*. *guttata*, *H*. *macropus*, *H*. *nordlandica*, *H*. *orentitomentosa*, *H*. *pubescens*, *H*. *scyphoides*, and *H. subspadicea*. Fourteen clusters composed of Chinese collection(s) are treated in this study (see Taxonomy). The other 26 clusters were suggested as putatively new species as currently no sporocarps are available for these species, or we were not able to examine the specimens in this study. They are accordingly marked as *Helvella* sp. 8–33. Notably, 14 species m occur in China, *i.e*., *Helvella* sp. 14–15, *Helvella* sp. 18, *Helvella* sp. 20, *Helvella* sp. 23–32. The others are from France, Germany, Italy, Japan, United States, South Korea, Spain, Switzerland, *etc*. (See Supplementary Fig. S3, Supplementary Table S5).

Lacunosa clade: Dataset V (ITS) was used to delimit and detect the *Helvella* species of the *Lacunosa* clade. This dataset comprised 247 sequences, including 29 sequences newly isolated from our *Helvella* specimens. The length of the dataset was 517 bp after alignment and exclusion of poorly aligned sites. Maximum likelihood and BI analyses yielded identical tree topologies; only the tree inferred from the ML analysis is shown (Supplementary Fig. S4). A total of 66 strongly supported clusters corresponding to 66 *Helvella* species were resolved in this clade. Of these, 39 clusters corresponded to known species because each cluster contains the authentic sequence(s) of these species. Twenty-nine species occur in China, *i.e*., *H. atra*, *H*. *austrooccidentalis*, *H*. *borealis*, *H. calycina*, *H. costifera*, *H*. *cystidiata*, *H*. *fulva*, *H*. *huangii*, *H*. *jizushanica*, *H. lacunosa*, *H*. *liui*, *H*. *lobata*, *H*. *magna*, *H*. *parva*, *H. philonotis*, *H*. *phlebophora*, *H*. *phlebophoropsis*, *H*. *plateata*, *H*. *ravida*, *H. rugosa*, *H. sublactea*, *H. subtinta*, *H*. *terricola*, *H. tianshanensis*, *H. tinta*, *H*. *varia*, *H*. *vitrea*, *H*. *vulgata* and *H*. *yunnanensis*. Two clusters composed of Chinese collections are described as new species in this study (see Taxonomy). The other 25 clusters were suggested as putatively new species as currently no sporocarps are available for these species, or we were not able to examine the specimens in this study. They are accordingly marked as *Helvella* sp. 34–58. Notably, one of these species occur in China, *i.e*., *Helvella* sp. 42. The others are respectively from Denmark, Germany, Hungary, Mexico, Norway, Sweden, United States, *etc*. (See Supplementary Fig. S4, Supplementary Table S6).

Species diversity of Helvella in China

Dataset VI (ITS/nrLSU) comprised 581 sequences with 574 sequences from Chinese samples, in which all Chinese *Helvella* species determined based on the phylogenetic analyses for Datasets I–V outlined above were included except for *H*. *palustris* (only having *hsp*) (Fig. 1, Supplementary Figs S1–S4). *Dissingia oblongispora* was selected as the outgroup. The length of the aligned dataset was 1 238 bp after exclusion of poorly aligned sites, with 529 bp for ITS and 709 bp for nrLSU. Maximum likelihood and BI analyses yielded identical tree topologies; only the tree inferred from the ML analysis is shown (Fig. 2).

Our phylogenetic analyses revealed 92 phylogenetic species from the Chinese collections, which were further clustered in four *Helvella* clades (Fig. 2). Of these, 57 clusters correspond to 57 species known from China (Ariyawansa *et al.* 2015, Zhao *et al.* 2015, Hyde *et al.* 2016, Wang *et al.* 2016, 2019, 2022, 2023a, Zhao *et al.* 2016a, b, Tibpromma *et al.* 2017, Zhuang *et al.* 2018, Xu *et al.* 2022, Lu *et al.* 2023, Yu *et al.* 2023), including five species new to China, *i.e*., *H*. *carnosa* (Fig. 2, Supplementary Fig. S3), *H*. *corbierei* (Fig. 2, Supplementary Fig. S3), *H*. *fistulosa* (Fig. 2, Supplementary Fig. S3), *H*. *nordlandica* (Fig. 2, Supplementary Fig. S3) and *H*. *scyphoides* (Fig. 2, Supplementary Fig. S3). Of the remaining 35 species, 18 species are described as new species (see Taxonomy section in this paper), and 17 are suggested as potentially undescribed species (marked as *Helvella* sp. 5 in Fig. 2 & Supplementary Fig. S2; *Helvella* sp. 14–15, *Helvella* sp. 18, *Helvella* sp. 20, *Helvella* sp. 23–32 in Figs 2 & S3; *Helvella* sp. 42. in Figs 2 & S4; *Helvella* sp. 59 in Figs 1 & 2). Notably, *H*. *floriforma* (Figs 1, 2, Datasets I, VI), *H*. *palustris* (Fig. 1, Dataset I), and *Helvella* sp. 59 (Figs 1, 2, Datasets I, VI) are not represented in the ITS dataset because there were no available ITS sequence of the three species.

TAXONOMY

Based on our phylogenetic and morphological data, 18 new species are described and illustrated, an epitype is designated for one species, and five species are newly recorded from China.

Helvella albopatella L. Fan, N. Mao & Y.Y. Xu, ***sp. nov.*** MycoBank MB 849609. Fig. 3.

Etymology: *albopatella*, *albo-*, white, *patella*, disc, referring to the white and disc-like cap of this species.

Apothecia stipitate-cupulate; cap regularly or irregularly discoid, slightly cumulate, or occasionally recurved, 0.4–0.7 cm high, 0.9–2.0 cm broad; hymenium white, grey white to pale white, becoming dark brown when dry; receptacle surface pubescent, concolourous with the disc, becoming yellowish when dry; stipe terete, 1.0–3.0 cm high, 0.15–0.3 cm broad, solid, greyish white to white, becoming yellowish when dry. *Ectal excipulum* 75–100 µm broad, of *textura angularis*, cells hyaline to pale brown, extending into fascicled hyphoid hairs in outer ectal excipulum, hairs multiseptated, cells elongate club-shaped, 15–35 × 11–16 µm. *Medullary excipulum* 225–300 µm broad, of interwoven *textura intricata*, hyphae 2.0–6.0 µm broad. *Asci* pleurorhynchous, tapering towards the base, 8-spored, 225–265 × 13–17 µm. *Ascospores* ellipsoid, with one large oil drop when mature, 16–18 × 11–12.5 µm, [Lm × Wm = 16.7 × 11.7 µm, Q = 1.32–1.56, Q_{av} = 1.42 ± 0.07]. *Paraphyses* filiform, septate, pale brown, 6.0–10.0 µm wide at clavate to subcapitate tips and 2.0–4.0 µm below.

Habitat: Scattered on the ground in broadleaf forest and coniferous forest.

Distribution: Known from Shanxi Province, Northern China.

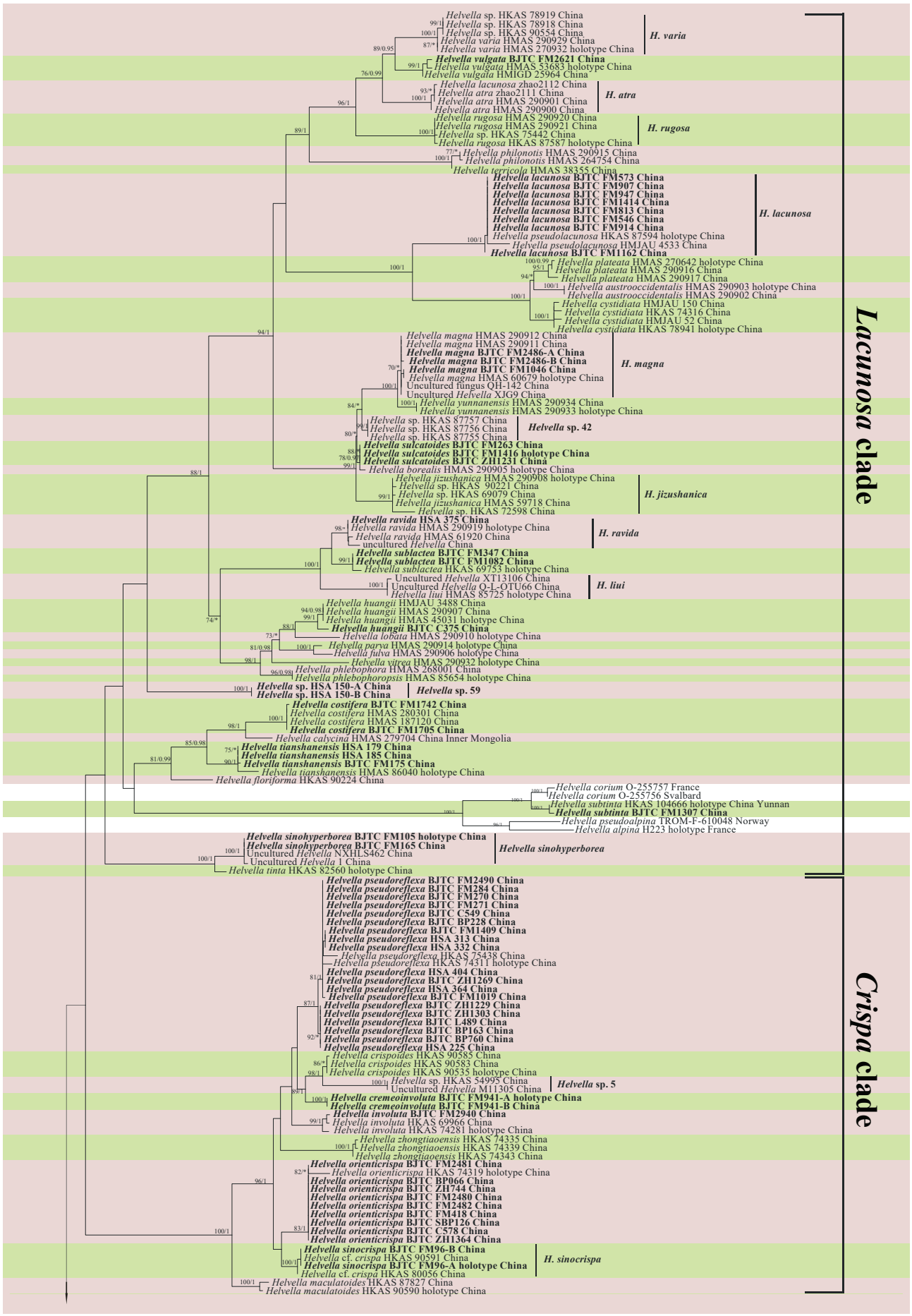

Fig. 2. Phylogeny of Chinese *Helvella* species inferred from the Dataset VI (ITS/nrLSU) using the maximum likelihood (ML) analysis. Numbers representing likelihood bootstrap support values (MLBS ≥ 70 %, left) and significant Bayesian posterior probability (BPP ≥ 0.95, right) are indicated above the nodes. New species are printed in **bold**.

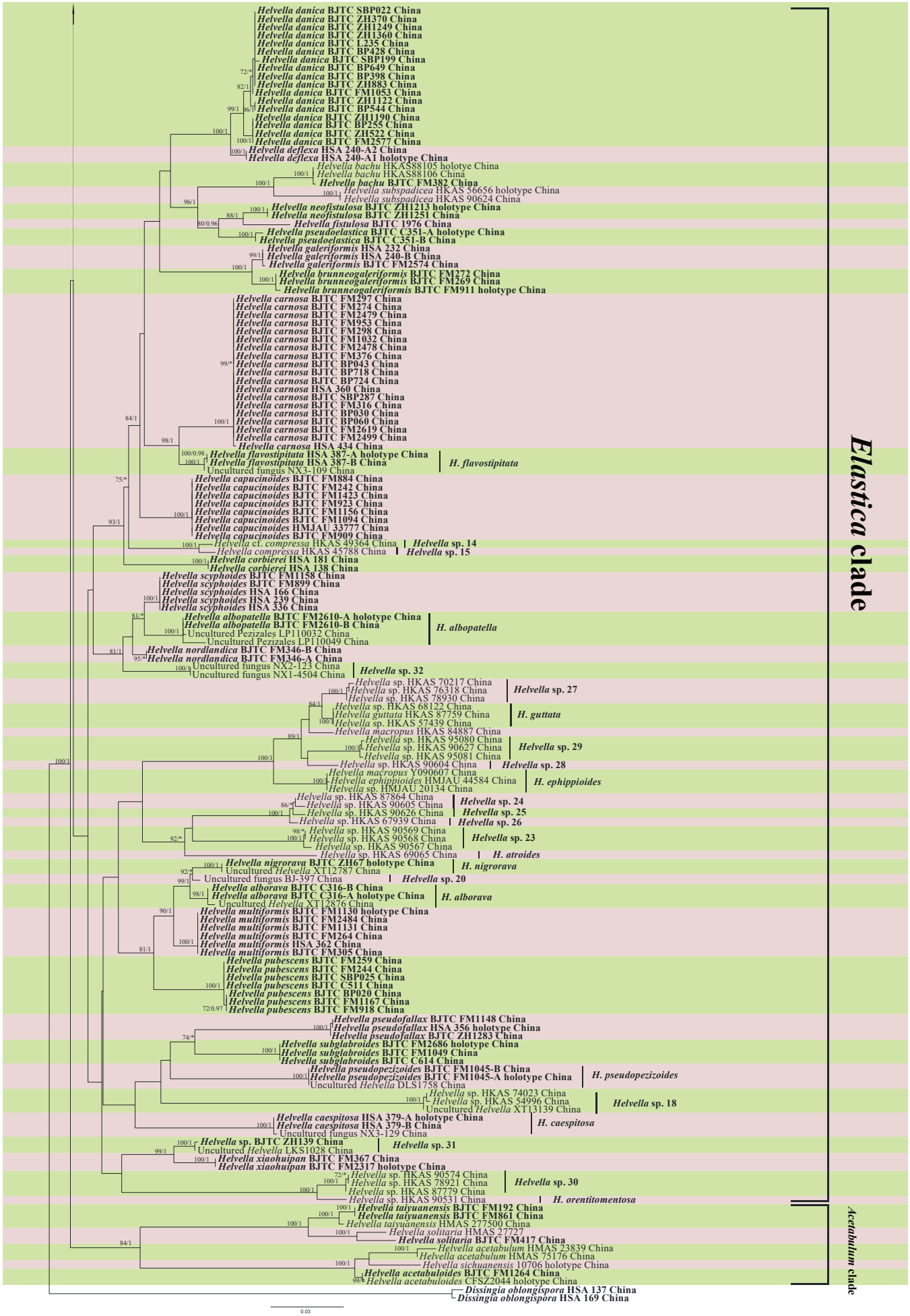

Fig. 2. (Continued).

Fig. 3. *Helvella albopatella* (BJTC FM2610-A, holotype). **A.** Apothecia. **B.** Ascospores in water. **C.** Ectal excipulum in Congo Red. **D.** Asci and paraphyses in Congo Red. **E.** Immature asci in Congo Red. Scale bars: A = 1 cm; B–E = 10 µm.

Specimens examined: **China**, Shanxi Province, Linfen City, Pu County, Wulushan mountains, on the ground in broadleaf forest dominated by *Quercus* sp., 36°56'23''N, 111°23'46''E, alt. 1 644.6 m, 26 Aug. 2022, *N. Mao* (**holotype** BJTC FM2610-A, GenBank Acc. No.: ITS = OR355082, nrLSU = OR355252, *tef1-α* = OR359014, *rpb2* = OR359137, *hsp* = OR366079); *ibid*., (BJTC FM2610-B).

Notes: *Helvella albopatella* is recognized by its disc-like cap and overall whitish ascomata with terete stipe. It is placed in the *hypocrateriformis* lineage, *Elastica* clade, sister to *H. nordlandica*, in our phylogenetic tree (Fig. 1). Morphologically, *H. albopatella* is distinguished from all other species in this lineage (including *H. nordlandica*) by its overall whitish ascomata with disc-like cap and a terete stipe. Molecularly, there are one *hsp*, three *rpb2*, five nrLSU, and 12 *tef1-α* substitutions between *H. albopatella* and *H. nordlandica*. Four ITS sequences downloaded from GenBank matched *H. albopatella* in our analysis (Fig. S3). These sequences are respectively extracted from ascomata or ectomycorrhizal root tips of *Quercus liaotungensis* and *Quercus* sp., from China. These results implied that *H. albopatella* is also occurs in another region of China and can form ectomycorrhizas with *Quercus* species. *Helvella albopatella* shares less than 94.87 % similarity in ITS region with other *Helvella* species.

Helvella alborava L. Fan, N. Mao & H. Zhou, ***sp. nov.*** MycoBank MB 849610. Fig. 4.

Etymology: *alborava, albo-,* means white, *rava*, means grey, referring to grey whitish ascomata.

Apothecia stipitate-capitate; cap regularly or irregularly saddle-shaped, sometimes regularly or irregularly cup-like, 0.6–2.0 cm high, 1.0–1.9 cm broad, at first margin adhered to stipe, then reflexed with age; hymenium greyish white to greyish, becoming brown to dark brown when dry; receptacle surface fine pubescent, concolourous with hymenium, becoming pale yellow to greyish brown when dry; stipe glabrous to fine pubescent, terete, 2.1–4.2 cm high, 0.2–0.5 cm broad, solid or hollow, greyish white, becoming pale brown to greyish brown when dry, towards base with inconspicuous grooves, base slightly enlarged. *Ectal excipulum* 80–120 µm broad, of *textura angularis*, cells hyaline to pale brown, extending into fascicled hyphoid hairs in outer ectal excipulum, hairs multiseptated, cells elongate club-shaped, 13–30 × 8–16 µm. *Medullary excipulum* 175–250 µm broad, of interwoven *textura intricata*, hyphae 2.0–4.0 µm broad. *Asci* pleurorhynchous, tapering, 8-spored, 215–275 × 13–19 µm. *Ascospores* ellipsoid, with one large oil drop when mature, 17–19 × 10–12 µm, [Lm × Wm = 17.9 × 10.9 µm,

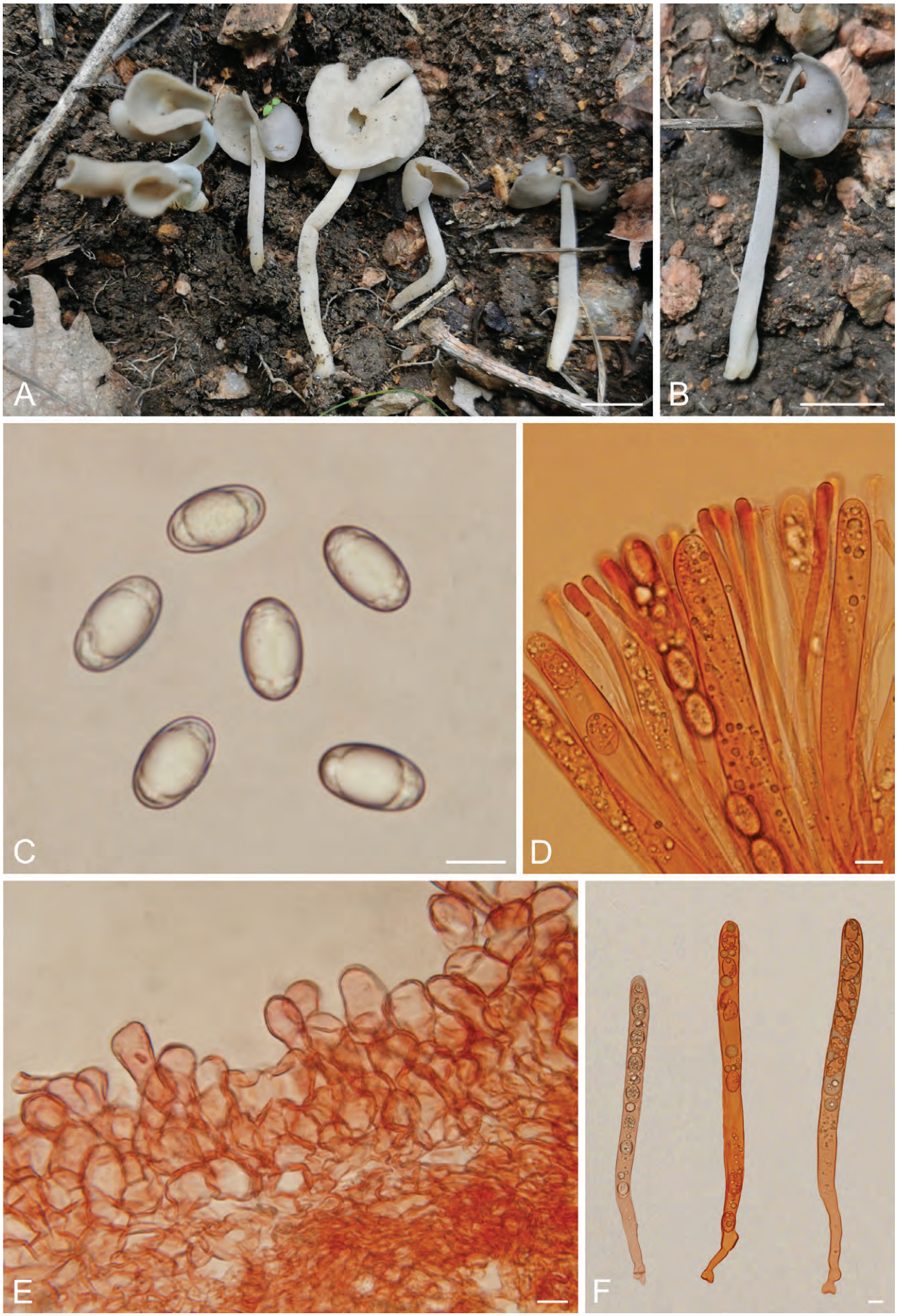

Fig. 4. *Helvella alborava* (BJTC C316-A, holotype). **A, B.** Apothecia. **C.** Ascospores in water. **D.** Asci and paraphyses in Congo Red. **E.** Ectal excipulum in Congo Red. **F.** Immature asci in Congo Red. Scale bars: A = 1 cm; B–F = 10 µm.

Q = 1.45–1.81, Q_{av} = 1.64 ± 0.09]. *Paraphyses* filiform, septate, pale brown, 4.0–6.0 µm wide at clavate to subcapitate tips and 2.0–3.5 µm below.

Habitat: Scattered on the ground in broadleaf forest.

Distribution: Known from Hebei Province, Northern China.

Specimens examined: **China**, Hebei Province, Xinglong County, on the ground in mixed broadleaf forest, alt. 898 m, 25 Aug. 2020, *G.Q. Chen* (**holotype** BJTC C316-A, GenBank Acc. No.: ITS = OR355106, nrLSU = OR355276, *tef1-α* = OR359033, *rpb2* = OR359155, *hsp* = OR366098), *ibid*., (BJTC C316-B).

Notes: *Helvella alborava* is phylogenetically nested in the *rivularis-sublicia* lineage, *Elastica* clade (Fig. 1). There are three other species in this lineage from China, *i.e*., *H*. *multiformis*, *H*. *nigrorava* and *H*. *pubescens*. *Helvella multiformis* is distinguished from *H. alborava* by its shape and colour of cap (cup to saddle, grey to black) and large spores (Lm × Wm = 19.1 × 11.9 µm); *Helvella nigrorava* by its dark grey to greyish black and saddle-shaped caps, and distinct pubescence on the surface of the receptacle and stipe (also see the comments on *H. nigrorava* in this paper); *Helvella pubescens* by its cup-like cap and stipe densely covered with pyramidal 'warts' (Skrede *et al.* 2017). In addition, seven *hsp*, three *rpb2*, five nrLSU, and 26 *tef1-α* substitutions separated *H*. *alborava* from *H*. *multiformis*; seven *hsp*, nine *rpb2*, 16 nrLSU substitutions and 41 *tef1-α* substitutions from *H*. *pubescens*. Two ITS ECM-sequences match *H*. *alborava* in our analysis (Fig. S3). They are extracted from the ectomycorrizal root tips of *Quercus variabilis*, and *Q. liaotungensis* from Shanxi Province and Beijing, Northern China. These indicate that *H*. *alborava* could form ectomycorrhizas with the two plant species. *Helvella alborava* shares less than 97.6 % similarity in ITS region with other *Helvella* species.

Helvella brunneogaleriformis L. Fan, N. Mao & Y.Y. Xu, ***sp. nov.*** MycoBank MB 849611. Fig. 5.

Etymology: *brunneogaleriformis*, because this species is phylogenetically closely related to *H. galeriformis* but with a brown cap.

Apothecia stipitate-capitate; cap irregularly umbrella-type, hemispheric to irregularly saddle-shaped, 0.5–2.2 cm high, 1.0–2.7 cm broad, at first margin adhered to stipe, then irregularly folded and free from stipe with age; hymenium ochre to brown when fresh, becoming dark brown to black brown when dry; receptacle surface glabrous, white, becoming yellow when dry; stipe terete 2.5–7.5 cm high, 0.3–0.7 cm broad, solid or hollow, white, or gradually becoming pale yellow brown to brown towards the base, becoming yellow when dry, base slightly enlarged, occasionally with a few shallow grooves. *Ectal excipulum* 80–130 µm broad, of *textura angularis*, cells hyaline to pale brown, arranged in rows turning out perpendicular to receptacle surface, outermost cells clavate, 23–56 × 13–29 µm. *Medullary excipulum* 150–230 µm broad, of interwoven *textura intricata*, hyphae 2.5–6.5 µm broad. *Asci* pleurorhynchous, tapering, 8-spored, 260–330 × 15–20 µm. *Ascospores* ellipsoid, with one large oil drop when mature, 17–20.5 × 10.5–12.5 µm, [Lm × Wm = 19 × 11.5 µm, Q = 1.5–1.8, Q_{av} = 1.65 ± 0.07]. *Paraphyses* filiform, 2.5–4.5 µm below, pale yellow to pale brown, septate, clavate to subcapitate, 6–13(–15) µm wide at tips.

Habitat: Scattered on the ground in coniferous forest.

Distribution: Known only from Shanxi Province, Northern China.

Specimens examined: **China**, Shanxi Province, Xinzhou City, Wutai County, Wutaishan mountains, on the ground in coniferous forest dominated by *Larix principis-rupprechtii* and *Picea asperata*, alt. 1 222 m, 27 Aug. 2019, *C. Yang* (**holotype** BJTC FM911, GenBank Acc. No.: ITS = OR355065, nrLSU = OR355235, *tef1-α* = OR359000, *rpb2* = OR359124, *hsp* = OR366062); *ibid*., Lvliang City, Jiaocheng County, Guandishan mountains, on the ground in coniferous forest dominated by *L. principis-rupprechtii* and *P. asperata*, alt. 2 003 m, 7 Sep. 2017, *Y.Y. Xu* (BJTC FM269); *ibid*., (BJTC FM272).

Notes: *Helvella brunneogaleriformis* is sister to *H. galeriformis* in the *capucina-danica* lineage, *Elastica* clade, as revealed in present analysis (Fig. 1). Morphologically, both species are similar in cap shape. However, the two species can be separated by the hymenium colour, which is ochre to brown in *H. brunneogaleriformis*, whereas grey blackish in *H. galeriformis*. *Helvella brunneogaleriformis* is similar to *H*. *elastica* and *H*. *carnosa* in its brown hymenium, and yellowish stipe. However, *H*. *elastica* and *H*. *carnosa* typically have a saddle-like cap, and *H*. *elastica* has lager asci (330–360 × 15–17 µm) and relatively longer ascospores (19–22 × 10.6–12.2 µm) (Skrede *et al.* 2017). *Helvella carnosa* has narrower asci (270–300 × 13–15 µm) and relatively narrower paraphyses at the apex (5–8 µm) (Skrede *et al.* 2017). In addition, six *hsp*, 13 *rpb2*, 16 nrLSU, and 20 *tef1-α* substitutions separated it from *H. elastica*; five *hsp*, 11 *rpb2*, 17 nrLSU substitutions, and 32 *tef1-α* substitutions from *H*. *carnosa*. *Helvella brunneogaleriformis* shares less than 97.8 % similarity in ITS region with other *Helvella* species.

Helvella caespitosa L. Fan, N. Mao & Y.Y. Xu, ***sp. nov.*** MycoBank MB 849612. Fig. 6.

Etymology: *caespitosa*, referring to its habit of growing in a cluster.

Apothecia stipitate-capitate; cap saddle-shaped, margin strongly deflexed, 0.4–1.0 cm high, 0.5–1.8 cm broad; hymenium dark grey to grey blackish, becoming greyish black when dry; receptacle surface pale grey, becoming greyish brown when dry; stipe pubescent, terete, 1.5–3.0 cm high, 0.2–0.3 cm broad, solid, pale grey, becoming greyish brown when dry, base often with white mycelia. *Ectal excipulum* 75–150 µm broad, of *textura angularis*, cells hyaline to pale brown, outermost cells club-shaped, 16–31 × 8–14 µm. *Medullary excipulum* 150–300 µm broad, of interwoven *textura intricata*, hyphae 2.0–5.5 µm broad. *Asci* pleurorhynchous, tapering, 8-spored, 210–300 × 14–21 µm. *Ascospores* ellipsoid, with one large oil drop when mature, 16.5–20 × 10–12 µm, [Lm × Wm = 18.5 × 11.1 µm, Q = 1.50–1.80, Q_{av} = 1.66 ± 0.07]. *Paraphyses* filiform, septate, pale brown, 5.0–9.0 µm wide at clavate to subcapitate tips and 1.5–3.5 µm below.

Habitat: Clustered or grouped on the ground in coniferous and broadleaf mixed forest dominated by *Betula* sp., *Pinus tabuliformis*, *Populus* sp., *Quercus wutaishansea*.

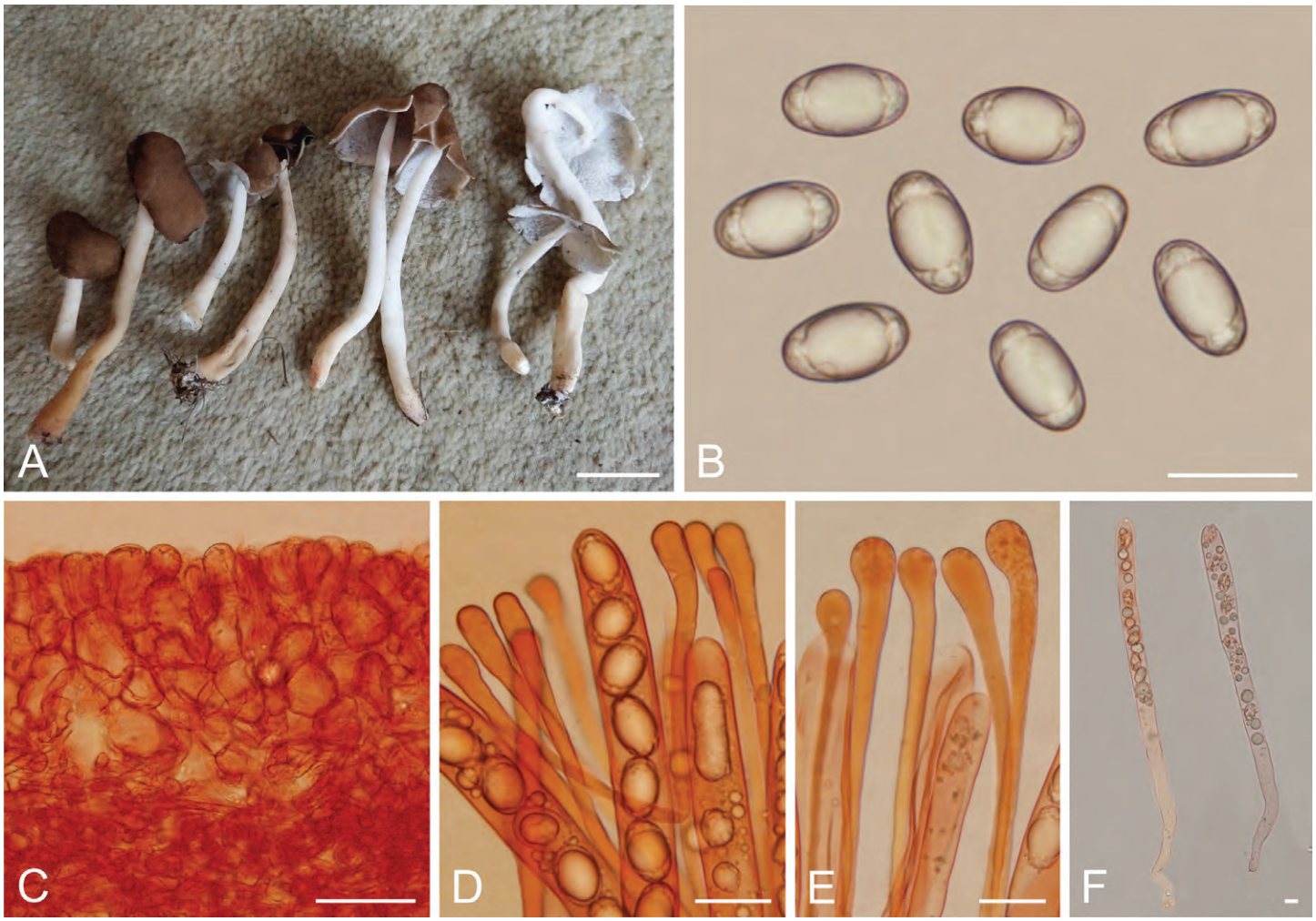

Fig. 5. *Helvella brunneogaleriformis* (BJTC FM911, holotype). **A.** Apothecia. **B.** Ascospores in water. **C.** Ectal excipulum in Congo Red. **D.** Asci and paraphyses in Congo Red. **E.** Paraphyses in Congo Red. **F.** Immature asci in Congo Red. Scale bars: A = 2 cm; B, D, E = 20 µm; C = 50 µm; F = 10 µm.

Distribution: Known from Shanxi Province, Northern China.

Specimens examined: **China**, Shanxi Province, Lvliang City, Xing County, Heichashan mountains, on the ground in coniferous and broadleaf mixed forest dominated by *Betula* sp., *Pinus tabuliformis*, *Populus* sp., *Quercus wutaishansea*, alt. 1 590 m, 6 Sep. 2018, *J.Z. Cao* (**holotype** HSA 379-A, GenBank Acc. No.: ITS = OR355091, nrLSU = OR355261, *tef1-α* = OR359022, *hsp* = OR366087); *ibid*., (HSA 379-B).

Notes: *Helvella caespitosa* is diagnosed by its grey blackish saddle-shaped cap with strongly deflexed margin, dark grey stipe with pubescent surface, and habit of growing in cluster. Our present analysis places *H. caespitosa* in the *fallax-pezizoides* lineage in the *Elastica* clade and sister to *H. bresadolae* and *H. pezizoides* (Fig. 1). *Helvella bresadolae* is easily confused with *H. caespitosa* in appearance of its cap. However, *H. bresadolae* is distinguished from *H. caespitosa* by its stipe base without white mycelia and relatively smaller asci (200–240 × 14–17 µm). The difference between *H. pezizoides* and *H. caespitosa* is in the cap margin of ascomata, which is inrolled in *H. pezizoides* but deflexed in *H. caespitosa* (Dissing 1966b). In addition, one *hsp* and 13 nrLSU substitutions separated it from *H. bresadolae*; 10 *hsp*, 13 nrLSU, and 19 *tef1-α* substitutions from *H. pezizoides*. Three ITS sequences downloaded from GenBank matched *H. caespitosa* in our analysis (Fig. S3). These sequences are respectively extracted from ectomycorrhizal root tips of *Picea crassifolia*, *Pinus tabuliformis*, and *Quercus liaotungensis*, from Ningxia Hui Autonomous Region, Northern China. These indicated that *H. caespitosa* also occurs in other regions of China, and has a wide host range. *Helvella caespitosa* shares less than 89.94 % similarity in ITS region with other *Helvella* species.

Helvella cremeoinvoluta L. Fan, N. Mao & Y.Y. Xu, ***sp. nov.*** MycoBank MB 849613. Fig. 7.

Etymology: *cremeoinvoluta*, referring to its high similarity to *H. involuta* in appearance of ascoma but pale grey-white to pale cream receptacle.

Apothecia stipitate-capitate; cap saddle-shaped to irregularly lobate, 0.5–1.3 cm high, 1.1–2.3 cm broad, margin strongly rolled upwards and completely wrapped the hymenium at first, then unrolled with age; hymenium glabrous, garish white to cream, becoming pale brown to yellowish brown when dry; receptacle surface subpubescent, pale grey white to pale cream, becoming yellowish when dry; stipe 2.6–4.8 cm high, 0.7–1.7 cm broad, white to yellowish white, becoming pale yellow to greyish yellow when dry, ribbed, blunt-edged, partly anastomosing and double-edged, with lacunae between ribs, chambered inside. *Ectal excipulum* 125–190 µm broad, of *textura angularis*, cells hyaline to pale brown, outermost cells catenuliform in long fascicled

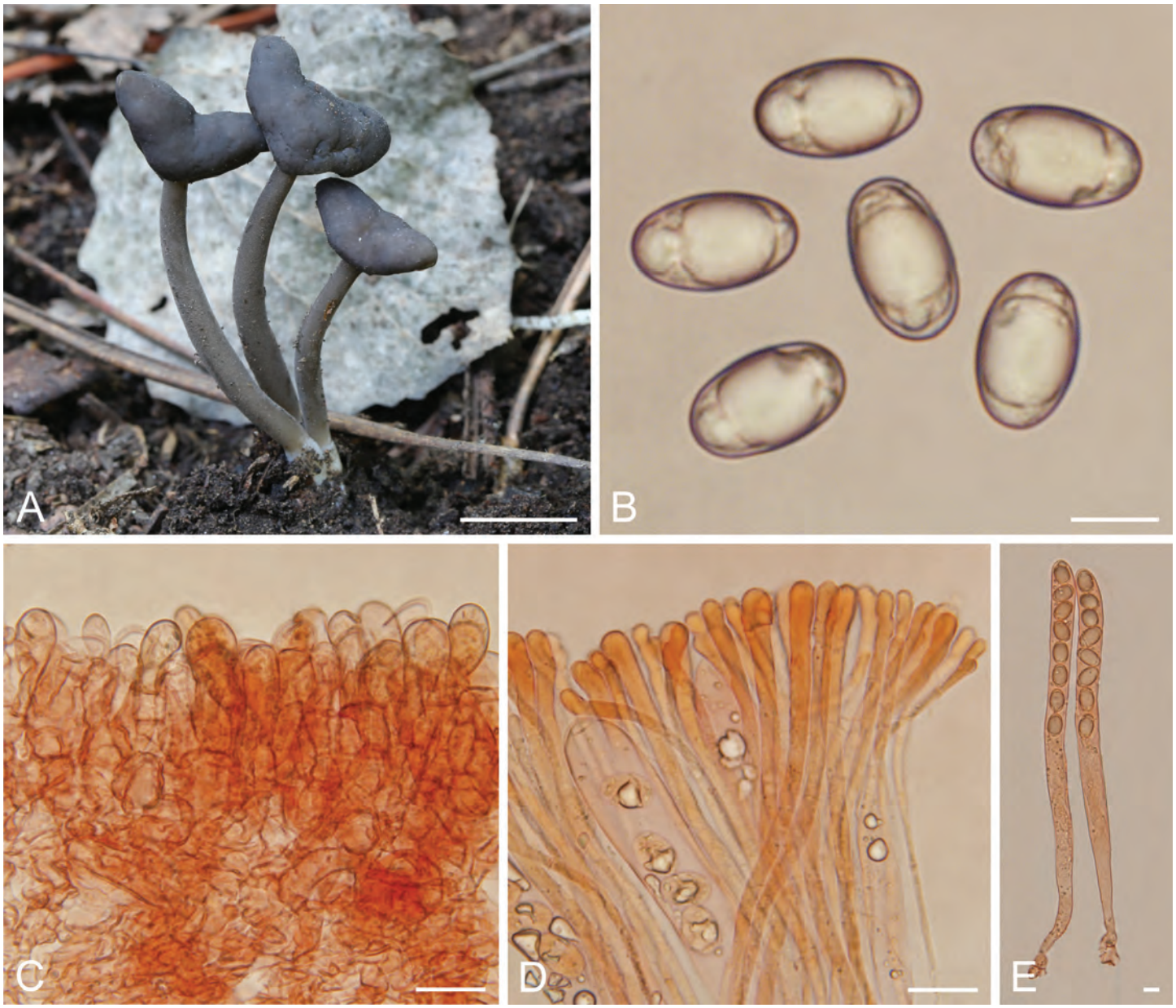

Fig. 6. *Helvella caespitosa* (HSA 379-A, holotype). **A.** Apothecia. **B.** Ascospores in water. **C.** Ectal excipulum in Congo Red. **D.** Asci and paraphyses in Congo Red. **E.** Asci in Congo Red. Scale bars: A = 1 cm; B, E = 10 µm; C, D = 20 µm.

tufts, with cylindrical to subclavate cells of 18–37 × 11–18 µm. *Medullary excipulum* 240–330 µm broad, of interwoven *textura intricata*, hyphae 3–7 µm broad. *Asci* pleurorhynchous, tapering, 8-spored, 225–275 × 13–18 µm. *Ascospores* ellipsoid, with one large oil drop when mature, 17–18.5 ×9.5–11 µm, [Lm × Wm = 17.6 × 10.1 µm, Q = 1.60–1.85, Q_{av} = 1.74 ± 0.10]. *Paraphyses* filiform, septate, hyaline to pale brown, 4–6 µm wide at tips and 2–4 µm below.

Habitat: Scattered to gregarious on the ground in coniferous forest dominated by *Larix principis-rupprechtii*.

Distribution: Known only from Shanxi Province, Northern China.

Specimens examined: **China**, Shanxi Province, Xinzhou City, Wutai County, Wutaishan mountains, on the ground in coniferous forest dominated by *Larix principis-rupprechtii*, 38°55'39''N, 113°35'43''E, alt. 1 543 m, 28 Aug. 2019, *Y. Shen* (**holotype** BJTC FM941-A, GenBank Acc. No.: ITS = OR355153, nrLSU = OR355324, *tef1-α* = OR359066, *rpb2* = OR359178, *hsp* = OR366131); *ibid*., 38°55'39''N, 113°35'40''E, alt. 1 543 m, 28 Aug. 2019, *Y. Shen* (BJTC FM941-B).

Notes: *Helvella cremeoinvoluta* and *H. crispoides* are closely related to each other in our phylogenetic analyses (Figs 1, 2). Morphologically, *H. crispoides* differs from *H. cremeoinvoluta* by its grey receptacle surface, white stipe, relatively shorter ascospores (15–17 × 9.5–11.5 µm), and broader paraphyses at the apex (6–7.5 µm) (Tibpromma *et al.* 2017). *Helvella involuta* is similar to *H. cremeoinvoluta* in cap shape and ascospores size, but the colour of its receptacle surface is clearly yellowish (Zhao *et al.* 2015), that is completely different from the present species (grey-white to pale cream). *Helvella cremeoinvoluta* shares less than 96.1 % ITS similarity with other *Hevella* species, supporting it is a distinct species.

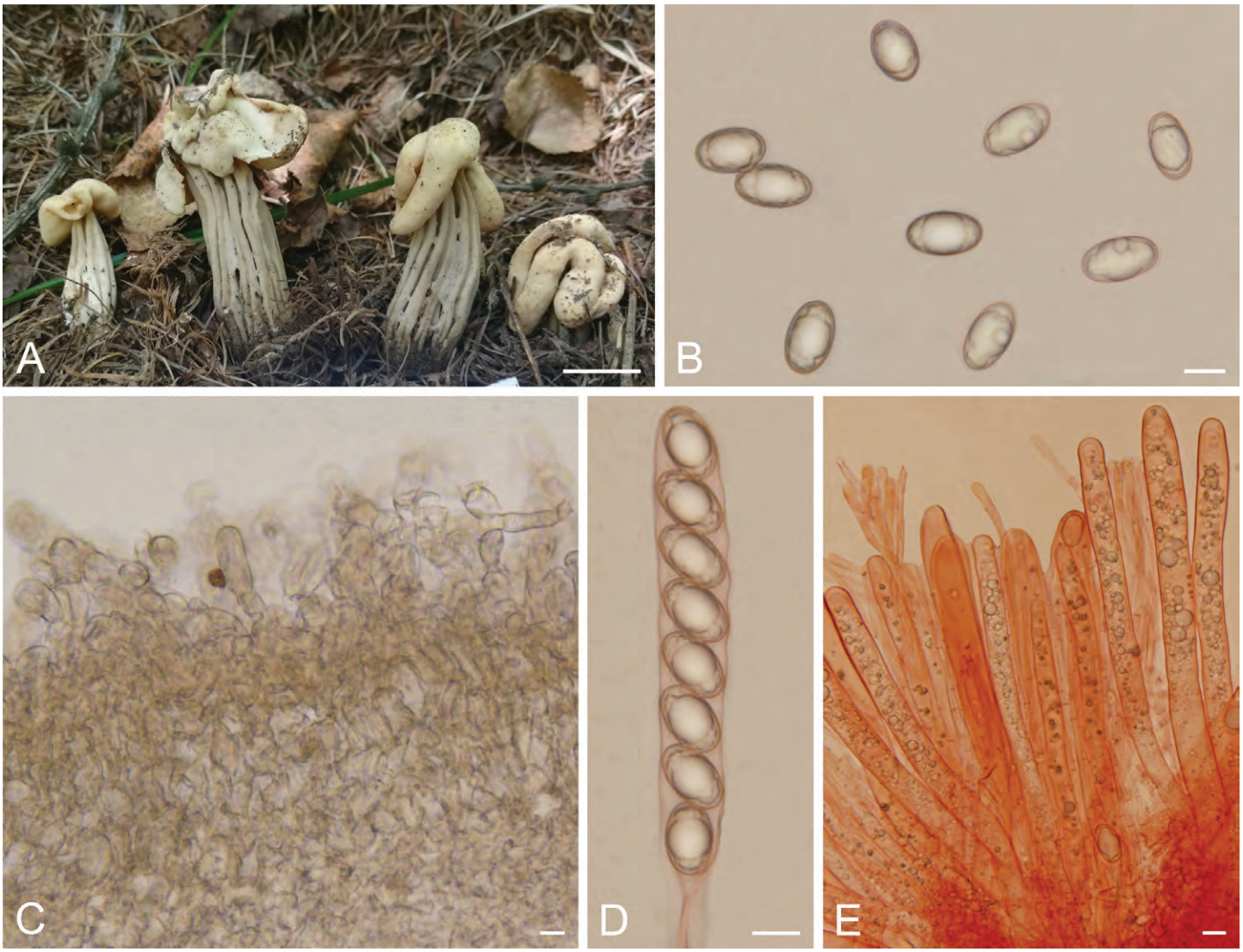

Fig. 7. *Helvella cremeoinvoluta* (BJTC FM941-A, holotype). **A.** Apothecia. **B.** Ascospores in water. **C.** Ectal excipulum in water. **D.** Asci in Congo Red. **E.** Immature asci and paraphyses in Congo Red. Scale bars: A = 1 cm; B–E = 10 µm.

Helvella deflexa L. Fan, N. Mao & Y.Y. Xu, ***sp. nov.*** MycoBank MB 849614. Fig. 8.

Etymology: *deflexa,* referring to the strongly deflexed margin of the cap.

Apothecia stipitate-capitate; cap saddle-shaped, 0.7–1.1 cm high, 2.0–3.0 cm broad, with a strongly deflexed margin; hymenium brown to dark brown; receptacle surface yellowish white; stipe terete, 1.5–3.0 cm high, 0.3–0.5 cm broad, solid or hollow, white to cream. *Ectal excipulum* 75–100 µm broad, of *textura angularis*, cells hyaline to pale brown, arranged in rows turning out perpendicular to receptacle surface, outermost cells elongate club-shaped, 21–50 × 10–20 µm. *Medullary excipulum* 100–125 µm broad, of interwoven *textura intricata*, hyphae 2.0–6.0 µm broad. *Asci* pleurorhynchous, tapering, 8-spored, 290–325 × 15–23 µm. *Ascospores* ellipsoid and with slightly narrow ends, with one large central oil drop and a few of small ones when mature, 19.5–23 × 12–14.5 µm, [Lm × Wm = 21.0 × 13.1 µm, Q = 1.46–1.81, Q_{av} = 1.60 ± 0.08]. *Paraphyses* filiform, septate, subhyaline to pale brown, 6.0–11.0 µm wide at clavate to subcapitate tips and 2.0–4.0 µm below.

Habitat: Scattered on the ground in coniferous and broadleaf mixed forest dominated by *Betula* sp. and *Larix principis-rupprechtii*.

Distribution: Known from Shanxi Province, Northern China.

Specimens examined: **China**, Shanxi Province, Lvliang City, Jiaocheng County, Pangquangou, on the ground in coniferous and broadleaf mixed forest dominated by *Betula* sp. and *Larix principis-rupprechtii*, alt. 2 160 m, 28 Aug. 2018, *L.J. Guo* (**holotype** HSA 240-A1, GenBank Acc. No.: ITS = OR355069, nrLSU = OR355239, *tef1-α* = OR359004, *rpb2* = OR359127, *hsp* = OR366066); *ibid*., (HSA 240-A2).

Notes: *Helvella deflexa* is recognized by its saddle-shaped cap with strongly deflexed margin, a long and white terete stipe and ascospores with slightly narrow ends. It is phylogenetically nested in the *capucina-danica* lineage of *Elastica* clade, closely related to *H. danica* (Fig. 1). *Hevlella danica* differs from *H. deflexa* by its campanulate cap and clustered habit (Skrede *et al.* 2017). Molecularly, one *hsp*, three *rpb2*, two nrLSU and seven *tef1-α* substitutions separated *H. deflexa* from *H. danica*. *Helvella deflexa* shares less than 96.16 % similarity in ITS region with other *Helvella* species.

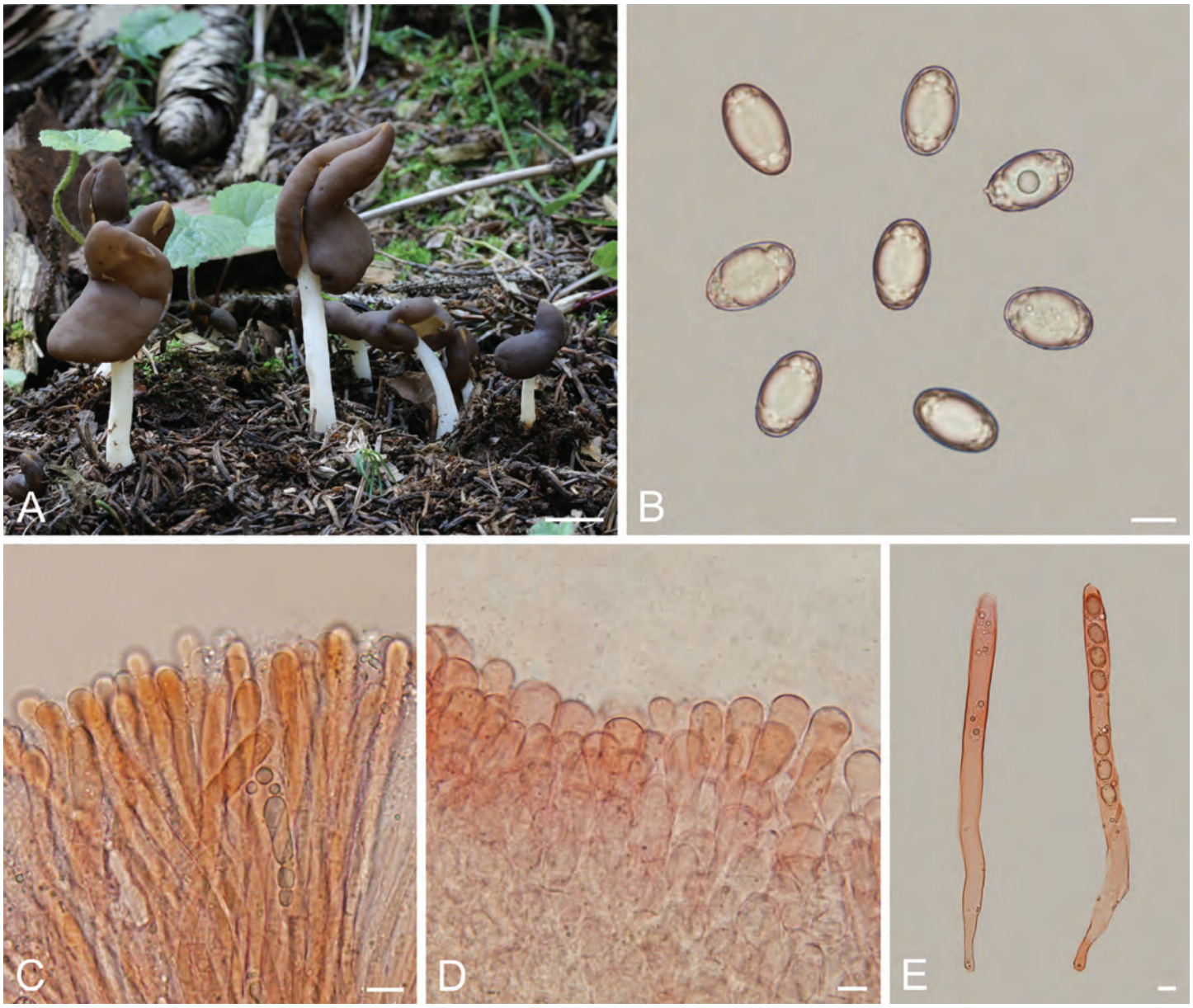

Fig. 8. *Helvella deflexa* (HSA 240-A1, holotype). **A.** Apothecia. **B.** Ascospores in water. **C.** Paraphyses in Congo Red. **D.** Ectal excipulum in Congo Red. **E.** Immature asci in Congo Red. Scale bars: A = 1 cm; B–D = 10 µm.

Helvella flavostipitata L. Fan, N. Mao & Y.Y. Xu, ***sp. nov.*** MycoBank MB 849615. Fig. 9.

Etymology: *flavostipitata*, *flavo-*, yellow, referring to the yellow stalk of this saddle fungus.

Apothecia stipitate-capitate; cap saddle-shaped, 2–2.4 cm high, 1.6–2.4 cm broad, margin adhered to stipe; hymenium yellowish brown to brown, becoming dark brown when dry; receptacle surface glabrous, pale grey to greyish yellow, becoming yellow when dry; stipe terete, 3.5–5.0 cm high, 0.3–0.4 cm broad, hollow, yellow, not change colour when dry, base often with white mycelia. *Ectal excipulum* 80–120 µm broad, of *textura angularis*, cells hyaline to pale brown, arranged in rows turning out perpendicular to receptacle surface, outermost cells clavate, 18–43 × 9–21 µm. *Medullary excipulum* 150–250 µm broad, of interwoven *textura intricata*, hyphae 2.0–7.0 µm broad. *Asci* pleurorhynchous, tapering, 8-spored, 250–310 × 14–20 µm. *Ascospores* ellipsoid, with one large oil drop when mature, 18–20.5 × 10.5–12.5 µm, [Lm × Wm = 19.3 × 11.5 µm, Q = 1.53–1.84, Q_{av} = 1.67 ± 0.08]. *Paraphyses* filiform, septate, pale yellow to pale brown, 5.5–9 µm wide at clavate to subcapitate tips and 2.0–4.0 µm below.

Habitat: Scattered on the ground in coniferous forest.

Distribution: Known from Shanxi Province, Northern China.

Specimens examined: **China**, Shanxi Province, Lvliang City, Jiaocheng County, Pangquangou, on the ground in coniferous forest dominated by *Picea* sp., alt. 1 860 m, 6 Sep. 2018, *H. Liu* (**holotype** HSA 387-A, GenBank Acc. No.: ITS = OR355035, nrLSU = OR355205, *tef1-α* = OR358976, *rpb2* = OR359103); *ibid*., (HSA 387-B).

Notes: *Helvella flavostipitata* is phylogenetically sister to *H. carnosa* in the *carnosa* lineage, *Elastica* clade (Fig. 1). Morphologically, both species have regularly saddle-shaped and brown caps, but *H. carnosa* has a receptacle surface

Fig. 9. *Helvella flavostipitata* (HSA 387-A, holotype). **A.** Apothecia. **B.** Ascospores in water. **C.** Ectal excipulum in Congo Red. **D.** Asci and paraphyses in Congo Red. **E.** Immature asci in Congo Red. Scale bars: A = 1 cm; B, E = 10 µm; C, D = 20 µm.

with delicate pubescence and relatively narrower asci (13–15 µm) (Skrede *et al.* 2017), whereas *H. flavostipitata* has a glabrous receptacle surface and wider asci (14–20 µm diam). Molecularly, *H. flavostipitata* deviates consistently in one *hsp*, five nrLSU, and nine *tef1-α* substitutions. Five ITS sequences from GenBank matched *H. flavostipitata* in our analysis (Fig. S3). These sequences are respectively extracted from ascomata or ectomycorrhizal root tips of *Pinus wallichiana* and *P. tabuliformis*, from China or Pakistan. These results implied that *H. flavostipitata* can form ectomycorrhizas with *Pinus* species. *Helvella flavostipitata* shares less than 91.5 % similarity in ITS region with other *Helvella* species.

Helvella multiformis L. Fan, N. Mao & Y.Y. Xu, ***sp. nov.*** MycoBank MB 849616. Fig. 10.

Etymology: *multiformis*, referring to the cap shape that includes cup and saddle.

Apothecia stipitate-cupulate; cap regular cupulate to saucer-shaped at first, then expanding to saddle-shaped, occasionally applanate, 0.7–2.2 cm high, 1.5–3.7 cm broad; hymenium, greyish black, dark brown, blackish to black, becoming dark brown to black when dry; receptacle surface pubescent, greyish to dark grey, becoming brown when dry; stipe terete, 2.0–5.0 cm high, 0.3–0.7 cm broad, solid or hollow, greyish white to greyish yellow, becoming greyish brown when dry, occasionally with grooves, base slightly enlarged. *Ectal excipulum* 120–200 µm broad, of *textura angularis*, cells hyaline to pale brown, sometimes extending into fascicled hyphoid hairs in outer ectal excipulum, hairs multiseptated, cells elongate club-shaped, 16–40 × 8–21 µm. *Medullary excipulum* 300–360 µm broad, of interwoven *textura intricata*, hyphae 3.0–6.0 µm broad. *Asci* pleurorhynchous, tapering, 8-spored, 250–300 × 17–20 µm. *Ascospores* ellipsoid, with one large oil drop when mature, 18–20.5 × 11–13 µm, [Lm × Wm = 19.1 × 11.9 µm, Q = 1.44–1.81, Q_{av} = 1.61 ± 0.09]. *Paraphyses* filiform, septate, subhyaline to pale

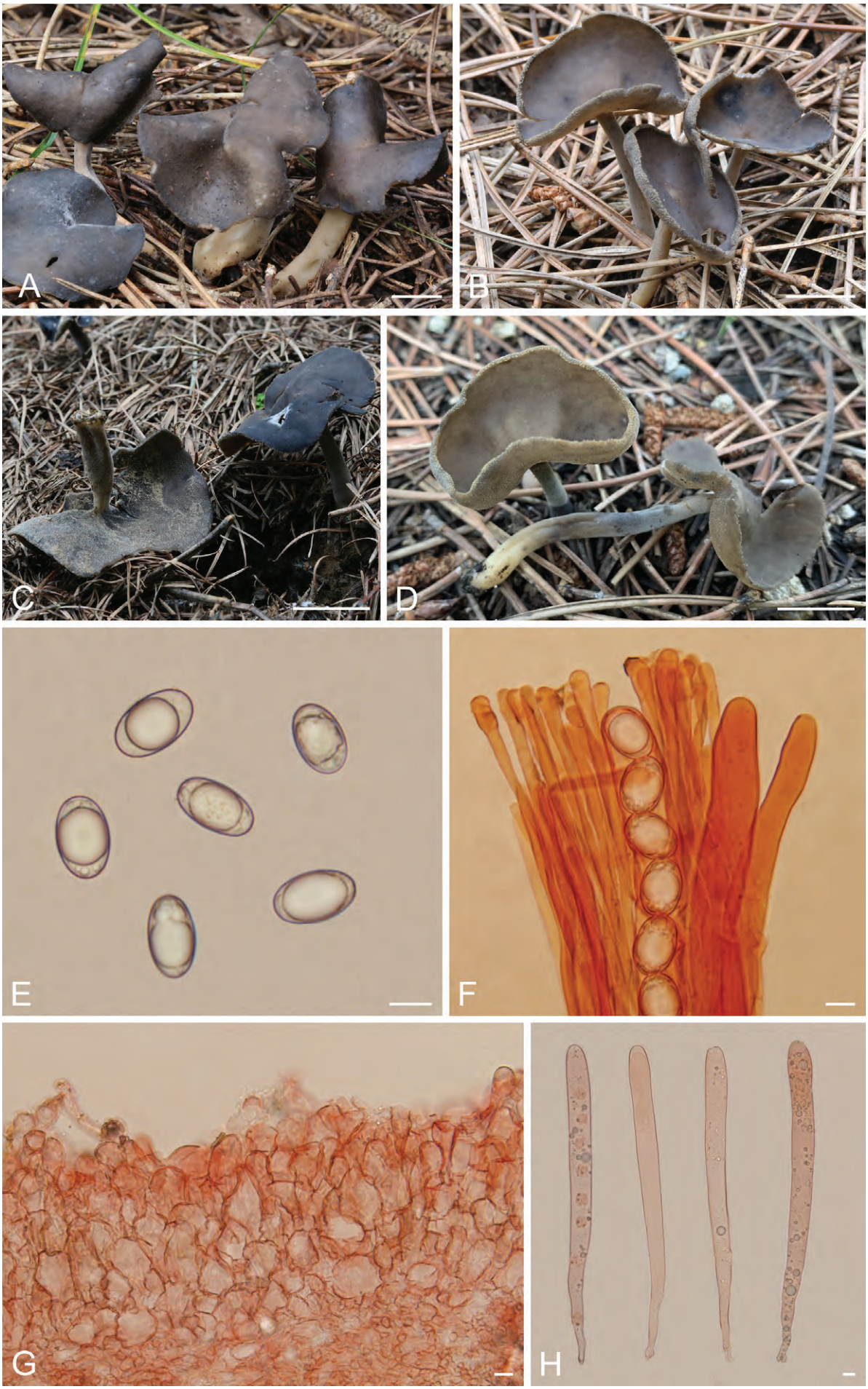

Fig. 10. *Helvella multiformis* (A, C, E–H. BJTC FM1130, holotype. B. BJTC FM1131. D. BJTC FM2484). **A–D.** Apothecia. **E.** Ascospores in water. **F.** Asci and paraphyses in Congo Red. **G.** Ectal excipulum in Congo Red. **H.** Immature asci in Congo Red. Scale bars: A–D = 1 cm; E–H = 10 µm.

brown, 4.5–7.0 µm wide at clavate to subcapitate tips and 2–4 µm below.

Habitat: Scattered on the ground in broadleaf forest and coniferous forest.

Distribution: Known from Shanxi Province, Northern China.

Specimens examined: **China**, Shanxi Province, Jincheng City, Qinshui County, Lishan mountains, on the ground in broadleaf forest dominated by *Quercus* sp., 35°29′4′′N, 112°1′25′′E, alt. 1 675m, 27 Aug. 2020, *N. Mao* (**holotype** BJTC FM1130, GenBank Acc. No.: ITS = OR355100, nrLSU = OR355270, *tef1-α* = OR359027, *rpb2* = OR359149, *hsp* = OR366092); *ibid*., (BJTC FM1131); *ibid*., Linfen City, Pu County, Wulushan mountains, on the ground in coniferous forest dominated by *Pinus* sp., 10 Sep. 2017, *X.Y. Yan* (BJTC FM305); *ibid*., Lvliang City, Jiaocheng County, Guandishan mountains, on the ground in coniferous forest dominated by *Larix principis-rupprechtii* and *Picea asperata*, alt. 2 003 m, 7 Sep. 2017, *J.Z. Cao* (BJTC FM264); *ibid*., Lvliang City, Xing County, Heicha mountains, on the ground in broadleaf forest dominated by *Populus* sp., alt. 1 590 m, 5 Sep. 2018, *L.J. Guo* (HSA 362); *ibid*., Taiyuan City, Loufan County, Yundingshan mountains, on the ground in coniferous forest dominated by *Pinus* sp., alt. 1 642 m, 23 Aug. 2022, *N. Mao* (BJTC FM2484).

Notes: *Helvella multiformis* is diagnosed by its variation of cap shape and colour (cup to saddle, grey to black). Phylogenetically it is nested in the *rivularis-sublicia* lineage, *Elastica* clade, and closely related to *H. poculiformis* and *H. sublicia* (Fig. 1). *Helvella poculiformis* is differentiated from *H. multiformis* by its cup-like and grey or grey-brown cap (never saddle-shaped and black), *H. sublicia* (syn. *Helvella ephippium*) by its whitish, greyish to dark grey cap (lacking black tints) (Skrede *et al.* 2020). Molecularly, five *hsp* and two *rpb2* substitutions separate this new species from *H. poculiformis*; five *hsp*, six *rpb2*, five nrLSU substitutions, and 11 *tef1-α* substitutions from *H. sublicia*. Four ITS sequences from GenBank matched *H. multiformis* in our analysis (Fig. S3). These sequences are respectively extracted from ascomata or ectomycorrhizal root tips of *Epipactis helleborine*, and *Pinus tabuliformis*, from Shanxi Province, Ningxia Hui Autonomous Region. These indicate that *H. multiformis* also occurs in other regions of China, and could form ectomycorrhiza with *E. helleborine* and *P. tabuliformis*. *Helvella multiformis* shares less than 95.35 % ITS similarity with other *Hevella* species, supporting it as a distinct species.

Helvella neofistulosa L. Fan, N. Mao & C.L. Hou, ***sp. nov.*** MycoBank MB 849617. Fig. 11.

Etymology: *neofistulosa*, *neo-*, new, because this species is phylogenetically closely related to *H. fistulosa.*

Apothecia stipitate-capitate; cap saddle-shaped, bi- to trilobate, or irregularly lobate, 0.6–2.5 cm high, 1.3–2.5 cm broad, at first margin adhered to stipe, then reflexed with age; hymenium grey to greyish yellow, becoming ochre to dark brown when dry; receptacle surface subpubescent, greyish white, becoming yellow when dry; stipe 1.3–5.3 cm high, 0.3–0.7 cm broad, solid or hollow, greyish white to cream, becoming yellow when dry, base slightly enlarged. *Ectal excipulum* 70–120 µm broad, of *textura angularis*, cells hyaline to pale brown, arranged in rows turning out perpendicular to receptacle surface, outermost cells clavate, 22–50 × 10–23 µm. *Medullary excipulum* 160–250 µm broad, of interwoven *textura intricata*, hyphae 2.3–4.5 µm broad. *Asci* pleurorhynchous, tapering, 8-spored, 250–300 × 14–21 µm. *Ascospores* ellipsoid, with one large oil drop when mature, 18–22.5 × 10.5–12.5 µm, [Lm × Wm = 20 × 11.6 µm, Q = 1.58–1.89, Q_{av} = 1.72 ± 0.08]. *Paraphyses* filiform, 2.5–4.5 µm below, septate, clavate to subcapitate, 6–11 µm wide at tips.

Habitat: Scattered on the ground in mixed broadleaf forest.

Distribution: Known from Beijing and Hebei Province, Northern China.

Specimens examined: **China**, Beijing, Huairou District, Labagoumen, on the ground in mixed broadleaf forest, alt. 1 250 m, 25 Aug. 2020, *H. Zhou* (**holotype** BJTC ZH1213, GenBank Acc. No.: ITS = OR355059, nrLSU = OR355229, *tef1-α* = OR358994, *rpb2* = OR359118, *hsp* = OR366056); Hebei Province, Chicheng county, Dahaituo, on the ground in mixed broadleaf forest, alt. 1 267 m, 25 Aug. 2020, *H. Zhou* (BJTC FM1251).

Notes: *Helvella neofistulosa* is placed in a position sister to *H. fistulosa* in the *capucina-danica* lineage, *Elastica* clade (Fig. 1). Morphologically, the two species can be separated by the cap colour, which is grey to greyish yellow in *H. neofistulosa* but brown in *H. fistulosa*. Molecularly, there are two *hsp*, one *rpb2*, three nrLSU, and 22 *tef1-α* substitutions between the two species (Skrede *et al.* 2017). Two ITS sequences downloaded from GenBank matched *H. neofistulosa* in our analysis (Fig. S3). The two sequences are respectively extracted from ascomata or ectomycorrhizal root tips of broadleaved trees, from China or Japan, implying that *H. neofistulosa* also occurs in Japan and can form ectomycorrhizas with broadleaved trees. *Helvella neofistulosa* shares less than 95.08 % ITS similarity with other *Hevella* species, supporting it is a distinct species.

Helvella nigrorava L. Fan, Y.Y. Xu & C.L. Hou, ***sp. nov.*** MycoBank MB 849618. Fig. 12.

Etymology: *nigrorava, nigro-,* means black, *rava,* means grey, referring to the blackish grey cap of this species.

Apothecium stipitate-capitate; cap saddle-shaped, 1.5 cm high, 1.2 cm broad; hymenium dark grey to greyish black, becoming black brown to black when dry; receptacle surface pubescent, concolourous with hymenium, becoming dark brown to black brown when dry; stipe pubescent, terete, 1.7 cm high, 0.2–0.35 cm broad, solid or hollow, greyish white to grey, becoming greyish brown to brown when dry, base slightly enlarged. *Ectal excipulum* 75–115 µm broad, of *textura angularis*, cells hyaline to pale brown, extending into fascicled hyphoid hairs in outer ectal excipulum, hairs multiseptated, cells elongate club-shaped, 11–37 × 9–16 µm. *Medullary excipulum* 135–200 µm broad, of interwoven *textura intricata*, hyphae 2.0–5.0 µm broad. *Asci* pleurorhynchous, tapering, 8-spored, 235–265 × 15–20 µm. *Ascospores* ellipsoid, with one large oil drop when mature, 16.5–18.5 × 11–12.5 µm, [Lm × Wm = 17.5 × 11.8 µm, Q = 1.40–1.63, Q_{av} = 1.49 ± 0.07]. *Paraphyses* filiform, septate, pale yellow to pale brown, 4.5–6.0 µm wide at clavate to subcapitate tips and 2.5–4.0 µm below.

Habitat: Scattered on the ground in broadleaf forest.

Distribution: Known from Beijing, Northern China.

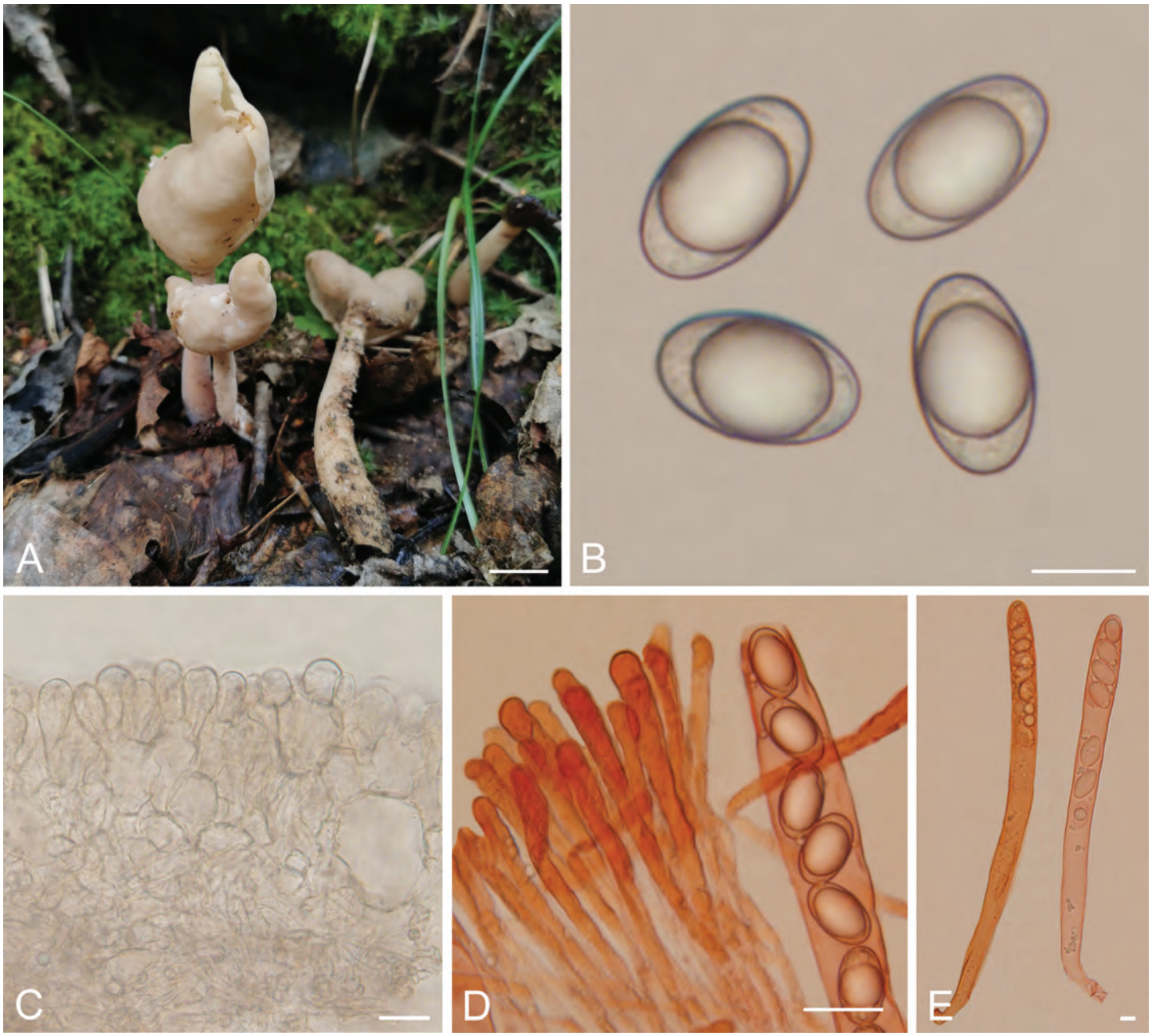

Fig. 11. *Helvella neofistulosa* (BJTC ZH1213, holotype). **A.** Apothecia. **B.** Ascospores in water. **C.** Ectal excipulum in water. **D.** Asci and paraphyses in Congo Red. **E.** Immature asci in Congo Red. Scale bars: A = 1 cm; B, E = 10 µm; C, D = 20 µm.

Specimen examined: **China**, Beijing, Changping District, Tiebiyinshan Mountains, on the ground in broadleaf forest, alt. 362 m, 14 Aug. 2019, *H. Zhou* (**holotype** BJTC ZH67, GenBank Acc. No.: ITS = OR355105, nrLSU = OR355275, *tef1-α* = OR359032, *rpb2* = OR359154, *hsp* = OR366097).

Notes: *Helvella nigrorava* was phylogenetically sister to *H. alborava*, a new species described in this study, in the *rivularis-sublicia* lineage, *Elastica* clade (Fig. 1). The two species can be separated by the cap shape and colour, which is saddle-shaped or irregularly cup-like and grey to greyish white in *H. alborava*, but regularly saddle-shaped and dark grey to greyish black in *H. nigrorava*. Also, *H. nigrorava* is more distinct pubescent on both of receptacle and stipe than that in *H. alborava.* Molecularly, there were four *hsp*, three *rpb2*, two nrLSU, and 20 *tef1-α* substitutions between the two species. One ITS sequence (GenBank MF405780) extracted from ectomycorrizal root tip of *Quercus variabilis* in Shanxi Province, Northern China matched this species (Fig. S3), indicating that *H. nigrorava* can form ectomycorrhizas with this plant species. *Helvella nigrorava* shares less than 95.9 % similarity in ITS region with other *Helvella* species.

Helvella pseudoelastica L. Fan, Y.Y. Xu & H. Zhou, ***sp. nov.*** MycoBank MB 849619. Fig. 13.

Etymology: *pseudoelastica*, referring to the similarity to *H. elastica* in appearance of ascomata.

Apothecia stipitate-capitate; cap saddle-shaped to bilobate, 0.7–1.2 cm high, 1.2–1.9 cm broad; hymenium greyish white, becoming brown when dry; receptacle surface greyish white, becoming yellowish when dry; stipe terete, 2.8–4.3 cm high, 0.2–0.4 cm broad, solid or hollow, white to yellowish white

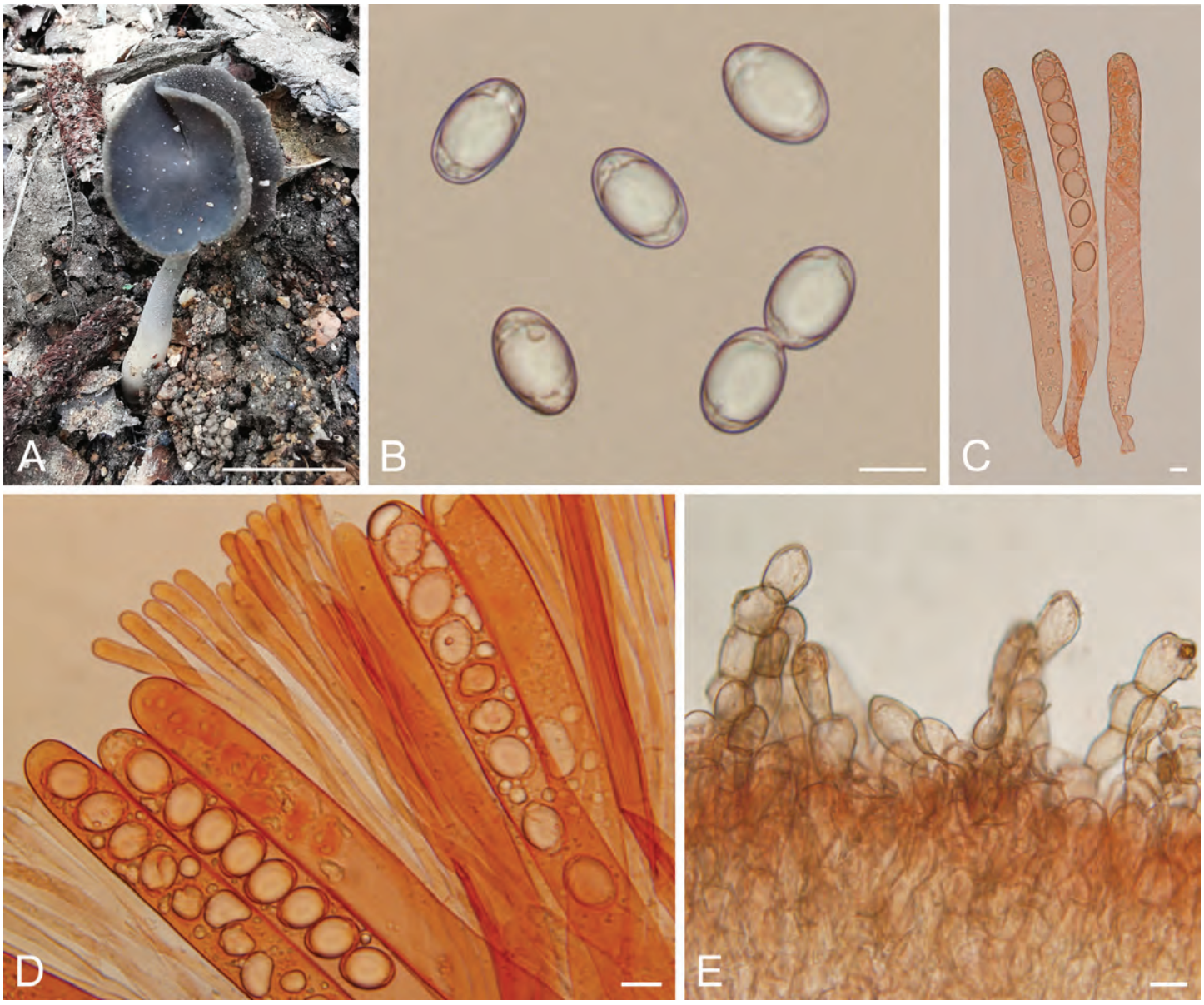

Fig. 12. *Helvella nigrorava* (BJTC ZH67, holotype). **A.** Apothecium. **B.** Ascospores in water. **C.** Asci in Congo Red. **D.** Asci and paraphyses in Congo Red. **E.** Ectal excipulum in Congo Red. Scale bars: A = 1 cm; B–E = 10 µm.

with distinct tints of pinkish especially near the base, becoming yellowish brown when dry. *Ectal excipulum* 85–115 µm broad, of *textura angularis*, cells hyaline to pale brown, arranged in rows turning out perpendicular to receptacle surface, outermost cells elongate club-shaped, 15–40 × 8–20 µm. *Medullary excipulum* 125–150 µm broad, of interwoven *textura intricata*, hyphae 2.0–5.0 µm broad. *Asci* pleurorhynchous, tapering, 8-spored, 260–290 × 16–21 µm. *Ascospores* ellipsoid, with one large oil drop when mature, 20–23 × 11–13 µm, [Lm × Wm = 21.5 × 12.1 µm, Q = 1.57–1.91, Q_{av} = 1.77 ± 0.11]. *Paraphyses* filiform, septate, pale brown, 5.0–8.0 µm wide at clavate to subcapitate tips and 2.0–4.0 µm below.

Habitat: Scattered on the ground in broadleaf forest.

Distribution: Known from Hebei Province, Northern China.

Specimens examined: **China**, Hebei Province, Xinglong County, on the ground in broadleaf forest, alt. 946 m, 22 Aug. 2020, *G.Q. Cheng* (**holotype** BJTC C351-A, GenBank Acc. No.: ITS = OR355170, nrLSU = OR355341, *tef1-α* = OR359078, *rpb2* = OR359189, *hsp* = OR366143); *ibid*., (BJTC C351-B).

Notes: *Helvella pseudoelastica* was nested in the *capucina-danica* lineage, *Elastica* clade (Fig. 1). Morphologically, it is difficult to separate *H. pseudoelastica* from the species of *capucina-danica* lineage, *bicolor-elastica* lineage and *carnosa* lineage in the *Elastica* clade by morphology alone. Most of these specimens had been misidentified as *H. elastica* during past decades. The stipe with distinct pinkish tint may be unique for this new species, but more specimens are needed to confirm this observation. *Helvella pseudoelastica* is closely related to *H. panormitana*, but there are two *hsp*, six *rpb2*, five nrLSU, and 12 *tef1-α* substitutions between them. *Helvella pseudoelastica* shares less than 93.08 % similarity in the ITS region with other *Helvella* species. An ITS specimen-sequence (GenBank KR673633) from South Korea matched *H. pseudoelastica* in our phylogenetic analysis (Fig. S3), which indicated that *H. pseudoelastica* also occurs in South Korea.

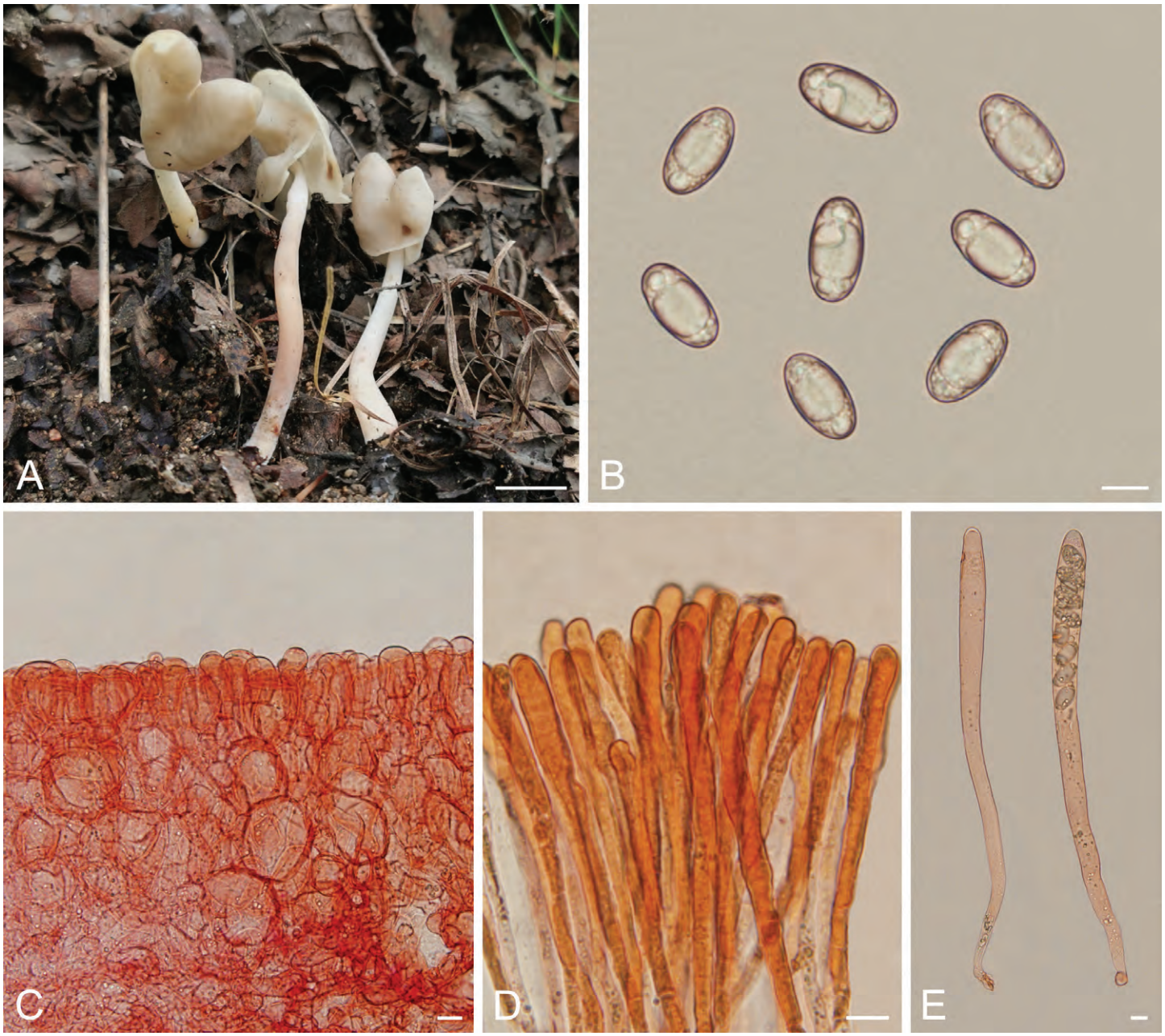

Fig. 13. *Helvella pseudoelastica* (BJTC C351-A, holotype). **A.** Apothecia. **B.** Ascospores in water. **C.** Ectal excipulum in Congo Red. **D.** Paraphyses in Congo Red. **E.** Immature asci in Congo Red. Scale bars: A = 1 cm; B–E = 10 µm.

Helvella pseudofallax L. Fan, N. Mao & Y.Y. Xu, ***sp. nov.*** MycoBank MB 849620. Fig. 14.

Etymology: *pseudofallax*, referring to its morphological similarity to *H. fallax*.

Apothecia stipitate-capitate; cap saddle-shaped or irregularly lobed, 0.6–1.0 cm high, 0.7–1.8 cm broad, at first margin adhered to stipe, then occasionally irregularly folded and free from stipe with age; hymenium grey, dark grey to blackish, becoming greyish black when dry; receptacle surface subpubescent, pale grey, becoming greyish black to black brown when dry; stipe subpubescent, terete, 1.5–5.0 cm high, 0.2–0.6 cm broad, solid or hollow, grey, becoming greyish black when dry. *Ectal excipulum* 150–200 µm broad, of *textura angularis*, cells hyaline to pale brown, extending into fascicled hyphoid hairs in outer ectal excipulum, hairs multiseptated, cells elongate club-shaped, 20–45 × 9–20 µm. *Medullary excipulum* of interwoven *textura intricata*, 200–350 µm thick, hyphae, 2.0–6.5 µm broad. *Asci* pleurorhynchous, tapering, 8-spored, 230–300 × 13–19 µm. *Ascospores* ellipsoid, with one large oil drop when mature, 15.5–19.5 × 9.5–11 µm, [Lm × Wm = 17.5 × 10.3 µm, Q = 1.55–1.90, Q_{av} = 1.70 ± 0.08]. *Paraphyses* filiform, septate, pale brown, 6.0–10.0 µm wide at clavate to subcapitate tips and 2.0–4.5 µm below.

Habitat: Scattered on the ground in broadleaf forest dominated by *Populus* sp.

Distribution: Known from Hebei and Shanxi Province, Northern China.

Specimens examined: **China**, Shanxi Province, Lvliang City, Xing County, Heichashan mountains, on the ground in broadleaf forest dominated

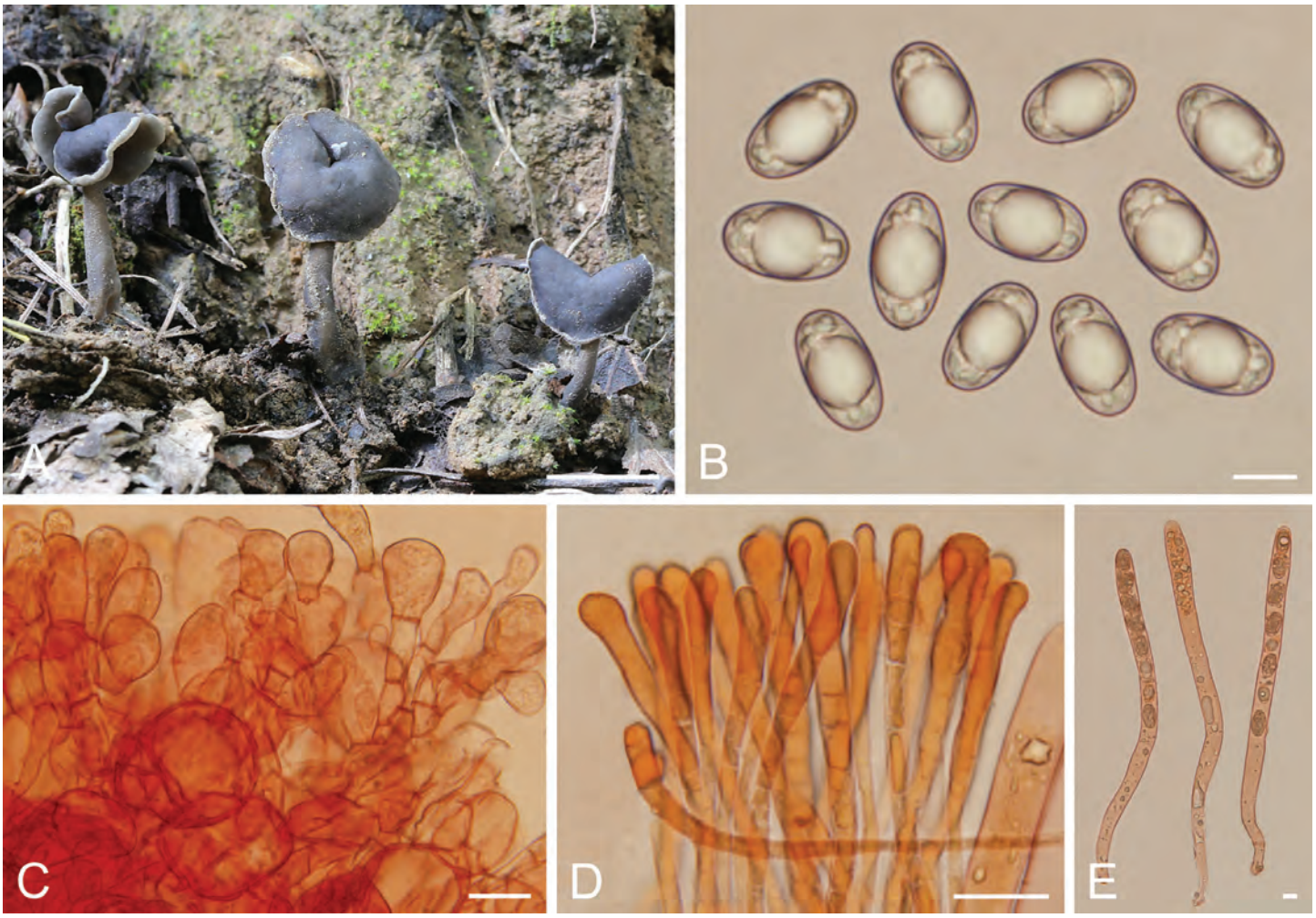

Fig. 14. *Helvella pseudofallax* (HSA 356, holotype). **A.** Apothecia. **B.** Ascospores in water. **C.** Ectal excipulum in Congo Red. **D.** Paraphyses in Congo Red. **E.** Immature asci in Congo Red. Scale bars: A = 1 cm; B, E = 10 µm; C, D = 20 µm.

by *Populus* sp., alt. 1 590 m, 5 Sep. 2018, *J.Z. Cao* (**holotype** HSA 356, GenBank Acc. No.: ITS = OR355083, nrLSU = OR355253, *tef1-α* = OR359015, *rpb2* = OR359138, *hsp* = OR366080); *ibid*., Xinzhou City, Wutai County, Wutaishan mountains, on the ground in broadleaf forest dominated by *Populus* sp., alt. 1 910 m, 3 Sep. 2020, *J.Z. Cao* (BJTC FM1148); Hebei Province, Zhangjiakou City, Chicheng County, on the ground in broadleaf forest, alt. 1 314 m, 26 Aug. 2020, *H. Zhou* (BJTC ZH1283).

Notes: *Helvella pseudofallax* was phylogenetically placed in the *fallax-pezizoides* lineage of the *Elastica* clade (Fig. 1). *Helvella fallax* and *H. pulla* are highly similar to the present species in morphology, but the pubescent receptacle and slightly reflexed cap margin separate it from the two former species (Skrede *et al.* 2017, 2020). In addition, six *hsp*, nine *rpb2*, 19 LSU, and 20 *tef1-α* substitutions separated this new species from *H. fallax*; 12 *hsp*, nine *rpb2*, and 21 LSU substitutions from *H. pulla*. *Helvella pseudofallax* shares less than 93.74 % similarity in the ITS region with other *Helvella* species.

Helvella pseudopezizoides L. Fan, N. Mao & Y.Y. Xu, ***sp. nov.*** MycoBank MB 849621. Fig. 15.

Etymology: *pseudopezizoides*, referring to the similarity to *H. pezizoides*.

Apothecia stipitate-capitate; cap saddle-shaped, or irregularly lobed, margin adnate to stipe, 0.9–2.0 cm high, 0.7–2.5 cm broad; hymenium grey, dark grey to grey blackish, becoming black when dry, slightly wrinkled with age; receptacle surface pubescent to villose, greyish black, becoming black when dry; stipe terete, 1.5–3.0 cm high, 0.2–0.7 cm broad, solid or hollow, concolourous with receptacle surface, becoming black when dry, occasionally with grooves. *Ectal excipulum* 100–200 µm broad, of *textura angularis*, cells hyaline to pale brown, extending into fascicled hyphoid hairs in outer ectal excipulum, hairs multiseptated, cells elongate club-shaped, 20–45 × 8–16 µm. *Medullary excipulum* 300–400 µm broad, of interwoven *textura intricata*, hyphae 2.0–6.0 µm broad. *Asci* pleurorhynchous, tapering, 8-spored, 230–300 × 13–18 µm. *Ascospores* ellipsoid, with one large oil drop when mature, 16–19.5 × 10.5–12 µm, [Lm × Wm = 18.1 × 11.2 µm, Q = 1.50–1.76, Q_{av} = 1.62 ± 0.06]. *Paraphyses* filiform, septate, pale brown, 6.0–11.0 µm wide at clavate to subcapitate tips and 2.0–4.5 µm below.

Habitat: Scattered on the ground in forest dominated by *Quercus* sp.

Distribution: Known from Shanxi Province, Northern China.

Specimens examined: **China**, Shanxi Province, Jingcheng City, Qinshui County, Shangwoquan Village, on the ground in broadleaf forest

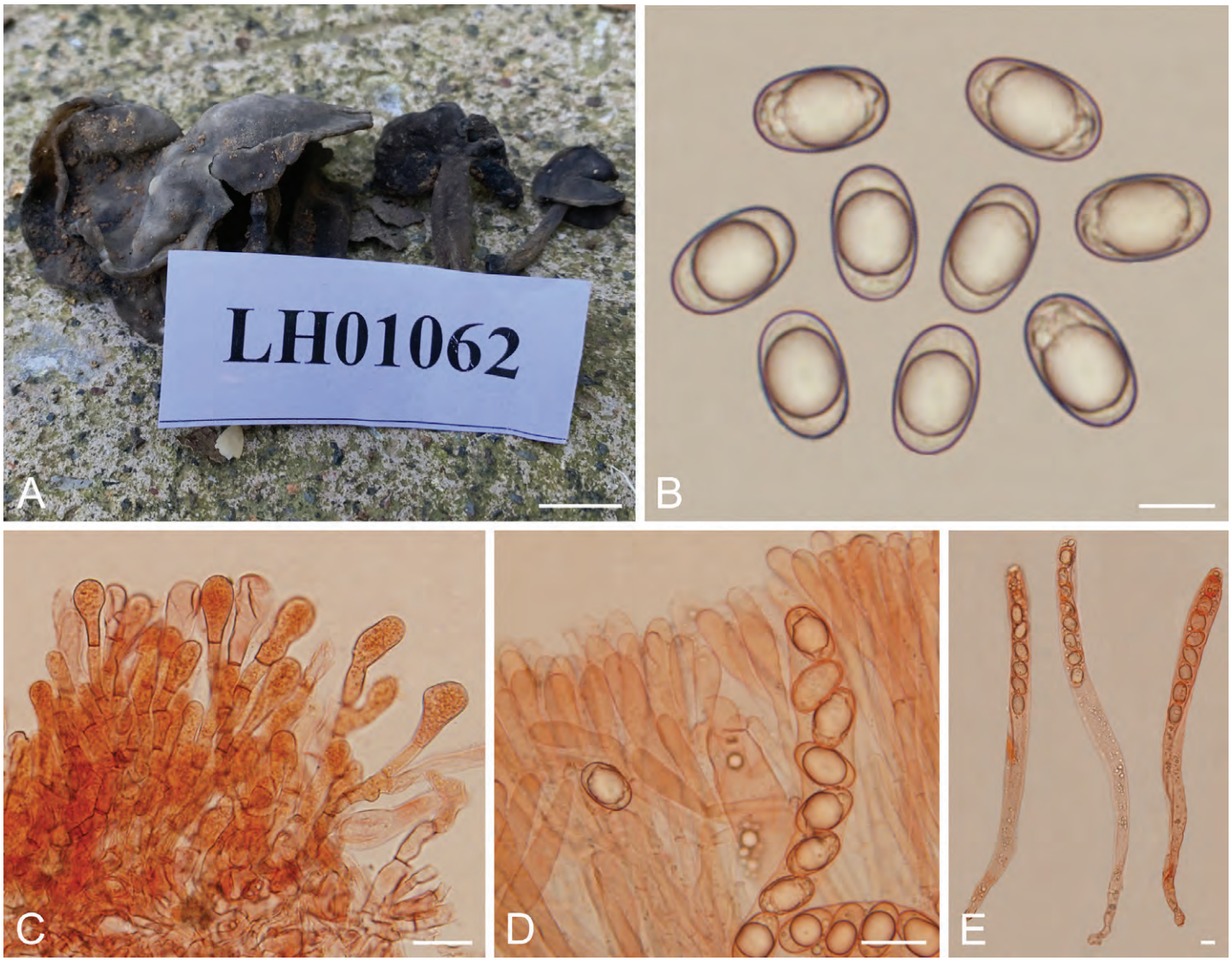

Fig. 15. *Helvella pseudopezizoides* (BJTC FM1045-A, holotype). **A.** Apothecia. **B.** Ascospores in water. **C.** Ectal excipulum in Congo Red. **D.** Asci and paraphyses in Congo Red. **E.** Asci in Congo Red. Scale bars: A = 1 cm; B, E = 10 µm; C, D = 20 µm.

dominated by *Quercus* sp., alt. 1 170 m, 25 Aug. 2020, *H. Liu* (**holotype** BJTC FM1045-A, GenBank Acc. No.: ITS = OR355089, nrLSU = OR355259, *tef1-α* = OR359020, *rpb2* = OR359143, *hsp* = OR366085); *ibid*., (BJTC FM1045-B).

Notes: *Helvella pseudopezizoides* is diagnosed by its overall dark grey to blackish ascomata with saddle-shaped or irregularly lobed cap and thin terete stipe. It was phylogenetically nested in the *fallax-pezizoides* lineage of the *Elastica* clade (Fig. 1). *Helvella pezizoides* is highly similar to the present species, but it differs by its somewhat inrolled cap margin, and smaller ascospores (14.5–16.5 × 8.5–9.6 µm) (Skrede *et al.* 2020). Other species in the *fallax-pezizoides* lineage are also somewhat similar in morphology, including *H. fallax*, *H. caespitosa*, *H. pseudofallax, H. pulla, H. subglabra*, *H. subglabroides,* but the cap colour in all of them is grey or dark grey, not blackish to black, then the stipe is pale at least near base (Skrede *et al.* 2017, 2020, the present study). In addition, three *hsp*, three *rpb2*, 20 nrLSU, and 16 *tef1-α* substitutions separated this new species from *H. fallax*; 14 *hsp*, and 26 nrLSU substitutions from *H. caespitosa*; 15 *hsp*, 11 *rpb2*, 28 nrLSU, and 26 *tef1-α* substitutions from *H. pezizoides*; 12 *hsp*, eight *rpb2*, 23 nrLSU, and 40 *tef1-α* substitutions from *H. pseudofallax*; seven *hsp*, three *rpb2*, and 23 nrLSU from *H. pulla*; four *hsp*, and five *rpb2* from *H. subglabra*; five *hsp*, three *rpb2*, 24 nrLSU, and 21 *tef1-α* substitutions from *H. subglabroides*. An ITS sequence (GenBank KX444420) from an ECM root tip of *Quercus liaotungensis* in Beijing matched this species (Fig. S3), indicating that this species could form ectomycorrhiza with this host. *Helvella pseudopezizoides* shares less than 89.95 % similarity in the ITS region with other *Helvella* species.

Helvella sinocrispa L. Fan, N. Mao & Y.Y. Xu, ***sp. nov.*** MycoBank MB 849622. Fig. 16.

Etymology: *sinocrispa*, referring to its similarity to *H. crispa* in morphology.

Apothecia stipitate-capitate; cap saddle-shaped to irregularly lobate, 1.4–2.5 cm high, 2.5–4 cm broad, at first margin rolled to hymenium, then expanded or cracked with age; hymenium glabrous, cream white to whitish, becoming brown to dark brown when dry; receptacle surface subpubescent, pale yellow to greyish yellow, becoming pale brown to yellowish brown when dry; stipe robust, 2.5–5.5 cm high, 1.0–2.6 cm broad, glabrous, white to dirty

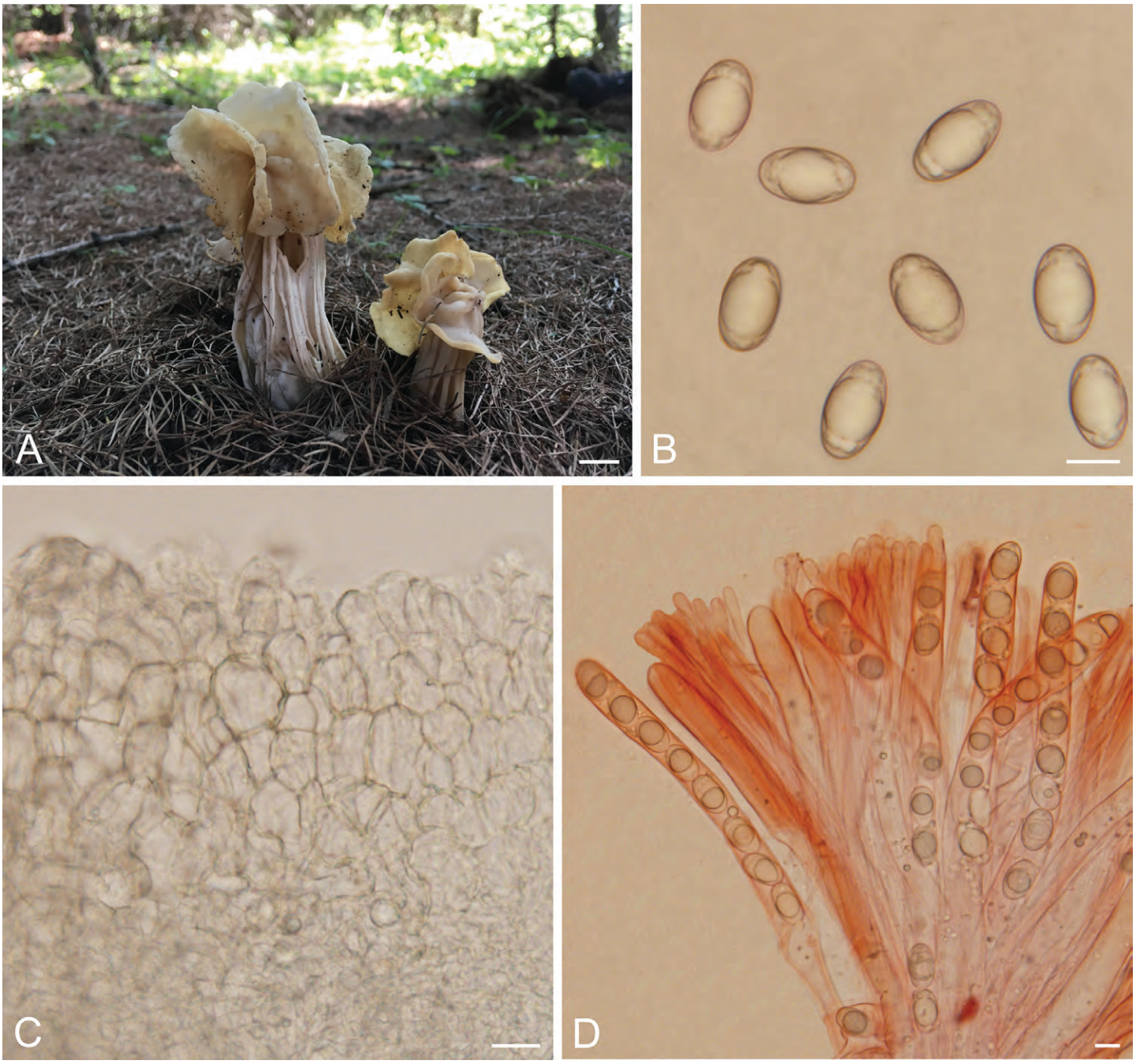

Fig. 16. *Helvella sinocrispa* (BJTC FM96-A, holotype). **A.** Apothecia. **B.** Ascospores in water. **C.** Ectal excipulum in water. **D.** Asci and paraphyses in Congo Red. Scale bars: A = 1 cm; B–D = 10 µm.

whitish, becoming pale yellow when dried, ribbed, blunt-edged, partly anastomosing and double-edged, with lacunae between ribs, chambered inside. *Ectal excipulum* 80–180 µm broad, of *textura angularis*, cells hyaline to pale brown, outermost cells catenuliform in long fascicled tufts, with cylindrical to subclavate, end cells 15–37 × 8.5–15 µm. *Medullary excipulum* 190–270 µm broad, of interwoven *textura intricata*, hyphae 2.5–5 µm broad. *Asci* pleurorhynchous, tapering, 8-spored, 255–285 × 13–16.5 µm. *Ascospores* ellipsoid, with one large oil drop when mature, 18–20 ×10.5–12 µm, [Lm × Wm = 19.3 × 11.2 µm, Q = 1.60–1.90, Q_{av} = 1.73 ± 0.08]. *Paraphyses* filiform, septate, hyaline to pale brown, 4.5–7 µm wide at tips and 2–3.5 µm below.

Habitat: Solitary or scattered on the ground in coniferous forest dominated by *Larix principis-rupprechtii* and *Picea asperata*.

Distribution: Known only from Shanxi Province, Northern China.

Specimens examined: **China**, Shanxi Province, Xinzhou City, Ningwu County, Guancenshan mountains, on the ground in coniferous forest dominated by *Larix principis-rupprechtii* and *Picea asperata*, alt. 2 230 m, 24 Aug. 2017, *M. Chen* (**holotype** BJTC FM96-A, GenBank Acc. No.: ITS = OR355155, nrLSU = OR355326, *tef1-α* = OR359068, *rpb2* = OR359180, *hsp* = OR366133); *ibid*., (BJTC FM96-B).

Notes: *Helvella sinocrispa* is recognized by its isolated phylogenetic position in the *Crispa* clade (Fig. 1). Morphologically it is highly similar to three other species of this clade, namely *H. crispa*, *H. orienticrispa*, and *H. pseudoreflexa*. In fact, it is difficult to distinguish these four species by morphology alone. DNA analysis is therefore needed to accurately identify

them. Molecularly, three *hsp*, six *rpb2*, five nrLSU, and 11 *tef1-α* substitutions separated this new species from *H. crispa*; three *hsp*, four *rpb2*, one nrLSU, and 12 *tef1-α* substitutions from *H. orienticrispa*; three *hsp*, four *rpb2*, two nrLSU, and 11 *tef1-α* substitutions from *H. pseudoreflexa*. Four ITS sequences downloaded from GenBank matched *H. sinocrispa* in our analysis (Fig. S2). These sequences are extracted from ascomata and ectomycorrhizal root tips from China, Europe or the USA. These results implied that *H. sinocrispa* is widely distributed in Northern Hemisphere. DNA analysis revealed that *H. sinocrispa* shares less than 94.04 % similarity in ITS region with other *Helvella* species, supporting it as a distinct species.

Helvella sinohyperborea L. Fan, N. Mao & Y.Y. Xu, ***sp. nov.*** MycoBank MB 849623. Fig. 17.

Etymology: *sinohyperborea*, referring to its close phylogenetic relationship to *H. hyperborea*.

Apothecia stipitate-cupulate; cap regular cupulate or irregularly undulate with wrinkled surface, 1.3–2.0 cm high, 2.1–6.0 cm broad; hymenium dark brown to blackish, becoming black when dry; receptacle surface upper part slightly lighter than the hymenium, below gradually white, becoming black when dry; stipe short, 1.0–2.5 cm high, 0.5–0.8 cm broad, hollow, white, becoming pale yellow to pale brown when dry, ribbed, blunt-edged, partly anastomosing and double-edged, occasionally with lacunae between ribs, ribs extending onto the receptacle. *Ectal excipulum* 100–150 µm broad, of *textura angularis*, cells hyaline to pale brown, extending into fascicled hyphoid hairs in outer ectal excipulum, hairs multiseptated, cells elongate club-shaped, 15–40 × 11–19 µm. *Medullary excipulum* 400–700 µm broad, of interwoven *textura intricata*, hyphae 2.0–6.0 µm broad. *Asci* pleurorhynchous, tapering, 8-spored, 240–300 × 13–19 µm. *Ascospores* ellipsoid, with one large oil drop when mature, 16–18.5 × 11–12.5 µm, [Lm × Wm = 17.5 × 11.8 µm, Q = 1.38–1.58, Q_{av} = 1.49 ± 0.05]. *Paraphyses* filiform, septate, pale brown, 4.5–6.0 µm wide at clavate to subcapitate tips and 1.5–3.5 µm below.

Habitat: Scattered on the ground in coniferous forest dominated by *Larix principis-rupprechtii.*

Distribution: Known from Shanxi Province, Northern China.

Specimens examined: **China**, Shanxi Province, Xinzhou City, Ningwu County, Guancen mountains, on the ground in coniferous forest dominated by *Larix principis-rupprechtii*, alt. 2 220 m, 24 Aug. 2017, *X.Y. Yan* (**holotype** BJTC FM105, GenBank Acc. No.: ITS = OR355132, nrLSU = OR355303, *tef1-α* = OR359056, *rpb2* = OR359170, *hsp* = OR366121); *ibid*., alt. 2 099 m, 25 Aug. 2017, *X.Y. Yan* (BJTC FM165).

Notes: *Helvella sinohyperborea* is characterized by the cup-like or undulate cap, the short robust ribbed stipe. Our present analysis places *H. sinohyperborea* in the *hyperborean-tinta* lineage in the *Lacunosa* clade, closely related to *H. hyperborea* and *H. tinta*. *Helvella hyperborea* is a Northern European species. It is differentiated from *H. sinohyperborea* by its regular cup-like cap, long stipe and pale brown hymenium (Skrede *et al.* 2017). *Helvella tinta* is a species known from southwestern China. It

Fig. 17. *Helvella sinohyperborea* (A, D–G. BJTC FM105, holotype. B, C. BJTC FM165). **A.** Apothecium. **B, C.** Apothecium infected by *Hypomyces* sp. **D.** Ascospores in water. **E.** Asci and paraphyses in Congo Red. **F.** Ectal excipulum in water. **G.** Immature asci in Congo Red. Scale bars: A–C = 1 cm; D–G = 10 µm.

is distinguished from *H. sinohyperborea* by its cup-like cap of ascomata with a consistently mottled, greyish to dark brown hymenium and receptacle surface (Hyde *et al.* 2016). Molecularly, two *hsp* and one *rpb2* substitutions separate this new species from *H. hyperborea*; four *hsp*, five nrLSU, and one *tef1-α* substitutions from *H. tinta*. *Helvella sinohyperborea* shared less than 97.83 % similarity in ITS region with other *Helvella* species. Two ITS sequences downloaded from GenBank matched *H. sinohyperborea* in our analysis (Fig. S4). These sequences are both extracted from ectomycorrhizal root tips of *Picea crassifolia*, from Inner Mongolia, Ningxia Hui Autonomous Region. This indicated that *H. sinohyperborea* also occurs in other regions of China, and could form ectomycorrhiza with *P. crassifolia*.

Helvella subglabroides L. Fan, N. Mao & Y.Y. Xu, ***sp. nov.*** MycoBank MB 849624. Fig. 18.

Etymology: *subglabroides,* referring to its high similarity to *H. subglabra* in appearance of its ascomata.

Apothecia stipitate-capitate; cap saddle-shaped, 0.7–2.5 cm high, 0.8–2.0 cm broad, at first margin adhered to stipe, then reflexed with age; hymenium grey to greyish yellow, becoming dark grey to greyish black when dry; receptacle surface glabrous to fine pubescent, concolourous with hymenium, becoming brown when dry; stipe terete, 2.0–5.0 cm high, 0.2–0.4 cm broad, solid, subpubescent, greyish white to grey, becoming dark grey when dry, base occasionally with inconspicuous grooves and white mycelia. *Ectal excipulum* 50–100 µm broad, of *textura angularis*, cells hyaline to pale brown, arranged in rows turning out perpendicular to receptacle surface, outermost cells clavate, 20–45 × 9–20 µm. *Medullary excipulum* 100–200 µm broad, of interwoven *textura intricata*, hyphae 2.5–6.5 µm broad. *Asci* pleurorhynchous, tapering,

Fig. 18. *Helvella subglabroides* (BJTC C614). **A.** Apothecia. **B.** Ascospores in water. **C.** Ectal excipulum in Congo Red. **D.** Asci and paraphyses in Congo Red. **E.** Immature asci in Congo Red. Scale bars: A = 1 cm; B, E = 10 µm; C, D = 20 µm.

8-spored, 200–260 × 12.5–18.5 µm. *Ascospores* ellipsoid, with one large oil drop when mature, 15–19.5 × 9–11 µm, [Lm × Wm = 17.2 × 10 µm, Q = 1.5–2, Q_{av} = 1.73 ± 0.10]. *Paraphyses* filiform, septate, yellowish brown, 5.5–11.5 µm wide at clavate to subcapitate tips and 2.5–4.0 µm below.

Habitat: Scattered on the ground in mixed coniferous and broadleaf forest.

Distribution: Known from Hebei, Shanxi, and Yunnan Province, China.

Specimens examined: **China**, Shanxi Province, Changzhi City, Qinyuan County, Lingkong mountains, on the ground in coniferous forest and broadleaf mixed forest, 15 Aug. 2022, *N. Mao* (**holotype** BJTC FM2686, GenBank Acc. No.: ITS = OR355088, nrLSU = OR355258, *tef1-α* = OR359019, *rpb2* = OR359142, *hsp* = OR366084); *ibid*., Jincheng City, Qinshui County, Shangwoquan Village, on the ground in broadleaf forest dominated by *Quercus* sp., 35°36′57″N, 112°3′7″E, alt. 1 170 m, 25 Aug. 2020, *H. Liu* (BJTC FM1049); Hebei Province, Zhangjiakou City, Chicheng County, Dahaituo Township, on the ground in coniferous forest and broadleaf mixed forest, alt. 1 222 m, 26 Aug. 2020, *G.Q. Cheng* (BJTC C614); Yunnan Province, Lijiang City, Jinshan mountains, 12 Sep. 2012, *Q. Zhao* (HKAS 78939); *ibid*., (HKAS 78940).

Notes: Our present analysis places *H. subglabroides* in the *fallax-pezizoides* lineage, *Elastica* clade, and is closely related to the North American *H. subglabra* (Fig. 1). Morphologically, *H. subglabroides* is also similar to *H. subglabra*, both having a saddle-shaped cap. However, the two species can be separated by their hymenium colour, which is grey to greyish yellow in the former but dark grey in the latter (Weber 1972). Molecularly, three *hsp*, four *rpb2*, eight nrLSU substitutions distinguish *H. subglabra* from *H. subglabroides*. *Helvella subglabroides* shares less than 96.15 % similarity in ITS region with other *Helvella* species.

Helvella sulcatoides L. Fan, N. Mao & Y.Y. Xu, ***sp. nov.*** MycoBank MB 849625. Fig. 19.

Etymology: *sulcatoides*, referring to its similarity to *H. sulcata.*

Apothecia stipitate-capitate; cap saddle-shaped, mostly bilobate, 1.3–1.8 cm broad, 1.3–2.0 cm high, margin attached to stipe;

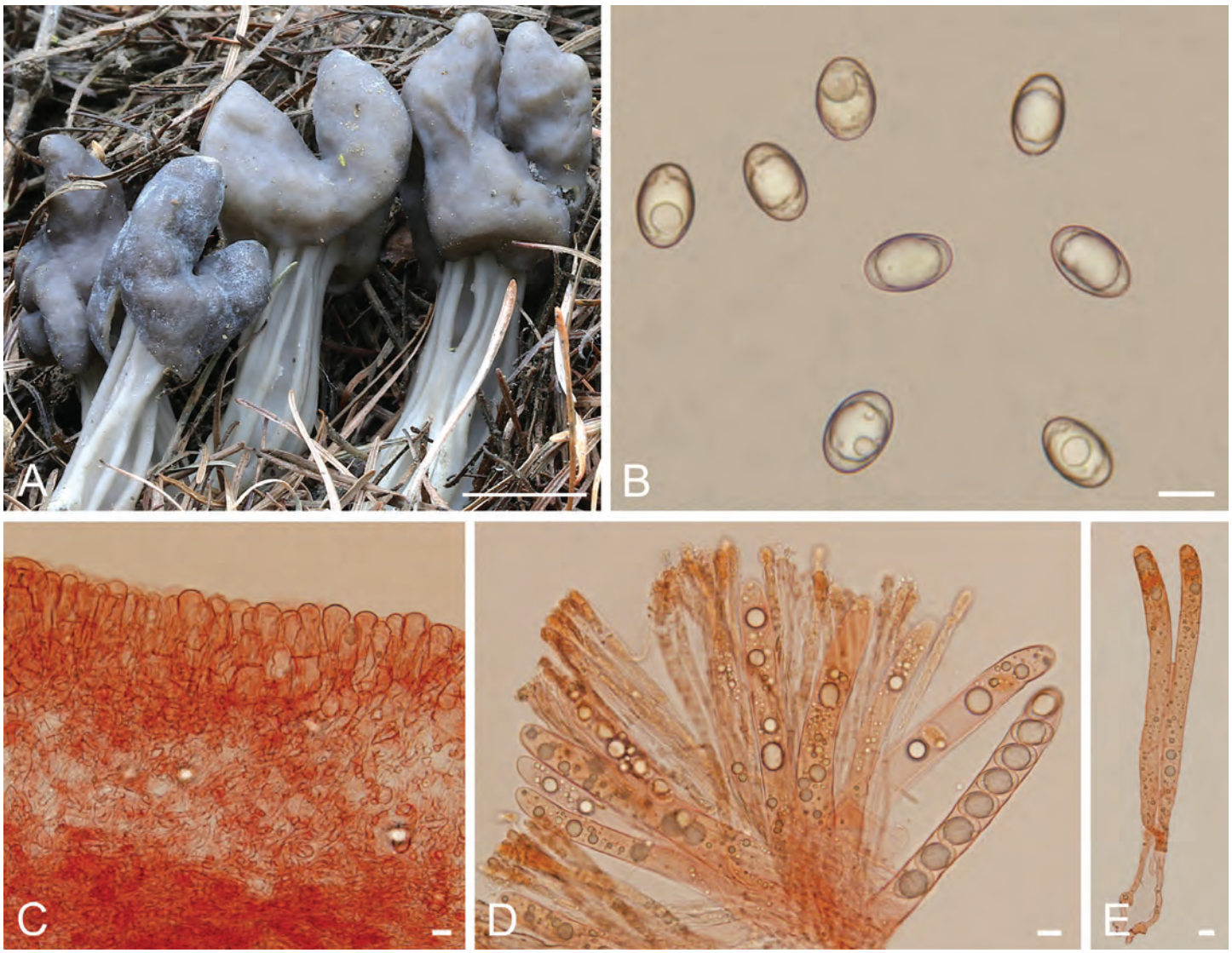

Fig. 19. *Helvella sulcatoides* (BJTC FM1416, holotype). **A.** Apothecia. **B.** Ascospores in water. **C.** Ectal excipulum in Congo Red. **D.** Asci and paraphyses in Congo Red. **E.** Immature asci in Congo Red. Scale bars: A = 1 cm; B–E = 10 µm.

hymenium grey, dark grey to black grey, becoming black when dried, slightly wrinkled; receptacle surface pale grey to greyish brown, becoming greyish brown when dried, smooth, without ribs on receptacle surface; stipe 0.5–0.9 cm broad, 1.2–2.4 cm high, greyish white to black grey, becoming dark brown to black brown when dry, ribbed, longitudinal ribs high and prominent, sharp, occasionally double-edged, sometimes with a few deep 'holes' between ribs. *Ectal excipulum* of *textura angularis*, 65–100 µm thick, cells hyaline to pale brown, arranged in rows turning out perpendicular to receptacle surface, outermost cells arranged in dense, club-shaped, 13–40 × 7–18 µm. *Medullary excipulum* of interwoven *textura intricata*, 130–200 µm thick, hyphae 2.5–6.5 µm broad. *Asci* pleurorhynchous, tapering, 8-spored, 225–275 × 14–18 µm. *Ascospores* ellipsoid, with one large oil drop when mature, 14.5–16.5 × 9–10.5 µm, [Lm × Wm = 15.9 × 9.9 µm, Q = 1.41–1.74, Q_{av} = 1.56 ± 0.08]. *Paraphyses* filiform, septate, hyaline to pale brown, 4–6 µm wide at tips and 2.5–4 µm below.

Habitat: Solitary or scattered on the ground in coniferous forest dominated by *Larix principis-rupprechtii* and *Picea asperata*.

Distribution: Known from Beijing and Shanxi Province, Northern China.

Specimens examined: **China**, Shanxi Province, Xinzhou City, Wutai County, Wutaishan mountains, on the ground in coniferous forest dominated by *Larix principis-rupprechtii* and *Picea asperata*., 11 Aug. 2020, *H. Liu* (**holotype** BJTC FM1416, GenBank Acc. No.: ITS = OR355119, nrLSU = OR355290, *tef1-α* = OR359043, *rpb2* = OR359160, *hsp* = OR366108); *ibid*., Lvliang City, Jiaocheng County, Guandishan mountains, 37°52′16′′N, 111°30′25′′E, alt. 2 003 m, 7 Sep. 2017, *J.Z. Cao* (BJTC FM263); Beijing, Huairou District, Labagoumen, alt. 1 345 m, 25 Aug. 2020, *H. Zhou* (BJTC ZH1231).

Notes: Phylogenetically, *H. sulcatoides* is placed in the *sulcata-phlebophoroides* lineage, *Lacunosa* clade (Fig. 1). It is closely related and similar to *H. borealis* and *H. sulcata*, but *H. borealis* is differentiated from *H. sulcatoides* by its grey white hymenium, slightly broader paraphyses at the apex (6.5–10.5 µm) and habit of growing on rotten wood (Wang *et al.* 2023a); *H. sulcata* by its black hymenium, large asci (290–320 × 13–16 µm), and broad spores (14.8–16.8 × 10.5–13.2 µm) (Skrede *et al.* 2017). *Helvella phlebophoroides*, a species recently described from Europe, is also closely related to *H. sulcatoides*, but can be separated by its irregularly radiating ribs on the receptacle surface, and large asci (280–320 × 12–15 µm) (Skrede *et al.* 2020). In addition, one *hsp*, five *tef1-α* substitutions separated *H. sulcatoides* from *H. borealis*; one *hsp*, four nrLSU, three *tef1-α* substitutions from *H. sulcata*; four *hsp*, six *rpb2*, and eight nrLSU substitutions from *H. phlebophoroides*.

Helvella xiaohuipan L. Fan, N. Mao & Y.Y. Xu, ***sp. nov.*** MycoBank MB 849626. Fig. 20.

Etymology: *xiaohuipan,* Chinese, meaning this *Helvella* is a small-sized and grey species with cup-like cap.

Apothecia stipitate-cupulate; regular cupulate to saucer-shaped, 0.3–0.7 cm high, 0.7–2.0 cm broad; hymenium grey to dark grey, becoming brown to black-brown when dry; receptacle surface pubescent, concolourous with hymenium, becoming greyish brown when dry; stipe terete, slender, 1.2–1.8 cm high, 0.15–0.35 cm broad, solid, yellowish white, becoming yellow when dry. *Ectal excipulum* 150–175 µm broad, of *textura angularis*, cells hyaline to pale brown, extending into fascicled hyphoid hairs in outer ectal excipulum, hairs multiseptated, cells elongate club-shaped, 12–37 × 10–20 µm. *Medullary excipulum* 250–300 µm broad, of interwoven *textura intricata*, hyphae 2.0–5.0 µm broad. *Asci* pleurorhynchous, tapering, 8-spored, 235–275 × 14–20 µm. *Ascospores* ellipsoid, with one large oil drop when mature, 17–19.5 × 10.5–12 µm, [Lm × Wm = 18 × 11.4 µm, Q = 1.46–1.72, Q_{av} = 1.58 ± 0.06]. *Paraphyses* filiform, septate, pale brown, 4.5–6.0 µm wide at clavate to subcapitate tips and 3.5–4.5 µm below.

Habitat: Scattered on the ground in broadleaf forest and coniferous forest.

Distribution: Known from Hebei and Shanxi Province, Northern China.

Specimens examined: **China**, Shanxi Province, Yuncheng City, Xia County, Sijiao Town, on the ground in broadleaf forest dominated by *Quercus* sp., 35°07′89′′N, 111°40′09′′E, alt. 970 m, 12 Aug. 2022, *N. Mao* (**holotype** BJTC FM2317, GenBank Acc. No.: ITS = OR355079, nrLSU = OR355249, *tef1-α* = OR359011, *rpb2* = OR359134, *hsp* = OR366076); Hebei Province, Tangshan City, Zhangzhuangzi Village, on the ground in broadleaf forest dominated by *Castanea mollissima*, 40°14′21′′N, 117°51′15′′E, alt. 107 m, 17 Sep. 2017, *T. Ling* (BJTC FM367).

Notes: *Helvella xiaohuipan* is characterized by its grey and cup-like cap, pubescent receptacle surface, yellowish white slender terete stipe and ellipsoid ascospores. *Helvella xiaohuipan* was phylogenetically nested in its own lineage (*xiaohuipan* lineage) in the *Elastica* clade, sister to the *fallax-pezizoides* lineage (Fig. 1). Currently, there are only two species recognized in this lineage, both from China. *Helvella fibrosa* (= *H. villosa*) in the *fibrosa-macropus* lineage is similar to *H. xiaohuipan* in colour and shape of ascomata (Dissing & Nannfeldt 1966). However, *H. fibrosa* differs from *H. xiaohuipan* by its grey stipe and ascospores longer than 20 µm. *Helvella pubescens* from the *rivularis-sublicia* lineage and *H. scyphoides* from the *hypocrateriformis* lineage also have a disk-like cap, but the colour of the cap is brown (Skrede *et al.* 2017) rather than grey as in *H. xiaohuipan*. Moreover, species in the *fallax-pezizoides* lineage have saddle-shaped ascocarps that make them easy to distinguish from the new species. An ITS specimen-sequence (GenBank JX462576, labelled as *Helvella cf. corium*) from China matched *H. xiaohuipan* in our phylogenetic analysis (Fig. S1), indicating that *H. xiaohuipan* also occurs in other regions of China. DNA analysis revealed that *H. xiaohuipan* shares less than 92.88 % similarity in ITS region with other *Helvella* species, supporting it as a distinct species.

Helvella galeriformis B. Liu & J.Z. Cao, *Acta Mycol. Sin*. **7**: 199. 1988, L. Fan, N. Mao & Y.Y. Xu, ***emend*.** Fig. 21.

Apothecia stipitate-capitate; cap irregularly hemisphere, irregularly umbrella type to irregularly saddle-shaped, 0.6–2 cm high, 1.5–3.5 cm broad, at first margin adhered to stipe, then more or less deflexed; hymenium greyish black, occasionally with olive green tinge; receptacle surface white, concolourous with stipe; stipe terete, 1.2–5.0 cm high, 0.3–0.7 cm broad, solid or hollow, cream to white, base slightly enlarged, with

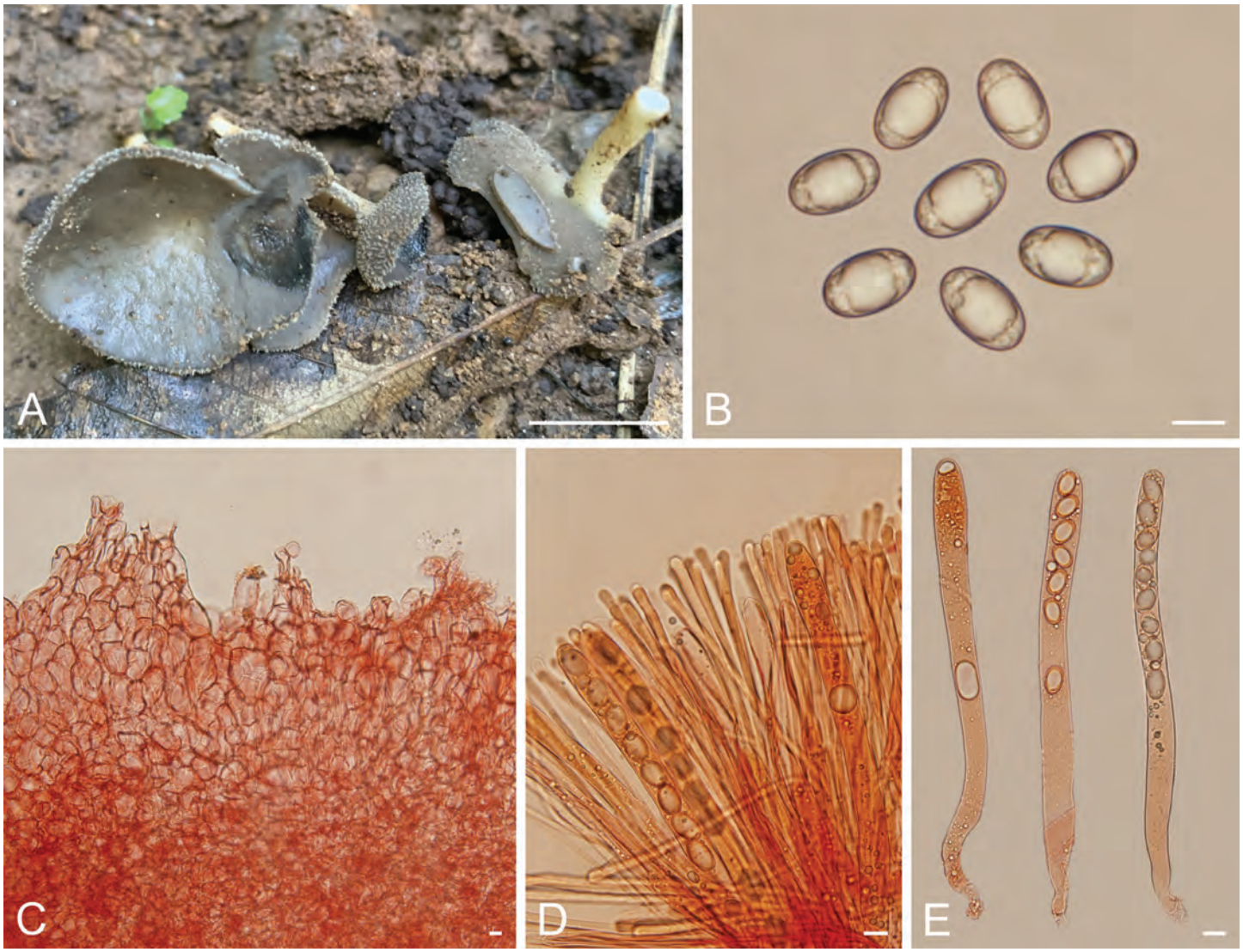

Fig. 20. *Helvella xiaohuipan* (BJTC FM2317, holotype). **A.** Apothecia. **B.** Ascospores in water. **C.** Ectal excipulum in Congo Red. **D.** Asci and paraphyses in Congo Red. **E.** Asci in Congo Red. Scale bars: A = 1 cm; B–E = 10 µm.

shallow grooves. *Ectal excipulum* 90–150 µm broad, of *textura angularis*, cells hyaline to pale brown, arranged in rows turning out perpendicular to receptacle surface, outermost cells clavate, 22–56 × 10–25 µm. *Medullary excipulum* 150–250 µm broad, of interwoven *textura intricata*, hyphae 2.5–6.5 µm broad. *Asci* pleurorhynchous, tapering, 8-spored, 300–360 × 15–20 µm. *Ascospores* ellipsoid, with one large oil drop when mature, 19–22.5 × 11.5–13.5 µm, [Lm × Wm = 20.8 × 12.5 µm, Q = 1.5–1.8, Q_{av} = 1.65 ± 0.07]. *Paraphyses* filiform, 2.5–4.5 µm below, pale yellow to pale brown, septate, clavate to subcapitate, 6–10 µm wide at tips.

Habitat: Scattered on the ground in mixed coniferous and broadleaf forest.

Distribution: Known only from Shanxi Province, Northern China.

Specimens examined: **Lectotype** here designated, Liu & Cao (1988), *Acta Mycol. Sin*. **7**: 199. 1988, fig. 2, MycoBank MBT 10014903. **China**, Shanxi Province, Lvliang City, Jiaocheng County, Guandishan mountains, on the ground in coniferous forest dominated by *Larix principis-rupprechtii* and *Betula* sp., alt. 2 160 m, 28 Aug. 2018, *H. Liu* (**epitype** here designated HSA 232, MycoBank MBT 10014391, GenBank Acc. No.: ITS = OR355066, nrLSU = OR355236, *tef1-α* = OR359001, *rpb2* = OR359125, *hsp* = OR366063); *ibid*., *L.J. Guo* (HSA 240-B); *ibid*., on the ground in coniferous forest dominated by *Picea* sp., alt. 1 875 m, 25 Aug. 2022, *N. Mao* (BJTC FM2574).

Notes: The holotype of *H. galeriformis* collected from Guancenshan Mountains (cited as 'Gaunqin Mountain') in Shanxi Province (MHSU 452) has been lost. However, because Liu & Cao (1988) provided an illustration (Liu & Cao 1988; fig. 2), this is here designated as lectotype, allowing us to introduce an epitype based on recently collected material (HSA 232). Recently, we collected several specimens in the same region of the holotype of *H. galeriformis* (Liu & Cao 1988), but the swollen cells in the medullary excipulum were not observed. However, the diagnosed colour and peculiar shape of ascomata matched well with the original description of *H. galeriformis*. Considering the collecting site, habitat and morphology, we regard these specimens as conspecific to *H. galeriformis*. Therefore, we designate a lectotype and epitype for *H. galeriformis* here. *Helvella galeriformis* is sister to *H. brunneogaleriformis* in our phylogenetic analyses (Figs 1, 2). Morphologically, *H. brunneogaleriformis* differs from *H. galeriformis* by its brown hymenium without blackish tint, smaller ascospores (17–20.5

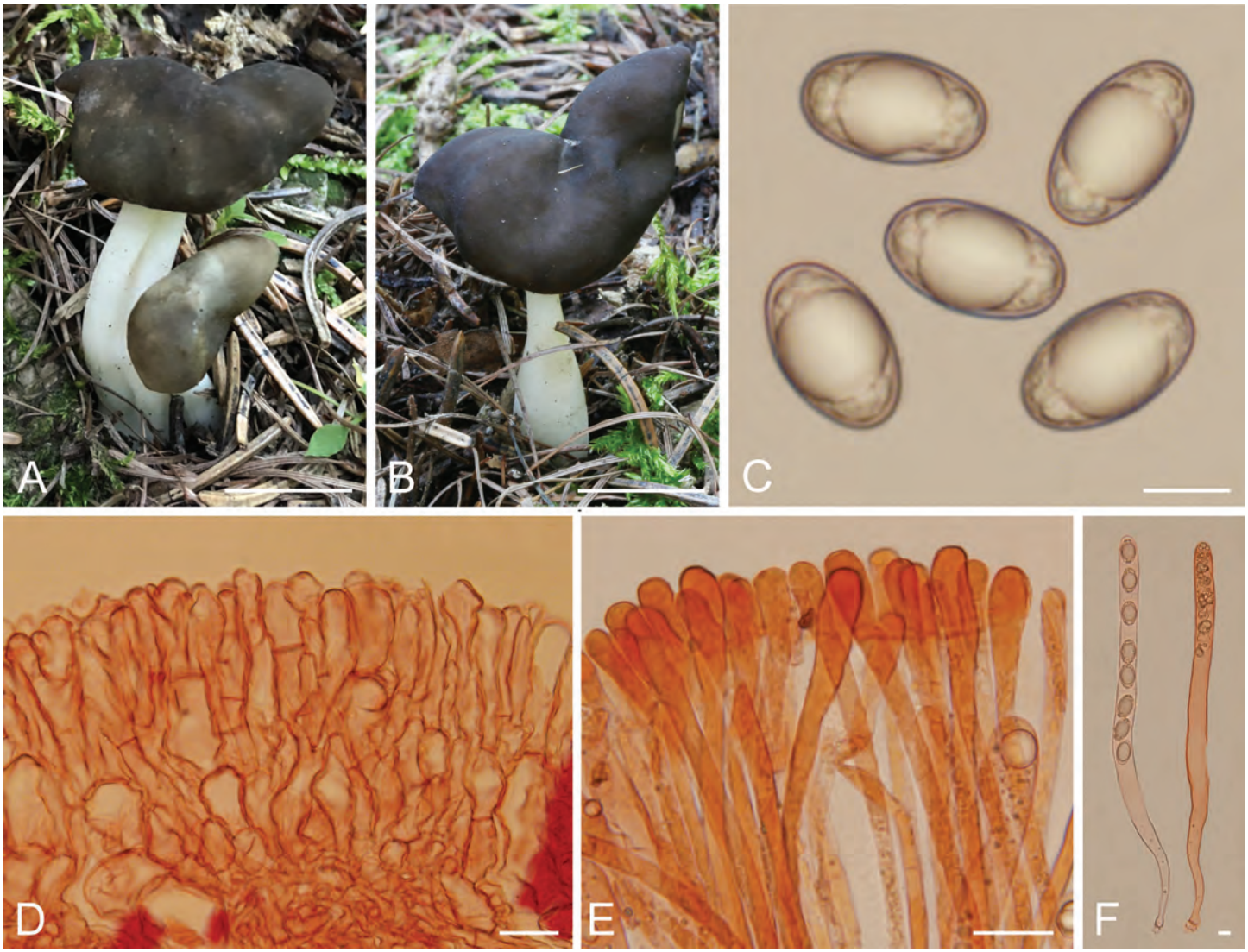

Fig. 21. *Helvella galeriformis* (HSA 232, epitype). **A, B.** Apothecium. **C.** Ascospores in water. **D.** Ectal excipulum in Congo Red. **E.** Paraphyses in Congo Red. **F.** Asci in Congo Red. Scale bars: A, B = 1 cm; C, F = 10 µm; D, E = 20 µm.

× 10.5–12.5 µm), and broader paraphyses at the apex (6–13 µm). Molecularly, *H. brunneogaleriformis* deviates consistently in one *hsp*, one *tef1-α*, and eight nrLSU substitutions from *H. galeriformis*. *Helvella galeriformis* shares less than 97.8 % similarity in the ITS region with *H. brunneogaleriformis*.

Helvella carnosa Skrede *et al*., *Persoonia* **39**: 237. 2017. Fig. 22.

Habitat: Scattered on the ground in coniferous forest or broadleaf forest.

Distribution: Known from Northern area in China.

Specimens examined: **China**, Beijing, Yanqing County, Songshan Mountains, alt. 812 m, 31 Aug. 2017, *C.L. Hou* (BJTC BP030); *ibid*., (BJTC BP043), *ibid*., alt. 816 m, *C.L. Hou* (BJTC BP060); *ibid*., alt. 919 m, 5 Sep. 2018, *C.L. Hou* (BJTC BP718); *ibid*., alt. 1 010 m, 5 Sep. 2018, *C.L. Hou* (BJTC BP724); *ibid*., Badaling, alt. 608 m, 6 Sep. 2018, *X.Y. Shen*. (BJTC SBP287); *ibid*., Shanxi Province, Xing County, Heichashan Mountains, on the ground in broadleaf forest, alt. 1 590 m, 5 Sep. 2018, *J.Z. Cao* (HSA 360); *ibid*., Pu County, Wulushan mountains, on the ground in coniferous forest, alt. 1 700 m, 9 Sep. 2018, *L.J. Guo* (HSA 434); *ibid*., Pu County, Wulushan mountains, 10 Sep. 2017, *Y.Y. Xu* (BJTC FM297); *ibid*., (BJTC FM298), *ibid*., *J.Z. Cao* (BJTC FM316); *ibid*., on the ground in coniferous forest, alt. 1 739 m, 26 Aug. 2022, *N. Mao* (BJTC FM2619); *ibid*., Lvliang City, Jiaocheng County, Guandishan Mountains, on the ground in coniferous forest, alt. 2 003 m, 7 Sep. 2017, *T. Li* (BJTC FM274); *ibid*., Ningwu County, Guancenshan Mountains, on the ground in coniferous forest, alt. 1 346 m, 15 Oct. 2017, *X.Y. Yan* (BJTC FM376), *ibid*., Wutai County, Wutaishan Mountains, alt. 1 376 m, 29 Aug. 2019, *H. Liu* (BJTC FM953); *ibid*., Qinshui County, Lishan mountains, on the ground in coniferous and broad-leaved mixed forest, alt. 1 650 m, 24 Aug. 2020, *N. Mao* (BJTC FM1032); *ibid*., Loufan County, Yunding Mountains, on the ground in coniferous forest, alt. 1 639 m, 23 Aug. 2022, *N. Mao* (BJTC FM2478); *ibid*., 1 642 m, 23 Aug. 2022, *N. Mao* (BJTC FM2479), *ibid*., on the ground in broad-leaved mixed forest, 1 861 m, 23 Aug. 2022, *N. Mao* (BJTC FM2499).

Notes: *Helvella carnosa* is a species recently described from Europe (Skrede *et al.* 2017). Our present analysis revealed that *H. carnosa* is common in Northern China (Fig. S3), and can form ectomycorrhiza with *Abies grandis* and *Pinus tabuliformis*, *Helvella carnosa* shares less than 91.86 % similarity in the ITS region with other *Helvella* species.

Fig. 22. Photographs of apothecia in their natural habitat. **A, B.** *Helvella carnosa* (A. BJTC BP060. B. BJTC FM2619). **C.** *H. corbierei* (HSA 181). **D.** *H. fistulosa* (BJTC 1976). **E.** *H. nordlandica* (BJTC FM346-A). **F.** *H. scyphoides* (HSA 239). Scale bars = 1 cm.

Helvella corbierei (Malençon) Van Vooren & Frund, *Bull. Mycol. Bot. Dauphiné-Savoie* **198**: 9. 2010. Fig. 22.

Habitat: Scattered on the ground in coniferous and broad-leaved mixed forest.

Distribution: Known from Northern area in China.

Specimens examined: **China**, Shanxi Province, Ningwu County, Dashidong, on the ground in coniferous forest, alt. 2 207 m, 2 Aug. 2018, *H. Liu* (HSA 138); *ibid*., Qiuqiangou, on the ground in coniferous and broad-leaved mixed forest, alt. 1 600 m, 4 Aug. 2018, *H. Liu* (HSA 181).

Notes: *Helvella corbierei* is widely distributed in Europe and North America. It is confirmed from China based on morphological and DNA evidence in this study. *Helvella corbierei* shares less than 95.59 % similarity in the ITS region with other *Helvella* species.

Helvella fistulosa Alb. & Schwein., *Consp. Fungorum Lusat*.: 299. 1805. Fig. 22.

Habitat: Scattered on the ground in coniferous and broad-leaved mixed forest.

Distribution: Known from the Southwest area in China.

Specimen examined: **China**, Yunnan Province, Kunming City, Jinning District, Shuibo Villa, on the ground in coniferous and broad-leaved mixed forest, 28 Aug. 2021, *T.H. Li* (BJTC 1976).

Notes: *Helvella fistulosa* is widely distributed in Europe, North America and Japan (Skrede *et al.* 2017). In this study, a specimen from Yunnan Province matched this species, which confirmed the occurrence of *H. fistulosa* in China. *Helvella fistulosa* shares less than 94.51 % similar in the ITS region with other *Helvella* species.

Helvella nordlandica Skrede & T. Schumach. *Fungal Syst. Evol*. **11**: 72. 2023. Fig. 22.

Habitat: Scattered on the ground in coniferous and broadleaf mixed forest.

Distribution: Known from Northern area in China.

Specimens examined: **China**, Shanxi Province, Linfen City, Pu County, Wulushan mountains, on the ground in coniferous and broadleaf mixed forest, 11 Sep. 2017, *T. Li* (BJTC FM346-A); *ibid*., (BJTC FM346-B).

Notes: *Helvella nordlandica* is a species recently described from Europe (Skrede *et al.* 2023). Our present analysis showed that *H. nordlandica* is a rare *Helvella* species in North China (Fig. 1). *Helvella nordlandica* shares less than 95.86 % similarity in the ITS region with other *Helvella* species.

Helvella scyphoides Skrede *et al*., *Persoonia* **39**: 237. 2017. Fig. 22.

Habitat: Scattered on the ground in coniferous and broad-leaved mixed forest.

Distribution: Known from Northern area in China.

Specimens examined: **China**, Shanxi Province, Ningwu County, Xiaoshidong, on the ground in coniferous forest, alt. 2 200 m, 3 Aug. 2018, *H. Liu* (HSA 166); *ibid*., Luyashan mountains, alt. 2 270 m, 4 Sep. 2018, *J.Z. Cao* (HSA 336); *ibid*., Jiaocheng County, Pangquangou, on the ground in coniferous and broad-leaved mixed forest, alt. 2 160 m, 28 Aug. 2018, *H. Liu* (HSA 239); *ibid*., Wutai County, Wutaishan mountains, 27 Aug. 2019, *Y. Shen* (BJTC FM899); *ibid*., on the ground in coniferous forest, alt. 2 040 m, 3 Sep. 2020, *N. Mao* (BJTC FM1158).

Notes: *Helvella scyphoides* is a species recently described from Europe (Skrede *et al.* 2017). Our present analysis revealed this species is common in Northern China (Figs 1, 2, S3). *Helvella scyphoides* shared less than 93.9 % similarity in the ITS region with other *Helvella* species.

DISCUSSION

The species diversity of *Helvella* in China

Our present study revealed that China is extremely rich in species of *Helvella*. Chinese species of *Helvella* were nested in all the four clades recognized based on the samplings worldwide, *i.e*., *Acetabulum* clade, *Crispa* clade, *Elastica* clade and *Lacunosa* clade (Fig. 1). There were 93 clusters, which corresponded to 93 phylogenetic species in China, recognized in our phylogenetic analyses based on five genes (Figs 1, 2, S1–S4). Among them, 58 species were identified as known species including five new to China, 18 species were described as new species in this study, and 17 species were proposed as potentially undescribed species and were not treated taxonomically due to the lack or poor condition of ascocarps. Moreover, there are 34 names of *Helvella* recorded in China before this study, and although their DNA data are unavailable for the time being, three of them at least are morphologically distinct according to our personal observations of specimens or literature (Liu & Cao 1988, Cao *et al.* 1990). Thus, we infer that the total number of the genus *Helvella* in China could reach to 96 species with the current diversity observed in the present study.

Phylogeny and morphological correspondence of *Helvella*

Our five-gene-based phylogenetic analysis resolved the species of *Helvella s. str.* (Hansen *et al.* 2019) into four distinct clades, *i.e*., *Acetabulum*, *Crispa*, *Elastica,* and *Lacunosa* clades (Fig. 1). Compared to the phylogeny proposed by Skrede *et al.* (2017), the combination of our *Acetabulum*, *Crispa* and *Lacunosa* clades corresponded to the Clade B suggested by Skrede *et al.* (2017). Among them, our *Acetabulum* clade corresponded to their *acetabulum-solitaria* lineage, our *Crispa* clade corresponded to their *crispa* lineage, our *Lacunosa* clade contained all the other remaining lineages in their Clade B. Our *Elastica* clade contained the Clade D plus Clade E suggested by Skrede *et al.* (2017).

The *Acetabulum* clade occupied a basal position in the phylogenetic tree of the genus *Helvella*, and is the least diverse clade in species and lineages. Currently a total of nine species are recognized, five species occur in China, and two lineages, *i.e*., *acetabulum* lineage and *solitaria* lineage, were recognized (Figs 1, S1). All the species of the *Acetabulum* clade are relatively

uniform in the appearance of the ascocarp that possess a regularly or irregularly cup-like cap with a robust and ribbed stipe. It is interesting that the species, nested in several lineages in the *Lacunosa* clade including the *costifera* lineage, *dalgeri* lineage and *tianshanensis* lineage, evolved highly convergent morphological features in ascocarp appearance with the species of the *Acetabulum* clade. The ascocarps of *H. acetabulum* (*acetabulum* lineage, *Acetabulum* clade), *H. costifera* (*costifera* lineage, *Lacunosa* clade) and *H. hyperborea* (*hyperborea* lineage, *Lacunosa* clade) are very similar so that the three species are often confused with one another (Harmaja 1978, 1979).

The *Crispa* clade is also a less diverse group in species and lineages compared to the *Elastica* and *Lacunosa* clades. A total of 13 species were recognized, including nine from China. The species *H. crispa* and its allies evolved as the core *crispa* lineage (Figs 1, S2). Morphologically, species of the *crispa* lineage in this clade usually have pale ascocarps. The caps of ascocarps are saddle-shaped or irregularly lobed, white, cream white and sometimes grey. The cap margin is completely free from the robust and sometimes chambered stipe. It is notable that some species of the *Lacunosa* clade also have white or cream-coloured ascocarps; for example, the European *H. lactea* and the Asian *H. sublactea* of the *lactea* lineage, or the European *H. pallescens* of the *atra-pallescens* lineage. However, all the white *Helvella* species in the *Lacunosa* clade possess a cap margin attached to the stipe at several points, by which they can be differentiated from the species of the *crispa* lineage in morphology. *Helvella maculata* from North America and *H. maculatoides* from China may represent their own lineage, because they each evolved an independent branch outside the *crispa* lineage (Fig. 1), and the cap surface (hymenium) of their ascocarps is brown or dark, which is quite different from the species of the *crispa* lineage.

The *Elastica* clade is a very diverse group in species and lineages. Our present analysis revealed eight evolving lineages in this clade (Fig. 1). Among them, six lineages, *i.e.*, *bicolor-elastica* lineage, *capucina-danica* lineage, *corbierei-stevensii* lineage, *fallax-pezizoides* lineage, *hypocrateriformis* lineage, *rivularis-sublicia* lineage, were suggested in a previous study (Skrede *et al.* 2017). The *carnosa* lineage was newly recognized in this study. The *macropus* lineage was split from the previous *fibrosa-macropus* lineage suggested by Skrede *et al.* (2017). *Helvella fibrosa* and its allies (with ellipsoid ascospores) were not included in the *macropus* lineage (with subfusiform ascospores), and their phylogenetic positions remain unresolved for the time being. Morphologically, the shared features of *Helvella* species in the *Elastica* clade included the terete stipe that is usually thin, solid and definitely lacks ribs and chambers, although a few of grooves can be observed sometimes, and the multiple shaped caps being typical cup-like to saddle-like. Most species in this clade have ellipsoid ascospores, but the species that evolved in the *macropus* lineage have fusiform to subfusiform ascospores, which seem unique for the species evolved in the *macropus* lineage in *Helvella*. The terete stipe is generally clearly thin, but in the European *H. leucopus*, the Chinese *H. bachu* and their allies it is robust. It is notable that the species evolved in the *alpina-corium* lineage, *alpestris-nannfeldtii* lineage and *alpicola* lineage within the *Lacunosa* clade also have a terete stipe, but their stipes are usually clearly shorter, and in that case, their caps are always cup-like and have a dark brown or blackish hymenium. Chinese species evolved in all of the eight lineages mentioned above. There are at least 66 species evolved in this clade based on our analysis (Figs 1, S3), of which 44 occur in China. Eighteen new species are described in this study, and 14 potentially species were proposed but not taxonomically treated for the time being. The *Elastica* clade is probably the second largest clade in species diversity of *Helvella*.

Lacunosa clade is the most diverse group in phylogeny and morphology of *Helvella*. There were at least 13 lineages evolved in this clade worldwide according to Skrede *et al.* (2017) and this study (Fig. 1). Among them, six lineages, *i.e.*, *atra-pallescens* lineage, *fusca-lactea* lineage, *lacunosa-helvellula* lineage, *palustris-philonotis* lineage, *sulcata-phlebophoroides* lineage, *phlebophora* lineage and the species *H. queletiana* were gathered into a strongly supported subclade. To improve the following discussion on this clade, we marked this subclade as subclade *lacunosa*, as in which *H. lacunosa* was included. The remaining seven lineages, *i.e.*, *alpestris-nannfeldtii* lineage, *alpicola* lineage, *alpina-corium* lineage, *costifera* lineage, *dalgeri* lineage, *hyperborea* lineage, *tianshanensis* lineage, and the species *H. floriforma* were treated as a group and marked as "*costifera* group" (Fig. 1). Among the 13 lineages of the *Lacunosa* clade, six lineages were suggested by Skrede *et al.* 2017, including *alpestris-nannfeldtii* lineage, *alpina-corium* lineage, *atra-pallescens* lineage, *fusca-lactea* lineage, *palustris-philonotis* lineage, *sulcata-phlebophoroides* lineage. The remaining seven lineages were newly recognized in this study. Both the *Lacunosa-nigra* lineage and *helvellula* lineage suggested by Skrede *et al*. (2017) merged into a strong support clade in our five-gene-based phylogeny (Fig. 1), which thus was proposed as a new lineage in this study, *i.e.*, *lacunosa-helvellula* lineage.

The species of the *Lacunosa* clade are greatly diverse in ascocarp appearance. They share various types of ascocarps with those species respectively evolved in the *Acetabulum*, *Crispa* and *Elastica* clades. In general, the species that evolved in subclade *lacunosa* possess the saddle-like or irregularly lobbed cap, and the cap margin attached to the stipe at several points except for a few species, such as the European *H. helvellua* and *H. iberica* and their allies, which have a free cap margin. The ascocarp of the species of the *costifera* group is clearly different from those species of the subclade *lacunosa*. Their ascocarp cap is never saddle-like or lobbed, but instead, regular or irregular cup-like. Some species of the *costifera* group have the same ascocarp type as those species in the *Acetabulum* clade. Their ascocarps have a robust and ribbed stipe, for example, the species in the *costifera* lineage, *dalgeri* lineage, *hyperborea* lineage and *tianshanensis* lineage. Some species have ascocarps with thin and terete stipes, which are the same as that in the *Elastica* clade, for example, the species in the *alpestris-nannfeldtii* lineage and *alpina-corium* lineage.

Some species with different phylogenetic positions in the *Lacunosa* clade showed a high morphological convergence. The typical example is *H. queletiana, H. phlebophora* and *H. phlebophoroides*, which are morphologically highly similar and easy confused with each other in the field, but are phylogenetically distantly related. Similarly, species of the *alpestris-nannfeldtii* lineage and *alpina-corium* lineage in the *Lacunosa* clade were morphological convergent with the species of the *fallax-pezizoides* lineage in the *Elastica* clade.

White species and white form in *Helvella*

The overall white or cream-coloured species are not very common in *Helvella*. Most of the white species are from the *Crispa* clade, like

H. crispa and its allies, or the *fusca-lactea* lineage in the *Lacunosa* clade, like *H. lactea* and *H. sublactea*. However, the white or whitish collections of some non-white species are available in this study, the samples include *H. capucinoides* (BJTC FM1156, BJTC FM1094, Fig. 23D, E) and *H. costifera* (BJTC FM1705, Fig. 23F). Currently, it remains unclear whether the white form of *Helvella* species is common or rare, pending further study.

Mottled hymenium and parasitism

The mottled hymenium has been checked and used to distinguish species in *Helvella* including *H. maculata* and *H. tinta* (Weber 1975, Hyde *et al*. 2016). We observed the mottled hymenium in individual apothecia of *H. tianshanensis* and *H. sinohyperborea* in this study (Figs 17, 24H, I). At the same time, the DNA sequences of the mycoparasitic fungi *Hypomyces cervinus* and *Hypomyces* sp. were extracted respectively from these apothecia, but not from the apothecia without mottled hymenia (hymenium colour is uniform). Parasitism is very common in *Helvella*, especially the species of *Hypomyces* (Abbott & Currah 1997, Nguyen *et al*. 2013). A mottled hymenium could thus be a consequence of such an infection.

The application of ITS sequence in species identification of *Helvella*

The ITS region is a universal barcode for fungi (Schoch *et al*. 2012). However, it has not been considered as a good barcode gene for *Helvella* species. One of the reasons may be the difficulty of obtaining ITS sequence data. In this study, we successfully sequenced almost all species recognized from our *Helvella* collections. Our molecular analyses also revealed that the topology of phylogenetic trees generated from ITS is almost identical to that generated from the five-gene-combined dataset (ITS/nrLSU/ *tef1-α/rpb2/hsp*) at clade level, lineage level and species level (Figs 1, 2, S1–S4). These results showed that the ITS region is effective at least for the delimitation of the Chinese *Helvella* species. In addition, BLASTn analyses for all of *Helvella* species identified in this study revealed that the intraspecific similarity in ITS sequence ranged from 86 % to 98 %.

Fig. 23. Photographs of apothecia in their natural habitat. **A.** *Helvella acetabuloides* (BJTC FM1264). **B, C.** *H. capucinoides* (B. BJTC FM242. C. BJTC FM1423). **D, E.** *H. capucinoides* (white form apothecia, D. BJTC FM1156. E. BJTC FM1094). **F.** *H. costifera* (white form apothecia, BJTC FM1705). **G, H.** *H. danica* (G. BJTC ZH883. H. BJTC ZH1190). **I.** *H. lacunosa* (BJTC FM907). Scale bars = 1 cm.

Fig. 24. Photographs of apothecia in their natural habitat. **A.** *Helvella magna* (BJTC FM2486-A). **B.** *H. orienticrispa* (BJTC FM2480). **C.** *H. pseudoreflexa* (HSA 332). **D.** *H. pubescens* (BJTC FM918). **E.** *H. ravida* (HSA 375). **F.** *H. solitaria* (BJTC FM417). **G.** *H. sublactea* (BJTC FM1082). **H.** *H. tianshanensis* (HSA 185). **I.** *H. tianshanensis* (apothecia infected by *Hypomyces cervinus*, BJTC FM175). **J.** *H. vulgata* (BJTC FM2621). Scale bars = 1 cm.

Therefore, we infer that 98 % ITS identity might be the threshold to delimitate *Helvella* species.

Previous studies suggested that the amplification success rate of ITS sequence is low, especially in old specimens (Skrede *et al.* 2017, Wang *et al*. 2019). Two primer pairs successfully used in our present work are provided in Table 1. We observed that the ITS sequences amplified using the primers of ITS1-F/ITS4 could result in an inaccurate sequence in several *Helvella* species, *i.e*., *H. solitaria*, *H. taiyuanensis*, and *Helvella* sp. 59. Amplifying the ITS2 sequence using the primers ITS3/ITS4 is, however, effective for these species.

Doubtful and excluded species of *Helvella* in China

A total of 90 *Helvella* species have been recorded in China before this study. Of these, 53 species were confirmed in this study. The remaining 37 species are documented as follows.

Helvella adhaerens Peck, *Ann. Rep. Reg. N.Y. St. Mus*. **54**: 956. 1902. [1901].

Hevella adhaerens is documented in China (Dai 1979, Zhuang WY 1998b) based on a specimen (HMAS 17262) collected from Beijing in 1955. We re-examined this specimen and identified it as the *H. elastica* complex according to morphological traits. The DNA sequence of this specimen was unsuccessfully sequenced in this study. As it is difficult and even impossible to identify species of the *H. elastica* complex accurately without DNA data according to our experience, the taxonomic treatment of this specimen awaits. *Hevella adhaerens* has been treated as a synonym of *H. elastica* (Dissing 1966b, Skrede *et al*. 2017).

Helvella albella Quél. [as '*Elvella*'], *C. r. Assoc. Franç. Avancem. Sci*. **24**: 621. 1896. [1895].

This species was reported based on two specimens deposited in the Mycological Herbarium of Shanxi University (MHSU456, MHSU457) (Liu & Cao 1988), but the specimens got lost according to the authors. *Helvella albella* has been treated as a synonym of *H. bicolor* (Skrede *et al*. 2017). None of Chinese collections matched *H. bicolor* in the present study.

Helvella albipes Fuckel, *Hedwigia* **5**: 15. 1866.
This species was reported in Mao's book (1998), but no specimen was cited. Recent work indicated that *H. albipes* is a heterotypic synonym of *H. monachella* (Skrede *et al.* 2017). *Helvella monachella* is a European species. Its most similar Chinese species is *H. bachu* (Zhao *et al.* 2016a).

Helvella chinensis (Velen.) Nannf. & L. Holm, in Lundell *et al.*, *Publications from the Herbarium, University of Uppsala, Sweden* **18**: 5. 1985.
This name was mentioned in several papers (Lundell *et al.* 1985, Zhuang 1995, Wang & Chen 2002) but no specimen was cited. No specimens are available for study.

Helvella compressa (Snyder) N.S. Weber, *Beih. Nova Hedwigia* **51**: 35. 1975.
Zhuang & Yang (2008) reported this species based on the specimen HKAS 45788, and HMAS 97524 from Tibet of China, but we are not able to re-examine the two specimens in this study.

Helvella confusa Harmaja, *Karstenia* **17**: 43. 1977.
This species was reported from China by Zhuang (1998b). This species has been transferred to the genus *Dissingia* as *D. confusa* (Hansen *et al.* 2019). The occurrence of *Dissingia confusa* in China has been confirmed by Wang *et al.* (2019).

Helvella corium (O. Weberb.) Massee, *Brit. Fungus-Fl.* **4**: 463. 1895.
This is a frequently encountered name of *Helvella* in Chinese papers (Dai 1979, Liu *et al.* 1985, Zhuang *et al.* 2018) but no specimen was cited. A Chinese collection (HKAS 69755) labelled as *Helvella cf. corium* matched *H. xiaohuipan*, a new species described in this study (Fig. S3). None of samples from China matched this species in our present molecular analyses. Moreover, according to Cao *et al.* (1990), the name *H. corium* is a misapplication for *H. rivularis* or *H. villosa* in China.

Helvella crispa (Scop.) Fr., *Syst. Mycol*. **2**: 14. 1822.
The name *H. crispa* is one of the commonest *Helvella* species in China. Almost all the white saddle-shaped species with robust ribbed stipe are identified as this species. Recent works revealed that the *H. crispa*-like saddle fungi represented a different phylogenetic species (Zhao *et al.* 2015, Tibpromma *et al.* 2017). Our present analysis also recognized two new species from the *H. crispa* complex. *Helvella crispa* is not confirmed in China in this study, but there are at least five species in China that are based on the *H. crispa*-like samples (Zhao *et al.* 2015, 2016b, this study). Moreover, some sequences from the USA gathered into isolated clusters, indicating the presence of undescribed species, such as *Helvella* sp. 3, *Helvella* sp. 4 (Fig. S2). Therefore, *H. crispa* might be a species endemic to Europe.

Helvella cupuliformis Dissing & Nannf., *Svensk Bot. Tidskr*. **60**: 326. 1966.
Zhuang (2004) reported this species based on specimens from Xinjiang of north-western China. No DNA sequences were obtained from these specimens in this study. This species has been treated as a synonym of *Helvella hypocrateriformis* (Skrede *et al*. 2017).

Helvella cupuliformis* var. *crassa W.Y. Zhuang, *Mycotaxon* **90**: 38. 2004.
We checked the type specimens (HMAS 83523, HMAS 83524) of this taxon, but their sequences are unsuccessfully isolated in this study. This name is listed as a synonym of *H. cupuliformis* (= *H. hypocrateriformis*, Skrede *et al*. 2017) in Index Fungorum.

Helvella dissingii Korf*, Mycotaxon* **31**: 381. 1988.
Li *et al*. (2015) listed this species from China but no specimen was cited. Currently, this species is treated as a synonym of *Helvella fibrosa* (Skrede *et al.* 2017).

Helvella elastica Bull.*, Herb. Fr.* (Paris) **6**: tab. 242. 1785.
Helvella elastica is one of the most common fungal names in China. However, our present study showed that no Chinese specimens matched to this species phylogenetically (Fig. 1). All the morphologically similar specimens are either introduced as new species, or matched other similar species in the *elastica-bicolor* lineage, *carnosa* lineage and *capucina-danica* lineage of the *Elastica* clade in this study (Fig. 1).

Helvella ephippium Lév., *Ann. Sci. Nat., Bot*., sér. 2, **16**: 240. 1841.
Helvella ephippium was reported in China by Cao (1988). Later, it was mentioned by Zhuang (1989, 2004) and Wang & Chen (2002). The specimen cited by Cao (1988) is lost according to the author. Recent work treated *Helvella ephippium* as a synonym of *H. sublicia* (Skrede *et al*. 2017).

Helvella fargesii Pat., *J. Bot.* **7**: 344. 1893.
Dai (1979) reported this species from China but without citing a specimen. Dissing (1966b) treated it as a synonym of *H. elastica*. It is treated as an uncertain species (Skrede *et al*. 2017).

Helvella fusca Gillet, *Champ. France Discomyc*. **1**: 9. 1879.
Helvella fusca was reported based on a specimen (HXZE515) from Tibet of China (Xu 2002). We have not re-examined this specimen in this study.

Helvella glutinosa B. Liu & J.Z. Cao, *Acta Mycol. Sin*. **7**: 198. 1988.
This species is described from Heilongjiang Province, north-eastern China based on a specimen under conifers (MHSU451, holotype) in September 1986 (Liu & Cao 1988). The only specimen had been lost, but according to the original description, it is a morphologically distinct species, which is diagnosed by the gel cap.

Helvella helvellula (Durieu) Dissing, *Rev. Mycol*. **31**: 204. 1966.
This species is recorded from Shanxi Province in Northern China based on a specimen under conifers (MHSU 275) (Liu & Cao 1988). The specimen had been lost, but according to the original description given by Liu & Cao (1988), the cap of this specimen is dark brown rather than black as in *H. helvellula*. It is notable that two specimens newly collected from the same locality are introduced as a new species *H. sinohyperborea* in this study (Fig. 1).

Helvella hyperborea Harmaja, *Karstenia* **18**: 57. 1978.
Xu (2002) reported this species from Tibet in China based on a specimen (HXZE1023). Wang *et al.* (2019) recognized this species again in China based on specimens from Shanxi and Xinjiang Provinces. Our present analysis showed that these

specimens cited by Wang *et al.* (2019) are identical with the newly introduced *H. sinohyperborea* in this study (Fig. 1).

Helvella jiaohensis J.Z. Cao *et al.*, *Acta Mycol. Sin*. **9**: 184. 1990.
This species was described from Jiling Province in north-eastern China based on a specimen (HBNNU 0700, holotype) deposited in the Northeast Normal University (Cao *et al.* 1990). We were not able to re-examine this specimen in this study. This species has subglobose to very broadly ellipsoid ascospores, which suggests it to be a distinct species (Cao *et al.* 1990).

Helvella jilinensis J.Z. Cao *et al.*, *Acta Mycol. Sin*. **9**: 185. 1990.
Helvella jilinensis is described from Jiling Province in north-eastern China based on a specimen (HBNNU 0738, holotype) deposited in Northeast Normal University (Cao *et al.* 1990). We were not able to re-examine this specimen in this study. According to Cao *et al.* (1990), this species is diagnosed mainly by its thick-walled hyphae in the medullary excipulum. However, whether this feature can be used in species delimitation in *Helvella* is questionable.

Helvella jimsarica W.Y. Zhuang, *Mycotaxon* **90**: 39. 2004.
This species was described from Xinjiang Uygur Autonomous Region (Zhuang 2004). No specimen is available for study.

Helvella lactea Boud., *Icon. Mycol., liste prélim*.: 2. 1904.
This species was reported from Shanxi Province, Northern China and Jiling Province, Northeast China based on two specimens (MHSU454, MHSU455) (Liu & Cao 1988). The two specimens had been lost according to one of the authors (Cao, pers. comm). It is notable that all the *H. lacteal*-like specimens newly collected from China matched *H. sublactea* in our phylogenetic analyses in this study.

Helvella latispora Boud., *Bull. Soc. Mycol. France* **14**: 16. 1898.
Helvella latispora was firstly reported based on a specimen from Tibet in Southwest China (HXZE1440). We were not able to re-examine this specimen in this study. Recently, *Helvella latispora* has been treated as a synonym of *H. levis* (Skrede *et al.* 2017).

Helvella leucomelaena (Pers.) Nannf., in Lundell & Nannfeldt, *Fungi Exsicc. Suecici Fasc.* **19–20**: 21, no. 952. 1941.
Helvella leucomelaena is documented from China (Teng 1963, Tai 1979, Zhuang 1998b), but it is actually not occurring in China according to Wang *et al.* (2019). *Helvella leucomelaena* has been transferred to *Dissingia* as *D. leucomelaena* (Hansen *et al.* 2019).

Helvella leucopus Pers., *Mycol. Eur*. **1**: 213. 1822.
This name in China has been shown to be a misapplication of the Chinese *H. bachu* (Zhao *et al.* 2016a). Currently, *H. leucopus* has been treated as a synonym of *H. monachella* (Skrede *et al*. 2017).

Helvella maculata N.S. Weber, *Beih. Nova Hedwigia* **51**: 27. 1975.
This species was reported based on two specimens (MHSU 062, MHSU 063) from Xinjiang in Northwestern China (Liu & Cao 1988). We could not re-examine the two specimens in this study.

Helvella oblongispora Harmaja, *Karstenia* **18**: 57. 1978.
This species has been transferred to the genus *Dissingia* as *D. oblongispora* (Hansen *et al.* 2019). The occurrence of *D. oblongispora* in China has been confirmed by Wang *et al.* (2019) and this study.

Helvella pezizoides Afzel., *Kongl. Vetensk. Acad. Nya Handl*. **4**: 308. 1783.
Cao (1988) reported this species from China. According to the author, the specimen is probably lost. Our present analysis showed that none of the Chinese specimens matched *H. pezizoides*.

Helvella pseudolacunosa Q. Zhao & K.D. Hyde, *Fungal Diversity* **75**: 142. 2015.
This species could be identical to *H. lacunosa* according to our study (Figs 1, S4) and Wang *et al*. (2023a).

Helvella rivularis Dissing & Sivertsen, *Bot. Tidsskr*. **75**: 101. 1980.
This species was reported based on a specimen from Shanxi Province in Northern China (Cao *et al.* 1990), but the specimen has been lost according to the author (Cao pers. comm.).

Helvella sinensis B. Liu & J.Z. Cao, *Acta Mycol. Sin*. **4**: 214. 1985.
This species is described from Shanxi Province in Northern China (Liu *et al.* 1985). The type specimen is lost according to the author (Cao, pers. comm.). *Helvella sinensis* is a species of the *H. crispa* complex, diagnosed by the red-brown apothecium and broad ascospores. DNA data is lacking for this taxon.

Helvella spadicea Schaeff. [as '*Elvela*'], *Fung. bavar. palat. nasc*. (Ratisbonae) **4**: 112. 1774.
The name *H. spadicea* is a misapplication for *H. bachu* or *H. subspadicea* in China (Zhao *et al.* 2016a). *Helvella spadicea* is treated as an uncertain species (Skrede *et al.* 2017).

Helvella subfusispora B. Liu & J.Z. Cao, *Acta Mycol. Sin*. **4**: 211. 1985.
This species is firstly introduced based on a specimen (HBSU 3319) from the Zhoushan islands of Zhejiang Province in Eastern China (Liu *et al.* 1985). The holotype was destroyed in a fire, thus the specimen HMAS 30483 from Sichuan Province of Southwestern China had been selected as the neotype (Cao *et al.* 1990). Attempts to obtain a sequence from the neotype was unsuccessful in this study. However, according to the original description, this is a morphologically distinct species, which is diagnosed by its saddle-shaped ascocarps with thin and terete stipe, and subfusiform ascospores.

Helvella subglabra N.S. Weber, *Michigan Bot*. **11**: 179. 1972.
The North American *H. subglabra* was reported based on five specimens from Southwestern and Northeastern China (Zhao *et al.* 2016b). Our present analysis based on the ITS phylogenetic analysis (Fig. S4) showed these Chinese samples cited by Zhao *et al.* (2016) matched the new species *H. subglabroides* described in this study.

Helvella ulvinenii Harmaja, *Karstenia* **19**: 42. 1979.
This species was reported from China based on a specimen from Yunnan (HKAS 90321) (Zhao *et al*. 2016b). *Helvella ulvinenii* has been treated as a synonym of *H. solitaria* (Skrede *et al*. 2017), and the sequence cited for this species by Zhao *et al*. (2016b) also matched *H. solitaria* in the present analysis (Fig. 1).

Helvella villosa (Hedw.) Dissing & Nannf., *Svensk bot. Tidskr*. **60**: 330. 1966.
Helvella villosa is popularly mentioned in China but without citation of specimens (Cao *et al*. 1990). Recently, *Helvella villosa* has been treated as a synonym of *H. fibrosa* (Skrede *et al*. 2017).

Helvella xinjiangensis J.Z. Cao *et al*., *Acta Mycol. Sin*. **9**: 186. 1990.
Attempts to obtain a sequence from the type specimen (HMAS 38353) was unsuccessful in this study. *Helvella xinjiangensis* is treated as a synonym of *H. elastica* (Zhuang 2004).

ACKNOWLEDGEMENTS

We are very grateful to Jinzhong Cao for his taxonomic and nomenclatural discussions and valuable suggestions to improve our work. We are thankful to Jing-Chong Lv, Hao-Yu Fu, Tao-Yu Zhao, Jia-Jia Yang, Ying Li, Hui-Min Ji for their help. Many thanks to the curator Lei Cai and staff Zhuo Du (HMAS), to the curator Tao Deng and staff Wen Zhang Ma (HKAS), and to the curator Tolgor Bau (HMJAU) for loan of specimens used in this study. This work was supported by the National Natural Science Foundation of China (No. 31750001, 31270058) and the Beijing Natural Science Foundation (No. 5172003).

Conflict of interest: The authors declare that there is no conflict of interest.

REFERENCES

Abbott SP, Currah RS (1997). The *Helvellaceae*: systematic revision and occurrence in northern and northwestern North America. *Mycotaxon* **62**: 1–125.

Alfaro ME, Zoller S, Lutzoni F (2003). Bayes or bootstrap? A simulation study comparing the performance of Bayesian Markov chain Monte Carlo sampling and bootstrapping in assessing phylogenetic confidence. *Molecular Biology and Evolution* **20**: 255–266.

Ariyawansa HA, Hyde KD, Jayasiri SC, *et al*. (2015). Fungal Diversity notes 111–252: taxonomic and phylogenetic contributions to fungal taxa. *Fungal Diversity* **75**: 27–274.

Cao JZ (1988). *The taxonomy and systematics of Helvellaceae in China*. MS thesis, Shanxi University, Taiyuan [In Chinese].

Cao JZ, Fan L, Liu B (1990). Some new species and new records of the genus *Helvella* from China II. *Acta Mycologica Sinica* **9**: 184–190.

Cao JZ, Liu B (1990). A new species of *Helvella* from China. *Mycologia* **82**: 642–643.

Dissing H, Nannfeldt JA (1966). *Helvella cupuliformis sp. nov., H. villosa* (Hedw. *ex* O. Kuntze) *comb. nov*., *H. macropus* (Pers. ex Fr.) Karst., and their allies. *Svensk Botanisk Tidskrift* **60**: 325–337.

Dissing H (1966a). A revision of collections of the genus *Helvella* L. *ex* St-Amans *emend*. Nannf. in the Boudier Herbarium. *Revue de Mycologie* **31**: 189–224.

Dissing H (1966b). The genus *Helvella* in Europe with special emphasis on the species found in Norden. *Dansk Botanisk Arkiv* **25**: 1–172.

Gardes M, Bruns TD (1993). ITS primers with enhanced specificity for basidiomycetes — application to the identification of mycorrhizae and rusts. *Molecular Ecology* **2**: 113–118.

Häffner J (1987). Die gattung *Helvella*, morphologie und taxonomie. *Beihefte zur Zeitschrift für Mykologie* **7**: 1–165.

Hall TA (1999). BioEdit: a user-friendly biological sequence alignment editor and analysis program for Windows 95/98/NT. *Nucleic Acids Symposium Series* **41**: 95–98.

Hansen K, Pfister DH (2006). Systematics of the *Pezizomycetes*–the operculate discomycetes. *Mycologia* **98**: 1029–1040.

Hansen K, Schumacher T, Skrede I, *et al*. (2019). *Pindara* revisited – evolution and generic limits in *Helvellaceae*. *Persoonia* **42**: 186–204.

Harmaja H (1978). New species and combinations in *Helvella* and *Gyromitra*. *Karstenia* **19**: 57.

Harmaja H (1979). Studies on cupulate species of *Helvella*. *Karstenia* **19**: 33–45.

Hillis DM, Bull JJ (1993). An empirical test of bootstrapping as a method for assessing confidence in phylogenetic analysis. *Systematic Biology* **42**: 182–192.

Hwang J, Zhao Q, Yang ZL, *et al*. (2015). Solving the ecological puzzle of mycorrhizal associations using data from annotated collections and environmental samples – an example of saddle fungi. *Environmental Microbiology Reports* **7**: 658–667.

Hyde KD, Hongsanan S, Jeewon R, *et al*. (2016). Fungal Diversity notes 367–490: taxonomic and phylogenetic contributions to fungal taxa. *Fungal Diversity* **80**: 1–270.

Katoh K, Frith MC (2012). Adding unaligned sequences into an existing alignment using MAFFT and LAST. *Bioinformatics* **28**: 3144–3146.

Korf RP (1972). Synoptic key to the genera of the *Pezizales*. *Mycologia* **64**: 937– 994.

Laessoe T, Hansen K (2007). Truffle trouble: what happened to the *Tuberales*? *Mycological Research* **111**: 1075–1099.

Landeros F, Iturriaga T, Guzmán-Dávalos L (2012). Type studies in *Helvella* (*Pezizales*) 1. *Mycotaxon* **119**: 35 – 63.

Landeros F, Iturriaga T, Rodriguez A, *et al*. (2015). Advances in the phylogeny of *Helvella* (*Fungi: Ascomycota*), inferred from nuclear ribosomal LSU sequences and morphological data. *Revista Mexicana de Boversidad* **86**: 856–871.

Landvik S, Kristiansen R, Schumacher T (1999). *Pindara*: a miniature *Helvella*. *Mycologia* **91**: 278–285.

Linnaeus C (1753). *Species Plantarum*. Vol. 2. Holmiae, Sweden.

Li Y, Li TH, Yang ZL, *et al*. (2015). *Atlas of Chinese Macrofungal Resources.* Central China Farmer's Publishing House, Zhengzhou. [in Chinese].

Liu B, Cao JZ (1988). Some new species and new records of the genus *Helvella* from China (I). *Acta Mycologica Sinica* **7**: 198–204.

Liu B, Du F, Cao JZ (1985). New species and new combination of the genus *Helvella*. *Acta Mycologica Sinica* **4**: 208–217.

Liu YJ, Whelen S, Hall BD (1999). Phylogenetic relationships among ascomycetes: evidence from an RNA polymerse II subunit. *Molecular Biology and Evolution* **16**: 1799–1808.

Løken SB, Skrede I, Schumacher T (2019). The *Helvella corium* species aggregate in Nordic countries – phylogeny and species delimitation. *Fungal Systematics and Evolution* **5**: 169–186.

Lu JR, Yu FM, Lei L, *et al*. (2023). A new species of *Helvella* (*Helvellaceae*, *Pezizomycetes*) within the *H. macropus* group from China. *Phytotaxa* **601**: 212–222.

Lundell S, Nannfeldt JA, Holm L (1985). *Fungi Exsiccati Suecici, Praesertim Upsalienses.* no. 3262. Pubis. *Herbarium University of Uppsala* **18**: 5.

Maia LC, Yano AM, Kimbrough JW (1996). Species of *Ascomycota* forming ectomycorrhiza. *Mycotaxon* **57**: 371–390.

Mao XL (1998). *Economic fungi of China*. Beijing: The Science Press.

Nguyen NH, Landeros F, Garibay-Orijel R, *et al*. (2013). The *Helvella lacunosa* species complex in western North America: cryptic species, misapplied names and parasites. *Mycologia* **105**: 1275 –1286.

Nylander J (2004). *MrModeltest 2.2*. Computer software distributed by the University of Uppsala. Evolutionary Biology Centre, Sweden.

Rambaut A (2000). Estimating the rate of molecular evolution: incorporating non-contemporaneous sequences into maximum likelihood phylogenies. *Bioinformatics* **16**: 395–399.

Rehner SA, Buckley E (2005). A *Beauveria* phylogeny inferred from nuclear ITS and *EF1-α* sequences: evidence for cryptic diversification and links to *Cordyceps* teleomorphs. *Mycologia* **97**: 84–98.

Ronquist F, Huelsenbeck JP (2003). MrBayes 3: Bayesian phylogenetic inference under mixed models. *Bioinformatics* **19**: 1572–1574.

Schoch CL, Seifert KA, Huhndorf S, *et al.* (2012). Nuclear ribosomal internal transcribed spacer (ITS) region as a universal DNA barcode marker for Fungi. *Proceedings of the National Academy of Sciences USA* **109**: 6241–6246.

Shameem N, Kamili AN, Ahmad M, *et al*. (2016). Antioxidant potential and DNA damage protection by the slate grey saddle mushroom, *Helvella lacunosa* (*Ascomycetes*), from Kashmir Himalaya (India). *International Journal of Medicinal Mushrooms* **18**: 631–636.

Skrede I, Ballester Gonzalvo L, Mathiesen C, *et al*. (2020). The genera *Helvella* and *Dissingia* (*Ascomycota*: *Pezizomycetes*) in Europe – Notes on species from Spain. *Fungal Systematics and Evolution* **6**: 65–93.

Skrede I, Carlsen T, Schumacher T (2017). A synopsis of the saddle fungi (*Helvella*: *Ascomycota*) in Europe – species delimitation, taxonomy and typification. *Persoonia* **39**: 201–253.

Skrede I, Løken SB, Mathiesen C, *et al.* (2023). Additions to the knowledge of the genus *Helvella* in Europe. New records and de novo description of five species from the Nordic region. *Fungal Systematics and Evolution* **11**: 71–84.

Stamatakis A (2014). RAxML version 8: a tool for phylogenetic analysis and post-analysis of large phylogenies. *Bioinformatics* **30**: 1312–1313.

Tai FL (1979). *Sylloge Fungorum Sinicorum*. Beijing: Science Press.

Tedersoo L, Hansen K, Perry BA, *et al*. (2006). Molecular and morphological diversity of pezizalean ectomycorrhiza. *New Phytologist* **170**: 581–596.

Teng SQ (1963). *The Fungi of China*. Beijing: Science Press.

Tibpromma S, Hyde KD, Jeewon R, *et al*. (2017). Fungal Diversity notes 491–602: taxonomic and phylogenetic contributions to fungal taxa. *Fungal Diversity* **83**: 1–261.

Vaidya G, Lohman DJ, Meier R (2011). SequenceMatrix: concatenation software for the fast assembly of multi-gene datasets with character set and codon information. *Cladistics* **27**: 171–180.

Vilgalys R, Hester M (1990). Rapid genetic identification and mapping of enzymatically amplified ribosomal DNA from several *Cryptococcus* species. *Journal of Bacteriology* **172**: 4238–4246.

Wang M, Zhao YC, Zhao Q, *et al*. (2016). *Helvella sublactea sp. nov*. (*Helvellaceae*) from southwestern China. *Phytotaxa* **253**: 131–138.

Wang TY, Wang JY, Meng JL, *et al.* (2023b). Three new records of *Helvella* in China. *Microbiology China* **50**: 3372–3381. [In Chinese].

Wang XC, Liu TZ, Chen SL, *et al*. (2019). A four-locus phylogeny of rib-stiped cupulate species of *Helvella* (*Helvellaceae*, *Pezizales*) with discovery of three new species. *MycoKeys* **60**: 45–67.

Wang XC, Zhuang WY, Zhao RL (2023a). Species diversity of *Helvella lacunosa* clade (*Pezizales*, *Ascomycota*) in China and description of sixteen new species. *Journal of Fungi* **9**: 697.

Wang YZ, Chen CM (2002). The genus *Helvella* in Taiwan. *Fungal Science* **17**: 11–17.

Weber NS (1972). The genus *Helvella* in Michigan. *The Michigan Botanist* **11**: 147–201.

Weber NS (1975). Notes on Western species of *Helvella*. I. *Beihefte Nova Hedwigia* **51**: 25–38.

White TJ, Bruns T, Lee S, *et al*. (1990). Amplification and direct sequencing of fungal ribosomal RNA genes for phylogenetics. In: *PCR Protocols, A guide to Methods and Applications* (Innis M, Gelfand D, Sninsky J, *et al.* eds). SanDiego Academic Press, SanDiego: 315–322.

Xu AS (2002). Notes on *Helvella* in Xizang. *Mycosystema* **21**: 188–191.

Xu RJ, Li Y, Zhao Q (2022). *Helvella cystidiata sp. nov*. (*Helvellaceae*, *Ascomycota*) from Tibetan Plateau, China. *Phytotaxa* **560**: 082–092.

Yu FM, Lei L, Luangharn T, *et al*. (2023). Four new additions to *Helvella* (*Helvellaceae*, *Pezizales*) from Northern Thailand. *Frontiers in Microbiology* **14**: 1182025.

Zhao Q, Sulayman M, Zhu XT, *et al.* (2016a). Species clarification of the culinary Bachu mushroom in western China. *Mycologia* **108**: 828–836.

Zhao Q, Tolgor B, Zhao Y, *et al*. (2015). Species diversity within the *Helvella crispa* group (*Ascomycota*: *Helvellaceae*) in China. *Phytotaxa* **239**: 130–142.

Zhao Q, Zhang X, Li S, *et al*. (2016b). New species and records of saddle fungi (*Helvella*, *Helvellaceae*) from Jiuzhaigou Natural Reserve, China. *Mycoscience* **57**: 422–430.

Zhuang WY, Wang Z (1998). Some new species and new records of discomycetes in China. VIII. *Mycotaxon* **66**: 429–438.

Zhuang WY, Yang ZL (2008). Some pezizalean fungi from alpine areas of southwestern China. *Mycologia Montenegrina* **10**: 235–249.

Zhuang WY (1989). Some common discomycetes in Shennongjia, Hubei Province. In: *Fungi and Lichens of Shennongjia. Mycological and Lichenological Expedition to Shennongjia.* (Anonymous, ed.). World Publishing Corp, Beijing: 98–106.

Zhuang WY (1995). Some new species and new records of discomycetes in China. V. *Mycotaxon* **56**: 31–40.

Zhuang WY (1996). Some new species and new records of discomycetes in China. VI. *Mycotaxon* **59**: 337–342.

Zhuang WY (1997). Fungal flora of the Daba Mountains: Discomycetes. *Mycotaxon* **61**: 3–12.

Zhuang WY (1998a). Notes on discomycetes from Qinghai Province, China. *Mycotaxon* **66**: 439–444.

Zhuang WY (1998b). A list of discomycetes in China. *Mycotaxon* **67**: 365–390.

Zhuang WY (2004). Preliminary survey of the *Helvellaceae* from Xinjiang, China. *Mycotaxon* **90**: 35–42.

Zhuang WY, Zheng HD, Zeng ZQ (2018). *Species catalogue of China*. *Volume 3 Fungi. Cup-Fungi.* Science Press.

Supplementary information

Fig. S1. Phylogeny of Chinese *Helvella* species of *Acetabulum* clade inferred from the Dataset II (ITS) using the maximum likelihood (ML) analysis. Numbers representing likelihood bootstrap support values (MLBS ≥ 70 %, left) and significant Bayesian posterior probability (BPP ≥ 0.95, right) are indicated above the nodes. New species are printed in **bold**.

Fig. S2. Phylogeny of Chinese *Helvella* species of *Crispa* clade inferred from the Dataset III (ITS) using the maximum likelihood (ML) analysis. Numbers representing likelihood bootstrap support values (MLBS ≥ 70 %, left) and significant Bayesian posterior probability (BPP ≥ 0.95, right) are indicated above the nodes. New species are printed in **bold**.

Fig. S3. Phylogeny of Chinese *Helvella* species of *Elastica* clade inferred from the Dataset IV (ITS) using the maximum likelihood (ML) analysis. Numbers representing likelihood bootstrap support values (MLBS ≥ 70 %, left) and significant Bayesian posterior probability (BPP ≥ 0.95, right) are indicated above the nodes. New species are printed in **bold**.

Fig. S4. Phylogeny of Chinese *Helvella* species of *Lacunosa* clade inferred from the Dataset V (ITS) using the maximum likelihood (ML) analysis. Numbers representing likelihood bootstrap support values (MLBS ≥ 70 %, left) and significant Bayesian posterior probability (BPP ≥ 0.95, right) are indicated above the nodes. New species are printed in **bold**.

Table S1. Specimens used in the five combined loci (ITS/nrLSU/*tef1-α*/*rpb2*/*hsp*) phylogenetic analysis and their GenBank accession numbers.

Newly generated sequences are in **bold**.

Table S2. Specimens used in the two combined loci (ITS/nrLSU) phylogenetic analysis and their GenBank accession numbers. Newly generated sequences are in **bold**.

Table S3. Specimens used in *Acetabulum* clade ITS phylogenetic analysis and their GenBank accession numbers. Newly generated sequences are in **bold**.

Table S4. Specimens used in *Crispa* clade ITS phylogenetic analysis and their GenBank accession numbers. Newly generated sequences are in **bold**.

Table S5. Specimens used in *Elastica* clade ITS phylogenetic analysis and their GenBank accession numbers. Newly generated sequences are in **bold**.

Table S6. Specimens used in *Lacunosa* clade ITS phylogenetic analysis and their GenBank accession numbers. Newly generated sequences are in **bold**.

Table S7. The list of *Helvella* species confirmed in China.

FUSE

Fungal Systematics and Evolution

Volume 12
DECEMBER 2023
PAGES 153–201

doi.org/10.3114/fuse.2023.12.09

A phylogeny for North American *Mallocybe* (*Inocybaceae*) and taxonomic revision of eastern North American taxa

P.B. Matheny[1*], L.V. Kudzma[2], M.G. Graddy[1], S.M. Mardini[1], C.R. Noffsinger[1], R.A. Swenie[1], N.C. Walker[1], S.R. Campagna[3], R. Halling[4], R. Lebeuf[5], M. Kuo[6], D.P. Lewis[7], M.E. Smith[8], M. Tabassum[3], S.A. Trudell[9], J. Vauras[10]

[1]Department of Ecology and Evolutionary Biology, University of Tennessee, Knoxville, Tennessee 37996-1610, USA
[2]37 Maple Avenue, Annandale, New Jersey 08801, USA
[3]Department of Chemistry, University of Tennessee, Knoxville, Tennessee 37996-1600, USA
[4]Institute of Systematic Botany, The New York Botanical Garden, Bronx, New York 10458-5126, USA
[5]Cercle des mycologues de Lanaudière et de la Mauricie, Saint-Casimir, Quebec G0A 3L0, Canada
[6]The Herbarium of Michael Kuo, Post Office Box 742, Athens, Ohio 45701, USA
[7]S.M. Tracy Herbarium, Texas A&M University, College Station, Texas 77843-2138, USA
[8]Department of Plant Pathology, University of Florida, Gainesville, Florida 32611, USA
[9]Herbarium, Burke Museum, University of Washington, Seattle 98195-5325, USA
[10]Biological Collections of Åbo Akademi University, Herbarium, University of Turku, FI-20014, Finland

*Corresponding author: pmatheny@utk.edu

Key words:
Agaricales
fungi
new taxa
secondary metabolites
systematics

Abstract: A multigene phylogenetic assessment of North American species of *Mallocybe* is presented based on analyses of *rpb1*, *rpb2*, ITS, and 28S rDNA nucleotide data. This framework enables a systematic revision of the genus for 16 eastern North American species and captures taxonomic and phylogenetic diversity in a global context. A grade of two unusual and poorly known North American species stems from the most recent common ancestor of the genus that gives rise to three core subgroups named here as clades Unicolores, Nothosperma, and Mallocybe. The grade of taxa includes the poorly known *Lepista praevillosa* from Florida and a new species from the southern Appalachians, *M. montana*, both of which appear to be narrow-range endemics. Clade Nothosperma is characterized by Australian and New Zealand species, whereas clade Unicolores is composed of six species from eastern North America and East Asia. Clade Mallocybe is dominated by numerous north temperate taxa and constitutes the sister group to clade Nothosperma. These major clades are distinguished by a combination of phylogeny, morphology, geographic distribution, and ecology. In addition, four North American species are described as new: *M. leucothrix, M. luteobasis, M. montana*, and *M. tomentella*. Several names originating in North America, long ignored or misunderstood in the literature, are revitalized and established by type comparisons and modern reference material collected from or near type localities. In addition, 11 species were subjected to mass spectrometry muscarine assays, none of which contained detectable amounts of muscarine except for two: *M. sabulosa* and *M. praevillosa*. This confirms a diffuse phylogenetic distribution of muscarine within the genus. Taxonomic descriptions are presented for 16 species, several synonymies proposed, and four new combinations made. A key to species of eastern North American *Mallocybe* is presented, along with illustrations of important diagnostic features.

Citation: Matheny PB, Kudzma LV, Graddy MG, Mardini SM, Noffsinger CR, Swenie RA, Walker NC, Campagna SR, Halling R, Lebeuf R, Kuo M, Lewis DP, Smith ME, Tabassum M, Trudell SA, Vauras J (2023). A phylogeny for North American *Mallocybe* (*Inocybaceae*) and taxonomic revision of eastern North American taxa. *Fungal Systematics and Evolution* **12**: 153–201. doi: 10.3114/fuse.2023.12.09
Received: 20 July 2023; **Accepted:** 24 August 2023; **Effectively published online:** 1 September 2023
Corresponding editor: P.W. Crous

INTRODUCTION

The genus *Mallocybe*, one of seven genera of *Inocybaceae*, was recently elevated to generic rank by Matheny *et al*. (2020). Species of *Mallocybe* are distinguished from other genera of *Inocybaceae* by a combination of the presence of necropigmented basida (basidia that collapse and fill with ochraceus or brownish yellow pigment), smooth basidiospores, a typically dark reaction to alkali solutions on the pileus surface, non-reddening context; cheilocystidia arising as terminal elements of hymenophoral trama that are, in most species, less than 50 µm long; and the absence of pleurocystidia. Previous work has shown that the toxin muscarine is present in some species but not detectable in others (Kosentka *et al*. 2013).

In the field many species of *Mallocybe* typically feature adnate or subdecurrent lamellae, a squamulose or tomentose pileus surface, and a short stipe relative to the width of the pileus. Coloration of most species is typically some shade of

brown, yellowish brown, or brownish yellow. However, several exceptions to this suite of features have been noted (*e.g*., Cripps *et al*. 2010, Matheny & Bougher 2017). The genus is a strongly supported monophyletic group and is widely distributed across the globe occurring in Africa, Asia, Australia, Europe, New Guinea, New Zealand, and North America (Matheny *et al.* 2020). New species of *Mallocybe* continue to be described from Africa, Asia, and Europe (Crous *et al*. 2020, Saba & Khalid 2020, Aignon *et al.* 2021, Mao *et al*. 2022, Hu *et al*. 2023), and new combinations continue to be made into the genus (Saba *et al*. 2020) raising the number of species to about 65 worldwide. *Mallocybe* is most diverse at temperate latitudes forming ectomycorrhizal associations with a number of different plant families (*e.g*., Daskalopoulos *et al.* 2021), and some species are important constituents of alpine and arctic systems (Favre 1955, Kühner 1988, Cripps *et al*. 2010). A few species have been described or documented from the Old-World tropics (Horak 1980, Matheny *et al*. 2009, Horak *et al*. 2015, Matheny & Bougher 2017, Aignon *et al*. 2021), but none have yet been described from the Neotropics and southern South America.

European *Mallocybe* have generally been recognized as a small group containing anywhere from 5 to 25 species. An early attempt to classify species attributable to *Mallocybe* was done by Heim (1931), who proposed "Stirpe dulcamara" in *Inocybe* sect. *Dulcamarae*. The stirps contained five species. Singer (1986) placed European species of *Mallocybe* in *Inocybe* sect. *Depauperatae* typified by *Inocybe delecta* and recognized five species in the group. Alessio & Rebaudengo (1980) treated 12 taxa, including several infraspecific varieties and forms.

Kuyper (1986) established *Inocybe* subg. *Mallocybe* in the sense used here but did not include a taxonomic treatment for the ten estimated species he accepted at that time from the northern hemisphere. Kühner (1988) described ten new species in *Inocybe* sect. *Dulcamarae* from alpine zones in central Europe, which doubled the number of known species in the group. Stangl (1989) recognized eight species in *Inocybe* subg. *Mallocybe* from central Europe, and Kobayashi (2002) recognized five including consideration of samples from East Asia. Jacobbson & Larsson (2012) treated 14 species of *Inocybe* subg. *Mallocybe* in northern Europe. Bon (1997), however, referenced 31 taxa (among 23 species) in his keys, and Ludwig (2017) recognized 25. In North America no extensive revision has been made of species of *Mallocybe*, but Cripps *et al*. (2010) documented six intercontinental Euro-American species from arctic-alpine settings in western North America. Bessette & Fatto (1998) attributed a new species they described from New York, *I. angustispora* (see also Bessette *et al*. 2001), to an alliance with what would be recognized as *Mallocybe* today. However, Matheny & Ammirati (2003) showed that *I. angustispora* was a later synonym of *Cortinarius aureifolius*, an atypically smooth-spored species of *Cortinarius*. A few new taxa were documented or described from the Old-World tropics as cited above, and Matheny & Bougher (2017) added five new species to *Inocybe* subgenus *Mallocybe* from Australian temperate and tropical regions. Horak (2018) included a description of a new species, *I. callichroa*, from New Zealand, which superficially resembles other species of *Mallocybe*. Lastly, five new species were recently described from China (Mao *et al.* 2022, Hu *et al.* 2023). Globally, about 65 species of *Mallocybe* can now be recognized since Matheny (2009) initially estimated *ca*. 30 species worldwide in the group.

Mallocybe has long been recovered as a single clade based on molecular phylogenetic analyses. Matheny (2005) sampled 12 species-level lineages of *Inocybe* subg. *Mallocybe* based on phylogenetic analyses of three gene regions, and Matheny *et al.* (2009) followed up on that study by including 25 species of *Inocybe* subg. *Mallocybe* worldwide. Cripps *et al.* (2010) reconstructed an rDNA phylogeny that sampled 13 species-level lineages of *Inocybe* subg. *Mallocybe*, and Ryberg *et al.* (2010) included about a dozen lineages based on analyses of nuclear and mitochondrial rDNA. All these treatments recovered *Mallocybe* as a strongly supported monophyletic group. However, Bandini *et al.* (2018) recently excluded *Inocybe stenospora* from *Mallocybe*, where it had been previously proposed (Stangl 1986), based on molecular phylogenetic evidence. Unfortunately, phylogenetic studies have varied on identification of the sister group to *Mallocybe* and have lacked strong evidence in favor of any sister group arrangement (Matheny 2005, Matheny *et al.* 2009, 2012, 2020, Alvarado *et al.* 2010, Ryberg *et al.* 2010). *Auritella*, *Tubariomyces*, and *Inosperma*, or some configuration of these taxa, have all been recovered as potential sister groups to *Mallocybe* but without strong support. In addition, no prior works have proposed any infrageneric molecular systematic treatment, although Hu *et al*. (2023) recovered three major clades within the genus (identified as clades A, B, and C) with an infrageneric multigene phylogeny based on combined analysis of ITS, 28S, and *rpb2* sequences.

Our objectives here are to: (1) present a global molecular phylogenetic assessment of *Mallocybe* based on *rpb1*, *rpb2*, ITS, and 28S data; (2) focus on identification of major lineages within *Mallocybe* incorporating North American taxa; (3) assay relative abundance of muscarine in North American samples; and (4) revise and document species that occur in eastern North America relative to those elsewhere. In addition, we also highlight the uniqueness of several lineages documented from western North America. To stabilize application of names based on old or poorly preserved type collections, we collected fresh specimens at or near type localities of species attributable to *Mallocybe* described by Peck, Murrill, and others in New York and Florida. Taxonomic descriptions of 16 species of *Mallocybe* from eastern North America are presented, including description of four new species, clade designations within the genus, a taxonomic key, and illustrations of diagnostic microscopic features and photographs of basidiomes. The work also provides a framework to revise *Mallocybe* species from western North America and elsewhere in the future.

MATERIALS AND METHODS

Morphology

Notes on fresh samples from the field were aided by reference to the color guides Munsell Soil Color Chart (1954) [*e.g*., 10YR 7/4), Ridgway (1912) [*e.g*., Dresden Brown], and Kornerup & Wanscher (1967) [*e.g*., 6E8]. "L" refers to the number of lamellae that reach the stipe. PDAB or *p*-dimethylaminobenzaldehyde (Matheny *et al.* 2013) and 5 % KOH (Kuyper 1986) were used to induce any microchemical reactions. After observation, fresh specimens were air-dried in a food dehydrator. Collections were accessioned at the Herbarium of the University of Tennessee (TENN) and the University of Washington Herbarium (WTU) or maintained in the private herbarium of L.V. Kudzma. Loans of specimens were obtained from the Royal Botanic Garden Edinburgh (E), the Fungarium of the Florida Museum of Natural

History (FLAS), the Herbarium of the University of Helsinki (H), the New York Botanical Garden (NY), and WTU. Herbarium codes follow Thiers [continuously updated]. Hand sections made with a razor and lamellar fragments were mounted in 5 % KOH to examine anatomical features such as the pileipellis, cheilocystidia, basidia, and basidiospore morphology and size (terminology following Kuyper 1986). Observations and measurements were made with a Nikon i80 Eclipse light microscope and Elements D software (Nikon Instruments Inc, Melville, New York). Outlier measurements constituting < 5 % of observations are indicated in parentheses, and mean values are italicized. Q-values are ratios of spore length to spore width and were calculated for each spore and then averaged. The total number of spores measured (x) and the number of specimens sampled (y) are indicated as x/y. Type collections were examined from FLAS, H, NY, TENN, and WTU.

DNA extractions and sequencing

Between 20 and 30 mg of dried pileal fragments were ground with liquid N and a pinch of sterile sand. In most cases, procedures for DNA extraction followed Judge *et al.* (2010) or Matheny *et al.* (2002). Recently collected samples underwent a rapid alkaline DNA extraction and PCR amplification as described by Matheny & Swenie (2018). ITS amplicons were amplified and sequenced using primers ITS1F and ITS4 (White *et al.* 1990). 28S amplicons were amplified using LR0R and LR7 and sequenced with these primers and LR5 (Vilgalys & Hesler 1990, Cubeta *et al.* 1991). The most variable region of *rpb1* was sequenced between conserved domains A and C using primers gAf (Stiller & Hall 1997) and fCr (Matheny *et al.* 2002). Both primers were used for sequencing along with internal primers int2F, int2.1F, and int2.1R (Frøslev *et al.* 2005). The most variable region of *rpb2* was amplified and sequenced between conserved domains 6 and 7 using primers b6F and b7.1R (Matheny 2005). For materials gathered in New Jersey, PCR procedures and sequencing followed Matheny & Kudzma (2019). For materials older than 30 years, the ITS spacers were amplified and sequenced separately following Sánchez-García *et al*. (2014). Chromatograms were constructed and edited in Sequencer v. 5.0.1 (Gene Codes Corp., Ann Arbor, Michigan). New sequences were submitted to GenBank and are shown in bold font in Table 1.

Taxon sampling

A list of taxa included in the phylogenetic analyses is presented in Table 1, including specimen-voucher number (where relevant), herbarium designation (if known), geographic origin, ecology (if known, including plant host information and edaphic factors), and GenBank accession numbers. DNA sequences of *rpb1*, *rpb2*, ITS, and 28S were used primarily from the following studies: Matheny *et al.* (2002, 2009), Matheny (2005), Ryberg *et al.* (2008), Larsson *et al.* (2009), Alvarado *et al.* (2010), Cripps *et al.* (2010), Ryberg *et al.* (2010), Vauras & Larsson (2011), Kosentka *et al.* (2013), Ariyawansa *et al.* (2015), Horak *et al.* (2015), Matheny & Bougher (2017), Crous *et al.* (2020), Aignon *et al.* (2021), Saba & Khalid (2020), Mao *et al.* (2022), and Hu *et al.* (2023). Blastn searches of sequences in GenBank that resulted in high similarity also led to inclusion of several *ad hoc* sequences (*e.g.*, Roy *et al.* 2009, Meza-Meneses *et al.* 2016), environmental sequences, and unpublished sequences. These are also included in Table 1.

Phylogenetic analyses

DNA sequences were aligned using ClustalX v. 2.0.9 (Larkin *et al.* 2007) and viewed and manually adjusted as nexus files in AliView v. 1.11 (Larson 2014). Outgroup sequences included *Auritella brunnescens*, *Crepidotus applanatus*, *Inosperma aff*. *mutatum*, *Inosperma rimosoides*, and *Tubariomyces* sp. following Matheny *et al.* (2020). Intron regions were identified following Matheny *et al.* (2002) and Matheny (2005). Data were partitioned by rDNA gene regions combined, 1st, 2nd, and 3rd codon positions separately, and RNA polymerase II intronic regions combined (Matheny *et al.* 2002, Matheny 2005). Because of their high divergence, sequences of ITS, intron-1 and intron-4 of *rpb1*, and intron-4 of *rpb2* were excluded from outgroups to facilitate alignments of the ingroup.

Three unlinked gene alignments were analyzed first. This included *rpb1* (conserved domains A to C), *rpb2* (conserved domains 6 to 7), and the ITS and 28S nuclear rDNA region combined. Maximum likelihood (ML) analyses were conducted in RAxML v. 8.2.9 (Stamatakis 2014) with 1 000 rapid bootstraps. Models of evolution used in ML analyses followed recommendations in the RAxML user manual (Stamatakis 2014), thus we applied a GTRCAT approximation to bootstrap trees, which was recommended for data sets with > 50 taxa. Any strongly intergenic conflicts (> 70 % bootstrap for incongruent groups) were noted before consideration of a final concatenated alignment.

We then assembled a 4-locus concatenated supermatrix partitioned into five-character sets (rDNA, the three codon positions separately, and RNA polymerase II introns combined) and conducted ML (see above) and Bayesian inference (BI) analyses in MrBayes v. 3.2.6 (Ronquist *et al.* 2012). Models used for each partition followed Matheny (2005). For all BI analyses, convergence diagnostics were examined to evaluate proper execution. These included examination of the standard deviation of split frequencies (reaching < 1.0 to ensure run convergence), potential scale reduction factors (PSRF) near 1.0, and effective samples size (ESS) > 100 for all parameters. Burn-in values of 25 % were applied, where tenable, or determined based on run convergence. We also performed a partitioned analysis of the 4-locus dataset in IQ-TREE v. 1.6.12 with 1 000 ultrafast (UF) bootstraps and the SH-aLRT test (SH) (Nguyen *et al.* 2015, Chernomor *et al.* 2016, Hoang *et al.* 2018). Any ML bootstrap proportions > 70 % were considered as evidence for strong support. Strong support was also noted if a clade received SH-aLRT > 80 % and UF bootstraps > 95 %.

The four alignments (*rpb1*, *rpb2*, nuc rDNA, 4-locus supermatrix), ML bipartition files including branch values and gene partitioning schemes, have been archived at FigShare (doi: 10.6084/m9.figshare.23604333).

Muscarine bioassays

Eleven samples of *Mallocybe* were subjected to mass spectrometry analysis for detection of muscarine, an alkaloid that stimulates the parasympathetic nervous system in animals (Kosentka *et al.* 2013). The samples included *M. heimii* (JV14932F), *M. isabellina* (NLB800/TENN-F-066800), *M. leucoblema* (PBM1539/WTU), *M. luteobasis sp. nov*. (PBM4437/TENN-F-075309), *M. montana sp. nov*. (PBM3872/TENN-F-067500/type), *M. myriadophylla* (JV5968F/WTU), *M. praevillosa comb. nov*. (FLAS-F-61523), *M. sabulosa* (NLB901/

TENN-F-066809), *M. squamosodisca comb. nov*. (PBM4621/TENN-F-075791), *M. subtomentosa comb. nov*. (PBM3910/TENN-F068440), and *Mallocybe* sp. 5 (PBM1922/WTU). These species were selected for this analysis because they are widely distributed across the *Mallocybe* phyogeny. The following samples were used as negative controls: *Psilocybe caerulipes* (DG21081110/TENN-F-076505, DG2108093/TENN-F-076504), *Inocybe picrosma* (RHM102910/TENN-F-066038), and *Inosperma mucidiolens* (PBM4323/TENN-F-074905) (Kosentka *et al.* 2013, Robbers *et al.* 1964, Strauss *et al.* 2022). Three positive controls were also used: *Inocybe occulta* (RAS920/TENN-F-76509), *I. aff. geophylla* (PBM4697/TENN-F-075834), and *Inosperma aff. maculatum* (PBM4522/TENN-F-075309). All three positive controls belong phylogenetically to inclusive groups known to contain muscarinic species (Kosentka *et al.* 2013).

The muscarine analyses were performed at the Biological Small Molecule Mass Spectrometry Core at the University of Tennessee Knoxville (RRID: SCR_021368). The analytical methodology was adapted from a previous study (Kosentka *et al*. 2013). Briefly, the ground samples ranging from 4–40 mg were placed into Eppendorf tubes, vortexed for 1 min, and extracted with 300 µL 4:1 Methanol:H_2O at -80 °C for 20 min. All solvents used were HPLC grade. The resulting suspension was centrifuged (16 100 rcf) for five min to remove particulates. The resulting supernatants were isolated, and an aliquot was diluted by a factor of 2 000. The diluted supernatant was stored at 4 °C until LCMS analysis in UltiMate 3 000 RS autosampler (Dionex, Sunnyvale, California).

An injection volume of 10 µL was used with reversed-phase chromatography utilizing a Phenomenex Gemini 5 µm C_{18} column (110 Å, 150 mm × 2 mm; Torrance, California). Ultra-high-performance liquid chromatography (UHPLC) was performed utilizing an UltiMate 3 000 pump. Separations were performed with a column temperature of 25 °C and a flow rate of 150 µL/min. The separation was carried out using water (solvent A) and acetonitrile (ACN) (solvent B) for 18 min creating a gradient elution profile as previously reported (Kosentka *et al*. 2013). The eluent was then introduced into a Thermo Scientific Q Exactive Orbitrap MS (Thermo Scientific, San Jose, California) for ion detection.

Electrospray ionization in positive ionization mode was used as described by Kosentka *et al*. (2013). Muscarine was detected using parallel reaction monitoring (PRM) for the unique product *m/z* 56.9857 ± 5 ppm at the collision energy *e*V 85. A 2.0 µM solution of muscarine was used as a standard (Fisher Scientific, Waltham, Massachusetts, USA). The muscarine standard was eluted from the column at a retention time of 1.9 min. Instrumental raw data files were converted to mzML format (Chambers *et al.* 2012). Peak areas were integrated from extracted ion chromatograms in the open-source software package El-MAVEN (Agrawal *et al*. 2019). Normalized peak areas refer to area count per mg or peak area per mg since the area after blank subtraction was sample mass normalized. Samples detected with abundance less than 2.5 times of the average abundance in the blank control were considered as below the limit of detection. Although the normalized peak area does not represent absolute concentration, it corresponds to the relative abundance in the samples.

RESULTS

DNA alignments

One hundred and ninety-seven new sequences (77 ITS, 53 28S, 33 *rpb1*, 34 *rpb2*) were produced. The *rpb1* dataset contained 55 taxa and 1 547 sites. The *rbp2* dataset contained 98 taxa and 774 sites. The rDNA dataset (ITS1-5.8S-ITS2+28S) included 304 taxa and 2 504 sites. The combined 4-gene region supermatrix included 304 taxa and 4 823 sites. Convergence diagnostics failed for the BI analysis of the 4-gene region supermatrix and resulted in spurious placements of several taxa represented by (partial) ITS data only. For this reason, we report phylogenetic results from the RAxML and IQ-TREE analyses only.

Murrill's *Inocybe* (*Lepista*) *praevillosa* is sister to *Mallocybe*

Both *rpb1* and *rpb2* gene trees (Supplementary Figs S1, S2, respectively) recovered *Mallocybe* as a strongly supported monophyletic group. Both trees indicated strong support for a grade of *Inocybe praevillosa*, originally described as *Lepista praevillosa* by W.A. Murrill, and the newly named *Mallocybe montana* giving rise to the remainder of *Mallocybe* described or documented from Asia, Australasia, Eurasia, and North America. Considerably denser taxon sampling of *Inocybaceae* and outgroups of *Crepidotaceae* and *Tubariaceae* reinforce these strongly supported results for both genes (unpubl. data). Both gene trees also recovered three main clades within the genus as previously shown by Hu *et al.* (2023). These three clades have yet to be named, but here we propose them informally as clades Unicolores, Nothosperma, and Mallocybe, and suggest they may be equivalent to potential subgenera depending on forthcoming revisions of European *Mallocybe.*

Both *rpb1* and *rpb2* recovered similar overarching topologies with respect to placement of *Inocybe* (*Lepista*) *praevillosa* and *M. montana* in position to the rest of *Mallocybe*. However, *rpb1* anchored clades Nothosperma and Unicolores as a monophyletic group with strong support, whereas *rpb2* recovered clades Nothosperma and Mallocybe as sister groups but with weak support. The rDNA-only tree did not recover *Mallocybe* as monophyletic due to the clustering of *I.* (*Lepista*) *praevillosa* among the outgroups, but this result was weakly supported. Clade Nothosperma was recovered as monophyletic with moderate support including a *Nothofagus*-associated sample from New Zealand sister to all other Australasian taxa. However, clade Mallocybe was found to be paraphyletic within which clade Unicolores and *M. montana* were placed.

A notable source of gene conflict was observed between the rDNA and *rpb2* gene trees. This concerned the placement of the recently described species *M. africana* (Aignon *et al.* 2021). Initial analyses of our rDNA and *rpb2* alignments (data not shown) placed it sister to *M. errata* with strong support (rDNA), or sister to the rest of *Mallocybe* with weak support (*rpb2*). Two *rpb2* sequences of *M. africana* from the same sample (MR00385) are available in GenBank, but these differ by 4.5 % percent identity. Because of concerns regarding gene duplication and paralogs, we excluded *M. africana* from further downstream analyses. A close relationship between *M. africana* (indicated as "*I. microdulcamara nom. prov.*") and *M. errata* and *M. heimii* was previously recovered by Matheny *et al.* (2009). Until new and additional *rpb1* and *rpb2* sequences can be produced, we regard *M. africana* as *incertae sedis* within the genus.

Table 1. Specimen data and DNA sequences analyzed for this study. New DNA sequences are in bold.

Species	Specimen-voucher (Herbarium)	Geographic origin	Ecology	GenBank Accession Numbers			
				ITS	28S	*rpb1*	*rpb2*
M. africana	96012 (PC0088767)	Zambia	Miombo woodland	**MN178510**	**MN178542**	—	—
	96204 (PC0088756)	Zambia	Miombo woodland	**MN178511**	EU569871	—	—
M. agardhii	EL88-04 (GB)	Sweden	*Salix*, calcareous	FJ904123	FJ904123	—	—
	JV7485F (WTU)	Finland	*Betula*, *Quercus*, gravel	—	AY380365	AY351792	AY333772
	JV13740 (WTU)	Finland	*Salix*, *Betula*, wet depression	—	AY380366	AY337362	AY337362
	AB980912 (GB)	Denmark	*Salix*	HM209790	HM209790	—	—
M. arenaria	EL250-08 (GB)	France	—	FN550937	FN550937	—	—
M. arthrocystis	BJ900815 (GB)	Sweden	*Salix*	—	GU980655	—	—
	CLC1141 (MONT)	Colorado	*Salix*	GU980653	GU980653	—	—
	CLC1356 (MONT)	Colorado	*Salix*	GU980649	GU980649	—	—
	CLC1357 (MONT)	Colorado	*Salix*	—	GU980652	—	—
	CLC1688 (MONT)	Colorado	*Salix*	GU980651	GU980651	—	—
	CLC1752 (MONT)	Colorado	*Salix*	GU980650	GU980650	—	—
	EL62-07 (GB)	Sweden	*Salix*	FN550941	FN550941	—	—
	PBM2397 (WTU)	Norway	*Picea*, *Betula*, *Salix*, eutrophic spruce forest	—	AY380394	AY351817	AY337402
	SJ06-011	Sweden	*Salix*	GU980654	GU980654	—	—
M. aurantiidisca	2020ZD01 (MHKMU)	Zhejiang	Mixed broad-leaved	OM179937	—	—	—
	NJ3109 (MHKMU)	Zhejiang	*Fagaceae* dominant	OM179935	OM138834	—	OM835751
	NJ3396 (MHKMU, **holotype**)	Zhejiang	*Pinus* dominant	OM179936	OM138835	—	OM835752
M. crassivelata	AH29788	Spain	*Castanea* forest	MN536810	—	—	—
	AH46622	Spain	*Quercus*, *Pinus*	MN536811	—	—	—
	MCVE 21499	Italy	*Picea* forest	MN536813	—	—	—
	MCVE 29561 (**holotype**)	Slovenia	*Fagus*	MN536812	MN537138	—	—
M. delecta	JV21393	Finland	*Pinus*, *Betula*, *Salix*, *Quercus*	OQ448534	OQ448534	—	—
	P. Karsten 1636 (H, **holotype**)	Finland	—	OQ448533	—	—	—
M. depressa	FM1300 (BJTC)	Shanxi	*Pinus* dominant	OM801895	OM801900	—	OM780099
	FM1695 (BJTC, **holotype)**	Shanxi	*Pinus* dominant	OM801899	OM801904	—	OM780100
M. errata	DED8022 (SFSU; ZT13034)	Thailand	*Pinus*, *Dipterocarpus*	EU569844	EU569844	—	—
	ZT9238	Thailand	*Pinus*, *Dipterocarpus*	—	EU569845	—	—
	ZT10108 (**type**)	Thailand	*Pinus*	—	GQ892935	—	—
M. fibrillosa (=*I. dulcamara sensu* Cripps *et al*. 2010)	CLC1131 (MONT)	Montana	*Salix*	GU980639	GU980639	—	—
	CLC1160 (MONT)	Montana	*Salix*	GU980642	—	—	—
	CLC1241 (MONT)	Colorado	*Salix*	GU980637	GU980637	—	—
	CLC1295 (MONT)	Colorado	*Salix*	GU980636	GU980636	—	—
	CLC1333 (MONT)	Colorado	*Salix*	GU980635	GU980635	—	—

Table 1. (Continued).

Species	Specimen-voucher (Herbarium)	Geographic origin	Ecology	GenBank Accession Numbers			
				ITS	28S	*rpb1*	*rpb2*
	CLC1364 (MONT)	Colorado	*Salix*	GU980641	—	—	—
	CLC1408 (MONT)	Colorado	*Salix*	GU980647	GU980647	—	—
	CLC1421 (MONT)	Colorado	*Salix*	GU980646	GU980646	—	—
	CLC1458 (MONT)	Colorado	*Salix*?	GU980638	GU980638	—	—
	CLC1581 (MONT)	Wyoming	*Salix*	GU980634	GU980634	—	—
	CLC1664 (MONT)	Colorado	*Dryas*?	GU980640	GU980640	—	—
	CLC1841 (MONT)	Colorado	*Salix*	GU980644	GU980644	—	—
	EL33-05 (GB)	Norway	*Salix*	GU980645	GU980645	—	—
	EL59-05 (GB)	Norway	*Betula*	GU980643	GU980643	—	—
	LVK14371	Maine	Mixed woods	**MN178498**	**MN178526**	**MN203504**	**MN203517**
	LVK14390	Maine	—	**MN178499**	**MN178527**	—	**MN203518**
	LVK15242	Maine	*Picea*, *Betula*	**MN178500**	—	—	—
	LVK22085	Maine	Mixed woods	**OP917925**	**OP918013**	—	—
	PBM2350 (WTU)	Washington	Conifers	—	EU600834	EU600832	EU600833
	REH10168 (TENN-F-073177)	New York	*Abies*, *Picea*, *Betula*, *Thuja*, *Pinus*	MH024850	MH024886	MK415442	MH577503
	2030506-001 (UBC F19167 as *I. gymnocarpa*)	British Columbia	—	HQ604785	HQ604785	—	—
M. fulviceps	DPL13914 (TENN-F-076539)	Louisiana	*Quercus nigra*	**OQ707213**	—	—	—
	MES-3773 (FLAS-F-66615)	Florida	*Quercus*, karst	**MZ404927**	—	—	—
	MES-2993 (FLAS-F-66574)	Florida	*Quercus*, karst	**MT415969**	—	—	—
	PBM4533 (TENN-F-075556)	Florida	*Quercus*, *Pinus*, karst	**MZ404928**	**MZ375430**	—	—
	PBM4542 (TENN-F-75565)	Florida	*Pinus*, *Quercus*, karst	**MZ404929**	**MZ375431**	**MZ404598**	**MZ405010**
	PBM4715 (TENN-F-F077389)	Florida	*Pinus*, *Quercus*, karst	**OQ208757**	—	—	—
	PBM4718 (TENN-F-077392)	Florida	*Pinus*, *Quercus*, karst	**OQ208758**	—	—	—
	PBM4722 (TENN-F-077396)	Florida	*Pinus*, *Quercus*, karst	**OQ208759**	—	—	—
	PBM4726 (TENN-F-077450)	Florida	*Carpinus*, *Quercus*, karst	**OQ208760**	—	—	—
M. fulvipes (subclade B *sensu* Cripps *et al*. 2010)	CLC1490 (MONT)	Colorado	*Salix*	GU980612	—	—	—
	CLC1566 (MONT)	Wyoming	*Salix*	GU980606	GU980606	—	—
	CLC1580 (MONT)	Wyoming	*Salix*	GU980608	GU980608	—	—
	CLC1844 (MONT)	Colorado	*Salix*	GU980611	GU980611	—	—
	EL83-07 (GB)	Sweden	*Salix*	FN550935	FN550935	—	—
	SJ84030 (GB – same field no. as *I. granulosa*)	Sweden	*Salix*	GU980609	GU980609	—	—
M. fuscomarginata	BJ890718 (GB)	Sweden	*Salix*	GU980656	GU980656	—	—
	EL109-06 (GB)	Sweden	*Salix*	FN550940	FN550940	—	—
	EL77-07 (GB)	Sweden	*Dryas*	GU980657	GU980657	—	—
M. granulosa	EL138-09 (GB, **type**)	Sweden	*Salix*, likely calcareous ground	KR029727	KR029727	—	—

Table 1. (Continued).

Species	Specimen-voucher (Herbarium)	Geographic origin	Ecology	GenBank Accession Numbers			
				ITS	28S	*rpb1*	*rpb2*
	Kuhner70-147 (as *I. squarrosoannulata*)	—	—	GU980610	GU980610	—	—
	SJ11008	Sweden	*Salix*	KR029726	KR029726	—	—
	SJ12916	Norway	—	KR029728	KR029728	—	—
	SJ12017	Norway	*Salix*	KR029729	KR029729	—	—
	SJ84030 (as *I. squarrosoannulata*)	Sweden	*Salix*	KR029725	KR029725	—	—
M. gymnocarpa	SJ980707 (GB)	Sweden	—	AM882866	AM882866	—	—
	16413	Italy	—	JF908161	—	—	—
	EL78-04 (GB; as "dulcamara")	Sweden	—	AM882865	—	—	—
M. heimii	JV14932 (WTU)	Italy	*Pinus*, sandy soil	—	AY380379	AY351804	AY337380
	G0256 (NL-0874)	Hungary	—	—	MK278231	—	—
M. isabellina	NLB420 (PERTH 08072442)	Western Australia	*Eucalyptus*, lawn	KP171139	KP170917	**MN203505**	KJ811583
	NLB836 (PERTH 08318441)	Western Australia	*Agonis*, *Spyridium*, *Acacia*, *Melalecua*, heath-scrub	KP171141	KP170920	**MN203506**	KJ811586
	E8290 (PERTH 07699255, **type**)	Western Australia	*Eucalyptus*, lawn	KP171137	KP170915	—	KJ811581
	NLB405 (PERTH 08096635)	Western Australia	Grassy parkland	KP171138	KP170916	—	KJ811582
	PBM3610 (PERTH 08319766)	Western Australia	*Eucalyptus*, *Corymbia*, Jarrah-Marri forest	—	KP170919	—	KJ811585
	E3730 (PERTH 07712758)	Western Australia	Sand dunes	**MN178501**	**MN178528**	—	MH618212
	NLB836 (PERTH 08318441)	Western Australia	*Agonis*, *Spyridium*, *Acacia*, *Melaleuca*, heath-scrub	KP171141	KP170920	—	KJ811586
	NLB800 (PERTH 08318832)	Western Australia	*Eucalyptus*, *Corymbia*, burned Jarrah-Marri forest	KP171140	KP170918	—	KJ811584
M. isabellina aff.	NLB491 (PERTH 08073287)	Western Australia	*Eucalyptus*, parkland	KP171142	KP170921	—	KJ811587
	PBM2207 / E7056 (TENN-F-066822)	Western Australia	*Corymbia*, lawn	—	AY380381	AY351806	AY337382
	PBM3595 (TENN-F-066498)	Western Australia	*Eucalyptus*, *Corymbia*, burned Jarrah-Marri forest	KP171143	KP170922	—	KP170922
M. latifolia	Nr. 3908 (M-0216716), EL3 (**type** *M. acystidiata*)	Germany	*Picea*, calcareous	**OR139041**	—	—	—
	Isolate 136	Shaanxi	*Populus simonsii* ECM root	LC013759	—	—	—
	Isolate 1969	Shaanxi	*Populus simonsii* ECM root	LC013761	—	—	—
	LVK22088	Maine	Mixed woods	**OP918037**	**OP918067**	**OQ870543**	—
	LVK22089	Maine	Mixed woods	**OP918038**	—	**OQ870544**	**OP924514**
	MO364156	Arizona	*Populus*, Cypress	MN177633	—	—	—
	M-0216738 (**type** *M. latifolia*)	Germany	*Betula*, *Picea*, calcareous	OQ976965	—	—	—
	PBM4535 (TENN-F-075558)	Florida	*Pinus*, *Quercus*	**MZ404930**	**MZ375432**	**MZ404599**	—
	PBM4537 (TENN-F-075560)	Florida	*Quercus*, *Pinus*, *Carpinus*	**MZ404931**	**MZ375433**	**MZ404600**	**MZ405011**
M. latispora	EL212-06 (GB)	France	—	FN550938	FN550938	—	—

Table 1. (Continued).

Species	Specimen-voucher (Herbarium)	Geographic origin	Ecology	GenBank Accession Numbers			
				ITS	28S	*rpb1*	*rpb2*
	EL190-08 (GB)	Sweden	—	KR029724	KR029724	—	—
	EL3-04 (GB)	Sweden	—	AM882859	—	—	—
	JV19684 (TENN-F-074801)	Finland	*Populus*, *Salix*, *Pinus* seedlings, on calcareous mull	**MN178502**	—	—	**MN203519**
	JV19640F (TENN-F-063757)	Finland	*Salix*, *Betula*, *Pinus*, *Populus*, *Picea*, calcareous soil	**MN178503**	**MN178529**	—	**MN203520**
	JV19642F (TENN-F-063523)	Finland	*Salix*, *Betula*, *Pinus*, *Populus*, *Picea*, calcareous soil	**MN178504**	**MN178530**	—	**MN203521**
	JV19650F (TENN-F-063759)	Finland	*Pinus*, *Betula*, *Picea*, *Salix*, near limestone quarry	**MN178505**	**MN178531**	**MZ404601**	**MN203522**
	STU-F-0901665 (**type** *M. plebeia*)	Germany	*Salix*, *Pinus*, calcareous soil	ON003442	—	—	—
M. leucoblema	CLC1721 (MONT)	Colorado	*Dryas*	GU980632	GU980632	—	—
	EL66-08 (GB)	Sweden	—	FN550936	FN550936	—	—
	EM29	Russia	*Epipogium aphyllum* root	—	EU711227	—	—
	JV16437 (WTU)	Finland	*Pinus*, *Picea*, *Salix*, *Betula*, *Populus*, calcareous soil	—	EU569858	AH013036	AY333310
	JV2898	Finland	*Picea*, *Betula*	HM209789	HM209789	—	—
	Moser 71123 (TENN-F-037075)	France	—	FJ601811 & FJ601812	**MN178532**	—	—
	PBM1522 (WTU)	Wyoming	*Picea*, *Abies*, calcareous soil	—	**MN178533**	—	MH577511
	PBM2737 (TENN-F-062549)	Colorado	*Picea*	HQ232481	**MN178534**	**MN203507**	—
	SEB97-09 (GB)	Sweden	*Pinus*	GU980631	GU980631	—	—
	SM2324 (GB)	Sweden	*Picea*	GU980630	GU980630	—	—
	TAA128324 (GB)	Estonia	*Salix*	GU980633	GU980633	—	—
M. leucoloma	CLC1232 (MONT)	Colorado	*Salix*	GU980624	GU980624	—	—
	CLC1355 (MONT)	Colorado	*Salix*	GU980623	GU980623	—	—
	CLC1431 (MONT)	Colorado	*Salix*	GU980619	GU980619	—	—
	CLC1442 (MONT)	Colorado	*Salix*	GU980620	GU980620	—	—
	CLC1703 (MONT)	Colorado	*Salix*	GU980617	GU980617	—	—
	CLC1869 (MONT)	Colorado	*Salix*	GU980618	GU980618	—	—
	CLC1877 (MONT)	Colorado	*Salix*	GU980621	GU980621	—	—
	EL40-07 (GB)	Sweden	*Salix*	GU980615	GU980615	—	—
	EL41-07 (GB)	Sweden	*Salix*	GU980615	GU980615	—	—
	EL50-05 (GB)	Norway	*Dryas*, *Salix*	AM882855	AM882855	—	—
	EL106-07 (GB)	Sweden	*Salix*	GU980627	GU980627	—	—
	EL107-07 (GB)	Sweden	*Salix*	GU980625	GU980625	—	—
	EL1-06 (GB)	Norway	*Salix*	GU980626	GU980626	—	—
	EL69-05 (GB)	Norway	*Dryas*, *Salix*	GU980616	GU980616	—	—

Table 1. (Continued).

Species	Specimen-voucher (Herbarium)	Geographic origin	Ecology	GenBank Accession Numbers			
				ITS	**28S**	***rpb1***	***rpb2***
	Kühner 63-36 (G, **type**)	France	*Dryas*, *Salix*	GU980614	GU980614	—	—
	PBM1574 (WTU)	Wyoming	*Salix*	—	EU555458	—	—
	PBM2296 (WTU)	Washington	Conifers mixed with *Betula*, *Populus*	—	AY380372	AY351798	AY337373
M. leucothrix sp. nov.	iNat131154234 (sp-AZ01)	Arizona	*Pinus*, *Quercus*, *Juniperus*, calcareous soil	OP784362	—	—	—
	iNat131155272 (sp-AZ01)	Arizona	*Pinus*, *Quercus*, *Juniperus*, calcareous soil	OP784312	—	—	—
	iNat131844666 (sp-AZ01)	Arizona	*Pinus*, *Quercus*, *Juniperus*, calcareous soil	OP784364	—	—	—
	PBM4541 (TENN-F-075564, **type**)	Florida	*Quercus*, *Pinus*, karst topography	**MZ404932**	**MZ375434**	**MZ404602**	**MZ405012**
	PBM4531 (TENN-F-075554)	Florida	*Quercus*, *Pinus*, karst topography	**MZ404933**	**MZ375435**	**MZ404603**	**MZ405013**
M. longicystis	FYG6371 (MHKMU)	Hainan	Fagaceous trees	OM179926	OM135609	—	OM835746
	FYG6373 (MHKMU)	Hainan	Fagaceous trees	OM179927	OM135610	—	OM747850
	FYG6374 (MHKMU, **type**)	Hainan	Fagaceous trees	OM179928	OM135611	—	OM835747
	FYG6376	Hainan	Fagaceous trees	OM179929	OM135612	—	OM835745
M. luteobasis sp. nov.	MK06071503 (TENN-F-073751)	Illinois	*Carya*, *Juniperus*	**MN178506**	**MN178535**	**MN203508**	**MN203523**
	MK06211102 (TENN-F-073749)	Illinois	*Quercus*, *Carya*	**MT239045**	—	—	—
	MK07140307 (TENN-F-073752)	Indiana	Deciduous woods	**MN178507**	**MN178536**	**MZ404604**	**MN203524**
	MK07180705 (TENN-F-073750, **type**)	Illinois	*Quercus*	**MN165953**	**MN178537**	**MZ404605**	**MN203525**
	Sayers *s.n.* (TENN-F-063525)	Kansas	*Quercus*	—	JN975028	—	MH577502
M. malenconii	EL807	Spain	—	FN550939	FN550939	—	—
	HMAS 262707	China	—	KJ810603	—	—	—
	IK-00018	Poland	—	KX602259	—	—	—
	JV4470F (WTU)	Finland	*Pinus sylvestris*, sandy soil	—	GQ906704	—	**MN203526**
	JV5498A (WTU)	Finland	—	—	EU569870	—	EU569869
	JV5824F (WTU)	Finland	*Picea*, *Betula*, *Salix*, sandy soil	—	**MN178538**	—	—
	JV23101 (WTU)	Finland	*Betula*, *Salix*, *Picea*	HM209787	HM209787	—	—
	LVK21286	New York	Mixed conifers and hardwoods	**OP046391**	**OP046370**	—	**OP060362**
	LVK22039	Maine	*Quercus*, *Pinus*	**OP918252**	—	—	—
	LVK22045	Maine	*Quercus*, *Pinus*	**OP913409**	—	—	—
	PAM98941302	France	*Betula*, *Pinus*	HM209788	HM209788	—	—
	SJ030822 (GB)	Sweden	*Pinus*	AM882862	—	—	—
	2020521-001 (UBC F19123)	British Columbia	—	HQ604776	HQ604776	—	—
M. montana sp. nov.	PBM3872 (TENN-F-067500, **type**)	North Carolina	Riverine hardwood forest	**OP046392**	**OP046371**	**OQ866119**	**OP060363**
	PBM4190 (TENN-F-074532)	North Carolina	*Pinus*, *Betula*	**MN178512**	—	—	—
	PBM4614 (TENN-F-075781)	North Carolina	*Tsuga*, *Pinus*, *Quercus*, *Betula*	**OP046393**	**OP046372**	**OP060357 & OP060358**	**OP060364**
M. multispora	CO4248 (CSU)	Oklahoma	*Quercus*, *Carya*, *Ulmus*, *Fraxinus*, sand	**MN178509**	**MN178540**	**MZ404606**	—
	DPL13518 (TENN-F-077876)	Texas	Bottomland hardwood forest near *Pinus*	**OQ707215**	—	—	—
	iNat126273738	Florida	*Quercus*, *Pinus*, sandy soil, karst	OP101166	—	—	—

Table 1. (Continued).

Species	Specimen-voucher (Herbarium)	Geographic origin	Ecology	GenBank Accession Numbers			
				ITS	28S	*rpb1*	*rpb2*
	iNat131720866	Arizona	*Pinus*, *Quercus*, *Juniperus*, calcareous	OQ023952	—	—	—
	FLAS-F-66616	Florida	*Quercus*, karst	**MZ404934**	—	—	—
	FLAS-F-61779	Florida	*Pinus*, *Sabal*, sandy pine flatlands	MH281884	MH620328	—	—
	FLAS-F-70016	Florida	—	OP580228	—	—	—
	MycoMap 10129	Indiana	hardwoods	OM473595	—	—	—
	MycoMap 10246	Indiana	*Pinus*, *Quercus*	OM473596	—	—	—
	PBM4717 (TENN-F-077391)	Florida	*Pinus*, *Quercus*, karst	**OQ208761**	—	—	—
M. myriadophylla	IK-00039	Poland	—	KX602263	—	—	—
	JV19652F (TENN-F-063760 – AFTOL-ID 482)	Finland	*Pinus*, *Betula*, *Picea*, *Salix*, calcareous mull soil	DQ221106	AY700196	DQ447917	AY803751
	JV19678 (TENN-F-063761, **type**)	Finland	*Pinus*, *Picea*, *Salix*, *Betula*, *Populus*	HM209793	HM209793	—	—
	JV5968F (WTU)	Finland	*Betula*, *Picea*, *Pinus*, calcareous ground	HM209794	HM209794	—	—
	SZ01	Germany	—	MF807958	—	—	—
M. nuptialis	STU-F-0901660	Austria	*Salix*, *Juniperus*, *Dryas*, *Pinus*, *Alnus*	ON003443	—	—	—
	STU-F-0901661 (**type**)	Austria	*Salix*	ON003444	ON003444	—	—
	STU-F-0901662	Germany	*Salix*	ON003445	—	—	—
M. pallidipes	FYG3736 (MHKMU, **type**)	Jilin	*Populus*	OM179924	OM137052	—	OM835749
	FYG3727 (MHKMU)	Jilin	*Populus*	OM179925	—	—	OM835750
M. piceae	FM555 (BJTC, **type**)	Shanxi	*Picea*	OM801896	OM801901	—	OM780096
	FM569 (BJTC)	Shanxi	*Picea*	OM801897	OM801903	—	OM780097
	FM896 (BJTC)	Shanxi	*Picea*	OM802898	OM801902	—	OM780098
M. praevillosa comb. nov.	FLAS-F-61523	Florida	*Pinus*, *Quercus*	MH211949 & **OP046394**	MH620294 & **OP046373**	**OP060359**	**OP060365**
	PBM4724 (TENN-F-077398)	Florida	*Quercus*, *Pinus*, karst	**OQ208762**	—	—	—
M. pygmaea	EL48-05 (GB)	Norway	*Dryas*, *Salix*	GU980628	GU980628	—	—
	J. Favre (**type**)	Switzerland	*Salix*	GU980629	—	—	—
M. pyrrhopoda	MDB F292/10 (PERTH 08383278)	Western Australia	*Antidesma*, *Glochidion*, *Melaleuca*, *Eucalyptus*, tropical forest	KP308814	KP170984	—	KM406224
	MDB F18s/13 (PERTH 08557764)	Western Australia	*Melaleuca*, tropical	KP308815	KP170986	—	KM406226
	PBM3759 (TENN-F-066987, **type**)	Queensland	*Melaleuca*, *Lophostemon*, *Corymbia*, tropical swamp	KP308813	KP170983	**MN203509**	KM406223
	PBM3740 (TENN-F-066972)	Queensland	*Corymbia*, *Eucalyptus*, tropical woodland	—	KP170985	—	KM406225
	REH9670	Queensland	*Eucalyptus*, subtropical	KP641622	KP171077	—	—
M. sabulosa	NLB986 (PERTH 08383308)	Western Australia	*Corymbia*, *Acacia*, gray sand limestone	—	KP170998	**MN203510**	KM406238
	NLB901 (PERTH 08320292)	Western Australia	*Acacia*, *Templetonia*, *Eucalyptus*, shrubland	KP308825	KP170997	—	KM406237
	E8178 (PERTH 07680732)	Western Australia	*Eucalyptus*, *Corymbia*, woodland	KP308822	JN974916	—	KM406235
	E8182 (PERTH 07680775)	Western Australia	*Eucalyptus*, suburban bushland	KP308823	KP170995	—	KM406236
	NLB898 (PERTH 08320322, **type**)	Western Australia	*Eucalyptus* (planted)	KP308821	KP170994	—	KM406234

Table 1. (Continued).

Species	Specimen-voucher (Herbarium)	Geographic origin	Ecology	GenBank Accession Numbers			
				ITS	28S	*rpb1*	*rpb2*
	MDB F7/11 (PERTH 08383057)	Western Australia	*Corymbia*, *Albizzia*, tropical woodland	KP308824	KP170996	—	—
Mallocybe sp. 1	uncultured	Alaska	*Dryas*	JX630703	—	—	—
	—	Alaska	*Dryas*	JX630716	—	—	—
	—	Alaska	*Dryas*	JX630710	—	—	—
Mallocybe sp. 2 (=*I. marmoripes sensu* N. Am. *auct.*, *non* G.F. Atk.)	BK06069724 (WTU)	Oregon	Conifers	—	AY380400	AY351825	MH577505
	BK06069725 (WTU)	Oregon	Conifers	—	**MN178541**	—	—
	LLN93063018 (WTU)	Washington	*Pinus*, *Salix*, *Alnus*	**OQ734476**	—	—	—
	2070626 (UBC F19439 as *I. malenconii* var. *megalospora*)	British Columbia	—	HQ604786	HQ604786	—	—
Mallocybe sp. 3	PBM1615	Washington	*Picea*, *Pseudotsuga*	—	AY038327	AF389549	AY337374
Mallocybe sp. 4	PBM2290 (WTU)	Washington	Conifers	—	EU555446	—	EU555445
Mallocybe sp. 5	JFA13285 (WTU)	Washington	*Picea*, *Pinus*, *Abies*	**MN178514**	**MN178543**	**MZ404607**	**MN203527**
	PBM1922 (WTU)	Washington	*Picea*, *Pinus*, *Tsuga*, *Pseudotsuga*	—	EU600879	—	EU600878
	SDA470 (TENN-F-074895)	Washington	*Abies*, *Pseudotsuga*, *Pinus* spp.	—	**ON478242**	—	—
Mallocybe sp. 6	ADP060305 (TENN-F-063537)	Washington	*Pseudotsuga*	**MN178513**	EU600877	—	EU600876
	PBM1444 (WTU)	Washington	*Populus*, *Abies*, *Pseudotsuga*	**OQ707214**	—	—	—
Mallocybe sp. 7	NS2563 (PDD 107312)	New Zealand	*Nothofagus*	**MN047372**	—	—	—
Mallocybe sp. 8	CFSZ12101	China	—	OP204682	—	—	—
	CFSZ12091	China	—	OP204681	—	—	—
	CFSZ22975	China	—	OP204687	—	—	—
	P20 “type”	China	—	ON045553	—	—	—
	PBM4749 (TENN-F-077511)	West Virginia	*Picea*	**OQ208763**	**OQ225230**	**OQ866120**	**OQ866121**
Mallocybe sp. 9	UBC F19404 (as *terrigena*)	British Columbia	*Pseudotsuga*, *Arbutus*	HQ604783	HQ604783	—	—
	UBC F19332 (as *terrigena*)	British Columbia	*Pseudotsuga*, *Thuja*	HQ604779	HQ604779	—	—
	UBC F19432 (as *terrigena*)	British Columbia	—	HQ604780	HQ604780	—	—
	DAVFP 28178 (as *terrigena*)	British Columbia	*Pseudotsuga*	HQ650752	—	—	—
	BK0306992 (UTC)	Washington	*Pseudotsuga*, *Arbutus*	—	AY038315	—	—
M. siciliana	AMB18273	Italy	*Salix*	MG757416	MG757418	—	—
	AMB18274	Italy	*Salix*	MG757417	MG757419	—	—
	JV7987 (WTU)	Finland	*Pinus*, *Picea*, *Salix*, *Betula*, *Alnus* on calcareous ground	—	EU569834	—	—
M. squamosodisca comb. nov.	LVK20133 (TENN-F-077383)	Maine	—	**MZ404935**	**MZ375436**	—	**MZ405014**
	LVK22053	Maine	*Quercus*, *Pinus*	—	—	—	—
	PBM4307 (TENN-F-074869)	Tennessee	*Quercus*, *Pinus*	**MT196944**	—	—	**MZ405015**
	PBM4591 (TENN-F-075758)	North Carolina	*Pinus*, *Tsuga*, *Quercus*, *Betula*	**OP046395**	**OP046374**	—	**OP060366**
	PBM4621 (TENN-F-075791)	New York	*Pinus*, *Abies*, *Betula*, *Populus*	**OP046396**	**OP046375**	—	—

Table 1. (Continued).

Species	Specimen-voucher (Herbarium)	Geographic origin	Ecology	GenBank Accession Numbers			
				ITS	28S	*rpb1*	*rpb2*
	REH7036 (NY01034397)	Costa Rica	*Quercus*, *Comarostaphylis*	**OP048953**	—	—	—
M. squarroso-annulata	Kuhner 63-236 (G, **type**)	Switzerland	—	HM209795	—	—	—
M. subflavospora	E5880 (PERTH 07609256, **type**)	Western Australia	*Eucalyptus*, dry sclerophyll	—	AY380396	AY351820	AY351821
	NLB1078 (PERTH 08578931)	Western Australia	*Allocasuarina*, *Eucalyptus*, woodland	**MN178515**	**MN178544**	—	MH577504
	NLB915 (PERTH 08320861)	Western Australia	*Eucalyptus*	KP641619	KP171074	—	KM656118
	PBM3791 (TENN-F-067023)	Queensland	*Eucalyptus*, wet sclerophyll	KP641620	KP171075	—	KM656119
	PBM3677 (PERTH 08319081)	Western Australia	*Allocasuarina*, dry sclerophyll	KP641621	KP171076	—	KM656120
M. subflavospora aff.	PBM3763 (TENN-F-066995)	Queensland	*Eucalyptus*, dry sclerophyll	—	**MN178545**	**MN203511**	MH618248
M. subgranulosa	EL11-12	Sweden	*Pinus*, *Salix*	OQ448535	OQ448535	—	—
	P. Karsten 2499 (H, **type**)	Finland	—	OQ448532	—	—	—
M. substraminipes	CLC1375 (MONT)	Colorado	*Salix*	GU980605	GU980605	—	—
	CLC1649 (MONT)	Colorado	*Dryas*	GU980602	GU980602	—	—
	CLC1731 (MONT)	Colorado	*Dryas*, *Salix*	GU980603	GU980603	—	—
	CLC2292 (MONT)	Colorado	*Salix*	GU980604	GU980604	—	—
	EL30-07 (GB)	Sweden	*Dryas*, *Salix*	GU980599	GU980599	—	—
	EL83-07 (GB)	Sweden	*Salix*	FN550935	FN550935	—	—
	EL99-07 (GB)	Sweden	*Salix*	GU980600	GU980600	—	—
	Kühner70-148 (G, **type**)	France	*Dryas*	GU980601	GU980601	—	—
	PBM1529 (WTU)	Wyoming	*Picea*, *Abies*	—	EU569835	—	—
	T10763 (WTU)	Alaska	*Salix*, *Alnus*	—	EU569836	—	—
M. subtilior	E00116332 (E)	Sabah (Malaysia)	in flower pot	**MN178516**	**MN178546**	—	—
	E9112 (PERTH 08095388)	Western Australia	—	KP641628	KP171082	—	—
	E4810 (PERTH 07660634)	Western Australia	*Eucalyptus*	KP641628	KP171083	—	—
	MDB F75/11 (PERTH 08383081)	Western Australia	*Corymbia*, *Acacia*, *Triodia*, red sand woodland	KP641629	KP171084	—	KM656125
	OKM24631 (PERTH 08561745, **type**)	Western Australia	*Eucalyptus*, sand	—	AY380398	AY351823	AY337406
M. subtomentosa comb. nov.	DPL13020	Mexico	*Pinus*	**OP046397**	—	—	—
	DPL13025	Mexico	*Pinus*	**OQ208764**	—	—	—
	LVK14251	Maine	*Pinus strobus*	**MN178517**	—	—	—
	LVK16004 (TENN-F-077382)	New Jersey	*Pinus*, *Quercus*	**MN178518**	**MN178547**	—	**MN203528**
	LVK16006	New Jersey	*Pinus*, *Quercus*	**MN178519**	**MZ375437**	—	**MZ405016**
	LVK16235	New Jersey	*Pinus*, *Quercus*	—	**MN178548**	**MN203512**	**MN203529**
	LVK17005	New Jersey	*Pinus*, *Quercus*	**MN178520**	—	—	—
	ME12_A6	Alaska	Arctic	JX436908	—	—	—
	MO207009	Pennsylvania	Conifer grove, grass	—	—	—	**MN203530**
	PBM2460 (TENN-F-062321)	Massachusetts	Mixed woods including *Pinus*, *Quercus*	**MN178521**	**MN178549**	**MN203513**	**MN203531**
	PBM3910 (TENN-F-068440)	North Carolina	*Pinus*, *Quercus*, *Betula*	**OP046398**	—	—	—
	PBM4701 (TENN-F-75838)	New York	Mixed conifers and hardwoods	**ON503076**	—	—	—
	PBM4763 (TENN-F-077551)	West Virginia	*Tsuga*, *Betula*, *Pinus strobus*, acidic soil	**OQ707212**	—	—	—

Table 1. (Continued).

Species	Specimen-voucher (Herbarium)	Geographic origin	Ecology	GenBank Accession Numbers			
				ITS	28S	*rpb1*	*rpb2*
	SAT9923301 (WTU)	New Mexico	*Pinus*, *Quercus*, *Pseudotsuga*	—	AY380373	AY351799	AY388644
M. terrigena	EL22-99 (GB)	Estonia	*Picea*, calcareous	AY586680	AY586680	—	—
	EL24-08 (GB)	Wyoming	*Salix*	GU980648	GU980648	—	—
	EL117-04 (GB)	Sweden	*Picea*, calcareous	AM882864	AM882864	—	—
	JV16431	Finland	*Pinus*, *Picea*, *Salix*, *Betula*, *Populus*, calcareous soil	—	AY380401	AY333301	AY333309
	PBM1563 (WTU)	Wyoming	*Picea*, *Abies*	—	**MN178550**	**MN203514**	—
M. tomentella sp. nov.	SAT0622810 (WTU)	Alberta	—	**MN178508**	**MN178539**	**OQ872543**	—
	PBM4690 (TENN-F-075826, **type**)	New York	Mixed conifers and hardwoods	**OP046400**	**OP046376**	**OP060360**	**OP060367**
	PBM4694 (TENN-F-075831)	New York	Mixed conifers and hardwoods	—	**ON478244**	—	—
M. tomentosula	GF2321 (TLXM)	Mexico	*Pinus cembroides*	KR817255	—	—	—
	HRL0027 (TENN-F-071134)	Quebec	*Pinus strobus*	KX897446	—	—	—
	PBM4138 (TENN-F-071837)	Tennessee	*Quercus*, *Juniperus*, limestone quarry	MG773814	MK421969	MK415443	MH577506
	RAS123 (TENN-F-071659)	Tennessee	*Quercus*, *Juniperus*, limestone quarry	MF992166	MF797642	—	—
M. umbrinofusca	Kühner70-38 (G, **type**)	France	*Salix*	GU980613	—	—	—
M. unicolor	iNAT:53190985 (TENN-F-076529)	Iowa	Hardwood forest	**ON503067**	**OP046377**	**OP060361**	**OP060368**
	MK06181501 (TENN-F-073747)	Illinois	*Quercus*	MH578008	—	—	—
	MK06231101 (TENN-F-073748)	Illinois	Hardwoods	MH578010	—	—	—
	MK08281401 (TENN-F-074753)	Illinois	*Quercus*, *Carya*	MH578009	—	—	—
	PBM1481 (WTU)	Missouri	*Quercus*, *Carya*, karst	—	AY380403	AY351827	AY337409
	PBM2645 (TENN-F-062476)	North Carolina	*Quercus*, *Fagus*	**MN178522**	**MN178551**	—	—
	PBM2940 (TENN-F-062698)	Tennessee	*Carya*, *Fagus*, karst	**MN178523**	**MN178552**	—	—
	PBM2974 (TENN-F-062732)	Tennessee	*Quercus*, lawn, karst	**MN178524**	JQ313569	**MN203515**	**MN203532**
	REH5532 (WTU)	New York	*Quercus*, *Fagus*	—	**MN178553**	—	**MN203533**
	RV7/4 (DUKE)	North Carolina	—	DQ490637	AF042617	—	—
	SH082407-01 (TENN-F-063553)	New Jersey	*Quercus*, lawn	**MN178525**	**MN178554**	**MN203516**	**MN203534**
M. velutina	MSM0048 (LAH310057, **type**)	Pakistan	*Pinus*	**MK990129**	**MK999927**	—	—
	MSM0049	Pakistan	*Pinus*	**MK990130**	**MK999928**	—	—
	MSM00050	Pakistan	*Pinus*	**MK990131**	**MK999929**	—	—
OUTGROUPS							
Auritella brunnescens	PBM3173 (TENN-F-065354)	New South Wales	*Eucalyptus*, dry sclerophyll	KJ702343	JQ313558	MK415420	KJ702348
Crepidotus applanatus	PBM717 (WTU)	Washington	Hardwood log, mixed *Pseudotsuga* forest	DQ202273	AY380406	AY333303	AY333311
Inosperma mutatum	PBM2542 (TENN-F-062387)	Massachusetts	*Quercus*	—	AY732212	DQ447917	DQ472729
Inosperma rimosoides	PBM2459 (TENN-F-062320)	New York	*Quercus*, *Pinus*, *Carya*, *Juniperus*, calcareous	DQ404391	AY702014	DQ447915	DQ385884
Tubariomyces sp.	BB6018 (PC)	Zambia	Miombo woodland	MK421964	EU600887	MK415448	EU600886

The 4-locus supermatrix provides a robust phylogeny of *Mallocybe*

Figure 1 provides a single-page phylogenetic overview of major clades and some species-level lineages within *Mallocybe* and the species that reside within each. Outgroups were pruned from this figure. Figure 2 was split into three parts detailing the entire phylogram. Phylogenetic analyses of the 4-gene supermatrix recovered an overall topology most similar to the *rpb2* gene tree with strong support for the union of clades Nothosperma and Mallocybe as a monophyletic group, and sister to it clade Unicolores. Similar to the *rpb1* and *rpb2* gene trees, both *Inocybe* (*Lepista*) *praevillosa* and *M. montana* formed a paraphyletic assemblage from which clades Unicolores and Nothosperma + Mallocybe emerged. Every one of these major nodes received strong support (> 77 % ML bootstrap) despite differences in taxon sampling depth per gene region. Overall, at least 55 species-level lineages were detected.

Murrill's *Inocybe* (*Lepista*) *praevillosa*, recombined below as *Mallocybe praevillosa*, was recovered as sister to all other species of *Mallocybe*. Murrill's taxon is distinguished by the relatively robust but brittle basidiomes, rooting stipe, the rather pale [originally described as pale pinkish by Murrill (1942)] allantoid to cylindric basidiospores, the presence of a low relative concentration of muscarine (Fig. 3), absence of necropigmented basidia, and elongated cheilocystidia. Cystidioid elements were found on the stipe, but these were not arranged in any way similar to those that characterize species of the genus *Tubariomyces* (Alvarado *et al.* 2010). Furthermore, the pileipellis was found to be a cutis giving rise to upright and interwoven hyphae, also unlike *Tubariomyces*, which forms a trichodermial palisade. The species was collected by us under *Quercus laurifolia* near the type locality on karst topography but also on sandhills with *Quercus* and *Pinus*.

Mallocybe montana (described below) was observed as sister to the remainder of *Mallocybe* with strong support. This species is characterized by elongated cheilocystidia, elongated cylindric basidiospores, necropigmented basidia, lack of a detectable amount of muscarine (Fig. 3), and occurrences on sandy acidic soils in mountainous regions of the Southern Appalachians.

Clade Unicolores (= Clade C in Hu *et al.* 2023) appeared sister to the other two major clades within *Mallocybe*. Here we documented that two additional species described by Murrill from Florida, *M. fulviceps* and *M. multispora*, belong to this clade. The American species in clade Unicolores are characterized often by elongated cheilocystidia, elongated cylindric spores, stipe length longer than the pileus width, and putative ectomycorrhizal relationships with *Quercus* and/or *Pinus* on limestone soils. *Mallocybe unicolor*, the third eastern North American species in clade Unicolores, seems to have a wide ecological amplitude, occurring abundantly in areas characterized by *Quercus* and *Tilia* on karst topography; however, the species has also been recorded, but with low basidiome abundance, on acidic soils in montane regions of the Southern Appalachians. Three East Asian species were also recovered in clade Unicolores, all of which are also characterized by elongated cheilocystidia (Hu *et al.* 2023). Their plant associations include *Fagaceae* (*e.g.*, *Castanopsis*) and Salicaceae (*Populus*).

The second major grouping, clade Nothosperma (= Clade B in Hu *et al.* 2023) contained five named species from Australia and/or Malaysia and one unidentified species from New Zealand. Two species – *M. subflavospora* and *M. pyrrhopoda* – were non-monophyletic. Within clade Nothosperma, the New Zealand sample (*Mallocybe* sp. 7) is sister to the Australian lineages with strong support. The unpublished *Mallocybe* sp. 7 is characterized by elongated cheilocystidia and an association with *Nothofagus*, unlike the Australian species in this clade, all of which have short cheilocystidia and associations with *Myrtaceae*, *Casuarinaceae*, and *Fabaceae* (Matheny & Bougher 2017). *Mallocybe callichroa* (recombined into *Mallocybe* below), another *Nothofagus* associate from New Zealand with clavate and elongated cheilocystidia, may belong to this clade as well, but molecular confirmation is lacking. *Mallocybe sabulosa* was found to contain relatively high amounts of muscarine (Fig. 3), whereas *M. isabellina* lacked any detectable amount of the toxin.

The third major group is referred to as clade Mallocybe (= Clade A in Hu *et al.* 2023) and includes the generic type *M. terrigena* and 40 other species-level lineages primarily from temperate regions of the northern hemisphere (and three from or extending into tropical latitudes). Several mostly strongly supported inclusive groupings were also observed in clade Mallocybe. The first of these was the Arthrocystis clade containing four species, only two of which are presently described – the European species *M. arthrocystis* and the East Asian *M. piceae*, and two undescribed species from the Pacific Northwest in western North America; all analyses recovered the Arthrocystis clade as monophyletic but only with moderate support (*e.g.*, 61 % ML bootstrap).The Fuscomarginata clade likewise included four species, two of which are known in Europe – *M. fuscomarginata* and *M. gymnocarpa*; two additional unclarified species were identified from the Pacific Northwest.

The core Mallocybe clade was recovered with strong support and was characterized by the inclusion of the Heimii clade, the Terrigena grade, and the highly diverse Delecta clade. The Heimii clade was strongly supported as sister to rest of the core Mallocybe clade with five species from the northern hemisphere including South Asia, whereas the Terrigena grade was recovered as a paraphyletic assemblage of *M. luteobasis* (described as new below), *M. terrigena*, *M. fibrillosa* (= *I. dulcamara sensu auct. p.p., non* Persoon), and *M. leucoblema.* The Delecta clade contains 24 species from north temperate regions, including high elevations in Central America. Within clade Mallocybe, six samples were assayed for the presence of muscarine, but the toxin was undetected in all of them (Fig. 3; see also further results below).

In total, 16 species of *Mallocybe* were recovered from eastern North America (four described as new below, but also one additional species that cannot be described here due to insufficient data). Of these 16 species, 11 were recovered in clade Mallocybe, three in clade Unicolores, and two corresponded to the Montana and Praevillosa lineages. Several additional and probably undescribed species were also recovered from western North America. These will be addressed and treated in a forthcoming study.

Overall, many species of *Mallocybe* have been characterized by broad intercontinental biogeographic distributions (Cripps *et al.* 2010). However, some local endemism by continent or regions of continents was suggested by our results. Species known currently only from eastern North America included several species described as new or recombined into *Mallocybe* below – *M. leucothrix*, *M. montana, M. praevillosa*, *M. squamosodisca* (including Costa Rica), *M. luteobasis*, and *M. tomentosula* (including Mexico), *M. unicolor*, and *M. fulviceps*.

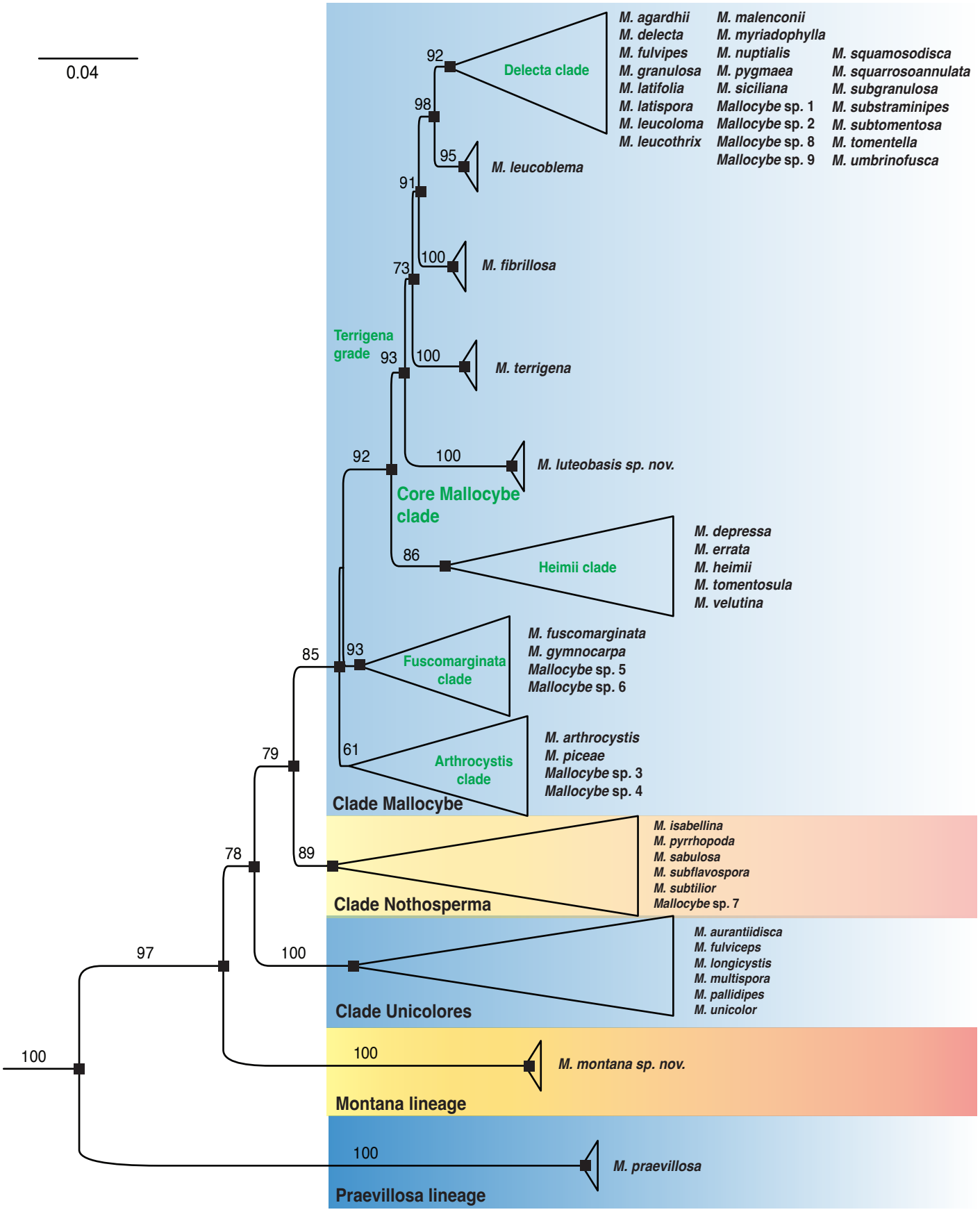

Fig. 1. Summary ML phylogram of *Mallocybe* based on a supermatrix of combined *rpb1, rpb2*, ITS, and 28S sequence data. Inclusive terminal groupings are cartooned to compress the figure for easier graphic presentation. Three major clades and two unresolved species-level lineages within *Mallocybe* are indicated: clades Mallocybe, Nothosperma, and Unicolores and the Montana and Praevillosa lineages. Within clade Mallocybe, several strongly supported nested groups were recovered: the Arthrocystis, Fuscomarginata, Heimii, core Mallocybe, and Delecta clades, in addition to a strongly supported paraphyletic group referred to as the Terrigena grade. Numbers above or below branches represent bootstrap proportions > 70 % except for the Arthrocystis clade. Black-filled squares indicate support values for internodes with SH-aLRT > 80 % and UF bootstraps > 95 %. The scale bar indicates the number of expected substitutions per site. Outgroups have been pruned.

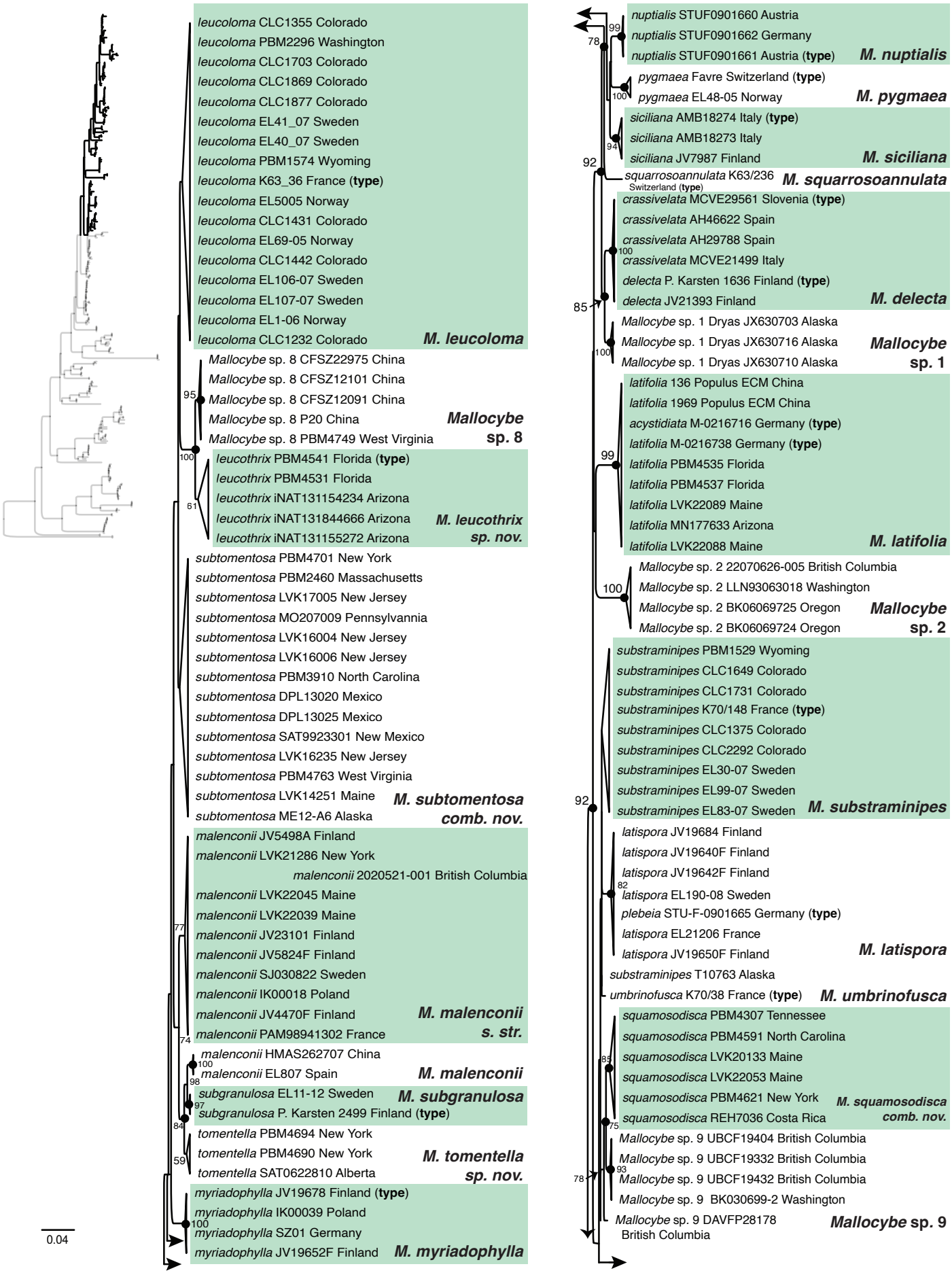

Fig. 2. The ML phylogeny of *Mallocybe* based on a supermatrix of combined *rpb1, rpb2*, ITS, and 28S sequence data. Numbers above or below branches indicate bootstrap proportions > 50 %. Black-filled circles indicate support values for internodes with SH-aLRT > 80 % and UF bootstraps > 95 %. The figure is divided into three parts (A, B, C). The scale bar equals the number of expected number of substitutions per site.

Fig. 2. (Continued).

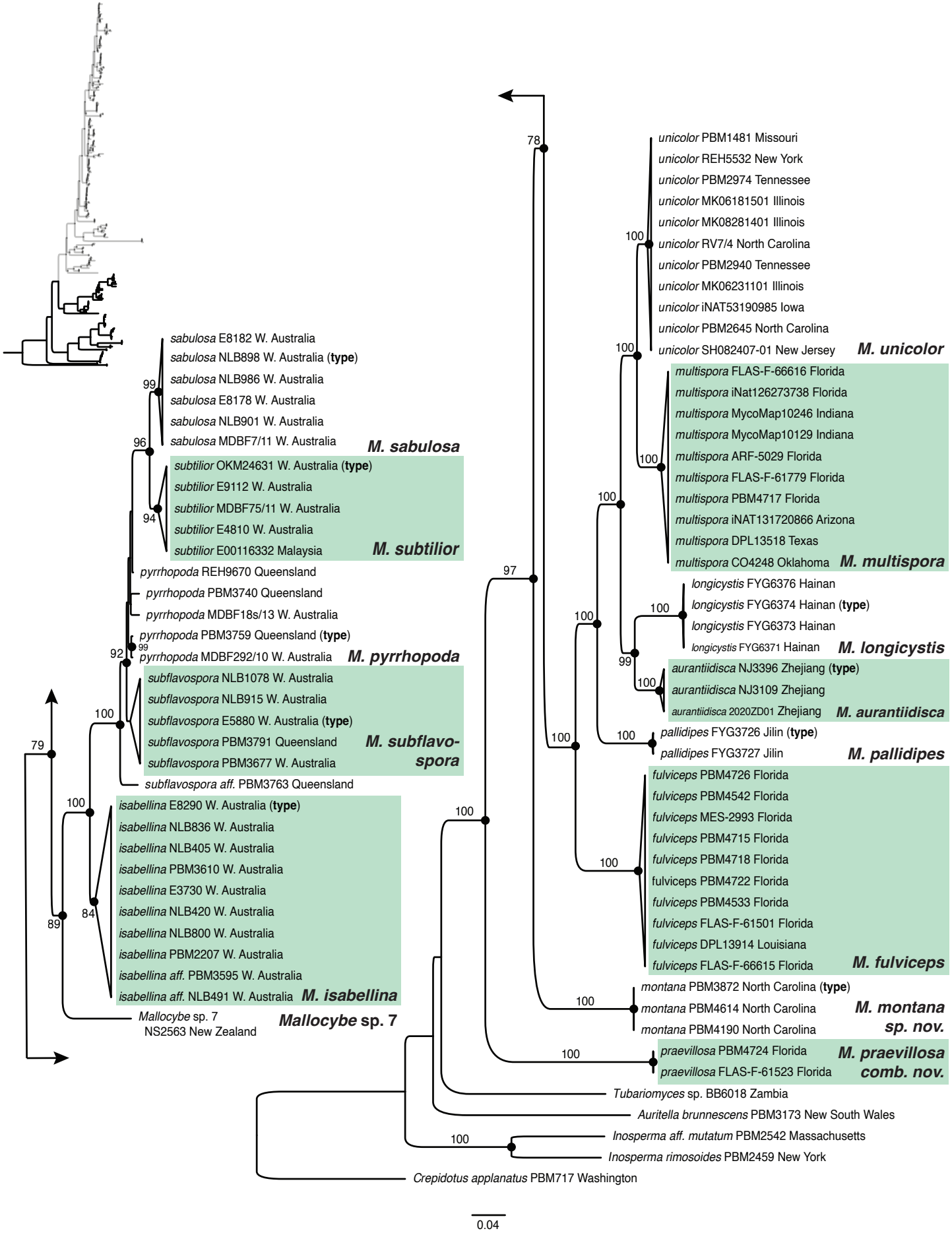

Fig. 2. (Continued).

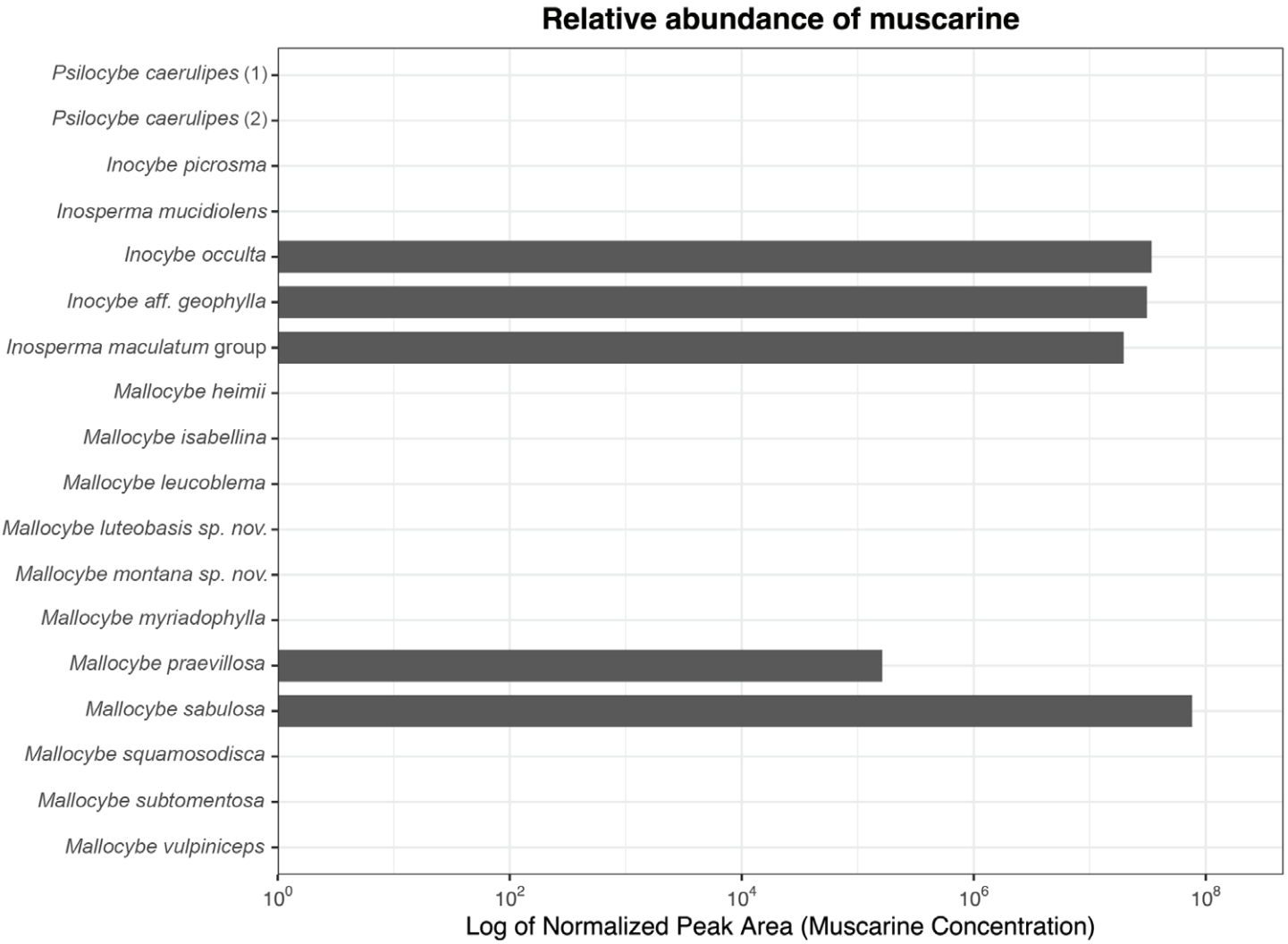

Fig. 3. Histogram showing the relative abundance of muscarine in select species of *Mallocybe* presented as a log normalized peak area, which refers to area count per mg or peak per mg since the aera after blank subtraction was sample mass normalized. Samples detected with abundance less than 2.5 times of the average abundance in the blank control were considered as below limit of detection. *Psilocybe caerulipes*, *Inocybe picrosma*, and *Inosperma mucidiolens* were used as negative controls, and *I. occulta*, *I. aff. geophylla*, and a species in the *Inosperma maculatum* group were used as positive controls. *Mallocybe unicolor* was also shown to lack muscarine by Kosentka *et al.* (2013). Of eastern North American species sampled, only *M. praevillosa* proved to contain a relative amount of muscarine but considerably lower than detected among the positive controls and the Australian species *M. sabulosa*. Stijve *et al.* (1985) also indicated the absence of muscarine from *M. terrigena*, the type of *Mallocybe*.

Two eastern North American species were also recorded from western regions and represent continental endemics to date: *M. tomentella* and *M. multispora*. All five described species from Australia appeared endemic to that continent, and the one species sampled from New Zealand is known thus far only from New Zealand.

Most species of *Mallocybe* lack detectable amounts of muscarine

Mass spectrometry revealed no detectable muscarine in samples of the following species: *Mallocybe heimii*, *M. isabellina*, *M. leucoblema*, *M. luteobasis*, *M. montana*, *M. myriadophylla*, *Mallocybe* sp. 5, *M. squamosodisca*, and *M. subtomentosa* (Fig. 3). A relatively high concentration of muscarine was detected in *M. sabulosa* and a relatively lower amount in *M. praevillosa*. As expected, none was detected in the negative controls *Psilocybe caerulipes*, *Inocybe picrosma*, and *Inosperma mucidiolens*. The three positive controls possessed relatively high concentrations of the toxin (Fig. 3).

TAXONOMY

Mallocybe (Kuyper) Matheny *et al*., *Mycologia* **112**: 94. 2020 [2019].
Synonym: *Inocybe* subg. *Mallocybe* Kuyper, *Persoonia* **3** (Suppl.): 22. 1986.

Typification: *Agaricus terrigenus* Fr., *Öfvers. K. Svensk. Vetensk.-Akad. Förhandl*. **8**(2): 46. 1851.

Description: Cheilocystidia often present and arising as terminal elements of the hyphae of hymenophoral trama, typically < 50

µm, rarely as short incrusted chains (if cheilocystidia > 50 µm long, this is generally a shared ancestral trait); pleurocystidia absent, basidia often necropigmented; lamellae usually broadly attached (adnate, uncinate, or subdecurrent), pileus typically woolly-squamulose or tomentose-fibrillose, surface often darkening with application of alkali solutions, context not reddening. Ectomycorrhizal with a wide range of plant families.

Notes: About 65 species are known in the genus and occur in Africa, Asia, Australia, Europe, New Zealand, and North America.

Mallocybe clade Mallocybe

Description: Includes *Mallocybe* species from the northern hemisphere, most of which are characterized by short clavate, pyriform, or cylindric cheilocystidia (often < 50 µm long). Common in north temperate zones, but also present in tropical areas of South Asia and high elevations in Central America. Muscarine not detected from most species assayed, including the type, but reported from other species: *M. agardhii*, *I. caesariata*, *I. dulcamara*, and *M. malenconii*. Putative plant family associates include *Betulaceae, Cistaceae, Dipterocarpaceae, Fagaceae, Pinaceae, Rosaceae*, and *Salicaceae*.

Currently included species (51 accepted): *M. abruptibulbosa*, *M. agardhii*, *M. arthrocystis*, *M. attenuatipes*, *M. cotoneovelata*, *M. delecta* (= *M. crassivelata*), *M. depressa*, *M. errata*, *M. fibrillosa* (= *I. dulcamara sensu auct. p.p., non* Persoon), *M. errata*, *M. fulvipes*, *M. fulvoumbonata*, *M. fuscomarginata*, *M. granulosa*, *M. gymnocarpa*, *M. hebelomoides*, *M. heimii* (=*M. arenaria*), *M. homomorpha*, *M. lagenicystidiata*, *M. latifolia* (= *M. acystidiata*), *M. latispora* (=*M. plebeia*), *M. leucoblema*, *M. leucoloma*, *M. leucothrix sp. nov.*, *M. luteobasis sp. nov*., *M. malenconii*, *M. megalospora*, *M. myriadophylla*, *M. nuptialis*, *M. pallidotomentosa*, *M. paludosa*, *M. parcesquamulosa*, *M. pelargoniodora*, *M. perbrevis*, *M. piceae*, *M. pseudodulcamara*, *M. pygmaea*, *M. siciliana*, *M. solidipes*, *M. squamosoannulata*, *M. squamosodisca comb. nov.*, *M. squarrosoannulata*, *M. subannulata*, *M. substraminipes*, *M. subtomentosa comb. nov.*, *M. terrigena*, *M. tomentella sp. nov.*, *M. tomentosula*, *M. umbrinofusca*, *M. velicoronata*, and *M. velutina*. *Inocybe favrei* Nespiak and *I. nespiaki* M. Bon are invalid names, but both species belong here. Note that *Inocybe stenospora* (contra Stangl 1989, Ludwig 2017), despite lacking pleurocystidia, belongs to the *Inocybe lanuginosa* group (Bandini *et al.* 2018) and not in *Mallocybe* as previously considered.

Notes: Most species of *Mallocybe* occur in clade Mallocybe upon consideration of their geographic distribution (non-Australasian), often short cheilocystidia (when present), and in most species average Q values for basidiospores < 2.0. In some species the stipe length is equal to or less than the pileus diameter. The clade includes all known arctic and alpine species. Daskalopoulos *et al*. (2021) noted some unique features to the ectomycorrhizal anatomy of *M. heimii* compared to other *Inocybaceae*: an open or variant anastomosis-type and presence of clamp connections on mantle hyphae.

Mallocybe clade Nothosperma

Etymology: *Nothosperma* (Gk.), southern seed, in reference to occurrence in the southern hemisphere.

Description: Includes *Mallocybe* species from the southern hemisphere (temperate and tropical regions) and tropical regions of southeast Asia (Malaysia) that associate with *Myrtaceae*, *Casuarinaceae*, and *Nothofagaceae*. Most species characterized by presence of short cheilocystidia (< 50 µm long); stipe often longer than the pileus diameter; pileipellis hyphae coarsely incrusted. Muscarine detected at relatively high concentration in *M. sabulosa*. No species have yet been recorded from South America.

Currently included species (seven accepted): *M. isabellina*, *M. pyrrhopoda*, *M. sabulosa*, *M. subflavospora*, and *M. subtilior* from Australia, *M. althofiae* from New Guinea, one unclarified species from Malaysia in association with *Allocasuarina*, and one unclarified species from New Zealand found with *Nothofagus*. *Inocybe callichroa* (Horak 2018) described from New Zealand, is placed here as well (see Taxonomy below). The occurrence of *M. cf. subtilior* in Sabah, Malaysia, was confirmed after sequencing a specimen from a flowerpot on bare earth (*leg*. *E.J.H. Corner*, 13 May 1964, E00116332). This species is likely introduced. However, another collection (E00116333) made by Corner from Johor, Malaysia, was made from bare sand in front of "*Casuarina*". This is an undescribed *Mallocybe* species characterized microscopically by large "laceroid" basidiospores (similar to *Inocybe lacera* in outline), 11.5–*12.4*–14(–14.5) × (5.5–)6-*6.2*–6.5(–7) µm, Q 1.85–*2.02*–2.33, short articulated cheilocystidia (28–45 × 12–25 µm), and presence of necrobasidia (Matheny 2003). No field notes accompanied the duplicate collection at Herbarium E. However, the combination of habit (stipe longer than the pileus diameter), small size, and coarsely incrusted pileipellis hyphae point to a relationship with Australian species of *Mallocybe*.

Mallocybe clade Unicolores

Etymology: *Unicolores* (L.), named after the oldest binomial in the clade, *Mallocybe unicolor.*

Description: A monophyletic group of *Mallocybe* species from East Asia and North America with distinct or elongated (> 50 µm long) cheilocystidia, stipe length generally longer than the pileus width, and association with angiosperms (*Fagales*, *Malvales*) and *Pinus*. Basidiospores with mean Q values > 1.90.

Currently included species (six accepted): *M. aurantiidisca*, *M. fulviceps*, *M. longicystis*, *M. pallidipes*, *M. multispora*, and *M. unicolor*. Known from eastern North America and East Asia.

Montana lineage

Description: A single stem lineage sister to clades Unicolores, Nothosperma, and Mallocybe. Characterized by elongated cheilocystidia, oblong-cylindric basidiospores, and narrow-range endemism in the Southern Appalachian Mountains in association with *Betulaceae*, *Fagaceae*, and/or *Pinaceae*. KOH dark on the pileus surface; necrobasidia present.

Currently included species (one accepted): *M. montana* (described as new below). Known only from the southeastern U.S.

Praevillosa lineage

Description: A single stem lineage sister to clades Unicolores, Nothosperma, and Mallocybe and the Montana lineage. Characterized by elongated cheilocystidia, oblong-cylindric to allantoid pale basidiospores, and narrow-range endemism in northern Florida in association with Fagaceae. KOH negative on pileus surface; necrobasidia not observed.

Currently included species (one accepted): *M. praevillosa* (recombined as new below). Known only from the southeastern U.S.

Mallocybe incertae sedis

Mallocybe africana Aïgnon, Yorou & Ryberg, *Phytotaxa* **478**: 53. 2021.

Species taxonomy

Mallocybe fibrillosa (Peck) Matheny & Esteve-Rav., *Mycologia* **112**: 106. 2019 [2020]. Figs 4A–C, 9A–C.
Basionym: *Inocybe fibrillosa* Peck, 1888, *non* (Cleland) Grgur., *Larger Fungi of South Australia*: 190. 1997.
Synonyms: *Inocybe dulcamara* Sacc., *Syll Fung* **5**:764. 1887 (*nom. illegit*., Art. 53.1), *non Inocybe dulcamara* (Pers.) P. Kumm., *Führ. Pilzk*.: 79. 1871.
Agaricus dulcamarus Alb. & Schwein., *Schr. Naturf. Ges, Leipzig*: no. 489. 1822 (*nom. illegit.* Art. 53.1), *non Agaricus dulcamarus* Pers., *Syn. Meth. Fung*. **2**: 324. 1801.
Inocybe subdecurrens Ellis & Everh., *J. Mycol*. **5**: 26. 1889.
Mallocybe subdecurrens (Ellis & Everh.) Matheny & Esteve-Rav., *Mycologia* **112**: 108. 2019 [2020].
Inocybe caesariata sensu Kauffman, *N. Am. Fl*. **10**(4): 255. 1924.

Pileus 15–40 mm wide, convex to plano-convex and eventually plane, margin incurved or inrolled at first and remaining so after expansion or becoming decurved, rarely subumbonate; surface dry, velipellis absent, heavily matted fibrillose to matted radially lanose or tomentose-fibrillose, disc at time with fibrillose scales, with white veil remnants when young; light brown (6C6–D6 or 6D5), brownish yellow, or fulvous throughout (10YR 5/6; Buckthorn Brown) brown with 3 % KOH, with cobwebby veil remnants at margin; context off-white, very pale brown, to yellowish white, unchanging where bruised, solid becoming hollow, *odor* mild or subtly sweet, *taste* mild. PDAB negative, guaiac dark olive green. *Lamellae* uncinate or subdecurrent to adnate, adnexed, close (up to 40 L) and with several tiers of lamellulae, light olive brown to olive brown (2.5Y 5/4–4/4), edges even or pallid and indistinctly fimbriate. *Stipe* 10–35 × 5–10 mm, equal, strict or curved; surface dry, heavily lanose to matted sublanose to squamulose, nowhere pruinose and not at all scaly, rarely peronate, with obvious partial veil remnants as a cortinate veil; light brown (lighter in color than the pileus surface) or with pale yellow ground color (2.5Y 2/4), white at the base; context solid becoming hollow, pale dingy yellow to olive yellow but nowhere bright yellow.

Basidia (26–)29–41 × 6–9 µm, 4-sterigmate, slenderly clavate, hyaline to ochraceous, necropigmented. *Basidiospores* (7.5–)8–*9.0*–9.5(–10) × 4.5–*5.0*–5.5(–6) µm, Q (1.50–)1.55–*1.76*–1.90(–2.24), smooth, elliptic, subphaseoliform, to (sub)amygdaliform with obtuse to bluntly pointed apices, with thickened walls, apiculus small and indistinct, ocher-buff to ochraceous-tawny (n = 53/3). *Pleurocystidia* absent. *Cheilocystidia* 16–45 × 9–14 µm, cylindric to clavate, occasionally flexuous, utriform, or short fusiform, apices obtuse or swollen, thin-walled, hyaline, edges of lamellae sterile. *Caulocystidia* not observed in the type but present as short clavate cells (at times elliptic or cylindric) at the extreme apex in *PBM2350*, usually hyaline, thin-walled; vesture hyphae brownish yellow in mass, incrusted, cylindric and up to 16 µm wide; stipe hyphae subhyaline in mass, refractive hyphae present. *Pileipellis* a cutis of parallel to subparallel hyphae, at times scattered upwards or tangled, tawny to brownish yellow in mass, hyphae cylindric, incrusted, 7–15 µm wide; tramal hyphae pale yellowish in mass, at times inflated, refractive hyphae present. *Lamellar trama* parallel, compact, pale yellowish or light yellowish brown in mass, hyphae cylindric and 7–15 µm wide. *Clamp connections* present.

Distribution: Widely distributed in the northeastern USA (Maine, New Jersey, New York), southeastern Canada (Quebec), the Pacific Northwest (British Columbia, Washington) and in the Rocky Mountains (Colorado, Wyoming), also northern Europe.

Habitat: On soil (at least some sites acidic) in mixed forests but with *Pinus* or other *Pinaceae* often present, also with *Salix*, and possibly *Dryas* in alpine areas of the USA, and with *Populus* in western subalpine areas, occurring with *Salix* or *Betula* in Europe. August–October in eastern North America, July–August in western North America.

Specimens examined: **USA**, Maine, Somerset Co., West Forks, Main Huts Trail (east end along Dead River), on ground in mixed woods, 19 Sep. 2014, *L.V. Kudzma*, LVK14371 (pers. herb.); Maine, Somerset Co., the Forks, Moxie Falls Trail, 20 Sep. 2014, *L.V. Kudzma*, LVK14390 (pers. herb.); *ibid.*, 22 Sep. 2015, *L.V. Kudzma*, LVK15242 (pers. herb.); Main, Limestone, Aroostook Co., Aroostook National Wildlife Refuge, on soil in mixed woods under *Picea*, *Abies*, *Betula*, *Larix*, *Populus*, 10 Sep. 2022, *L.V. Kudzma*, LVK22085 (pers. herb.); New Jersey, Gloucester Co., Newfield, under overhanging limbs of Norway spruce (*Picea*), Oct. 1887, *Ellis & Everhart* (**holotype** of *Inocybe subdecurrens*, NY 00775657, 00775658, 007775659, 00775660); Somerset Co., Woods Road School, under pine, 7 Oct. 1995, *R.M. Fatto*, RMF908 (NY 673247); *ibid.*, under conifers, 12 Oct. 1996, *R.M. Fatto*, RMF1009 (NY 673246); New York, Albany Co., Bethlehem, Corning Farm, on damp mossy banks in woods, Aug. (no day and year), *C.H. Peck s.n.* (**isotype** WTU part of NYSf1175); Essex Co., Peck Foray at the State University of New York (SUNY) College of Environmental Forestry (EFS) Newcomb Campus, Huntington Forest Preserve, 43.96929 -74.22022, 507 m elev., gregarious on soil under *Abies*, *Picea*, *Betula*, *Thuja*, *Pinus*, no date, *R.E. Halling*, REH10168 (NY 2861422, TENN-F-073177); Washington, King Co., exit 47 off Interstate 90, Pratt Lake Trail, scattered along moist bank along trail in second growth conifer forest dominated by *Pseudotsuga* and *Tsuga*, 25 Aug. 2002, *P.B. Matheny*, PBM2350 (WTU).

Other specimens examined (*Mallocybe delecta*): **Finland**, Tavastia australis, Tammela, Syrjä, no date, *P.A. Karsten*, 1636 (**holotype** of *Agaricus delectus*, H); *ibid*., *P.A. Karsten*, 1637 (**isotype** of *Agaricus delectus*, H).

Notes: The name *Mallocybe fibrillosa* (syn. *I. fibrillosa* Peck) has not been widely used since synonymized with *I. caesariata* by Kauffman (1924) but in our judgement conforms to application of the name *Inocybe dulcamara* used by Cripps *et al*. (2010;

Fig. 4. Basidiomes of *Mallocybe* from eastern North America. **A.** *M. fibrillosa* (LVK14371, photo L. Kudzma). **B.** *M. fibrillosa* (REH10168, photo R. Halling). **C.** *M. fibrillosa* (PBM2350, photo B. Matheny). **D.** *M. fulviceps* (DPL13914, photo D. Lewis). **E.** *M. fulviceps* (PBM4533, photo B. Matheny). **F.** *M. fulviceps* (PBM4726, photo B. Matheny). **G.** *M. latifolia* (LVK22088, photo L. Kudzma). **H.** *M. latifolia* (PBM3731, photo B. Matheny). **I.** *M. latifolia* (MES3796, photo M. Smith). **J.** *M. leucothrix* (PBM4541, holotype, photo B. Matheny). **K.** *M. leucothrix* (PBM4531, photo B. Matheny). Scale bars = 1 cm.

see further discussion below about conflicting concepts for this species). We suggest that modern extant material studied from New York (NY 2861422) and elsewhere in northeastern states serves as adequate reference material for Peck's *Inocybe fibrillosa* originally described from the greater Albany area in New York. The species is characterized generally by the tomentose-fibrillose pileus, olivaceous hues to the moderately spaced lamellae, the tomentose to lacerate-fibrillose stipe with a white base, and, according to Cripps *et al.* (2010, as *I. dulcamara*), an odor of honey or burnt sugar. Washington material of *M. fibrillosa* exhibited a sweet earthy smell. The spores are not oblong and have a mean Q value less than 2.0. The cheilocystidia

are short and generally cylindric. Cripps *et al.* (2010) reported the presence of 2-sterigmate basidia in some alpine collections and thus larger spores. Ecologically, the species is widespread, occurring in northern Europe and eastern and western North America at high latitudes or high elevation, including alpine areas (as confirmed by molecular data). The species may have a circumboreal distribution. The plant host range overall is somewhat broad and includes *Pinaceae*, particularly *Pinus* but also other genera, *Salicaceae* (*Salix*, *Populus*), *Betulaceae* (*Betula*), and *Rosaceae* (*Dryas*). Among other species that occur in eastern North America, *M. subtomentosa* differs from *M. fibrillosa* by the stipe length that is longer than the pileus width and the nearly smooth pileus. *Malllocybe squamosodisca* can be distinguished from *M. fibrillosa* by the cracked-areolate pileus surface that develops with age, longer spores on average, and the lack of any odor as well.

Our concept of *M. fibrillosa* is the same as that documented from western North America and Europe as *I. dulcamara* by Cripps (1997, in the sense of Albertini and Schweinitz) without molecular data and by Cripps *et al.* (2010, as *I. dulcamara* (Alb. & Schwein.) P. Kumm.) with molecular data. However, *Agaricus dulcamarus* Alb. & Schwein. 1822 is a later homonym of *Agaricus dulcamarus* Pers. 1801 and thus an illegitimate name per ICN Art. 53.1. Neither name was included in any sanctioning works of Fries. *Inocybe dulcamara* Sacc. 1887 is a homotypic synonym of *Agaricus dulcamarus* Alb. & Schwein. and is illegitimate because it is a later homonym of *Inocybe dulcamara* (Pers.) P. Kumm. 1871.

Agaricus dulcamarus Pers. represents a different species than interpreted by many modern authors including Ricken (1915), Heim (1931), Kühner & Romagnesi (1953), Favre (1955), Malloch (1973), Cripps *et al.* (2010), and that documented by Favre (1955), per Cripps and colleagues, as *I. dulcamara* 'forma typique'. The description in Persoon's protologue (Persoon 1801), and later an icon (Persoon 1803–1806) of *Agaricus dulcamarus* Pers. conflicts with the later interpretation of *I. dulcamara sensu auct. p.p.* (Matheny 2003). Persoon's fungus may actually represent *Inosperma cervicolor* (T.W. Kuyper, pers. comm.). Fries (1828) interpreted *A. dulcamarus* as his *A. lucifugus*, a name treated by Kuyper (1986) as a *nomen dubium.* Singer (1986) preferred to use the name *Inocybe delecta* in lieu of *I. dulcamara* (Alb. & Schwein.) P. Kumm. We examined the type collections of *Agaricus delectus* [H, No. 1636 (holotype) and 1637 (isotype)] and found the spores to be somewhat narrower and more oblong (8–*9.0*–10 × 4–*4.6*–5 µm, Q 1.80–*1.95*–2.13(–2.38)) than in *M. fibrillosa*. Since our examination of the types, Ellen Larsson (University of Gothenburg) was able to produce a molecular annotation (ITS) from the type of *Mallocybe delecta* (H, No. 1636; OQ448533) and modern reference material (JV21393; OQ448534 – ITS and 28S). Sequences from both samples cluster with strong support in a species-level lineage with *M. crassivelata*. Thus, we can safely eliminate the possibility of any conspecificity between *M. fibrillosa* and *M. delecta*.

The application of the name *I. dulcamara* (Fr.) Quél. by Stuntz (1947; Stz. 805), collected under high-elevation conifers in Washington, likely represents a different species, possibly *M. gymnocarpa* or a closely related species, based on the large size of the basidiomes, spore morphology, and absence of a veil.

Stuntz (1947) considered *I. subdecurrens* and *I. tomentosa* Ellis & Everh. (*non* Quél.) as synonymous, as others did before him (Kauffman 1924, Smith 1939), and applied the name *I. subdecurrens* to a single lowland collection under *Alnus* from lowland Washington state. From this single collection Stuntz noted a white ample cortina, the stipe longer than the pileus width, relatively narrow spores (8–10 × 4.5–5.5 µm), and pyriform to short-clavate articulated cheilocystidia. Stuntz' collection may fit *M. leucoloma* (see discussion under *M. subtomentosa*). Peck published *Inocybe fibrillosa* in 1888, which precedes by one year the publication of *I. subdecurrens*, hence, when considering the two as synonymous, *I. fibrillosa* has priority.

In the study by Matheny *et al.* (2020), *M. fibrillosa* was referred to as *I. subdecurrens*. The holotype of *I. subdecurrens* comprises three packets and four elements, all from the same original gathering and fixed to a single sheet at NY. Attempts to sequence two elements of the holotype (775657 and 775658) failed due to poor quality reads and sequence heterogeneity. We did not attempt to sequence the type of *I. fibrillosa*. Because we cannot distinguish the two species morphologically and ecologically, we regard them as the same with *M. fibrillosa* holding nomenclatural priority by a single year.

Phylogenetic analyses (Fig. 2A) support multiple samples from North America and Europe, including alpine and non-alpine populations, as a strongly supported clade. The geographic and ecological extent of *M. fibrillosa* in Europe awaits further revision.

Mallocybe fulviceps (Murrill) Matheny & Esteve-Rav., *Mycologia* **112**: 106. 2019 [2020]. Figs 4D–F, 9D–I.
Basionym: *Inocybe fulviceps* Murrill, *Quart. J. Florida Acad. Sci*. **8**: 187. 1945.
Synonyms: *Inocybe pertomentosa* Murrill, *Quart. J. Florida Acad. Sci*. **8**: 189. 1945.
Inocybe vialis Murrill, *Quart. J. Florida Acad. Sci*. **8**: 191. 1945.

Pileus 10–28 mm wide, obtusely conical to convex or subexpanded with a small pointed or low broad umbo; margin incurved, becoming decurved with age; surface dry, appressed tomentose-fibrillose to fibrillose-scaly, velipellis absent; fulvous or yellowish brown (10YR 5/6; near Buckthorn Brown or a shade lighter), at times paler over the disc, dark brown with 5 % KOH; context very thin, pallid with a pale yellow tone, *odor* spermatic, at least when first cut, or somewhat acidulous. *Lamellae* sinuate to uncinate, subdistant to moderately close with *ca*. 20–24 L and several tiers of lamellulae, ventricose, broad; pallid to yellowish brown becoming dark yellowish brown with age; edges pallid, indistinctly fimbriate. *Stipe* 10–33 × 2–3 mm, equal, not bulbous; surface dry, cortina fugacious and composed of fulvous fibrils, tattered fibrillose entire length, not scaly but on occasion with scattered bands of fibrils; pale yellow (2.5Y 7/4); context solid, pale yellow throughout including in the base.

Basidia 27–35 × 9–10 µm, 4-sterigmate, clavate, hyaline or necropigmented. *Basidiospores* (9.5–)10–*11.0*–13(–14) × (4.5–)5–*5.1*–5.5(–6) µm, Q 1.90–*2.15*–2.56 (n = 85/5), smooth, oblong-elliptic, oblong-phaseoliform, less often subamygdaliform, with obtuse apices; thick-walled, ochraceous-buff, apiculus small and indistinct. *Pleurocystidia* absent. *Cheilocystidia* 28–48 × 11–16(–22) µm, clavate to utriform but saccate and obovate cells also observed; thin-walled, hyaline; edges sterile. *Caulocystidia* in clusters, similar to cheilocystidia; stipe hyphae yellowish in mass, cylindric, 4–9 µm wide, weakly incrusted, refractive hyphae not observed. *Pileipellis* a cutis of parallel hyphae, yellowish brown to ochraceous in mass, hyphae cylindric, up to 15 µm wide, incrusted. *Lamellar trama* parallel, pale yellowish brown to subhyaline in mass, hyphae cylindric, up to 15 µm wide. *Clamp connections* present.

Distribution: Southeastern USA (Florida, Louisiana).

Habitat: Scattered to gregarious, singly or in small clusters on sandy soil on karst topography in mixed forests of *Quercus* and *Pinus* or under hardwoods such as *Carpinus* and *Quercus*, including *Q. nigra*, also in disturbed areas such as roadsides. July–December.

Specimens examined: **USA**, Florida, Alachua Co., Gainesville, 11 Aug. 1944, *W.A. Murrill*, F18506 (**isotype** of *Inocybe fulviceps* WTU, **isotype** TENN-F-021186); Alachua Co., Gainesville, gregarious in a path shaded by frondose trees, 20 Sep. 1944, *W.A. Murrill*, F20017 (**isotype** of *Inocybe vialis* WTU, **holotype** FLAS-F-20017); Alachua Co., Gainesville, gregarious to caespitose in moist shaded soil, no date, *W.A. Murrill*, F19657 (**isotype** of *Inocybe pertomentosa* WTU, **isotype** TENN-F-021192); Alachua Co., Gainesville, University of Florida, Natural Area Teaching Lab, 29.63389 -92.368728, 25 Aug. 2017, Florida Mycological Foray (FLAS-F-61501); Alachua Co., Wood Creek neighborhood, Gainesville, under *Quercus virginiana*, *Q. nigra*, 19 Sep. 2020, *M.E. Smith*, MES-3773 (FLAS-F-66615); Alachua Co., Alachua, Mill Creek Preserve, West Trail, on sandy soil under *Pinus palustris*, other *Pinus*, and *Quercus*, 6 Jul. 2022, *R.A. Swenie*, PBM4715 (TENN-F-077389); *ibid. P.B. Matheny*, PBM4718 (TENN-F-077392); *ibid.*, *P.B. Matheny*, PBM4722 (TENN-F-077396); Alachua Co., Gainesville, on sandy soil under *Carpinus*, *Quercus*, Blues Creek Ravine Preserve, 7 Jul. 2022, *P.B. Matheny*, PBM4726 (TENN-F-077450); Polk Co., Circle B Bar Reserve, Lakeland, on soil near a trail, 22 Oct. 2016, *S.-Y Wu*, MES2993 (FLAS-F-66574); Putnam Co., Ordway-Swisher Biological Station (UF), near west entrance, 45 m elev., gregarious to scattered singly or in small clusters on sandy soil on side of road under *Quercus* spp., *Pinus elliottii*, 12 Dec. 2020, *M.E. Smith & P.B. Matheny*, PBM4533 (TENN-F-075556); *ibid*., near Goose Lake, 12 Dec. 2020, *P.B. Matheny*, PBM4542 (TENN-F-075565); Louisiana, St. Landry Parish, Thistlethwaite Wildlife Management Area, Peckham Road, gregarious on soil under *Quercus nigra*, 17 Jul. 2021, *D.P. Lewis*, DPL13914 (TENN-F-076539).

Notes: This is the first documentation of *Mallocybe fulviceps* since it was described from northern Florida by Murrill in 1945. The species is characterized by the small basidiomes (pileus < 30 mm wide, stipe up to 3 mm thick), the often umbonate fulvous pileus, the pale stipe, oblong basidiospores with a mean Q > 2.0, and occurrence under *Quercus* and *Pinus* on sandy calcareous soil. A comparison of the types of *M. fulviceps*, *I. pertomentosa*, and *I. vialis* indicate all share the same brown color (7.5YR 4/4 or umber brown with a slight reddish tinge), similar small basidiome size, similar pileus surface, stipe texture, and basidiospore morphology. *Inocybe pertomentosa* shows a somewhat clustered habit that we also observed in freshly collected material near the type localities. We regard all three as synonymous taxa, yet all have equal priority as they were published in the same study by Murrill (1945). We choose *I. fulviceps* for priorable purposes because this epithet most accurately describes the species morphologically.

Phylogenetically, *M. fulviceps* is nested within clade Unicolores with strong support, and nine samples of the species from Florida and Louisiana form a strongly supported clade (Figs 1, 2C). The species is sister to the remainder of the Unicolores clade also with strong support. *Mallocybe multispora* (documented below) differs from *M. fulviceps* mainly by the slenderly clavate to subcylindric cheilocystidia. *Mallocybe unicolor* differs from *M. fulviceps* by the granulose-scaly pileus surface, presence of dark colored bands of fibrils and scales on the lighter colored stipe, and elongated cheilocystidia.

Descriptions of *M. perbrevis* by Heim (1931) and Stangl (1989) (both as *Inocybe perbrevis*) seem most similar to *M. fulviceps* including the small umbo, small stature, gregarious habit, and association with hardwoods like *Populus*, *Carpinus*, and *Fagus* in Europe. The basidiospores of *M. fulviceps* (including *I. vialis* and *I. pertomentosa*) are narrower than depicted by Heim (1931) but similar to those described by Stangl (1989). Modern molecular comparisons are needed between *bona fide* collections of *M. perbrevis* and *M. fulviceps*.

Mallocybe fulvoumbonata (Murrill) Matheny & Esteve-Rav., *Mycologia* **112**: 106. 2019 [2020].
Fig. 9J, K.
Basionym: *Inocybe fulvi-umbonata* Murrill, *Quart. J. Florida Acad. Sci*. **8**: 187. 1945.

Pileus up to 15 mm wide, convex to nearly expanded and with a small but prominent umbo; margin even, entire; surface dry, tomentose, isabelline with a fulvous umbo; context very thin, pallid. *Lamellae* plane, adnate, medium distant, inserted, pallid [dried specimens dark yellowish brown], fimbriate, broad. *Stipe* 30 × 2–3 mm, longer than the pileus width, equal, dry, fibrillose, isabelline.

Basidia 26–45 × 7–10 µm, clavate, hyaline or necropigmented, 4-sterigmate. *Basidiospores* 8–*8.7*–9(–10.5) × 4.5–*5.1*–5.5(–6) µm, smooth, Q (1.50–)1.55–*1.76*–1.91(–2.00) (n = 52/2), smooth, many phaseoliform or subamygdaliform, at times elliptic, pale brown, with thickened wall, apiculus small and indistinct. *Pleurocystidia* absent. *Cheilocystidia* 22–26 × 13–15 µm, reviving poorly, broadly clavate, thin-walled, hyaline (gill edges fimbriate per Murrill), in some sections none observed. *Stipitipellis* composed of a vesture of loose interwoven hyphae, these cylindric, weakly incrusted, thin-walled, mostly 5–10 µm wide, caulocystidia not observed. *Pileipellis* a cutis of cylindric hyphae, these cylindric, weakly incrusted, thin-walled, mostly 5–12 µm wide, yellowish brown in mass. *Lamellar trama* parallel, subhyaline or very pale brown in mass, hyphae cylindric. *Clamp connections* present.

Distribution: Southeastern USA (Florida).

Habitat: Under *Quercus laurifolia*. July.

Specimens examined: **USA**, Florida, Alachua Co., Gainesville, 8 Jul. 1944, *W.A. Murrill* (**holotype** FLAS-F-24503, **isotype** TENN-F-021187).

Notes: Initially, we mistook *M. latifolia* (documented below) as *M. fulvoumbonata*, but upon examination of the holotype and isotype, we believe it is more appropriate to maintain them as separate taxa. Thus, despite our efforts to re-collect Murrill species from Gainesville in July, none of our specimens matched *M. fulvoumbonata*. Therefore, *M. fulvoumbonata*, known only from the type collection, appears to be best characterized by the lack of any substantial veil remnants over the pileus, the small but prominent umbo, the stipe length longer than the pileus width, the relatively short clavate cheilocystidia, and the noticeably pale brown to light yellow spores that are mostly 8–9 × 5 µm in size.

The other small mallocyboid species described by Murril (*viz*., *M. fulviceps*, *M. multispora*) differ principally by their elongated,

darker, narrow spores and/or cheilocystidia with a different morphology. *Mallocybe latifolia* produces larger basidiomes without a distinct umbo and larger basidiospores (mostly 9–11 × 5.5–6.5 µm) that are more darkly pigmented (yellowish brown). *Mallocybe leucothrix* also produces larger basidiomes without a distinct umbo, and both the pileus and stipe are overlain with superficial whitish fibrils.

Mallocybe latifolia (E. Ludw.) Matheny & Esteve-Rav., *Mycologia* **3**: 107. 2020 [2019]. Figs 4G–I, 9L, M.
Basionym: *Inocybe latifolia* E. Ludw., *Pilzkompendium* (Eching) **4**: 153. 2017.
Synonyms: *Inocybe acystidiata* E. Ludw., *Pilzkompendium* (Eching) **4**: 152. 2017.
Mallocybe acystidiata (E. Ludw.) Matheny & Esteve-Rav., *Mycologia* **3**: 105. 2020 [2019].

Pileus 15–42 mm wide, convex to obtusely conical, expanding to plane in age with an obtuse umbo or depressed at the center; margin inrolled to incurved in youth, later decurved and with the edge remaining inrolled at times; surface dry, tomentose-fibrillose due to superficial thin white covering throughout, the covering wearing away with age, occasionally breaking up into appressed scales or becoming cracked-areolate, never rimose; ground color fulvous or brownish yellow to yellowish brown; context firm, whitish, unchanging where bruised, odor not remarkable. *Lamellae* adnate to uncinate, close to subcrowded with about 34–40 L and several tiers of lamellulae, medium to somewhat broad; light yellowish brown to light olive brown when young, becoming brown with age; edges whitish-fimbriate. *Stipe* 30–40 × 2–6 mm, equal, generally not longer than the pileus diameter after pileus expansion; surface dry, usually without a well-developed superior ring-zone (at times a weak ring-zone may be present); cortina white, fugacious; surface white when young due to the presence of superficial silky fibrils throughout, these wearing away, surface becoming coarsely fibrillose or tattered-fibrillose and revealing an isabelline or light yellowish brown ground color with age, base white, not yellow; context solid to hollow, pale brown.

Basidia 28–47 × 7–10 µm, slenderly clavate to subclavate, hyaline or necropigmented, 4-sterigmate. *Basidiospores* (8–)9–*10*–11(–12) × 5.5–*5.9*–6.5(–7) µm, Q (1.34–)1.50–*1.68*–1.88(–2.08) elliptic, subamygdaliform, or subphaseoliform, yellowish brown, with thickened wall, apices often obtuse, apiculus small and indistinct (n = 119/4). *Pleurocystidia* absent. *Cheilocystidia* 19–34 × 12–22 µm, clavate to saccate or pyriform, subtending cells often hyphal (not densely articulated), hyaline but many ocher-brown and/or incrusted or appearing with wrinkled walls, thin-walled or with slightly thickened walls, often collapsed in revived dried mounts. *Caulocystidia* 27–46 × 12–18 µm, pyriform to clavate or subcylindric, in scattered but dense clusters, often brownish incrusted, thin-walled or with slightly thickened walls. *Pileipellis* a cutis, ochraceous-tawny in mass, hyphae with thin to slightly thickened walls, incrusted, mostly 6–15 µm wide. *Lamellar trama* parallel, pale buff in mass, hyphae cylindric, smooth, mostly 5–15 µm wide. *Clamp connections* present.

Distribution: Eastern and western USA (Arizona, Florida, Maine), southeastern Canada (Quebec), north-central China (Shaanxi), and central Europe (Germany, type), broad and intercontinental.

Habitat: On calcareous soils in mixed forest of *Quercus*, *Pinus*, under planted *Quercus*, *Pinus*, or in mixed conifer forests including *Populus*, also under *Populus* at high elevation (Arizona) and with *Populus simonsii* (ectomycorrhizal roots) in Shaanxi Province, China; in Europe on calcareous soil under *Picea*. July–December in eastern USA.

Specimens examined: **USA**, Florida, Alachua Co., Gainesville, gregarious singly on soil under *Pinus*, *Quercus*, in suburban neighborhood, B'nai Israel Synagogue, 3830 NW 16th Blvd, ca. 29.645, -82.327, 9 Dec. 2020, *M.E. Smith*, MES-3796 (=PBM4535) (TENN-F-075558; FLAS-F-67923); Putnam Co., Melrose, Ordway-Swisher Biological Station, gregarious, often singly, on disturbed soil along roadside under *Quercus* and *Pinus*, 12 Dec. 2020, *M.E. Smith*, PBM4537 (TENN-F-075560); *ibid.,* by west gate entrance, 19 Oct. 2017, *M.E. Smith* (FLAS-F-61869); Maine, Aroostook Co., Limestone, Aroostook National Wildlife Refuge, Durepo Look Trail, in mixed forest under *Picea*, *Abies*, *Larix*, *Betula*, and *Populus*, 10 Sep. 2022, *L.V. Kudzma*, LVK22088 (pers. herb.); *ibid*., LVK22089 (pers. herb.).

Notes: Phylogenetic analysis of ITS data obtained from two German type collections (*Mallocybe acystidiata* and *M. latifolia*) form a strongly supported monophyletic group with sequences from basidiomes collected under *Populus* in Arizona and a mixed conifer forest including *Populus* in Maine, and from ectomycorrhizal root tip sequences of *Populus* from north-central China (Fig. 2A). In addition, the species has been recently confirmed from Quebec (J. Landry, pers. comm.). No American or Asian names are available for this species-level clade, but there are two equally competing names from Europe (*M. acystidiata* and *M. latifolia*) published in the same work (Ludwig 2017) that can be applied to it. We choose *M. latifolia* over *M. acystidiata* because cheilocystidia were actually observed in several samples, including a re-examination of the type of *M. acystidiata* (Bandini, unpubl. data). Overall, the species has a broad intercontinental distribution with a wide range of plant associates. Phylogenetically, *M. latifolia* is nested within the greater core Mallocybe clade.

Mallocybe latifolia can be distinguished from other eastern North American *Mallocybe* by the presence of a thin white vesture, occurrence on calcareous soils probably in association with *Populus*, *Pinus*, and *Picea* (and possibly *Quercus*), the relatively large basidiospores (9–11 × 5.5–6.5 µm), and the cheilocystidia that are collapsed in revived mounts. The species closely resembles *M. fibrillosa* but lacks the odor (like burnt sugar or honey) of that species. *Mallocybe leucothrix* also possesses a distinct white vesture but differs from *M. latifolia* by the smaller basidiospores (8–10 × 4.5–5.5 µm) and phylogenetic affinities with *M. leucoloma*.

Mallocybe leucothrix Matheny & M.E. Sm., ***sp. nov.*** MycoBank MB 847416. Figs 4J, K, 10A, B.

Etymology: *leucothrix* (Gk.), white hairs, in reference to the whitish veil encompassing the basidiomata and close phylogenetic relationship to *M. leucoloma*.

Typus: **USA**, Florida, Putnam Co., Ordway-Swisher Biological Station, east of Ashley Prairie near Goose Lake, Melrose, on disturbed soil at side of road under *Quercus*, *Pinus elliottii*, 29.705, -81.967, 12 Dec. 2020, *M.E. Smith*, PBM4541 (**holotype** TENN-F-075564).

Diagnosis: Distinguished from closely related species by the combination of the whitish veil enclosing medium-sized basidiomata, basidiospores with mean Q values < 2.0, presence of short cylindric to clavate cheilocystidia, and occurrence on calcareous soils with *Quercus* and *Pinus* in Florida and Arizona. Forming a unique monophyletic group apart from closest relatives including *M. leucoloma*, *M. subtomentosa*, and the undescribed *Mallocybe* sp. 8.

Pileus 15–55 mm wide, obtusely conical or pulvinate in youth, expanding to broadly convex and plano-convex, at last plane to depressed at the center with age, umbo absent; margin incurved and usually remaining so or decurved when plane; surface dry, appressed tomentose-fibrillose, not at all scaly; color a mixture of various shades of very pale brown, pale brown, or light yellowish brown due to variable coating of a white velipellis, at times with a dull olive tone in areas (10YR 7/3–6/3–6/4; overall near clay color to isabella color where velipellis is exposed); surface dark brown with KOH, fleetingly brown with ammonia; context firm and with a pale yellow tone, confluent with the stipe, unchanging where bruised, *odor* absent or indistinct. *Lamellae* adnate to subdecurrent, close; pale olive (5YR 6/3) to grayish olive, becoming yellowish brown (10YR 5/4; clay color), edges indistinctly pallid-fimbriate. *Stipe* 20–35 × 3–6 mm, equal, often longer than the pileus width (but not always); cortina white and fugacious, not leaving a distinct annular zone; dry, surface overlain with a white vesture of superficial fibrils part of the overall veil, these wearing away revealing a pale brown to yellowish brown ground color, white at the base (not yellow); solid, becoming hollow, pallid with a pale yellow tone like the pileus context.

Basidia 30–35 × 6–15 µm, 4-sterigmate, slenderly clavate, hyaline or necropigmented. *Basidiospores* (7.5–)8–*9.1*–10(–11) × 4.5–*5.1*–5.5 µm, Q (1.50–)1.55–*1.78*–2.04(–2.08) (n = 41/2), smooth, mostly amygdaliform to somewhat phaseoliform due to a ventral depression, occasionally ovate, apices bluntly pointed, yellowish brown to brownish yellow in KOH, apiculus small and indistinct, wall slightly thickened. *Pleurocystidia* absent. *Cheilocystidia* 18–32 × 6–10 µm, cylindric to clavate or short-cylindric to short-clavate, arising from short hyphal segments or articulated hyphae, thin-walled, hyaline, edges of lamellae sterile or nearly so. *Caulocystidia* present at the extreme apex of the stipe, similar to cheilocystidia. *Pileipellis* an interwoven cutis, rusty brown to tawny in mass; hyphae cylindric, noticeably incrusted, thin-walled or slightly thick-walled, mostly 5–14 µm wide. *Lamellar trama* parallel, hyphae mostly 3–19 µm wide, cylindric to inflated, light yellowish brown in mass, thin-walled, smooth. *Clamp connections* present.

Distribution: Southeastern (Florida) and southwestern USA (Arizona).

Habitat: Scattered to gregarious on karst topography under *Quercus virginiana*, other *Quercus* spp., and *Pinus elliottii* in Florida, also on calcareous soils under *Pinus engelmannii* and *Quercus hypoleucoides* in Arizona. August (Arizona) and December (Florida).

Other specimen examined: **USA**, Florida, Putnam Co., Ordway-Swisher Biological Station, east of Ashley Prairie near Goose Lake, Melrose, 29.705, -81.967, 12 Dec. 2020, *C.R. Noffsinger & P.B. Matheny*, PBM4531 (TENN-F-075554).

Notes: *Mallocybe leucothrix* forms a monophyletic group with moderate support based on five samples collected under *Quercus* and *Pinus* on calcareous soils in Florida and Arizona. The species is most closely related to an undescribed species that differs ecologically by association with *Picea* on acidic soils in West Virginia, Quebec, and China. Because of the phylogenetic and ecological differences, we recognize both clades as separate species even though both are united as a strongly supported monophyletic group. Both species are closely related to the intercontinental species *M. leucoloma*, which to date has been observed in western North America in alpine settings with shrub and dwarf *Salix* and in conifer forests mixed with *Betula* and *Populus*. Several similarities with *M. leucoloma* include the relatively distinct white veil covering of the basidiomata, white cortina, white stipe base, and the stipe length at times longer than the pileus width. *Mallocybe leucoblema* can be distinguished from *M. leucothrix* generally by the more robust size, occurrence on calcareous soils in alpine and montane regions of western North America and Europe, and unique phylogenetic position sister to the Delecta clade.

Mallocybe subtomentosa differs from *M. leucothrix* by the subsmooth pileus, occurrence on acidic soils with *Quercus* and/or *Pinus*, and by phylogenetic position. *Mallocybe tomentella* (described as new below) differs from *M. leucothrix* by the bicolorous pileus, presence of a cortinate ring-zone on the stipe, occurrence on acidic soils, and phylogenetic association with members of the *M. malenconii* group.

Mallocybe luteobasis Matheny & M. Kuo, ***sp. nov*.** MycoBank MB 847417. Figs 5A–C, 10C, D.

Etymology: *luteobasis* (L.), yellow base, in reference to the yellow base of the stipe.

Typus: **USA**, Illinois, Coles Co., Charleston, Fox Ridge State Park, on soil under *Quercus*, 18 Jul. 2007, *M. Kuo*, MK07180705 (**holotype** TENN-F-073750).

Diagnosis: Distinguished from closely related species by the combination of the medium-sized basidiomata often with large appressed scales, yellow stipe base or yellow basal mycelium, the broad basidiospores with a mean Q value < 2.0, elongate digitiform cheilocystidia, and occurrence on calcareous soils under fagaceous trees. Forming a monophyletic group within the Terrigena grade.

Pileus 20–55 mm wide, convex becoming plano-convex to plane, margin inrolled; surface dry, appressed-squamose to appressed-fibrillose; scales reddish brown, strong brown, or fulvous against a lighter background color, center at times reddish brown; gray or dark brown with KOH; context up to 3 mm thick under the disc, pale yellow, unchanging where bruised, *odor* none or not distinctive. *Lamellae* broadly adnate to uncinate, moderately close, lamellulae frequent; pale yellow when young or whitish to brownish yellow or with olivaceous tone, becoming olive-brown (Dresden Brown) with age; edges noticeably fimbriate, white to yellowish. *Stipe* 25–60 × 3–9 mm, more or less equal or tapered to the base; apex with decurrent lamellar lines; veil cortinate and thick and fibrillose covering the lamellae entirely when young, this becoming a cortinate ring-zone at times but not always; surface dry, fibrillose-scaly or shaggy-fibrillose below the veil, at times fibrils forming bands; fibrils and scales brownish

Fig. 5. Basidiomes of *Mallocybe* from eastern North America. **A.** *M. luteobasis* (MK0611102, photo M. Kuo). **B.** *M. luteobasis* (MK07180705, holotype, photo M. Kuo). **C.** *M. luteobasis* (G. Sayers *s.n.*, photo G. Sayers). **D.** *M. malenconii* (LVK21286, photo L. Kudzma). **E.** *M. montana* (PBM4585, photo B. Matheny). **F.** *M. montana* (PBM3872, holotype, photo B. Matheny). **G.** *M. montana* (PBM4190, photo B. Matheny). **H.** *M. multispora* (PBM4717, photo B. Matheny). **I.** *M. multispora* (FLAS66616, photo M. Smith). Scale bars = 1 cm.

to reddish brown against a dull yellowish ground color; basal mycelium sulphur yellow, especially beneath the soil; context pale yellow, unchanging where bruised, typically yellow at the base when fresh.

Basidia 36–41 × 7–8 µm, 4-sterigmate, slenderly clavate, soon collapsed, becoming necropigmented. *Basidiospores* (8.5–)9–*9.6*–10(–12) × (5–)5.5–*5.6*–6(–7) µm, Q (1.50–)1.64–*1.71*–1.90(–2.18) (n = 45/3), smooth; elliptic, subphaseoliform, or nearly amygdaliform, at times with a ventral depression; thick-walled, brownish in KOH, apiculus indistinct. *Pleurocystidia* absent. *Cheilocystidia* 18–60(–65) × 4–10 µm, many digitiform or irregularly cylindric with a flexuous outline and tapered apices, at times mixed with shorter cylindric cells or apices obtuse or rarely swollen, thin-walled (rarely slightly thickened), hyaline or infrequently ochraceous. *Stipitipellis* a vesture of superficial hyphae, these dark russet or dark tawny in mass, 5–12 µm wide, weakly incrusted or smooth, thin-walled, *caulocystidia* not observed; tramal hyphae hyaline, smooth, thin-walled, cylindric. *Pileipellis* a turf or interwoven cutis of dark russet or dark rusty colored hyphae in mass, these cylindric and mostly 5–12 µm wide, weakly incrusted or smooth, thin-walled. *Lamellar trama* parallel, pale yellow to subhyaline in mass, hyphae cylindric, many 4–10 µm wide, smooth, thin-walled. Lamellar trama parallel. *Clamp connections* present.

Distribution: Midwestern (Illinois, Indiana, Kansas) and southeastern states (Tennessee), USA.

Habitat: On calcareous ground under hardwoods including *Quercus*, *Fagus*, *Carpinus*, and/or *Carya*. June–September.

Other specimens examined: **USA**, Illinois, Coles Co., Charleston, Lakeview Park, on ground under *Quercus* mixed with *Carya* and *Juniperus*, 21 Jun. 2011, *M. Kuo*, MK06211102 (TENN-F-073749); *ibid*., 29 Jul. 2020, *M. Kuo*, MK07292005 (herb. Kuo); Marion Co., gregarious under *Carya glabra*, *Ulmus rubra*, *Juniperus virginina*, 7 Jun. 2015, *M. Kuo*, MK06071503 (TENN-F-074751); Indiana, Parke Co., on soil in deciduous woods, 14 Jul. 2003, *M. Kuo*, MK07140307 (TENN-F-074752); Kansas, locality unknown, in mixed hardwood forest under *Quercus*, 7 Aug. 2008, *G. Sayers s.n.* (TENN-F-063525); Tennessee, Anderson Co., Norris Dam State Park, Clear Creek Trail, on soil in hardwood forest under *Quercus*, *Fagus*, *Carpinus*, *Carya*, 21 Sep. 2018, *P.B. Matheny*, PBM4194 (TENN-F-074601); *ibid.* 8 Aug. 2019, *P.B. Matheny & R.A. Swenie*, PBM4312 (TENN-F-074884); *ibid*. 16 Aug. 2020, *P.B. Matheny*, PBM4437 (TENN-F-075309); *ibid*. 3 Sep. 2020, *P.B. Matheny*, PBM4479 (TENN-F-075351); Knox County, William Hastie Natural Area, on soil on karst topography under *Quercus*, *Carya*, *Pinus virginiana*, 5 Jul. 2023, *R.A. Swenie*, RAS1119 (TENN-F-078399).

Notes: *Mallocybe luteobasis* is described here as new to accommodate a species recognized by the conspicuous reddish brown to fulvous appressed scales against a lighter background pileus color, dark colored fibrils and scales on the stipe, the yellow stipe base, pale yellow context, and occurrence under hardwoods (*Fagales*) on calcareous soils in midwestern and southeastern states of the USA. The spores are somewhat wider than all other eastern North American *Mallocybe* and have an average Q value less than 2.0. An additional distinctive feature of *M. luteobasis* is the digitiform or subcylindric cheilocystidia that may be elongated. The species could be confused with *M. unicolor*, but the latter differs from *M. luteobasis* by the granulose-scaly pileus surface, whitish stipe base, the typically oblong spores, and the differently shaped cheilocystidia (irregularly cylindric to fusiform at times with subcapitate apices). The two species are sympatric and co-occur at the same localities but are distantly related. *Mallocybe fulvipes* (Cripps *et al.* 2010) is somewhat similar given the squamulose-fibrillose reddish brown pileus and yellow stipe base, but this species can be distinguished from *M. luteobasis* by its occurrence in alpine regions with *Salix* in western North America and Europe and phylogenetic position within the Delecta clade.

Phylogenetically, *M. luteobasis* represents the first split in the Terrigena grade (Fig. 1) where it is strongly supported as sister to the rest of the core Mallocybe clade. Four specimens sequenced from Illinois (type), Indiana, and Kansas form a strongly supported group. Samples from Tennessee have also been observed.

Smith & Hesler (1968) drew some similarities between *Pholiota sola* and *Inocybe*. *Pholiota sola* is similar to *M. luteobasis* in outward appearance other than the notably elongated stipe in relation to the pileus width in *P. sola*. This species was described based on a single collection with the type from Michigan, not Washington D.C. as stated in the protologue. The spores are somewhat narrower compared to *M. luteobasis*, and chrysocystidia and pleurocystidia were described as present, which would support placement in *Pholiota*. Smith & Hesler (1968) also noted the dry pileus and the absences of gelatinous tissues and of a germ pore in *P. sola*, similarly to *Mallocybe*.

Mallocybe malenconii (R. Heim) Matheny & Esteve-Rav., *Mycologia* **112**: 107. 2019 [2020]. Figs 5D, 10E, F.
Basionym: *Inocybe malenconii* R. Heim, *Encyclopédie Mycol*. **1**: 163. 1931.
Synonym: *Inocybe marmoripes sensu N. Am. auct. p.p.*

Pileus 10–25 mm wide, convex to plano-convex or almost plane, never depressed at the center, margin incurved for long durations but not inrolled; surface dry, center decorated with prominent, short, woolly tufts of fibrils that are concolorous with or slightly darker than the rest of the surface, at first simply fibrillose; center dark reddish brown to yellowish red (Argus Brown to Amber Brown (5YR 3/4–4/6), shading to Buckthorn Brown (10YR 5/6–5/8) towards the margin (Sienna color per Heim); context fleshy, firm, pale ocher-pink; *odor* and *taste* indistinct. *Lamellae* adnate or mostly uncinate, moderately close, ventricose but somewhat narrow; cinnamon but becoming much darker with age, edges pallid. *Stipe* 15–40 × 3–5 mm, irregularly cylindric, usually flexuous, often curved or twisted, equal towards the base; surface dry, in age with darker brown scattered fibrillose tufts; light brownish or paler at the apex and at the base; context fibrous, tough, not putrescent, more or less hollow.

Basidia 20–32 × 6–9 µm, 4-sterigmate, slenderly clavate to subcylindric, hyaline but becoming necropigmented. *Basidiospores* (9–)9.5–*10.7*–12 × 4–*4.5*–5 µm, Q (2.11–)2.20–*2.39*–2.75(–2.88) (n = 50/3), smooth; oblong-cylindric, oblong-subphaseoliform, or oblong-amygdaliform ("laceroid"), often with a ventral depression and obtuse to bluntly pointed apices; brownish yellow to pale brown, wall slightly thickened, apiculus small and indistinct. *Pleurocystidia* absent. *Cheilocystidia* 17–26 × 10–16(–20) µm, short clavate or short cylindric to sphaeropedunculate or obclavate, thin-walled, hyaline to ochraceous, rarely brownish incrusted; lamellar edges sterile. *Caulocystidia* similar to cheilocystidia, restricted to the extreme apex of the stipe (possibly just an extension of the hymenium

at the extreme stipe apex); superficial hyphae sparse, yellowish brown to ochraceous in mass, cylindric, 6–13 µm wide, weakly incrusted. *Pileipellis* composed of tufts of trichodermial hyphae, these Tawny to Ochraceous-Tawny in mass, cylindric to inflated and mostly 10–18 µm wide, incrusted to coarsely so, with slightly thickened walls. *Lamellar trama* parallel; hyphae light yellowish in mass, 10–18 µm wide, smooth, thin-walled. *Clamp connections* present.

Distribution: Northern regions of eastern and western North America (British Columbia, Maine, New York, Quebec, Washington). Also, northern and central Europe (type), eastern Russia, Korea.

Habitat: On sandy acidic soils under mixture of conifers (*Pinus*, *Picea*) and/or *Salix* and *Betula*. April–May in the Pacific Northwest, August–September in the northeast USA and southeastern Canada.

Specimens examined: **Canada**, British Columbia, Cranbrook, on trail to Lloyds Meadows off Crowsnest Highway, 1 100 m elev., 21 May 2002, *O. Ceska*, 2020521-001 (UBC F19123; image only). **Finland**, Pohjois-Häme, Saarijärvi, Linnankylä, along margin of road 13, in sandy soil on bank of road near *Pinus sylvestris* and young *Betula pubescens*, *Salix caprea*, and *Salix phylicifolia*, 18 Aug. 1989, *J. Vauras*, JV3590F (TURA, WTU); Satakunta, Kankaanpää, Niinisalo, the spring Yskänlähde, on sandy soil near *Pinus sylvestris*, 24 Jul. 1990, *J. Vauras*, JV4470F (TURA, WTU); Perä-Pohjanmaa, Rovaniemi rurual commune, Jaatila, Jaatilanvaara, near Savioja, edge of the main road near young *Picea abies*, *Betula*, and *Salix* on sandy soil, 24 Aug. 1991, *J. Vauras*, JV5824F (TURA, WTU). **USA**, Maine, Medway, Penobscot Co., Route 11 south of Grindstone Falls Rest Area, on soil along roadside under *Quercus*, *Pinus*, 9 Sep. 2022, *L.V. Kudzma*, LVK22039 (pers. herb.); *ibid.*, LVK22045 (pers. herb.); New York, Essex Co., Bloomingdale, in sandy soil under mixed conifers and hardwoods, 13 Aug. 2021, *L.V. Kudzma*, LVK21286 (pers. herb.); Washington, Snohomish Co., Point Wells, near Richmond Beach, 2 Apr. 1941, *D.E. Stuntz*, 948 (WTU).

Other specimen examined (Inocybe subgranulosa): **Finland**, Tavastia australis, Tamella, Barrskog., på brända sandmarker (Mustiala på Syrjä), 2 Oct. 1892, *P. Karsten* (**holotype** H 2499).

Notes: The gross morphological description of *M. malenconii* is taken mainly from Heim (1931, as *Inocybe malenconii*) but modified to fit the formatting here and supplemented with observations from material collected in the USA. No other previously described North American taxon appears to match this species though it is very closely related to what we now interpret here as *M. tomentella* described as new below. Several studied European specimens agree morphologically and genetically with North American samples from the Pacific Northwest, New York, and Maine and thus, for the first time, confirm the presence of *M. malenconii* from North America. It has also been recently confirmed in Quebec (J. Landry, pers. comm.). Where the ecology is known, the species appears to occur on sandy acidic soils.

Mallocybe malenconii resembles forms of *Inocybe lacera* in outward appearance, and microscopically has similar oblong "laceroid" basidiospores with an average Q value > 2.00. However, the absence of pleurocystidia and presence of necrobasidia easily distinguish the species from *I. lacera*. The species in a restricted sense is monophyletic with strong support, but references to collections of *M. malenconii* from China and Spain are very closely related to those of *M. subgranulosa* (including its type) from Sweden and Finland (Fig. 2A). *Mallocybe malenconii* differs from *M. tomentella* morphologically by the narrower "laceroid" shaped spores, however, both were observed to co-occur in the same sandy acidic soil habitats in New York.

Mallocybe malenconii has been reported from Kamchatka in Russia (Peintner & Horak 2002) and Korea (Cho *et al*. 2021) and thus would have a broad circumboreal distribution, however, Asian samples have yet to be confirmed in the *M. malenconii* clade in the strict sense. Kauffman (1924) and Stuntz (1940) recognized the species from the Pacific Northwest but under the broadly misapplied name of *Inocybe marmoripes*. The latter, as interpreted by Kauffman (1924) and Stuntz (1940), actually included two species (*M. malenconii* and *Mallocybe* sp. 2 in Fig. 2A). Upon inspection of these materials, *Mallocybe* sp. 2 was found to differ from *M. malenconii* genetically and by the longer basidiospores. Note that *Inocybe marmoripes* is considered a later synonym of *M. unicolor* (see below).

Mallocybe megalospora differs from *M. malenconii* by the wider spores and association with *Salix* and *Alnus* in Europe (Stangl & Bresinsky 1983). This taxon has not been confirmed from North America. An unpublished sequence (GenBank HQ604786) under this name has been reported from British Columbia, but that sequence represents *Mallocybe* sp. 2, which appears to be endemic to the Pacific Northwest.

Mallocybe montana Matheny, ***sp. nov.*** MycoBank MB 847419. Figs 5E–G, 10G, H.

Etymology: *montana* (L.), mountain, in reference to occurrence in the southern Appalachian Mountains.

Typus: **USA**, North Carolina, Haywood Co., Great Smoky Mountains National Park, Big Creek, Baxter Creek Trail, scattered to gregarious on sandy acidic soil in riverbed under hardwoods in a riparian hardwood forest, 518 m elev., 9 Aug. 2012, *P.B. Matheny*, PBM3872 (**holotype** TENN-F-067500).

Diagnosis: Characterized by the small to medium-sized basidiomata, finely velutinous pileus, lighter colored stipe, cylindric basidiospores with a mean Q value > 2.0, presence of elongated cheilocystidia that are pale brown in mass in KOH, and occurrence on poor, sandy, acidic soils in Appalachian montane mixed forests. Distinguished phylogenetically as the sister lineage to clades Unicolores, Nothosperma, and Mallocybe.

Pileus 8–35 mm wide, convex at first, occasionally obtusely conical, expanding to broadly convex or nearly plane with age, umbo absent, center slightly depressed with age; margin incurved to decurved, entire; surface dry, velipellis and veil remnants absent, finely tomentose to finely velutinous or matted woolly tomentose under a hand lens, appearing subsmooth to the naked eye; strong brown (7.5YR 4/4) to yellowish brown or dark yellowish brown (10YR 5/6–5/8–6/6–4/4; Prout's Brown to Dresden Brown), brownish with 5 % KOH; context watery pale brown to olive-yellow when moist, up to several mms thick under the disc, not changing color where bruised; *odor* noticeable when first cut, nearly acidulous but with an unpleasant component, at times not remarkable; PDAB negative. *Lamellae* adnate to uncinate, seceding, subdistant with 18–22 L and several tiers of lamellulae; brown to

yellowish brown (10YR 5/3–5/4) or dark yellowish brown with age; medium, up to 4 mm deep; edges crenate or nearly so, not white but colored pale brown like the faces. *Stipe* 14–40 × 2–5 mm at the apex, equal, not bulbous, cortina not observed; surface dry, with scattered fine brown fibrils against a pale brown or pale yellow (buff) to light yellowish brown ground color (2.5Y 7/4, 10YR 6/3–6/4), overall paler than the pileus; context not confluent, pale brown throughout, base encased in sand, basal mycelium white, solid.

Basidia 42–60 × 7–10 µm, 4-sterigmate, slenderly clavate to subcylindric, necropigmented. *Basidiospores* (10–)11–*12.2*–13.5(–14) × (4.5–)5–*5.4*–6 µm, Q (1.82–)1.92–*2.27*–2.55(–2.80) (n = 60/4), smooth, oblong-amygdaliform or cylindric, yellowish brown with thickened walls, apiculus not distinctive. *Cheilocystidia* 26–74 × 8–16 µm, slenderly clavate or elongate-clavate to somewhat cylindric, arising from short articulated cells, apices often swollen or subcapitate, thin-walled or weakly thickened in places, pale brown in mass, on occasion with fine apical incrustations, necropigmented with age. *Pleurocystidia* absent. *Stipitipellis* with clusters of dense short clavate to subcylindric caulocystidia, 27–40 × 8–12 µm, these thin-walled and hyaline; or without caulocystidia, composed of scattered interwoven brownish to ocher-tawny tufts of terminal hyphae similar to pileipellis hyphae; terminal cells cylindric, not particularly cystidioid, pigmented and smooth to incrusted, mostly 8–20 µm wide; with numerous refractive hyphae present in stipe trama. *Pileipellis* a tangled interwoven trichoderm or short turf, composed of loose chains of hyphae, ocher-tawny in mass in KOH; hyphae cylindric, mostly 8–20 µm wide, walls thin or slightly thickened and often with pale brownish to ocher-tawny pigment, at times incrusted or coarsely so, terminal cells occasionally cystidioid or differentiated in appearance. *Lamellar trama* parallel; hyphae pale yellowish in mass, 4–15 µm wide, smooth or weakly incrusted. *Clamp connections* present.

Distribution: Southeastern USA (North Carolina).

Habitat: Scattered singly or in pairs, often on very sandy acid soil in mixed forests of *Quercus*, *Pinus*, *Betula*, and *Tsuga* or under hardwoods in sandy riparian areas. July–September.

Other specimens examined: **USA**, North Carolina, Macon Co., Highlands, Wahalla Road, Blue Valley Road, scattered singly on sandy acid soil on side of dirt road under *Pinus strobus*, *Betula alleghaniensis*, *Quercus*, 760 m elev., 8 Sep. 2018, *P.B. Matheny*, PBM4190 (TENN-F-074532); *ibid.*, on sandy acid soil on side of dirt road under *Quercus, Pinus*, 760 m elev., 26 Jul. 2021, *R.A. Swenie & P.B. Matheny*, PBM4585 (TENN-F-075751); North Carolina, Macon Co., Nantahala National Forest, Rock Gap, Appalachian Trail near Standing Indian Campground, scattered singly on acid soil in mixed forest under *Tsuga*, *Pinus strobus*, *Quercus*, *Betula*, 885 m elev., 30 Jul. 2021, *P.B. Matheny*, PBM4614 (TENN-F-075781).

Notes: *Mallocybe montana* is an unusual species of *Mallocybe* characterized by the elongated, clavate, pale brown pigmented cheilocystidia, long basidia, and narrow oblong spores. The species is currently only known from the southern Appalachian Mountains at several different localities in western North Carolina where it occurs on acidic and often sandy soils. To the eye, the pileus may seem almost smooth but is velutinous to woolly-tomentose under a hand lens, and no veil remnants have yet been observed. It matches none of the prior descriptions of species made by North American workers, thus the species is described here as new.

Mallocybe montana represents a significant discovery because, together with *M. praevillosa* (see below), it forms a strongly supported grade (paraphyletic group) from which the remainder of *Mallocybe* is derived (Figs 1, 2C). Three samples of *M. montana* collected in different regions of western North Carolina form a strongly supported monophyletic group. *Mallocybe multispora* is somewhat similar but differs from *M. montana* by the hyaline or rarely ochraceous cheilocystidia, convex to conical pileus with a small conical or subacute umbo, the more tomentose to scaly pileus covering, occurrence at lower elevations in mixed pine-oak or hardwood forests, and phylogenetic placement in clade Unicolores sister to *M. unicolor*.

Mallocybe multispora (Murrill) Matheny & Esteve-Rav., *Mycologia* **112**: 107. 2019 [2020]. Figs 5H, I, 10I, J.
Basionym: *Inocybe multispora* Murrill, *Proc. Florida Acad. Sci*. **7**:122. 1944.

Pileus 7–20 mm wide, convex to conical and often with a distinct (sub)conical or subacute umbo, margin incurved in youth, soon decurved or nearly straight; surface dry, umbo covered with a grayish velipellis, with appressed fibrillose scales at the center, coarsely fibrillose or tomentose towards the margin, not rimose but margin occasionally split; pale isabelline to fulvous or ochraceous tan (yellowish brown or fulvous when dried 10YR 5/6–5/8 or 7.5YR 5/6); context thin, *odor* sweet [in protologue], "fishy" when cut, or mild. *Lamellae* adnexed to adnate, moderately close, broad, edges white and fimbriate, yellowish brown to brown. *Stipe* 15–35 × 1.5–3 mm, subequal above a small bulb or swollen to enlarged, dry, ochraceous-buff, roughened with longitudinal fibrils; context concolorous, not hollow.

Basidia 30–40 × 7–10 µm, 4-sterigmate, slenderly clavate, hyaline or necropigmented. *Basidiospores* 10–*11.3*–13(–14) × 4.5–*5.3*–6(–6.5) µm, Q 1.82–*2.14*–2.47(–2.55) (n = 43/2), smooth, yellowish-brown, oblong-elliptic, oblong-subphaseoliform, or oblong-amygdaliform, often with a ventral depression, apices obtuse to bluntly pointed, germ pore absent, thick-walled, apiculus small and indistinct. *Pleurocystidia* absent. *Cheilocystidia* 27–55 × 8–15(–20) µm, subcylindric or slenderly clavate with obtuse to subcapitate apices, thin-walled, hyaline (rarely ochraceous), edges of lamellae sterile. *Caulocystidia* absent, numerous opaque refractive hyphae present among stipe hyphae. *Pileipellis* a cutis forming trichodermial fascicles, hyphae cylindric to inflated, many 7–12(–20) µm wide and coarsely incrusted and with thickened walls, bright tawny or bright fulvous in KOH. *Lamellar trama* parallel, yellowish brown in mass, hyphae cylindric and up to 11 µm wide. *Clamp connections* present.

Distribution: Southern USA (Florida, Oklahoma, Texas).

Habitat: Gregarious on sandy soil, at times pure sand, on calcareous soils (where known) under *Quercus*, *Pinus*, palms, or in hardwood forests including *Quercus* and *Carya*. June–November.

Other specimens examined: **USA**, Florida, Alachua Co., Gainesville, gregarious under a palm, 8 Jun. 1938, *W.A. Murrill*, F17380 (**isotype** TENN-F-021190, **isotype** WTU); *ibid*., Green Acres Park, under *Quercus*

virginiana and *Q. nigra*, 14 Jun. 2020, *M.E. Smith & O. Smith*, MES3732 (FLAS-F-66616); Alachua Co., Alachua, Mill Creek Preserve, West Trail, on sandy soil under *Pinus palustris*, other *Pinus*, and *Quercus*, 6 Jul. 2022, *P.B. Matheny*, PBM *4717* (TENN-F-77391); Martin Co., Jonathan Dickson State Park, on sandy moist pine flatlands with abundant *Sabal etonia* (Scrub Palmetto) and forbs, 22 Nov. 2017, *L. Kaminsky* (FLAS-F-61779); Oklahoma, Pontotoc Co., Pontotoc Ridge Nature Preserve, 15.5 miles south of Ada, gregarious on soil in mixed hardwoods under *Quercus*, *Carya*, *Ulmus*, *Fraxinus*, 21 Sep. 2002, *C.L. Ovrebo*, CO4248 (CSU); Texas, Newton County, Bleakwood, Lewis properties front lot by state highway 87, on soil in bottomland hardwood forest near *Pinus*, 36 m elev., 3 Jun. 2020, *D.P. Lewis*, DPL13581 (TENN-F-0778786).

Notes: This is the first report of *Mallocybe multispora* since the species was described from northern Florida in the 1940s (Murrill 1944). We confirm, based on morphological comparisons, extant collections from Florida, Oklahoma, and Texas. Of the available names in *Mallocybe* (under the genus *Inocybe*) originally described by Murrill, *M. multispora* matches the modern samples best by virtue of the gregarious habit, small basidiome size, pileus with a conical umbo, pallid stipe, and subcylindric to slenderly clavate cheilocystidia. Murrill also described (from a single collection) the presence of a bulbous stipe base for *M. multispora*, a feature, however, we did not observe in fresh material. *Mallocybe fulviceps* is very similar to *M. multispora*, and closely related to it but differs by the shorter clavate, utriform, or saccate cheilocystidia and phylogenetic position. *Mallocybe montana* is similar microscopically to *M. multispora*, but the pileus is not umbonate, the cheilocystidia are often pale brown pigmented, and it occurs on acidic soils in mountainous areas of the Southern Appalachians.

Of European species, *M. multispora* seems most similar to *M. perbrevis* reported in association with hardwoods (Heim 1931, Stangl 1989). This species, like *M. multispora* and *M. fulviceps*, is also depicted with a small pointed umbo, small stature, and gregarious habit similar to *M. multispora*. Until direct molecular comparisons can be made with *bona fide* reference material of *M. perbrevis*, we prefer to point to the superficial similarities but maintain the autonomy of the two American species. *Mallocybe arthrocystis*, a pan-north temperate species with oblong or cylindric-shaped spores, associates with *Salix* in western North America in alpine settings (Cripps *et al.* 2010). It differs from *M. multispora* by the short articulated cheilocystidia, bell-shaped pileus, and white lamellae in youth.

Phylogenetically, *M. multispora* is confirmed with strong support as a closely related sister species to *M. unicolor* (Figs 1, 2C) in clade Unicolores. *Mallocybe unicolor* differs from *M. multispora* and *M. fulviceps* by the larger basidiomes, pileus without a conical umbo, distinctly granulose-squamulose pileus surface, bands of dark colored fibrils on the stipe, and elongated cheilocystidia.

The ecology of *M. multispora* is still coming into focus. The subtropical Florida sample was collected in pure sand among pines and palms, whereas our more recent material was collected under oaks. Murrill's protologue states the type was collected under a palm, a non-ectomycorrhizal plant; however, the Oklahoma material was found in mixed hardwoods under *Quercus*, *Carya*, *Ulmus*, and *Fraxinus* on sandy soil. The evidence from recent collections suggest that this taxon is likely an ectomycorrhizal associate of *Fagales*, but we cannot rule out associations with *Pinaceae* as well.

Mallocybe praevillosa (Murrill) Matheny, ***comb. nov.*** MycoBank MB 84723. Figs 6A, 10K–N.

Basionym: *Lepista praevillosa* Murrill, *Lloydia* **5**: 155. 1942.

Synonym: *Inocybe praevillosa* Murrill (Murrill), *Mycologia* **36**: 122. 1944.

Pileus 15–47 mm wide, habit tricholomatoid, convex, broadly convex to conico-convex, expanding to plano-convex with age, not umbonate, margin incurved to decurved; surface dry, villous to fine suede-like smooth over the disc and towards the margin, not rimose, margin entire and at times finely fibrillose, velipellis absent, matt, dull; very pale brown (10YR 7/4) to yellow (2.5Y 7.6) or light yellowish brown (2.5Y 6/4) or Cream-Buff to Chamois or Honey Yellow with Isabella Color tones (2.5Y 5/4–5/6) in places with age, surface negative with 5 % KOH; context thick, white, not changing color where bruised, firm, tough, confluent with the stipe, *odor* and *taste* somewhat unpleasant, remaining unpleasant after dried. *Lamellae* sinuate to uncinate, close to nearly crowded with few tiers of lamellulae, narrow to somewhat broad, brittle, very pale brown to pale brown or light yellowish brown (10YR 7/4–6/3–6/4), edges pallid but indistinctly fimbriate. *Stipe* 40–80 × 8–11 mm, equal, terete, at times slightly curved, much of the lower part buried in sand; surface dry, rough, scurfy-fibrillose, no veil observed even in a young button; whitish to white throughout, KOH negative on surface; context white, confluent with pileus. *Spore print* "pale-purplish in mass" per the protologue.

Basidia 31–36 × 7–9 µm, slenderly clavate, 4-spored, hyaline, at times collapsed but none necropigmented. *Basidiospores* (8–)8.5–*9.7*–11(–12) × 3.5–*4.2*–4.5(–5) µm, 1.89–*2.30*–2.67(–2.75) (n = 62/3), allantoid to oblong-cylindric or oblong-phaseoliform in profile, oblong-cylindric to minimally angular in face view, apices obtusely conical, very pale brown in KOH (noticeably pale), no reaction in Melzer's, apiculus not distinctive. *Pleurocystidia* absent. *Cheilocystidia* 25–61 × 12–22 µm, broadly clavate to broadly fusiform or utriform, at times fusiform, occasionally long-pedicellate, apices often smooth and obtuse but on occasion developing a filiform appendage, thin-walled, hyaline, edges of lamellae sterile. *Stipitipellis* with protruding cylindric, fusiform, and irregularly cylindric terminal cells 37–66 × 6–8 µm but not appearing in tufts or in a gregarious hymenial formation, these hyaline, more or less thin-walled. *Pileipellis* a cutis giving rise to trichodermial tufts or interwoven upturned hyphae, thin-walled or slightly thick-walled, 5–12 µm wide, lacking any noticeable incrustations, light yellowish brown or brownish yellow to ocher-tawny in mass (not darkening appreciably in KOH mounts and no exudation of pigment), terminal cells mostly cylindric to slightly clavate. *Lamellar trama* parallel, dull yellow in mass, hyphae smooth in appearance, thin-walled, up to 10 µm wide. *Clamp connections* present.

Distribution: Southeastern USA (Florida).

Habitat: Solitary to scattered or gregarious in calcareous sand or sandy soil in high oak-pine forests and sandhill habitat under *Pinus palustris* and *Quercus* or under *Quercus laurifolia*. July–August.

Specimens examined: **USA**, Florida, Alachua Co., Gainesville, solitary in high *Pinus-Quercus* woods, 12 Jul. 1939, *W.A. Murrill* (**holotype** FLAS-F-19723); *ibid*., same habitat as above, 6 Jul. 1939, *W.A. Murrill* (FLAS-F-19703); Alachua Co., Alachua, Mill Creek Preserve, West Trail,

Fig. 6. Basidiomes of *Mallocybe* from eastern North America. **A.** *M. praevillosa* (PBM4724, photo B. Matheny). **B.** *Mallocybe* sp. 8 (PBM4749, photo B. Matheny). **C.** *M. squamosodisca* (PBM4307, photo B. Matheny). **D.** *M. squamosodisca* (LVK20133, photo L. Kudzma). **E.** *M. subtomentosa* (SAT-99-233-01, photo S. Trudell). **F.** *M. subtomentosa* (LVK16004, photo L. Kudzma). Scale bars = 1 cm.

on sandy soil under *Quercus laurifolia* with *Pinus palustris* in the general vicinity, 6 Jul. 2022, *C.R. Noffsinger*, PBM4724 (TENN-F-077398); Putnam Co., Ordway-Swisher Biological Station, by Blue Pond, 29.71008 -81.992526, in sandhill habitat under *Quercus*, *Pinus palustris*, 28 Aug. 2017, *L. Kaminsky & D. Borland* (FLAS-F-61523).

Notes: Comparisons of two recent collections from northern Florida with the holotype of *Lepista praevillosa* indicates they are conspecific with the holotype based on the similar basidiome morphology, ecology, and microscopic features. Blast searches using ITS (GenBank MH211949) and 28S (GenBank MH620294) sequences produced from the modern reference materials were inconclusive and did not provide confident generic placement for this unusual species. Indeed, our rDNA phylogeny placed samples of this species outside *Mallocybe* among outgroups but with poor support (Supplementary Fig. S3). However, we re-extracted DNA from FLAS-F-61523 and PBM4724 and produced longer 28S reads than GenBank MH620294, as well as and partial

rpb1 and *rpb2* sequences. In Figs 1 and 2C, one can now see that *Lepista praevillosa* forms the sister species to the remainder of *Mallocybe*. Classification of *Lepista praevillosa* in *Mallocybe* appears warranted by the rather robust tricholomatoid basidiomes, smooth basidiospores, absence of pleurocystidia, and presence of distinct cheilocystidia. However, the species exhibits some features that deviate from most other species of *Mallocybe*: (i) the basidia are not necropigmented; (ii) the pileus surface does not darken with application of 5 % KOH; and (iii) the basidiospores are lighter pigmented. One might consider placing *L. praevillosa* in a separate genus, but this would require description of a new genus to accommodate a single species, so at this time we prefer to classify it in *Mallocybe*, which is supported by our phylogenetic analyses.

The species shares a few features in common with *Tubariomyces*, including the allantoid to oblong-cylindric spores and occurrence in sandy soils and sand in oak-pine habitats subject to disturbance by fire (Villarreal *et al.* 1998, Alvarado *et al.* 2010, Vizzini *et al.* 2012, Matheny & Bougher 2017). Species of *Cistaceae* (genera *Lechea* and *Crocanthemum*) do occur in sandhill habitats in northern Florida where one reference specimen was made, so we cannot rule out the possibility of an ectomycorrhizal association with *Cistaceae*, a feature of some Mediterranean *Tubariomyces*. However, other key features of *Tubariomyces* are not found in *M. praevillosa*, namely, the omphalinoid habit, the broadly attached to decurrent lamellae, and the presence of caulocystidia on the entire length of the stipe.

Index Fungorum mistakenly indicates *Inocybe praefarinacea* (Murrill) Singer as the current name for *I. praevillosa*. However, the former is a smooth-spored metuloid-bearing species similar to *Inocybe serotina* but is phylogenetically allied with the *I. metrodii* group (Eberhardt *et al.* 2023).

Our muscarine assay detected its presence in *M. praevillosa* but at a low relative concentration compared to the only other species of *Mallocybe* in which we detected the compound, *M. sabulosa*. The relative muscarine concentration in *M. sabulosa* was 760 times greater than that found in *M. praevillosa.*

***Mallocybe* sp. 8.** Figs 6B, 11A, B.

Pileus 11–47 mm wide, hemispherical in youth, becoming convex and expanding to nearly plane with age, umbo absent, margin incurved to decurved; surface dry, covered with white, superficial, floccose-tomentose fibrils when young, these relegated to the margin after expansion, not scaly, becoming smooth over the disc; generally fulvous to brown; odor slightly acidulous. *Lamellae* sinuate-uncinate, close to subcrowded, light olive brown to yellowish brown, edges white-fimbriate. *Stipe* 25–40 × 3–6 mm, often longer than or equal to the pileus width, equal, terete; surface dry, cortina whitish (not yellow), coarsely fibrillose to lacerate-fibrillose, colored like the pileus, base white mycelioid; context solid, becoming hollow, light yellowish brown.

Basidia 25–34 × 7–9 µm, 4-sterigmate, slenderly clavate, hyaline, necropigmented with age. *Basidiospores* (8–)8.5–*8.9*–9.5(–10.5) × 4.5–*5.0*–5.5 µm, Q (1.60–)1.70–*1.79*–1.93(–2.00) (n = 31/1), smooth, subphaseoliform, subamygdaliform, or elliptic, rarely compressed or subangular, apices often bluntly pointed, wall slightly thickened, apiculus small and not very distinct, yellowish brown. *Pleurocystidia* absent. *Cheilocystidia* 20–33 × 10–16 µm, mostly clavate, at times utriform or pyriform, hyaline, thin-walled. *Pileipellis* a cutis of cylindric incrusted hyphae with slightly thickened walls, mostly 6–11 µm wide, russet brown to tawny in mass. *Lamellar trama* regular; hyphae cylindric, smooth, thin-walled, 4–14 µm wide. *Clamp connections* present. *Distribution*: Central Appalachian Mountains of the eastern USA (West Virginia), also China.

Habitat: On acidic soil under *Picea rubens* in conifer forest, *ca*. 1 500 m elev. August.

Specimen examined: **USA**, West Virginia, Pendleton County, Spruce Knob, Whispering Spruce Trail, gregarious to scattered singly on acidic soil under *Picea rubens*, *ca*. 1 500 m elev., 8 Aug. 2022, *P.B. Matheny*, PBM4749 (TENN-F-077511).

Notes: We initially took this single collection as representative of *M. subtomentosa* in the field but noted the relatively conspicuous white fibrils especially towards the margin of the pilei. Blast searches of sequence data and phylogenetic analyses, however, revealed our West Virginia sample as conspecific with several unidentified samples from China forming a monophyletic group with strong support. The species is very closely related and sister to *M. leucothrix* (Fig. 2A). Both species, as well as *M. leucoloma*, which is also closely related, share the relatively distinct white veil covering of the basidiomata, white cortina, white stipe base, and the stipe length often longer than the pileus is wide. *Mallocybe leucoloma* differs from these by the longer spores and occurrence primarily with *Salix* and/or *Dryas* in alpine and montane regions of western North America and Europe. *Mallocybe leucothrix* associates with *Quercus* and/or *Pinus* in Florida and Arizona and occurs in areas with karst topography. By contrast, *Mallocybe* sp. PBM4947 was observed on acidic soils under *Picea* but does share a similar spore size and shape with that of *M. leucothrix. Mallocybe subtomentosa* has a less pronounced initial whitish covering, a subsmooth pileus, and principally occurs with *Quercus* and *Pinus*.

As we know the species from only a single sample, we defer to our Asian colleagues to provide a more thorough account and description of this species.

Mallocybe squamosodisca (Peck) Matheny & Kudzma, ***comb. nov*.** MycoBank MB 847424. Figs 6C, D, 11C, D.
Basionym: *Inocybe squamosodisca* Peck, *Bull. N.Y. St. Mus*. **75**: 18. 1904.

Pileus 10–50 mm wide, convex to broadly so, umbo absent, margin incurved and inrolled throughout all stages at least when young, becoming decurved; surface dry, velipellis absent, tomentose-fibrillose, at times breaking into areolate or cracked scales; yellowish brown to ochraceous buff (10YR 5/6–5/8; Buckthorn Brown to Dresden Brown, 6E8–4B4), dark brown with KOH; context whitish with a pale yellow tone (Colonial Buff, 4B4), not confluent with the stipe, rather firm, unchanging where bruised, *odor* mild or not remarkable. *Lamellae* adnate to ascending adnexed or sinuate, close with ca. 38–42 L and several tiers of lamellulae, pale yellow (5Y 8/4–7/4, Colonial Buff to Deep Colonial Buff, 5C3) to yellowish brown (10YR 5/6, 6E5); edges even, not fimbriate, more or less concolorous with the faces, medium to broad. *Stipe* 10–50 × 3–12 mm, short or typically not longer than the pileus width, equal or tapered towards the base, not bulbous, terete; cortina yellowish brown, fugacious; surface dry, nowhere pruinose, heavily silky fibrillose to coarsely fibrillose or villose with scattered tufts of fibrils,

becoming lacerate; cortina and/or annular zone buff (5A4–B4); overall brownish yellow (10YR 6/6), somewhat lighter than or nearly concolorous with the pileus but with yellowish brown fibrils; context solid becoming hollow, pale yellow or whitish overall mixed with a pale yellow tone, with a whitish to yellow interior at the base.

Basidia 26–39 × 6–9 µm, (2–)4-spored, slenderly clavate, hyaline to ochraceous. *Basidiospores* (8–)8.5–*9.6*–10.5(–12.5) × (4.5–)5–*5.3*–5.5(–6) µm, Q (1.60–)1.67–*1.82*–2.00(–2.27) (n = 69/5), smooth, phaseoliform to elliptic or subamygdaliform, at times subcylindric and weakly angular, apiculus indistinct, slightly thick-walled, ochraceous buff to brownish yellow, the occasional long and cylindric spore presumably from 2-spored basidia. *Pleurocystidia* absent. *Cheilocystidia* 12–38 × 7–14 µm, short-cylindric, clavate, to obovate, fusiform, or filiform, at times subtended by articulated hyphal cells, thin-walled, hyaline to ochraceous. *Pileipellis* an irregular or interwoven cutis including tufts of uplifted hyphae, these tawny in mass, cylindric to somewhat inflated, 5–18 µm wide, incrusted and at times coarsely so, thin-walled to slightly thickened. *Caulocystidia* not observed; superficial hyphae similar to pileipellis hyphae, often coarsely incrusted. *Lamellar trama* parallel; hyphae ochraceous to pale yellow in mass, cylindric to inflated, 4–19 µm wide. *Clamp connections* present.

Distribution: Eastern USA (Maine, New York, North Carolina, Tennessee), extending southwards into high elevation oak forests in Costa Rica.

Habitat: On acidic soils under *Quercus*, *Pinus*. June–September.

Other specimens examined: **Costa Rica**, Cartago, Prusia, Parque Prusia, west slope of Volcan Irazu, on acidic soil under *Quercus costaricensis*, *Comarostaphylis*, *Vaccinium*, 20 Jul. 1993, *R.E. Halling*, REH7036 (NY). **USA**, Maine, Somerset Co., Appalachian Trail near Pleasant Pond, Caratunk, on soil, 1 Sep. 2020, *L.V. Kudzma*, LVK20133 (TENN-F-077383); Maine, Penobscot Co., Route 11 south of Grindstone Falls Rest Area, on soil along roadside under *Quercus*, *Pinus*, 9 Sep. 2022, *L.V. Kudzma*, LVK22053 (pers. herb.); North Carolina, Macon Co., Highlands, Cliffside Lake Recreation Area, on acidic soil in mixed woods under *Pinus strobus*, *Tsuga*, *Quercus*, 27 Jul. 2021, *P.B. Matheny*, PBM4591 (TENN-F-074869); Tennessee, Cumberland County I-40 Rest Area, near Crab Orchard, on soil among bryophytes under *Quercus* and near planted *Pinus*, 3 Aug. 2019, *P.B. Matheny*, PBM4307 (TENN-F-074869); New York, Franklin Co., Paul Smith's Visitor Interpretive Center, Barnum Brook Trail, 9 Aug. 2021, *S. Hopkins*, PBM4621 (TENN-F-075791); New York, Adirondack Park, Sacandaga Lake, gregarious under pine trees on lakeshore, 17 Aug. *ca*. 1903, *C.H. Peck* (**isotype** WTU, **isotype** MICH 11088; image only).

Notes: *Inocybe squamosodisca* is broadly distributed in the eastern USA and Central America and occurs typically with *Quercus* and/or *Pinus*. ITS data from our materials are 98 % similar to sequences of *M. substraminipes* (*fulvipes* group A; Cripps *et al.* 2010) and sequences mislabeled "*M. terrigena*" (here labeled as *Mallocybe* sp. 9) from the Pacific Northwest based on blast searches. Phylogenetically, our samples clustered independently in the Delecta clade (Fig. 1) apart from *M. substraminipes*, *M. latispora*, and their close relatives (Fig. 2A). Morphologically, our specimens feature stipe context with a pale yellow tone and with white (when very young) or yellow in the stipe base similar to *M. substraminipes* and allies in *fulvipes* group A of Cripps *et al.* (2010). Peck's protologue made no mention of the color of the stipe context but did describe the pileus context as whitish or yellowish white, consistent with our observation of fresh specimens. In addition, these collections are consistent microscopically with the type, and some of the specimens show a cracked-areolate pileus surface with age. These features, in combination with the longer spores on average and lack of any noticeable odor, serve to distinguish the species from *M. fibrillosa*.

Smith (1939) considered *Inocybe squamosodisca* as a possible synonym of *I. caesariata sensu* Kauffman. This latter name has been applied in various ways by North American authors (Kauffman 1924, Lincoff 1981), but the stipe has generally been recognized as scaly, a feature at odds with *I. squamosodisca*. Application of the name *I. caesariata* in Europe is not clear (Stangl 1989). However, the protologue describes the stipe as fibrillose, not scaly. Given the range of materials observed and similarities with the type, including the cracked-areolate pileus surface that develops with age and microscopic similarities, we prefer to recognize this unique phylogenetic entity as Peck's *I. squamosodisca*, hence, the recombination in *Mallocybe*. Specimens from New York and Maine studied by us and sequenced here serve credibly as reference material for this species.

Mallocybe subtomentosa (Peck) Matheny & Kudzma, ***comb. nov.*** MycoBank MB 847425. Figs 6E, F, 7A, B, 11E–H.
Basionym: *Inocybe subtomentosa* Peck, *Ann. Rep. NY St. Mus*. **48**: 109. 1897 [1895].

Pileus 8–35 mm wide, conical to obtusely conical, margin incurved, umbo absent or rarely low and obtuse; surface dry, not hygrophanous, finely fibrillose, not at all scaly, almost smooth with age, velipellis usually absent; yellowish brown (10YR 5/4–5/6–5/8 or Buckthorn Brown), mixed with some light olive brown tones (2.5Y 5/4 or Isabella Color) or dark yellowish brown (10YR 4/4) at the center, surface brown with 3 % KOH; context pallid with pale yellowish tinge, not changing color where bruised, *odor* faintly acidulous or not remarkable. *Lamellae* adnate with slight decurrent tooth, moderately close with several tiers of lamellulae (up to 40 L), light olive buff to pale brown, becoming yellowish brown to dark yellowish brown with age (10YR 5/4–4/4), edges pallid but at most indistinctly fimbriate. *Stipe* 20–40 × 3–5 mm at apex, longer than pileus width, tapered below or equal, terete; cortina forming thin, silky, cobwebby, white fibrils, fugacious; surface dry, scurfy at extreme apex, elsewhere fibrillose, at times with fine silky white vesture, mostly light yellowish brown (2.5Y 6/4) mixed with light olivaceous tones (Isabella Color) or whitish with dull yellow tones (2.5Y 8/4; Cream-Buff), extreme base with whitish appressed mycelium; context solid becoming hollow, whitish throughout, *not* yellow at the base.

Basidia 24–33 × 6–9 µm, 4-sterigmate, slenderly clavate, ochraceous or hyaline. *Basidiospores* 7.5–*8.9*–9.5(–11) × 4.5–*5.0*–5.5 µm, Q 1.55–*1.77*–1.90(–2.00) (n = 52/5) smooth, subphaseoliform, subamygdaliform, or elliptic, apices often obtuse, yellowish brown, with slightly thickened wall, apiculus not distinct. *Cheilocystidia* 13–40 × 7–17 µm, short clavate or pyriform (*Opuntia*-like), arising from articulated hyphae, occasionally utriform. *Pleurocystidia* absent. *Caulocystidia* not observed; stipitipellis composed of a vesture of tangled, sparse, cylindric hyphae, similar to hyphae of the pileipellis, refractive

hyphae not observed. *Pileipellis* a cutis of repent to tangled hyphae, these cylindric and up to 13 µm wide, faintly incrusted with thin or slightly thickened walls, ochraceous-tawny to tawny in mass, refractive hyphae frequent. *Lamellar trama* parallel, yellowish in mass, hyphae cylindric to inflated and mostly 5–12 µm wide, thin-walled, smooth. *Clamp connections* present.

Distribution: Northern regions of North America (Alaska, Maine, Massachusetts, New York, New Jersey, Pennsylvania, Quebec), and at higher elevations in the central and southern Appalachian Mountains (North Carolina, West Virginia), and in montane regions of New Mexico and Mexico (Michoacán).

Habitat: On soil (probably acidic) often under *Pinus* or *Pinus* mixed with *Quercus*. June–September.

Other specimens examined: **Mexico**, Michoacán, Tlalpujahua, Municipio San Felipe del Progresso, Centro Ceremonial Mazahua, on soil in pine forest, 2 889 m elev., 8 Aug. 2018, *D.P. Lewis*, DPL13020 (TENN-F-074582); *ibid*., *D.P. Lewis*, DPL13025 (TENN-F-074575). **USA**, Maine, Ogunquit Museum of Art, on soil under *Pinus strobus*, 4 Aug. 2014, *L.V. Kudzma*, LVK14251 (pers. herb.); Massachusetts, Northbridge, scattered singly on soil among woodchips along roadside in mixed woods including *Pinus* and *Quercus*, 26 Sep. 2003, *J.C. Slot*, PBM2460 (TENN-F-062321); New Jersey, Brendan T. Byrne State Forest near Pakim Pond parking area, on soil under *Pinus* and *Quercus*, 15 May 2017, *L.V. Kudzma*, LVK17005 (pers. herb.); *ibid.*, 17 May 2017, *L.V. Kudzma*, LVK16004 (TENN-F-077382); *ibid.*, *L.V. Kudzma*, LVK16006 (pers. herb.); New Mexico, Santa Fe National Forest, Jemez Mountains, Camp Shaver (YMCA), near Battleship Rock, 5 km south of La Cueva, in mixed forest of *Pinus ponderosa*, *Pseudotsuga*, *Quercus gambelii*, *Juniperus*, 2 060 m elev., 21 Aug. 1999, *S.A. Trudell*, SAT-99-233-01 (WTU); New York, Rouses Point (near the Canadian border), gregarious or subcaespitose in gravelly soil among fallen leaves, Sep. (day and year not known), *C.H. Peck* (**isotype** WTU 018341); Franklin County, Paul Smith's Visitor Interpretive Center, Barnum Brook Trail, on acid soil in mixed woods under conifers, including *Pinus strobus*, *Betula*, *Fagus*, *Populus*, 14 Aug. 2021, *P.B. Matheny & S. Hopkins*, PBM4701 (TENN-F-075838); Franklin County, Hayes Brook Truck Trail, near Paul Smith's VIC, scattered singly to clustered on acidic sandy soil under conifers including *Pinus sylvestris*, *Abies*, 14 Aug. 2021, *S. Hopkins* & *L. Kudzma*, PBM4703 (TENN-F-075840); North Carolina, Little Switzerland, Blue Ridge Parkway, on acid soil in mixed forest under *Quercus*, *Pinus*, *Betula, ca*. 1 000 m elev., 22 Sep. 2012, *B.P. Looney & M. Sánchez-García*, PBM3910 (TENN-F-068440); Tucker Co., Blackwater Falls State Park, Davis, Lindy Point Overlook Trail, on acid soil in hemlock forest under *Tsuga*, *Pinus strobus*, *Betula*, 11 Aug. 2022, *R.A. Swenie*, PBM4763 (TENN-F-077551).

Notes: Numerous samples of *M. subtomentosa* from the eastern USA and western regions of North America form a weakly supported monophyletic group sister to *M. leucoloma* and *M. leucothrix*, all of which are placed in the Delecta clade within the core Mallocybe clade (Fig. 2A). The species has also been recorded in central Mexico at high elevation, as well as in Quebec (J. Landry, pers. comm.). Of Peck's available names, this species best fits the protologue of *Inocybe subtomentosa*. Based on composite data, *M. subtomentosa* is characterized by the small basidiome size, almost smooth pileus surface, the stipe length longer than the pileus width, the merely fibrillose to scurfy stipe surface, white fugacious cortina, white stipe base, and relatively narrow spores with Q-values less than 2.0. Compared to *M. fibrillosa*, the pileus of *M. subtomentosa* is almost smooth, a seemingly distinctive feature. Both *M. fibrillosa* and *M. squamosodisca* also have short stipes in relation to the width of the pileus, unlike *M. subtomentosa*. *Mallocybe squamosodisca* can be further distinguished from *M. subtomentosa* by the pale yellow tone to the stipe context and usually yellowish stipe base. *Mallocybe subtomentosa* was described with a white mycelioid base, which we observe here consistently among the collections examined.

Mallocybe leucoloma and *M. leucothrix* can be distinguished from *M. subtomentosa* by the presence of a superficial covering of white tissue when young that remains on the pileus margin or stipe with age (Cripps *et al.* 2010; see also under *M. leucothrix*). As in *M. subtomentosa*, the cortina is white and often copious and the odor faint or not noticeable. In North America, *M. leucoloma* is distributed in western states better known from alpine areas of the Rockies, but the species also occurs in montane conifer forests of Wyoming and Washington.

Stuntz's application of the name *Inocybe subdecurrens* (Stuntz 1947) could fit our concept of *M. subtomentosa* given the ample white cortina, stipe length longer than the pileus width, similar spore size, and the short articulated cheilocystidia. A single collection (Stz. 604) was cited under *Alnus* and *Acer* in lowland Washington state. Stuntz described the pileus as campanulate to plane with a small obtuse umbo and densely appressed lanuginose forming squamules toward the margin. This last feature deviates from all the material we have observed and is more consistent with *M. fibrillosa*, of which we consider *I. subdecurrens* a synonym, or Stz. 604 could represent a non-alpine *M. leucoloma*.

We observed many single nucleotide polymorphic sites (SNPs) across samples of *M. subtomentosa* in our concatenated alignment at ITS (5), 28S (4), *rpb1* (8), and *rpb2* (30) loci. Taxon sampling was uneven across the four loci sequenced, but the relatively consistent occurrence of SNPs at all four loci may suggest some degree of hybridization among divergent populations within *M. subtomentosa* or with closely related species.

Mallocybe tomentella Matheny & Kudzma, ***sp. nov***. MycoBank MB 847421. Figs 7C, D, 11I, J.

Etymology: *tomentella* (L.), somewhat hairy, in reference to the fibrillose-tomentose pileus.

Typus: **USA**, New York, Franklin Co., Bloomingdale, Bloomingdale Bog, scattered to gregarious, singly or in pairs, on very sandy acidic soil along roadside under mixture of trees including *Picea*, *Abies*, *Pinus strobus*, *Larix*, *Populus*, *Betula*, *Alnus*, 490 m elev., 13 Aug. 2021, *S. Hopkins & P.B. Matheny*, PBM4690 (**holotype** TENN-F-075826).

Diagnosis: Pileus generally tomentose-fibrillose, at times bicolorous due to accumulation of cobwebby whitish fibrils at the margin; *odor* absent; stipe often with a distinct apical cortinate ring-zone, context light yellowish brown to isabelline; differing from *Mallocybe malenconii* by the shorter, wider, and differently shaped basidiospores, these mostly 8–10.5 × 4.5–5.5 µm (Q value < 2.00); cheilocystidia < 40 µm long, hyaline; on poor acidic sandy soils under *Picea*, *Populus*.

Pileus 12–40 mm wide, pulvinate with an incurved margin at first, becoming convex, soon plane, at times depressed at the center and with somewhat raised margins, with or without a low obtuse umbo; surface dry, velipellis absent, generally

Fig. 7. Basidiomes of *Mallocybe* from North America. **A.** *M. subtomentosa* (PBM4703, photo B. Matheny). **B.** *M. subtomentosa* (LVK16006, photo L. Kudzma). **C.** *M. tomentella* (PBM4690, holotype, photo B. Matheny). **D.** *M. tomentella* (SAT-06-228-10, photo S. Trudell). **E.** *M. tomentosula* (PBM4138, photo B. Matheny). **F.** *M. tomentosula* (HRL0027, photo R. Lebeuf). Scale bars = 1 cm.

tomentose-fibrillose, exceptionally forming minute floccose scales; often bicolorous (at least when fresh) with the center yellowish brown (10YR 5/8; Buckthorn Brown) and the margin light yellowish brown (10YR 6/4) or noticeably pale due to the accumulation of radially, cobwebby, whitish fibrils; with age the center may be dark brown or umbrinous but also ranging to fulvous or almost so throughout; surface dark brown with 5 % KOH; context dull dingy pale brown, not yellow, unchanging color where bruised, PDAB negative, *odor* absent. *Lamellae* adnate to weakly subdecurrent, close with several tiers of lamellulae, narrow to medium, not broad; pale brown to brown (10YR 6/3–5/3), yellowish brown with age (10YR 5/4), at times with olivaceous tones. *Stipe* 25–45 × 2–6 mm, equal or at times with a slightly swollen base, cortina whitish and often forming a distinct apical or superior cortinate ring-zone, veil remnants appendiculate along the margin of the pileus at times; surface dry, nowhere pruinose, fibrillose to coarsely so or tattered fibrillose, the superficial fibrils silky and pallid against the light yellowish brown to isabelline ground color; context soon hollow, colored like the stipe ground color.

Basidia 24–30 × 7–9 µm µm, 4-sterigmate, slenderly clavate to subcylindric, hyaline or necropigmented.

Basidiospores 8–*9.0*–10.5(–11) × 4.5–*5.0*–5.5 µm, Q (1.48–)1.60–*1.81*–2.00(–2.09) (n = 76/3), elliptic to subphaseoliform or subamygdaliform, at times suboblong, not at all or rarely subangular, apices obtuse or bluntly pointed, brownish yellow to yellowish brown, with a slightly thickened wall. *Pleurocystidia* absent. *Cheilocystida* 20–34 × 11–16 µm, mostly clavate to broadly so (not short-clavate) to saccate or spheropedunculate, thin-walled, hyaline. *Caulocystidia* not observed. *Pileipellis* a cutis of cylindric hyphae, these often coarsely incrusted and with slightly thickened walls and 7–17 µm wide, russet brown in mass. *Lamellar trama* parallel; hyphae pale yellow in mass, cylindric, thin-walled, mostly 4–12 µm wide. *Clamp connections* present.

Distribution: Northern regions of eastern and western North America (New York, Quebec, Alberta).

Habitat: On poor, sandy, acidic soils under *Picea*, *Populus tremuloides*, or in mixed forests including these trees. August.

Other specimens examined: **Canada**, Alberta, Division No. 14, Bighorn Recreation Trail, Robb Road/Cold Creek Road, near Hinton, on soil in *Picea-Populus tremuloides* forest, 1 160 m elev., 16 Aug. 2010, *S.A. Trudell*, SAT0622810 (TENN-F-071587). **USA**, New York, Franklin Co., Bloomingdale, Bloomingdale Bog, scattered to gregarious, singly or in pairs, on very sandy acidic soil along roadside under mixture of trees including *Picea*, *Abies*, *Pinus strobus*, *Larix*, *Populus*, *Betula*, *Alnus*, 490 m elev., 13 Aug. 2021, *S. Hopkins & P.B. Matheny*, PBM4694 (TENN-F-075831).

Notes: *Mallocybe tomentella* is characterized namely by the white cobwebby fibrils covering the pileus margin and darker disc when fresh, depressed pileus center usually with a small umbo, long incurved pileus, presence of a cortinate ring-zone, basidiospores with Q value < 2.00 on average, and putative association with *Picea* and possibly *Populus* on acidic soils. Our phylogenetic analyses support a broad northerly distribution between Alberta on one hand and New York and Quebec on the other [the latter as *Inocybe* sp. RL8 (GenBank MN992187)].

Both *M. malenconii* and *M. subgranulosa* can be distinguished from *M. tomentella* by the fine scaly pilei and narrow laceroid or minimally angular basidiospores with higher Q values. Support values for the clade of *M. tomentella* are only moderate, but together the samples form a robustly supported monophyletic group with *M. subgranulosa* and two orphaned samples of *M. malenconii* from China and Spain (Fig. 2A). However, given the differences in morphology, including the pileus surface structure (not granulose) and basidiospore morphology (not subangular and "laceroid"), we prefer to recognize *M. tomentella* as a distinct taxon. Further samples from Asia, Europe, and North America, including more genetic data, will be needed to ascertain whether the group might be a complex of entities surrounding *M. subgranulosa*. This *M. subgranulosa* "complex" is sister to *M. malenconii s.str.* with strong support.

A similar species, *M. tomentosula*, is presented below. The two species share the presence of cortinate ring-zone and non-laceroid basidiospores with mean Q values < 2.00. However, *M. tomentosula* differs from *M. tomentella* by occurring on limestone soils with *Quercus* and/or *Pinus strobus*. It also differs from *M. tomentella* by the darker colored pileus, phenology, and phylogenetic position where it occurs in a well-supported group containing *M. heimii*, *M. velutina*, *M. depressa*, and *M. errata* (*viz*., the Heimii clade; Fig. 1).

Mallocybe tomentosula Matheny & Esteve-Rav., *Mycologia* **112**: 109. 2019 [2020]. Figs 7E, F, 11K–M.
Basionym: *Inocybe tomentosa* Ellis & Everh., *J. Mycol*. **5**: 26. 1889, *nom. illegit*., Art. 53.1, *non Inocybe tomentosa* Quél. 1888.

Pileus 12–45 mm wide, convex or obtusely conical in youth, soon expanding to plano-convex or plane with age, umbo generally absent, center occasionally depressed, margin incurved at first and remaining slightly so when expanded or decurved with age; surface dry, velipellis absent, densely fibrillose-tomentose, at times with few scattered appressed scale-like aggregates of fibrils, not rimose; yellowish brown or fulvous (10YR 5/6–5/8) to strong brown or nearly rusty brown (7.5YR 4/4) with age, after drying specimens noticeably umbrinous; context whitish to olivaceous or with olivaceous streaks, *odor* none. *Lamellae* adnate or uncinate, close with 40–50 L and several tiers of lamellulae; light yellowish brown to light olive brown (2.5Y 6/4–5/4–5/6) to rusty brown with age, edges even and not appearing fimbriate, medium (2–4 mm deep). *Stipe* 10–35 × 3–5 mm, equal, cylindric, not bulbous; surface cortinate in youth, cortina composed of fine whitish silky fibrils, often leaving a superior annular zone; nowhere pruinose, dry, fibrillose to coarsely so, nowhere scaly, colored more or less like the pileus or with isabelline areas; base not yellow.

Basidia 24–36 × 7–8 µm, 4-sterigmate, slenderly clavate to cylindrico-clavate, hyaline or necropigmented. *Basidiospores* (8–)8.5–*9.4*–10.5(–11) × (4.5–)5–*5.4*–6(–6.5) µm, Q (1.50–)1.61–*1.74*–1.98(–2.04) (n = 71/3), smooth, subamygdaliform to elliptic, at times subphaseoliform due to a ventral depression, apices bluntly pointed or obtuse, yellowish brown, wall slightly thickened, apiculus small and not very distinct. *Pleurocystidia* absent. *Cheilocystidia* 14–34 × 8–13 µm, short-cylindric to short-clavate or pyriform, arising from articulated hyphal cells, hyaline or brownish incrusted, thin-walled, edges of lamellae becoming pigmented with age. *Pileipellis* a cutis of regularly to somewhat tangled and coarsely incrusted hyphae, russet or dark tawny in mass, hyphae cylindric and mostly 7–17 µm wide, more or less thin-walled; tramal hyphae light yellowish brown in mass, smooth, thin-walled. *Caulocystidia* not observed. *Lamellar trama* parallel, hyaline in mass, hyphae mostly 4–12 µm wide, smooth, thin-walled. *Clamp connections* present.

Distribution: Eastern North America (Quebec, New Jersey, Tennessee), including Mexico (Tlaxcala).

Habitat: On calcareous soils in Tennessee and Mexico, under *Quercus*, *Pinus strobus* or *P. cembroides* (plantation), and/or *Juniperus*; type recorded near *Picea abies* in New Jersey, soil conditions unknown. April and November (southern range), July–September (northern range).

Specimens examined: **Canada**, Quebec, Saint-Alban, under *Pinus strobus* sandy soil, 20 Sep. 2006, *R. Lebeuf*, HRL0027 (TENN-F-071134); **USA**, New Jersey, Gloucester, Newfield, in grass around Norway spruce, Sep. 1888 (no day and no collector cited) [**holotype** NY 00775649, 00775650, 0075656, 00775651 (**isotype** ex Barnard College)]; Tennessee, Knox County, Knoxville, Ijams Nature Center, on dry gravelly soil under *Quercus montana* and *Juniperus virginianus* at a limestone quarry, *ca*. 300 m elev., 17 Apr. 2016, *R.A. Swenie*, RAS123 (TENN-F-071659); *ibid.*, 11 Nov. 2017, *P.B. Matheny*, PBM4138 (TENN-F-071134).

Notes: *Mallocybe tomentosula* is most closely related to the European species *M. heimii*, the South Asian species *M. velutina* (Saba & Khalid 2020), and the East Asian *M. depressa* from China (Mao *et al.* 2022) (Fig. 2B). This strongly supported assemblage forms a sister group to *M. errata* from Thailand. *Mallocybe fuscomarginata* is superficially similar to *M. tomentosula* in that both may be characterized by the presence of brownish incrusted cheilocystidia, the cigar brown colored pileus, and the veil in *M. fuscomarginata* that at times forms a thin ring-zone (Jacobbson & Larsson 2012). However, both the spores and cystidia of *M. fuscomarginata* are larger than in *M. tomentosula*, and the gill edges of the latter are not noticeably dark brown. The two species are distantly related (Fig. 2B).

Mallocybe tomentosula has a wide geographic distribution ranging from Quebec to central Mexico (Meza-Meneses *et al.* 2016), where it associates with species of *Pinus* subg. *Strobus* and *Quercus* on limestone soils where known. The ecology, in combination with the medium sized basidiomes, the presence of a superior cortinate ring-zone, spores mostly 8.5–10.5 × 5–6 µm, and the short articulated cheilocystidia that become brownish with age, serve to distinguish it from other eastern North American *Mallocybe*. In addition, the phenology of *M. tomentosula* is unusual in that it has been recorded as early as April in Tennessee on multiple occasions, and again in November. In Quebec the species was recorded with *Quercus*, *Populus*, *Salix*, and/or *Picea* in city parks and forested areas between July and September (J. Landry, pers. comm.). The soil conditions of the Canadian samples are not known.

Matheny *et al*. (2020) introduced *Mallocybe tomentosula* Matheny & Esteve-Rav. as a *nom. nov*. for *I. tomentosa* Ellis & Everh., an illegitimate name due to the publication of the same binomial, *I. tomentosa* Quél. during the prior year. The ecology of the type is not clear with the mention only that the species occurred near planted Norway spruce in New Jersey.

The holotype of *I. tomentosa* comprises four parts on a single sheet, all from the same original gathering, one of which is an ex-isotype, since rejoined with the holotype, from Barnard College. Attempts to produce molecular annotations by Sanger sequencing (775651 and 775656) failed due to very poor quality and heterogeneous nature of the reads. All four elements resemble each other and are consistently light yellowish brown overall. We could not glean any data regarding the cheilocystidia morphology from the holotype, but the spore shape and size are consistent with our other observations of what we interpret as this species. Unpublished observations of the type of *I. tomentosa* by D.E. Stuntz in Feb. 1964 featured clavate to spheropedunculate cheilocystidia 28–36 × 12–14 µm in size. This feature is also consistent with our other studied specimens. Thus, the presence of a cortinate ring-zone, probable association with *Quercus* and *Pinus* (and possibly other plants), spore and cystidium morphology, and geography (New Jersey) are all consistent with sequenced samples studied by us from Quebec and Tennessee.

Kauffman (1924) and Smith (1939) considered *I. tomentosa* (our *M. tomentosula*) as synonymous with *I. subdecurrens*, however, we recognize the latter as a later synonym of *Mallocybe fibrillosa.* Our interpretation of *M. fibrillosa* differs from *M. tomentosula* in that *M. fibrillosa* lacks a cortinate ring-zone and tends to feature a (subtly) sweet odor. Phylogenetically, the two species are distantly related (see commentary below).

Mallocybe unicolor (Peck) Matheny & Esteve-Rav., *Mycologia* **112**: 109. 2019 [2020]. Figs 8A–D, 12A–F.
Basionym: *Inocybe unicolor* Peck, *Ann. Rep. NY St. Mus*. **50**: 104. 1897.
Synonyms: *Inocybe lorillardiana* Murrill, *Mycologia* **3**: 101. 1911.
Inocybe marmoripes G.F. Atk., *Am. J. Bot*. **5**: 213. 1918.
Inocybe caesariata sensu N. Am. auct. p.p., *non* Kauffman 1924.

Illustrations: Lincoff (1981, as *I. caesariata*); Phillips (2010, as *I. caesariata*).

Pileus 15–50 mm wide, deeply convex when young to obtusely conical or parabolic to conical, becoming subcampanulate and finally plane, an obtuse umbo sometimes present, margin incurved to decurved; surface dry, granulose due to very fine recurved or appressed squamules (resembling *Cystoderma*), at times velvety in appearance, margin entire (not rimose), dark brown with 3–5 % KOH (pale or light brown with 10 % NH_4OH); the scales dark yellowish brown or strong brown (Cinnamon Brown) at the center (10YR 4/4–7.5YR 4/4) against a yellowish brown or fulvous ground color (10YR 5/6–5/8; Buckthorn Brown), on occasion faded to light yellowish brown; context up to 3 mm thick beneath the disc, whitish, not confluent with stipe; *odor* and *taste* not remarkable. *Lamellae* narrowly adnate to uncinate, moderately close with 24–30 L and several tiers of lamellulae; cream colored or pale yellow when young (2.5 Y7/4), becoming light olive brown or isabelline (2.5Y 5/4) to dark yellowish brown (10YR 4/4) with an olive tinge or olive brown (2.5Y 4/4); equal to subventricose, up to 6 mm deep; edges white and fimbriate. *Stipe* 30–50 × 2–7 mm, often longer than the pileus diameter, terete or compressed, usually equal but occasionally slightly swollen or tapered at the base; cortina yellowish brown, fugacious; surface dry, densely fibrillose when very young but soon breaking up into yellowish brown or cinnamon brown squamules, these recurved at times, against a pale yellowish brown ground color (contrasting with the darker colored scales), dark brown with 5 % KOH; apex of stipe finely fibrillose, not pruinose; context solid becoming hollow but with a tough cortex, dingy whitish or with slight yellowish tinge, unchanging color where bruised or exposed. Context negative with guaiac and PDAB.

Basidia 28–38 × 7–10 µm, 4-sterigmate, clavate hyaline but becoming necropigmented. *Basidiospores* (8.5–)9.0–*9.9*–11.5(–12) × (4.0–)4.5–*5.0*–5.5(–6.0) µm, Q 1.64–*1.97*–2.33(–2.44) (n = 72/4), smooth, oblong-elliptic to oblong-subamygdaliform or oblong-subphaseoliform, at times with a ventral depression, apices obtuse or bluntly pointed, thick-walled to slightly thick-walled, brownish yellow (Ochraceous-Buff), apiculus small and indistinct. *Pleurocystidia* absent. *Cheilocystidia* 32–65 × 9–13 µm, irregularly cylindric, at times strangulated, or fusiform, narrowly utriform to lageniform, apices often swollen or indistinctly subcapitate, thin-walled, hyaline, edges of lamellae sterile. *Caulocystidia* not observed, superficial hyphae on stipe forming a trichoderm or interwoven layer of cylindric hyphae, these 4–10 µm wide, ocher-tawny in mass, end cells undifferentiated or at times flexuous or lageniform; subtending hyphae pale yellow brown to hyaline in mass, up to 14 µm wide, with walls that appear smooth. *Pileipellis* a cutis giving rise to fascicles of trichodermial elements that are ocher-tawny in mass; hyphae cylindric to inflated and up to 18 µm wide, incrusted, with slightly thickened walls; hyphae of subpellis up to 25 µm wide. *Lamellar trama* parallel, pale yellowish brown to hyaline in mass, hyphae

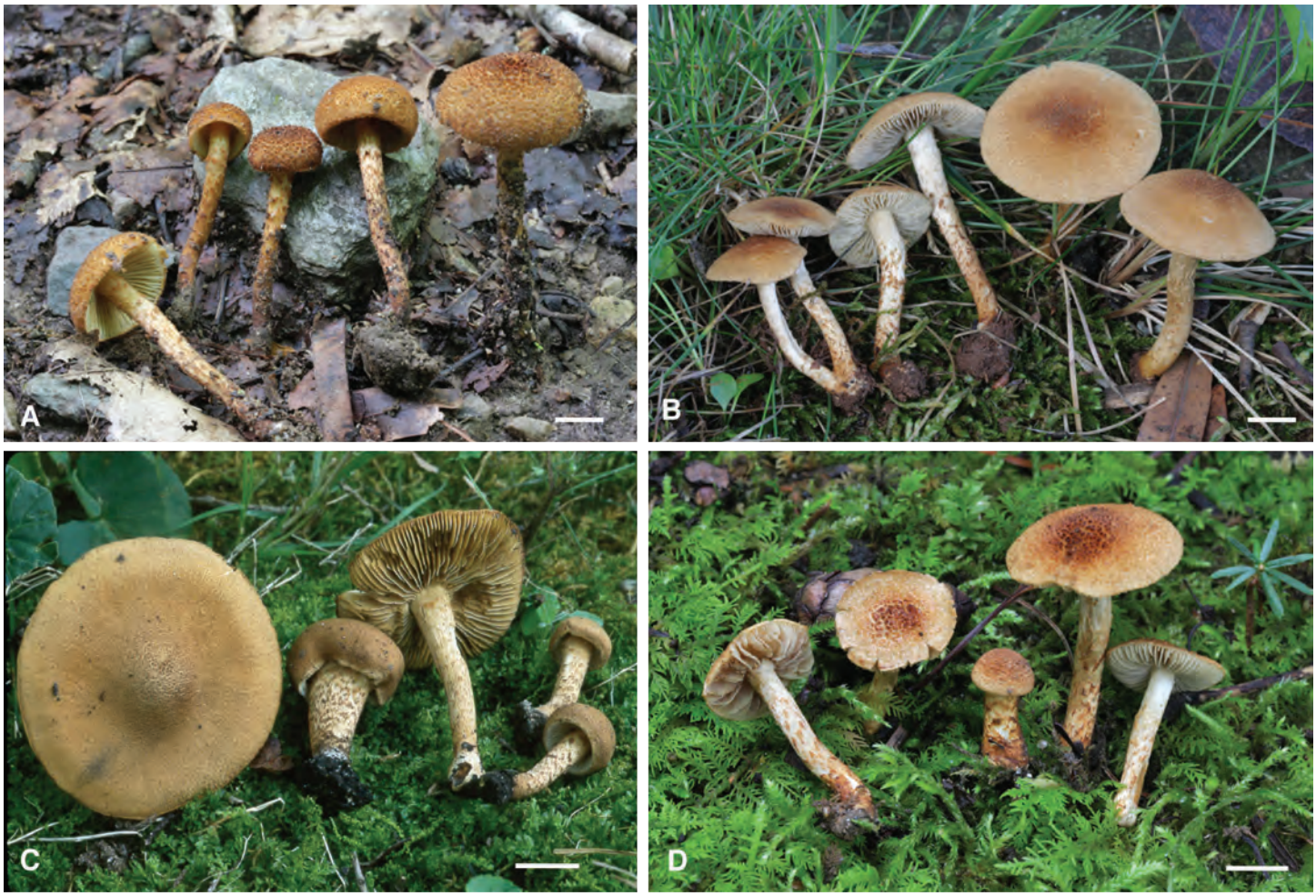

Fig. 8. Basidiomes of *Mallocybe unicolor* from eastern North America (all photos by B. Matheny). **A.** PBM4013. **B.** PBM3794. **C.** PBM1481. **D.** PBM4451. Scale bars = 1 cm.

cylindric and up to 12 µm wide, rusty colored refractive hyphae present. *Clamp connections* present.

Distribution: Throughout eastern North America. Common.

Habitat: Scattered to gregarious, at times forming troops, singly or in small groups on calcareous soil under *Quercus*, *Carya*, and *Carpinus*, or under planted *Quercus* or *Tilia*, at times on lawns in grass, generally in oak-hickory forests, or mixed mesic forests including *Quercus* and *Tsuga* on acidic soils. June–October.

Specimens examined: **USA**, Illinois, Coles Co., Charleston, First and Harrison, gregarious in grass under *Quercus*, 18 Jun. 2015, *M. Kuo*, MK06181501 (TENN-F-073747); Coles Co., Charleston, Fox Ridge State Park, picnic area, on gravelly soil under *Quercus*, *Carya*, 28 Aug. 2014, *M. Kuo*, MK08281401 (TENN-F-074753); *ibid.*, 28 Aug. 2014, *M. Kuo*, MK08281401 (TENN-F-074753); Iowa, Linn County, Mount Vernon, Palisades-Kepler State Park, on karst topography in hardwood forest, 15 Jul. 2020, *S. DeLong-Duhon*, iNAT53190985 (TENN-F-076529); Missouri, Taney Co., Mark Twain National Forest, Ozark Mountains, Coy Bald Trail at Hercules Glen, on soil in campground along creek in under *Quercus*, *Carya*, *Juglans*, 4 Jul. 1999, *P.B. Matheny*, PBM1481 (WTU); New York, Menands, on clay soil, July, *C.H. Peck s.n.* (**isotype** of *I. unicolor*, WTU); Bronx Co., New York Botanical Garden, on soil in lawn under *Quercus*, *Fagus*, *Acer*, 20 Sep. 1987, *R.E. Halling*, REH5532 (WTU); New York City, in front of museum building, caespitose in grass under *Carya*, 25 Jul. 1916, *W.A. Murrill s.n.* (WTU 63030); Tompkins Co., near Glenwood (suburb of Ithaca), west of Cayuga Lake, solitary to subcaespitose on ground in woods, July, *B. Walker*, Atk24275 (**isotype** of *I. marmoripes*, WTU); North Carolina, Haywood Co., Great Smoky Mountains National Park, Baxter Creek Trail, 11 Sep. 2004, *P.B. Matheny*, PBM2645 (TENN-F-062476); *ibid.*, 7 Jul. 2015, *P.B. Matheny*, PBM3997 (TENN-F-70346); Macon Co., Highlands Biological Research Station, under *Pinus Quercus*, and *Rhododendron* on acid soil, 29 Jul. 2021, *C.R. Noffsinger*, PBM4604 (TENN-F-075771); Yancey Co., Burnsville, Carolina Hemlocks campground, in hemlock dominant forest under *Quecus*, *Tsuga*, *Rhododendron* on acid soil, 20 Aug. 2020, *P.B. Matheny*, PBM4452 (TENN-F-075323); Tennessee, Anderson Co., Norris Dam State Park, Clear Creek Trail, under *Quercus*, *Carpinus*, *Fagus*, *Carya*, 11 Oct. 2009, *P.B. Matheny*, PBM3331 (TENN-F-063892); Blount Co., Great Smoky Mountains National Park, Schoolhouse Gap Trail, 8 Jun. 2012, *C.C. Braaten*, CCB48 (TENN-F-067079); *ibid.*, 17 Jul. 2019, *R.A. Swenie & S.R. Warwick*, PBM4301 (TENN-F-074863); Cocke Co., Great Smoky Mountains National Park, Low Gap Trail, 10 Oct. 2010, *M.G. Wood*, MGW869 (TENN-F-065333); Cumberland Co., Interstate 40 rest area between exits 324-325, on ground under *Quercus*, 23 Jul. 2018, *P.B. Matheny*, PBM4167 (TENN-F-074483); Knox Co., west Knoxville, residential area, on soil in grass under planted *Quercus phellos*, 29 Jul. 2008, *P.B. Matheny*, PBM2974 (TENN-F-062732 – muscarine assay); Knox Co., University of Tennessee campus, the Hill, in lawn on soil under planted *Tilia americana*, 7 Aug. 2009, *P.B. Matheny*, PBM3322 (TENN-F-063887); Knox Co., Sharp's Ridge Memorial Park, on soil under hardwoods, 2 Aug. 2022, *R.A. Swenie*, RAS1007 (TENN-F-077502); Sevier Co., Great Smoky Mountains National Park, Alum Cave Bluffs Trail, 11 Aug. 2005, *E.B. Lickey* (TENN-F-061152); Virginia, Shenandoah National

Fig. 9. Microscopic features of *Mallocybe*. **A.** Basidiospores of *M. fibrillosa* (isotype). **B.** Cheilocystidia of *M. fibrillosa* (isotype). **C.** Basidiospores of *M. fibrillosa* (isotype of *Inocybe subdecurrens*). **D.** Basidiospores of *M. fulviceps* (isotype). **E.** Cheilocystidia of *M. fulviceps* (isotype). **F.** Cheilocystidia of *M. fulviceps* (isotype of *I. pertomentosa*). **G.** Basidiospores of *M. fulviceps* (isotype of *I. pertomentosa*). **H.** Basidiospores of *M. fulviceps* (isotype of *I. vialis*). **I.** Cheilocystidia of *M. fulviceps* (isotype of *I. vialis*). **J.** Basidiospores of *M. fulviumbonata* (holotype). **K.** Cheilocystidia of *M. fulvioumbonata* (holotype). **L.** Basidiospores of *M. latifolia* (PBM4537). **M.** Cheilocystidia of *M. latifolia* (PBM4537). Scale bars = 10 µm for spores; 25 µm for cystidia.

Park, north park entrance, Dickey Ridge Trail, 600 m elev., on clay soil in Oak-Hickory forest (*Quercus*, *Carya*, *Juglans*, *Liriodendron*, *Robinia*), 22 Jun. 2002, *P.B. Matheny & E.C. Durman*, PBM2320 (WTU).

Notes: *Mallocybe unicolor* is easy to recognize in the field due to the granulose-scaly pileus, the dark colored fibrillose scales on the stipe, the dull olivaceous to brownish lamellae, and habitat typically under oaks. The species is also characterized by the elongated cheilocystidia and oblong spores with mean Q-values ranging mostly between 1.90 and 2.25. *Mallocybe unicolor* is widespread in eastern North America and common in Oak-Hickory forests and urban habitats in lawns under planted *Quercus*, *Carya*, and *Tilia*, typically on karst topography. To a lesser extent it has been found in mixed mesic Hemlock

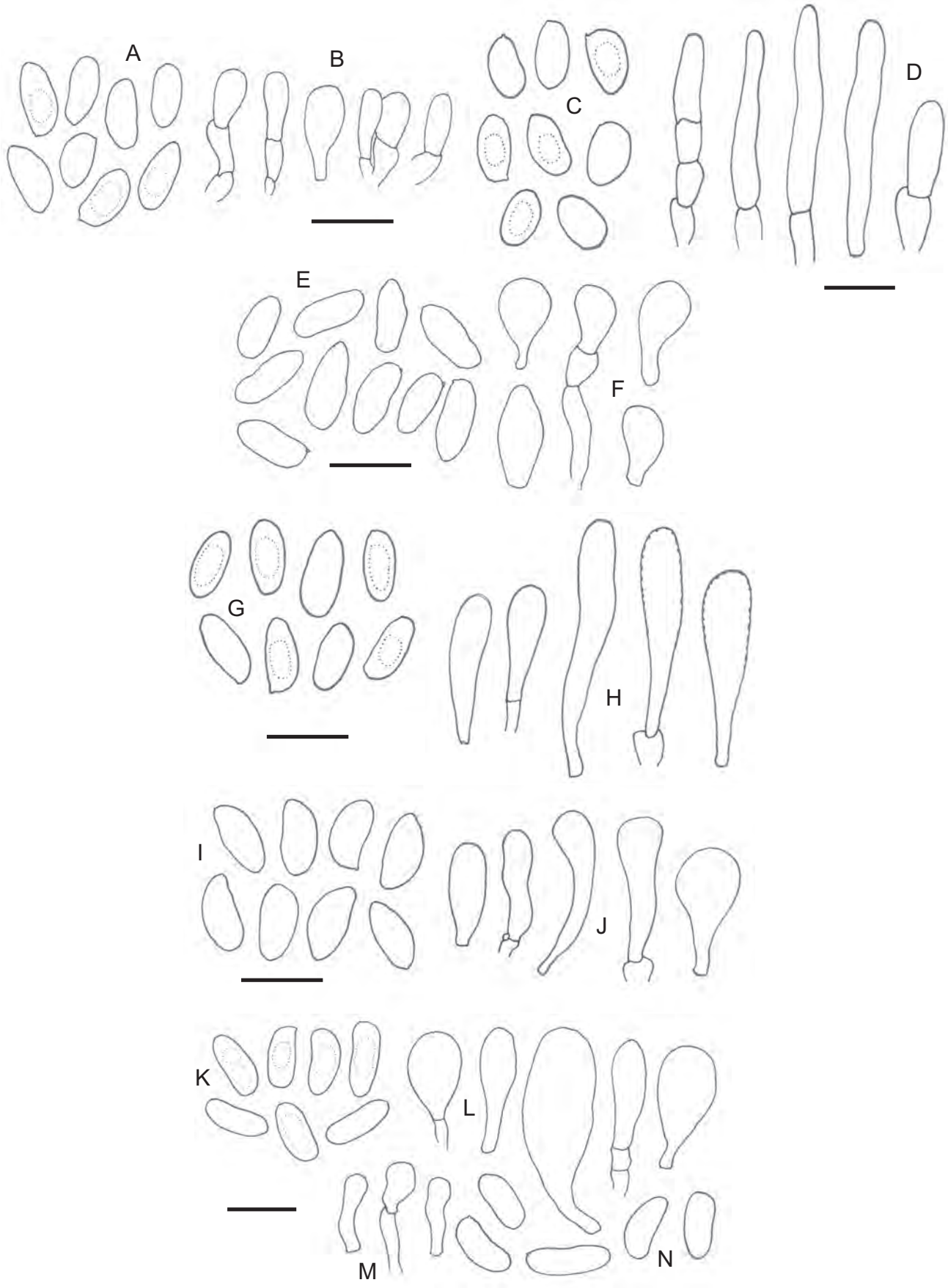

Fig. 10. Microscopic features of *Mallocybe*. **A.** Basidiospores of *M. leucothrix* (paratype – PBM4531). **B.** Cheilocystidia of *M. leucothrix* (paratype – PBM4531). **C.** Basidiospores of *M. luteobasis* (paratype – Sayers *s.n.*). **D.** Cheilocystidia of *M. luteobasis* (paratype – PBM4312). **E.** Basidiospores of *M. malenconii* (JV4470F). **F.** Cheilocystidia of *M. malenconii* (JV4470F). **G.** Basidiospores of *M. montana* (holotype). **H.** Cheilocystidia of *M. montana* (holotype). **I.** Basidiospores of *M. multispora* (isotype). **J.** Cheilocystidia of *M. multispora* (isotype). **K.** Basidiospores of *M. praevillosa* (FLAS-F-61523). **L.** Cheilocystidia of *M. praevillosa* (FLAS-F-61523). **M.** Caulocystidia of *M. praevillosa* (PBM4724). **N.** Basidiospores of *M. praevillosa* (holotype). Scale bars = 10 µm for spores; 25 µm for cystidia.

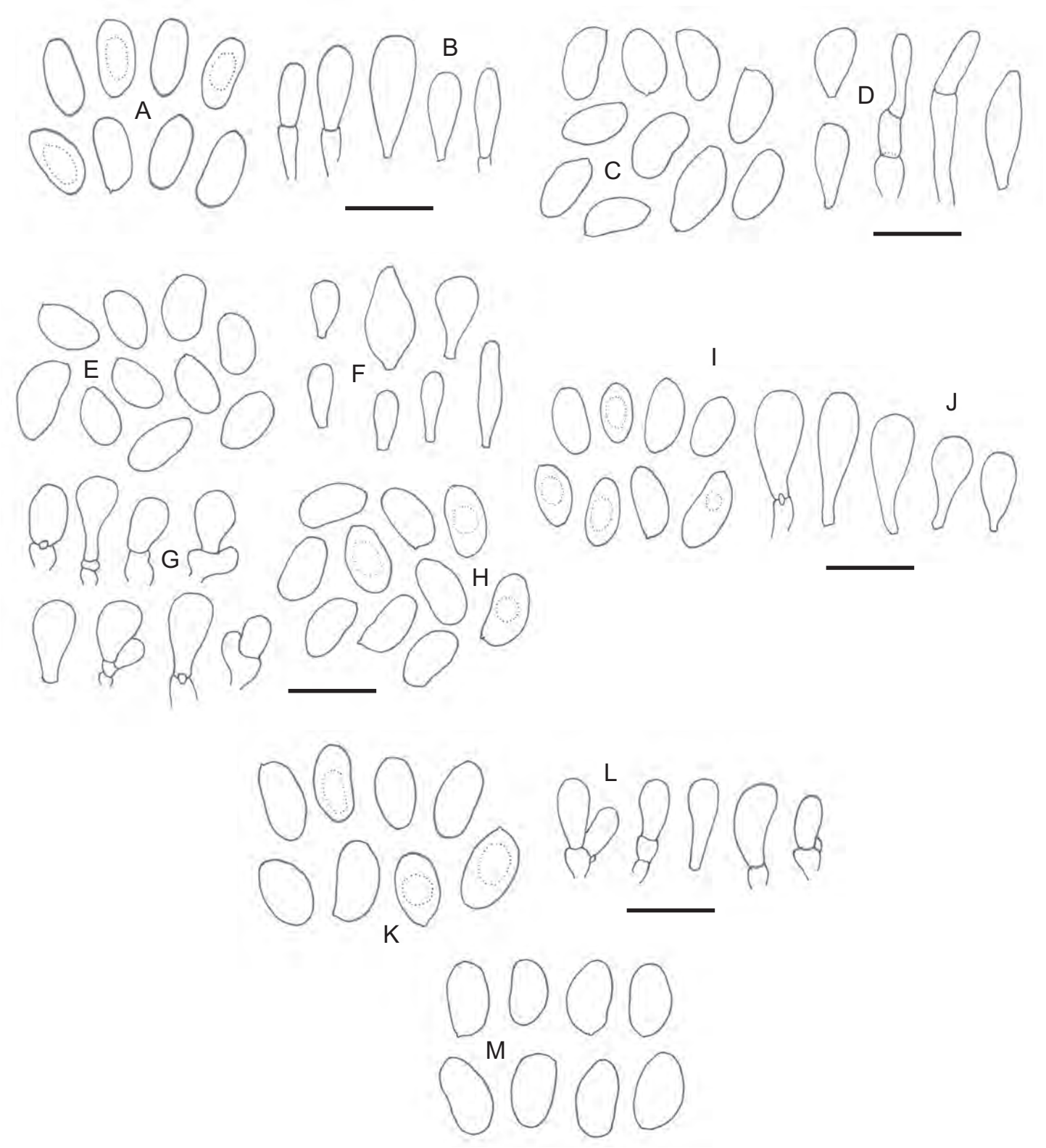

Fig. 11. Microscopic features of *Mallocybe*. **A.** Basidiospores of *Mallocybe* sp. 8 (PBM4749). **B.** Basidiospores of *Mallocybe* sp. (PBM4749). **C.** Basidiospores of *M. squamosodisca* (isotype). **D.** Cheilocystidia of *M. squamosodisca* (isotype). **E.** Basidiospores of *M. subtomentosa* (isotype). **F.** Cheilocystidia of *M. subtomentosa* (isotype). **G.** Cheilocystidia of *M. subtomentosa* (SAT-99-233-01. **H.** Basidiospores of *M. subtomentosa* (SAT-99-233-01). **I.** Basidiospores of *M. tomentella* (holotype). **J.** Cheilocystidia of *M. tomentella* (holotype). **K.** Basidiospores of *M. tomentosula* (RAS123). **L.** Cheilocystidia of *M. tomentosula* (RAS123). **M.** Basidiospores of *M. tomentosula* (holotype of *Inocybe tomentosa* - 00775651). Scale bars = 10 µm for spores; 25 µm for cystidia.

(*Tsuga*) forests including *Quercus* and *Betula* on acidic soils characterized by presence of *Rhododendron*. It is unknown at this time if these ecological differences correspond to divergent populations.

Because the species is so common throughout eastern North America, it is not surprising it has been described as new independently by several early 20th century taxonomists. Under incandescent light the scales of *M. unicolor* could be interpreted

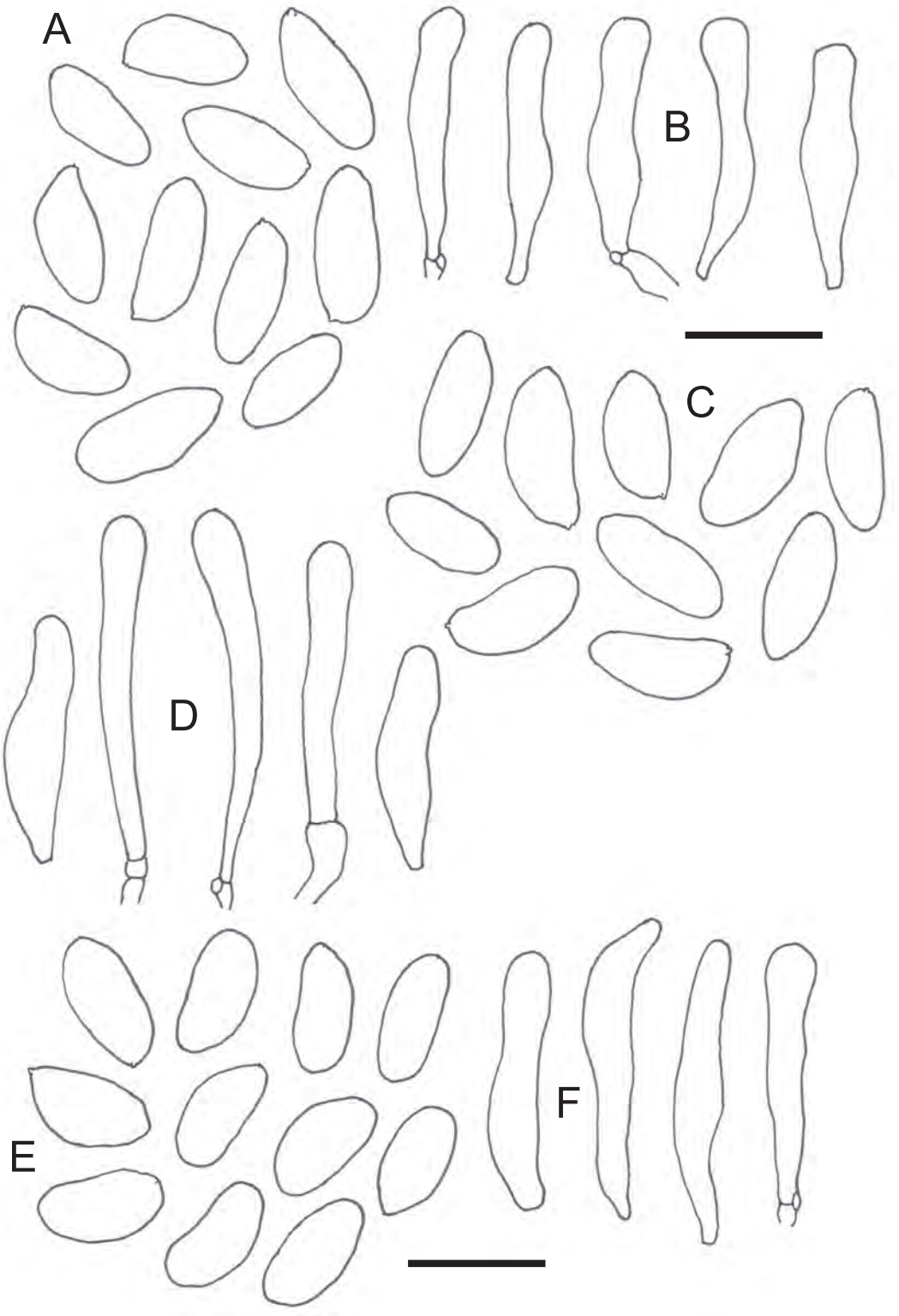

Fig. 12. Microscopic features of *Mallocybe unicolor*. **A.** Basidiospores (isotype). **B.** Cheilocystidia (isotype). **C.** Basidiospores (isotype of *Inocybe marmoripes*). **D.** Cheilocystidia (isotype of *I. marmoripes*). **E.** Basidiospores (isotype of *I. lorillardiana*). **F.** Cheilocystidia (isotype of *I. lorillardiana*). Scale bars = 10 µm for spores; 25 µm for cystidia.

as "ferrugineous" as described by Murrill for *Inocybe lorillardiana* based on examination of authentic material gathered by Murrill from the type locality. Bessette & Fatto (1998) presented a thorough study of the holotype of *I. marmoripes* consistent with our evaluation of the isotype at WTU. The basidiospore dimensions of *I. marmoripes* fall within range of the collections studied here, although the mean Q value (2.25) is longer than those of some other collections (1.86–1.89), but similar to the Virginia material (2.12) and the type of *M. unicolor* (2.09). At present, DNA sequences from numerous samples of *M. unicolor* form a cohesive strongly supported monophyletic group (Fig. 2C), but some separation was noted for two samples from New York and Missouri (REH5532 and PBM1481) characterized by the shorter Q values (1.86–1.89). Murrill's collection of *I. lorillardiana*

also shares the shorter spores (mean Q 1.86). However, based on current sampling, we regard these differences as indicative of population-level variability based on current sampling. Additional collections, backed by further genetic data, are needed to determine if there is any taxonomic significance to the shorter-spored variants consistent with *I. lorillardiana*, and whether these might be correlated with edaphic factors.

Kauffman (1924) reported *I. marmoripes* from Maryland and Washington, however, his description of the cheilocystidia as clavate is not in concordance with the type. Kauffman's concept of *I. marmoripes* was a broad one including *M. malenconii* and the undescribed *Mallocybe* sp. 2 from Oregon and British Columbia (the latter reported as *M. malenconii* var. *megalospora* by its GenBank authors). Stuntz (1940) applied the name *I. marmoripes* to what we interpret as *M. malenconii*, which can be distinguished from *M. unicolor* by the smaller basidiomes (pileus up to 20 mm wide), short clavate cheilocystidia, and slightly narrower and somewhat angular basidiospores (9–12 × 4–5 µm) similar to those of *Inocybe lacera* in appearance.

The name *Inocybe caesariata* (Fr.) P. Karst. (*non* Kauffman) has been widely applied to *M. unicolor* by Hesler (1936), Lincoff (1981), Phillips (2010), and Roberts & Evans (2011). Use of the name *I. caesariata* by Kauffman (1924) in our opinion corresponds to *M. fibrillosa* Peck.

One MyCoPortal record (CMMF002038) from Quebec is misidentified as *I. unicolor*. The photograph of the specimens resembles those of *M. subtomentosa*.

A liquid chromatography-tandem mass spectrometry assay by Kosentka *et al.* (2013) did not detect muscarine in sample TENN-F-062732 (PBM2974).

Extralimital taxa

Mallocybe callichroa (E. Horak) Matheny, ***comb. nov***. MycoBank MB 847422.
Basionym: *Inocybe callichroa* E. Horak, *Westerdijk Biodiversity Series* **16**: 76. 2018.

Notes: *Inocybe callichroa* (Horak 2018) bears many features indicative of *Mallocybe*: the overall ocher-brown coloration of the basidiomes, the slenderly clavate basidia, the smooth slenderly phaseoliform basidiospores with an average Q value at or near 2.00, the absence of pleurocystidia, the presence of cheilocystidia and clamp connections, and a cutis to trichoderm type of pileipellis. Furthermore, the pileus was described as velutinous to minutely squamulose and the odor as indistinct. All of these features are consistent with *Mallocybe*. Horak, however, did note that KOH failed to darken the pileus surface, and no explicit statement of the presence of necrobasidia was made. Despite this, and given the overall combination of features above, placement in *Mallocybe* seems most warranted, hence the new combination above. The species is a *Nothofagus* associate, and the first species of *Mallocybe* described from New Zealand.

Key to Eastern North American species of *Mallocybe*

1a. Pileus granulose-scaly and stipe with bands of dark colored fibrillose-scales against a lighter background ..... ***M. unicolor***
1b. Pileus and stipe not as above **2**

2a. Basidiospores oblong, mean Q > 2.0 ..... **3**
2b. Basidiospores not oblong, mean Q < 2.0 ..... **6**

3a. Basidiomes robust (mature stipe 8–10 mm wide), flesh tough, lamellae brittle, pileus surface not darkening with application of KOH solution, basidiospores pale brown in KOH ..... ***M. praevillosa***
3b. Basidiomes not robust (mature stipe < 8 mm wide), flesh soft and lamellae soft, pileus surface darkening with KOH, basidiospores yellowish brown in KOH **4**

4a. Pileus convex to plano-convex at first and not umbonate; cheilocystidia short-clavate, pyriform to short-cylindric (< 30 µm long); on acidic soil in northern forests ..... ***M. malenconii***
4b. Pileus convex to broadly convex and not umbonate; cheilocystidia elongated (> 30 µm long); on acidic soil in southern Appalachian montane forests ..... ***M. montana***
4c. Pileus conical at first and umbonate, cheilocystidia differently shaped than above (> 30 µm long); on calcareous soil, northern Florida in oak-pine forests **5**

5a. Cheilocystida subcylindric or slenderly clavate with obtuse to subcapitate apices ..... ***M. multispora***
5b. Cheilocystidia clavate (not slenderly so), utriform, saccate, and/or obovate ..... ***M. fulviceps***

6a. Stipe base yellow and/or stipe context with pale yellow tone **7**
6b. Stipe base white and stipe context without a yellow tone **8**

7a. Basidiospores 6–6.5 µm wide, on karst topography under oak-hickory ..... ***M. luteobasis***
7b. Basidiospores 5–5.5 µm wide, on acid soils under oaks, pine, ericaceous trees and/or shrubs, or other conifers (*Pseudotsuga*) ..... ***M. squamosodisca***

8a. Stipe with a distinct cortinate ring-zone **9**
8b. Stipe without a distinct cortinate ring-zone **10**

9a. Pileus brown to dark brown, not bicolorous, in areas with limestone under *Quercus* or *Pinus* ..... ***M. tomentosula***
9b. Pileus two-toned or bicolorous with a brown disc and whitish margin due to heavy accumulation of superficial fibrils, on acidic soils under *Picea* or in mixed forests including *Picea* ..... ***M. tomentella***

10a. Pileus subsmooth in age and often without an umbo, on acidic soils **11**
10b. Pileus tomentose-fibrillose to squamulose, at times umbonate, soil type various **12**

11a. Under *Quercus* and/or *Pinus* ..... ***M. subtomentosa***
11b. Under *Picea* ..... ***Mallocybe* sp. PBM4749**

12a. On acidic soils in northern and alpine regions, odor often sweet ..... ***M. fibrillosa***
12b. On calcareous soils in various regions (Maine, Florida, Arizona) but not alpine; odor not remarkable **13**

13a. Pileus not umbonate, with a distinct hairy white vesture; basidiospores 8–10 × 4.5–5.5 µm, yellowish brown in KOH; cheilocystidia < 12 µm wide ..... ***M. leucothrix***
13b. Pileus at most weakly umbonate, with a distinct hairy white vesture; basidiospores 9–11 × 5.5–6.5 µm, yellowish brown in KOH; cheilocysatidia > 12 µm wide ..... ***M. latifolia***
13c. Pileus with a small but prominent umbo, without a distinct hairy white vesture; basidiospores 8–9 × 4.5–5.5 µm, very pale brown to light yellow in KOH; cheilocystidia > 12 µm wide ..... ***M. fulvoumbonata***

Unclarified species of *Mallocybe* from North America, Asia, and Australasia

Nine insufficiently known species, seven from western North America, one from eastern North America, and one from New Zealand, are recognized from one or few collections or are known only from environmental samples. These species will be documented taxonomically elsewhere pending evaluation of additional data.

Mallocybe sp. 1 was recovered from three environmental root system samples of *Dryas integrifolia* in the Alaskan arctic by Timling *et al.* (2012); the species is very closely related to *M. delecta* (syn. *M. crassivelata*), a European species found in hardwood and conifer forests (Crous *et al.* 2020). We are unaware of any collections associated with *Mallocybe* sp. 1 at this point. *Inocybe marmoripes sensu* D.E. Stuntz (Stuntz 1940) undoubtedly represents *Mallocybe* sp. 2, which we have documented from Oregon and confirmed from British Columbia (see discussion above under *M. unicolor*). Sufficient collections are on-hand eventually to describe this species. *Mallocybe* sp. 3 (PBM1615) is known from a single collection under montane conifers in Washington state and is the sister species to the northern European species *M. arthrocystis* (FIG. 2B) with strong support. *Mallocybe* sp. 4 (PBM2290) is yet another likely undescribed species from Washington state that is also in the Arthrocystis clade, but it is known only from one collection. *Mallocybe* sp. 5 (JFA13285, PBM1922, SDA470) is likewise an independent lineage collected under montane conifers from Washington state and is sister to *M. fuscomarginata* from Europe; we intend to present a formal description of this species at a later date. *Mallocybe* sp. 6 (ADP060305, PBM1444) is yet another montane conifer-associate found in Washington state; it is strongly supported in a sister position to all other species in the Fuscomarginata clade and will be formally described in forthcoming works. *Mallocybe* sp. 7 represents an unclarified species with an omphalinoid habit from New Zealand found in likely association with *Nothofagus.* It does not appear to match any of the previously described species attributed to *Mallocybe* from this region (Horak 2018); it is known from a single collection at this time. *Mallocybe* sp. 8 is represented by one known American collection studied by us from West Virginia and several samples from China and Quebec (the latter communicated by J. Landry); this species is probably undescribed. *Mallocybe* sp. 9 is known from several samples from the Pacific Northwest to which the name *Inocybe terrigena* has been misapplied; this entity forms a paraphyletic group in our analyses but deserves further scrutiny. Lastly, the status of some collections documented from Australia by Matheny & Bougher (2017) related to *M. isabellina*, *M. subflavospora*, and *M. pyrrhopoda* await further revision.

Excluded Eastern North American species attributed to *Mallocybe*

Inocybe angustispora Bessette & Fatto, *Mycotaxon* **66**: 123. 1998.
Synonym: *Inocybe taedophilia* Murrill, *Proc. Florida Acad. Sci*. **7**: 122. 1944.

Both *I. angustispora* and *I. taedophila* are later synonyms of *Cortinarius aureifolius* Peck (Matheny 2003, Matheny & Ammirati 2003). Gene sequences of 28S, *rpb1*, and *rpb2* have been produced from the holotype of *I. angustispora*.

Inocybe ferruginosa A.H. Sm., *Pap. Mich. Acad. Sci*. **24**: 93. 1939.

Ammirati (1972) synonymized *I. ferruginosa* and *Cortinarius uliginosus* var. *nauseosus* with *Cortinarius uliginosus*. However, Niskanen (2014) combined *I. ferruginosa* in *Cortinarius*. An ITS sequence has been produced from the holotype, which supports assignment of the species in *Cortinarius*.

Inocybe weberi Murrill, *Proc. Florida Acad. Sci*. **7**: 123. 1944.

The punctate elliptic to subamygdaliform basidiospores (8–9 × 5–5.5 µm), in combination with the yellowish lamellae and presence of anthraquinone interhyphal pigment deposits, suggest the type is synonymous with *Cortinarius croceus* (Matheny 2003).

DISCUSSION

This study is the first systematic revision of *Mallocybe* as it occurs in eastern North America. We used four different gene regions for phylogenetic analyses and considered taxon sampling across the globe. Our intent was to revise first those species that occur in eastern North America and generate a useful and predictive infrageneric systematic arrangement. To facilitate stable application of names, we have produced sequenced reference specimens for seven species described in historical works by Peck, Ellis & Everhart, and Murrill. Some authors have had success with molecular annotation of types and other historical collections of *Inocybe* (Cripps *et al.* 2010, Matheny & Swenie 2018, Matheny & Kudzma 2019). However, the process to do so must take steps to avoid contamination from non-target fungi (*e.g.*, *Aspergillus*) and laboratory aerosols and equipment. These problems can be mitigated with careful laboratory procedures and taxon-specific primers. Even with these approaches, the success rate is still low for collections made by Murrill from northern Florida in the 1930s and 1940s (Looney 2014). This is probably due to poor preservation technique by the original collector, the age of the specimens, or degradation of DNA over time. Moreover, some of Murrill's types are scanty or composed of single basidiomes. In addition, recent studies by Eberhardt *et al*. (2022, 2023) were only able to produce partial molecular annotations for one of six species of *Inocybaceae* described by Peck more than 100 years ago, and only a few *Inocybaceae* described by Murrill could be partially annotated. While epitypification is a useful tool to ultimately clarify and stabilize species recognition (Hyde & Zhang 2008), we avoided this procedure because interpretation of North American types attributable to *Mallocybe* could be accomplished based on morphology and ecology, most often in comparison to modern reference materials collected by us at or near type localities. As a consequence, several unused names attributable to *Mallocybe* have been resurrected in this study based on our interpretations of the types (*M. fibrillosa*, *M. subtomentosa*, *M. squamosodisca*, and *M. unicolor* of Peck; *M. fulvoumbonata*, *M. fulviceps,* and *M. multispora* of Murrill; and *M. tomentosula*, a replacement name based on the type of *Inocybe tomentosa* Ellis & Everh.). In addition, we were able to resuscitate the Murrill name *Lepista praevillosa* and recombine it in *Mallocybe*, which was discovered as the sister species to all other *Mallocybe*. Despite resurrecting several old names, we still detected undescribed lineages to which no prior names could be applied and described four of those as new – *M. leucothrix*, *M. luteobasis*, *M. montana*, and *M. tomentella*. We are also aware of additional species from eastern North America (*e.g.*, *Mallocybe* sp. 8) that remain unclarified or possibly undescribed but are not yet sufficiently documented.

Our study also recovered three strongly supported clades within *Mallocybe* that could correspond to subgenera (clades Mallocybe, Nothosperma, and Unicolores) but await formal description pending efforts at revision of additional taxa. Clade Mallocybe contains the bulk of known *Mallocybe* species, and these primarily originate from temperate regions of the northern hemisphere and are often characterized by presence of short cheilocystidia. Clade Nothosperma contains species known from Australasia (Australia, New Zealand, New Guinea) and Malaysia; most of these species too are primarily characterized by the presence of short cheilocystidia. Clade Unicolores contains six species, three of which are endemic to eastern North America and characterized by spores with mean Q values near or greater than 2.00 and often elongated cheilocystidia (> 50 µm in length) (Hu *et al.* 2023).

One challenge we encountered during this work was the phylogenetic placement of the recently described western and southern African tropical species *M. africana* (Aignon *et al.* 2021). We have been aware of this species for some time (see Matheny *et al.* 2009 where it was treated as "*I. microdulcamara nom. prov.*") based on nuclear ribosomal DNA sequences only and found the species to cluster with another Old World tropical lineage from south Asia, *M. errata*, with strong support (Matheny *et al.* 2009). Aignon *et al.* (2021) were able to generate *rpb2* data from recent materials, but our phylogenetic analysis of RNA polymerase II data only (not shown) placed *M. africana* in a sister position to all other species of *Mallocybe*. Unfortunately, gene sampling across *Mallocybe* is uneven (*e.g.*, *rpb2* data could not be generated for *M. errata*, and we could not independently obtain new *rpb2* and *rpb1* sequences from *M. africana* either), so we cannot exclude the possibility that uneven gene and taxon sampling could impact the placement of this unusual species, or that existing data provide conflicting phylogenetic signal. Thus, we treat *M. africana* as *incertae sedis* within *Mallocybe*. Additional specimens and loci (*e.g.*, *rpb1*) of *M. africana* will need to be produced and re-analyzed, and data produced from *M. althoffiae* by the senior author but analyzed by Aignon *et al.* (2021) should be discarded as artifacts (Matheny *et al.* 2020).

Our rDNA phylogeny (Supplementary Fig. S3) was ambiguous about the placement of *Mallocybe praevillosa*, where it clustered with weak support among outgroup taxa. However, individual analyses of *rpb1* and *rpb2* (Supplementary Figs S1, S2) and analyses of the combined data (Figs 1, 2), strongly supported *M. praevillosa* as sister to all other *Mallocybe* in this work. *Mallocybe praevillosa* possesses some character states unlike other *Mallocybe* in that (i) the pileus surface did not darken with KOH, (ii) the basidia were not necropigmented, and (iii) the flesh of the basidiomes was tough and the lamellae brittle. In addition to these features, the basidiospores were found to be noticeably pale, but this trait has been noted in other species (*e.g.*, *M. subflavospora*, *M. fulvoumbonata*). Furthermore, *M. praevillosa* was the only eastern North American sample for which we detected muscarine. One might consider accommodation of *M. praevillosa* in a separate (new) genus apart from *Mallocybe* due to the unique combination of traits highlighted above, but we decided against this decision owing to taxonomic redundancy (viz, establishing a monotypic genus), the few specimens studied, and the fact that the species forms a strongly supported clade with the rest of *Mallocybe*.

This work also recapitulates and highlights some significant evolutionary and ecological findings. Hu *et al.* (2023) demonstrated that the presence of elongated cheilocystidia was a shared ancestral state in *Mallocybe*. Our study reinforces this result even with the discoveries of *M. montana* and *M. praevillosa*. The shift to short-clavate or short-pyriform cystidia may have occurred in the most recent common ancestor of clades Mallocybe and Nothosperma or perhaps independently in these groups. We also find it notable that species of the Montana and Praevillosa lineages, as well as those in clade Unicolores, exhibit relative narrow ranges of endemism, and all either originate in eastern North America or east Asia. The Australasian species in clade Nothosperma likewise exhibit narrow-range endemism either restricted to Australia or New Zealand. By contrast, many species in the core Mallocybe clade

exhibit broad intercontinental geographic distributions as noted previously by Cripps *et al.* (2010).

Our work also provides a multigene phylogenetic framework to continue studies and revision of additional taxa from other parts of the world. For example, we detected seven species-level lineages that occur in western North American conifer forests that are likely undescribed. In addition, further attention is necessary to clarify some Australasian species of *Mallocybe* (Matheny & Bougher 2017).

Detection of the secondary metabolite muscarine varies within *Mallocybe.* Here we report the non-detection of muscarine in nine of the 11 species sampled. Muscarine was detected at relatively high amounts in two distantly related species (*M. sabulosa* from Australia and *M. praevillosa* from Florida). Kosentka *et al.* (2013) and Stijve *et al.* (1985) also reported the lack of detectable amounts of muscarine from *M. unicolor* and *M. terrigena*, respectively. The evolutionary and ecological significance of the absence and sporadic presence of muscarine across the genus are poorly understood at this time. Future efforts are needed to assess the relative concentrations of the toxin among multiple samples within species and confirm the taxonomy and earlier reports of muscarine-containing *Inocybe* attributable to *Mallocybe* today (Stijve *et al.* 1985, Gurevich & Nezdoiminogo 1992), including species *M. agardhii*, *I. caesariata*, *I. dulcamara*, and *M. malenconii* (Kosentka *et al*. 2013).

ACKNOWLEDGMENTS

This study was supported by grants from the Daniel E. Stuntz Memorial Foundation, the Tennessee Herbarium Hesler Endowment Fund, and the National Science Foundation (DEB-2030779). The authors thank Shannon Adams, Joe Ammirati, Christine Braaten, Cathy Cripps, Sarah DeLong-Duhon, Django Grootmyers, Alicia Hobbs, Sigrid Jakob, Jacob Kalichman, Hailee Korotkin, Jacques Landry, Danny Miller, Dick Morrison, and Aaron Wolfenbarger for their laboratory assistance or sharing materials for this study. Marcos Caiafa, Rosanne Healy, Susan Hopkins, and Caro Willis kindly assisted with field work. We also thank Jerry Cooper and Noah Siegel for sharing specimen-voucher information and ITS data for New Zealand material, and acknowledge the contribution of ITS and morphological data kindly shared by Christiane Baschien, Ditte Bandini, and Ursula Eberhardt from Erhard Ludwig's herbarium materials. The authors are also indebted to Ellen Larsson, who shared ITS data from type collections made by Petter Karsten. We appreciate the support from herbarium directors and staff at FLAS, H, NY, TENN, and WTU and the provision of loans for this study. We also acknowledge support from Katarina Jones and Hector Castro for their assistance at the Biological Small Molecular Mass Spectometry Core at the University of Tennessee (RRID: SCR_021368). Comments from two reviews improved an earlier draft version.

Conflict of interest: The authors declare that there is no conflict of interest.

REFERENCES

Agrawal S, Sahil K, Raghav S, *et al*. (2019). El-MAVEN: A fast, robust, and user-friendly mass spectrometry data processing engine for metabolomics. *Methods in Molecular Biology (Clifton, N.J.)* **1978**: 301–321.

Aignon HL, Naseer AJ, Matheny PB, *et al*. (2021). *Mallocybe africana* (*Inocybacae*, *Fungi*), the first species of *Mallocybe* described from Africa. *Phytotaxa* **478**: 49–60.

Alessio CL, Rebaudengo E (1980). *Inocybe*. – *Iconographica Mycologica* Vol. 29, Suppl. 3. Museo Tridentino di Science Naturalis, Trento, Italy.

Alvarado P, Manjón JL, Matheny PB, *et al*. (2010). *Tubariomyces*, a new genus of *Inocybaceae* from the Mediterranean region. *Mycologia* **12**: 1389–1397.

Ammirati JF (1972). *The section Dermocybe of Cortinarius in North America*. PhD dissertation. University of Michigan, Ann Arbor, USA.

Ariyawansa H, Hyde K, Jayasiri S, *et al*. (2015). Fungal diversity notes 111–252—taxonomic and phylogenetic contributions to fungal taxa. *Fungal Diversity* **75**: 27–274.

Bandini D, Oertel B, Ploch S, *et al.* (2018). Revision of some central European species of *Inocybe* (Fr.: Fr.) Fr. subgenus *Inocybe*, with the description of five new species. *Mycological Progress* **18**: 247–294.

Bessette AE, Fatto RM (1998). Two narrow-spored Inocybes. *Mycotaxon* **66**: 121–126.

Bessette AR, Bessette AE, Neill WJ (2001). *Mushrooms of the Cape Cod and the National Seashore*. Syracuse University Press, Syracuse, New York, USA.

Bon M (1997). Clé monographique du genre *Inocybe* (Fr.) Fr. *Documents Mycologiques* **27**(105): 1–51.

Chambers MC, Maclean B, Burke R, *et al.* (2012). A cross-platform toolkit for mass spectrometry and proteomics. *Nature Biotechnology* **30**: 918–920.

Chernomor O, von Haesler A, Minh BQ (2016). Terrace aware data structure for phylogenomic inference from supermatrics. *Systematic Biology* **65**: 997–1008.

Cho S-E, Kway Y-N, Han S-K, Kim CS (2021). Seven newly recorded macrofungi of *Inocybaceae* (*Agaricales, Basidiomycota*) in Korea. *The Korean Journal of Mycology* **49**: 139–153.

Cripps CL (1997). The genus *Inocybe* in Montana aspen stands. *Mycologia* **89**: 670–688.

Cripps CL, Larsson E, Horak E (2010). Subgenus *Mallocybe* (*Inocybe*) in the Rocky Mountain alpine zone with molecular reference to European arctic-alpine material. *North American Fungi* **5**: 97–126.

Crous PW, Wingfield MJ, Chooi Y-H, *et al*. (2020). Fungal Planet description sheets: 1042–1111. *Persoonia* **44**: 301–459.

Cubeta MA, Echandi E, Abernethy T, *et al*. (1991). Characterization of anastomosis groups of binucleate *Rhizoctonia* species using restriction analysis of an amplified ribosomal RNA gene. *Molecular Plant Pathology* **81**: 1395–1400.

Daskalopoulos V, Polemis E, Fryssouli V, *et al*. (2021). *Mallocybe heimii* ectomycorrhizae with *Cistus criticus* and *Pinus halepensis* in Mediterranean littoral sand dunes – assessment of phylogenetic relationships to *M. arenaria* and *M. agardhii*. *Mycorrhiza* **31**: 497–510.

Eberhardt U, Schütz, Bartlett P, *et al.* (2022). 96 North American taxa sorted – Peck's *Hebeloma* revisited. *Mycologia* **114**: 337–387.

Eberhardt U, Grilli E, Schütz N, *et al.* (2023). Old but not obsolete: A new life for some of Murrill's (*Hebeloma*) names. *Mycologia* **115**: 375–426.

Favre J (1955). Les champignons supérieurs de la zone alpine du Parc National Suisse. *Ergebnisse der Wissenschaftlichen Untersuchungen des Schweizerrischen Nationalparks* **5**: 1–212.

Fries E (1828). *Elenchus fungorum*. Vols. I & II. Greifswald, Germany.

Frøslev TG, Matheny PB, Hibbett DS (2005). Lower level relationships in the mushroom genus *Cortinarius* (*Basidiomycota, Agaricales*): a comparison of *RPB1*, *RPB2*, and ITS phylogenies. *Molecular Phylogenetics and Evolution* **37**: 602–618.

Gurevich LS, Nezdoiminogo EL (1992). Psilocybin and muscarine as possible chemotaxonomic markers for the genus *Inocybe* (Fr.) Fr. *Mycologija i Phytopathologija* **262**: 88–97.

Heim R (1931). *Le genre Inocybe, Encyclopédie Mycologique* I. Paul Lechevalier & Fils, Paris, France.

Hesler LR (1936). Notes on southern Appalachian fungi. *Journal of the Tennessee Academy of Sciences* **11**: 107–122.

Hoang DT, Chernomor O, von Haeseler A, Minh BQ, Vinh LS (2018). UFBoot2: Improving the ultrafast bootstrap approximation. *Molecular Biology and Evolution* **35**: 518–522.

Horak E (1980). *Inocybe* (*Agaricales*) in Indomalaya and Australasia. *Persoonia* **11**: 1–37.

Horak E (2018). *Fungi of New Zealand / Ngā Hekaheka o Aotearoa*. Vol. 6. *Agaricales* (*Basidiomycota*) of New Zealand. 2. Brown spored genera *p.p. Crepidotus*, *Flammulaster*, *Inocybe*, *Phaeocollybia*, *Phaeomarasmius*, *Pleuroflammula*, *Pyrrhoglossum*, *Simocybe*, *Tubaria* and *Tympanella*. Westerdijk Biodiversity Series. 16. Westerdijk Fungal Biodiversity Institute, Utrecht, The Netherlands.

Horak E, Matheny PB, Desjardin DE, *et al*. (2015). The genus *Inocybe* (*Inocybaceae, Agaricales, Basidiomycota*) in Thailand and Malaysia. *Phytotaxa* **230**: 201–238.

Hu J-H, Yu W-J, Deng L-S, *et al.* (2023). The detection of major clades and new species of *Mallocybe* (*Inocybaceae, Agaricales*) from China with elongate cheilocystidia. *Mycological Progress* **22**: 15.

Hyde KD, Zhang Y (2008). Epitypification: should we epitypify? *Journal of Zhejiang University Science B* **9**: 842–846.

Jacobsson S, Larsson E (2012). *Inocybe* (Fr.) Fr. In: *Funga Nordica: Agaricoid, boletoid, clavarioid, cyphelloid and gastroid genera*. Nordsvamp, Copenhagen, Denmark: 981–1021.

Judge BS, Ammirati JF, Lincoff GH, *et al*. (2010). Ingestion of a newly described North American mushroom species from Michigan resulting in chronic renal failure: *Cortinarius orellanosus*. *Clinical Toxicology* **48**: 545–549.

Kauffman CH (1924). *Inocybe*. *North American Flora* **10**: 227–260.

Kobayashi T (2002). The taxonomic studies of the genus *Inocybe*. *Nova Hedwigia* **124**: 1–146.

Kornerup A, Wanscher JK (1967). *Methuen Handbook of Colour*. 2nd edn. Methuen & Co. Ltd., London, U.K.

Kosentka P, Sprague SL, Ryberg M, *et al*. (2013). Evolution of the toxins muscarine and psilocybin in a family of mushroom-forming fungi. *PLoS ONE* **8**(5): e64646.

Kühner R (1988). Diagnoses de quelques nouveaux Inocybes récoltés en zone alpine de la Vanoise (Alpes françaises). *Documents Mycologiques* **19**(74): 1–27.

Kühner R, Romagnesi H. (1953). *Flore analytique des champignons supérieurs*. Masson et Cie, Paris, France.

Kuyper TW (1986). A revision of the genus *Inocybe* in Europe. I. Subgenus *Inosperma* and the smooth-spored species of subgenus *Inocybe*. *Persoonia* **3**(Suppl.): 1–247.

Larkin MA, Blackshields G, Brown NP, *et al*. (2007). Clustal W and Clust X version 2.0 *Bioinformatics* **23**: 2947–2948.

Larson A (2014). AliView: a fast and lightweight alignment viewer and editor for large data sets. *Bioinformatics* **30**: 3276–3278.

Larsson E, Ryberg M, Moreau P-A, *et al*. (2009). Taxonomy and evolutionary relationships within species of section *Rimosae* (*Inocybe*) based on ITS, LSU and mtSSU sequence data. *Persoonia* **23**: 86–98.

Lincoff G (1981). *National Audubon Society field guide to North American mushrooms*. Alfred A. Knopf, New York, USA.

Looney B (2014). Molecular annotation of type specimens of *Russula* species described by W.A. Murrill from the southeast United States. *Mycotaxon* **129**: 255–268.

Ludwig E (2017). *Pilzkompendium*. Bd. 4. Fungicon-Verlag, Berlin, Germany.

Malloch D (1973). *Inocybe dulcamara*. Fungi Canadenses No. 3, Agriculture Canada, Ottawa, Canada.

Mao N, Xu Y-Y, Zhao T-Y, *et al*. (2022). New species of *Mallocybe* and *Pseudosperma* from North China. *Journal of Fungi* **8**: 256.

Matheny PB (2003). *Molecular systematics and taxonomic contributions towards the Inocbybaceae*. PhD dissertation. Department of Botany, University of Washington, USA.

Matheny PB (2005). Improving phylogenetic inference of mushrooms using *RPB1* and *RPB2* sequences (*Inocybe*, *Agaricales*). *Molecular Phylogenetics and Evolution* **35**: 1–20.

Matheny PB, Aime MC, Bougher NL, *et al.* (2009). Out of the Palaeotropics? Historical biogeography and diversification of the cosmopolitan ectomycorrhizal mushroom family Inocybaceae. *Journal of Biogeography* **36**: 577–592.

Matheny PB, Ammirati JF (2003). *Inocybe angustispora*, *I. taedophila*, and *Cortinarius aureifolius*: an unusual inocyboid *Cortinarius*. *Mycotaxon* **88**: 401–407.

Matheny PB, Bougher NL (2017). *Fungi of Australia: Inocybaceae*. Australia Biological Resources Study, Canberra. CSIRO Publishing, Melbourne, Australia.

Matheny PB, Hobbs AM, Esteve-Raventós F (2020). Genera of *Inocybaceae*: New skin for the old ceremony. *Mycologia* **112**: 83–120.

Matheny PB, Kudzma LV (2019). New species of *Inocybe* (*Inocybaceae*) from eastern North America. *Journal of the Torrey Botanical Society* **146**: 213–235.

Matheny PB, Liu YJ, Ammirati JF, *et al*. (2002). Using RPB1 sequences to improve phylogenetic inference among mushrooms (*Inocybe*, *Agaricales*). *American Journal of Botany* **89**: 688–698.

Matheny PB, Norvell LL, Giles EC (2013). A common new species of *Inocybe* in the Pacific Northwest with a diagnostic PDAB reaction. *Mycologia* **105**: 436–446.

Matheny PB, Pradeep CK, Vrinda KB, *et al.* (2012). *Auritella foveata*, a new species of *Inocybaceae* (*Agaricales*) from tropical India. *Kew Bulletin* **67**: 119–125.

Matheny PB, Swenie RA (2018). The *Inocybe geophylla* group in North America: a revision of the lilac species surrounding *I. lilacina*. *Mycologia* **110**: 618–634.

Meza-Meneses Y, Flores GG, Pérez JLM, *et al*. (2016). Molecular characterization and RFLP profile of an *Inocybe* (*Inocybaceae, Agaricales*) species isolated from Tlaxcala (Mexico): evidence for a new species in the subgenus *Mallocybe*. *Nova Hedwigia* **103**: 475–490.

Munsell Soil Color Charts (1954). Munsell Color Co., Baltimore, Maryland, USA.

Murrill WA (1942). New fungi from Florida. *Llyodia* **5**: 136–157.

Murrill WA (1944). New Florida fungi. *Proceedings of the Florida Academy of Sciences* **7**: 107–128.

Murrill WA (1945) New Florida fungi. *Quarterly Journal of the Florida Academy of Sciences* **8**: 175–198.

Nguyen L-T, Schmidt HA, von Haeseler A, Minh BQ (2015). IQ-TREE: A fast and effective stochastic algorithm for estimating maximum likelihood phylogenies. *Molecular Biology and Evolution* **32**: 268–274.

Niskanen T (2014). Nomenclatural novelties. *Index Fungorum* **197**: 1–4.

Peintner, Horak E (2002). *Inocybe* (*Basidiomycota*, *Agaricales*) from Kamchatka (Siberia, Russia): taxonomy and ecology. *Sydowia* **54**: 198–241.

Persoon CH (1801). *Synopsis methodica fungorum*, parts 1 & 2. Göttingen, Germany.

Persoon CH (1803–1806). *Icones pictae specierum rariorum fungorum*. Chez Amand Koenig, Libraire, Paris, France.

Phillips R (2010). *Mushrooms and other fungi of North America*. Reprint edn. Firefly Books, Richmond Hill, Ontario, Canada.

Ricken A (1915). *Die Blatterpilze*. Leipzig: Verlag von Theodor Oswald Weigel.

Ridgway R (1912). *Color standards and nomenclature*. Published by the author, Washington D.C., USA.

Robbers JE, Brady L, Tyler Jr V (1964). A chemical and chemotaxonomic evaluation of *Inocybe* species. *Lloydia* **27**: 192–202.

Roberts P, Evans S (2011). *The book of fungi*. University of Chicago Press, Chicago, Illinois, USA.

Ronquist F, Teslenko M, van der Mark P, *et al*. (2012). MrBayes 3.2: efficient Bayesian phylogenetic inference and model choice across a large model space. *Systematic Biology* **61**: 539–542.

Roy M, Yagame T, Yamato M, *et al*. (2009). Ectomycorrhizal *Inocybe* species associate with the mycoheterotrophic orchid *Epipogium aphyllum* but not its asexual propagules. *Annals of Botany* **104**: 595–610.

Ryberg M, Nilsson RH, Kristiansson E, *et al*. (2008). Mining metadata from unidentified ITS sequences in GenBank: A case study in *Inocybe* (*Basidiomycota*). *BMC Evolutionary Biology* **8**: 50.

Ryberg M, Larsson E, Jacobsson S (2010). An evolutionary perspective on morphology and ecological characters in the mushroom family *Inocybaceae* (*Agaricomycotina, Fungi*). *Molecular Phylogenetics and Evolution* **55**: 431–442.

Saba M, Haelewaters D, Pfister DH, *et al.* (2020). New species of *Pseudosperma* (*Agaricales, Inocybaceae*) from Pakistan revealed by morphology and multi-locus phylogenetic reconstruction. *MycoKeys* **69**: 1–31.

Saba M, Khalid AN (2020). *Mallocybe velutina* (*Agaricales, Inocybaceae*), a new species from Pakistan. *Mycoscience* **61**: 348–352.

Sánchez-García M. Matheny PB, Palfner G, *et al*. (2014). Deconstructing the *Tricholomataceae* (*Agaricales*) and introduction of the new genera *Albomagister*, *Corneriella*, *Pogonoloma* and *Pseudotricholoma*. *Taxon* **65**: 993–1007.

Singer R (1986). *The Agaricales in modern taxonomy*. 4th edn. Koeltz Scientific Books., Koenigstein, Germany.

Smith AH (1939) Certain species of *Inocybe* in the herbarium of the University of Michigan. *Papers of the Michigan Academy of Science, Arts and Letters* **34**: 93–105.

Smith AH, Hesler LR (1968). *The North American species of Pholiota*. Hafner, New York, USA.

Stamatakis A (2014). RAxML 8: a tool for phylogenetic analysis and post-analysis of large phylogenies. *Bioinformatics* **30**: 1312–1313.

Stangl J (1989). Die Gattung *Inocybe* in Bayern. *Hoppea* **46**: 1–409.

Stangl J, Breskinsky A (1983). *Inocybe stenospora spec. nov.* und *Inocybe malenconii* Heim var. *megalospora var. nov. Hoppea* **41**: 409–421.

Stiller JW, Hall BD (1997). The origin of red algae: implications for plastid evolution. *Proceedings of the National Academy of Sciences USA* **94**: 4520–4525.

Stijve T, Klan J, Kuyper TW (1985). Occurrence of psilocybin and baeocystin in the genus *Inocybe* (Fr.) Fr. *Persoonia* **12**: 469–473.

Strauss D, Ghosh S, Murray Z, *et al.* (2022). An overview on the taxonomy, phylogenetics and ecology of the psychedelic genera *Psilocybe*, *Panaeolus*, *Pluteus* and *Gymnopilus*. *Frontiers in Forests and Global Change* **5**: 813998.

Stuntz DE (1940). *The genus Inocybe in western Washington*. PhD dissertation. Department of Forestry, Yale University, USA.

Stuntz DE (1947). Studies in the genus *Inocybe*. I. New and noteworthy species from Washington. *Mycologia* **39**: 21–55.

Thiers B [continuously updated]. *Index herbariorum: A global directory of public herbaria and associated staff*. New York Botanical Garden's virtual herbarium. https://sweetgum.nybg.org/ih/

Timling I, Dahlberg A, Walker DA, *et al*. (2012). Distribution and drivers of ectomycorrhizal fungal communities across the North American arctic. *Ecosphere* **3**: 111.

Vauras J, Larsson E (2011). *Inocybe myriadophylla*, a new species from Finland and Sweden. *Karstenia* **51**: 31–36.

Vilgalys R, Hester M (1990). Rapid genetic identification and mapping of enzymatically amplified ribosomal DNA from several *Cryptococcus* species. *Journal of Bacteriology* **173**: 4238–4246.

Villarreal M, Esteve-Raventós F, Heykoop M, *et al.* (1998). *Inocybe expectata*, a new and unusual species of subgenus *Mallocybe*. *Mycological Research* **102**: 479–482.

Vizzini A, Maggiora MD, Tolaini F, Ercole E (2012). A new cryptic species in the genus *Tubariomyces* (*Inocybaceae*, *Agaricales*). *Mycological Progress* **12**: 375–381.

White TJ, Bruns T, Lee S, *et al*. 1990. Amplification and direct sequencing of fungal ribosomal RNA genes for phylogenetics. In: *PCR protocols: a guide to the methods and applications*. (Innis MA, Gelfand JJ, Sninsky, *et al*., eds). Academic Press, New York, USA: 315–322.

Supplementary information

Fig. S1. ML *rpb1* gene phylogeny of *Mallocybe*. Numbers above or below branches indicate bootstrap proportions > 50 %.

Fig. S2. ML *rpb2* gene phylogeny of *Mallocybe*. Numbers above or below branches indicate bootstrap proportions > 50 %.

Fig. S3. ML ITS+28S rDNA gene phylogeny of *Mallocybe*. Numbers above or below branches indicate bootstrap proportions > 50 %.

FUSE

Fungal Systematics and Evolution

Volume 12
DECEMBER 2023
PAGES 203–217

doi.org/10.3114/fuse.2023.12.10

Plasmopara echinaceae, a new species of downy mildew affecting cone flowers (*Echinacea purpurea*) in the United States

C. Salgado-Salazar[1*], M.K. Romberg[2], B. Hudelson[3]

[1]Mycology and Nematology Genetic Diversity and Biology Laboratory, U.S. Department of Agriculture, Agriculture Research Service (USDA-ARS), 10300 Baltimore Avenue, Beltsville MD, 20705, USA
[2]National Identification Services, Plant Protection and Quarantine, U.S. Department of Agriculture, Animal and Plant Health Inspection Service (USDA-APHIS), 10300 Baltimore Avenue, Beltsville, MD, 20705, USA
[3]Plant Disease Diagnostics Clinic, Department of Plant Pathology, University of Wisconsin-Madison, 1630 Linden Drive Madison, WI, 53706, USA

*Corresponding author: Catalina.Salgado@usda.gov

Key words:
Asteraceae
new taxon
obligate biotrophs
Oomycetes
ornamental plants
Peronosporaceae

Abstract: Downy mildew is one of the most important diseases of commercial sunflower and other *Asteraceae* hosts, including ornamental *Rudbeckia*. *Plasmopara halstedii* has historically been identified as the causal agent of this disease, considered a complex of species affecting nearly 35 genera in various tribes. However, with the use of molecular DNA characters for phylogenetic studies, distinct lineages of *P. halstedii* in the *Asteraceae* have been identified, confirmed as distinct or segregated as new species. During August of 2022, a downy mildew was observed on potted *Echinacea purpurea* grown in a retail greenhouse in Jefferson County, Wisconsin, USA. Phylogenetic analyses of the cytochrome c oxidase subunit 2 (*cox2*) and nuclear large subunit ribosomal RNA (nc LSU rDNA) gene regions indicated these *Plasmopara* sp. isolates are not conspecific with *P. halstedii*. Based on phylogenetic evidence and new host association, the *Plasmopara* isolates from *E. purpurea* are here described as *Plasmopara echinaceae*. Diagnostic morphological characters for this new species were not observed when compared with other isolates of *P. halstedii* or other *Plasmopara* species found on *Asteraceae* hosts, and therefore a list of species-specific substitutions in the *cox*2 region are provided as diagnostic characters. As this study corresponds to the first observation of downy mildew in cone flowers, it is recommended to follow the required disease prevention guidelines to prevent outbreaks and the establishment of this plant pathogen in production sites.

Citation: Salgado-Salazar C, Romberg MK, Hudelson B (2023). *Plasmopara echinaceae*, a new species of downy mildew affecting cone flowers (*Echinacea purpurea*) in the United States. *Fungal Systematics and Evolution* **12**: 203–217. doi: 10.3114/fuse.2023.12.10
Received: 14 June 2023; **Accepted:** 31 August 2023; **Effectively published online:** 22 September 2023
Corresponding editor: M. Thines

INTRODUCTION

The genus *Echinacea* (coneflowers) belongs to the daisy family *Asteraceae* and includes flowering herbaceous perennials. Many are drought-tolerant species. The genus is native and endemic to North America, occurring primarily in the eastern and central US and in southern Canada (Flagel *et al.* 2008). Coneflower plants are also increasingly used in ornamental gardens where they can remain in bloom for long periods of time, are adaptable to a range of soil types and pH and are hardy from U.S.D.A. Zones 3–8 (Baskin *et al.* 1992). The coneflower seedheads attract birds, and the flowers attract multiple pollinator communities, with bees as the most important group (Erickson *et al.* 2021). The species *E. purpurea* or purple coneflower is the most well-known species in the genus *Echinacea*, being widely cultivated as an ornamental (Lim 2014). Other *Echinacea* species also cultivated as ornamentals but to a lesser degree, include *E. angustifolia* (Black samson), *E. pallida* (pale purple coneflower), the endemic and endangered *E. tennesseensis* (Tennessee purple coneflower), and *E. paradoxa* (yellow coneflower). In contrast to *E. purpurea*, none of these latter species have been developed as ornamentals beyond the wild type (Ault 2007). In addition to their ornamental use, coneflowers have been frequently used as medicinal plants and their preparations are widely used in herbal medicines (Bruni *et al.* 2018). These plants produce large levels of active compounds with different therapeutic uses including treatment of common cold, flu, typhoid, diphtheria, and rheumatoid arthritis as well as various skin problems (Billah *et al.* 2019). For pharmacological applications, the species *E. angustifolia* var. *angustifolia*, *E. pallida* and *E. purpurea* are the most extensively studied and used (Xu *et al.* 2014).

Echinacea purpurea, a perennial prairie wildflower and the best-known species, was first described from specimens collected in Virginia (Binns *et al.* 2001, 2002). This species is characterized by erect main stems up to 2 meters in height, alternate leaves on long stalks, coarse hairs, and solitary spiny, reddish orange flowers surrounded by purplish bracts. *Echinacea purpurea* is cultivated widely throughout the United States, Canada, and Europe, especially in Germany, for ornamental uses as well as for its reported medicinal properties (Sharifi-Rad *et al.*

2018). *Echinacea purpurea* is generally considered to have few disease or insect problems; however increased cultivation for both ornamental and pharmaceutical uses can increase the rate at which new and re-emerging diseases are reported. Current diseases of *E. purpurea* are caused mostly by fungi, with a few caused by bacteria, phytoplasmas, viruses, nematodes, and insects (Davenport 2009, Moorman 2016). To date, there are no reports of diseases of *Echinacea* caused by oomycetes, including downy mildews (Farr & Rossman 2023), even though downy mildew diseases are prevalent in many plant genera in the *Asteraceae*. Several genera and species in the *Peronosporaceae* are known to cause downy mildew on host plants in the family *Asteraceae* (Peck 1889, Shaw 1951, Kenneth & Palti 1984, Constantinescu 1996, Voglmayr *et al.* 2004, Constantinescu & Thines 2010, Choi & Thines 2015, Salgado-Salazar *et al.* 2019, Farr & Rossman 2023). Downy mildews in these hosts result in severe economic losses for high value crops due to yield and quality reduction and downgrading of market value. Affected high value crops include oilseed (annual and cultivated sunflowers, *P. halstedii*; Gascuel *et al.* 2015), leafy vegetables (lettuce, *Bremia lactucae*, Spring *et al.* 2018), and ornamental crops (ornamental *Rudbeckia*, *Coreopsis*, *etc*.; Choi *et al.* 2009c, Rivera *et al.* 2016, Salgado-Salazar *et al.* 2019), among others.

In August of 2022, *Echinacea purpurea* (purple coneflowers) with foliar symptoms and signs of downy mildew caused by *Plasmopara* spp. were observed at a retail greenhouse in Jefferson County, Wisconsin, USA. To date, there are no reports of downy mildew on purple coneflower caused by *Plasmopara* or any other downy mildew species in the USA (Farr & Rossman 2023). Traditionally, *P. halstedii* has been designated as causing downy mildew on other species in the *Asteraceae* that are closely related to *Echinacea*. These include commercially important plants such as sunflowers (*Helianthus* sp.), ornamental Coreopsis (*Coreopsis* sp.), Black eyed Susan (*Rudbeckia* sp.), Velvet plants (*Gynura* sp.), floss flower (*Ageratum* sp.), among others (Choi *et al.* 2009c, Duarte *et al.* 2013, Palmateer *et al.* 2015, Pisani *et al.* 2019, Rivera *et al.* 2014, 2015, 2016, Salgado-Salazar *et al.* 2019). Since previous studies have found that *P. halstedii* is likely to be an assemblage of many cryptic species (Rivera *et al.* 2016), we used both morphological and molecular phylogenetic approaches to determine if the downy mildew isolates affecting *E. purpurea* were *P. halstedii* or if they constitute an undescribed species.

MATERIALS AND METHODS

Sample collection and morphological characterization

Echinacea purpurea plants (purple coneflower) showing symptoms and signs of downy mildew disease were observed in a greenhouse in Jefferson County, Wisconsin, USA. A total of five individual plants were examined. Using an entomological pin, sporangial masses were scraped from sporulating lesions on the abaxial leaf surface, mounted in a drop of 85 % lactic acid on a microscope slide and covered with a glass coverslip. Microscope slides were incubated on a warming plate set at 50 °C for 30 min before examination with a Zeiss Axio Imager M2 compound microscope (Zeiss, Jena, Germany). Pieces of leaf tissue with downy mildew lesions (approx. 5 × 5 mm) were examined microscopically for the presence of oospores. Tissue lesions were cleared using a solution of 95 % ethanol-acetic acid-glycerol (75:15:10 v/v) for 2 h or enough time for the tissue to be clear of pigment. Cleared tissue pieces were placed in 85 % lactic acid on a microscope slide, pressed gently with a cover slip to disrupt tissue, and observed with the compound microscope. Measurements of morphological characters are given as (minimum) – standard deviation towards minimum – average – standard deviation towards the maximum – (maximum) with the number of measurements given in brackets, as recommended by Choi *et al.* (2009b). Additional diseased tissue for all five sample specimens was deposited at the US National Fungus Collection (BPI, Table 1).

DNA extraction, PCR amplification and sequencing

Extraction of total DNA from leaf samples was performed by excising *ca*. 10 mm^2 discrete leaf sections colonized by downy mildew structures (mycelia, sporangia) using a sterile razor blade. The plant lesions were homogenized into a fine powder using liquid nitrogen in a sterile ceramic mortar and pestle. DNA was extracted using the E.Z.N.A. HP Fungal DNA Kit (Omega Bio-tek, Inc, Norcross, GA, USA) following the manufacturer's instructions. Amplification products were generated using the primer pairs cox2-F/Cox-RC4 (*cox*2; Hudspeth *et al.* 2000, Choi *et al.* 2015), OomCox1-levup/ OomCox1-levlo (*cox1*; Robideau *et al.* 2011) LR0R (Vilgalys & Hester 1990) and LR6-O (ncLSU rDNA; Riethmüller *et al.* 2002) and ITS1-O (Rouxel *et al.* 2013) and LR-O (ncITS rDNA; Moncalvo *et al.* 1995). Amplification reactions were performed in 20 µL volumes containing 10 µL of Platinum™II Hot-Start PCR Master Mix (2X) (Thermo Fisher Scientific, Waltham, MA, USA), 0.4 µL of each primer (10 µM), 5–10 ng of template DNA (1–2 µL), and 7–8 µL of PCR-grade water. Amplification was performed in a C1000 Touch PCR Thermal Cycler (Bio-Rad, Hercules, CA) using PCR cycle conditions described by Salgado-Salazar & Thines (2022). Amplicons were bi-directionally sequenced using a BigDye™ v. 3.1 Terminator Cycle sequencing kit on an Applied Biosystems SeqStudio Genetic Analyzer (Thermo Fisher Scientific, Waltham, MA, USA). Sequences were visually inspected and assembled using CLC Main Workbench v. 23 (QIAGEN, Inc, Germantown, MD, USA).

Phylogenetic analyses

DNA sequences for *cox2* and LSU markers obtained from the *E. purpurea* specimens, as well as sequence data from related species including those of downy mildew species affecting other hosts in the *Asteraceae* and other plant families, were downloaded from GenBank (Table 1). Individual alignments were obtained using MAFFT v. 7 (http://mafft.cbrc.jp/alignment/server/; Katoh & Standley 2013) using the algorithm G-INS-i. The amino acid substitution model best fitting each dataset was estimated using RAxML GUI v. 2.0.10 (Stamatakis 2006, Silvestro & Michalak 2012) based on the Akaike Information Criterion AIC, with GTR+I+G4 identified for *cox2* and LSU. Phylogenetic analyses were run individually for each gene using two different methods. Maximum likelihood (ML) phylogenetic analyses were performed in RAxML GUI v. 2.0.10 (Stamatakis 2006, Silvestro & Michalak 2012) with 1 000 bootstrap replicates. Bayesian inference (BI) phylogenetic trees were obtained using MrBayes v. 3.2.5. Analyses were initiated from random starting trees, run for 10 M generations with four chains (Metropolis-coupled Markov chain Monte Carlo) (Huelsenbeck & Rannala 2004), and sampled every 1 000th generations for a total of 10 000 tree samples per run. Default priors were used on all analyses and two independent Bayesian inference (BI) analyses were run. To evaluate stationarity and convergence between runs, log-likelihood

Table 1. List of isolates used in this study.

Species	Isolate number	Host	Country	*cox2*	LSU	Reference
Plasmopara ampelopsidis	H5	*Ampelopsis grandulosa* var. *brevipedunculata*	USA, Maryland	OK631956	OK631721	Salgado-Salazar & Thines (2022)
	H6	*Ampelopsis grandulosa* var. *brevipedunculata*	USA, Maryland	OK631957.1	OK631721	Salgado-Salazar & Thines (2022)
Plasmopara angustiterminalis	HOH HUH 674	*Xanthium strumarium*	Hungary	HM628742.1	n/a	Schroeder *et al.* (2011)
	KUS-F 24490	*Xanthium strumarium*	South Korea	MT731364.1	MT729826.1	Lee *et al.* (2020)
	MTX03A1	*Xanthium strumarium*	Hungary	HM628741.1	EU826113.1	Schroeder *et al.* (2011); Goeker (2008)
	SOMF07198	*Xanthium strumarium*	Bulgaria	EU743812	n/a	Choi *et al.* (2009b)
Plasmopara australis	Wallace2876	*Luffa cylindrica*	USA, North Carolina	KT159463.1	KT159461.1	Wallace *et al.* (2016)
Plasmopara baudysii	H.V. 571	*Berula erecta*	Austria	EU826098.1	n/a	Voglmayr *et al.* (2004)
Plasmopara carveri	MI	*Vitis riparia*	USA, New York	HM628757.1	HM628772.1	Schröder *et al.* (2011)
	U375	*Vitis riparia*	USA, Iowa	HM628755.1	n/a	Schröder *et al.* (2011)
Plasmopara densa	H.V. 2232 (WU)	*Rhinanthus alectorolophus*	Germany	n/a	EF553464.1	Voglmayr & Constantinescu (2008)
	MG 6-1	*Rhinanthus alectorolophus*	Germany	DQ365754.1	AY250175.1	Göker *et al.* (2007); Voglmayr *et al.* (2004)
***Plasmopara echinaceae* Type**	**EchDM1/ BPI 911239**	***Echinacea purpurea***	**USA, Wisconsin**	**OR004814**	**OR030905**	**This study**
	EchDM2/ BPI 911240	***Echinacea purpurea***	**USA, Wisconsin**	**OR004815**	**OR030906**	**This study**
Plasmopara euphrasiae	WU30283 / H.V. 2226	*Euphrasia stricta*	Sweden	KF041006.1	EF553465.1	Voglmayr & Constantinescu (2008)
Plasmopara halstedii	AR 179	*Flaveria bidentis*	Bolivia	n/a	AY178534.1	Spring *et al.* (2003)
	C1G1	*Coreopsis grandifolia*	USA, Tennessee	MH807829.1	MH807830.1	Salgado-Salazar *et al.* (2019)
	C2-hap1	*Helianthus annuus*	n/a	OM273733.1	n/a	Kitner *et al.* (2023)
	C2-hap2	*Helianthus annuus*	n/a	OM273734.1	n/a	Kitner *et al.* (2023)
	C2-hap3	*Helianthus annuus*	n/a	OM273735.1	n/a	Kitner *et al.* (2023)
	C2-hap4	*Helianthus annuus*	n/a	OM273736.1	n/a	Kitner *et al.* (2023)
	GynF	*Gynura aurantiaca*	USA, Florida	n/a	KR028988.1	Palmateer *et al.* (2015)
	H.V. 921	*Helianthus ×laetiflorus*	Germany	n/a	AY178529.1	Spring *et al.* (2003)
	KUS-F 18911	*Helianthus annuus*	Korea	EU743813.1	EU743803.1	Choi *et al.* (2009b)
	KUS-F 23701	*Coreopsis lanceolata*	Korea	n/a	FJ638471.1	Choi *et al.* (2009c)
	Ph110	*Helianthus annuus*	Germany	HM628743.1	n/a	Schröder *et al.* (2011)
	PUL F2909	*Ageratum houstonianum*	USA, Florida	n/a	KX096708.1	Pisani *et al.* (2019)
	RDM-FR-1	*Rudbeckia fulgida "Goldstrum"*	USA, Maryland	n/a	KF927152.1	Rivera *et al.* (2014)
	RDM1	*Rudbeckia fulgida "Goldstrum"*	USA, Connecticut	KU232282.1	n/a	Rivera *et al.* (2016)
	RDM37	*Rudbeckia fulgida "Goldstrum"*	USA, Maryland	KU232281.1	n/a	Rivera *et al.* (2016)
	RDM4	*Rudbeckia fulgida "Goldstrum"*	USA, Ohio	KU232283.1	n/a	Rivera *et al.* (2016)
	RDM5	*Rudbeckia fulgida "Goldstrum"*	USA, Maryland	KU232284.1	n/a	Rivera *et al.* (2016)
	RWB1050	*Gerbera jamesonii*	Brazil	KC690148.1	n/a	Duarte *et al.* (2013)
	SDM1	*Helianthus annuus*	n/a	KU232275.1	n/a	Rivera *et al.* (2016)

Table 1. (Continued).

Species	Isolate number	Host	Country	*cox2*	LSU	Reference
	SDM142	*Helianthus annuus*	n/a	KU232276.1	n/a	Rivera *et al.* (2016)
	SDM146	*Helianthus annuus*	n/a	KU232277.1	n/a	Rivera *et al.* (2016)
	SDM147	*Helianthus annuus*	n/a	KU232278.1	n/a	Rivera *et al.* (2016)
	SDM33	*Helianthus annuus*	USA, North Dakota	KU232280.1	n/a	Rivera *et al.* (2016)
	SDM74	*Helianthus annuus*	USA, North Dakota	KU232279.1	n/a	Rivera *et al.* (2016)
Plasmopara invertifolia	RWB1049	*Helichrysum bracteatum*	Brazil	KC841910.1	n/a	Duarte *et al.* (2014)
	RWB975	*Helichrysum bracteatum*	Brazil	KC841909.1	n/a	Duarte *et al.* (2014)
Plasmopara majewskii	DAR 69721	*Arctotis* sp.	Australia	HM628759.1	HQ402933.1	Schröder *et al.* (2011); Constantinescu & Thines (2010)
	VPRI20080a	*Arctotis* sp.	Australia	n/a	HQ402932.1	Constantinescu & Thines (2010)
Plasmopara megasperma	MG 39-4	*Viola rafinesquii*	USA, Tennessee	DQ365755.1	n/a	Göker *et al.* (2007)
Plasmopara muralis	BPI 911208	*Parthenocissus quinquefolia*	USA, Maryland	MN807253.1	n/a	Salgado-Salazar & Thines (2022)
	HOH HUH 1024	*Parthenocissus tricuspidata*	Germany	KJ654170.1	n/a	Choi *et al.* (2015)
	PmPtL12	*Parthenocissus tricuspidata*	Poland	MH492326.1	n/a	Mirzwa-Mróz *et al.* (2019)
Plasmopara nivea	AR 233	*Aegopodium podagraria*	Germany	n/a	AY250162.1	Voglmayr *et al.* (2004)
	HOH HUH 586	*Aegopodium podagraria*	Germany	HM628761.1	n/a	Schröder *et al.* (2011)
	MG 7-2	*Aegopodium podagraria*	Germany	DQ365756.1	n/a	Göker *et al.* (2007)
Plasmopara obducens	H.V. 207	*Impatiens noli-tangere*	n/a	n/a	EF196869.1	Voglmayr & Thines (2007)
	H.V. 306	*Impatiens noli-tangere*	n/a	DQ365757.1	n/a	Göker *et al.* (2007)
	KUS-F 23732	*Impatiens walleriana*	Korea	n/a	FJ638470.1	Choi *et al.* (2009a)
Plasmopara pimpinellae	H.V. 634	*Pimpinella major*	Austria	DQ365758.1	AY035519.2	Göker *et al.* (2007); Riethmueller *et al.* (2002)
Plasmopara pusilla	MG 8-10	*Geranium pratense*	Germany	DQ365759.1	AY035521.2	Göker *et al.* (2007); Riethmueller *et al.* (2002)
	WU30280 / H.V. 140	*Geranium sibiricum*	Austria	n/a	DQ148402.1	Voglmayr *et al.* (2006)
Plasmopara siegesbeckiae	KUS-F 21312	*Siegesbeckia glabrescens*	Korea	EU743814.1	EU743805.1	Choi *et al.* (2009)
Plasmopara sp.	HV-2014a	*Plumeria pudica*	Austria	KC774622.1	n/a	Voglmayr & Esquivel (2013)
	KUS-F 23331	*Ambrosia artemisiifolia*	Hungary	EU743820.1	EU743811.1	Choi *et al.* (2009)
	KUS-F 23333	*Ambrosia artemisiifolia*	Hungary	EU743819.1	EU743810.1	Choi *et al.* (2009)
	KUS-F 23334	*Ambrosia artemisiifolia*	Canada	EU743815.1	EU743806.1	Choi *et al.* (2009)
	KUS-F 23337	*Ambrosia artemisiifolia*	USA: Pennsylvania	EU743817.1	EU743808.1	Choi *et al.* (2009)
Plasmopara sphagneticolae	BPI 919166	*Lipochaeta integrifolia*	USA: Hawaii	MT292790.1	n/a	Davis *et al.* (2020)
	BRIP 61010	*Sphagneticola trilobata*	Australia	KM085175.1	KM085176.1	McTaggart *et al.* (2015)
Plasmopara viticola	MG 11-5	*Vitis vinifera*	Germany	DQ365760.1	n/a	Göker *et al.* (2007)
	PvI	*Vitis vinifera*	USA: New York	HM628749.1	HM628764.1	Schröder *et al.* (2011)
	TxI	*Vitis vinifera*	USA: Texas	HM628748.1	HM628762.1	Schröder *et al.* (2011)
Plasmoverna pygmaea	AR 86	*Anemone ranunculoides*	n/a	n/a	AF119605.2	Riethmueller *et al.* (1999)
	MG 4-6	*Anemone ranunculoides*	Germany	DQ365761.1	n/a	Göker *et al.* (2007)

scores were plotted using TRACER v. 1.6 (Rambaut *et al.* 2013). After stationarity evaluation, 25 % of the trees were removed from the analyses. The remaining trees were used to calculate posterior probabilities (PP) and were summarized in a 50 % majority rule consensus tree. Phylogenetic trees were visualized and edited using FigTree v. 1.4.3 (Rambaut 2014). *Plasmoverna pygmaea* was used as outgroup taxon to root the *cox2*, LSU rDNA and concatenated phylogenetic trees (Table 1). Sequence alignments for *cox2* and LSU rDNA datasets, are available through the National Agricultural Library AgData Commons (https://doi.org/10.15482/USDA.ADC/1529170).

RESULTS

Phylogenetic analyses

The nucleotide sequences generated in this study were deposited in GenBank (Table 1). Sequence data could only be obtained for two out of 5 samples examined. In addition to *cox2* and LSU, the markers *cox1* and ITS were also obtained; however, they were not used for the phylogenetic inference. The *cox*1 and ITS sequences were deposited in GenBank (*cox1*: OR004816 & OR004817; ITS: OR031840 & OR031841) to be used as supplementary barcodes for further studies. The *cox2* dataset contained the higher number of taxa as this marker has been extensively used as molecular barcode for oomycetes (Choi *et al.* 2015). The final *cox2* alignment contained 56 taxa including outgroup, consisted of 539 characters of which 310 were conserved, 229 variable and 188 parsimony informative. The final LSU alignment contained 36 taxa including outgroup and consisted of 1 209 characters of which 1 016 were conserved, 191 variable, and 144 parsimony informative. A concatenated *cox2*-LSU dataset using all taxa on Table 1 and a reduced (subset of taxa without missing data) *cox2*-LSU concatenated were also constructed. The concatenated dataset containing all taxa studied consisted of 1 748 characters, of which 1 326 were conserved, 420 variable and 332 parsimony informative. The reduced concatenated dataset contained 23 taxa and consisted of 1 748 characters of which 1 367 were conserved, 379 variable, and 264 parsimony informative.

The best-scoring ML tree topologies obtained from analysis of the *cox2* and LSU datasets are shown in Figs 1 & 2 and includes the branch support values for the ML and BI analyses (bootstrap and posterior probabilities). The phylogenetic reconstructions based on the *cox2* dataset indicated the *Plasmopara* sp. found on *E. purpurea* are not conspecific with *P. halstedii* and/or other species of *Plasmopara* found on *Asteraceae* hosts included in this study, such as *P. angustiterminalis*, *P. majewskii*, *P. invertifolia*, *P. siegesbeckiae* and *P. sphagneticola*. Specimens of *Plasmopara* on *E. purpurea* form a separate, well supported clade, closely related to *P. australis*, although this relationship lacks significant branch support (Fig. 1). The phylogenetic reconstruction using the LSU dataset showed the isolates from *E. purpurea* form a well-supported, monophyletic clade and are closely related to *P. halstedii* and *P. sphagneticolae*, as opposed to what was observed for the *cox2* dataset (Fig. 2). An isolate of *P. halstedii* on *Flaveria bidentis* appears as sister single isolate lineage to *Plasmopara* on *E. purpurea* (Fig. 2). The phylogenetic analyses of the concatenated *cox2*-LSU dataset produced trees with well supported terminal lineages, including specimens of *Plasmopara* on *E. purpurea* (Figs 3, 4). The concatenated *cox2*-LSU dataset with and without missing data showed the same general relationships and support among *Plasmopara* species, although branch supports obtained from the analysis of combined dataset without missing data showed better resolution for interior nodes in the phylogenies (Fig. 4). The individual *cox2* and LSU phylogenies, as well as those of concatenated *cox2*-LSU datasets, show *Plasmopara* species found on *Asteraceae* hosts do not form a monophyletic group, and are distributed throughout the tree (Figs 3, 4).

Disease symptoms and morphological characterization

Symptoms of downy mildew were investigated in a total of five affected plants (BPI numbers 911239, 911240, 911241, 911242, 911243). However, the microscopic observation of morphological features of the purple coneflower downy mildew pathogen (Fig. 5) were based on samples taken from two of the specimens showing disease signs, *i.e.*, active abaxial sporulation (specimens BPI 911239 holotype and BPI 911240). The remaining specimens showed only initial symptoms of the disease without any signs of the pathogen. Plants affected by the downy mildew show symptoms on the upper side of the leaves, including foliar vein delimited lesions that start as chlorotic spots, later turning dark brown due to necrosis (Fig. 5). As disease progresses, necrotic leaf lesions coalesce causing complete necrosis of leaves. White downy growth can be observed on the lower surface of the leaves, with active sporulation observed during the initial stages prior to necrosis. In necrotic tissues, the downy growth of the pathogen turned dark brown or completely dislodged from the leaf tissue (Fig. 5).

Plasmopara isolates on *E. purpurea* showed sporangiophore lengths ranging from 219–460 µm (291.8–)325.4–378.1–430.8(–460.4) µm, and (6.5–)7.4–9.3–11.2(–12.5) µm width at the base (av. 378.1 × 9.3 µm, n = 103). These sporangiophores were monopodially branched with terminal branchlets at right angles, (5.9–)7.2–8.8–10.4(–12) µm in length (av. 8.8 µm, n = 61). The observed sporangia sizes ranged from (17.4–)19.8–23.9–28(–34.3) × (12.6–)15.5–18.4–21.3(–24.8) µm, L/W ratio (0.9–)1.2–1.3–1.5(–1.7), (av. 23.9 × 18.4 µm, n = 77, Fig. 5). The isolates here designated as *P. echinaceae sp. nov*. showed no significant morphological variations to those included in the *P. halstedii* protologue (sporangiophores 300–750 µm long and 11–15 µm width at the base, sporangia 19–30 µm long, and 16–26 µm wide, av. 24.5 × 20.5 µm) (Saccardo 1888). No differences were observed also for *P. halstedii* isolates found on other plants in the tribes *Arctotideae*, *Eupatorieae, Heliantheae* and *Mutisieae* (Table 2), for example *P. halstedii* on *Ageratum houstonianum* (Pisani *et al.* 2019), *Coreopsis* sp. (Choi *et al.* 2009c, Salgado-Salazar *et al.* 2019), *Gerbera jamesonii* (Duarte *et al.* 2013), *Gynura aurantica* (Palmateer *et al.* 2015), *Helianthus* ×*laetiflorus*, and *Rudbeckia fulgida* (Rivera *et al.* 2014, 2015). Based on the phylogenetic analyses of single genes and combined datasets, the species *P. australis* on *Luffa cylindrica* and *P. halstedii* on *F. bidentis* are closely related to the *Plasmopara* isolates on *E. purpurea*. No information about morphological characters could be found for *Plasmopara* on *F. bidentis* (Spring *et al.* 2003), and *P. australis* shows smaller sporangia when compared to those of *Plasmopara* on *E. purpurea*. Related to other species of *Plasmopara* found on other *Asteraceae* hosts, *P. angustiterminalis* (Lee *et al.* 2020), *P. invertifolia* (Duarte *et al.* 2014), *P. siegesbeckia* (Lee *et al.* 2020), and *P. spagneticolae* (McTaggart *et al.* 2015), seem to be the only species showing morphological differences by producing sporangia smaller than those of *Plasmopara* from *E. purpurea* or *P. halstedii* on other *Asteraceae* hosts (Table 2) (see Notes in Taxonomy section).

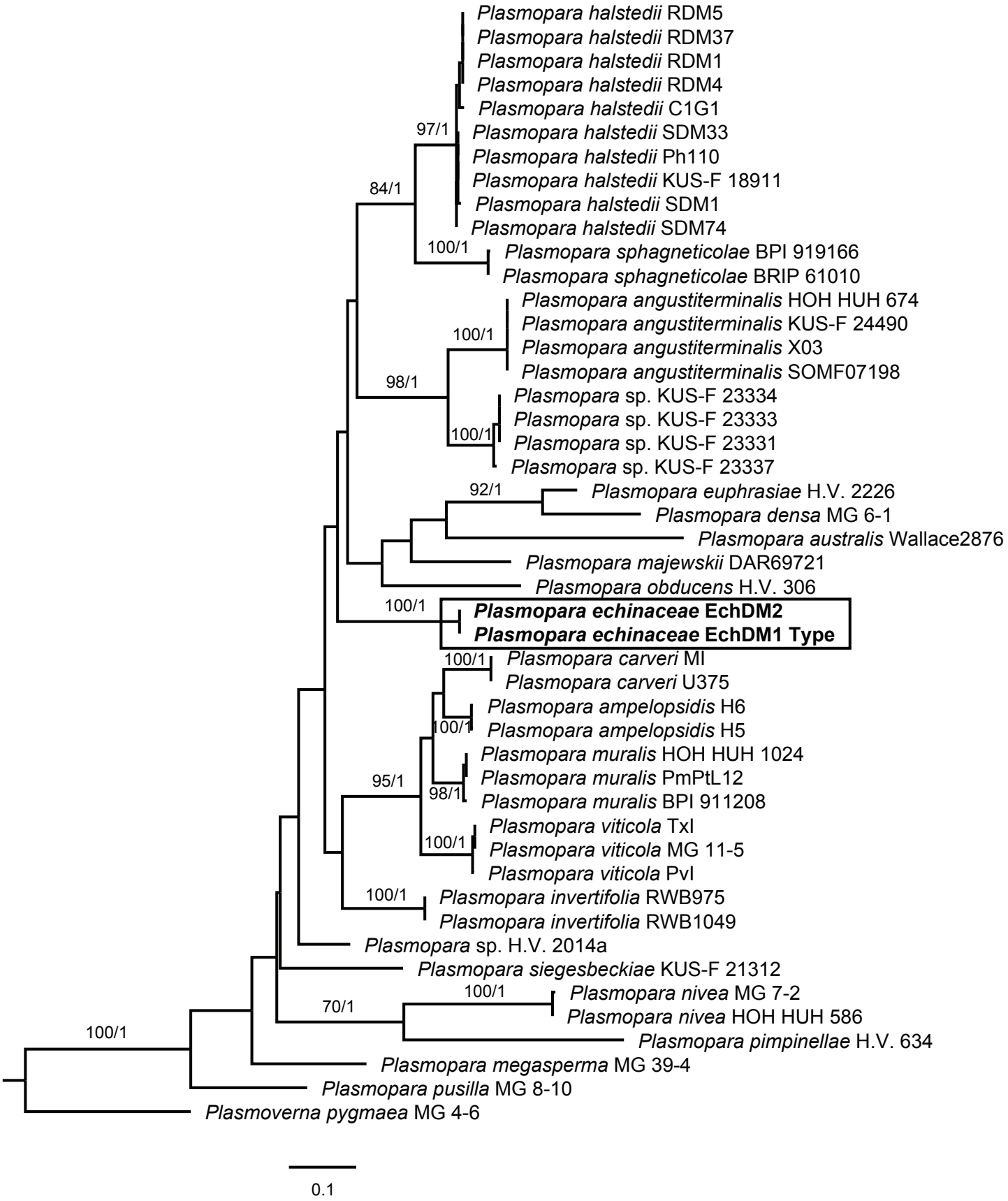

Fig. 1. Phylogenetic reconstruction (ML, BI) based on the *cox2* sequence data. Support values (bootstrap and posterior probabilities) are indicated above branches (ML/BI). Lack of support value indicates the branch was not supported at values higher than 0.95 PP, and 70 % bootstrap. *Plasmoverna pygmaea* was used as outgroup.

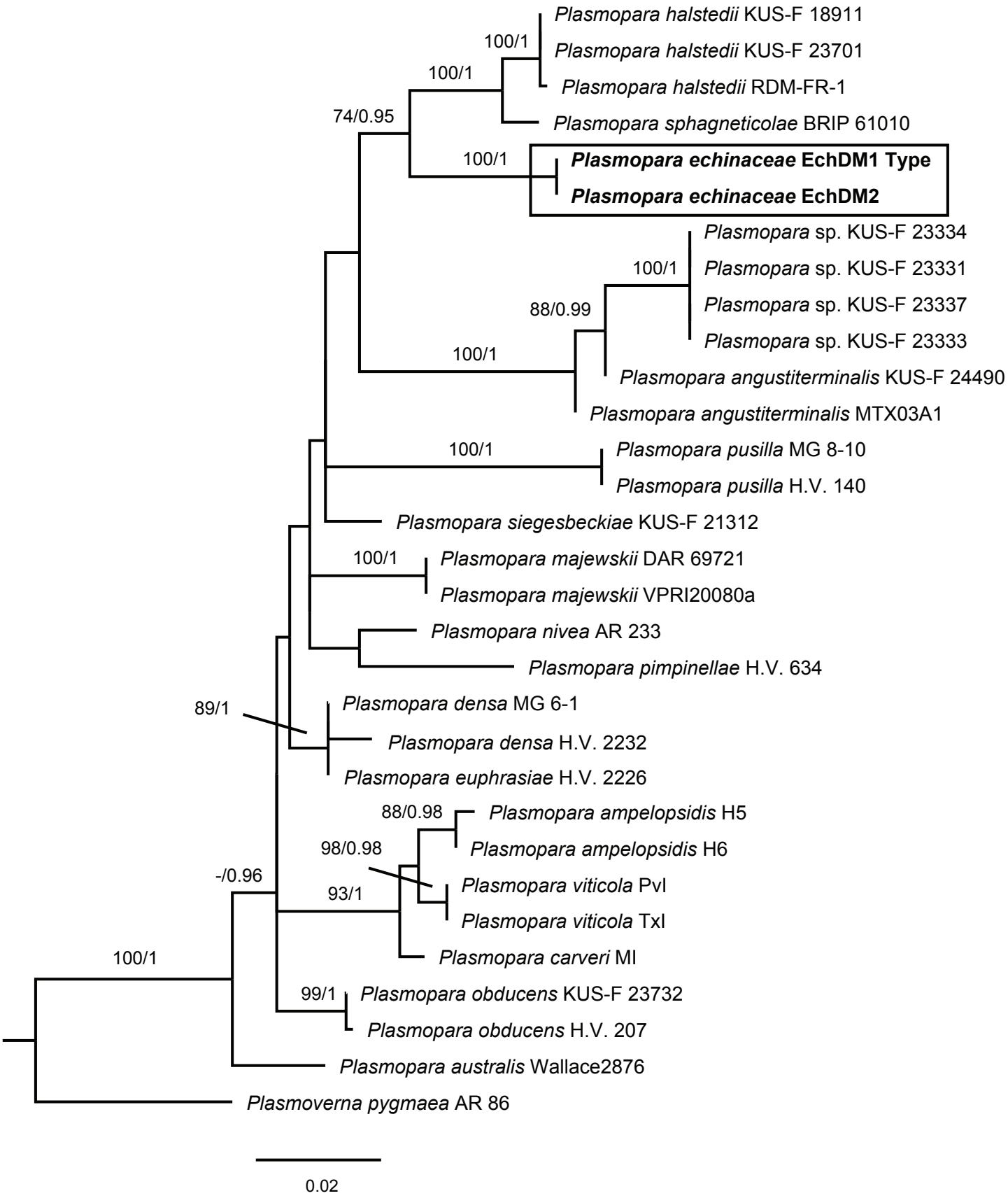

Fig. 2. Phylogenetic reconstruction (ML, BI) based on the LSU sequence data. Support values (bootstrap and posterior probabilities) are indicated above branches (ML/BI). Lack of support value indicates the branch was not supported at values higher than 0.95 PP, and 70 % bootstrap. *Plasmoverna pygmaea* was used as outgroup.

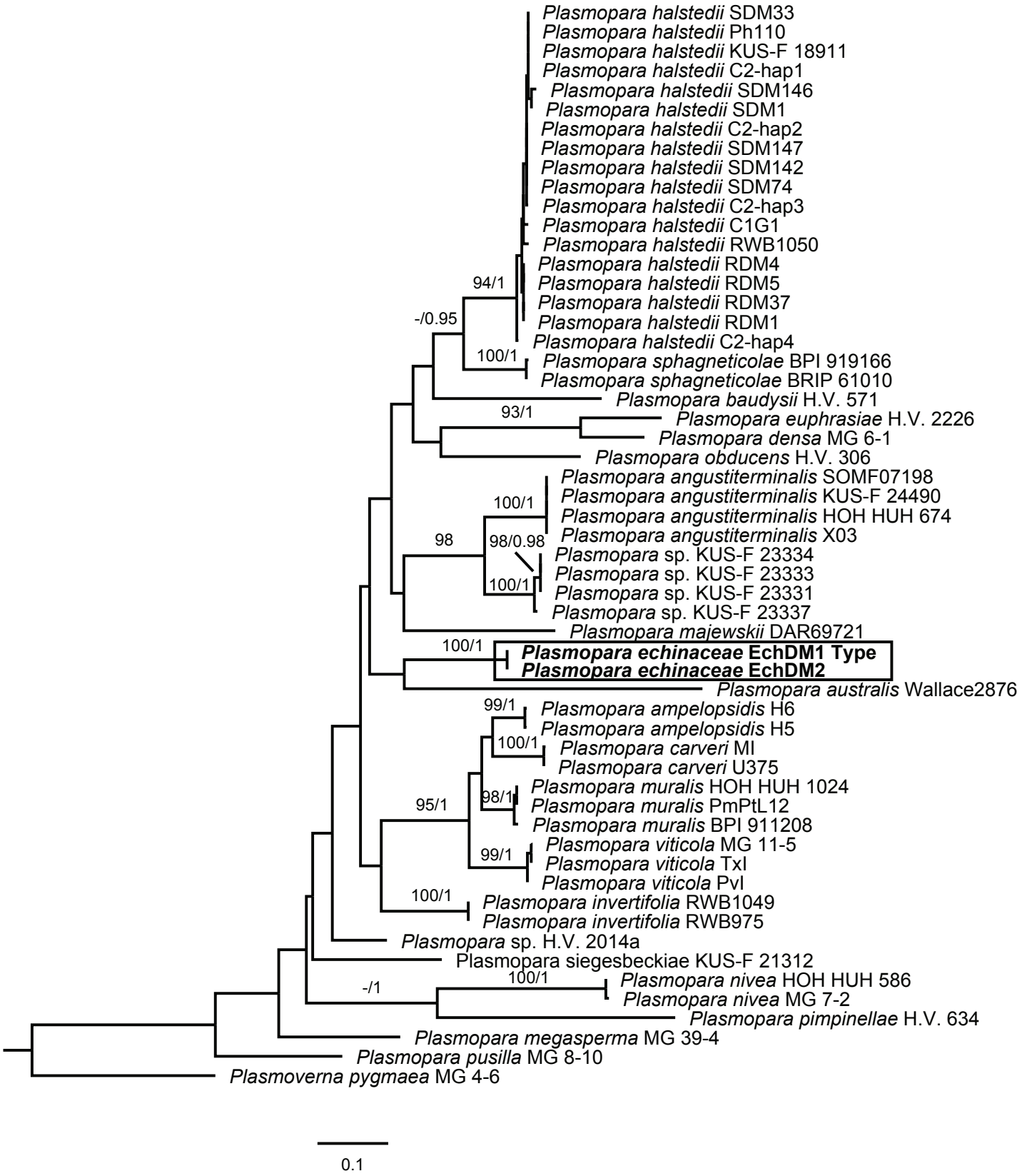

Fig. 3. Phylogenetic reconstruction (ML, BI) based on the *cox2* – LSU concatenated analysis with missing data. Support values (bootstrap and posterior probabilities) are indicated above branches (ML/BI). Lack of support value indicates the branch was not supported at values higher than 0.95 PP, and 70 % bootstrap. *Plasmoverna pygmaea* was used as outgroup.

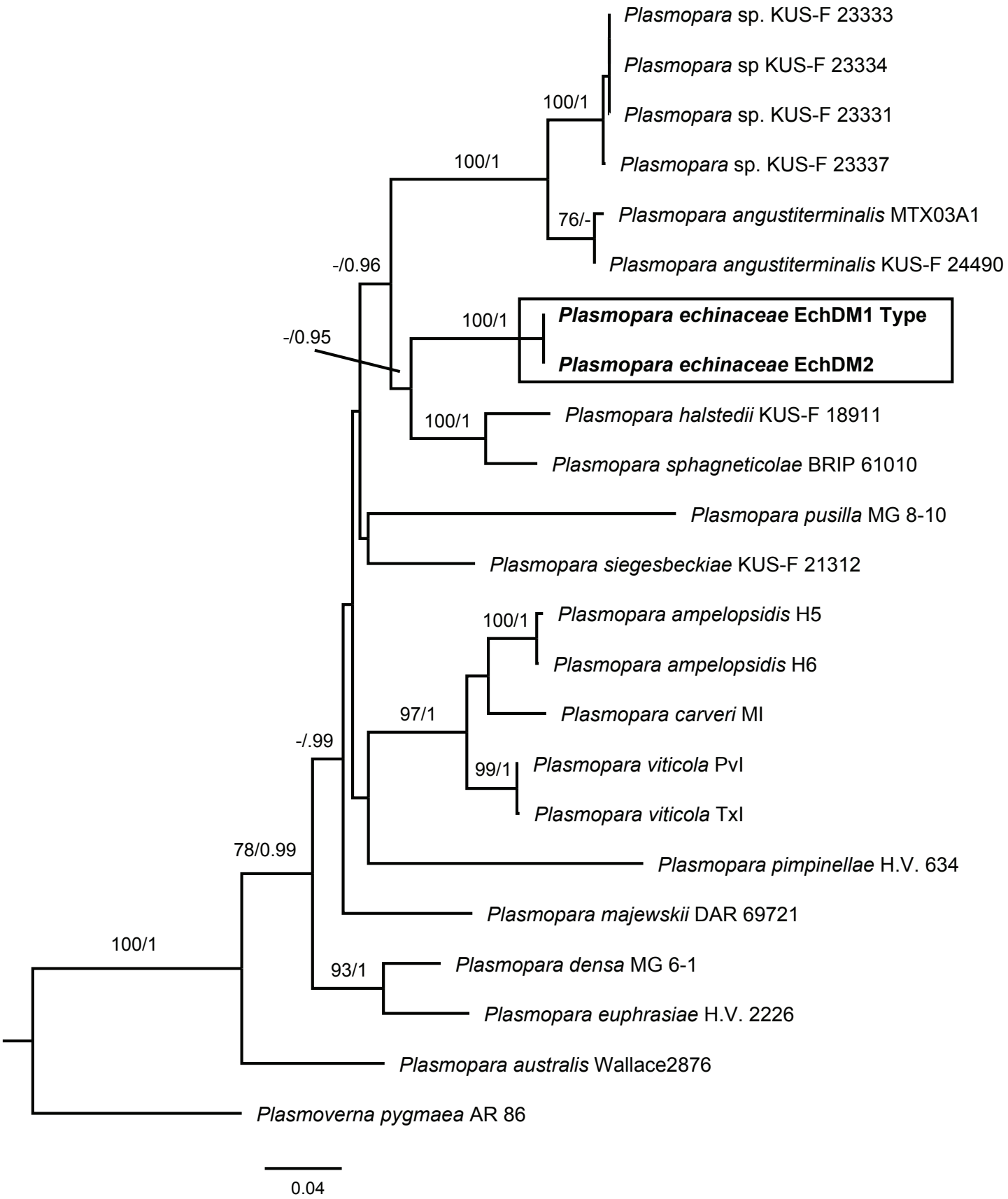

Fig. 4. Phylogenetic reconstruction (ML, BI) based on the *cox2* – LSU reduced concatenated sequence data. Support values (bootstrap and posterior probabilities) are indicated above branches (ML/BI). Lack of support value indicates the branch was not supported at values higher than 0.95 PP, and 70 % bootstrap. *Plasmoverna pygmaea* was used as outgroup.

Table 2. Comparative measurements of sporangiophores and sporangia from *Plasmopara halstedii* and other *Plasmopara* species on *Asteraceae* hosts.

Species (host species)	Sporangiophores	Sporangia	Reference
Plasmopara echinaceae (*Echinacea purpurea*)	291–460 µm, base 6.5–12.5 µm	19–28 × 15–21 µm (av. 23–18 µm)	This study
Plasmopara halstedii (Protologue)	300–750 µm, base 11–15 µm	19–30 × 15–26 µm (av. 24–20 µm)	Saccardo (1888)
Plasmopara halstedii (*Helianthus laetiflorus*)	450–700 µm, base 8–12 µm	av. 25 × 20 µm	Spring *et al.* (2003)
Plasmopara halstedii (*Rudbeckia fulgida*)	261–904 µm, base n/a	av. 24 × 20 µm	Rivera *et al.* (2014, 2015)
Plasmopara halstedii (*Ageratum houstonianum*)	Up to 550 µm, base 8.5–14.4 µm	16–24 × 12–18 µm (av. 20–15 µm)	Pisani *et al.* (2019)
Plasmopara halstedii (*Coreopsis grandiflora*)	344–579 µm, base 7–13 µm	15–22 × 13–19 µm (av. 18–16 µm)	Salgado-Salazar *et al.* (2019)
Plasmopara halstedii (*Coreopsis lanceolata*)	350–500 µm, base 7–13.5 µm	19–26 × 16–21 µm (av. 22–20 µm)	Choi *et al.* (2009c)
Plasmopara halstedii (*Gerbera jamesonii*)	Up to 650 µm, base 6.5–13 µm	20–28 × 13–18 µm (av. 24–20 µm)	Duarte *et al.* (2013)
Plasmopara halstedii (*Gynura aurantica*)	n/a	21–29 × 17–21 µm (av. 25–19 µm)	Palmateer *et al.* (2015)
Plasmopara angustiterminalis (*Xanthium* sp.)	200–550 µm, base 6–10 µm	19–22 × 13–15 µm (av. 20–14 µm)	Lee *et al.* (2020)
Plasmopara invertifolia (*Helichrysum bracteatum*)	Up to 670 µm, base 7.5–12 µm	9–20 × 9–18 µm (av. 14–13 µm)	Duarte *et al.* (2014)
Plasmopara majewskii (*Arctotis* sp., Type)	360–650 µm, base up to 13 µm	20–27 × 16–22 µm (av. 23–19 µm)	Constantinescu & Thines (2010)
Plasmopara siegesbeckia (*Siegesbeckia glabrescens*)	150–550 µm, base up to 11 µm	18–22 × 13–16 µm (av. 20–14 µm)	Lee *et al.* (2020)
Plasmopara spagneticolae (*Spagneticola trilobata*, Type)	300–50 µm, base 7–13 µm	15–27 × 14–20 µm (av. 21–17 µm)	McTaggart *et al.* (2015)
Plasmopara spagneticolae (*Lipochaeta integrifolia*)	n/a	15–24 × 12–19 µm (av. 19–15 µm)	Davis *et al.* (2020)
Plasmopara sp. (*Ambrosia artemisiifolia*)	220–490 µm, base up to 15 µm	19–26 × 15–19 µm (av. 22–17 µm)	Choi *et al.* (2009)
Plasmopara aff. *australis* (*Luffa cylindrica*)*	348–771 µm, base 8–16 µm	13–18 × 11–15 µm (av. 15–13 µm)	Wallace *et al.* (2016)
Plasmopara baudysii (*Berula erecta*)*	90–250 µm, base 8–12 µm	21–31 × 17–21 µm (av. 26–19 µm)	Skalicky (1954)

* not on *Asteraceae.*

Taxonomy

Based on the phylogenetic analyses of two molecular markers, morphological data, and host distribution, we describe here a new *Plasmopara* species infecting *Echinacea purpurea* (Purple cone flower).

Plasmopara echinaceae C. Salgado & B. Hudelson, ***sp. nov.*** MycoBank MB 849048. Fig. 5.

Etymology: The name refers to the genus of the host plant where this species can be found (*Echinacea purpurea*).

Typus: **USA**, Wisconsin, Jefferson County, on leaves of *Echinacea purpurea* in greenhouse retailer, Aug. 2022, *B. Hudelson* UWPDDC-I475/ EchDM1 (**holotype** BPI 911239).

Diagnosis: *Plasmopara echinaceae* has only been found on *E. purpurea*. Additionally, it can be diagnosed by the following species-specific nucleotide characters, which are fixed in *cox2* sequences between *P. echinaceae* and other downy mildew species on *Asteraceae*, including *P. halstedii* on various hosts, *P. angustiterminalis*, *P. invertifolia*, *P. majewskii*, *P. siegesbeckia*, *P. sphagneticolae*, *Plasmopara* sp. on *Ambrosia*, by positions 39 (G:A), 129 (A:T), 235 (C:T), 237 (G:A), 300 (C:T), 304 (T:C), 312 (A:T), 347 (T:C/A), 396 (G:A/T), 435 (C:T), 489 (T:A/C). This alignment is available through the National Agricultural Library AgData Commons (https://doi.org/10.15482/USDA.ADC/1529170).

Description: *Sporangiophores* emerging through stomata, hyaline, straight or slightly curved, 219–460 length × 6–12 µm width at the base (av. 378.1 × 9.3 µm); basal end of sporangiophore not differentiated to slightly bulbous, callose plugs often present. Branches straight, monopodial. Ultimate branchlets 2–3 base not inflated or slightly swollen, diverging at 70–90 º angle, 8.8 µm length on average. *Sporangia* subglobose to broadly ellipsoidal, hyaline, 17.4–34.3 µm length × 12.6–24.8 µm width (av. 23.9 × 18.4 µm), L/W ratio 0.9–1.7, sporangia tip round or slightly apiculate; covered by a lenticular or outwardly convex papilla. *Sexual structures* (oospores) not seen.

Additional specimen examined: **USA**, Wisconsin, Jefferson County, on leaves of *Echinacea purpurea*, August 2022, *B. Hudelson* EchDM2 (BPI 911240).

Host: Echinacea purpurea.

Geographic distribution: USA, Wisconsin.

Barcodes: *cox2*: OR004814, OR004815; LSU: OR030905, OR030906. Additional molecular markers *cox1*: OR004816, OR004817; ITS: OR031840, OR031841.

Notes: Phylogenetic analyses of *cox2* and LSU datasets showed *P. echinaceae* is genetically close to *P. australis* and *P. baudysii*. However, these species are known to cause disease in members of the families *Cucurbitaceae* and *Apiaceae*, respectively. This, together with the provided single nucleotide polymorphisms in the *cox2* gene, can distinguish *P. echinaceae* from these downy mildew species, as well as from others found on other *Asteraceae* hosts. The *cox2* alignment used to define the species-specific nucleotides is deposited at USDA AgData Commons (https://doi.org/10.15482/USDA.ADC/1529170).

DISCUSSION

The molecular differences and new host information indicated the presence of a separate and new species on the *Asteraceae* species *Echinacea purpurea*, here named *Plasmopara echinaceae*. Traditionally, downy mildew pathogens occurring on several hosts in the *Asteraceae* were initially labeled as *P. halstedii*, however, phylogenetic and population genetic studies carried out in the last 20 years (*e.g.*, Spring *et al.* 2003, 2006, Choi *et al.* 2009b, Rivera *et al.* 2016) have shown that *P. halstedii* is a complex of cryptic species. Even though advocacy for the split of *P. halstedii* into several species has existed for many decades (Novotel'nova 1962a, b, 1963), only the inclusion of molecular data in phylogenetics has allowed researchers to understand and correctly apply species limits in this group. Examples of independent lineages in *P. halstedii sensu lato* segregated into distinct species include *P. angustiterminalis* on *Xanthium* spp., *P. invertifolia* on *Helichrysum bracteatum*, *P. majewskii* on *Arctotis* × *hybrida*, and *P. spagneticolae* on *Spagneticola trilobata*, among others. Despite the segregation of some lineages into different species, *P. halstedii* as of now still shows a wide range host that includes plants in the subtribes *Eupatorieae*, *Heliantheae*, *Milleriae,* and *Mutisieae* (Choi *et al.* 2009c, Duarte *et al.* 2013, Rivera *et al.* 2014, 2015, Palmateer *et al.* 2015, Pisani *et al.* 2019, Salgado-Salazar *et al.* 2019).

Plasmopara halstedii sensu lato and other *Plasmopara* species found on *Asteraceae* are examples of morphologically conservative species. In this study we observed that sizes of morphological characters showed no significant differences among species of *Plasmopara* affecting this host family. Morphology is strongly linked to functional demands, which are in turn dependent on the environment. Consequently, lack of significant morphological variation is considered a strong indicator of the specific ecological preferences and function of downy mildew species (Voet *et al.* 2022). In this study we could observe that published sizes of morphological characters among different *P. halstedii* isolates and among other *Plasmopara* species found on *Asteraceae*, do not have enough size variation to allow individuals to be identified based on morphology. Kulkarni *et al.* (2009) reported in a comparative analysis of the sizes of various morphological characters in *P. halstedii* that isolates displaying virulence differences, did not show significant differences in sporangiophore length and sporangia size, as these showed overlapping values, and slight differences were due to intraspecific variation. Lack of morphological characters used for systematic studies has required the incorporation of single nucleotide polymorphisms at mitochondrial DNA gene regions, phylogenetic divergence, and host association as species delimiting characters.

Systematic and taxonomic studies of downy mildew species in the *Peronosporaceae* are increasing with the purpose of verifying taxonomic entities, updating nomenclature, and establishing species limits, especially for species groups previously described using only comparative morphology. Even after this renewed interest, molecular DNA data to be used in phylogenetic studies is still scarce in data repositories like GenBank, where either most data found is restricted to one gene or is specifically abundant for isolates of species which detrimental effect in

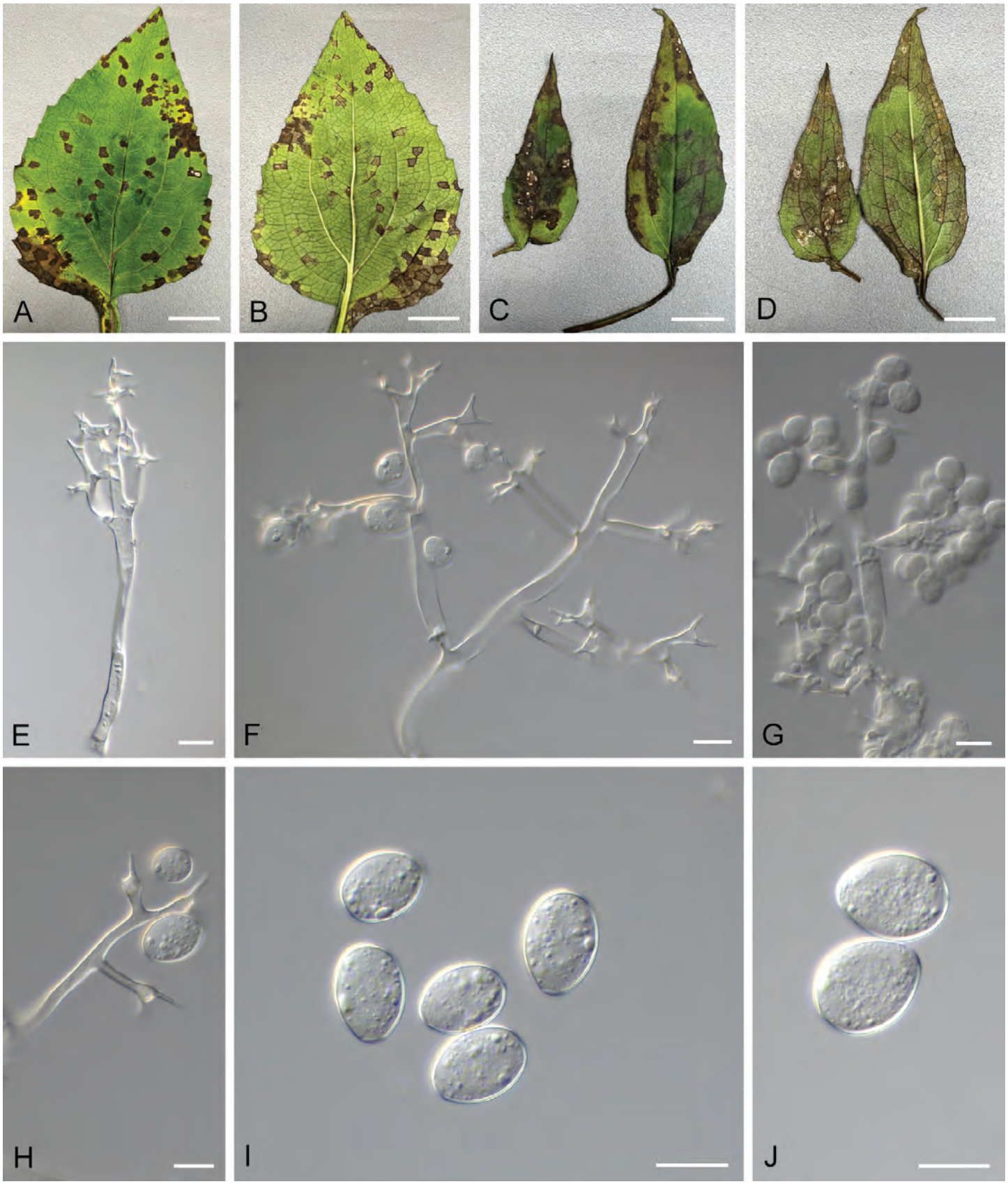

Fig. 5. Symptoms and signs of downy mildew affecting *Echinacea purpurea*. **A–D.** Diseased leaves displaying vein delimited, dark brown spots surrounded by chlorotic tissues around lesions. **E, F.** Sporangiophores. **G, H.** Close-up image of sporangiophore ramifications showing sporangia developing and ultimate branchlets. **I, J.** Sporangia. Scale bars: A–D = 1 cm; E–J = 20 µm.

agriculture has high economic impact (*i.e.*, *Plasmopara viticola*, *P. halstedii* on sunflower, *Pseudoperonospora cubensis*). Due to this limitation, multi-locus phylogenetic analysis of species of certain genera or host groups would require the introduction of missing data in the phylogenetic analysis. Still, it is important to include in this kind of studies species for which there is little to no data. In this study, the introduction of missing data in the multilocus analysis, or the analysis of a reduced multi-locus did not have an effect in the designation of the *Plasmopara* isolates on *E. purpurea* as new species. We also observed that not all *Plasmopara* species found on *Asteraceae* hosts cluster in the same group or have a single common ancestor, which is the case for *P. invertifolia*. We could also observe that *Plasmopara* species not found on *Asteraceae* hosts, such as *P. baudysii*, clustered in the main group containing *P. halstedii*, *P. angustiterminalis*, and *P. sphagneticola*. Consequently, based on previous and current studies, the evolutionary origin of downy mildew species on *Asteraceae*, patterns of species diversification, and species relationships remain unresolved.

Downy mildew diseases caused by *Plasmopara* species are some of the most severe and destructive diseases of ornamental plants, impacting the quality of product, making it a major constraint for the ornamental industry. Herbaceous perennial plants remain popular for its use in private gardens and in commercial landscapes in the United States, and it was estimated that the value of herbaceous perennials for wholesale operations with $100 000+ in sales in 36 selected states within the U.S. was estimated to be $4.63 billion for 2018, compared with $4.37 billion for 2015. Production in California and Florida account for 46 percent of the total value and the number of producers for 2018 was up 8 % compared with 2015 (Source: USDA - NASS Floriculture Crops 2018 Summary, May 2019). Downy mildew species particularly affect the floriculture and ornamental plants industry, especially those grown under protected environments (greenhouses). In these conditions, downy mildews can be common and can cause significant economic losses, by reducing yield and quality of crops and downgrading the value of ornamentals (Daughtrey & Benson 2005). Delimiting and describing new species of downy mildews and recording their current and new geographical distribution is fundamental for the study of emergent and re-emergent threats to agricultural, horticultural, or natural ecosystems. Taxonomic knowledge has a direct impact on epidemiological studies (spore trapping, disease survey and weather monitoring), and facilitates the development of integrated pest management and a predictive model for downy mildew occurrence on horticultural crops.

ACKNOWLEDGEMENTS

This work was supported by funds from USDA-ARS project 8042-22000-298-00-D. Mention of trade names or commercial products in this publication is solely for the purpose of providing specific information and does not imply recommendation or endorsement by the USDA. The USDA is an equal opportunity provider and employer.

Conflict of interest: The authors declare that there is no conflict of interest.

REFERENCES

Ault JR (2007). Coneflower. In: *Flower Breeding and Genetics* (Anderson NO, ed.). Springer, Dordrecht: 801–824.

Baskin CC, Baskin JM, Hoffman GR (1992). Seed dormancy in the prairie forb *Echinacea angustifolia* var. *angustifolia* (*Asteraceae*): after ripening pattern during cold stratification. *International Journal of Plant Sciences* **153**: 239–243.

Billah MdM, Hosen MdB, Khan F, *et al.* (2019). *Echinacea*. Chapter. 3.13 In: *Nonvitamin and Nonmineral Nutritional Supplements* (Nabavi SM, Silva AS, eds.). Academic Press: 205–210.

Binns SE, Baum BR, Arnason JT (2001). Typification of *Echinacea purpurea* (L.) Moench (*Heliantheae: Asteraceae*) and implications for the correct naming of two *Echinacea* taxa. *Taxon* **50**: 1169–1175.

Binns SE, Baum BR, Arnason JT (2002). A taxonomic revision of *Echinacea* (*Asteraceae: Heliantheae*). *Systematic Botany* **27**: 610–632.

Bruni R, Brighenti V, Caesar LK, *et al.* (2018). Analytical methods for the study of bioactive compounds from medicinally used *Echinacea* species. *Journal of Pharmaceutical and Biomedical Analysis* **160**: 443–477.

Choi Y-J, Beakes G, Glockling S, *et al.* (2015). Towards a universal barcode of oomycetes – a comparison of the *cox1* and *cox2* loci. *Molecular Ecology Resources* **15**: 1275–1288.

Choi YJ, Han JG, Park MJ, *et al.* (2009a). Downy mildew of *Impatiens balsamina* and *I. walleriana* in Korea. *The Plant Pathology Journal* **25**: 433.

Choi YJ, Kiss L, Vajna L, *et al.* (2009b). Characterization of a *Plasmopara* species on *Ambrosia artemisiifolia*, and notes on *P. halstedii*, based on morphology and multiple gene phylogenies. *Mycological Research* **113**: 1127–1136.

Choi YJ, Park MJ, Shin HD (2009c). First Korean report of downy mildew on *Coreopsis lanceolata* caused by *Plasmopara halstedii*. *Plant Pathology* **58**: 1171.

Choi YJ, Thines M (2015). Host jumps and radiation, not co-divergence drives diversification of obligate pathogens. A case study in downy mildews and *Asteraceae*. *PLoS ONE* **10**: e0133655.

Constantinescu O (1996). *Paraperonospora apiculata sp. nov*. *Sydowia* **48**: 105–110.

Constantinescu O, Thines M (2010). *Plasmopara halstedii* is absent from Australia and New Zealand. *Polish Botanical Journal* **55**: 293–298.

Davenport M (2009). *Echinacea*. Clemson Cooperative Extension, Home and Garden Information Center. Available at: https://hgic.clemson.edu/factsheet/echinacea/

Daughtrey ML, Benson DM (2005). Principles of plant health management for ornamental plants. *Annual Review of Phytopathology* **43**: 141–169.

Davis WJ, Ko M, Ocenar, JR, *et al.* (2020). First report of *Plasmopara sphagneticolae* on the native Hawaiian plant *Lipochaeta integrifolia*. *Australasian Plant Disease Notes* **15**: 29.

Duarte LL, Choi Y-J, Barreto RW (2013). First report of downy mildew caused by *Plasmopara halstedii* on *Gerbera jamesonii* in Brazil. *Plant Disease* **97**: 1382–1382.

Duarte LL, Choi Y-J, Soares DJ, *et al.* (2014). *Plasmopara invertifolia sp. nov*. causing downy mildew on *Helichrysum bracteatum* (*Asteraceae*). *Mycological Progress* **13**: 285–289.

Erickson E, Patch HM, Grozinger CM (2021). Herbaceous perennial plants can support complex pollinator communities. *Scientific Reports* **11**: 17352.

Farr DF, Rossman AY (2021). *Fungal Databases, U.S. National Fungus Collections, ARS, USDA*. Retrieved March 13, 2021, from https://nt.ars-grin.gov/fungaldatabases/

Flagel LE, Rapp RA, Grover CE, *et al.* (2008). Phylogenetic, morphological, and chemotaxonomic incongruence in the North American endemic genus *Echinacea*. *American Journal of Botany* **95**: 756–765.

Gascuel Q, Martinez Y, Boniface M-C, *et al.* (2015). *Plasmopara halstedii*, sunflower downy mildew. *Molecular Plant Pathology* **16**: 109–122.

Göker M, Voglmayr H, Riethmüller A, *et al.* (2007). How do obligate parasites evolve: A multi-gene phylogenetic analysis of downy mildews. *Fungal Genetics and Biology* **44**: 105–122.

Huelsenbeck JP, Rannala B (2004). Frequentist properties of Bayesian posterior probabilities of phylogenetic trees under simple and complex substitution models. *Systematic Biology* **53**: 904–913.

Hudspeth DSS, Nadler SA, Hudspeth MES (2000). A *cox2* molecular phylogeny of the *Peronosporomycetes*. *Mycologia* **92**: 674–684.

Katoh K, Standley DM (2013). MAFFT multiple sequence alignment software version 7: improvements in performance and usability. *Molecular Biology and Evolution* **30**: 772–780.

Kenneth RG, Palti J (1984). The distribution of downy and powdery mildews and of rusts over tribes of *Compositae* (*Asteraceae*). *Mycologia* **76**: 705–718.

Kitner M, Thines M, Sedlarova M, *et al.* (2023). Genetic structure of *Plasmopara halstedii* populations across Europe and South Russia. *Plant Pathology* **72**: 361–375.

Kulkarni S, Hegde YR, Kota RV (2009). Pathogenic and morphological variability of *Plasmopara halstedii*, the causal agent of downy mildew in sunflower. *Helia* **32**: 85–90.

Lee JS, Shin HD, Choi Y-J (2020). Rediscovery of seven long-forgotten species of *Peronospora* and *Plasmopara* (*Oomycota*). *Mycobiology* **48**: 331–340.

Lim TK (2014). *Echinacea purpurea*. In: *Edible Medicinal and Non-Medicinal Plants*. Springer, Dordrecht.

McTaggart AR, Shuey LS, McKenna SG, *et al.* (2015). *Plasmopara sphagneticolae sp. nov.* (*Peronosporales*) on *Sphagneticola* (*Asteraceae*) in Australia. *Australasian Plant Pathology* **44**: 81–85.

Mirzwa-Mróz E, Kukuła W, Kuźma K, *et al.* (2019). First report of downy mildew caused by *Plasmopara muralis* on Boston Ivy (*Parthenocissus tricuspidata*) in Poland. *Plant Disease* **103**: 1793.

Moncalvo J-M, Wang H-H, Hseu R-S (1995). Phylogenetic relationships in *Ganoderma* inferred from the Internal Transcribed Spacers and 25S Ribosomal DNA sequences. *Mycologia* **87**: 223–238.

Moorman GW (2016). *Echinacea diseases*. PennState Extension. Available at: https://extension.psu.edu/echinacea-diseases

Novotel'nova NS (1962a). K woprosu o loznoj mucˇnistoj rose podsolnecˇnika [Downy mildew on sunflowers]. Sbornik Dokla dov Naucˇnoj Konferencii po Zasˇcˇita Rastenij (Tallinn): 129–138.

Novotel'nova NS (1962b). Plasmopara *halstedii* as a composite species (the basis for the taxonomic division of the genus *Plasmopara* on *Compositae*). *Botanicheskii Zhurnal* **47**: 970–981.

Novotel'nova NS (1963). Nowye widy *Plasmopara* na *Compositae*. *Botanic´eskie materially Otdela sporvykh rastenij Botanicheskogo instituta Akademii nauk SSSR* **16**: 72–83.

Rambaut A (2014). *FigTree v. 1.4.3.* http://tree.bio.ed.ac.uk/software/figtree/

Rambaut A, Suchard M, Drummond A (2013). *Tracer v. 1.6.* http://tree.bio.ed.ac.uk/software/tracer/

Palmateer AJ, Cating RA, Lopez P (2015). First report of downy mildew on *Gynura aurantiaca* by *Plasmopara halstedii sensu lato* in Florida. *Plant Disease* **99**: 1279.

Peck CH (1889). Report of the Botanist. In: *Annual Report of the Reagents*: 74. Albany, J.B. Lyon, State Printer, 1890–1903.

Pisani C, Patel PC, Rosskopf EN, *et al.* (2019). First report of downy mildew caused by *Plasmopara halstedii* on *Ageratum houstonianum* in the United States. *Plant Disease* **103**: 2968.

Riethmüller A, Voglmayr H, Göker M, *et al.* (2002). Phylogenetic relationships of the downy mildews (*Peronosporales*) and related groups based on nuclear large subunit ribosomal DNA sequences. *Mycologia* **94**: 834–849.

Riethmüller A, Weiss M, Oberwinkler F (1999). Phylogenetic studies of *Saprolegniomycetidae* and related groups based on nuclear large subunit ribosomal DNA sequences. *Canadian Journal of Botany* **77**: 1790–1800.

Rivera Y, Creswell TC, Ruhl G, *et al.* (2015). First report of downy mildew caused by *Plasmopara halstedii* on native *Rudbeckia fulgida* Aiton var. *speciosa* (Wender.) Perdue in Indiana. *Plant Disease* **99**: 1278–1278

Rivera Y, Rane K, Crouch JA (2014). First report of downy mildew caused by *Plasmopara halstedii* on Black-eyed Susan (*Rudbeckia fulgida* cv. 'Goldstrum') in Maryland. *Plant Disease* **98**: 1005.

Rivera Y, Salgado-Salazar C, Gulya T, *et al.* (2016). Emergent rudbeckia downy mildew epidemics caused by *Plasmopara halstedii* are genetically distinct from the pathogen populations infecting sunflower. *Phytopathology* **106**: 752–761.

Robideau GP, De Cock AW, Coffey MD, *et al.* (2011). DNA barcoding of oomycetes with cytochrome c oxidase subunit I and internal transcribed spacer. *Molecular Ecology Resources* **11**: 1002–1011.

Rouxel M, Mestre P, Baudoin A, *et al.* (2014). Geographic distribution of cryptic species of *Plasmopara viticola* causing downy mildew on wild and cultivated grape in Eastern North America. *Phytopathology* **104**: 692–701.

Rouxel M, Mestre P, Comont G, *et al.* (2013). Phylogenetic and experimental evidence for host-specialized cryptic species in a biotrophic oomycete. *New Phytologist* **197**: 251–263.

Saccardo PA (1888). *Sylloge Fungorum Omnium Hucusque Cognitorium Digessit* **7**: 242.

Salgado-Salazar C, Creswell TC, Ruhl G, *et al.* (2019). First report of *Plasmopara halstedii* on *Coreopsis grandiflora* in the United States. *Plant Disease* **103**: 775.

Salgado-Salazar C, Thines M (2022). Two new species of *Plasmopara* affecting wild grapes in the United States. *Mycological Progress* **21**: 63.

Schröder S, Telle S, Nuck P, *et al.* (2011). Cryptic diversity of *Plasmopara viticola* (*Oomycota*, *Peronosporaceae*) in North America. *Organisms Diversity and Evolution* **11**: 3–7.

Sharifi-Rad M, Mnayer D, Bezerra Morais-Braga MF, *et al.* (2018). *Echinacea* plants as antioxidant and antibacterial agents: From traditional medicine to biotechnological applications. *Phytotherapy Research* **32**: 1653–1663.

Silvestro D, Michalak I (2012). raxmlGUI: a graphical front-end for RAxML. *Organisms Diversity and Evolution* **12**: 335–337.

Skalicky V (1954). Studies on the parasitic family *Peronosporaceae* II: New *Plasmopara* species of the phylogenetic compass of the species *Plasmopara umbelliferarum*. *Ceska Mykologie* **8**: 176–179.

Shaw CG (1951). New Species of the *Peronosporaceae*. *Mycologia* **43**: 445–455.

Spring O, Bachofer M, Thines M, *et al.* (2006). Intraspecific relationship of *Plasmopara halstedii* isolates differing in pathogenicity and geographic origin based on ITS sequence data. *European Journal of Plant Pathology* **114**: 309–315.

Spring O, Gomez-Zeledon J, Hadziabdic D, *et al.* (2018). Biological characteristics and assessment of virulence diversity in pathosystems of economically important biotrophic oomycetes. *Critical Reviews in Plant Sciences* **37**: 439–495.

Spring O, Voglmayr H, Riethmüller A, *et al.* (2003). Characterization of a *Plasmopara* isolate from *Helianthus* × *laetiflorus* based on cross infection, morphology, fatty acid and molecular phylogenetic data. *Mycological Progress* **2**: 163–170.

Stamatakis A (2006). RAxML-VI-HPC: maximum likelihood-based phylogenetic analyses with thousands of taxa and mixed models. *Bioinformatics* **22**: 2688–2690.

Vilgalys R, Hester M (1990). Rapid genetic identification and mapping of enzymatically amplified ribosomal DNA from several *Cryptococcus* species. *Journal of Bacteriology* **172**: 4238–4246.

Voet I, Denys C, Colyn M, *et al.* (2022). Incongruences between morphology and molecular phylogeny provide an insight into the diversification of the *Crocidura poensis* species complex. *Scientific Reports* **22**: 10531.

Voglmayr H, Constantinescu O (2008). Revision and reclassification of three *Plasmopara* species based on morphological and molecular phylogenetic data. *Mycological Research* **112**: 487–501.

Voglmayr H, Fatehi J, Constantinescu O (2006). Revision of *Plasmopara* (*Chromista, Peronosporales*) parasitic on *Geraniaceae. Mycological Research* **110**: 633–645.

Voglmayr H, Riethmüller A, Göker M, *et al.* (2004). Phylogenetic relationships of *Plasmopara*, *Bremia* and other genera of downy mildew pathogens with pyriform haustoria based on Bayesian analysis of partial LSU rDNA sequence data. *Mycological Research* **108**: 1011–1024.

Voglmayr H, Thines M (2007). Phylogenetic relationships and nomenclature of *Bremiella sphaerosperma* (*Chromista, Peronosporales*). *Mycotaxon* **100**: 11–20.

Wallace E, Choi YJ, Thines M, *et al.* (2016). First report of *Plasmopara* aff. *australis* on *Luffa cylindrica* in the United States. *Plant Disease* **100**: 537.

Xu CG, Tang TX, Chen R, *et al.* (2014). A comparative study of bioactive secondary metabolite production in diploid and tetraploid *Echinacea purpurea* (L.) Moench. *Plant Cell, Tissue and Organ Culture* **116**: 323–332.

FUSE

Fungal Systematics and Evolution

Volume 12
DECEMBER 2023
PAGES 219–246

doi.org/10.3114/fuse.2023.12.11

Molecular phylogeny and morphology reveal two new graminicolous species, *Curvularia aurantia sp. nov.* and *C. vidyodayana sp. nov*. with new records of *Curvularia* spp. from Sri Lanka

H.S. Ferdinandez[1], D.S. Manamgoda[1*], D. Udayanga[2], M.S. Munasinghe[1], L.A. Castlebury[3]

[1]Department of Botany, Faculty of Applied Sciences, University of Sri Jayewardenepura, Gangodawila, Nugegoda, Sri Lanka
[2]Department of Biosystems Technology, Faculty of Technology, University of Sri Jayewardenepura, Pitipana, Homagama, Sri Lanka
[3]Mycology and Nematology Genetic Diversity and Biology Laboratory, United States Department of Agriculture, Agricultural Research Service, Beltsville, MD, USA

*Corresponding author: dsmanamgoda@sjp.ac.lk

Key words:
dematiaceous hyphomycetes
new taxa
phylogeny
Poaceae

Abstract: Despite being a small island, Sri Lanka is rich in fungal diversity. Most of the fungi from Sri Lanka have been identified as pathogens of vegetables, fruits, and plantation crops to date. The pleosporalean genus *Curvularia* (*Dothideomycetes*) includes phytopathogenic, saprobic, endophytic, and human/animal opportunistic pathogenic fungal species. The majority of the plant-associated *Curvularia* species are known from poaceous hosts. During the current study, 22 geographical locations of the country were explored and collections were made from 10 different poaceous hosts. Morphology and molecular phylogeny based on three loci, including nuclear internal transcribed spacers 1 and 2 with 5.8S nrDNA (ITS), glyceraldehyde-3-phosphate dehydrogenase (*gapdh*), and translation elongation factor 1-α (*tef1*) supported the description of two new species of fungi described herein as *C. aurantia sp. nov*. and *C. vidyodayana sp. nov*. Moreover, novel host-fungal association records for *C. chiangmaiensis*, *C. falsilunata*, *C. lonarensis*, *C. plantarum*, and *C. pseudobrachyspora* are updated herein. In addition, five species within the genus *Curvularia*, *viz*., *C. asiatica*, *C. geniculata*, *C. lunata*, *C. muehlenbeckiae*, and *C. verruculosa* represent new records of fungi from Sri Lanka.

Citation: Ferdinandez HS, Manamgoda DS, Udayanga D, Munasinghe MS, Castlebury LA (2023). Molecular phylogeny and morphology reveal two new graminicolous species, *Curvularia aurantia sp. nov.* and *C. vidyodayana sp. nov*. with new records of *Curvularia* spp. from Sri Lanka. *Fungal Systematics and Evolution* **12**: 219–246. doi: 10.3114/fuse.2023.12.11
Received: 10 June 202; **Accepted:** 28 August 2023; **Effectively published online:** 28 September 2023
Corresponding editor: P.W. Crous

INTRODUCTION

The genus *Curvularia*, typified by *C. lunata*, is a species-rich genus in the family *Pleosporaceae* (*Pleosporales, Dothideomycetes*) (Manamgoda *et al.* 2012b, 2015). It is known that pathogenic species of *Curvularia* can cause plant diseases such as black kernels, grain molds, leaf blights, seedling blights, leaf spots, and opportunistic human infections (Sivanesan 1987, Manamgoda *et al.* 2012b, 2015, Madrid *et al.* 2014). The development of sympodial conidiophores with tretic, terminal, and intercalary conidiogenous cells as well as transversely septate, often curved conidia characterise species of *Curvularia* morphologically. Asymmetrically swollen intermediate cells control the characteristic curvature of conidia; however, species with straight conidia have also been reported (Sivanesan 1987, Marin-Felix *et al.* 2017b). The delimitation of species in *Curvularia* remains ambiguous due to the overlapping morphological characters among closely related taxa. Thus, it is recommended to incorporate molecular data assessments to accurately identify species (Manamgoda *et al.* 2014, 2015, Tan *et al.* 2014, 2018, Marin-Felix *et al.* 2017b, 2020). Members of the genus are associated with a variety of host plants around the world and display varied life modes, including saprophytic, endophytic, and pathogenic lifestyles. Most of the species are known from poaceous hosts (Ellis 1971, Sivanesan 1987, Manamgoda *et al.* 2014, Tan *et al.* 2016).

It is widely accepted that Sri Lanka has a variety of ecosystems and only a small portion of the country's microbial biodiversity has been documented. Only 3 000 species of fungi are currently recognised, despite the estimated 25 000 species of local mycobiota present. There are 404 species of plant pathogenic fungi listed in the most recent checklist on "Plant pathogenic fungi and *Oomycota* in Sri Lanka" by Adikaram & Yakandawala (2020). According to the United States National Fungus Collections database and previous publications, only 14 species of *Curvularia* have been reported so far from Sri Lanka including *Curvularia alcornii, C. eleusinicola*, *C. eragrostidis*, *C. fallax*, *C. hawaiiensis*, *C. lunata*, *C. pallescens*, *C. panici-maximi*, *C. plantarum*, *C. pseudointermedia*, *C. ravenelii*, *C. senegalensis, C. simmonsii*, and *C. tuberculata* (Salim & Mahindapala 1981, Sivanesan 1987, Richardson 1990, Adikaram & Yakandawala 2020, Ferdinandez *et al.* 2021, Farr

& Rossman 2022, Jayawardena *et al.* 2022). Therefore, the objective of this work is to collect *Curvularia* species from poaceous hosts and identify them using morphological and molecular data.

MATERIALS AND METHODS

Sample collection, isolation, and morphological identification

From 2018 to 2021, numerous field surveys were conducted spanning 22 different geographical locations in Anuradhapura, Galle, Gampaha, Hambantota, Kurunegala, Matale, Monaragala, and Puttalam districts in Sri Lanka. Samples with leaf lesions, infected panicles, grains, and associated dead plant materials were collected from various poaceous hosts and brought to the laboratory for further processing. Single spore isolation (Chomnunti *et al.* 2011) was followed to obtain pure cultures of emerging fungi and maintained on potato dextrose agar (PDA, HiMedia-India). The colony characters were determined after inoculating cultures in triplicate on three different media: PDA, corn meal agar (CMA, HiMedia-India), and malt extract agar (MEA, Criterion-USA), at 25 °C, with a 12 h light and 12 h dark light regimen. The Rayner (1970) colour chart was used to record colony colours. Digital images of fungal structures were captured using a Carl Zeiss compound light microscope equipped with an AxioCam digital camera and ZEN lite software (Carl Zeiss Microscopy, Thornwood, NY, USA). The statistical data (mean, standard deviation, minimum, and maximum) for each morphological measurement utilised in the morphological descriptions were recorded. The specimens collected were deposited in USJ-H (University of Sri Jayewardenepura Herbarium) and the living fungal cultures are maintained in USJCC (University of Sri Jayewardenepura Culture Collection). Two taxonomic novelties were registered in MycoBank (www.MycoBank.org; Crous *et al.* 2004).

DNA extraction, PCR, and sequencing

Genomic DNA was extracted from all the isolates following the method described in Ferdinandez *et al.* (2021). The nuclear ribosomal internal transcribed spacers 1 and 2 with 5.8S nrDNA region (ITS) and translation elongation factor 1-α (*tef1*) loci were amplified according to the protocols described in Manamgoda *et al.* (2012b). The glyceraldehyde-3-phosphate dehydrogenase (*gapdh*) locus was amplified using the PCR conditions mentioned in Ferdinandez *et al.* (2021). All the amplificatoin reactions were performed using GoTaq® Green Master Mix (Promega-USA) and PCR products were visualised by agarose gel electrophoresis, in a 2 % gel, with a 100 bp DNA ladder (Promega-USA). The amplified products were purified and sequenced at the Sanger DNA sequencing facility provided by Macrogen (Seoul, Korea).

Sequence alignment, phylogenetic analyses, and species recognition

Raw sequences generated for fresh isolates were assembled with BioEdit v. 7.0.5 for MS Windows (Hall 1999). All the available accepted ex-type and reference DNA sequences for the genus based on numerous publications were included and used in the analyses (Table 1). DNA sequence alignments were performed by MAFFT v. 7 using default settings (http://mafft.cbrc.jp/alignment/server/) (Katoh & Standley 2013). Preliminary identifications of the fresh isolates were determined using newly generated ITS, *gapdh*, and *tef1* sequences using NCBI BLAST. Novel species from the current study were further analysed with their respective closely related taxa from pairwise DNA sequence comparisons using the BLAST tool with default settings (Table 2). Phylogenetic reconstructions were performed using both Maximum parsimony (MP) and Maximum likelihood (ML) criteria as described in Ferdinandez *et al.* (2022). Initially, single-locus trees were generated and compared to visually find out whether the three loci used are congruent with respect to the placement of each species. As no remarkable incongruence was noted, loci were combined in a concatenated alignment. The multi-locus concatenated alignment included 204 strains of *Curvularia* and other members of *Pleosporaceae*, *i.e*., *Alternaria alternata*, *Bipolaris maydis*, *Pyrenophora poae*, *Exserohilum turcicum*, *Johnalcornia aberrans*, and *Porocercospora seminalis* (Marin-Felix *et al.* 2020, Ferdinandez *et al.* 2021). The DNA sequence alignments and phylogenetic trees are available in TreeBASE (study S30416). All DNA sequences were submitted to GenBank (Table 1).

RESULTS

The concatenated three loci sequence alignment comprised 204 *Curvularia* strains and six other pleosporalean taxa as out-groups. Out of the number of 204 *Curvularia* strains in the alignment, 36 in-group strains were fresh isolates collected from the current study. Alignment statistics for the parsimony analysis are as follows: 2 236 total characters, with 1 431 constant characters, 588 parsimony-informative characters, and 217 variable parsimony uninformative characters. Tree statistics for equally most parsimonious tree resulting from the parsimony analysis of the combined dataset with bootstrap 50 % majority rule consensus are as follows: TL = 3 961, CI = 0.327, RI = 0.757, RC = 0.247, HI = 0.673. The resulting phylogram (Fig. 1) from the multi-locus phylogenetic analyses revealed that two lineages from the fresh isolates are distinct from closely related taxa and all other members of the genus, which are described as novel species below (*Curvularia aurantia sp. nov*. and *C. vidyodayana sp. nov*). The remaining 33 isolates obtained were identified as *C. asiatica, C. chiangmaiensis*, *C. falsilunata*, *C. geniculata*, *C. lonarensis*, *C. lunata*, *C. muehlenbeckiae*, *C. plantarum*, *C. pseudobrachyspora*, and *C. verruculosa*.

TAXONOMY

In this section, morphological descriptions, notes on taxonomy, and phylogeny with illustrations are provided for two novel species and 10 other species isolated from Sri Lanka with new host and geographic distribution records.

Curvularia aurantia Ferdinandez, Manamgoda & Udayanga, ***sp. nov.*** MycoBank MB 848300. Fig. 2.

Etymology: Species is named after the latinised term for orange colour "*aurantia*"; colour of the pigment diffused to PDA.

Table 1. GenBank and culture collection accession numbers of *Curvularia* isolates used in this study. Sequences generated in this study are in bold.

Species	Isolate/Culture Collection[1]	Host/Substratum	Country	GenBank accessions			References
				ITS	*gapdh*	*tef1*	
C. aeria	CBS 294.61^{T}	Air	Brazil	HF934910	HG779148	–	Amaradasa *et al.* (2014), Madrid *et al.* (2014)
C. affinis	CBS 154.34^{T}	Unknown	Indonesia	KJ909780	KM230401	KM196566	Manamgoda *et al.* (2015)
C. ahvazensis	CBS 144673^{T}	*Zinnia elegans*	Iran	KX139029	MG428693	MG428686	Mehrabi-Koushki *et al.* (2018)
C. akaii	CBS 318.86^{T}	Unknown	Japan	LT631340	LT715797	–	Hernandez-Restrepo *et al.* (2018)
C. akaiiensis	BRIP 16080^{T}	Unknown	India	KJ415539	KJ415407	KJ415453	Tan *et al.* (2014)
C. alcornii	MFLUCC 10-0703^{T}	*Zea mays*	Thailand	JX256420	JX276433	JX266589	Manamgoda *et al.* (2012a)
C. americana	UTHSC 08-3414^{T}	Human ankle	USA	HE861833	HF565488	–	da Cunha *et al.* (2013)
C. andropogonis	CBS 186.49^{T}	*Andropogon nardus*	Indonesia	LT631354	LT715835	–	Hernandez-Restrepo *et al.* (2018)
C. angsiewkeeae	BRIP 72449a^{T}	*Scleria sp.*	Australia	OK638993	OK655929	OK655924	–
C. annelliconidiophori	CGMCC 3.19352^{T}	*Saccharum officinarum*	China	MN215641	MN264077	MN263935	Raza *et al.* (2019)
C. arcana	CBS 127224^{T}	Unknown	Unknown	MN688801	MN688828	MN688855	Marin-Felix *et al.* (2020)
C. asiatica	MFLUCC 10-0711^{T}	*Panicum* sp.	Thailand	JX256424	JX276436	JX266593	Manamgoda *et al.* (2012a)
	USJCC–0072	***Oryza sativa***	**Sri Lanka**	**OQ275214**	**OQ269625**	**–**	**This study**
	USJCC–0074	***Oryza sativa***	**Sri Lanka**	**OQ275215**	**OQ269626**	**OQ332408**	**This study**
	USJCC–0075	***Oryza sativa***	**Sri Lanka**	**OQ275216**	**OQ269627**	**–**	**This study**
C. aurantia sp. nov.	**USJCC–0096^{T}**	***Zea mays***	**Sri Lanka**	**OQ275217**	**OQ269628**	**OQ332409**	**This study**
C. australiensis	BRIP 12044^{T}	*Oryza sativa*	Australia	KJ415540	KJ415406	KJ415452	Tan *et al.* (2014)
C. australis	BRIP 12521^{T}	*Sporobolus caroli*	Australia	KJ415541	KJ415405	KJ415451	Tan *et al.* (2014)
C. austriaca	CBS 102694^{T}	Human nasal cavity	Austria	MN688802	MN688829	MN688856	Marin-Felix *et al.* (2020)
C. bannonii	BRIP 16732^{T}	*Jacquemontia tamnifolia*	USA	KJ415542	KJ415404	KJ415450	Tan *et al.* (2014)
C. beasleyi	BRIP 10972^{T}	*Chloris gayana*	Australia	MH414892	MH433638	MH433654	Tan *et al.* (2018)
C. beerburrumensis	BRIP 12942^{T}	*Eragrostis bahiensis*	Australia	MH414895	MH433634	MH433657	Tan *et al.* (2018)
C. boeremae	IMI 164633^{T}	*Portulaca oleracea*	India	MH414911	MH433641	–	Tan *et al.* (2018)
C. borreriae	CBS 859.73^{T}	Volcanic ash soil	Chile	LT631355	LT715838	–	Hernandez-Restrepo *et al.* (2018)
C. bothriochloae	BRIP 12522^{T}	*Bothriochloa bladhii*	Australia	KJ415543	KJ415403	KJ415449	Tan *et al.* (2014)
C. brachyspora	CBS 186.50^{T}	Soil	Java	HG778983	KM061784	KM230405	Madrid *et al.* (2014), Manamgoda *et al.* (2014)
C. buchloes	CBS 246.49^{T}	*Buchloe dactyloides*	USA	KJ909765	KM061789	KM196588	Manamgoda *et al.* (2014)
C. cactivora	CBS 580.74^{R}	Member of *Cactaceae*	Republic of Suriname	MN688803	MN688830	MN688857	Marin-Felix *et al.* (2020)
C. canadensis	CBS 109239^{T}	Overwintered grass	Canada	MN688804	MN688831	MN688858	Marin-Felix *et al.* (2020)
C. caricae-papayae	CBS 135941^{T}	*Carica papaya*	India	LT631350	LT715816	–	Hernandez-Restrepo *et al.* (2018)
C. chiangmaiensis	CPC 28829^{T}	*Zea mays*	Thailand	MF490814	MF490836	MF490857	Marin-Felix *et al.* (2017b)
	USJCC–0022	***Panicum virgatum***	**Sri Lanka**	**MT410574**	**MZ971270**	**MZ971256**	**This study**

Table 1. (Continued).

Species	Isolate/Culture Collection[1]	Host/Substratum	Country	GenBank accessions			References
				ITS	*gapdh*	*tef1*	
	USJCC–0064	***Pennisetum pedicellatum***	**Sri Lanka**	**MZ948818**	**MZ971264**	**–**	**This study**
	USJCC–0069	***Cyperus rotundus***	**Sri Lanka**	**OQ275218**	**OQ269629**	**–**	**This study**
	USJCC–0070	***Oryza sativa***	**Sri Lanka**	**OQ275219**	**OQ269630**	**OQ332410**	**This study**
	USJCC–0087	***Panicum virgatum***	**Sri Lanka**	**OQ275220**	**OQ269631**	**–**	**This study**
	USJCC–0144	***Ischaemum* sp.**	**Sri Lanka**	**OQ275221**	**OQ269632**	**–**	**This study**
C. chlamydospora	UTHSC 07-2764^{T}	Human toenail	USA	HG779021	HG779151	–	Madrid *et al.* (2014)
C. chonburiensis	MFLUCC 16-0375^{T}	*Pandanus* sp.	Thailand	MH275055	MH412747	–	Tibpromma *et al.* (2018)
C. chuasooengiae	BRIP 72482a^{T}	*Scleria* sp.	Australia	OK638997	OK655933	–	–
C. clavata	BRIP 61680b	*Oryza rufipogon*	Australia	KU552205	KU552167	KU552159	Khemmuk *et al.* (2016)
C. coatesiae	BRIP 24261^{T}	*Litchi chinensis*	Australia	MH414897	MH433636	MH433659	Tan *et al.* (2018)
C. coicicola	HSAUP 990901	*Coicis lacryma-jobi*	China	AB453880	–	–	Zhang & Zhang (2004)
C. coicis	CBS 192.29^{T}	*Coix lacryma-jobi*	Japan	HF934917	HG779130	JN601006	Amaradasa *et al.* (2014), Madrid *et al.* (2014)
C. coimbatorensis	SZMC 22225^{T}	Human cornea	India	MN628310	MN628306	MN628302	Kiss *et al.* (2020)
C. colbranii	BRIP 13066^{T}	*Crinum zeylanicum*	Australia	MH414898	MH433642	MH433660	Tan *et al.* (2018)
C. comoriensis	CBS 110673	Unknown	Unknown	LT631357	LT715841	–	Hernandez-Restrepo *et al.* (2018)
C. crassiseptata	CBS 503.90^{T}	Plant material	Nigeria	LT631310	LT715882	MN688859	Hernandez-Restrepo *et al.* (2018), Marin-Felix *et al.* (2020)
C. crustacea	BRIP 13524^{T}	*Sporobolus* sp.	Indonesia	KJ415544	KJ415402	KJ415448	Tan *et al.* (2014)
C. curculiginis	YZU 181230^{R}	*Curculigo capitulata*	China	MK507796	MK507794	MK507795	Liu *et al.* (2019)
C. cymbopogonis	CBS 419.78^{T}	*Yucca* sp.	Netherlands	HG778985	HG779129	–	Madrid *et al.* (2014)
C. dactyloctenicola	CPC 28810^{T}	*Dactyloctenium aegyptium*	Thailand	MF490815	MF490837	MF490858	Marin-Felix *et al.* (2017b)
C. dactyloctenii	BRIP 12846^{T}	*Dactylocteniumradulans*	Australia	KJ415545	KJ415401	KJ415447	Tan *et al.* (2014)
C. determinata	CGMCC 3.19340^{T}	*Saccharum officinarum*	China	MN215653	MN264088	MN263947	Raza *et al.* (2019)
C. deightonii	CBS 537.70^{T}	*Sorghum vulgare*	Denmark	LT631356	LT715839	–	Hernandez-Restrepo *et al.* (2018)
C. eleusinicola	USJCC–0005^{T}	*Eleusine coracana*	Sri Lanka	MT262877	MT393583	MT432925	Ferdinandez *et al.* (2021)
C. elliptiformis	CGMCC 3.19351^{T}	*Saccharum officinarum*	China	MN215656	MN264091	MN263950	Raza *et al.* (2019)
C. ellisii	CBS 193.62^{T}	Air	Pakistan	JN192375	JN600963	JN601007	Manamgoda *et al.* (2011)
C. eragrostidicola	BRIP 12538^{T}	*Eragrostis pilosa*	Australia	MH414899	MH433643	MH433661	Tan *et al.* (2018)
C. eragrostidis	CBS 189.48^{T}	*Sorghum*	Java	HG778986	HG779154	–	Madrid *et al.* (2014)
C. falsilunata	CGMCC 3.19329^{T}	*Saccharum officinarum*	China	MN215660	MN264093	MN263954	Raza *et al.* (2019)
	USJCC–0053	***Zea mays***	**Sri Lanka**	**MN044758**	**MN053041**	**MN053010**	**This study**
	USJCC–0067	***Echinochloa crus-galli***	**Sri Lanka**	**MZ948820**	**MZ971266**	**–**	**This study**
	USJCC–0140	***Panicum maximum***	**Sri Lanka**	**OQ275222**	**OQ269633**	**–**	**This study**

Table 1. (Continued).

Species	Isolate/Culture Collection[1]	Host/Substratum	Country	GenBank accessions			References
				ITS	*gapdh*	*tef1*	
C. flexuosa	CGMCC 3.19447[T]	*Saccharum officinarum*	China	MN215663	MN264096	MN263957	Raza *et al.* (2019)
C. frankliniae	BRIP 72476a[T]	*Sorghum timorense*	Australia	OK638995	OK655931	OK655926	–
C. fraserae	BRIP 64708a[T]	*Bothriochloa insculpta*	Australia	OM809867	OM721558	OM714552	Tan *et al.* (2022)
C. geniculata	CBS 187.50[T]	*Andropogon sorghum*	Indonesia	KJ909781	KM083609	KM230410	Manamgoda *et al.* (2015)
	USJCC–0021	***Oryza sativa***	**Sri Lanka**	**MT410573**	**MZ971269**	**MZ971255**	**This study**
	USJCC–0037	***Sorghum* sp. (Traditional-Swayanjatha)**	**Sri Lanka**	**MZ948816**	**MZ971262**	**MZ971252**	**This study**
	USJCC–0039	***Zea mays***	**Sri Lanka**	**ON514026**	**ON561896**	**–**	**This study**
	USJCC–0063	***Panicum virgatum***	**Sri Lanka**	**MZ948817**	**MZ971263**	**–**	**This study**
	USJCC–0073	***Saccharum officinarum***	**Sri Lanka**	**ON514024**	**ON561894**	**–**	**This study**
	USJCC–0084	***Ischaemum* sp.**	**Sri Lanka**	**OQ275223**	**OQ269634**	**–**	**This study**
C. gladioli	CBS 210.79	*Gladiolus* sp.	Romania	LT631345	LT715802	–	Hernandez-Restrepo *et al.* (2018)
C. graminicola	BRIP 23186a[T]	*Aristida ingrata*	Australia	JN192376	JN600964	JN601008	Manamgoda *et al.* (2012b)
C. guangxiensis	CGMCC 3.19330[T]	*Saccharum officinarum*	China	MN215667	MN264100	MN263961	Raza *et al.* (2019)
C. gudauskasii	DAOM 165085	Unknown	Unknown	AF071338	AF081393	–	–
C. harveyi	BRIP 57412[T]	*Triticum aestivum*	Australia	KJ415546	KJ415400	KJ415446	Tan *et al.* (2014)
C. hawaiiensis	BRIP 11987[T]	*Oryza sativa*	USA	KJ415547	KJ415399	KJ415445	Tan *et al.* (2014)
C. heteropogonicola	BRIP 14579[T]	*Heteropogon contortus*	India	KJ415548	KJ415398	KJ415444	Tan *et al.* (2014)
C. heteropogonis	CBS 284.91[T]	*Heteropogon contortus*	Australia	KJ415549	JN600969	JN601013	Tan *et al.* (2014)
C. hominis	UTHSC 09-464[T]	Human cornea	USA	HG779011	HG779106	–	Madrid *et al.* (2014)
C. homomorpha	CBS 156.60[T]	Air	USA	JN192380	JN600970	JN601014	Manamgoda *et al.* (2012b)
C. hustoniae	BRIP 72486a[T]	*Heteropogon triticeus*	Australia	OK638999	OK655935	OK655928	–
C. inaequalis	CBS 102.42[T]	Soil	France	KJ922375	KM061787	KM196574	Manamgoda *et al.* (2014)
C. intermedia	CBS 334.64	*Avena versicolor*	USA	HG778991	HG779155	–	Madrid *et al.* (2014)
C. iranica	IRAN 3487C[T]	*Bougainvillea spectabilis*	Iran	MT551122	MN266487	MN266490	Safi *et al.* (2020)
C. ischaemi	CBS 630.82[T]	*Ischaemum indicum*	Solomon Islands	HG778992	HG779131	–	Madrid *et al.* (2014)
C. kenpeggii	BRIP 14530[T]	*Triticum aestivum*	Australia	MH414900	MH433644	MH433662	Tan *et al.* (2018)
C. khuzestanica	CBS 144736[T]	*Atriplex lentiformis*	Iran	MH688044	MH688043	–	Song *et al.* (2019)
C. kusanoi	CBS 137.29[T]	*Eragrostis major*	Japan	JN192381	LT715862	KM196592	Manamgoda *et al.* (2011), Hernandez-Restrepo *et al.* (2018)
C. lamingtonensis	BRIP 12259[T]	*Microlaena stipoides*	Australia	MH414901	MH433645	MH433663	Tan *et al.* (2018)
C. lolii	CMAA 1785[T]	*Lolium multiflorum*	Brazil	MT849336	MT889299	MT881706	Victoria Arellano *et al.* (2021)
C. lonarensis	CBS 140569[T]	Lonar lake	India	KT315408	KY007019	–	Sharma *et al.* (2016)

Table 1. (Continued).

Species	Isolate/Culture Collection[1]	Host/Substratum	Country	GenBank accessions			References
				ITS	*gapdh*	*tef1*	
	USJCC–0082	***Saccharum officinarum***	**Sri Lanka**	**OQ275224**	**OQ269635**	**OQ332411**	**This study**
C. lunata	CBS 730.96^{T}	Human lung biopsy	USA	JX256429	JX276441	JX266596	Manamgoda *et al*. (2012b)
	USJCC–0023	***Panicum virgatum***	**Sri Lanka**	**MT410575**	**MZ971271**	**MZ971257**	**This study**
	USJCC–0132	***Zea mays***	**Sri Lanka**	**OQ275225**	**OQ269636**	**–**	**This study**
C. lycopersici	Strain 11	*Solanum lycopersicum*	Egypt	KY883347	KY883345	–	Ismail *et al.* (2016)
C. manamgodae	CGMCC 3.19446^{T}	*Saccharum officinarum*	China	MN215677	MN264110	MN263971	Raza *et al*. (2019)
C. malina	CBS 131274^{T}	*Zoysia matrella*	USA	JF812154	KP153179	KR493095	Tomaso-Peterson *et al*. (2016)
C. mebaldsii	BRIP 12900^{T}	*Cynodon transvaalensis*	Australia	MH414902	MH433647	MH433664	Tan *et al.* (2018)
C. micrairae	BRIP 17068a^{T}	*Micraira subulifolia*	Australia	OM421618	OM373204	OM373205	–
C. micropus	CBS 127235^{T}	*Paspalum notatum*	USA	HE792934	LT715859	–	da Cunha *et al.* (2012), Hernandez-Restrepo *et al*. (2018)
C. microspora	GUCC 6272^{T}	*Hippeastrum striatum*	China	MF139088	MF139106	MF139115	Liang *et al.* (2018)
C. millisiae	BRIP 71718a^{T}	*Cyperus aromaticus*	Australia	OK661031	OK636415	OK636413	Tan *et al.* (2022)
C. miyakei	CBS 197.29^{T}	*Eragrostis pilosa*	Japan	KJ909770	KM083611	KM196568	Manamgoda *et al*. (2014)
C. moringae	CPC 38873^{T}	*Moringa ovalifolia*	Namibia	MW175363	MW173105	–	Crous *et al.* (2020)
C. mosaddeghii	IRAN 3131C^{T}	*Syzygium cumini*	Iran	MG846737	MH392155	MH392152	Heidari *et al*. (2018)
C. muehlenbeckiae	CBS 144.63^{T}	*Muehlenbeckia* sp.	India	HG779002	HG779108	–	Madrid *et al.* (2014)
	USJCC–0027	***Sorghum* sp. (Traditional-Swayanjatha)**	**Sri Lanka**	**MZ948813**	**MZ971259**	**MZ971250**	**This study**
C. nanningensis	GUCC 11005^{T}	*Cymbopogon citratus*	China	MH885321	MH980005	MH980011	Zhang *et al*. (2020)
C. neergaardii	BRIP 12919^{T}	*Oryza sativa*	Ghana	KJ415550	KJ415397	KJ415443	Tan *et al.* (2014)
C. neoindica	IMI 129790^{T}	*Brassica nigra*	India	MH414910	MH433649	MH433667	Tan *et al.* (2018)
C. nicotiae	BRIP 11983^{T}	Soil	Algeria	KJ415551	KJ415396	KJ415442	Tan *et al.* (2014)
C. nodosa	CPC 28800^{T}	*Digitaria ciliaris*	Thailand	MF490816	MF490838	MF490859	Marin-Felix *et al.* (2017b)
C. nodulosa	CBS 160.58	*Eleusine indica*	USA	JN601033	JN600975	JN601019	Manamgoda *et al.* (2015)
C. oryzae	CBS 169.53^{T}	*Oryza sativa*	Vietnam	KP400650	HG779156	KM196590	Madrid *et al*. (2014), Manamgoda *et al.* (2015)
C. oryzae-sativae	CBS 127725^{T}	*Oryza sativa*	Argentina	MN688808	MN688835	MN688863	Marin-Felix *et al.* (2020)
C. ovariicola	BRIP 15882	*Eragrostis schultzii*	Australia	JN192384	JN600976	JN601020	Manamgoda *et al.* (2012b)
C. pallescens	CBS 156.35^{T}	Air	Indonesia	KJ922380	KM083606	KM196570	Manamgoda *et al*. (2012b)
C. palmicola	MFLUCC 14-0404^{T}	*Acoelorrhaphe wrightii*	Thailand	MF621582	–	–	Hyde *et al*. (2017)
C. pandanicola	MFLUCC 15-0746^{T}	*Pandanus* sp.	Thailand	MH275056	MH412748	MH412763	Tibpromma *et al.* (2018)
C. panici	Strain OKI-1	*Panicum repens*	Japan	AB164703	–	–	Chung & Tsukiboshi (2005)
C. panici-maximi	USJCC–0006^{T}	*Panicum maximum*	Sri Lanka	MN044757	MN053040	MN053009	Ferdinandez *et al*. (2021)
C. papendorfii	CBS 308.67^{T}	*Acacia karroo*	South Africa	KJ909774	KM083617	KM196594	Manamgoda *et al.* (2014)

Table 1. (Continued).

Species	Isolate/Culture Collection[1]	Host/Substratum	Country	GenBank accessions			References
				ITS	*gapdh*	*tef1*	
C. paraverruculosa	FMR 17656^{T}	Soil	Mexico	LR736641	LR736646	LR736649	Iturrieta-González *et al.* (2020)
C. patereae	CBS 198.87^{T}	*Triticum durum*	Argentina	MN688810	MN688837	MN688864	Marin-Felix *et al.* (2020)
C. penniseti	CBS 528.70	Unknown	Unknown	MH859833	LT715840	–	Hernandez-Restrepo *et al.* (2018), Vu *et al.* (2019)
C. perotidis	CBS 350.90^{T}	*Perotis rara*	Australia	HG778995	HG779138	KM230407	Madrid *et al.* (2014), Manamgoda *et al.* (2014)
C. petersonii	BRIP 14642^{T}	*Dactyloctenium aegyptium*	Australia	MH414905	MH433650	MH433668	Tan *et al.* (2018)
C. phaeospara	CGMCC 3.19448^{T}	*Saccharum officinarum*	China	MN215686	MN264118	MN263980	Raza *et al.* (2019)
C. pisi	CBS 190.48^{T}	*Pisum sativum*	Canada	KY905678	KY905690	KY905697	Marin-Felix *et al.* (2017a)
C. plantarum	CGMCC 3.19342^{T}	*Saccharum officinarum*	China	MN215688	MN264120	MN263982	Raza *et al.* (2019)
	USJCC–0033	***Oryza sativa***	**Sri Lanka**	**OQ275226**	**OQ269637**	**–**	**This study**
	USJCC–0054	***Zea mays***	**Sri Lanka**	**OQ275227**	**OQ269638**	**–**	**This study**
	USJCC–0068	***Echinochloa crus-galli***	**Sri Lanka**	**OQ275228**	**OQ269639**	**–**	**This study**
	USJCC–0078	***Zea mays***	**Sri Lanka**	**OQ275229**	**OQ269640**	**–**	**This study**
	USJCC–0091	***Zea mays***	**Sri Lanka**	**OQ275230**	**OQ269641**	**–**	**This study**
	USJCC–0097	***Zea mays***	**Sri Lanka**	**OQ275231**	**OQ269642**	**–**	**This study**
C. platzii	BRIP 27703b^{T}	*Cenchrus clandestinum*	Australia	MH414906	MH433651	MH433669	Tan *et al.* (2018)
C. polytrata	CGMCC 3.19338^{T}	*Saccharum officinarum*	China	MN215691	MN264123	MN263984	Raza *et al.* (2019)
C. portulacae	BRIP 14541^{T}	*Portulaca oleracea*	USA	KJ415553	KJ415393	KJ415440	Tan *et al.* (2014)
C. prasadii	CBS 143.64^{T}	*Jasminum sambac*	India	KJ922373	KM061785	KM230408	Manamgoda *et al.* (2014)
C. protuberans	CGMCC 3.19360^{T}	*Saccharum officinarum*	China	MN215693	MN264125	MN263986	Raza *et al.* (2019)
C. protuberata	CBS 376.65^{T}	*Deschampsia flexuosa*	Scotland	KJ922376	KM083605	KM196576	Manamgoda *et al.* (2014)
C. pseudobrachyspora	CPC 28808^{T}	*Eleusine indica*	Thailand	MF490819	MF490841	MF490862	Marin-Felix *et al.* (2017b)
	USJCC–0024	***Zea mays***	**Sri Lanka**	**MT410576**	**MZ971272**	**MZ971258**	**This study**
	USJCC–0085	***Panicum virgatum***	**Sri Lanka**	**OQ275232**	**OQ269643**	**OQ332412**	**This study**
C. pseudoclavata	CBS 539.70^{T}	*Oryza sativa*	Denmark	MN688817	MN688844	MN688869	Marin-Felix *et al.* (2020)
C. pseudoellisii	CBS 298.80^{T}	*Sorghum bicolor*	Sudan	MN688818	MN688845	MN688870	Marin-Felix *et al.* (2020)
C. pseudointermedia	CBS 553.89^{T}	Soil	Brazil	MN688819	MN688846	MN688871	Marin-Felix *et al.* (2020)
C. pseudolunata	UTHSC 09-2092^{T}	Human nasal sinus	USA	HE861842	HF565459	–	da Cunha *et al.* (2013)
C. pseudoprotuberata	CBS 385.69^{T}	Soil	Canada	MN688821	MN688848	MN688873	Marin-Felix *et al.* (2020)
C. pseudorobusta	UTHSC 08-3458	Human nasal sinus	USA	HE861838	HF565476	–	da Cunha *et al.* (2013)
C. radici-foliigena	CGMCC 3.19328^{T}	*Saccharum officinarum*	China	MN215695	MN264127	MN263988	Raza *et al.* (2019)
C. radicicola	CGMCC 3.19327^{T}	*Saccharum officinarum*	China	MN215699	MN264131	MN263992	Raza *et al.* (2019)
C. ravenelii	BRIP 13165^{T}	*Sporobolus fertilis*	Australia	JN192386	JN600978	JN601024	Manamgoda *et al.* (2012b)
C. reesii	BRIP 4358^{T}	Air	Australia	MH414907	MH433637	MH433670	Tan *et al.* (2018)

Table 1. (Continued).

Species	Isolate/Culture Collection[1]	Host/Substratum	Country	GenBank accessions			References
				ITS	*gapdh*	*tef1*	
C. richardiae	BRIP 4371[T]	*Richardia brasiliensis*	Australia	KJ415555	KJ415391	KJ415438	Tan *et al.* (2014)
C. robusta	CBS 624.68[T]	*Dichanthium annulatum*	USA	KJ909783	KM083613	KM196577	Manamgoda *et al.* (2014)
C. rouhanii	CBS 144674[T]	*Syngonium vellozianum*	Iran	KX139030	MG428694	MG428687	Mehrabi-Koushki *et al.* (2018)
C. ryleyi	BRIP 12554[T]	*Sporobolus creber*	Australia	KJ415556	KJ415390	KJ415437	Tan *et al*. (2014)
C. saccharicola	CGMCC 3.19344[T]	*Saccharum officinarum*	China	MN215701	MN264133	MN263994	Raza *et al.* (2019)
C. sacchari-officinarum	CGMCC 3.19331[T]	*Saccharum officinarum*	China	MN215705	MN264137	MN263998	Raza *et al.* (2019)
C. senegalensis	CBS 149.71	Unknown	Nigeria	HG779001	HG779128	–	Madrid *et al.* (2014)
C. sesuvii	CGMCC 3.9578[T]	*Sesuvium portulacastrum*	China	EF175940	–	–	Zhang & Li (2009)
C. shahidchamranensis	SCUA-8-Marun[T]	Soil	Iran	MH550084	MH550083	–	Dehdari *et al*. (2018)
C. sichuanensis	Strain BN9	Air	China	MH483998	–	–	Zhang *et al.* (2007)
C. siddiquii	CBS 196.62[T]	Air	Pakistan	MN688823	MN688850	–	Marin-Felix *et al*. (2020)
C. simmonsii	USJCC–0002[T]	*Panicum maximum*	Sri Lanka	MN044753	MN053011	MN053005	Ferdinandez *et al*. (2021)
C. soli	CBS 222.96[T]	Soil	Papua New Guinea	KY905679	KY905691	KY905698	Marin-Felix *et al*. (2017a)
C. sorghina	BRIP 15900[T]	*Sorghum bicolor*	Australia	KJ415558	KJ415388	KJ415435	Tan *et al.* (2014)
C. spicifera	CBS 274.52	Soil	Spain	JN192387	JN600979	JN601023	Manamgoda *et al.* (2012b)
C. sporobolicola	BRIP 23040b[T]	*Sporobolus australasicus*	Australia	MH414908	MH433652	MH433671	Tan *et al*. (2018)
C. stenotaphri	BRIP 71303[T]	*Stenotaphrum secundatum*	Australia	MZ681952	MZ695824	MZ695819	Crous *et al.* (2021b)
C. subpapendorfii	CBS 656.74[T]	Soil	Egypt	KJ909777	KM061791	KM196585	Manamgoda *et al.* (2015)
C. suttoniae	FMR 10992[T]	Human leg wound	USA	HE861828	HF565479	LR736651	Iturrieta-González *et al.* (2020)
C. tamilnaduensis	SZMC 22226[T]	Human cornea	India	MN628311	MN628307	MN628303	Kiss *et al.* (2020)
C. tanzanica	IMI 507176[T]	*Cyperus aromaticus*	Tanzania	MW396857	MW388669	–	Crous *et al.* (2021a)
C. templetoniae	BRIP 72453a[T]	*Hyparrhenia hirta*	Australia	OK442370	OK655930	OK655925	–
C. thailandicum	MFLUCC 15-0747[T]	*Pandanus* sp.	Thailand	MH275057	MH412749	MH412764	Tibpromma *et al*. (2018)
C. tribuli	CBS 126975[T]	*Tribulus terrestris*	South Africa	MN688825	MN688852	MN688875	Marin-Felix *et al.* (2020)
C. trifolii	ICMP 6149	*Setaria glauca*	New Zealand	KM230395	KM083607	JX266600	Manamgoda *et al.* (2012b, 2015)
C. tripogonis	BRIP 12375[T]	*Tripogon loliiformis*	Australia	JN192388	JN600980	JN601025	Manamgoda *et al.* (2011)
C. tropicalis	BRIP 14834[T]	*Coffea arabica*	India	KJ415559	KJ415387	KJ415434	Tan *et al*. (2014)
C. tsudae	ATCC 44764[T]	*Chloris gayana*	Japan	KC424596	KC747745	KC503940	Tan *et al*. (2018)
C. tuberculata	CBS 146.63[T]	*Zea mays*	India	JX256433	JX276445	JX266599	Manamgoda *et al.* (2012b)
C. umbiliciformis	CGMCC 3.19346[T]	*Saccharum officinarum*	China	MN215711	MN264142	MN264004	Raza *et al.* (2019)
C. uncinata	CBS 221.52[T]	*Oryza sativa*	Vietnam	HG779024	HG779134	–	Madrid *et al.* (2014)
C. variabilis	CPC 28815[T]	*Chloris barbata*	Thailand	MF490822	MF490844	MF490865	Marin-Felix *et al*. (2017b)

Table 1. (Continued).

Species	Isolate/Culture Collection[1]	Host/Substratum	Country	GenBank accessions			References
				ITS	*gapdh*	*tef1*	
C. verruciformis	CBS 537.75	*Vanellus miles*	New Zealand	HG779026	HG779133	–	Madrid *et al.* (2014)
C. verrucosa	CBS 422.93	Air	Cuba	MN688826	MN688853	MN688876	Marin-Felix *et al*. (2020)
C. verruculosa	CBS 150.63	*Punica granatum*	India	KP400652	KP645346	KP735695	Manamgoda *et al.* (2015)
	USJCC–0028	***Oryza sativa***	**Sri Lanka**	**MZ948815**	**MZ971261**	**MZ971251**	**This study**
	USJCC–0031	***Zea mays***	**Sri Lanka**	**MZ948814**	**MZ971260**	**–**	**This study**
	USJCC–0103	***Saccharum officinarum***	**Sri Lanka**	**OQ275233**	**OQ269644**	**–**	**This study**
C. vidyodayana sp. nov.	**USJCC–0029^{T}**	***Oryza sativa***	**Sri Lanka**	**OQ275234**	**OQ269645**	**OQ332413**	**This study**
	USJCC–0062	***Oryza sativa***	**Sri Lanka**	**OQ275234**	**OQ269646**	**–**	**This study**
C. vietnamensis	FMR 17659^{T}	Unidentified dead leaves	Vietnam	LR736642	LR736644	LR736647	Iturrieta-González *et al*. (2020)
C. warraberensis	BRIP 14817^{T}	*Dactyloctenium aegyptium*	Australia	MH414909	MH433653	MH433672	Tan *et al*. (2018)
C. xishuangbannaensis	KUMCC 17-0185^{T}	*Pandanus amaryllifollus*	Thailand	MH275058	MH412750	MH412765	Tibpromma *et al*. (2018)
C. yamadana	COAD 375	*Cyperus rotundus*	Brazil	MN954704	–	MT008259	Ferreira & Barreto (2020)
Outgroups							
Alternaria alternata	CBS 916.96^{T}	Unknown	Unknown	KF465761	–	–	Lecellier *et al.* (2014)
Bipolaris maydis	CBS 137271/C5^{T}	*Zea mays*	USA	AF071325	KM034846	KM093794	Berbee *et al.* (1999), Manamgoda *et al.* (2014)
Exserohilum turcicum	CBS 690.71^{T}	*Zea mays*	Germany	LT837487	LT882581	LT896618	Hernandez-Restrepo *et al*. (2018)
Johnalcornia aberrans	CBS 510.91^{T}	*Eragrostis parviflora*	Australia	KJ415522	KJ415424	–	Tan *et al*. (2014)
Porocercospora seminalis	CPC 21305^{T}	*Bouteloua dactyloides*	USA	HF934942	–	–	Amaradasa *et al*. (2014)
Pyrenophora poae	BRIP 10953	Member of *Poaceae*	Australia	KJ415566	KJ415380	KJ415427	Tan *et al*. (2014)

[1]Culture collections: ATCC: American Type Culture Collection, Virginia, USA; BRIP: Queensland Plant Pathology Herbarium, Queensland, Australia; CBS: CBS-KNAW Fungal Biodiversity Centre, Utrecht, The Netherlands; CGMCC: China General Microbiological Culture Collection, Institute of Microbiology, Chinese Academy of Sciences, Beijing, China; CMAA: Collection of Microorganisms of Agricultural and Environmental Importance at Embrapa Environmental research unit (Embrapa Meio-Ambiente), Brazil; COAD: Universidade Federal de Viçosa - Coleção Octávio de Almeida Drumond; CPC: working collection of P.W. Crous, housed at the Westerdijk Fungal Biodiversity Institute, Utrecht, the Netherlands; DAOM: Plant Research Institute, Department of Agriculture (Mycology), Ottawa, Canada; FMR: Medical School of the Rovira i Virgili University, Reus, Spain; GUCC: Department of Plant Pathology, Agriculture College, Guizhou University, P.R. China; HSAUP: Herbarium of Shandong Agricultural University, Department of Plant Pathology, China; ICMP: International Collection of Micro-organisms from Plants, Landcare Research, Auckland, New Zealand; IMI: International Mycological Institute, Kew, UK; IRAN: Iranian Fungal Culture Collection, Iranian Research Institute of Plant Protection, Iran; KUMCC: Kunming Institute of Botany Culture Collection; MFLUCC: Mae Fah Luang University culture collection, Thailand; SCUA: the Collection of Fungal Cultures, Department of Plant Protection, Shahid Chamran University of Ahvaz, Iran; SZMC: Szeged Microbiology Collection, Hungary; YZU: Culture Collection of Yangtze University Jingzhou, China; USJCC: University of Sri Jayewardenepura Culture Collection, Sri Lanka; UTHSC: Fungus Testing Laboratory, University of Texas Health Science Center, San Antonio, Texas. ^{R} and ^{T} indicate reference and ex-type strains, respectively.

Table 2. Pairwise comparison of the loci analysed for novel species described in the current study with closely related taxa.

Novel species	Closely related taxa	Locus, Identity and Gaps (both with percentages)					
		ITS		*gapdh*		*tef1*	
		Identity and percentage	Gaps	Identity and percentage	Gaps	Identity and percentage	Gaps
Curvularia aurantia sp. nov. (USJCC–0096)	*C. coicis*	551/565 (98 %)	6/565 (1 %)	360/373 (97 %)	0/373 (0 %)	910/914 (99 %)	0/914 (0 %)
	C. ischaemi	452/487 (93 %)	16/487 (3 %)	497/502 (99 %)	0/502 (0 %)	–	–
	C. crassiseptata	455/485 (94 %)	15/485 (3 %)	336/345 (97 %)	1/345 (0 %)	868/891 (97 %)	0/891 (0 %)
	C. comoriensis	453/486 (93 %)	16/486 (3 %)	517/542 (95 %)	6/542 (1 %)	–	–
	C. heteropogonicola	385/405 (95 %)	10/405 (2 %)	355/370 (96 %)	1/370 (0 %)	781/804 (97 %)	0/804 (0 %)
	C. cymbopogonis	454/485 (94 %)	15/485 (3 %)	325/337 (96 %)	1/337 (0 %)	–	–
Curvularia vidyodayana sp. nov. (USJCC–0029)	*C. affinis*	506/509 (99 %)	1/509 (0 %)	542/551 (98 %)	0/551 (0 %)	898/899 (99 %)	0/899 (0 %)
	C. soli	499/509 (98 %)	5/509 (0 %)	579/587 (99 %)	0/587 (0 %)	918/921 (99 %)	0/921 (0 %)
	C. thailandicum	496/507 (98 %)	6/507 (1 %)	335/347 (97 %)	0/347 (0 %)	901/909 (99 %)	1/909 (0 %)
	C. xishuangbannaensis	493/504 (98 %)	5/504 (0 %)	528/537 (98 %)	1/537 (0 %)	876/883 (99 %)	2/883 (0 %)
	C. millisiae	504/514 (98 %)	5/514 (0 %)	564/576 (98 %)	0/576 (0 %)	972/978 (99 %)	1/978 (0 %)
	C. asiatica	460/467 (99 %)	5/467 (1 %)	483/487 (99 %)	0/487 (0 %)	913/916 (99 %)	0/916 (0 %)
	C. senegalensis	504/514 (98 %)	5/514 (0 %)	536/545 (98 %)	0/545 (0 %)	–	–
	C. geniculata	504/514 (98 %)	5/514 (0 %)	443/448 (99 %)	0/448 (0 %)	821/822 (99 %)	0/822 (0 %)

On leaf lesions (2–5 cm long) of *Zea mays*. *Asexual morph*: On CMA *hyphae* 4–5 µm wide, subhyaline to pale brown, septate, branched. *Stroma* 3–8 mm long, dark brown to black, elongated, branched, dense hypha. *Conidiophores* (115–)161–500(–611) × 5–8(–9) µm ($\bar{x}$ = 330 × 6 µm, *n* = 20), hyaline to pale brown, micronematous to macronematous, septate, simple or branched, straight or flexuous, sometimes geniculate at the apex. *Conidiogenous cells* (4–)5–10(–15) × 4–6(–7) µm ($\bar{x}$ = 8 × 5 µm, *n* = 20), hyaline to pale brown, smooth-walled, subcylindrical to slightly swollen, terminal or intercalary, mono- to polytretic. *Conidia* (18–)23–26(–30) × (10–)11–13(–16) µm ($\bar{x}$ = 24 × 12 µm, *n* = 30), hyaline to pale brown, curved, asymmetrical, sometimes Y-shaped, enlarged middle cells, 3–4-distoseptate; *hila* inconspicuous. *Microconidiation* observed. *Sexual morph* not observed.

Culture characteristics: Colonies on PDA reaching 36 mm diam after 7 d at 25 °C, colonies from above: irregular, margin irregular, slightly raised, velvety appearance, dark brown at the margin, mouse grey aerial mycelia, producing orange colour pigment which defuse to the media; dark brown to black elongated, branched stroma observed above the media after about 5 d, reverse: dark brown at the margin, black in the centre. Colonies on CMA reaching 40 mm diam after 7 d at 25 °C, colonies from above: circular, margin irregular, flat, hairy appearance, white at the margin, grey in the centre, concentric ring growth; reverse: pale brown centre to margin. Colonies on MEA reaching 50 mm diam after 7 d at 25 °C, colonies from above: circular, margin mostly irregular, flat, hairy appearance, dark green and dark grey concentric ring growth, mouse grey in the centre; reverse: brown at the margin, black in the centre.

Typus: **Sri Lanka**, Central Province, Matale District, Dambulla, N 7.903257 E 80.670494, on leaf spots of *Zea mays*, 15 Aug. 2019, *H.S. Ferdinandez* (**holotype** USJ-H-087, culture ex-type USJCC–0096).

Known host and distribution: *Zea mays* in Sri Lanka (this study).

Notes: Based on the phylogenetic analyses and pairwise DNA sequence comparison results (Table 2), *C. aurantia* (USJCC–0096) is closely related to *C. coicis* and *C. ischaemi*. Pairwise DNA sequence comparison revealed that *C. aurantia* is distinct from its closely related taxa. *Curvularia aurantia* differs by having smaller conidia compared to those of *C. ischaemi* (22.5–)24–35(–40) × (11.5–)13–17.5(–18.5) µm and of *C. coicis* 40–64 × 17–23 µm (Sivanesan 1987). Conidia of *C. ischaemi* are 3-distoseptate while in *C. coicis* they are 4–5-distoseptate. Moreover, when compared to *C. aurantia* both taxa have shorter conidiophores; *C. ischaemi* up to 375 µm long and *C. coicis* up to 200 µm long. *Curvularia coicis* has been reported from several *Coix* spp. and *Zea mays* (Farr & Rossman 2022). *Curvularia ischaemi* has only been reported from *Ischaemum* spp. (Farr & Rossman 2022). *Curvularia aurantia* was collected from *Zea mays* during this study. Therefore, based on molecular data and morphology, *C. aurantia* is described herein as a new species.

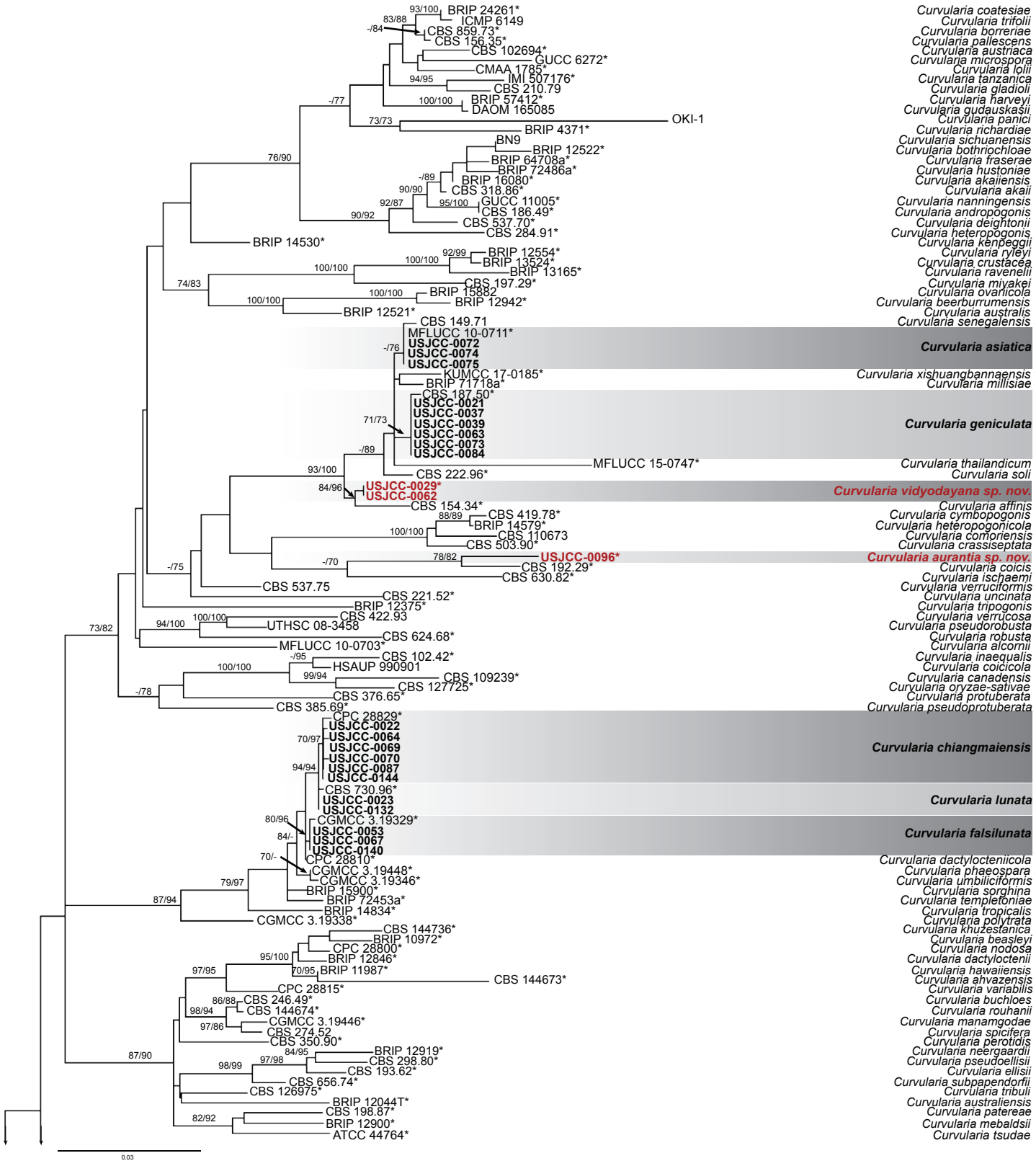

Fig. 1. Phylogram of *Curvularia* spp. based on the combined ITS, *gapdh*, and *tef1* alignment. Maximum parsimony and RAxML bootstrap support values above 70 % are shown at the nodes respectively. Type cultures are marked with an asterisk. Novel species from the current study are indicated in red. New records are in bold. The tree is rooted with other members of *Pleosporaceae* (*Alternaria alternata*, *Bipolaris maydis*, *Pyrenophora poae*, *Exserohilum turcicum*, *Johnalcornia aberrans,* and *Porocercospora seminalis*); the root branches were shortened to facilitate layout by the factor indicated on them.

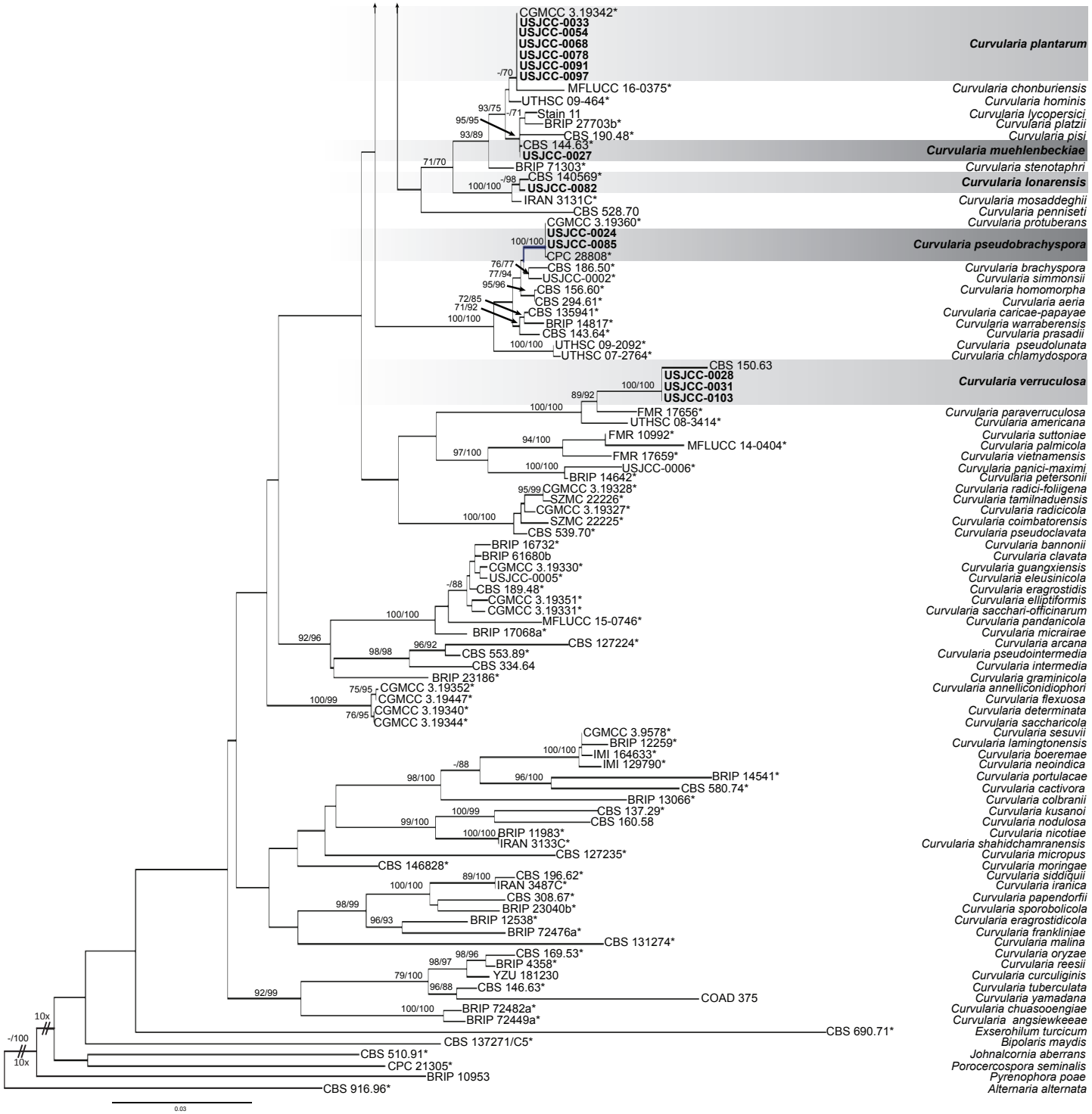

Fig. 1. (Continued).

Curvularia vidyodayana Ferdinandez, Manamgoda & Udayanga, ***sp. nov.*** MycoBank MB 848301. Fig. 3.

Etymology: Name refers to the Vidyodaya, former name of the University of Sri Jayewardenepura where this research study was carried out.

Saprobic on grains of *Oryza sativa*. *Asexual morph*: On CMA *hyphae* 4–6 µm wide, hyaline, septate, branched. *Conidiophores* 51–232(–432) × (4–)5–6 µm ($\bar{x}$ = 142 × 5 µm, *n* = 20), hyaline to brown, micronematous to macronematous, septate, simple or branched, straight or flexuous, swollen at the apex. *Conidiogenous cells* (9–)10–16(–20) × (4–)5–6 µm ($\bar{x}$ = 13 × 5 µm, *n* = 20), hyaline to pale brown, smooth-walled, subcylindrical to swollen, terminal or intercalary, mono- to polytretic. *Conidia* (16–)19–25(–27) × (7–)8–10(–11) µm ($\bar{x}$ = 22 × 9 µm, *n* = 30), hyaline immature conidia, pale brown to brown mature conidia, slightly curved, mostly ellipsoidal with broadly tapering ends, mostly enlarged third cell from the base, usually 3-, occasionally 4-distoseptate; *hila* 2–3 µm wide, slightly protruding, darkened. *Chlamydospores* 10–12 µm diam, dark brown, globose to subglobose or cylindrical, grouped as chain, thick-walled, terminally and intercalary. *Sexual morph* not observed.

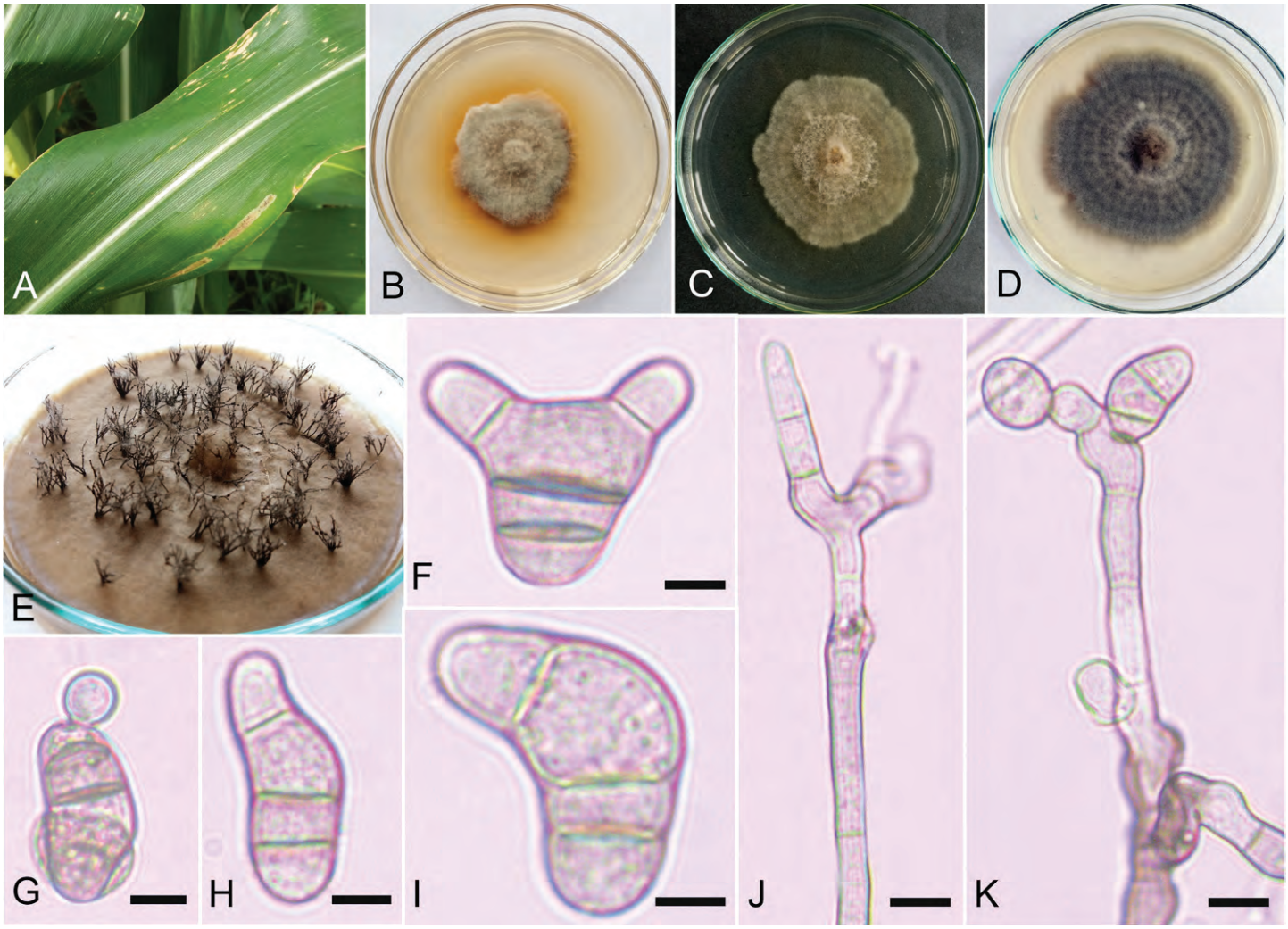

Fig. 2. *Curvularia aurantia* (USJCC–0096, ex-type). **A.** Host: lesions on leaf blade of *Zea mays*. **B–D.** Seven-day-old colony on PDA, CMA, and MEA, respectively. **E.** Stroma on 14-d-old colony on PDA. **F–I.** Conidia. **J.** Conidiophore. **K.** Conidiophore with immature conidia. Scale bars: F–I = 6 µm; J, K = 9 µm.

Culture characteristics: Colonies on PDA reaching 41 mm diam after 7 d at 25 °C, colonies from above: circular, margin entire, slightly raised, cottony appearance, pale brown at the margin, mouse grey in the centre, reverse: brown at the margin, black in the centre. Colonies on CMA reaching 68 mm diam after 7 d at 25 °C, colonies from above: circular, margin entire, flat, hairy appearance, white at the margin, pale brown and grey concentric ring growth; reverse: pale brown centre to margin. Colonies on MEA reaching 73 mm diam after 7 d at 25 °C, colonies from above: circular, margin entire, convex, cottony appearance, dark brown at the margin, white to dark green centre to periphery; reverse: brown at the margin, black in the centre.

Typus: **Sri Lanka**, Southern Province, Galle District, Yakkalamulla, N 6.078573 E 80.373524, on grains of *Oryza sativa*, 25 Aug. 2018, *H.S. Ferdinandez* (**holotype** USJ-H-009, culture ex-type USJCC–0029); *ibid.* (**isotype** USJ-H-010, culture USJCC–0062).

Known host and distribution: *Oryza sativa* in Sri Lanka (this study).

Notes: Based on the phylogenetic analyses and pairwise DNA sequence comparison results (Table 2), *C. vidyodayana* is closely related to *C. affinis*. The pairwise DNA sequence comparison revealed that *C. vidyodayana* is distinct from its closely related taxa. In the comparison of morphological characters with *C. affinis*, *C. vidyodayana* has smaller (19–25 µm), 3–4-distoseptate conidia while *C. affinis* has 27–49 × 8–13 µm, 4–5-distoseptate conidia. *Curvularia affinis* is a cosmopolitan fungus and has been recorded in Asian countries from several poaceous hosts including *Oryza sativa* (India, Malaysia, and Taiwan), *Pennisetum typhoides* (India), *Sorghum vulgare* (Taiwan) and *Zea mays* (Malaysia) (Farr & Rossman 2022). *Curvularia vidyodayana* was recorded on dried grains of *Oryza sativa*. Because of the disparities among *C. affinis* and *C. vidyodayana*, both in morphological and molecular data, we propose *C. vidyodayana* as a new species.

Curvularia asiatica Manamgoda *et al.* [as '*asianensis*'], *Sydowia* **64**: 262. 2012. MycoBank MB 545037. Fig. 4.

Saprobic on dried grains *Oryza sativa*. *Asexual morph*: On CMA *hyphae* 3–4 µm wide, hyaline, septate, branched. *Conidiophores* (99–)131–368(–495) × (4–)6–9(–12) µm ($\bar{x}$ = 249 × 8 µm, *n* = 20), pale brown to dark brown, micronematous to macronematous, septate, simple or branched, straight or flexuous, swollen at the apex. *Conidiogenous cells* (5–)6–8(–9) × (3–)4–6(–7) µm ($\bar{x}$ = 7 × 5 µm, *n* = 20), hyaline to pale brown, smooth-walled,

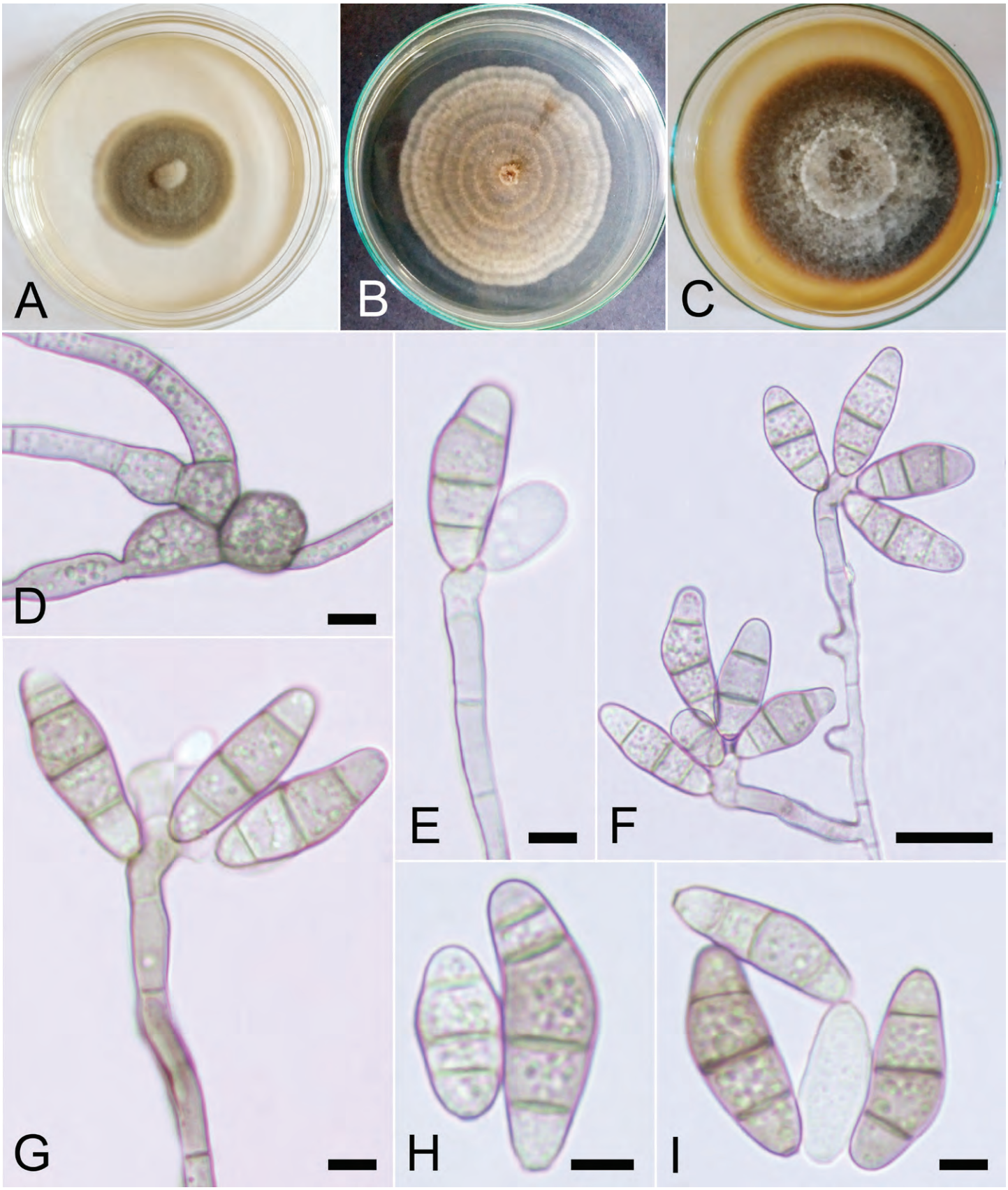

Fig. 3. *Curvularia vidyodayana* (USJCC–0029, ex-type). **A–C**. Seven-day-old colony on PDA, CMA, and MEA, respectively. **D.** Chlamydospores. **E–G.** Conidia attached to conidiophores. **H, I.** Conidia. Scale bars: D, E, G–I = 5 µm; F = 15 µm.

swollen, terminal or intercalary, mono- to polytretic. *Conidia* (16–)20–26(–34) × (7–)9–11(–14) µm ($\bar{x}$ = 23 × 10 µm, *n* = 30), hyaline to pale brown apical and basal cells, pale brown to dark brown matured conidia, straight or curved, asymmetrical, sometimes clavate, enlarged middle cells, dark brown septa, 3–4-distoseptate; *hila* 1–2 µm wide, protruding, darkened. *Sexual morph* not observed.

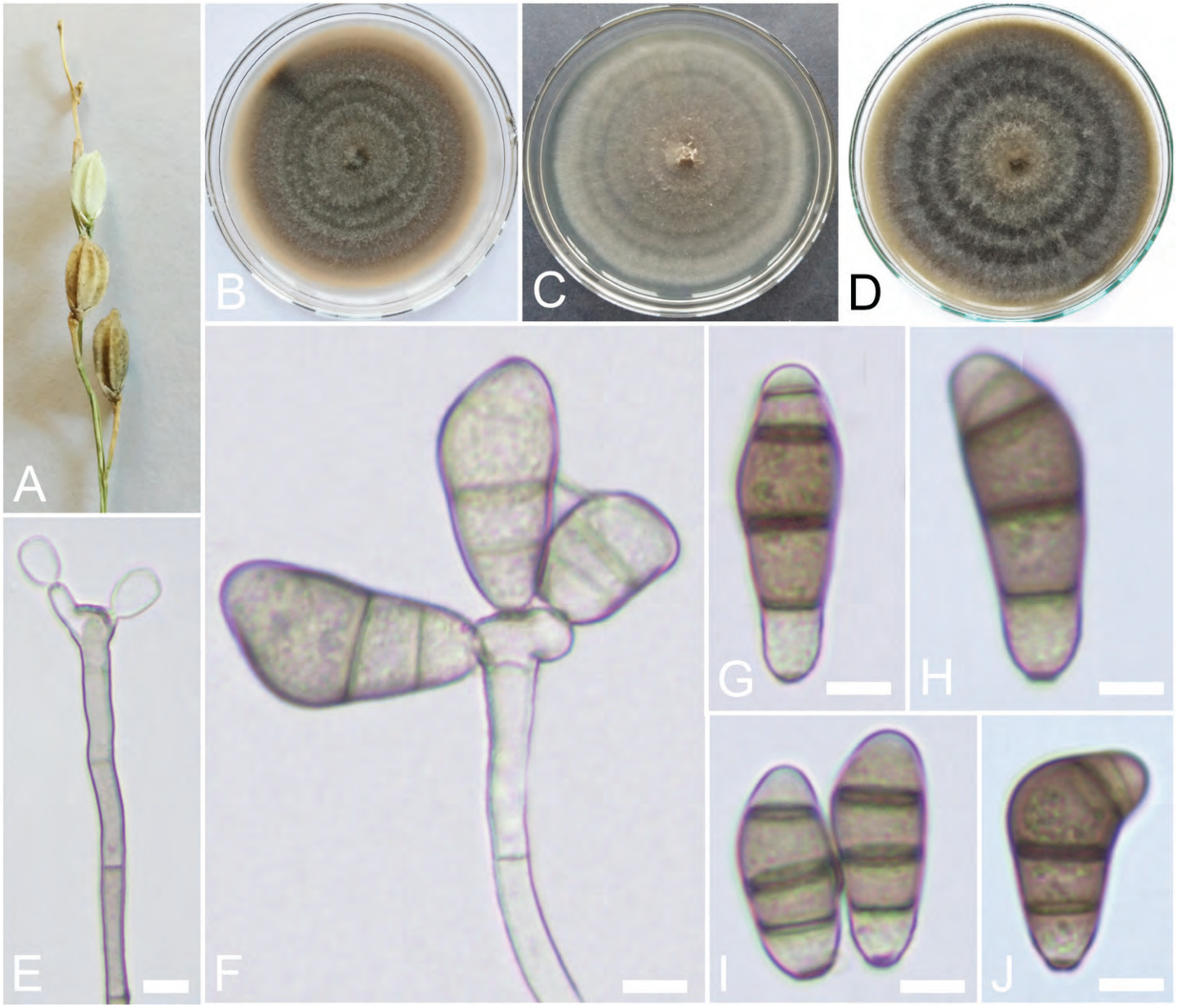

Fig. 4. *Curvularia asiatica* (USJCC–0075). **A.** Host: black spore masses on dried grains of *Oryza sativa*. **B–D.** Seven-day-old colony on PDA, CMA, and MEA, respectively. **E.** Immature conidia on conidiophore. **F.** Conidia attached to conidiophore. **G–J.** Conidia. Scale bars: E–H = 5 µm; I, J = 6 µm.

Culture characteristics: Colonies on PDA reaching 84 mm diam after 7 d at 25 °C, colonies from above: circular, margin entire, slightly convex, cottony appearance, dark brown at the margin, grey aerial mycelia, concentric ring growth; reverse: dark brown at the margin, black in the centre. Colonies on CMA reaching 90 mm diam after 7 d at 25 °C, colonies from above: circular, margin entire, flat, hairy appearance, white at the margin, pale brown in the centre, concentric ring growth; reverse: pale brown at the margin, dark brown in the centre. Colonies on MEA reaching 86 mm diam after 7 d at 25 °C, colonies from above: circular, margin entire, convex, cottony appearance, dark brown and brown concentric ring growth, mouse grey in the centre; reverse: dark brown at the margin, black in the centre.

Materials examined: **Sri Lanka**, North Western Province, Kurunegala District, Pilessa, N 7.464732 E 80.401004, on dried grains of *Oryza sativa*, 19 Feb. 2019, *H.S. Ferdinandez*, USJ-H-057, living culture USJCC–0075; *ibid.*, USJ-H-052, living culture, USJCC–0074; *ibid.*, USJ-H-045, living culture USJCC–0072.

Known hosts and distribution: Oryza sativa in Australia (Khemmuk *et al.* 2016); *Epipremnum pinnatum* (Wang *et al*. 2018) and *Saccharum officinarum* (Raza *et al.* 2019) in China; *Sansevieria trifasciata* in Malaysia (Kee *et al*. 2020); *Panicum* spp., *Saccharum officinarum,* and *Oryza sativa* in Thailand (Manamgoda *et al*. 2012a); *Festuca* sp., *Microstegium* sp., and *Paspalum* sp. in USA (Manamgoda *et al*. 2015); *Oryza sativa* in Sri Lanka (this study).

Notes: Isolates USJCC–0072, USJCC–0074, and USJCC–0075 were identified as *C. asiatica*. Fresh isolates were collected from dried grains of *Oryza sativa*. *Curvularia asiatica* has so far been recorded in Australia, China, Malaysia, Thailand, and USA (Farr & Rossman 2022). To our knowledge, this is the first record of *C. asiatica* from Sri Lanka.

Curvularia chiangmaiensis Y. Marín *et al*., *Mycosphere* **8**: 1565. 2017. MycoBank MB 822082. Fig. 5.

Fig. 5. *Curvularia chiangmaiensis* (USJCC–0064). **A.** Host: lesions on leaf of *Pennisetum pedicellatum*. **B–D.** Seen-day-old colony on PDA, CMA, and MEA, respectively. **E.** Conidiophore. **F, G.** Conidia attached to conidiophores. **H–J.** Conidia. Scale bars: E = 6 µm, F, G = 8 µm, H–J = 3 µm.

On leaf lesions of *Pennisetum pedicellatum*. *Asexual morph*: On CMA *hyphae* 4–5 µm wide, hyaline, septate, branched. *Conidiophores* (65–)91–262(–427) × (3–)4–6(–8) µm ($\bar{x}$ = 177 × 5 µm, *n* = 20), pale brown to dark brown, mostly subhyaline at the apex, micronematous to macronematous, septate, simple or branched, straight or flexuous with subnodulose and nodulose intercalary swellings, geniculate at the apex. *Conidiogenous cells* (6–)7–11(–13) × 4–5(–6) µm ($\bar{x}$ = 9 × 5 µm, *n* = 20), subhyaline, rarely brown, smooth-walled, subcylindrical to slightly swollen, terminal, mono- to polytretic. *Conidia* (20–)21–24(–25) × (7–)8–10(–11) µm ($\bar{x}$ = 22 × 9 µm, *n* = 30), hyaline to pale brown, mostly ellipsoidal, straight, sometimes curved, mostly enlarged third cell from base, 3-distoseptate; *hila* 1–2 µm wide, flat, darkened. *Sexual morph* not observed.

Culture characteristics: Colonies on PDA reaching 51 mm diam after 7 d at 25 °C, colonies from above: circular, margin entire, convex, cottony appearance, white at the margin, grey aerial mycelia; reverse: brown at the margin, black in the centre. Colonies on CMA reaching 73 mm diam after 7 d at 25 °C, colonies from above: circular, margin entire, flat, hairy appearance, white at the margin, pale brown concentric ring growth; reverse: pale brown at the margin, brown in the centre. Colonies on MEA reaching 70 mm diam after 7 d at 25 °C, colonies from above: circular, margin entire, convex, cottony appearance, dark green and grey concentric ring growth, mouse grey in the centre; reverse: dark brown at the margin, black in the centre.

Materials examined: **Sri Lanka**, North Western Province, Kurunegala District, Dambadeniya, N 7.378799 E 80.161981, on leaves of *Pennisetum pedicellatum*, 24 Oct. 2018, *H.S. Ferdinandez*, USJ-H-018, living culture USJCC–0064; Western Province, Gampaha District, Minuwangoda, N 7.170841 E 79.942587, on leaves of *Panicum virgatum,* 24 Oct. 2018, *H.S. Ferdinandez*, USJ-H-017, living culture USJCC–0022; Western Province, Gampaha District, Minuwangoda, N 7.170841 E 79.942587, on leaves of *Cyperus rotundus*, 24 Oct. 2018, *H.S. Ferdinandez*, USJ-H-037, living culture USJCC–0069; Western Province, Gampaha District, Ja-Ela, N 7.079222 E 79.906035, on leaves of *Oryza sativa*, 31 Jan. 2019, *H.S. Ferdinandez*, USJ-H-040, living culture USJCC–0070; North Central Province, Anuradhapura District, Thuruwila, N 8.247372 E 80.419233, on dried leaves of *Panicum virgatum,* 13 Jun. 2019, *D.S. Manamgoda*, USJ-H-074, living culture USJCC–0087; Uva Province, Monaragala District, Wellawaya, N 6.729670 E 81.104552, on leaves of *Ischaemum* sp., 21 Dec. 2021, *H.S. Ferdinandez*, USJ-H-116, living culture USJCC–0144.

Known hosts and distribution: *Saccharum officinarum* in China (Raza *et al.* 2019); *Zea mays* in Thailand (Marin-Felix *et al.* 2017b); *Cyperus rotundus, Ischaemum* sp., *Oryza sativa, Panicum virgatum,* and *Pennisetum pedicellatum* in Sri Lanka (this study).

Notes: Isolates USJCC–0022, USJCC–0064, USJCC–0069, USJCC–0070, USJCC–0087, and USJCC–0144 were identified as *C. chiangmaiensis*. So far, *C. chiangmaiensis* has only been recorded from *Saccharum officinarum* (Raza *et al.* 2019) and *Zea mays* (Marin-Felix *et al.* 2017b). All six fresh isolates collected from *Cyperus rotundus, Ischaemum* sp., *Oryza sativa, Panicum virgatum*, and *Pennisetum pedicellatum* in Sri Lanka update the novel host-fungal association records herein. To our knowledge, this is the first record of *C. chiangmaiensis* from Sri Lanka.

Curvularia falsilunata M. Raza *et al*., *Fungal Diversity* **99**: 54. 2019. MycoBank MB 556659. Fig. 6.

Leaf blight on *Zea mays*. *Asexual morph*: On CMA *hyphae* 3–4 µm wide, hyaline, septate, branched. *Conidiophores* (71–)87–244(–318) × 4–7(–9) µm ($\bar{x}$ = 166 × 5 µm, *n* = 20), hyaline to pale brown, micronematous to macronematous, septate, simple or branched, mostly straight, sometimes flexuous. *Conidiogenous cells* (7–)8–13(–16) × 4–5(–6) µm ($\bar{x}$ = 11 × 5 µm, *n* = 20), hyaline to pale brown, smooth-walled, subcylindrical, terminal or intercalary, mono- to polytretic. *Conidia* (18–)21–24(–26) × (5–)7–9(–10) µm ($\bar{x}$ = 23 × 8 µm, *n* = 30), hyaline to pale brown, ellipsoidal, slightly curved, 3-distoseptate; *hila* inconspicuous. *Chlamydospores* 11–16 µm diam, pale brown to dark brown,

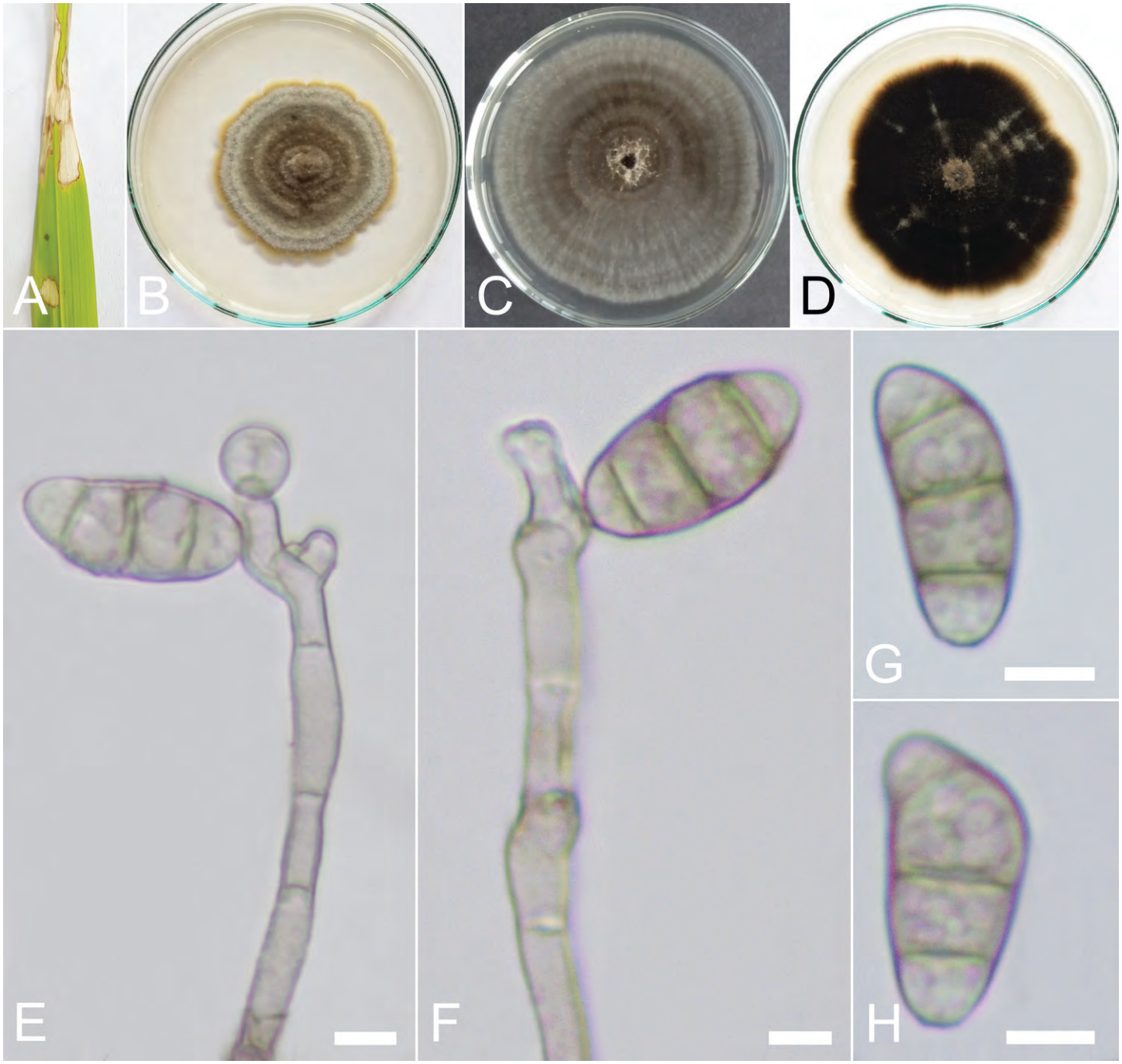

Fig. 6. *Curvularia falsilunata* (USJCC–0053). **A.** Host: leaf blights on *Zea mays*. **B–D.** Seven-day-old colony on PDA, CMA, and MEA, respectively. **E, F.** Conidia attached to conidiophores. **G, H.** Conidia. Scale bars: E, F = 6 µm; G, H = 7 µm.

globose to subglobose, thick-walled, grouped as chains or clumps, terminally and intercalary. *Sexual morph* not observed.

Culture characteristics: Colonies on PDA reaching 57 mm diam after 7 d at 25 °C, colonies from above: circular, margin undulate, slightly convex, cottony appearance, pale brown at the margin, dark brown and mouse grey concentric ring growth; reverse: dark brown at the margin, black in the centre. Colonies on CMA reaching 74 mm diam after 7 d at 25 °C, colonies from above: circular, margin entire, flat, hairy appearance, white at the margin, brown in the centre concentric ring growth; reverse: pale brown at the margin, dark brown in the centre. Colonies on MEA reaching 71 mm diam after 7 d at 25 °C, colonies from above: circular, margin undulate, flat, hairy appearance, dark brown at the margin, black in the centre; reverse: black in the centre to margin.

Materials examined: **Sri Lanka**, North Western Province, Kurunegala District, Nagollagama, N 7.728825 E 80.291368, leaf blights on *Zea mays*, 19 Dec. 2018, *H.S. Ferdinandez*, USJ-H-035, living culture USJCC–0053; North Western Province, Kurunegala District, Nagollagama, N 7.727944 E 80.280785, leaf spots on *Echinochloa crus-galli*, 19 Dec. 2018, *H.S. Ferdinandez*, USJ-H-034, living culture USJCC–0067; Uva Province, Monaragala District, Siyambalanduwa, N 6.892415 E 81.5454107, leaf blight on *Panicum maximum*, 21 Dec. 2021, *H.S. Ferdinandez*, USJ-H-112, living culture USJCC–0140.

Known hosts and distribution: *Saccharum officinarum* in China (Raza *et al.* 2019); *Echinochloa crus-galli*, *Panicum maximum,* and *Zea mays* in Sri Lanka (this study).

Notes: Isolates USJCC–0053, USJCC–0067, and USJCC–0140 were identified as *C. falsilunata*. *Saccharum officinarum* is the only reported host for *C. falsilunata* so far (Raza *et al.* 2019). The fresh isolates were collected from *Echinochloa crus-galli*, *Panicum maximum* and *Zea mays* during this study. Thus, novel host-fungal association records are updated herein. To our knowledge, this is the first record of *C. falsilunata* from Sri Lanka.

Curvularia geniculata (Tracy & Earle) Boedijn*, Bull. Jard. Bot. Buitenz*, 3 Sér. **13**: 129. 1923. MycoBank MB 265873. Fig. 7.
Basionym: *Helminthosporium geniculatum* Tracy & Earle, *Bull. Torrey Bot. Club* **23**: 207. 1896
Synonyms: *Cochliobolus geniculatus* R.R. Nelson, *Mycologia* **56**: 778. 1964.
Pseudocochliobolus geniculatus (R.R. Nelson) Tsuda *et al.*, *Mycologia* **69**: 1118. 1978.

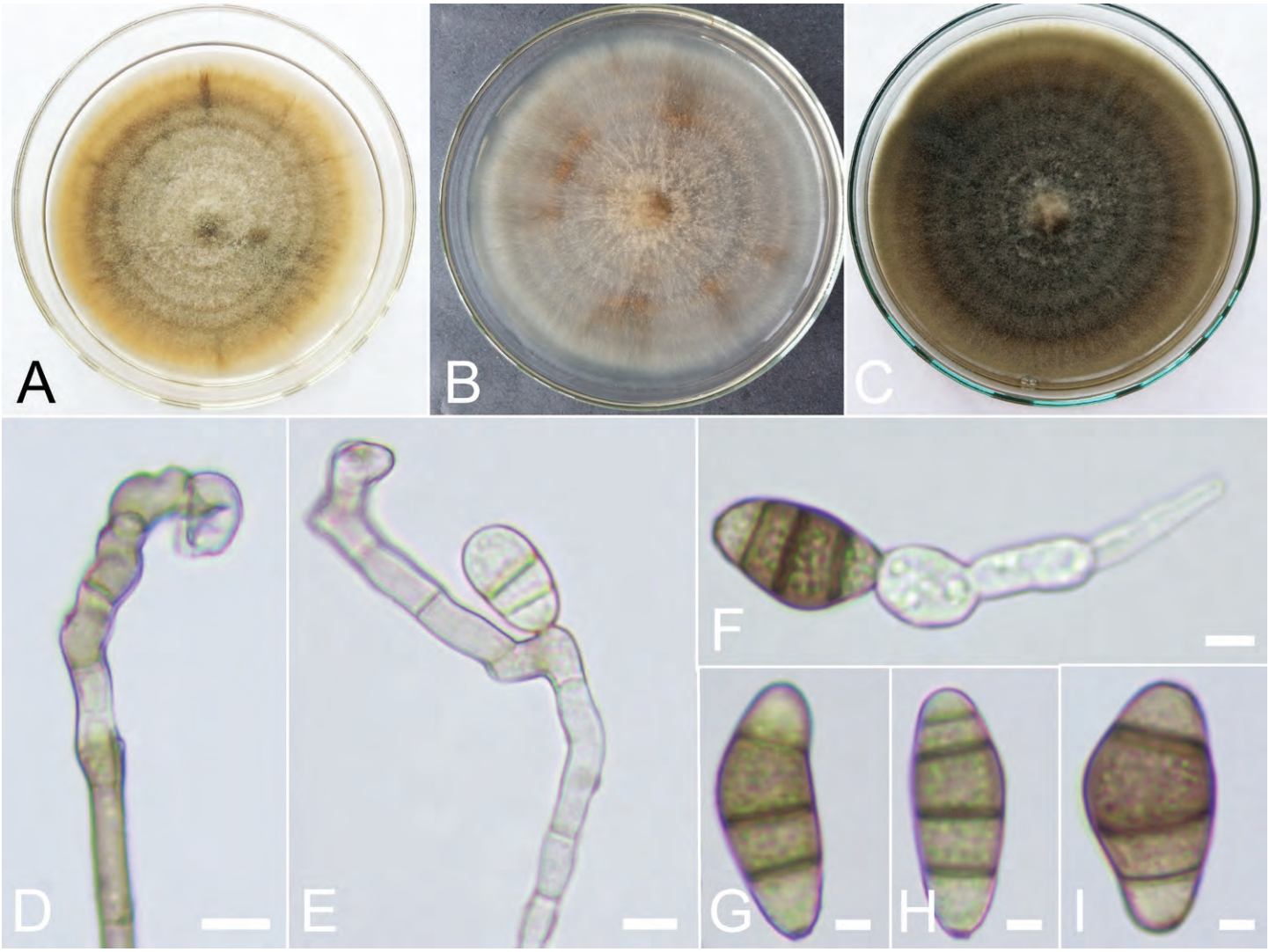

Fig. 7. *Curvularia geniculata* (USJCC–0073). **A–C.** Seven-day-old colony on PDA, CMA, and MEA, respectively. **D.** Conidiophore. **E.** Immature conidium attached to conidiophore. **F.** Germinating conidium. **G–I.** Conidia. Scale bars: D, E = 7 µm; F = 6 µm; G–I = 3 µm.

On leaves of *Saccharum officinarum*. *Asexual morph*: On CMA *hyphae* 3–4 µm wide, hyaline, septate, branched. *Conidiophores* (60–)104–274(–355) × 5–8(–9) µm ($\bar{x}$ = 189 × 6 µm, *n* = 20), pale brown to dark brown, micronematous to macronematous, septate, simple or branched, straight or flexuous, geniculate at the apex. *Conidiogenous cells* 6–10(–11) × (4–)5–6 µm ($\bar{x}$ = 8 × 5 µm, *n* = 20), subhyaline to pale brown, smooth-walled, subcylindrical, terminal or intercalary, mono- to polytretic. *Conidia* (15–)17–23(–29) × (7–)8–11(–13) µm ($\bar{x}$ = 20 × 9 µm, *n* = 30), hyaline to pale brown apical and basal cells, dark brown middle cells in matured conidia, straight or slightly curved, mostly ellipsoidal, sometimes obovoid, dark brown middle septa, enlarged middle cells, 3–4-distoseptate; *hila* 2–3 µm wide, protruding, darkened. *Sexual morph* not observed.

Culture characteristics: Colonies on PDA reaching 67 mm diam after 7 d at 25 °C, colonies from above: circular, margin entire, slightly raised, cottony appearance, pale brown at the margin, white and grey in the centre; reverse: pale brown at the margin, dark brown in the centre. Colonies on CMA reaching 76 mm diam after 7 d at 25 °C, colonies from above: circular, margin entire, flat, hairy appearance, white at the margin, mouse grey and pale brown in the centre; reverse: white at the margin, pale brown in the centre. Colonies on MEA reaching 77 mm diam after 7 d at 25 °C, colonies from above: circular, margin entire, slightly raised, cottony appearance, dark brown at the margin, black in the centre; reverse: black centre to margin.

Materials examined: **Sri Lanka**, Uva Province, Monaragala District, Sewanagala, N 6.404432 E 80.833103, on leaves of *Saccharum officinarum*, 20 Feb. 2019, *H. S. Ferdinandez*, USJ-H-046, living culture USJCC–0073; Western Province, Gampaha District, Yakkala, N 7.073656 E 80.032788, on grains of *Oryza sativa*, 20 Aug. 2018, *H.S. Ferdinandez*, USJ-H-004, living culture USJCC–0021, Western Province, Gampaha District, Minuwangoda, N 7.170841 E 79.942587, on leaves of *Panicum virgatum*, 24 Oct. 2018, *H.S. Ferdinandez*, USJ-H-012, living culture USJCC–0063; Central Province, Matale District, Palapathwela, N 7.556333 E 80.610611, on panicle of *Sorghum* sp. (Traditional-Swayanjatha), 12 Mar. 2019, *D.S. Manamgoda*, USJ-H-058, living culture USJCC–0037; Southern Province, Hambantota District, Mamadala, N 6.163880 E 80.957413, on leaf of *Zea mays*, 7 Aug. 2019, *H.S. Ferdinandez*, USJ-H-080, living culture USJCC–0039; North Central Province, Anuradhapura District, Thambuttegama, N 8.180449 E 80.321654, on leaves of *Ischaemum* sp., 13 Jun. 2019, *H. S. Ferdinandez*, USJ-H-071, living culture USJCC–0084.

Known hosts and distribution: Plurivorous and cosmopolitan (Farr & Rossman 2022); *Ischaemum* sp., *Oryza sativa*, *Panicum virgatum*, *Saccharum officinarum*, *Sorghum* sp. (Traditional-Swayanjatha), and *Zea mays* in Sri Lanka (this study).

Notes: Isolates USJCC–0021, USJCC–0063, USJCC–0073, USJCC–0037, USJCC–0084 and USJCC–0039 were identified as *C. geniculata*. *Curvularia geniculata* has been recorded as cosmopolitan fungus that most common in tropical regions from various host plant families. Six fresh isolates mentioned here were collected from *Ischaemum* sp., *Oryza sativa*, *Panicum virgatum*, *Saccharum officinarum*, *Sorghum* sp. (Traditional-Swayanjatha), and *Zea mays*. To our knowledge, this is the first record of *C. geniculata* from Sri Lanka.

Curvularia lonarensis Roh. Sharma & Rah. Sharma, *Front. Microbiol*. **7**: 10. 2016. MycoBank MB 814557. Fig. 8.

On leaf spots (approx. 5 cm long) of *Saccharum officinarum*. *Asexual morph*: On CMA *hyphae* 4–5 µm wide, hyaline, septate, branched. *Conidiophores* (75–)132–260(–321) × (4–)5–7(–8) µm ($\bar{x}$ = 196 × 6 µm, *n* = 20), pale brown to dark brown, micronematous to macronematous, septate, simple or branched, straight or flexuous, geniculate at the apex. *Conidiogenous cells* (6–)8–15(–18) × 5–6(–7) µm ($\bar{x}$ = 11 × 6 µm, *n* = 20), subhyaline to pale brown, subcylindrical to swollen, terminal or intercalary, mono- to polytretic. *Conidia* (19–)20–26(–32) × (7–)8–12(–13) µm ($\bar{x}$ = 23 × 10 µm, *n* = 30), hyaline to pale brown basal cell, dark brown matured conidia, straight or curved, mostly asymmetrical, sometimes Y-shaped, dark brown septa, enlarged middle cells, 3-distoseptate; *hila* 1–2 µm wide, flat, darkened. *Sexual morph* not observed.

Culture characteristics: Colonies on PDA reaching 87 mm diam after 7 d at 25 °C, colonies from above: circular, margin entire, flat, black centre, dark green at the margin; reverse: black centre to margin. Colonies on CMA reaching 86 mm diam after 7 d at 25 °C, colonies from above: circular, margin entire, flat, cottony appearance, white at the margin, grey and brown concentric ring growth; reverse: pale brown at the margin, dark brown in the centre. Colonies on MEA reaching 87 mm diam after 7 d at 25 °C, colonies from above: circular, margin entire, flat, dark brown to black from centre to margin; reverse: black from centre to margin.

Material examined: **Sri Lanka**, North Central Province, Anuradhapura District, Thuruwila, N 8.251407 E 80.421112, on leaf of *Saccharum officinarum*, 13 Jun. 2019, *H.S. Ferdinandez*, USJ-H-068, living culture USJCC–0082.

Known hosts and distribution: From a hyper alkaline and saline lake called "Lonar" in India (Sharma *et al.* 2016); *Saccharum officinarum* in Sri Lanka (this study).

Notes: Isolate USJCC–0082 was identified as *C. lonarensis*. The fresh isolate was collected from a leaf spot on *Saccharum officinarum*. *Curvularia lonarensis* has only recorded from a sample collected from a lake called "Lonar" in India. To our knowledge, this is a novel host record of *C. lonarensis* on *Saccharum officinarum* and first report from Sri Lanka.

Curvularia lunata (Wakker) Boedijn, *Bull. Jard. Bot. Buitenz*, 3 Sér. **13**: 127. 1933. MycoBank MB 269889. Fig. 9.
Basionym: *Acrothecium lunatum* Wakker, *De Ziektan van het Suikerriet op Java*: **196**. 1898.
Synonyms: *Cochliobolus lunatus* R.R. Nelson & F.A. Haasis, *Mycologia* **56**: 316. 1964.
Pseudocochliobolus lunatus (R.R. Nelson & F.A. Haasis) Tsuda *et al.*, *Mycologia* **69**: 1118. 1978.
Helminthosporium caryopsidum Sacc, *Ann. Mycol.* **12**: 313. 1914
Curvularia caryopsidum (Sacc.) S.C Teng., *Bull. Soc. Sci. Nat. Saône-et-Loire, ser. 2*: 760. 1964.

On leaf spots (approx. 0.5 cm long) of *Zea mays*. *Asexual morph*: On CMA *hyphae* 3–4 µm wide, hyaline, septate, branched. *Conidiophores* (59–)64–95(–116) × 3–4 µm ($\bar{x}$ = 80 × 4 µm, *n* = 20), hyaline to pale brown, micronematous to macronematous, septate, simple or branched, straight, sometimes flexuous,

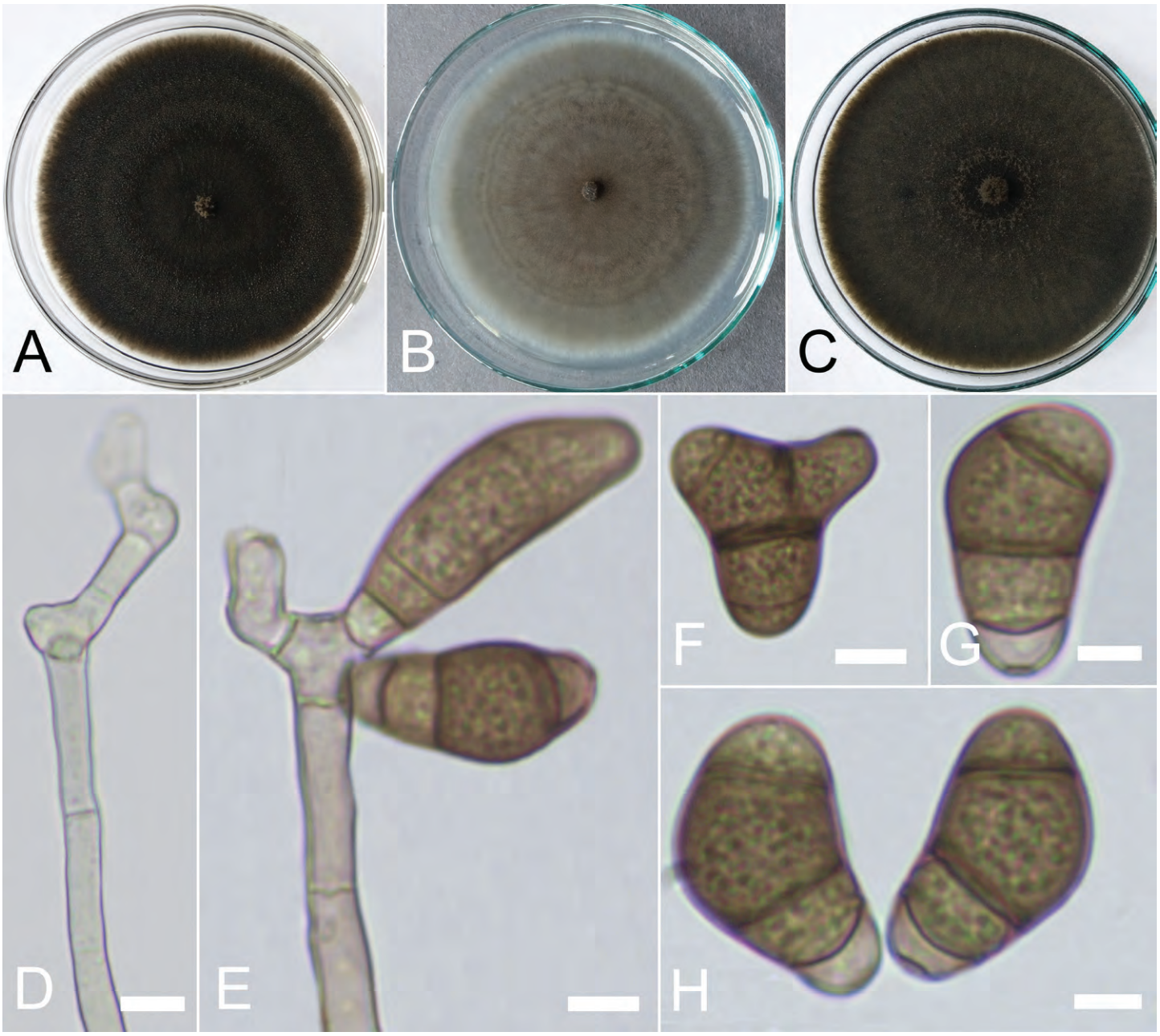

Fig. 8. *Curvularia lonarensis* (USJCC–0082). **A–C.** Seven-day-old colony on PDA, CMA, and MEA, respectively. **D.** Conidiophore. **E.** Conidia attached to conidiophore. **F–H.** Conidia. Scale bars: D, E, G, H = 6 µm; F = 7 µm.

swollen at the base and apex. *Conidiogenous cells* (6–)7–11(–12) × 4–7(–8) µm ($\bar{x}$ = 9 × 6 µm, *n* = 20), hyaline, smooth-walled, swollen, terminal or intercalary, mono- to polytretic. *Conidia* (16–)19–23(–26) × (6–)7–9 µm ($\bar{x}$ = 21 × 8 µm, *n* = 30), hyaline to pale brown, straight or curved, ellipsoidal, asymmetrical, enlarged third cell from base, 3–4-distoseptate; *hila* 1–2 µm wide, flat, darkened. *Chlamydospores* 7–10 µm diam, dark brown, globose, rarely subcylindrical, grouped as clumps, terminal or intercalary. *Sexual morph* not observed.

Culture characteristics: Colonies on PDA reaching 83 mm diam after 7 d at 25 °C, colonies from above: circular, margin entire, slightly convex, cottony appearance, pale brown at the margin, brown and grey mycelia in concentric ring growth; reverse: dark brown at the margin, black in the centre. Colonies on CMA reaching 85 mm diam after 7 d at 25 °C, colonies from above: circular, margin entire, flat, hairy appearance, white at the margin, pale brown and grey concentric ring growth; reverse: pale brown at the margin, dark brown in the centre. Colonies on MEA reaching 87 mm diam after 7 d at 25 °C, colonies from above: circular, margin entire, flat, cottony appearance, dark green margin, dull green to dark brown centre; reverse: dark brown at the margin, black in the centre.

Materials examined: **Sri Lanka**, Uva Province, Monaragala District, Wellawaya, N 6.609018 E 81.134455, on leaf spots of *Zea mays*, 21 Dec. 2021, *H.S. Ferdinandez*, USJ-H-124, living culture USJCC–0132; North Western Province, Kurunegala District, Uhumiya, N 7.466806 E 80.303167, on leaf of *Panicum virgatum*, 24 Oct. 2018, *H.S. Ferdinandez*, USJ-H-019, living culture USJCC–0023.

Known hosts and distribution: Plurivorous and cosmopolitan (most common in tropical regions) (Farr & Rossman 2022); *Panicum virgatum* and *Zea mays* (this study).

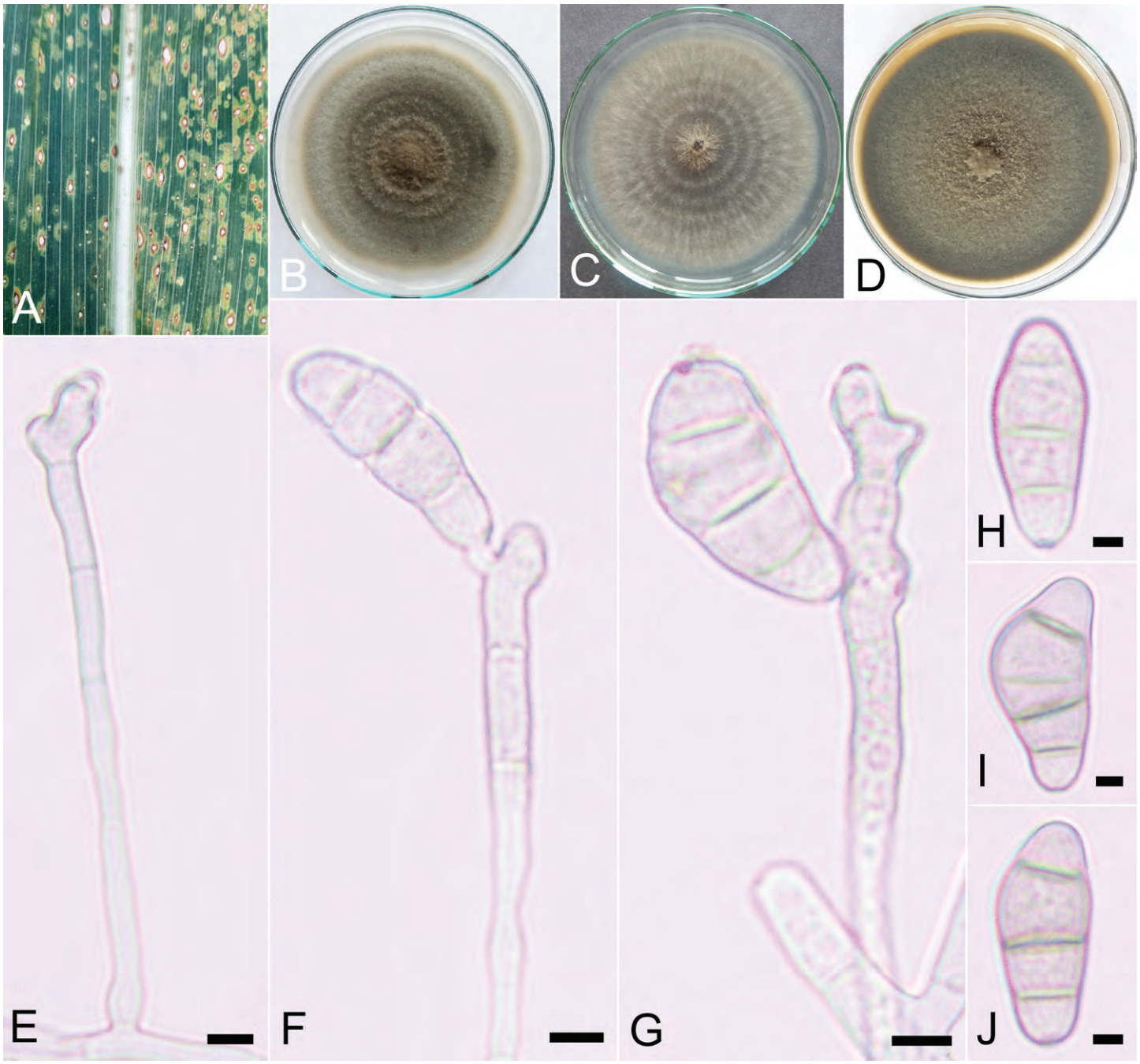

Fig. 9. *Curvularia lunata* (USJCC–0132). **A.** Host: small leaf spots on *Zea mays*. **B–D.** Seven-day-old colony on PDA, CMA, and MEA, respectively. **E.** Conidiophore. **F, G.** Conidia attached to conidiophore. **H–J.** Conidia. Scale bars: E–G = 5 µm; H–J = 3 µm.

Notes: Isolates USJCC–0132 and USJCC–0023 were identified as *C. lunata.* The fresh isolates were collected from *Panicum virgatum* and *Zea mays*. So far, *C. lunata* was recorded from *Oryza sativa* in Sri Lanka (Sivanesan 1987, Adikaram & Yakandawala 2020). To our knowledge, this is the first record of *C. lunata* from *Panicum virgatum* and *Zea mays* in Sri Lanka.

Curvularia muehlenbeckiae Madrid *et al*., *Persoonia* **33**: 56. 2014. MycoBank MB 806055. Fig. 10.

Saprobic on dried panicle of *Sorghum* sp. (Traditional-Swayanjatha). *Asexual morph*: On CMA *hyphae* 3–4 µm wide, hyaline, septate, branched. *Conidiophores* (94–)113–212(–255) × (5–)6–8 µm ($\bar{x}$ = 162 × 7 µm, *n* = 20), hyaline to pale brown, micronematous to macronematous, septate, simple or branched, flexuous, sometimes geniculate at the apex. *Conidiogenous cells* (6–)8–14(–17) × (4–)5–7(–8) µm ($\bar{x}$ = 11 × 6 µm, *n* = 20), hyaline to pale brown, smooth-walled, subcylindrical to irregularly shaped, terminal or intercalary, mono- to polytretic. *Conidia* (17–)19–22(–27) × (9–)10–12(–14) µm ($\bar{x}$ = 21 × 11 µm, *n* = 30), hyaline to pale brown apical and basal cells, pale brown to dark brown middle cells, straight or curved, usually ellipsoidal, sometimes asymmetrical or Y-shaped, rarely clavate, dark brown middle septa, enlarged middle cells, 3-distoseptate; *hila* inconspicuous. *Sexual morph* not observed.

Culture characteristics: Colonies on PDA reaching 79 mm diam after 7 d at 25 °C, colonies from above: circular, margin entire, flat, hairy appearance, pale brown at the margin, dark green to olive green from centre to periphery, concentric ring growth; reverse:

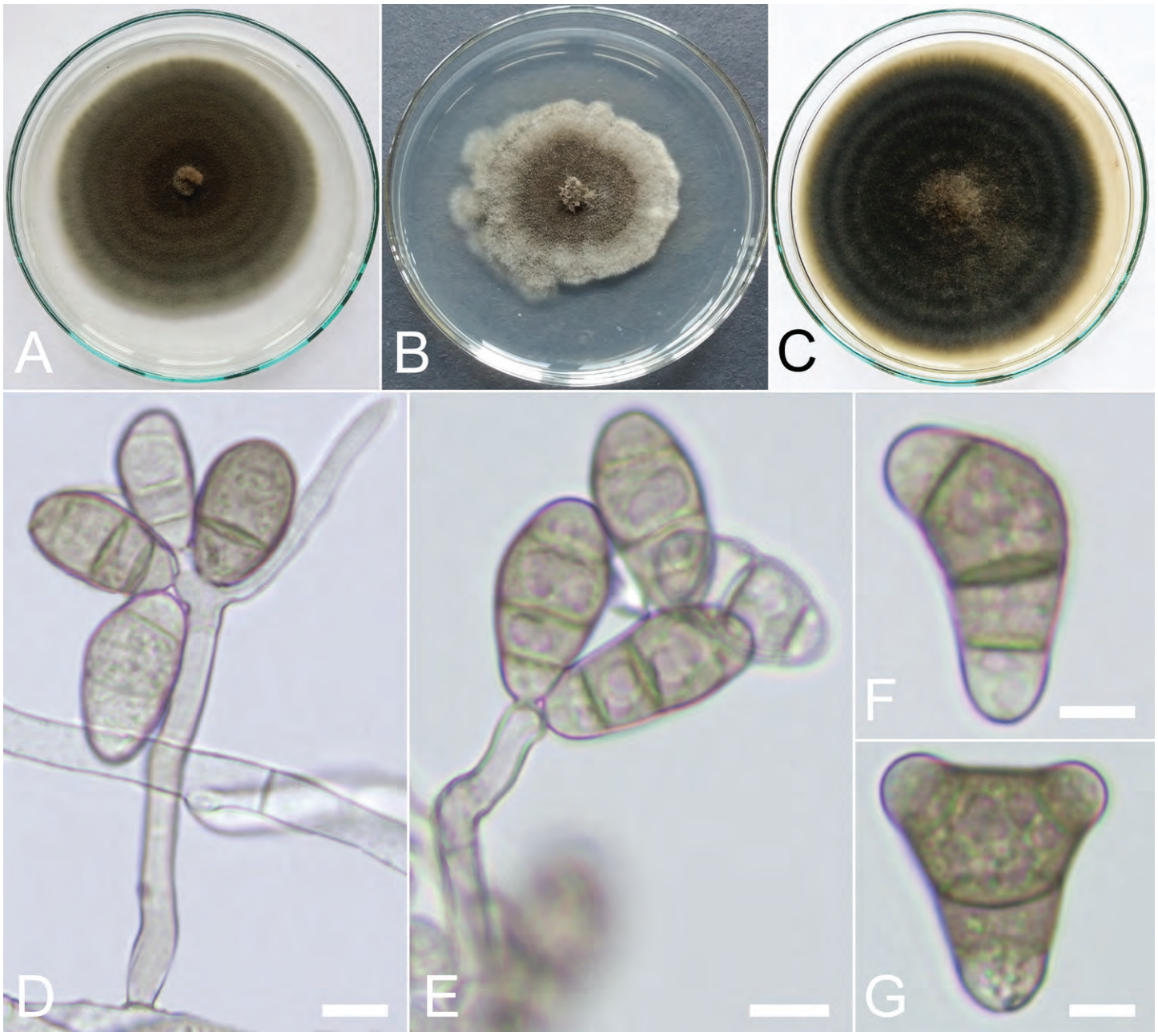

Fig. 10. *Curvularia muehlenbeckiae* (USJCC–0027). **A–C.** Seven-day-old colony on PDA, CMA, and MEA, respectively. **D, E.** Conidia attached to conidiophore. **F, G.** Conidia. Scale bars: D = 7 µm; E = 8 µm; F, G = 6 µm.

olive green at the margin, dark brown in the centre. Colonies on CMA reaching 61 mm diam after 7 d at 25 °C, colonies from above: circular, margin irregular, flat, hairy appearance, white at the margin, grey in the centre; reverse: grey at the margin, black in the centre. Colonies on MEA reaching 84 mm diam after 7 d at 25 °C, colonies from above: circular, margin entire, flat, hairy appearance, dark green and olive green concentric ring growth, black in the centre; reverse: pale brown at the margin, black in the centre.

Material examined: **Sri Lanka**, Central Province, Matale District, Palapathwela, N 7.556333 E 80.61061, on panicle of *Sorghum* sp. (Traditional-Swayanjatha), 12 Mar. 2019, *D.S. Manamgoda*, USJ-H-061, living culture USJCC–0027.

Known hosts and distribution: *Oryza* sp. in Australia (Khemmuk *et al.* 2016); *Cunninghamia lanceolate* (Cui *et al.* 2020), *Saccharum officinarum* (Raza *et al.* 2019), and *Zizania latifolia* (Chen *et al.* 2021) in China; *Muehlenbeckia* sp. in India (Madrid *et al.* 2014); *Sorghum bicolor* in Japan (Heidari *et al.* 2018); *Sorghum halepense* in Mexico (Olivas-Peraza *et al.* 2022); *Sorghum* sp. in USA (Heidari *et al.* 2018); *Sorghum* sp. (Traditional-Swayanjatha) in Sri Lanka (this study).

Notes: Isolate USJCC–0027 was identified as *C. muehlenbeckiae*. The fresh isolate was collected on a dried panicle of *Sorghum* sp. (Traditional-Swayanjatha). *Curvularia muehlenbeckiae* has so far recorded in Australia, China, India, Japan, Mexico, and USA (Farr & Rossman 2022). To our knowledge, this is the first record of *C. muehlenbeckiae* from Sri Lanka.

Curvularia plantarum M. Raza *et al*., *Fungal Diversity* **99**: 61. 2019. MycoBank MB 556664. Fig. 11.

Leaf spots on *Zea mays*. *Asexual morph*: On CMA *hyphae* 3–4 µm wide, hyaline, septate, branched. *Conidiophores* (142–)167–312(–410) × 5–7 µm ($\bar{x}$ = 240 × 6 µm, *n* = 20), pale brown, hyaline towards the apex, septate, simple or branched, flexuous, micronematous to semi-macronematous, geniculate. *Conidiogenous cells* (5–)6–11(–13) × (3–)4–5(–6) µm ($\bar{x}$ = 8 × 5 µm, *n* = 20), hyaline to pale brown, smooth-walled, subcylindrical to irregularly shaped, terminal or intercalary, mono- to polytretic. *Conidia* (19–)21–25(–28) × (7–)9–11(–12) µm ($\bar{x}$ = 23 × 10 µm, *n* = 30), hyaline apical and basal cells, pale brown to dark brown middle cells, mostly ellipsoidal, sometimes Y-shaped or ovate, straight or curved, enlarged middle cells, 3–4-distoseptate; *hila* 1–2 µm wide, slightly protruding. *Sexual morph* not observed.

Culture characteristics: Colonies on PDA reaching 82 mm diam after 7 d at 25 °C, colonies from above: circular, margin entire, flat, glistening surface, hairy appearance, pale olivaceous grey to white at the margin, olivaceous black and malachite green concentric ring growth; reverse: dark brown at the margin, black in the centre. Colonies on CMA reaching 87 mm diam after 7 d at 25 °C, colonies from above: circular, margin entire, flat, hairy appearance, white at the margin, grey and white concentric ring growth; reverse: pale brown at the margin, dark brown in the centre. Colonies on MEA reaching 83 mm diam after 7 d at 25 °C, colonies from above: circular, margin entire, flat, hairy appearance, pale olivaceous grey at the margin, olivaceous green in the centre; reverse: black in the centre to margin.

Materials examined: **Sri Lanka**, Southern Province, Galle District, Imaduwa, N 6.008556 E 80.373444, on leaves of *Zea mays*, 30 Aug. 2018, *H.S. Ferdinandez*, USJ-H-011, living culture USJCC–0054; North Western Province, Kurunegala District, Nagollagama, N 7.727944 E 80.280785, leaf spots on *Echinochloa crus-galli*, 19 Dec. 2018, *H.S. Ferdinandez*, USJ-H-036, living culture USJCC–0068; North Central Province, Anuradhapura District, Thuruwila, N 8.247372 E 80.419233, on leaf of *Zea mays*, 13 Jun. 2019, *H.S. Ferdinandez*, USJ-H-064, living culture USJCC–0078; Southern Province, Hambantota District, Mamadala, N 6.163880 E 80.957413, on leaf spots of *Zea mays*, 7 Aug. 2019, *H.S. Ferdinandez*, USJ-H-081, living culture USJCC–0091; Central Province, Matale District, Dambulla, N 7.903257 E 80.670494, on leaf spots of *Zea mays*, 15 Aug. 2019, *H.S. Ferdinandez*, USJ-H-088, living culture USJCC–0097; North Western Province, Puttalam District, Garayakgama, N 7.793702 E 79.955101, on panicles of *Oryza sativa,* 29 Jan. 2020, *H.S. Ferdinandez*, USJ-H-092, living culture USJCC–0033.

Known hosts and distribution: *Saccharum officinarum* in China (Raza *et al.* 2019); *Eleusine coracana, Oryza sativa, Panicum virgatum*, and *Paspalum* sp., in Sri Lanka (Ferdinandez *et al.* 2021); *Echinochloa crus-galli*, *Oryza sativa,* and *Zea mays* in Sri Lanka (this study).

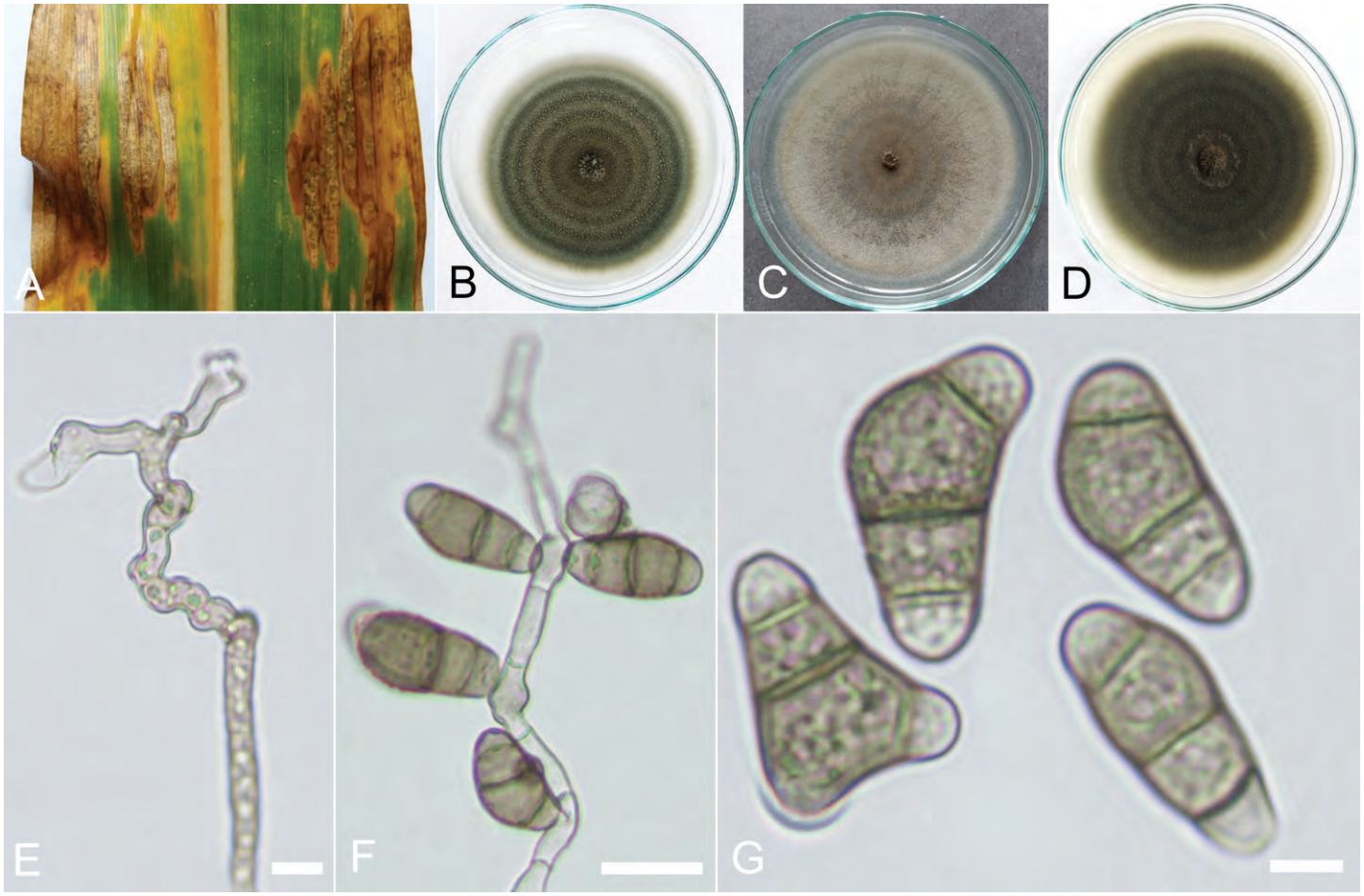

Fig. 11. *Curvularia plantarum* (USJCC–0091). **A.** Host: leaf lesions on *Zea mays*. **B–D.** Seven-day-old colony on PDA, CMA, and MEA, respectively. **E.** Conidiophore. **F.** Conidia attached to conidiophore. **G.** Conidia. Scale bars: E = 8 µm; F = 16 µm; G = 5 µm.

Notes: Fresh isolates USJCC–0054, USJCC–0091, USJCC–0078, and USJCC–0097 which were collected from *Zea mays*, USJCC–0068 from *Echinochloa crus-galli*, and USJCC–0033 from *Oryza sativa* were identified as *C. plantarum*. *Curvularia plantarum* was first reported from *Saccharum officinarum* in China. Later on, Ferdinandez *et al*. (2021) reported *C. plantarum* in Sri Lanka from *Eleusine coracana, Oryza sativa, Panicum virgatum*, and *Paspalum* sp. Thus, the occurrence of *C. plantarum* on *Echinochloa crus-galli*, and *Zea mays* update the novel host-fungal association records herein.

Curvularia pseudobrachyspora Y. Marín *et al*., *Mycosphere* **8**: 1569. 2017. MycoBank MB 822085. Fig. 12.

Saprobic on panicles of *Zea mays*. *Asexual morph*: On CMA *hyphae* 3–4 µm wide, hyaline, septate, branched. *Conidiophores* (70–)98–184(–204) × 5–6 µm ($\bar{x}$ = 141 × 6 µm, *n* = 20), pale brown to brown, micronematous to macronematous, simple, septate, straight or flexuous. *Conidiogenous cells* (6–)7–13(–16) × (3–)4–5(–6) µm ($\bar{x}$ = 10 × 5 µm, *n* = 20), hyaline to pale brown, smooth-walled, subcylindrical to swollen, terminal or intercalary, mono- to polytretic. *Conidia* (16–)19–23(–25) × (7–)8–9(–10) µm ($\bar{x}$ = 21 × 9 µm, *n* = 30), hyaline or pale brown basal and apical cells, pale brown to dark brown middle cells, straight or curved, ellipsoidal or asymmetrical, 3-distoseptate; *hila* inconspicuous. *Sexual morph* not observed.

Culture characteristics: Colonies on PDA reaching 49 mm diam after 7 d at 25 °C, colonies from above: circular, margin entire, flat, hairy appearance, pale brown at the margin, dull green and mouse grey concentric ring growth; reverse: brown at the margin, dark green in the centre. Colonies on CMA reaching

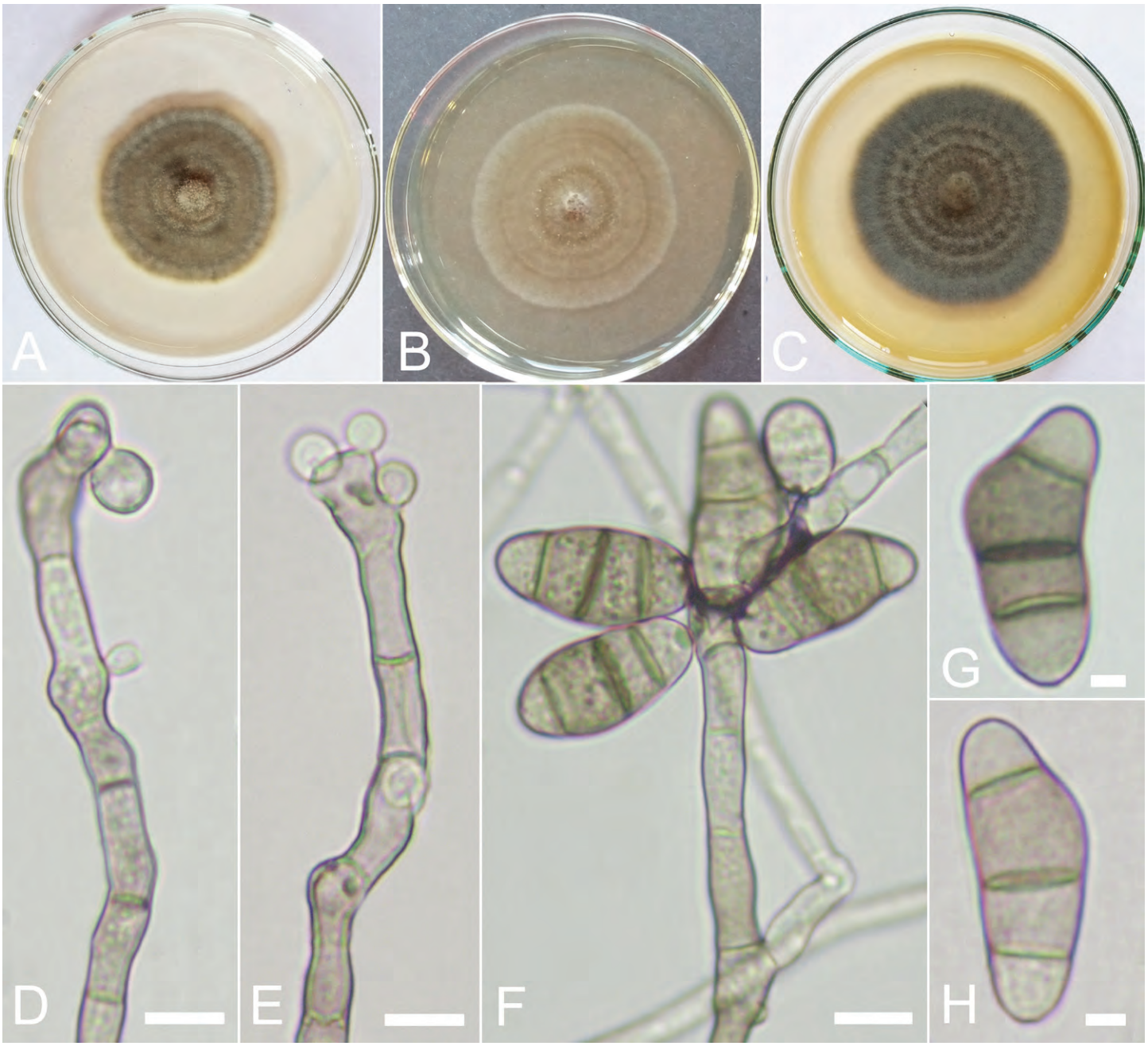

Fig. 12. *Curvularia pseudobrachyspora* (USJCC–0024). **A–C.** Seven-day-old colony on PDA, CMA, and MEA, respectively. **D, E.** Conidiophores with immature conidia. **F.** Conidia attached to conidiophore. **G, H.** Conidia. Scale bars: D, E = 7 µm; F = 9 µm; G, H = 3 µm.

57 mm diam after 7 d at 25 °C, colonies from above: circular, margin entire, flat, hairy appearance, white at the margin, grey and brown concentric ring growth; reverse: grey at the margin, brown in the centre. Colonies on MEA reaching 67 mm diam after 7 d at 25 °C, colonies from above: circular, margin entire, flat, velvety appearance, dull green and brown concentric ring growth; reverse: dark brown in the centre to margin.

Materials examined: **Sri Lanka**, Central Province, Matale District, Palapathwela, N 7.556333 E 80.61061, on panicle of *Zea mays*, 8 Nov. 2018, *D.S. Manamgoda*, USJ-H-030, living culture USJCC–0024; North Central Province, Anuradhapura District, Thuruwila, N 8.247372 E 80.419233, on leaves of *Panicum virgatum,* 13 Jun. 2019, *D.S. Manamgoda*, USJ-H-072, living culture USJCC–0085.

Known hosts and distribution: *Pennisetum* sp. in Denmark (Marin-Felix *et al.* 2020); *Cocos nucifera* in Ghana (Lekete *et al.* 2022); *Acorus calamus* in India (Srivastava *et al.* 2019); *Areca catechu* (Wang *et al.* 2019) and *Lilium brownii* var. *viridulumin* (Zeng *et al.* 2020) in China; *Eleusine indica* (Marin-Felix *et al.* 2017b) and *Oryza sativa* (Marin-Felix *et al.* 2020) in Thailand; *Agropyron repens* (Marin-Felix *et al.* 2020), *Cannabis sativa* (Marin *et al.* 2020), *Pennisetum glaucum*, and *Trisetum* sp. in USA (Marin-Felix *et al.* 2020); *Panicum virgatum* and *Zea mays* in Sri Lanka (this study).

Notes: Isolates USJCC–0024 and USJCC–0085 were identified as *C. pseudobrachyspora.* According to the phylogram (Fig. 1), two fresh isolates are closely related to *C. pseudobrachyspora* and *C. protuberans.* Ellipsoidal to obovoid conidia of *C. pseudobrachyspora* [(16–)21.5–27(–28.5) × 8–14 µm] are closer to morphological data from the fresh isolates in this study. Conidia of *C. protuberans* are obovoid to asymmetrical and smaller (9.5–25.5 × 6–19.5 µm) than the above-mentioned species. To date, *C. pseudobrachyspora* has never been reported from *Panicum virgatum* and *Zea mays.* Thus, novel host-fungal association records are updated herein. To our knowledge, this is the first record of *C. pseudobrachyspora* from Sri Lanka.

Curvularia verruculosa Tandon & Bilgrami *ex* M.B. Ellis, *Mycol. Pap.* **106**: 20. 1966. MycoBank MB 329454. Fig. 13.

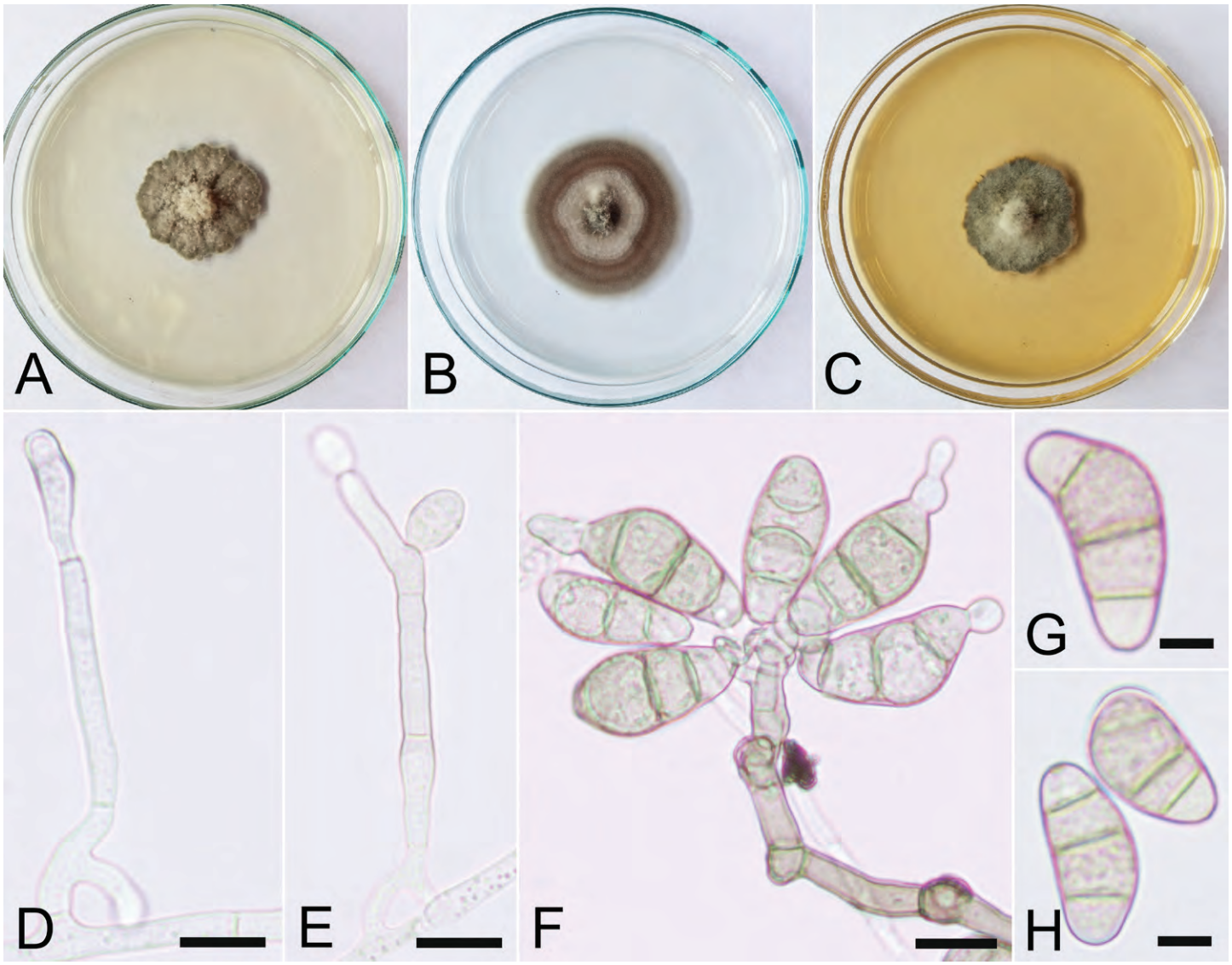

Fig. 13. *Curvularia verruculosa* (USJCC–0028). **A–C.** Seven-day-old colony on PDA, CMA, and MEA, respectively. **D.** Conidiophore. **E.** Conidiophore with immature conidia **F.** Conidia attached to conidiophore. **G, H.** Conidia. Scale bars: D–F = 12 µm; G, H = 6 µm.

Leaf blights on *Oryza sativa*. *Asexual morph*: On CMA *hyphae* 3–4 µm wide, hyaline, septate, branched. *Conidiophores* (50–)85–248(–333) × 4–7(–8) µm ($\bar{x}$ = 167 × 5 µm, *n* = 20), hyaline to pale brown, micronematous to macronematous, septate, simple, forming clamps at the base, straight or flexuous. *Conidiogenous cells* (7–)9–19(–22) × 4–6(–7) µm ($\bar{x}$ = 14 × 5 µm, *n* = 20), hyaline to pale brown, smooth-walled, subcylindrical to slightly swollen, terminal or intercalary, mono- to polytretic. *Conidia* (18–)22–28(–31) × (6–)8–10(–11) µm ($\bar{x}$ = 25 × 9 µm, *n* = 30), hyaline to pale brown, curved, obovoid or asymmetrical, enlarged middle cells, 3-distoseptate; *hila* inconspicuous. *Chlamydospores* 12–15 µm diam, dark brown, subglobose or cylindrical, thick-walled, terminally and intercalary. *Microconidiation* is observed. *Sexual morph* not observed.

Culture characteristics: Colonies on PDA reaching 26 mm diam after 7 d at 25 °C, colonies from above: irregular, margin undulate, slightly convex, velvety appearance, dull green at the margin, mouse grey in the centre; reverse: dark green at the margin, black in the centre. Colonies on CMA reaching 37 mm diam after 7 d at 25 °C, colonies from above: circular, margin entire, flat, hairy appearance, white at the margin, grey in the centre, dark brown to periphery, concentric ring growth; reverse: pale brown at the margin, dark brown in the centre. Colonies on MEA reaching 28 mm diam after 7 d at 25 °C, colonies from above: circular, margin undulate, convex, velvety appearance, dull green at the margin, grey in the centre; reverse: black centre to margin.

Materials examined: **Sri Lanka**, North Western Province, Puttalam District, Eluwankulama, N 8.273258 E 79.875740, leaf blights on *Oryza sativa*, 29 Jan. 2020, *H.S. Ferdinandez*, USJ-H-100, living culture USJCC–0028; Southern Province, Hambantota District, Mamadala, N 6.163880 E 80.957413, on leaf of *Zea mays*, 7 Aug. 2019, *H.S. Ferdinandez*, USJ-H-090, living culture USJCC–0031; North Western Province, Puttalam District, Garayakgama, N 7.793702 E 79.955101, leaf spots on *Saccharum officinarum*, 29 Jan. 2020, *H.S. Ferdinandez*, USJ-H-098, living culture USJCC–0103.

Known hosts and distribution: Plurivorous and cosmopolitan (Farr & Rossman 2022), *Oryza sativa, Saccharum officinarum*, and *Zea mays* in Sri Lanka (this study).

Notes: Isolates USJCC–0028, USJCC–0031, and USJCC–0103 were identified as *C. verruculosa*. It has been recorded from subtropical and tropical regions all over the world from a variety of host plant families. The fresh isolates were collected from *Oryza sativa, Saccharum officinarum,* and *Zea mays* during this study. To our knowledge, this is the first record of *C. verruculosa* from Sri Lanka.

DISCUSSION

The pleosporalean genus *Curvularia* is a well-established monophyletic genus in the *Dothideomycetes* with a wide geographic range. However, morphological characters and ITS sequences alone are insufficient to accurately identify individual species. Thus, majority of the recent publications have effectively used additional markers [*i.e.* 28S/large subunit of the nuclear ribosomal DNA (LSU), *gapdh*, second-largest subunit of RNA polymerase II (*rpb2*), and *tef1*] (Hernández-Restrepo *et al.* 2018, Manamgoda *et al.* 2012, 2015, Madrid *et al.* 2014, Marin-Felix *et al.* 2017a, 2017b, Tan *et al.* 2018, Marin-Felix *et al.* 2020). During the last five years, a considerable number of new *Curvularia* species have been introduced (Hyde *et al.* 2017, Marin-Felix *et al.* 2017a, b, 2020, Dehdari *et al.* 2018, Heidari *et al.* 2018, Liang *et al.* 2018, Mehrabi-Koushki *et al.* 2018, Tan *et al.* 2018, Tibpromma *et al.* 2018, Kiss *et al.* 2020, Raza *et al.* 2019, Zhang *et al.* 2020, Ferdinandez *et al.* 2021).

In this study, sequences of 36 fresh isolates were compared with those from type cultures as well as published reference cultures for species of *Curvularia*. Multi-locus phylogenetic analyses from a combined data set of ITS, *gapdh*, and *tef1* along with morphological attributes were employed to identify species and confirm the morphological differences of novel species. Both novel species *C. aurantia* and *C. vidyodayana* were collected from specimens of two major poaceous crops in Sri Lanka, *Zea mays* and *Oryza sativa*, respectively. Other than the novel species, new host records were updated for *C. chiangmaiensis*, *C. falsilunata*, *C. lonarensis*, *C. plantarum*, and *C. pseudobrachyspora*. Moreover, five species (*C. asiatica*, *C. geniculata*, *C. lunata*, *C. muehlenbeckiae*, and *C. verruculosa*) represent new records for the mycobiota of Sri Lanka. These new records reveal the need for redefining the host range and geographic distribution of species within the genus. Even though the species described here are generally minor pathogens, endophytes or saprobes, more concern should be noted as they can cause devastating diseases by switching life modes (Rai & Agarkar 2016). The present study is helpful as it conveys information necessary for future studies on control and management of fungi occurring in commercially important poaceous crops including *Oryza sativa*, *Saccharum officinarum*, *Sorghum* sp., and *Zea mays*. Moreover, description of these species improves knowledge of their host ranges and updates the checklist of fungi from Sri Lanka.

ACKNOWLEDGMENTS

The authors gratefully acknowledge the University of Sri Jayewardenepura for Research Grant ASP/01/RE/SCI/2018/036 and ASP/01/RE/SCI/2021/014 to work on the dematiaceous hyphomycetous fungi of Sri Lanka. The Department of Botany, Faculty of Applied Sciences and Department of Biosystems Technology, Faculty of Technology are thanked for laboratory facilities. The use of trade, firm, or corporation names in this publication is for the information and convenience of the reader. Such use does not constitute an official endorsement or approval by the United States Department of Agriculture or any other affiliated institute of the authors. The USDA is an equal opportunity employer. LAC is funded by USDA-ARS National Program 303, Project # 8042-22000-323-00D.

Conflict of interest: The authors declare that there is no conflict of interest.

REFERENCES

Adikaram NKB, Yakandawala DMD (2020). A checklist of plant pathogenic fungi and *Oomycota* in Sri Lanka. *Ceylon Journal of Science* **49**: 93–123.

Amaradasa BS, Madrid H, Groenewald JZ, *et al*. (2014). *Porocercospora seminalis gen. et comb. nov*., the causal organism of buffalo grass false smut. *Mycologia* **106**: 77–85.

Berbee ML, Pirseyedi M, Hubbard S (1999). *Cochliobolus* phylogenetics and the origin of known, highly virulent pathogens, inferred from ITS and glyceraldehyde-3-phosphate dehydrogenase gene sequences. *Mycologia* **91**(6): 964–977.

Chen X, Tang T, Chen C, *et al*. (2021). First report of *Curvularia* leaf spot caused by *Curvularia muehlenbeckiae* on *Zizania latifolia* in China. *Journal of Plant Pathology* **103**: 1073–1073.

Chomnunti P, Schoch CL, Aguirre-Hudson B, *et al*. (2011). *Capnodiaceae*. *Fungal Diversity* **51**: 103–134.

Chung WH, Tsukiboshi T (2005). A new species of *Curvularia* from Japan. *Mycotaxon* **91**: 49–54.

Crous PW, Cowan DA, Maggs-Kölling G, *et al*. (2020). Fungal Planet description sheets: 1112–1181. *Persoonia* **45**: 251–409.

Crous PW, Cowan DA, Maggs-Kölling G, *et al*. (2021a). Fungal Planet description sheets: 1182–1283. *Persoonia* **46**: 313–528.

Crous PW, Gams W, Stalpers JA, *et al*. (2004). MycoBank: an online initiative to launch mycology into the 21st century. *Studies in Mycology* **50**: 19–22.

Crous PW, Osieck ER, Jurjevi Ž, *et al*. (2021b). Fungal Planet description sheets: 1284–1382. *Persoonia* **47**: 178–374.

Cui WL, Lu XQ, Bian JY, *et al*. (2020). *Curvularia spicifera* and *Curvularia muehlenbeckiae* causing leaf blight on *Cunninghamia lanceolata*. *Plant Pathology* **69**: 1139–1147.

da Cunha KC, Sutton DA, Fothergill AW, *et al*. (2012). Diversity of *Bipolaris* species in clinical samples in the United States and their antifungal susceptibility profiles. *Journal of Clinical Microbiology* **50**: 4061–4066.

da Cunha KC, Sutton DA, Fothergill AW, *et al*. (2013). *In vitro* antifungal susceptibility and molecular identity of 99 clinical isolates of the opportunistic fungal genus *Curvularia*. *Diagnostic Microbiology and Infectious Disease* **76**: 168–174.

Dehdari F, Mehrabi-Koushki M, Hayati J (2018). *Curvularia shahidchamranensis sp. nov*., a crude oil-tolerant fungus. *Current Research in Environmental & Applied Mycology* **8**: 572–584.

Ellis MB (1971). *Dematiaceous Hyphomycetes*. Commonwealth Mycological Institute, Kew, UK.

Farr DF, Rossman AY (2022). *Fungal databases, U.S. National Fungus Collections, ARS, USDA. USA*. https://nt.ars-grin.gov/fungaldatabases/ (accessed 10 November 2022).

Ferdinandez HS, Manamgoda DS, Udayanga D, *et al*. (2021). Molecular phylogeny and morphology reveal three novel species of *Curvularia* (*Pleosporales*, *Pleosporaceae*) associated with cereal crops and weedy grass hosts. *Mycological Progress* **20**: 431–451.

Ferdinandez HS, Manamgoda DS, Udayanga D, *et al*. (2022). Molecular phylogeny and morphology reveal two new graminicolous species, *Bipolaris adikaramae sp. nov.* and *B. petchii sp. nov*., with new records of fungi from cultivated rice and weedy grass hosts. *Mycological Progress* **21**: 1–15.

Ferreira BW, Barreto RW (2020). Debunking *Duosporium*. *Mycological Progress* **19**: 715–723.

Hall TA (1999). BioEdit: A user-friendly biological sequence alignment editor and analysis program for Windows 95/98/NT. *Nucleic Acids Symposium Series* **41**: 95–98.

Heidari K, Mehrabi-Koushki M, Farokhinejad R (2018). *Curvularia mosaddeghii sp nov*., a novel species from the family *Pleosporaceae*. *Mycosphere* **9**: 635–646.

Hernandez-Restrepo M, Madrid H, Tan YP, *et al*. (2018). Multi-locus phylogeny and taxonomy of *Exserohilum*. *Persoonia* **41**: 71–108.

Hyde KD, Norphanphoun C, Abreu VP, *et al*. (2017). Fungal diversity notes 603–708: taxonomic and phylogenetic notes on genera and species. *Fungal Diversity* **87**: 1–235.

Ismail AM, Essa TA, Kamel SM, *et al.* (2016). First report of *Curvularia spicifera* causing leaf spot on tomato (*Solanum lycopersicum* L.) in Egypt. *Journal of Plant Pathology* **98**: 679.

Iturrieta-González I, Gené J, Wiederhold N, *et al*. (2020). Three new *Curvularia* species from clinical and environmental sources. *MycoKeys* **68**: 1–21.

Jayawardena RS, Hyde KD, Wang, S. *et al.* (2022). Fungal diversity notes 1512–1610: taxonomic and phylogenetic contributions on genera and species of fungal taxa. *Fungal Diversity* **117**: 1–272.

Katoh K, Standley DM (2013). MAFFT multiple sequence alignment software version 7: improvements in performance and usability. *Molecular Biology and Evolution* **30**: 772–780.

Kee YJ, Zakaria L, Mohd MH (2020). *Curvularia asianensis* and *Curvularia eragrostidis* associated with leaf spot of *Sansevieria trifasciata* in Malaysia. *Journal of Phytopathology* **168**: 290–296.

Khemmuk W, Shivas RG, Henry RJ, *et al*. (2016). Fungi associated with foliar diseases of wild and cultivated rice (*Oryza* spp.) in northern Queensland. *Australasian Plant Pathology* **45**: 297–308.

Kiss N, Homa M, Manikandan P, *et al*. (2020). New species of the genus *Curvularia*: *C. tamilnaduensis* and *C. coimbatorensis* from fungal keratitis cases in South India. *Pathogens* **9**: 1–14.

Lecellier A, Mounier J, Gaydou V, *et al.* (2014). Differentiation and identification of filamentous fungi by high-throughput FTIR spectroscopic analysis of mycelia. *International Journal of Food Microbiology* **168–169**: 32–41.

Lekete E, Osekre EA, Andoh-Mensah E (2022). First report of *Curvularia pseudobrachyspora* causing leaf spots disease on coconut (*Cocos nucifera* L.) seedlings in Ghana. *American Journal of Plant Sciences* **13**: 972–983.

Liang Y, Ran SF, Bhat J, *et al*. (2018). *Curvularia microspora sp. nov*. associated with leaf diseases of *Hippeastrum striatum* in China. *MycoKeys* **29**: 49–61.

Liu HF, Zha QC, Huang TC, *et al*. (2019). *Curvularia curculiginis* causes leaf spot and blight on *Curculigo capitulata* in China. *Australasian Plant Disease Notes* **14**: 1–5.

Madrid H, Da Cunha KC, Gené J, *et al*. (2014). Novel *Curvularia* species from clinical specimens. *Persoonia* **33**: 48–60.

Manamgoda DS, Cai L, Bahkali AH, *et al*. (2011). *Cochliobolus*: an overview and current status of species. *Fungal Diversity* **51**: 3–42.

Manamgoda DS, Cai L, McKenzie EHC, *et al*. (2012a). Two new *Curvularia* species from northern Thailand. *Sydowia* **64**: 255–266.

Manamgoda DS, Cai L, McKenzie EH, *et al*. (2012b). A phylogenetic and taxonomic re-evaluation of the *Bipolaris-Cochliobolus-Curvularia* complex. *Fungal Diversity* **56**: 131–144.

Manamgoda DS, Rossman AY, Castlebury LA, *et al*. (2014). The genus *Bipolaris*. *Studies in Mycology* **79**: 221–288.

Manamgoda DS, Rossman AY, Castlebury LA, *et al*. (2015). A taxonomic and phylogenetic re-appraisal of the genus *Curvularia* (*Pleosporaceae*): human and plant pathogens. *Phytotaxa* **212**: 175–198.

Marin MV, Wang NY, Coburn J, *et al*. (2020). First report of *Curvularia pseudobrachyspora* causing leaf spot on hemp (*Cannabis sativa*) in Florida. *Plant Disease* **104**: 3262.

Marin-Felix Y, Groenewald JZ, Cai L, *et al*. (2017a). Genera of phytopathogenic fungi: GOPHY 1. *Studies in Mycology* **86**: 99–216.

Marin-Felix Y, Hernández-Restrepo M, Crous PW (2020). Multi-locus phylogeny of the genus *Curvularia* and description of ten new species. *Mycological Progress* **19**: 559–588.

Marin-Felix Y, Senwanna C, Cheewangkoon R, *et al*. (2017b). New species and records of *Bipolaris* and *Curvularia* from Thailand. *Mycosphere* **8**: 1556–1574.

Mehrabi-Koushki M, Pooladi P, Eisvand P, *et al*. (2018). *Curvularia ahvazensis* and *C. rouhanii spp. nov.* from Iran. *Mycosphere* **9**: 1173–1186.

Olivas-Peraza DD, Leyva-Madrigal KY, Maldonado-Mendoza IE, *et al*. (2022). *Curvularia muehlenbeckiae* causing leaf spot on Johnson grass in Mexico. *Mycological Progress* **21**: 1–10.

Rai M, Agarkar G (2016). Plant–fungal interactions: what triggers the fungi to switch among lifestyles? *Critical Reviews in Microbiology* **42**: 428–438.

Rayner RW (1970). *A mycological colour chart*. Commonwealth Mycological Institute, UK

Raza M, Zhang ZF, Hyde KD, *et al*. (2019). Culturable plant pathogenic fungi associated with sugarcane in southern China. *Fungal Diversity* **99**: 1–104.

Richardson MJ (1990). *An annotated list of seed-borne diseases*. International Seed Testing Association, Zurich.

Safi A, Mehrabi-Koushki M, Farokhinejad R (2020). *Amesia khuzestanica* and *Curvularia iranica spp. nov*. from Iran. *Mycological Progress* **19**: 935–945.

Salim N, Mahindapala R (1981). Leaf blight disease of coconut 2. Studies on *Curvularia* sp. *Ceylon Coconut* **32**: 96–104.

Sharma R, Prakash O, Sonawane MS, *et al*. (2016). Diversity and distribution of phenol oxidase producing fungi from soda lake and description of *Curvularia lonarensis sp. nov*. *Frontiers in Microbiology* **7**: 1–19.

Sivanesan A (1987). Graminicolous species of *Bipolaris, Curvularia, Drechslera*, *Exserohilum* and their teleomorphs. *Mycological Papers* **158**: 1–261.

Song J, Liang JF, Mehrabi-Koushki M, *et al*. (2019). Fungal systematics and evolution: FUSE 5. *Sydowia* **71**: 141–245.

Srivastava AK, Saroj A, Nishad I, *et al*. (2019). First report of *Acorus calamus* leaf spot caused by *Curvularia pseudobrachyspora* in India. *Plant Disease* **103**: 767.

Tan YP, Bishop-Hurley SL, Shivas RG *et al*. (2022). Fungal Planet description sheets: 1436–1477. *Persoonia* **49**: 261–350.

Tan YP, Crous PW, Shivas RG (2016). Eight novel *Bipolaris* species identified from John L. Alcorn's collections at the Queensland Plant Pathology Herbarium (BRIP). *Mycological Progress* **15**: 1203–1214.

Tan YP, Crous PW, Shivas RG (2018). Cryptic species of *Curvularia* in the culture collection of the Queensland Plant Pathology Herbarium. *MycoKeys* **35**: 1–25.

Tan YP, Madrid H, Crous PW, *et al*. (2014). *Johnalcornia gen. et. comb. nov*., and nine new combinations in *Curvularia* based on molecular phylogenetic analysis. *Australasian Plant Pathology* **43**: 589–603.

Tibpromma S, Hyde KD, McKenzie EH, *et al*. (2018). Fungal diversity notes 840–928: micro-fungi associated with *Pandanaceae*. *Fungal Diversity* **93**: 1–160.

Tomaso-Peterson M, Jo YK, Vines PL, *et al*. (2016). *Curvularia malina sp. nov*. incites a new disease of warm-season turf grasses in the southeastern United States. *Mycologia* **108**: 915–924.

Victoria Arellano AD, Guatimosim E, da Silva GM, *et al*. (2021). Fungi causing leaf spot diseases in *Lolium multiflorum* in Brazil. *Mycological Progress* **20**: 1175–1190.

Vu D, Groenewald M, De Vries M, *et al*. (2019). Large-scale generation and analysis of filamentous fungal DNA barcodes boosts coverage for kingdom fungi and reveals thresholds for fungal species and higher taxon delimitation. *Studies in Mycology* **92**: 135–154.

Wang H, Xu L, Zhang Z, *et al*. (2019). First report of *Curvularia pseudobrachyspora* causing leaf spots in *Areca catechu* in China. *Plant Disease* **103**: 150.

Wang Y, Pan XJ, Zhang Q, *et al*. (2018) First report of *Curvularia asianensis* causing leaf blotch of *Epipremnum pinnatum* in Guangxi autonomous region of China. *Plant Disease* **102**: 1854.

Zeng H, Li R, Lu Q, *et al*. (2020). First report of bulb rot on lily caused by *Curvularia pseudobrachyspora* in China. *Plant Disease* **104**: 291.

Zhang J, Li M (2009). A new species of *Bipolaris* from the halophyte *Sesuvium portulacastrum* in Guangdong Province, China. *Mycotaxon* **109**: 289–300.

Zhang M, Wu H, Pei Z, *et al*. (2007). A new species and a new variety of *Curvularia* in China. Southwest China. *Journal of Agricultural Sciences* **20**: 1144– 1145.

Zhang M, Zhang T (2004). Taxonomic studies of *Curvularia* from China I. A new species and a new Chinese record on *Gramineae*. *Mycosystema* **23**: 328–330.

Zhang Q, Yang ZF, Cheng W, *et al*. (2020). Diseases of *Cymbopogon citratus* (*Poaceae*) in China: *Curvularia nanningensis sp. nov*. *MycoKeys* **63**: 49–67.

FUSE

Fungal Systematics and Evolution

Volume 12
DECEMBER 2023
PAGES 247–254

doi.org/10.3114/fuse.2023.12.12

Ducellieriales ord. nov. and evidence for a novel clade of endobiotic pollen-infecting "lagenidiaceous" *Peronosporomycetes*

A.T. Buaya[1,2*], M. Thines[1,2]

[1]Goethe-Universität Frankfurt am Main, Department of Biological Sciences, Institute of Ecology, Evolution and Diversity, Max-von-Laue Str. 13, D-60438 Frankfurt am Main, Germany
[2]Senckenberg Biodiversity and Climate Research Centre, Senckenberganlage 25, D-60325 Frankfurt am Main, Germany

*Corresponding author: anthony.buaya@senckenberg.de

Key words:
biotrophic oomycetes
chlorophyte algae
Ducellieria
new order
Oomycetes
phylogeny
xanthophyte algae

Abstract: The genus *Ducellieria* (*Ducellieriaceae*) contains three species (*D. chodatii, D. tricuspidata, D. corcontica*), and a single variety (*D. chodatii* var. *armata*) of obligate endobiotic pollen parasites. These organisms have been first assigned to the green alga genus *Coelastrum*, as they form very similar spherical structures, but the observation of heterokont zoospores has led to their reclassification to the phylum *Oomycota*. However, despite their widespread nature, these organisms are only known from their descriptive morphology, and life cycle traits of some species still remain incompletely known. Only the type species, *D. chodatii*, has been rediscovered several times, but the phylogeny of the genus remains unresolved, since none of its species has been studied for their molecular phylogeny. At present the genus is still included in some algal databases. To clarify the evolutionary affiliation of *Ducellieria*, efforts were undertaken to isolate *D. chodatii* from pollen grains, to infer its phylogenetic placement based on nrSSU sequences. By targeted isolation, the pollen endoparasitoid was rediscovered from three lakes in Germany (Mummelsee, Okertalsperre, Knappensee). Apart from the typical coelastrum-like spheroids, oomycetes sporulating directly from pollen grains in a lagenidium-like fashion were observed, and molecular sequences of both types of oomycetes were obtained. Phylogenetic reconstruction revealed that coelastrum-like and lagenidium-like forms are unrelated, with the former embedded within the deep branching early-diverging lineages, and the later stage forming a distinct clade in *Peronosporales*. Consequently, the life cycle of *D. chodatii* needs careful revision using single-spore isolates of the species, to infer if previous lifecycle reconstructions that involve various different thallus types are stages of a single species or potentially of several ones.

Citation: Buaya AT, Thines M (2023). *Ducellieriales ord. nov.* and evidence for a novel clade of endobiotic pollen-infecting "lagenidiaceous" *Peronosporomycetes*. *Fungal Systematics and Evolution* **12**: 247–254. doi: 10.3114/fuse.2023.12.12
Received: 12 July 2023; **Accepted:** 31 August 2023; **Effectively published online:** 19 October 2023
Corresponding editor: P.W. Crous

INTRODUCTION

Freshwater holocarpic oomycetes are diverse and widespread (Karling 1942, Sparrow 1960, Dick 2001, Buaya & Thines 2020). They are mostly obligate biotrophic endobiotic parasites, infecting various hosts, including diatoms (Sparrow 1960, Buaya *et al*. 2019a, Buaya & Thines 2019b, 2020, 2021, Thines & Buaya 2022), filamentous macroalgae (Zopf 1884, de Wildeman 1893, 1896, 1897, Scherffel 1925), cyanobacteria (Ingold 1949), plants (Zopf 1887, Karling 1981), oomycetes (Cornu 1872, Barrett 1912, McLarty 1941, Whiffen 1942, 1946, Sparrow 1950, Buaya *et al*. 2019d), and invertebrate animals (Sparrow 1939, Drechsler 1940, Karling 1944, Barron 1980, Glockling & Beakes 2000). Most of the species belong to the early-diverging lineages of oomycetes (*e.g. Diatomophthora, Olpidiopsis*), while others are in the crown clades of *Saprolegniomycetes* (*e.g. Aphanomycopsis, Ectrogella*) and *Peronosporomycetes* (*e.g. Lagena, Lagenidium*) (Karling 1942, Sparrow 1960, Dick 2001, Buaya & Thines 2000). But despite recent progress, the taxonomic affiliations of most freshwater holocarpic oomycetes remain obscure, since many species have not been investigated with respect to their molecular phylogeny (Beakes & Thines 2017, Buaya & Thines 2020).

In particular, the pollen-parasitic oomycetes, of which less than a dozen species have been reported, remain unresolved, despite their widespread occurrence and potential ecological role for carbon cycling in freshwater environments (Kagami *et al*. 2014, Masigol *et al*. 2019). Records of pollen inhabiting oomycetes are known from both gymnosperm and angiosperm plants, and almost none of them have been rediscovered, to date (Sparrow 1960). These include two varieties classified in the genus *Lagenidium*, (*L. pygmaeum* var. *pygmaeum, L. pygmaeum* var. *pygmaeoides*) (Zopf 1887, Karling 1981), one each from *Aphanomycopsis* (*A. saprophytica*) (Karling 1968), and *Anisolpidium* (*A. saprobium*) (Karling 1968), a handful of enigmatic species classified into genus *Ducellieria* (*D. chodatii*, *D. corcontica, D. tricuspidata*) (Teiling 1957, Kusel Fetzmann & Nouak 1981, Hesse *et al.* 1989, Matula 1980), and the

provisional genus *Lagenidicopsis* (*L. arctica*) (Artemchuk 1972). Dick (2001) subsequently reclassified some of these parasites, and reassigned *L. pygmaeum* to *Cornumyces*, *L. pygmaeum* var. *pygmaeoides* to *Pleocystidium*, *A. saprophytica* to *Hyphochytrium*, and introduced the family *Ducellieriaceae* to accommodate the pine pollen pathogen *D. chodatii* within *Oomycota*. However, there are no molecular data supporting the placement of these species, including also the type species of the genus *Ducellieria*, *D. chodatii*, which is still sometimes listed as a member of the yellow-green algae family *Botryochloridaceae* of the class *Xanthophyceae* (Teiling 1957, Coute 1984) in algae databases (*e.g.* AlgaeBase) and papers in phycology (Wehr & Sheath 2003, Ettl 2009, Godínez Ortega 2017).

The genus *Ducellieria* was described by Teiling in 1957. It currently comprises three species, its types species, *Ducellieria chodatii*, and with two additional species, *D. corcontica* and *D. tricuspidata* (Matula 1980), along with a variety, *D. chodatii* var. *armatum*. In addition, one species, *D. bicuspidata*, has not been validly described, as no type specimen had been indicated (Oblinger 2005). In any case, the description provided does not contain enough detail to infer if it can be considered a member of the genus. *Ducellieria* is primarily characterized by forming colourless, multicellular, coelastrum-like spherical aggregates, connected by hollow spines, and outward-directed spines (Kusel Fetzmann & Nouak 1981, Hesse *et al.* 1989). The spherical aggregate is formed at the tip of a discharge tube from an endobiotic non-septate holocarpic thallus (Kusel Fetzmann & Nouak 1981, Hesse *et al*. 1989, Stoyneva *et al.* 2013). *Ducellieria chodatii* recurs seasonally in parallel to the peak of the pollen bloom of *Pinus* and *Picea* species, but has only rarely been reported (Kusel Fetzmann & Nouak 1981, Hesse, Kusel Fetzmann & Carniel 1989, Gorbulin 2012, Stoyneva *et al.* 2013, Bancsó 2023).

Ducellieria with its type species, *D. chodatii*, has been reclassified multiple times into different taxonomic lineages. Originally described as *Coelastrum chodatii* by Ducellier (1915) in the green algae family *Chlorophyceae* (Ducellier 1915, Bourelly 1968, Komarek & Fott 1983), the parasite has been reclassified into *Ducellieria chodatii* by Teiling (1957) with its own genus in the yellow-green algae family *Xanthophyceae* containing three species (*D. chodatii, D. corcontica, D. tricuspidata*) (Teiling 1957, Matula 1980), and one variety, *D. chodatii* var. *armata* (Teiling 1957), of which only *D. chodatii* has been proven to be an oomycete by electron microscopy (Hesse *et al.* 1989). Subsequently, a detailed re-examination of its life cycle and cellular ultrastructure confirmed its identification as an oomycete, and it was initially placed in the *Saprolegniales* (Hesse *et al.* 1989). Dick (2001) reclassified the species into its own family (*Ducellieriaceae*), provisionally assigning it to the *Leptomitales*, but excluding *D. tricuspidata* and *D. chodatii* var. *armata*.

In order to resolve the phylogeny of the type species of *Ducellieria*, attempts were made to isolate this oomycete from different freshwater environments and geographic locations in Germany. While screening for holocarpic oomycete parasites from pollen grains from the lakes Mummelsee, Okertalsperre, and Knappensee, the species was rediscovered, and it was the aim of this study to clarify its phylogenetic placement.

MATERIALS AND METHODS

Isolation, characterisation, and host and parasite dual culture attempts

Dense pollen films (predominantly from *Pinus sylvestris* and *Picea abies*) were collected from shores of the lake Mummelsee, in the state of Baden-Württemberg, Southwest Germany (48°35’53.1”N, 8°12’03.9”E), the reservoir Okertalsperre in the state of Sachsen-Anhalt, Central Germany (51°51’02.9”N, 10°27’33.0”E), the lake Knappensee (50°26’27.3”N, 8°53’55.2”E), and the pond Forbachteich (50°22’47.2”N, 8°36’45.1”E) in the state of Hessen, Central Germany. Pollen clusters with living aggregates of *Ducellieria chodatii* were collected in June 2020 from Mummelsee, Knappensee, and Forbachteich, and in June 2021 from Mummelsee and Okertalsperre, by directly collecting masses of floating pollen grains using multiple 50 mL sterile plastic tubes (Sarstedt, Nümbrecht, Germany). About 10 mL of pollen concentrates were poured onto several Petri dishes (150 × 20 mm) (Sarstedt, Nümbrecht, Germany) on the day of collection, and 100 mL of autoclaved distilled water were added to dilute the samples. Subsequently, samples were screened for *D. chodatii* using an inverted compound light microscope (AE31, Motic, Xiamen, China) and were individually picked using a 10 µL pipette (Brandt, Wertheim, Germany), rinsed multiple times in autoclaved deionized water, and transferred to 2 mL tubes containing 0.5 mL RNA*Later* solution (Invitrogen, Thermo Fisher, Lithuania) or 70 % ethanol (VWR, France) for subsequent DNA extraction. Approximately 100 spherical coelastrum-like aggregates, and pine pollen grains with endobiotic oomycete thalli were collected in this manner for DNA extraction. Samples preserved in 70 % ethanol were deposited in the herbarium collection of the Senckenberg Museum of Natural History (Herbarium Senckenbergianum, FR), Cryptogams Section, Frankfurt am Main (accession numbers (Forbachteich 2020 isolate FR-0046136, Knappensee 2020 isolate FR-0046137) for pollen grains with endobiotic thalli, and (Mummelsee 2021 isolate FR-0046135, Okertalsperre 2021 isolate FR-0046156) for coelastrum-like spheroids). Morphological characterisation of the parasite was done as described earlier (Buaya *et al*. 2022) using a compound light microscope (Imager2, Carl Zeiss Göttingen, Germany) with DIC, and photographs were taken using a Zeiss Axiocam MRc5 (Carl Zeiss, Göttingen, Germany), or an SLR digital camera (EOS 500D, Canon, Tokyo Japan) for life cycle observations, mounted on the inverted compound light microscope. To inhibit motility of freshly released zoospores for microscopic photography, small amounts of Sorbitol (Carl Roth GmbH, Karlsruhe, Germany) solution (2 mg/mL) were added to the slides.

Parasite cultures with pollen grains were also attempted using living spherical aggregates of *D. chodatii* and pine pollen directly collected from pine trees (*P. sylvestris*) in 15 mL Petri dishes (60 × 15mm), with the addition of 50 µg/mL ampicillin or 100 µg/mL rifampicin (Carl Roth GmbH, Karlsruhe, Germany) and 50 mg/L Benomyl (Edgington *et al*. 1971) (Sigma-Aldrich Chemie GmbH, Steinheim, Germany) to control unwanted microbial contaminants. Culture replicates were incubated in a climate chamber (CMP 6010, Conviron, Canada) at 16 °C and 12 °C, 14 h in light and in 10 h darkness (1 000 lux, Narva, bio-vital, Germany), respectively, per day cycle. To these cultures, new pine pollen and autoclaved water were added regularly. However, long term culture trials to obtain single spore cultures from living spherical aggregates of *D. chodatii* were unsuccessful.

DNA extraction, PCR amplification, and phylogenetic analyses

DNA extraction was performed using an innuPREP Plant DNA extraction Kit (analytikjena, Jena, Germany), as previously described (Buaya *et al*. 2017) on isolated living spherical coelastrum-like aggregates and endobiotic oomycete thalli. Initially, the collected thalli were centrifuged at maximum speed (19 000 *g*) for 2 min at 22 °C to concentrate the cells. Subsequently, RNA*Later* or 70 % ethanol was carefully removed using 1 000 µL pipette tips, and 400 µL SLS buffer from the extraction kit was added. About 100 mg of sterile 0.1 mm Silica Glass Beads (Carl Roth GmbH, Karlsruhe, Germany) were added into each 2 mL tube (Sarstedt, Nümbrecht, Germany) and the samples were homogenized at 25 Hz for 25 min in a Retsch Mixer Mill MM 200 (Retsch GmbH, Haan, Germany). DNA extraction of all samples was conducted following the manufacturer's instructions of the innuPREP Plant DNA extraction Kit. The PCR amplification of the partial nuclear encoding small subunit (18S; nrSSU) was performed as described in Buaya *et al*. (2019a) using Mango*Taq*™ DNA Polymerase (Bioline, London, UK) with the 18S primer pair EUK422-445 and EUK1422-1440_R (Wang *et al*. 2014) on all samples. Subsequently, all positive amplicons were sent for sequencing to the laboratory centre of the Senckenberg Biodiversity and Climate Research Centre, Frankfurt am Main (SBiK-F, Frankfurt, Germany) using the 18S primers used in the PCR. In addition, direct PCRs (putting cells of the oomycete directly into PCR tubes without prior DNA extraction) using 18S primers (Wang *et al*. 2014) were also done as described in Buaya *et al*. (2019a). To obtain high quality nrSSU sequence data for *D. chodatii* coelastrum-like aggregates, PCR amplicons were cloned into competent *Escherichia coli* (Agilent Technologies, Santa Clara, United States) using a StrataClone TA cloning kit (Agilent Technologies, Santa Clara, United States) following instructions of the manufacturer. Single bacterial colonies were picked into 20 µL molecular grade water (Life Technologies, USA) and colony PCR was carried out with the Mango*Taq*™ DNA Polymerase using M13-F and M13-R plasmid primers with amplification conditions set to an initial denaturation at 96 °C for 10 min, 36 cycles at 96 °C for 20 s, 56 °C for 20 s and 72 °C for 60 s, and concluding with a final elongation at 72 °C for 10 min. Amplicons were sent for sequencing to the laboratory centre of the Senckenberg Biodiversity and Climate Research Centre (Frankfurt am Main, Germany) using M13 (M13-F, M13-R), T7 and T3 plasmid primers.

The resulting sequences were edited using Geneious v. 5.6, and the assembled sequences of *D. chodatii* were aligned together with sequences of various members of the *Pythiales, Saprolegniales,* and early-diverging oomycete lineages, using MAFFT v. 7 (Katoh & Stanley 2013), employing the Q-INS-i algorithm. The final alignment can be found on FigShare (doi: 10.6084/m9.figshare.24185379). Minimum Evolution phylogenetic inference with 1 000 bootstrap replicates was computed using MEGAX (Kumar *et al*. 2018) with pairwise deletion, the Tamura-Nei substitution model, and all other parameters set to default. Phylogenetic analyses using the GTR model were done on the TrEase webserver (http://thines-lab.senckenberg.de/trease/, Mishra *et al*. 2023) using RAxML v. 8 (Stamatakis 2014) for Maximum Likelihood inference with 1 000 bootstrap replicates. Bayesian inference was done on the same server using MrBayes v. 3.2 (Ronquist *et al*. 2012) and 5 M generations, while other parameters were set to default. Partial nrSSU sequences obtained in this study were deposited in GenBank under the accession numbers given in the phylogenetic tree.

RESULTS

Screening and observation

Floating pollen collected during spring of 2020 and 2021 from Mummelsee, Knappensee, and Okertalsperre in Germany were found to contain abundant *Pinus sylvestris* and *Picea abies* pollen grains, living spherical coelastrum-like aggregates of *Ducellieria chodatii*, and endobiotic oomycete thalli in the pollen grains. Spherical aggregates of *D. chodatii* were highly abundant on pollen samples from Mummelsee and Okertalsperre, but very rare in samples from Knappensee, while pollen from all sites contained dense clusters of endobiotic oomycete thalli and epibiotic thalli of monocentric fungi (*e.g. Chytridiomycota*), as well as filamentous oomycetes (*e.g. Aphanomyces*, *Lagenidium*, *Pythium*). All samples were further incubated for 2–4 wk under controlled conditions, with the addition of freshly collected pollen of *Pinus sylvestris.* Every week, about 50 mL of autoclaved deionised water and pine pollen were added to prevent desiccation and to provide continuous substrate for *D. chodatii*. These culture plates were screened daily, and after more than a week, spherical coelastrum-like aggregates of *D. chodatii* became more abundant, especially on Mummelsee samples. Two weeks after this, the amount of coelastrum-like aggregates declined rapidly and finally they disappeared from all culture plates. In all samples both colonial and single-celled varieties of algae were common. During zoospores release, some protists become attracted to the newly released mass of zoospores, centrally located within the cage of empty aggregates of pentagonal or triangular shaped cells (as seen from above or the side, respectively). Often, the cage provided an effective barrier against the external predators, protecting the newly released zoospores, before they attained full motility. However, sometimes other unicellular eukaryotes penetrated into the cage after multiple attempts, but frequently remained trapped, and sometimes died within the cage.

Axenic host and pathogen dual cultures of *D. chodatii* were attempted using freshly collected *Pinus sylvestris* pollen. For this living spherical coelastrum-like aggregates were isolated and inoculated into freshly collected and autoclaved pollen grains of *Pinus sylvestris*. Subsequently, cultures were inspected daily for 1 wk for the presence of the pathogen and production of coelastrum-like spherical aggregates. However, diverse microbial contaminants, especially filamentous oomycetes *e.g. Aphanomyces, Lagenidium*, *Pythium* and fungal organisms *e.g.* chytrids, filamentous ascomycetes, and yeasts, quickly colonised all the substrates, despite application of antibiotics, and no coelastrum-like aggregates of *D. chodatii* were observed after more than 2 wk of incubation in multiple attempts. In addition, growth of the pathogen was neither observed on autoclaved pollen grains nor on pollen grains treated with freezing at -80 °C after more than 2 wk of incubation.

While the development of the endobiotic thalli (Fig. 1A) seemed to show features of several genera, including *Aphanomyces*, *Ducellieria*, and *Lagenidium*, the development of the coelastrum-like form (Fig. 1A, B) was always in line with previous descriptions of *D. chodatii* (Kusel-Fetzmann & Nouak 1981, Kusel-Fetzmann & Carniel 1984, Hesse *et al*. 1989, Stoyneva *et al*. 2013). As we assume that multiple species of oomycetes were causing the endobiotic thalli in this study, only the coelastrum-like form is described here. The number of cells in a spherical aggregate varied, likely reflecting the nutritional

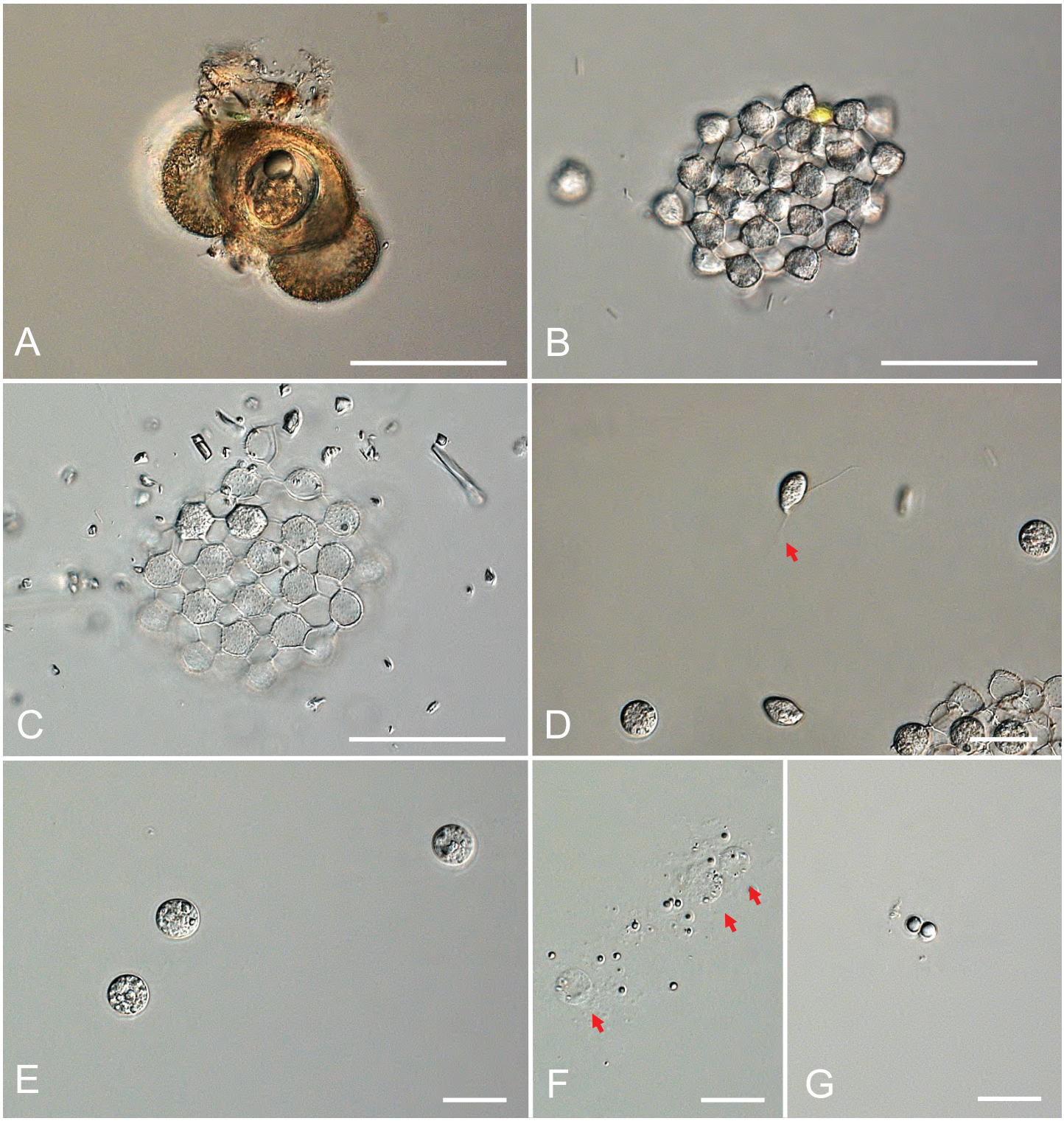

Fig. 1. DIC light micrographs of parasites of coniferous pollen. **A.** Representative of an endobiotic parasite thallus within a *Pinus* sp. pollen grain. **B–G.** Development of the coelastrum-like state of *Ducellieria chodatii*, at different stages **B.** Fully developed spherical aggregate. **C.** Spherical aggregate after most zoospore have been released. **D.** Biflagellate zoospores (red arrow pointing to the forward-directed tinsel flagellum). **E.** Zoospores resting after encystation. **F.** Empty cysts with scattered granular globules (**F, G**) after disintegration. Scale bars: A–C = 50 µm; D–G = 20 µm.

state of the thallus from which they were formed, and, thus, probably depending on the size of the pollen grains consumed. *Pinus* pollen grains, which are much smaller than those of *Picea*, usually produced smaller aggregates. The hollow coelastrum-like aggregates from *Picea* pollen grains usually consisted of more than 20 cells, with a diameter of about 50–80 µm (Fig. 1B, C). The warty to papillate individual cells usually measured 10–15 µm diam, as seen from above, each cell forming 4–6 connections to neighbouring cells. Cells in aggregates were hyaline, at maturity contained fine granules with mixtures of larger droplets (Fig. 1B). In conventional light microscopy, the spore ball sometimes appears light yellow or faint yellow green. After some time, each cell of the aggregate developed a single zoospore almost simultaneously, which escaped into the inner side of the sphere. The newly released spores usually remained in the hollow centre of the sphere for a while, initially weakly

moving inside the sphere. Subsequently, zoospore motility became more intense, and after 10–15 min zoospores swam away in an irregular motion, escaping through from the cage formed by the cell connections, leaving an empty spherical aggregate behind (Fig. 1C). The zoospores were about 8–13 µm long and 7–10 µm diam, broadly limoniform to pyriform or reniform, biflagellate with two subapically inserted flagella, of which one was forward-directed (Fig. 1D, red arrow). The heterokont zoospores usually swam for several minutes before they settled down, becoming aflagellate and spherical in shape, surrounded by thin cell wall (Fig. 1E). Sometimes, the spherical resting cysts fragmented into minute spherical globules (Fig. 1F, G) after several minutes leaving behind empty cysts (Fig. 1F, red arrows).

Molecular phylogeny

In the phylogenetic reconstructions inferred from partial nrSSU sequences (Fig. 2), the coelastrum-like form of *Ducellieria chodatii* and the endobiotic thalli belonged to different oomycete lineages, in line with the observation that in the samples obtained most endobiotic thalli showed a lagenidium-like spore discharge. *Ducellieria chodatii* coelastrum-like isolates had identical sequences and formed a monophyletic group with maximum support. This group was resolved as a member of the early-diverging oomycete lineages, forming separate, deep-branching clade. The clade was grouped with *Olpidiopsidales* and *Miraculales*, but without support. The lagenidium-like thalli were imbedded within the crown oomycete order *Peronosporales* with lacking to weak support and no clear affinities to any of the genera of the *Peronosporales* sequenced so far.

TAXONOMY

Based on the life-cycle traits and phylogenetic placement, *Ducellieria chodatii* is a *bona fide* member of the early-diverging oomycete lineages. Thus, the provisional placement of the parasitoid in the *Leptomitales* by Dick (2001) cannot be upheld, and the assignment is revised in the present study by reclassifying *D. chodatii* to an order of its own.

Ducellieriales A.T. Buaya & Thines, ***ord. nov.*** MycoBank MB 849453.

Obligate biotrophic parasite of *Pinus* and *Picea* pollen grains, thallus holocarpic, forming hollow sphere at discharge, which at maturity forms a multicellular hollow spherical aggregate, individual cells with a thin, colourless wall, ornamented with warts and spines directed outwards; zoospores single per individual cell, biflagellate and heterokont.

Type genus: *Ducellieria* Teiling

Type species: *Ducellieria chodatii* (F. Ducell.) Teiling, *Svensk bot. Tidskr*. **51**: 209. 1957.

The typification of Dick (2001) was made by choice of an iconotype, the figures in Hesse *et al*. (1989). Thus, no molecular phylogenetic investigation of the type can be done to clarify if morphologically similar and divergent species are conspecific. Therefore, FR-0046135 (**Germany**, Baden-Württemberg, Black Forest, Mummelsee, 14 Jun. 2021, *M. Thines,* ex type partial nrSSU sequence deposited in GenBank under thre accession number OR282458) deposited in the Herbarium Senckenbergianum (FR), is here designated as an **epitype** (MBT 10014079).

DISCUSSION

Holocarpic parasites of plant pollen are widespread in freshwater aquatic environments and ecologically important for carbon cycling (Karling 1942, Sparrow 1960, Dick 2001). Despite their ubiquitous nature, none of these organisms have been investigated for molecular phylogeny, leaving their taxonomic placement largely unresolved (Beakes & Thines 2017, Buaya & Thines 2020). Arguably the most enigmatic of these organisms belong to the genus *Ducellieria* (*D. chodatii*, *D. chodatii* var. *armata, D. corcontica, D. tricuspidata*), which forms a unique coelastrum-like sporangial state that has led to a classification of the pathogen in green and later golden-green algae (Ducellier 1915, Teiling 1957, Karling 1968, Artemchuk 1972, Matula 1980).

Originally, the type species of the genus was classified as *Coelastrum chodatii* in the *Chlorophyceae* by Ducellier (1915). It was later transferred to a new genus in the *Xanthophyceae*, *Ducellieria*, by Teiling (1957). However, the placement of *D. chodatii* among algae was questioned by subsequent investigators (Kusel-Fetzmann & Nouak 1981, Kusel-Fetzmann & Carniel 1984) due to the lack of plastids, absence of solid connection between cells (unlike *Coelastrum*), and other traits of its complex life cycle evidently divergent from algae (*e.g*. the formation of a holocarpic thallus). After detailed re-examination of its life cycle and cellular ultrastructure, its affiliation to the *Oomycota* was confirmed by Hesse *et al*. (1989). The pathogen was initially thought to be a member of the *Saprolegniales* (Kusel-Fetzmann & Nouak 1981). However, Dick (2001) reclassified the species to the order *Leptomitales* in separate family (*Ducellieriaceae*), excluding other related species originally included by Teiling (1957), due to the difference in the structure of connections between cells (*D. chodatii* var. *armata*), or incomplete life cycle observations by the original author (*D. tricuspidata*).

The isolate investigated in the present study agrees well with the description of previous investigators (Kusel Fetzmann & Nouak 1981, Hesse *et al*. 1989, Stoyneva *et al*. 2013), in terms of morphology and parasitism to coniferous plant pollen. However, it is noteworthy that the coelastrum-like forms co-occurred with a widespread lagendium-like form and several other pollen parasites of both chytrids and oomycetes (*e.g*. an aphanomyces-like pathogen). The possibility of confusing *D. chodatii* with other species has already been pointed out before (Kusel Fetzmann & Nouak 1981, Kusel Fetzmann & Carniel 1984, Hesse *et al*. 1989, Stoyneva *et al*. 2013), but it also seems possible, that forms attributed to the life cycle of *D. chodatii* might actually represent other oomycetes or fungi, since drifting gymnosperm pollen harbours a great diversity of fungi and oomycetes (Sparrow 1960, Sparrow 1968, Czeczuga & Muszyńska 2004, Wurzbacher *et al*. 2014, Van den Wyngaert *et al*. 2022), as we have also observed in all our samples. Due to the cage-like nature of the aggregates it seems possible that even isolations of single spheroids might contain additional organisms able to infect pollen grains. Thus, until dual cultures using single zoospore isolates confirm the various stages previously reported, only cycle “A” and “B” from Hesse *et al*. (1989) featuring the coelastrum-like phase and the fact that thalli can develop within pollen grains can be considered doubtless, while variations of the endobiotic stage

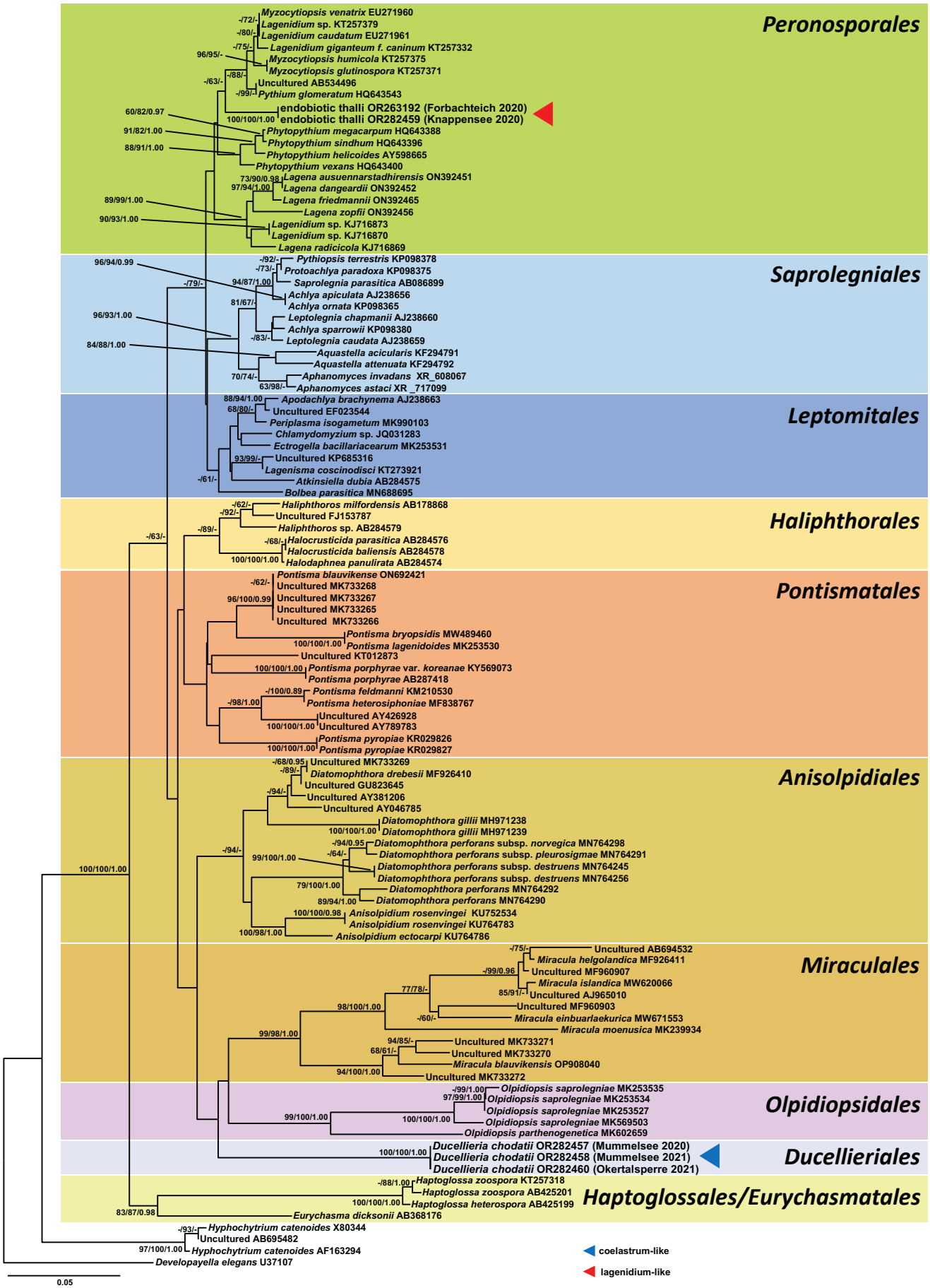

Fig. 2. Molecular phylogeny using Minimum Evolution inferred from partial nrSSU sequences. The numbers at the branches denote bootstrap support values from Maximum Likelihood and Minimum Evolution analyses, in respective order. A hyphen (-) indicates less than 60 % bootstrap support or a conflicting topology. The third number refers to posterior probabilities equal to or greater than 0.95 from the Bayesian phylogenetic inference. Also in this case, a hyphen (-) sign denotes lack of support for the presented or an alternate topology.

and the additional stages (A1, B1, D1) found by Stoyneva (2013) should be confirmed with single spore isolates. This might not always be easy, as it is conceivable, that the formation of these stages depends on environmental conditions. Also, the resting stage reported (*e.g.* Hesse *et al.* 1989) should be considered as not conclusively belonging to *D. chodatii*, as Hesse *et al.* (1989) did not succeed to trigger the formation of coelastrum-like forms from these. The exclusion of *D. tricuspidata* (basionym: *Coelastrum tricuspidatum*), and *D. chodatii* var. *armata* (basionym: *Coelastrum augustae* var. *armata*) from *Ducellieria* by Dick (2001) also requires re-evaluation. Considering the similarities with respect to the formation of a coelastrum-like stage, these species are probably better retained in the genus until a re-evaluation of their life cycle and molecular phylogenetic reconstructions can clarify their evolutionary affinities.

ACKNOWLEDGEMENTS

ATB and MT are thankful to Stefan Wötzel and Tetyana Tsykun for pollen collection at Mummelsee Lake, Baden-Württemberg, Germany in June 2020, and to José Luis Godínez-Ortega for pollen collection at the Zempoala Lagoon Mexico in 2021, even though *Ducellieria* could not be retrieved from there.

Conflict of interest: M. Thines is a senior editor of the journal. However, he was not involved in the handling or review process of this manuscript.

REFERENCES

Artemchuk JA (1972). The fungi of the White Sea. III New Phycomycetes, discovered in the Great Salma Strait of the Kandalakshial Bay. *Veröffentlichungen des Instituts fur Meeresforschung in Bremerhaven* **13**: 231–237.

Bancsó S (2023). Adatok a *Ducellieria chodatii* nyugat-magyarországi előfordulásához. *Kitaibelia* **28**: 3–10.

Barrett JT (1912). Development and sexuality of some species of *Olpidiopsis* (Cornu) Fischer. *Annals of Botany London* **26**: 209–238.

Barron GL (1980). A new *Haptoglossa* attacking rotifers by rapid injection of an infective sporidium. *Mycologia* **72**: 1186–1194.

Beakes GW, Thines M (2017). *Hyphochytriomycota and Oomycota*. In: *Handbook of the Protists* (Archibald JM, Simpson AGB, eds). Springer Verlag, Germany: 435–505.

Bourelly P (1968). Les algues d'eau douce. Inition á la systématique. II. Les algues jaunes et brunes. *Boubée ed. Paris*: 1–438.

Buaya AT, Ploch S, Hanic L, *et al*. (2017). Phylogeny of *Miracula helgolandica gen. et sp. nov.* and *Olpidiopsis drebesii sp. nov*. two basal oomycete parasitoids of marine diatoms, with notes on the taxonomy of *Ectrogella*-like species. *Mycological Progress* **16**: 1041–1050.

Buaya AT, Ploch S, Thines M (2019a). Rediscovery and phylogenetic placement of *Olpidiopsis gillii* (de Wildeman) Friedmann, a holocarpic oomycete parasitoid of freshwater diatoms. *Mycoscience* **60**: 141–146.

Buaya AT, Thines M (2019b). *Miracula moenusica*, a new member of the holocarpic parasitoid genus from the invasive freshwater diatom *Pleurosira laevis*. *Fungal Systematics and Evolution* **3**: 19–33.

Buaya AT, Kraberg A, Thines M (2019c). Dual culture of the oomycete *Lagenisma coscinodisci* Drebes and *Coscinodiscus* diatoms as a model for plankton/parasite interactions. *Helgoland Marine Research* **73**: 92.

Buaya AT, Ploch S, Inaba S, *et al* (2019d). Holocarpic oomycete parasitoids of red algae are not *Olpidiopsis*. *Fungal Systematics and Evolution* **4**: 21–31.

Buaya AT, Thines M (2020). An overview on the biology and phylogeny of the early-diverging oomycetes. *Philippine Journal of Systematic Biology* **14**: 1–20.

Buaya AT, Thines M (2021). *Miracula einbuarlaekurica sp. nov.*, a new holocarpic endoparasitoid species from pennate freshwater diatoms in Iceland. *Mycology* **13**: 1–9.

Buaya AT, Tsai I, Thines M (2022). *Pontisma blauvikense sp. nov.* the first member of the early-diverging oomycete genus *Pontisma* parasitizing brown algae. *Journal of Eukaryotic Microbiology* **70**: e12957.

Choi YJ, Beakes G, Glocking S, *et al.* (2015). Towards a universal barcode of oomycetes – a comparison of the *cox1* and *cox2* loci. *Molecular Ecology Resources* **15**: 1275–1288.

Cobelas MA (1984). Catalogo de las algas continentales Españolas. II. *Craspedophyceae*, *Cryptophyceae*, *Chrysophyceae*, *Dinophyceae*, *Euglenophyceae*, *Haptophyceae*, *Phaeophyceae*, *Rhodophyceae*, *Xanthophyceae*. *Acta Botánica Malacitana* **9**: 27–40.

Cornu M (1872). Monographie des Saprolégniées, étude physiologique et systematique. *Annales des Sciences Naturelles Botanique* **15**: 1–198.

Coute A (1984). Premiéres observations au M.E.T. et au M.E.B. sur la cytologie de *Ducellieria chodatii* (Ducell.) Teiling (*Xanthophyceae*, *Mischococcoales*, *Chlorobotrydaceae*). *Nova Hedwigia* **39**: 651–662.

Czeczuga B, Muszyńska E (2004). Aquatic zoosporic fungi from baited spores of cryptogams. *Fungal Diversity* **16**: 11–22.

de Wildeman E (1893). Notes mycologiques I. *Annales de la Société Belge de Microscopie* **17**: 5–30.

de Wildeman E (1896). Notes mycologiques VII. *Annales de la Société Belge de Microscopie* **20**: 21–64.

de Wildeman E (1897). Notes mycologiques IX. *Annales de la Société Belge de Microscopie* **21**: 3–31.

Dick MW (2001). *Straminipilous Fungi*. Kluwer, Netherlands.

Drechsler C (1940). Three fungi destructive to free-living terricolous nematodes. *Journal of the Washington Academy of Sciences* **30**: 240–254.

Ducellier F (1915). Note sur un nouveau *Coelastrum*. *Bulletin de la Sociéte Botanique de Genéve, 2. Serie* **7**: 73–74.

Edgington LV, Khew KL, Barron GL (1971). Fungitoxic spectrum of benzimidazole compounds. *Phytopathology* **61**: 42–44.

Ettl H (2009). *Xanthophyceae.* In: *Suwasserflora von Mitteleuropa* (Ettl H, Gerloff J, Heynig H, eds). Fischer, Stuttgart, Germany: 1–530.

Glockling SL, Beakes GW (2000). An ultrastructural study of sporidium formation during infection of a rhabditid nematode by large gun cells of *Haptoglossa heteromorpha*. *Journal of Invertebrate Pathology* **76**: 208–215.

Godínez-Ortega JL, Oliva-Martínez MG, Escobar-Oliva MA, *et al.* (2017). Diversidad algal del Parque Nacional Lagunas de Zempoala, México, excepto diatomeas. *Hidrobiológica* **27**: 45–58.

Gorbulin OS (2012). Ecological and biological characteristics of *Xanthophyta* of Ukraine inland water bodies. *The Journal of V.N. Karazin Kharkiv National University. Series: Biology* **15**: 50–66.

Hesse M, Kusel-Fetzmann E, Carniel K (1989). Life cycle and ultrastructure of *Ducellieria chodatii* (*Oomycetes*). *Plant Systematics and Evolution* **165**: 1–15.

Hudspeth DSS, Nadler SA, Hudspeth MES (2000). A *cox*2 molecular phylogeny of the *Peronosporomycetes*. *Mycologia* **92**: 674–684.

Ingold CT (1949). On the genus *Resticularia*. *Annals of Botany. London. N.S.* **13**: 435–443.

Kagami M, Miki T, Takimoto G (2014). Mycoloop: chytrids in aquatic food webs. *Frontiers in Microbiology* **5**: 1–9.

Karling JS (1942). *The simple holocarpic biflagellate Phycomycetes*. JS Karling, USA.

Karling JS (1944). New lagenidiaceous parasites of rotifers from Brazil. *Lloydia (Cincinnati)* **7**: 328–342.

Karling JS (1968). Zoosporic fungi of Oceania. II. Two saprophytic species of *Aphanomycopsis*. *Mycologia* **60**: 271–284.

Karling JS (1981). Some zoosporic fungi from soils of Sri Lanka. *Nova Hedwigia* **35**: 107–116.

Katoh K, Standley DM (2013). MAFFT multiple sequence alignment software version 7: improvements in performance and usability. *Molecular Biology and Evolution* **30**: 772–780.

Komarek J, Fott B (1983). *Chlorophyceae* (Grünalgen); Ordnung: *Chlorococcales.* In: *Die Binnengewässer 16. Das Phytoplankton des Süßwassers* (Huber Pestalozzi, ed). Schweizerbartsche Verlagsbuchhandlung, Stuttgart, Germany: 1–1044.

Kumar S, Stecher G, Li M, *et al.* (2018). MEGA X: Molecular Evolutionary Genetics Analysis across Computing Platforms. *Molecular Biology and Evolution* **35**: 1547–1549.

Kusel-Fetzmann E-L, Nouak H (1981). *Ducellieria chodatii* - Alge oder Pilz? *Plant Systematics and Evolution* **138**: 199–207.

Kusel-Fetzmann E-L, Carniel K (1984). Beiträge zur Biologie und Ultrastruktur von *Ducellieria Chodatii*. *Mitteilungsband d. Tagung der Deutschen Botanischen Gesellschaft in Wien, Kurzfassung der Beiträge*: 107.

Masigol H, Khodaparast SA, Woodhouse JN, *et al.* (2019). The contrasting roles of aquatic fungi and oomycetes in the degradation and transformation of polymeric organic matter. *Limnology and Oceanography* **64**: 2662–2678.

Matula J (1980). *Ducellieria chodatii* (Ducel.) Tell. and *D. corcontica* Mat. *nova sp.* (*Xanthophyceae*) found in a peat bog in the Karkonosze Mts. *Fragmenta Floristica et Geobotanica* **26**: 349–353.

McLarty DA (1941). Studies in the family *Woroninaceae*. I. Discussion of a new species including a consideration of the genera *Pseudolpidium* and *Olpidiopsis*. *Bulletin of the Torrey Botanical Club* **68**: 49–66.

Mishra B, Ploch S, Weiland C, Thines M (2023). The TrEase web service – inferring phylogenetic trees with ease. *Mycological Progress* **22**: 81.

Oblinger H (2005). Über die Kleinlebewelt in den Hochmoorgewässem des Haspelmoores und des Mödishofer Moores. *Berichte des naturwissenschaftlichen Vereins für Schwaben, Augsburg* **109**: 124–133.

Ronquist F, Teslenko M, van der Mark P, *et al.* (2012). MrBayes 3.2: efficient Bayesian phylogenetic inference and model choice across a large model space. *Systematic Biology* **6**: 539–542.

Scherffel A (1925). Endophytische Phycomycetenparasiten der Bacillariaceen und einige neue Monadinen. Ein Beitrag zur Phylogenie der Oomyceten (Schröter). *Archiv für Protistenkunde* **52**: 1–141.

Sparrow FK (1939). A new species of *Lagenidium* parasitic in rotifer eggs. *Mycologia* **31**: 527–532.

Sparrow FK (1950). Some Cuban *Phycomycetes*. *Journal of the Washington Academy of Sciences* **40**: 50–55.

Sparrow FK (1960). *Aquatic Phycomycetes*. *The University of Michigan Press*, Ann Arbor Michigan, USA.

Sparrow FK (1968). Remarks on the *Thraustochytriaceae*. *Veröffentlichungen des Instituts for Meeresforschung in Bremerhaven, Sonderband* **3**: 7–18.

Stamatakis A (2014). RAxML version 8: a tool for phylogenetic analysis and post-analysis of large phylogenies. *Bioinformatics* **30**: 1312–1313.

Stoyneva MP, Uziunov BA, Gärtner G (2013). First record of the parasitic oomycete *Ducellieria chodatii* from Pirin Mts (Bulgaria) with notes on its taxonomy, life cycle and ecology. *Sydowia* **65**: 1–12.

Teiling E (1957). Some little known Swedish phytoplankters. *Svensk Botanisk Tidskrift* **51**: 207–222.

Thines M, Buaya AT (2022). *Lagena* - an overlooked oomycete genus with a wide range of hosts. *Mycological Progress* **21**: 66.

Van den Wyngaert S, Ganzert L, Seto K, *et al.* (2022). Seasonality of parasitic and saprotrophic zoosporic fungi: linking sequence data to ecological traits. *ISME Journal* **16**: 2242–2254.

Wang Y, Tian RM, Gao ZM, *et al.* (2014). Optimal eukaryotic 18S and universal 16S/18S ribosomal RNA primers and their application in a study of symbiosis. *PLoS ONE* **9**: e90053.

Wehr J, Sheath RG (2003). *Freshwater Algae of North America: Ecology and Classification*. Academic Press.

Whiffen AJ (1942). A discussion of some species of *Olpidiopsis* and *Pseudolpidium*. *American Journal of Botany* **29**: 607–611.

Whiffen A J (1946). Two new terricolous phycomycetes belonging to the genera *Lagenidium* and *Blastocladiella. Journal of the Elisha Mitchell Scientific Society* **62**: 54–58.

Wurzbacher C, Rösel S, Rychla A, *et al.* (2014). Importance of saprotrophic freshwater fungi for pollen degradation. *PLoS ONE* **9**: e94643.

Zopf W (1884). Zur Kenntniss der Phycomyceten. I. Zur Morphologie und Biologie der Ancylisteen und Chytridiaceen. *Novorum actorum Academia Caesareae Leopoldinae-Carolinae Germanicae Naturae Curiosorum* **47**: 143–236.

Zopf W (1887). Über einige niedere Algenpilze (Phycomyceten) und eine neue Methode ihre Keime aus den Wasser zu isolieren. *Abhandlungen der naturforschenden Gesellschaft zu Halle* **17**: 77–107.

FUSE

Fungal Systematics and Evolution

Volume 12
DECEMBER 2023
PAGES 255–269

doi.org/10.3114/fuse.2023.12.13

A phylogenetic assessment of a fungicolous lineage in *Coniocybomycetes*: *Chaenotricha*, a new genus of *Trichaptum*-inhabiting species

A. Suija[1,2*], R.T. McMullin[3], P. Lõhmus[1]

[1]Institute of Ecology and Earth Sciences, University of Tartu, J. Liivi 2 (Oecologicum), EE50409 Tartu, Estonia
[2]Mycological collections, Natural History Museum and Botanical Garden, University of Tartu, Vanemuise 46, EE50410, Tartu, Estonia
[3]Research and Collections, Canadian Museum of Nature, P.O. Box 3443, Station D, Ottawa, Ontario K1P 6P4, Canada

*Corresponding author: ave.suija@ut.ee

Key words:
Ascomycota
epimycotic
lichens
new taxa
polypores
sporocarp-inhabiting fungi

Abstract: The globally distributed genus *Trichaptum* is one of the most species-rich among polypores in terms of hosting other fungi. Among *Trichaptum*-associates, there is a group of mazaediate lichenized fungi (*Coniocybomycetes*, *Ascomycota*) that previously had an uncertain phylogenetic position. DNA sequences – mitochondrial small subunit (mtSSU), nuclear large subunit rDNA (nuLSU), and internal transcribed spacer (ITS) – were obtained from 29 specimens collected from Europe and North America. Maximum likelihood and Bayesian inference analyses of these three gene loci were used to infer phylogenetic position and relationships among lineages. Statistical tests were used to find which phenotypical characteristics distinguish species. The molecular sequence data provide evidence that the fungicolous specimens form a distinct lineage within *Coniocybomycetes* sister to the combined clade of *Chaenotheca s. lat.* and *Sclerophora.* Considering its phylogenetic placement and strict specialization, we describe a new genus – *Chaenotricha*. This fungicolous lineage contains three species based on molecular characteristics. Morphological characters mostly overlap except for spore size and stalk length of apothecia. We provide a new combination, *Chaenotricha obscura,* for the only previously described species for which we designate an epitype, and introduce a new species – *Chaenotricha cilians*. The third lineage remains undescribed because of a small sample size, which did not allow us to clearly delineate species boundaries.

Citation: Suija A, McMullin RT, Lõhmus P (2023). A phylogenetic assessment of a fungicolous lineage in *Coniocybomycetes*: *Chaenotricha*, a new genus of *Trichaptum*-inhabiting species. *Fungal Systematics and Evolution* **12**: 255–269. doi: 10.3114/fuse.2023.12.13
Received: 27 September 2023; **Accepted:** 2 November 2023; **Effectively published online:** 22 November 2023
Corresponding editor: P.W. Crous

INTRODUCTION

The surface of polypore sporocarps can be a substratum for many organisms such as epiphytic algae (Zavada & Simoes 2001, Stonyeva *et al*. 2015, Vondrák *et al*. 2023), non-lichenized (*e.g*., Hutchison 1987, Sun *et al*. 2019, Maurice *et al*. 2021) and lichenized fungi (Hawksworth *et al.* 2014), forming so-called epimycotic or fungicolous communities (Stonyeva *et al*. 2015, Maurice *et al*. 2021). For example, a globally distributed genus of poroid white-rotting fungi, *Trichaptum* (*Hymenochaetales*, *Agaricomycetes*, *Basidiomycota*; Larsson *et al*. 2006), may host more than 20 green algal (*Chlorophyta*) species (Mukhin *et al*. 2018) and is one of the richest among polypores in terms of associated fungicolous fungi (Maurice *et al*. 2021). Among these, there are at least three lichenized *Chaenotheca* species, *C. gracillima* (Spribille *et al*. 2010), *C. trichialis* (Selva 2014), and *C. obscura* (= *C. balsamconensis*; Merrill 1909, Allen & McMullin 2015, Selva & McMullin 2020), reported as growing on *Trichaptum* sporocarps.

The genus *Chaenotheca*, together with the genus *Sclerophora*, belongs to the early diverging lichenized lineage *Coniocybomycetes*, species of which are characterized by having stalked and mazaediate ascomata (Prieto *et al*. 2013), and their closest relatives belong to *Lichinomycetes* (Prieto *et al*. 2013, Díaz-Escandón *et al*. 2022). The oldest report of a *Chaenotheca* species growing on *Trichaptum* sporocarps was made by Fries (1865), who mentioned a *Trichaptum*-inhabiting variant called *Chaenotheca brunneola β cilians* due to its similarities to eyelashes. Unfortunately, the original material of this taxon is lost (L. Tibell & A. Thell, pers. comm.). The second oldest evidence comes from North America, where Merrill (1909) described *Calicium obscurum* (= *Chaenotheca obscura*) growing on *Trichaptum.* In 2015, Allen & McMullin (2015) described *C. balsamconensis* from North America, but after examining Merrill's type material, Selva & McMullin (2020) concluded that this species is conspecific with *C. obscura* and synonymized accordingly. At the same time, a study by Suija *et al*. (2016) tested if morphologically similar, but ecologically distinct (wood inhabiting *vs*. fungal sporocarp-inhabiting) specimens belong to the same species – *Chaenotheca brunneola*. A single-gene (full-length ITS) analysis in that study showed that all *Trichaptum*-dwelling specimens, including the type of *C. balsamconensis* from North America, form a distinct lineage sister to the rest of *Chaenotheca* and *Sclerophora* species. Moreover, there was

a clear distinction in nucleotide sequences between European and North American specimens, suggesting that these two may represent different species.

In the current study, we aimed to clarify the taxonomic position of these fungi within *Coniocybomycetes*. We analyzed slow- and fast-evolving ribosomal DNA markers as well as their morphological characteristics. We also sampled widely to better understand the distribution of these *Trichaptum*-inhabiting fungi.

MATERIAL AND METHODS

Taxon sampling and morphological examination

We examined chaenotheca-like lichenized fungi growing on *Trichaptum* sporocarps. The specimens are deposited in BILAS, CANL, DAU, M, NY, UPS, TRH and TUF (fungarium acronyms follow Index Herbariorum; https://sweetgum.nybg.org/science/ih/). In total, we studied the morphology and anatomy of 29 specimens collected from Europe and North America (Table 1), including an isotype of *Chaenotheca obscura* from the exsiccate series *Merrill, Lich. Exs. Ser. II. 92*. (M0205375 and CANL) and the holotype of *C. balsamconensis* (NY02359896).

We selected 28 morpho-anatomical characters to describe the specimens (Supplementary Table S1). For each specimen, we recorded the thallus type (immersed or episubstratal), shape (granular or farinaceous) and presence of thallus cortex; if thallus was visible, we also tested thallus color reactions with standard spot tests with reagents following protocols described by Brodo *et al*. (2001): potassium hydroxide *ca*. 10 % solution (K), para-phenylenediamine ethanol solution (Pd) and commercial bleach containing sodium hypochlorite (C). The abbreviation KC refers to a color reaction after applying K and then C immediately afterwards to the same location. We examined up to five apothecia per specimen (the number examined depended on the availability/abundance of apothecia). We also recorded the location of the apothecia on the *Trichaptum* fruitbodies and stalk pigment reaction in K. For each apothecium, we described 13 characteristics: presence of pruina on the stalk, stalk color (dull or shining black), capitulum shape (spherical or obconical), development of excipulum (well or weakly), color of mazaedium (dark brown or black) and its structure (powdery or granular), height and width of the stalk and capitulum, shape of the asci (cylindrical or clavate) and its length (without stipe), shape of the ascospores (spherical, slightly elliptical or both), ascospore surface (smooth, with fissures or both) and diameter of ascospores. We calculated the average length-width ratio of the stalk based on up to five apothecia per specimen. Average size of ascospores and asci were calculated using 10 ascospores and four asci (if possible) for each apothecium to a maximum of 20 asci and 50 ascospores per specimen. Variable values were given as (min–)mean ±SD(–max) where SD is the standard deviation, and min and max are minimum and maximum values respectively.

We examined the anatomical characters of ascomata and ascospores in squash preparations under a Leica DM1000 LED compound light microscope. Our measurements were made in tap water with a precision of 1 µm using 10× objectives for apothecia and 100× (water) objectives for asci and ascospores. We produced scanning electron micrographs from air-dried material mounted on stubs coated with a thin layer of gold and observed using a FEI INSPECT Scanning Electron Microscope (The National Museum of Natural Sciences [MNCN, CSIC], Madrid). Our character selection and terminology of morphological and anatomical characteristics follows Schmidt (1970), Tibell (1980, 1999) and Allen & McMullin (2015).

Using a Mann-Whitney U Test, we assessed the difference in morphological and anatomical variables (except two variables with extremely low sample size) between two taxon groups with Statistica® v. 6.0 software (StatSoft 1984–2001).

DNA extraction, amplification, and sequencing

We extracted total DNA from 29 specimens growing on the sporocarps of *Trichaptum abietinum, T. fuscoviolaceum* and *T. biforme* and from several *Chaenotheca* and *Sclerophora* specimens (Table 1). For DNA extraction, we removed four to five ascomata per specimen from the substratum and placed them into a 1.5 mL test tube. We used a High Pure PCR Template Preparation Kit (Roche Applied Science®) and followed the protocol provided by the manufacturer.

We amplified two nuclear (full-length internal transcribed spacer [ITS] and partial large subunit [nuLSU]), and one mitochondrial (small subunit (mtSSU)) ribosomal DNA regions. To amplify these loci, we used the following primer pairs: ITS0F / ITS4, ITS0F / LA-W or ITS1 / LA-W (White *et al*. 1990, Tedersoo *et al*. 2008) for ITS, LR0R / LR7 or LR0R / LR5 (Vilgalys & Hester 1990) for nuLSU, and mrSSU1 / mrSSU3r (Zoller *et al*. 1999) for mtSSU. The PCR mix (25 µL) consisted of 5 µL 5× HOT FIREPol Blend Master Mix (Solis BioDyne, Tartu, Estonia), 0.5 µL of both primers, 3–8 µL of target-DNA and the rest of distilled water. We visualized the PCR products on a 1 % agarose gel stained with ethidium bromide. For the purification of PCR products, we added 1 µL of FastAP and 0.5 µL of Exonuclease I (Thermo Scientific, Waltham, MA, USA) to each tube and the tubes were incubated at 37 °C for 45 min, and the enzymes were deactivated by heating at 85 °C for 15 min. We sequenced both complementary strands of ITS using primer pairs ITS4 and ITS5 (White *et al.* 1990), and nuLSU with CTB6 (Garbelotto *et al*. 1997) and LR7, and mtSSU with the same primers as amplified. We performed DNA extraction, amplification, and purification in the molecular lab of mycology at the University of Tartu (TU, Estonia) and we Sanger sequenced the amplicons by Macrogen Inc. (Amsterdam, the Netherlands).

We used Sequencher v. 4.10.1. (GeneCodes Corp.®, Ann Arbor, MI, USA) or CodonCode Aligner v. 8.0.2 (CodonCode Corporation®, Centerville, MA, USA) to check, assemble, and manually edit the sequence fragments. To avoid misidentifications, we compared the consensus sequences with those available in the nucleotide database of the National Center for Biotechnology Information (NCBI; https://www.ncbi.nlm.nih.gov/) using the 'megablast' algorithm (Altschul *et al*. 1990). We deposited the newly generated DNA sequences in NCBI and UNITE (Abarenkov *et al.* 2010) data repositories. The sequenced voucher specimens are in DAU, TUF, NY, TRH, UPS, and the extracted DNA samples in the DNA and Environmental Sample Collection of the Natural History Museum in Tartu University (TUE). We also provide UNITE Species Hypotheses (SH; Kõljalg *et al.* 2013) at a distance value of 1.5 %, and a reference sequence for each recognized taxon.

Table 1. Information about voucher specimens (taxon name, voucher ID, country of origin, lab code, and morpho ID), and NCBI accession codes of the new and downloaded DNA sequences (full-length ITS, nuLSU and mtSSU) used for reconstruction of phylogeny presented on Figs 1 and 2. "—" means sequence not generated or not available for this specimen. The type specimens are in **bold.**

Taxon name	Voucher ID	Country	Lab code	Morpho ID	ITS	LSU	mtSSU
Chaenotheca biesboschii	A.v.d. Pluijm 3244 (UPS)	Netherlands			MK514539	—	—
	A.v.d. Pluijm 3244 (UPS)	Netherlands			MK376459	—	—
Chaenotheca brachypoda	Tibell 22193 (UPS)	Sweden			AF297963	—	—
	Tibell 17062 (UPS)	Sweden			AF297962	—	—
Chaenotheca brunneola	Tibell 22202 (UPS)	Sweden			AF297964	—	—
	TUF076414	Estonia	CB22		KX348121	—	—
	TUF076421	Estonia	CB14		KX348125	—	—
Chaenotheca chlorella	Tibell 16867 (UPS)	Sweden			—	AY804191	—
	Tibell 22372 (UPS)	Estonia			AF445356	—	—
	Tibell 22187 (UPS)	Sweden			AF297966	—	—
Chaenotheca chrysocephala	Tibell 21799 (UPS)	Sweden			AF298121	—	—
	PRA-Vondrak26008	Austria			OQ717362	—	—
Chaenotheca cinerea	TUF039194	Estonia	BF18		KX348119	—	—
	Tibell 22374 (UPS)	Estonia			AF421201	—	—
	Jonsson & Nordin (UPS)	Sweden			AF298122	—	—
Chaenotheca deludens	Tibell 16575	New Zealand			AF408678	—	—
Chaenotheca ferruginea	TUF089549	Estonia	CH463		OR661708	OR661698	—
	Tibell 22276 (UPS)	Sweden			AF298123	—	—
Chaenotheca furfuracea	Wedin 6366 (UPS)	Unspecified			—	JX000087	JX000121
	TUF091901	Estonia	AS899		OR661703	—	—
	Tibell 22364	Sweden			AF445357	—	—
Chaenotheca gracilenta	Wedin 7022 (S)	Unspecified			JX000100	JX000084	JX000119
	TUF030149	Estonia	BF30		KX348118	—	—
Chaenotheca gracillima	TUF091585	Estonia	CH289		OR661701	—	OR661671
	Tibell 16725 (UPS)	New Zealand			AF408682	—	—
	Tibell 17614 (UPS)	Argentina			AF408679	—	—
Chaenotheca hispidula	TUF051093	Latvia	CH361		OR661707	—	—
	Tibell 21900 (UPS)	India			AF298128	—	—
Chaenotheca hygrophila	TNS:YO9596	Japan			LC669601	—	—
	Thor 15612	Japan			AF298129	—	—
Chaenotheca laevigata	Tibell 21998b (UPS)	India			AF298131	—	—
	Tibell 22176 (UPS)	Sweden			AF298130	—	—
Chaenotheca nitidula	Tibell 21490 (UPS)	USA			AF492388	—	—
	Koffman 170 (UPS)	Canada			AF492387	—	—
Chaenotheca phaeocephala	Tibell 22291 (UPS)	Sweden			AF446045	—	—
	Tibell 21819 (UPS)	Sweden			AF445360	—	—
Chaenotheca sp.	Tibell 22113 (UPS)	India			AF298135	—	—
Chaenotheca sphaerocephala	Tibell 21939 (UPS)	India			AF298134	—	—
Chaenotheca stemonea	Tibell 22191 (UPS)	Sweden			AF408683	—	—
	WSL:BC-087-3	Switzerland			KX133006	—	—
Chaenotheca subroscida	Tibell 22150 (UPS)	Sweden			AF298136	—	—
	TUF049310	Estonia	CH760		OR661702	—	—
Chaenotheca trichialis	Prieto 3028 (S)	Unspecified			JX000102	JX000085	JX000120
	Tibell 22384 (UPS)	Sweden			AF421207	—	—
	KR-0051902	Unspecified			MW325680	—	—

Table 1. (Continued).

Taxon name	Voucher ID	Country	Lab code	Morpho ID	ITS	LSU	mtSSU
Chaenotheca xyloxena	Selva 7753 (UMFK)	Canada			AF421213	—	—
	Tibell 22329 (UPS)	Sweden			AF421212	—	—
Chaenotricha cilians	TUF095043	Norway	AS972		OR661716	—	OR661678
	UPS-L-941561	Sweden	CH419		OR661713	OR661686	OR661659
	TUF091610	Estonia	CH99		—	OR661699	—
	TUF089479	Canada	CH484	1	—	—	OR661670
	TUF050023	Estonia	AS699	2	OR661715	OR661694	OR661676
	TUF076412	Estonia	CH168	3	KX348131	—	—
	TUF076423	Estonia	CH98	4	KX348120	OR661693	OR661672
	TUF091611	Estonia	CH290	5	—	—	OR661669
	TUF091612	**Estonia**	**CH288**	**6**	**OR661721**	**OR661692**	**OR661665**
	DAU0602050	Latvia	CH310	7	OR661717	—	OR661666
	DAU0602051	Latvia	CH311	8	—	—	OR661667
	DAU0602052	Latvia	CH312	9	—	—	OR661668
	TUF089401	Latvia	CH481	10	—	OR661689	OR661662
	TUF090000	Latvia	CH480	11	OR661712	OR661688	OR661661
	TRH-L-18707	Norway	CH435	12	OR661709	OR661687	OR661660
	TRH-L-18708	Norway	CH434	13	OR661711	OR661690	OR661663
	TUF050022	Norway	AS698	14	OR661714	OR661695	OR661675
	TUF095044	Norway	AS973	15	OR661719	—	OR661677
	BILAS	Russia	CH436	16	—	OR661691	OR661664
	UPS-L-867275	Sweden	CH418	17	OR661710	—	—
	UPS-L-872283	Sweden	CH420	18	OR661718	—	—
	TUF076413	Estonia	CB1		KX348130	—	—
	TUF076417	Estonia	CB3		KX348129	—	—
	TUF076416	Estonia	CB5		KX348128	—	—
	TUF076420	Estonia	CB15		KX348124	—	—
	TUF076419	Estonia	CB19		KX348123	—	—
	TUF076422	Estonia	CB21		KX348122	—	—
Chaenotricha obscura	TUF089391	Canada	CH488	24	OR661720	OR661684	OR661657
	NY02359896	**USA**	**CH174**	**25**	**KX348132**	**OR661679**	**OR661652**
	NY02439109 (epitype)	**USA**	**CH175**	**26**	**KX348133**	**OR661680**	**OR661653**
	CANL20337 (lectotype)	**USA**		**27**	—	—	—
Chaenotricha sp.	TUF089393	Canada	CH490	19	—	OR661681	OR661654
	TUF089480	Canada	CH485	20	—	OR661682	OR661655
	TUF089481	Canada	CH486	21	—	OR661696	OR661674
	TUF089547	Estonia	CH461	22	—	OR661683	OR661656
	TUF089548	Estonia	CH462	23	—	OR661685	OR661658
Lempholemma polyanthes	Zoladeski & Lutzoni 11294-L1(2/2) (CANL	Unspecified			—	AF356691	AY584709
Peltula auriculata	B. Büdel 24902	Venezuela			MF766344	MF766385	MF766303
	Herb. B. Büdel 24901	Venezuela			—	DQ832330	DQ922953
Peltula rodriguesii	B. Büdel 15901	Namibia			MF766373	—	—
Sclerophora amabilis	PRA-Vondrak24780	Czechia			OQ718083	—	—
	PRA-Vondrak24776	Czechia			OQ718082	—	—
Sclerophora farinacea	TUF086803	Estonia	SC406		OR661706	OR661700	—
	TUF055034	Estonia	BF32		OR661705	—	—

Table 1. (Continued).

Taxon name	Voucher ID	Country	Lab code	Morpho ID	ITS	LSU	mtSSU
Sclerophora pallida	EDNA09-01585	United Kingdom			FR799288	—	—
	EDNA09-01513	United Kingdom			FR799287	—	—
Sclerophora peronella	TUF051090	Estonia	SC362		OR661704	OR661697	OR661673
	TUF038050	Estonia	BF16		KX348134	—	—

Phylogenetic analysis

We successfully generated 72 new sequences (18 ITS, 24 nuLSU and 30 mtSSU; Table 1). Sequence blasting in NCBI indicated that our specimens belong to *Coniocybomycetes*. We therefore downloaded sequences of *Chaenotheca* and *Sclerophora* from NCBI and UNITE data repositories (Table 1) to assess the phylogenetic position of these *Trichaptum*-habiting specimens. We included the closest relatives to *Coniocybomycetes*, species of *Lichinomycetes* – *Peltula auriculata* and *P. rodriguesii* to root the ITS-based phylogeny, and *P. auriculata* and *Lempholemma polyanthes* to root the three-locus phylogeny. Approximately 50 *Chaenotheca* species and seven *Sclerophora* species are described (Index Fungorum; https://www.indexfungorum.org; accessed 6 Sep. 2023; and salient literature), of them DNA sequences are available for 21 and four species respectively in publicly accessible repositories.

We aligned sequences with the online version of MAFFT v. 7 (Katoh *et al*. 2019; https://mafft.cbrc.jp/alignment/server/) using default options and then manually adjusted them in Seaview v. 3.2 (Gouy *et al*. 2010) or AliView v. 1.27 (Larsson 2014). We refined the nuLSU and mtSSU alignments, *i.e*., eliminated poorly aligned positions and divergent regions by using Gblocks v. 0.91b (Talavera & Castresana 2007; http://www.phylogeny.fr/). In Gblocks, we used relaxed settings by allowing gap positions within the final blocks and less strict flanking positions. From the ITS alignment, we used ITSx (Bengtsson-Palme *et al*. 2013) in the PlutoF workbench (https://plutof.ut.ee) for extraction of neighboring conservative rDNA regions.

We reconstructed single-gene phylogenies with Maximum Likelihood (ML) using IQ-TREE v. 2 (Trifinopoulos *et al*. 2016; http://iqtree.cibiv.univie.ac.at) to detect possible conflicts among individual genes. We selected GTR+I+G4+F as the nucleotide substitution model and tested branch support with ultrafast bootstrapping (Minh *et al*. 2013) by applying 1 000 iterations. No incongruences were found, so we concatenated the mtSSU, nuLSU and ITS alignments. In the concatenated alignment, we considered gaps as missing characters. Next, we analyzed these two datasets, *i.e*., the concatenated mtSSU+nuLSU+ITS (37 specimens; 2 229 characters, of which 714 bp are mtSSU, 816 bp nuLSU, and 669 bp ITS) and ITS (69 sequences: 737 characters, of which 117 were parsimony informative) datasets. We used both datasets to 1) assess the phylogenetic position of the fungicolous lineage in relation to *Sclerophora* and *Chaenotheca s. lat.*; and 2) evaluate the species limits within the fungicolous group. We deposited the alignments in the TreeBASE repository (study ID S30840).

Next, based on the concatenated alignment, we inferred the phylogenetic relationships and the tree confidence by using two different methodologies: the Metropolis coupled Markov Chain Monte Carlo (MCMC) approach implemented in MrBayes v. 3.2.1. (Ronquist *et al*. 2012) and Maximum Likelihood (ML) in RAxML (Stamatakis 2006), using RAxML-NG v. 1.0.0 software (Kozlov *et al*. 2019; https://raxml-ng.vital-it.ch/). We calculated the best-fit nucleotide substitution model using PartitionFinder v. 2.1.1 (Lanfear *et al*. 2012). The best-fit models according to the lowest value of the Akaike Information Criterion (AICc) were TrN+I+G for nuLSU and GTR+I+G for mtSSU and ITS. The settings for MCMC were as follows: two parallel, simultaneous runs with four incrementally heated chains starting with a random tree; *ngen* = 1 M generations, *samplefreq* and *diagnfreq* = 500, *printfreq* = 2 000. We ran the analysis until the standard deviation of split frequencies (SDSF) was below 0.01 and the potential scale reduction factor (PSRF) was close to 1 indicating convergence of the chains. We discarded the first 25 % as 'burn-in' and a consensus tree and posterior probabilities (PP) were calculated from the remaining tree distribution. We calculated Maximum Likelihood (ML) using a GTR+F0+G nucleotide substitution model, bootstrap support of the ML topology was obtained using *bootstrapping* with 1 000 pseudo-replicates (bootstrap cut-off was 0.01). In the phylogenetic trees, we considered clades supported when posterior probabilities (PP) were ≥ 0.95 and bootstrap values (BS) ≥ 70 %. Our consensus trees were visualized using FigTree v. 1.4.4 (Rambaut 2014) and annotated with Adobe Illustrator v. 13.0.0 CS3®.

RESULTS AND DISCUSSION

The analysis of two datasets (concatenated mtSSU+nuLSU+ITS and ITS only) indicate that the *Trichaptum*-dwelling specimens form a distinct, highly supported lineage sister to the *Chaenotheca-Sclerophora* clade (mtSSU+nuLSU+ITS: BS = 100 %, PP = 1; ITS: BS = 99 %) and in all combinations the *Sclerophora* clade is nested within *Chaenotheca s. lat.* (Figs 1, 2). In both analyses, the closest relatives are species in the *Chaenotheca brunneola* group (*i.e.*, *C. brunneola, C. deludens, C. ferruginea, C. hygrophila*, *C. sphaerocephala* and *C. stemonea*), but this relationship is supported only in the ITS-based phylogeny (Figs 1, 2). Following the smaller genus concepts of Tibell *et al*. (2019) based on an ITS-phylogeny and morphology, and instead of incorporating all species of *Coniocybomycetes* under the single name *Chaenotheca*, we describe a new genus – *Chaenotricha* – to accommodate all *Trichaptum*-specialists (see the Taxonomy section). This allows us to retain *Sclerophora* as a separate taxonomic unit without combining it with *Chaenotheca*.

The Bayesian and ML trees were topologically concordant and revealed three lineages within *Chaenotricha* (Fig. 2), instead of the previously recognized two (Suija *et al*. 2016). One of the groups includes the holotype of *C. balsamconensis* (= *C.*

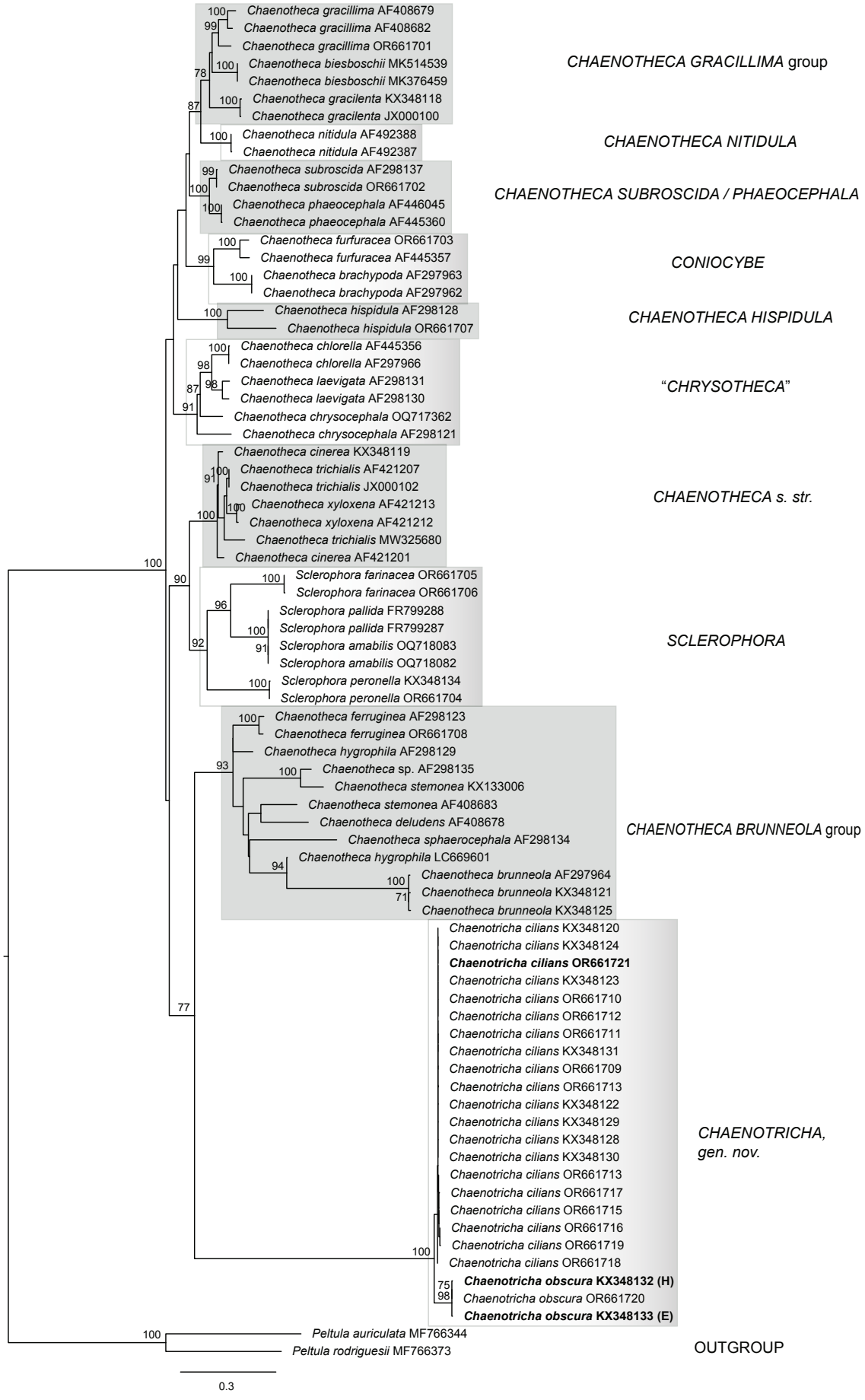

Fig. 1. Maximum likelihood (ML) phylogeny based on rDNA ITS sequences generated for this study and derived from NCBI and UNITE database (Table 1) and showing the position of *Chaenotricha* in relation to other "taxa" within *Coniocybomycetes*. The names of the clades follow Tibell *et al.* (2019); bootstrap support values (BS) ≥ 70 % are above branches. Letters "H" and "E" in brackets indicate the holotype of *Chaenotheca balsamconensis* (= *Chaenotricha obscura*) and epitype of *Chaeotricha obscura*, respectively.

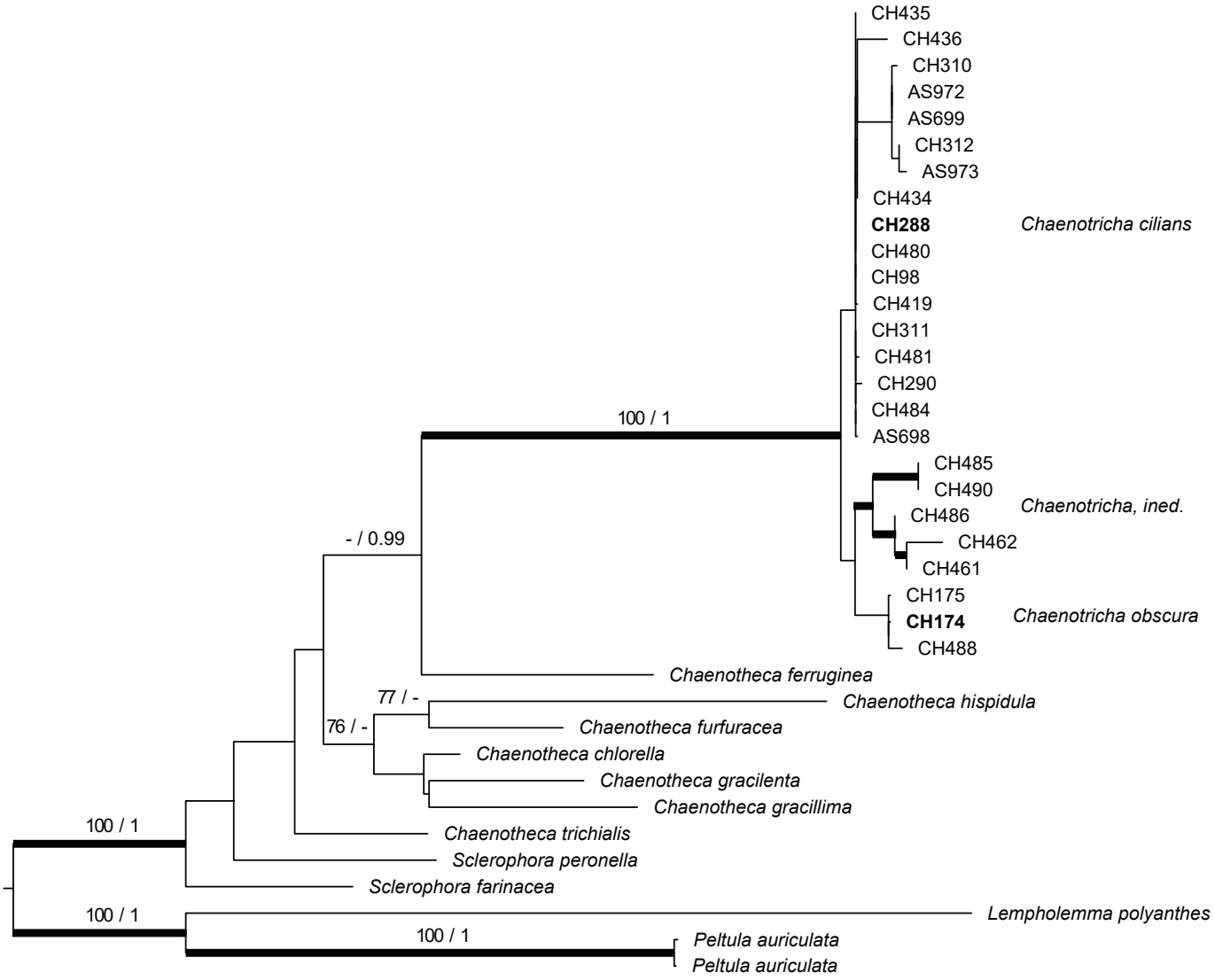

Fig. 2. Three-locus phylogeny (mtSSU+nuLSU+ITS) based on the Maximum Likelihood consensus tree showing the position of *Chaenotricha* within *Coniocybomycetes* and three clades within it corresponding to *Chaenotricha* species. The branches with posterior probabilities (PPs) ≥ 0.95 and bootstrap values (BS) ≥ 70 % are considered as supported and indicated with a thicker line. Support values are above branches. Species of *Lichinomycetes* form an outgroup. Type specimens are in **bold**. CH174 - holotype of *Chaenotheca balsamconensis*; CH175 - epitype of *Chaenotricha obscura*.

obscura, combined with *Chaenotricha* here), and two other specimens from USA and Canada. The second group includes 18 specimens from Europe (Estonia, Latvia, Norway, Sweden, European Russia), and one from Canada, and the third group is from Canada and Estonia (five specimens). The specimens in the second group have smaller ascospores and shorter stalk lengths compared to *C. obscura* (Fig. 3, Table 2). Also, the pairwise comparison of ITS sequences revealed that there are 23 parsimony informative characters (4.6 % of 504 bp, n = 25) separating these two groups as distinct species (Table 3). The third group is also well-supported molecularly, but we failed to obtain ITS sequences from any of these specimens. However, the sequences of slow-evolving genes were divergent enough not to incorporate these specimens under the names *C. cilians* or *C. obscura* (Fig. 2, Table 3). We found that the morphological characteristics of these specimens are somewhat intermediate between *C. obscura* and *C. cilians* (Fig. 3, Table 2), but because of the small sample size, we are only describing the two species that are morphologically distinct for now.

Taxonomy

Chaenotricha Suija, McMullin & P. Lõhmus, ***gen. nov.*** MycoBank MB 850355. Figs 4–7; fig. 1 in Allen & McMullin (2015).

Etymology: The name combines two genus names – *Chaenotheca*, a genus in which the type species was originally settled, and *Trichaptum*, a genus on which the lichenized species grow.

Type species: *Chaenotricha obscura* (G. Merr.) Suija, McMullin & P. Lõhmus

Typus: *Calicium (Allodium) obscurum* Merrill. Merrill, Lichenes Exsiccati prepared by G.K. Merrill no. 92. **USA**, Rockland, Maine, on dead fungus, 5 Sep. 1909, *G.K. Merrill* (**lectotype** designated here CANL 20337!, *vidi*, MBT 10016450; isotype M0205375!, *vidi*).

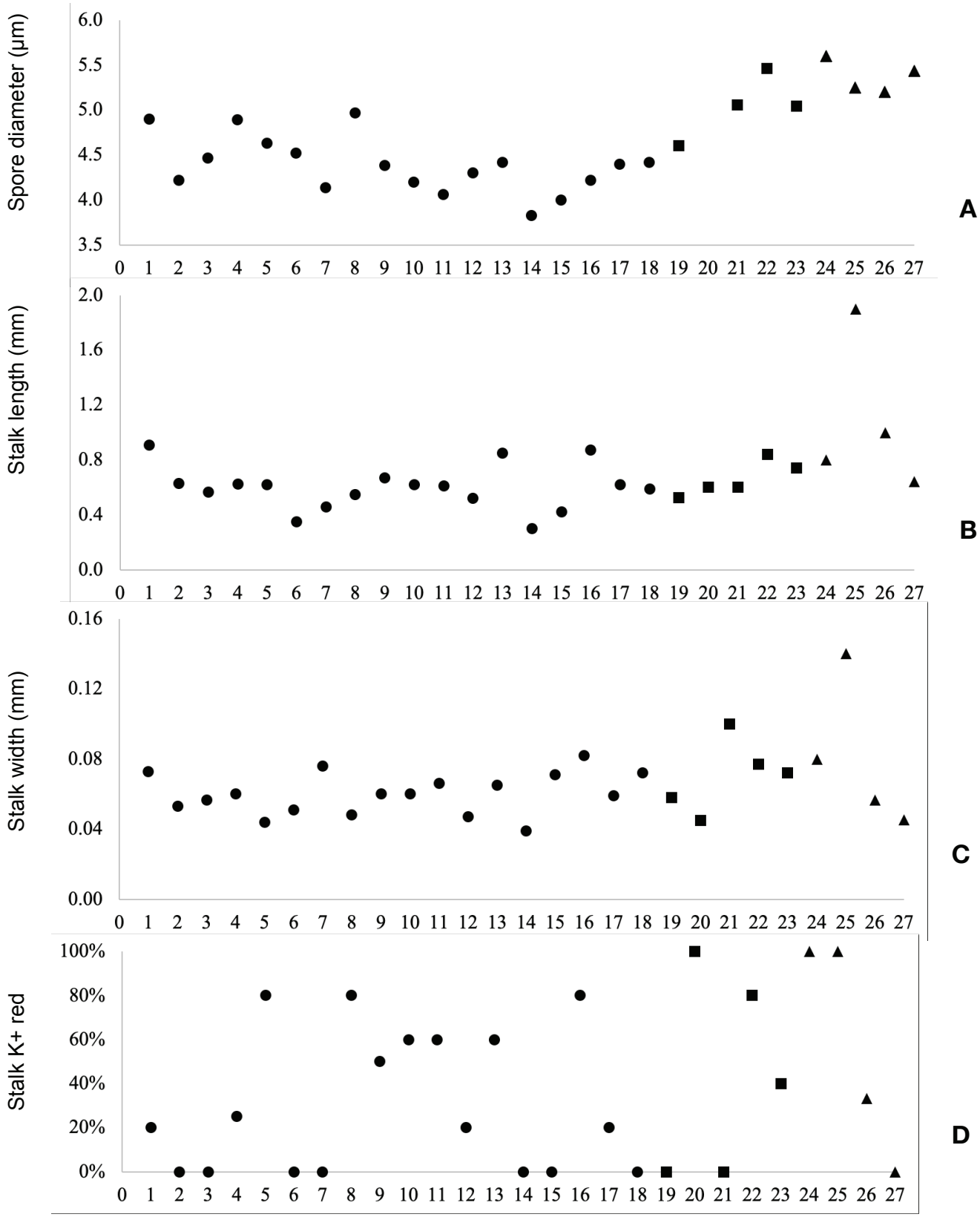

Fig. 3. Average values of anatomical (**A**) and morphological (**B**, **C**) characters and the proportion of apothecia with stalks that have a K+ red reaction (**D**) of the studied specimens of *Chaenotricha cilians* (●), *Chaenotricha* sp. (■) and *C. obscura* (▲). Specimen ID numbers correspond to vouchers in Table 1. Five apothecia were surveyed per specimen, except for ID #4 (four apothecia), #3, #26–27 (three), and #20, #24, #25 (one). Type specimen of *C. cilians* is ID #6. Spore data are missing for #20.

Table 2. Morphological and anatomical apothecial characters for three *Chaenotricha* species. Sample size (N) represents the number of specimens studied (for each specimen, up to five apothecia were studied; also see corresponding illustrations in Fig. 3).

Character	*Chaenotricha cilians*					*Chaenotricha* sp.					*Chaenotricha obscura*				
	N	min	**Mean**	max	SD	N	min	**Mean**	max	SD	N	min	**Mean**	max	SD
Stalk with K+ red (%)	18	0	**31**	80	32	5	0	**44**	100	46	4	0	**58**	100	50
Stalk+capitulum length (mm)	18	0.4	**0.7**	1.0	0.2	5	0.6	**0.8**	1.0	0.2	4	0.8	**1.3**	2.3	0.7
Stalk length (mm)	18	0.3	**0.6**	0.9	0.2	5	0.5	**0.7**	0.8	0.1	4	0.6	**1.1**	1.9	0.6
Stalk width (mm)	18	0.04	**0.06**	0.08	0.01	5	0.05	**0.07**	0.10	0.02	4	0.05	**0.08**	0.14	0.04
Stalk length to width ratio	18	6	**10**	14	2	5	6	**10**	13	3	4	10	**14**	18	3
Capitulum length (mm)	18	0.03	**0.08**	0.12	0.03	4	0.10	**0.12**	0.13	0.01	4	0.05	**0.19**	0.40	0.15
Capitulum width (mm)	18	0.1	**0.2**	0.3	0.0	4	0.2	**0.3**	0.3	0.0	4	0.1	**0.3**	0.6	0.2
Mazaedium length (mm)	18	0.03	**0.08**	0.16	0.04	4	0.08	**0.14**	0.22	0.06	2	0.05	**0.07**	0.08	0.02
Ascus length (µm)	17	16	**18**	20	1	4	18	**20**	21	1	2	16	**23**	30	10
Ascospore diameter (µm)	18	3.8	**4.4**	5.0	0.3	4	4.6	**5.0**	5.5	0.4	4	5.2	**5.4**	5.6	0.2

Table 3. An overview of the single-gene alignments (full-length ITS, nuLSU, and mtSSU) for the *Trichaptum*-specialized specimens characterized by the number of sequences in the alignment, number of base pairs in the alignment (length), number and percentage of variable nucleotide positions and parsimony informative nucleotide positions.

Locus	No. of sequences	Length (bp)	Variable (%)	Informative (%)
ITS	25	504	25 (5.0)	23 (4.6)
nuLSU	18	1 242	38 (3.1)	18 (1.5)
mtSSU	25	818	7 (1.3)	5 (0.9)

Diagnosis: Species in this genus grow exclusively on sporocarps of *Trichaptum*, which distinguishes it from the rest of *Coniocybomycetes*. It differs from the species in the *Chaenotheca brunneola* group by having ascospores without fissures and cracks.

Description: *Thallus* immersed or inconspicuous, forming loose associations with unicellular green algae on the surface of *Trichaptum* sporocarps or infrequently episubstratal forming ecorticate, granular aggregations of hyphae and algae. *Ascomata* stalked, stalk dark brown to black, mostly shiny, straight to somewhat curved, consisting of periclinally arranged brown hyphae, surface uneven, stalk K– or K+ red (color bleeds from the stalk). *Capitulum* spherical to obconical, epruinose. Mazaedium powdery. True excipulum and hypothecium well-developed, brown to dark brown, formed as a continuation of the stalk, with similar hyphal structure. *Hamathecium* consists of asci dissolving at the early stage of development, and paraphyses. *Asci* cylindrical, raising singly and directly from the ascogenous hyphae, no croziers, consisting of eight uniseriately arranged ascospores, stalked. *Paraphyses* hyaline, straight, not swollen at tips, without septa. *Ascospores* aseptate, at the early stage of development hyaline, brown when mature, smooth, spherical to irregularly spherical. *Asexual morph* not observed.

Fig. 4. Isotype of *Chaenotricha obscura* from Merrill, Lich. Exs. Ser. I 92 (CANL). Scale bar = 0.5 mm.

Chaenotricha obscura (G. Merr.) Suija, McMullin & P. Lõhmus, ***comb. nov.*** MycoBank MB 850356.
Basionym: *Calicium obscurum* G. Merr., *Bryologist* **12**: 107. 1909.
Synonyms: *Chaenotheca obscura* (G. Merr.) Nádv., *Stud. Bot. Čechoslov*. **5**: 124. 1942.
Chaenotheca balsamconensis J.L. Allen & McMullin, *Bryologist* **118**: 55. 2015.
Epitype: **USA**, Michigan, Chippewa county, Hiawatha National Forest, FS3343 1.5 mi E of jct w/ MI-123, 1.9 mi NE of Trout Lake, 4.3 mi NW of Old Dick (45.21444°N, 84.889722°W), bog dominated by *Pinus banksiana* with additional hardwoods (*Acer*, *Betula*, *Populus*, *Salix*) and conifers (*Abies*, *Larix*, *Picea*), on *T. abietinum* on dead *Pinus banksiana*, *leg. J.C. Lendemer*, #45283-A (**epitype** designated here NY02439109, *vidi*, MBT 10016475).

Species hypothesis: SH1265129.09FU.

Reference sequence from the epitype: ITS (GenBank KX348133), other available gene sequences nuLSU (GenBank OR661680), mtSSU (GenBank OR661653).

Materials examined: **Canada,** Lunenburg County, *ca*. 1 km N of Crouse's Settlement, *ca*. 1 km NE of Crouse's Settlement Road, 8 m E of Old Wood's Road (44.3561°N, 64.4050°W), coastal mature mixed-wood forest, on *T. abietinum*, on a dead *Abies balsamea*, *leg*. *F. Anderson*, *det*. *T. R. McMullin* (TUF089391). **USA**, North Carolina, Yancey County: Mount Mitchell State Park, Balsam Cone summit and vicinity, *ca*. 2 mi N of Mount Mitchell, *ca*. 3 mi W of US80 (35.7894°N, 82.2559°W), spruce (*Picea*)-fir (*Abies*) forest with *Betula, Rhododendron*, and *Sorbus* on top of narrow ridge with scattered, large rock outcrops, on *T. abietinum*, on dead *Abies*, *leg*. *J.L. Allen & J.C. Lendemer*, J. Allen #4108 (**holotype** of *C. balsamconensis* NY02359896).

Chaenotricha cilians Suija, McMullin & P. Lõhmus, ***sp. nov.*** MycoBank MB 850357. Figs 5–7, and fig. 1 in Suija *et al*. (2016).

Etymology: The epithet *cilians* was used by Theodor Magnus Fries (1832–1913) for a variant of *Chaenotheca brunneola* inhabiting *Trichaptum* sporocarps. The name was adopted by him due to the resemblance to eyelashes.

Diagnosis: This species differs from *Chaenotricha obscura* by having shorter stalks on average 0.6 mm *vs*. 1.1 mm, and slightly smaller ascospores, on average 4.5 µm *vs*. 5.5 µm. The species is similar to *Chaenotheca brunneola* (lignicolous) except inhabiting fruitbodies of *Trichaptum* spp., having exclusively cylindrical asci with uniseriately arranged smooth ascospores and stalks K– or with a K+ red reaction (bleeds from the stalk).

Typus: **Estonia**, Tartu Co., Kardla village (58.4204°N 26.5604°E), *Aegopodium* boreo-nemoral forest site type, 66-yr-old Norway spruce dominated forest, on *Trichaptum* on a *Picea abies* snag, 2 Jun. 2017, *leg. P. Lõhmus*, Kardla ID27 (**holotype** TUF091612).

Species hypothesis: SH1265130.09FU.

Reference sequence: ITS (UNITE: UDB0801842; GenBank OR661721), other gene sequences nuLSU (GenBank OR661692), mtSSU (GenBank OR661665).

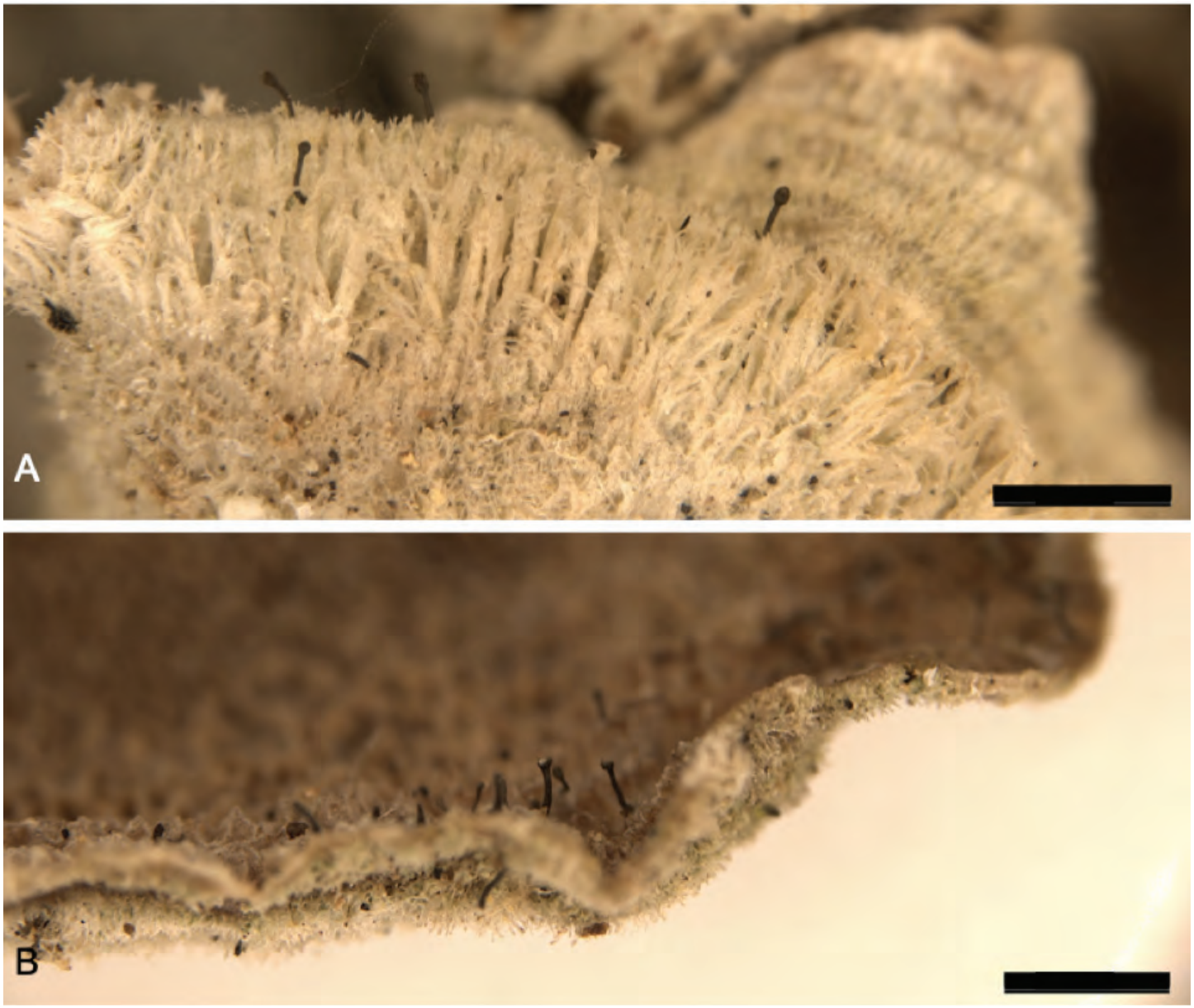

Fig. 5. *Chaenotricha cilians sp. nov*. **A.** Ascomata of *C. cilians* on the upper side of the *Trichaptum* fruitbodies (TUF091612, holotype). **B.** Ascomata on the hymenophore layer of the *Trichaptum* fruitbodies (TUF050023). Scale bars = 20 mm.

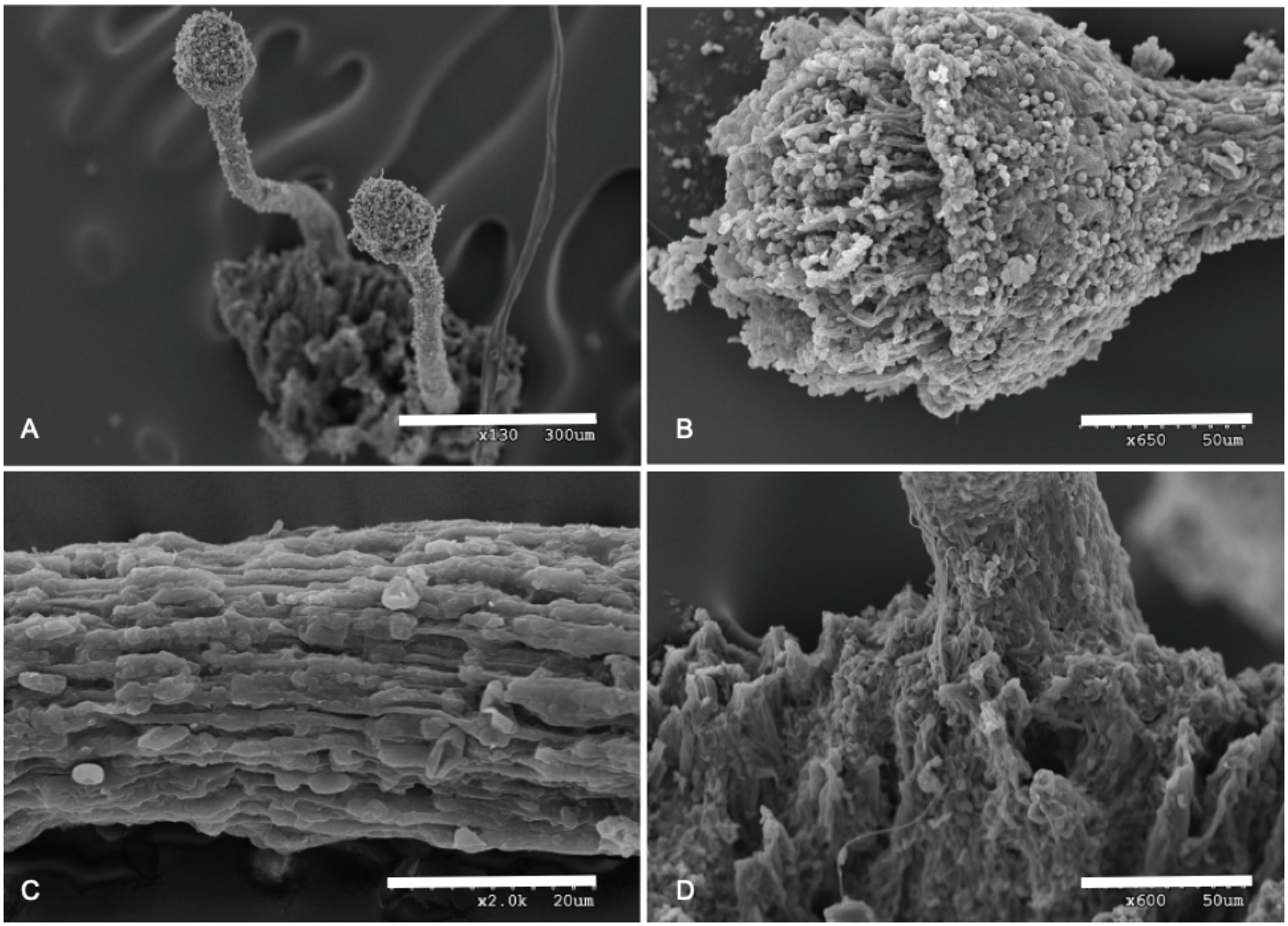

Fig. 6. Scanning electron microscopy of *Chaenotricha cilians* (specimen TRH-L-18708). **A.** Ascomata (note the obovate shape of the mazaedium). **B.** Exciple surrounding the hamathecium. **C.** Periclinally arranged hyphae of the stalk. **D.** Base of ascomatal stalk. Scale bars: A = 300 µm; B, D = 50 µm; C = 20 µm.

Description: *Thallus* inconspicuous, mycobiont hyphae loosely connected with cells of trebouxioid algae on the sporocarp surface. *Ascomata* developed on the upper surface and at the edge of the fungal sporocarp. *Stalk* epruinose, dark brown, K–, (0.35–)0.4 ± 0.07(–0.5) mm in length × (0.045–)0.05 ± 0.01(–0.06) mm in width, length to width ratio (6–)7 ± 1(–8). *Capitulum* spherical to obconical, (0.10–)0.13 ± 0.01(–0.14) mm in diameter (n = 5). *Excipulum* well developed, mazaedium dark brown, powdery. *Asci* cylindrical, born singly on a stalk, (15–)19.3 ± 4.4(–30) µm in length (n = 20); some measured asci (n = 9) had a stipe, (5–)5.6 ± 1.7(–10) µm long. *Ascospores* arranged within the ascus uniseriately, hyaline when young, brown, smooth, spherical to irregularly spherical, (3–)4.5 ± 0.6(–5) µm diam (n = 50). *Asexual morph* not observed.

Ecology and Distribution: *Chaenotricha cilians* grows on the sporocarps of three *Trichaptum* species, *T. abietinum, T. fuscoviolaceum* and *T. biforme.* So far, the distribution includes European countries (Denmark, Estonia, Latvia, Lithuania, Norway, Russia, Sweden) but there is also one record from Canada. *Chaeotricha cilians* is reported from hemiboreal and boreal forests and bog areas, on *Trichaptum* sporocarps inhabiting standing dead trunks, mainly of Norway spruce and Scots pine and rarely on birch.

Notes: Eighteen specimens were examined (see Table 1), and on a few occasions ascomata were produced on the hymenophore surface (Fig 4B), and in those cases, we did not find associations with algae using a compound light microscope. Moreover, we did not locate living or dead algal cells in the area around the ascomata. Life-style switching is common among fungi, and optional and weak lichenization has been demonstrated for several groups of ascomycetes (*e.g.*, Wedin *et al.* 2006, Pérez-Ortega *et al*. 2016). Our results suggest that *C. cilians* may be an example of optional lichenization. Genome screening, metatranscriptomics, and other techniques may provide further information about the relationships of this tri-partite association.

The intensity of the K+ red pigment reaction of the stalks and the degree of shininess can vary within and among specimens (Fig. 3D, Table 2). The length of apothecia (and other anatomical and morphological characters) may vary slightly among specimens (Fig. 3, Table 2); for example, the type specimen has 0.2 mm shorter stalks than the average length measured for 18 specimens (Table 2). The species differs significantly from *Chaenotricha obscura* by its 1 µm smaller spores, respectively (Table 2; Mann-Whitney U test, U = 7.00, p = 0.013) and in the length of the stalk, which is significantly shorter than that of *C. obscura* (on average 0.5 mm, Table 2; U = 0, p = 0.002), However,

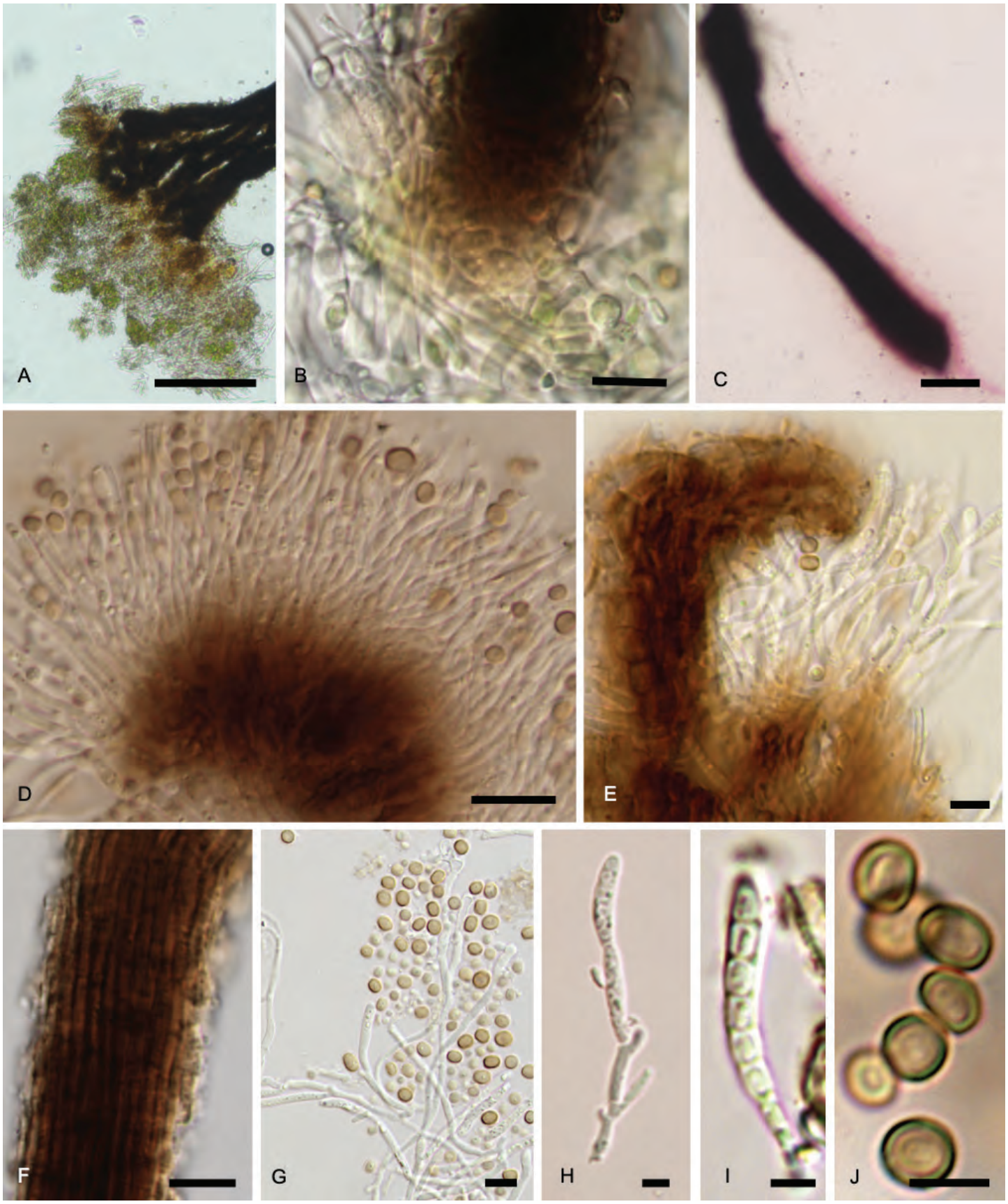

Fig. 7. Micromorphological characters of *Chaenotricha cilians* (TUF050023). **A, B**. Base of the stalk. **C.** K+ bleeding red reaction of the apothecium. **D.** Hypothecium and hamathecium consisting of asci at different developmental stages and paraphyses, and single liberated ascospores. **E.** Exciple. **F.** Stalk structure (note periclinally arranged hyphae and uneven surface of the stalk). **G.** Developing asci, paraphyses and ascospores **H.** Ascus (immature) developing singly from the ascogenous cells. **I.** Immature ascus with developing ascospores. **J.** Mature ascospores. Scale bars: A, C = 50 µm; B, F = 20 µm; D, E, G = 10 µm; H–J = 5 µm.

because of very unequal (and small) sample sizes of species groups, the results of statistical tests should be interpreted with caution.

Materials examined (selected): **Denmark**, North Denmark Region, Thisted Municipality, Nationalpark Thy (56.9769°N, 8.4274°E), on *Trichaptum* sp. on *Pinus contorta*, 14 Oct. 2023, *leg. P. Lõhmus & A. Suija* (TUF095157); *ibid*., Thagaard plantation (56.9817°N, 8.4283°N), on *T. abietinum* on standing corticated *Pinus cf. mugo*, 14 Oct. 2023, *leg. N. Johansson* (TUF095158). **Estonia**, Pärnu county, Saarde community (58.1224°N, 25.0914°E), on *T. abietinum* on a *Picea abies* snag, 18 Aug. 2014, *leg. P. Lõhmus* (TUF076419; TUF076420); Surju comm. (58.3099°N, 24.9826°E), on *T. abietinum* on a *P. sylvestris* snag, 26 May 2014, *leg. P. Lõhmus* (TUF076423); Tartu co., Puhja comm. (58.3337°N, 26.2631°E), on *T. abietinum* on snag of *P. sylvestris*, 10 Jun. 2014, *leg. P. Lõhmus* (TUF076422); Tartu comm., Valmaotsa village, Selli-Sillaotsa hiking trail, Alam-Pedja Nature Reserve, (58.4411°N, 26.2662°E), on *Trichaptum* sp. on a snag of *Betula*, 7 Aug. 2022, *leg. A. Suija & M. Suija* (TUF050023). **Latvia**, Alūksne Municipality, Liepna Parish, young boggy birch forest (57.4110°N 27.4843°E), on *T. abietinum* on *P. sylvestris*, unknown collection date, *leg. R. Moisejevs* (DAU0602050); *ibid*. (DAU0602051); Jēkabpils Municipality, Sauka Parish (56.3187°N 25.3954°E), on *T. abietinum* on *P. sylvestris*, unknown collection date, *leg. R. Moisejevs* (DAU0602052); Drabeši parish (57.2638°N, 25.1108°E), spruce forest, on *Trichaptum* sp. on natural spruce stump, 2020, *leg. P. Degtjarenko & R. Moisejevs* (TUF090000). **Lithuania**, Trakai district, Plomenai bog. close to Sibirka village (54.6425°N, 24.9004°E), on sporocarps of *Trichaptum* sp. growing on *Pinus*, 6 Feb. 2022, *leg. M. Ryla* (TUF095099, ex BILAS 11108). **Norway,** Steinkjer Municipality, W of Strukstadmyra (63.9873°N, 11.5801°E), boreal rainforest, on *Trichaptum* on dead spruce (*P. abies*), 9 Aug. 2018, *leg. A. Frisch* (TRH-L-18707); Vefsn Municipality, Langmoen, NW of Fustvatnet (65.912°N, 13.28372°E), on *Trichaptum* sp. on a spruce snag, 26 Jun. 2018, *leg. A. Frisch* (TRH-L-18706); Grong Municipality, Solemsmoen naturreservat, Kvernbekken (64.5760°N, 12.5557°E), boreal rainforest, on *T. abietinum* on *P. abies*, 16 Aug. 2019, *leg. H. Holien* (TRH-L-18708); Nordre Follo, Ås (59.6715°N,10.8846°E), on *T. fuscoviolaceum* on dead *P. sylvestris* in *Sphagnum* bog, 28 Jan. 2023, *leg. A. K. Ruud* (TUF050022); Fredrikstad Municipality, Askedalstangen (59.1367°N,11.0780°E), on *T. fuscoviolaceum* on pine, 5 Nov. 2022, *leg. A.G. Helle* (TUF095043); Moss, Vardasen nature reserve (59.3529°N,10.6764°E), on *T. fuscoviolaceum* on pine, 29 Jan. 2023, *leg. A.G. Helle & M. Angard* (TUF095044). **Russia,** Krasnoznamensky District, SE to Krasnoznamensk, forest "Michurinsky", near Kaban'e bog" (54.8892°N, 22.5622°E), old-growth pine forest with *Sphagnum* spp. and *Carex* sp., with mosses and *Vaccinium myrtillis* on hummocks, with young birches and spruce undergrowth, with upturned trees and big log, on *T. biforme* on trunk of *Betula* sp., 27 Sep. 2019, *leg. I. Stepanchikova & D. Himelbrant* (BILAS). **Sweden,** Uppsala, Kvarnbo (59.8410°N, 17.5668°E), on *T. fuscoviolaceum*, 21 Apr. 2019, *leg. R. Elleby* (UPS-L-941561); Åmål Municipality, Edelskog par., Baljasen Nature Reserve, *ca*. 750 m NW of the folk museum Petersborg (59.0812°N, 12.4657°E), on *T. abietinum* on the trunk of *P. abies*, 14 Apr. 2017, *leg. M. Westberg & C. Kannesten* (UPS-L-867275); Uppsala, Hammarparken, (59.8424°N, 17.5981°E), on *T. fuscoviolaceum*, 16 Mar. 2019, *leg. H. Lernefalk & B. Kühn* (UPS-L-941560); Uppland, Vänge par., Fiby urskog (59.8899°N, 17.3525°E), on *T. abietinum* on *P. abies*, 7 Apr. 2016, *leg. J. C. Zamora, M. Svensson, S. Ekman, M. Westberg & G. von Hirschheydt* (UPS-L-872283).

***Chaenotricha* sp.**

Five specimens that we examined form a well-supported clade in the three-marker phylogenetic tree (Fig. 2). These specimens have an intermediate set of morphological characteristics between the other two *Chaenotricha* species. They are similar to *C. cilians* in stalk length, and other morpho-anatomical characters (Fig. 3, Table 2), but they differ by having larger (average 5 µm) ascospores similar to those to *C. obscura* (for additional results see the Notes of *C. cilians*).

Distribution: Five localities in North America (Canada, USA) and Europe (Estonia) are known.

Specimens examined: **Canada**, Lunenburg County, *ca*. 1 km N of Crouse's Settlement, *ca*. 1 km NE of Crouse's Settlement Road, 3 m E of Old Wood's Road (44.3555°N, 64.4045°W), coastal mature mixed-wood forest, on *T. abietinum*, on an *Abies balsamea* snag, 30 Aug. 2020, *leg. R.T. McMullin* (TUF089393); Ontario, Thunder Bay District, Sibley Peninsula, Sleeping Giant Provincial Park, between park cabin 5 and the Marie Louise Lake Campground, (48.4584°N, 88.7368°W), 16 Oct. 2018, *leg. R.T. McMullin* (TUF089481). **Estonia**, Saaremaa, Lussu village (58.4575°N, 22.4370°E), on *T. fuscoviolaceum* on *P. sylvestris*, 12 Nov. 2019, *leg. M. Nõmm* (TUF089547); Järise village (58.4920°N, 22.3916°E), on *T. fuscoviolaceum*, on log of *P. sylvestris*, 31 Oct. 2019, *leg. M. Nõmm* (TUF089548). **USA**, Haywood County, Great Smoky Mountains National Park, McKee Branch Trail, 0.48 km (linear) SE of junction with Caldwell Fork Trail (35.5952°N, 83.0991°W), mature mixed-wood forest, deciduous dominated in protected river valley, on *T. abietinum*, 27 Oct. 2017, *leg. R.R. McMullin* (TUF089480).

ACKNOWLEDGEMENTS

The curators of BILAS, UPS, TRH and M are thanked for loans of herbarium specimens, Irina Stepanchikova, Dmitry Himelbrant, Anja Karine Ruud, Andres Gunnar Helle, Rolands Moisejevs, Polina Degtjarenko, Maarja Nõmm, Mindaugas Ryla and Niko Johansson for collecting material from Russia, Norway, Latvia, Estonia, Lithuania and Denmark. Rasmus Puusepp and Marju Vahter are thanked for laboratory work, Kadri Runnel (all from University of Tartu) for determining species of *Trichaptum*, and Yolanda Ruíz León (RJB, Madrid) for performing Scanning Electron Microscopy. Funding for AS was provided by the European Regional Development Fund (Centre of Excellence EcolChange), by Estonian Research Council grant PRG1170 by SYNTHESYS+ project (http://www.synthesys.info/) financed by European Community Research Infrastructure Action under the H2020 Integrating Activities Programme, Project number 823827 at the Real Jardín Botánico & Museo Nacional de Ciencias Naturales (CSIC) SYNTHESYS grant ES-TAF-1280.

Conflict of interest: The authors declare that there is no conflict of interest.

REFERENCES

Abarenkov K, Tedersoo L, Nilsson RH, *et al*. (2010). PlutoF – a Web Based Workbench for Ecological and Taxonomic Research, with an Online Implementation for Fungal ITS Sequences. *Evolutionary Bioinformatics* **6**: 189–196.

Allen JL, McMullin RT (2015). *Chaenotheca balsamconensis*, a new calicioid lichen on *Trichaptum abietinum* from North America that is benefiting from widespread conifer fatalities. *Bryologist* **118**: 54–58.

Altschul SF, Gish W, Miller W, *et al*. (1990). Basic local alignment search tool. *Journal of Molecular Biology* **215**: 403–410.

Bengtsson-Palme J, Veldre V, Ryberg M, *et al*. (2013). ITSx: improved software detection and extraction of ITS1 and ITS2 from ribosomal ITS sequences of fungi and 880 other eukaryotes for use in environmental sequencing. *Methods in Ecology and Evolution* **4**: 914–919.

Brodo IM, Sharnoff SD, Sharnoff S (2001). *Lichens of North America*. Yale University Press.

Darriba D, Taboada GL, Doallo R, *et al*. (2012). jModelTest 2: more models, new heuristics and parallel computing. *Nature Methods* **9**: 772.

Díaz-Escandón D, Tagirdzhanova G, Vanderpool D, *et al*. (2022). Genome-level analyses resolve an ancient lineage of symbiotic ascomycetes. *Current Biology* **32**: 5209–5218.

Fries TM (1865). 3. Nya skandinaviska laf-arter. *Botaniska Notiser*: 38–40.

Garbelotto MM, Lee HK, Slaughter G, *et al*. (1997). Heterokaryosis is not required for virulence of *Heterobasidion annosum*. *Mycologia* **89**: 92–102.

Gouy M, Guindon S, Gascuel O (2010). SeaView version 4: a multiplatform graphical user interface for sequence alignment and phylogenetic tree building. *Molecular Biology and Evolution* **27**: 221–224.

Hutchison LJ (1987). Studies on *Phaeocalicium polyporaeum* in North America. *Mycologia* **79**: 786–789.

Kalyaanamoorthy S, Minh BQ, Wong TKF, *et al.* (2017). ModelFinder: Fast model selection for accurate phylogenetic estimates. *Nature Methods* **14**: 587–589.

Katoh K, Rozewicki J, Yamada KD (2019). MAFFT online service: multiple sequence alignment, interactive sequence choice and visualization. *Brief Bioinformatics* **20**: 1160–1166.

Kauserud H, Schumacher T (2003). Regional and local population structure of the pioneer wood-decay fungus *Trichaptum abietinum*. *Mycologia* **95**: 416–425.

Kozlov AM, Darriba D, Flouri T, *et al.* (2019). RAxML-NG: A fast, scalable, and user-friendly tool for maximum likelihood phylogenetic inference. *Bioinformatics* **35**: 4453–4455.

Lanfear R, Calcott B, Ho SYW, *et al.* (2012). PartitionFinder: combined selection of partitioning schemes and substitution models for phylogenetic analyses. *Molecular Biology and Evolution* **29**: 1695–1701.

Larsson A (2014). AliView: a fast and lightweight alignment viewer and editor for large data sets. *Bioinformatics* **30**: 3276–3278.

Larsson K-H, Parmasto E, Fischer M, *et al*. (2006). *Hymenochaetales*: a molecular phylogeny for the hymenochaetoid clade. *Mycologia* **98**: 926–936.

Maurice S, Arnault G, Nordén J, *et al.* (2021). Fungal sporocarps house diverse and host-specific communities of fungicolous fungi. *ISME Journal* **15**: 1445–1457.

Merrill GK (1909). Lichen notes No. 14. Three New Forms of *Calicium*. *Bryologist* **12**: 107–108.

Minh BQ, Nguyen MAT, von Haeseler A (2013). Ultrafast approximation for phylogenetic bootstrap. *Molecular Biology and Evolution* **30**: 1188–1195.

Mukhin VA, Neustroeva NV, Patova EN, *et al.* (2018). Lichen-like symbiotic associations of wood-decaying fungi and algae. I. In: *The fourth International Scientific Conference on Ecology and Geography of Plants and Plant Communities*. KnE Life Sciences: 134–142.

Pérez-Ortega S, Garrido-Benavent I, Grube M *et al*. (2016). Hidden diversity of marine borderline lichens and a new order of fungi: *Collemopsidiales* (*Dothideomyceta*). *Fungal Diversity* **80**: 285–300.

Prieto M, Baloch E, Tehler A, *et al.* (2013). Mazaedium evolution in the *Ascomycota* (*Fungi*) and the classification of mazaediate groups of formerly unclear relationship. *Cladistics* **29**: 296–308.

Rambaut A (2014). FigTree v. 1.4.2. Software available from author, http://tree.bio.ed.ac.uk/software/ figtree/.

Ronquist F, Teslenko M, van der Mark P, *et al*. (2012). MrBayes 3.2: efficient bayesian phylogenetic inference and model choice across a large model space. *Systematic Biology* **61**: 539–542.

Schmidt A (1970). Anatomisch-taxonomische Untersuchungen an europaeischen Arten der Flechtenfamilie *Caliciaceae*. *Mitteilungen der Staatsinstitut für Allgemeine Botanik Hamburg* **13**: 111–166.

Selva SB (2014). The calicioid lichens and fungi of the Acadian Forest Ecoregion of northeastern North America, II. The rest of the story. *Bryologist* **117**: 336–367.

Selva SB, McMullin RT (2020). An update of G.K. Merrill's 1909 "Lichen notes no. 14". *Mycotaxon* **135**: 333–337.

Spribille T, Pérez-Ortega S, Tønsberg T, *et al.* (2010). Lichens and lichenicolous fungi of the Klondike Historic Park, Alaska, in a global biodiversity context. *Bryologist* **113**: 439–515.

Stamatakis A (2006). RAxML-VI-HPC: maximum likelihood-based phylogenetic analyses with thousands of taxa and mixed models. *Bioinformatics* **22**: 2688–2690.

Stonyeva MP, Uzunov BA, Gärtner G (2015). Aerophytic green algae, epimycotic on *Fomes fomentarius* (L. ex Fr.) Kickx. *Annuals of Sofia University "St. Kliment Ohridski". Faculty of Biology* **99**: 19–25.

Suija A, Suu A, Lõhmus P (2016). Substrate specificity corresponds to distinct phylogenetic lineages: The case of *Chaenotheca brunneola*. *Herzogia* **29**: 355–363.

Sun JZ, Liu XZ, McKenzie EHC, *et al*. (2019). Fungicolous fungi: terminology, diversity, distribution, evolution, and species checklist. *Fungal Diversity* **95**: 337–430.

Talavera G, Castresana J (2007). Improvement of phylogenies after removing divergent and ambiguously aligned blocks from protein sequence alignments. *Systematic Biology* **56**: 564–577.

Tedersoo L, Jairus T, Horton BM, *et al*. (2008). Strong host preference of ectomycorrhizal fungi in a Tasmanian wet sclerophyll forest as revealed by DNA barcoding and taxon-specific primers. *New Phytologist* **180**: 479–490.

Tibell L (1980). The lichen genus *Chaenotheca* in the northern hemisphere. *Symbolae Botanicae Upsalienses* **23**: 1–63.

Tibell L (1999). Calicioid lichens and fungi. In: *Nordic Lichen Flora. Volume 1. Introductory Parts. Calicioid Lichens and Fungi* (Ahti, T, Jørgensen PM, Kristinsson H, *et al.*, eds). Nordic Lichen Society, Uddevalla, Sweden: 20–94.

Tibell L, Tibell S, van der Pluijm A (2019). *Chaenotheca biesboschii* a new calicioid lichen from willow forests in the Netherlands. *Lichenologist* **51**: 123–135.

Trifinopoulos J, Nguyen L-T, von Haeseler A, *et al.* (2016). W-IQ-TREE: a fast online phylogenetic tool for maximum likelihood analysis. *Nucleic Acids Research* **44** (W1): W232–W235.

Vilgalys R, Hester M (1990). Rapid genetic identification and mapping of enzymatically amplified ribosomal DNA from several *Cryptococcus* species. *Journal of Bacteriology* **172**: 4238–4246.

Vondrák J, Svoboda S, Zíbarová L, *et al.* (2023). Alcobiosis, an algal-fungal association on the threshold of lichenisation. *Scientific Reports* **13**: 2957.

Wedin M, Döring H, Gilsenstam G (2006). *Stictis s. lat*. (*Ostropales*, *Ascomycotina*) in northern Scandinavia, with a key and notes on morphological variation in relation to lifestyle. *Mycological Research* **110**: 773–789.

White TJ, Bruns T, Lee S, *et al*. (1990). Amplification and direct sequencing of fungal ribosomal RNA for phylogenetics. In: *PCR protocols: a guide to methods and applications* (Innis MA, Gelfand DH, Sninsky JJ, *et al*., eds). Academic Press Inc., New York, USA: 315–322.

Zavada MS, Simoes SP (2001). The possible demi-lichenization of the basidiocarps of *Trametes versicolor* (L.: Fries) Pilat (*Polyporaceae*). *Northeast Naturalist* **8**: 101–112.

Zoller S, Scheidegger C, Sperisen C (1999). PCR primers for the amplification of mitochondrial small subunit ribosomal DNA of lichen-forming ascomycetes. *Lichenologist* **31**: 511–516.

Supplementary Material: http://fuse-journal.org/

Table S1. List of evaluated morphological characters.

FUSE

Fungal Systematics and Evolution

Volume 12
DECEMBER 2023
PAGES 271–322

doi.org/10.3114/fuse.2023.12.14

A revised genus-level classification for *Cerrenaceae* (*Polyporales, Agaricomycetes*)

O. Miettinen[1*], J. Vlasák[2], E. Larsson[3], J. Vlasák Jr.[4], J.S.S. Seelan[5], Hernawati[6], Q. Levicky[7], K.-H. Larsson[8], V. Spirin[1]

[1]Finnish Museum of Natural History, P.O. Box 7, 00014 University of Helsinki, Finland
[2]Biology Centre, Academy of Sciences of the Czech Republic, Branišovská 31, CZ 37005, České Budějovice, Czech Republic
[3]Biological and Environmental Sciences, University of Gothenburg, and Gothenburg Global Biodiversity Centre, Box 461, 40530 Gothenburg, Sweden
[4]207 Silverbrook Dr., Schwenksville, PA, USA
[5]Mycology and Pathology Laboratory, Institute for Tropical Biology and Conservation (ITBC), Universiti Malaysia Sabah, 88400 Kota Kinabalu, Sabah, Malaysia
[6]Fakultas Kehutanan (Faculty of Forestry), Universitas Muhammadiyah Sumatera Barat, Padang, Sumatera Barat 25172, Indonesia
[7]The Royal Botanic Gardens, Kew, Richmond, TW9 3AB, UK
[8]Natural History Museum, University of Oslo, P.O. Box 1172 Blindern, 0318 Oslo, Norway

*Corresponding author: otto.miettinen@helsinki.fi

Key words:
hydnoid fungi
hyphal system
new taxa
pathogenic fungi
polypore
root rot disease
systematics
taxonomy

Abstract: *Cerrenaceae* is a small family of polypores and hydnoid fungi in the order *Polyporales* (*Basidiomycota*). The family consists of white-rot fungi, some of which are serious tree pathogens. Combining morphological evidence with a phylogenetic dataset of six genetic markers, we revise generic concepts in the family and propose a seven-genus classification system for the family. Two genera are introduced as new: the monotypic *Acanthodontia* for *Radulodon cirrhatinus*, and *Lividopora* for the *Rigidoporus vinctus* complex. We re-introduce the name *Somion* for the *Spongipellis delectans* complex. Other recognized genera in the family are *Cerrena, Irpiciporus, Pseudolagarobasidium*, and *Radulodon*. New species introduced are *Irpiciporus branchiformis* from Tanzania, *Lividopora armeniaca*, and *L. facilis* from Southeast Asia, and *Somion strenuum* from East Asia. We provide nomenclatural comments on all the names combined to the above *Cerrenaceae* genera and typify *Cerrena unicolor*, *C. zonata*, *Polyporus carneopallens* (= *L. vincta*), *Somion occarium*, and *S. unicolor*. The genus *Hyphoradulum* belongs to *Cystostereaceae* (*Agaricales*), and we transfer the type species *H. conspicuum* to *Crustomyces*. Our study highlights the importance of integrating different basidiocarp types in analyses when revising genus classification in macrofungi.

Citation: Miettinen O, Vlasák J, Larsson E, Vlasák J Jr., Seelan JSS, Hernawati, Levicky Q, Larsson K-H, Spirin V (2023). A revised genus-level classification for *Cerrenaceae* (*Polyporales*, *Agaricomycetes*). *Fungal Systematics and Evolution* **12**: 271–322. doi: 10.3114/fuse.2023.12.14
Received: 5 August 2023; **Accepted:** 28 November 2023; **Effectively published online:** 29 November 2023
Corresponding editor: P.W. Crous

INTRODUCTION

A phylogenetic framework became available to mycologists in the 1990s with the onset of easy and low-cost DNA sequencing. Its impact has step by step penetrated fungal systematics and classification. Hibbett *et al.* (2007) established a classification system at the order level and above. Justo *et al.* (2017) extended the phylogeny-based classification to the family level in the order *Polyporales*, which is dominated by macrofungal basidiocarp types, polypores and crusts (corticioid fungi). Family concepts in this scheme are monophyletic groups defined by their genetic similarity; morphology was not – and one could argue cannot be – a leading principle when designing fungal classification at the higher levels.

Yet DNA-based phylogenetics does not liberate us from considering morphological or ecological characters in taxonomy. Most species can be and are being defined by morphological or ecological traits. Some of the families might be characterized morphologically, others not; but between the family and species level there is a space, genus-level and intermediary ranks, where morphology and phylogenetics both can and should define classification. The question how to define monophyletic genera so that they would be morphologically identifiable whenever possible is an important consideration when revising classification. Each family is likely to represent a unique dilemma in this sense, and it is becoming evident that only suboptimal solutions exist in some cases, thus is the level of morphological plasticity in fungi.

The subject of our paper is one of the families Justo *et al*. (2017) established, the *Cerrenaceae*. This small family includes wood decomposers and tree pathogens. Basidiocarp morphology varies from polypores such as *Antrodiella p.p.*, *Cerrena*, *Rigidoporus p.p.*, and *Spongipellis p.p.* (Fig. 1) to hydnoid fungi such as *Pseudolagarobasidium* and *Radulodon* (Fig. 2). When establishing the genus, Justo *et al*. did not elaborate on how the family might be delimited morphologically or how to classify species diversity within it. Here we have studied most of the species complexes and all the genera in the *Cerrenaceae*, and propose a genus classification for the family. This task exemplifies the problem of balancing morphological signal with phylogenetics – in essence between the extremes of many small

Fig. 1. Poroid members of the *Cerrenaceae*. **A.** *Cerrena albocinnamomea* (*Niemelä 6372*). **B.** *Cerrena unicolor* (*Miettinen 16901*). **C.** *Cerrena zonata* (*Miettinen 13798*). **D.** *Lividopora benetosta* (*Miettinen 18135*). **E.** *Somion occarium* (*Overall*, K(M) 159049). **F.** *Somion strenuum* (holotype). **G.** *Somion tomsovskyi* (*Vlasák Jr.*, JV 1307/8). Scale bars = 1 cm.

Fig. 2. Hydnoid and irpicoid representatives of *Cerrenaceae*. **A.** *Acanthodontia cirrhatina* (*Miettinen 13717*). **B.** *Irpiciporus pachyodon* (*Spirin 13785*). **C.** *Radulodon erikssonii* (*Miettinen 10977*). **D.** *Pseudolagarobasidium subvinosum* in herbarium (*Wu 8609*). Scale bars = 1 cm.

genera or a few larger ones. As we will show below, neither solution is perfect. Both solutions would create a situation where morphological genus definition is difficult, and yet one of them has to be implemented to avoid non-phylogenetic genera.

If polypores and hydnoid fungi would be viewed in isolation, one could arrive at two classification systems that do a good job creating monophyletic, morphologically easy-to-recognize genera within the *Cerrenaceae*. However, these two schemes would not be mutually compatible (phylogenetically logical). We argue that genus taxonomy should be revised in overview papers such as Justo & Hibbett (2011), Miettinen *et al.* (2012), Chen *et al.* (2021), Savchenko *et al*. (2021) and Li *et al.* (2022) to mention a few good examples from corticioid fungi and polypores. These papers are based on large, multi-marker, and taxonomically inclusive datasets. In contrast, many current taxonomic papers treat each case in isolation and routinely erect new genera for newly-discovered clades in the most recent phylogram without the benefit of a wider perspective.

Following is a short introduction to currently recognized genera in the *Cerrenaceae*.

Antrodiella is a polypore genus that historically included dimitic white-rot species with small pores and spores. Miettinen *et al.* (2012) suggested a narrower, monophyletic concept for the genus, a concept that was adopted by some subsequent authors (Yuan 2014, Westphalen *et al*. 2019) but not all (Ryvarden 2018, 2020a). *Antrodiella sensu stricto* belongs to the *Steccherinaceae*. In his paper on Chinese *Antrodiella*, Yuan (2014) showed that *A. albocinnamomea* and *A. zonata* are related to *Cerrena* and transferred them to *Cerrena*, though without wider consideration of genus classification in the *Cerrena* clade (*Cerrenaceae*). We show in this paper that *A. multipileata* also belongs to the *Cerrenaceae*.

Cerrena, as currently recognized, is a small polypore genus perhaps best known for *Cerrena unicolor*, a wide-spread temperate species in the northern hemisphere. *Cerrena unicolor* has two relatives (*C. cystidiata* and *C. 'gilbertsonii'*). As mentioned, Yuan (2014) also included two former *Antrodiella* species in the genus as *C. albocinnamomea* and *C. zonata*. In our experience, *Cerrena unicolor* is a phytopathogen, and Dai *et al*. (2007) list *C. zonata* as a heartwood rotter of living trees. *Cerrena unicolor* has been studied for its enzymatic capabilities (Janusz *et al*. 2007, Elisashvili *et al*. 2010, Lisova *et al.* 2010, Hartikainen *et al*. 2016, Janusz *et al*. 2018), as has *C. albocinnamomea* (Yuan *et al*. 2012).

Pseudolagarobasidium contains nine temperate to tropical species with thin, hydnoid basidiocarps. The current genus concept derives from Hallenberg *et al*. (2008) and Nakasone & Lindner (2012). Two species are known to be tree pathogens, causing root rot (Jang & Chen 1985, Wood & Ginns 2006), while others have been reported as endophytes and saprotrophs (Hallenberg *et al*. 2008).

Radulodon contains several light-coloured hydnoid species. Nakasone & Lindner (2012) narrowed the genus concept by excluding a set of species, and we continue here, leaving two temperate species and a recently described species from the Eastern Himalayas (Wang & Dai 2022). *Radulodon* spp. are apparently saprotrophs of angiosperms.

Rigidoporus in the traditional sense is a highly polyphyletic genus. Species placed under it are found in two orders (*Hymenochaetales* and *Polyporales*) and within the *Polyporales* in several families, the largest of which is the *Meripilaceae* (Justo *et al*. 2017, Wu *et al*. 2018). Justo *et al*. (2017) showed that the *Rigidoporus vinctus* complex belongs to the *Cerrenaceae*. It is clear that *Rigidoporus* in the strict sense is not related, and consequently a better-fitting genus has to be found for the *R. vinctus* complex. This species group includes effused polypores mostly found in the tropics. Several species (previously called varieties) are known as tree pathogens in the tropics and New Zealand ("red root-rot", Setliff & Mesner 1971, Setliff 1972b, Hood & Dick 1988). They have also been detected as endophytes of rubber (Martin *et al*. 2015). We revise this species complex here.

Spongipellis is a small genus of polypores comprising about 10 species. Its current concept was introduced by Bondartsev & Singer (1941), but their concept has been shown to be polyphyletic and their species concepts outdated (Tomšovský 2012, Dvořák *et al*. 2014). *Spongipellis* in the strict sense is related to *Meripilaceae*, whereas the species complexes *S. delectans* and *S. pachyodon* are in the *Cerrenaceae* (Justo *et al*. 2017, Kotiranta *et al*. 2017). The genus name *Irpiciporus* is available for the *S. pachyodon* species complex and has been put in use recently (Wang & Dai 2022). Species of the *S. delectans* complex have been reported to be serious tree pathogens of oaks (Ljubarsky 1934, Černý 1979, Dai *et al.* 2007). Wang & Dai (2022) recently described the genus *Pseudospongipellis* for the *S. delectans* complex. We re-introduce here the older genus name *Somion* for this clade. Nakasone & Ortiz-Santana (2022) added several species.

In this paper, we comment on all names combined to *Cerrena*, *Irpiciporus*, *Pseudolagarobasidium*, and *Radulodon*. For *Spongipellis* nomenclature, see Spirin *et al*. (2022), who focused on *Spongipellis sensu stricto*. We comment further on *Spongipellis* names here, including all names we know are associated with the *Cerrenaceae*, but provide no exhaustive checklist for this genus.

MATERIALS AND METHODS

We studied 152 specimens from the following fungaria: H, O, BPI, CFMR, DAOM, FH, FLOR, GB, K, NY, PC, PRM, and W (Thiers 2023). JV refers to the personal fungarium of Josef Vlasák. The basic mountant used in microscopic descriptions is Cotton Blue (CB). We measured 30 basidiospores per specimen and 20 hyphae for each hyphal type for each specimen used in making the descriptions. When presenting measurements of basidiospores, 5 % extreme values from both ends of variation are given in parentheses. For hyphal measurements, the 20 % tails are placed in parentheses. The following abbreviations are used in descriptions below: L – mean spore length, W – mean spore width, Q – L/W ratio, n – number of measurements per specimens. For more details on microscopic routine, consult Miettinen *et al*. (2018).

DNA extractions were performed as described in Miettinen *et al*. (2012), Spirin *et al.* (2013), and Gutaker *et al*. (2017). The nuclear ribosomal internal transcribed spacer (ITS) region was amplified by PCR and sequenced using primers ITS1, ITS2, ITS5, ITS4, and LR22; nuclear large subunit or 28S (LSU) with CTB6, LR5 and LR7; and mitochondrial small subunit or 16S (mtSSU) with MS1 and MS2 (White *et al*. 1990, Vilgalys lab 1992 https://sites.duke.edu/vilgalyslab/rdna_primers_for_fungi, Garbelotto *et al.* 1997); mitochondrially encoded ATP synthase membrane subunit 6 (*ATP6*) with ATP6-1, -3, and -4 (Kretzer & Bruns 1999); DNA-directed RNA polymerase II largest subunit RPB1 encoding gene (*RPB1*) with rpb1-gAf and rpb1-fCr (Matheny *et al*. 2002); and translation elongation factor 1-alpha (*TEF1*) with EF1-983F (Rehner & Buckley 2005) and EFgr (Rehner, GCAATGTGGGCRGTRTGRCARTC). Sanger sequencing was mostly conducted at Macrogen (Korea and Netherlands) and the Academy of Sciences of the Czech Republic (České Budějovice, Czech Republic). Also, Illumina NextSeq data were used to retrieve markers from partial genome sequences for a few specimens as described in Viner *et al.* (2021). Newly created sequences were submitted to GenBank (Sayers *et al.* 2022, Table 1).

Table 1. List of specimens with DNA sequences used in this study. Codes refer to INSDC or UNITE accession numbers. Newly produced sequences are printed in **bold**. Asterisk (*) denotes cultures as the origin of the sequences. Abbreviation of provinces/states follows ISO 3166-2.

Species	Specimen / culture*	Country (province/state)	GenBank accession numbers					
			ITS	LSU	mtSSU	*ATP6*	*RPB1*	*TEF1*
Acanthodontia cirrhatina	**holotype**	**Malaysia**	**OR262205**	—	—	—	—	—
	Miettinen 13717	**Indonesia (SB)**	**OR262179**	**OR262179**	—	**OR296385**	**OR296392**	**OR296407**
Cerrena albocinnamomea	**Miettinen 10511**	**China (JL)**	**OR262168**	**OR262168**	**OR295446**	**OR296382**	—	**OR296402**
	holotype of *C. aurantiopora*	South Korea	FJ821532	—	—	—	—	—
		—	KC485522	KC485539	—	—	—	—
Cerrena cystidiata		Brazil	MZ649034	MZ649034	—	—	—	—
Cerrena 'gilbertsonii'	**D. Vlasák (JV 1609/29)**	**Guadeloupe**	**OR262202**	—	—	—	**OR296399**	—
	Vandevender 94-144	**Mexico**	**OR262171**	**OR262171**	**OR295447**	—	—	—
Cerrena multipileata	**J. Vlasák (JV 1407/63)**	**Costa Rica**	**OR262201**	**OR262201**	—	—	**OR296398**	—
	Ryvarden 43881	**Costa Rica**	**OR262155**	**OR262155**	**OR295442**	—	—	—
	Kout (JV 0611/A36)	**Guatemala**	**OR262203**	—	—	—	—	—
Cerrena sp1		China	KX527879	—	—	—	—	—
		China	MK247953	—	—	—	—	—
		China	MT908560	—	—	—	—	—
		Vietnam	MT269762	—	—	—	—	—
		Vietnam	MT269763	—	—	—	—	—
Cerrena sp2		China	OP022000	—	—	—	—	—
		Indonesia	KJ654531	—	—	—	—	—
		Taiwan	MN592928	—	—	—	—	—
Cerrena unicolor		Antarctica	HM589361	—	—	—	—	—
		Argentina (TF)	MH019790	—	—	—	—	—
		Canada (ON)	MH855029	—	—	—	—	—
		China (XJ)	OM100740	OM083972	ON417068	—	ON424672	ON424825
		China	JQ798288	—	—	—	—	—
		China	MW467890	—	—	—	—	—
		Czech Republic	FJ821536	—	—	—	—	—
		Finland	FN907915	FN907915	—	—	—	—
		Italy	MK581063	—	—	—	—	—
		Japan	LC415531	—	—	—	—	—
	Uotila 47558	**Kyrgyzstan**	**OR262167**	—	—	—	—	—
		Serbia	MW485440	—	—	—	—	—
		South Korea	MN294859	—	—	—	—	—
		Sweden	JN710525	JN710525	JN710663	JN710614	—	JX109891

Table 1. (Continued).

Species	Specimen / culture*	Country (province/state)	GenBank accession numbers					
			ITS	LSU	mtSSU	*ATP6*	*RPB1*	*TEF1*
		Turkey	MK120293	—	—	—	—	—
		United Kingdom	MZ159683	—	—	—	—	—
		USA (MA)	KP135304	KP135209	—	—	KP134874	—
		Uzbekistan	MT526291	—	—	—	—	—
Cerrena zonata	**Genevieve Gates 39555**	**Australia (TAS)**	**OR262160**	**OR262160**	—	—	—	—
		Bhutan	UDB0780153	—	—	—	—	—
	Miettinen 9773	**China (YN)**	**OR262157**	**OR262157**	—	—	—	—
	Miettinen 9889/OMC 13*	**China (YN)**	**OR262158**	**OR262158**	**OR295443**	**OR296380**	**OR296390**	**OR296401**
	Miettinen 13798	**Indonesia (SB)**	**OR262166**	**OR262166**	—	—	—	—
		Japan	LC631683	—	—	—	—	—
		New Zealand	HQ533016	—	—	—	—	—
		South Korea	MN294861	—	—	—	—	—
		Vietnam	OP985107	—	—	—	—	—
Crustomyces albidus	holotype	China (YN)	ON117191	ON117175	—	—	—	—
Crustomyces isabellinus		Vietnam	ON117185	ON117170	—	—	—	—
Crustomyces laminiferus		Costa Rica	EU118622	—	—	—	—	—
Crustomyces sp.		China	ON117190	ON117174	—	—	—	—
Crustomyces subabruptus		France	MF183941	—	—	—	—	—
	Spirin 4826	**Russia (LEN)**	**OR262177**	—	—	—	—	—
Crustomyces tephroleucus	holotype	China (HI)	MF290417	MF290415	—	—	—	—
Cymatoderma sp.		USA (FL)	KY948826	KY948872	—	—	KY948971	—
Cymatoderma africanum	**Niemelä 8803**	**Mozambique**	**OR236211**	**OR236211**	**OR295457**	**OR296389**	—	**OR296425**
Cymatoderma caperatum		Venezuela	JN710529	JN710529	JN710666	JN710617	—	—
Cystostereum crassisporum	holotype	China (GX)	ON117193	ON117179	—	—	—	—
Cystostereum murrayi		Germany	MH855588	MH867098	—	—	—	—
Cystostereum submurrayi	holotype	China (JX)	ON117192	ON117177	—	—	—	—
Effusomyces thailandicus		Thailand	ON117194	ON117180	—	—	—	—
Hyphoradulum conspicuum	**holotype**	**Czech Republic**	**OR262206**	—	—	—	—	—
Irpiciporus branchiformis	**holotype**	**Tanzania**	**OR262193**	**OR262193**	—	—	—	**OR296421**
Irpiciporus mollis	**Dollinger 770**	**USA (FL)**	**OR262192**	—	—	—	—	**OR296420**
		USA (MA)	KP135302	KP135288	—	—	KP134875	—
	J. Vlasák (JV 0709/174)	**USA (VA)**	**OR359379**	**OR359379**	—	—	—	**OR387174**

Table 1. (Continued).

Species	Specimen / culture*	Country (province/state)	GenBank accession numbers					
			ITS	LSU	mtSSU	*ATP6*	*RPB1*	*TEF1*
		USA	DQ249277	AY629322	AFTOL705	EU339271	—	DQ028599
Irpiciporus pachyodon	**Heilmann-Clausen 07-286**	**Bulgaria**	**OR262165**	**OR262165**	—	—	—	—
	J. Vlasák (JV 9311/1)	**Czech Republic**	**OR262191**	**OR262191**	—	—	—	**OR296419**
	Kotlaba (JV 1611/1)	**Czech Republic**	**OR253988**	**OR253988**	**OR295456**	**OR296388**	**OR296395**	**OR296422**
		Czech Republic	HQ728293	HQ729003	—	—	—	—
		Italy	AY849307	—	—	—	—	—
Irpiciporus sinuosus	holotype	China (YN)	KX161649	KX161658	—	—	—	OM982699
		Thailand	MK589288	—	—	—	—	—
Irpiciporus sp.		Ecuador	KX161650	KX161659	—	—	—	—
Lividopora armeniaca	**isotype**	**Malaysia**	KY953211	KY953211	**OR291311**	**OR296404**	KY953212	**OR296384**
Lividopora benetosta		Cameroon	KJ831816	—	—	—	—	—
		Cameroon	KJ831817	—	—	—	—	—
		Cameroon	KJ831819	—	—	—	—	—
		Cameroon	KJ831837	—	—	—	—	—
		Cameroon	KJ831838	—	—	—	—	—
		China (GD)	KU904221	—	—	—	—	—
		China (HI)	KX013197	—	—	—	—	—
		China (HK)	KU194316	—	—	—	—	—
	Härkönen K778	**China (HN)**	**OR262204**	—	—	—	—	—
	Härkönen K8	**China (HN)**	**OR262170**	—	—	—	—	—
	Miettinen 10225	**China (YN)**	**OR262178**	—	—	—	—	—
		French Polynesia	MZ996950	—	—	—	—	—
		French Polynesia	MZ996951	—	—	—	—	—
		French Polynesia	MZ996952	—	—	—	—	—
		India	OM033590	—	—	—	—	—
	Miettinen 8823.2	**Indonesia (RI)**	**OR262156**	—	—	—	—	—
		Indonesia (RI)	KJ654526	—	—	—	—	—
		Indonesia (RI)	KJ654534	—	—	—	—	—
	Miettinen 9166.5	**Indonesia (PA)**	**OR262162**	**OR262162**	**OR295445**	**OR296381**	—	—
	Miettinen 9176.2	**Indonesia (PA)**	**OR262163**	—	—	—	—	—
		Malaysia	HQ400710	—	—	—	—	—
	Hallenberg 15301	**New Zealand**	**OR262161**	—	—	—	—	—

Table 1. (Continued).

Species	Specimen / culture*	Country (province/state)	GenBank accession numbers					
			ITS	LSU	mtSSU	*ATP6*	*RPB1*	*TEF1*
	ICMP 18224*	**New Zealand**	**OR262169**	—	—	—	—	—
		New Zealand	MN007016	—	—	—	—	—
		Papua New Guinea	KR015166	—	—	—	—	—
		Papua New Guinea	KR015237	—	—	—	—	—
		Papua New Guinea	KR016181	—	—	—	—	—
		Philippines	MK817568	—	—	—	—	—
		Philippines	MT597859	—	—	—	—	—
	Miettinen 18035	**Puerto Rico**	**OR262175**	**OR262175**	**OR295450**	—	—	—
	Miettinen 18135	**Puerto Rico**	**OR262176**	—	—	—	—	**OR296406**
		Taiwan	MZ423082	—	—	—	—	—
		Thailand	LC269928	—	—	—	—	—
		Thailand	MG545057	—	—	—	—	—
Lividopora facilis	**isotype**	**Indonesia (RI)**	**OR262154**	**OR262154**	**OR295441**	**OR296379**	—	**OR296400**
Lividopora subvincta	**holotype**	**Zimbabwe**	**OR262197**	—	—	—	—	—
	Savchenko 171129/1309A	**Kenya**	**OR262196**	—	—	—	—	—
	CFMR ECS-194-R*	**Tanzania**	KY948734	KY948873	**OR295449**	—	**KY948953**	—
Lividopora vincta	**Gazis *et al.* NHB39***	**Brazil (PA)**	**OR262173**	—	—	—	—	—
	J. Vlasák (JV 1704/102)	Costa Rica	OM669884	—	—	—	—	—
		Mexico	KU747939	—	—	—	—	—
	Gazis *et al.* MS512*	**Peru**	**OR262172**	**OR262172**	—	—	—	—
		Peru	KJ831895	—	—	—	—	—
		Peru	KJ831906	—	—	—	—	—
		Peru	KJ831912	—	—	—	—	—
		Peru	KJ831915	—	—	—	—	—
		Peru	KJ831927	—	—	—	—	—
		Peru	KJ831935	—	—	—	—	—
		Peru	KJ831950	—	—	—	—	—
		Peru	KJ832036	—	—	—	—	—
	Miettinen 17916/OMC 1567*	**USA (FL)**	KY948735	KY948874	—	—	**KY948954**	**OR296405**
Panus conchatus		Finland	JN710579	JN710579	JN710695	JN710643	—	—
		Puerto Rico	OM337524	OM337524	—	—	JACDTX010000312	JACDTX010000141
Panus lecomtei		USA (AZ)	KP135328	KP135233	—	—	KP134877	—

Table 1. (Continued).

Species	Specimen / culture*	Country (province/state)	GenBank accession numbers					
			ITS	LSU	mtSSU	*ATP6*	*RPB1*	*TEF1*
Parvodontia austrosinensis		China (GX)	ON117195	ON117183	—	—	—	—
Pseudolagarobasidium acaciicola		China	MK247443	—	—	—	—	—
		China	MT814716	—	—	—	—	—
		India (AP)	KR149461	—	—	—	—	—
		India	HQ323693	—	—	—	—	—
		India	JX886000	—	—	—	—	—
		India	KP297894	—	—	—	—	—
		India	MK163558	—	—	—	—	—
		South Africa	DQ517882	EU569321	—	—	—	—
		South Africa	DQ517883	—	—	—	—	—
		Thailand	KF673346	—	—	—	—	—
Pseudolagarobasidium baiyunshanensis		China (GD)	MT428549	MT428547	—	—	—	—
		China (GD)	MT428550	MT428548	—	—	—	—
Pseudolagarobasidium belizense	isotype	Belize	JQ070173	—	—	—	—	—
	Gazis *et al.* VPB197*	**Brazil (PA)**	**OR262174**	**OR262174**	**OR295448**	**OR296383**	**OR296391**	**OR296403**
		China (GD)	KM278016	—	—	—	—	—
Pseudolagarobasidium sp.		China	MK790683	—	—	—	—	—
		China	MK790684	—	—	—	—	—
		China	MK790685	—	—	—	—	—
		India	KM053237	—	—	—	—	—
		Thailand	MK589289	—	—	—	—	—
		Vietnam	KM234009	—	—	—	—	—
Pseudolagarobasidium venustum	holotype of *P. pallens*	Brazil (RS)	MZ649030	MZ649030	—	—	—	—
		Brazil (RS)	MZ649031	MZ649031	—	—	—	—
		Brazil (SP)	MZ649033	—	—	—	—	—
	Carranza 120929	**Costa Rica**	**OR262150**	**OR262150**	—	—	—	—
	K.H. Larsson 11363	**Costa Rica**	**OR262151**	**OR262151**	—	—	—	—
	K.H. Larsson 10040	**Puerto Rico**	**OR262152**	**OR262152**	—	—	—	—
Radulodon americanus		USA (MN)	JQ070174	—	—	—	—	—
		USA (MT)	JQ070175	—	—	—	—	—
Radulodon casearius		China (YN)	MK404494	—	—	—	—	—
		USA (FL)	KY948752	KY948871	—	—	KY948943	—

Table 1. (Continued).

Species	Specimen / culture*	Country (province/state)	GenBank accession numbers					
			ITS	LSU	mtSSU	*ATP6*	*RPB1*	*TEF1*
Radulodon erikssonii	**Pennanen 3794**	**Finland**	**OR262200**	—	—	—	—	**OR296426**
	Pennanen 3886	**Finland**	**OR262199**	—	—	—	—	—
		Norway	KY415963	KY415963	KY415964	KY415971	—	—
		Sweden	MH864059	—	—	—	—	—
	Martini (GB 0181279)	**Switzerland**	**OR359377**	**OR359377**	—	—	—	—
Radulodon yunnanensis	holotype	China (YN)	OM971916	OM971936	—	—	—	OM982705
		China (YN)	OM971915	OM971897	—	—	—	OM982704
		China (YN)	OM971917	OM971898	—	—	—	OM982706
Somion delectans		India	MG719295	—	—	—	—	—
		India	MT126488	—	—	—	—	—
		USA	MH856070	—	—	—	—	—
		USA (KY)	MN430947	—	—	—	—	—
		USA (MD)	HQ728301	—	—	—	—	—
		USA (MD)	KY948750	—	—	—	—	—
	CFMR FP-101579-Sp*	**USA (MD)**	**OR262198**	—	—	—	—	—
		USA (MI)	KP135301	KP135287	—	—	KP134876	—
		USA (MS)	HQ728299	—	—	—	—	—
	J. Vlasák (JV 0809/62)	**USA (NH)**	**OR262183**	**OR262183**	—	—	—	**OR296411**
	J. Vlasák Jr (JV 1507/22)	**USA (PA)**	**OR262182**	**OR262182**	—	—	—	**OR296410**
		USA (PA)	HQ728297	—	—	—	—	—
		USA (PA)	HQ728298	—	—	—	—	—
		USA (PA)	HQ728300	HQ729007	—	—	—	—
Somion formosanum	**ATCC MYA-262*, ex-holotype**	**Taiwan**	JQ070094	JQ070165	—	—	**OR296396**	**OR296423**
Somion litschaueri		Austria	HQ728304	—	—	—	—	—
		Austria	HQ728306	HQ729009	—	—	—	—
		Austria	UDB0802574	—	—	—	—	—
		China (BJ)	FJ789779	—	—	—	—	—
		China	MH425279	—	—	—	—	—
		China	OM971907	—	—	—	—	—
		China	OM971912	—	—	—	—	—
	J. Vlasák (JV 1309/1)	**Czech Republic**	**OR262189**	**OR262189**	—	—	—	**OR296417**
		Czech Republic	HQ728303	—	—	—	—	—

Table 1. (Continued).

Species	Specimen / culture*	Country (province/state)	GenBank accession numbers					
			ITS	LSU	mtSSU	*ATP6*	*RPB1*	*TEF1*
		Czech Republic	HQ728305	—	—	—	—	—
		Czech republic	HQ728307	—	—	—	—	—
		Czech Republic	HQ729014	HQ729014	—	—	—	—
		Russia (PRI)	UDB0780498	—	—	—	—	—
	J. Vlasák (JV 1309/7)	**Slovakia**	**OR262190**	**OR262190**	—	—	—	**OR296418**
		—	MH860539	—	—	—	—	—
Somion occarium	**epitype**	**Czech Republic**	**OR262180**	**OR262180**	—	—	—	**OR296408**
	J. Vlasák (JV 1310/23)	**Czech Republic**	**OR262181**	**OR262181**	—	—	—	**OR296409**
		Czech Republic	HQ728294	HQ729004	—	—	—	—
		Czech Republic	HQ728295	HQ729005	—	—	—	—
		Czech republic	HQ728296	—	—	—	—	—
	K.H. Larsson 14261	**Sweden**	**OR262194**	—	—	—	—	—
		—	AJ006670	—	—	—	—	—
Somion strenuum	**holotype**	**Russia (KHA)**	**OR262186**	**OR262186**	**OR295451**	—	**OR296394**	**OR296414**
	Dai 3041	China (LN)	KY415961	KY415961	KY415966	KY415969	—	—
	Miettinen 10546	**China (LN)**	**OR262164**	**OR262164**	—	—	—	—
		China (LN)	KY415961	—	—	—	—	—
	Spirin 6112	**Russia (KHA)**	**OR262187**	**OR262187**	—	—	—	**OR296415**
Somion tomsovskyi	**J. Vlasák Jr (JV 1209/55)**	**USA (AZ)**	**OR236210**	**OR236210**	**OR295455**	**OR296387**	—	**OR296413**
	J. Vlasák Jr (JV 1307/8)	**USA (AZ)**	**OR262184**	**OR262184**	—	**OR296386**	**OR296393**	**OR296412**
		USA (AZ)	KY948751	—	—	—	KY948942	—
Somion unicolor		France	FJ349625	—	—	—	—	—
		USA (AZ)	HQ728302	—	—	—	—	—
		USA (GA)	OL142241	—	—	—	—	—
		USA (LA)	HQ728312	—	—	—	—	—
		USA (MI)	HQ728311	—	—	—	—	—
		USA (MO)	HQ728310	—	—	—	—	—
	J. Vlasák Jr (JV 1304/1)	**USA (NJ)**	**OR262188**	**OR262188**	—	—	—	**OR296416**
	J. Vlasák Jr (JV 1708/10)	**USA (NJ)**	**OR262195**	**OR262195**	—	—	**OR296397**	**OR296424**
		USA (VA)	HQ729011	HQ729011	—	—	—	—
		USA (WI)	HQ728308	—	—	—	—	—
		USA (WI)	HQ728309	—	—	—	—	—

Table 1. (Continued).

Species	Specimen / culture*	Country (province/state)	GenBank accession numbers					
			ITS	LSU	mtSSU	*ATP6*	*RPB1*	*TEF1*
			HQ728313					
			MH854650					
Somion cf. unicolor		USA (AZ)	OP297810					
Somion sp.		China	MW554292					
			AY089734					

We compiled eight sequence datasets for phylogenetic analysis. Selection was based on ITS and LSU sequence similarity searches for each *Cerrenaceae* species in GenBank (using BLAST; Altschul *et al.* 1997) and UNITE (Nilsson *et al.* 2018) implemented in PlutoF (using BLAST and species hypothesis annotation; Abarenkov *et al.* 2010). We referred to Justo *et al*. (2017) when selecting the outgroup (the closest relative *Panaceae*) for the family-level dataset. For the other datasets (genus-level trees), which were compiled mainly for species delimitation, we used mid-point rooting without an outgroup. Since genetic distances between genera are generally large, including outgroup sequence with a divergent ITS sequence would have decreased the number of homologous (alignable) characters significantly, reducing species resolution.

We aligned the sequences with PRANK v. 170427 (Löytynoja 2021) or the MAFFT online service with E-INS-I (Katoh *et al.* 2017), each marker individually, and adjusted them manually in PhyDE v. 0.9.7.1 (Müller *et al*. 2010). We excluded characters from the 6-marker dataset manually when judged as non-homologous. The datasets, with the final alignment length and the number of parsimony informative sites calculated in MEGA v. 7 (Kumar *et al*. 2016) are as follow: i) a 6-marker dataset of *Cerrenaceae* (1 091 parsimony informatic characters/5 228 total characters), ii) *Cerrena* ITS (72/618), iii) *Irpiciporus* ITS (32/588), iv) *Irpiciporus* ITS+*TEF1* (63/1 604), v) *Lividopora* ITS (39/604), vi) *Pseudolagarobasidium* ITS (61/564), vii) *Radulodon* ITS (11/597), viii) *Somion* ITS (32/542), ix) *Somion* ITS+*TEF1* (138/1 684), and x) *Cystostereaceae* ITS (93/708).

The 6-marker dataset of the *Cerrenaceae* contained nrDNA ITS and LSU, mtSSU, *ATP6*, *TEF1* and *RPB1*. Two of the markers are mitochondrial (mtSSU and *ATP6*), and all, except for ITS and LSU, independently evolving. To reduce gaps in the alignment, data within five species were fused so that for *Cerrena 'gilbertsonii'*, GenBank OR296399 was used for *RPB1* while the rest of the markers were from *Vandevender 94-144* (GenBank OR262171, *etc*.); GenBank KP134874 was used for *RPB1* of *Cerrena unicolor* while the rest were from the collection *Larsson* (GenBank JN710525, *etc*.); GenBank KP134876 for *RPB1* of *Somion delectans* while the rest of the markers were from the collection *Vlasák Jr.* JV 1507/22 (GenBank OR262182, *etc*.); GenBank KY948942 for *RPB1* of *Somion tomsovskyi* while the rest of the markers were from *Vlasak* JV 1209-55 (GenBank OR236210, *etc*.); and GenBank OR296426 for *TEF1* of *Radulodon erikssonii* while the rest were from *Hofton 09820* (GenBank KY415963, *etc*.). In all these cases, the ITS similarity was > 99.5 %. Thus compiled, marker data were missing for 27 % of the maximum 180 marker sequences. At the level of genera, only one marker sequence out of 54 (mtSSU of *Acanthodontia*) was missing.

Models for the phylogenetic analyses were selected for each marker and dataset by AICc ModelTest-NG v. 0.2.0 (Darriba *et al*. 2020). We inferred phylogenies with MrBayes v. 3.2.7a (Ronquist *et al*. 2012) and RAxML-NG v. 1.1.0 (Kozlov *et al*. 2019). Bootstrap support values for the RAxML maximum likelihood analyses were calculated from 1 000 replicas. MrBayes v. 3.2.7a was run with three parallel runs of 8 chains each for 2–4 million generations, sampling every 10 000 generations. Good convergence (standard deviation of split frequencies < 0.01) was reached in all cases and the standard 25 % burnin was used when compiling the consensus tree. All computations were run at the CSC – IT Centre for Science (Espoo, Finland) computing environment. The alignments, with model information included in their nexus blocks, are available at PlutoF (doi: 10.15156/BIO/2938061).

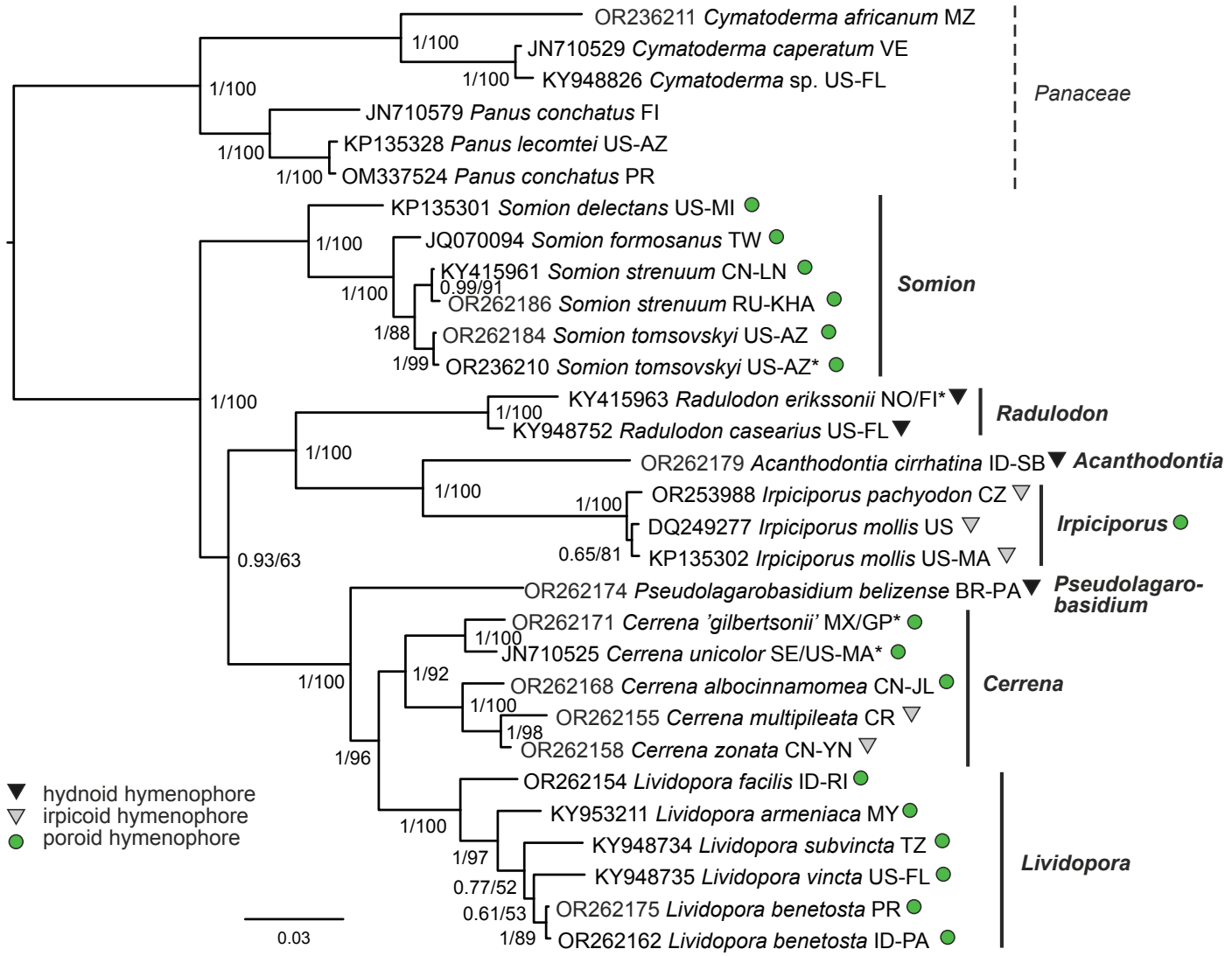

Fig. 3. Bayesian consensus phylogram of the *Cerrenaceae* based on four nuclear (ITS, nLSU, *RPB1, TEF1*) and two mitochondrial (mtSSU, *ATP6*) genetic markers. Decimal support values denote posterior probabilities, while values over 50 % denote bootstrap support. The INSDC accession numbers for each leaf refer to ITS. Leaves with asterisk (*) contain data of several specimens (see Material and Methods). Countries (and states) of origin are denoted with ISO 3166 codes.

RESULTS

The 6-marker phylogenetic estimate confirms the *Cerrenaceae* as a well-supported family (Fig. 3). It resolves three main clades within the family: *Somion* containing *Spongipellis delectans* and relatives, *Irpiciporus-Radulodon* and *Cerrena-Pseudolagarobasidium*. Individual marker phylogenies mostly confirm this, but *TEF1* and *RPB1* do not support monophyly of the *Irpiciporus-Radulodon* clade (Supplementary Figs S1–S5).

How should genera in the family be delimited in the light of this information? Our analysis provides several possible solutions in balancing morphology with phylogenetic information. We have assumed here that phylogenetic distance must be reflected in genus limits. Thus, we consider all clades of equal phylogenetic distance consistently as genera within the family, requiring all clades above a threshold be treated equally when deciding on their generic status. Under this condition, and by maximizing morphological distinctiveness and minimizing nomenclatural change, we have divided the family into seven genera, two of them newly described: *Acanthodontia gen. nov.*, *Cerrena*, *Irpiciporus*, *Lividopora gen. nov.*, *Pseudolagarobasidium*, *Radulodon*, and *Somion* (Table 2). ITS-based trees of all the genera (except the monotypic *Acanthodontia*) are provided in the taxonomy section.

Cerrena-Pseudolagarobasidium clade

The 6-marker phylogeny supports dividing the *Cerrena-Pseudolagarobasidium* clade into three to four parts: *Cerrena unicolor* and relatives, *Cerrena zonata* and relatives, *Rigidoporus vinctus* and relatives, and *Pseudolagarobasidium* (Fig. 3). When analyzed individually (Supplementary Figs S1–S5), only *RPB1* (Supplementary Fig. S4) produces a similar topology as the 6-marker dataset (supporting a clade containing *C. unicolor* and *C. zonata*). However, also the ITS+LSU and *ATP6* datasets support division into the above-mentioned four subclades, albeit with a different branching order (Supplementary Figs S1, S3). The rest of the markers, mtSSU and *TEF1*, fail to recover the four clades (Supplementary Figs S2, S5). None of the individual marker phylogenies contradicts the 6-marker phylogeny, and differences are due to the lack of support for most nodes.

Table 2. Morphological comparison of accepted genera in the *Cerrenaceae*.

Genus	Basidiocarp	Hymenial surface	Hyphal system	Cystidia	Spores	Other
Acanthodontia	Effused-reflexed, whitish	**Regular long spines**	**Dimitic** but dominated by generatives, gen. hyphae slightly thick-walled, uniform, neatly arranged	**Tramal cystidia** slightly thick-walled, bend into hymenium	Slightly thick-walled, with guttula	Subhymenium well developed
Cerrena	Effused to reflexed, whitish to brown-gray	Regularly **poroid** to irpicoid	**Dimitic**	Hymenial thin-walled, staining cystidia	Thin-walled, no guttula	—
Lividopora	Effused, red to brown to gray	Regularly **poroid**, **small-pored**	**Dimitic**	1) **Encrusted skeletocystidia**, 2) hymenial thin-walled stained cystidia	Thin-walled, no guttula	**Clamps absent**
Pseudolagarobasidium	**Effused**, whitish tobrownish-grayish, thin	**Hydnoid** with short blunt teeth to irpicoid	Monomitic & microbinding hyphae	1) **Tramal cystidia** slightly thin-walled, bend into hymenium, 2) hymenial thin-walled, staining cystidia	**Thin-walled**, **no guttula**	—
Radulodon	**Effused**, whitish	**Regular spines**	Monomitic, **messy**, hyphae thin- to slightly thick-walled	**Hymenial cystidia**, thin-walled	**Slightly thick-walled**, **with guttula**	—
Irpiciporus	Effused-reflexed to reflexed, relatively **thin**, whitish	**Irpicoid** to sinuous pores	**Monomitic**, **neat**, hyphae slightly thick-walled, uniform	**None**	**Slightly thick-walled**, with guttula	Subhymenium almost nonexistent; **basidia long** (> 20 µm)
Somion	Reflexed, **thick**, context duplex, whitish	**Pores regular to sinuous**	**Monomitic**, **neat**, with a mix of thin- and **thick-walled hyphae**	**None**	**Thick-walled**, with guttula	Subhymenial cells differentiated; basidia short (mostly < 20 µm)

The resulting phylogeny leaves us with four well-supported options in delimiting genera in the *Cerrena-Pseudolagarobasidium* clade. First, phylogenetically perhaps the simplest solution would be to include all species in this clade in one genus (*Cerrena*). All the species in this clade share some morphological characters: dimitic hyphal structure, thin-walled, ellipsoid, middle-sized spores, and thin-walled hymenial cystidia ("gloeocystidia"). They are all aggressive wood-rotters, and there are tree pathogens in all the subclades. Species in the clade grow fast on malt agar and are enzymatically active (Nobles 1948, Westhuizen 1963, Setliff 1972a, Maekawa 2002, Wood & Ginns 2006). However, morphological differences of basidiocarps between the extremes are still quite significant (see below), and one large genus would be at odds with the current traditions of defining polypore and corticioid genera morphologically.

Second, the genus could be divided into hydnoid and near-monomitic *Pseudolagarobasidium* on one hand, and dimitic polypores of *Cerrena* and *Rigidoporus vinctus* on the other. Thus delimited, *Cerrena* would be better morphologically defined, but still quite heterogenous. This option would induce minimal name changes.

The third option is to divide the clade into three genera: hydnoid, effused, nearly monomitic *Pseudolagarobasidium*, dimitic *Cerrena* with clamped hyphae and irregular/dentate pores (including *C. unicolor* and *C. zonata* subclades), and dimitic but simple septate *Rigidoporus vinctus* coll. with encrusted skeletocystidia and regular, small pores. Thus defined, the three groups are distinct and easy to separate from each other. We consider this the best solution currently and describe here the genus *Lividopora* for the *R. vinctus* subclade.

Lastly, the fourth option would be to divide the clade into four genera: *Cerrena sensu stricto* (*C. unicolor* and relatives), a new genus for *C. zonata* and relatives, *Lividopora*, and *Pseudolagarobasidium*. This option, too, has merits. Morphologically, there are some differences between the *C. unicolor* and *C. zonata* clades: more pronounced pigmentation in *Cerrena sensu stricto*, duplex context, more distinct gloeocystidia in the *C. zonata* subclade, and subtle differences in hyphal structure. However, these characters (except duplex context) are subject to gradation. In our experience, they are not as informative phylogenetically as, for instance, the presence of skeletocystidia or type of septation, which are more reliable and easier to interpret among polypores. Furthermore, as shown under taxonomy part of *Cerrena*, diversity in the *C. zonata* clade exceeds the currently described species and our material. Hence, a genus description for this clade would be outdated from the start – a clear argument for sticking to larger

genera. Finally, if the *Cerrena-Pseudolagarobasidium* clade would be divided into four genera, and we would define all similarly distant clades in the family as separate genera, the *Somion* clade (*Spongipellis delectans* and relatives) would also be split into two, morphologically very similar sister genera, which we think is unnecessary.

Radulodon-Irpiciporus clade

The *Radulodon-Irpiciporus* clade is divided phylogenetically into three subclades: *Radulodon sensu typi*, *R. cirrhatinus*, and *Irpiciporus*. This clade is morphologically fairly homogenous: basidiocarps are light-coloured, hydnoid or irpicoid, (nearly) monomitic with clamps, hymenial cells relatively large, and spores slightly thick-walled. Placing these species in one genus would be a good option from this perspective. Phylogenetically the three parts are distant, however. Considering our genus concepts in the *Cerrena-Pseudolagarobasidium* clade, *i.e.*, division of that clade into several genera, the three parts of the *Radulodon-Irpiciporus* clade must be considered separate genera. We describe here a monotypic genus *Acanthodontia* for *Radulodon cirrhatinus*. Despite similarities, there are some differences between the genera: *Acanthodontia* and *Radulodon* are fully hydnoid whereas *Irpiciporus* are irpicoid to poroid; cystidia and rare skeletal hyphae are found in *Acanthodontia* and *Radulodon*. The latter two differ for instance in their hyphal structure and nature of skeletal hyphae (Table 2).

Somion clade

Spongipellis delectans and its relatives form a distinct clade and clearly merit recognition at the genus level. They are monomitic polypores with clamps and loose structure, thick-walled spores and big, light-coloured caps, somewhat similar to *Spongipellis sensu stricto*, which belongs to a different family, *Meripilaceae* (Spirin *et al.* 2022). Wang & Dai (2022) reached similar conclusion about this clade's generic status and described *Pseudospongipellis*. We adopt the genus name *Somion* as the correct name for this clade. *Somion delectans* and its European sibling *S. occarium* are phylogenetically distinct from the rest of the species, but since morphological differences are small, we see no reason to split this genus further.

Taxonomy

Acanthodontia Miettinen & Spirin***, gen. nov.*** MycoBank MB 849641.

Type species: *Acanthodontia cirrhatina* (Hjortstam & Spooner) Miettinen & Spirin

Etymology: Derived from ἄκανθος (Greek, noun), thorn, and -odon derived from the Greek word for sharp teeth, ὀδοντιάω.

Pileate, sessile, white to cream *basidiocarps* with long spines underneath. *Hyphal system* dimitic with clamps in all septa of generative hyphae, but skeletal hyphae found in context and subiculum only, otherwise monomitic and dominated by slightly thick-walled generative hyphae, in trama subparallel. Long, slightly thick-walled sack-like *cystidia* embedded in trama and hymenium. *Basidiospores* ellipsoid, mid-sized, smooth, slightly thick-walled, with a large guttule, cyanophilous.

Acanthodontia cirrhatina (Hjortstam & Spooner) Miettinen & Spirin, ***comb. nov.*** MycoBank MB 849642. Figs 2, 4.
Basionym: *Radulodon cirrhatinus* Hjortstam & Spooner, Kew Bull. 45: 312, 1990.

Typus: **Malaysia**, Sabah, Danum Valley, on a fallen log, 30 Nov. 1985, *Spooner 295** (**holotype** K(M) 62575, studied).

Basidiocarp resupinate to half-resupinate, caps white, with a rough but hairless upper surface, projecting up to 2 cm; resupinate patches up to 10 cm wide. Hymenophore consists of regular conical spines, 4–15 mm long and 2 per mm, white to cream when fresh with reddish brownish tints upon drying. Subiculum white, uniform, 0.5–1 mm thick, cap context 1–2 mm thick, up to 7 mm at the base. Margin distinct, often with a 1–2 mm wide zone of sterile subiculum visible.

Hyphal system dimitic, but skeletal hyphae rare and concentrated in cap context, clamps present. Generative hyphae homogenous, slightly thick-walled, (2.2–)2.8–4.4(–5.8) µm diam in subiculum, (2.4–)3.0–4.2(–5.3) µm in trama. Subiculum structure similar to context, but skeletal hyphae fewer. Context a loose, interwoven structure with segments of skeletal hyphae here and there, (2.0–)2.4–3.1(–3.9) µm diam. Tramal hyphae subparallel, structure rather loose; a distinct subhymenial layer consisting of strongly interwoven hyphae, 20–50 µm thick. *Cystidia* clavate, tramal or rarely subhymenial in origin, bending into hymenium, projecting up to 10 µm, slightly thick-walled basally when young, thick-walled and cyanophilous when old, often with constrictions when old, occasionally tapering but always blunt, sometimes with a deep root, 38–135 × 9–17 µm (up to 70 µm long without the root). Similar, swollen cells embedded in context. *Basidia* clavate, some constricted, (14–) 16–26 × 5.5–6.8 µm, with 4 sterigmata. *Basidiospores* ellipsoid, slightly thick-walled (walls 0.2–0.3 µm), uniguttulate, slightly to distinctly cyanophilous, 4.0–5.1(–5.2) × (3.4–)3.5–4.2(–4.3) µm, L = 4.69 µm, W = 3.79 µm, Q = 1.21–1.26.

Distribution and ecology: The two known finds are from lowland rainforests in insular Southeast Asia, *viz*. Borneo and Sumatra.

Notes: *Acanthodontia cirrhatina* is easy to identify by its long spines, effused-reflexed basidiocarps and tramal cystidia that penetrate the hymenium. This monotypic genus is morphologically quite similar to its sister taxon, *Irpiciporus*. The phylogenetic distance to *Irpiciporus* is sufficiently large and consistent throughout genetic markers that *A. cirrhatina* should warrant its own genus. They share very similar cyanophilous spores, hymenium, and the tramal construction of loosely arranged, subparallel hyphae. Basidiocarp habit is also quite similar, but the *A. cirrhatina* hymenophore consists of regular, slender, conical spines, whereas *Irpiciporus* spp. have poroid to irpicoid hymenophore. Microscopically, skeletal hyphae and cystidia of *Acanthodontia* are lacking in basidiocarps of *Irpiciporus*. Subhymenial layer appears more visible and thicker than in *Irpiciporus* spp.

The next closest kin, *Radulodon* spp., form fully effused, thinner basidiocarps. Microscopically, the interwoven, messy-looking hyphal structure is different, and skeletal hyphae are much narrower. Cystidia are a shared character between the two genera, and along with the hydnoid hymenophore the reason why *A. cirrhatina* was described in *Radulodon*.

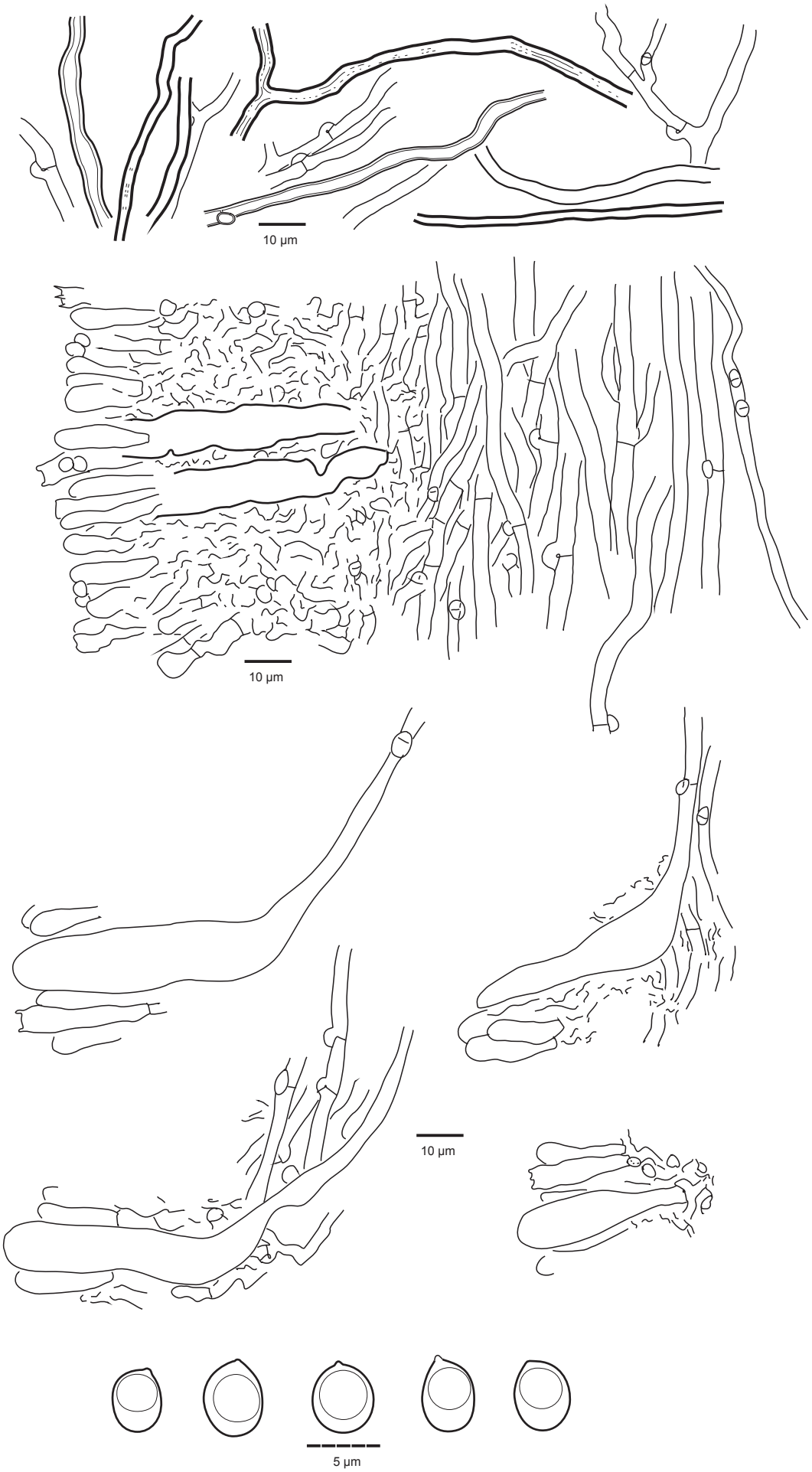

Fig. 4. Microscopic structures of *Acanthodontia cirrhatina* (*Miettinen 13717*). Subicular skeletal and generative hyphae, trama and hymenium, cystidia, and spores.

Nakasone (2001) studied the type specimen and accurately described skeletal hyphae; later she considered the species monomitic with sclerified segments of generative hyphae (Nakasone & Ortiz-Santana 2022). In our view, those segments and hyphae should be called skeletal hyphae. They are found in old cap context, and do not dominate structure anywhere. Another slightly younger specimen (*Miettinen 13717*) has so few skeletal hyphae that we found them only after specifically looking for them in context. Vegetative mycelial mats associated with the latter specimen are dominated by narrow skeletal hyphae with occasional thin-walled branches that branch at right angles, reminiscent of (but not fully similar to) the microbinding hyphae documented by David (1969) in *Irpiciporus pachyodon*.

Cerrena Gray, *A natural arrangement of British plants* 1: 649. 1821.

Type species: *Boletus unicolor* Bull.

Pileate to resupinate polypores with cream, brownish to grey *basidiocarps* with a cottony context. *Pores* mid-sized, irregular in old specimens, in some species irregular already when young. *Hyphal system* dimitic with clamps; intermediary hyphae and branching skeletal hyphae may be present. Hyphae CB(+), IKI-, KOH-, CRB lilac. Hymenial, thin-walled cystidia with a stained inclusion ("gloeocystidia") present, though may be absent in young specimens. *Basidiospores* ellipsoid, mid-sized, with thin or distinct walls. Aggressive white rotters.

Notes: *Cerrena* can remind of other polypore genera with pilei and dimitic hyphal structure, such as *Antrodiella*, *Funalia*, and *Trametes*. However, thin-walled hymenial cystidia are not present in *Funalia* or *Trametes*, and the latter genus is distinctly trimitic. Furthermore, ellipsoid spores are rare in *Trametes* and not known from *Funalia*. In *Antrodiella sensu stricto*, thin-walled hymenial cystidia ("gloeocystidia") may be present in older basidiocarps, but spore and basidial size is consistently smaller and so is mostly pore size.

Two subclades can be distinguished in *Cerrena* as we define it (Fig. 3): the *Cerrena unicolor* complex (incl. *C. cystidiata* and *C. 'gilbertsonii'*) with brownish-greyish basidiocarps, and the *C. zonata* complex (incl. *C. albocinnamomea* and *C. multipileata*) with light-colored basidiocarps. The latter complex was placed in *Antrodiella* (Dai & Niemelä 1997, Nuñez & Ryvarden 2001, Ryvarden 2015), until Yuan (2014) moved some of them to *Cerrena* solely on phylogenetic grounds. We considered two separate genera for these clades, but we decided against splitting. Microscopically, the larger *Cerrena* is quite homogenous. Irregular pores are also shared by all species. Colour difference of basidiocarps is also not a clear separating character: *C. albocinnamomea*, as the name implies, turns brownish when old, and young specimens of *C. unicolor* are white. ITS data (Fig. 5) show that more species than described here are present, forming a third clade, but we have no information about their morphology. All these arguments support a larger genus. Duplex context is a unique character for the *C. unicolor* clade within the genus.

When Gray (1821: 649) described *Cerrena*, he accepted only one species, *Cerrena cinerea* (Pers.) Gray. He mentioned *Sistotrema cinereum* Pers. and *Boletus unicolor* Sowerby (= *B. unicolor* Bull.) as synonyms of the aforementioned species. Both are available for typification of the genus (ICN Shenzhen art. 10.2). The lectotypification is traditionally assigned to Murrill (1903: 91), who chose *Daedalea unicolor* (Bull.) Fr. as the genus type. Later he mentioned *S. cinereum* as the type (Murrill 1908). Recent changes in the International Code of Nomenclature suppress typifications by Murrill (art. 10.5, 10.7). The next oldest typification we could trace is by Bondartsev (1953: 45), who selected "*Cerrena unicolor* (Bull.) Murrill" as the type species.

Fries (1821, 1828) considered *Sistotrema cinereum* Pers. a synonym of *Daedalea unicolor* (Bull.) Fr. The latter name is thus sanctioned. Fries also accepted *Daedalea cinerea* as a separate species, but with a different identity than *S. cinereum*, even though he considers part of Persoon's concept of *S. cinereum* to belong to his *D. cinerea*. Formally, the identity of *D. cinerea* Fr. is not relevant for the typification of *Cerrena*. To conclude, the correct, sanctioned name for the type species of *Cerrena* is *C. unicolor* (Bull.) Murrill.

The relationship of *Cerrena* and *Trametes* has been a subject of discussion due to their morphological similarity (Ryvarden 1991). The two genera are not closely related as DNA phylogenies reveal. Bipolar mating system (Westhuizen 1963, Nobles 1965), broad ellipsoid spore shape (rare in *Trametes*), and less clearly trimitic hyphal system are some of the characters that separate *Cerrena* from *Trametes*.

The hyphal system in *Cerrena unicolor* does not readily fit into terminology of hyphal system types. Gilbertson & Ryvarden (1986) and Bernicchia (2005), for instance, call it trimitic and Niemelä (2005) di-trimitic. The context and lower trama consist of long, straight, wide skeletal hyphae intermixed with generative and narrower, winding, and occasionally branching skeletal hyphae ("binding hyphae"). The structure appears trimitic initially, but it is not as distinct as in *Trametes*, where skeletal and binding hyphae can usually be separated with ease. In the case of *Cerrena*, the distinction between the two "types" is not clear-cut, and intermediary hyphae occur – sometimes a single hypha may turn from skeletal to "binding". In his detailed study Westhuizen (1963) finds two types of hyphae but points out that clamps are found on the thick-walled hyphae. He goes on to define this species monomitic. We have also observed that thick-walled clamps at the start/end of skeletal segments are rather common (not so in *Trametes*). In our view, the hyphal structure in *C. unicolor* is best described as dimitic, with some intermediary hyphae and branching of skeletal hyphae.

Cerrena albocinnamomea (Y.C. Dai & Niemelä) H.S. Yuan, *Mycol. Progr*. **13**: 362. 2013. [2014]. Fig. 1.
Basionym: *Antrodiella albocinnamomea* Y.C. Dai & Niemelä, *Mycotaxon* **64**: 70. 1997.
Synonym: *Cerrena aurantiopora* J.S. Lee & Y.W. Lim. *Mycologia* **102**: 212. 2010.

Typus: **China**, Jilin, Antu, Changbaishan, on stump of *Acer*, 5 Sep. 1993, *Dai 1063* (**holotype** of *Antrodiella albocinnamomea* H).

Notes: For description, see Dai & Niemelä (1997). This temperate East Asian species with resupinate basidiomes can be mistaken for *Antrodiella*. The cottony subiculum and sterile, even fimbriate margin, relatively large size of basidiomes and a bit larger spore size separate it from *Antrodiella sensu stricto*. The hymenial cystidia, although present, can be rare and difficult to find.

Cerrena cystidiata Rajchenb. & Meijer, *Mycotaxon* **38**: 176. 1990.

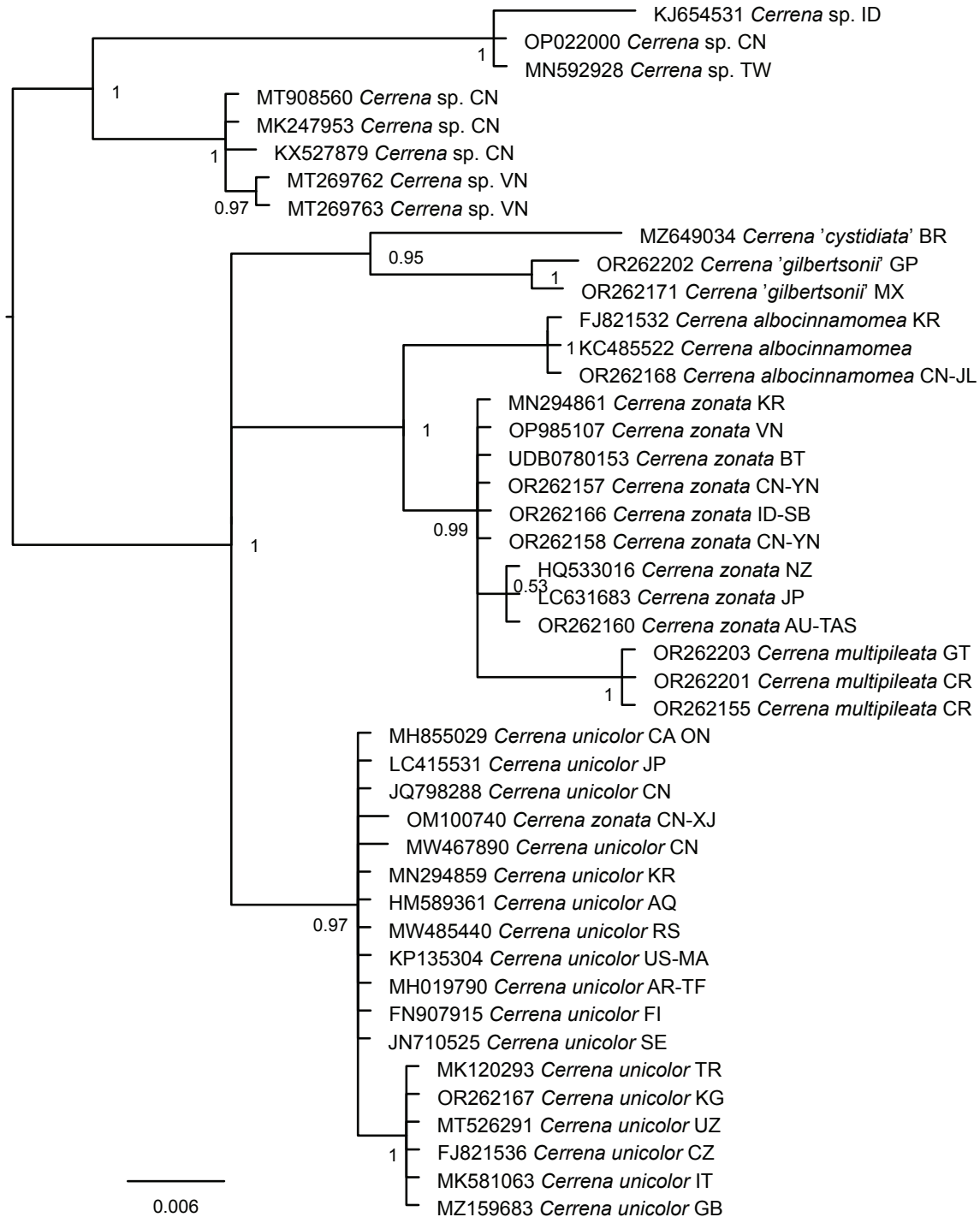

Fig. 5. Bayesian consensus phylogram of *Cerrena* spp. based on ITS sequences. For each leaf, the GenBank accession number, the species name (as available), and the ISO 3166 country code of the country of origin are shown.

Typus: **Brazil**, Paraná, São José dos Pinhais, Reserva Biológica Cambuí, dead and standing *Sebastia connersoniana*, 22 May 1988, *de Meijer 1169* (**holotype** BAFC 31626).

Notes: Westphalen & Motato-Vásquez (2022) provide a sequence they have labelled as *C. cystidiata* from the south of Brazil, where the type was collected. They do not mention if they have compared it with the type, nor do they provide a description. The sequence is unique and closely related to *C. 'gilbertsonii'* and *C. unicolor* (Fig. 5). It is not out of the question that *C. 'gilbertsonii' sensu* Ryvarden could be found in Brazil as well, so comparison with the type is needed to confirm if the Brazilian specimen or *C. 'gilberstonii'* actually belong to this species. Looking at the protologue, we cannot readily point to any clear differences to separate *C. cystidiata* from *C. 'gilbertsonii'*.

Cerrena 'gilbertsonii' Ryvarden, ***nom. prov.*** Fig. 6.

Typus: **Mexico**, Sonora, Alamos area, Rio Cuchujaqui, El Guyabo crossing, on *Croton cf. niveus*, 14 Mar. 1994, *Vandevender 94-144* (**holotype** ARIZ, **isotype** O* studied).

Notes: When Ryvarden (2012) first described this species, he omitted holotype herbarium information, making the description invalid from a nomenclatural perspective (ICN Art. 40.7). In Ryvarden (2015) he amended his description with the holotype information to validate the name, but without supplying a digital identifier, which is required since 2013 (ICN Art. F.5.1). Thus, the name remains invalid. Since the identity of *C. cystidiata vs*. *C. 'gilberstonii'* is unclear, we refrain from validating the name, but use it as *nomen provisorum* to denote a good species separate from *C. unicolor*.

Cerrena 'gilbertsonii' is very close to *C. unicolor* phylogenetically and morphologically. As Ryvarden (2012) describes, usually its basidiocarps are smaller and thinner and more hydnoid than those of *C. unicolor*. However, variation in *C. unicolor* is considerable and equally hydnoid specimens are found in the latter species as well. Its basidiocarps may also be small and thin. Judging by the few samples we have seen, the upper surface is consistently brown and hairs shorter than in *C. unicolor*, whose caps are initially much lighter in colour and never as evenly brown. Ryvarden (2015) mentions the presence of gloeocystidia as a separating character. Gloeocystidia are also found in *C. unicolor*, and they are notoriously unreliable as a character for identification, being sometimes absent and highly dependent on basidiocarp age. Spore shape and size, however, seem to be reliable microscopic characters: spores in *C. unicolor* are narrower (on average about 3 µm, Q > 1.5) than in *C. 'gilbertsonii'* (width about 3.5 µm, Q < 1.5; Table 3, Fig. 6).

Cerrena multipileata (C.L. Leite & J.E. Wright) Miettinen, *comb. nov.* MycoBank MB 849643.
Basionym: *Antrodiella multipileata* C.L. Leite & J.E. Wright, *Mycotaxon* **41**: 167. 1991.

Typus: **Brazil**, Santa Catarina, Florianópolis, Morro da Lagoa da Conceicão, 27 Jul. 1998, *Leite & Furlani 251* (**holotype** FLOR 10633, studied).

Notes: This species is an American counterpart of *C. zonata* from Asia. We have not been able to find morphological differences between the two species, but it should be said we have limited material of *C. multipileata* at hand. Our sequenced specimens of *A. multipileata* are not from the type area in South Brazil but rather from Central America. ITS sequences differ slightly (7 bp, 1.3 %) between the two species. For the time being, we retain *C. multipileata* as a distinct, geographically defined species.

Cerrena unicolor (Bull.) Murrill, *North American Flora* **9**(2): 124. 1908. Figs 1, 6.
Basionym: *Boletus unicolor* Bull., *Herbier de la France* **9**: t. 408. 1789; sanctioned as *Daedalea unicolor* (Bull.) Fr., *Syst. Mycol.* **1**: 336. 1821.
Synonyms: *Polystictus prosector* Lloyd, *Mycological Writings* **7**(67): 1147. 1922. See MycoBank for additional synonyms.

Typus: **Lectotype** of *Daedalea unicolor* designated here, plate 408 of Bulliard (1789) cited in the sanctioning work (Fries 1821), MBT 10014555.

Notes: *Cerrena unicolor* is a variable species, abundant in the boreal zone and rather frequent in the temperate zone. For a description, see Ryvarden & Melo (2016).

It would appear that the northern specimens are on average more robust and less irpicoid than the southern ones. ITS variation (Fig. 5) does not suggest more than one species in Eurasia. The same species is also found in North America. Nuñez & Ryvarden (2001) list *C. cystidiata* for East Asia, though it is unclear if their description is based on Asian material (the species was described from South America). Our sequenced specimen from Kyrgyzstan fits their description yet it represents *C. unicolor*. As mentioned under *'C. gilbertsonii'*, gloeocystidia are not a reliable character for separating species in this complex. The type of *Polystictus prosector* from China is a similar, thin, small-pored specimen with many gloeocystidia, and for the time being we consider it a synonym of *C. unicolor*.

We have not been able to locate a proper typification for the species *Daedalea unicolor*. Ryvarden (1991) selected a neotype (his "lectotype" from 1850 must be considered a neotype), but a neotype should only be selected if no original material is in existence (ICN art. 9.8). The illustrations cited in the protologue and the sanctioning work are part of such original material and, in the absences of specimens, must be used for lectotypification (art. 9.4). Thus, we select here the plate 408 of Bulliard (1789) cited in the sanctioning work (Fries 1821) as the lectotype of *D. unicolor* (Bull.) Fr. The current species concept of *C. unicolor* in Europe and the lectotype illustrations are clear enough that we see no need for an epitype.

Murrill (1903) did not accept *Cerrena* as a good genus, and therefore his 1903 combination of *C. unicolor* is invalid (ICN art. 33.1). In Murrill (1908: 124) he does accept *Cerrena* and this should be considered the correct publication for the valid combination.

Cerrena zonata (Berk) H.S. Yuan, *Mycol. Progr.* **13**: 363. 2013. [2014]. Figs 1, 7.
Basionym: *Irpex zonatus* Berk., *Hook. J. Bot*. **6**: 168, 1854.
Synonyms: *Irpex consors* Berk., *J. Linn. Soc. Bot*. **16**: 51. 1877.
Cerrena consors (Berk.) K.S. Ko & H.S. Jung, *FEMS Microbiol. Lett*. **170**: 185. 1999.
Irpiciporus consors (Berk.) Murrill, *Mycologia* **1**: 166. 1909.
Irpiciporus japonicus Murrill, *Mycologia* **1**: 166. 1909.

Typus: **Nepal**, Ilam district, 8 Nov. 1848, *Hooker* (**lectotype** of *Irpex zonatus* designated here K(M) 147643, MBT 10014532, studied).

Notes: This species is easy to recognize by its pilei with an irpicoid hymenophore combined with dimitic structure with clamps and cystidia. Ryvarden (1992) provided a description and compiled a comprehensive treatise on the nomenclature. He studied types of *I. zonatus* and eight other species described from Australia, Indian Himalayas, Japan, and New Zealand. He found them to represent the same taxon, for which the oldest name is *I. zonatus*. Ryvarden gives a good description of the species, and we trust his concept of the species. Our ITS dataset (Fig. 5) contains sequences of this species among others from New Zealand, Australia, Sumatra, Vietnam, Bhutan, Japan, and Chinese Himalayas, and these specimens show little ITS variation, supporting the conclusion about one wide-spread species, excluding Neotropics, where the sister species *C. multizonata* is found.

In his otherwise comprehensive paper, Ryvarden (1992) did not lectotypify *I. zonatus*. Also Maas Geesteranus (1974: 503) left the matter open, and in his type studies Ryvarden (1977) does not deal with the species. Berkeley's species description

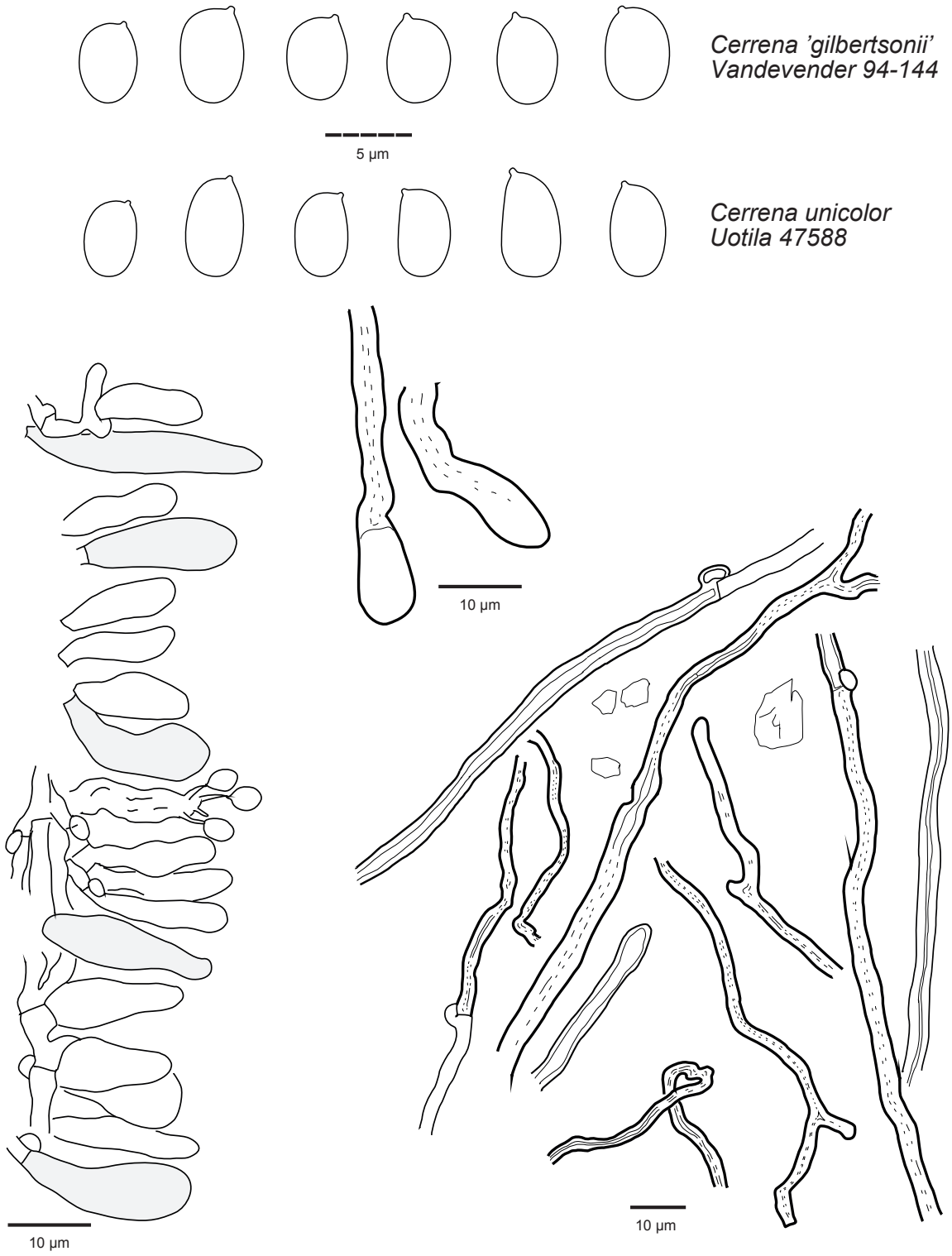

Fig. 6. Spores of *Cerrena gilbertsonii* and *C. unicolor*. Other hyphal structures, gloeocystidia, swollen skeletal hyphal ends, context skeletal hyphae, belong to *Cerrena unicolor* (*Uotila 47588*).

seems to mention two specimens, one from Sikkim and another from East Nepal collected by Hooker: "Sikkim; East Nepal. November 8. (Dr. Hooker.)" (Berkeley 1854). There are two specimens marked as syntypes in Kew, one from Sikkim, another from East Nepal, collected on 8 November. The envelope from Sikkim contains only remnants of context glued to paper, but the latter is a good-sized specimen. We designate here the specimen "East Nepal, November 8", K(M) 147643 as the lectotype of *Irpex zonatus*. The lectotype is sterile and mouldy, but recognizable. According to Hooker's travel journal, it was collected between "Jummanoo" [Jamuna?] and "Sakkiazung" [Sakhejung?] villages, in today's Ilam district of Nepal (Hooker 1854).

Irpiciporus Murrill, *Bull. Torrey Bot. Club* **32**: 471. 1905.

Basidiocarps annual or biennial, sessile, effused-reflexed or completely resupinate, light-coloured, watery in fresh condition, rather tough after drying. Context duplex, with softer upper and more compact lower layer. *Pores* range from regular angular when young, splitting to irregular pores in some species, to

Table 3. Spore measurements of studied specimens of the *Cerrenaceae*.

Species / specimen	Length	L	Width	W	Q	n
Acanthodontia cirrhatina	**4.0–5.1(–5.2)**	**4.69**	**(3.4–)3.5–4.2(–4.3)**	**3.79**	**1.24**	**65/2**
holotype	(4.0–)4.2–4.9(–5.0)	4.48	(3.4–)3.5–4.1	3.71	1.21	30
Miettinen 13717	(4.2–)4.6–5.2	4.86	3.4–4.2(–4.3)	3.87	1.26	35
Cerrena gilbertsonii	**(4.5–)4.7–5.4(–5.6)**	**5,00**	**(3.2–)3.3–4.0(–4.7)**	**3.68**	**1.36**	**64/2**
isotype	4.5–5.4	4.94	3.2–3.8(–3.9)	3.52	1.40	34
Vlasák (JV 1609/29)	(4.6–)4.7–5.6	5.05	(3.5–)3.6–4.1(–4.7)	3.87	1.31	30
Cerrena multipileata	**(3.5–)3.7–5.0(–5.4)**	**4.16**	**(2.4–)2.5–3.1(–4.4)**	**2.79**	**1.49**	**93/3**
de Meijer 2623	(3.9–)4.0–5.2(–5.4)	4.49	(2.5–)2.7–3.2	2.88	1.56	30
Ryvarden 43881	(3.6–)3.7–4.7	4.11	2.4–3.1(–4.4)	2.76	1.49	32
Vlasák (JV 1407/63)	3.5–4.5(–5.0)	3.90	2.4–3.0	2.73	1.43	31
Cerrena unicolor	**(3.9–)4.2–5.6(–6.2)**	**4.86**	**(2.5–)2.6–3.3(–3.8)**	**2.93**	**1.66**	**150/5**
Miettinen 16729	(4.4–)4.6–5.2(–5.5)	4.83	(2.6–)2.7–3.2	2.97	1.63	30
Niemelä 30 Jun. 1970	4.0–5.3(–5.4)	4.83	2.5–3.1(–3.2)	2.84	1.70	30
Niemelä 5352	(3.9–)4.2–5.3(–5.5)	4.80	2.5–3.0	2.74	1.75	30
Niemelä 6098	4.1–6.0(–6.2)	4.82	2.6–3.3(–3.4)	2.90	1.66	30
Uotila 47588	(4.2–)4.4–5.8(–6.2)	5.03	(2.8–)2.9–3.7(–3.8)	3.19	1.58	30
Cerrena zonata	**(3.7–)4.0–5.5(–6.4)**	**4.66**	**(2.5–)2.6–3.4(–3.6)**	**2.95**	**1.58**	**103/3**
Gates *s.n.*	(4.0–)4.2–5.2(–5.5)	4.62	2.6–3.6	2.93	1.58	30
Miettinen 13798	3.7–4.7(–4.8)	4.24	(2.5–)2.6–3.2	2.86	1.48	33
Miettinen 9773	4.3–5.7(–6.4)	5.04	2.8–3.4(–3.5)	3.05	1.65	40
Irpiciporus branchiformis	**(4.4–)4.7–6.0(–6.2)**	**5.30**	**4.0–5.2(–5.3)**	**4.67**	**1.14**	**62/2**
holotype	(4.4–)4.6–5.7(–5.8)	5.17	4.0–5.1(–5.2)	4.65	1.11	32
Niemelä 5937	(4.6–)4.8–6.1(–6.2)	5.43	(4.0–)4.1–5.2(–5.3)	4.69	1.16	30
Irpiciporus mollis	**(4.8–)5.1–6.2(–6.3)**	**5.45**	**(4.0–)4.3–5.3(–6.0)**	**4.84**	**1.13**	**121/4**
lectotype	5.1–6.2(–6.3)	5.60	(4.2–)4.3–5.6(–6.0)	4.97	1.13	30
Vlasák (JV 0108/115)	(5.0–)5.2–6.0(–6.2)	5.54	(4.3–)4.4–5.2	4.87	1.14	30
Vlasák (JV 0709/174)	(4.8–)5.0–5.9(–6.1)	5.34	(4.2–)4.3–5.2(–5.3)	4.72	1.13	30
Vlasák (JV 0808/45)	(5.0–)5.1–5.8(–5.9)	5.34	(4.0–)4.2–5.3(–5.5)	4.80	1.11	31
Irpiciporus pachyodon	**(5.2–)5.5–6.5(–7.4)**	**6.02**	**(4.2–)4.5–5.6(–6.4)**	**5.09**	**1.18**	**122/4**
Heilmann-Clausen 07–286	(5.4–)5.5–6.3(–6.5)	5.87	(4.3–)4.4–5.3(–5.6)	4.94	1.19	30
Melo 327	5.4–6.8(–6.9)	6.02	(4.7–)4.8–5.6(–6.1)	5.21	1.15	30
Spirin 13785	(5.2–)5.3–6.3(–6.8)	6,00	(4.2–)4.4–5.4(–5.6)	4.94	1.22	30
Vlasák (JV 9311/1)	(5.6–)5.8–7.2(–7.4)	6.17	(4.6–)4.8–5.7(–6.4)	5.25	1.18	32
Lividopora armeniaca	**(3.7–)3.8–4.6(–4.8)**	**4.10**	**3.3–4.0(–4.2)**	**3.61**	**1.14**	**38**
Lividopora benetosta	**(3.2–)3.4–4.6(–4.9)**	**3.94**	**(2.9–)3.0–3.9(–4.3)**	**3.46**	**1.14**	**220/8**
Hallenberg 15301	3.7–4.4	4.10	3.2–3.8(–3.9)	3.48	1.18	30
Härkönen K778	4.0–4.8(–4.9)	4.43	3.0–3.9(–4.1)	3.62	1.22	20
Lloyd 5042	3.6–4.3	4.02	3.1–3.8	3.44	1.17	10
Miettinen 10394,1	3.8–4.6	4.14	3.3–3.9	3.60	1.15	5
Miettinen 13647,1	(3.3–)3.5–4.8(–4.9)	4.03	(3.0–)3.1–4.2(–4.3)	3.63	1.11	32
Miettinen 13891	3.7–4.6	4.08	3.3–3.8	3.59	1.14	20
Miettinen 18035	3.2–3.8(–3.9)	3.52	(2.9–)3.0–3.5	3.21	1.10	34
Miettinen 18135	(3.4–)3.5–4.1(–4.2)	3.82	(3.1–)3.2–3.8(–4.0)	3.48	1.10	30
Miettinen 8823,2	3.5–4.2	4.04	3.0–3.5	3.24	1.25	5
Miettinen 9023,2	3.7–4.3	3.91	3.2–3.8	3.46	1.13	24
Miettinen 9166,5	3.6–4.2(–4.6)	3.90	2.9–3.7	3.34	1.17	30
Miettinen 9978,2	3.6–3.9	3.70	3.3–3.6	3.48	1.06	8
Lividopora facilis	**3.2–4.0**	**3.50**	**2.5–3.0**	**2.69**	**1.30**	**33**

Table 3. (Continued).

Species / specimen	Length	L	Width	W	Q	n
Lividopora subvincta	**(3.4–)3.6–4.6(–5.2)**	**4.02**	**(2.6–)2.9–3.4(–3.5)**	**3.13**	**1.28**	**90/3**
holotype	(3.6–)3.7–4.6	4.02	(2.8–)2.9–3.3	3.10	1.30	30
Savchenko 171124/1505	(3.4–)3.5–4.2	3.87	2.9–3.5	3.17	1.22	30
Savchenko 171129/1309X	(3.5–)3.6–5.1(–5.2)	4.18	(2.6–)2.8–3.4(–3.5)	3.14	1.33	30
Lividopora vincta	**(3.2–)3.3–4.2(–4.5)**	**3.80**	**(2.8–)2.9–3.4(–3.5)**	**3.13**	**1.21**	**62/2**
Lowe (CFMR L-13218-Sp)	(3.6–)3.7–4.2(–4.5)	3.95	2.9–3.4(–3.5)	3.22	1.23	30
Miettinen 17916,1	(3.2–)3.3–4.0(–4.3)	3.65	2.8–3.3(–3.5)	3.06	1.20	32
Somion delectans	**(5.8–)6.0–7.3(–7.6)**	**6.60**	**(5.0–)5.1–6.6(–6.8)**	**5.64**	**1.17**	**90/3**
isotype	(5.8–)6.0–7.4(–7.6)	6.59	(5.0–)5.1–6.7(–6.8)	5.66	1.16	30
Thaxter 799	6.0–7.2(–7.3)	6.61	(5.1–)5.2–6.7	5.72	1.16	30
Vlasák 1507/22	(6.0–)6.1–7.2(–7.3)	6.61	(5.0–)5.1–6.5(–6.6)	5.55	1.19	30
Somion litschaueri	**(6.6–)6.8–8.6(–9.1)**	**7.71**	**(4.9–)5.2–7.0(–7.7)**	**6.00**	**1.28**	**120/4**
holotype	(6.8–)6.9–8.6(–9.1)	7.77	(4.9–)5.0–7.2(–7.7)	6.14	1.27	30
Vampola 198	6.6–8.1(–8.2)	7.28	(5.4–)5.5–6.3(–6.4)	5.94	1.23	30
Vlasák (JV 1309/1)	(6.7–)7.0–8.8(–8.9)	7.69	(5.0–)5.1–6.3(–6.6)	5.79	1.33	30
Vlasák (JV 1309/7)	(6.8–)7.3–8.8(–9.1)	8.08	(5.3–)5.4–7.0(–7.1)	6.16	1.31	30
Somion occarium	**(5.3–)6.0–7.2(–7.6)**	**6.60**	**(3.9–)4.3–5.5(–6.2)**	**5.02**	**1.31**	**120/4**
holotype	(5.3–)5.8–7.1(–7.5)	6.47	(4.2–)4.3–5.6(–6.2)	5.06	1.28	60
Vampola 149	6.0–7.5(–7.6)	6.78	(3.9–)4.0–5.5(–5.6)	4.94	1.37	30
Vlasák 0511/8	(5.9–)6.0–7.2(–7.3)	6.68	(4.4–)4.6–5.3(–5.6)	5.03	1.33	30
Somion strenuum	**(5.0–)5.2–6.4(–7.2)**	**5.90**	**(4.1–)4.2–5.3(–6.0)**	**4.80**	**1.23**	**120/4**
Miettinen 10456	(5.1–)5.2–6.3(–7.1)	5.89	(4.1–)4.2–5.2(–5.7)	4.69	1.26	30
Spirin 10989	(5.0–)5.1–6.8(–7.2)	5.75	(4.1–)4.2–5.6(–6.0)	4.82	1.19	30
Spirin 6112	(5.2–)5.4–6.3(–6.4)	6.03	(4.1–)4.2–5.5(–5.7)	4.90	1.23	30
Spirin 7330	(5.2–)5.3–6.5(–6.8)	5.94	(4.1–)4.2–5.3(–5.4)	4.77	1.25	30
Somion tomsovskyi	**(6.4–)6.8–8.3(–8.7)**	**7.50**	**(5.1–)5.5–6.8(–7.1)**	**6.11**	**1.23**	**60/2**
Vlasák Jr. (JV 1209/55)	(6.4–)6.8–8.2(–8.7)	7.47	(5.2–)5.4–6.9(–7.1)	6.05	1.23	30
Vlasák Jr. (JV 1307/8)	6.8–8.3(–8.6)	7.55	(5.1–)5.5–6.8(–7.1)	6.18	1.22	30
Somion unicolor	**(5.2–)5.3–7.1(–7.3)**	**6.13**	**(4.0–)4.2–5.4(–5.9)**	**4.78**	**1.28**	**90/3**
Lewis DAOM 9080	(5.3–)5.8–7.2(–7.3)	6.38	(4.1–)4.2–5.5(–5.6)	4.77	1.34	30
Vlasák (JV 1708/10)	5.2–6.7(–6.8)	5.88	(4.0–)4.1–5.4(–5.9)	4.82	1.22	30
Vlasák Jr. (JV 1304/1)	(5.4–)5.5–6.9(–7.0)	6.11	(4.1–)4.2–5.3(–5.8)	4.74	1.29	30

incomplete, becoming dentate or spathulate in others. *Hyphal structure* monomitic, loose, homogenous, hyphae clamped and slightly cyanophilous, thin- to thick-walled, subparallel in trama. *Basidia* long-clavate, 20–45 × 5–8 µm, four-spored, with guttulate contents. *Basidiospores* broadly ellipsoid to subglobose, slightly thick-walled (wall 0.2–0.3 µm thick), with a central oil-drop, slightly to distinctly cyanophilous. Causes a white rot of living and dead dicot trees.

Genus type: *Irpex mollis* Berk. & M.A. Curtis

Notes: *Irpiciporus* spp. have completely monomitic basidiocarps, but David (1969) has shown that when cultured *I. pachyodon* produces microbinding hyphae similar to *Pseudolagarobasidium* and *Radulodon*. She does not report similar hyphae for *Somion occarium* (as *"Spongipellis delectans"*).

We accept here five *Irpiciporus* species, but from available DNA data it is evident that at least one additional species also belongs to the core *Irpiciporus* (Fig. 8). Zhao *et al.* (2017) published a sequence under the name *Tyromyces xuchilensis* from Ecuador (*Ryvarden 44669*, studied, GenBank KX161650). This sequence belongs to *Irpiciporus* in the close vicinity of *I. sinuosus* – but not to *T. xuchilensis* (see Excluded taxa). It might belong to *Tyromyces irpiceus*, which is possibly a species of *Irpiciporus* as indicated by Corner (1989) himself. *Irpiciporus sinuosus* and the Ecuadorian material have regularly poroid hymenophore unlike the other species, which are truer to the genus name in having an irpicoid hymenophore of splitting pores. Otherwise, basidiocarp configuration, colouration, and micromorphology are very similar among all the species in the genus.

Nakasone & Ortiz-Santana (2022) combined three hydnoid species in the genus. We accept one of those species (*Irpiciporus revolubilis*) in *Irpiciporus*, but we show here that *Irpiciporus africanus* (Ipulet & Ryvarden) Nakasone belongs to *Hypochnicium* rather than to the *Cerrenaceae*. We treat the third species (*I. decolorans*) as insufficiently known (see Excluded taxa).

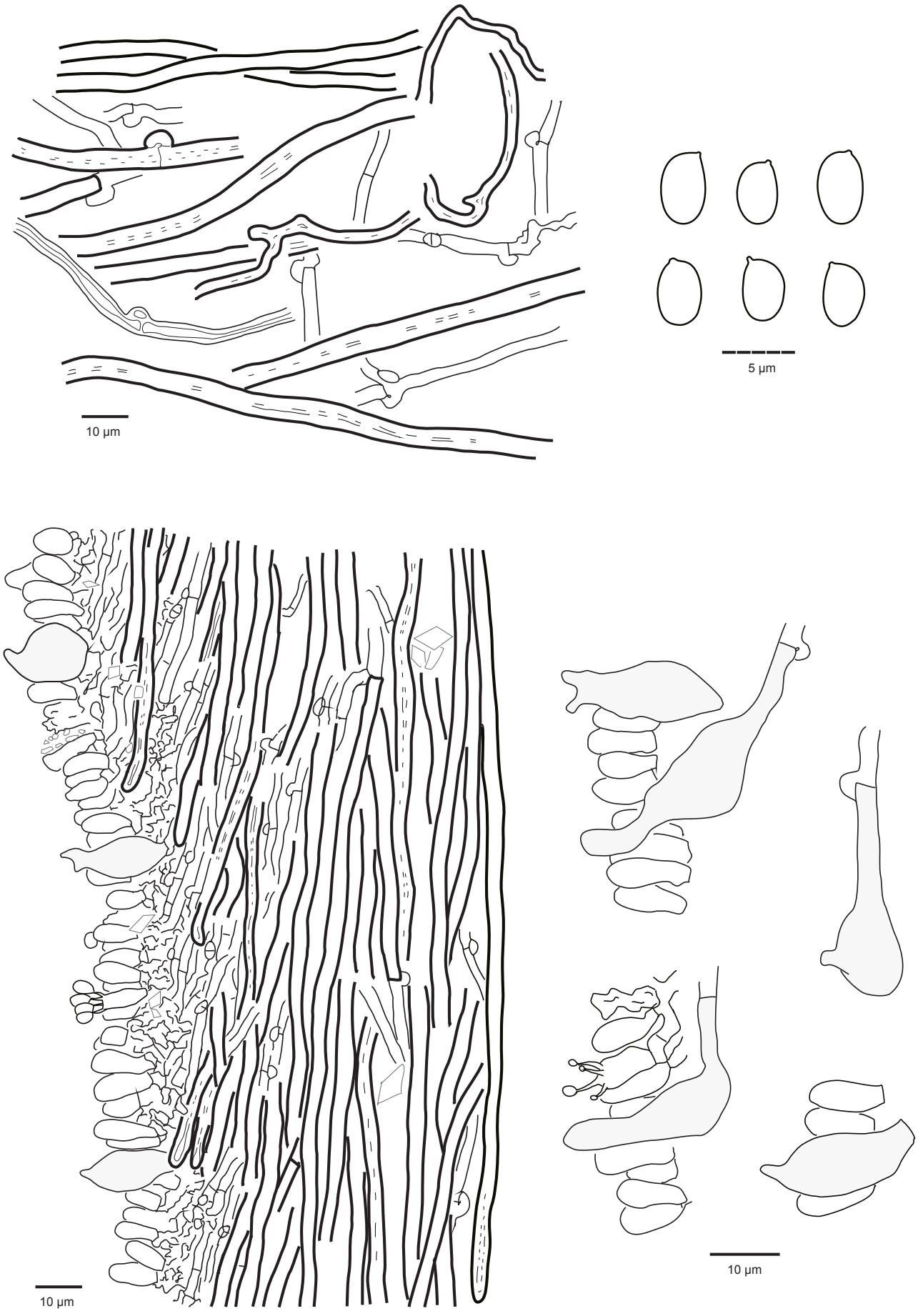

Fig. 7. *Cerrena zonata* (*Miettinen 9773*). Context hyphae, tube trama and hymenium, hymenial cystidia and spores.

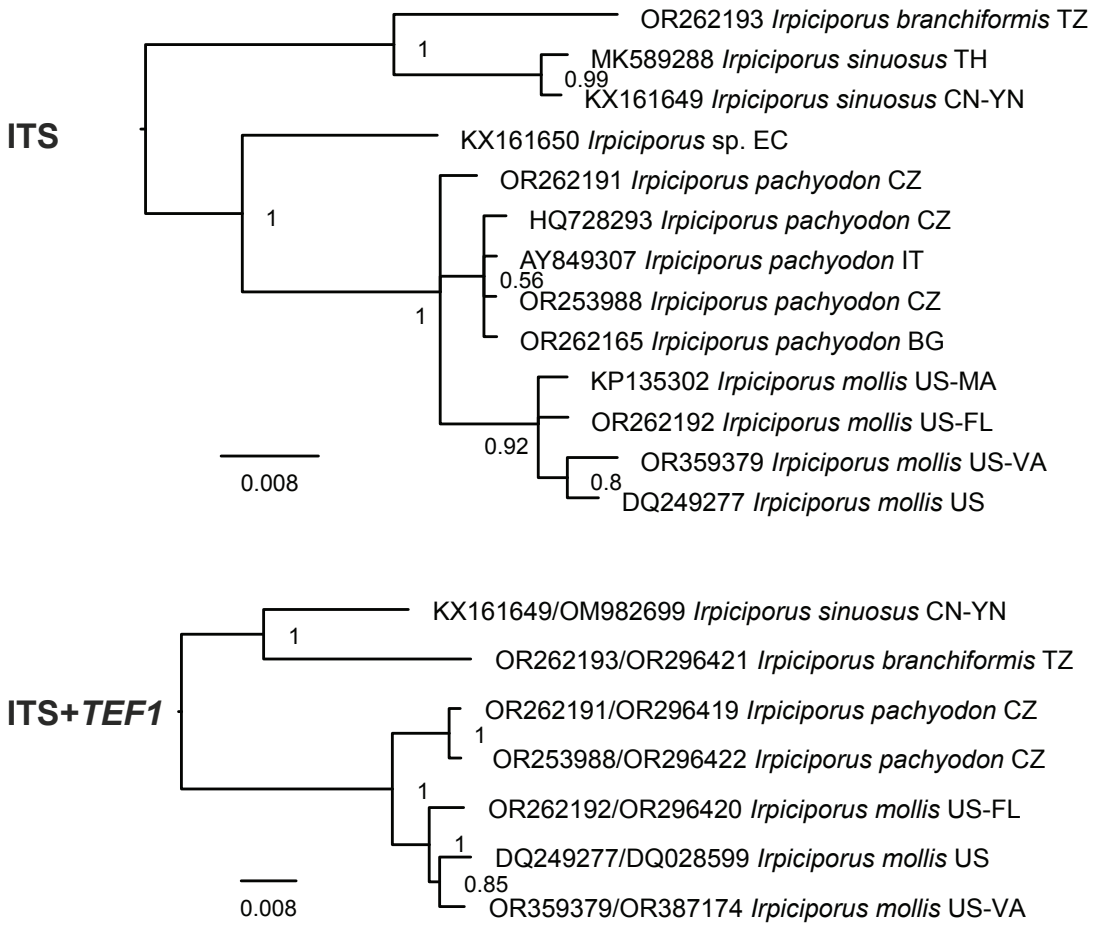

Fig. 8. Bayesian consensus phylograms of *Irpiciporus* spp. based on ITS and ITS+ *TEF1* datasets. Countries (and states) of origin are denoted with ISO 3166 codes.

After describing the genus, Murrill used *Irpiciporus* as a replacement for *Irpex*. From *Irpiciporus sensu* Murrill, only the type species is in the *Cerrenaceae*, and the rest of the species are a variable set of unrelated irpicoid polypores (Donk 1974). All names combined to *Irpiciporus* are commented either as recognized species or synonyms or under Excluded taxa.

Irpiciporus branchiformis Miettinen & Spirin, ***sp. nov.*** MycoBank MB 849644. Fig. 9.

Typus: **Tanzania**, Tanga, Lushoto, Mazumbai Forest Res., -4.8075° : 38.5032° ± 300 m, alt. 1 500–1 600 m, lower montane rainforest, fallen log of *Ocotea usambarensis*, 17 Apr. 1991, *Saarimäki 869* (**holotype** H 7200355).

Etymology: *Branchiformis* (Lat., adj.), reminiscent of fish gills, in reference to the irpicoid caps of the species.

Basidiocarps annual or biennial, sessile, pilei projecting up to 3 cm. Upper surface pubescent, azonate, cream coloured. Edge of pileus sharp, fertile, concolourous with pileal surface. Hymenial surface more or less concave, cream coloured to pale ochraceous; pores incomplete, shallow, present only in marginal areas, 2–3 per mm, quickly becoming dentate to spathulate and finally transforming to flattened, sharp-pointed spines, 2–3 per mm. Section: context cream coloured, soft, indistinctly fibrillose, up to 0.5 mm thick; hymenial layer soft, concolourous or slightly paler than hymenial surface, up to 0.7 cm thick.

Hyphal structure monomitic, all septa with clamp connections. Context hyphae slightly thick-walled, interwoven to subparallel, (3.0–)3.8–4.4(–5.3) µm diam. Tramal hyphae thin- to slightly thick-walled, subparallel, (2.9–)3.1–4.1(–4.6) µm diam. Subhymenial hyphae not differentiated from tramal ones. *Basidiospores* slightly thick-walled, subglobose to more rarely broadly ellipsoid, (4.4–)4.7–6.0(–6.2) × 4.0–5.2(–5.3) µm, L = 5.3 µm, W = 4.67 µm, Q = 1.11–1.16.

Distribution and ecology: The species is so far known only from two localities in East Africa (Tanzania), inhabiting decorticated wood of angiosperms.

Notes: *Irpiciporus branchiformis* differs from two other irpicoid species of the genus (*I. mollis* and *I. pachyodon*) in having fragile, thinner basidiocarps, more densely arranged pores/spines, and smaller basidiospores (Table 3).

Irpiciporus mollis (Berk. & M.A. Curtis) Murrill, Bull. Torrey Bot. Club 32: 471, 1905. Fig. 9.
Basionym: *Irpex mollis* Berk. & M.A. Curtis, Hooker's J. Bot. 1: 236, 1849.

Typus: **USA**, South Carolina, Santee River, unknown collection date, leg. *Ravenel*, herb. *Curtis 1729* (**lectotype** K(M) 64592, studied – selected by Murrill 1905: 471).

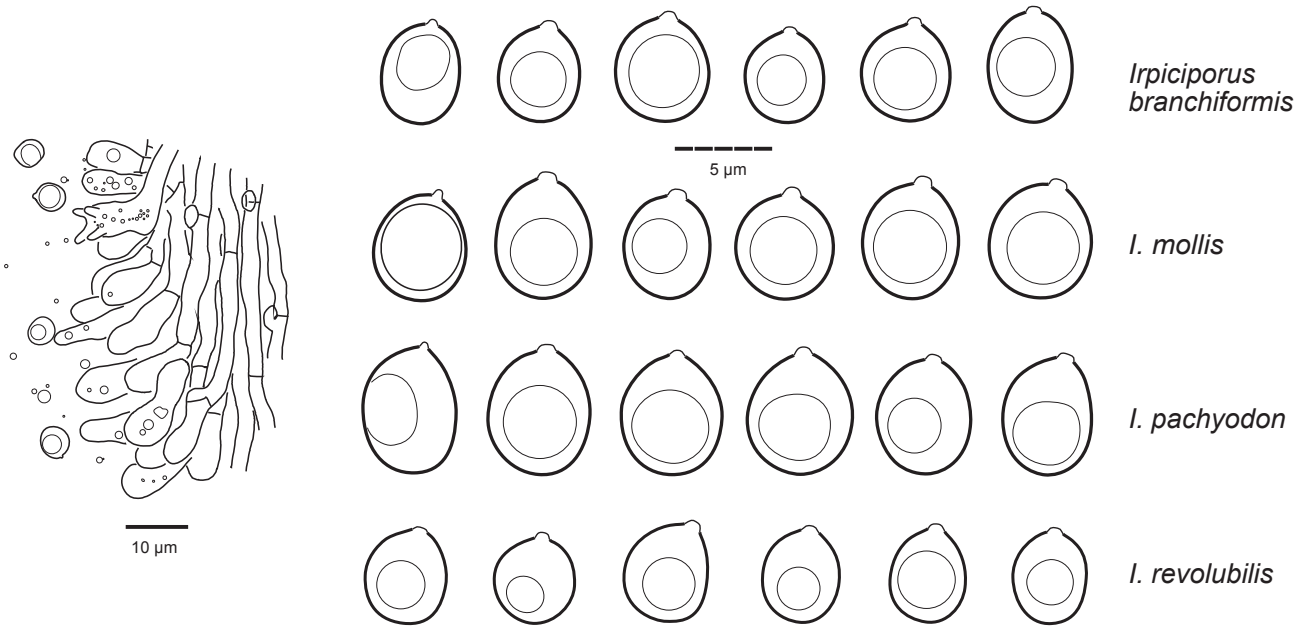

Fig. 9. *Irpiciporus* microscopic structures. Tube trama, hymenium and spores of *I. branchiformis* (holotype), and spores of *I. mollis* (*Vlasák*, JV 0808/45), *I. pachyodon* (*Vlasák*, JV 9311/1) and *I. revolubilis* (holotype).

Basidiocarps annual or biennial, sessile or effused-reflexed, rarely completely resupinate, pilei projecting up to 3 cm. Upper surface pubescent, azonate, cream coloured to pale ochraceous, in oldest parts almost smooth. Edge of pileus sharp, fertile, concolourous with pileal surface. Hymenial surface more or less concave, cream coloured to pale ochraceous, in very old basidiocarps brownish; pores incomplete, shallow, present only in marginal areas, 1–2 per mm, quickly becoming dentate to spathulate and finally transforming to flattened, sharp-pointed spines, about 1 per mm. Section: context cream coloured, in old herbarium specimens pale ochraceous, watery in fresh condition, firm, distinctly fibrillose and sometimes indistinctly zonate when dry, up to 2 cm thick; hymenial layer tough, concolourous with or slightly paler than hymenial surface, up to 1.5 cm thick.
Hyphal structure monomitic; all septa with clamp connections. Context hyphae very thick-walled, interwoven to subparallel, (4.3–)5.2–6.2(–6.7) µm diam. Tramal hyphae slightly to distinctly thick-walled (lumen wide to capillary), subparallel, (2.8–)3.4–4.3(–5.2) µm diam. Subhymenial hyphae thin- to slightly thick-walled, some short-celled and inflated, 3–5 µm diam. *Basidiospores* slightly thick-walled, broadly ellipsoid to subglobose, (4.8–)5.1–6.2(–6.3) × (4.0–)4.3–5.3(–6.0) µm, L = 5.45 µm, W = 4.84 µm, Q = 1.11–1.14.

Distribution and ecology: Widely distributed in the eastern part of North America, reaching Florida at the southernmost limit of its distribution. Occurs on many angiosperm tree species, and Gilbertson & Ryvarden (1987) report it from living trees, but we have not been able to find any reference that it would be pathogenic. It also grows on dead trees.

Notes: This species was originally described from South Carolina (Berkeley & Curtis 1849) and recognized as such until Kotlaba & Pouzar (1957) placed it among the synonyms of the European species *I. pachyodon*. However, both morphological and DNA data confirm that they are different species, whose distribution areas do not seem to overlap. *Irpiciporus mollis* is distributed in the eastern part of USA and Canada (Gilbertson & Ryvarden 1987, as S. pachyodon). According to Murrill (1905) and Maas Geesteranus (1974), *Irpex crassus* Berk. & Curtis and *Irpex crassitatus* Lloyd are conspecific with *I. mollis*. Ryvarden (2020b) lists further junior synonyms.

Irpiciporus pachyodon (Pers.) Kotl. & Pouzar, *Česká Mykol*. **11**: 156. 1957. Figs 2, 9.
Basionym: *Hydnum pachyodon* Pers., *Mycol. Europaea* **2**: 174. 1825.
Synonym: *Hydnum schestunovii* Nikol., *Notulae Syst. Sect. Cryptogam. Inst. Bot*. **6**: 38. 1949 (*fide* Nikolaeva 1964).

Typus: **France**, *Delastre* (**lectotype** of *Hydnum pachyodon* L 910.263–1321 – selected and studied by Maas Geesteranus 1974: 491).

Basidiocarps annual or biennial, effused-reflexed to completely resupinate, pilei projecting up to 5 cm. Upper surface pubescent, azonate, cream coloured to pale ochraceous, in oldest parts almost smooth. Edge of pileus sharp to rather blunt, fertile, concolourous with pileal surface. Hymenial surface more or less concave, cream coloured or yellowish, in very old basidiocarps pale ochraceous; pores incomplete, shallow, present only in marginal areas, 0.5–1 per mm, quickly becoming dentate to lamellate and finally transforming to flattened, sharp-pointed spines, 0.5–1 per mm. Section: context almost white to cream coloured, tough in fresh condition, compact when dry, up to 3 cm thick; hymenial layer tough, concolourous with or slightly paler than hymenial surface, up to 2 cm thick.

Hyphal structure monomitic; all hyphae with clamp connections. Context hyphae thin- or only slightly thick-walled, easily collapsing, interwoven to subparallel, (4.7–)4.9–6.0(–6.8) µm diam. Tramal hyphae thin- or slightly thick-walled, subparallel, (3.0–)3.3–4.1(–4.5) µm diam. Subhymenial hyphae thin-walled, some short-celled and slightly inflated, 3.0–4.5 µm diam. *Basidiospores* slightly thick-walled, broadly ellipsoid to

subglobose, (5.2–)5.5–6.5(–7.4) × (4.2–)4.5–5.6(–6.4) µm, L = 6.02 µm, W = 5.09 µm, Q = 1.15–1.22.

Distribution and ecology: *Irpiciporus pachyodon* is a temperate European species inhabiting mostly living oak trees (Ryvarden & Melo 2014). It has also been reported from Caucasus (Nikolaeva 1964).

Notes: *Irpiciporus pachyodon* is the European counterpart of North American *I. mollis*. Morphological differences between these species are subtle: tramal hyphae of *I. pachyodon* are slightly narrower than in *I. mollis* and not so thick-walled, and its basidiospores are slightly larger.

Irpiciporus revolubilis (Hjortstam & Ryvarden) Nakasone, *Lilloa* **59** (Suppl.): 97. 2022. Fig. 9.
Basionym: *Radulodon revolubilis* Hjortstam & Ryvarden, *Syn. Fungorum* **23**: 88. 2007.

Typus: **Venezuela**, Aragua, Parque National Henri Pittier, Rancho Grande Research Station, on decayed hardwood, 14 Apr. 1999, *Ryvarden 41417* (**holotype** O, studied).

Basidiocarps annual, effused, up to 5 cm in longest dimension. Margin sharply compact, delimited, up to 1 mm, detaching and rolling in dry basidiocarps. Hymenial surface cream coloured to pale ochraceous; hymenophore irpicoid, spines sharp to rather blunt, 3–5 per mm, partly fusing together and forming dentate or spathulate projections. Section: context cream-colored, soft, up to 0.5 mm thick; hymenial layer soft, concolourous with or slightly paler than hymenial surface, up to 0.3 cm thick.

Hyphal structure monomitic, all septa with clamp connections. Context hyphae slightly to distinctly thick-walled, interwoven to subparallel, (3.4–)4.1–5.0(–5.6) µm diam. Tramal hyphae slightly to distinctly thick-walled, predominantly subparallel, (2.5–)2.7–4.1(–5.1) µm diam. Subhymenial hyphae not differentiated from tramal ones. *Basidiospores* slightly thick-walled, ellipsoid to broadly ellipsoid, more rarely subglobose, (4.2–)4.3–5.0(–5.1) × (3.3–)3.5–4.3(–4.4) µm, L = 4.63 µm, W = 3.98, Q = 1.17.

Notes: We agree with Nakasone & Ortiz-Santana (2022) that this species belongs to *Irpiciporus*. It has the smallest spores among the species in the genus and reminds closely of the African *I. branchiformis*.

Irpiciporus sinuosus Y.C. Dai & Chao G. Wang, *Mycol. Progr.* **21**(73): 8. 2022.

Typus: **China**, Yunnan, Puer, Laiyanghe Forest Park, angiosperm, 6 Jun. 2011, *Dai 12234* (**holotype** BJFC 010517).

Notes: This species has well-developed pores, even though they start to split soon (Zhao *et al.* 2017). It is the first truly poroid species confirmed to belong to *Irpiciporus*.

Lividopora Miettinen, ***gen. nov.*** MycoBank MB 849645.

Type species: *Lividopora facilis* Miettinen

Etymology: Derived from *lividum* (Lat., adjective), livid, refers to the greyish (dull) tint of the basidiocarps.

Resupinate annual to short-lived perennial *polypores* with reddish to grey colours, leathery tough when fresh, drying hard, with a distinct margin. *Pores* regular, mid-sized to small (5–15 per mm) thin-walled and entire. Brown, black or red basal layer present. *Hyphal system* dimitic, clamps absent, weakly to moderately cyanophilous, IKI-, KOH-, CRB lilac. Skeletal hyphae interwoven but not agglutinated, with a visible narrow lumen, generative hyphae slightly thick-walled, dominating in lower tube trama. The overall impression of hyphal structure is messy. Two main types of *cystidia*: tramal encrusted skeletocystidia are clavate, abundant and conspicuous, embedded or penetrating hymenium; thin-walled, often mamillate, slightly projecting, sack-like hymenial cystidia also present, often with a stained plasma and could be called gloeocystidia. In addition to these, encrusted and naked hyphidia in hymenium. *Basidia* with four sterigmata, barrel-like to clavate. *Basidiospores* ellipsoid to subglobose, smooth, mid-sized, thin-walled or with distinct walls, devoid of guttulae.

Notes: Incorporation of ITS sequences from public nucleotide databases in our analyses (Fig. 10) shows that two *Lividopora* species are widespread, *L. benetosta* in the Paleotropics and Caribbean, and *L. vincta* in the Neotropics. We could not find public sequences of the other three species. Both *L. benetosta* and *L. vincta* show some ITS variation, but differences are small, giving no reason to recognize more species in the genus.

Species of *Lividopora* are similar microscopically, and in many cases macroscopic characters of the basidiocarp such as colour (Fig. 11) and pore size are more useful for identification. Geographic origin too is of help, since all but one species seem to be restricted to some part of the tropics. However, young specimens, for instance in the Caribbean where both *L. benetosta* and *L. vincta* occur, can be very difficult or even impossible to identify with certainty by their morphology.

Table 4 provides key identification characters. For cultural characters and further morphological characters of the group, we recommend Setliff (1972a, b). He notes that *L. vincta* coll. produce clamps in culture.

Skeletocystidia (Figs 12, 13) appear first as thin-walled, swollen hyphal ends with sparse encrustation, often in hymenium, though rooted in trama. At this stage, they may appear similar to the permanently thin-walled hymenial cystidia ("gloeocystidia"). Later in development the skeletocystidia become thick-walled and obtain a coarse and thick crystal cover that finally obscures view to the hyphae inside the cystidia. The two types are easy to distinguish in slides, even though, pending on developmental stage, the thin-walled "gloeocystidia" may be rare or only found in some parts of the basidiocarp. Cystidial encrustation is very persistent, visible even in otherwise destroyed (old, mouldy, or sterile) specimens.

Lividopora spp. have been included in *Rigidoporus* by Ryvarden (1972b) and Corner (1987) as *R. vinctus* and *R. hypobrunneus* (= *L. benetosta* below). Even though not closely related, the two genera share morphological characters such as cyanophilous simple-septate hyphae in basidiocarps, ellipsoid to subglobose spores, short and broad, barrel-like hymenial cells, and heavily encrusted, thick-walled club-like tramal cystidia. Their main difference is in the hyphal structure, which is distinctly dimitic in *Lividopora* spp. and monomitic or indistinctly dimitic in *Rigidoporus* spp. The structure of trama is different: hyphae are parallel in most *Rigidoporus* spp. and related *Physisporinus* spp. but interwoven in *Lividopora*. Spores of *Rigidoporus* are

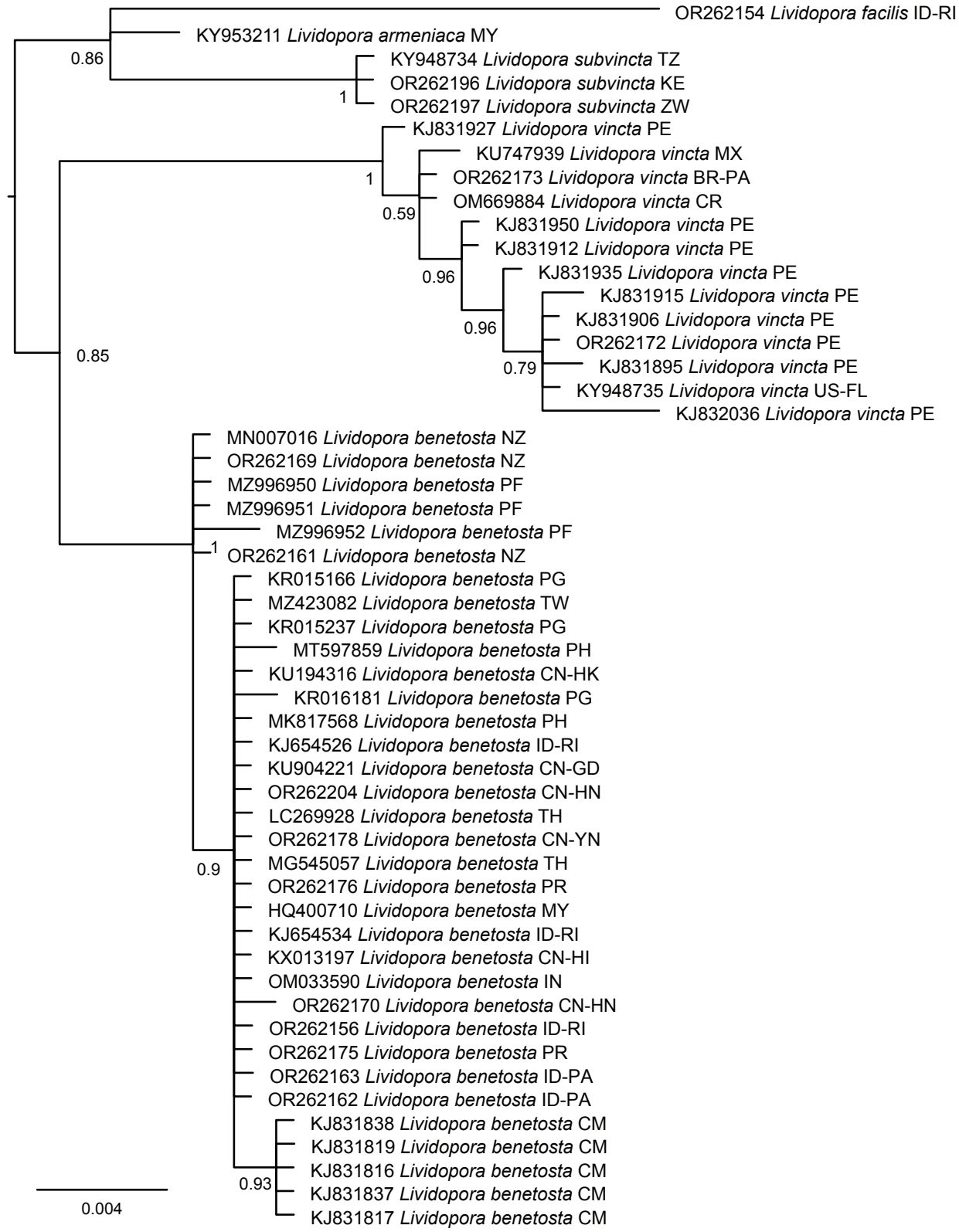

Fig. 10. Bayesian consensus phylogram of *Lividopora* spp. based on ITS sequences. Countries (and states) of origin are denoted with ISO 3166 codes.

cyanophilous and usually slightly thick-walled, whereas in *Lividopora* spp. they are thin-walled and acyanophilous.

Ryvarden (1972b) considered the hyphal system of *L. vincta* monomitic, consisting of apparent skeletal hyphae or their segments, but with transitions to generative hyphae. He softened his stand later, settling for "apparently dimitic" (Gilbertson & Ryvarden 1987). Intermediary hyphae are not a rare phenomenon in dimitic polypores. In our view, the intermediary hyphae are not prevalent in *Lividopora*, and for all practical purposes (normal morphological examination and functionality for the fungus), the structure may be called dimitic.

Lividopora armeniaca Miettinen & J. S. Seelan, ***sp. nov.*** MycoBank MB 849646. Figs 11–13.

Table 4. Comparison of morphological characters of *Lividopora* spp.

Species	Encrusted cystidia (L and W in µm)	Pore size (60 % mid range)	Spores (L and W in µm)	Color	Tramal skeletal hyphae (µm in diameter, 60 % mid range)	Other
L. armeniaca	**Narrow, L = 23, W = 7.2**	10–12	**Subglobose, L = 4.10, W = 3.61, Q = 1.14**	Orange when fresh, dries brick	Yellowish, **narrow**, 2.5–3.0	—
L. benetosta	Most very broad and short (Q < 2), L = 34, W = 14.9	8–13	**Subglobose, L = 3.94, W = 3.46, Q = 1.14**	Faded reddish when young, **brownish-grayish** when old	Yellow to brown, wide, 3.0–4.0	Gloeocystidia commonly > 10 µm wide
L. facilis	**Narrow, L = 21, W = 9.7**	**5–6**	**Ellipsoid, L = 3.5 µm, W = 2.69 µm, Q = 1.30**	Faded reddish, dries brown	Almost hyaline, narrow, 2.8–3.3	—
L. subvincta	Broad and long, L = 32, W = 11	9–11	**Ellipsoid, L = 4.02 µm, W = 3.13 µm, Q = 1.28**	**Dark gray**	Brown, wide, 3.2–4.2	—
L. vincta	Broad and long, L = 47, W = 14.6	9–11	**Ellipsoid, L = 3.80, W = 3.13, Q = 1.21**	**Reddish**	Yellowish, wide, 3.7–4.5	—

Typus: **Malaysia**, Sabah, Ranau. Kinabalu Park, Timpohon peak trail, 6.02775° 116.54527°, alt. 1 880 m, upper montane rainforest, on a fallen crown of a dicot (24 cm diam, decay stage 3/5), 14 Jun. 2013, *Miettinen 16136 & Seelan* (**holotype** SNP33533, **isotype** H 7200338*).

Etymology: *Armeniacus* (Lat., adj.), apricot-coloured, refers to basidiocarp colour.

Basidiocarps resupinate, apricot-coloured when fresh, drying dull reddish brown, patches up to 7 × 3 cm and 2 mm thick. Consistency hard woody when dry, curving inwards upon drying, detaching from wood. Pores thin-walled, regular, angular, mouths smooth, (10–)11–12(–13) per mm, up to 1.2 mm long. Subiculum cream-colored, in contrast to darker tubes, 0.2–0.6 mm thick. Basal layer in dry state a dark, reddish waxy film, orange when fresh.

Hyphal structure dimitic, clamps absent. Generative hyphae thin- to slightly thick-walled, frequently septate, uniform except in basal layer, 2.0–3.0(–3.6) µm diam. Subiculum dominated by skeletal hyphae, interwoven, winding, yellowish to hyaline, tissue rather loose; basal layer about 20 µm, strongly agglutinated, brown, (2.7–)3.3–4.2(–4.5) µm diam, with a distinct lumen third to sixth of the total cell width. Tramal tissue dense, hyphae interwoven to subparallel, dominated equally by slightly thick-walled generative hyphae and slightly yellowish skeletal hyphae (2.1–)2.5–3.0(–3.5) µm diam, towards tube mouths by generative hyphae. *Cystidia*: Tramal skeletocystidia abundant, often bending into hymenium, (7–)15–30(–47) × (5.3–)6.3–8(–12) µm, L = 23.0 µm, W = 7.2 µm (n = 37). Thin-walled hymenial cystidia rather narrow, clavate, few mamillate, heavily but finely encrusted, 11–40 × 4.7–8.8 µm, W = 6.1 µm (n = 13). Basidia barrel-like, 8–10 × 4.2–5.5 µm. *Basidiospores* broadly ellipsoid, thin-walled, (3.7–)3.8–4.6(–4.8) × 3.3–4.0(–4.2) µm, L = 4.10 µm, W = 3.61 µm, Q = 1.14.

Distribution and ecology: Known from dead wood from a montane rainforest in Sabah, North Borneo.

Notes: The type specimen reminded of a thin *Rigidoporus microporus* specimen when fresh. *Lividopora benetosta* may look similar, for differences see Table 4. The type is well developed but does not contain any old parts. This should be taken into account when interpreting cystidial characters, which are age-dependent in *Lividopora*.

Lividopora benetosta (Berk.) Miettinen, ***comb. nov.*** MycoBank MB 849647. Figs 1, 11–13.
Basionym: *Polyporus benetostus* Berk., *Bot. J. Linn. Soc.* **16**: 52. 1877.
Synonyms: *Poria fulvobadia* Pat., *J. Bot. (Morot)* **11**: 340. 1897.
Poria fumosa Bres. & Pat., *Mycological Writings* **1**(6): 49. 1901.
Poria porphyrophaea Bres., *Hedwigia* **56**: 296. 1915.
Poria hypobrunnea Petch, *Ann. Roy. Bot. Gard*. (Peradeniya) **6**: 137, 1916.
Poria vincta var. *cinerea* (Bres.) Setliff, *Mycologia* **64**: 695. 1972, *pro parte*.

Typus: **French Polynesia**, Tahiti, on bark, 24 Sep. 1875, *Challenger Expedition* (**holotype** of *Polyporus benetostus* K(M) 192246, ex herb. Berkeley, studied). **Vietnam**, Thanh Hóa, 20 Apr. 1892, *Bon 5294* (**lectotype** of *Poria fulvobadia* FH 290623 – selected by Ryvarden (1983), studied). **Samoa**, *Lloyd 5042* (**lectotype** of *Poria fumosa* BPI US0318515 – selected by Stevenson & Cash 1936: 1940, **isotype** FH

Fig. 11. Species of *Lividopora*. **A.** *L. armeniaca* (holotype). **B.** *L. benetosta*, young basidiocarp (*Miettinen 18133*). **C.** *L. benetosta*, old basidiocarp (*Miettinen 13011.3*). **D.** *L. facilis* (holotype). **E.** *L. subvincta* (*Savchenko 171124/1505*). **F.** *L. vincta* (*Vlasák 1704/102*). Scale bars = 1 cm.

290621 studied). **Philippines**, Mindanao. Zamboanga, San Ramon, 12 May 1904, *Copeland 743* (**lectotype** of *Poria porphyrophaea* NY 00742723 – selected by Ryvarden 1988). **Sri Lanka**, Gangaruwa, Dec. 1913, *Petch 3930* (**lectotype** of *Poria hypobrunnea* K(M) 56199 – selected by Setliff (1972b), studied).

Basidiocarps resupinate, annual or more rarely lasting for 2–3 growth seasons, juvenile fruiting bodies nearly white, quickly attaining reddish-greyish colour ranging from nearly orange, purplish or pinkish to brick-colour with a grey overlay, later dark brown or grey; colours fade after drying, patches from a few cm to a couple of dm, 0.5–2(–4) mm thick. Old basidiocarps curving and bone-hard when dry, tough leathery when fresh. Pores regular, rounded, thin-walled, (7–)9–13(–16) per mm, median 8–15 so quite variable between specimens. Subiculum cream coloured when young, brown when old, cottony, topped by a brown, agglutinated basal layer, which is also visible between annual layers, 0.2–0.5 mm. Margin abrupt, very narrow, if any sterile part at all, sometimes a narrow beige or cream-colored band of younger growth in contrast to darker old pores.

Hyphal structure dimitic, clamps absent. Generative hyphae slightly thick-walled, yellowish, (1.5–)2.0–3.4(–4.2) µm diam. Subiculum dominated by interwoven brownish skeletal hyphae, (2.4–)3.0–4.3(–5.4) µm diam with a usually distinct lumen, 1/4 to 1/6 of total width. Tramal tissue dense, interwoven, difficult to study but not agglutinated, lower trama dominated by generative hyphae or equally by skeletal hyphae, (2.0–)3.0–4.0(–4.8) µm diam. *Cystidia:* Skeletocystidia abundant and persistent, embedded in trama, heavily encrusted, encrustation commonly short but wide, (12–)20–45(–155) × (8–)11.5–18(–26), L = 33.6 µm, W = 14.9 µm (n = 134/15), width up to 17 µm when naked; in slides it is typical to see only large ellipsoid crystal clumps and not the root of the cystidia. Hymenial gloeocystidia mamillate, varying in number but often numerous, broad and conspicuous, (10–)14–19.5(–31) × (5–)9–11.2(–16), W = 10.1 µm (n = 44/11). *Basidia* clavate to barrel-shaped, 7.5–17 × 4.6–6.5 µm. *Basidiospores* broad ellipsoid to subglobose, (3.2–)3.4–4.6(–4.9) × (2.9–)3.0–3.9(–4.3) µm, L = 3.94 µm, W = 3.46 µm, Q = 1.10–1.22.

Distribution and ecology: Widely distributed in tropical and subtropical areas in the Old World and Pacific, in the southern hemisphere reaching Australia and New Zealand. In the Neotropics known from the Caribbean. Basidiocarps develop on dead wood of various angiosperms but known also for attacking living trees.

Notes: Hymenophore colour changes drastically with age from light-coloured to brown or grey. Specimens have a pink or purple tinge combined with dull greyness, except in senescent specimens that lose all reddish colour. Microscopically, subglobose spores and wide but short cystidial encrustation are characteristic. Young specimens, where cystidial characters and grey colour are not well developed, might be difficult to tell apart from *L. vincta*.

Lividopora benetosta is a very common species in old world tropics. *Poria vincta* var. *cinerea* of Setliff (1972a, b) is largely based on *L. benetosta*, but also on *L. subvincta* and possibly other species as well. Corner (1987) adopted *Poria hypobrunnea* for this species. Corner's description and the type of this species fit well our concept of *L. benetosta*. However, *Poria hypobrunnea* is just one name in a long list of synonyms of *Lividopora benetosta*, and one of the most recent ones.

The reports on *Acacia* heartwood rot caused by *Rigidoporus hypobrunneus* (Lee & Noraini Sikin 1999) probably refer to *L. benetosta* as defined here. Data by Martin *et al.* (2015) on endophytic fungi shows that *L. benetosta* is rather common on living rubber trees (*Hevea brasiliensis*) in Cameroon, and we speculate that it could be a pest of rubber plantations.

Lividopora facilis Miettinen, ***sp. nov.*** MycoBank MB 849648. Figs 11, 12.

Typus: **Indonesia**, Riau, Indragiri Hulu, Bukit Aluran Babi, -0.83541° : 102.2278° ± 140 m, alt. 150 m, secondary, half-open forest on moist, level ground, fallen branch on the ground (*Anthocephalus*?, 3 cm diam, decay stage 2/5), 29 Jun. 2004, *Miettinen 8742** (**holotype** BO, **isotype** H 7200351).

Etymology: *Facilis* (Lat., adj.), easy, referring to easy identification of this species.

Basidiocarps resupinate, greyish pinkish or faded brick colour, like a dull version of *Steccherinum collabens*, in senescent parts light ochraceous brown, patches of 2–5 × 1–2 cm, 0.4–1 mm thick. Consistency tough, woody when dry. Pores rather regular in size, thin-walled, rounded angular; mouths whitish pruinose due to projecting hyphal ends, 5–6(–7) per mm. Subiculum very thin, white, lighter in colour than pores, ≤ 0.1 mm thick. A thin basal layer with a reddish-brownish colour present.

Hyphal structure dimitic, clamps absent. Generative hyphae uniform, thin- to slightly thick-walled, (1.5–)1.8–2.8(–3.2) µm diam. Subiculum dominated by interwoven, faintly yellowish to hyaline skeletal hyphae, (2.5–)2.6–3.3(–5.0) µm diam, their lumen visible and 1/6–1/3 of total width, tissue rather loose. A very tightly packed basal layer of 20–40 µm composed of slightly thick-walled generative hyphae is found next to the substrate. Tramal hyphae interwoven to subparallel, skeletal hyphae (2.4–)2.8–3.3(–3.9) µm diam, tissue rather dense but not agglutinated. Dominance of skeletal hyphae fades towards tube mouths, which are nearly monomitic. *Cystidia:* Encrusted hyphal ends in trama, occasionally bending into hymenium, when young slightly thick-walled generative hyphal ends that later develop into larger thick-walled skeletocystidia, (7–)12.5–27.6(–55) × (6–)8.7–10.8(–14) µm, L = 20.8 µm, W = 9.7 µm (n = 24), up to at least 10 µm wide without encrustation. The second type of cystidia ("gloeocystidia") often mamillate, 9.4–20 × 5–8, µm W = 6.3 µm (n = 18), projecting up to 10 µm beyond hymenium. *Basidia* clavate to cylindrical, 8.5–14 × 4.3–5.5 µm. *Basidiospores* thin-walled, ellipsoid, 3.2–4.0 × 2.5–3.0 µm, L = 3.5 µm, W = 2.69 µm, Q = 1.3.

Distribution and ecology: Known from dead dicot wood from a secondary lowland rainforest in Sumatra.

Notes: Larger pores and clearly narrower spores separate *L. facilis* from other *Lividopora* species.

Lividopora subvincta (Ryvarden) Miettinen, ***comb. nov.*** MycoBank MB 849649. Figs 11–13.
Basionym: *Rigidoporus subvinctus* Ryvarden, *Syn. Fungorum* **40**: 105. 2020.
Synonym: *Poria vincta* var. *cinerea* (Bres.) Setliff, *Mycologia* **64**: 695. 1972. *pro parte*.

Typus: **Zimbabwe**, Manicaland, Vumba, Leopard rock, angiosperm, 14 Mar. 1995, *Ryvarden 37098** (**holotype** of *Rigidoporus subvinctus* O-F-76331, studied).

Basidiocarps resupinate, annual to biennial, dark grey, patches of a few cm to dm, 0.5–2 mm thick. Consistency hard when dry, curving inwards upon drying. Pores regular, round, (7–)9–12(–14) per mm. Subiculum brown, in younger parts cream coloured, basal layer a thin, waxy black line, visible between annual layers, 0.2 mm. Margin abrupt or an up to 1 mm wide light-coloured sterile zone.

Hyphal structure dimitic, clamps absent. Generative hyphae slightly thick-walled, (1.9–)2.2–2.8(–3.4) µm diam. Subiculum dominated by interwoven, brown skeletal hyphae, basal layer with partly parenchymatic tissue, apparently consisting of both skeletal and generative hyphae, skeletal hyphae (3.4–)3.7–4.8(–5.6) µm diam, with a distinct lumen 1/3–1/6 of total width. In trama skeletal hyphae similar to subicular hyphae, interwoven,

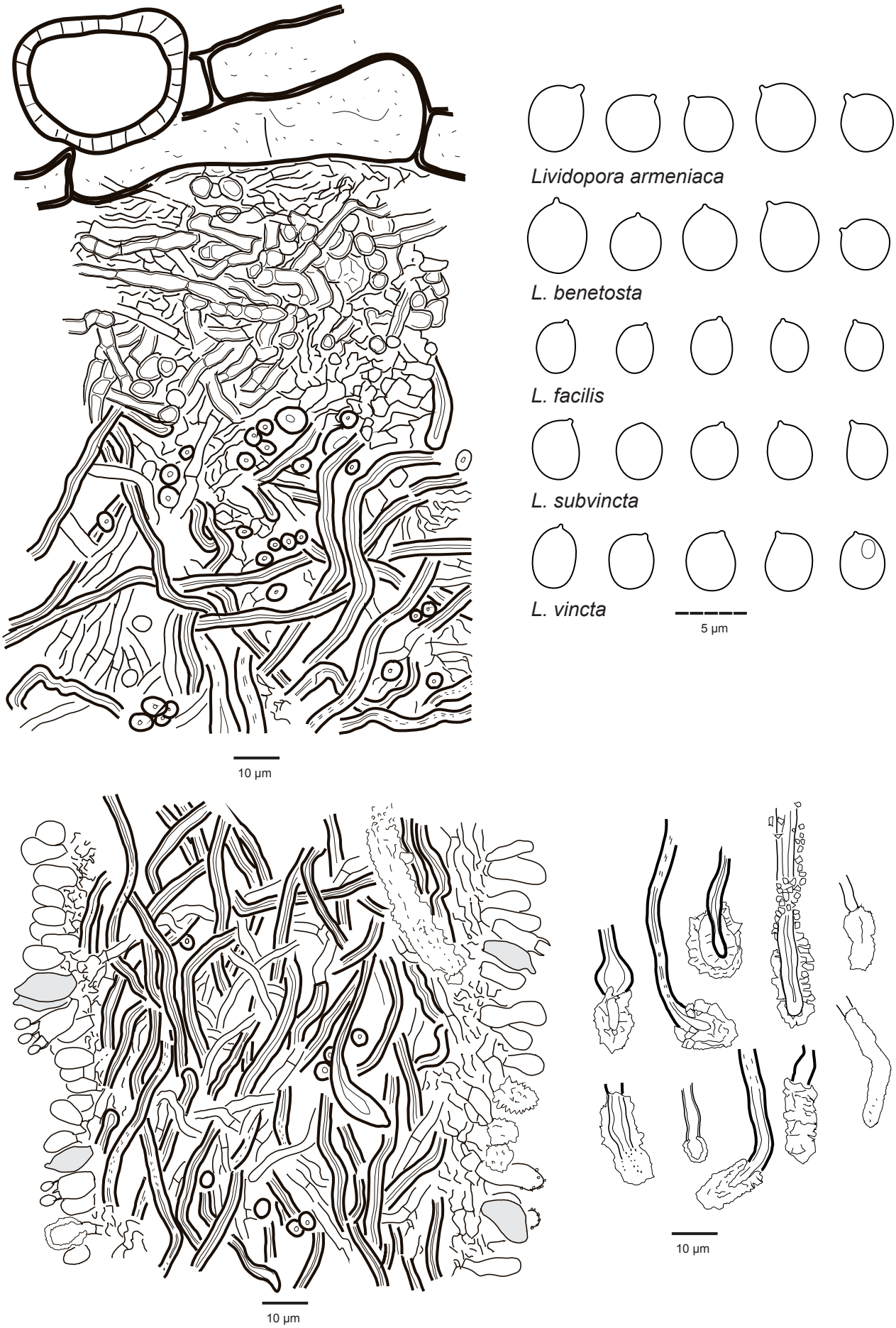

Fig. 12. *Lividopora facilis* basidiome hyphal structures (subiculum, trama, and encrusted cystidia) and spores of the five *Lividopora* species treated here.

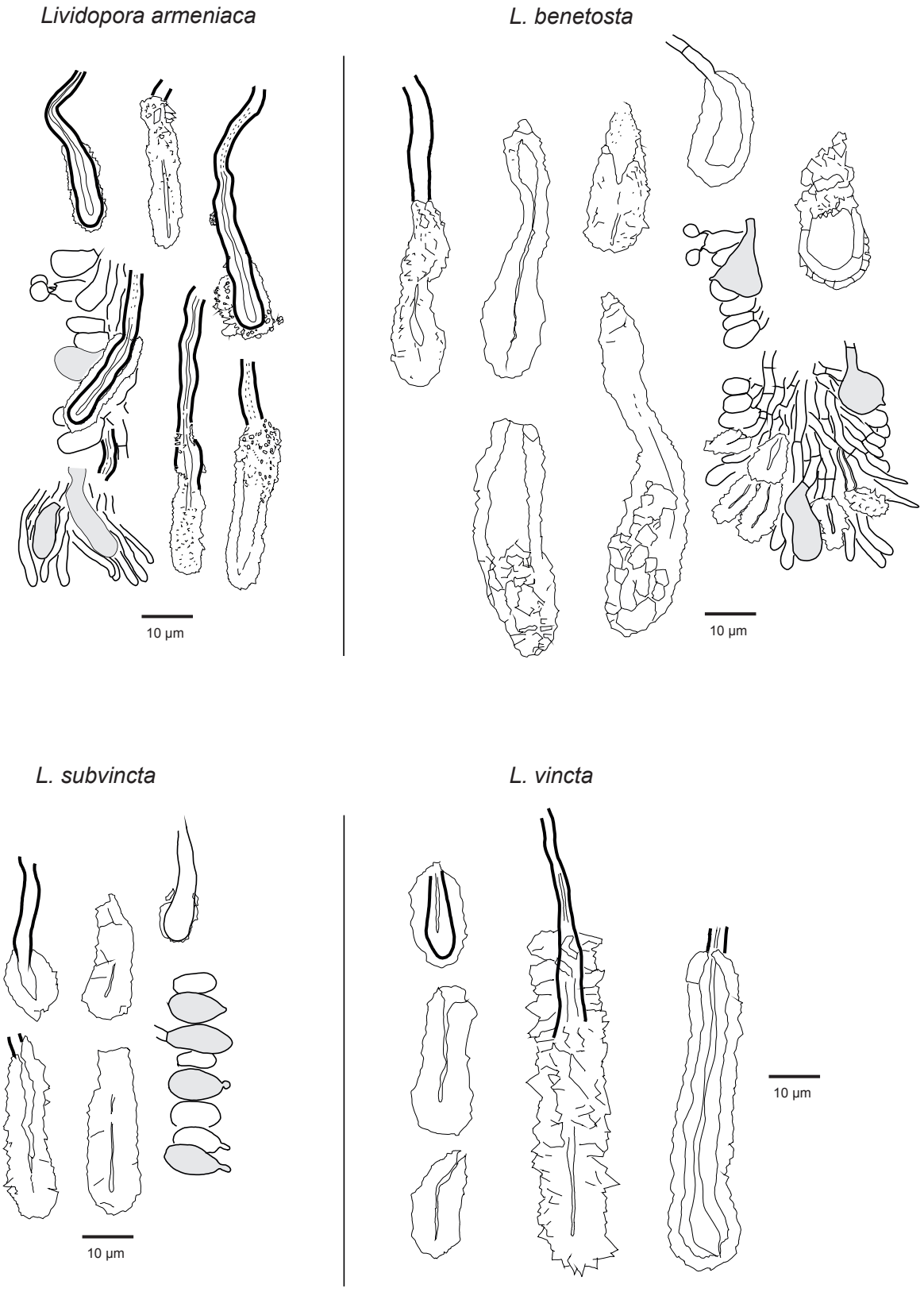

Fig. 13. Cystidia of *Lividopora* spp.

dominant in upper trama, (2.4–)3.2–4.2(–5.0) µm diam; generative hyphae dominate close to tube mouths. *Cystidia:* Skeletocystidia abundant, encrusted heavily, ranging from mid-sized to broad, usually encrustation long, (9.5–)23–42(–58) × (6.8–)9.4–12(–17) µm, L = 31.6 µm, W = 11.0 µm, (n = 75/3), up to at least 9.5 µm in width without encrustation. Stained thin-walled hymenial cystidia variable in numbers, may be locally abundant close to tube mouths, round, partly mamillate, (13–)14–18.3(–40) × (5.5–)6.8–8.2(–8.8) µm, W = 7.4 µm (n = 27/3). Basidia clavate to barrel-shaped, 8.8–10 × 5.4–6 µm. *Basidiospores* broad ellipsoid to subglobose, with distinct walls and no guttulae, (3.4–)3.6–4.6(–5.2) × (2.6–)2.9–3.4(–3.5) µm, L = 4.02 µm, W = 3.13 µm, Q = 1.22–1.30.

Distribution and ecology: Known from Kenya, Tanzania, and Zimbabwe from *Cupressus* and dicot wood; tree pathogen causing root rot.

Notes: This species is dark already when young unlike the other African species of *Lividopora*, *L. benetosta*. Basidiocarps are darker than in *L. benetosta* also when older. According to Ryvarden (2020a), this species is different from "*Rigidoporus vinctus*" by having two types of cystidia, while the latter has only one type. This is incorrect, as we have shown here that all *Lividopora*, including *L. vincta*, have two types of cystidia. His concept of *R. vinctus* may be mixed (including some *Meripilaceae*), but he quite correctly likened the two species when describing *L. subvincta*. Microscopic differences include slightly narrower spores in *L. subvincta* (Q > 1.2) and shortly but widely encrusted skeletocystidia in *L. benetosta* as opposed to long encrustation in *L. subvincta*.

Setliff & Mesner (1971) report this species as *Poria vincta* var. *cinerea* as a tree plantation pest from Mt. Meru, Tanzania. We sequenced a Tanzanian strain of Setliff (ECS-194-R) very likely associated with this study. Later their concept of the aforementioned variety included also *L. benetosta*, as can be deduced from their list of studied specimens (Setliff 1972b).

Lividopora vincta (Berk.) Miettinen, ***comb. nov.*** MycoBank MB 849650. Figs 11–13.
Basionym: *Polyporus vinctus* Berk., *Ann. Mag. Nat. Hist*. **9**: 196. 1852.
Synonym: *Polyporus carneopallens* Berk., *Hooker's J. Bot. Kew Gard. Misc*. **8**: 235, 1856.

Typus: **Dominican Republic**, Santo Domingo, unknown collection date, *Sallé 34* (**holotype** of *Polyporus vinctus* K(M) 167866, studied). **Brazil**, Amazon, Rio Uaupés, Ipanoré ("Panuré"), on dead trees, Feb. 1853, *Spruce 178* (**lectotype** of *Polyporus carneopallens* designated here K(M) 192248, MBT 10014556, studied; **isolectotype** FH 00290615, studied).

Basidiocarps resupinate, orange reddish or pinkish when fresh, drying duller reddish ochraceous, 1–2.5 mm thick. Consistency hard when dry. Pores regular, rounded, (7–)8–10(–12). Subiculum ochraceous, 0.2–1 mm thick, basal waxy, red to black layer present, 20–100 µm thick. Margin cream coloured.

Hyphal structure dimitic, clamps absent. Generative hyphae slightly thick-walled, CB(+), (1.7–)2.2–3.0(–3.8) µm diam. Subiculum dominated by interwoven, yellowish skeletal hyphae, loose to rather tight, (2.3–)3.1–4.6(–5.4) µm diam, with a distinct lumen of 1/3–1/6 total width. Basal layer monomitic, composed of agglutinated, thick-walled generative hyphae, (3.2–)3.7–4.7(–5.0) µm diam. Tramal skeletal hyphae interwoven, (2.0–)3.7–4.6(–5.9) µm diam, dominate in upper trama, less so towards tube mouths where hyphae are subparallel, tissue dense but not agglutinated. *Cystidia:* Skeletocystidia clavate, large and heavily encrusted, (17–)31–60(–105) × (7–)9.8–20(–23) µm, L = 46.1 µm, W = 14.8 µm (n = 94/5), up to 12.5 µm in width when naked. Thin-walled hymenial cystidia clavate to mamillate, (10–)14–40(–46) × (4.6–)7.0–9.5(–12.4) µm, W = 8.2 µm (n = 34/5). *Basidia* not seen, basidioles 7.5–10.5 × 4.5–5.3. *Basidiospores* broad ellipsoid, with thin to distinct walls, (3.2–)3.3–4.2(–4.5) × (2.8–)2.9–3.4(–3.5) µm, L = 3.80 µm, W = 3.13 µm, Q = 1.20–1.23.

Distribution and ecology: Found in tropical and warm temperate Americas. Endophyte DNA data of Martin et al. (2015) show that *L. vincta* appears to be common on living *Hevea brasiliensis* in natural forests in Brazil and Peru.

Notes: The name *Rigidoporus vinctus* has been interpreted confusingly in the literature and herbaria, and we know from our own experience that it covers many species. Part of the material under this name belongs to *Meripilaceae*, and part of it to *Lividopora*.

The distributions of *L. benetosta* and *L. vincta* overlap at least in the Caribbean. *Lividopora vincta* is lighter in colour than *L. benetosta*, its spores are narrower and its cystidia are long, not short and wide as often seen in *L. benetosta* (Table 4).

There is some ITS variation in *L. vincta* (Fig. 10), and it would be interesting to see a more in-depth study of this species with more specimens and several markers. It may yet turn out to be a species complex, but ITS variation is small and gradual enough to be the result of geographic spread of sequenced specimens or quality issues.

Pseudolagarobasidium J.C. Jang & T. Chen, *Trans. Brit. Mycol. Soc.* **85**: 374. 1985.

Type species: *Pseudolagarobasidium subvinosum* (Berk. & Broome) Sheng H. Wu

Notes: Hallenberg *et al.* (2008) showed that *Pseudolagarobasidium*, a genus of hydnoid wood-inhabiting resupinate fungi, is related to *Cerrena*. Nakasone & Lindner (2012) gave a taxonomic treatment of the genus recently, and good illustrations of *Pseudolagarobasidium* species can be found in Maekawa & Hasebe (2002) and Wood & Ginns (2006). Nakasone & Ortiz-Santana (2022) expanded the genus so that in their view it includes 11 species. We have shown here that *Acanthodontia cirrhatina* does not belong to *Pseudolagarobasidium*, as they suggested, and we exclude *Hyphoradulum conspicuum* from the genus.

The genus would require a revision with properly sequenced material to ascertain the real species number. In particular, the paleotropical *Pseudolagarobasidium* species should be revised, and historical names should be checked against newly described species. It would appear there are several closely related species parasitic on *Fabaceae*. Currently, the six species listed below have been sequenced and described reliably enough that we conclude that they belong to the genus. They are listed below. For two of them, only LSU data is available, making integrative species-level comparison within the genus problematic at present. We consider the remaining names as insufficiently known taxa.

Our ITS-based tree of all publicly available sequences (Fig. 14) represents nominally four species (*P. acaciicola*, *P. baiyunshanensis*, *P. belizense*, and *P. pallens*). We find it difficult to interpret these results. Species number may vary between three and seven. We suggest future papers utilize another marker beside ITS to delimit species.

Thin-walled hymenial cystidia just like those shared by other genera of the *Cerrena* clade are found in the genus. *Pseudolagarobasidium* species are also dimitic and their blunt, raduloid ("subporoid") hymenophore reminds of old, irpicoid *Cerrena* a lot. However, hyphal structure in *Pseudolagarobasidium* is mostly monomitic and skeletal hyphae are found only in the basal part of the basidiocarp. These skeletal hyphae are furthermore peculiar "microbinding hyphae", *i.e*. narrow and regularly branching, quite unlike the regular, rarely branching skeletal hyphae in *Cerrena*.

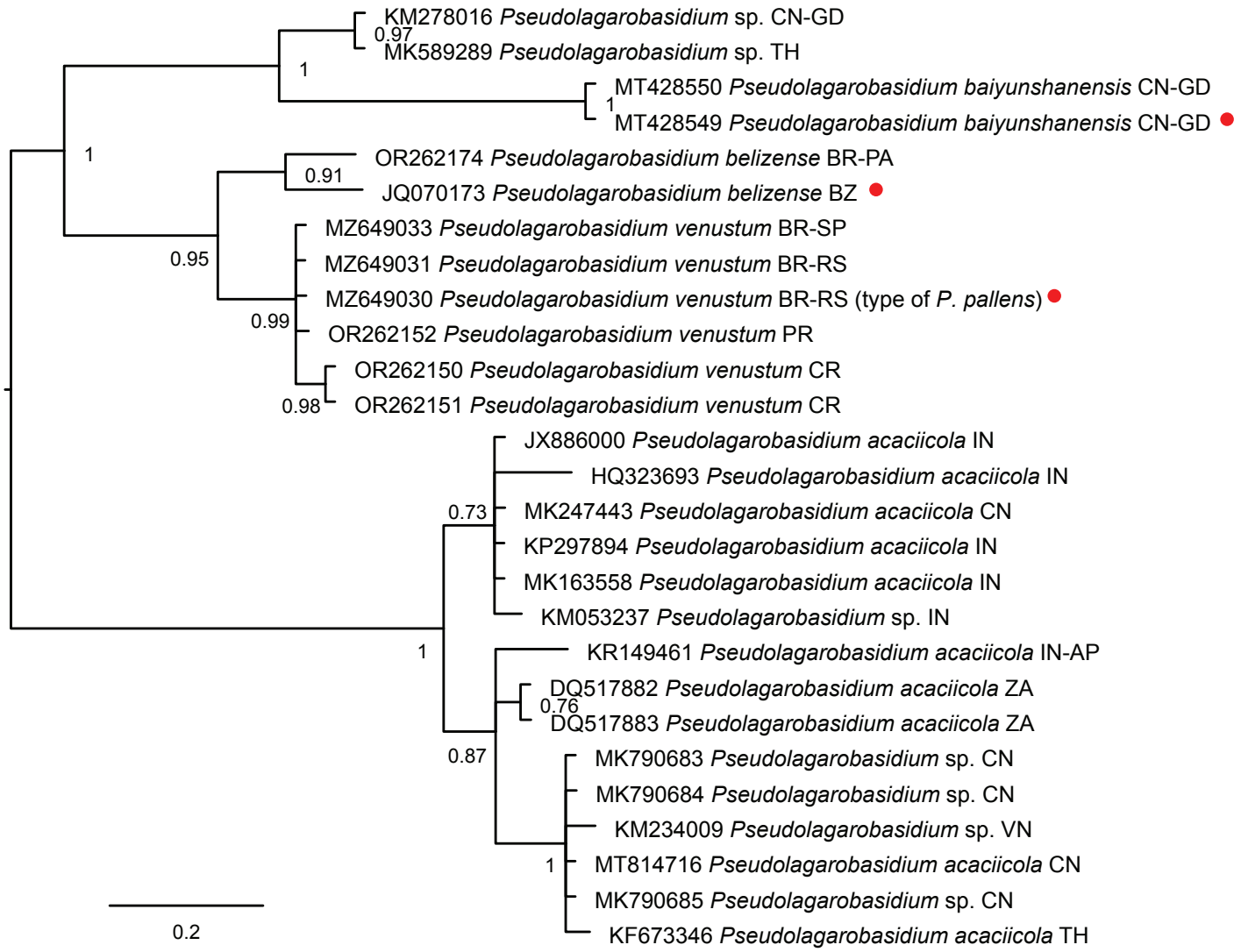

Fig. 14. Bayesian consensus phylogram of *Pseudolagarobasidium* spp. based on ITS sequences. Red circles denote type specimens. Countries (and states) of origin are denoted with ISO 3166 codes.

Accepted species with DNA sequences available

Pseudolagarobasidium acaciicola Ginns, *Canad. J. Bot*. **84**: 752. 2006.

Note: Even though Wood & Ginns (2006) do not mention sequence accession numbers, they published ITS sequences of two paratypes (GenBank DQ517882, DQ517883), complemented with a LSU (GenBank EU569321) by Hallenberg *et al*. (2008).

Pseudolagarobasidium baiyunshanense M.L. Han, L.S. Bian & Q. An, *Phytotaxa* **483**: 171. 2021.

Pseudolagarobasidium belizense Nakasone & D.L. Lindner, *Fungal Diversity* **55**: 158. 2012.

Pseudolagarobasidium subvinosum (Berk. & Broome) Sheng H. Wu, *Acta Bot. Fenn*. **142**: 113. 1990. Fig. 2.
Basionym: *Hydnum subvinosum* Berk. & Broome, *J. Linn. Soc., Bot*. **14**(73): 60. 1873 [1875].
Synonym: *Pseudolagarobasidium leguminicola* J.C. Jang & T. Chen, *Trans. Brit. Mycol. Soc.* **85**: 374. 1985.

Typus: **Sri Lanka**, Peradeniya, Nov. 1867, no. 180 (**holotype** of *Hydnum subvinosum* K). **Taiwan**, Hua-Ling, Fung-Ping, *Leucaena leucocephala*, Feb. 1983, *Jang & Chen* (**holotype** of *Pseudolagarobasidium leguminicola* TAI 9020).

Notes: This species is distinctive enough that we trust the conclusion of Nakasone & Lindner (2012) that the generic type *P. leguminicola* and *P. subvinosum* belong to the same species, or at least are closely related. An LSU sequence (GenBank EU569319) was published by Hallenberg et al. (2008).

Pseudolagarobasidium pronum (Berk. & Broome) Nakasone & D.L. Lindner, *Fungal Diversity* **55**: 162. 2012.

Notes: Hallenberg *et al*. (2008) provide an LSU sequence (GenBank EU569320) based on a Taiwanese specimen of Wu identified as *P. calcareum*, a species described from the southern part of Australia. This LSU sequence clearly belongs to *Pseudolagarobasidium*. We have studied Wu's Taiwanese collection of *P. calcareum*, the same one studied by Nakasone & Lindner (2012), and it is very similar to *P. belizense* and thus a true *Pseudolagarobasidium*. Nakasone & Lindner (2012) concluded that this species is a synonym of *P. pronum*, which was described

from Sri Lanka. Now that species diversity in the genus has increased, also the identity of *P. calcareum* against *P. pronum* should be re-assessed. We have not studied the types involved. If they belong to separate species of *Pseudolagarobasidium*, an affinity of Taiwanese material to Sri Lankan *P. pronum* appears more likely than to the South Australian *P. calcareum*.

Pseudolagarobasidium venustum (Hjortstam & Ryvarden) Nakasone & D.L. Lindner, *Fungal Diversity* **55**: 165. 2012.
Basionym: *Radulodon venustus* Hjortstam & Ryvarden, *Mycotaxon* **74**: 250, 2000.
Synonym: *Pseudolagarobasidium pallens* Motato-Vazq. & Westphalen, *Phytotaxa* **555**: 163. 2022.

Typus: **Brazil**, São Paulo, Reg. Santos, Cananeia, Ilha do Cardoso, on bark of palm, 2 Feb. 1987, *Hjortstam 16838* (**holotype** of of *Radulodon venustus* K(M) 77909, studied).

Notes: Our sequenced material from Costa Rica and Puerto Rico agrees well with the type. The sequences are near identical with the Brazilian material that Westphalen & Motato-Vásquez (2022) described as *P. pallens*. They cited as main differences yellow to orange colour and smaller spores of *P. venustum*, though apparently without studying the type of *P. venustum*. The protologue of *P. venustum* states that the colour is at first whitish and later straw-coloured. Their statement about colour probably refers to Nakasone & Lindner (2012), who studied the type but also included other specimens in their description, none of which was sequenced, and whose identity we cannot confirm. Spores are of equal width and a bit longer in *P. pallens* than reported for the type of *P. venustum*. Spore length can vary, and we think it is highly likely *P. pallens* is conspecific with *P. venustum*. Both were described from the same area in southern Brazil.

Radulodon Ryvarden, *Canad. J. Bot.* **50**: 2073. 1972.

Genus type: *Radulodon americanus* Ryvarden

Notes: Nakasone & Lindner (2012) showed that most species of *Radulodon sensu lato* belong to *Pseudolagarobasidium* instead. As currently recognized, the genus contains 3–4 boreal to temperate species, depending on whether *R. americanus* is recognized as a separate species. The differences in ITS sequences within the genus are small (Fig. 15).

Phylogenetically, *Radulodon* is a sister genus to *Irpiciporus* (Fig. 3). We have retained the genus here, though alternatively it would be possible to include it in *Irpiciporus*. Our reasons relate to the overall generic arrangement of the *Cerrenaceae* – even though sister taxa, the two are genera are genetically distant (see Results). We suspect our dataset is lacking a lot of species diversity around *Radulodon*, and hence minimal nomenclatural change is justified until wider genetic and morphological datasets may indicate otherwise.

As defined here, *Radulodon* is characterized by rather thin, hydnoid basidiocarps as opposed to larger, effused-reflexed found in *Acanthodontia* and *Irpiciporus*. Microscopically, cystidia and dense, interwoven subhymenial structure are characteristic. Cystidia are found in *Acanthodontia* also, but its hyphal structure is consistently looser and more regular as in *Irpiciporus*, which lacks cystidia. The differences are small, however.

Radulodon casearius (Morgan) Ryvarden, *Canad. J. Bot*. **50**: 2075. 1972.
Basionym: *Hydnum casearium* Morgan, *J. Cincinnati Soc. Nat. Hist*. **10**: 11, 1887.

Typus: **USA**, Ohio, Cincinnati, *Carya*, unknown collection date, *A. P. Morgan* (**holotype** BPI US0324642, C. G. Lloyd herb. 16737 – selected by Stevenson & Cash 1936: 74).

Notes: See Nakasone (2001) for a description. Smaller spores separate it from the other species of the genus. This species is known from south temperate United States so far.

Radulodon erikssonii Ryvarden, *Canad. J. Bot*. **50**: 2075. 1972. Fig. 2.

Typus: **Norway**, Oslo, Sørkedalen, *Populus tremula*, 24 Oct. 1968, *Ryvarden* (**lectotype** O – selected by Nakasone (2001), studied; **isotypes** in DAOM, L).

Notes: See Eriksson *et al.* (1981) for a description. ITS sequences of *Radulodon americanus* and *R. erikssonii* are nearly identical (2 bp difference in our set of seven sequences). Morphologically, material from North America and Eurasia are indistinguishable; the characters outlined by Ryvarden (1972a) do not separate these species (presence of cystidia, basidiocarp thickness). North temperate to boreal distribution with a continental preference and *Populus tremula/tremuloides* as a host also join the two. Hence, we consider it likely that *R. americanus* and *R. erikssonii* are synonyms, but we would like to see this confirmed with more extensive sampling and several genetic markers. The two species were described in the same paper, but *R. erikssonii* has been used more widely than *R. americanus*, and it is included in red lists of several European countries. We recommend therefore maintaining *R. erikssonii* over *R. americanus*, if the two are synonymized.

Radulodon yunnanensis Y.C. Dai & Chao G. Wang, *Mycol. Progr*. **21**(73): 11. 2022.

Typus: **China**, Yunnan, Pingbian, Daweishan Forest Park, *Castanea*, 5 Jun. 2011, *Dai 12204* (**holotype** BJFC 010487).

Notes: Wang & Dai (2022) described this species from the mountains of Yunnan, China, *i.e*. eastern Himalayas. It is genetically distinct, but the morphological characters (fimbriate margin, spine density) that the authors list do not separate it from *R. erikssonii*. Notably, the authors cite one collection from *Pinus*, while the rest are from angiosperms. This is the only collection of conifer-dwelling *Radulodon* known to us.

Somion Adans., *Familles des plantes* **2**: 5. 1763.

Genus type: *Hydnum occarium* Batsch, chosen by Donk (1974: 175).

Etymology: σώμα (Gr., noun) derives from body, torso, flesh, evidently referring to fleshy basidiocarps.

Basidiocarps annual or biennial, sessile to effused-reflexed, light-colored, watery in fresh condition, rather tough after drying. *Context* duplex, with softer upper and more compact lower

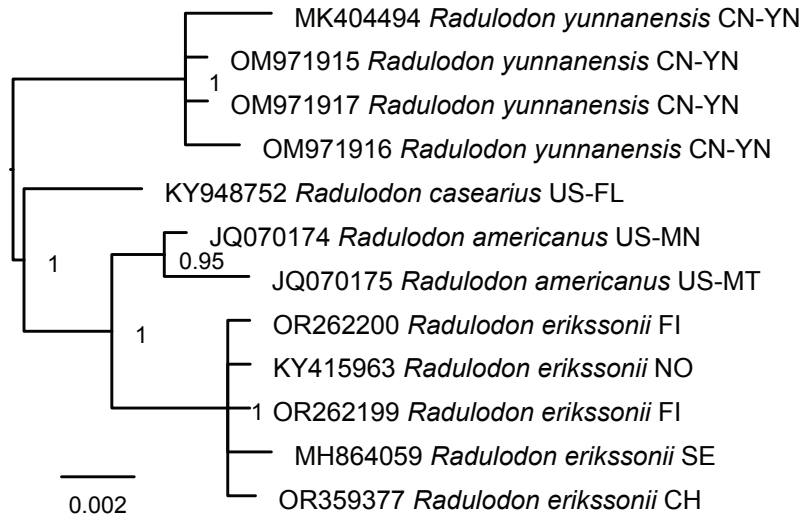

Fig. 15. Bayesian consensus tree of *Radulodon* spp. based on ITS sequences. Countries (and states) of origin are denoted with ISO 3166 codes.

layers. *Pores* angular to sinuous, 1–4 per mm. *Hyphal structure* monomitic, hyphae clamped and slightly cyanophilous, distinctly thick-walled in both context and trama. *Basidia* short-clavate, 13–25 × 5–8 µm, four-spored, with guttulate contents, quickly collapsing. *Basidiospores* ellipsoid or ovoid to subglobose, thick-walled (spore wall up to 1 µm thick), with a large central oil-drop, cyanophilous. Causes a white rot of living and dead deciduous trees.

Notes: *Somion* is a sister clade to the rest of the *Cerrenaceae* (Fig. 3). Being so distinct phylogenetically if not morphologically, this clade clearly requires its own genus, whose nomenclature is discussed below. Phylogenetically, the genus is divided in two groups: *S. delectans* and *S. occarium* form a clade distinct from the rest. ITS sequences alone are not sufficient to separate all species in the genus, in particular *S. formosanum*, *S. litschaueri,* and *S. strenuum* (Fig. 16). However, *TEF1* and the joint *TEF1*-ITS dataset show clear support for dividing this complex into seven species overall (Fig. 17). For identification of species within the genus, see Table 5.

Dismantling traditional, morphology-based genera requires not only a re-consideration of their younger synonyms (*e.g. Irpiciporus* in the case of *Spongipellis sensu lato*) but also a careful revision of suppressed older names. Recent DNA-based revisions of the corticioid genera *Hyphodontia* and *Tomentella*, both conserved *versus* their older synonyms, made it necessary to restore some suppressed generic names (*e.g.*, *Kneiffiella*, *Odontia*, and *Xylodon*). This restoration is allowed if the type species of the conserved and the suppressed genus cannot be anymore considered congeneric (ICN Shenzhen code art. 14.6). In the case of *Spongipellis*, the older name which requires further examination is *Somion* Adans. against which *Spongipellis* has been conserved (ICN Appendix III). We show below that the type species of *Somion* cannot belong to *Spongipellis sensu stricto* (*Meripilaceae*), and thus the name is available for use and must be considered when *Spongipellis sensu lato* is being divided into several genera.

The genus *Somion* was described by Adanson (1763: 5) based on three illustrations published by Micheli (1729: Tabula 64, figs 3–5). No binomial species names were addressed to the genus in the protologue; nevertheless, *Somion* meets the requirements for a validly published generic name (see Donk 1960: 283). The name may have gone unnoticed because Ryvarden's index to generic names does not contain it (Ryvarden 1991). The three aforementioned Micheli's figures were the basis for the subsequent introduction of four species names: *Hydnum occarium* Batsch (fig. 3 – Batsch (1783: 113), sanctioned by (Fries 1821: 412), *H. orbiculatum* Pers. (fig. 5 – Persoon 1801: 559), sanctioned by Fries (1821: 412) and *H. pectinatum* Fr. (fig. 4 – Fries 1821: 412). Batch's *H. pectiniforme* is based on figs 4 and 5, but Fries considers it as a synonym of *H. orbiculatum*, so the latter as a conserved name has priority over the former and *H. pectiniforme* is obsolete.

Donk (1974: 175) selected *H. occarium* as a lectotype of *Somion* (at that time a devalidated generic name) and treated it as a synonym of *Spongipellis* – he had suggested earlier that *H. occarium* might be a synonym of *Spongipellis pachyodon* (Donk 1960: 176). Changing the starting point for validly published fungal genera from 1821 to 1753 (ICBN Sydney code 1981) made *Somion* available for use although under the aforementioned condition only. The identity of *H. occarium* decides whether *Somion* is going to be kept as a suppressed synonym of *Spongipellis* or whether it should be put in use as an independent genus.

The protologue by Batsch (1783) and the subsequent redescription of *H. occarium* by Fries (1821) introduced it as a white, large fungus with hairy upper surface and flat, thick and blunt "aculei"; additionally, Fries describes the consistence of *H. occarium* as "probably fleshy" ('substantia … forsan carnosa'), and size being 3 inches wide and projecting 1–1.5 inches. The generic name *Somion* refers to a fleshy fungus, which may be the origin of Fries's statement. The measurements probably derive from Persoon (1801). Micheli's drawing, which may serve as a lectotype of the species (ICN art. 9.3, 9.4), shows three pileate, mid-sized caps with something like irpicoid or blunt hydnoid hymenophore viewed from the side.

There are not many non-stipitate pileate, light-coloured hydnoid-irpicoid fungi in Europe. *Climacodon septentrionalis*, *Donkia pulcherrima*, and *Hericium cirrhatum* have sharp, rather small teeth in contrast to descriptions of Batsch (1783) and Fries (1821). Old caps of *Cerrena unicolor* may be irpicoid but then also grey, not light-coloured, and caps are rather thin. *Irpex lacteus*, *Irpicodon pendulus*, and *Steccherinum oreophilum* fruiting bodies are much too small to fit the description. *Trametopsis cervina* has daedaleoid pores that may turn irpicoid, but its caps

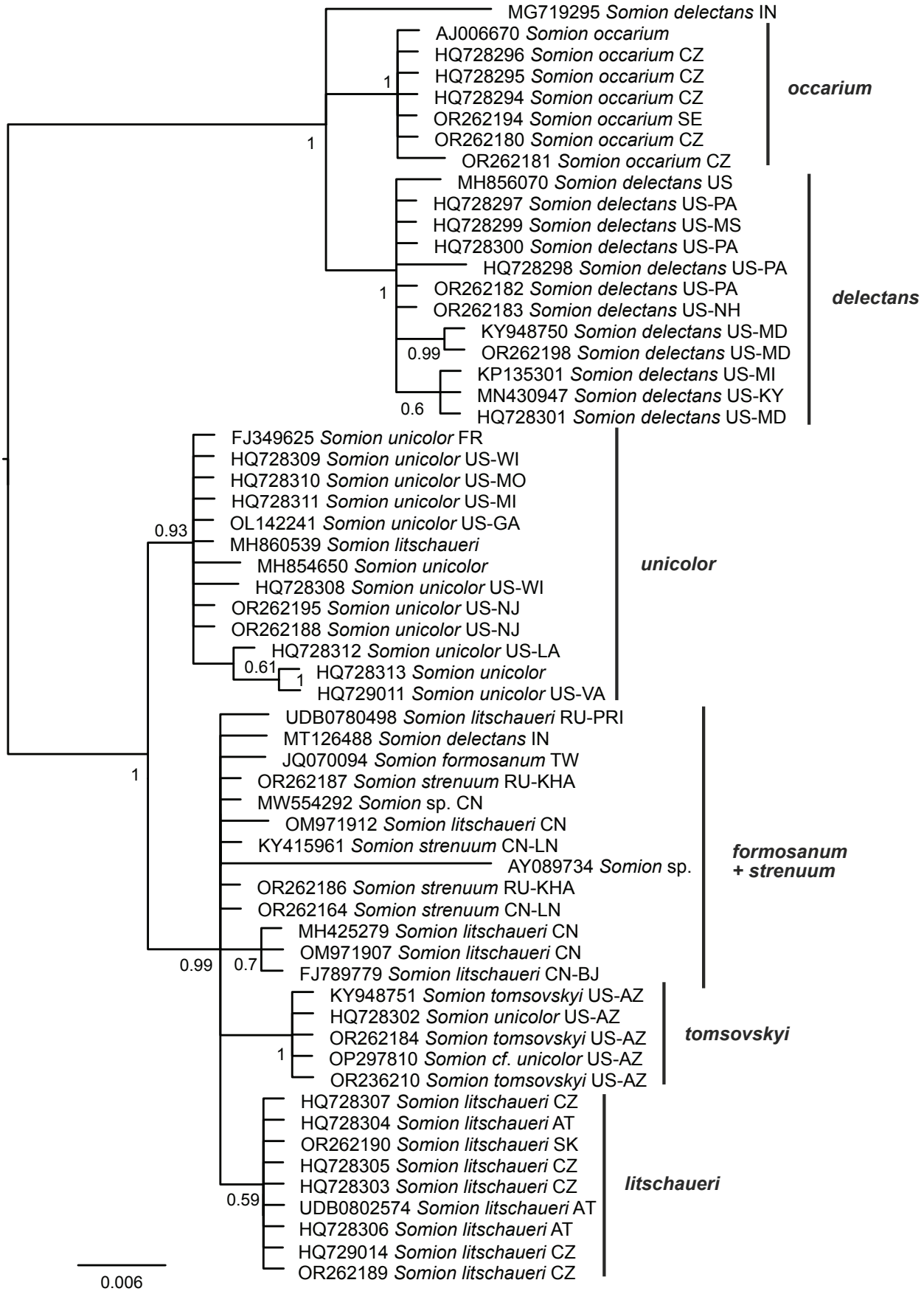

Fig. 16. Bayesian consensus phylogram of *Somion* spp. based on ITS sequences. Countries (and states) of origin are denoted with ISO 3166 codes.

are usually quite thin, projecting less than described, and not fleshy, so this species is not the most likely candidate either.

Turning to *Spongipellis*, the hymenophore construction precludes the two European species of *Spongipellis sensu stricto*, *S. profissilis* and *S. spumea* (Spirin *et al*. 2022). They both possess normal poroid hymenophore, which cannot be interpreted as having tooth-like appearance, and thus synonymy of *Somion* and *Spongipellis* is excluded. The illustration and description

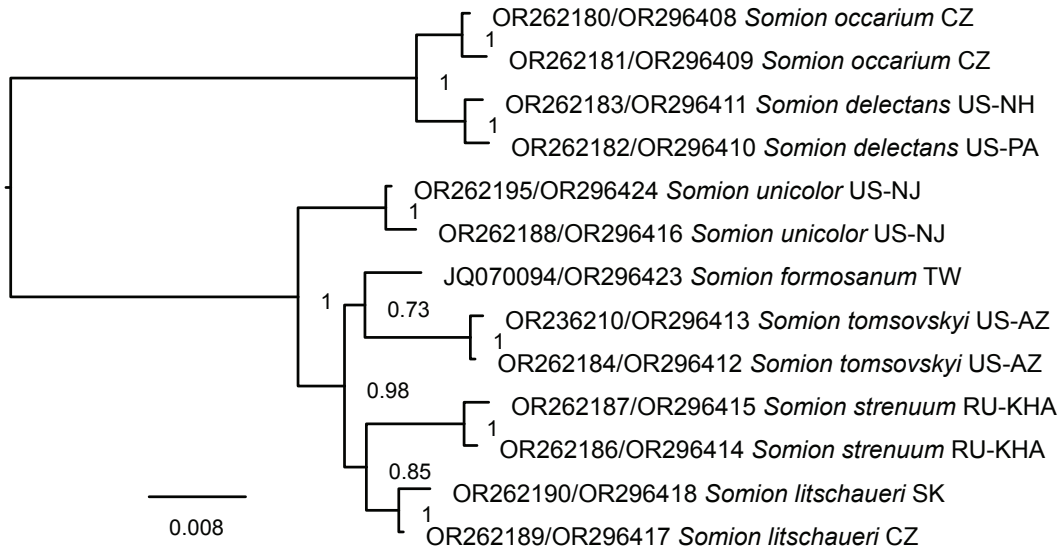

Fig. 17. Bayesian consensus phylogram of *Somion* spp. based on ITS and *TEF1* sequences. Countries (and states) of origin are denoted with ISO 3166 codes.

of the hymenophore would fit well to *Spongipellis* (*Irpiciporus*) *pachyodon*. However, all the specimens we have seen have smooth (or near so) pileal surface, and this seems to be the case in the literature as well: Bernicchia (2005) describes the upper surface as tomentose to smooth, and Rivoire (2020) as cottony to felt-like. The relatively small size of caps in *S. pachyodon* does not fit the descriptions of *H. occarium* either.

The European taxon so far called *S. delectans* but proven to represent a good species in this study, is yet another option. It has nearly white, substantial basidiocarps with often strigose pileal surface (Fig. 1E) and large, irregular pores that may become dentate (described as irpicoid by Bernicchia 2005 and Rivoire 2020). Micheli, Batsch, and Fries (who apparently never saw specimens) might have described such a hymenophore as consisting of blunt teeth. We find the European *S. delectans* as the most credible option for typifying *H. occarium* in that it does not contradict any element of the protologue and agrees well in many. Consequently, we designate here an epitype to supplement the lectotype illustration among the European material of *S. delectans.*

As a result, *Somion* becomes the oldest name available for the *S. delectans* complex, which requires its own genus. The correct species name of European *S. delectans* is then *Somion occarium* (Batsch) Spirin & Miettinen.

Somion delectans (Peck) Vlasák & Spirin, ***comb. nov.*** MycoBank MB 849651. Fig. 18.
Basionym: *Polyporus delectans* Peck, *Bull. Torrey Bot. Club* **11**: 26. 1884.

Typus: **USA**, Ohio, Cincinnati, fallen log, unknown collection date, *Morgan 106* (**holotype** NYS, **isotype** BPI US 0207202, studied).

Basidiocarps annual, sessile or effused-reflexed, up to 15 cm in widest dimension. Upper surface finely pubescent, later almost smooth, azonate, cream coloured to pale ochraceous. Edge of pileus sharp to rather blunt, sterile, concolourous with pileal surface. Hymenial surface even to more-or-less concave or rarely convex, cream coloured to pale ochraceous; pores angular to somewhat elongated, 2–3 per mm, dissepiments rather thin, first even, later serrate. Section: context white to cream coloured or pale ochraceous (old herbarium specimens only), watery in fresh condition, firm, indistinctly fibrillose and azonate when dry, up to 1 cm thick; tube layer soft, concolourous with pore surface, up to 1 cm thick.

Hyphal structure monomitic; all hyphae with clamp connections. Context hyphae very thick-walled, arranged in subparallel bundles, a few thin-walled, (4.1–)4.7–6.2(–7.7) µm diam. Tramal hyphae thick-walled (lumen capillary to indistinct), subparallel, (3.2–)3.8–4.7(–5.2) µm diam. Subhymenial hyphae more or less thin-walled, 2.7–4.0 µm diam. *Basidiospores* thick-walled, broadly ellipsoid to subglobose, (5.8–)6.0–7.3(–7.6) × (5.0–)5.1–6.6(–6.8) µm, L = 6.6 µm, W = 5.64 µm, Q = 1.16–1.19.

Distribution and ecology: Found in temperate forests in the eastern part of North America, uncommon. Occurs on still standing trees and fallen logs of various angiosperms.

Notes: Morphologically, *S. delectans* is the most similar to the European *S. occarium*. Both species share sessile or effused-reflexed, rather thin and pale coloured (compared with other *Somion* species) basidiocarps. However, pores of *S. delectans* are not as irregular in size and shape as in *S. occarium*, and on average smaller, 2–3 per mm. Moreover, basidiospores of the first species are slightly wider than in *S. occarium* although these differences are merely statistical.

Polyporus delectans was described from Ohio (Peck 1884) and later reported from the US Northeast and adjacent parts of Canada (Lowe 1975, as *Tyromyces delectans*). It inhabits living and fallen deciduous trees from many genera (Gilbertson & Ryvarden 1987). Its earlier records from the Pacific Northwest and Alaska should be confirmed.

Somion formosanum (T.T. Chang & W.N. Chou) Miettinen & Vlasák, ***comb. nov.*** MycoBank MB 849652.
Basionym: *Tyromyces formosanus* T.T. Chang & W.N. Chou, *Mycol. Res*. **103**: 675. 1999.

Typus: **Taiwan**, Nantou, Meifeng, hardwood, Dec. 1997, *Chou TFRI c2873* (**holotype** "TAIF").

Table 5. Identification table for *Spongipellis s.l.* All species have slightly thick-walled tramal hyphae and grow on a variety of dicots unless otherwise indicated. Excludes *Somion formosanum*, which we only know from a sequence from Taiwan. Information for *Irpiciporus sinensis* from Wang & Dai (2022).

Species	Distribution	Hosts	Caps	Pores (per mm)	Basidia	Basidiospores (L and W in µm)	Other
Aurantiporus s.l.	temperate to tropical	—	Thick, often reddish	Regular, 2–4	Short	Thin-walled, mid-sized	Tramal hyphae thin-walled, oil abundant
Irpiciporus branchiformis	East Africa, tropical	—	Thin, effused	Irpicoid, 2–3	Long	Slightly thick-walled, L = 5.19, W = 4.69, Q = 1.11	—
Irpiciporus mollis	American Northeast, temperate to subtropical	Preferably *Fagaceae*	Thin, effused	Irpicoid, 1	Long	Slightly thick-walled, L = 5.46, W = 4.84, Q = 1.14	Tramal hyphae thick-walled
Irpiciporus pachyodon	Europe and Caucasus, temperate	Preferably *Fagaceae*	Thin, effused	Irpicoid, 0.5–1	Long	Slightly thick-walled, L = 6.00, W = 5.14, Q = 1.17	—
Irpiciporus sinuosus	Southeast Asia, subtropical to tropical	—	Thin, reflexed	Sinuous, 4–5	Long	Slightly thick-walled, L = 5.31, W = 4.42, Q = 1.20	—
Somion delectans	American Northeast, temperate	—	Thick, context duplex	Regular to elongated, 2–3	Short	Slightly thick-walled, L = 6.61, W = 5.64, Q = 1.18	Tramal hyphae thick-walled
Somion litschaueri	Central Europe, Caucasus, temperate	*Quercus*	Thick, context duplex, hirsute	Regular to elongated, 1–3	Short	Thick-walled, L = 7.68, W = 5.96, Q = 1.29	Tramal hyphae thick-walled
Somion occarium	Europe, North Africa, temperate to subtropical	Preferably *Fagaceae*	Thick, context duplex	Regular to sinuous, 1–3	Short	Thick-walled, L = 6.60, W = 5.02, Q = 1.32	Tramal hyphae thick-walled
Somion strenuum	East Asia, temperate	*Quercus*	Thick, context duplex, hirsute	Regular, 3–4	Short	Thick-walled, L = 5.90, W = 4.80, Q = 1.23	Tramal hyphae thick-walled
Somion tomsovskyi	American Southwest, temperate to subtropical	*Quercus*	Thick, context duplex, hirsute	Regular, 1–2	Short	Thick-walled, L = 7.51, W = 6.12, Q = 1.24	Tramal hyphae thick-walled, interwoven
Somion unicolor	American Northeast, temperate	*Quercus*	Thick, context duplex, hirsute	Regular to sinuous, 1–2	Short	Thick-walled, L = 6.12, W = 4.78, Q = 1.29	Tramal hyphae thick-walled
Spongipellis ambiens	East Asia, boreal to temperate	Preferably *Populus*	Rather thick, hirsute	Regular, 4–6	Rather long	Slightly thick-walled, L = 5.18, W = 4.31, Q = 1.20	—
Spongipellis occidentalis	North America, temperate	Type from *Fagus*	Thick, hirsute	Regular, 4–6	Rather long	Slightly thick-walled, L = 6.24, W = 5.00, Q = 1.25	—
Spongipellis profissilis	East Asia, boreal to temperate	Preferably *Populus*	Thick	Regular, 3–4	Rather long	Slightly thick-walled, often ovoid, L = 7.31, W = 5.24, Q = 1.41	—
Spongipellis spumea	Europe, temperate	—	Thick, hirsute	Regular, 3–4	Rather long	Slightly thick-walled, L = 6.14, W = 5.02, Q = 1.23	—
Spongipellis variispora	East Asia, temperate	Preferably *Ulmus*	Thick, hirsute	Regular, 4–6	Rather long	Slightly thick-walled, L = 6.24, W = 5.29, Q = 1.19	—

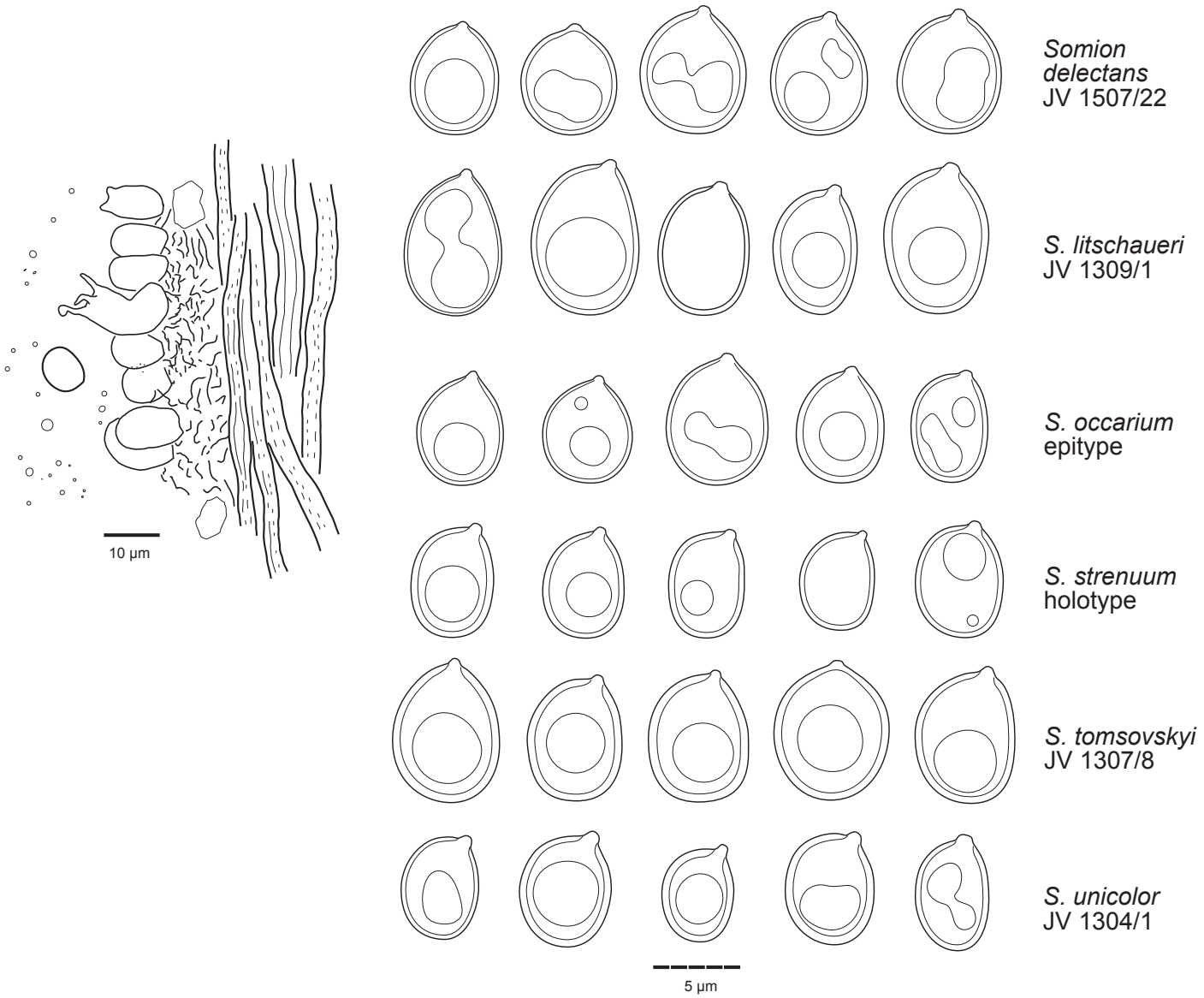

Fig. 18. Spores of *Somion* spp. and hyphal structure, tube trama, with subhymenium and hymenium, of *S. strenuum* (holotype).

Notes: This species was described as a member of *Tyromyces*, at that time a collective genus for all fleshy mono/dimitic polypores causing a white rot. ITS and *TEF1* sequences show that *T. formosanus* is a member of *Somion* and does not belong to any other species of the genus recognized here. The type is supposedly stored in the herbarium TAIF of the Taiwan Forest Research Institute, where Dr T.T. Chang worked. We wrote to TAIF requesting the type on loan in 2016 – so 17 years after the publication of the species – but were informed that no fungal material is stored in the herbarium. The herbarium staff suggested that the type specimen may still be with Dr Chang, who never replied to us. Under these circumstances, we were not able to get the type on loan. According to the original description (Chang & Chou 1999), *S. formosanum* is morphologically the most similar to *S. unicolor*. However, DNA data indicate that it is more closely related to *S. litschaueri* and *S. strenuum*. So far, *S. formosanum* is known only from two collections from the type locality.

Somion litschaueri (Lohwag) Vlasák & Spirin, ***comb. nov.*** MycoBank MB 849653. Fig. 18.

Basionym: *Spongipellis litschaueri* Lohwag, *Arch. Protistenk*. **75**: 301, 1931.

Typus: **Austria**, Burgenland: Sankt Margarethen im Burgenland, broken standing tree of *Quercus* sp., Oct. 1930, *K. Jusa* (**holotype** W 0132387, studied).

Basidiocarps annual, sessile, pilei projecting up to 10 cm. Upper surface tomentose to hirsute, azonate, yellowish to pale or bright ochraceous. Edge of pileus blunt, sterile, concolourous with pileal surface. Hymenial surface even to more-or-less convex, cream coloured to ochraceous or pale brown; pores angular to irregularly elongated, 1–3 per mm, dissepiments rather thick, first more or less even, later serrate. Section: context white to cream coloured or pale ochraceous (old herbarium specimens only), watery in fresh condition, firm, distinctly fibrillose and zonate when dry, up to 3 cm thick; tube layer tough, concolourous with pore surface, up to 3 cm thick.

Hyphal structure monomitic; all hyphae with clamp connections. Context hyphae very thick-walled, interwoven or arranged in subparallel bundles, (3.9–)4.8–5.8(–7.4) µm diam.

Tramal hyphae thick-walled (lumen narrow to rather wide), subparallel, (2.8–)3.2–4.1(–5.2) µm diam. Subhymenial hyphae slightly thick-walled, 2.0–2.5 µm diam. *Basidiospores* thick-walled, broadly ellipsoid to ovoid, (6.6–)6.8–8.6(–9.1) × (4.9–)5.2–7.0(–7.7) µm, L = 7.71 µm, W = 6.00 µm, Q = 1.27–1.33.

Distribution and ecology: Widely distributed in Central Europe although rare. Inhabits old living and recently fallen logs of *Quercus* spp., especially *Q. cerris* (Kotlaba & Pouzar 1965).

Notes: This species was described from Austria (Lohwag 1931, as *Spongipellis litschaueri*) and later reported from several countries of Central Europe (summarized in Tomšovský 2012). Another *Somion* species from Europe, *S. occarium*, differs from *S. litschaueri* in having thinner and paler, often effused-reflexed basidiocarps, sinuous pores, wider tramal hyphae and smaller basidiospores. Older records of *S. litschaueri* from European part of Russia, Ukraine, and Caucasus (Bondartsev 1953) should be reconfirmed.

Somion occarium (Batsch) Spirin & Miettinen, ***comb. nov.*** MycoBank MB 849654. Figs 1, 18.
Basionym: *Hydnum occarium* Batsch, *Elenchus fungorum*: 113. 1783 (conserved by Fries 1821: 412).
Synonyms: Spongipellis suberis Pat., *Catalogue Raisonné des Plantes Cellulaires de la Tunisie* **7**: 48. 1897.
Leptoporus bredecelensis Pilát ex Pilát, *Acta Musei Nat. Pragae* **9B**(2): 103. 1953.

Typus: Micheli, *Nova plantarum genera*: table 64, fig. 3, 1729 (**lectotype** of *Hydnum occarium* selected here, MBT 10014533). **Czech Republic**, Jihomoravský kraj, Břeclav, Valtice, 48.74931 16.79226, dead, uprooted *Quercus cerris*, 18 Nov. 2005, *Vlasák** (**epitype** of *Hydnum occarium* designated here H 7200694, MBT 10014534, studied, isoepitype JV 0511/8). **Tunisia**, El Fedja, *Quercus suber*, Jan. 1893, herb. *Patouillard* (**lectotype** of *Spongipellis suberis* FH, studied – selected by Ryvarden 1983). **Ukraine**, Zakarpatska Reg., Dilove, Mt. Menchul, *Fagus sylvatica*, Aug. 1934, *Pilát* (**holotype** of *Leptoporus bredecelensis* PRM 623854, studied).

Basidiocarps annual, sessile or effused-reflexed, up to 10 cm in widest dimension. Upper surface finely pubescent, sometimes indistinctly warted or striate, later almost smooth, azonate, cream coloured to pale ochraceous. Edge of pileus sharp to rather blunt, sterile, concolourous with pileal surface. Hymenial surface even to more or less concave or rarely convex, almost white to cream coloured; pores angular to sinuous, 1–3 per mm, dissepiments rather thin, serrate to dentate. Section: context white to cream coloured or pale ochraceous (old herbarium specimens only), watery in fresh condition, firm, indistinctly fibrillose and azonate when dry, up to 1 cm thick; tube layer soft, concolourous with pore surface, up to 2 cm thick.

Hyphal structure monomitic; all hyphae with clamp connections. Context hyphae very thick-walled, arranged in subparallel bundles, (4.2–)5.0–6.3(–10.4) µm diam. Tramal hyphae thick-walled to more rarely slightly thick-walled (lumen distinct to capillary), subparallel, (3.0–)3.6–4.7(–5.4) µm diam. Subhymenial hyphae thin-walled, 3–4 µm diam. Basidiospores thick-walled, broadly ellipsoid to ovoid, a few subglobose, (5.3–)6.0–7.2(–7.6) × (3.9–)4.3–5.5(–6.2) µm, L = 6.60 µm, W = 5.02 µm, Q = 1.28–1.37

Distribution and ecology: *Somion occarium* inhabits many deciduous trees, both living and already dead but it seems to prefer *Fagus* (Ryvarden & Gilbertson 1994, as *S. delectans*). Its distribution stretches from the Mediterranean in the south to the southern part of Sweden in the north.

Notes: See remarks under the genus for nomenclatural details. *Somion occarium* is the European counterpart of North American *S. delectans*. Differences between these species are listed under the latter species.

Somion strenuum Spirin & Vlasák, ***sp. nov.*** MycoBank MB 849655. Figs 1, 18.

Typus: **Russia**, Khabarovsk Reg., Solnechnyi Dist., Sonakh, 51.450 : 135.321, alt. 230 m, low, bushy oak forest with fire history, on living *Quercus mongolica* (basal diameter 20 cm), 15 Aug. 2014, *Spirin 7330** (**holotype** H 7200353).

Etymology: *Strenuus* (Lat., adj.) – strenuous, tough.

Basidiocarps annual or short-living perennial, sessile, pilei projecting up to 12 cm. Upper surface tomentose to hirsute, azonate, yellowish to pale ochraceous, in oldest parts fading to grey. Edge of pileus blunt, sterile, concolourous with pileal surface. Hymenial surface even to more or less concave, yellowish to pale ochraceous; pores angular, 3–4 per mm, dissepiments rather thick, uneven to serrate. Section: context cream coloured to pale ochraceous, watery in fresh condition, firm, indistinctly fibrillose and zonate when dry, up to 3 cm thick; tube layer tough, indistinctly stratified, concolourous with or slightly paler than pore surface, up to 2 cm thick.

Hyphal structure monomitic; all hyphae with clamp connections. Context hyphae very thick-walled, interwoven or in subparallel bundles, (3.3–)4.2–5.1(–6.3) µm diam. Tramal hyphae very thick-walled (lumen capillary to indistinct), subparallel, (2.7–)3.2–3.8(–4.2) µm diam. Subhymenial hyphae thin- to slightly thick-walled, 3–4 µm diam. *Basidiospores* thick-walled, ellipsoid to broadly ellipsoid, (5.0–)5.2–6.4(–7.2) × (4.1–)4.2–5.3(–6.0) µm, L = 5.90 µm, W = 4.80 µm, Q = 1.19–1.26.

Distribution and ecology: *Somion strenuum* is distributed in temperate East Asia and restricted to *Quercus* spp. Lyubarsky & Vassilieva (1975) treated this species (as *S. litschaueri*) from oak forests and plantations in Russian Far East, where it attacks living, often rather young trees of *Q. mongolica*.

Notes: *Somion strenuum* has the smallest pores in the whole genus. Microscopically, it is the most similar to the North American *S. unicolor*, which has much larger pores.

Somion tomsovskyi (Nakasone & Ortiz-Santana) Vlasák & Spirin, ***comb. nov.*** MycoBank MB 849656. Figs 1, 18.
Basionym: *Pseudospongipellis tomsovskyi* Nakasone & Ortiz-Santana, *Lilloa* **59** (Suppl.): 104. 2022.

Typus: **USA**, Arizona, Cochise County, Coronado National Forest, Chiricahua Mountains, Rucker Canyon, on *Quercus emoryi*, 27 Oct. 1967, *Gilbertson 7701* (**holotype** ARIZ AN010813; **isotype** CFMR).

Basidiocarps annual, sessile, pilei projecting up to 10 cm. Upper surface tomentose to hirsute, azonate, yellow to pale ochraceous, in oldest parts fading to grey. Edge of pileus blunt, sterile, concolourous with pileal surface. Hymenial surface even to more-or-less convex, yellow to pale ochraceous; pores angular, 1–1.5 per mm, dissepiments thick, uneven to serrate. Section: context cream coloured to pale ochraceous, in old herbarium specimens pale brown, watery in fresh condition, firm, distinctly fibrillose and zonate when dry, up to 4 cm thick; tube layer tough, concolourous with or slightly paler than pore surface, up to 2 cm thick.

Hyphal structure monomitic; all hyphae with clamp connections. Context hyphae very thick-walled, rather loosely interwoven, a few arranged in subparallel bundles, (3.1–)3.6–4.7(–5.3) µm diam. Tramal hyphae slightly or distinctly thick-walled (lumen wide to narrow), densely interwoven, (3.2–)3.8–4.8(–5.1) µm diam. Subhymenial hyphae thin- to slightly thick-walled, 3–5 µm diam. *Basidiospores* thick-walled, ellipsoid to broadly ellipsoid, (6.4–)6.8–8.3(–8.7) × (5.1–)5.5–6.8(–7.1) µm, L = 7.5 µm, W = 6.11 µm, Q = 1.22–1.23.

Distribution and ecology: So far known from the US Southwest and adjacent areas of Mexico inhabiting living and recently dead logs of *Quercus* spp.

Notes: *Somion tomsovskyi* is a close relative of *S. unicolor*. These species differ primarily in their distribution areas (US Southwest and Mexico *vs*. the North American Northeast). Microscopically, *S. tomsovskyi* differs from the rest of *Somion* species in having interwoven (not subparallel) tramal hyphae with a well-visible lumen. Two other species from North America, *S. delectans* and *S. unicolor*, have smaller basidiospores. Description and spore measurements of *S. unicolor* given by Gilbertson & Ryvarden (1987) refer to *S. tomsovskyi*.

Somion unicolor (Fr.) Spirin & Miettinen, ***comb. nov.*** MycoBank MB 849657. Fig. 18.
Basionym: *Polyporus unicolor* Fr., *Epicrisis Systematis Mycologici*: 458. 1838.
Synonym: *Boletus unicolor* Schwein., *Schriften der Naturforschenden Gesellschaft zu Leipzig* **1**: 97. 1822.

Typus: **USA**, North Carolina, Salem (**lectotype** of *Polyporus unicolor* selected here PH 00063495, MBT10014535, photo studied in plants.jstor.org).

Basidiocarps annual, sessile, pilei projecting up to 10 cm. Upper surface tomentose to hirsute, azonate, yellowish to pale ochraceous, in oldest parts fading to pale grey. Edge of pileus blunt, fertile, concolourous with pileal surface. Hymenial surface even to more-or-less convex, yellowish to pale ochraceous or brownish; pores angular to sinuous, in largest basidiocarps with a tendency to radial arrangement, 1–1.5 per mm, dissepiments thick, serrate to dentate. Section: context cream coloured to pale ochraceous, in old herbarium specimens pale brown, watery in fresh condition, firm, distinctly fibrillose and zonate when dry, up to 2 cm thick; tube layer tough, concolourous with or slightly paler than pore surface, up to 3 cm thick.

Hyphal structure monomitic; all hyphae with clamp connections. Context hyphae very thick-walled, arranged in subparallel bundles, (3.7–)4.2–5.3(–6.2) µm diam. Tramal hyphae very thick-walled (lumen capillary), subparallel, (3.4)–4.0–4.7(–5.3) µm diam. Subhymenial hyphae thin- to slightly thick-walled, some inflated, 3–6 µm diam. *Basidiospores* thick-walled, ellipsoid to ovoid, (5.2–)5.3–7.1(–7.3) × (4.0–)4.2–5.4(–5.9) µm, L = 6.13 µm, W = 4.78 µm, Q = 1.22–1.34.

Distribution and ecology: Widely distributed in the North-American Northeast inhabiting still living or recently dead trees of *Quercus* spp.

Notes: Schweinitz (1822) described *Boletus unicolor* from North Carolina. This name is invalid due to *Boletus unicolor* Bull. 1789. Fries (1836–1838), however, technically validated the name when he treated it as *Polyporus unicolor*, and should be cited as the valid author of the species. Schweinitz's protologue does not mention specimens. We select the single collection from the Schweinitz herbarium in PH as the lectotype. The basidiocarp is thick and with initially regular pores that split with age, 5–10 pores per cm (median 7), *i.e*., 0.5–1 per mm. The two other *Somion* species in North America do not come into question: *S. tomsovskyi* is not found in the east coast, and *S. delectans* has smaller, less regular pores and thinner fruiting bodies. Thus, the lectotype agrees with the modern concept of the species.

Somion unicolor has been reported from many localities in the US Northeast and adjacent part of Canada (Lowe 1975). It seems to be restricted to *Quercus* spp. Earlier records of *S. unicolor* from the US Southwest belong to *S. tomsovskyi* (see above). *Somion delectans*, sharing the same distribution area with *S. unicolor*, differs from it in having thinner, often effused-reflexed basidiocarps, smaller pores and wider basidiospores.

Excluded and insufficiently known species

Cerrena maxima (Mont.) L. Hansen, *Nat. Hist. Renell Isl. Solomon Isls*: 129. 1960.
Synonym: *Trametes maxima* (Mont.) A. David & Rajchenb., *Mycotaxon* **22**: 315. 1985.

Typus: **Cuba**, de la Sagra (**holotype** of *Trametes maxima* PC, herb. Montagne 1413, studied).

Notes: Ryvarden & Johansen (1980) retained this and the two following species in *Cerrena*. *Trametes maxima* is a typical member of *Trametes*.

Cerrena meyenii (Klotzsch) L. Hansen, *Nat. Hist. Renell Isl. Solomon Isls*: 129. 1960.
Synonym: *Trametes meyenii* (Klotzsch) Lloyd, *Mycological Writings* **5**(67): 14. 1918.

Notes: While this species has been placed in *Cerrena*, our morphological analysis and preliminary sequence data place it in the *Polyporaceae*. For now, *Trametes* is the best available genus for it.

Cerrena sclerodepsis (Berk.) Ryvarden, *Mem. New York Bot. Gard*. 28: 204. 1976.
Basionym: *Trametes sclerodepsis* Berk., Hooker's J. *Bot. Kew Gard. Misc*. **8**: 236. 1856.

Notes: Our morphological analysis and preliminary sequence data place this species in the *Polyporaceae*. For now, *Trametes* is the best available genus for it.

Irpiciporus africanus (Ipulet & Ryvarden) Nakasone, *Lilloa* **59** (Suppl.): 94. 2022.
Basionym: *Spongipellis africana* Ipulet & Ryvarden, *Syn. Fungorum* **20**: 97. 2005.
Hypochnicium africanum (Ipulet & Ryvarden) Miettinen, ***comb. nov.*** MycoBank MB 849658.

Typus: **Uganda**, Kanungu, Bwindi Impenetrable NP, Byumba, rotting log, 24 May 2003, *Ipulet F1683** (**holotype** of *Spongipellis africana* O, studied).

Notes: This species with hydnoid, effused-reflexed basidiocarps has septate cystidia and thick-walled, cyanophilous spores. It does not belong to the *Cerrenaceae* or *Spongipellis s. str*. Micromorphology and nrDNA sequence of the type specimen point towards *Hypochnicium* and not to *S. pachyodon* (*i.e. Irpiciporus*) as suggested by Ipulet & Ryvarden (2005) and Nakasone & Ortiz-Santana (2022). In the scheme of Maekawa *et al.* (2023), the species might belong to *Gyrophanopsis* or to a genus of its own, but we prefer a larger concept of *Hypochnicium* for now, including *Gyrophanopsis* and *H. africanum.*

Irpiciporus cubensis (Berk. & M.A. Curtis) Murrill, *N. Amer. Fl.* **9**: 15. 1907.
Basionym: *Irpex cubensis* Berk. & M.A. Curtis, *J. Linn. Soc., Bot*. **10**: 326. 1869.

Typus: **Cuba**, summit of Lomo del Gaso, on rotting logs, unknown collection date, *Wright 240*, Fungi Cubensis Wrightiani no. 355 (**lectotype** K – selected by Maas Geesteranus 1974: 470, **isotype** FH 00301398).

Notes: Description of the type were given by Maas Geesteranus (1974) and Nakasone & Ortiz-Santana (2022). According to their descriptions, the type is small and sterile, with unclear affinity. Maas Geesteranus specifically excludes conspecificity with *Cerrena zonata* and notes the specimen is irpicoid, dimitic, with clamped septa and oil-filled hyphal ends. Nakasone and Ortiz-Santana add that cylindrical cystidia (or oil hyphae) project from the hymenium. We have not seen the type, but it seems unlikely that it belongs to any genus treated here.

Irpiciporus decolorans (Cooke) Nakasone, *Lilloa* **59** (Suppl.): 95. 2022.
Basionym: *Irpex decolorans* Cooke, *Grevillea* **19**(92): 109. 1891.

Typus: **Cuba**, on rotting logs, unknown collection date, *C. Wright 835* (**lectotype** K(M) 62571 – selected by Maas Geesteranus 1974: 471).

Notes: Nakasone (2012) and Nakasone & Ortiz-Santana (2022) provide descriptions of the type, which we have not studied here. According to them, the type is richly fertile though the hymenium is degraded. Nakasone & Lindner (2012) describe a dense structure of agglutinated hyphae, small ellipsoid spores, brown colour and relatively short, and small spines. They placed it in *Cristinia* (*Agaricales*). Nakasone & Ortiz-Santana (2022) place the species in *Irpiciporus* and state that the basidiomes "change from white to brown on drying". Where this information comes from is unclear, since already Cooke in the protologue describes the caps as sooty, *i.e.* dirty brown ("*fuligineus*"). These characters make it highly unlikely that this species belongs to *Irpiciporus* with white, rather big basidiomes and open structure. Hjortstam & Larsson (1995) suggest this species is related to *Radulodon*, though Nakasone does not describe cystidia as present in *Radulodon* spp. Ryvarden (2020b) claims it represents *Cerrena zonata*, a dimitic species. These opinions are all conflicting and the identity of this species remains ambiguous.

Irpiciporus lacteus (Fr.) Murrill, *North American Flora* **9**: 15. 1907.
Synonym: *Irpex lacteus* (Fr.) Fr., *Elenchus Fungorum* **1**: 145. 1828.

Note: This type species of *Irpex* belongs to *Irpicaceae*, *Polyporales* (Justo *et al*. 2017).

Irpiciporus noharae Murrill, *Mycologia* **1**: 166. 1909.
Synonym: *Lopharia mirabilis* (Berk. & Broome) Pat., *Bull. Soc. Mycol. France* **11**: 14. 1895.

Notes: Nakasone & Ortiz-Santana (2022), who studied the type, conclude it represents *Lopharia mirabilis*, a distinctive species in the *Polyporaceae*. This is also the conclusion of Ryvarden (2020b).

Irpiciporus rajchenbergii Nakasone, *Lilloa* **59** (Suppl.): 95. 2022.

Typus: **Brazil**, São Leopoldo, 1931, *Rick* (**holotype** BPI 0259635).

Notes: Nakasone described this species without sequence data and based on an old specimen of Rick from southern Brazil (Nakasone & Ortiz-Santana 2022). The description points towards *Irpiciporus*, but since her concept of the genus is heterogeneous, another opinion on its identity would be desirable.

Irpiciporus tanakai Murrill, *Mycologia* **1**: 167. 1909.
Synonym: *Antrodia tanakae* (Murrill) Spirin & Miettinen, [as '*tanakai*'], *Mycologia* **105**: 1572. 2013 [2014].

Note: This species belongs to *Antrodia sensu stricto* (*Fomitopsidaceae*, *Polyporales*; Spirin *et al*. 2013).

Irpiciporus tulipiferae (Schwein.) Murrill, *Bull. Torrey Bot. Club* **32**: 472. 1905.
Synonym: *Irpex lacteus* (Fr.) Fr., *Elenchus Fungorum* **1**: 145. 1828.

Note: Maas Geesteranus (1974) showed the type belongs to *Irpex lacteus*.

Irpiciporus xuchilensis (Murrill) Y.C. Dai & Chao G. Wang, *Mycol. Progr*. **21**(73): 8. 2022.
Basionym: *Coriolus xuchilensis* Murrill, *Bull. New York Bot. Gard*. **8**: 143, 1912.
Bjerkandera xuchilensis (Murrill) Miettinen, ***comb. nov.*** MycoBank MB 849659.

Typus: **Mexico**, Veracruz, Xuchiles, near Cordoba along Rio Blanco, 17 Jan. 1910, *WA & EL Murrill 1171* (**holotype** of *Coriolus xuchilensis* NY 00705008, studied).

Notes: Zhao *et al*. (2017) and Wang & Dai (2022) published *Irpiciporus* sequences of one Ecuadorian specimen under this name (GenBank KX161650, KX161659). Those sequences are unique among the available sequences, so this specimen

represents another species in the genus *Irpiciporus*. However, the correct name is not *I. xuchilensis*. We have studied the type of *C. xuchilensis*. It clearly belongs to *Bjerkandera*, though it is beyond the scope of this paper to determine to which of the currently recognized species in that genus. New species of *Bjerkandera* have been recently described from tropical Americas, and they should be reviewed against this older species name. Coming back to the *Irpiciporus* specimen, we leave it formally without a name, since we consider it possible that older names may exist for it for instance among the species Murril described.

Polyporus albostygius Berk. & M.A. Curtis, *J. Linn. Soc., Bot*. **10**: 309. 1869.
Synonym: *Rigidoporus albostygius* (Berk. & M.A. Curtis) Rajchenb., *Revista de Investigaciones Agropecuarias Serie 5, Patología vegetal*: 72. 1984.

Typus: **Cuba**, unknown collection date, *Wright 583* (K – **lectotype** of *Rigidoporus albostygius* designated by Ryvarden (1984), **isotype** FH 290626, studied).

Note: Though sometimes listed as a synonym of *Lividopora vincta*, this species belongs to *Meripilaceae*.

Polyporus bistratosus Berk. & Cooke, *J. Linn. Soc. Bot*. **15**: 384. 1877.

Typus: **Brazil**, Amazon, Paricatuba, River Purua, 8 Sep. 1974, *Trail 74* (**holotype** K(M) 192256, studied).

Notes: Another species sometimes listed as a synonym of *L. vincta*. It belongs to *Meripilaceae*.

Polyporus hyposclerus Berk. ex Cooke, *Grevillea* **10**(55): 103. 1882.

Typus: **Australia**, Queensland, Brisbane, unknown collection date, *Broome* (**holotype** K(M) 192252, studied).

Notes: A supposed synonym of *L. vincta*. The type is sterile and in bad condition, but it is a species of *Fomitopsis*.

Pseudolagarobasidium calcareum (Cooke & Massee) Sheng H. Wu, *Acta Bot. Fenn*. **142**: 112. 1990.

Notes: Nakasone & Lindner (2012) suggested that this species is a synonym of *P. pronum* described from Sri Lanka. Its status as a separate species should be revised; see further notes under *P. pronum*.

Pseudolagarobasidium concentricum (Cooke & Ellis) Hjortstam, *Mycotaxon* **54**: 190. 1995.
Synonym: *Pirex concentricus* (Cooke & Ellis) Hjortstam & Ryvarden, *Mycotaxon* **24**: 289. 1985.

Note: This North American species is the type of *Pirex* and belongs to *Phanerochaetaceae* (*Polyporales;* Justo et al. 2017).

Pseudolagarobasidium conspicuum (Pouzar) Nakasone, *Mycotaxon* **130**: 378. 2015.
Basionym: *Hyphoradulum conspicuum* Pouzar, *Česká Mykol*. **41**: 26. 1987.

Crustomyces conspicuus (Pouzar) K.H. Larss., ***comb. nov.*** MycoBank MB 849660.

Typus: **Czech Republic**, Central Bohemia, Karlštejn, Velka Hora, *Cornus mas*, 2 Oct. 1981, *Pouzar* (**holotype** of *Hyphoradulum conspicuum* PRM 834886; **isotype** GB*, studied).

Notes: This is the type species of the monotypic genus *Hyphoradulum* Pouzar. Nakasone (2015) placed it in *Pseudolagarobasidium*. We managed to generate an ITS sequence from an isotype deposited in herb. GB. BLAST searches against GenBank showed close affinity with *Crustomyces*, which belongs to *Cystostereaceae*, *Agaricales*. Li *et al*. (2022) recently published a phylogenetic analysis of *Cystostereaceae*. We conducted a phylogenetic analysis of the ITS region from a selection of the dataset used in Li *et al.* along with the *H. conspicuum* sequence and a few new *Crustomyces* sequences (Fig. 19). *Hyphoradulum conspicuum* was recovered as a sister taxon to *Crustomyces tephroleucus* within a strongly supported clade corresponding to the expanded genus concept of *Crustomyces* introduced by Li *et al.* (2022). This wider *Crustomyces* includes *Cystidiodontia* (type *Cystidiodontia artocreas* = *C. laminifera*) and *Rigidotubus* (type *Rigidotubus tephroleucus*). We follow this circumscription of *Crustomyces* and suggest that also *Hyphoradulum* should be placed there.

Radulodon acaciae G. Kaur, Avneet P. Singh & Dhingra, *Mycotaxon* **127**: 111. 2014.

Notes: This species likely belongs to *Pseudolagarobasidium*, and Nakasone & Ortiz-Santana (2022) considered it a synonym of *P. acaciicola* based on the original description. In our view the protologue (Kaur et al. 2014) is not sufficient to make any firm conclusions about its identity.

Radulodon americanus Ryvarden, *Canad. J. Bot*. **50**: 2074. 1972.

Typus: **Canada**, British Columbia, Prince George, *Populus tremuloides*, 25 Aug. 1945, *Foster* (**holotype** DAOM 16599, studied).

Note: Type species of *Radulodon*, but possibly a synonym of *R. erikssonii*, see remarks under that species.

Radulodon copelandii (Pat.) N. Maek., *Rep. Tottori Mycol. Inst*. **31**: 93. 1993.
Synonym: *Radulomyces copelandii* (Pat.) Hjortstam & Spooner, *Kew Bulletin* **45**: 314. 1990.

Notes: This species described from the Philippines belongs to *Radulomyces* (Nakasone 2001). Nakasone *et al.* (2021) provide sequences under this name from southern China.

Radulodon indicus Jyoti & Dhingra, *Syn. Fungorum* **32**: 38. 2014.

Notes: Described from Jammu, India. Its authors compare the species to *Radulodon pseudomucidus*, which is a synonym of *Radulomyces copelandii* (Nakasone *et al.* 2021). We have not seen material, but the description points towards *Radulomyces*.

Radulodon licentii (Pilát) Ryvarden, *Česká Mykol*. **30**(1): 40. 1976.
Synonym: *Radulomyces licentii* (Pilát) Parmasto, *Conspectus Systematis Corticiacearum*: 111. 1968.

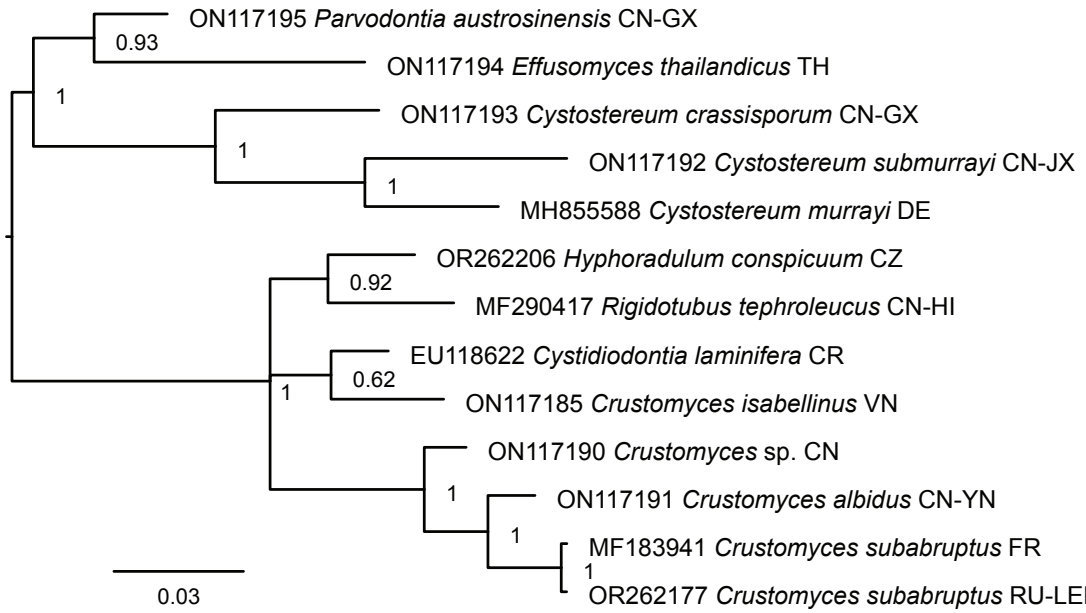

Fig. 19. Bayesian consensus phylogram of *Cystostereaceae* based on ITS sequences. Countries (and states) of origin are denoted with ISO 3166 codes.

Note: Nakasone *et al.* (2021) accept this species described from North China in *Radulomyces* (*Agaricales*) and provide DNA data from Southwest China and Taiwan.

Radulodon pseudomucidus (Petch) Stalpers, *Folia Cryptog. Estonica* **33**: 137. 1998.

Note: Nakasone *et al*. (2021) consider this a synonym of *Radulomyces copelandii* (*Agaricales*).

Radulodon subquercinus (Henn.) Hjortstam & Ryvarden, *Mycotaxon* **10**: 285. 1980.

Notes: Type of the genus *Phaneroites*, this acystidiate species reminds *Phanerochaete sensu lato* and does not belong to the *Cerrenaceae*. Hjortstam (1987) considered *Phanerochaete radulans* Hallenb. a synonym.

Rigidoporus hypobrunneides Corner, *Beih. Nova Hedwigia* **86**: 165. 1987.

Typus: **Malaysia**, Pahang, Cameron Highland, 31 Jul. 1934, *Corner* (**holotype** E 00159712, photograph studied).

Notes: As the name indicates, Corner (1987) considers this species similar to *R. hypobrunneus* (= *Lividopora benetosta*). He mentions that it has bigger pores, which brings *Lividopora facilis* to mind. We have not studied the type under microscope, but the photograph is of a light-colored resupinate polypore, whose mid-sized tubes have turned partly brown. Corner mentions that *R. hypobrunnea* has thick-walled, heavily encrusted cystidia ("extrahymenial setae"), while he only mentions thin-walled, narrow cystidia in *R. hypobrunneides*. This tells us that *R. hypobrunneides* is not a species of *Lividopora* and certainly not an older name for *L. facilis.* It could rather be a member of the *Meripilaceae*. Hattori (2001), who studied the type, mentions that it is moldy, indicating that Corner's spore measurements may refer to mold spores. Hattori left the specimen as *Rigidoporus* sp.

Spongipellis caseosa (Pat.) Ryvarden, *Occas. Pap. Farlow Herb. Cryptog. Bot*. **18**: 11. 1983.
Basionym: *Leptoporus caseosus* Pat., *Ann. Mycol*. **5**(4): 365. 1907.

Typus: **Brazil**, São Paulo, Caminas, Mar. 1897, *Noack* (**lectotype** FH 00258975, studied – typified by Ryvarden 1983).

Notes: Light-coloured, monomitic with thick-walled generative hyphae, spores slightly cyanophilous and slightly thick-walled, ellipsoid. Hymenium has collapsed in the type. These characters may imply *Somion*, but we cannot exclude *Ryvardenia*. Spores are smaller than in the described species of *Ryvardenia* (Rajchenberg 1994) or *Somion*. Modern collections and/or revision of the type material are needed to confirm its identity.

Spongipellis eberhardtii Pat., *Bull. Soc. Mycol. France* **36**: 176. 1920.

Typus: **Vietnam**, Annam, Lang Biang, sur Pin, Eberhardt 196 (**lectotype** FH 00258973, studied – typified by Ryvarden 1983).

Notes: Fleshy mid-sized polypore with regular, pinkish pores, large, ellipsoid, thick-walled spores, monomitic with very wide and thick-walled, clamped hyphae, partly agglutinated, changing colour upon drying. We do not know the true affinity of this species, and we are not aware of any modern collections. In our opinion it does not belong to any genus in the *Cerrenaceae* or *Spongipellis sensu stricto*.

Tyromyces irpiceus Corner, *Beih. Nova Hedwigia* **96**: 143. 1989.

Notes: Corner (1989) described this species from Brazil. According to his description, the species has small pilei and lamellate to irpicoid hymenophore, and Corner compares it with *Irpiciporus* and *Spongipellis sensu lato*. According to the protologue, the species is acystidiate and monomitic with thick-walled clamped hyphae. Corner describes the ellipsoid, mid-sized spores as thin-walled. We have not seen the type, but this species should be kept in mind when dealing with Neotropical

Irpiciporus and *Somion*. Hattori (2002) did not mention this species in his type studies.

Tyromyces sublamellatus Corner, *Beih. Nova Hedwigia* **96**: 199. 1989.

Notes: Corner (1989) likens this Malaysian species to *T. irpiceus*, which in turn he considers similar to *Irpiciporus*. Judging from Corner's description, this might be a species of *Irpiciporus*. However, Hattori (2003) reports the species as dimitic and having gloeocystidia, relating it to *Abortiporus roseus*. Clearly this species does not belong to *Irpiciporus*.

Specimens studied

Acanthodontia cirrhatina. **Malaysia**, Sabah (see **holotype**). **Indonesia**, Sumatera Barat, Sijunjung, Bukit Tujuh, alt. 550 m, dicot, 23 Jul. 2009, *Miettinen 13717** (ANDA, H).

Cerrena albocinnamomea. **China**, Jilin, Antu, Changbai Mts, on *Tilia*, 3 Sep. 1993, *Dai 997* (H, **paratype**); *Acer*, 5 Sep. 1993, *Dai 1085* (H, **paratype**); *Acer mono*, 15 Sep. 1998, *Niemelä 6372* (H); dicot, 26 Aug. 2005, *Miettinen 10511** (H).

Cerrena 'gilbertsonii'. **Guadeloupe**, Basse-Terre, Grande Anse, dicot, unknown collection date, *D. Vlasák** (JV 1609/29, H). **Mexico** (see type).

Cerrena multipileata. **Brazil**, Parana, Mandirituba, alt. 850 m, 20 Apr. 1993, *de Meijer 2623* (O, H); Santa Catarina (see type). **Costa Rica**, San José, Cerro Vueltas, alt. 2 000 m, 18 Jul. 2001, *Ryvarden 43881* (O, H*); Puntarenas, Santa Elena, dicot, 28 & 29 Jul. 2014, *Vlasák** (JV 1407/63, H). **Guatemala**, Huehuetenango, San Mateo Ixtatán, alt. nearly 3 000 m, 21 Nov. 2006, *Kout A36** (JV 0611/A36).

Cerrena unicolor. **China**, *Hu* (**lectotype** of *Polystictus prosector* BPI 0315073, LC23787, selected by Stevenson & Cash 1936: 137). **Finland**, Etelä-Häme, Lammi, Pappilankylä, *Betula*, 10 Sep. 1997, *Niemelä 6098* (H); Pohjois-Karjala, Tohmajärvi, Rouanaho, *Betula*, 30 Jun. 1970, *Niemelä* (H); Kainuu, Hyrynsalmi, Latvakorvensuo, *Betula pubescens*, 26 Sep. 2010, *Miettinen 14197* (H); Suomussalmi, Soidinkangas, *B. pubescens*, 30 Sep. 2004, *Miettinen 9443** (H); Kittilän Lappi, Kittilä, Pallas-Ounas National Park, *B. pubescens*, 21 Aug. 1990, *Niemelä 5352* (H). **Kyrgystan**, Jalal-Abad, Aksy, Arkyt village, *Craetagus*, 31 Jul. 2007; *Uotila 47588** (H 7200336). **USA**, Minnesota, Waseca, Janesville, Willis Lake, dicot, 21 Aug. 2013, *Miettinen 16729* (H 7005991); New York, Essex Co., Huntington wildlife forest, Arbutus lake, dicot, 17 Sep. 2013, *Miettinen 16901* (H).

Cerrena zonata. **Australia**, Trowutta Arch, 17 Apr. 2008, *Gates** (H). **China**, Yunnan, Kunming Bot. Garden, 30 Jul. 2005, *Miettinen 9773** (H); Chuxiong, Zixishan, dicot, 2 Aug. 2005, *Miettinen 9889.1** (H). **Indonesia**, Sumatera Barat, Lima Puluh Kota, Gunung Sago, dicot, 25 Jul. 2009, *Miettinen 13798** (ANDA, H). **Japan**, Tokyo, *Quercus*, Oct. 1908, *Kusano & Nohara* (**type** of *Irpiciporus japonicus* Murrill NY 00985353). **Nepal** (see type).

Crustomyces conspicuus. **Czech Republic** (see type).

Crustomyces subabruptus. **Russia**, Leningrad reg, Tikhvin, Gorodokskoe, *Populus tremula*, 28 Jul. 2012, *Spirin 4826** (H).

Irpiciporus branchiformis. **Tanzania**, Tanga, Lushoto, Mazumbai Forest Res., dense forest, on dead wood, 15 Dec. 1995, *Niemelä 5937* (H)*; see also type.

Irpiciporus mollis. **USA**, Florida, Escambia Co., Pensacola, *Quercus* sp., 25 Nov. 1914, *Bartholomew* (Fungi Columbiani #4545, H); Manatee Co., Braden river trail, dicot, 8 May 2016, *Dollinger 770** (JV, H), Bradenton, dicot, 10 Oct. 2016, *Dollinger 962* (JV); Massachusetts, Worcester Co., Worcester, *Acer saccharum*, 20 Oct. 2013, *Miettinen 17338* (H); New Hampshire, Carroll Co., Chocorua, *Acer* sp., Aug. 1908, *Farlow 334* (H ex FH); New Jersey (?), *Quercus* sp., Sep. 1879, *Ellis* (North American Fungi #320, H); Pennsylvania, Philadelphia, Wissahickon Creek, *Fagus virginiana*, Aug. 2008, *Vlasák* (JV 0808/45, H); Bucks Co., Ralph Stover State Park, *Quercus* sp., Aug. 2001, *Vlasák* (JV 0108/115, H); South Carolina, Santee River, *Ravenel* (herb. *Curtis 1729* in K – **lectotype**); Virginia, Prince William Co., Woodbridge, *Liriodendron tulipifera*, Sep. 2007, *Vlasák** (JV 0709/174, H).

Irpiciporus pachyodon. **Bulgaria**, Burgas, Strandzha Nat. Park, *Quercus* sp., 25 Oct. 2007, *Heilmann-Clausen 07–286** (H). **Czech Republic**, Jihočeský kraj, Hluboká nad Vltavou, *Quercus petraea*, Nov. 1993, *Vlasák** (JV 9311/1, H); Středočeský kraj, Průhonický park, *Quercus rubra*, 1 Nov. 2016, *Kotlaba** (JV 1611/1); Vysočina, Velký Špičák, *Fagus sylvatica*, 2 Oct. 2004, *Vampola 199* (H ex MJ). **France**, Var, Forêt de Janas, *Q. suber*, 20 Dec. 1987, *David* (H, O ex LY). **Italy**, Piedmont, Alessandria, Bosio, Capanne di Marcarolo Nat. Regional Park, *Quercus* sp., 16 Oct. 2019, *Spirin 13785* (H). **Portugal**, Estremadura, Setúbal, Alto da Guerra, *Q. suber*, 8 Apr. 1978, *Melo 327* (H ex LISU).

Lividopora armeniaca. **Malaysia** (see type).

Lividopora benetosta. **China**, Hunan, Sangzhi, Badagongshan NR, 23 Sep. 2000, *Härkönen K778** (H); Wulingyuan World Heritage Site, 15 Sep. 1999, *Härkönen K8** (H); Yunnan, Xishuangbanna, Botanical Garden, dicot, 5 Aug. 2005, *Miettinen 9978.2* (H); 6 Aug. 2005, Miettinen 10020 (H); Biosphere Reserve, Menglun, *Moraceae*?, 9 Aug. 2005, *Miettinen 10142.1* (H); Jinghong, Mandian village, 15 Aug. 2005, *Miettinen 10333* (H); Mandian Water Fall surroundings near Jinghong, 17 Aug. 2005, *Miettinen 10394.1*, *10396.2* (H); Primeval Forest Park near Jinghong, 13 Aug. 2005, *Miettinen 10225** (H). **French Polynesia** (see type). **Indonesia**, Nusa Tenggara Barat, Lombok Utara, Bentek, dicot, 29 Dec. 2011, *Miettinen 15238* (BO, H), *15243* (BO, H); *Theobroma cacao*, 29 Dec. 2011, *Miettinen 15252* (BO, H); Papua, Jayapura Reg, Cyclop Mountains, *Fabaceae* (?), 22 Aug. 2004, *Miettinen 9127.1* (H); dicot, 29 Aug. 2004, *Miettinen 9176.2** (H); *Sapindaceae/Meliaceae* (?), 29 Aug. 2004, *Miettinen 9166.5** (H); dicot, 29 Aug. 2004, *Miettinen 9188.1* (H); 14 Dec. 2007, *Miettinen 12080.1* (MAN, H); Papua Barat, Manokwari Reg, Amberbaken, River Anjii/Wepai near Saukorem, dicot, 1 Nov. 2010, *Miettinen 14287* (H); Riau, Indragiri Hulu, Bukit Aluran Babi, dicot, 2 Jul. 2004, *Miettinen 8823.2** (H); Pelalwan, Teluk Meranti, dicot, 25 Jul. 2004, *Miettinen 9026.2* (BO, H); Sumatera Barat, Pesisir Selatan, Muara Sako, dicot, 22 Apr. 2002, *Miettinen 6026* (BO, H); Padang, Limau Manis, 13 Jul. 2008, *Miettinen 13011.3* (ANDA, H); Ulu Gadut, dicot, 28 Jul. 2009, *Miettinen 13884.1*, *13891* (ANDA, H); Sijunjung, Bukit Sebelah, 22 Jul.

2008, *Miettinen 13674.1* (ANDA, H). **Malaysia**, Sabah, Ranau, Poring, dicot, 19 Jun. 2013, *Miettinen 16397.2* (SNP 33655, H), *Miettinen 16416* (SNP 33667, H). **New Zealand**, Rotorua, between lakes Rotoiti-Rotoehu, Hongi's track, 14 Apr. 2004, *Hallenberg 15301** (O). **Philippines**, Zamboanga, San Ramon, 12 May 1904, *Copeland 743* (**type** of *Poria porphyrophaea* NY 00742723). **Puerto Rico**, Luquillo, El Yunque National Forest, Bisley, *Dacryodes excelca* (?), 7 Jan. 2014, *Miettinen 18019* (H); Sabana, *Cecropia*, 8 Jan. 2014, *Miettinen 18035** (H); 12 Jan. 2014, *Miettinen 18133* (H); 14 Jan. 2014, *Miettinen 18140* (H); Yokahú tower, 14 Jan. 2014, *Miettinen 18135** (H). **Samoa**, unknown collection date, *Lloyd 5042* (**lectotype** of *Poria fumosa* BPI US0318515, **isotype** FH 290621). **Sri Lanka**, Gangaruwa, Dec. 1913, *Petch 3930* (**lectotype** of *Poria hypobrunnea* K(M) 56199). **US Virgin Islands**, St John, Virgin Islands NP, 8 Feb. 2012, *Justo 513** (H). **Vietnam**, Thanh Hóa, 20 Apr. 1892, *Bon 5294* (**lectotype** of *Poria fulvobadia* FH 290623).

Lividopora facilis. **Indonesia**, Riau (see type).

Lividopora subvincta. **Kenya**, Taita-Taveta, Taita Hills, Ngangao, dicot, 24 Nov. 2017, *Savchenko 171124/1505* (H 7008794); dicot, 29 Nov. 2017, *Savchenko 171129/1309A** (H 7008878). **Zimbabwe** (see type).

Pseudolagarobasidium belizense. **Brazil**, Pará, Vicinal Das Paranarense, Municipio de Aveiro, *Hevea brasiliensis*, unknown collection date, *Gazis VPB197** (H). **Costa Rica**, Guanacaste, Reserva Biologica Lomas Barbudal, angiosperm, 14 Jul. 2001, *KH Larsson 11363** (O, H).

Lividopora vincta. **Brazil**, Amazon, Rio Uaupés, Ipanoré ("Panuré"), on dead trees, Feb. 1853, *Spruce 178* (**lectotype** of *Polyporus carneopallens* K(M) 192248, **isotype** FH 00290615). **Costa Rica**, San José, Ciudad Colon, alt. 800 m, 23 Jul. 1963, *Lowe L-13218-Sp* (CFMR). Puntarenas, Tarcoles, Villa LaPaz, dicot, 22 Apr. 2017, *Vlasák** (JV 1704/102). **Dominican Republic** (K, type). **USA**, Florida, Alachua Co., Gainesville, dicot, 24 Nov. 2013, *Miettinen 17916.1** (H).

Pseudolagarobasidium calcareum. **Taiwan**, Nantou, Sun-Moon Lake, *Castanopsis kusanoi*, 26 Oct. 1988, *Wu 88102*6–*18* (H 7003571).

Pseudolagarobasidium subvinosum. **Taiwan**, Hualien, Hsiulin Hsiang, *Leucaena leucocephala*, Sep. 1986, *Wu 8609* (H 7003570).

Pseudolagarobasidium venustum. **Brazil**, São Paulo, Cananeia, Ilha do Cardoso, dicot, 2–5 Feb. 1987, *Ryvarden 24717* (GB, **paratype**), see also **holotype**. **Colombia**, Magdalena, Parque Nacional Tayrona, Estacion Canaveral, 17–19 Jun. 1978, *Ryvarden 15910B* (GB, paratype). **Costa Rica**, unknown collection date, *Carranza 120929** (O); Guanacaste, Tempisque, Reserva Biologica Lomas Barbudal, on decaying dicot wood, 14 Jul. 2001, *K.H. Larsson 11363** (GB). **Puerto Rico**, Luquillo, Sabana, Bisley, dicot, 6 Jun. 1997, *K.H. Larsson 10040** (GB).

Radulodon americanus. **Canada** (see type).

Radulodon casearius. **USA**, Fungi Caroliniani Exsiccati by H.W. Ravenel, fasc. III, 20. "*Hydnum trichodontium*", *Quercus* sp. (H).

Radulodon erikssonii. **Finland**, Pohjois-Häme, Vesijaon luonnonpuisto, 21 Sep. 2018, *Pennanen 3886** (H); Pohjois-Savo, Savonlinna, Haukiniemi, *Populus tremula*, 9 Nov. 2018, *Pennanen 3794** (H); Pieksänmaa, Kivimäki, *P. tremula*, 29 Sep. 2006, *Miettinen 10977* (H). **Norway** (see type). **Switzerland**, Ticino, Losone, Maia, *P. tremula*, 30 Apr. 1988, *Martini** (GB 0181279).

Somion delectans. **USA**, Maine. York Co., Kittery Point, *Carya ovata*, Oct. 1922, *Thaxter 799* (H ex FH); New Jersey, Carroll Co., North Conway, *Betula* sp., Sep. 2008, *Vlasák 0809/62** (JV); Ohio, Cincinnati, fallen log, unknown collection date, *Morgan 106* (BPI – **isotype**); Pennsylvania, Montgomery Co., Green Lane State Park, *Carya* sp., Jul. 2015, *J. Vlasák Jr.** (JV 1507/22, H); Chester Co., Phoenixville, *Acer rubrum*, Nov. 2018, *J. Vlasák Jr.** (JV 1811/9).

Somion litschaueri. **Czech Republic**, Jihomoravský kraj, Valtice, *Quercus cerris*, 10 Sep. 1998, *Vampola 198* (H ex MJ); 3 Sep. 2013, *Vlasák** (JV 1309/1, H). **Slovakia**, Zvolen, Čertova Skala Nat. Res., *Quercus* sp., 4 Sep. 2013, *Vlasák** (JV 1309/7, H).

Somion occarium. **Czech Republic**, Jihočeský kraj, Jindřichův Hradec, Suchdol nad Lužnicí, *Fagus sylvatica*, Oct. 2013, *Hlásek** (JV 1310/23, H); Jihomoravský kraj (see epitype); Vysočina, Doupě, *F. sylvatica*, 17 Nov. 1994, *Vampola* (H ex MJ, *Polyporales* Exsiccati Čechoslaviacae 149). **Sweden**, Skåne, Kullaberg, Brunnby, *F. sylvatica*, 20 Nov. 2009, *KH Larsson 14261** (GB). **Tunisia**, El Fedja, *Quercus suber*, Jan. 1893, herb. *Patouillard* (**lectotype** of *Spongipellis suberis* FH). **Ukraine**, Zakarpatska Reg., Dilove, Mt. Menchul, *F. sylvatica*, Aug. 1934, *Pilát* (**holotype** of *Leptoporus bredecelensis* PRM 623854).

Somion strenuum. **China**, Liaoning, Anshan, Qian Mts. Park, *Quercus* sp., 22 Aug. 2005, *Miettinen 10456** (H). **Russia**, Khabarovsk Reg., Komsomolsk Dist., Boktor, *Quercus mongolica*, 18 Aug. 2013, *Spirin 6112** (H); Solnechnyi Dist., Igdomi, *Q. mongolica*, 6 Sep. 2016, *Spirin 10989* (H); Sonakh (see type); Ulchskii Dist., Susanino, *Q. mongolica*, 27–29 Aug. 1976, *Alanko 31049*, *31153* (H).

Somion tomsovskyi. **Mexico**, San Luis Potosí, Ciudad de Maiz, 23 May 1963, *Lemke* (H ex O). **USA**, Arizona, Cochise Co., Chiricahua, *Quercus hypoleucoides*, 6 Oct. 1967, *Gilbertson 7638* (H ex O); 5 Sep. 2012, *J. Vlasák Jr.** (JV 1209/55, H); *Quercus* sp., 19 Jul. 2013, *J. Vlasák Jr.** (JV 1307/8, H); Pima Co., Madera Canyon, *Quercus* sp., 20 Nov. 2016, *J. Vlasák Jr.** (JV 1611/1).

Somion unicolor. **Canada**, Ontario, Renfrew Co., Petawawa Forest Station, *Quercus borealis*, Aug. 1937, *Lewis* (H ex DAOM 9080). **USA**, Missouri, Perry Co., Perryville, dead logs, 1884, *Demetrio* (Rabenhorst-Winter's Fungi Europaei #3330, H); New Jersey, Atlantic Co., Hammonton, Wharton State Forest, *Quercus* sp., 15 Apr. 2013, *J. Vlasák Jr. 1304/1** (JV, H); Burlington Co., Batsto Village, *Quercus* sp., Aug. 2017, *J. Vlasák Jr.* 1708/10* (JV, H); *Acer rubrum*, Jan. 2021, *J. Vlasák Jr. 2102/2** (JV).

Trametes meyenii. **Indonesia**, Nusa Tenggara Barat, Lombok Utara, Bentek, dicot, 29 Dec. 2011, *Miettinen 15249* (BO, H); Papua Barat, Teluk Wondama, Werianggi-Werabur, 7 Sep. 2004, *Miettinen 9274* (BO, H).

Trametes sclerodepsis. **Ecuador**, Orellana, Yasuni NP, 12 Mar. 2002, *Ryvarden 44671A* (O, H).

DISCUSSION

We have inferred a phylogeny of the family *Cerrenaceae* with a 6-marker dataset to revise its classification at the genus level. Balancing morphological data and phylogenetic information, we have adopted a scheme of seven genera. Other schemes would also be feasible for the family: three large genera (*Cerrena*, *Irpiciporus*, and *Somion*), six genera (as in the seven-genus solution but *Lividopora* included in *Cerrena*) or nine small genera (as in the seven-genus solution, but *Cerrena* and *Somion* divided into two each). The latter are fairly similar phylogenetically to the seven-genus solution, but genera in them would be more difficult to define morphologically. The phylogenetically simplest three-genus solution is worthy of further comments.

Nomenclaturally, the three-genus option would cause many more changes to the *status quo* than the other options. On the positive side, the three genera would be phylogenetically more distinct (distant) than in the other solutions, and therefore likely more robust over time, when more species are discovered and added to the phylogenetic estimate. In the other schemes, compulsory modifications are more likely, when species that do not fit to genera, for instance within the *Cerrena-Pseudolagarobasidium* clade, turn up. However, we cannot work with the unknown, and the above-mentioned point of view should not be overemphasized. Our sampling covers all forested continents and is tolerably representative of genus diversity in the family.

If we were to define genera for the hydnoid members of the family in isolation, then division into *Irpiciporus* (incl. *Radulodon*) and *Pseudolagarobasidium* would be well justified both morphologically and phylogenetically. However, once polypores are added, either *Pseudolagarobasidium* would need to be included in a morphologically heterogeneous *Cerrena* (the three-genus solution), or the *Irpiciporus* clade would need to be divided into three genera (the seven-genus solution we have adopted, Fig. 3). Either way, the solution no longer appears optimal from the isolationist perspective.

Defining genera from the polypore perspective, division into four (*Irpiciporus*, *Somion*, *Cerrena*, and *Lividopora*) is the most natural solution morphologically, and the one we have adopted here, even if it causes splitting of hydnoid taxa. The three-genus solution (*Cerrena* incl. *Lividopora*, *Irpiciporus*, and *Somion*) could be morphologically somehow justified. Again, when hydnoid taxa are added, the *Irpiciporus* concept becomes more diluted and *Cerrena sensu lato* would include nearly monomitic, hydnoid species of *Pseudolagarobasidium*, making it a yet more difficult concept morphologically.

We have chosen here the seven-genus solution as the one optimizing morphological recognition with phylogenetic signal, while minimizing nomenclatural changes. In doing so we have had to abandon easy-to-define genera for hydnoid fungi. This underlies the importance of integrating different morphogroups and their research traditions when making conclusions on higher-level taxonomy. Polypores and corticioid fungi in particular are very often intermixed above the genus level, as is the case of the *Cerrenaceae*, *Irpicaceae*, *Polyporaceae*, and *Steccherinaceae* to give a few examples from the *Polyporales*. Our seven-genus solution avoids placing strictly hydnoid and poroid species in the same genus, which would have been the case for the three-genus solution.

Can the family *Cerrenaceae* be defined morphologically? Definition in the strict sense is not feasible, as is the case for most families in the *Polyporales*. A few general characters are shared by all the known species: mid-sized spores that are slightly cyanophilous if they are thick-walled, mid-sized to large basidia, hyphal structure that is never agglutinated, aggressive white rot; many, if not all species, are tree parasites or pathogens. These characters are found in many other families in *Agaricomycetes* and even as a combination are not unique to the *Cerrenaceae*.

We have focused on morphological and phylogenetic characters of the *Cerrenaceae*. Ecologically this family contains only species that inhabit trees, though quite many species are able to colonize living trees already and some are considered tree diseases. Some wood decay fungi are able to grow in soil as well, but this does not seem to be the case with the *Cerrenaceae*. When compiling ITS sequences for this study, we searched the UNITE database for species that belong to this family. UNITE contains many unique sequences, mostly soil-derived, not available through GenBank, but only few additional sequences were found through UNITE in this case, indicating that they are not an important component of soil funga.

Representatives of all the genera in the *Cerrenaceae* have been studied for their cultural morphology in varying degree with the exception of *Acanthodontia,* which has not been cultivated to our knowledge. In particular, *Cerrena unicolor* has been studied for its enzymes associated with white rot (see Introduction). When grown on agar plates, members of the family produce fast-growing, white, well-spaced mycelium cottony on the surface, with clamps in part of the septa, conidia, and they show signs of laccase and peroxidase activity (David 1969, Setliff 1972a, Stalpers 1978, Woods & Ginns 2006). In this sense the *Cerrenaceae* are rather uniform, but with the current sampling of a single specimen and species per genus, little can be said on how the genera differ in their cultural characters, if at all. The above-mentioned set of characters is also not unique to the *Cerrenaceae*, and for instance in the key of Stalpers (1978), the family appears in different parts of the key intermixed with unrelated species. It would appear that cultural characters are not very useful for the systematics of the *Cerrenaceae*.

Surprisingly, only one high-quality genome sequence, *Cerrena unicolor*, has been produced for the whole family, by the US Joint Genome Institute. Even this genome is not yet public, though it is visible in the Mycocosm database (Grigoryev *et al*. 2013). It is a typical white-rot polypore genome in size and in its gene count of carbohydrate active enzymes such as class II peroxidases and other genes associated with wood decomposition. Considering how easy the *Cerrenaceae* are to culture and due to their economic importance as tree pathogens, we would expect more high-quality genome sequences to be published soon, enabling comparative genomics.

We will end this paper with a note on the intriguing ecology of the *Cerrenaceae*. *Cerrena unicolor* is spread by several species of the woodwasp (*Siricidae*) genera *Tremex* and *Eriotremex* (Stillwell 1964, Tabata & Abe 1995, Pažoutová & Šrůtka 2007, Schiff *et al*. 2012). The symbiosis between woodwasp and *Amylostereum* (*Russulales*) is well-documented, but so far, no other fungi than *Amylostereum* and *Cerrena* are known to be associated with woodwasps. Could other species of *Cerrena* be associated with insects in a similar manner? And to expand, many species in this family attack living trees as mentioned in the introduction. In addition to *Cerrena*, also *Pseudolagarobasidium* and *Somion* are pathogenic; *Lividopora* spp. are known to be

tree pathogens but also endophytes, *i.e.* present as mycelium in healthy plant tissues. Could insect association provide a route for these species to enter living trees?

ACKNOWLEDGEMENTS

We would like to thank Genevieve Gates, Romina Gazis, Jacob Heilmann-Clausen and Alfredo Justo for generously sharing their material, Yu-Cheng Dai and his research group for joint field work, University of Andalas for arrangements of field trips in Sumatra, Matthew Smith for hosting OM in Florida, Jean Lodge and the US forest service for making field work in Puerto Rico possible, and Alfredo Justo for sequences. Rolinus Paulous assisted during the field work in Malaysia. We are indebted to Alexander Sennikov and Konstanze Bensch for their advice on nomenclatural questions. Gaurav Sablok assembled genomes that provided some sequences for this study. Andy Overall provided us a photo of *Somion occarium*, as did Tuomo Niemelä for *C. albocinnamomea*. We acknowledge Abbot Oghenekaro for help in sequencing and IT Center for Science, Finland, for computational resources. Funding for this project was provided by the European Research Council (Marie Curie International Outgoing Fellowship), National Science Foundation project PolyPEET, institutional support of the Academy Sciences of the Czech Republic RVO: 60077344, Academy of Finland project grant 315927, University of Helsinki 3-year research grant, and White Rose mechanistic biology DTP. Finnish Barcode of Life (FinBOL) ITS data were utilized here. Malaysian collections were made under Sabah Biodiversity Council permit JKM/MBS.1000-2/2 JLD.11(3).

Conflict of interest: The authors declare that there is no conflict of interest.

REFERENCES

Abarenkov K, Tedersoo L, Nilsson RH, *et al.* (2010). PlutoF – a web based workbench for ecological and taxonomic research, with an online implementation for fungal ITS sequences. *Evolutionary Bioinformatics* **6**: EBO.S6271.

Adanson M (1763). *Familles des plantes.* Vincent, Paris.

Altschul SF, Madden TL, Schäffer AA, *et al.* (1997). Gapped BLAST and PSI-BLAST: a new generation of protein database search programs. *Nucleic Acids Research* **25**: 3389–3402.

Batsch AJGK (1783). *Elenchus fungorum*. Halle.

Berkeley MJ (1854). Decades of fungi. Decades XLIV–XLVI. Indian fungi. *Hooker's Journal of Botany and Kew Garden Miscellany* **6**: 161–174.

Bernicchia A (2005). *Polyporaceae s.l.*, vol 10. Fungi Europaei. Candusso, Alassio.

Bondartsev AS (1953). *Trutovye griby evropeiskoi chasti SSSR i Kavkaza*. Academy of the Sciences of the USSR, Moscow-Leningrad.

Bulliard P (1789). *Herbier de la France*, vol 9. Bulliard, Paris.

Černý A (1979). Bělochoroš bukový - *Sponipellis delectans* (Peck) Murr. - nový choroš pro ČSSR. *Česká Mykologie* **33**: 99–105.

Chen C-C, Chen C-Y, Wu S-H (2021). Species diversity, taxonomy and multi-gene phylogeny of phlebioid clade (*Phanerochaetaceae, Irpicaceae, Meruliaceae*) of *Polyporales*. *Fungal Diversity* **111**: 337–442.

Corner EJH (1987). Ad Polyporaceas IV. *Beihefte zur Nova Hedwigia* **86**: 1–276.

Corner EJH (1989). Ad Polyporaceas V. *Beihefte zur Nova Hedwigia* **96**: 1–218.

Dai Y-C, Cui B-K, Yuan H-S, *et al.* (2007). Pathogenic wood-decaying fungi in China. *Forest Pathology* **37**: 105–120.

Dai Y-C, Niemelä T (1997). Changbai wood-rotting fungi 6. study on *Antrodiella*, two new species and notes on some other species. *Mycotaxon* **64**: 67–81.

Darriba D, Posada D, Kozlov AM, *et al.* (2020). ModelTest-NG: A new and scalable tool for the selection of DNA and protein evolutionary models. *Molecular Biology and Evolution* **37**: 291–294.

David A (1969). Caractères culturaux et cytologiques d'espèces du genre *Spongipellis* Pat. et affines. Bulletin Mensuel de la Société Linnéenne de Lyon **38**: 191–201.

Donk MA (1960). The generic names proposed for *Polyporaceae*. *Persoonia* **1**: 173–302.

Donk MA (1974). *Check-list of European polypores*. North-Holland Pub. Comp., Amsterdam.

Dvořák D, Běťák J, Tomšovský M (2014). *Aurantiporus alborubescens* (*Basidiomycota, Polyporales*) – first record in the Carpathians and notes on its systematic position. *Czech Mycology* **66**: 71–84.

Elisashvili V, Kachlishvili E, Khardziani T, *et al.* (2010). Effect of aromatic compounds on the production of laccase and manganese peroxidase by white-rot basidiomycetes. *Journal of Industrial Microbiology & Biotechnology* **37**: 1091–1096.

Eriksson J, Hjortstam K, Ryvarden L (1981). *The Corticiaceae of North Europe 6*. *Phlebia-Sarcodontia*. Fungiflora, Oslo.

Fries EM (1821). *Systema mycologicum* 1. Ex officina Berlingiana, Lund.

Fries EM (1828). *Elenchus fungorum*. Sumptibus E. Mauritii.

Fries EM (1836–1838). *Epicrisis systematis mycologici*. Typographia Academica, Uppsala.

Garbelotto MM, Lee HK, Slaughter G, *et al.* (1997). Heterokaryosis is not required for virulence of *Heterobasidion annosum*. *Mycologia* **89**: 92–102.

Gilbertson RL, Ryvarden L (1986). *North American Polypores Vol. 1*. *Abortiporus* to *Lindtneria*. Fungiflora, Oslo.

Gilbertson RL, Ryvarden L (1987). *North American Polypores Vol. 2*. *Megasporoporia* to *Wrightoporia*. Fungiflora, Oslo.

Gray SF (1821). *Natural arrangement of British plants, vol 1*. Baldwin, Cradock and Joy, London.

Grigoriev IV, Nikitin R, Haridas S, *et al.* (2013). MycoCosm portal: gearing up for 1000 fungal genomes. *Nucleic Acids Research* **42**: D699–D704.

Gutaker RM, Reiter E, Furtwängler A, *et al.* (2017). Extraction of ultrashort DNA molecules from herbarium specimens. *Biotechniques* **62**: 76–79.

Hallenberg N, Ryberg M, Nilsson RH, *et al.* (2008). *Pseudolagarobasidium* (*Basidiomycota*): on the reinstatement of a genus of parasitic, saprophytic, and endophytic resupinate fungi. *Botany* **86**: 1319–1325.

Hartikainen ES, Miettinen O, Hatakka A, *et al.* (2016). Decolorization of six synthetic dyes by fungi. *American Journal of Environmental Sciences* **12**: 77–85.

Hattori T (2001). Type studies of the polypores described by E.J.H. Corner from Asia and West Pacific Areas II. Species described in *Gloeophyllum*, *Heteroporus*, *Microporellus*, *Oxyporus*, *Paratrichaptum*, and *Rigidoporus*. *Mycoscience* **42**: 19–28.

Hattori T (2002). Type studies of the polypores described by E.J.H. Corner from Asia and West Pacific Areas. IV. Species described in *Tyromyces* (1). *Mycoscience* **43**: 307–315.

Hattori T (2003). Type studies of the polypores described by E.J.H. Corner from Asia and West Pacific Areas. VI. Species described in *Tyromyces* (3), *Cristelloporia, Grifola, Hapalopilus, Heterobasidion, Ischnoderma, Loweporus,* and *Steccherici*um. *Mycoscience* **44**: 453–463.

Hibbett DS, Binder M, Bischoff JF, *et al.* (2007). A higher-level phylogenetic classification of the *Fungi*. *Mycological Research* **111**: 509–547.

Hjortstam K (1987). A check-list of genera and species of corticioid fungi (*Hymenomycetes*). *Windahlia* **17**: 55–85.

Hjortstam K, Larsson K-H (1995). Annotated check-list to genera and species of corticioid fungi (*Aphyllophorales, Basidiomycotina*) with special regards to tropical and subtropical areas. *Windahlia* **21**: 1–75.

Hood IA, Dick M (1988). *Junghuhnia vincta* (Berkeley) *comb. nov*., root pathogen of *Pinus radiata*. *New Zealand Journal of Botany* **26**: 113–116.

Hooker JD (1854). *Himalayan journals; or, Notes of a naturalist in Bengal, the Sikkim and Nepal Himalayas, the Khasia Mountains, vol 1*. J. Murray, London.

Ipulet P, Ryvarden L (2005). New and interesting polypores from Uganda. *Synopsis Fungorum* **20**: 87–99.

Jang JC, Chen T (1985). *Pseudolagarobasidium leguminicola gen. et sp. nov.* on *Leucaena* in Taiwan. *Transactions of the British Mycological Society* **85**: 374–377.

Janusz G, Mazur A, Wielbo J, *et al.* (2018). Comparative transcriptomic analysis of *Cerrena unicolor* revealed differential expression of genes engaged in degradation of various kinds of wood. *Microbiological Research* **207**: 256–268.

Janusz G, Rogalski J, Szczodrak J (2007). Increased production of laccase by *Cerrena unicolor* in submerged liquid cultures. *World Journal of Microbiology and Biotechnology* **23**: 1459–1464.

Justo A, Hibbett D (2011). Phylogenetic classification of *Trametes* (*Basidiomycota, Polyporales*) based on a five-marker dataset *Taxon* **60**: 1567–1583.

Justo A, Miettinen O, Floudas D, *et al.* (2017). A revised family-level classification of the *Polyporales* (*Basidiomycota*). *Fungal Biology* **121**: 798–824.

Katoh K, Rozewicki J, Yamada KD (2017). MAFFT online service: multiple sequence alignment, interactive sequence choice and visualization. *Briefings in Bioinformatics* **20**: 1160–1166.

Kaur G, Singh AP, Dhingra GS (2014). *Radulodon acaciae sp. nov*. from India. *Mycotaxon* **127**: 111–113

Kotiranta H, Kulju M, Miettinen O (2017). *Caudicicola gracilis* (*Polyporales, Basidiomycota*), a new polypore species and genus from Finland. *Annales Botanici Fennici* **54**: 159–167.

Kotlaba F, Pouzar Z (1957). Nové nebo málo známé choroše pro Československo. *Česká Mykologie* **9**: 214–224.

Kotlaba F, Pouzar Z (1965). *Spongipellis litschaueri* Lohwag a *Tyromyces kmetii* (Bres.) Bond. et Sing., dva vzácné bělochoroše v Československu (*Spongipellis litschaueri* Lohwag and *Tyromyces kmetii* (Bres.) Bond. et Sing., two rare polypores in Czechoslovakia). *Česká Mykologie* **19**: 69–78.

Kozlov AM, Darriba D, Flouri T, *et al.* (2019). RAxML-NG: a fast, scalable and user-friendly tool for maximum likelihood phylogenetic inference. *Bioinformatics* **35**: 4453–4455.

Kretzer AM, Bruns TD (1999). Use of *atp6* in fungal phylogenetics: an example from the *Boletales*. *Molecular Phylogenetics and Evolution* **13**: 483–492.

Kumar S, Stecher G, Tamura K (2016). MEGA7: Molecular Evolutionary Genetics Analysis Version 7.0 for bigger datasets. *Molecular Biology and Evolution* **33**: 1870–1874.

Lee SS, Noraini Sikin Y (1999). Fungi associated with heart rot of *Acacia mangium* trees in Peninsular Malaysia and East Kalimantan. *Journal of Tropical Forest Science* **11**: 240.

Li Y, Nakasone KK, Chen C-C, *et al.* (2022). Taxonomy and phylogeny of *Cystostereaceae* (*Agaricales, Basidiomycota*): a new genus, five new species, and three new combinations. *Journal of Fungi* **8**: 1229.

Lisova ZA, Lisov AV, Leontievsky AA (2010). Two laccase isoforms of the basidiomycete *Cerrena unicolor* VKMF-3196. Induction, isolation and properties. *Journal of Basic Microbiology* **50**: 72–82.

Ljubarsky D (1934). On fungal plant deceases and wood-rotters in the South Ussuri area. *Vestnik DVFAN SSSR* **9**: 75–104. [translated from Russian]

Lowe JL (1975). *Polyporaceae* of North America. The genus *Tyromyces*. *Mycotaxon* **2**: 1–82.

Löytynoja A (2021). Phylogeny-aware alignment with PRANK and PAGAN. In: Katoh K (ed) *Multiple sequence alignment: methods and protocols*. Springer US, New York, NY: 17–37.

Maas Geesteranus RA (1974). Studies in the genera *Irpex* and *Steccherinum*. *Persoonia* **7**: 443–581.

Maekawa N (2002). *Pseudolagarobasidium calcareum*: Japanese records and cultural characteristics. *Mycoscience* **43**: 271–275.

Maekawa N, Hasebe K (2002). *Pseudolagarobasidium calcareum*: Japanese records and cultural characteristics. *Mycoscience* **43**: 271–275.

Maekawa N, Sugawara R, Kogi H, *et al.* (2023). *Hypochnicium sensu lato* (*Polyporales, Basidiomycota*) from Japan, with descriptions of a new genus and three new species. *Mycoscience* **64**: 19–34.

Martin R, Gazis R, Skaltsas D, *et al.* (2015). Unexpected diversity of basidiomycetous endophytes in sapwood and leaves of *Hevea*. *Mycologia* **107**: 284–297.

Matheny PB, Liu YJ, Ammirati JF, *et al.* (2002). Using RPB1 sequences to improve phylogenetic inference among mushrooms (*Inocybe*, *Agaricales*). *American Journal of Botany* **89**: 688–698.

Micheli PA (1729). *Nova plantarum genera*. Florence.

Miettinen O, Larsson E, Sjökvist E, *et al.* (2012). Comprehensive taxon sampling reveals unaccounted diversity and morphological plasticity in a group of dimitic polypores (*Polyporales*, *Basidiomycota*). *Cladistics* **28**: 251–270.

Miettinen O, Vlasák J, Rivoire B, Spirin V (2018). *Postia caesia* complex (*Polyporales*, *Basidiomycota*) in temperate Northern Hemisphere. *Fungal Systematics and Evolution* **1**: 101–129.

Murrill WA (1903). A historical review of the genera of *Polyporaceae*. *Journal of Mycology* **9**: 87–102.

Murrill WA (1905). The *Polyporaceae* of North America: XII. A synopsis of the white and bright-colored pileate species. *Bulletin of the Torrey Botanical Club* **32**: 469–493.

Murrill WA (1908). *Polyporaceae*, Part 2. *North American Flora* **9**: 73–173.

Müller J, Müller K, Quandt D (2010) PhyDE – Phylogenetic Data Editor, version 0.997. http: //phyde.de.

Nakasone K, Ortiz-Santana B (2022). New species and combinations in the *Cerrenaceae* (*Polyporales*, *Basidiomycota*). *Lilloa* **59** (Suppl.): 89–113.

Nakasone KK (2001). Taxonomy of the genus *Radulodon*. *Harvard Papers in Botany* **6**: 163–177.

Nakasone KK (2012). Type studies of corticioid *Hymenomycetes* (*Basidiomycota*) with aculei – Part II. *Czech Mycology* **64**: 23–42.

Nakasone KK (2015). Taxonomic studies in *Chrysoderma*, *Corneromyces*, *Dendrophysellum*, *Hyphoradulum*, and *Mycobonia*. *Mycotaxon* **130**: 369–397.

Nakasone KK, Lindner DL (2012). Taxonomy of *Pseudolagarobasidium* (*Polyporales*, *Basidiomycota*). *Fungal Diversity* **55**: 155–169.

Nakasone KK, Ortiz-Santana B, He S-H (2021). Taxonomic studies of crust fungi with spines in *Radulomyces*, *Sarcodontia*, and the new genus *Noblesia*. *Mycological Progress* **20**: 1479–1501.

Niemelä T (2005). Käävät, puiden sienet. Polypores, lignicolous fungi. *Norrlinia* **13**: 1-320

Nikolaeva TL (1964). Новый и впервые обнарушенные в СССР Виды ежовиковых грибов (сем. Hydnaceae) (Novyy i vpervye obnarushennye v SSSR vidy ezhovikovyh gribov (sem. Hydnaceae)). *Novosti Sistematiki Nizshikh Rastenii* **1**: 168–175.

Nilsson RH, Glöckner FO, Saar I, *et al.* (2018). The UNITE database for molecular identification of fungi: handling dark taxa and parallel taxonomic classifications. *Nucleic Acids Research* **47**: D259–D264.

Nobles MK (1948). Studies in forest pathology VI. Identification of cultures of wood-rotting fungi. *Canadian Journal of Research C* **26**: 281–431.

Nobles MK (1965). Identification of cultures of wood-inhabiting *Hymenomycetes*. *Canadian Journal of Botany* **43**: 1097-1139.

Nuñez M, Ryvarden L (2001). East Asian polypores, volume 2 - *Polyporaceae s. lato*. *Synopsis Fungorum* **14**: 169–522.

Pažoutová S, Šrůtka P (2007). Symbiotic relationship between *Cerrena unicolor* and the horntail *Tremex fuscicornis* recorded in the Czech Republic. *Czech Mycology* **59**: 83–90.

Persoon CH (1801). *Synopsis methodica fungorum*. Göttingen.

Rajchenberg M (1994). A taxonomic study of the subantarctic *Piptoporus* (*Polyporaceae*, *Basidiomycetes*) I. *Nordic Journal of Botany* **14**: 435–449.

Rehner SA, Buckley E (2005). A *Beauveria* phylogeny inferred from nuclear ITS and EF1-α sequences: evidence for cryptic diversification and links to *Cordyceps* teleomorphs. *Mycologia* **97**: 84–98.

Rivoire B (2020). *Polypores de France et d'Europe*. Mycopolydev, Orliénas.

Ronquist F, Teslenko M, van der Mark P, *et al.* (2012). MrBayes 3.2: efficient Bayesian phylogenetic inference and model choice across a large model space. *Systematic Biology* **61**: 539–542.

Ryvarden L (1972a). *Radulodon*, a new genus in the *Corticiaceae* (*Basidiomycetes*). *Canadian Journal of Botany* **50**: 2073–2076.

Ryvarden L (1972b). Studies on the *Aphyllophorales* of the Canary Islands with a note on the genus *Perenniporia* Murr. *Norwegian Journal of Botany* **19**: 139–144.

Ryvarden L (1977). Type studies in the *Polyporaceae* 10. Species described by J. M. Berkeley, either alone or with other authors, from 1844 to 1845. *Norwegian Journal of Botany* **24**: 213–230.

Ryvarden L (1983). Type studies in the *Polyporaceae* 14. species described by N. Patouillard, either alone or with other mycologists. Occasional papers of the Farlow Herbarium of Cryptogamic Botany. Harvard University Herbaria, Cambridge, MA.

Ryvarden L (1984). Type studies in the *Polyporaceae* 16. Species described by J. M. Berkeley, either alone or with other mycologists from 1856 to 1886. *Mycotaxon* **20**: 329–363.

Ryvarden L (1988). Type studies in the *Polyporaceae*. 20. Species described by G. Bresadola. *Mycotaxon* **33**: 303–327.

Ryvarden L (1991). Genera of polypores. Nomenclature and taxonomy. *Synopsis Fungorum* **5**: 1–363.

Ryvarden L (1992). On *Irpex zonatus*. *Boletin de la Sociedad Argentina de Botánica* **28**: 227–231.

Ryvarden L (2012). Studies in neotropical polypores 33. *Cerrena gilbertsonii* nov. sp. *Synopsis Fungorum* **30**: 44–45.

Ryvarden L (2015). Neotropical polypores, part 2. *Polyporaceae*, *Abortiporus-Nigroporus*. *Synopsis Fungorum* **34**: 232–443.

Ryvarden L (2018). Studies in African *Aphyllophorales* 25. New species from East and Central Africa. *Synopsis Fungorum* **38**: 25–32.

Ryvarden L (2020a). *Aphyllophorales* 36 - more new African polypores. *Synopsis Fungorum* **40**: 101–105.

Ryvarden L (2020b). The genus *Irpex* - a synopsis. *Synopsis Fungorum* **41**: 33–49.

Ryvarden L, Johansen I (1980). *A preliminary polypore flora of East Africa*. Fungiflora, Oslo.

Ryvarden L, Melo I (2016). *Poroid fungi of Europe*. vol 37, 2nd revised edition edn. Fungiflora, Oslo.

Savchenko A, Zamora JC, Shirouzu T, *et al.* (2021). Revision of *Cerinomyces* (*Dacrymycetes, Basidiomycota*) with notes on morphologically and historically related taxa. *Studies in Mycology* **99**: 1–72.

Sayers EW, Bolton EE, Brister JR, *et al.* (2022). Database resources of the National Center for Biotechnology Information in 2023. *Nucleic Acids Research* **51**: D29–D38.

Schiff NM, Goulet H, Smith DR, *et al.* (2012). *Siricidae* (*Hymenoptera: Symphyta: Siricoidea*) of the Western Hemisphere. *Canadian Journal of Arthropod Identification* **21**: 1–305.

Schweinitz LD (1822). Synopsis fungorum Carolinae Superioris. *Schriften der Naturforschenden Gesellschaft zu Leipzig* **1**: 21–122.

Setliff EC (1972a). Cultural characteristics of *Poria vincta*. *Mycologia* **64**: 641–646.

Setliff EC (1972b). The taxonomy and morphology of *Poria vincta*. *Mycologia* **64**: 689–701.

Setliff EC, Mesner W (1971). A root rot disease of forest trees caused by *Poria vincta* var. *cinerea*. *Plant Disease Reporter* **55**: 257–260.

Spirin V, Vlasák J, Niemelä T, *et al.* (2013). What is *Antrodia sensu stricto*? *Mycologia* **105**: 1555–1576.

Spirin V, Vlasák J, Niemelä T, Miettinen O (2022). Studies in *Spongipellis sensu stricto* (*Polyporales, Basidiomycota*). *Lilloa* **59** (Suppl.): 341–358.

Stevenson JA, Cash EK (1936). The new fungus names proposed by C. G. Lloyd. *Bulletin of the Lloyd library and museum* **35**: 1–209.

Stillwell MA (1964). The fungus associated with woodwasps occurring in beech in New Brunswick. *Canadian Journal of Botany* **42**: 495–496.

Tabata M, Abe Y (1995). *Cerrena unicolor* isolated from the mycangia of a horntail, *Tremex longicollis*, in Kochi Prefecture, Japan. *Mycoscience* **36**: 447–450.

Thiers B (2023) *Index Herbariorum*. http://sweetgum.nybg.org/science/ih. Accessed 24 Apr. 2023.

Tomšovský M (2012). Delimitation of an almost forgotten species *Spongipellis litschaueri* (*Polyporales*, *Basidiomycota*) and its taxonomic position within the genus. *Mycological Progress* **11**: 415–424.

Viner I, Bortnikov F, Ryvarden L, *et al.* (2021). On six African species of *Lyomyces* and *Xylodon*. *Fungal Systematics and Evolution* **8**: 163–178.

Wang C-G, Dai Y-C (2022). Phylogeny and taxonomy of *Spongipellis* (*Polyporales*, *Basidiomycota*) and its micromorphological similar genera. *Mycological Progress* **21**: 73.

Westhuizen GCAvd (1963). The cultural characters, structure of the fruit body, and type of interfertility of *Cerrena unicolor* (Bull. ex Fr.) Murr. *Canadian Journal of Botany* **41**: 1487–1499.

Westphalen MC, Motato-Vásquez V (2022). A new species of *Pseudolagarobasidium* from Brazil and new insights on *Cerrena* (*Basidiomycota*, *Cerrenaceae*). *Phytotaxa* **555**: 2.

Westphalen MC, Tomsovsky M, Gugliotta AM, *et al.* (2019). An overview of *Antrodiella* and related genera of *Polyporales* from the Neotropics. *Mycologia* **111**: 813–831.

White TJ, Bruns T, Lee S, *et al.* (1990). Amplification and direct sequencing of fungal ribosomal RNA genes for phylogenetics. In: Innis MA, Gelfand DH, Sinisky JJ, *et al.* (eds) *PCR protocols, a guide to method and application*. Academic Press, San Diego: 315–322.

Wood AR, Ginns J (2006). A new dieback disease of *Acacia cyclops* in South Africa caused by *Pseudolagarobasidium acaciicola sp. nov*. *Canadian Journal of Botany* **84**: 750–758.

Wu F, Chen J-J, Ji X-H, *et al.* (2018). Phylogeny and diversity of the morphologically similar polypore genera *Rigidoporus*, *Physisporinus*, *Oxyporus*, and *Leucophellinus*. *Mycologia* **109**: 749–765.

Yuan H-S (2014). Molecular phylogenetic evaluation of *Antrodiella* and morphologically allied genera in China. *Mycological Progress* **13**: 353–364

Yuan H-S, Dai Y-C, Steffen K (2012). Screening and evaluation of white rot fungi to decolourise synthetic dyes, with particular reference to *Antrodiella albocinnamomea*. *Mycology* **3**: 100–108.

Zhao C-l, Liu S-l, Ren G-j, *et al.* (2017). Three species of wood-decaying fungi in *Polyporales* new to China. *Mycotaxon* **132**: 29–42.

Supplementary Material: http://fuse-journal.org/

Fig. S1. Bayesian consensus tree of *Cerrenaceae* based on nrDNA ITS and LSU sequences. Countries (and states) are denoted with ISO 3166 codes.

Fig. S2. Bayesian consensus tree of the *Cerrenaceae* based on mitochondrial SSU sequences.

Fig. S3. Bayesian consensus tree of the *Cerrenaceae* based on mitochondrial *ATP6* sequences.

Fig. S4. Bayesian consensus tree of the *Cerrenaceae* based on nuclear *RPB1* sequences.

Fig. S5. Bayesian consensus tree of the *Cerrenaceae* based on nuclear *TEF1* sequences.

Fungal Systematics and Evolution (ISSN: 2589-3823, E-ISSN: 2589-3831)

About Fungal Systematics and Evolution

Fungal Systematics and Evolution has an OPEN ACCESS publishing policy. All manuscripts will undergo peer review before acceptance, and will be published as quickly as possible following acceptance. There are no page charges or length restrictions, or fees for colour plates. The official journal language is English. All content submitted to Fungal Systematics and Evolution is checked for plagiarism.

For more information and ordering of other books and publications, see www.fuse-org.com and www.wi.knaw.nl.

About the Westerdijk Fungal Biodiversity Institute

The Westerdijk Fungal Biodiversity Institute is the largest expertise centre for microfungi in the world. Our renowned researchers dedicate themselves to enriching and expanding our Fungal Biobank. We explore the fungal kingdom to gain a better understanding of their fungal characteristics and their potential applications, especially in the fields of industry, agriculture and healthcare.

The Westerdijk Fungal Biodiversity Institute is part of the Royal Netherlands Academy of Arts and Sciences (KNAW).

Explore - study - preserve - explore